DTIC FILE COPY

PROCEEDINGS
OF THE
33rd ANNUAL SYMPOSIUM ON FREQUENCY CONTROL

HELD IN ~~1979~~ ATLANTIC CITY, NEW JERSEY
ON 30 MAY - 1 JUNE 1979.

AD-A213 544

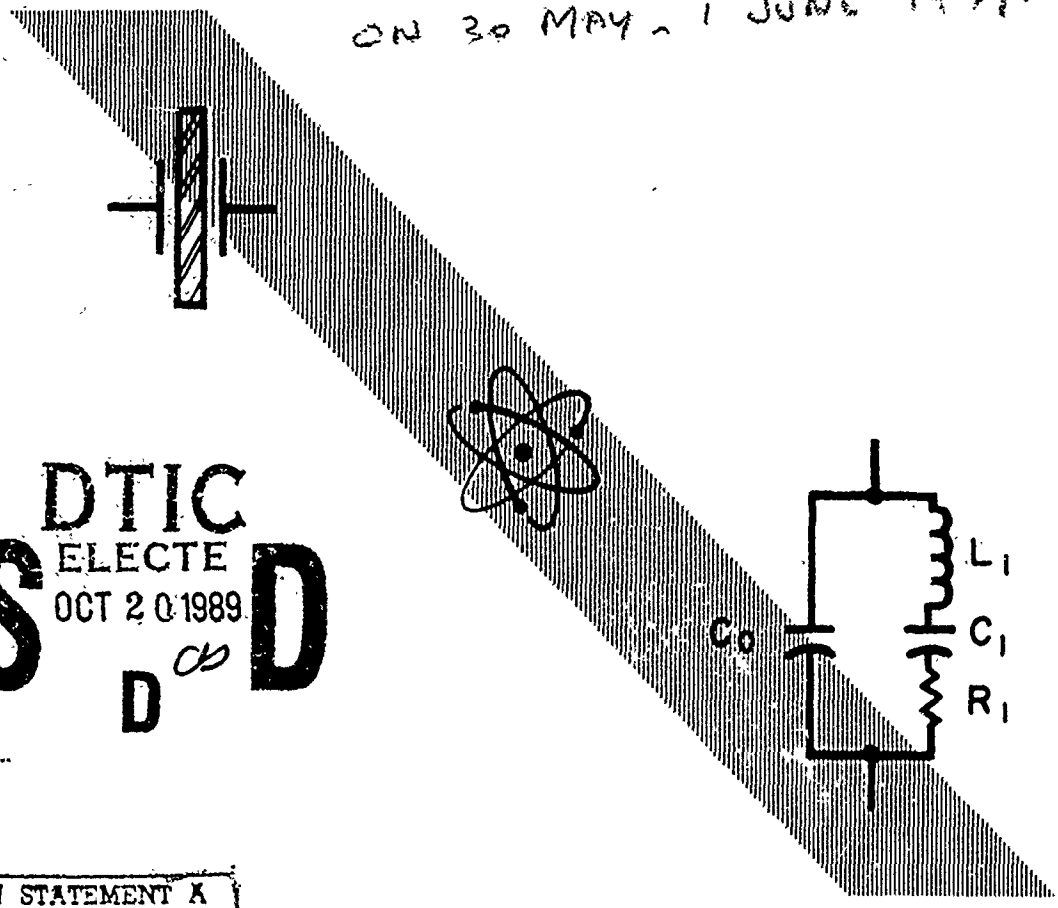

DTIC
ELECTE
OCT 2 0 1989
S D
D CD

DISTRIBUTION STATEMENT A
Approved for public release;
Distribution Unlimited

30 May - 1 June 1979

U.S. Army Electronics Research And Development Command

89 10 20 248

PROCEEDINGS

of the

THIRTY SECOND ANNUAL FREQUENCY CONTROL SYMPOSIUM

1979

Sponsored by

DTIC
COPY
INSPECTED
4

U.S. ARMY ELECTRONICS RESEARCH AND DEVELOPMENT COMMAND
Major General Charles D. Daniel, Jr.
Commanding

ELECTRONICS TECHNOLOGY AND DEVICES LABORATORY
Dr. C. G. Thornton
Director

© Electronic Industries Association 1979
All rights reserved
Printed in U.S.A.

Accession For
NTIS GRA&I
DTIC TAB
Unannounced
Justification
By per form 50
Distribution/
out of stock
Availability Codes
Dist | Avail and/or special
A-1

Copies of the Proceedings are available from:

Electronic Industries Association
2001 Eye Street, N.W.
Washington, D.C. 20006

~~PRICE PER COPY: $12.50~~

None of the papers contained in the Proceedings may be reproduced in whole or in part, except for the customary brief abstract, without permission of the author, and without due credit to the Symposium.

30 MAY - 1 JUNE 1979

Boardwalk Regency Hotel
Atlantic City, New Jersey

THIRTY THIRD ANNUAL FREQUENCY CONTROL SYMPOSIUM

Sponsored By

U.S. ARMY ELECTRONICS RESEARCH AND DEVELOPMENT COMMAND
ELECTRONICS TECHNOLOGY AND DEVICES LABORATORY

Fort Monmouth, New Jersey

30, 31 MAY – 1 JUNE, 1979
Boardwalk Regency Hotel
Atlantic City, New Jersey

SYMPOSIUM EXECUTIVE COMMITTEE

Chairman — Dr. Erich Hafner
Executive Secretary — Mrs. Lee Hildebrandt

TECHNICAL PROGRAM COMMITTEE

Dr. Erich Hafner – Chairman
U.S. Army Electronics Technology and Devices Laboratory

Mr. E. J. Alexander
Bell Laboratories

Dr. A. Ballato
U.S. Army, ERADCOM

Dr. J. A. Barnes
National Bureau of Standards

Dr. M. Bloch
Frequency Electronics, Inc.

Mr. A. R. Chi
NASA – Goddard Space Flight Center

Dr. L. T. Claiborne
Texas Instruments

Dr. L. S. Cutler
Hewlett-Packard

Mr. M. E. Frerking
Rockwell International – Collins Radio Corp.

Mr. V. L. Friedrich
OFC, Asst. Sec'y of the Army (R&D)

Dr. H. Hellwig
Frequency & Time Systems

Mr. J. D. Holmbeck
Northern Engineering Laboratories

Dr. W. H. Horton
Piezo Technology, Inc.

Mr. T. Joseph
Hughes Aircraft Co.

Mr. A. Kahan
U.S. Air Force, RADC

Mr. E. Kentley
Hi-Q Quartz Products Limited

Dr. J. C. King
Sandia Laboratories

Mr. J. A. Kusters
Hewlett-Packard

Mr. E. Mariani
U.S. Army, ERADCOM

Dr. T. Meeker
Bell Laboratories

Mr. D. Reifel
Motorola, Inc.

Mr. S. S. Schodowski
U. S. Army, ERADCOM

Dr. J. R. Vig
U. S. Army, ERADCOM

Dr. G. M. R. Winkler
U. S. Naval Observatory

CHAIRMEN FOR TECHNICAL SESSIONS

PLENARY SESSION

Dr. A. McCoubrey, National Bureau of Standards

PROPERTIES OF PIEZOELECTRIC RESONATOR MATERIALS

Dr. J. C. King, Sandia Laboratories

FILTERS and MEASUREMENTS AND SPECIFICATIONS

Dr. W. H. Horton, Piezo Technology, Inc.

THEORY AND DESIGN OF CRYSTAL RESONATORS I TEMPERATURE EFFECTS; MINIATURE RESONATORS

Dr. T. R. Meeker, Bell Telephone Laboratories

THEORY AND DESIGN OF CRYSTAL RESONATORS II RESONATOR THEORY; EXTERNAL FORCE EFFECTS

Dr. R. D. Mindlin, Columbia University

RESONATOR PROCESSING and SURFACE ACOUSTIC WAVE DEVICES

Dr. D. L. Hammond, Hewlett-Packard

OSCILLATORS AND CIRCUITS

Mr. M. Beach, Frequency Electronics

FREQUENCY AND TIME and ATOMIC AND MOLECULAR FREQUENCY STANDARDS I

Dr. L. S. Cutler, Hewlett-Packard

ATOMIC AND MOLECULAR FREQUENCY STANDARDS II

Dr. J. A. Barnes, National Bureau of Standards

DISCUSSION PANEL ON FILTERS

Chairman — M. Dishal, ITT Avionics

F. J. Witt, Bell Laboratories
R. C. Smythe, Piezo Technology, Inc.
R. T. Enderby, Motorola, Inc.
C. H. Hewes, Texas Instruments, Inc.
R. Rosenfeld, SAWTEK, Inc.
E. M. Frymoyer, Rockwell International Inc.

This symposium included [illegible]

TABLE OF CONTENTS

Page

Plenary Session

The Sesquicentennial of the First Crystal Plate Equations
- R. D. Mindlin, Columbia University 1

Relativity and Clocks
- C. Alley, University of Maryland 4

1/f (Flicker) Noise: A Brief Review
- R. F. Voss, IBM 40

The Domestic and International Use of the Radio Spectrum
- D. M. Jansky, National Telecommunications and Information Administration..... 47

Properties of Piezoelectric Resonator Materials

Radiation Effects in Berlinite
- L. E. Halliburton, Oklahoma State University, L. A. Kappers, University of Connecticut, A. F. Armington and J. Larkin, Rome Air Development Center 62

Bulk and Surface Acoustic Wave Propagation in Berlinite
- J. Detaint, M. Feldmann, J. Henaff, H. Poignant and Y. Toudic, CNET 70

Piezoelectric Properties of Single Crystal Berlinite
- E. J. Ozimek and B. H. T. Chai, Allied Chemical Corporation 80

Solubility, Crystal Growth and Perfection of Aluminum Orthophosphate
- E. D. Kolb, R. L. Barnes, J. C. Grenier*, and R. A. Laudise, Bell Telephone Laboratories 88

Point Defects and Radiation Damage Processes in a-Quartz
- D. L. Griscom, Naval Research Laboratory 98

A High-Sensitivity AC Dilatometer for the Direct Measurement of Piezoelectricity and Electrostriction
- K. Uchino and L.E. Cross, The Pennsylvania State University 110

Radiation-Induced Frequency Transients In AT, BT and SC Cut Quartz Resonators
- D. R. Koehler, Sandia Laboratories 118

Radiation Effects in Swept Premium-Q Quartz Material, Resonators and Oscillators
- H. G. Lipson, F. Euler and P. A. Ligor, Rome Air Development Center 122

Radiation-Induced Mobility of Interstitial Ions in Synthetic Quartz
- J. J. Martin, S. P. Doherty, L.E. Halliburton, M. Markes, N. Koumvakalis and W. A. Sibley, Oklahoma State University and R. N. Brown and A. Armington, Rome Air Development Center 134

Filters

Monolithic Crystal Filters With High Q Factor and Low Spurious Level
- R. Lefevre, CNET 148

A Four-Frequency Process for Accurately Measuring Coupled-Dual Resonator Crystals
- G. E. Roberts, General Electric Company 159

New Discrete Crystal Filters for Bell System Analog Channel Banks
- D. I. McLean , A. F. Graziani and J. J. Royer, Bell Telephone Laboratories 166

The Design and Application of Electromechanical Single Silicon Beam Filters
- M. F. Hribsek, University of Belgrade 173

Measurements and Specifications

A Review of the New IEEE Standard on Piezoelectricity
- T. R. Meeker, Bell Telephone Laboratories 176

Trim Sensitivity - A Useful Characterization of a Resonator
- J. H. Sherman, Jr., General Electric 181

Page

New Metal Enclosures for Resistance Welding Developed to Meet Mil-Specifications
- D. Fuchs and K.H. Mucke, Jenaer Glaswerk Schott & Gen. 186

Quartz Crystal Measurements by a 'Phase-Amplitude' Method
- W. D. Beaver, W. E. Van Loben Sels, M. Wang, Comtec Economation, Inc. 189

Automatic Measurement of Parameters of VHF Quartz Crystal Resonators
- Y. Tsuzuki, M. Toki, T. Adachi and H. Yamagi, Yokohama National University 201

Discussion Panel on Filters

Digital Filters - An Overview
- F. J. Witt, Bell Telephone Laboratories 206

Modern Crystal Filters
- R. C. Smythe, Piezo Technology Inc. 209

CCD and Switched Capacitor Filters
- C. R. Hewes, Texas Instruments Inc. 214

Surface Acoustic Wave (SAW) Bandpass Filter Review
- R. C. Rosenfeld, Sawtek, Inc. 220

Mechanical Filters
- E. M. Frymoyer, Rockwell International 223

Theory and Design of Crystal Resonators I

Temperature Effects;

Temperature Induced Frequency Changes in Electroded Contoured Quartz Crystal Resonators
- B. K. Sinha and H. F. Tiersten, Rensselaer Polytechnic Institute 228

Frequency Response of a Quartz Oscillator to Temperature Fluctuation
- Y. Teramachi, M. Horie, H. Kataoka and T. Musha, Tokyo Institute of Technology 235

Dynamic Thermal Behavior of Quartz Resonators
- G. Theobald, G. Marianneau, R. Pretot and J. J. Gagnepain, CNRS 239

New Quartz Tuning Fork with Very Low Temperature Coefficent
- E. Momosaki, S. Kogure, M. Inoue and T. Sonoda, Suwa Seikosha Co., Ltd. 247

Miniature Resonators

A New Quartz Crystal Cut for Contour Mode Resonators
- J. Hermann and C. Bourgeois, Centre Electronique Horloger S.A. 255

Three-Dimensional Variational Analysis of Small Crystal Resonators
- R. F. Milsom, Philips Research Laboratories 263

Frequency Temperature Characteristics of Rectangular At-Cut Quartz Plates
- T. Kato and H. Ueda, Citizen Watch Co., Ltd. 271

New Frequency-Temperature Characteristics of 4.19MHz Beveled Rectangular At-Cut Quartz Resonator
- S. Yamashita, S. Motte, K. Takahashi, N. Echigo, A. Watanabe, K. Kubota, Daini Seikosha Co., Ltd. 277

Theory and Design of Crystal Resonators II

Resonatory Theory

Extension, Flexure, and Shear Modes in Rotated X-Cut Quartz Rectangular Bars
- T. R. Meeker, Bell Telephone Laboratories 286

Nonlinear Vibrations of Quartz Rods
- H. F. Tiersten, Rensselaer Polytechnic Institute and A. Ballato, USERADCOM 293

Temperature Dependence of the Force Frequency Effect for the Rotated X-Cut
- E. P. EerNisse, Sandia Laboratories 300

Page

External Force Effects

Low "g" Sensitivity Crystal Units and Their Testing
- A. Warner, B. Goldfrank, M. Meirs and M. Rosenfeld, Frequency Electronics, Inc. 306

Resonators for Severe Environments
- T. J. Lukaszek and A. Ballato, USAERADCOM 311

Resonators Compensated for Acceleration Fields
- A. Ballato, USAERADCOM 322

Design of a Bulk Wave Quartz Resonator Insensitive to Acceleration
- R. Beeson, ENSCMB, J. J. Gagnepain, LPMO, D. Janiaud and M. Valdois, ONERA 337

A Comparison of the Effects of Bending Moments on the Vibrations of AT and SC (or TTC) Cuts of Quartz
- E. D. Fletcher and A. J. Douglas, Philips Research Laboratories..... 346

Resonator Processing

Etching Studies on Singly and Doubly Rotated Quartz Plates
- J. R. Vig, Ronald J. Brandmayr and R. L. Filler, USAERADCOM 351

Anisotropy of Etching Rate for Quartz in Ammonium Bifluoride
- P. Suda, A. E. Zumsteg and W. Zingg, Omega 359

A Microprocessor Assisted Anodizing Apparatus for Frequency Adjustments
- Dick Ang, Tyco Crystal Products Inc. 364

Continuous Vacuum Processing System for Quartz Crystal Resonators
- R. J. Ney, General Electric Company, Neutron Devices Department and E. Hafner, USAERADCOM 368

Surface Acoustic Wave Devices

Hybrid Saw Oscillator Fabrication and Packaging
- S. J. Dolochycki, E. J. Staples, J. Wise, J. S. Schoenwald, and T. C. Lim, Rockwell International..... 374

Stability of Phase Shift on Quartz Saw Devices
- T. E. Parker and D. L. Lee, Raytheon Research Division 379

Analysis of Shallow Bulk Acoustic Wave Excitation by Interdigital Transducers
- K. F. Lau, K. H. Yen, J. Z. Wilcox and R. S. Kagiwada, TRW Defense and Space Systems Group 388

L-Band Low Loss Saw Filters
- B. R. Potter, Texas Instruments 396

A New Cut of Quartz with Orthogonal Temperature-Compensated Propagation Directions for Surface Acoustic Wave Applications
- R. M. O'Connell, Rome Air Development Center 402

Oscillators and Circuits

Performance Results of an Oscillator Using the SC Cut Crystal
- R. Burgoon and R. L. Wilson, Hewlett-Packard Company 406

Design Aspects of an Oscillator Using the SC Cut Crystal
- R. Burgoon and R. L. Wilson, Hewlett-Packard Company 411

An Analysis of Unwanted Frequency Oscillation in a Crystal Controlled Oscillator
- S. Kodama and Y. Sato, Nippon Electric Company, Ltd. 417

A Non-Interative Solution for a Two-Thermistor TCXO
- C. T. Swanson and E. S. McVey, University of Virginia 425

The Application of Microprocessors to Communications Equipment Design
- M. E. Frerking, Rockwell International 431

Use of Fiber Optic Frequency and Phase Determining Elements in Radar
- A. M. Levine, ITT Gilfillan 436

Page

Bulk Acoustic Resonators for Microwave Frequencies
- R. A. Moore, F. W. Hopwood, T. Haynes, B. R. McAvoy, Westinghouse Electric Company 444

The Effect of the Sampling Action of Phase Comparators on Frequency Synthesizer Performance
- M. J. Underhill and R. I. H. Scott, Philips Research Laboratories, UK 449

An m/n Frequency Divider Using a Lambda (Λ) - Shaped Three-Terminal Negative Resistance Device
- Y. Sekine, M. Suyama, K. Nakamura, H. Sekine and Y. Sakuta, Nihon University 458

Frequency and Time

A New Approach to Data Management and Its Impact on Frequency Control Requirements
- D. L. Blanchard, A. J. Fuchs and A. R. Chi, NASA-Goddard Space Flight Center 468

Two-Way Time Transfers Between National Research Council (Ottawa) and Paris Observatory Via the "Symphonie" Satellite
- C. C. Costain, J.-S. Boulanger, H. Daams, L. G. Miller, National Research Council, G. Freon, P. Parcelier, Laboratoire Primaire du Temps et des Frequences, M. Brunet, Bureau International de L'Heure, J. Azoubib and B. Guinot Bureau International de l'Heure 473

Atomic and Molecular Frequency Standards, I

Study of the Dependence of Frequency Upon Microwave Power of Wall-Coated and Buffer-Gas-Filled Passive Rb^{87} Frequency Standards
- A. Risley and S. Jarvis, Jr., National Bureau of Standards and J. Vanier, Universite Laval 477

Development of a Light Weight, Military, Cesium Standard
- I. Pascaru and M. Meirs, Frequency Electronics, Inc. 484

New Cesium Beam Tube Utilizing Hexapole / Double-Dipole Optics
- D. A. Emmons and P. J. Rogers, Frequency and Time Systems, Inc. 490

Laser to Microwave Frequency Division Using Synchrotron Radiation II
- J. C. Bergquist and D. J. Wineland, National Bureau of Standards 494

Atomic and Molecular Frequency Standards II

An Improved Multiplier Chain For Precise Frequency Measurements Up to 20 THz
- A. Godone, A. De Marchi, E. Bava, Istituto Elettrotecnico Nazionale 498

Comparison of Different Tuning and Modulation Techniques for F.I.R. Lasers
- A. De Marchi, A. Godone, E. Bava, Istituto Elettrotecnico Nazionale 504

Research With a Cold Atomic Hydrogen Maser
- R.F.C. Vessot, E. M. Mattison and E. L. Blomberg, Smithsonian Astrophysical Observatory.. 511

Amplitude Noise in Passively and Actively Operated Masers
- P. Lesage and C. Audoin, CNRS and M. Tetu, Universite Laval 515

Hydrogen Frequency Standard Using Free-Induction Technique
- H. T. M. Wang, Hughes Research Laboratories 536

Compact Cavity for Hydrogen Frequency Standard
- H. T. M. Wang and J. B. Lewis, Hughes Research Laboratories and S. B. Crampton, Williams College 543

Design, Construction and Testing of a Small Passive Hydrogen Maser
- E. M. Mattison, E. L. Blomberg, G. U. Nystrom and R. F. C. Vessot, Smithsonian Astrophysical Observatory 549

A Small, Passively Operated Hydrogen Maser
- D. A. Howe, F. L. Walls, H. E. Bell, and H. Hellwig, National Bureau of Standards 554

"Passive H Maser"
- G. Busca and H. Brandenberger, Ebauches S. A. 563

THE SESQUICENTENNIAL OF THE FIRST CRYSTAL PLATE EQUATIONS

R. D. MINDLIN
Professor Emeritus, Columbia University

Abstract

1979 marks the one hundred and fiftieth anniversary of Cauchy's differential equations of motion of crystal plates. In this talk, the main developments which preceded and followed Cauchy's contribution are reviewed; beginning with those of Galileo on the strength of beams, in 1638, and three generations of the Bernoulli family from Jacques, in 1691, on the equation of the elastica, to his great-nephew of the same name who published the first attempt at equations of flexure of plates - 1788. Included in the contributions stemming from the Bernoullis was Daniel Bernoulli's addition of the acceleration term to the beam equation, in 1735, and a variational derivation by Leonhard Euler - at one time a fellow student, with Daniel, under the tutelage of Daniel's father Jean. The 1788 equation of flexure of isotropic plates, by Daniel's nephew Jacques, was improved during 1811-1816 by Germain and Lagrange and, finally, the correct derivation was produced by Navier in 1820 - the year before he presented his invention of the general, three-dimensional, equations of elasticity from which, after some improvement, Cauchy deduced the equations of motion of crystal plates. Cauchy's equations, as we now know, are limited in application to very low frequencies. Extensions of his equations to higher frequencies did not appear until more than a century later - influenced by the intervening work of Rayleigh and Lamb in 1889, Lamb in 1917 and Timoshenko in 1921. The isolated paper by Ekstein, in 1945, was followed by a great flood of contributions starting in 1951. Beginning in 1956, most of the new advances were published in the Proceedings of these Annual Symposia on Frequency Control - many of the contributions by authors whose names appear in these Proceedings.

who inserted this garbage?

The following is an annotated bibliography for readers interested in further study of the history of the theory of plates.

1638 Galileo Galilei, "Discorsi e Dimonstrazioni Matematiche, intorno à due nuove scienze", in Leida, Appresso gli Elfevirii, 1638. English translation by H. Crew and A. de Salvio: "Dialogues Concerning Two New Sciences", Macmillan, New York, 1914. The two new sciences were those of motion and of strength of materials.

1798 P. S. Girard, "Traité analytique de la résistance des solides et des solides d'égale resistance", Paris 1798. The first book on strength of materials; contains a historical introduction of 47 pages.

1821 C. L. M. H. Navier, Mémoire sur les lois de l'équilibre et du mouvement des corps solides élastique", Presented to the Academy of Sciences on May 14, 1821, published 1827. First paper on the mathematical theory of elasticity.

1829 A. L. Cauchy, "Sur l'équilibre et le mouvement d'une plaque elastique dont l'elasticite n'est pas la même dans tous les sens", Exercices de Mathématiques, Quatrième Année, Bure Frères, Paris 1829; Oeuvres, Ser. 2, Vol 9, pp 9-22. First two-dimensional equations of motion of anisotropic plates (deduced from the three-dimensional equations and limited to low frequencies).

1852 G. Lamé, "Leçons sur la théorie mathématique de l'élasticité des corps solides", Gauthier-Villars, Paris, 1852. The first book on the mathematical theory of elasticity. Contains the solution for the equivoluminal modes of vibration of rectangular parallelepipeds with all faces traction-free. (rediscovered almost 100 years later by A. Sommerfeld, see below.) Lamé exhibits other solutions for vibrations of rectangular parallelepipeds, but the faces are not traction-free. All the solutions are for isotropic materials.

1859 J. A. C. Bresse, "Cours de mécanique appliquée", Première Partie, Mallet-Bachelier, Paris, 1859. Contains the equations of motion of curved bars including terms for rotatory inertia and transverse shear deformation. Overlooked for almost 100 years. See Timoshenko, below.

1864 Saint Venant-Navier, "Résumé des leçons donnée à l'écoles des ponts et chaussées...." Troisième édition, avec des notes et des appendices par M. Barré de Saint-Venant, Dunod, Paris, 1964. Saint-Venant's ten-fold expansion of Navier's "Leçons". Contains a 227 page historical introduction. Section 53 of the introduction covers the development of equations of vibrations of strings and blades by Taylor, Daniel Bernoulli and Euler. Section 59 does the same for isotropic membranes and plates (low frequencies) by Euler, Jacques Bernoulli, Germain, Lagrange,

Poisson and Navier.

1883 Saint Venant-Clebsch, "Théorie de l'élasticité des corps solides de Clebsch..... avec des notes étendues de M. de Saint-Venant", Dunod, Paris 1883. Saint Venant's three-fold expansion of A. Clebsch's "Theorie der Elasticität fester Körper", B. G. Teubner, Leipzig, 1862. Contains Saint Venant's 64 page "Note Finale due § 73: Théorie de la flexion et des autres petites déformations des plaques élastiques planes minces, tirée directment des équations differentielles générales de l'équilibre d'élasticité des solides." See Cauchy, above.

1886 I. Todhunter and K. Pearson, "A History of the Theory of Elasticity and of the Strength of Materials from Galilei to the Present Time, Vol. 1, Galilei to Saint-Venant 1639-1850", Cambridge, 1886.

1889 Lord Rayleigh, "On the Free Vibrations of an Infinite Plate of Homogeneous, Isotropic, Elastic Matter", Proc. London Mathematical Society, Vol. 20, 1889, pp 225-234. Derivation of the transcendental equation relating frequency and wave-length. Analyzes only the long wave, low frequency limit.

1890 H. Lamb, "On the Flexure of an Elastic Plate", Proc. London Mathematical Society, Vol. 21, 1890, pp 70-90. In a paper on the old controversy of three versus two boundary conditions in classical plate theory, he re- that he had obtained Rayleigh's solution more than a year before.

1892 A. E. H. Love, "A Treatise on the Mathematical Theory of Elasticity", Vol. 1, Cambridge, 1892. Contains a 34 page historical introduction.

1917 H. Lamb, "On Waves in an Elastic Plate". Proc. Royal Society, London, Series A, Vol. 93, 1917, pp. 114-128. An elegant derivation of the Rayleigh-Lamb frequency equation. Includes some study of the higher modes.

1921 S. Timoshenko, "On the Correction for Shear of the Differential Equations for Transverse Vibrations of Primatic Bars", Philosophical Magazine, Series 6, Vol. 41, pp. 774-746. Rediscovery of the Bresse-type equations.

1945 H. Ekstein, "High Frequency Vibrations of Thin Crystal Plates", Physical Review, Vol. 68, 1945, pp. 11-23. Derivation, within the framework of the three-dimensional theory, of the transcendental equation relating frequency to wave-length for anisotropic plates of the type of rotated-Y-cuts of quartz. Analysis of the branch at the fundamental thickness-shear cut-off frequency.

1945 E. Reissner, "The Effect of Transverse Shear Deformation on Bending of Elastic Plates", Journal of Applied Mechanics, Vol. 12, 1945, pp. 69-77. Static equations for isotropic plates. Aimed at extending two dimensional stress-concentration problems to thick plates.

1947 A. Sommerfeld, "Spezielle Lösungen des Problems der elastischen Eigenschwingungen beim Quader und Würfel", S. -B. Math. -Nat. Abt. Bayerische Akad. Wiss., 1947, pp. 81-88. Rediscovery of Lamé modes.

1948 Y. S. Uflyand, "The Propagation of Waves in Transverse Vibrations of Bars and Plates", P. M. M., Vol. 12, 1948, pp 287-300. Early work on isotropic plates including rotatory inertia and transverse shear deformation.

1951 A. N. Holden, "Longitudinal Modes of Elastic Waves in Isotropic Cylinders and Slabs", Bell System Technical Journal, Vol. 30, No. 4, Part 1, 1951, pp. 956-969. Contains the beginning of a detailed study of a family of the higher branches of the Rayleigh-Lamb frequency equation for the infinite, isotropic plate.

1951 R. D. Mindlin, "Thickness-shear and Flexual Vibrations of Crystal Plates", Journal of Applied Physics, Vol. 22, 1951, pp. 316-323. Extension of the Bress-Timoshenko beam equations to include anisotropic plates. Includes an application to an AT-cut quartz plate with a pair of free edges.

1952 R. D. Mindlin, "Forced Thickness-shear and Flexural Vibrations of Piezoelectric Crystal Plates", Journal of Applied Physics, Vol. 23, 1952, pp. 83-88. Extension of the results in the preceding paper to include piezoelectric terms.

1956-1979: Proceedings of the Annual Symposia on Frequency Control. Most of the developments of new equations of motion of plates and new solutions appear, or are referred to, in these Proceedings.

Recent Books

1953 Stephen P. Timoshenko, History of Strength of Materials, with a brief account of the history of theory of elasticity and theory of structures, McGraw-Hill, New York, 1953.

1960 C. Truesdell, The Rational Mechanics of Flexible or Elastic Bodies, 1638-1788, Introduction to Leonhardi Euleri Opera Omnia, Vol. X et XI, Seriei Secundae, Societatis Scientiarum Naturalium Helveticae, Orell Füssli Turici, Switzerland, 1960.

1961 R. F. S. Hearman, An Introduction to Applied Anisotropic Elasticity, Oxford, 1961.

1969 Richard Holland and E. P. EerNisse, Design of Resonant Piezoelectric Devices, M.I.T. Press, Cambridge, Mass. 1969.

1969 Arthur W. Leissa, Vibration of Plates, Scientific and Technical Information Division, Office of Technological Utilization, National Aeronautics and Space Administration, NASA SP-180, Washington, D.C. 1969.

1969 H. F. Tiersten, Linear Piezoelectric Plate Vibrations, Plenum Press, New York, 1969.

1973 J. D. Achenbach, Wave Propagation in Elastic Solids, North-Holland, American Elsevier, New York, 1973.

1973 B. A. Auld, Acoustic Fields and Waves in Solids, Wiley, New York, 1973.

1978 Julius Miklowitz, The Theory of Elastic Waves and Waveguides, North-Holland, Elsevier North-Holland, New York, 1978.

RELATIVITY AND CLOCKS

Carroll O. Alley

University of Maryland
College Park, Maryland

Summary

In this centennial year of the birth of Albert Einstein, it is fitting to review the revolutionary and fundamental insights about time which he gave us in the Restricted Theory of Relativity (1905) and in the conseqences of the Principle of Equivalence ("...The happiest thought of my life...") which he developed (1907-1915) into his theory of gravity as curved space-time, the General Theory of Relativity.

It is of particular significance that the extraordinary stability of modern atomic clocks has recently allowed the experimental study and accurate measurement of these basic effects of motion and gravitational potential on time. Experiments with aircraft flights and laser pulse remote time comparison (Alley, Cutler, Reisse, Williams, et al, 1975) and an experiment with a rocket probe (Vessot, Levine, et al, 1976) are briefly described.

Proper understanding and allowance for these remarkable effects is now necessary for accurate global time synchronization using ultrastable clocks, transported by aircraft, and for the correct operation of navigational systems such as the NAVSTAR/Global Positioning System.

Introduction

It is an honor to be asked to review the subject of relativity and clocks for the 33rd Frequency Control Symposium in this centennial year of the birth of Albert Einstein which occurred in Ulm, Germany on March 14, 1879. I am pleased to attempt a brief summary of the subject.

The plan is to recall first some of the significant events in Einstein's intellectual life by showing his photographs at various ages. Next, the restricted ("special") theory of relativity (restricted, that is, to inertial frames of reference) will be sketched, followed by the implications of the Principle of Equivalence that gravity curves light beams and affects the rate of clocks, the clues that led to the idea of gravity as curved space-time, the General Theory of Relativity. Recent experiments which have been able to measure and study some of the effects of motion and gravity on time will be briefly described. Finally, the practical matter of including relativity in modern clock synchronization and navigational systems will be mentioned.

The international timekeeping community should take great pride in the fact that the great stability of contemporary atomic clocks requires the first practical applications of Einstein's General Theory of Relativity. This circumstance can be expected to produce a better understanding among physicists and engineers of the physical basis of gravity as curved space-time. For slow motions and weak gravitational fields, such as we normally experience on the earth, the primary curvature is that of time, not space. A body falls, according to Einstein's view, not because of the Newtonian force pulling it to the earth, but because of the properties of time: clocks run slower when moving and run faster or slower, the higher or lower respectively they are in the earth's gravity field.

Some Events in Einstein's Intellectual Development

Figure 1 shows Einstein in his study in Berlin several years after he had brought the General Theory of Relativity to its complete form in 1915. He always regarded this theory as his major accomplishment, although his other outstanding contributions to physics would place him among the greatest physicists of this century even without the General Theory. His stature as a scientist and his character as a man are appropriately symbolized in the cartoon of Herblock which appeared in The Washington Post shortly after his death on April 18, 1955. (Figure 2). This drawing is included here for an additional reason.

Imagine someone observing the Earth from the position of Herblock's observer, taken to be a space ship far removed from the solar system, located among the nearby stars but at great distances from each of them, not moving with respect to the Sun, and equipped with standard cesium atomic clocks with which to measure time. This observer is clearly aware of Einsteinian time. The one hundred years which have elapsed on Earth since Einstein's birth would be recorded by the Herblock observer to be about 46 seconds longer due to the effects of gravitational potential difference (29 seconds from the Sun's potential and 62 seconds from the Earth's potential) and orbital motion of the Earth (~15 seconds). In the next section, I wish to recall and explain these fundamental effects on time which Einstein originally revealed to us by pure thought.

To continue with Einstein's life, Figure 3 shows his earliest known picture at the age of about 5. This is when he first saw a magnetic compass and began to wonder about its behavior. Figure 4 shows him in elementary school in Munich at the age of 10. He is second from the right in the front row. Figure 5 shows him at the age of 14. He had begun to read Euclidean Geometry two years earlier and a year later was to become a high school dropout because of dissatisfaction with the methods of teaching in his Munich gymnasium. He spent a happy year in Northern Italy where his family had moved, travelling and continuing his own studies. At the age of 16, he attempted to enroll in the Swiss Federal Institute of Technology (Eidgenössische Technische Hochschule) in Zurich, but failed the entrance examination overall, although he impressed the examiners with his knowledge and ability in physics and mathematics. These examiners recommended that he spend a year in the high school in Aarau, Switzerland, and then enter the ETH, since no entrance examination was required of graduates of Swiss secondary schools. Figure 6 shows the 16 year old Albert Einstein (far right, first row) in the Aarau classroom of an excellent teacher, Dr. Jost Winteler. It was during this period that Einstein began to think about what a beam of light would look like if somehow he were able to move fast enough to catch up with it. Figure 7 shows him as a student at the ETH in Zurich, where he succeeded in disappointing and alienating his professors by attending the required classes only sporadically while pursuing independent studies. (He particularly liked to spend time in the electricity and magnetism laboratory and in the study of Maxwell's Theory of the electromagnetic field, which was not then taught at the ETH). He passed the few required examinations only with the help of his friend, Marcel Grossmann, who was a model student, attending lectures and taking careful notes, which he lent to Einstein. The famous mathematician, Hermann Minkowski, who lectured at the ETH and later contributed the geometrical point of view to space-time and relativity, said,[1] on learning of Einstein's 1905 paper on restricted relativity, "Oh, that Einstein, always missing lectures - I really would not have believed him capable of it!" On another occasion, he referred to Einstein as "a lazy dog".

Because of these attitudes, which seem to have been shared by other members of the faculty, Einstein could not obtain an academic position or a permanent job of any sort for about a year and a half after he graduated. (As a teacher in a university, I reflect often, when looking at these pictures of Einstein during his student years, how easy it is to completely misjudge a student's true abilities. Conventional teaching in universities has changed little since Einstein's student days, and we have yet to react to his criticisms. A recent essay by Martin Klein[2] on Einstein and the Academic Establishment is particularly pertinent as are Einstein's own essays on education[3]). Finally, his good friend Marcel Grossmann prevailed on Grossmann's father who was acquainted with the director of the Swiss Patent Office in Bern to intercede and obtain an interview for Einstein. This led to employment there for seven fruitful years from 1902 until 1909. He had a natural aptitude for evaluating the feasibility of the patent applications, leaving time and energy to wonder about physics. Often in later life when asked for advice by young scientists, he would recommend, with his experience at the patent office in mind, that they not be dependent for their livelihood on the production of scientific results because of his concern with the corrupting influence of the need to be successful. In Figure 8, he is shown at the age of 26 at his desk at the Patent Office in the year 1905 when he published three remarkable papers in the Annalen der Physik: One introducing the light quantum into physics, one discussing the theory of the Brownian Motion and providing the clinching argument for skeptics of the existence of atoms, and the third, "On the Electrodynamics of Moving Bodies," containing his revolutionary insight about the relative nature of simultaneity and the non-absolute nature of time, the fundamental key to his restricted theory of relativity. About his years at the Patent Office, and Marcel Grossmann's help in obtaining the position, he wrote in a letter of condolence to Grossmann's widow in 1936, "...This saved my life; not that I would have died without it, but I would have been intellectually stunted", and, in the last year of his life, "The greatest thing that Marcel Grossmann did for me as a friend". There was, however, a third major thing that Grossmann did for Einstein. When he needed to learn differential geometry and the tensor calculus in order to give mathematical form to his idea of gravity as curved space-time, he turned to Grossmann who had specialized in the subject and was a member of the faculty of mathematics at the same ETH in Zurich when Einstein was a member of the physics faculty there from 1912 to 1914. Figure 9 shows Einstein in a playful mood at the California Institute of Technology in the early 1930's while Figure 10 shows him at the Institute for Advanced Study in Princeton where he spent the last twenty-two years of his life.

If these tidbits have stimulated you to want to learn more about Einstein's life, there is no better book to begin with than the brilliant biography by Professor Banesh Hoffmann, Albert Einstein, Creator and Rebel.[4] Many of the facts stated above, along with many of the photographs, were taken from this book. It has the added virtue of explaining Einstein's physics in a particularly clear way. Some of the remarks in the next sections of this talk follow the approach of Hoffmann.

Brief Review of Restricted ("Special") Relativity

This review will be much too concentrated for those people who may be encountering the ideas for the first time. However, I shall assume that most people in this audience have had some prior contact with the subject so that we can recall the fundamental concepts quickly.

The restriction is to reference systems which move with respect to one another with constant

velocity, and in any one of which a body at rest remains at rest and a freely moving body moves in a straight line - the so-called inertial systems. The adjacent diagram shows the conventional repre-

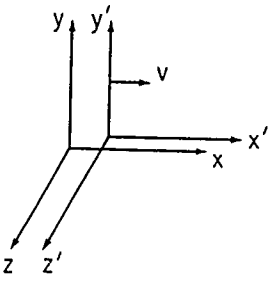

sentation of two such systems in relative motion. A fundamental postulate is that the laws of physics, electromagnetism and all other parts of physics, as well as dynamics, are to be the same in every inertial system. This has the consequence that no experiment carried out within an inertial system can distinguish it from any other such system. This is the restricted (special) Principle of Relativity.

The second fundamental postulate which Einstein identified had to do with the velocity of light in empty space.[8] Light travels with a definite speed ($c = 3 \times 10^8$ meters per second) for every inertial observer which does not depend on the motion of its source.

These two postulates appear to be hopelessly in conflict. Consider the two inertial systems illustrated, each of which has a light source at

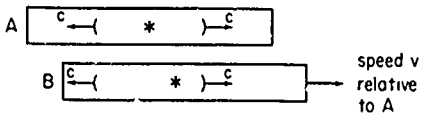

its center. When the two light sources are abreast of each other, let them flash simultaneously, sending out light wave fronts in the forward and back directions for observer A and for observer B. (These could be railroad cars, in Einstein's own example, or space ships, appropriate to our own epoch. For simplicity, we are limiting ourselves to only one dimension.) In his own system, A would see the pulses reaching the ends at the same time, but he would observe the backward travelling wave front reach the back end of system B before the forward travelling wave front reaches the front end of system B. How could observer B measure that the speed of light was c in both directions, as A would surely measure? Does this not violate the postulate of relativity, by which A and B should agree on the laws of physics?

You know well the resolution of this dilemma, which came to Einstein after many years of musing and bafflement. On awaking one morning during his time at the Patent Office, he sat bolt upright in bed with the realization that time is not absolute. The situation described is only "apparently irreconcilable". The simultaneity of separated events is relative to the inertial observer. Different inertial observers will not agree on whether two spatially separated events are simultaneous. For some observers, they may be simultaneous, but other observers will not even agree on which event occurs before the other. This fundamental realization about time has had profound consequences for all of physics!!

Einstein's Prescription for Comparison of Time (Clock Readings) for Separated Events

The following illustration shows Einstein's prescription for time comparison and affords the opportunity of introducing space-time diagrams:

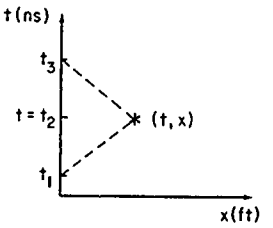

Let the vertical axis measure time in nano-seconds and the horizontal axis measure distance (one dimension) in feet (≈30 cm). Then the plot of a moving light pulse will make an angle of 45° since $c \approx 1$ foot per nano-second. The prescription is simple. Send out a pulse at time t_1, let it be reflected at the distant event, and return to the observer at time t_3. One assumes that the time of reflection assigned by the observer in midway between t_1 and t_3:

$$t = t_2 = t_1 + \frac{1}{2}(t_3 - t_1) = t_1 - \frac{1}{2}t_1 + \frac{1}{2}t_3$$
$$= \frac{1}{2}(t_1 + t_3) \qquad (1)$$

The same measurements of time will also yield the distance to the event by using the radar equation:

$$x = \frac{c}{2}(t_3 - t_1) \qquad (2)$$

The diagram is called a Minkowski diagram after Einstein's distinguished professor of Mathematics at the ETH who developed this geometric way of looking at space-time in 1907.

Modern Observers and Minkowski Diagrams

The modern observer will be equipped with:

1. Atomic Clocks
2. Short Pulse Lasers
3. Fast Photo-detectors
4. Event Timers

The k-Calculus. By sending and receiving short light pulses and recording the times (epochs) of such events, one can measure the space-time coordinates of distant events, as we have just seen. In addition, the technique lends itself to a very clear way of developing the conceptual structure of relativity, as was first done by Bondi.[5] Consider the following diagram in which the world line of B is represented in the space-time diagram of A.

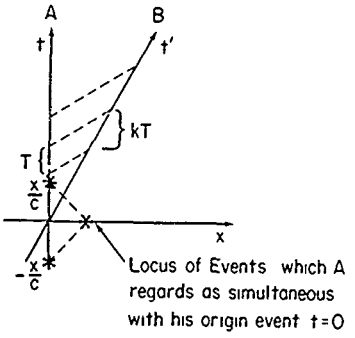

Observer B has the same equipment as A, in particular a standard atomic clock. Because of the motion of B relative to A, light pulses emitted by A with a time interval T between them will be received by B with a stretched time interval kT because of the additional distance travelled by B between reception of pulses. This is just the familiar Doppler effect.[6] It is an easy exercise to show that the relativistic Doppler factor k is given by

$$k = \sqrt{\frac{1 + v/c}{1 - v/c}} \qquad (3)$$

The locus of the events which A regards as simultaneous with his origin event t = 0 as determined by the operation shows in the above diagram, a pulseless effect at t = -x/c being received back at t = x/c. This constitutes A's x-axis. If observer B carries through the same operation, as shown in the following diagram, emitting a pulse at t' = -x'/c and receiving it back at t' = x'/c,

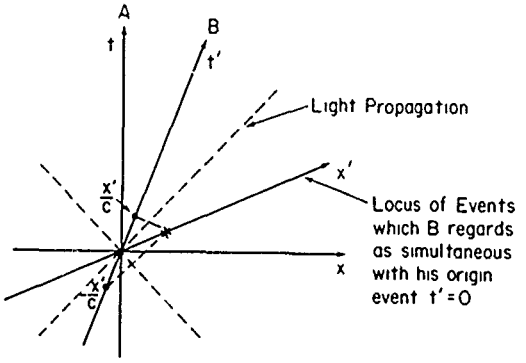

Space-Time

the locus of all such reflection are the events he regards as simultaneous with his origin even to t' = 0. (The same even t to which A assigns t=0). This x'-axis makes the same angle with respect to the locus of light propagation, the 45^{o} line, as the t'-axis. The light propagation lines, shown dashed in the figure, are the same for both observers because of the invariance of the speed of light. They are often called the light cone.

The geometrization of space-time, as pointed out by Minkowski in 1907, amounts to this: There is an absolute space-time, which is "sliced up" by different inertial observers in different ways, as shown in the following diagram (for one space dimension)

Minkowski's Absolute Space-Time (1907)

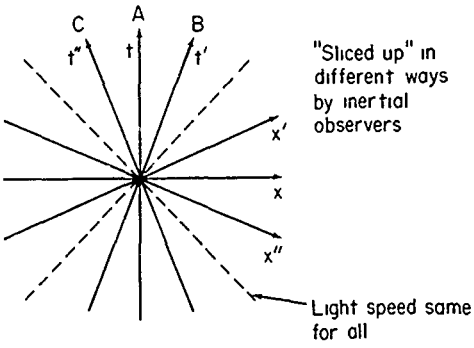

Some reference event is chosen and a light cone is associated with it. If this reference event is chosen as the origin event for several inertial observers, their time and space axis are plotted as shown. Observer C is moving to the left with respect to observer A. The distance in the diagram along the time and space axes which corresponds to unity will be different for each inertial observer[7]. The coordinates for an event are determined by parallel projection onto the time and space axes for any inertial observer, as shown in the following diagram

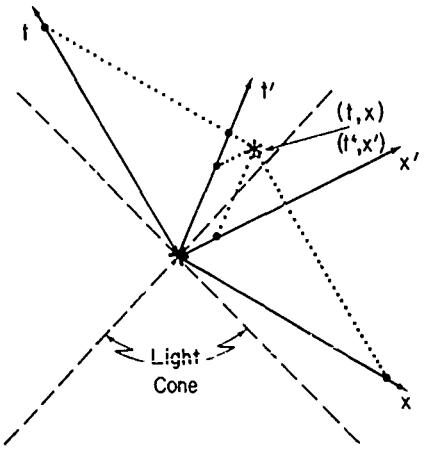

Minkowski showed a very remarkable property: even though $t' \neq t$ and $x' \neq x$ in the above diagrams, there is an expression which is the same for both observers, namely[8]

$$s^2 \equiv c^2 t^2 - x^2 - c^2 t'^2 - x'^2 \qquad (4)$$

This is called the square of the invariant interval between the origin event (0,0) and the event (t,x) or (t', x'). For any two events whose separation in time is Δt or $\Delta t'$ and whose separation in space is Δx^2 or $\Delta x'$, it is easily shown that

$$(\Delta s)^2 = c^2(\Delta t)^2 - (\Delta x)^2 = c^2(\Delta t')^2 - (\Delta x')^2 \qquad (5)$$

Even though $\Delta t \neq \Delta t'$ and $\Delta x \neq \Delta x'$, all inertial observers will get the same result for $(\Delta s)^2$ as defined by equation (5)! In three spatial dimensions, $(\Delta s)^2$ becomes

$$\begin{aligned}(\Delta s)^2 &= c^2(\Delta t)^2 - (\Delta x)^2 - (\Delta y)^2 - (\Delta z)^2 \\ &= c^2(\Delta t')^2 - (\Delta x')^2 - (\Delta y')^2 - (\Delta z')^2\end{aligned} \qquad (6)$$

and continues to be invariant for all inertial observers.

This is an extremely important result because it provided the mathematical basis for Einstein's later development of his theory of gravity - a curvature of the flat space-time that we have been discussing in terms of the preceding diagrams - as we shall discuss later on. Minkowski characterized his development of the geometry of space-time during an address to the 80th Assembly of German Natural Scientists and Physicians in Cologne on the 21st of September, 1908 in the following famous excerpt:

> "The views of Space and Time which I wish to lay before you have sprung from the soil of experimental physics, and therein lies their strength. Henceforth, space by itself, and time by itself, are doomed to fade away into mere shadows, and only a kind of union of the two will preserve an independent reality."

He was, of course, talking about the slicing up of space-time by different inertial observers, accompanied by the invariance of the interval, as we have just discussed.

The Effect of Motion on Clocks

This is most readily described by using the invariant interval. Consider the following Minkowski space-time diagram which represents the motion of a clock with respect to some arbitrary inertial observer whose coordinate time and space axes are displayed. The world line of the moving clock is just the locus of the events at which

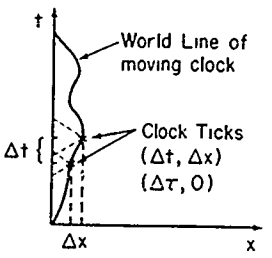

Reading of moving clock is its own time. Proper Time. Denote by τ.

it is present. The curvature of the world line shows that it experiences accelerations. Two neighboring events along the world line of the clock are shown representing "ticks" of the clock (every second, or better, every nanosecond). With respect to the inertial observer, they have a time separation Δt and a spatial separation Δx. For the moving observer accompanying the clock, the time separation between ticks is the time interval actually recorded by the moving clock, which is called its proper time interval and given the symbol $\Delta\tau$. The spatial separation between the ticks for the observer moving with the clock will be zero, since the clock is always at the origin of the moving coordinate system. If the two tick events are close together, the moving observer can be regarded as an inertial observer since his instantaneous velocity v will change very little during the interval between ticks. Then, denoting the time and space measurements of the moving observer with primes,

$$(\Delta s)^2 = c^2(\Delta t)^2 - (\Delta x)^2 = c^2(\Delta t')^2 - (\Delta x')^2 \qquad (7)$$

But

$$\begin{aligned}\Delta t' &= \Delta\tau \\ \Delta x' &= 0\end{aligned} \qquad (8)$$

and

$$\Delta x = v\Delta t \qquad (9)$$

Equation (7) thus becomes

$$\begin{aligned}c^2(\Delta\tau)^2 &= c^2(\Delta t)^2 - (v\Delta t)^2 \\ &= (c^2 - v^2)(\Delta t)^2\end{aligned} \qquad (10)$$

or

$$(\Delta\tau)^2 = \left(1 - \frac{v^2}{c^2}\right)(\Delta t)^2$$

$$\Delta\tau = \sqrt{1 - \frac{v^2}{c^2}}\ \Delta t \qquad (11)$$

relating the proper time increment $\Delta\tau$ of the moving clock to the coordinate time increment Δt of the inertial observer. Note that this important result has been obtained with very little mathematics. The author has successfully taught these ideas to introductory physics students, given several weeks for them to be absorbed gradually.

If two identical clocks are synchronized to read the same when they are together, and observed to have the same rate when together, they will not exhibit the same reading after being separated and experiencing different routes in space-time before being brought together again, even though their rates will again be the same. The situation is illustrated below for clocks A and B.

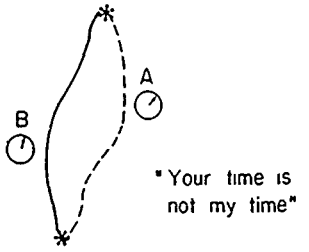

The difference in proper times for clocks A and B will be

$$\tau_A(\text{final}) - \tau_B(\text{initial}) = \int d\tau_a = \int \sqrt{1 - v_A^2/c^2}\ dt$$

$$\tau_B(\text{final}) - \tau_B(\text{initial}) = \int d\tau_b = \int \sqrt{1 - v_B^2/c^2}\ dt \qquad (12)$$

Where t represents the coordinate time of some inertial observer and v_A and v_B are the instantaneous velocities of A and B with respect to that inertial observer. The elapsed proper time will be different for clocks A and B since their histories or routes are different. There is a route dependence of elapsed proper time. Colloquially, to paraphrase a once popular song, "Your time is not my time"!

Note in equation (12) that there is no explicit dependence on the acceleration or higher derivatives of the motion of the clocks, but only the instantaneous velocity. This is sometimes referred to in the literature of relativity as the "clock hypothesis". There clearly must be some acceleration for the clocks to separate and be brought back together again. Any real clock will be influenced by acceleration to some extent. For example, a watch dropped on a hard floor from a sufficient height will probably stop running! However, it is possible in real situations to keep accelerations small enough to avoid significant rate changes by careful packaging to reduce shocks and vibrations and by sufficiently slow motions of the vehicle (e.g. aircraft) carrying the clock. The important point is that there is no specific dependence on the instantaneous acceleration in the theory predicting the elapsed proper time for an arbitrary motion of a clock in space-time.

Einstein's 1905 Prediction

In the 1905 paper, "On the Electrodynamics of Moving Bodies", referred to earlier, Einstein made the following statement after developing his ideas about time:

> "Thence we conclude that a balance-clock* at the equator must go more slowly, by a very small amount, than a precisely similar clock situated at one of the poles under otherwise identical conditions.
>
> *Not a pendulum clock, which is physically a system to which the earth belongs. This case had to be excluded."

The situation is sketched below. The equatorial

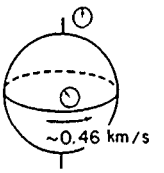

surface velocity is about 0.46 meters/second. Equation (12) evaluated in an inertial frame (non-rotating) with origin at the center of the earth yields, to first order in v^2/c^2.

$$\tau(\text{final}) - \tau(\text{initial}) \approx \int \left(1 - \frac{v^2}{2c^2}\right) dt \approx t - \frac{v^2}{2c^2}\, t \qquad (13)$$

At a pole, $v = 0$, but at the equator $v^2/2c^2 = 1.18 \times 10^{-12}$. If t is one day, the equatorial clock would run slow with respect to the polar clock by about 102 nanoseconds.

If atomic clocks had existed in 1905 with the stability we have today (~2 ns/day) so that the prediction could have been tested, it would have been found to be wrong! Why? Because the effect of gravity had not been included! Two years were

to go by before Einstein discovered the Principle of Equivalence in 1907 and drew the conclusion about the influence of gravitational potential on time. The oblateness of the spinning earth causes a decrease in the gravitational potential as one moves from the equator to a pole, getting nearer to the center of the earth. It is remarkable that the effect of this change on clocks is predicted to offset exactly the effect of the change of surface velocity, so that the correct prediction is a null effect. We have performed an experiment recently, transporting clocks from Washington, D.C. to Thule, Greenland and back, which supports this null prediction, and will describe it later.

The Principle of Equivalence
(Einstein's "Happiest Thought")

Let us now turn to the incorporation of gravity into the structure of space-time which in Einstein's hands produced the General Theory of Relativity - no longer restricted to inertial frames of reference. It is my experience that the best way to understand Einstein's theory of gravity is through the historical route actually followed by Einstein. The physical ideas came before the full mathematical formulation of curved space-time involving the tensor calculus, which took eight more years to develop. The key idea came to Einstein in 1907 when he was working on a summary essay concerning the special theory of relativity for the yearbook for Radioactivity and Electronics. He described his train of thought in an essay written in 1919, "The Fundamental Idea of General Relativity in its Original Form", which is not yet published, but an excerpt was printed in the New York Times[9] in 1972 when the planned editing and publication of all his papers was announced.

> "I tried to modify Newton's theory of gravitation in such a way that it would fit into the theory. Attempts in this direction showed the possibility of carrying out this enterprise, but they did not satisfy me because they had to be supported by hypotheses without physical basis. At that point, there came to me the happiest thought of my life [emphasis added] in the following form:
>
> Just as in the case where an electric field is produced by electromagnetic induction, the gravitational field similarly has only a relative existence. Thus, for an observer in free fall from the roof of a house there exists, during his fall, no gravitational field - at least not in his immediate vicinity. If the observer releases any objects, they will remain, relative to him, in a state of rest, or in a state of uniform motion, independent of their particular chemical and physical nature.* The observer is therefore justified in considering his state as one of "rest".
>
> The extraordinarily curious, empirical law that all bodies in the same gravitational field fall with the same acceleration immediately took on, through this consideration, a deep physical meaning. For if there is even one thing which falls differently in a gravitational field than do the others, the observer would discern by means of it that he is in a gravitational field, and that he is falling in it. But if such a thing does not exist - as experience has confirmed with great precision - the observer lacks any objective ground to consider himself as falling in a gravitational field. Rather, he has the right to consider his state as that of rest, and his surroundings (with respect to gravitation) as field-free.
>
> The fact, known from experience, that acceleration in free fall is independent of the material, is therefore a mighty argument that the postulate of relativity is to be extended to coordinate systems that are moving non-uniformly relative to one another.

*In this consideration one must naturally neglect air resistance."

The following simple diagrams illustrate the point made by Einstein and allow profound consequences to be drawn with little or no mathematics! Consider a laboratory falling freely as shown below. Objects released with no initial velocity

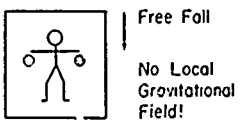

will remain at rest. If the initial velocity is not zero, the path of the object will be a straight line. This is now very familiar to us from television and movies of the U.S. astronauts in Skylab and the Apollo spacecraft, and the Soviet cosmonauts in Salyut and the Soyuz spacecraft. The freely falling spacecraft constitutes a true (local) inertial system. If one imagines the spacecraft in a region of space free of gravity but subject to the acceleration produced by a rocket engine, as shown on the left below (the "Aclab" of Banesh Hoffmann), the observer inside will experience effects similar to those in a stationary lab-

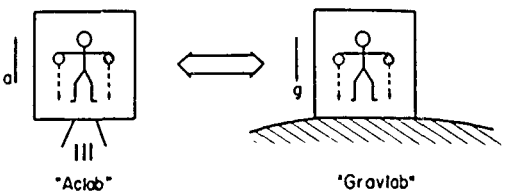

oratory on the surface of a body like the earth where there is an acceleration of gravity g. In both cases, objects released will move to the floor with accelerated motion. In the "Aclab" case, the floor accelerates to the released object, so that any object, regardless of its composition, will behave in the same way. In the "Gravlab" case, it has been measured with increasing accuracy by Galileo, Newton, Eötvös, Dicke, and Braginsky, that all bodies at the surface of the earth fall with the same acceleration. The latest measurements,[10] using torsion balance techniques to compare aluminum and gold at Princeton University and to compare aluminum and platinum at Moscow State University give

$$\left|\frac{g_{al} - g_{au}}{g}\right| < 10^{-11} \quad \text{(Dicke, 1964)}$$

$$\left|\frac{g_{al} - g_{pt}}{g}\right| < 10^{-12} \quad \text{(Braginsky, 1972)} \qquad (14)$$

Implications for Light Propagation

Einstein proposed that the equivalence idea should hold, not only for dynamics, but for all of physics, and, in particular, for electromagnetic phenomena, including light. If this is the case, one can draw some conclusions without using any mathematics at all as illustrated in the following diagram. Since the "Aclab" is accelerating with

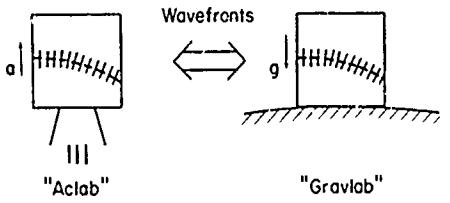

respect to an inertial system, and a beam of light would propagate in a straight line in that system, to an observer in the "Aclab", the light would appear to follow a curved path. If the equivalence to the "Gravlab" is correct, the prediction would be that light follows a curved path when propagating in a gravitational field. In addition, by noting that the wave fronts associated with the light beam must move like ranks of soldiers when turning, the outer soldiers moving faster than the inner ones, the conclusion follows that the speed of light should increase with height in a gravitational field!!

Implications for the Rate of Clocks

Imagine two atomic clocks of identical construction to be at the top and bottom of an "Aclab" as shown below, their readings being compared by modern observers equipped with short pulse lasers, fast photo-detectors, and event timers as discussed earlier. The rates can be calculated using the

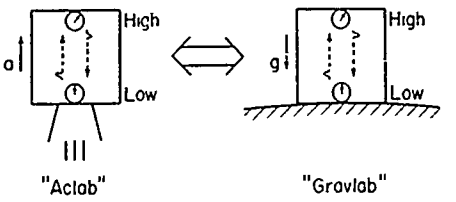

techniques of restricted relativity discussed earlier (accelerated motion can be analyzed by using a succession of inertial frames having the instantaneous velocity of the accelerated object). The conclusion, as we will show below, is that the high clock will run fast with respect to the low clock. Therefore, by the principle of equivalence, in the "Gravlab", the high clock will run fast with respect to the low clock. A clock's rate is predicted to depend on its position in a gravitational field!!

Since we have presented earlier all the mathematical machinery needed to draw this conclusion, let us run briefly through the analysis. Construct a space-time diagram for the low and high observers in the "Aclab" referred to time and space axes of an inertial observer, as shown on the left below. The curvature of the world lines represents

Comparison of Clocks in "Aclab"

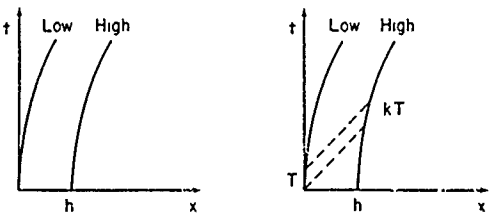

their acceleration with respect to the observer establishing the time and space coordinates. They are separated by a vertical distance h when t = 0. Let two successive light pulses be emitted by the low observer separated by a time interval T on his clock. The pulses will be received by the high observer separated by a time interval kT in accordance with our earlier discussion of the Doppler factor, equation (3). The velocity which should be used to evaluate k in that of the high observer when the first pulse reaches him.

$$v = at \simeq ah/c \qquad (15)$$

where a is the acceleration of the "Aclab" and the approximation is made that the separation is still h at this later time so the transit time $\simeq h/c$. It is further assumed that during the time T the velocity will not change appreciably.

Then

$$k = \sqrt{\frac{1 + v/c}{1 - v/c}} \approx \sqrt{1 + 2v/c} \approx \sqrt{1 + \frac{2ah}{c^2}} \qquad (16)$$

Now, by the Principle of Equivalence, a = g, the acceleration of gravity, so k becomes

$$k = \sqrt{1 + \frac{2gh}{c^2}} \qquad (17)$$

Recall that gh is just the Newtonian potential difference ϕ if h is small,

$$\phi \equiv gh \qquad (18)$$

so that

$$k = \sqrt{1 + \frac{2\phi}{c^2}} \qquad (19)$$

By the Principle of Equivalence, the situation would be as shown in the following space-time diagram. The low and high clocks are not moving

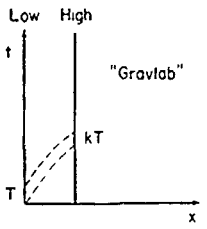

so their world lines are straight. The light propagation lines are curved because of the increase of the speed of light with height. The time interval T becomes stretched to kT, where

$$k = \sqrt{1 + \frac{2gx}{c^2}} \qquad (20)$$

This circumstance is what can be called the "curvature of time." The elapsed proper time of a clock depends on where it is located in the gravitational field and differs from the elapsed coordinate time established by an observer, at the surface of the earth, for example, with the aid of light signals. The following diagram shows the relation for vertical distances.

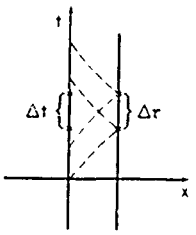

The observer on the ground at x = 0 can establish the coordinates (t, x) of any event by sending out a light pulse to be reflected back at the time of the event and received at a later time. The time he assigns to the event is halfway between his emission and reception events as described by equation (1). (This is still valid even though the speed of light is not constant in a gravitational field; the time required for the light pulse to go out is the same as that for it to return). If the procedure is repeated an interval of coordinate time Δt later, it will define an interval of proper time $\Delta\tau$ at the higher position, as shown in the diagram. The essential property is that

$$\Delta t \neq \Delta\tau \qquad (21)$$

Time Curvature

It is possible to generalize the expression for the square of the invariant interval in restricted relativity, equations (5) and (6), to allow for this effect, and that is just what Einstein did, writing now

$$\Delta s^2 = \left(1 + \frac{2gx}{c^2}\right)c^2 (\Delta t)^2 - (\Delta x)^2 \qquad (22)$$

For three spatial dimensions, and using the Newtonian potential ϕ to include non-uniform gravitational fields

$$\Delta s^2 = \left(1 + \frac{2\phi}{c^2}\right)c^2 (\Delta t)^2 - (\Delta x)^2 - (\Delta y)^2 - (\Delta z)^2 \qquad (23)$$

Einstein retained the interpretation of Δs as measuring the interval between two events in space-time, so for the interval between two ticks of a clock,

$$\Delta s = c\Delta\tau \qquad (24)$$

where $\Delta\tau$ is the interval of proper time recorded by the clock. If the clock is not moving

$$(\Delta s)^2 = c^2(\Delta\tau)^2 = \left(1 + \frac{2\phi}{c^2}\right)c^2 (\Delta t)^2 \qquad (25)$$

or

$$\Delta\tau = \sqrt{1 + \frac{2\phi}{c^2}}\ \Delta t \qquad (26)$$

which is the same as equation (19), giving the relation between increments of proper time and coordinate time. If the clock is moving,

$$\Delta x = v_x \Delta t,\ \Delta y = v_y \Delta t,\ \Delta z = v_z \Delta t \qquad (27)$$

and equation (23) becomes

$$(\Delta s)^2 = c^2(\Delta\tau)^2 = \left(1 + \frac{2\phi}{c^2}\right) c^2 (\Delta t)^2 - \{v_x^2 + v_y^2 + v_z^2\} (\Delta t)^2 \quad (28)$$

which leads to

$$\Delta\tau = \sqrt{1 + \frac{2\phi}{c^2} - \frac{v^2}{c^2}}\ \Delta t \quad (29)$$

as the relation between proper time and coordinate time increments for a clock in motion.

As Einstein developed these concepts during the years 1907 - 1915, and especially during the collaboration with Marcel Grossmann from 1912 - 1914, he realized there would also be a curvature of space produced by a gravitational field. This would be represented by coefficients of the $(\Delta x)^2$, $(\Delta y)^2$, and $(\Delta z)^2$ terms of the expression for $(\Delta s)^2$ which would also be functions of position, just as the coefficient of the $c^2(\Delta t)^2$ term. The values of these coefficients are determined by his field equations for a given distribution of matter. For a spherically symmetric mass distribution, the famous Schwarzschild solution of the field equations is

$$(\Delta s)^2 = \left(1 + \frac{2\phi}{c^2}\right) c^2 (t)^2 - \frac{(r)^2}{\left(1 + \frac{2\phi}{c^2}\right)} - r^2 \cos^2\beta(\Delta\alpha)^2 - r^2 (\Delta\beta)^2 \quad (30)$$

where

$$\phi = -\frac{GM}{r} \quad (31)$$

with M the mass of the central body, r the radial distance, α the longitude, and β the latitude. For motions in weak gravitational fields such that

$$\frac{|\phi|}{c^2} << 1, \quad (32)$$

and for slow motions,

$$\frac{v^2}{c^2} << 1, \quad (33)$$

one can neglect the coefficients of the spatial increments, and one is left with the equation (23) containing only the curvature of time.

Under the conditions of low velocity and weak gravity expressed by equations (32) and (33), one can approximate equation (29) as

$$\Delta\tau = \left(1 + \frac{\phi}{c^2} - \frac{v^2}{2c^2}\right) \Delta t \quad (34)$$

All of the experiments with atomic clocks which have been done recently, and which we will describe below, are a testing of the relationship (34) between proper time and coordinate time.

Analogy of Time Curvature to the Curvature of a Sphere

Consider a sphere, like the earth, whose curved surface possesses a coordinate system of latitude and longitude, as shown in the following diagrams. The coordinates of longitude α runs through the range 0 to 360.

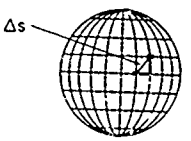

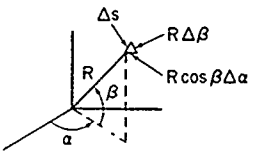

The coordinate of latitude runs from -90° to 90°. R is the radius of the sphere. What is the distance Δs between two neighboring points on the surface of the sphere, differing by $\Delta\alpha$ and $\Delta\beta$? It is <u>not</u> given by

$$(\Delta s)^2 = (\Delta\alpha)^2 + (\Delta\beta)^2 \quad \text{(Wrong!)} \quad (35)$$

but rather by

$$(\Delta s)^2 = R^2 \cos^2\beta(\Delta\alpha)^2 + R^2 (\Delta\beta)^2 \quad (36)$$

There are <u>metric coefficients</u>, which depend on position, multiplying the square of the coordinate differentials to give the true measure of length, or <u>proper length</u>, between the points. The actual proper length will be different for different locations on the sphere, even though the coordinate differentials are the same. For example, consider $\Delta\alpha = 1^\circ$ and $\Delta\beta = 0$, as shown in the following exaggerated diagram.

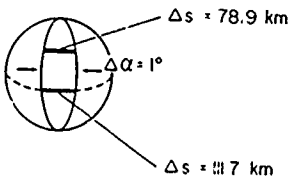

At the equator, Δs will be 111.7 km, while at the latitude of 45°, Δs will be 78.9 km. The relation between the proper time increment $\Delta\tau$ and coordinate

time increment Δt in curved space-time is very closely analogous to the relation between the proper length increment Δs and the coordinate of longitude increment $\Delta\alpha$ on the curved surface of the sphere. The coefficients in relativity are also called metric coefficients. For a network of curvilinear coordinates, x_1 and x_2, on an arbitrary curved surface as shown the proper length Δs is

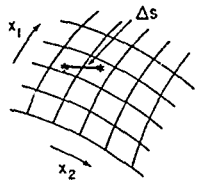

expressed as:

$$(\Delta s)^2 = g_{11}(\Delta x_1)^2 + 2g_{12}(\Delta x_1)(\Delta x_2) + g_{22}(\Delta x_2)^2 \quad (37)$$

The great mathematician Gauss made many contributions to the differential geometry of two-dimensional curved surfaces, in particular showing that the curvature can be calculated from the variation of the metric coefficients g_{ij} on the surface only.[11] These results were generalized to an arbitrary number of coordinates describing n-dimensional curved space by Riemann. This Riemannian geometry furnished many mathematical tools which Einstein and Grossmann used in the final form of General Relativity.

Brief Summary of the Curved Space-time Theory of Gravity

In the curved space-time produced by the presence of matter, the metric coefficients in the expression for $(\Delta s)^2$ being determined by the Einstein field equations, a free object will move in such a way that if one imagines it carrying a clock, the path it follows in space-time will make its elapsed proper time a maximum. In technical terms, it will follow a so-called geodesic path which is the analog of a great circle on a sphere. Locally, the path will be as straight as possible in the curved space-time. In the words of Professor John Wheeler,

> "Matter tells space-time how to curve; Curved space-time tells objects how to move."

This is graphically represented by the following picture and analogy taken from the book Gravitation by Misner, Thorne, and Wheeler.[12] The curved surface of the apple may be thought of as caused by the stem (analog of mass). The ants moving on the curved surface try to move locally as straight as possible (geodesics). The result is that the ants end up moving in curved paths about the stem (planet orbiting the sun).

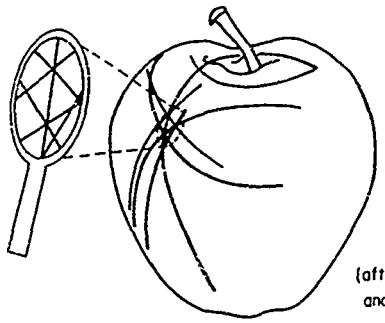

(after Misner, Thorne, and Wheeler)

There is another way of looking at free motion in the curved space-time produced by masses. Recall from Einstein's essay that the Principle of Equivalence allows the local cancellation of the effects of gravity by going to a freely falling frame of reference. It can only be local because gravitational fields in the real world are not uniform, as the following diagrams indicate. The extent of the local freely falling frame in both time and space will depend on the accuracy with

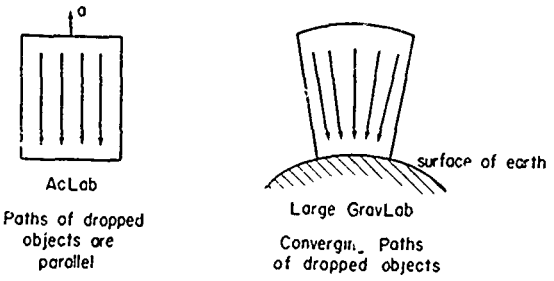

which measurements are made. These local freely falling frames obviously are local inertial systems in that freely moving objects will move in straight lines as discussed earlier. Inertial systems must be local because only non-uniform gravitational fields exist in the real world. The inertial systems of large extent as discussed in restricted relativity are a fiction. An object moving freely in a non-uniform gravitational field (curved space-time) can be thought of as moving in straight lines in the flat space-time of restricted relativity in each of a succession of local freely falling systems which differ in both direction and velocity of motion. It is clear from equations (12) and associated diagrams that such straight line motion in an inertial system between two events in space-time produces a proper time difference greater than curvilinear motion, since there is some inertial system in which it would be at rest. Hence, the conclusion that free motion in curved space-time follows a path which produces a maximum proper time difference. Bertrand Russell[13] has referred to this as the "Principle of Cosmic Laziness."

Einstein's theory of gravity as curved space-time does away with the concept of Newtonian gravitational forces. A body falls to the earth because it follows the locally straightest path in curved

space-time. We have seen that for low velocities and weak fields, as exist for most motions on earth, the primary curvature is that of time. Thus, from the Einsteinian point of view, bodies fall because of the properties of time and the behavior of clocks which we are discussing. The essential property is the relation between proper time and coordinate time, equation (34). The curved world line of a falling body results from the elapsed proper time associated with the body

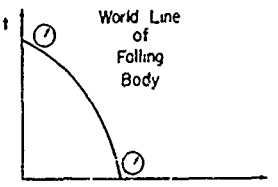

Curved Space-Time

$$\tau(\text{final}) - \tau(\text{initial}) = \int d\tau \approx \int \left(1 + \frac{\phi}{c^2} - \frac{v^2}{2c^2} \right) dt \qquad (38)$$

having a maximum value for that path as compared with other paths between the same initial and final events.

The following diagram shows a plot of gravitational potential ϕ/c^2 for the sun as a function of distance from its center, along with a schematic representation of the change in rate of clock as a function of position. This is one way of indicating the curvature of time. At the surface of the sun $\phi/c^2 \approx -2 \times 10^{-6}$. Using the value at the earth of the solar gravitational potential, the earth gravitational potential ($\phi/c^2 \approx -7 \times 10^{-10}$ at its surface) and the velocity of the earth in its orbit around the sun (~30 km/s), the additional 46 seconds since Einstein's birth as observed by Herblock's distant cosmic observer, (whose proper time will be the same as coordinate time), was calculated using equation (38) for the freely falling earth.

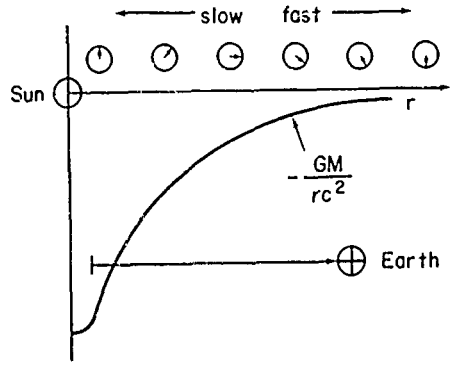

In the popular literature on general relativity, the curvature of space is referred to almost exclusively since it is somewhat easier to visualize than the curvature of time. However, this is quite misleading, since the curvature of time leads to all of Newtonian physics for low speeds and weak fields in Einstein's theory, and in this sense can perhaps be regarded as the primary curvature. One should regard most of these references to the curvature of space as shorthand for the curvature of space-time. Now that it is possible to measure accurately with modern atomic clocks, as described in the next sections, the remarkable properties of Einsteinian time, and as the properties are, of necessity, used more and more in global timekeeping systems, we can hope for more intuitive understanding of the physics of general relativity.

Experimental Measurements

Introduction

The experiments which will mainly be described are those of the author and his collaborators with modern cesium beam atomic clocks in aircraft and the experiment with a hydrogen maser in a rocket probe conducted by Vessot and Levine. These experiments were designed to measure primarily the effects of gravitational potential, although the effects of motion were necessarily present and were also measured. They used macroscopic oscillators controlled by atomic resonances. Before describing them, it is appropriate to mention for completeness some of the earlier observations using direct radiation from atoms and nuclei.

Optical Spectroscopy

Solar Redsnift Observations. The first tests[14] of the properties of time as affected by gravitational potential were sought in the shift toward the red of the frequency of optical radiation emitted by atoms on the sun and received and compared on earth with radiation from similar atoms. The potential difference would predict a shift $\Delta f/f \sim 2 \times 10^{-6}$. It was very difficult to establish this value with any confidence because of lack of accurate knowledge of pressure-induced frequency shifts in the sun's atmosphere and the complications of Doppler shifts due to turbulent motions of the emitting gas atoms and the surface velocity of the sun due to its rotation. A brief summary with references of these older observations and the attempts to interpret them is given by Pauli.[15]

The choice of atoms whose spectral lines are little affected by pressure, and the use of rapid switching in the earth laboratory from solar radiation to laboratory sources has allowed measurements with a believable accuracy of about 5%. The experiments were done at Princeton University by J. Brault (1963)[16], in France by J. Blamont and F. Roddier (1965)[17], and in the U.S.A. at Oberlin College by J. Snider (1972)[18].

White Dwarf Redshifts. These observations have suffered from lack of precise knowledge of the size and mass of the objects from which to calculate the surface gravitational potential. Sirius B provides the comparison most widely known, although there are others, such as 40 Eridani B. The accuracy is probably no better than 15 to 20%.[19,20]

Moving Atoms. The first controlled measurements of the relativistic effects of motion were carried out by H.E. Ives and G.R. Stilwell (1941).[21] They measured the "transverse Doppler effect" (that is, the difference between coordinate time and proper time by examining the light from excited atoms moving in a collimated beam, much care being taken to average out the first order Doppler effect. The accuracy of comparison with theory is difficult to assess -- perhaps 5 to 10%. Similar experiments have been performed by G. Otting (1939).[22] H.L. Mandelberg and L. Witten (1962)[23] quote an accuracy of 5% in their more recent version of the experiment.

Using a beam of high velocity Na atoms and laser techniques for the cancellation of first order Doppler effects, the "time dilation" has been recently measured by J.J. Snyder and J.L. Hall (1975)[24] to 0.5%.

With Helium-Neon lasers stabilized by Methane, the expected shift of frequency of 0.542 per degree in the Methane due to the change of rms velocity with temperature has been observed with an uncertainty of 10% by S.N. Bagayev and V.P. Chebotayev (1972).[25]

Mössbauer Gamma Ray Spectroscopy

Effect of Gravitational Potential. The discovery by Mössbauer that the frequency shift associated with the recoil of the nucleus when emitting or absorbing a γ-ray photon could be very small when the nucleus transferred its momentum to the solid of which it was a part opened the way to very high resolution γ-ray spectroscopy. The application of the technique to a terrestrial measurement was first made by R.V. Pound and G.A. Rebka (1960)[26] using a 22.6 meter vertical path in a tower at Harvard University. The potential difference produces a frequency shift $\Delta f/f \sim 2.5 \times 10^{-15}$, which was measured with about 10% accuracy. Later Pound and J. Snider (1965)[27] improved the measurements to an accuracy of about 1%.

Motional Effects. The temperatures of the materials hosting the γ-ray emitting and absorbing nuclei in the above experiments need to be measured with precision and kept closely equal to prevent the motional effects on time of the lattice vibrations from masking the gravitational effect. Complications of solid state physics and temperature measurement do not allow a very accurate measurement, but the temperature dependence of the shift in resonant frequency provides evidence for the difference between coordinate time and proper time. The Mössbauer technique has been used to demonstrate the effect of velocity on time in centrifuge experiments by H.J. Hay, J.P. Schiffer, T.E. Cranshaw, and P.A. Egelstaff (1960);[28] by W. Kündig (1963);[29] and also by K.C. Turner and H.A. Hill (1964)[30] while studying other aspects of relativity. The centrifuge technique has produced an accuracy of comparison with theory of about 1%.

The very large accelerations associated with these motional effects, as well as the acceleration of the muons in storage rings discussed below, have no intrinsic effect on the relation between proper time and coordinate time as given in equation (11).

Astronomical Observations from the Moving Earth

The analysis of many types of observations involves the transformation from a reference system "attached" to the center of mass of the solar system in which calculations are more easily done, to the reference system associated with the earth. Such observations include the measurement of changing pulsar periods, very long baseline interferometry, lunar laser ranging, deep space tracking of spacecraft, and planetary ranging. All involve the use of stable atomic clocks on the earth. The difference between proper time on the earth and coordinate time in the solar system is therefore essential in the analysis of the results of the observations. A particularly clear discussion of the transformation is given by J.B. Thomas (1976).[31]

High Energy Physics

Charged Pion Lifetime. This has been measured by A.J. Greenberg, et al, (1969)[32] in a beam from the Lawrence Radiation Laboratory's 184-inch cyclotron where the factor $(1 - v^2/c^2)^{-\frac{1}{2}}$ had the value 2.4. The accuracy of the lifetime determination compared with the previously measured value of 26 nanoseconds for the lifetime at rest agrees with the relativistic prediction to 0.4%.

Moving Muons. The difference between coordinate time intervals and proper time intervals has been measured using the decay of muons. The lifetime of rapidly moving muons increased by the factor $(1 - v^2/c^2)^{-\frac{1}{2}}$. The most accurate measurement, about 2%, has been made in a storage ring at Center for Nuclear Research (CERN) in Geneva by Farley, et al, (1966).[33] The factor $(1 - v^2/c^2)^{-\frac{1}{2}}$ had a value of 12. Earlier, but much less accurate, measurements had been made as early as 1941 by Rossi and Hall[34] by studying as a function of altitude the survival of muons produced by cosmic rays in the upper part of the earth's atmosphere. They would not survive to sea level except for the relativistic effect since their life time at rest is only about 2 microseconds.

Relativistic Dynamics. The design of particle accelerators and the analysis of high energy experiments uses concepts of relativistic energy and momentum which are based squarely on the invariance of the interval, equation (6) above. Thus, high energy physics makes continuing use of the Einsteinian concept of time.

Atomic Clocks Carried in Commercial Aircraft on Around the World Flights

In October of 1971, J.C. Hafele and R.E. Keating[35] first demonstrated the relativistic effects on time for macroscopic atomic clocks by carrying an ensemble of four commercial cesium beam clocks (Hewlett-Packard Model No. 5061) belonging to the U.S. Naval Observatory around the world on scheduled airline flights, first in the eastward direction, and six days later in the westward direction. The combination of the surface velocity of the earth due to its rotation with the velocity of the jet aircraft leads to the prediction of an asymmetry in the relativistic effects for the different circumnavigation senses. The gravitational potential effect due to the altitude of the aircraft needs to be included. The following table gives their published values of the predicted effects:

Effect	Eastward	Westward
Potential	144 ± 14 ns	179 ± 18 ns
Velocity	-184 ± 18 ns	96 ± 10 ns
Net	- 40 ± 23 ns	275 ± 21 ns
Trip duration	65.4 hrs.	80.3 hrs.

The uncertainties are from a lack of sufficiently detailed knowledge of the velocity, altitude, and position of the airplanes during the flights.

The ensemble of clocks were intercompared to 1 ns once an hour in order to identify any rate changes of individual clocks with respect to the average. Several such rate changes were identified and corrected for in arriving at the measured results. The systematic error in this procedure is given as ±30 ns. Corrections for temperature and pressure changes were not made. The measured values of the average time difference with respect to the stay-at-home clocks at the U.S. Naval Observatory are given as:

Eastward -59 ns
Westward ±273 ns

The comparison with the predictions seems to show an uncertainty of about 13% for the westward direction, but much worse for the eastward direction. It is difficult to assign an uncertainty for the comparison of the individual potential and velocity effects, but their existence is certainly demonstrated.

Atomic Clocks Carried in an Aircraft on Local Flights with Radar Tracking and Laser Pulse Time Comparison

Participants. These experiments were conducted[36] by the author and L.S. Cutler, R.A. Reisse, R.E. Williams, J.D. Rayner, C.A. Steggerda, J. Mullendore, S. Davis, L. Small and B. Duvall (all at the University of Maryland except L.S. Cutler, who is at Hewlett-Packard) during the period from May, 1975 through January, 1976 with the support of the U.S. Navy,[37] especially the Time Services Division of the U.S. Naval Observatory and its Director, G.M.R. Winkler. The Hewlett-Packard Model 5061 High Performance (Option 004) cesium atomic clocks used were provided by the observatory. They were modified to improve their performance under the guidance of L.S. Cutler,[38] who had been responsible for the original design at Hewlett-Packard. We were kindly lent two hydrogen masers for the ground clock set made by H. Peters by the Goddard Space Flight Center,[39] which also lent us the trailer used in the experiments. Three rubidium optically pumped frequency standards made by Efratom were included in each clock set.[40]

Theoretical Framework. Our experiments measured the difference in proper time recorded by the aircraft clock set, τ_A, and the proper time recorded by the ground clock set, τ_G. The prediction of general relativity is

$$\tau_A = \int_0^T (1 + \phi_A/c^2 - v_A^2/2c^2)\, dt \qquad (39)$$

$$\tau_G = \int_0^T (1 + \phi_A/c^2 - v_G^2/2c^2)\, dt \qquad (40)$$

$$\tau_A - \tau_G = \int_0^T ((\phi_A - \phi_G)/c^2 - (v_A^2 - v_G^2)/2c^2)dt \qquad (41)$$

We used short pulses of laser light to carry out the comparison of clock readings between the ground and the airplane as prescribed by Einstein, equation (1) above. The appropriate spacetime diagram for the laser pulse time comparison is shown below.

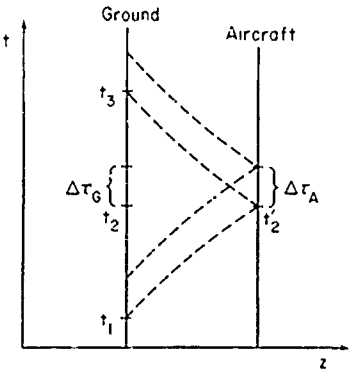

The inertial system in which the integral (41) is to be evaluated is centered on the freely falling earth and is non-rotating with respect to distant matter, as shown in the following diagram.

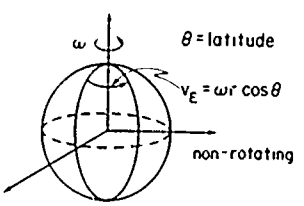

The vector velocity $\vec{v}_A$ in the inertial system is given by

$$\vec{v}_A = \vec{v}_A^{\,*} + \vec{\omega} \times \vec{r} \qquad (42)$$

whose $\vec{v}_A^{\,*}$ is the velocity of the aircraft with respect to the surface of the earth and $\vec{\omega} \times \vec{r}$ is the surface velocity of the rotating earth whose angular velocity is $\vec{\omega}$. The radius vector to the location of the aircraft is $\vec{r}$. When v is squared to insert in equation (41), one obtains

$$v_A^2 = v_A^{*2} + \underline{2\,\vec{v}_A^{\,*} \cdot (\vec{\omega} \times \vec{r})} + (\vec{\omega} \times \vec{r})^2 \qquad (43)$$

The underlined term in the above equation is just twice the eastward component of $\vec{v}_A^{\,*}$ multiplied by the eastward surface velocity $v_E = \omega r \cos\theta$, where θ is the latitude. It is this term which leads to the asymmetry in the around the world flights described above, since it is positive for eastward flights and negative for westward flights. In our local flights, its integral was too small to be measured.

Airborne Equipment. A schematic diagram of the experiment is given below. The aircraft was a Navy P3C anti-submarine patrol plane, capable of flights of 15 to 16 hours duration at altitudes up to 35,000 feet. Figure 11 is a picture of our aircraft, P3C 912, in flight. On board the plane was an ensemble of three Hewlett-Packard cesium clocks

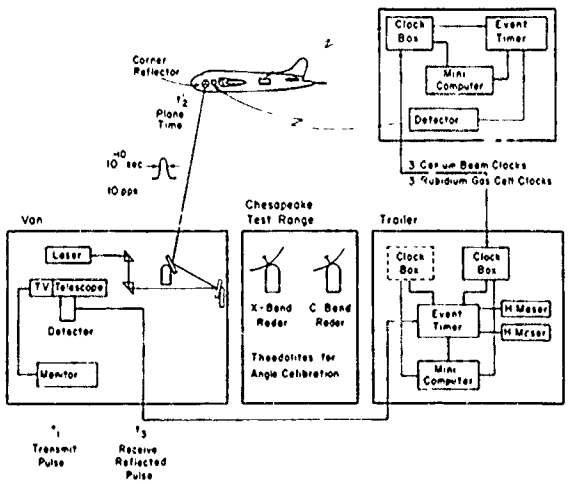

carefully packaged to provide a very well controlled environment along with an environmentally controlled set of three Efratom rubidium clocks, the entire collection of clocks and environmental package being called a "clock box." This is shown in Figure 12 in position on the aircraft. Also on board were an event timer, capable of measuring the epoch of an event with a precision of 0.1 nanosecond, a NOVA 2 minicomputer and associated LINC magnetic tape unit, a strip chart recorder for visual monitoring of clock phases and temperatures, a dry nitrogen tank for the pressure control system, and a non-environmentally controlled traveling clock. This equipment is shown in Figure 13. Intercomparison of the epochs of the zero-crossings of the 5 MHz clock outputs was made every 200 seconds. The reflection of laser light pulses from the aircraft was accomplished by placing an optical corner reflector of the type developed for the lunar laser ranging experiment[41] beside the forward observing window on the aircraft as shown in Figure 14. A photomultiplier equipped with neutral density filters and a 100 Angstrom band pass filter was housed as shown in Figure 15 so that it could be pointed by hand from inside the forward observing window toward the laser transmitter on the ground. The epoch of the received laser pulses on the plane was measured by the event timer in the proper time of the plane and stored in the computer where it could be read out and communicated to the ground by voice radio link.

Ground Equipment. On the ground at the Patuxent Naval Air Test Center, a trailer contained an identical clock box (Figure 16); event timer and NOVA 2 minicomputer with standard magnetic tape, disk, and tektronix graphics terminal for analyzing and displaying the data (Figure 17); and two hydrogen masers (Figure 18). Figure 19 shows the aircraft parked alongside the trailer for direct comparison by coaxial cable of the aircraft and ground clock sets before and after flights. Between flights in the absence of the aircraft, both clock boxes and the airborne electronics were housed in the trailer. On the five separate fifteen hour flights, one box was flown three times and the other twice. Figure 20 shows Dr. Williams and Dr. Reisse preparing to transfer a clock box to the plane, into which it had to be inserted through the narrow hatch shown in Figure 21. The installation of the electronics and clock box in the P3C aircraft typically required a day and a half.

Laser Light Pulse Time Comparison. The laser transmitting and receiving equipment was located in the van at the corner of the hangar in Figure 19. The beam directing optics is pictured in Figure 22 and illustrated schematically in the above diagram. Underneath the laser was located a 7.5 inch telescope[42] which was used with a beam splitter both to detect the reflected laser light with a photomultiplier tube and to track the plane with closed circuit television. This equipment in the van is shown in Figure 23. The laser is a frequency doubled neodymium YAG system utilizing a mode-locked oscillator with pulse extraction and subsequent amplification, emitting a pulse 10 times a second with energy of 0.5 millijoules and duration of 100 picoseconds. The aircraft was flown mainly at night with its landing lights on to enhance the contrast for acquiring and tracking it visually. The flights approximated the path in a clockwise sense shown in the following map. The cone shows the acceptance angle for the laser light pulse to be reflected back by the corner reflector. The time comparisons were made on the near side of each circuit, with occasional gaps due to cloud cover or equipment difficulties. The aircraft was acquired optically

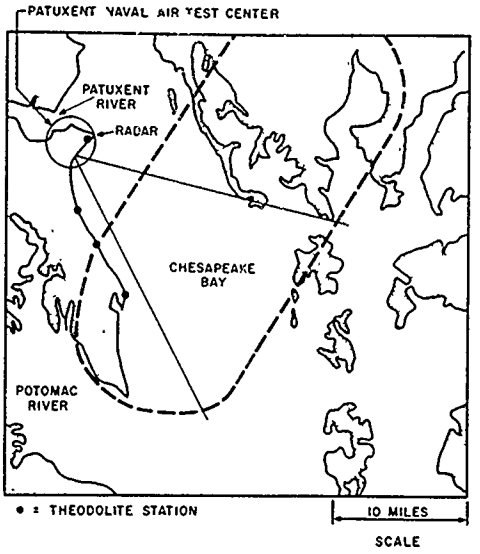

shortly before the laser time comparison by pointing in the direction communicated by the Chesapeake Test Range which tracked the aircraft continuously with radar. The laser beam had a divergence of about 0.5 milliradians, which illuminated about one-half the length of the aircraft at the slant range of about twelve miles. The required precision pointing was provided by Steve Davis working with coarse and fine Heath kit model airplane controllers setting elevation and azimuth rates for the beam directing optics. The controllers and closed circuit TV display are shown in Figure 24, while Figure 25 displays the landing lights as seen on the TV screen. When the laser pulse was hitting the corner reflector, the return flashes were seen on the screen and could also be seen by the eye if one stood next to the laser beam. At the plane, the laser light was very bright (but considerably below eye damage levels), actually casting shadows in the darkened interior of the plane. An inadequate view of the laser transmitter and runways as seen from the plane at twilight is shown in Figure 26. (This is one frame from a color motion picture film. It can be seen, along with other parts of the experiments, in the BBC TV program, "Einstein's Universe," presented on public television as part of the Einstein Centennial activities).

Radar Tracking. An essential part of the experiment was the continuous measurement of the aircraft altitude and velocity during flight by radars at the Chesapeake Test Range located about two miles from the ground clock set. At intervals during flights, the angular measurements of the radars were calibrated by optical theodolities. The radar data was used to compute the relativistic time integral, equation (41), with an accuracy considerably better than that of the atomic clock measurements themselves, so that the clock performance itself determined the accuracy of the comparison with general relativity. The Chesapeake Test Range and a closeup of one of the antennas are shown in Figures 27 and 28.

Clock Performance. Typical atomic clock stabilities of 2 to 3 parts in 10^{14} for an averagir time of one day were achieved with commercial Hewlett-Packard 5061 high performance standards by making several modifications to them and by maintaining a rigorously controlled environment. A plot of the experimentally measured Allan variance σ (2; τ) for five separate standards compared with the sixth is given below. The modifications consisted of a proprietary change in the beam tube

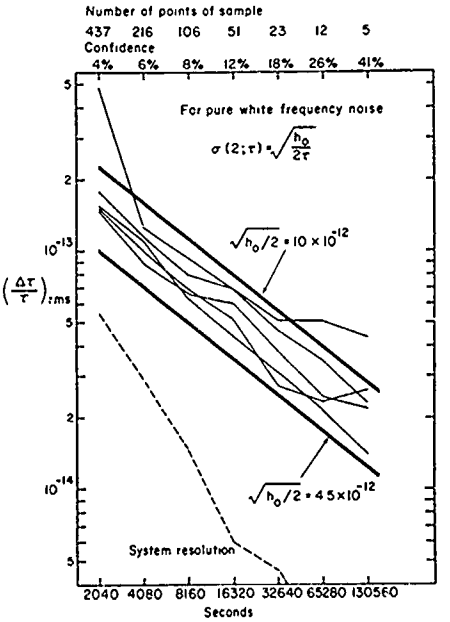

which is now standard on all HP5061 high performance units; the addition of an additional integration in the quartz crystal control loop to reduce frequency offset due to steps or ramps in the crystal frequency, (now available as an option from Hewlett-Packard); and the increase of the beam current by a factor of about two by raising the oven temperature (also available as an option from Hewlett-Packard), which increases short term frequency stability at the expense of tube lifetime. A simple block diagram of the standard is given below showing the extra integration and additional buffer amplification to aid in the intercomparison of the clocks. The modifications were carried out at Maryland with the supervision and active participation of L.S. Cutler. Figure 29 shows him tuning up the ensemble of clocks before they were inserted into the clock boxes.

BLOCK DIAGRAM OF HP 5061 CESIUM BEAM ATOMIC CLOCK

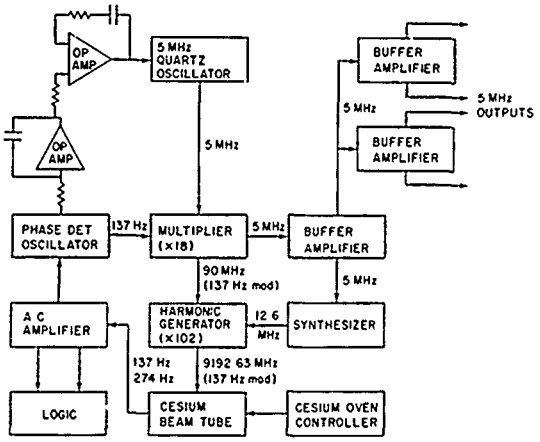

Clock Packaging for Environmental Control. Careful environmental control was maintained to keep small any changes in temperature, pressure, magnetic fields, or supply voltages. Isolation from vibrations and shocks was provided. These controls were accomplished by mounting each set of three clocks in a clock box, shown opened in Figure 30. The objective was to control the environment so that any changes would affect the clock stability by less than 10^{-14}. The clocks were mounted vertically in individual magnetic shields of 60 mil thick Mo-Permalloy. After the magnetic lid was put on (See Figure 31), individual clocks were degaussed. To remove heat from the clocks, and to control their temperature, air was circulated by an individual fan through each of the magnetic shields, entering at the top through the hoses shown in Figures 31 and 32 after passing a heater controlled by feedback from a distributed array of thermistors within the magnetic shield. The air exited a shield through holes at its bottom and flowed along the interior bottom of the pressure controlled aluminum clock box, losing heat to the outside through conduction. Variable speed fans controlled the flow of external air over the bottom of the clock box, the rate being controlled automatically by the external temperature. (We are indebted to Dr. J.P. Richard of the University of Maryland for this and other advice concerning the temperature control). The temperature at individual points in the clocks was kept constant to about 0.060°K. The temperature of the air changed by about 10° in flowing through a magnetic shield.

The clock box was nearly hermetically sealed when the lid was attached and either dry nitrogen or dry air was fed to it from a Granville-Phillips feedback controlled value to keep the pressure constant to less than 1 Torr at a value slightly above sea level atmospheric pressure. To allow for possible decompression of the aircraft cabin pressure at high altitudes, the clock box was made very strong with walls of ½ inch thick aluminum. This also isolated the clocks from acoustic noise.

The isolation against vibration and shock was achieved by mounting the box on four pneumatic Barry mounts which gave a resonant frequency of about 3 Hz. Almost critical damping was achieved by using expansion cylinders following an adjustable orifice, which led to an increase of isolation of 12 db per octave. The characteristic frequencies of the aircraft were around 80 Hz. Sway of the box in the aircraft was restrained by a cushioned retainer ring acting on a vertical post extended upward from the box. Strong flexible cables were fastened around the pneumatic isolaters to restrain the 1000 lb. box in the event of an accident.

The clock box lid carried the voltage regulation and pressure control equipment as well as the environmental control box for the Efratom rubidium clocks, which can be seen on the left in Figure 33. Similar control procedures were followed for these clocks, but they proved much more susceptible than the cesium standards to the shocks of landing and take-off, those events producing rate changes. For this reason, the rubidium data is not very useful for relativity measurements and will not be presented here.

Significant Features. Some of the significant features of the experiments are listed below:

*Ensembles of Clocks on Ground and in Aircraft

Clocks in each ensemble intercompared among themselves every 200 seconds.

*Careful Environmental Control

-Temperature stability $\Delta T < 0.060^{\circ}$K (rms)
-Pressure stability $\Delta P < 1$ Torr
-Magnetic shielding
-Vibration and shock isolation
-Voltage regulation

Effect on clock stability $< 10^{-14}$
No need for systematic corrections

*Return of Clocks for Post Flight Comparison

No rate changes observed for cesium standards beyond statistical expectation for stationary clocks.

*Repeated Measurements

-Clock Box 1: 3 flights
-Clock Box 2: 2 flights
-5 Test flights of ~2 hours duration each to study and improve performance of experiment.

*Laser Light Pulse Time Comparison During Flights

-No Doppler Effect Complications
-Technique of value for future space experiments since optical pulses are little affected by the ionosphere and solar corona.
-First realization of Einstein's 1905 prescription for comparing separated

clocks with light pulses.

*Flying Clocks Experience ∿ 1 g of Most of Time

-No relaxation of stresses as occurs in free fall.
-Periods of steady acceleration limited to take-off and landing.
-Plane's rotations made slowly to avoid Coriolis effects on cesium beams.

Experimental Results. Although much detailed data exists from the five 15 hour flights, only a representative sampling can be given here, which is taken from the flight of November 22, 1975. Shown below is a plot of the predicted effect of gravitational potential and of velocity on the rate of the aircraft clock set with respect to the ground clock set calculated from the radar tracking data.

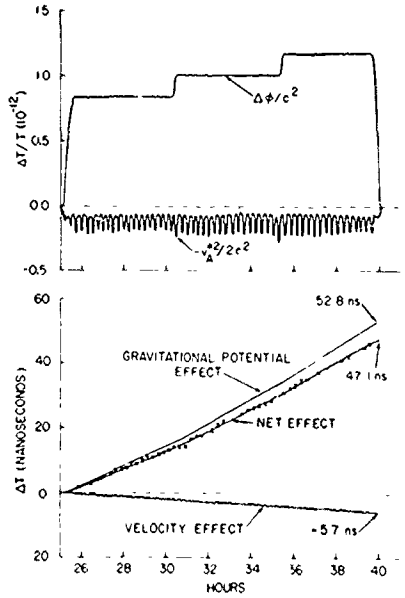

The upper curve is a plot of $(\phi_A - \phi_G)/c^2$ which is seen to average about 10^{-12}. The steps in this quantity are caused by the need of the aircraft to remain at 25,000 feet for 5 hours while burning off fuel to enable it to climb to 30,000 feet for another 5 hours, before being light enough to climb to 35,000 feet for the final 5 hours. The lower curve is a plot of $V_A^{*2}/2c^2$, the velocity effect due to motion of the plane with respect to the ground at the Chesapeake Test Range. The oscillations are due to the effect of winds as the plane circles. The average value of this effect is seen to be about 10^{-13}, corresponding to an average speed of 138 m/s. The second and third terms of equation (43) are not plotted since $\vec{V}_A^* \cdot (\vec{\omega} \times \vec{r})$ will integrate to zero and $(\vec{\omega} \times \vec{r})^2$ will be nearly cancelled by a similar term for the ground clocks. The lower plots are the integrals of the upper curves over the 15 hour flight, showing the time difference $\Delta\tau = \tau_A - \tau_G$ as it was predicted to develop during the flight for the gravitational and velocity effects separately and for the net effect. The plotted points with error bars (± ∿ 0.3 ns) are the laser light pulse comparisons.

The direct comparison measurements of the 5 MHz clock phases before and after the flight are shown in the following plot along with the laser pulse comparisons which were made when the plane was on the ground as well as in the air. The solid lines are the comparison of the "paper clocks,"

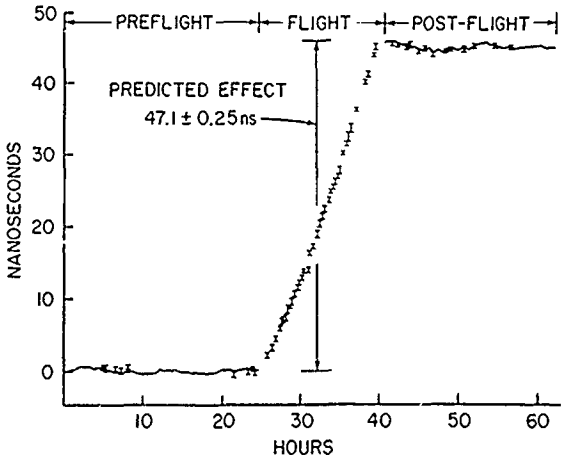

that is the averages of the three cesium clocks in each clock set. The irregular form is due to the intrinsic clock time fluctuations. In this plot, the difference in rates between the clock sets established before the flight has been subtracted out. The actual rates are shown in the following plot of the laser time comparison.

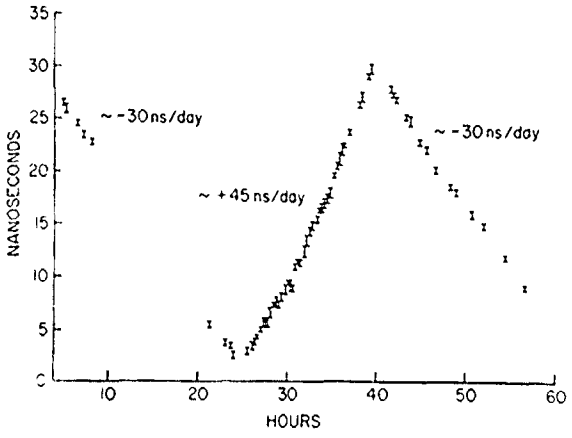

The gap in the preflight data was caused by the need of the laser operator to sleep before the flight. The effect of the steps in altitude on the flying clock rates can be seen by plotting the laser comparisons during flight in an expanded

scale as is done below. The only change the clocks

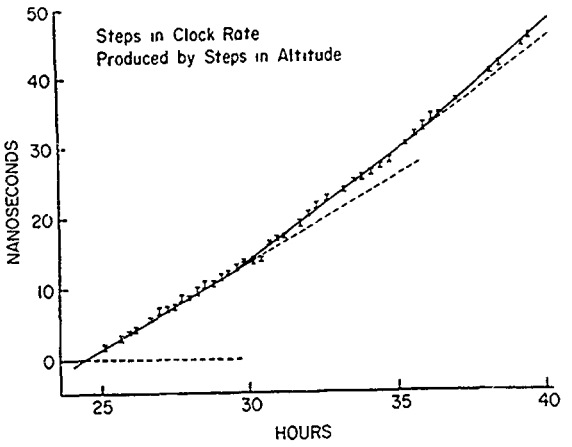

experienced was the change in gravitational potential.

It is also of interest that the flying clocks continued to behave with respect to one another exactly the same during the flights as before and after. This is illustrated by the following plot of the time of flying clock #3 with respect to the average of the three flying clocks. Similar data exists for each clock on each flight. When compared to the ground paper clock, however, flying

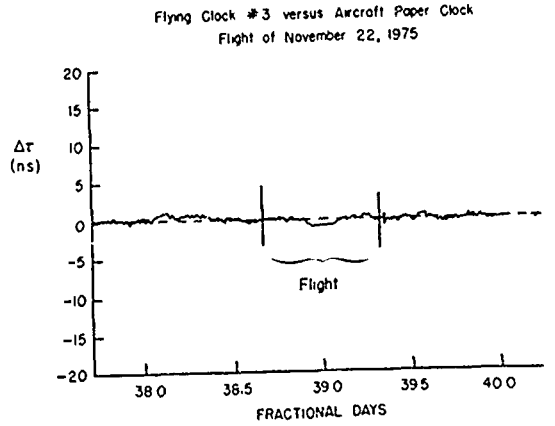

clock #3 showed a step as seen in the next plot. (The black marks fusing into a thick bar are recorded when a data point is absent for the direct comparison of the 5 MHz phases, as was the case during the flight). The step in $\tau_A - \tau_G$ is, of course, the result of the relativistic effects during the flight.

If one treats each cesium clock on each of the five flights as an individual measurement,

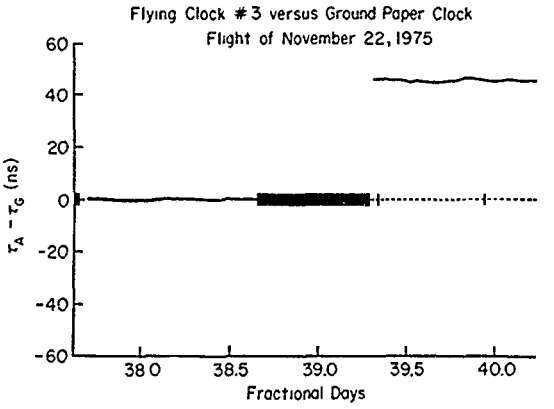

there is some scatter. Below is plotted a histogram for the ratio of the measured time difference to that calculated from General Relativity using the radar data. The predictions had an uncertainty no

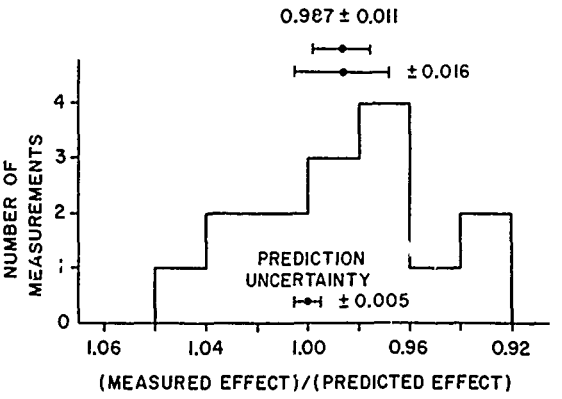

more than ± 0.5%. The formal standard deviation of the mean was 0.011. To allow for possible systematic efforts, we are currently estimating (conservatively) an uncertainty of ± 0.016. The result is:

$$\frac{\text{Measured Effect}}{\text{Calculated Effect (General Relativity)}} = 0.987 \pm 0.016$$

The measured behavior of macroscopic clocks in aircraft flights - a "human scale" type of situation - exhibits the remarkable properties of Einsteinian time within the accuracy of measurement of about 1%!

Atomic Clocks Carried in an Aircraft on Global Flights With Inertial Navigation and Radar Altimetry.

Participants. The flights were conducted in June and July, 1977 by the same group (from the University of Maryland and Hewlett-Packard) which conducted the local flights described above with similar equipment. The Air Force joined the Navy in supporting the experiments by

43

providing a C141 long range transport aircraft from the Wright Patterson Air Force Base, assistance in reconfiguring the equipment, and ground support facilities at the Andrews Air Force Base in Maryland near Washington, D.C.

Purpose. The purpose of the flights was to study experimentally the implications of General Relativity for the elapse of proper time at different latitudes on the spinning earth, freely falling towards the sun as it moves in its orbit. Clear understanding of these implications is of great practical importance for worldwide time keeping, and will be discussed later. Clarification of the concepts by means of simple experiments aids in the development of physical intuition.

Null Change of Proper Time with Latitude. On the spinning earth, general relativity predicts a null effect on proper time as one moves a clock from the equator to the pole along the mean ocean surface. This was discussed earlier in the sections on theory in relation to Einstein's discovery of the effect of gravity on time. His 1905 prediction that a clock at the equator would run slow with respect to one at the pole ignores the influence of gravitational potential since he did not discover it until 1907. If the earth were a homogeneous perfect sphere as shown, the gravitational potential would be the same everywhere on the earth's

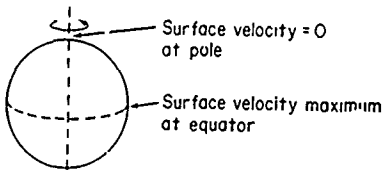

surface and the 1905 prediction would be correct. However, the earth has the shape, to first order, of an oblate ellipsoid due to its spin, as shown in exaggerated form in the following sketch. The gravitational potential ϕ_{pole}, at the pole is less

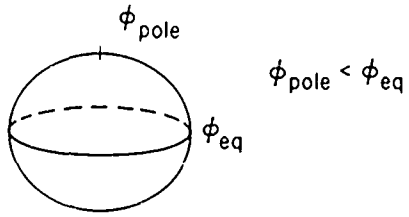

than that of the equator, ϕ_{eq}, since the pole is closer to the center of the earth. The surface of the oceans of the earth is determined by the "geopotential," $\phi - V_s^2/2$, where V_s is the surface speed of the rotating earth. $V_s^2/2$ is the "centrifugal potential, and ϕ is the gravitational potential, both of which change with latitude such that the combination has a constant value independent of latitude,

$$\phi - \frac{V_s^2}{2} = \text{constant} \qquad (44)$$

along the ocean surface. From the earlier discussion of the theory, it will be recalled that the relation between a proper time increment $\Delta\tau$ and a coordinate time increment Δt is

$$\Delta\tau = \left(1 + \frac{\phi}{c^2} - \frac{V^2}{2c^2}\right) \Delta t \qquad (45)$$

for the weak gravity and slow velocities which exist at the earth's surface. Thus, along a surface of constant geopotential, the relation of proper time to coordinate time is

$$\Delta\tau = \left(1 + \frac{\text{constant}}{c^2}\right) \Delta t \qquad (46)$$

and all standard clocks at mean sea level are predicted to run at the same rate independent of latitude.

Experimental Results for Flight to Thule. To check this null prediction, a clock box containing three cesium standards was transported in an Air Force C141 from Washington, D.C. to Thule Air Force Base in Greenland as shown in the polar photograph of a globe in Figure 34, this being the largest conveniently accessible latitude change in one hemisphere. The latitude of Thule is 76° 32' and that of Washington is 38° 49'. After a number of local test flights with the reconfigured equipment in the C141 aircraft, the flight to Thule was undertaken on June 23, 1977, after several days of problem-free comparison with the ground clocks, as a combination of long test flight and global measurement. The plane was kept on the ground at Thule for four days and returned on June 27. Although the radar altimeter failed about 2 hours before arrival at Thule and had to be replaced by one flown in on a regular Air Force flight, the experiment was generally successful. Using the inertial navigation data and radar and pressure altimeters to evaluate the relativistic integral, equation (41), and making direct electrical comparisons of the aircraft and ground clock sets before and after the flight as had been done for the local flights from the Patuxent Naval Air Test Center, but with pre and post flight periods of several days, the following comparison was obtained.

Measured: $\tau_A - \tau_G = 38 \text{ ns} \pm 5 \text{ ns}$

Calculated: $\tau_A - \tau_G = 35 \text{ ns} \pm 5 \text{ ns}$

The time difference measured agrees within errors with that predicted for the flights to and from Thule. There is no evidence for any anomalous latitude effect. The "Einstein Error" of 1905 - not including the gravitational effects - would have predicted a time difference of an additional 56 ns per day, or a total of 224 ns for the four day dwell time! Because the aircraft had to be used for other purposes starting August 1, it was not possible to repeat the Thule flight or to make flights from Washington to Panama to check further the null prediction. It was deemed more important to use the remaining time to transport the clocks to Christ Church, New Zealand.

Reconfigured Equipment for C141 Aircraft. Before describing the purpose and results of the northern to southern hemisphere flights, the reconfigured equipment and the ground base at the Andrews Air Force Base will be briefly discussed. Figure 35 shows a front view of the equipment being assembled on an aluminum frame in the shop of the University of Maryland.[44] The clock box, seen on the left, was rewired to meet rigorous Air Force requirements. It was also mounted on improved pneumatic supports at the height of its center of mass to reduce the sway encountered with the former bottom mounting. The minicomputer, event timer, tape recorder, chart recorder, and other electronics were mounted in an Air Force furnished rack which included some vibration and shock isolation between the inner structure and the outer structure which was bolted to the main frame.

Figure 36 is a rear view of the frame and equipment. A special regulated power supply capable of working from either 60Hz or 400Hz was constructed to power the clocks and other equipment. It included enough Sears Die Hard batteries in a special vented container to operate the clocks for at least 12 hours in the event of failure of other sources. This apparatus is seen on the left, being worked on by technician Lyndon Small.

The entire frame was surrounded by double wall plywood panels containing insulation and was mounted on a standard Air Force 7 foot by 9 foot cargo pallet. Figure 37 is a picture of the complete assembly in a prefabricated garage structure built at the Andrews Air Force Base to contain the equipment between flights. The hoses on the back panel circulate temperature controlled air into and out of the large insulated enclosure. Two Sears window air conditioners provide cooling. Heaters in the flat plenum on the left were used for fine temperature control which could be maintained to a few degrees. This enclosure solved one of the major problems -- the large variation with time of the temperature within the aircraft during flights, and on the ground. The mounting on the cargo pallet allowed the equipment to be placed on the C141 or removed from it in about 10 minutes compared with about one and a half days for the earlier experiments with the Navy P3C aircraft. Figure 38 shows the C141, garage, trailer housing the ground clocks, and van containing the ground computer equipment. Figure 39 shows the tail assembly of the C141 with the petal doors which can open to receive the pallet with its clock equipment. The first transfer of the equipment (without its front insulating panel) from the garage to the plane is shown in Figures 40 through 44. The installed equipment with Len Cutler standing in front is seen in Figure 45. During an actual flight, the equipment is shown from the front in Figure 46 and from the rear in Figure 47. Enough seats were installed to accommodate the eight University of Maryland people and fourteen Air Force personnel who went on each flight. In addition to the crew for operating the plane, there were technicians to operate and maintain the gasoline powered portable electrical generators, portable air conditioners, and portable heaters needed to power the plane and provide temperature control of its interior during dwell times on the ground at the remote sites and at Andrews Air Force Base before and after flights. The transportation of this equipment, some of it in duplicate, required the large storage capacity of the aircraft. It was essential in maintaining continuous operation of the clocks in an adequate environment in the interior of the plane at the remote sites, and during the 12 hour layovers in Hawaii on Christ Church flights.

Two Carousel IV inertial navigation systems, a radar altimeter, and a pressure altimeter were installed on the aircraft to provide accurate measurements of latitude and longitude, velocity with respect to the ground, and altitude above the ground. This information was recorded automatically in digital form every 0.6 second on magnetic tape recorders. In addition, there was provision for manual readout which was logged every 15 minutes. This log was used with a Hewlett-Packard 97 calculator to compute a running integral of the difference between the proper time on the aircraft and the proper time at the Andrews Air Force Base as the flights proceeded. The recording and readout equipment is seen in Figure 48. At Thule it was possible to place the aircraft in a hangar, shown in Figure 49.

The midnight sun was very high in the sky at Thule since we were there only a few days after the summer solstice. Figure 50 showing the C141 which brought our replacement radar altimeter was taken just before midnight. The relatively short shadows cast by the sun at midnight are shown in Figure 51. The $23^{\circ}.5$ tilt of the earth's spin axis which causes this summer solstice on the 21st of June each year in the northern hemisphere made possible another experiment which required flying the clock from the northern to the southern hemisphere.

Does the Gravitational Potential of the Sun Affect Proper Time on the Freely Falling Earth? The following diagram shows that at the time of the summer solstice the North Pole and points in

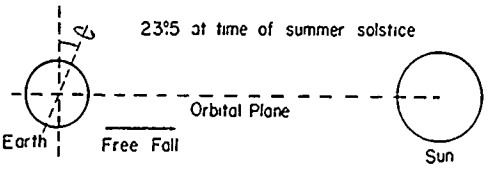

the northern hemisphere are closer to the sun on the average (due to the spin of the earth) than the South Pole and points in the southern hemisphere. Since the earth is falling freely towards the sun as it moves in its yearly orbit around the sun, the nearly fixed direction of the spin axis affords the opportunity of conducting experiments in a freely falling laboratory -- the earth as Einstein's freely falling elevator. At the time of the Summer Solstice, the northern hemisphere is the "floor" and the southern hemisphere is the "ceiling," with the positions reversed at the Winter Solstice.

Recalling the earlier discussion about Einstein's Principle of Equivalence, one can ask: is the gravitational field of the sun transformed away for experiments on the freely falling earth? In particular, will clocks on the "floor" run at the same rate as clocks on the "ceiling" even though they are at different distances from the sun? Here we are taking for granted the effect of gravitational potential difference on clock rates as established by other experiments. The question can be answered experimentally by transporting clocks from the northern to the southern hemisphere near the epoch of a solstice, letting them dwell for a while, and then returning them for comparison with the stay-at-home clocks. From the theoretical point of view, the Principle of Equivalence seems to provide a clear answer: on the freely falling earth (strictly, the earth-moon system, but we ignore this complication since its effects are small) the gravitational effects of the sun are not experienced, to first order, just as in the freely falling Skylab in orbit about the earth the astronauts experienced no effects of the gravity field of the earth, to first order. Mathematically, this means that in the plot of gravitational potential ϕ as a function of distance from the sun, as shown in the sketch below, the slope, or linear

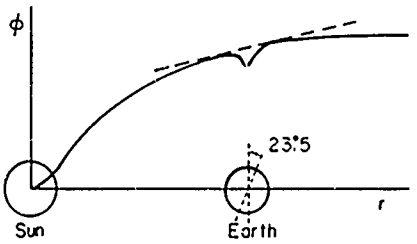

term in the Taylor's Series expansion of ϕ about the center of the earth is subtracted away, leaving only the second order terms.[31] These terms produce the tides, but the difference in ϕ which they yield across the earth's diameter would produce a rate difference in proper times of only 7×10^{-17} or 0.62 picoseconds per day. However, the linear term, if it affected phenomena on earth, would produce a day to night shift in clock rates of about 8×10^{-13} or about 75 ns per day. This question was studied carefully by Professor Banesh Hoffmann (author of the biography of Einstein recommended in the first section of this paper[4]) in 1957.[45] He predicted that no such effect would be measured in the reference frame of the earth, but called for experiments to check the prediction when clocks of sufficient accuracy became available.

In 1976 the question was examined again by Professor Roman Sexl[46] who was seeking an explanation for an erroneous report of a dependence of atomic clock rates on latitude.[47] He concluded that there should be a seasonal effect caused by the tilt in the earth's spin axis, described by the equation

$$\frac{d\tau_1}{dt} - \frac{d\tau_2}{dt} = 14.8\{\sin \theta_2 - \sin \theta_1\} \cdot \cos\left[\frac{t - 21\ \text{June}}{365}\right] \text{ ns/day} \qquad (47)$$

where τ_1 and τ_2 are the proper times at latitudes θ_1 and θ_2 (southern latitudes being taken as negative). This equation results from the incorrect retention of the linear term in the expansion of the sun's potential as just discussed. It would be correct for observations conducted from a frame of reference attached to the sun, but is wrong for observations carried out on the earth. Professor Sexl now acknowledges his error.[48]

Experimental Results for Flights to Christ Church. Figure 52 shows on a globe tilted at 23°.5 the path taken by our C141 in transporting the clocks to Christ Church, New Zealand (latitude -43°29') from Washington, D.C. (latitude 38°48') and the different average distances of these locations from the sun. The first trip was made from July 10 to July 17 and a second trip from July 23 to July 30. Three days were required for the travel out and back, including ∿12 hour stopovers in Hawaii each way and a 2 hour stopover at the Travis Air Force Base in California on the westward journey. This allowed a dwell time in Christ Church of four days. Figure 53 shows the aircraft on the ground at the Operation Deep Freeze Antarctic support base in Christ Church surrounded by some of the portable electrical generating and heating equipment (it was winter in New Zealand) it had carried with it.

The data for the time differences $\tau_A - \tau_G$ are displayed in the following table:

	Measured Value (ns)	Calculated Value (ns)	Alleged Effect of Sun (ns)
Flight 1	115 ± 8	129 ± 5	80 ± 5
Flight 2	131 ± 8	118 ± 5	70 ± 5

The data is still being analyzed to correct the readings of the radar altimeter over the varying topography of the continental U.S. to give altitude above the ellipsoid rather than above the local topography, but the changes in the above numbers will not be large. There is no evidence, with a detection sensitivity of about 10% when the measured and calculated effects are compared, of the alleged effect of the sun.

Hydrogen Maser Carried on Suborbital Rocket Flight With Doppler Cancellation Tracking

In June 1976, a hydrogen maser was carried as payload in a suborbital flight by a Scout rocket launched from the Wallops Test Center of NASA in an experiment designed and conducted by R.F.C. Vessot, M. Levine and others of the Harvard/Smithsonian Center for Astrophysics.[49] The purpose was to measure with high accuracy by ground tracking the large change in frequency of the maser caused by the large change in gravitational potential as it ascended to an altitude of about one and a half earth radii above the earth's surface and fell back into the Atlantic Ocean in a flight lasting just under two hours. A sketch of the trajectory is given below. The ground path of the flight is shown in the following map. Ground tracking with microwave frequencies was carried out from stations

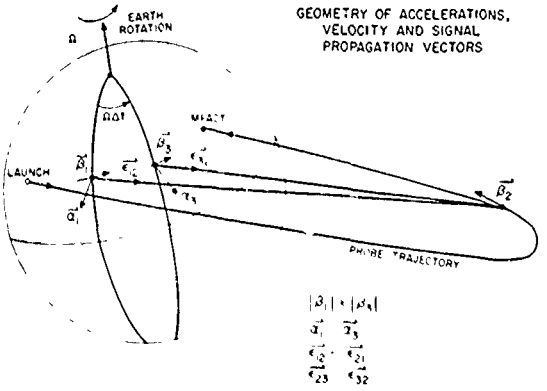

at Wallops Island, Bermuda and Florida equipped with hydrogen masers. In terms of relativistic frequency changes, it is readily shown that they are expressible as the integrand of equation (41)

$$\frac{f_{Probe} - f_{Ground}}{f_{Ground}} = \frac{\Delta f}{f} = \frac{\phi_{Probe} - \phi_{Ground}}{c^2} - \frac{V^2_{Probe} - V^2_{Ground}}{2c^2} \qquad (48)$$

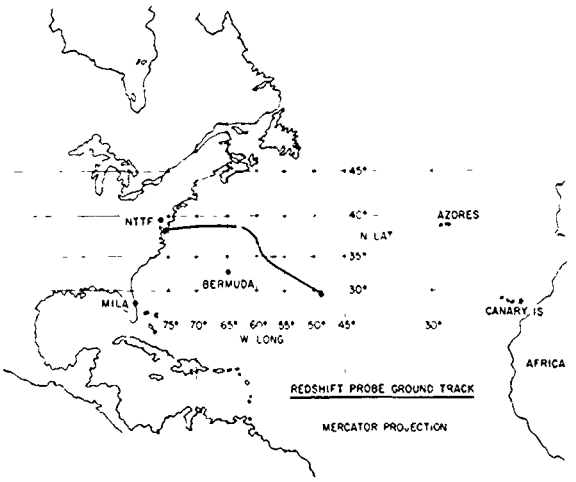

In this case, the gravitational potential difference causes the frequency of the probe maser to be shifted to higher values than the reference masers on the ground -- a violet shift rather than a red shift, but it is still convenient to speak of the effect as "redshift." The value of the gravitational shift as a function of height above the earth is plotted below. The received microwave frequency

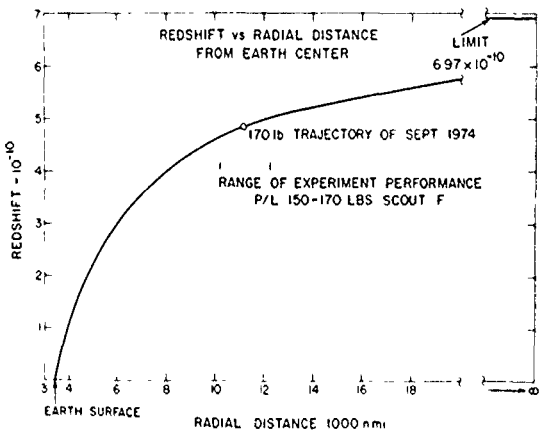

will be strongly affected by the ordinary Doppler effect which is just the rate of change of slant range divided by the speed of light. For a typical planned trajectory, the Doppler shift in frequency could be as high as 2×10^{-5} as shown in the following plot. Since the gravitational relativistic effect would be about 4×10^{-10} and the expected stability of the hydrogen maser was hoped to be $\sim 10^{-14}$, extraordinary measures had to be taken to measure or cancel the Doppler shift. Also, the large and variable effects of the earth's ionosphere causing phase shifts in the propagated microwave signals had to be considered.

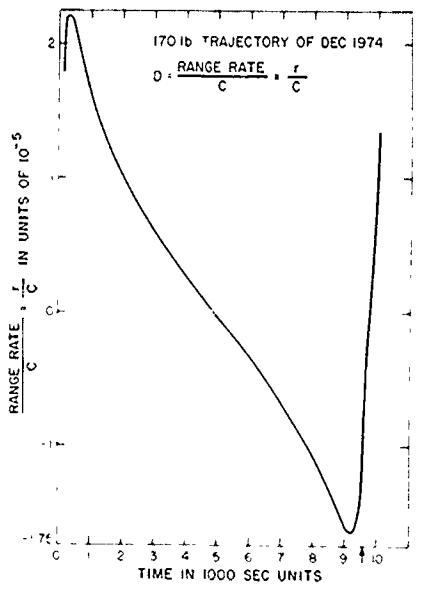

A very ingeneous arrangement of three microwave links at different frequencies as shown in the simplified block diagram below solved these problems.

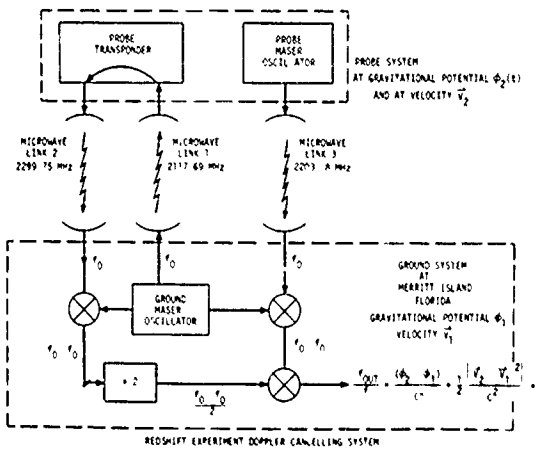

It was possible to achieve real time cancellation so that the redshift was evident during the flight as shown by the following quick look beat frequency data. The break in the data just before the end of the flight is due to tracking station problems and interrupted the phase continuity. It could not subsequently be recovered, so the remaining data is not useful for analysis. The combination of potential and velocity effects produced zero beats during both ascent and descent. The ascent zero beat data is shown in Figure 54. The rotation and nutation of the spinning payload can be clearly distinguished. Figure 55 shows the environmentally controlled hydrogen maser package which was flown

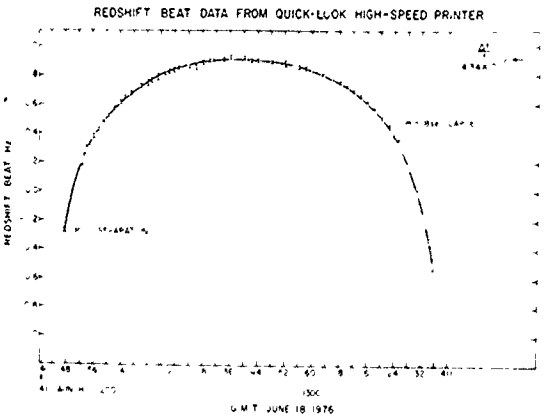

(and not recovered!) being held by its makers, Bob Vessot (on the right) and Marty Levine. Figure 56 is a picture of the rocket during launch.

Careful analysis of the ground tracking data to determine the actual rocket trajectory and comparison of the measured frequency shift as a function of time with that predicted by general relativity has yielded the following value[50] for the gravitational frequency shift (the velocity effects were assumed given)

$$\frac{\Delta f}{f} = \{1 + (5 \pm 126) \times 10^{-6}\} \frac{\Delta\phi}{c^2} \qquad (49)$$

This is the most accurate measurement of the relativistic effects on frequency. A plot of the residuals at the early stage of the analysis is given in Figure 57.

Other Atomic Clock Measurements

Mountain to Valley Experiments. The first such measurement was made in 1975 in Italy between Torino and a cosmic ray laboratory at Plateau Rosa 3250 m higher by L. Briatore and S. Leschiutta[51] using one cesium beam clock at each location. Comparison was achieved by receiving the same TV signal at each site and by direct comparison before and after the 66 day dwell time at Plateau Rosa. Although no stringent environmental control was attempted, nor were systematic corrections made for environmental changes, a 15% measurement was achieved, agreeing with the general relativistic calculation within that uncertainty.

The second measurement was made in Japan in June and July, 1977 by S. Iijima and K. Fujiwara[52] of the Tokyo Astronomical Observatory. One Hewlett-Packard 5061 High Performance standard was transported from the Tokyo Observatory (altitude 58 m above sea level) to the Norikura Corona Station (altitude 2876 m above sea level) on two successive occasions and left to operate for one week. Before and after those trips, one week comparisons were

made with a similar clock at the observatory. Systematic corrections were made for the effect of different environmental conditions at the different sites on the rate of the clock. They also paid close attention to the placement of the clocks in the local magnetic field and took great pains to keep environmental control during the 8 hour transport time in a cushioned and air conditioned van. Their results were

$$\frac{\text{Measured Effect}}{\text{Calculated Effect}} = 0.94 \pm 0.05, \qquad (50)$$

a verification at the 5% level.

These experiments measured purely the effect of gravitational potential difference.

Comparison of Absolute Frequency Determinations. Since the early 1970's, the National Bureau of Standards in Boulder, Colorado, at an altitude of about 6000 feet above sea level, has been including the gravitational effect $\Delta\phi/c^2 \sim 2 \times 10^{-13}$ in the determination of the absolute cesium frequency with its laboratory beam tubes. Other standards laboratories are at much lower altitudes so the effect is not yet significant in terms of achievable accuracies for them. However, the international definition of the second is based on the value of the cesium ground state hyperfine transition at sea level, so the gravitational shift of 1.09×10^{-16} per meter must be included in any absolute measurement. Inclusion of the effect in the NBS measurements does result in smaller differences in current international comparisons.

Practical Applications

Global Timekeeping

At the level of 0.1 microsecond, the relativistic effects of clock transport by aircraft are quite significant. For example, in the global measurements involving trips to Christ Church, New Zealand from Washington, D.C. and back, the relativistic time difference produced was ~120 nanoseconds. It is interesting to give a breakdown of the calculated relativistic effect for each leg:

Washington to California:	+29 ns	}	E→W
California to Hawaii :	+31 ns		
Hawaii to New Zealand :	+52 ns		
New Zealand to Hawaii :	+16 ns	}	W→E
Hawaii to Washington :	- 6 ns		

The asymmetry between E→W and W→E is very apparent. It is clear that even for short flights, the effects are important at the ten's of nanoseconds level. The U.S. Naval Observatory is now using an algorithm to estimate these effects for its transportable clock trips.

NAVSTAR/Global Positioning System[53]

This is a new navigation system under development by the United States Department of Defense. It is shown in artist's conception, together with some facts about it in Figures 58 and 59. There will be 24 satellites placed in 12 hour period circular orbits, 8 in each of 3 orbital planes inclined at 63° to the equator and equally spaced around it. Each of these satellites will carry a very stable atomic clock (with several spares) and will transmit a pseudo-random noise code with a bit repetition frequency controlled by the atomic clock. Information about the orbit of the satellite is also transmitted. User equipment will receive signals from four or more GPS satellites simultaneously, or sequentially, locking on to the transmitted code by shifting a local clock which steps the same pseudo-random noise code in the receiver. Large scale integrated solid state electronic circuits in the receiver package can then calculate the position, velocity, and time for any user.

The stable atomic clocks in orbit are the heart of the system. In order for all of them to remain synchronized with each other and with the ground clocks at the U.S. Naval Observatory which sets time worldwide for the Defense Department, the effects of general relativity must be included. When placed in such an orbit, a standard clock will run fast with respect to an identical one on the ground by 44,000 nanoseconds per day! This effect was first measured with the NTS-2 satellite carrying a cesium atomic clock.[54] The clocks must be adjusted to run slow by that amount before being placed in orbit in order to keep in synchronization with atomic clocks on the earth's surface. Furthermore, periodic change in distance from the center of the earth for a satellite in a slightly elliptic orbit can lead to significant effects. For an eccentricity of 0.005, the peak to peak time difference will be 24 nanoseconds. This translates into a range uncertainty of 24 feet which is very significant in a system whose present design goal is 10 meters, and must be included in the system operation.

The fact that standard clock rates are constant at mean sea level on the ellipsoidal surface of the spinning earth as discussed earlier allows the establishment of a coordinate time for the Global Positioning System which can be made the same as Universal Time on the surface of the earth. The standard atomic clocks in orbit will keep this GPS time when they are offset by the ~44,000 ns/day discussed above and corrected for the relativistic effects of the elliptic orbit. Stationary standard clocks on the ground must have their rates compensated, depending on their distance above or below the mean ocean surface ellipsoid by $\pm 1.09 \times 10^{-16}$ per meter in order to keep GPS coordinate time.

Significance

The two applications discussed briefly above are among the first non-scientific uses of Einstein-

ian Time. That the remarkable behavior of clocks as predicted by General Relativity is now required to be included in practical applications is an intellectual milestone, made possible by the extraordinary stability of modern atomic clocks.

References and Notes

1. Quoted in Hilbert, by Constance Reid. Published by Springer-Verlag: New York, Heidelberg, Berlin, 1970, page 105.

2. Martin Klein, "Einstein and the Academic Establishment," in Einstein, A Centenary Volume, edited by A.P. French, Harvard University Press, Cambridge, Massachusetts, 1979, page 209. (Figure 6 is taken from this essay)

3. Albert Einstein, "On Education" in Out of My Later Years, New York Philosophical Library, 1950. Reprinted in the commemorative volume cited in reference 2, page 315.

4. Banesh Hoffmann, Albert Einstein, Creator and Rebel. The Viking Press, New York, 1972. Paperback edition, New American Library, New York, London, and Scarborough, Ontario, 1973.

5. Hermann Bondi, Relativity and Common Sense, A New Approach to Einstein, Anchor Book Science Study Series, Doubleday and Company, Inc., Garden City, New York, 1964.

6. Consider the following spacetime diagram in which observer B is moving with constant velocity v with respect to observer A.

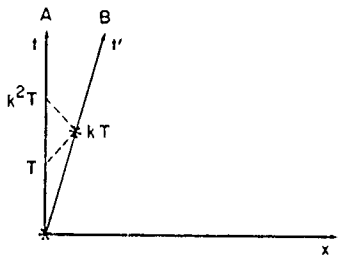

When B is at the same position as A, they set their identical clocks to read 0. At time T later A emits a light pulse which is received by B at time kT and immediately transmitted back to A who receives it at time $k(kT) = k^2T$ since the Doppler stretching has operated twice. By equations (1) and (2), the position of B as determined by A when B receives and reflects the pulse is

$$x = \frac{c}{2}(k^2 T - T) = \frac{c}{2}(k^2 - 1)\,T$$

and the time of this reception event by B according to A is

$$t = \frac{1}{2}(T + k^2 T) = \frac{1}{2}(k^2 + 1)\,T$$

The velocity $v = x/t = c\,(k^2 - 1)/(k^2 + 1)$ and the result in the text follows by solving for k.

7. The distances corresponding to the units on the time and space axes are determined by plotting branches of the rectangular hyperbolae

$$t^2 - x^2 = \pm 1$$

with respect to the light cone as shown in the following diagram:

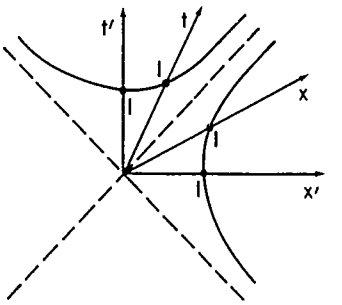

Intersection of the time and space axes for an inertial observer yields the calibration points.

8. This is shown very easily with the "k-calculus" and the following diagram

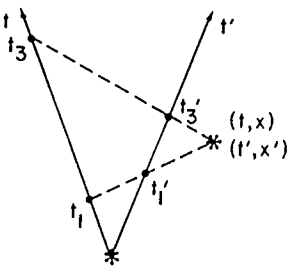

The spatial axes have been suppressed. It is clear from equations (1) and (2) in the text that

$$t_1 = t - x/c \qquad t_1' = t' - x'/c$$

$$t_3 = t + x/c \qquad t_3' = t' + x'/c$$

It is also clear from the definition of the Doppler factor k, that

$$t_1' = kt_1$$

$$t_3 = kt_3'$$

These two equations may be written as

$$t - x/c = \frac{1}{k}(t' - x'/c)$$

$$t + x/c = k(t' + x'/c)$$

Multiplying these equations together and multiplying the result by c^2, one has the result stated as equation (4) in the text. If one solves this pair of simultaneous equations for t' and x' in terms of t and x, the Lorentz transformation is obtained.

9. New York Times, March 28, 1972; page 32. The first part of this excerpt is also very illuminating, so we reproduce it here:

> "In the development of special relativity theory, a thought - not previously mentioned - concerning Faraday's work on electromagnetic induction played for me a leading role.
>
> According to Faraday, when a magnet is in relative motion with respect to a conducting circuit, an electric current is induced in the latter. It is all the same whether the magnet moves or the conductor; only the relative motion counts, according to the Maxwell-Lorentz theory. However, the theoretical interpretation of the phenomenon in these two cases is quite different:
>
> If it is the magnet that moves, there exists in space a magnetic field that changes with time and which, according to Maxwell, generates closed lines of electric force -- that is, a physically real electric field; this electric field sets in motion movable electric masses (that is, electrons) within the conductor.
>
> However, if the magnet is at rest and the conducting circuit moves, no electric field is generated; the current arises in the conductor because the electric bodies being carried along with the conductor experience an electromotive force, as established hypothetically by Lorentz, on account of their (mechanically enforced) motion relative to the magnetic field.
>
> The thought that one is dealing here with two fundamentally different cases was, for me, unbearable. The difference between these two cases could not be a real difference, but rather, in my conviction, could be only a difference in the choice of reference point. Judged from the magnet there certainly were no electric fields; judged from the conducting circuit there certainly was one. The existence of an electric field was therefore a relative one, depending on the state of motion of the coordinate system being used, and a kind of objective reality could be granted only to the electric and magnetic field together, quite apart from the state of relative motion of the observer or the coordinate system. The phenomenon of the electromagnetic induction forced me to postulate the (special) relativity principle."

10. P.G. Roll, R. Krotkov, and R.H. Dicke, "The Equivalence of Inertial and Passive Gravitational Mass," Ann. Phys (U.S.A.) 26, 442-517 (1964).

    V.B. Braginsky and V.I. Panov, "Verification of the Equivalence of Inertial and Gravitational Mass," Zh. Eksp. & Teor. Fiz. 61, 873-879 (1971). English translation in Sov. Physics - JETP Lett. 10, 280-283 (1972).

11. C.F. Gauss, "Disquitiones Generales circa Superficies Curvas," Göttingen, 1827. There has just appeared a modern translation of "General Investigations of Curved Surfaces" in Astérisque 62: "150 Years After Gauss," by P. Dombrowski, published by the Société Mathématique de France, 1979.

12. C.W. Misner, K.S. Thorne, and J.A. Wheeler, Gravitation, W.H. Freeman and Company, San Francisco, 1973. Cover drawing and page 4.

13. Bertrand Russell, The ABC of Relativity, Third Revised Edition, New York, New American Library Mentor Book, 1959, page 80. (Original edition, 1925).

14. J. Evershed, Bulletin of the Kodaikanal Observatory, 36 (1914).

15. W. Pauli, Theory of Relativity. Pergamon Press; New York, London, Paris, Los Angeles. 1958, Page 153.

16. J. Brault, Bulletin of the American Physical Society, 8, page 28 (1963).

17. F. Roddier, Annals of Astrophysics, 28, page 463 (1965).

18. J.L. Snider, Physical Review Letters, 28, page 853 (1972).

19. J.L. Greenstein, J.B. Oke, and H.L. Shipman, Astrophysical Journal, 169, page 563 (1971).

    J.L. Greenstein and V. Trimble, Astrophysical Journal, 149, p. 283 (1967).

20. A discussion of the problems involved is given by S. Weinberg, Gravitation and Cosmology, John Wiley and Sons, Inc., New York, London, Sydney, Toronto. 1972. Pages 79ff.

21. H E. Ives and G.R. Stilwell, "An Experimental Study of the Rate of a Moving Atomic Clock," (I and II) Journal of the Optical Society of America, 28, p. 215 (1938); 31, page 369 (1941).

22. G. Otting, Physikalische Zeitschrift, 40, page 681 (1939).

23. H.I. Mandelberg and L. Witten, Journal of the Optical Society of America, 52, page 529 (1962).

24. J.J. Snyder and J.L. Hall, Laser Spectroscopy, Proceedings of the Second International Conference, 23-27 June, 1975, Mégève, France, Springer-Verlag: Berlin, Heidelberg, New York, 1975. Page 6.

25. S. N. Bagayev and V.P. Chebotayev, Pis 'ma Zh. Eksp. i Teor. Fiz., 16, page 614 (1972).

26. R.V. Pound and G.A. Rebka, Physical Review Letters, 3, page 439 (1959); 4, page 337 (1960).

27. R.V. Pound and J.L. Snider, Physical Review Letters, 13, page 539 (1964); Physical Review 13, 140, page 788 (1965). See also R.V. Pound, "Terrestrial Measurements of the Gravitational Red Shift," in Albert Einstein's Theory of General Relativity, edited by G. Tauber, Crown Publishers, Inc., New York, 1979. Pages 32ff.

28. H.J. Hay, J.P. Schiffer, T.E. Cranshaw, and P.A. Egelstaff, "Measurement of the Red Shift in an Accelerated System Using the Mössbauer Effect in Fe," Physical Review Letters, 4, page 165 (1960).

29. W. Kündig, "Measurement of the Transverse Doppler Effect in an Accelerated System," Physical Review, 129, page 2371 (1963).

30. K.C. Turner and H.A. Hill, "New Experimental Limit on Velocity Dependent Interactions of Clocks and Distant Matter," Physical Review B, page 134 (1964).

31. J.B. Thomas, "Reformulation of the Relativistic Conversion Between Coordinate Time and Atomic Time," Astronomical Journal, 80, No. 5, p. 405 (1975).

32. A.J. Greenberg, D.S. Ayres, A.M. Commach, R.W. Kenny, D.O. Cadwell, V.B. Elings, W.P. Hesse, and K.J. Morrison, "Charged Pion Lifetime and a Limit on a Fundamental Length," Physical Review Letters, 23, page 1267 (1969).

33. F.J.M. Farley, J. Bailey and E. Picasso, "Experimental Verifications of the Special Theory of Relativity," Nature, 217, page 17 (1968).

34. B. Rossi and D.B. Hall, "Variation of the Rate of Mesotrons with Momentum," Physical Review, 59, page 223 (1941).

35. J.C. Hafele and R.E. Keating, Science, 177, page 166 and page 168 (1972).

36. In addition to the main participants listed in the text, the following people participated from the University of Maryland: J.P. Richard and D.G. Currie advised on some technical questions; F. Meraldi mounted the corner reflectors; and J.J. Giganti and J. Mathews did some electronic design and construction.

A detailed account of the measurements is contained in two University of Maryland Ph.D. dissertations:

R. E. Williams, "A Direct Measurement of the Relativistic Effects of Gravitational Potential on the Rates of Atomic Clocks Flown in an Aircraft," (May, 1976).

R. A. Reisse, "The Effect of Gravitational Potential on Atomic Clocks as Observed with a Laser Pulse Time Transfer System," (May, 1976).

The work has also been described in talks at meetings and symposia, including: Precise Time and Time Interval Meeting, Goddard Space Flight Center, December, 1976; 30th Frequency Control Symposium, Atlantic City, June, 1976 (During Round Table Discussion on Remote Time Comparison); Second Symposium on Frequency Standards and Metrology, Copper Mountain, Colorado, July, 1976; Meeting of Commission 31 (Time) at the XVI General Assembly of the International Astronomical Union, Grenoble, France, August, 1976; Meeting on Experimental Gravitation, Sponsored by the Accademia Nazionale dei Lincei, Pavia, Italy, September, 1976; Symposium on Time and Frequency at the 19th General Assembly of the International Union of Radio Science, Helsinki, Finland, August, 1978.

37. The support of the U.S. Navy has come from many organizations in addition to the U.S. Naval Observatory, including its Directors Kai Strand and Gart Westerhout. These include:

The Naval Materiel Command
James Probus, Director of Navy Laboratories
Norris Keeler, Director of Navy Technology
The Office of Naval Research
John Dardis, Project Monitor
Doran Padgett, Project Monitor
William Condell, Physics Branch Chief
Fred Quelle, Boston Office
The Naval Air Development Center
Kenneth Lobb, Technical Director
Ronald Vaughn, Richard Sheklin } Navigation Laboratory
Patuxent Naval Air Test Center
Robert Merritts, Project Engineer (He worked night and day along with the principal participants and contributed much to the success of the experiments).
Pilots, Flight Engineers, Crew Chiefs, and Airmen for P3C-912.

38. The modifications were carried out at Maryland with R. Hyatt and J. Bourdet of Hewlett-Packard assisting L.S. Cutler and the Maryland group.

39. Frequent assistance in maintenance was provided by D. Kaufman and J. Soucy of the Goddard Space Flight Center.

40. We are indebted to Ernst Jechert and Hans Badura of Efratom for the loan of these standards.

41. The development of this experiment is described by C.O. Alley in Adventures in Experimental Physics, Alpha, 1972. Edited by B. Maglich. The major scientific result of the lunar laser ranging experiment is a test of the Principle of Equivalence for massive bodies (Earth and Moon both falling to the sun): J.G. Williams, R.H. Dicke, P.L. Bender, C.O. Alley, W.E. Carter, D.G. Currie, D.H. Eckhardt, J.E. Faller, W.M. Kaula, J.D. Mulholland, H.H. Plotkin, S.K. Poultney, P.J. Shelus, E.C. Silverberg, W.S. Sinclair, M.A. Slade, and D.T. Wilkinson, Physical Review Letters, 36, page 551 (1976).

42. We are indebted to Dr. Frank Hoge of the Wallops Center of NASA for the loan of this telescope.

43. The Air Force organizations providing support included:

    The Air Force Systems Command
    Maj. Gen. G. Hendricks, Director of Laboratories
    Dr. Bernard Kulp, Chief Scientist
    The Air Force Office of Scientific Research
    Major Richard Gullickson, Project Monitor
    Col. R. Detwiler, Physics Branch Chief
    4950th Test Wing, Wright Patterson Air Force Base
    Lt. Steve Stratton, Test Director (He worked closely with the major participants, contributing much to the success of the measurements).
    Col. William Odgers. Commander
    Instrumentation Branch
    Modification Center
    Pilots, Navigators, Flight Engineer, Loadmasters, Crew Chiefs, and Airmen for C141 -- 779.

44. The entire Mechanical Development Design group and machine shop personnel of the Department of Physic and Astronomy of the University of Maryland performed in an outstanding manner to accomplish the reconfiguration of the equipment to very exacting Air Force requirements in the short time available between the authorization of the project in early April and the beginning of the experiments in late May. The following people deserve special recognition: Frank Desrosier, Jerome Massé, Ernest Grossenbacher, Wade Hay, Ben Scesa, Dan Koch, Karl Harzer and Edward Gorsky.

45. B. Hoffmann, "Noon - Midnight Red Shift," Physical Review, 121, page 337 (1961).

46. R.U. Sexl, "Seasonal Differences Between Clock Rates," Physics Letters, 61B, page 65 (1976).

47. W.H. Cannon and O.G. Jensen, "Terrestrial Timekeeping and General Relativity: A New Discovery," Science, 188, page 317 (1975). The errors in this paper have been pointed out in many letters in a subsequent issue of Science: "Acceleration and Clocks," Science, 191, pages 489-491 (1976). The authors have retracted their claims.

48. R.U. Sexl, private communication, August, 1977.

49. R.F.C. Vessot and M.W. Levine, Gravitazione Sperimentale, Accademia Nazionale dei Lincei, Rome, page 371 (1977).

50. R.F.C. Vessot, presented at Second Marcel Grossmann Meeting on Recent Developments in General Relativity, Trieste, Italy, July, 1979.

51. L. Briatore and S. Leschiutta, "Evidence for the Earth Gravitational Shift by Direct Atomic-Time-Scale Comparison," Il Nuovo Cimento, 37B, No. 2 (1977).

52. S. Iijima and K. Fujiwara, "An Experiment for the Potential Blue Shift at the Norikura Corona Station," Annals of the Tokyo Astronomical Observatory, Second Series, Volume XVII, Number 2, (1978).

53. The NAVSTAR/Global Positioning System is fully described by seventeen articles in the GPS special issue of Navigation, Journal of the Institute of Navigation, Vol. 25, No. 2, Summer, 1978.

54. T. McCaskill, J. White, S. Stebbins, and J. Buisson, "NTS-2 Frequency Stability Results," Proceedings of the 32nd Frequency Control Symposium, 1978.

1. Albert Einstein in his study in Berlin.

2. Herblock drawing in the Washington Post after Einstein's death in 1955.

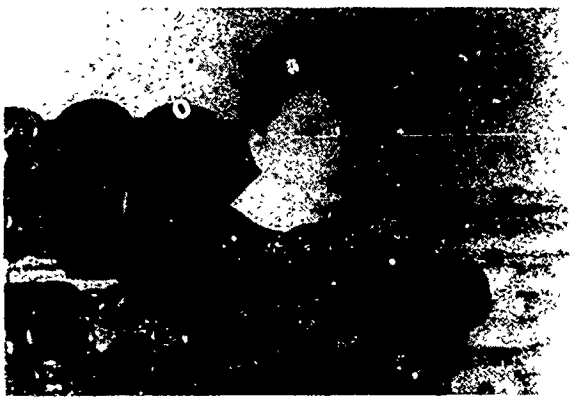

3. The earliest known picture of Einstein - age around 5 years.

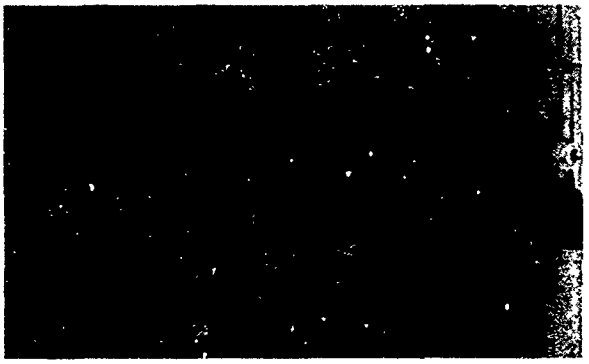

4. Einstein in elementary school in Munich at the age of 10 (Second from right, first row).

5. Einstein at the age of 14.

6. The classroom of Dr. Jost Winteler in Aarau. Einstein at age 16 is at right.

7. Einstein as a student at the ETH in Zurich.

8. Einstein at his desk in the Swiss Patent Office in Bern at age 26.

9. Einstein in a playful mood at the California Institute of Technology in the early 1930's.

10. Einstein in his later years at the Institute for Advanced Study in Princeton.

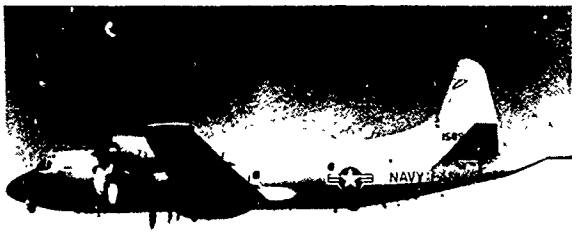

11. Navy P3C Orion Aircraft 912 used in the experiments.

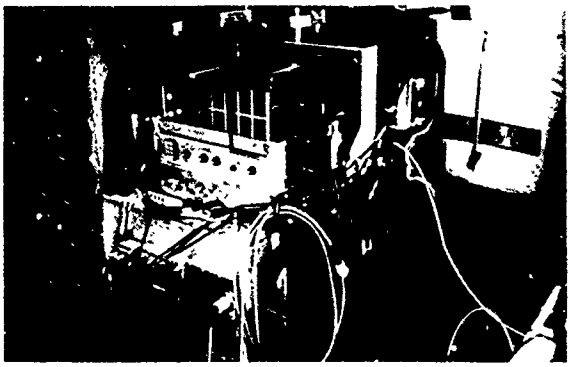

12. Clock Box installed on aircraft.

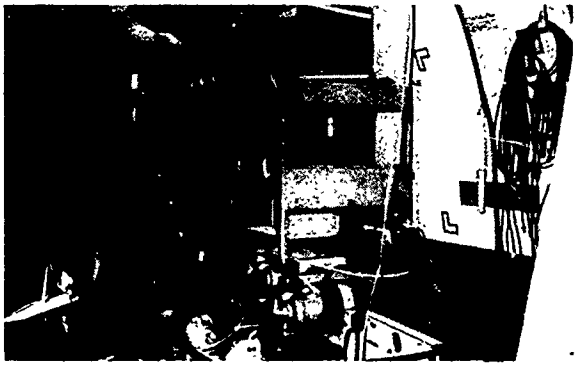

13. Electronic racks installed on aircraft.

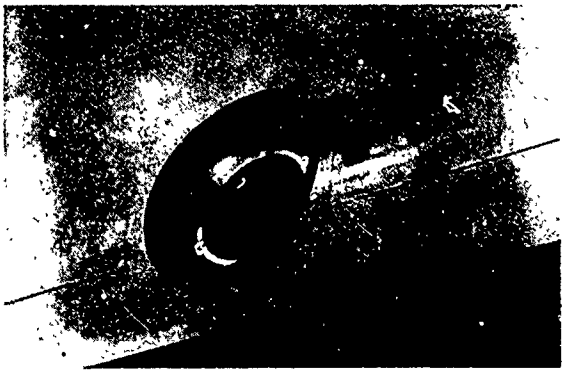

14. Optical corner reflector on the aircraft of the type used for the Apollo Lunar Laser Ranging Retro-Reflectors.

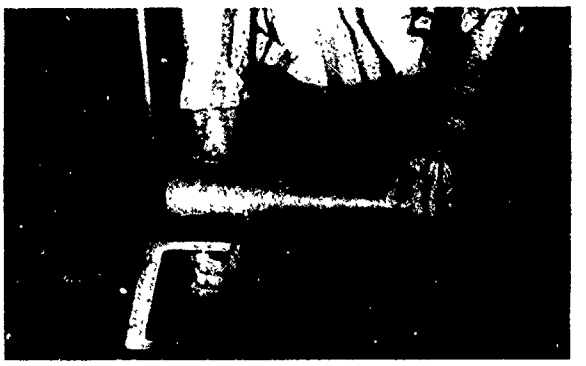

15. Housing of photo-multiplier for detection of laser light pulses on the aircraft.

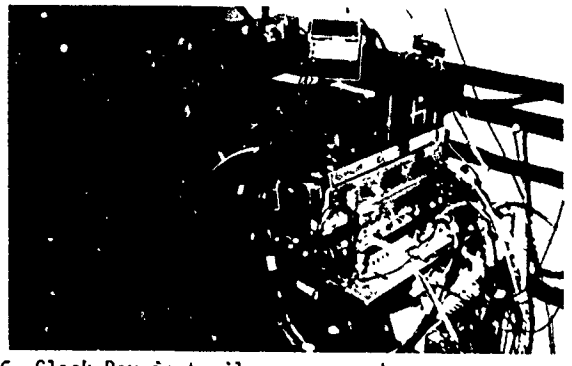

16. Clock Box in trailer on ground.

17. Ground computer system, event timer, and strip chart monitoring displays in trailer. (R.E. Williams, left and R.A. Reisse).

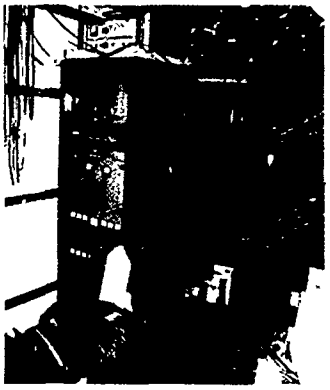

18. Two hydrogen masers made by Harry Peters on loan from the Goddard Space Flight Center.

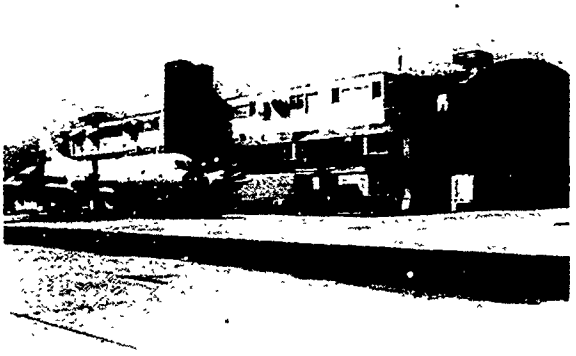

19. Aircraft on ground near trailer containing atomic clocks and van containing laser equipment.

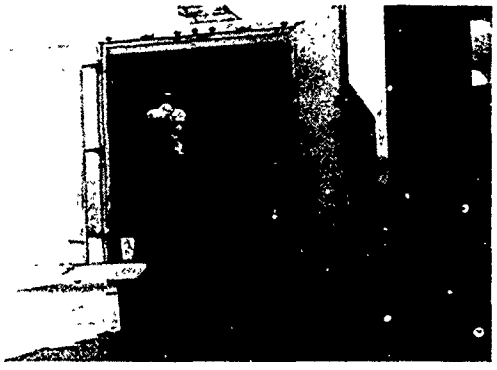

20. Clock Box being removed from trailer.

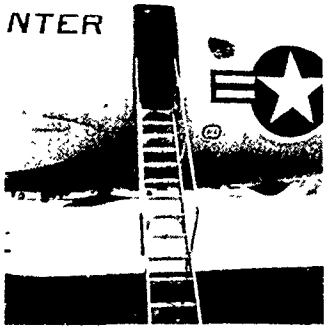

21. Narrow hatch of aircraft.

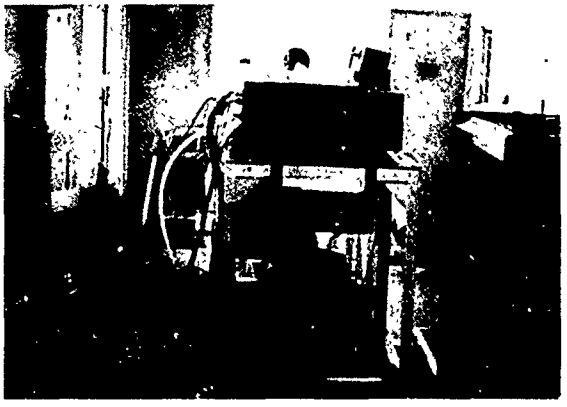

22. Laser Beam directing and receiving optics.

23. Laser equipment and receiving optics in van.

24. Closed circuit TV display with coarse and fine joysticks for aircraft tracking.

25. Landing lights of plane on TV display during tracking.

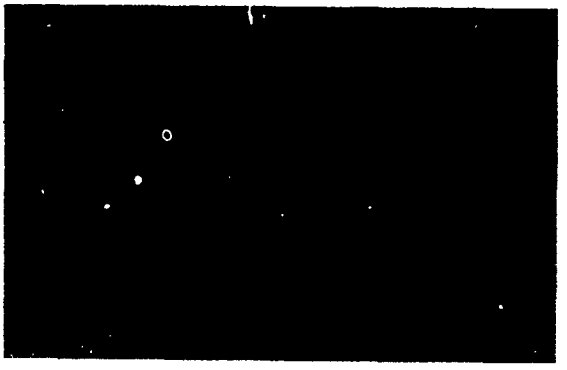

26. Laser transmitter and runways as seen from the airplane at twilight.

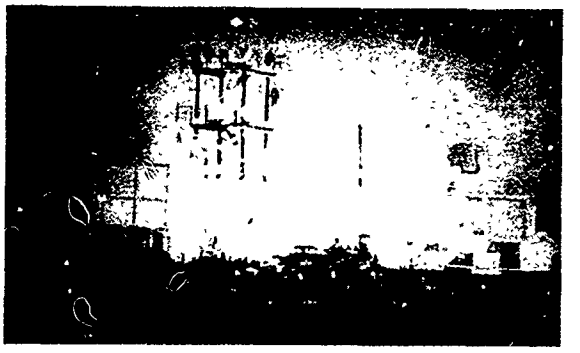

27. Chesapeake Test Range.

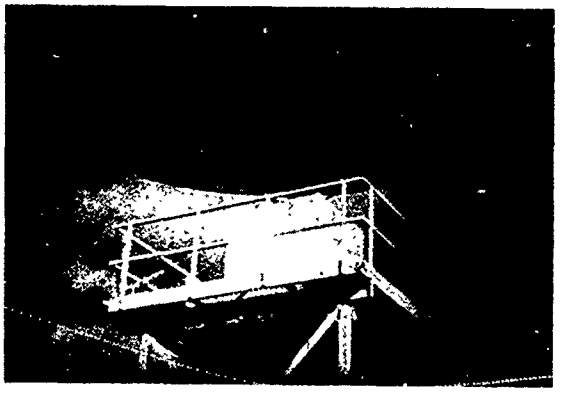

28. Ground tracking antenna at the Chesapeake Test Range.

29. L.S. Cutler adjusting ensemble of modified Hewlett-Packard 5061A atomic clocks.

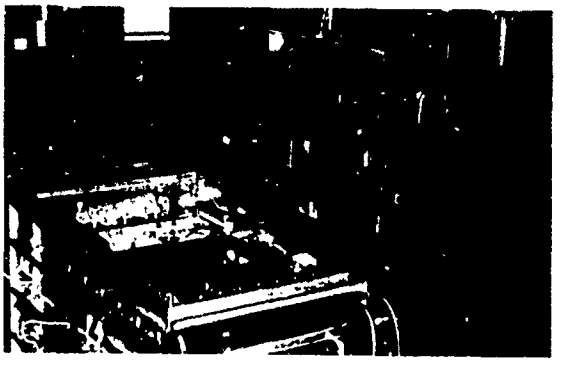

30. Interior of Clock Box.

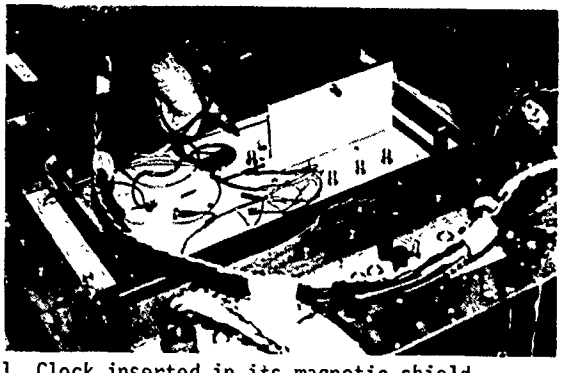

31. Clock inserted in its magnetic shield.

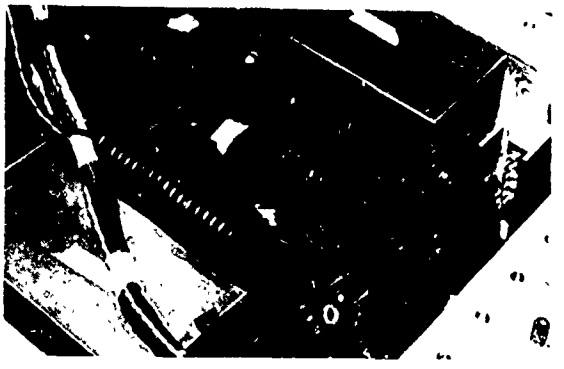

32. Air flow hoses for controlling temperatures and removing heat from clocks.

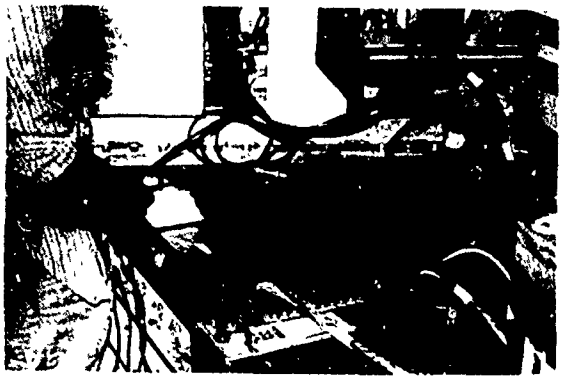

33. Lid carrying Efratom rubidium atomic clocks and voltage and pressure regulation equipment.

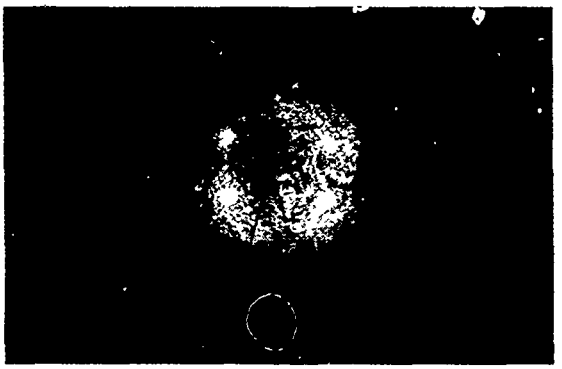

34. Polar photograph of globe showing distances of Washington and Thule from the Earth's spin axis.

35. Airborne equipment being reconfigured for C141 cargo pallet (Front View).

36. Airborne equipment being reconfigured for C141 cargo pallet (Back View) (Technician Lyndon Small at left).

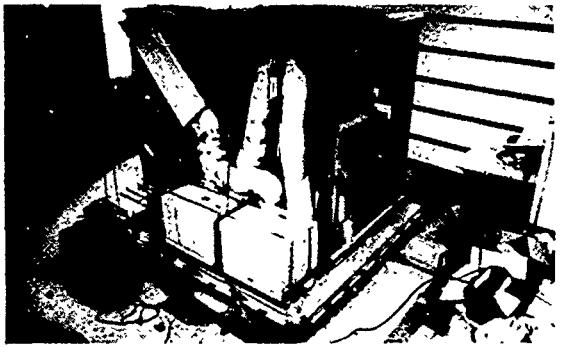

37. Airborne equipment on cargo pallet housed in pre-fabricated garage of Andrews Air Force Base.

38. Air Force C141 Starlifter Aircraft 779 at Andrews Air Force Base next to garage, trailer, and van.

39. Tail of C141 with petal doors through which equipment was loaded.

40. Preparing to transfer equipment from garage.

41. Front lift carrying pallet to aircraft.

42. Petal door open to receive pallet.

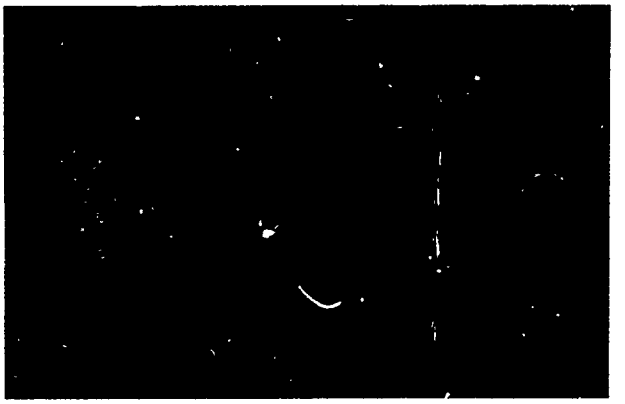

43. Matching of pallet to aircraft roller tracks.

44. Rolling pallet to forward part of aircraft.

45. Len Cutler beside installed pallet on aircraft.

46. Clock Box Assembly during flight. (Seen from rear of plane).

47. Clock Box Assembly during flight. (Seen from front of plane).

48. Recording and readout equipment for inertial navigation units and altimeters.

49. Preparing to place aircraft in hangar at the Thule Air Force Base.

50. A C141 at Thule just before midnight on June 25.

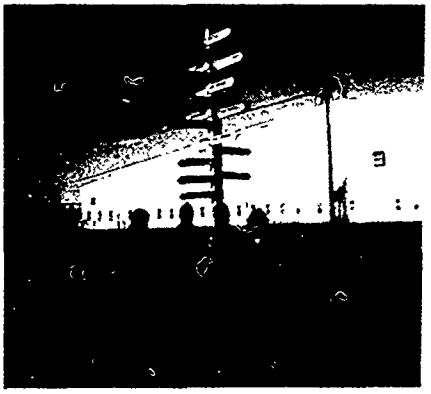

51. Midnight shadows cast by sun at Thule on June 25.

52. Globe tilted at 23°.5 showing relation between Washington and Christ Church at time of summer solstice (Sun to right).

53. C141 779 on ground at Christ Church surrounded by support equipment.

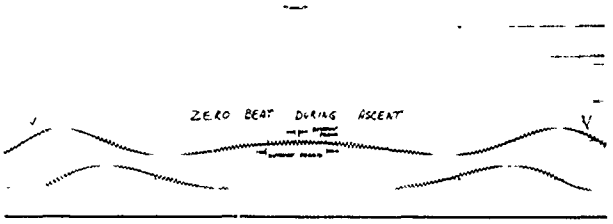

54. Zero beat during ascent of hydrogen maser on rocket probe.

55. Environmentally packaged hydrogen maser to be carried by Scout rocket being held by R. F. C. Vessot (right) and M. Levine.

56. Launch of Scout rocket carrying hydrogen maser.

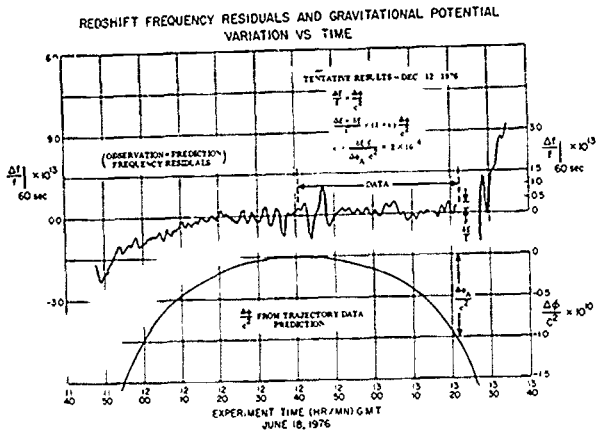

57. Residuals during an early stage of the analysis of the hydrogen maser rocket probe data.

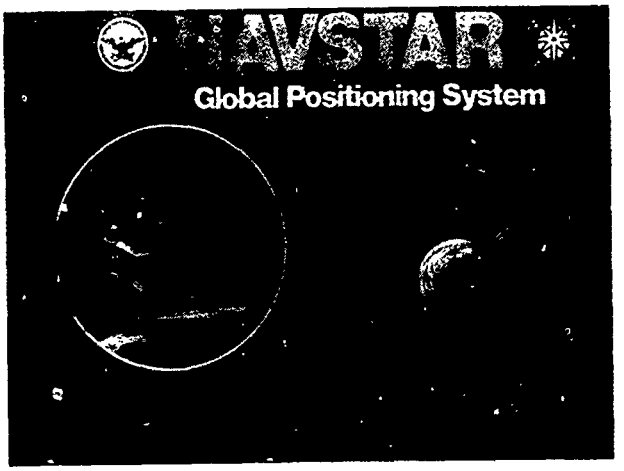

58. Artist's drawing of NAVSTAR/Global Positioning System.

59. Major segments of the NAVSTAR system.

1/f (FLICKER) NOISE: A BRIEF REVIEW

Richard F. Voss
IBM Thomas J. Watson Research Center
Yorktown Heights, New York 10598

ABSTRACT

Noise mechanisms limit the accuracy of precision measurements. Although many sources of noise are well understood, the origin of the "1/f" or "flicker" noises remains, in general, a mystery in spite of their remarkably widespread occurance in nature. In this paper a review is given of the systems exhibiting 1/f noise and the postulates researchers have made about its origin.

INTRODUCTION

All physical measurements are ultimately limited by fluctuations or "noise" in either the system being measured or the measuring apparatus. Although there are many sources of noise, both classical and quantum mechanical, the common noises found in nature fall into three general classes according to their spectral densities Figure 1 shows samples of noise from these classes together with logarithmic plots of their spectral densities vs frequency. The spectral density (also known as "power spectrum"), $S_V(f)$, of a quantity V(t) fluctuating in time is a measure of the mean square variation in a unit bandwidth centered on the frequency f. $S_V(f)$ may be measured by passing V(t) through a narrow bandpass filter at frequency f with bandwidth Δf. $S_V(f)$ is then the average of the squared output of the filter divided by Δf. $S_V(f)$ provides information about the time correlations of the fluctuating process. A slowly varying process has more "power" at lower frequencies.

Figure 1(a) shows a trace of a "white noise." Like a "white" light, white noise shows equal amounts of fluctuations at all frequencies. It has the most random appearance of the three and is the simplest to understand mathematically. Its fluctuation at any instant of time is independent of the fluctuations at other times. It can be described by a complete lack of correlation. Figure 1(c) shows a trace of a $1/f^2$ noise. Such a trace might represent the position of a particle undergoing one dimensional Brownian motion The $1/f^2$ noise is much more slowly varying and much more correlated in time than the white noise. Yet, like the white noise, its mathematical description is simple. A $1/f^2$ noise results from the superposition of uncorrelated increments (a random walk). It is just the integral of a white noise. Both white and $1/f^2$ noises are well known and understood (Johnson noise, shot noise, Brownian motion). Figure 1(b), on the other hand, shows the subject of this paper, a 1/f or flicker noise. In appearance the 1/f noise is intermediate between the white and $1/f^2$ noises and exhibits a balance between randomness and correlation on all time scales. A 1/f noise is characterized by a simple power law spectral density with an exponent close to -1 Unlike the other noises and inspite of its seemingly ubiquitous occurrence, a universal explanation of 1/f noise has eluded scientists

EARLY HISTORY

The first spectral density measurement of a 1/f noise was published by J. B. Johnson in 1925[1]. Interestingly, this is the same J. B. Johnson who, several years later[2], would make the first experimental verification of Nyquist's prediction of equilibrium noise in conductors[3] to earn his namesake noise. In his 1925 paper Johnson was experimentally studying Schottky's prediction of shot noise in vacuum tubes[4] At high frequencies the measured noise agreed with prediction (2eI) but at lower frequencies was substantially greater The magnitude of the excess spectral density varied as the current squared and, although he made no comment on the frequency dependence, his published data show the excess to be proportional to 1/f. He ascribed the effect to "irregular temporal changes in the cathode emissivity."

The first "theory" of Johnson's excess noise was advanced the following year (1926) by W. Schottky[5] who also proposed the name "flicker effect " According to Schottky, "if we had to do with emission of light instead of electrons, we would speak of a chaotic variation of light intensity taking place over the surface of the cathode, a phenomenon which we should describe by the word 'flicker'." Schottky also set a precedent in either misunderstanding or simply not believing the experimental data by trying to fit the data to a $1/f^2$ spectral density with a process characterized by a single correlation time

Also in a 1925 paper on the shot effect Hull and Williams[6] made the observation that replacing the vacuum tube by an India ink resistance (standard grid leak) gave an excess noise of the same magnitude as the shot effect while a wire resistance did not. Although they presented no spectral density measurements, India ink resistors are, in fact, excellent sources of flicker noise Figure 2 shows a recent measurement by the author of the spectral density of the resistance fluctuations of

an India ink resistor. The spectral density varies as $1/f^{1.21}$ over 10 decades. Figure 2 not only demonstrates the remarkably large frequency range over which the spectral density can vary as a simple power law but also shows that the dependence need not be exactly 1/f.

By the 1930's it was generally accepted that thin film granular resistors produced an excess noise in the presence of current. In one study G. W. Barnes[7] attempted to verify a suggestion by Dr. W. F. G. Swann that the excess noise was essentially shot noise. They believed that "if conduction in these films takes place by leaps of electricity between aggregates or groups of molecules in the film, the phenomena ought to partake of the nature of a Schottky effect, but with the electronic charge replaced by an apparent electronic charge of much larger magnitude " However, it was not until the spectral density of such thin films was measured by J. Bernamont[8] that it was realized that the excess noise was of the flicker as opposed to shot variety. Bernamont's work was remarkable both for its completeness and for the early realization that the 1/f behavior could not be approximated by a Lorentzian (single correlation time) as suggested by Brillouin[9] but required a distribution of times. Bernamont and Brillouin also anticipated later work by postulating that 1/f noise was inversely proportional to the total number of charge carriers in the sample.

At about the same time Christensen and Pearson[10] at Bell Labs and Otto[11] and Meyer and Thiede[12] in Germany published extensive experimental studies of the excess noise in carbon microphones (such as those used in telephones) and other granular resistors Christensen and Pearson showed that the noise was proportional to current squared and had a spectral density varying as 1/f They attributed the noise to resistance fluctuations at the contacts between grains and called the noise "contact noise." They also referred to a 1919 paper by Kawamoto at Western Electric who characterized the electrical disturbances in carbon transmitters as "carbon burning" at high voltages or more generally as "carbon roar" which described the "continuous rushing sound which is always present no matter how well the transmitter is shielded from external disturbances."

Since these early measurements, fluctuations with a $1/f^{\beta}$ spectral density have been found for virtually all of the electronic devices made possible by the advances in solid state physics Continuous metal films[13], semiconducting films[14], metal contacts[15], semiconducting contacts[16], ionic solutions[17], thermocells[18], concentration cells[17], PN junctions[19], Schottky[20], Zener[21], and tunnel diodes[22], bipolar[19,23] and field effect transistors[24], flux flow in superconductors[25] and Josephson junctions[26] all exhibit what has come to be known as "1/f noise."

1/f noise limits the accuracy of precision time standards including quartz oscillators, atomic clocks, and superconducting cavity resonators[27]. Even modern measurements on the ancient time standard, the hourglass[28], show that the flow of sand fluctuates as 1/f. The Allan variance[29], is more often used to characterize the fluctuations of precision time or frequency standards than the spectral density. The Allan variance of a quantity V(t) is given by

$$\sigma_V^2(\tau) = \frac{1}{2}\overline{(V_{k+1}-V_k)^2},$$

where V_k is the average of the fluctuation V(t) over a time τ.

$$V_k = \frac{1}{\tau}\int_{k\tau}^{k\tau+\tau} V(t)dt.$$

Whereas the typical spectral (Fourier) analysis of a fluctuating quantity measures the mean square of the convolution of the fluctuation with a sine wave, the Allan variance measures the convolution with one period of a square wave. The Allan variance is thus approximately the spectral density at $f \simeq 1/2\tau$ times a bandwidth $\Delta f \simeq 1/2\tau$

$$\sigma_V^2(\tau) \cong S_V(\frac{1}{2\tau})\frac{1}{2\tau}.$$

For a 1/f spectrum, the Allan variance is independent of τ. Typical measurements show an Allan variance that decreases as a function of increasing τ until the "flicker floor" is reached where σ^2 becomes independent of τ corresponding to a low frequency 1/f limit.

1/f noise is by no means limited to the world of electronics It is found for the fluctuations of the earth's rate of rotation[30], undersea currents[31], and traffic on Japanese expressways[32]. A 1/f spectral density is common for hydrological variables where the persistence of the fluctuations prompted Mandelbrot[33] to refer to it as the "Joseph effect." One example is given in Fig. 3 which shows the spectral density of the minimum and maximum flood levels of the river Nile as compiled from yearly records of the ancient Egyptians[34] As first shown by Verveen and Dirkson[35], 1/f noise also plays a dominant role in the fluctuations across nerve membranes, and is of current importance in fundamental studies of nerve processes[36].

It is just this ubiquity of the 1/f spectral density that suggests an answer to a question that has long troubled philosophers In the words of Plato, " for when there are no words (accompanying music) it is very difficult to recognize the meaning of the harmony and rhythm, or to see that any worthy object is imitated by them," (*Laws*, Book II). The arts were assumed to be imitative and, although it was clear how painting, sculpture, or drama imitated nature, it was not at all obvious just what music imitated At least a partial answer is that

music imitates the way our world changes in time. These changes are characterized by a $1/f^{\beta}$ spectral density. In fact, such a spectral density is found for the loudness and pitch fluctuations of speech and music[37]. As shown in Fig 4, a 1/f spectral density is common to music of all cultures and, as shown in Fig. 5, is common to the development of western music. Indeed, 1/f noise provides a remarkably good staring point for stochastic music composition.

Although rarely mentioned in the classroom, the power law (non-exponential) decays of correlation associated with 1/f noise are common to many fields of science. Two examples are worthy of specific mention since they predate 1/f noise measurements by at least a century. A decay varying as $1/t^n$ where $n \approx 1$ is common in the field of dielectric relaxation and is now referred to as the "universal dielectric response"[38]. Early measurements were concerned with the decay of charge in Leydon jars and by 1907 the decays were followed to 200 days[39] before the experimenter (von Schweidler) lost patience. Similar effects are observed for the decay of perturbations in viscoelastic media[40]. Remarkably, the explanations for these phenomena are of the same unsatisfactory nature as those for 1/f noise, that of a distribution of characteristic times (Hopkinson for dielectric relaxation[41] and Boltzman for elasticity[42]). The relation between 1/f noises and power law correlations in geometric shapes (Fractals) is described by Mandelbrot in a recent essay[43].

CORRELATION TIMES

In addition to the spectral density, the time correlations of V(t) may also be characterized by the autocorrelation function $\langle V(t)V(t+\tau)\rangle$. $\langle V(t)V(t+\tau)\rangle$ is a measure of how the fluctuations at times t and $t+\tau$ are related. For a stationary process $\langle V(t)V(t+\tau)\rangle$ is independent of t and depends only on the time difference τ. In this case $S_V(f)$ and $\langle V(t)V(t+\tau)\rangle$ are related by the Wiener-Khintchine relation[44]

$$\langle V(t)V(t+\tau)\rangle = \int_0^\infty S_V(f)\cos(2\pi f\tau)df.$$

Setting $\tau = 0$ in the above equation gives a normalization condition on the fluctuations

$$\langle V^2\rangle = \int_0^\infty S_V(f)df.$$

The mean square fluctuation is just the sum of each of the spectral components. For an exact 1/f spectrum the integral diverges at both low and high frequencies. The high frequency limit presents no problem since real systems are limited in how fast physical processes can occur. Many researchers, however, have sought the low frequency limit to 1/f noise. Although exceptional systems do show such a cutoff most continue as 1/f down to the limit of either the experimenters apparatus or patience. In the case of semiconductor devices the spectral density has been measured down to $10^{-6.3}$ Hz[45]. The Nile river flood levels extend the spectrum to 10^{-10} Hz. The apparent divergence does not, however, imply an anomalous physical process or infinite energy. It merely means that $\langle V^2\rangle$ is not a well defined quantity. For example, in a one dimensional Brownian motion (a very well understood process) the position, x(t), has an exact $1/f^2$ spectral density at low frequencies

One of the major difficulties in understanding 1/f noise is the inability of simple physical models to naturally predict a 1/f spectrum. The reason is that most fluctuating physical processes can be characterized by a correlation time, τ_c. In such a case the autocorrelation function typically takes the form:

$$\langle V(t)V(t+\tau)\rangle = \langle V^2\rangle e^{-|\tau|/\tau_c}$$

and Wiener-Khintchine relation gives a Lorentzian spectral density:

$$S_V(f) = \frac{4\langle V^2\rangle\tau_c}{1+(2\pi\tau_c f)^2}.$$

This spectral density is shown in Fig. 6. For $f >> 1/2\pi\tau_c$ $S_V(f) \propto 1/f^2$ while for $f << 1/2\pi\tau_c$ $S_V(f)$ is independent of f. Thus, a 1/f spectrum cannot come from a process characterized by a correlation time, τ_c. In fact, a 1/f spectrum requires a specific distribution of independent processes with different τ's For such a distribution, $g(\tau)d\tau$,

$$S_V(f) \propto \int \frac{\tau g(\tau)d\tau}{1+(2\pi\tau f)^2}$$

An exact 1/f spectrum requires

$$g(\tau) \propto \frac{1}{\tau}.$$

This superposition of Lorentzian spectra of different τ is valid only if the physical processes at different τ's are independent, otherwise the spectral density is dominated by the smallest τ.

Although the idea that 1/f noise corresponds to such a distribution of τ's can be considered little more than a mathematical identity, it is continually being rediscovered and advanced as the "explanation" of 1/f noise Indeed the first postulation of the distribution of τ's goes back to Bernamont[8] in 1937. The problem remains to find a physical basis for the specific $1/\tau$ distribution

Two approaches seem physically reasonable. A thermally activated process characterized by

$$\tau = \tau_0 e^{E/kT}$$

yields a $1/\tau$ distribution from a uniform distribution in energy E. Such a postulate was advanced independently in 1950 by du Pre[46] and van der Ziel[47]. One might expect then that ther-

mally activated processes would play a dominant role in 1/f noise This does not appear to be the case. Many thermal activation models, such as carrier traps, are not statistically independent Moreover, the thermal activation model predicts a relatively strong temperature dependence (at least $\propto$ T) for the 1/f noise. In practice, however, most systems exhibit little temperature dependence One notable exception is recent work on 1/f noise in continuous metal films where the thermal activation model is once again being resurrected[48].

A second approach involves the assumption that the τ's are determined by quantum mechanical tunneling or overlap of wavefunctions. In this case

$$\tau = \tau_0 e^{x/\lambda},$$

where λ is the characteristic decay length of the wavefunction. Such a model was originally proposed by McWhorter for the trapping times of traps located a distance x from a semiconductor-oxide interface[49]. A uniform distribution of traps in x gives $g(\tau) \propto 1/\tau$. The McWhorter model has remained the most accepted "explanation" of 1/f noise. In particular, it appears to explain the dependence of 1/f noise in field effect transistors (FETs) on surface states. More recent measurements, however, on FETs with lower surface state densities indicate that the 1/f noise is not due to trapping but is an intrinsic property of the conduction along the channel[50].

GENERAL CHARACTERIZATIONS

It is possible to make several generalizations about the behavior of 1/f noise in simple conducting systems One of the most useful characterizations is given by Hooge[51]:

$$\frac{S_V(f)}{V^2} = \frac{2\times10^{-3}}{N_c}\frac{1}{f}.$$

Although this relation has been shown to be incorrect in some cases, it does summarize a large amount of experimental data and give a reasonable estimate of the size of the 1/f noise. The dependence of $S_V(f)$ on N_c^{-1} where N_c is the total number of carriers in the sample demonstrates that 1/f noise is a size effect. Small samples have large amounts of 1/f noise. A large current passing through a small constriction (bad contact) is noisy Semiconductors, with fewer carriers are noisier that metals The fact that $S_V(f) \propto V^2$ suggests that the noise is due to resistance fluctuations as is now generally accepted. The resistance fluctuations appear to be due to mobility fluctuations of the carriers rather than changes in N_c[52]. Moreover, it has been shown that these resistance fluctuations can be a thermal equilibrium property of the system being studied[53]. The current used in measuring the 1/f noise does not generate the fluctuations but only serves as a probe of the resistance changes. The same spectral density for resistance fluctuations is observed both by measuring fluctuations in Johnson noise power (no power dissipated in the sample) and by probing with a current.

Other workers have sought more natural ways of arriving at a 1/f spectrum than the distribution of τ's. One likely candidate is a diffusion process which is typically "slow" and is not characterized by a single τ. Richardson[54] showed, however, that diffusion processes do not, in general, give a 1/f spectrum although power law spectra of the form $1/f^{1/2}$ or $1/f^{3/2}$ are common. More recently Voss and Clarke[55] showed that many of the experimental properties of 1/f noise in metal films could be accounted for by equilibrium temperature fluctuations modulating the resistance. They demonstrated that the decay of a temperature perturbation in a metal film could, in fact, give the logarithmic time dependence of the 1/f noise autocorrelation function. They also showed that certain correlated diffusion mechanisms could theoretically give a 1/f spectrum. Recently, Hooge[56] has modified his relation to account for the fact that only scattering of charge carriers by phonons contributes to the 1/f noise. Although he is unwilling to call this effect temperature fluctuations, he does state that, "the number of phonons fluctuates with a 1/f spectrum." It is also known that a one dimensional diffusion process driven by a single localized white noise source produces a 1/f spectrum at high frequencies. Such a model cannot, however, account for the equilibrium 1/f noise where the sources must be distributed throughout the sample.

Although such attempts at physically characterizing the 1/f noise in specific systems has met with moderate success, the results are not of the universal nature that the ubiquity of 1/f noise seem to beg. Attempts at universal theories have not been successful The inability of linear theories to naturally predict the 1/f spectrum has lead several researchers to postulate general non-linear mechanisms as the origin of 1/f noise[57]. An experimental measurement of statistical non-linearities in several 1/f noise producing systems showed that some (but not all) 1/f noise mechanisms are associated with non-linearities[58]. When a non-linearity was detected it was associated with a non-Gaussian amplitude distribution.

In conclusion, the widespread occurrence of 1/f or flicker noise remains unexplained. It seems almost certain that there is no single physical mechanism for the 1/f noise in so many different systems. One hopes, however, for an underlying mathematical unity more satisfying than the oft-resurrected distribution of τ's.

REFERENCES

1. J. B. Johnson, *Phys. Rev.* 26, 77 (1925).
2. J. B. Johnson, *Phys. Rev.* 32, 97 (1928).
3. H. Nyquist, *Phys. Rev.* 32, 110 (1928).
4. W. Schottky, *Ann. Phys.* 57, 541 (1918).

5. W. Schottky, *Phys Rev* **28**, 74 (1926).
6 A. W. Hull and N H. Williams, *Phys Rev* **25**, 147 (1925).
7 G W Barnes, *J Franklin Inst* **219**, 100 (1935)
8. J Bearnamont, *C R. Acad Sci., Paris* **198**, 1755, 2144 (1934); *Proc. Phys. Soc* **49**, 138 (1937); *Ann. de Phys* 7, 71 (1937)
9 L Brillouin, *Helv phys Acta* 7, 47 (1934).
10 C J. Christensen and G L Pearson, *Bell Sys Tech J* **15** 197 (1936).
11. R. Otto, *Hochfrequenztechnik und Elektroakustik* **45**, 187 (1935).
12 E Meyer and H. Thiede, *Elekt Nach Tech* **12**, 237 (1935)
13 F N. Hooge and A M H Hoppenbrouwers, *Physica* **45**, 386 (1969); J Clarke and R F Voss, *Phys. Rev Lett.* **33**, 24 (1974).
14. H C. Montgomery, *Bell Sys Tech. J.* **31**, 959 (1952)
15. F. N Hooge and A M. H Hoppenbrouwers, *Phys. Lett*, **29A**, 642 (1969).
16. F N. Hooge, *Physica* **83**, 14 (1976)
17 F N. Hooge and J L. Gaal, *Philips Res Rep* **26**, 77 (1971).
18 Th G M. Kleinpenning, *Physica* 77, 78 (1974)
19 A van der Ziel, *Proc. IEEE* **58**, 1178 (1970)
20 S T Hsu, *IEEE Trans Elec Dev* **ED-17**, 496 (1970).
21 T J Boehm, H. R. Bilger, and J. L Tandon, *Proc. Symp on 1/f Fluct.* Tokyo, Japan (1977)
22 T Yajima and L. Esaki, *J. Phys. Soc. Jap* **13**, 1281 (1958)
23 H Higuchi and S. Ochi, *Proc Symp on 1/f Fluct.*, Tokyo, Japan (1977)
24 H Fu and C Sah, *IEEE Trans on Elec Dev.*, **ED-1°**, 273 (1972).
25 J R Clem, *Phys Rev* **B1**, 2140 (1970).
26 J Clarke and G Hawkins, *Phys Rev.* **B14**, 2826 (1976)
27 A good review is found in: D. W Allan, *Proc Symp. on 1/f Fluct* Tokyo, Japan (1977).
28 K L Schick and A A Verveen, *Nature* **251**, 599 (1974)
29 J A Barnes, *et al*, *IEEE Trans. on Instrum and Meas.* **IM-20**, 105 (1971).
30 J A Barnes and D W Allan, *Frequency* **5**, 15 (1967); N Matsunami and K Nakajima, *Proc Symp on 1/f Fluct* Tokyo, Japan (1977).
31 B A Tait, *et al*, *Deep Sea Res* **21**, 403 (1974)
32 T. Musha and H Higuchi, *Jap J Appl Phys* **15**, 1271 (1976).
33. B B Mandelbrot and J. R Wallis, *Water Resour. Res.* **4**, 909 (1968); **5**, 321 (1969).
34 O Toussoun, *Memoires de l'Institut d'Egypt* **8-10**, Cairo (1925).
35 A A. Verveen and H. E Dirkson, *Proc. IEEE* **56**, 906 (1968).
36 B Neumcke, *Biophys Struct Mechanism* **4**, 179 (1978).
37. R. F Voss and J Clarke, *Nature* **258**, 317 (1975), *J Accoust. Soc Am* **63**, 258 (1978). This work is also discussed by Martin Gardner in *Scientific American* April, 1978.
38 A K. Johnscher, *Nature* **267** 673 (1977).
39. E von Schweidler, *Anal d. Physik* **24**, 711 (1907)
40 Early experiments go back to W Weber, *Ann Phys Chem* **34**, 247 (1835). A more recent summary is given by H. Leaderman, *Rhelogy Vol II*, F R. Eirich, ed., Academic Press, New York (1958).
41. J. Hopkinson, *Proc Roy. Soc (London)*, 489, (1876), 549 (1877).
42. L Boltzmann, *Ann. Phys Chem Erg* 7, 624 (1876)
43 B B Mandelbrot, *Fractals: Form, Chance, and Dimension*, Freeman, San Francisco, (1977)
44. A good review is given in. F. Reif, *Fundamentals of Statistical and Thermal Physics*, McGraw-Hill, New York, (1965).
45. M. A Caloyannides, *J. Appl Phys* **45**, 307 (1974).
46 F. K. du Pre, *Phys. Rev.* **78**, 615 (1950).
47. A. van der Ziel, *Physica* **16**, 359 (1950)
48. P. Dutta and P M Horn, *Bull Am Phys. Soc.* **24**, 358 (1979).
49 A L McWhorter, *Semiconductor Surface Physics*, R H Kingston, ed., Univ. Penn Press, Philadelphia, 207 (1957).
50 R F. Voss, *Proc. Symp. on 1/f Fluct* Tokyo, Japan, 132 (1977)
51. F. N Hooge, *Phys Lett.* **29A**, 139 (1969)
52 F N. Hooge, *Physica* **60**, 130 (1972)
53 R F Voss and J. Clarke, *Phys Rev Lett* **36**, 42 (1976)
54. J M Richardson, *Bell Sys Tech J* **29**, 117 (1950)
55 R F Voss and J Clarke, *Phys Rev* **B13**, 556 (1976).
56 F N Hooge and L K J Vandamme, *Phys Lett* **66A**, 315 (1978)
57. S Putterman, *Phys Rev. Lett* **39**, 585 (1977) and S Teitler and M F M Osborne, *Phys. Rev Lett* **27**, 912 (1971)
58 R F Voss, *Phys Rev Lett* **40**, 913 (1978)

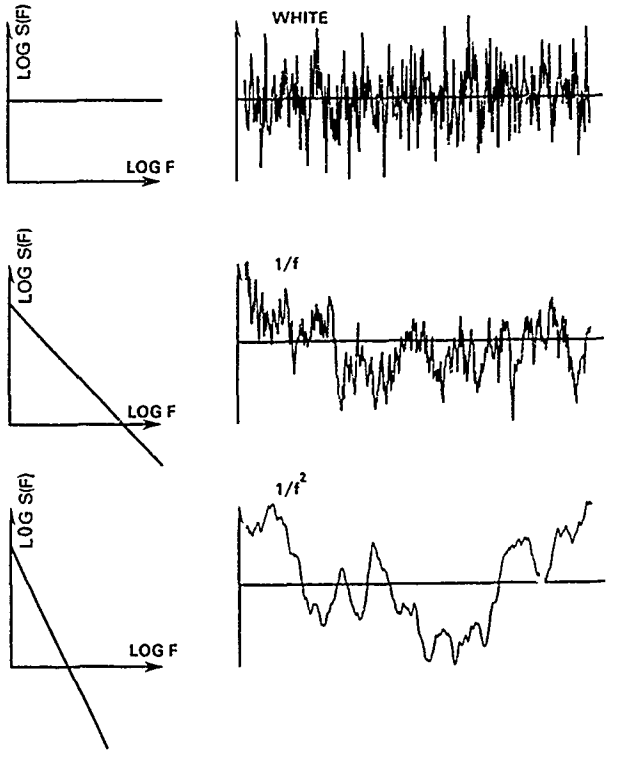

Figure 1. Samples of common noises and their spectra.

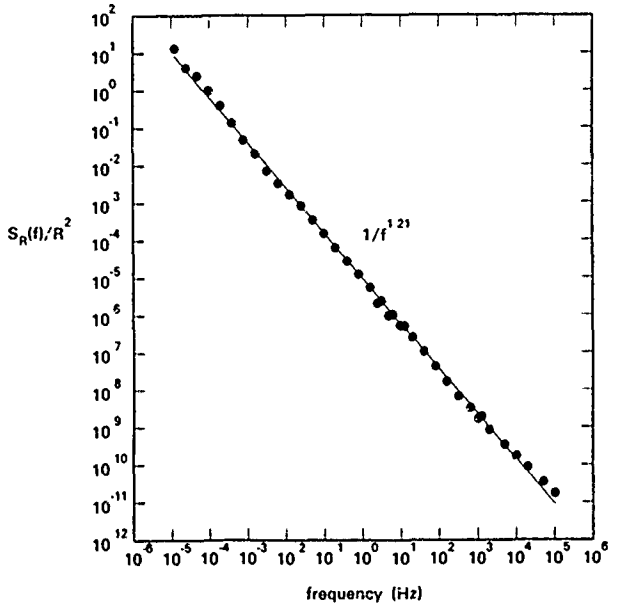

Figure 2. Relative resistance fluctuation spectrum, $S_R(F)/R^2$, for a 56K India ink resistor. The spectrum is fit to $1/f^{1.21}$ over 10 decades.

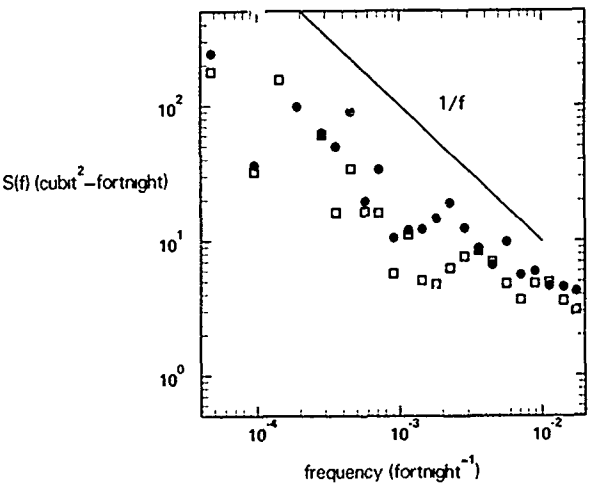

Figure 3. Spectral density of Nile river flood levels as recorded by the ancient Egyptians.

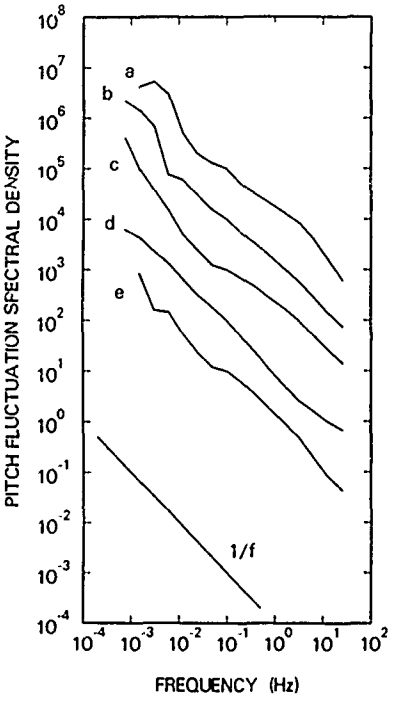

Figure 4. Pitch fluctuations from different musical cultures:

a) the Ba-Benzele Pygmies

b) traditional music of Japan

c) classical ragas of India

d) folk songs of old Russia

e) American blues

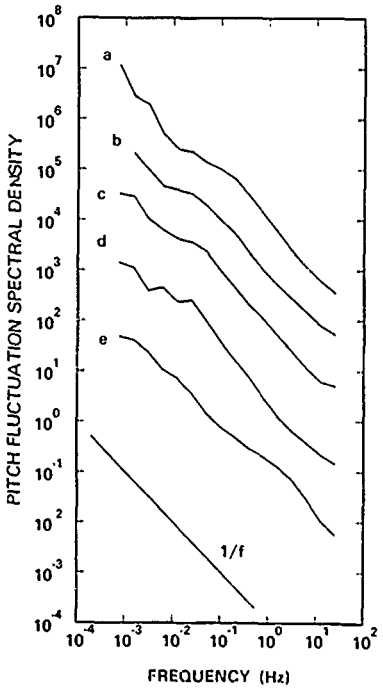

Figure 5. Pitch fluctuations in western music:

a) Medieval music up to 1300

b) Beethoven, 3rd Symphony

c) Debussey, piano works

d) R. Strauss, ein Heldenlebe

e) the Beatles, Sgt. Pepper

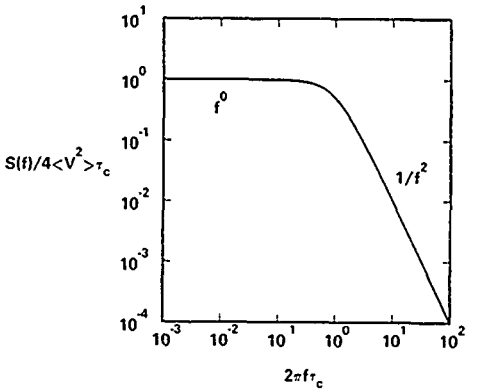

Figure 6. Spectral density, $S_V(f)$ for a process characterized by a correlation time, τ_c.

THE DOMESTIC AND INTERNATIONAL USE OF THE RADIO SPECTRUM

Donald M. Jansky

National Telecommunications and
Information administration

This paper will address the policy structure and organizations by which the radio frequency spectrum is managed and utilized in the United States. These mechanisms will be illustrated through a description of activities taking place to prepare for the 1979 World Administrative Radio Conference (WARC-79). Particular emphasis on allocation proposals associated with the scientific and engineering management will be discussed.

The electromagnetic spectrum has served man for over 50 years. This paper describes the domestic and international use which has evolved to effectively manage the availability of spectrum to provide continued services. Figure 1 depicts the evolution of use. The modern era began at the Atlantic City Radio Conference 1947 - giving form to the modern structure of international radio regulations. Figure 2 illustrates the numerous propagation modes for radio signals; and Figure 3 the kind of services now being performed throughout the spectrum. Starting from two services, there are now over 40.

The International Telecommunication Union (ITU) was born over 100 years ago; now has 154 member nations (Figure 4). It is a one-nation-one-vote organization, providing international structure for coordination/regulation of the spectrum.

Its structure is indicated in Figure 5. The most important parts are WARC's since they are treaty conferences for modification of the Radio Regulations. The principle technical body is the CCIR (Figure 6). The present WARC '79 will be described later. U.S. policy in the ITU is established by NTIA, FCC, and State (Figure 7). These organizations are focal points of policy because of their domestic responsibilities.

Domestic policy and structure of spectrum management derives from the Communications Act of 1934 (Figure 8). FCC has no formal spectrum management structure. The basic functions of allocation, licensing and assignment are dispersed among the several bureaus and is carried out under the Administrative Procedures Act.

Executive Branch policy and management is carried out in NTIA (Figure 9). Its predecessors have been a Presidential Special Assistant (Truman); OCDM (Eisenhower); OTM (Johnson); and OTP (Nixon). Its overall functions are shown in the referenced figure.

It is assisted by IRAC, which is the oldest Federal advisory committee (Figure 10). It represents the largest Federal users of spectrum; has liaison representation from the FCC. The chairman and all subcommittees are provided by NTIA. Basic spectrum policy is recommended here.

The basic functions of national spectrum management are shown in Figure 11. These are accomplished in NTIA by an organization indicated in Figure 12, with assistance from many government agencies.

Basic frequency authorizing is in accordance with rules and regulations of the NTIA manual, which is modified three times annually upon recommendations of IRAC. There are 4-6,000 assignment actions monthly overseen by the Frequency Assignment Subcommittee. The process for obtaining a frequency assignment is Figure 13; distribution of users is Figure 14.

Preliminary to authorizing, major systems must pass system review. The purpose is to show that:

- o the new systems will work;
- o it won't hurt others; and
- o will husband spectrum.

The review procedure is intended to prevent what happened to TDRSS (Figures 15 and 16). Today, the procedure permits the authorizing of JTIDS in bands used by safety of life services (Figure 17).

Internationally major coordination is carried out with respect to earth stations and satellite networks in accordance with provisions of Articles 9A, 7, Appendices 1A, 1B, 28 and 29 of the radio regulations. These regulations have been incorporated into NTIA and FCC rules and regulations. Figure 18 illustrates earth station coordination.

The domestic and international radio conference structures merge in the context of a World Administrative Radio Conference. The preparatory process structure is Figure 19. After over three years, eight Notices of Inquiry, hundreds of committee meetings, the U.S. sent forth to Geneva, this year, 300+ pages of proposals. The structure of the conference is in Figures 20 and 21. The U.S. has proposed new allocations in many services. To be successful the U.S. must take into account the needs of other countries. To this end, discussions have been held with countries in Figure 22.

Spectrum management is a never-ending process of coordination and accommodation seeking ways to serve man through radio--Figure 23.

FIGURE 1

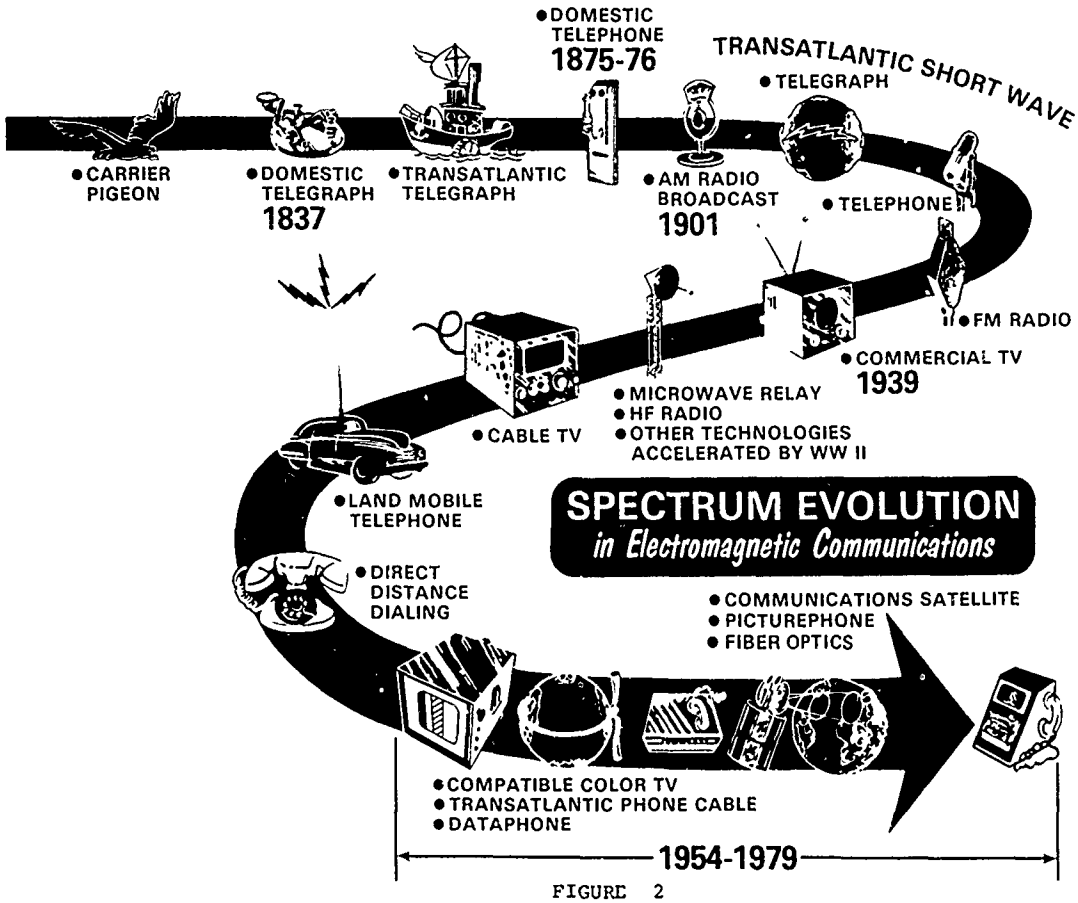

FIGURE 2

TELECOMMUNICATION PROPAGATION MODES

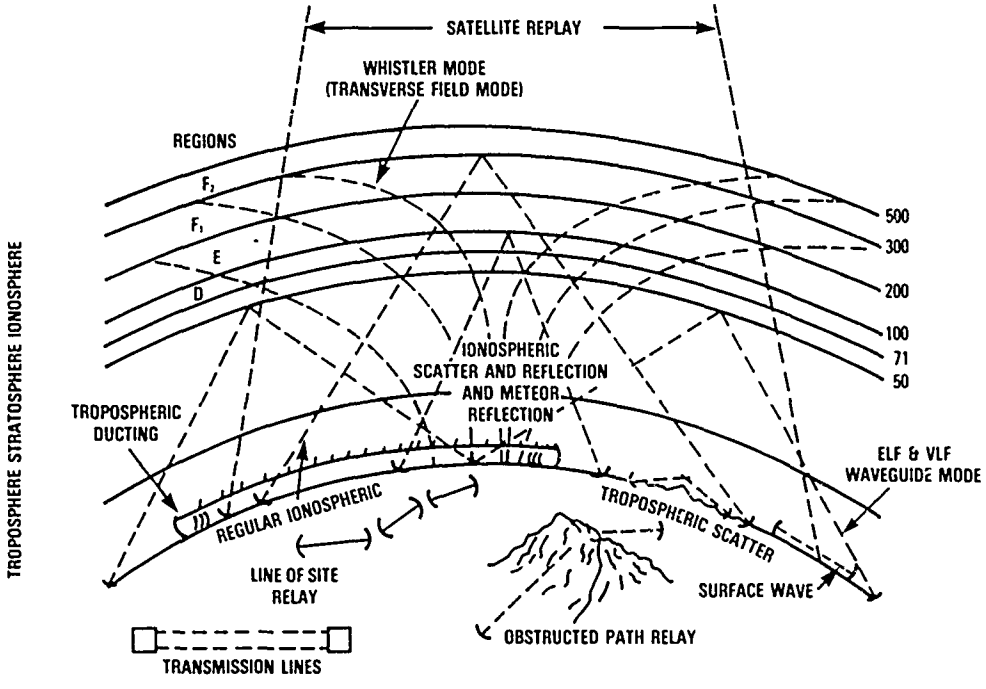

FIGURE 3

Typical Uses of Radiofrequency Bands

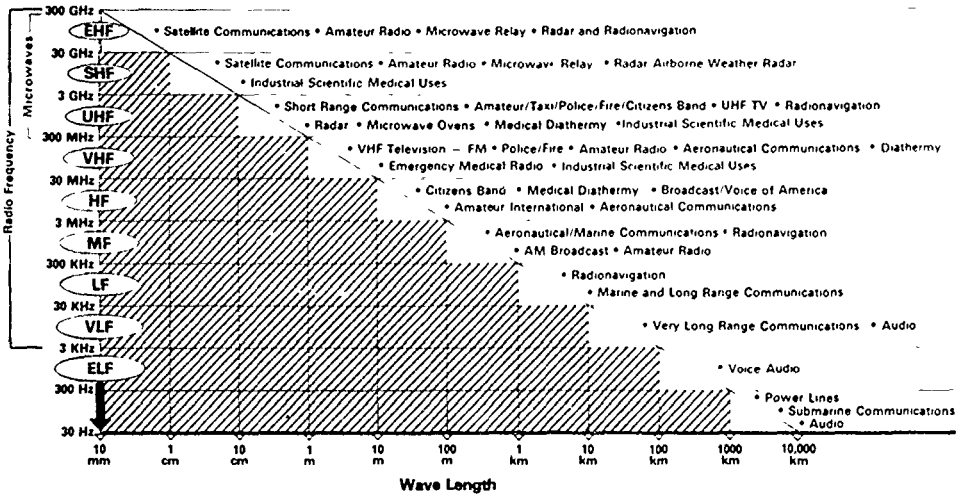

FIGURE 4

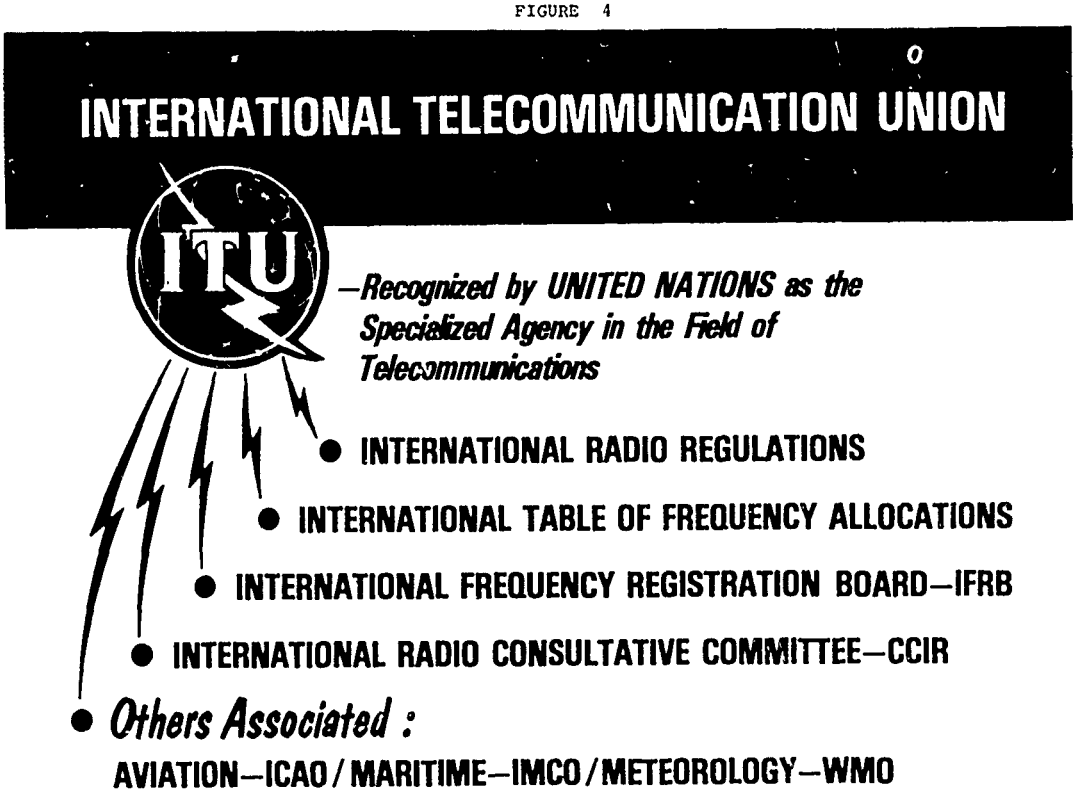

FIGURE 5

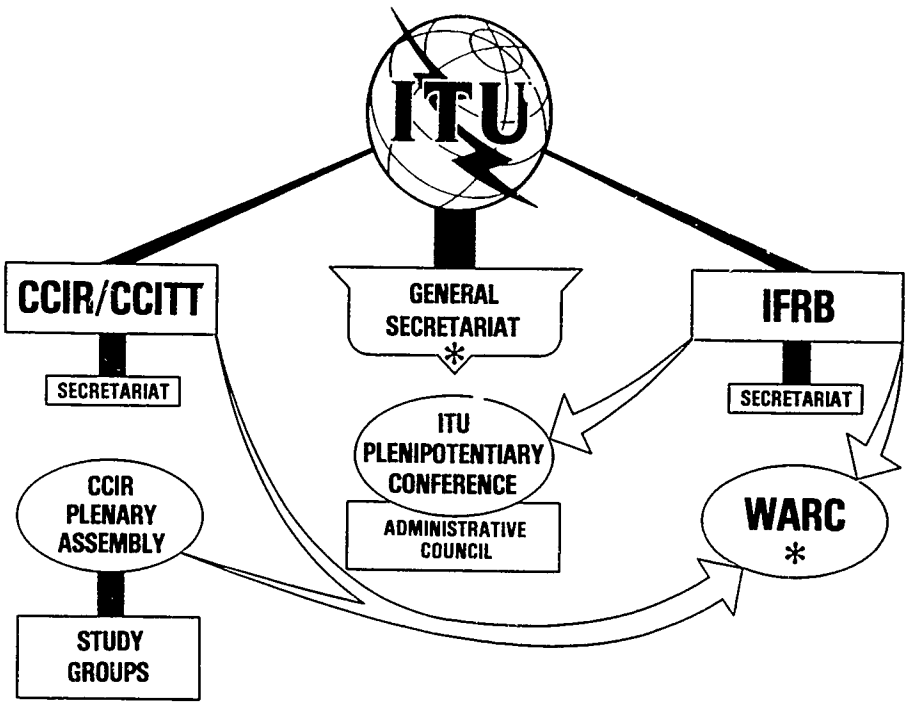

* Processes National Proposals to/from the World Administrative Radio Conference.

FIGURE 6

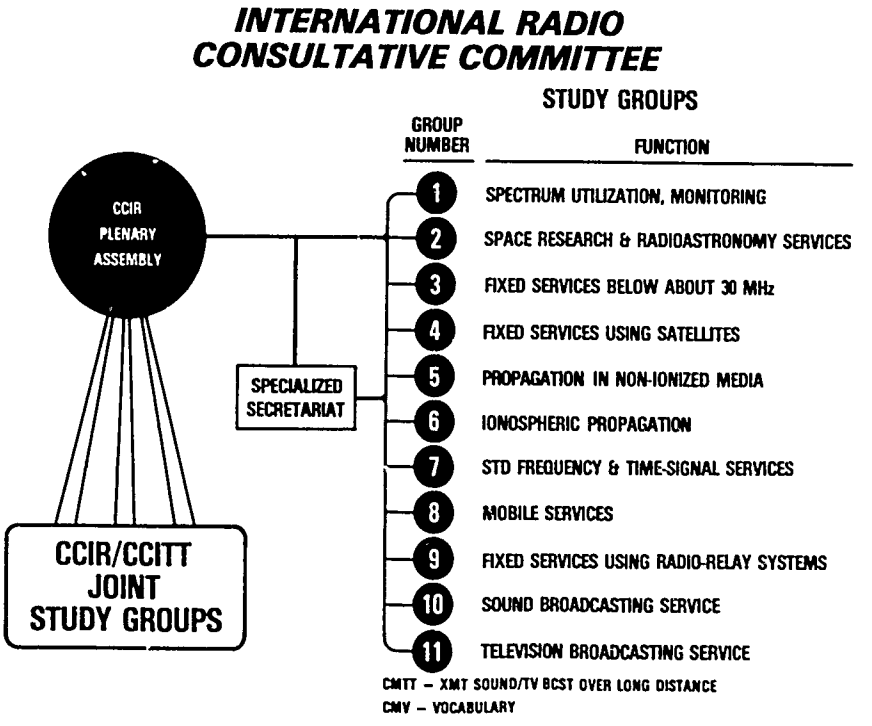

FIGURE 7

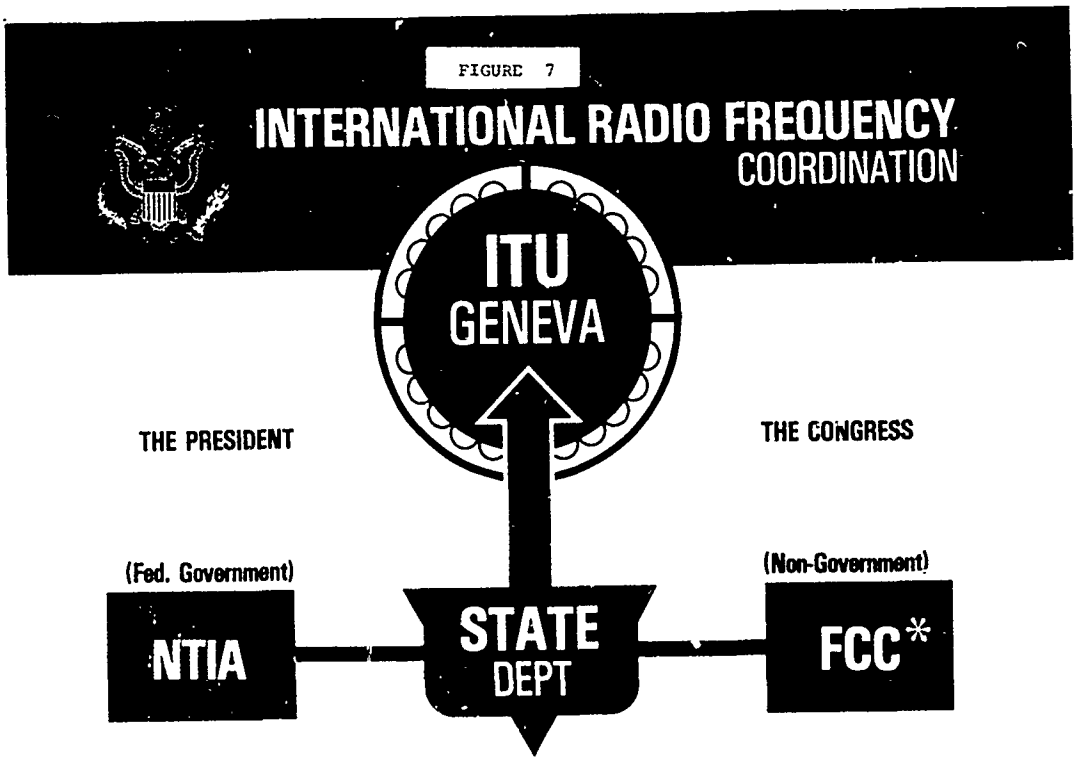

* Processes National Frequency Notification & Registration Actions to/from the IFRB-ITU.

FIGURE 8

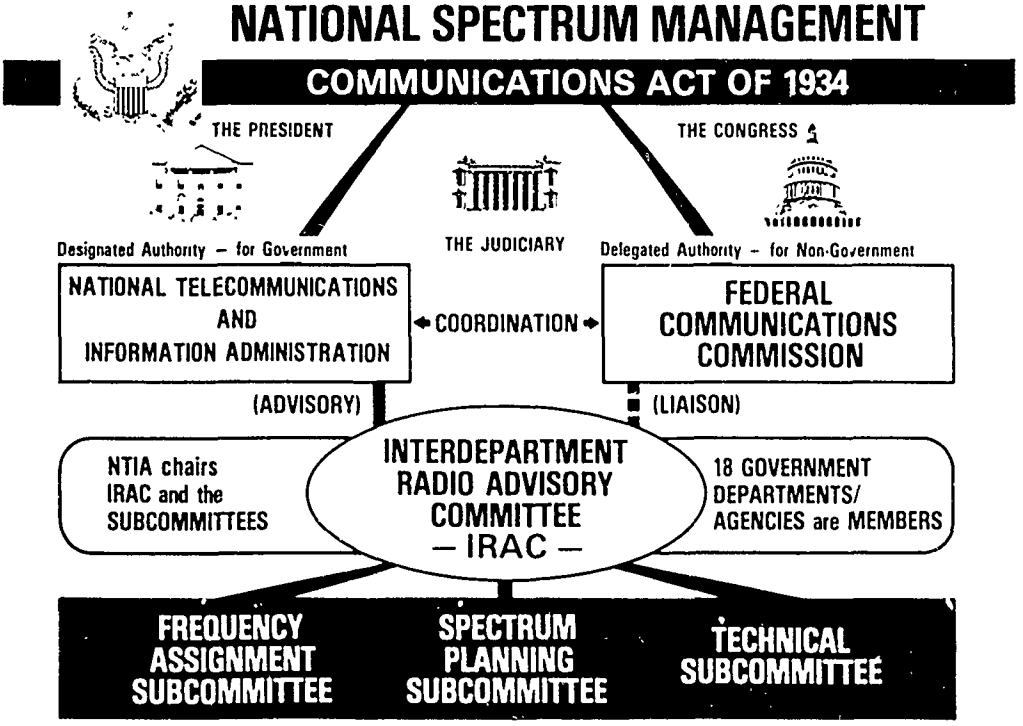

FIGURE 9

NTIA FUNCTIONS AS THE PRESIDENT'S PRINCIPAL ADVISOR ON TELECOMMUNICATIONS POLICY

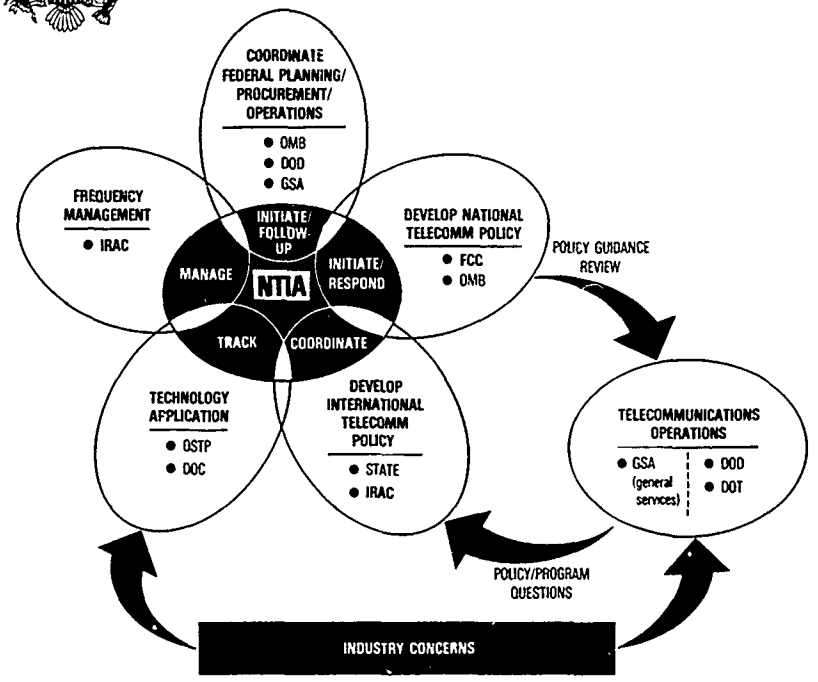

FIGURE 10

INTERDEPARTMENT RADIO ADVISORY COMMITTEE

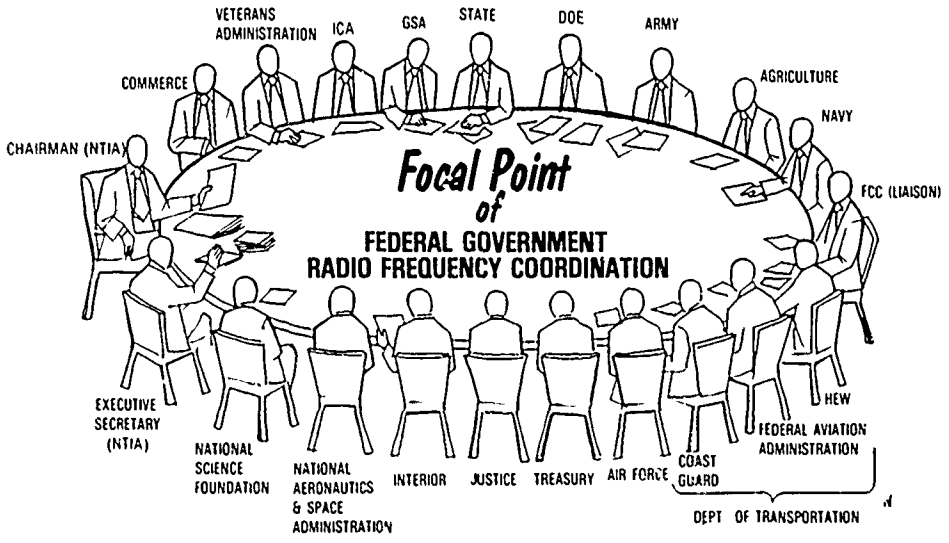

FIGURE 11

COORDINATED FEDERAL GOVERNMENT
SPECTRUM MANAGEMENT

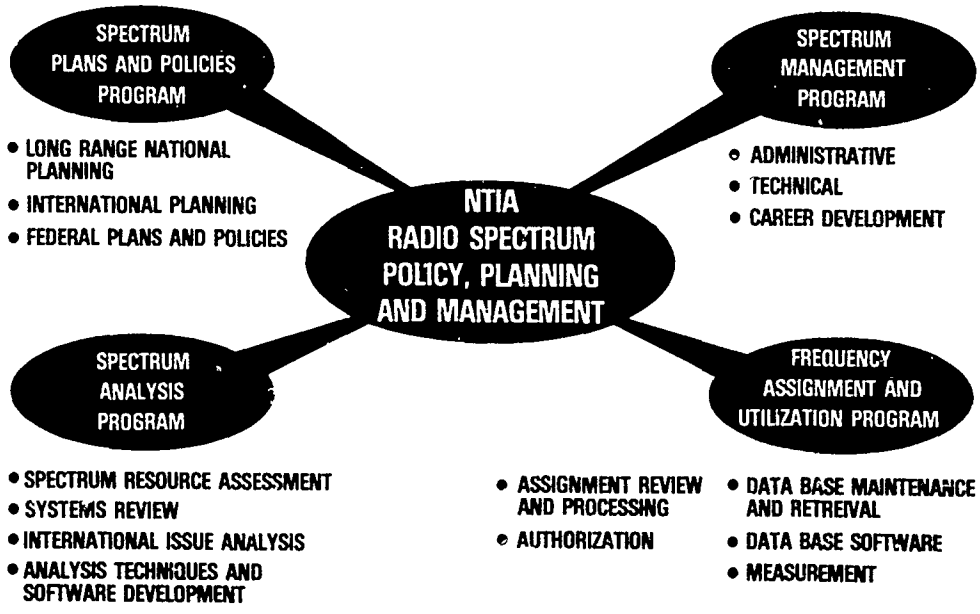

FIGURE 12

NATIONAL TELECOMMUNICATIONS AND INFORMATION ADMINISTRATION

FEDERAL SYSTEMS AND SPECTRUM MANAGEMENT

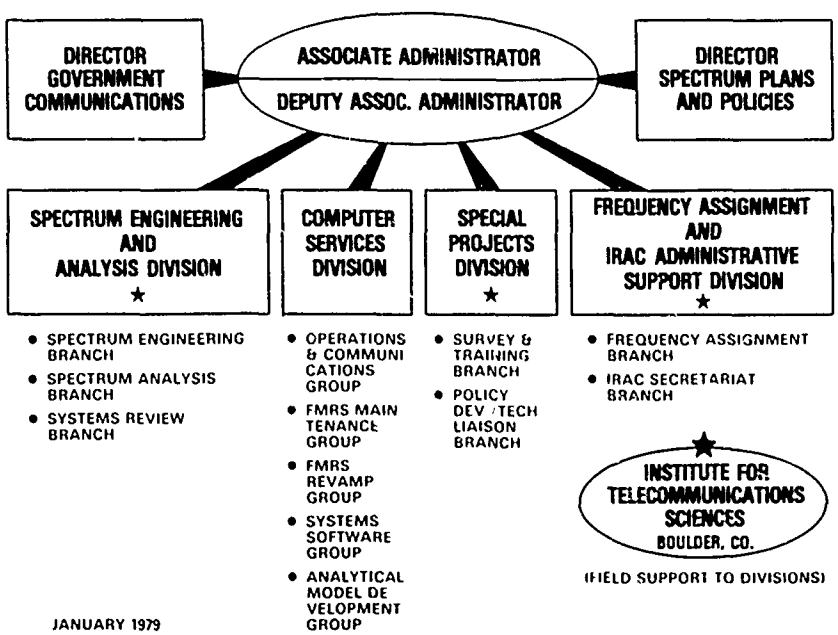

JANUARY 1979

FIGURE 13

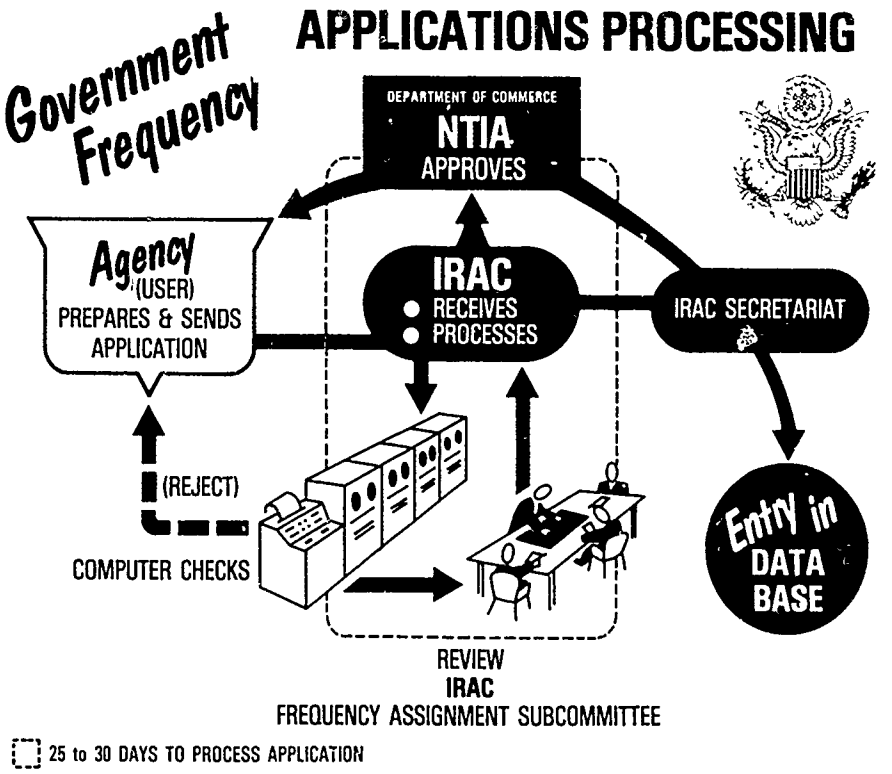

FIGURE 14

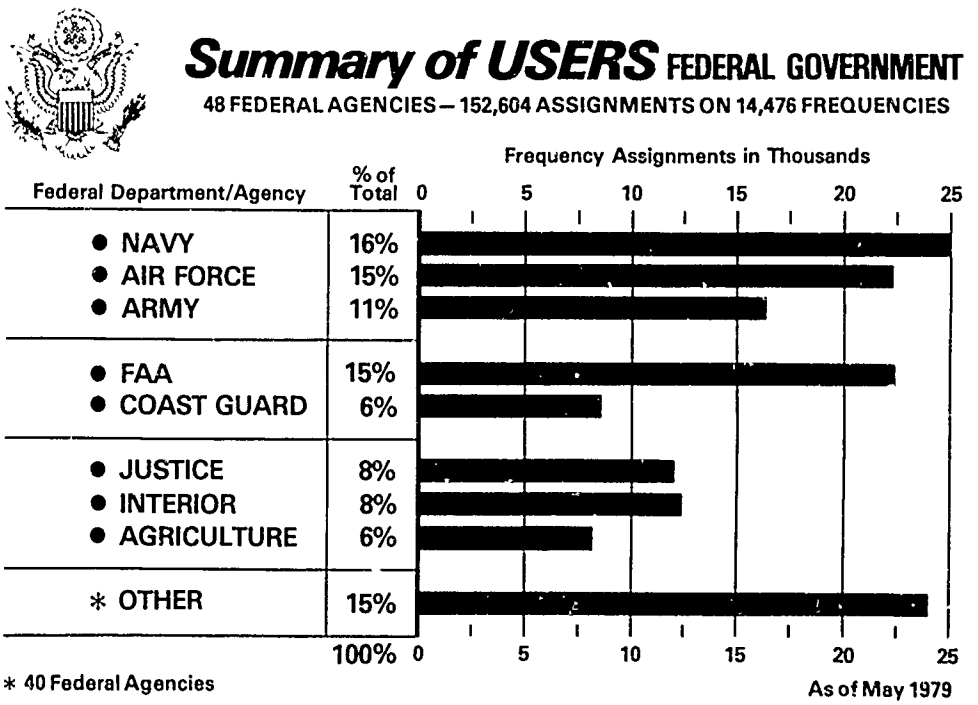

FIGURE 15

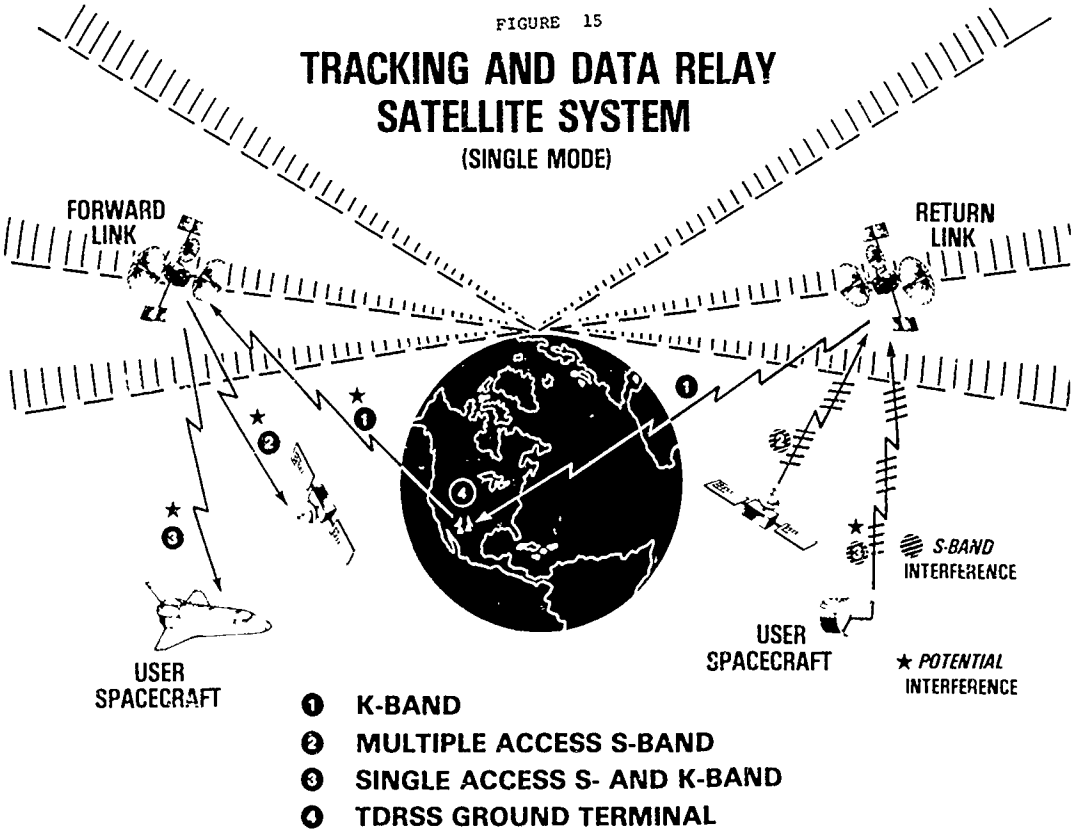
TRACKING AND DATA RELAY SATELLITE SYSTEM
(SINGLE MODE)
FORWARD LINK
RETURN LINK
USER SPACECRAFT
USER SPACECRAFT
S-BAND INTERFERENCE
★ POTENTIAL INTERFERENCE
❶ K-BAND
❷ MULTIPLE ACCESS S-BAND
❸ SINGLE ACCESS S- AND K-BAND
❹ TDRSS GROUND TERMINAL

FIGURE 16

A $100-Million Mistake: Radar Would 'Jam' Satellites

By Thomas O'Toole
Washington Post Staff Writer

The National Aeronautics and Space Administration, which had planned to launch two giant satellites in 1980 to communicate with all of its other orbiting craft, has belatedly discovered that because of interference from Russian radar in Europe the satellites will not work.

The space agency is now redesigning the satellites' electronic systems, the engineering model of which had already been built. It now expects the launch to be delayed at least three months and the extra cost to amount to $100 million.

The tracking and data relay satellite is a giant orbiting transmitter and receiver whose two umbrella-like antennas weigh 50 pounds apiece and unfurl in space to a diameter of 185 feet. The satellites are being built to replace 60 percent of the antennas NASA uses on earth at an estimated saving of more than $100 million a year.

NASA's plans call for an eventual total of six of the 5,000-pound satellites, and it awarded a $386 million contract to Western Union to build and operate them.

The electronic interference, which is not deliberate but comes from routine activities of the large Soviet radar installations that ring Eastern Europe, was not identified as a problem until last December, well after the contract had been awarded.

"The people involved did not fully understand the environment and the effects it would have on the system," said C. Curtis Johnson, tracking and data relay satellite project manager at Goddard Space Flight Center. "Otherwise, we would have been more careful in the specifications of the system."

The first satellite was scheduled to be carried into orbit in July 1980 by the space shuttle. The three-month delay is important because NASA wants the satellite to be communicating with the shuttle as shuttle flights increase in 1981. And tracking station contracts NASA has with other countries will be expiring about that time.

White House and Capitol Hill sources said that part of the reason for the belated discovery of the problem is that Pentagon and the Central Intelligence Agency never alerted NASA to the size and scope of the radio interference caused by Soviet radars in the high orbit regions to be occupied by the tracking and data relay satellites.

Sources said this is one reason the White House two weeks ago set up a policy review committee of 16 federal agencies to make sure space project chiefs were fully aware of all the issues that might have an impact on them.

The Senate committees are looking into the reasons for the sudden cost increase in the NASA satellite pro-

See SATELLITE, A7, Col. 1

The Washington Post

Satellite Error To Cost the U.S. $100 Million

SATELLITE, From A1

gram. They are the Select Committee on Intelligence and the Commerce Committee, whose subcommittee on science and space is chaired by Sen. Adlai E. Stevenson (D-Ill.).

According to the way the Interference has been described by NASA to Congress, the giant Soviet radars from the Baltic to the Black Sea transmit beams that converge high over the Atlantic and Pacific at precisely the same locations NASA wants to put its tracking and data relay satellites.

These are spots 22,400 miles above the earth in what are called geosynchronous orbits, meaning the satellites move around the earth at the same speed the earth rotates. This keeps the satellites "hovering" over the same spot on earth all the time.

NASA could relocate the satellites but they would be in slots any place else. What NASA wants the satellites to do is provide complete radio cover with its orbiting space shuttle and 30 other satellites that are orbiting the earth at lower altitudes.

The tracking satellite is being built to replace obsolete and expensive ground antennas on Ascension Island in the South Atlantic, Quito, Ecuador; Santiago, Chile, and Guam, and it will replace other antennas in Alaska, North Carolina and Bermuda.

The satellite will be a great improvement. It will allow controllers on the ground to "talk" to other satellites and the astronauts in the space shuttle during more than 90 percent of each orbit of the earth. As things are now, satellites in low orbit are out of touch with the ground 40 percent of the time.

What must be redesigned to accommodate the radar interference are the integrated electronic circuits built into the satellite to "process" the endless signals from other satellites in lower orbits. The satellite is designed to accept 300 million "bits" of information every second, the equivalent of 6,200 encyclopedias.

"What we're redesigning are the electronics that unmix all those signals and sort them out before sending them to the ground," Johnson said.

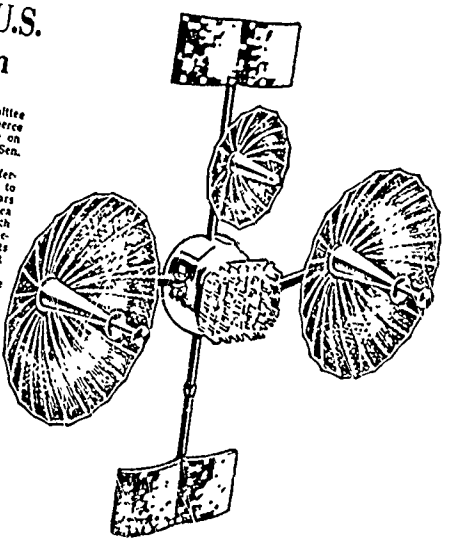

Rendering of tracking and data relay satellite national space agency is building

"That amounts to 20 percent of the hardware on this satellite."

The way the electronics were originally designed they would be overwhelmed by the Soviet radar signals, at least in part because the electronics would be unable to "lock onto" the Russian radar in time to sort it out of the other signals the satellite was receiving.

The space agency estimates the redesign to harden the electronics against the Soviet radar will cost in the tens of millions of dollars. Capitol Hill sources say the expense will be "at least $100 million."

The contract to build six of the satellites is held by Western Union, which sublet the work to TRW Inc., Harris Electronics Corp. and Watkins-Johnson Co. in Palo Alto, Calif., where most of the electronics design was done.

The $386 million contract signed by NASA with Western Union is a fixed price contract, meaning that whatever extra costs are incurred in the redesign of the electronics and the spacecraft must be renegotiated.

NASA is considering reducing the number of spacecraft its ordered from six to four. One of the six was to be a spare in orbit and another was to be "ready" for launch in case one of the in-orbit satellites failed.

Eliminating two production satellites would save $100 million, the estimated cost of the redesign.

FIGURE 17

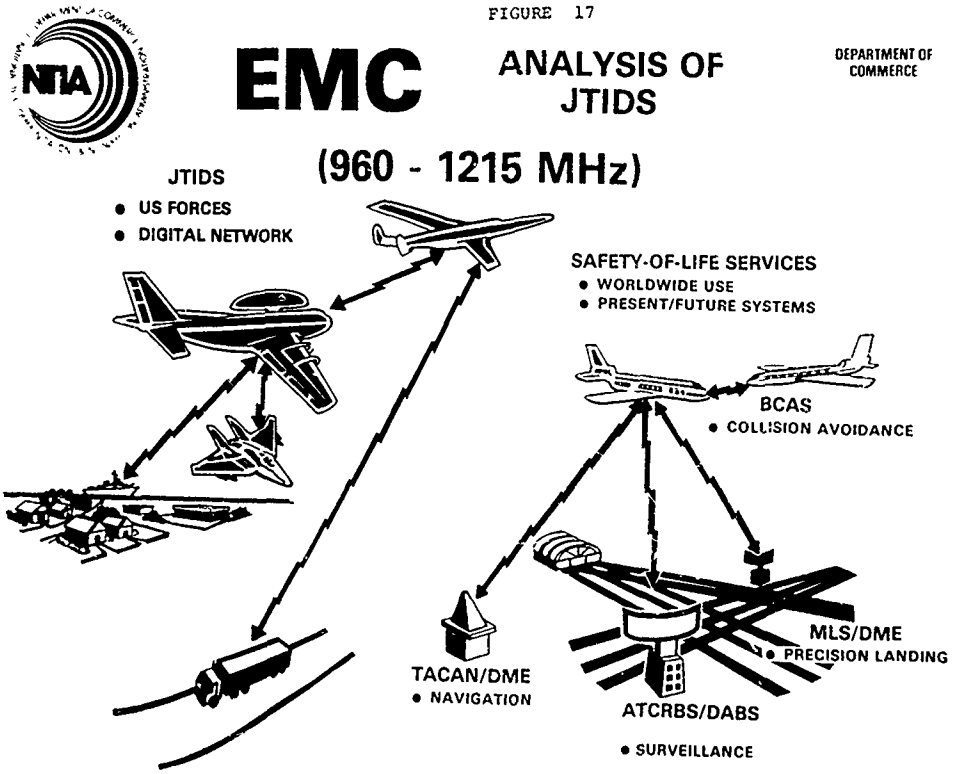

FIGURE 18

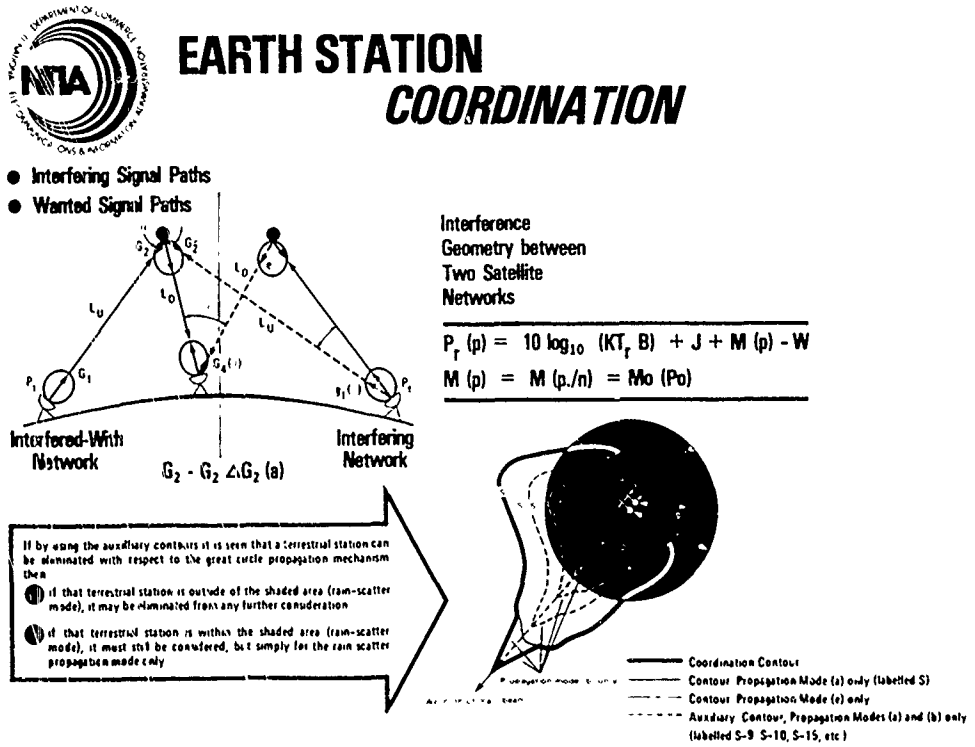

FIGURE 19

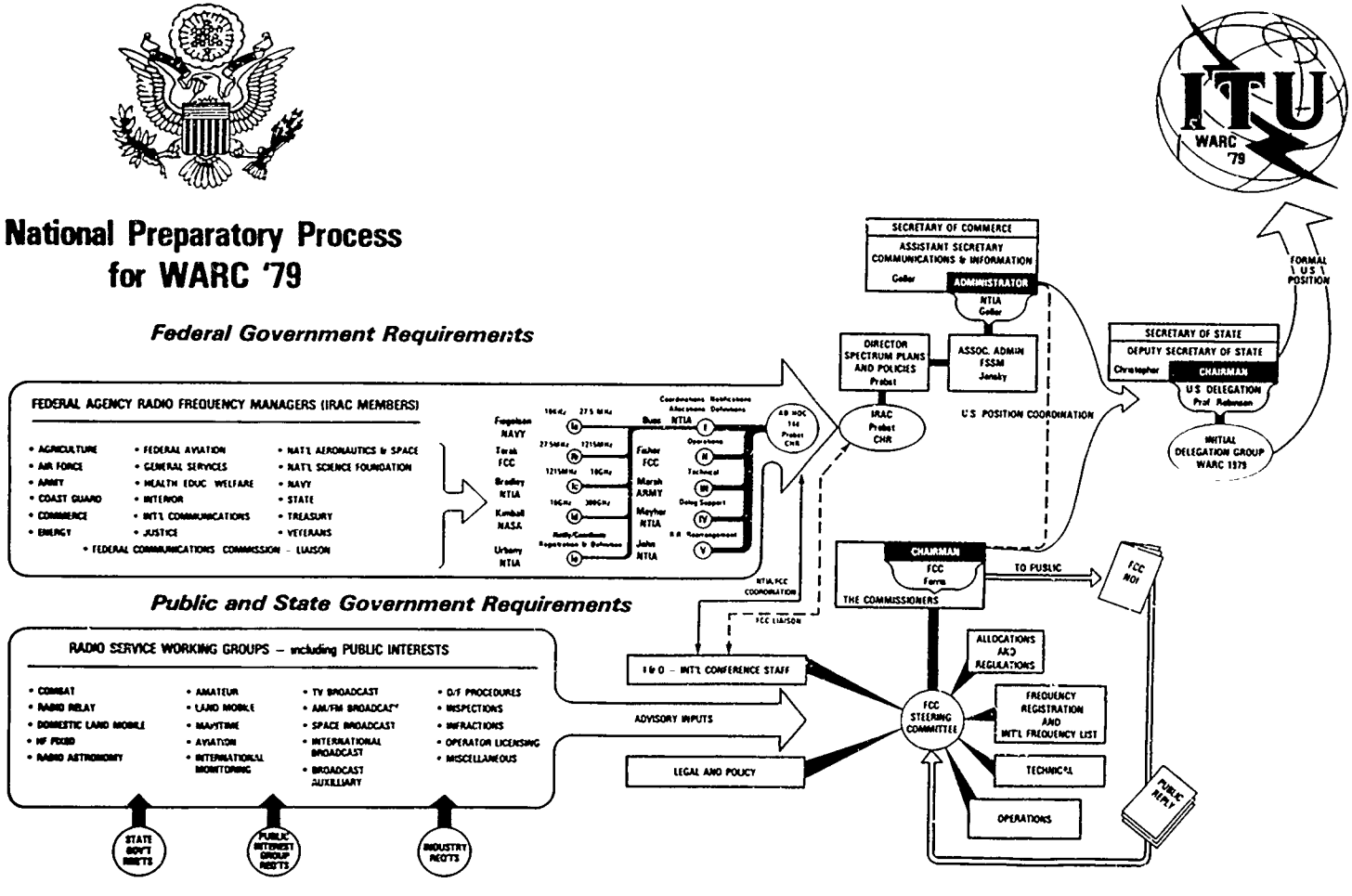
National Preparatory Process
for WARC '79
ITU
WARC '79
Federal Government Requirements
FEDERAL AGENCY RADIO FREQUENCY MANAGERS (IRAC MEMBERS)
• AGRICULTURE
• AIR FORCE
• ARMY
• COAST GUARD
• COMMERCE
• ENERGY
• FEDERAL AVIATION
• GENERAL SERVICES
• HEALTH EDUC WELFARE
• INTERIOR
• INT'L COMMUNICATIONS
• JUSTICE
• NAT'L AERONAUTICS & SPACE
• NAT'L SCIENCE FOUNDATION
• NAVY
• STATE
• TREASURY
• VETERANS
• FEDERAL COMMUNICATIONS COMMISSION – LIAISON
Fogelson NAVY
Tarsk FCC
Bradley NTIA
Kimball NASA
Urbany NTIA
Fisher FCC
Marsh ARMY
Meyher NTIA
John NTIA
Bass NTIA
Operations
Technical
Doing Support
R.R. Rearrangement
SECRETARY OF COMMERCE
ASSISTANT SECRETARY COMMUNICATIONS & INFORMATION
Geller
ADMINISTRATOR
NTIA
Geller
DIRECTOR SPECTRUM PLANS AND POLICIES
Probst
ASSOC. ADMIN FSSM
Jansky
IRAC
Probst
CHR
U.S. POSITION COORDINATION
SECRETARY OF STATE
DEPUTY SECRETARY OF STATE
Christopher
CHAIRMAN
U.S. DELEGATION
Prof Robinson
INITIAL DELEGATION GROUP WARC 1979
FORMAL U.S. POSITION
Public and State Government Requirements
RADIO SERVICE WORKING GROUPS – including PUBLIC INTERESTS
• COMBAT
• RADIO RELAY
• DOMESTIC LAND MOBILE
• HF FIXED
• RADIO ASTRONOMY
• AMATEUR
• LAND MOBILE
• MARITIME
• AVIATION
• INTERNATIONAL MONITORING
• TV BROADCAST
• AM/FM BROADCAST
• SPACE BROADCAST
• INTERNATIONAL BROADCAST
• BROADCAST AUXILLIARY
• O/F PROCEDURES
• INSPECTIONS
• INFRACTIONS
• OPERATOR LICENSING
• MISCELLANEOUS
STATE GOVT INPUTS
PUBLIC INTEREST GROUP INPUTS
INDUSTRY INPUTS
ADVISORY INPUTS
I & O – INT'L CONFERENCE STAFF
LEGAL AND POLICY
NTIA/FCC COORDINATION
FCC LIAISON
CHAIRMAN
FCC
Ferris
THE COMMISSIONERS
TO PUBLIC
FCC NOI
FCC STEERING COMMITTEE
ALLOCATIONS AND REGULATIONS
FREQUENCY REGISTRATION AND INT'L FREQUENCY LIST
TECHNICAL
OPERATIONS
PUBLIC INPUT

FIGURE 20

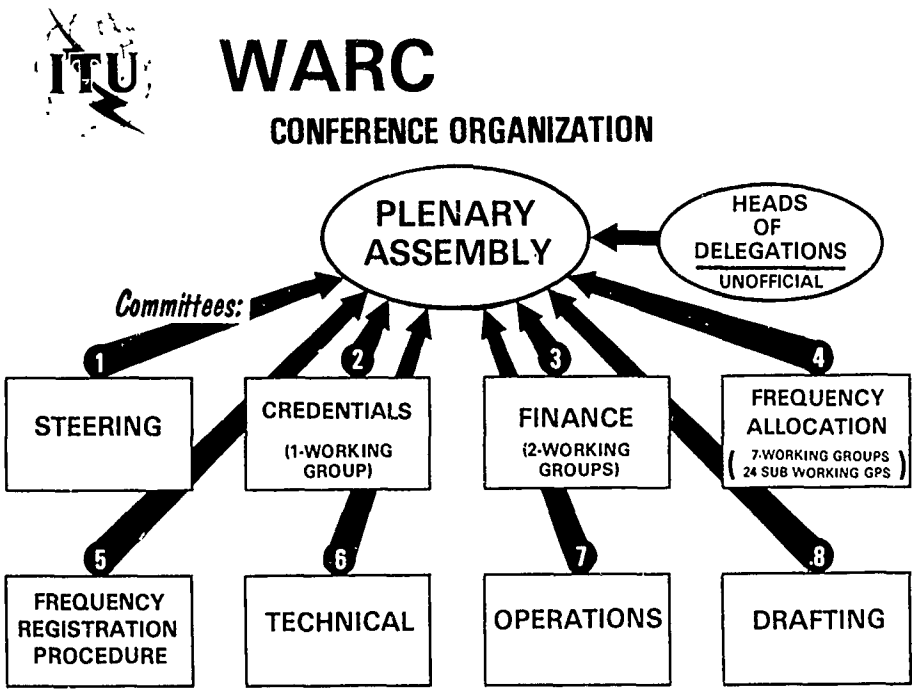

FIGURE 21

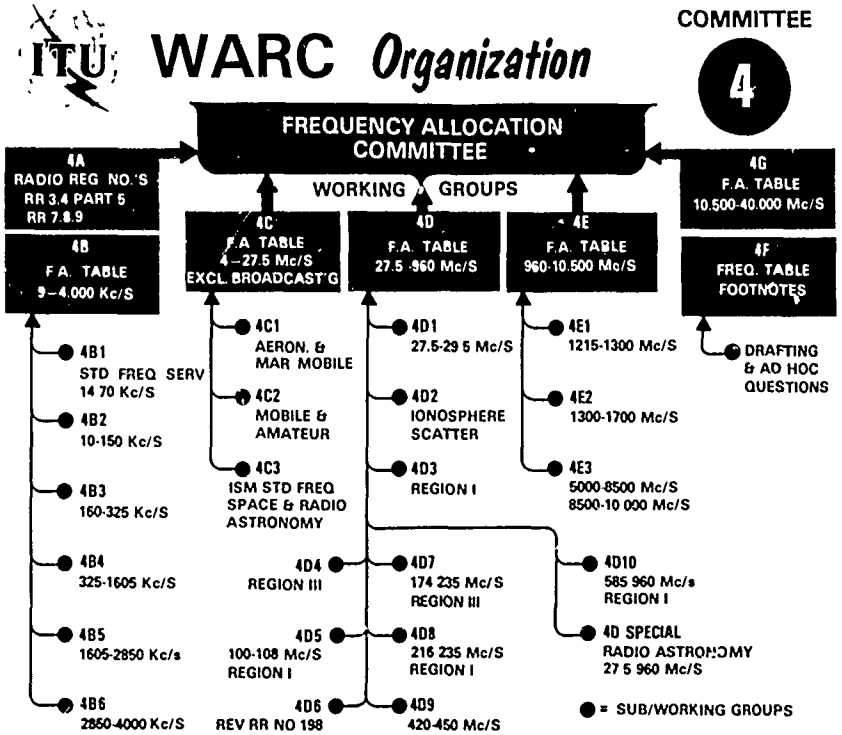

FIGURE 22

WARC-'79
International COORDINATION

CATALYST – TECHNICAL EXCHANGE – FAMILIARITY

REGION I	CAMEROON	IVORY COAST	SUDAN
	DENMARK	KENYA	SWEDEN
	EGYPT	LIBERIA	SWITZERLAND
	FRANCE	MOROCCO	TURKEY
	GERMANY (FRG)	NETHERLANDS	UNITED KINGDOM
	GHANA	NIGERIA	USSR
	GREECE	NORWAY	ZAIRE
	ISRAEL	SAUDI ARABIA	
	ITALY	SENEGAL	
REGION II	ARGENTINA	COLOMBIA	URUGUAY
	BRAZIL	MEXICO	VENEZUELA
	CANADA	PANAMA	
	CHILE	PERU	
REGION III	AUSTRALIA	IRAN	PAKISTAN
	CHINA	JAPAN	PHILIPPINES
	INDIA	KOREA	SINGAPORE
	INDONESIA	NEW ZEALAND	

- THREE NATO JOINT CIVIL/MILITARY MEETINGS
- CEPT COUNTRIES MEETING
- THREE ITU REGIONAL SEMINARS
- ITU - SPEC. PREPARATORY MEETING
- CITEL MEETING

FIGURE 23

RADIO FREQUENCY MANAGEMENT IS DONE BY EXPERTS WHO MELD YEARS OF EXPERIENCE WITH A CURIOUS BLEND OF REGULATIONS, ELECTRONICS, POLITICS AND NOT A LITTLE BIT OF LARCENY. THEY JUSTIFY REQUIREMENTS, HORSE-TRADE, COERCE, BLUFF AND GAMBLE WITH AN INTUITION THAT CANNOT BE TAUGHT OTHER THAN BY LONG EXPERIENCE.

VICE ADMIRAL JON L. BOYES
U.S. NAVY

RADIATION EFFECTS IN BERLINITE

L. E. Halliburton
Physics Department, Oklahoma State University
Stillwater, Oklahoma, 74074

L. A. Kappers
Physics Department, University of Connecticut
Storrs, Connecticut, 06268

and

A. F. Armington and J. Larkin
Rome Air Development Center (RADC/ET)
Hanscom AFB, Massachusetts, 01731

Summary

Electron spin resonance (ESR), electron-nuclear double resonance (ENDOR), and optical absorption have been used to investigate radiation effects in synthetic crystals of berlinite. Crystals from seeded and unseeded growth were included in the study and impurities in both types of samples were determined by emission spectrographic techniques. The presence of significant concentrations of Fe^{3+} ions was verified by ESR measurements, and the relative amount of random strain in each crystal was determined from the Fe^{3+} spin resonance spectrum. When the berlinite samples were irradiated at 300 K with 1.7 MeV electrons, six distinct hole-like centers were created. The ESR spectrum of one of these centers, labeled B-1, could only be observed at temperatures below 30 K because of line-broadening due to rapid motional effects. The other five centers, B-2 through B-6, also showed motional effects but could be observed with ESR at 77 K. At room temperature the ESR signals from the six centers were broadened beyond recognition. Thermal anneal studies revealed the centers decay in two groups; centers B-1 through B-4 decay near 425 K while B-5 and B-6 decay at 550 K. All six centers exhibited a hyperfine interaction with a 100% abundant I = 1/2 nucleus. The irradiation induced a light orange coloration in the crystals and optical absorption spectra revealed a band at 520 nm along with additional absorption in the ultraviolet region. When the samples were irradiated at 77 K, two additional defects were produced which are not stable at room temperature. One of these centers is identified as atomic hydrogen stabilized at an interstitial site in the c-axis channel. The hydrogen atom thermally decays near 125 K. The second center, labeled B-7, is hole-like and slowly decays as the temperature is increased from 100 K to 300 K.

Introduction

In recent years, berlinite ($AlPO_4$) has been suggested to be an excellent candidate for use as a surface acoustic wave (SAW) substrate material.[1-4] It has been shown to have temperature-compensated cuts and has piezoelectric coupling coefficients greater than ST quartz. However, berlinite occurs only rarely in nature and, moreover, has proved difficult to synthesize in the form of large high-quality crystals.[5] Thus, before this material can be successfully incorporated into SAW-device technology, these problems of large-scale crystal growth must be resolved.

Evaluation of the quality of grown crystals, both from the macroscopic and microscopic viewpoints, is an important source of information to be used in selecting optimum material preparation and growth techniques. Macroscopic evaluation (i.e., characterization of extended defects such as voids, cracks, surface damage, inclusions, etc.) provides, of course, the most valuable and easily obtained information about crystal quality in the initial stages of a crystal growth project. As the quality of the crystals improves, the need increases for microscopic evaluation (i.e., characterization of the number and nature of isolated point defects) to provide further information on which to base improvements in growing techniques.

The most direct microscopic evaluation technique is elemental impurity analysis. However, it is often advantageous to know the valence state and local environment of the various impurities as well, and this latter information can usually be obtained from optical and magnetic resonance techniques. Another dimension is added to the microscopic evaluation process when ionizing radiation is considered. In many cases, radiation will change the charge state of an existing defect or will trap an electron or hole adjacent to an existing defect and, thus, make the defect "visible" in subsequent spectroscopic measurements. In magnetic resonance experiments, for example, superhyperfine interactions which result from an adjacent unpaired electron may allow diamagnetic impurities to be directly observed.

With the goal of helping to determine the optimum growth conditions, we have begun a research program designed to investigate the fundamental properties of point defects in single crystal

$AlPO_4$, including those defects and impurities present in the as-grown crystals as well as defects introduced by radiation. In the present paper, we compare the microscopic defect behavior of berlinite samples grown by two different techniques. The major impurities have been identified by emission spectrographic techniques; while electron spin resonance (ESR), electron-nuclear double resonance (ENDOR), and optical absorption have been used to further characterize the paramagnetic impurities and radiation-induced defects. The temperature dependence of the radiation effects has been monitored and models for the defects are discussed.

Samples

Berlinite has the same crystal structure as quartz, the difference being half the silicons are replaced by aluminum and half by phosphorus. As further evidence of their similarities, the $\alpha \leftrightarrow \beta$ phase change occurs at 581°C for berlinite and at 573°C for quartz. Berlinite has a single three-fold axis, and three separate two-fold axes lying in the basal plane. There are four oxygens around each cation and each oxygen links an aluminum and a phosphorus ion. The oxygen-cation separations are divided into short and long bond lengths; 1.7327 Å and 1.7452 Å for the oxygen-aluminum bonds and 1.5124 Å and 1.5394 Å for the oxygen-phosphorus bonds.[6] The aluminum-oxygen-phosphorus bond angles are 142.6° and 142.9° at room temperature.

Single crystals of berlinite used in the present study were obtained from the Naval Weapons Center (located at China Lake, California) and from Airtron (located at Morristown, New Jersey). Starting materials for the Naval Weapons Center samples were hydrated alumina, $Al(OH)_3$, and phosphoric acid. The resulting solution was sealed in a pyrex ampoule and the crystals grew as the temperature was slowly increased from 145°C to 180°C at a 0.5°C per day rate. No seed was used for the Naval Weapons Center samples. In the case of the Airtron samples, the starting material was produced by reacting concentrated phosphoric acid with $Al(OH)_3$ in an autoclave at increasing elevated temperature, the final temperature being approximately 200°C. The Airtron samples were then grown from seeds in a standard pressure autoclave using a temperature gradient. In this latter technique, it was noted that faster crystal growth occurred in the 170-200°C range.

A sample from the Naval Weapons Center and one from Airtron were chemically analyzed using emission spectrographic techniques and the results are shown in Table I. Both samples contained significant amounts of transition-metal ions as well as calcium and magnesium.

Experimental

The ESR spectrometer used in this work consisted of a home-built homodyne microwave bridge and a 9-inch Fieldial-regulated Varian magnet. The magnetic field modulation frequency was 100 kHz. An NMR proton probe and microwave frequency counter were used to measure the g_c and A_c values. The ESR spectrometer was modified for ENDOR operation by adding an HP 8601A sweep generator and a Nicolet 1073 signal averager.

TABLE I. Impurity analysis in ppm atomic.

	AIRTRON	NAVAL WEAPONS CENTER
Calcium	10	10
Copper	20	10
Chromium	30	--
Iron	100	200
Gallium	40	80
Magnesium	80	30
Manganese	30	80
Nickel	20	40
Titanium	10	50

All the irradiations of ESR samples were 4 minutes in duration and used 1.7 MeV electrons from a Van de Graaff accelerator. The current on the sample was approximately 0.2 $\mu A/cm^2$. Each ESR sample was 3 x 3 x 5 mm^3 in size and, during a 77 K irradiation, was immersed directly in liquid nitrogen. Following an irradiation, the ESR sample was either returned to, or kept at, 77 K and placed in a spring-loaded Delrin sample holder. The sample and holder were transferred into a liquid nitrogen-filled finger Dewar which, in turn, was inserted in a Varian V-4531 rectangular microwave cavity. When ESR spectra were obtained below 77 K, an Air Products Heli-Tran LTD-3-110 variable temperature system was used instead of the finger Dewar. A Varian V-4557 variable temperature accessory was used for the thermal anneal studies between 77 K and room temperature. For each step of the anneals above room temperature, the sample was removed from the microwave cavity and heated in a separate furnace.

Optical absorption data were taken at room temperature and at 77 K using a Cary 14R spectrophotometer. Both x-rays (15 mA, 50 kV) and 1.7 MeV electrons were separately used for defect production in the optical studies. The samples were mounted on a cold-finger of an optical cryostat and measurements were taken with light polarized perpendicularly to the c-axis.

Results and Discussion

Prior to any irradiation, a prominent electron spin resonance spectrum was found in both the Naval Weapons Center sample and the Airtron sample. At 77 K with the magnetic field parallel to the c-axis, this X-band spectrum consists of a series of lines of varying intensity extending from 1000 gauss to near 9000 gauss and has been attributed to isolated Fe^{3+} ions located at substitutional sites.[7,8] The Fe^{3+} spectrum from each of the two samples is shown in Fig. 1; the ESR spectrometer was operated with identical settings in both cases to allow direct comparison. The $-1/2 \leftrightarrow +1/2$ transition, which occurs near 1575 gauss, is insensitive to random strain within the crystal and, thus, provides a measure of the relative concentration of Fe^{3+} in the two samples. The data in Fig. 1 suggest the

Naval Weapons Center sample contains a factor of 1.6 more iron than the Airtron sample and, thus, lends support to the emission spectrographic analysis summarized in Table I, where the Naval Weapons Center sample was estimated to contain a factor of two more iron than the Airtron sample.

Even more importantly, the random strain within the crystal can be determined directly from the Fe^{3+} spectrum. The 3/2 ↔ 5/2 type transition, occurring near 8620 gauss, is the most sensitive to random strain, and by comparing linewidths of the 3/2 ↔ 5/2 transition and the -1/2 ↔ +1/2 transition, a relative measure of the random strain within the crystal is obtained. Changes in linewidth are easily detected as changes in intensity and examination of the spectra in Fig. 1 yields 0.15 and 0.34 for the intensity ratio of the two previously mentioned transitions for the Airtron and the Naval Weapons Center samples, respectively. In a crystal having no detectable strain this intensity ratio[9] becomes 0.56. Thus, our data show a significant increase in strain for the Airtron sample as compared to the Naval Weapons Center sample; a result in agreement with expectation for seeded versus non-seeded crystal growth.

The optical absorption spectrum of an unirradiated Naval Weapons Center sample is shown in Fig. 2a. The sample is transparent throughout the visible region but shows a broad absorption peaking at 5.7 eV. This ultraviolet band may be due to transition-metal impurities such as Fe^{3+} or oxygen-vacancy-related defects. When this same sample is exposed to x-rays for 15 hours at room temperature, additional absorption bands appear near 2.4, 4.0, and 5.9 eV as illustrated in Fig. 2b. These radiation-induced bands give the crystal a light orange coloration. Further irradiation with 1.7 MeV electrons (4 minutes, 0.2 $\mu A/cm^2$) at room temperature greatly enhances the absorption throughout the visible and ultraviolet as shown in Fig. 2c.

Additional information concerning the structure of the radiation-induced defects in $AlPO_4$ can be obtained from analysis of their ESR spectra. Electron irradiation of an Airtron sample at 77 K gives rise to the ESR spectrum shown in Fig. 3 when the magnetic field is parallel to the c-axis. In addition to the Fe^{3+} lines discussed earlier, a widely split pair of lines labeled E' as well as a set of very intense lines near g = 2.0 are observed. The lines labeled E' have a c-axis splitting of 4350 gauss, exhibit only a small angular dependence, and are thought to arise from an unpaired electron interacting with a 100% abundant I = 1/2 nucleus. From such a large splitting, one can infer the hyperfine interaction is with a phosphorus nucleus and that the unpaired electron is strongly localized on the phosphorus.[10] From analogy with quartz, we believe the model for this defect consists of an oxygen vacancy with an unpaired electron trapped in an sp^3 hybrid orbital of the adjacent phosphorus. This proposed model is illustrated in Fig. 4.

The intense lines observed near g = 2.0 following electron irradiation at 77 K are shown on an expanded scale in Fig. 5. The data presented in Fig. 5 was obtained from a Naval Weapons Center sample and the Airtron sample gave nearly identical results. Two distinct doublets are observable and neither show any angular dependence. The outer doublet is split by 508.3 gauss; a value very characteristic of hydrogen atoms. The analogous spectrum in quartz has been assigned to interstitial hydrogen atoms located in the c-axis channels[11] and we believe a similar model applies in berlinite. The doublet with the smaller splitting in Fig. 5 is labeled the B-7 center. (The symbol B is taken from the word berlinite.) The g_c value for the B-7 center is 2.0106, thus making it hole-like, and the c-axis splitting is 34.0 gauss. The relatively large linewidth of the B-7 center suggests the presence of considerable unresolved hyperfine effects.

In Fig. 6, the spin resonance spectrum obtained after 77 K irradiationis compared with that obtained after 300 K irradiation. Both traces were taken at 77 K. The dominant spectrum very near the g = 2.0 region following a 77 K irradiation is the B-7 doublet as shown in the top trace. In the lower trace, after a 300 K irradiation, the B-7 center is not seen; but instead, a series of other doublets appear with the most prominent being labeled B-2, B-3 and B-4. The latter three centers all have hole-like g shifts and similar doublet splittings, varying between 36 and 39 gauss. Table II contains the c-axis g values and c-axis splittings, g_c and A_c, for all the B-type centers observed in the present investigation.

TABLE II. The c-axis g values and c-axis hyperfine splittings for the radiation-induced B centers.

Center	g_c	A_c(gauss)
B-1	2.0618	35.3
B-2	2.0422	38.8
B-3	2.0276	36.6
B-4	2.0104	38.0
B-5	2.0134	8.3
B-6	2.0093	9.0
B-7	2.0106	34.0

The three doublets, B-2, B-3 and B-4, were distinguished by their different line-broadening characteristics. Following a 300 K irradiation of a Naval Weapons Center sample, ESR spectra were measured at 90 K and 45 K as shown in Fig. 7. At 90 K, the B-4 center predominates while the other centers are broadened nearly beyond recognition At 45 K, both the B-2 and the B-4 centers are easily seen but the B-3 center is reduced in relative intensity when compared to the 77 K spectrum shown in the lower portion of Fig. 6. When spectra of this same crystal were taken at 38 K and 15 K a new doublet, labeled B-1 in Fig. 8, becomes observable. The B-1 doublet is only partially resolved at 38 K, but has narrowed and completely dominates the spectrum at 15 K. Because of the large intensity of the B-1 center at 15 K, the spectrometer gain was reduced by a factor of 50 in the lower trace of Fig. 8. At 77 K, the B-1 center is broadened beyond recognition and thus, its presence cannot be determined by electron spin resonance at

this temperature even though it is one of the dominate defects in the crystal.

The c-axis splitting of the B-1 center, given in Table II, is very similar to that of the B-2, B-3, B-4, and B-7 centers. In order to verify that this splitting was a hyperfine effect and to identify the specific nucleus involved, an electron-nuclear double resonance (ENDOR) experiment was performed. At 5 K, the B-1 center was sufficiently saturated by microwave power to obtain the ENDOR spectrum shown in Fig. 9. Two ENDOR lines, separated by 12.0 MHz, were observed when the magnitude of the magnetic field was 3241 gauss and the direction was parallel to the c axis. A splitting of 11.2 MHz is predicted for the free phosphorus nucleus and higher order corrections in the spin Hamiltonian bring the predicted value into agreement with the observed value. The only other reasonable candidate for the nucleus was hydrogen, but its ENDOR splitting would have been 27.6 MHz.

These ENDOR results clearly identify phosphorus as the nucleus giving rise to the resolved hyperfine splitting in the ESR spectrum of the B-1 center and, by inference, in the spectra of the B-2, B-3, B-4, and B-7 centers. We suggest that these B centers may be variations of a basic defect consisting of a hole trapped in a non-bonding oxygen p orbital. This hole would be stabilized within the lattice by an unidentified entity replacing the adjacent aluminum ion. On the other side of the hole, there would be the normal phosphorus ion to give the observed hyperfine splittings. The lack of observable hyperfine interaction with an aluminum nucleus, at least in the case of the B-1, B-2, B-3, and B-4 centers, also supports the belief that the adjacent aluminum ion has been replaced. This proposed model for these B centers is illustrated in Fig. 10. Each B center would most likely have a different stabilizing entity, but at this time their identities are unknown.

Two additional B-type centers are resolved by annealing a sample to 475 K for 5 minutes following a room temperature irradiation. The ESR spectra taken before and after the high temperature anneal are shown in Fig. 11. These two remaining overlapping doublets are labeled B-5 and B-6 and their g_c and A_c parameters are given in Table II. The fact that there are actually two overlapping doublets left after the 475 K anneal was verified by taking additional data at 20 GHz where the two doublets are easily distinguished from each other. Since the c-axis splitting for the B-5 and B-6 centers is approximately 4 times smaller, it is not clear that the model proposed for the other B centers would be valid for the B-5 and B-6 centers.

The thermal stabilities of the various radiation-induced defects in $AlPO_4$ are summarized in Fig. 12. Only the hydrogen atom H^o and the B-7 center were produced by the initial irradiation at 77 K. The hydrogen atom decayed near 125 K while the B-7 center slowly decays over the 100 to 300 K temperature range. However, if the sample is irradiated at room temperature, then the B-1 through B-6 group of centers are created. The decay of these centers occurs in two distinct temperature regions. The B-1, B-2, B-3 and B-4 centers all decay near 425 K. In addition to having the same decay temperature, these four centers also have nearly the same c-axis hyperfine splittings of approximately 35 to 38 gauss. On the other hand, the B-5 and B-6 centers both decay near 550 K and have about the same c-axis splittings of 9 gauss.

This work was supported in part by the U. S. Air Force under contract F19628-77-C-0171 and by NSF Grant DMR77-08465.

References

1. Z. P. Chang and G. R. Barsch, "Elastic Constants and Thernal Expansion of Berlinite," IEEE Trans. on Sonics and Ultrasonics, SU-23, 127, 1976.

2. R. M. O'Connell and P. H. Carr, "High Piezoelectric Coupling, Temperature Compensated Cuts of Berlinite, $AlPO_4$, for SAW Applications," IEEE Trans. on Sonics and Ultrasonics SU-24, 376, 1977.

3. R. M. O'Connell and P. H. Carr, "Progress in Closing the Lithium Niobate - ST Cut Quartz Piezoelectric Coupling Gap," Proc. of the 32nd Annual Symp. on Frequency Control, p. 189, 1978.

4. D. G. Morency, W. Soluch, J. F. Vetelino, S. D. Mittleman, D. Harmon, S. Surek, J. C. Field, and G. Lehmann, "Experimental Measurement of the SAW Properties of Berlinite," Appl. Phys. Lett., 33, 117, 1978.

5. E. D. Kolb and R. A. Laudise, "Hydrothermal Synthesis of Aluminum Orthophosphate," J. Crystal Growth, 43, 313, 1978.

6. Von D. Schwarzenbach, "Verfeinerung der Struktur der Tiefquarz-Modifikation von $AlPO_4$," Zeitschrift für Kristallographie, 123, 161, 1966.

7. U. Krauss and G. Lehmann, "EPR of Fe^{3+} in Low Quartz Isomorphs $A(III)B(V)O_4$," Z. Naturforsch. Teil A, 30, 28, 1975.

8. R. Lang, C. Calvo, and W. R. Datars, "Phase Transformation in $AlPO_4$ and Quartz Studied by Electron Paramagnetic Resonance of Fe^{3+}," Can. J. Phys., 55, 1613, 1977.

9. J. E. Wertz and J. R. Bolton, "Electron Spin Resonance; Elementary Theory and Practical Applications," (McGraw-Hill, New York, 1972).

10. G. D. Watkins, "Electron Paramagnetic Resonance of Point Defects in Solids, with Emphasis on Semiconductors," in "Point Defects in Solids" edited by J. H. Crawford and L. M. Slifkin, Vol. 2, Chapter 4, (Plenum Press, New York, 1975).

11. R. A. Weeks and M. M. Abraham, "Electron Spin Resonance of Irradiated Quartz: Atomic Hydrogen," J. Chem. Phys., 42, 68, 1965.

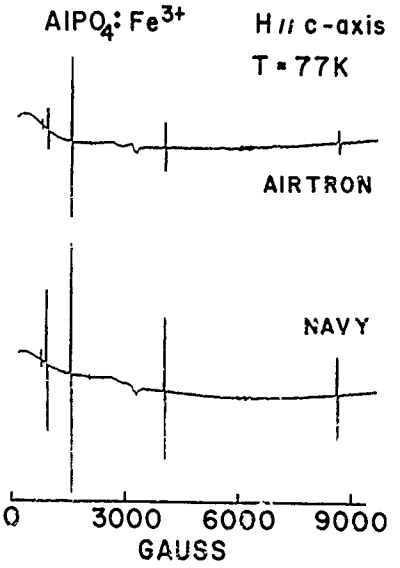

Figure 1.

ESR spectrum of Fe^{3+} in two different berlinite crystals.

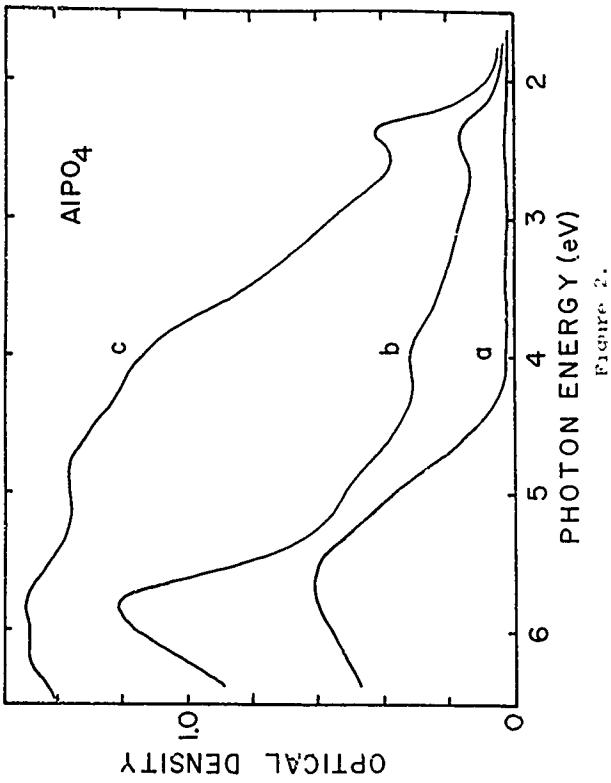

Figure 2.

Optical absorption of a Naval weapons Center sample (a) before irradiation, (b) after x-irradiation, and (c) after additional electron irradiation.

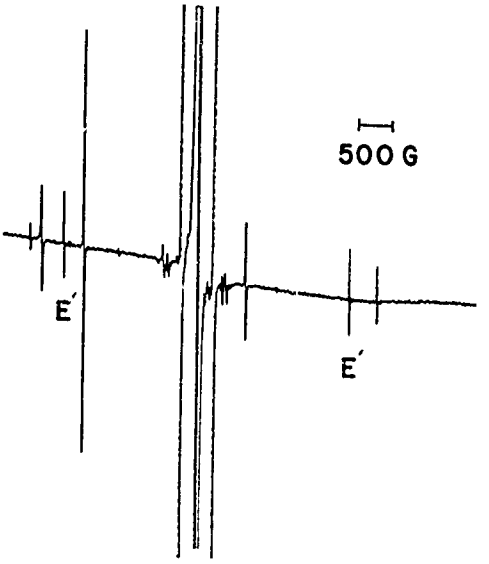

Figure 3.

Airtron sample after electron irradiation at 77 K.

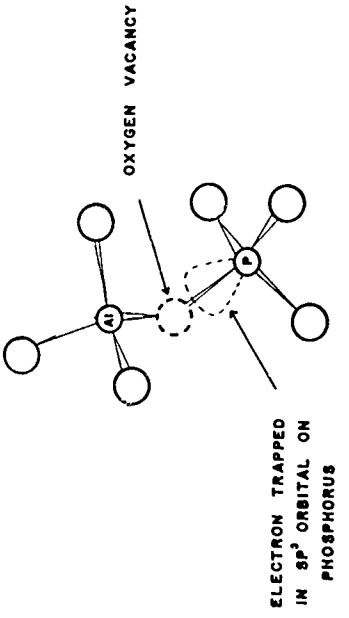

MODEL FOR E' CENTER

Figure 4. Proposed model for E' center in berlinite.

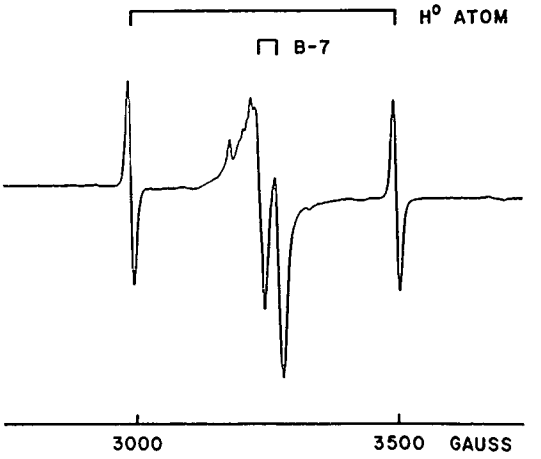

Figure 5. Naval Weapons Center sample after electron irradiation at 77 K. The microwave frequency is 9.14 GHz.

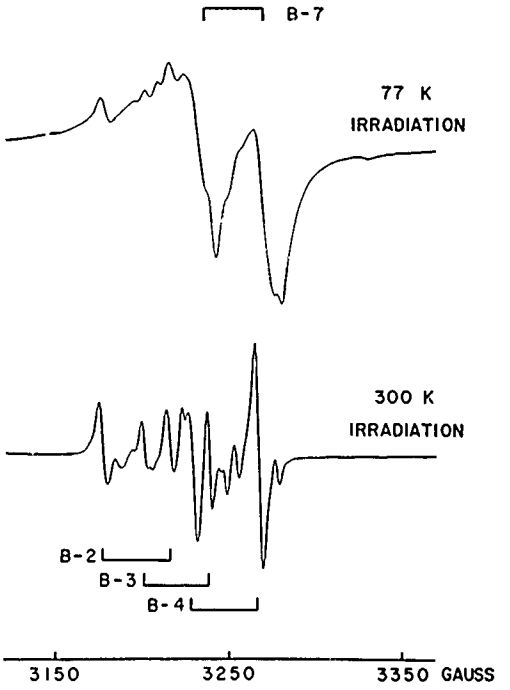

Figure 6.

Comparison of 77 K irradiation and 300 K irradiation.

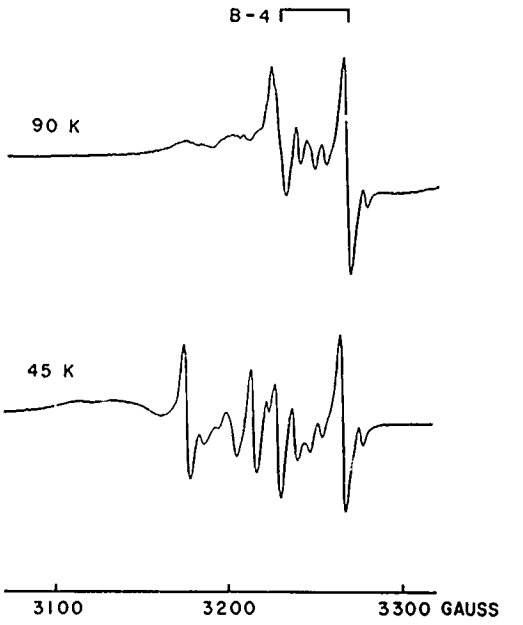

Figure 7.

ESR spectra of berlinite taken at 90 K and 45 K following a room temperature electron irradiation. The microwave frequency is 9.27 GHz.

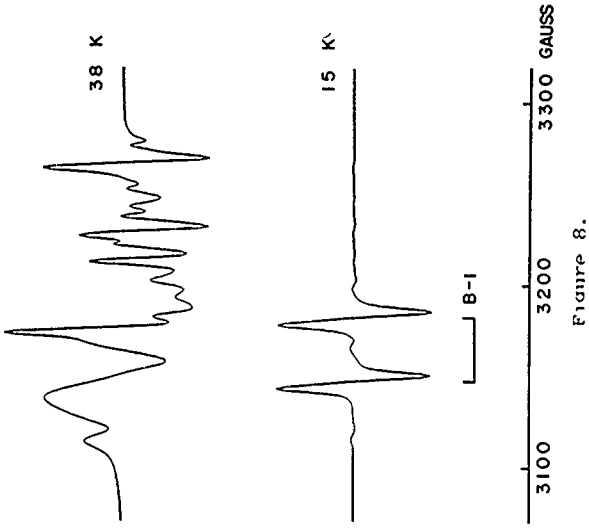

Figure 8.

ESR spectra taken at 38 K and 15 K following a room temperature electron irradiation. The microwave frequency is 9.27 GHz.

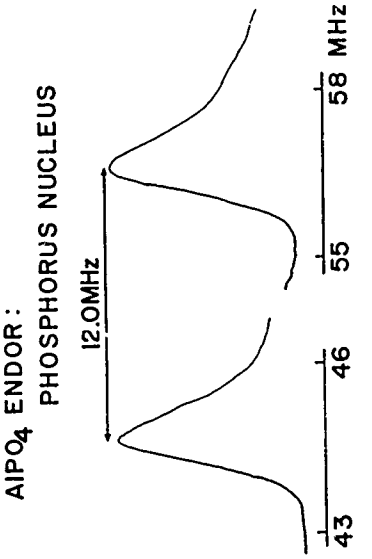

Figure 9.

Electron-nuclear double resonance (ENDOR) spectrum of the B-1 center.

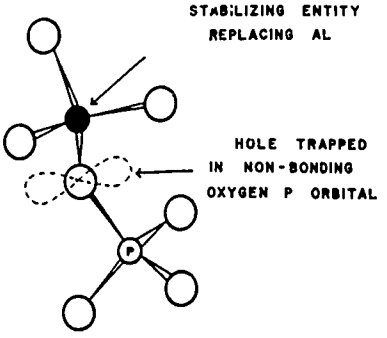

MODEL FOR B-TYPE CENTERS

Figure 10. Proposed model for the B-type centers.

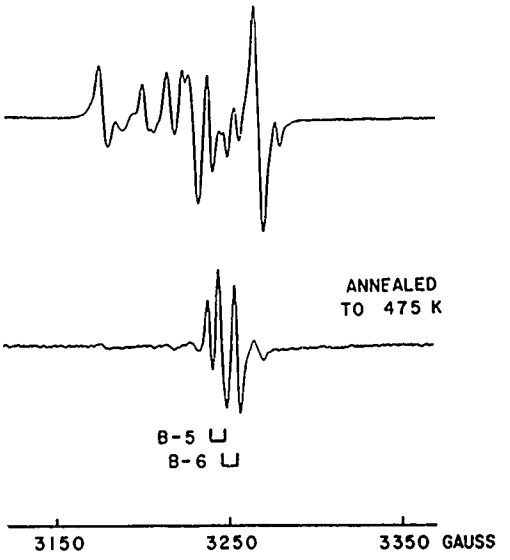

Figure 11.

Comparison of room-temperature electron-irradiated berlinite sample before and after anneal to 475 K.

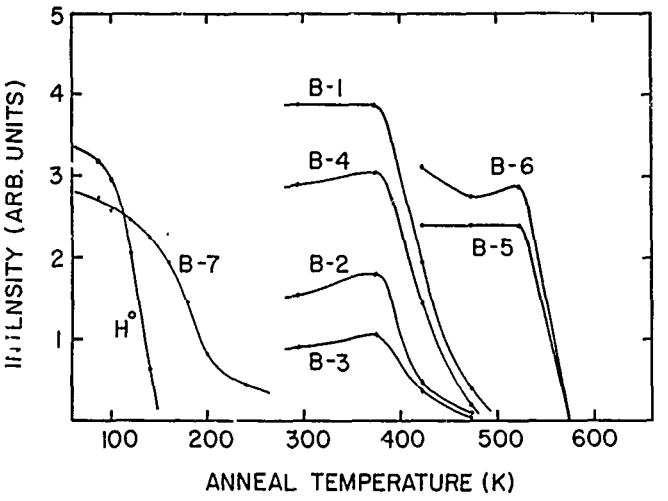

Figure 12. Thermal anneal behavior of radiation-induced defects in berlinite.

BULK AND SURFACE ACOUSTIC WAVE PROPAGATION IN BERLINITE

J. DETAINT
M. FELDMANN
J. HENAFF

H . POIGNANT
Y. TOUDIC

Centre National d'Etudes des Télécommunications
Dépt TCR/DEF
92131 Issy-les-Moulineaux (France)

Dépt CPM/PMT
22301 Lannion (France)

Summary

Samples of berlinite ($AlPO_4$) have been grown by two different methods from the solution $AlPO_4/H_3PO_4$ in an autoclave of 250 cm^3 capacity. At the present time, typical sizes are in the centimeter range. Such plates have been measured in both bulk and surface configurations and the results have been compared with the computed values.

From computation of the first order bulk frequency temperature coefficients (FTC) a zero TC cut behaviour was expected for (Y + 0) - plates with $\theta \simeq 30°$. This condition is slightly different for open and short circuit resonant frequencies. Experiments have been carried out at 7.5 MHz. The Q-factor of the resonators was found to be about 1000, and the resonant frequencies exhibit a cubic variation versus temperature.

In addition, the SAW propagation parameters have been recalculated. The experimental results presently available concern Y-cut X-propagation delay lines operating at 225 MHz. Good agreement between theory and experiment has been obtained. Furthermore, this experimental configuration is a zero - FTC - cut. Its second order FTC is one magnitude higher than the ST-quartz value. Other theoretical zero-FTC cuts have been found (with up to 0.8 % coupling coefficient). These results show that $AlPO_4$ has very interesting properties with regard to practical applications, but they also indicate the need for further experimental investigations.

I- Introduction

For both bulk and surface wave devices, research on high - coupling material with a good temperature stability and satisfactory mechanical properties continues to attract attention. Some recent published results for berlinite ($AlPO_4$) have demonstrated the potential interest of this material.

Berlinite is a trigonal crystal with 32symmetry, like quartz. Its acoustic velocity is lower but it has zero temperature coefficients of frequency (FTC) in both surface and bulk propagation. Also, its coupling is roughly four times higher than that of quartz.

This paper describes theoretical and experimental results concerning this crystal. Berlinite has been grown by hydrothermal methods in the Brittany laboratories of CNET, and the methods will be described below. Samples have been tested on bulk and surface wave devices at the Issy-les-Moulineaux laboratories. Computed results are compared here with experiments.

II - Crystal Growth

Owing to its 580° C phase transition, Berlinite is conveniently grown by the hydrothermal method at low temperature. We have used $AlPO_4$ /H_3PO_4 solutions [1] , below 250°C and H_3PO_4 concentrations lower than 10 M. As shown on Fig. 1, solubility decreases with temperature, and therefore at least two methods are relevant : slow increase of temperature of the saturated solution as used by Stanley [2] and later by Kolb et al [3] , and the reverse temperature gradient method. Both methods have been tested, using 250 cm^3 autoclaves lined with PTFE, Ag or Pt to prevent corrosion. Two independant heater windings allow the control of the temperature and its gradient.

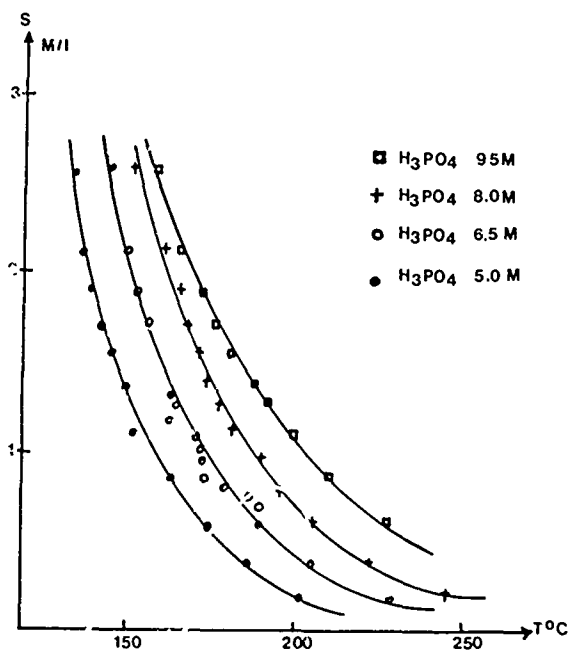

Fig. 1. Solubility curve of $AlPO_4$ in H_3PO_4 versus temperature (Pressure < 20 bar).

The method of slow heating has been studied under various conditions. The amount of $AlPO_4$ (MERCK SELECTIPUR) in the solvent H_3PO_4 is such that it produces a saturated solution at the beginning of the heating cycle (Tc). This solution, including seeds, is first rapidly raised up to the crystallization temperature (to prevent unwanted dissolving of the crystal) and then slowly heated at a selected rate during the growth period.

Similarly, at the end of the process, the autoclave is rapidly quenched in cold water and the crystals immediately removed. We finally selected the conditions given in Table I and obtained crystals up to 3 cm along the c-axis (Fig. 2). The growth rate is given on Fig. 3.

Table I

$[H_3 PO_4]$	6.5 M	9.5 M
$[AlPO_4]$	1.54 M/l	2.5 M/l
$T_1 - T_2$ (Cumulative)	154 - 184°C	160 - 130°C
Δ T/day	2	1.5

Experimental conditions selected for the 1st method

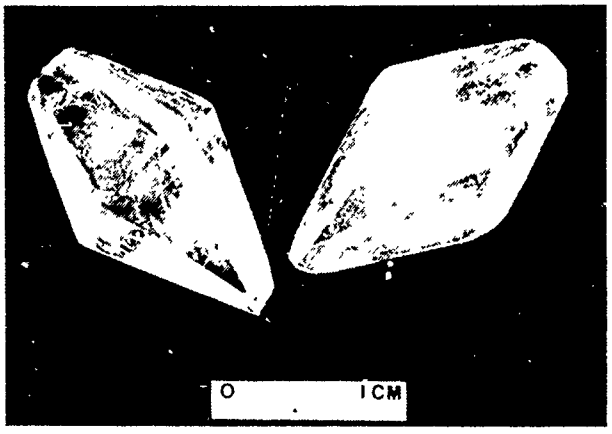

Fig. 2. $AlPO_4$ crystals grown on cut (001) seeds, after two successive growth generations, by slow heating in following conditions :
- *1.54 Mole of $AlPO_4$ in $H_3 PO_4$ 6.5M*
- *Heating rate : 3°C/ day*
- *Initial Temperature : Ti = 154°C*
- *Final Temperature : Tf = 198°C.*

The second method tends to produce larger and more homogeneous samples since the experimental conditions are constant during the growth. The experimental set up using a 80 % filled autoclave, is shown in Fig. 4. The nutrient obtained from previous nucleations is at the top of the autoclave and the seeds are at the bottom. Transfer of material is then the result of free convection of the solution. Various conditions have been examined by varying the temperature, the gradient and the solvent concentration. The finally selected conditions and the resulting rates are summarized on Tables II and III, and Figs 5-6. In addition, the activation energy Q =-14 Kcal/Mole has been obtained from the plot of the growth rate versus temperature

$\left[\text{Log } v_{0001} = f\ (1/Tf)\right]$.

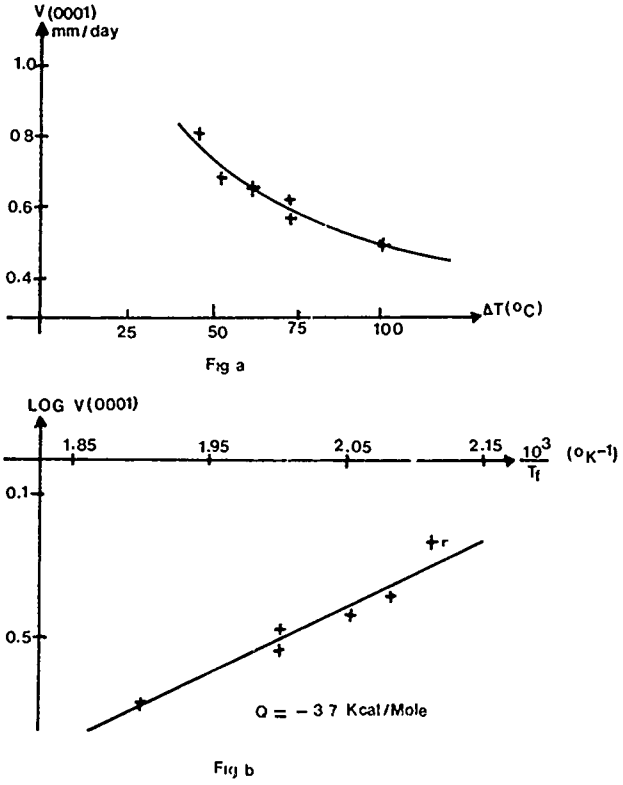

Fig. 3. Dependence of growth rate (0001) on ΔT (Δ T = Tf - Ti) (figure a) and plot of log V (0001) as a function of $\left(\frac{1}{Tf}\right)$ (figure b).

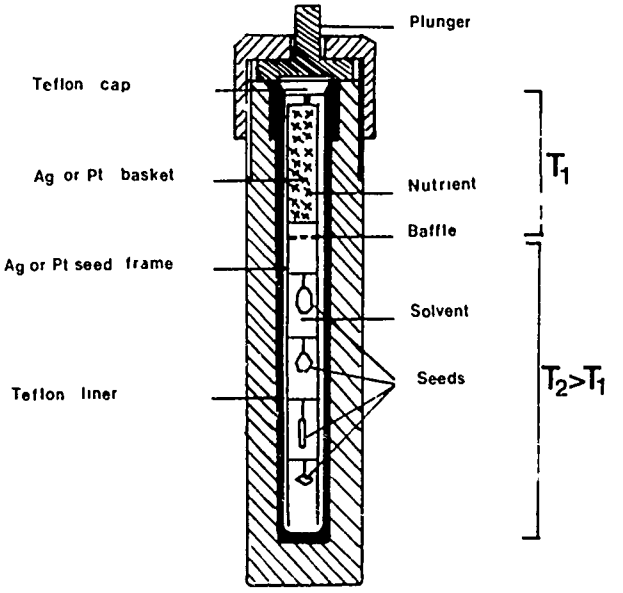

Fig. 4. Schematic of hydrothermal system used for $AlPO_4$ growth with a reverse temperature gradient ($T_2 > T_1$).

Table II

	orientations		
	0001	$10\bar{1}0$	$10\bar{1}1$
1st method (5°C/day)	0.5-0.8		
2nd method	0.7	0.3	0.1

Growth rates for different orientations (in mm/day)

Table III

$[H_3PO_4]$	6.5 M
T_1	169° C
T_2	174° C
filling	80 %

Selected conditions for the 2nd method

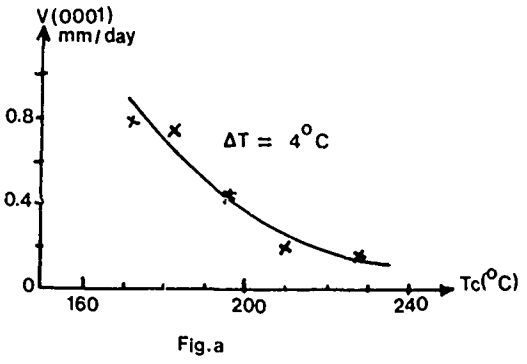

Fig.a

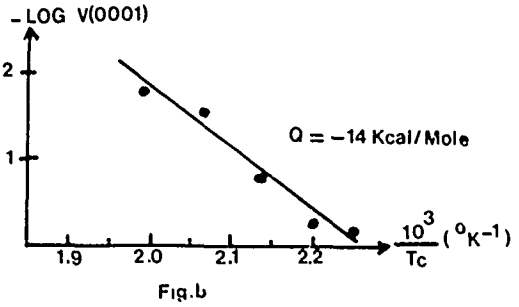

Fig.b

Fig. 5. Dependence of growth rate (0001) on the temperature of crystallization temperature Tc (figure a) and plot of log v (0001) as a function of $\left(\frac{1}{Tc}\right)$

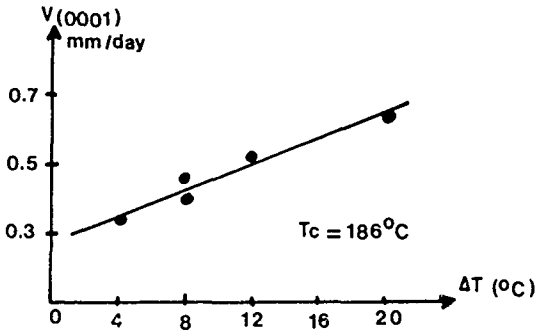

Fig. 6. Dependence of growth rate (0001) on the temperature gradient T (crystallization temperature Tc = 186°C).

Several samples have been already tested for acoustic propagation. At present, most of the results concern samples obtained by the first method. These crystals are about 1.5 cm long. The best zones have been selected by X ray-topography, etching and polarizing microscopy.

Crystals of relatively small size obtained from the second method are already available (fig. 7.). Their quality is very good and they are currently under investigation.

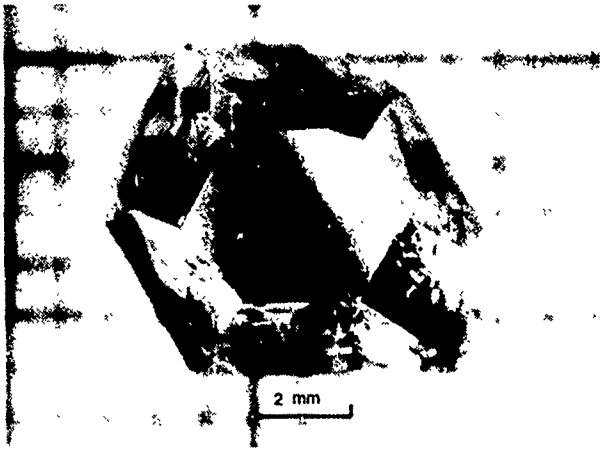

Fig. 7. $AlPO_4$ crystal grown on (0001) seed, by the temperature gradient method, in following conditions : Tc = 174°C
Td = 169°C
H_3PO_4 6.5M (saturated à 174°C with dissolved $AlPO_4$)
0/0 fill : 80

III - Bulk Wave Propagation

In the bulk wave field the results of Chang and Barsch [4] and Ballato [5] have pointed out the attractive properties of Y-rotated and doubly rotated cuts of Berlinite in terms of its large coupling coefficient (twice that of quartz), with the constraint of zero first order frequency temperature coefficient (F T C). We have investigated the behaviour of this crystal with respect to its 2nd order FTC.

It is well known that the attraction of quartz is due to the simultaneous cancellation of the 1st and 2nd order FTC in the AT cut and in some doubly rotated cuts [6] . Similar conditions hold in Berlinite.

For our computations we use the classical model of an infinite plate with massless electrodes, which leads to the well known impedance formula [7 - 8]

$$\bar{z}(j\omega) = \frac{1}{jC_0\omega}\left[1 - \sum k_i^2 \frac{\operatorname{tg}\Theta i}{\Theta i}\right],$$

where C_0 is the high frequency capacitance k_i is the coupling coefficient of mode i and $\Theta_i = \frac{\omega h}{2v_i}$ depends upon the angular frequency ω, the phase velocity of mode i and the thickness h of the plate. Poles and zeros of $\bar{z}(j\omega)$ defines the antiresonance and resonance frequencies of the plate. The FTC are obtained from the frequencies computed for temperatures around the reference point. For each antiresonance or resonance frequency (any mode and any order of overtone) a polynomial approximation technique is used to obtain a temperature law from which the FTC of orders up to the 3rd are computed.

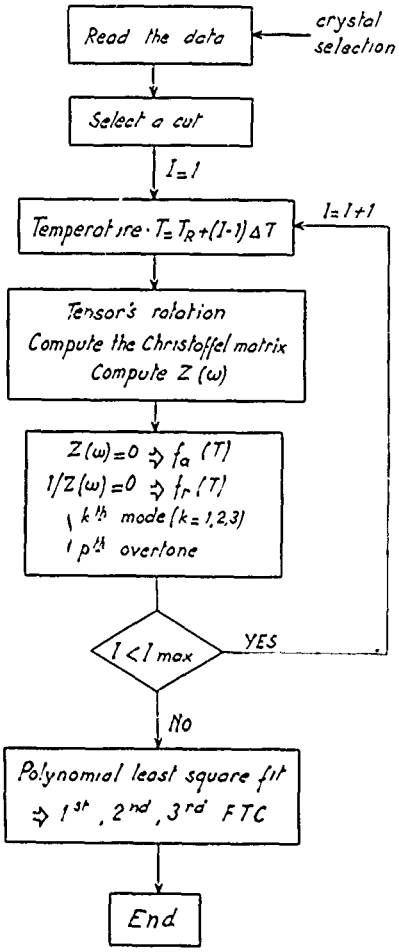

Fig.8. Flow Chart of the computer program used to Compute the F.T.C.

The computer program written (Fig. 8) for this purpose was checked against the results published for high order FTC of Y rotated quartz by Bechmann et al [6] .

The material constants were obtained from Ref. [4] with 2nd and 3rd order temperature coefficients of the elastic constants calculated from Table IV of this reference by polynomial least square analysis. The values used are given in Table IV where it can be seen that high order TC are much larger than for quartz.

Table IV

Constants	1st order coefficients
C(1,1) = .64013 E+11	TIC(1,1) = -77.8E-6
C(1,2) = .0724 E+11	TIC(1,2) = -1409.E-6
C(1,3) = .09554 E+11	TIC(1,3) = -127.2E-6
C(1,4) = .12347 E+11	TIC(1,4) = 62.4E-6
C(3,3) = .85754 E+11	TIC(3,3) = -223.5E-6
C(4,4) = .43171 E+11	TIC(4,4) = -169.74 E-6
C(6,6) = .28381 E+11	TIC(6,6) = 88.74 E-6
E(1,1) = - .30	TIE(1,1) = -266.E-6
E(1,4) = .13	TIE(1,4) = -561.E-6
EPS (1,1) = 5.19 E-11	TIL(1,1) = 15.9E-6
EPS (3,3) = 5.19 E-11	TIL(3,3) = 9.7E-6
2nd order coefficients	**3rd order coefficients**
T2C(1,1) = 353.E-9	T3C(1,1) = -1495.E-12
T2C(1,2) = 3800.E-9	T3C(1,2) = 27037.E-12
T2C(1,3) = 8419.E-9	T3C(1,3) = 67000.E-12
T2C(1,4) = -1558.E-9	T3C(1,4) = -9272.E-12
T2C(3,3) = -388.E-9	T3C(3,3) = 2138.E-12
T2C(4,4) = -555.E-9	T3C(4,4) = -1603.E-12
T2C(6,6) = -885.E-9	T3C(6,6) = 4835.E-12
T2L(1,1) = 7.62E-9	
T2L(2,2) = 7.62E-9	
T2L(3,3) = 7.54E-9	

Constants of $AlPO_4$ obtained from ref [4] and recomputed for the determination of higher order temperature coefficients.

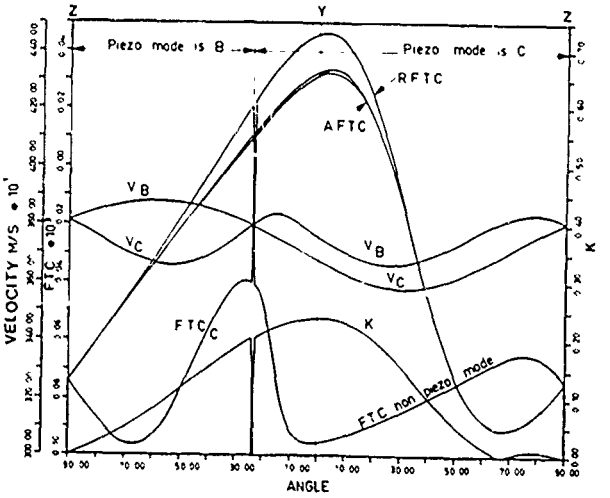

Fig. 9. Properties of Y rotated plates (phase velocities, coupling coefficient, 1st order FTC) for the transverse modes B and C.

The results concerning the first order FTC are plotted in Fig.9. for the fast transverse (B) and the slow transverse (C) branches. These results are consistent with previously published data[4-5]. It should be emphasized that the FTC for the resonant and antiresonant frequencies are significantly different. This is due to the relatively large coupling coefficient as shown by Onoe [9] . This is emphasized on Fig. 10. The 2nd order FTC is plotted on Fig. 11 for Y rotated cuts. The computed thermal behaviour of several Y rotated resonators is given on Fig.12.

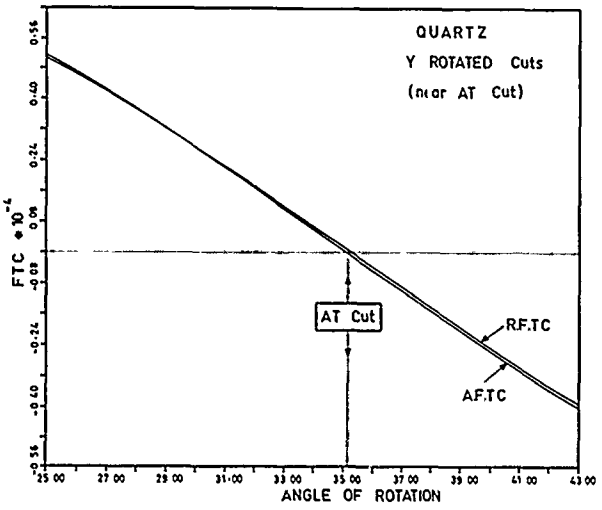

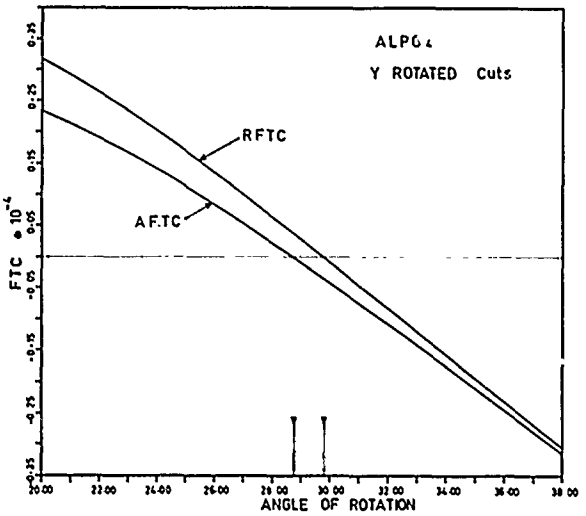

Fig. 10. Computed first order RFTC and AFTC of Y rotated plates of quartz and $AlPO_4$ in the vicinity of their AT cuts.

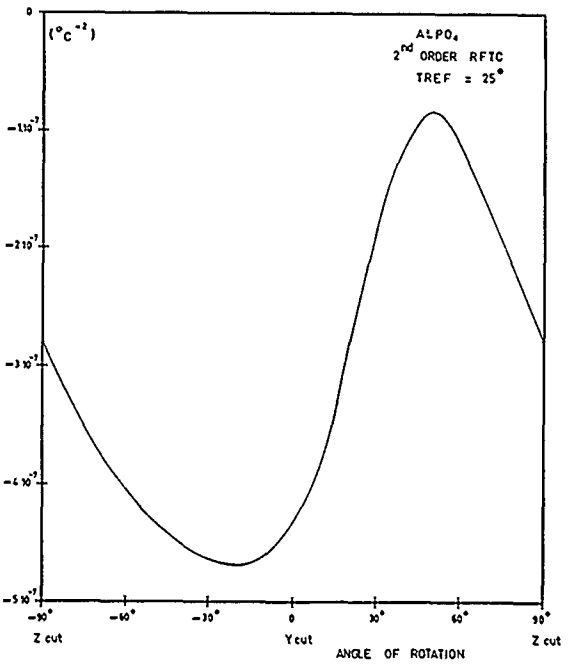

Fig. 11. Computed 2nd order R.F.T.C. of Y rotated plates of Berlinite (Piezo mode only).

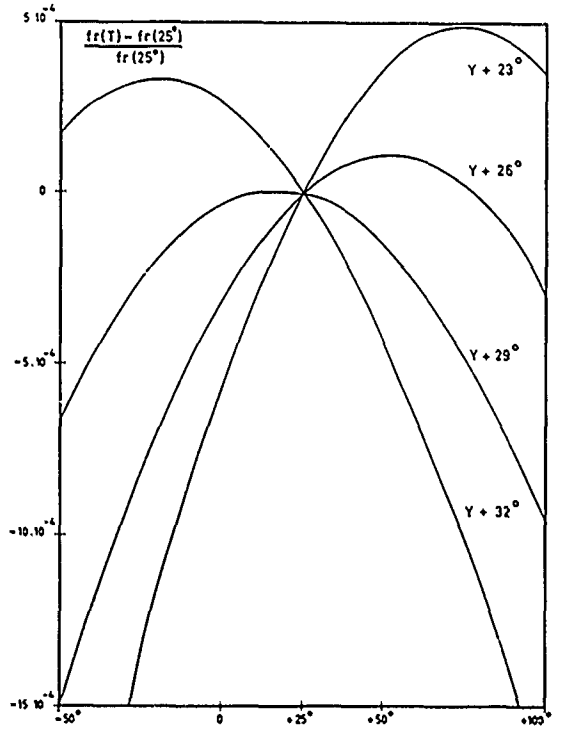

Fig. 12. Computed thermal behaviour of some Y rotated plates.

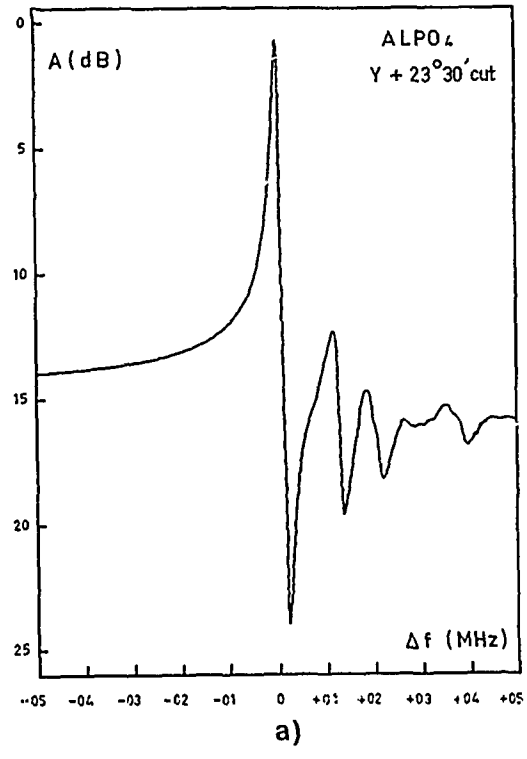

Fig. 13. Amplitude frequency response of Y rotated resonators.[a) Y + 23°30', b) Y + 29°45'; with static capacitance compensated in a bridge].

Resonators with Y, Y + 29°45 , Y + 23°30 orientations have been measured on several samples in each case. The plates used were 0.2 mm thick with thin gold electrodes of 1 to 3 mm diameter deposited on plate regions free from macroscopic twining. For the best samples the Q factor was around 1000. The electrical response is clean and typical of trapped energy resonators (Fig. 13). Experimental evidence of the occurence of conventional energy trapping was obtained by X-ray-topography of the vibrating samples (Fig. 14). The observed coupling coefficients are somewhat dispersed. The maximum value of 24 %, measured with Y cut resonators, is consistent with theory. The experimental frequency versus temperature behaviour of Y + 29°45 resonators is plotted on Fig. 15. A comparison with computed results is summarized in Table V.

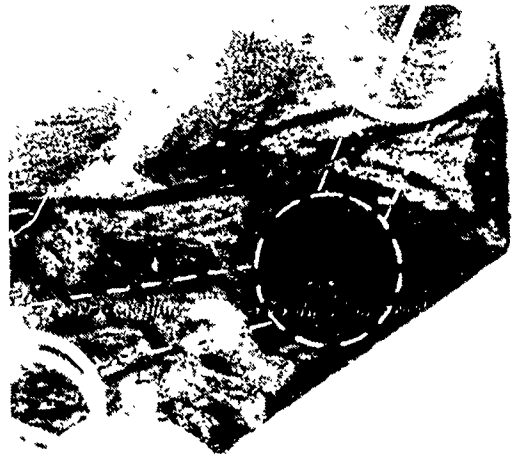

Fig. 14. X ray topography of a vibrating Y + 23°30' resonator.

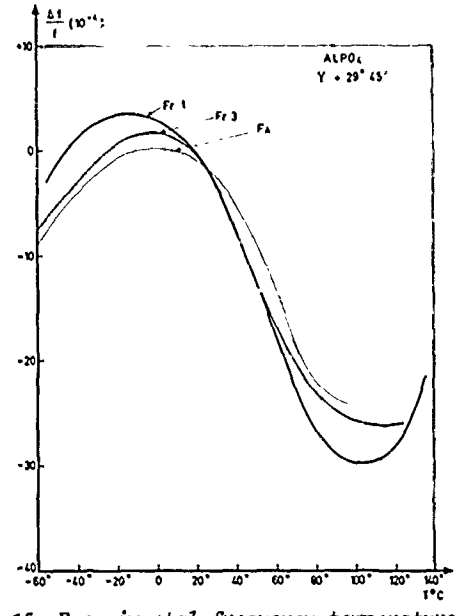

Fig. 15. Experimental frequency temperature behaviour of Y + 29°45' cut.

Table V

a) Y + 29°45'

	Experimental	Computed
1st R.F.T.C(°C-1)	- . 28 10^{-4}	. 47 10^{-5}
2nd R.F.T.C(°C-2)	- . 47 10^{-6}	-.18 10^{-6}
K (%)	∿ 7	16
NFA (KHz.mm)	1435.	1437.
NFR (KHz.mm)	1433.	1432.

b) Y + 23°30'

	Experimental	Computed
1st R.F.T.C(°C-1)	. 29 10^{-4}	. 27 10^{-4}
2nd R.F.T.C(°C-2)	-. 22 10^{-6}	- .24 10^{-6}
K (%)	7.3	19
NFA (KHz.mm)	1458.	1466.
NFR (KHz.mm)	1455.	1443.

Results for the Y + 29°45' and Y + 23°30' Cuts.

Our experimental results indicate that a 3rd order behaviour, not foreseen from computation, holds in the vicinity of the Y + 29°45' cut. A precise determination of the optimal cut and of its properties may require further refinement of the thermal derivatives of the material constants. This would be of particular interest for large crystal of high perfection (such as those grown by the second synthesis method), since the question arises as to whether or not the high order TC of the material constants are independant of impurities and of crystal perfection. These points are currently under investigation.

IV - Saw propagation

The properties of berlinite have been also investigated with regard to surface wave propagation. The potential applicability of berlinite to SAW devices was first noted by P.H. Carr et al [10] and A. Jhunjhunwala et al [11] .

Using the constants of Ref.[4] , we first computed the complete atlas of configurations (cut and propagation directions, Fig. 16) in terms of coupling coefficient k^2 , 1st and 2nd order FTC and power flow angle ψ . The method is substantially the same as that described by Campbell and Jones [12] . The flow chart for this program is shown on Fig. 17. Results are given in terms of stereographic maps as described elsewhere [13- 14]. For example, such a map for a propagation direction located in the (x,y) plane is plotted on Fig. 18. We then selected several cuts with coupling up to 0.8 % and zero 1st order FTC, as summarized on Table VI.

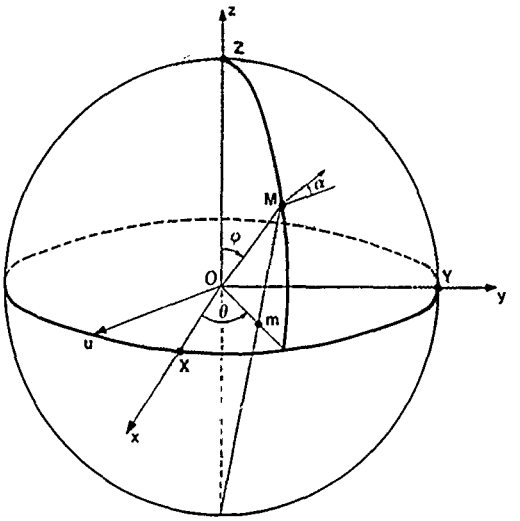

Fig. 16. Characteristic angles (α, θ , φ) Each configuration is characterized by 3 angles α , θ and φ described in Ref [13-14] . θ and φ are the spherical coordinates of the cut, and α the departure of the propagation direction from the xOy plane.

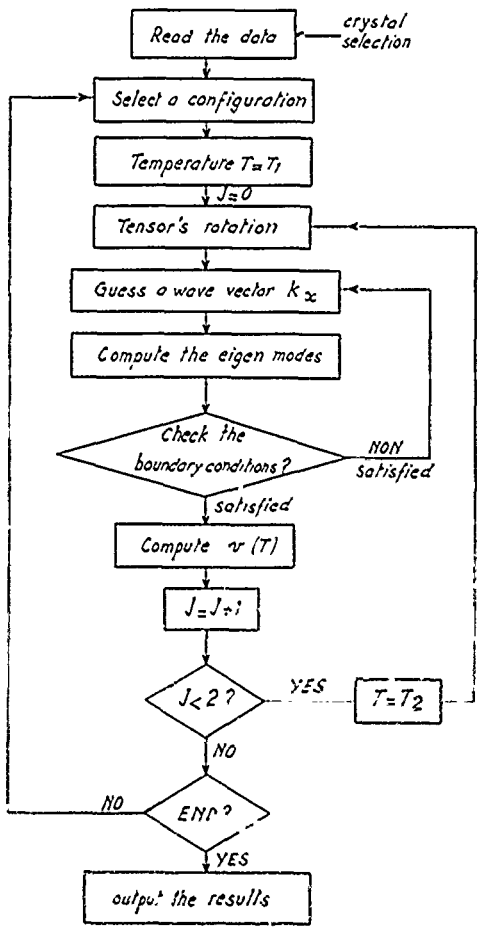

Fig. 17. FTC flowchart of computer program.

Table VI

	Angles			Cut			Propagation			v	k^2	$\varepsilon_{LF}/\varepsilon$	ψ	β	Ti
	α	θ	φ	X	Y	Z	X	Y	Z	m/s	%			10^{-8} K^{-2}	C
A	6°75	90	90	0	1	0	-.993	0	0.117	2752.6	0.57	6.14	4°36	1.34	20
B	22°3	0	90	1	0	0	0	-.925	-.379	2756.6	0.55	6.11	0°76	0.7	18
C	6°875	45	45	.5	.5	.707	.762	.642	.085	3060.6	0.86	6.04	4°36	1.25	20
ST	0	90	87.1	0	.999	.050	-1	0	0	2736.5	0.56	6.14	0	2.06	19
D	0	90	90	0	1	0	1	0	0	2739.6	0.58	6.14	0	2.	25

Main parameters of the selected cuts of $AlPO_4$

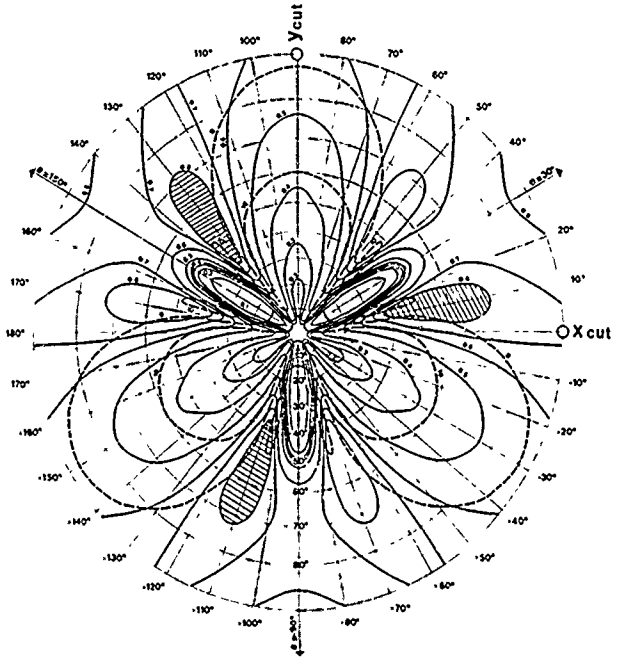

Fig. 18. Stereographic projection of equal $-k^2$ and equal - FTC corresponding to the azimuth angle $\alpha = 0°$ - solid lines : k^2 in % - broken lines : FTC in ppm.

Actually, it has been found convenient to use also the temperature coefficients of the constants given on Table IV. Qualitatively, the results are only slightly modified but the discrepancy is significant for the second order FTC. This is of particular interest for the (YX) configuration, which has a zero 1st order FTC. In order to check the above computations several samples of berlinite have been tested in this particular configuration. We have fabricated a SAW delay-line with two interdigital transducers of 181 and 361 fingers of 12.192 µm wavelength and 0.5 mm aperture. For the best samples the response is particularly clean as shown on Figs 19 and 20. Rejection is everywhere > 40-50 dB. The matched insertion loss is as low as 8 dB, showing a fair coupling coefficient k^2 and negligible propagation loss.

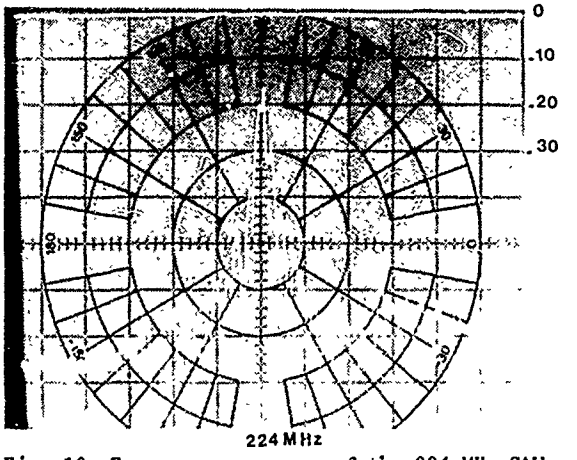

Fig. 19. Frequency response of the 224 MHz SAW delay line without matching
horizontal scale F : 5 MHz/div.
vertical scale I.L. : 10 dB/div.

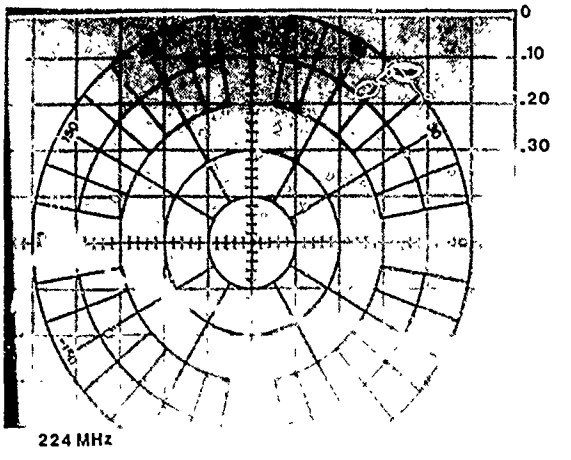

Fig. 20. Frequency response of the 224 MHz SAW delay line with inductance-tuned ports, showing an insertion loss as low as 8dB and a very clean response.
horizontal scale F : 50 MHz/div.
vertical scale I.L. : 10 dB/div.

From impedance measurements (Fig. 21a and b) it is possible to evaluate the coupling coefficient (k^2> 0.5 %), which is in good agreement with the theory (0.56 %) for the best sample. To find the velocity,we placed the delay line in a feedback loop with a broadband amplifier and measured the oscillation frequency : 224.75 MHz. This corresponds to a velocity of 2740 m/s, very close to the theoretical value of v_∞ = 2739. 6 m/s.

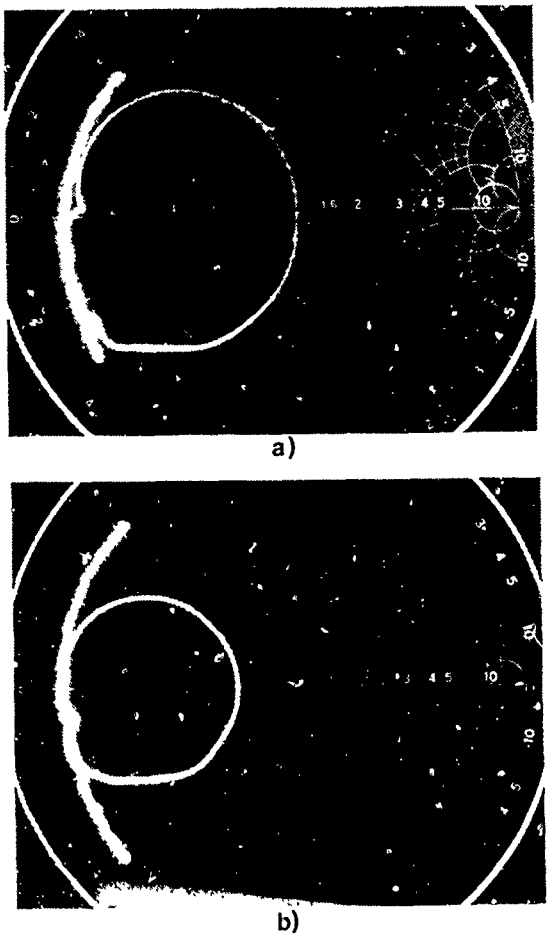

a)

b)

Fig. 21. Smith' chart of the two transducers of the 224 MHz SAW-delay line for evaluation of the coupling coefficient

a : 361 fingers IDT
b : 181 fingers IDT

We have similarly investigated the temperature stability. The experimental results are summarized on Fig. 22. for the best sample, together with theoretical curves computed with constants from Ref [4] (cf. Fig. 22a) and the present work (compare Fig. 22b). It is seen that YX berlinite is similar to ST-quartz. The turnover temperature depends upon the samples and varies in our experiments from 14 to 24°C. The second order FTC is one order of magnitude higher than for quartz :

experimental : $\beta_c = 2.1 \times 10^{-7}$
theoretical : a) $\beta_a = 2.10^{-8}$, b) $\beta_b = 2.3\ 10^{-7}$

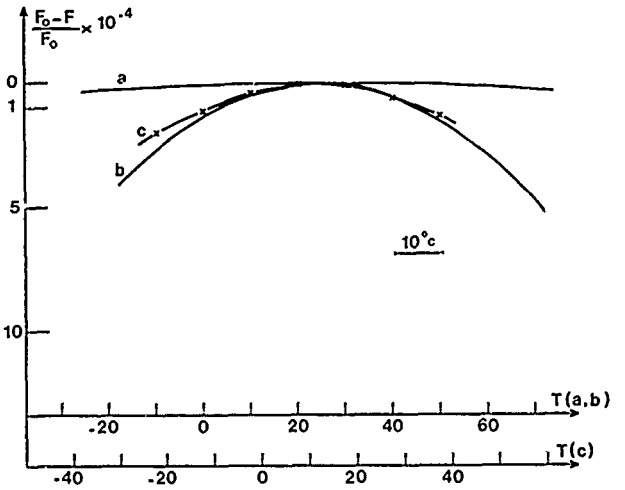

Fig. 22. Plot of the fractional oscillation frequency [(Fo - F)/Fo X 10^{-4}] versus temperature. (10°C/division).

a : theory neglecting 2nd order temperature coefficients ($\beta = 0.2 \times 10^{-7}$)

b : theory with 2nd order temperature coefficients (cf. Table IV) ($\beta = 2.3 \times 10^{-7}$)

c : experiment ($\beta = 2.1 \times 10^{-7}$)

There is a good agreement between theory and experiment regarding velocity, coupling coefficient, first and second order temperature coefficients. The only discrepancy, which is slight, concerns the turn-over temperature which differs for different samples. Just as in bulk wave propagation, this indicates the need of further investigation of crystals obtained by the second method which is capable of producing more homogeneous samples.

V - Conclusion

As pointed out by several authors, berlinite is an attractive material for frequency control devices. A reproducible method for growing homogeneous samples is available and will be applied to obtain larger crystals than those available at present.

Compared with quartz, berlinite is very similar, but with two distinctive features :

- the coupling is 2 to 4 times larger
- the second order FTC are one order of magnitude larger.

Due to these properties, berlinite meet the requirements of relatively large bandwidth devices. In terms of design parameters, both an AT-cut for bulk wave and an ST-cut for SAW propagation are available. The exact cuts and orientations are currently under determination since this implies further investigations on reproducible samples.

Références

1. *H. POIGNANT, L. LE MARECHAL and Y.TOUDIC : "Etude de la solubilité du phosphate d'aluminium ($AlPO_4$) dans des solutions hydrothermales d'acide orthophosphorique (H_3PO_4)", The Materials Research Bulletin, vol. 14, n°5 (1979) (to be published).*

2. *J.M. STANLEY : "Hydrothermal synthesis of large aluminium phosphate crystals", Industr. Eng. Chem., vol. 46, 8,pp. 1684-1689 (1954).*

3. *E.D.KOLB and R.A. LAUDISE : "Hydrothermal synthesis of aluminium orthophosphate", J. of crystal growth, vol. 43, pp. 313-319 (1978).*

4. *Z.P. CHANG and G.R. BARSCH : "Elastic constants and thermal expansion of berlinite", IEEE Trans. on Sonics and Ultrasonics, vol. SU - 23, n°2 pp. 127-135 (1976).*

5. *A.D. BALLATO and G.J. IAFRATE : "The angular dependance of piezoelectric plate frquencies and their temperature coefficients", Proc. 30th frequency control Symposium, pp. 141-156 (1976).*

6. *R. BECHMANN, A.D. BALLATO and T.J. LUKASZEK : "High order temperature coefficients of the elastic stiffnesses and compliance of α-quartz" Proc. IRE, vol. 50, pp. 1812-1822 (1962).*

7. *H.F. TIERSTEN : "Thickness vibration of piezoelectric plates", J. Acoust. Soc. Am., vol. 35, pp. 53-58, (1963).*

8. *A. GLOWINSKI : "Vibrations d'épaisseur des lames piezoelectriques", Ann. Telecommuni., Vol. 27, n°s 3-4, pp. 147-157 (1972).*

9. *M. ONOE : "Relationship between temperature behaviour of resonant frequencies and electromechanical coupling factors of piezoelectric resonators", Proc. IEEE, vol. 57, n° 4, pp. 702-703 (1969).*

10. *P.H. CARR and Lt R.M. O' CONNELL : "New temperature compensated materials with high piezoelectric coupling", Proc. 30 thFrequency Control Symposium, pp. 129 - 131 (1976).*

11. *A. JHUNJHUNWALA, J.F. VETELINO and J.C. FIELD : "Berlinite, a temperature compensated material for surface acoustic wave applications", Proc. 1976 Ultrasonics Symposium, IEEE Cat. ## 76 CH 1120 - 5SU, pp. 523 - 527 (1976).*

12. *J.J. CAMPBELL and W.R. JONES : "A method for estimating optimal crystal cuts and propagation directions for excitation of piezoelectric surface waves", IEEE Trans. Sonics and Ultrasonics, vol. SU-15, pp. 209 - 217 (1968).*

13. *J. HENAFF and M. FELDMANN : "New acoustic-surface-wave zero-temperature cuts in Tl_3VS_4", Electron. Lett., vol. 13, n°10, pp. 300 - 302 (1977).*

14. *M. FELDMANN and J. HENAFF : "Propagation des ondes élastiques de surface", Revue de Physique Appliquée, vol. 12, pp. 1775-1787 (1977).*

PIEZOELECTRIC PROPERTIES OF SINGLE CRYSTAL BERLINITE

E. J. Ozimek and B. H. T. Chai
Corporate Research Center
Allied Chemical Corporation
P.O. Box 1021R
Morristown, New Jersey 07960

Summary

Chang and Barsch, O'Connell and Carr, and others have shown that berlinite (α-$AlPO_4$) is one of the better candidates for SAW substrate materials. The investigation of berlinite in our laboratory has involved the synthesis of high quality berlinite single crystals as well as the characterization of their fundamental material properties. The single crystals were grown by the transport method by using oriented plates of berlinite as the seed material and coarse granular crystalline α-$AlPO_4$ as the nutrient. Phosphoric acid is used as the transport medium.

Crystals with large areas free of imperfections such as veiling, inclusions, twinning, cracks and surface damage have been successfully grown. A number of Y resonator plates were prepared. The samples were placed in the series arm of a π-resistance network in accord with the IEEE Standard No. 177 for Piezoelectric Vibrators. A stable frequency synthesizer was used to drive the crystal over a broad band of frequencies and the output signals were recorded.

As a means of comparison, a number of α-quartz Y resonator plates were fabricated and mounted in an identical manner to the berlinite samples. From a recording of the transmission response, a $Q \geq 14\,000$ has been observed for a berlinite Y plate at 6.8 MHz fundamental frequency. Other parameters were found to be in accord with published values. Identically prepared quartz Y resonator plates gave a Q of 61 000.

In addition, spectrophotometric studies have been done over the ultraviolet, visible and infrared regions for selected samples. Absorption in the 250 nm region is believed to be associated with transition metal impurities. The IR spectrum shows a broad absorption shoulder in the region 2600-3600 cm^{-1}. No sharp peaks attributable to OH^- have been observed either at room or liquid-N_2 temperatures.

Introduction

The ideal material for large bandwidth SAW devices must possess high electromechanical coupling, low energy loss (high material Q), and high temperature stability (zero temperature coefficient to second order). Chang and Barsch,[1] O'Connell and Carr[2-5] and others[6-9] have shown that berlinite (α-$AlPO_4$) is one of the better candidates for SAW substrate materials. This conclusion is based on the fact that the crystal structure of berlinite is isomorphic with α-quartz with half of the silicon positions occupied by Al^{3+} and the other half by P^{5+}. Therefore, there must be temperature compensated cuts as for α-quartz. Indeed, experimental work does show that such orientations exist.[1,6,7] Theoretical calculation of the behavior of surface acoustic waves on berlinite also show that along the same temperature-compensated orientation, the electromechanical coupling can be as much as 4 times that of ST-cut quartz. In addition, the relatively high hardness, low water solubility, chemical inertness, and high acoustic wave propagation velocity make berlinite a very attractive material for an SAW device substrate.

These superior properties projected for berlinite over other substrate materials have caused the start up of programs for the growth of berlinite in many places, namely the Air Force, DOD Research Laboratories,[10] Bell Laboratories,[11-13] Airtron Inc., and the Allied Chemical Corp. Recent information indicates that similar projects have also been started in other countries. The investigation of berlinite at the Allied Chemical Corp. involved the synthesis of high quality berlinite single crystals as well as the characterization of their fundamental material properties.

Crystal Synthesis

Berlinite crystals were first synthesized by Huttenlocher in 1935.[14] The largest crystals he grew were about 4 mm in length. The first actual attempt to grow berlinite crystals to a usable size was made by Joseph M. Stanley in 1954.[15] However, the technique he used was direct precipitation from solution and requires many manhours and, therefore, is very costly. It was decided by us to use the transport technique which has been well established in hydrothermal synthesis of quartz crystals. This technique requires the use of coarse granular crystalline α-$AlPO_4$ as nutrient material. Since this nutrient material is not available commercially, it is synthesized in this laboratory.

Nutrient Synthesis

The starting materials can either be $Al(OH)_3$ or Al_2O_3 and phosphoric acid. Typical synthesis time is two to three weeks. The reaction is always completed in each synthesis experiment.

No residuals of starting material or any solid phase other than α-$AlPO_4$ were found. A typical run started with 1350 grams Al_2O_3 will yield twice as much in weight of crystalline α-$AlPO_4$. The crystalline nutrient material is then sieved into three size fractions. Those fractions greater than 50 mesh are the standard nutrient material for growth. Those fractions between 50 to 90 mesh are considered marginal. However, it was recently found that the finer mesh material is also satisfactory for growth. Those fractions below 90 mesh are unacceptable for growth. The weight fraction of a typical load after synthesis is 38% (>50 mesh), 50% (50-90 mesh) and 12% (<90 mesh). The synthesis technique is still under refinement in order to reduce further the synthesis time and to increase the coarse grain size fractions.

The impurity level of the nutrient material depends on the starting material. Emission spectroscopic analysis of the synthesized nutrient material gives the following result: Si (<20 ppm), B (20 ppm), Ga (70 ppm), transition metals (<100 ppm), alkaline earths (<30 ppm), and alkalies (<20 ppm). It should be noted that "less" means below the detectable limit of the instrument employed. Therefore, the major impurities of the α-$AlPO_4$ nutrient material are B and Ga as would be expected on the basis of the ionic size and charge of these elements.

Crystal Growth

The initial seed crystals were synthesized by spontaneous nucleation and then grown by transport process. The usable seeds had to have a minimum length of 5 mm. The increase in crystal size is achieved by repeated overgrowth of these seeds. When the crystals exceeded 2 cm in length, they were cut into seed plates and used for further growth. The growth of berlinite crystals is based on a transport process arising from the difference in solubility of berlinite in two regions of different temperature. Since berlinite has a retrograde solubility in phosphoric acid,[15] seed crystals are hung at the warmer part of the autoclave and the crystalline nutrient is placed at the cooler part of the autoclave in reverse of that of the arrangement for quartz growth. A baffle is inserted in between the two regions to maintain the temperature gradient. The growth rate of a berlinite crystal is much slower than that of quartz. The average growth rate of a berlinite plate varies from 0.15 mm to 0.4 mm.

Crystal Defects

Although we have grown berlinite crystals in excess of 6 cm in this laboratory, the quality of the crystal has still not reached the necessary perfection. The defects found in berlinite crystals can be classified into five categories:

1) Twinning: Twinning is a very common feature in almost all the crystals grown. Both types of interpenetration twins found in quartz crystals, namely, the Dauphiné (electrical) twin and the Brazil (optical) twin, are also found in berlinite. The twinning boundaries of these two twin laws are shown in Fig. 2 and Fig. 3. Similar to quartz, the twinning boundary of a Dauphiné twin is generally irregular, but the twinning boundary of a Brazil twin is very regular. These twins generally form an intricate, complex zig-zag pattern and in many cases the twinning can be so fine down to a micron scale. As a surprise, it was found that the Brazil twin is more common than the Dauphiné twin in berlinite crystals. This result is just the reverse of the result for quartz crystals.

2) Crevicing (or channeling): This defect is typical of most basal plate growth before the completion of capping. The amount of this type of defect is a function of growth rate. This type of defect can be effectively eliminated if the growth rate is reduced to less than 0.3 mm/day.

3) Veiling: This defect consists of small liquid--gas inclusions less than 10 μ in diameter arranged in a veil-like structure. One type of veiling forms along the junction of original seed and the overgrowth portion similarly to that found in the growth of quartz crystals. The other type of veiling is distributed in random curved surfaces which give a fuzzy milky appearance to the crystal. It is believed to be the result of a partially healed crack inside the crystal.

(4) Cracking: These defects are stress cracks which are generated during the rapid quenching at the end of each run. There is also evidence that some cracks are formed during the growth period. In fact, veils seem to be the relics of such cracks. Cracking is caused by twinning, by locally high dislocation density, and by the Pt seed hanging wire.

(5) Surface damage: Because of the retrograde solubility, the crystal surface is always subject to back-dissolution during cooling. The amount of etching which occurs is proportional both to the crystal quality and to the total time of cooling. Etching is localized at the dislocations, at the twinning boundaries as well as at the surface traces of the cracks. When etching is severe, a white opaque material also forms inside the pits. It is believed that this white opaque material is aluminum phosphate hydrates.

Despite all of these defects, it was possible to find areas of crystals which are free from any visible defects and also large enough for crystal oscillator fabrication. However, the dislocation density in these areas is still very high, as is evidenced by the high etching pits density (Figs. 2 and 3). We estimate that the dislocation density can be two to three orders of magnitude higher than that of good hydrothermally grown quartz crystals, which, we believe, will affect somewhat the performance of the crystal.

Piezoelectric Measurements

The experimental evaluation of the piezoelectric vibrators followed closely the procedures set forth in the IEEE Standard No. 177[16] for piezoelectric vibrators and Publication 444[17] of the International Electrotechnical Commission. Figure 4 shows a block diagram of the various components associated with the transmission network. A highly stable (1 part in 10^9/day), programmable General Radio GR-1061 frequency synthesizer was used to drive the piezoelectric vibrator which was in the series arm of a π network. The frequency of the output signal was constantly monitored with a highly stable Hewlett Packard 5248L electronic counter. In order to improve the signal-to-noise ratio, synchronous detection was used. A broad band P.A.R. lock-in amplifier Model 5202 made it possible to monitor simultaneously both vector amplitude and phase of the output signal from the π network. A -1/2 to +5 volt, variable time, voltage ramp was used to drive the frequency synthesizer over a selected band of frequencies, as well as to provide the horizontal drive for an X-Y recorder. The detected amplitude and/or phase signal was recorded on the ver-

tical axis of the chart recorder.

(I) Transmission Measurement:

Up to the time of preparation of this article, the growth of large, high quality, single crystal berlinite has not been fully accomplished. However, we were able to obtain areas large enough to fabricate several 7.94 mm diameter circular Y resonator plates. The plates were carefully ground to 0.25 mm in thickness with a Hoffman lapper. A few plates showed chipped edges, small cracks, and small twinning areas after lapping. Chromium and gold contact electrodes were vacuum deposited on the crystals prior to mounting the units. Both bellows contacts and wire mounts (HC-6/U and HC-25/U) were used in the course of the evaluation.

After being mounted in the π-network, transmission responses of the fundamental, 3rd harmonic and 5th harmonic resonances were recorded. From the shape of the transmission spectra, it was possible to estimate the material Q value from the 1/2 power points (i.e., $f/\Delta f$). These values showed relatively good agreement with those calculated by the capacitance substitution method. In order to make a comparison, Y resonators of a known high quality quartz rod ($Q>1.8 \times 10^6$) from Valtec were also prepared in identical size and fashion. The transmission data for both quartz and berlinite Y resonator plates are shown in Figure 5. A Q value of about 14 000 was obtained for berlinite based on $f/\Delta f$ evaluation. The corresponding quartz Y-resonator plate gave a Q about 61 000, which was slightly lower than it should be.[18] It is not surprising that the berlinite oscillators of a similar cut show a lesser Q value considering that these have a larger electromechanical coupling coefficient. Compared to transmission data reported previously, these samples show an improvement of two orders of magnitude. Due to the effects of stray capacitance, the antiresonant frequency could not be accurately determined either by amplitude or by phase measurement. While this limitation prevents an accurate determination of the electromechanical coupling coefficient k, it does not seriously affect the measurement of the material quality factor.

(II) IR and UV Spectrophotometric and Raman Scattering Measurements:

The correlation between the infrared absorption around the 3500 cm^{-1} region and the material Q value of α-quartz crystals has long been well established.[19-22] It is assumed that H^+ enters the quartz lattice as OH^- and is the main cause for the acoustic loss. However, it is not clear whether the same relationship also holds for berlinite, simply because it is an isomorph of quartz. Thin plates of berlinite were prepared and submitted for both infrared and ultraviolet transmission measurements. Berlinite is transparent throughout the visible region of the spectrum but shows strong absorption in the 250 nm region. It is believed that this absorption is associated with the transition metal impurities, such as Fe and Cr in particular. The crystal purity has to be further improved in order to increase its optical transparency in the UV region.

Infrared transmittance spectra of berlinite was also measured in the 4000-2000 cm^{-1} region with a Nicolet 7199 Fourier transform infrared spectrophotometer. A 4.31 mm thick berlinite slab was first used for the measurement. The transmittance decrease sharply at 3700 cm^{-1} and no transmittance was detectable beyond 3600 cm^{-1}. The sample thickness has to be reduced to less than 1 mm before any reasonable transmittance can be detected by the instrument. Thinner samples of berlinite (0.38 mm thick) were prepared for IR measurement. In order to enhance any sharp absorption peak, IR spectra were measured at both room temperature and at liquid nitrogen temperature (77 K).

To make a comparison, quartz samples were also prepared for IR measurement. The IR transmittance results for both quartz and berlinite samples are illustrated in Figure 6. Two types of quartz crystals were used. One was Valtec quartz from Sawyer Research Products with a guaranteed Q of over 1.8×10^6. The other one was a large cracked quartz blank of an unknown origin. All the principal absorption band peaks[23] (i.e., 3581, 3438, 3396, 3348 cm^{-1}) associated with O-H stretching vibrations were observed in both quartz samples. In addition, the quartz sample of unknown origin also showed a broad absorption shoulder from 3600 cm^{-1} to 2900 cm^{-1}. In the case of berlinite, no distinct absorption peaks were observed even at liquid-nitrogen temperature, except possibly a weak absorption peak at around 3515 cm^{-1}. Instead, only a broad absorption shoulder from 3600 cm^{-1} to 2600 cm^{-1} was observed.

Berlinite parallelpipeds ($4 \times 6 \times 7$ mm^3) with polished faces normal to X, Y, Z directions were also prepared for a Raman Scattering study.[24] Again, only a broad Raman spectrum structure from 3600 to 2600 cm^{-1} was observed. No distinct peaks were found. The spectrum is very similar to that reported[25] for a quartz sample X257-23. This material was grown hydrothermally in a KOH solution in a silver tube[26] with estimated total of $OH^- + H_2O$ content of 220 ppm by weight. Correlation of this result for quartz with the berlinite result was difficult because the vertical intensity scale of the Raman spectrum was not given in the paper.[25] However, the paper suggested that most of the H^+ content in this particular quartz sample existed as H_2O molecules. The IR spectrum[26] of this quartz sample also showed a broad absorption band from 3700 to 2900 cm^{-1} without noticeable absorption peaks. On the basis of all the evidence collected, it is suggested that the H^+ incorporated into berlinite structure is present as H_2O molecules not OH^-. This conclusion is also consistent with the argument that most H^+ incorporated in the quartz structure is present to charge compensate for ions with a valence of less than four, such as Fe^{3+} and Al^{3+}, which replace Si^{4+}. These transition metal impurities when incorporated in the berlinite structure do not require charge compensation since they replace Al^{3+}.

IR absorption has been used successfully to evaluate the acoustic Q of quartz.[19-23] It is not clear whether the same relationship is also applicable to berlinite. The IR transmittance data obtained here give a Q value of 1.12×10^6 for Valtec quartz which corresponds to about 8 ppm total $OH^- + H_2O$ by weight. This value of Q is lower than the specification. The IR spectrum of the unknown quartz blank seems to indicate that large quantities of both OH^- and H_2O are present. The total $OH^- + H_2O$ content is estimated to be about 120 ppm which corresponds to a Q of about 1.0×10^5. The IR transmittance result for berlinite gives a total H_2O content of about 110 ppm. By using the same formula as for quartz, the Q of berlinite at the present H_2O level is estimated to be in the 10^5 range.

Conclusions

The possible use of berlinite (α-$AlPO_4$) as an alternative to α-quartz in many piezoelectrical device applications has been well documented. Unfortunately, the growth of large, high quality, single crystals of berlinite has not been fully accomplished. This endeavor is a continuing objective in our laboratory. The preliminary results of the growth, defect characterization, and physical property evaluation of berlinite crystals have been presented. Although our process is not at a point of perfection, it is felt that the crystal quality and the piezoelectric response data for the fabricated resonators represent some of the best results obtained for berlinite. With a continuing improvement in crystal quality, berlinite promises to become an ideal candidate for many SAW as well as bulk wave devices.

ACKNOWLEDGEMENT

The authors would like to express their appreciation to M. A. Gilleo for his suggestions and critical review of the article; to J. J. Flynn and E. Beuhler for assistance and perfection of the growth process; to B. D. Forman and J. D. Witt for the IR and UV measurements; to M. L. Shand for the Raman Scattering measurement, to J. J. Bezak and J. T. Fleming for cutting and polishing the samples; to M. J. Markuson for the impurity measurement; and to J. E. Macur for the SEM study.

References

1. Z. P. Chang and G. R. Barsch, IEEE Trans. Sonics Ultrason. SU-23, 127 (1976).
2. R. M. O'Connell and P. H. Carr, 1978 Frequency Control Symposium, Atlantic City, p. 189.
3. R. M. O'Connell and P. H. Carr, 1977 Frequency Control Symposium, Atlantic City, p. 182.
4. R. M. O'Connell and P. H. Carr, IEEE Trans. Sonics Ultrason. SU-24, 376 (1977).
5. P. H. Carr and R. M. O'Connell, 1976 Frequency Control Symposium, Atlantic City, p. 129.
6. D. G. Morency, W. Soluch, J. F. Vetelino, S. D. Mittleman, D. Harmon, S. Surek, J. C. Field, and G. Lehmann, Appl. Phys. Lett. 33, 117 (1978).
7. D. G. Morency, W. Soluch, J. F. Vetelino, S. D. Mittleman, D. Harmon, S. Surek, J. C. Field, 1978 Frequency Control Symposium, Atlantic City, p. 196.
8. A. Jhunjhunwala, J. F. Vetelino and J. C. Field, 1976 IEEE Ultrasonics Symposium Proceedings, Annapolis, p. 523.
9. A. Jhunjhunwala, J. F. Vetelino and J. C. Field, J. Appl. Phys. 48, 87 (1977).
10. W. R. McBride and M. E. Hills, ICCG-5, Boston, Abst. Ø65, (1977).
11. E. D. Kolb and R. A. Laudise, 1977 Frequency Control Symposium, Atlantic City, p. 178.
12. E. D. Kolb and R. A. Laudise, J. Cryst. Growth 43, 313 (1978).
13. E. D. Kolb and R. A. Laudise, 1979 Frequency Control Symposium, Atlantic City, in press.
14. H. F. Huttenlocher, Z. Krist. 90, 508 (1935).
15. J. M. Stanley, Ind. Engr. Chem. 46, 1684 (1954).
16. IEEE Standard No. 177, May 1966.
17. International Electrotechnical Commission Pub. 444, 1973.
18. M. E. Frerking, Crystal Oscillator Design and Tempture Compensation, Van Nostrand Reinhold Co., p. 240 (1978).
19. D. L. Wood, J. Phys. Chem. Solids 13, 326 (1960).
20. D. M. Dodd and D. B. Fraser, J. Phys. Chem. Solids 26, 673 (1965).
21. B. Sawyer, IEEE Trans. Sonics Ultrason. SU-19, 41 (1972).
22. N. C. Lias, E. E. Grudenski, E. D. Kolb, and R. A. Laudise, J. Crystal Growth 18, 1 (1973).
23. H. G. Lipson, F. Euler, and A. F. Armington, 1978 Frequency Control Symposium, Atlantic City, p. 11.
24. M. L. Shand and B. H. T. Chai, in preparation.
25. G. E. Walrafen and J. P. Luongo, Spex Speaker XX, No. 3, September 1975.
26. A. A. Ballman, D. M. Dodd, N. A. Kuebler, R. A. Laudise, D. L. Wood, and D. W. Rudd, Applied Optics 7, 1387 (1968).

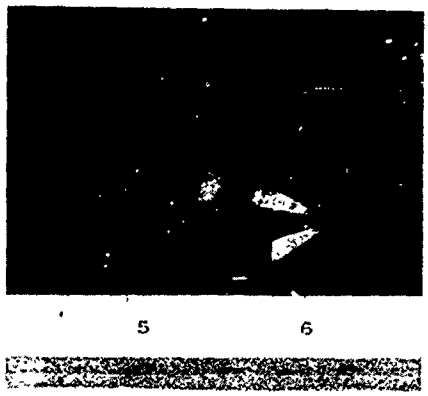

Fig. 1. Photograph of as-grown berlinite crystals. (scale : inches)

Dauphiné (Electric) Twin

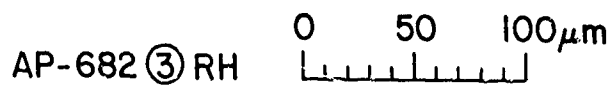

Fig. 2. Etching figures on the minor z ($01\bar{1}1$) face of an as-grown berlinite crystal showing the Dauphiné (electric) twinning law. Notice the irregular twin boundary.

Brazil (Optical) Twin

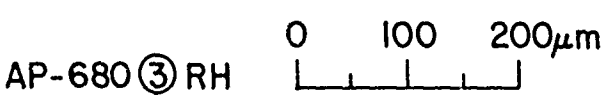

Fig. 3. Etching figure on the minor z ($01\bar{1}1$) face of an as-grown berlinite crystal showing the Brazil (optical) twinning law. Notice the very regular laminar twin boundaries.

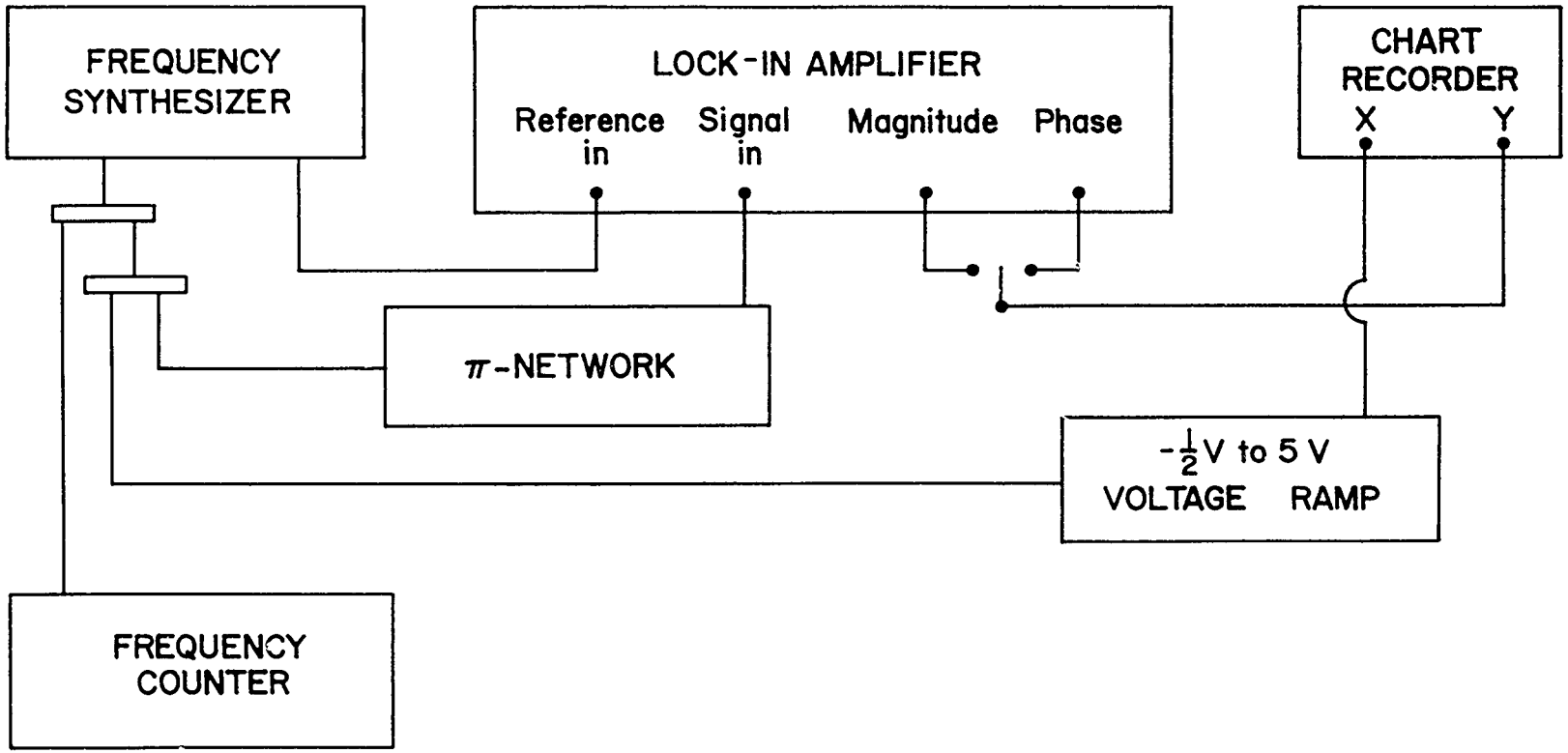

Fig. 4. Block diagram of the equipments used in transmission measurement of resonator plates.

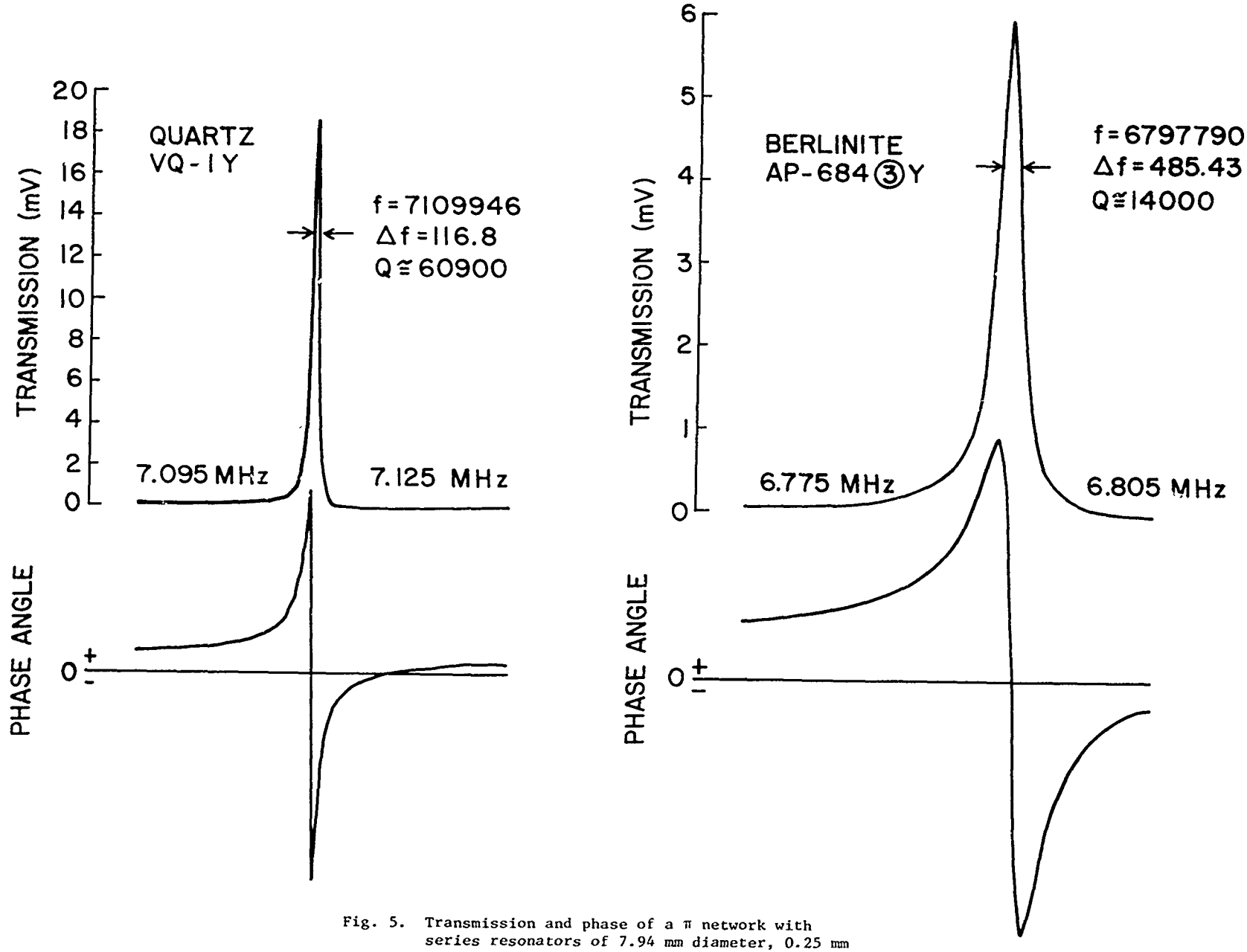

Fig. 5. Transmission and phase of a π network with series resonators of 7.94 mm diameter, 0.25 mm thick circular Y plates of α-quartz and berlinite.

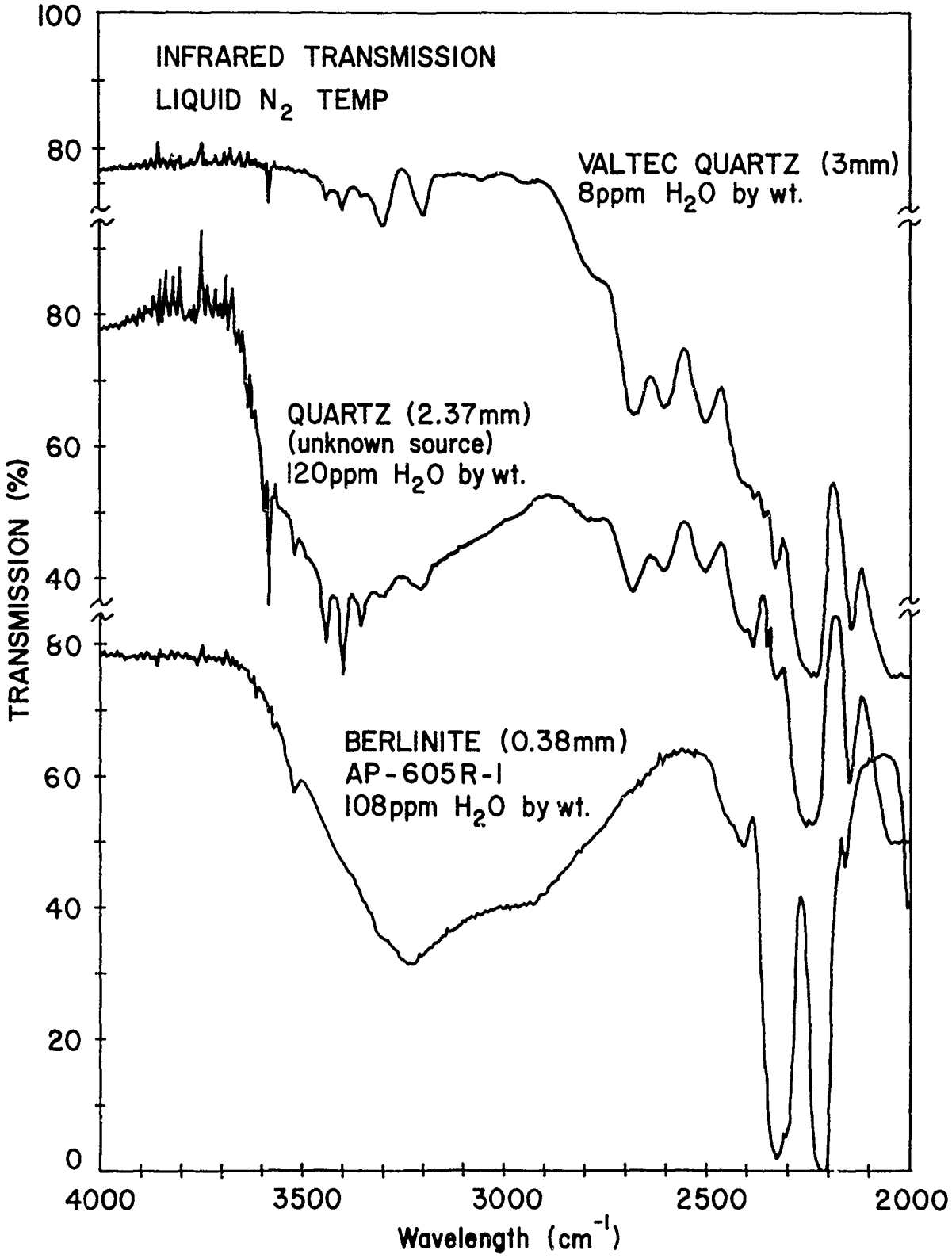

Fig. 6. IR transmittance spectra of Valtec quartz, unknown quartz blank, and berlinite crystals in the range from 4000 to 2000 cm^{-1}.

SOLUBILITY, CRYSTAL GROWTH AND PERFECTION OF ALUMINUM ORTHOPHOSPHATE

E. D. Kolb, R. L. Barns, J. C. Grenier*, and R. A. Laudise

Bell Laboratories
Murray Hill, New Jersey 07974

Summary

In order to improve hydrothermal techniques for the crystallization of $AlPO_4$, we have made studies of its solubility. Contrary to reports in the literature, the temperature coefficient of solubility is negative over this range. However, the magnitude of the solubility is adequate to the crystal growth. Seeded growth was investigated on three seed orientations. The rates were basal - 0.5 mm/da, x - 0.25 mm/da, y - 0.18 mm/da. The quality was substantially better for x and y growth. Voids, cracks, and liquid bubble inclusions were observed. These imperfections are correlated with growth conditions and suggestions for their minimization are made. Etching studies revealed sectoring shallow etch pits and twins, x-ray linewidth studies showed that seeds were severely damaged during cutting and lapping. Etching techniques for preparing undamaged seeds were developed.

Introduction

Aluminum orthophosphate, $AlPO_4$, continues to be of high interest because of its large piezoelectric coefficients and small temperature coefficients of appropriately cut resonators. [1] Because of these properties, use in surface acoustic wave and other devices is likely. However the material which is under investigation in a number of laboratories in the United States and Europe is proving rather difficult to grow reproducibly as large high quality single crystals. Kolb and Laudise [2] reported their extensions of the original hydrothermal synthesis of Stanley [3] and the unpublished work of McBride. [4] This work described techniques for preparing high quality small crystals (nutrient) by reacting aluminum containing compounds in H_3PO_4 and reported methods for the growth of large crystals by dissolving this nutrient in H_3PO_4 and recrystallizing on seeds. These methods were designed to overcome the well known negative temperature coefficient of solubility exhibited by $AlPO_4$ in H_3PO_4. The earliest reported growth of $AlPO_4$ due to Jahn and Kordes [5] suggested methods of growth based on temperature-pressure conditions where the temperature coefficient of solubility was apparently positive and Kolb and Laudise [2] grew crystals under these conditions.

In order to understand and improve hydrothermal techniques for the growth of $AlPO_4$ and to explore whether conditions exist where the temperature coefficient of solubility is truly positive, we decided to make systematic measurements of solubility. With the hope of improving quality and growth rates, we decided it was worthwhile to investigate the effect of seed orientation. With a view toward correlating growth conditions with perfection, we also examined grown crystals visually in an index matching immersion medium, and studied perfection by the use of etching, x-ray diffraction line widths and x-ray topographs.

Experimental

Growth experiments were carried out in Pt lined Morey-type [6] autoclaves of the sort reported previously. [2] Furnaces, temperature control and measurement and general procedures have already been described. [2]

Solubility measurements were carried out by weight loss method we have used for other materials. [7-10] In this method a crystal is kept in equilibrium with an appropriate solution at the desired pressure-temperature conditions for a period of time greater than that necessary to establish equilibrium. Following a rapid quench to room temperature the remaining crystal is weighed and the weight loss is taken to be a measure of the solubility. When the temperature coefficient of solubility is positive, this method is satisfactory provided: (1) regrowth from the solution does not take place on the crystal during or after the quench, (2) but one fluid phase coexists in equilibrium with the solid phase and (3) the crystal is indeed the stable phase at the conditions of the experiment. If the temperature coefficient of solubility is negative these conditions must be met but additional further complications to be discussed below must be considered.

In our earlier work [7] we found that, with a small sacrifice in precision and much less effort, it is possible to carry out weight loss solubility determinations (at least where the solubility is above $\sim$ 1%) in small welded Pt capsules whose volume is one cm^3 or less. The procedure used has been described so that only a brief outline is

*Permanent address: Laboratoire de Chimie du Solide, Universite de Bordeaux 1, 33405 TALENCE, Cedex.

needed here. One or more weighed crystals of $AlPO_4$ together with an appropriate volume of mineralizer were added to a small (0.50 cm ID x 3.8 cm long) open ended Pt capsule. The $AlPO_4$ crystals were prepared by reaction of aluminum oxide or hydroxide with H_3PO_4 under hydrothermal conditions using the techniques previously described for making nutrient.[2] X-ray powder patterns were used to confirm identity. The H_3PO_4 mineralizer molarity was determined by titration against NaOH. Mineralizer volume (typically 0.15 cm^3) was determined with a micro-syringe. The capsule was crimped and welded shut with a D.C. micro-arc welder and placed in a 0.63 cm ID x 20 cm length Tuttle[11] cold seal test tube type autoclave manufactured by Tempress, Inc., State College, Pa. A steel rod partly filled the unused volume of the autoclave in the region above the capsule so as to reduce convection and make the capsule as isothermal as possible. The capsule was pressurized on the outside using water pumped by an air driven intensifier and brought to temperature with a resistance heated furnace and an appropriate temperature controller. Temperatures were measured with chromel-alumel thermocouples contained in a thermocouple well in the bottom of each autoclave. Temperatures are judged to be accurate ±3°C. Pressures were measured with Bourdon gauges (calibrated with a dead weight tester) and are judged to be accurate ±0.5%. The external pressure was chosen so as to approximately balance the internal pressure in the capsule at operating conditions. Balance was estimated from capsule examination following preliminary runs-burst or obviously crushed capsules being evidence of poor balance. Following a run the autoclaves were quenched in ice water, the crystallites were removed from the capsule, quickly rinsed, dried and weighed. Careful examinations for foreign phases, glassy residues (indicating two immiscible fluid phases) and capsule leaks were made at appropriate stages.

Special problems might be expected to be associated with determining the solubility of materials with a negative temperature coefficient. Primarily one must consider the possibility of further weight loss of the specimen due to increased solubility during the quench or even at room temperature before it is removed from the capsule. A series of replicate runs were made to establish equilibrium time and to assure ourselves that weight loss after equilibration at the desired temperature was not contributing significant errors. Redissolving resulting in a few tenths of a percent apparent increase in solubility at all temperatures could give a significant relative error at temperatures where solubilities are low. Under typical conditions, we found that from the beginning of the quench to weighing no more than five minutes were required. In experiments where the weighing was delayed as long as 15 min. no significant difference in solubility was obtained. From this we conclude that the kinetics of dissolution are slow enough during quench and at room temperature that our measurements would not be perturbed by a negative temperature coefficient of solubility. Varying the time that specimens were held at the desired p-T conditions established that for the range of our experiments, equilibrium was established in less than three days. Our equilibrium times were never less than three days.

Results and Discussion

Solubility

Solubility was measured as a function of temperature, pressure and mineralizer concentration over the range 170 - 525°C, 1 - 30 Kpsi (69 - 2070 bar), 0 - 14.6 m (molar) H_3PO_4. H_3PO_4 is the "traditional" solvent for $AlPO_4$ having been used by Stanley,[3] McBride,[4] Jahn and Kordes,[5] Kolbe and Laudise[2] and being used in most current growth studies known to us. It may not be the only useful solvent, but we felt it the one currently most worthy of systematic investigation. Transport and nutrient crystallization measurements have been conducted from 150°-400°C and up to ∿10 m H_3PO_4 establishing $AlPO_4$ as the stable phase. We assumed from the absence of foreign phases in our capsules that $AlPO_4$ is probably stable over the entire range of our experiments. It is well known that $AlPO_4 \cdot nH_2O$[12] phases are stable below about 150°C and $AlPO_4$ in the tridymite form above ∿584°C[13] at 1 atm pressure.

Figures 1(a) and (b) show the solubility of $AlPO_4$ as a function of temperature in 7.58 m H_3PO_4 at various pressures. In general three replicate experiments were made at each temperature, the bar heights indicate the spread in solubilities obtained. These data reveal several features of importance to crystal growth. Solubilities above ∿2% do not occur much above about 300°C suggesting that growth much above that temperature is likely to be impractical. The temperature coefficient of solubility is everywhere negative even over the range of Jahn and Kordes[7] "positive temperature coefficient" growth experiments. Indeed Jahn and Kordes report solubilities with a positive temperature coefficient between 300° and 350°C in 10 - 50% (∿1-7 m) H_3PO_4 at estimated pressures up to ∿200 atm. Their solubilities were typically lower (∿0.1 - 0.6 wgt %) than ours. Their slope was positive everywhere but began to approach 0 at 7 m H_3PO_4. They reported experimental difficulties, did not fully replicate runs and their solubility experiments were in a large autoclave and at a constant percent fill (i.e., constant density*).

Indeed it is possible that while $(\partial s/\partial T)_p$, the temperature coefficient of solubility at constant pressure is negative, $(\partial s/\partial T)_\rho$ the temperature coefficient of solubility at constant density (or percent fill) is positive. Figure 2 shows Kennedy's[14] solubility data for quartz in pure water at several pressures. As can be seen $(\partial s/\partial T)_p$ is negative in some p-T regions. Indeed this "retrograde" solubility behavior for quartz is often considered the classic example of such solubility relationships in hydrothermal systems. No mineralizer was present, so the solubilities are quite low. Since the concentration of solute in the solutions of Fig. 2 is low, it is reasonable to assume that the pressures approximate those of pure water and that the published[15] pressure-volume-temperature data for pure water applies. Thus, these data can be used to establish temperatures where the pressures of Fig. 2 give a constant density (or constant percent fill). This procedure was used to plot the solubility at several densities as a function of temperature (the dashed lines of Fig. 2). As can be seen $(\partial s/\partial T)_\rho$ is everywhere positive. Thus, at least for SiO_2-H_2O, the "mysterious" retrograde solubility behavior is a consequence of the p-v-T characteristics of the solution and does not obtain at constant density. Indeed the solubility data of Laudise and Ballman[16] for the system SiO_2-H_2O-NaOH measured at constant density do not show any retrograde behavior. However, these data cannot be converted to solubility at constant pressure because the concentrations of solute are too high for the p-v-T data of pure water to be applicable and complete pressure data for the system are unavailable. It is worth pointing out that solubility data for Al_2O_3,[7] ZnO,[8] ZnS,[9] and other materials[10] under hydrothermal conditions at constant pressure all show $(\partial s/\partial T)_p$ to be positive. No equation of state for $AlPO_4$-H_3PO_0-H_2O is available so that $(\partial s/\partial T)_\rho$ cannot be determined from the data of Fig. 1. Nevertheless, it is possible that in common with the system SiO_2-H_2O $(\partial s/\partial T)_\rho$ is positive.

*When the fluid is pure water and the autoclave is at conditions when only one fluid phase is present the density = (1/% fill) x 100.

However, as we show from the following considerations, $(\partial s/\partial T)\rho$ for $AlPO_4$ cannot be positive over at least some of the conditions of actual growth. Hydrothermal growth experiments are at constant pressure if growth is by transport in a temperature differential (ΔT) with seeds and nutrient kept at different temperatures. In such a system a density gradient between regions of differing temperatures will allow the equation of state of the particular fluid to be locally obeyed. When growth is by programming the temperature over intervals of many days and over temperature ranges of many tens or hundreds of degrees, the pressure will change with time so that growth is at constant density (neglecting small effects due to deliberate or accidental ΔT's in the system). Thus, it is important to point out that since the commonly used programming sequence[2] wherein crystal growth is achieved by heating autoclaves from ~150-300°C (in 6.1 m H_3PO_4 with fills from 80-82% fill) suggests that for these conditions $(\partial s/\partial T)\rho$ is negative.

Finally we must mention that Jahn and Kordes[5] report growing $AlPO_4$ under the following conditions: 7.58 m H_3PO_4, 70% fill, 326°C (nutrient) bottom of the autoclave temperature and 300°C top of the autoclave (seed) temperature. We[2] attempted to reproduce these results where the nutrient was hotter than the seeds and obtained low growth rates and lack of reproducibility. Indeed it was our experience that growth strategies both at constant percent fill (programmed increases in temperature used to produce supersaturation) and at constant pressure (temperature differences between seed and nutrient used to produce supersaturation with the nutrient colder than the seeds) based on the premise that the coefficient of solubility was negative were always successful. On the contrary, growth strategies assuming a positive coefficient were never reproducibly successful. Thus, if there is a region where $(\partial s/\partial T)\rho$ is positive, it must be rather small in extent.

Figure 3 shows log s vs 1/T for $AlPO_4$ in 7.58 m H_3PO_4 at several pressures. As can be seen, the Van't Hoff equation is quite well obeyed between 150 and 300°C with ΔH, the heat of "solution" or better the heat of reaction with the mineralizer, from the slopes of Fig. 3 being -8.8 ± 0.5 Kcal/mol. Above 300°C either a second linear region with a slope suggesting a ΔH of about -3 Kcal/mol or a departure from linearity occurs. It is tempting to suggest that the temperature and water pressure dependence of the ortho-meta-pyro equilibria in the phosphoric acids:

$$2H_3PO_4 \rightleftarrows H_4P_2O_7 + H_2O \qquad (1)$$

$$H_4P_2O_7 \rightleftarrows 2HPO_3 + H_2O \qquad (2)$$

could produce appropriate changes in the solvent at 300°C so as to cause a relatively abrupt change in the dissolving reaction.*

Figure 4 shows the dependence of $AlPO_4$ solubility on H_3PO_4 concentration. It is well known that insoluable alkali metal phosphates are solubilized in acid media by the formation of acid phosphates. The formation of the soluble "super phosphate" fertilizer, $Ca(HPO_4)$, from apatite, $Ca_3(PO_4)_2$ is an economically important example.[17] Thus it is not unreasonable to associated the dissolving of $AlPO_4$ with a reaction of the type:

$$AlPO_4 + 2H_3PO_4 \rightleftarrows Al(H_2PO_4)_3 \qquad (3)$$

Analogous reactions could form $Al_2(HPO_4)_3$ and appropriate reaction products with $H_4P_2O_7$, and HPO_3. In the past we[18] have discovered a number of hydrothermal systems where the mineralizer reactions analogous to Eq. (3) go essentially to completion allowing one to determine the number of moles of mineralizer reacting with each mole of solute so as to give credence to the choice of dissolving reaction and to the nature of the dissolved species. In Fig. 5 we have replotted data of Fig. 4 as molarity of $AlPO_4$ vs molarity of H_3PO_4. The slope of the plots of Fig. 5 suggests that the mole ratio $H_3PO_4/AlPO_4$ varies from ~5 for H_3PO_4 concentrations above 7 m at 170°C and 10 Kpsi. If at these conditions the dissolving reaction goes to completion, a possible reaction is:

$$AlPO_4 + 5H_3PO_4 \rightleftarrows Al(H_2PO_4)_6^{-3} + 3H^+ \qquad (4)$$

However, whatever the dissolving reaction(s) the ΔH's calculated from Fig. 3 suggest they are exothermic. It might be pointed out that exothermic heats of solution (negative temperature coefficients of solubility) are rather common for soluble phosphates and acid phosphates at ambient pressure.

Figure 6 shows the effect of pressure on solubility and indicates the greatest increase with pressure at the lower temperatures. If Eq. (3) or Eq. (4) describes the dissolving reaction it would be expected that the volume of the species on the right is smaller leading to an increase in solubility with pressure.

Growth and Perfection

Seed Orientation

In order to investigate the effect of seed orientation on growth rate and perfection, a series of runs using seeds of various orientations was carried out. The condtions were: 6.1 m H_3PO_4, 82% fill, ΔT between seeds and nutrient 2-5°C with the seeds in the lower portion of the autoclave and the nutrient contained in a bsaket in the upper portion which was always at a lower temperature and rate of temperature increase 1.6-2°C/da. (see ref. 2) for details of this growth procedure). All experiments began with the seed region 151 ± 1°C and in general concluded when the seed region was at ~210°C. The growth rates obtained for seeds whose faces are as indicated were:

(0001) (basal plane) - 10-20 mil/da (0.25-0.50 mm/da)

$(11\bar{2}0)$(X cut)* - 9-12 mil/da (0.23-0.30 mm/da)

$(10\bar{1}0)$(Y cut)* - 5-6 mil/da (0.12-0.15 mm/da)

$(01\bar{1}1)$(minor rhombohedral face) - 5 mil/da (0.12 mm/da)

$(10\bar{1}1)$(major rhombohedral face) - 6 mil/da (0.15 mm/da).

*Although no data are available for hydrothermal conditions, at ambient the ionization constants of the first H^+ for the acids are $K_{H_3PO_4} > K_{H_4P_2O_7} > K_{HPO_4}$. Data for mono-basic acids[18] under hydrothermal conditions show that ionization constants decrease rapidly as temperature is raised and increase with pressure. Quantitative calculation of these effects for the phosphoric acids awaits appropriate data.

*X and Y are the crystallographic axes in the I.R.E. nomenclature (see R. A. Heising "Quartz Crystals for Electrical Circuits" Electronic Indus. Ass., Washington, 1946, p. 60 ff).

The relative growth rates are in general agreement with the morphology of the equilibrium form as judged from observing spontaneously nucleated crystals. Spontaneously nucleated crystals are bounded by small prism $(10\bar{1}0)$ faces and terminated by minor and major rhombohedral faces. Thus, it would be expected that the rates on prism, major and minor faces are smaller than for $(11\bar{2}0)$ and (0001) faces since the latter two do not exist as bounding equilibrium surfaces.

Perfection Studies

Much can be learned by macroscopic examination of grown crystals. The two principal imperfections readily observable are "crevice flawing" and cracks. Figure 7 illustrates rather severe crevice flawing on an X-cut seed. Growth conditions and growth rates for the crystals examined for perfection are quoted in the previous section. When growth is on a nonequilibrium face there is a tendence for higher growth rates and the formation of "hillocks" which tend to protrude across the solute depleted diffusion layer near the growing face. The tips of such hillocks experience a higher supersaturation and tend to grow faster than the regions between hillocks. This phenomenon is the hydrothermal analogue of constitutional supercooling and may be viewed as a kind of dendritic growth.[19,20] Entrapment of solution between hillocks leads to bubbles of solution in the grown material which are observed as "veils" Thus, growth at slower growth rates and on equilibrium faces would be expected and was observed to produce a greatly reduced tendency for crevice flawing.

Cracks of the sort shown in Fig. 8 are often observed in hydrothermally grown material. In the case of quartz[21] we found that they were associated with strain caused either by strain in the seed propagating into the grown crystal or by strain associated with dislocations arising at inclusions in the new growth. It was further observed in quartz[21] that disordered regions in seeds propagated into crystals and strain free seeds were much less likely to produce cracked growth. Polariscopic examination of $AlPO_4$ of the sort used on quartz[21] revealed that strain was generally present and tended to be localized near cracks and veils. Since veils are caused by local bubble inclusions where solvent is trapped in the grown crystal, it is reasonable that these inclusions will be a source of strain which, if excessive, will lead to cracks. Thus, processes designed to reduce bubbles and veils have proved helpful in reducing cracking. Systematic screening of seeds in a polariscope once seed quality is high enough to permit a reasonable yield of strain free crystals would also be indicated.

Based on the above macroscopic observations of grown crystals, we decided that in order to improve the evaluation of $AlPO_4$, it was important to develop a suite of techniques capable of distinguishing:

(1) microscopic imperfections such as veils, bubbles and foreign phases within the interior of the crystal.

(2) twinning and low angle grain boundaries in seeds and grown material,

(3) damage in seeds as a result of seed preparation,

(4) dislocations in seeds and grown material.

To evaluate imperfections within the crystal, we have found that both macroscopic and microscopic examinations in index matching immersion oil can be a most useful technique. Figure 9 shows an example of a rather imperfect crystal as viewed in immersion oil. It is worth pointing out that many of the imperfections revealed in Fig. 9 would have escaped observation in the absence of the index matching fluid. The imperfections are principally "veils". Observation at higher magnification (Fig. 10) shows, as expected, that the veils are composed of microscopic bubbles entrapping hydrothermal fluid. It is interesting to note that the degree of fill of the bubbles approximates that of the autoclave growth conditions, thus, substantiating the procedures used by geochemists, such as Roedder[22] where degree of fill of liquid inclusions in minerals is taken as a fair measure of the density of the growth solution.

Twinning and low angle grain boundaries are best revealed by etching. An appropriate etch is a saturated aqueous solution of NH_4HF_2 at room temperature. Etching times of the order of 30 min. reveal many features. Figure 11 shows two sorts of features best revealed by such etching, misoriented regions (Fig. 11a) and growth striae (Fig. 11b). Misoriented regions propagate from the seeds so that careful seed inspection and selection using etching is necessary. Growth striae could result in inhomogeneities in the crystal affecting, for example, acoustic Q and may need to be taken into account in interpreting such measurements.

As a result of etching studies, we become concerned that the seed damage caused by sawing and lapping might be propagating into grown material. To evaluate such damage, x-ray diffraction linewidth measurements were used. A single crystal diffractometer having very narrow source slits and a wide area detector was used with CuK_α radiation. Seeds were cut with a diamond impregnated wire using silicon carbide slurry in water and lapped with 600 mesh silicon carbide. Figure 12 (curve A) shows the diffraction curve for the (200) reflection following this procedure. Experience indicated that linewidths of the magnitude shown in Fig. 12 (curve A) were associated with fairly severe damage. The sample of Fig. 12 was further lapped with 303-1/2 and 305 Al_2O_3 and then etched with saturated NH_4HF_2 at room temperature for 30 min. The linewidths of Fig. 1 (curve B) result. Experience with other mateials such as Si indicates that a linewidth of the magnitude of curve B can only be obtained from a material with negligible damage. Thus, Al_2O_3 lapping and etching were adopted as standard seed preparation procedures.

Dislocations are a common feature of hydrothermal crystals and have been extensive studied in quartz.[23,25] Therefore, using CuK_α radiation and procedures previously described for quartz,[25] we decided to take preliminary Lang x-ray topographs of $AlPO_4$. An example is shown in Fig. 13. As can be seen, the dislocation density is very high. The dark vertical lines of Fig. 13 are reflections and should not be associated with regions of unusual dislocation density. It would be expected that processes analogous to those used in quartz growth (seed selection, etching to remove damage in seeds, avoiding inclusions, etc.) would be effective in reducing and perhaps even eliminating dislocations in $AlPO_4$.

By combining the procedures to improve quality described above, it is possible to grow crystals which, while not perfect, are nevertheless of quite respectable quality as shown in Fig. 14. Important features in obtaining improved quality are as follows: (1) Growth on orientations other than (0001), especially X and Y-cut seeds produce crystals more free of misoriented regions, veils and cracks. This is understandable since (0001) is the fastest growing surface with a higher tendency for growth hillocks, dendritic growth and bubble inclusions. (2) Imperfections present in seeds tend to propagate into grown crystals so that seed screening by means of etching should be

used to select seeds free of disordered regions. Etching to remove saw and lapping damage should also be used as standard seed preparation procedure. As the quality of seeds improves, polariscopic examination and x-ray topography become appropriate for seed selection. (2) Past experience with other materials would suggest that slower growth rates and further attention to the chemical purity of starting materials would be profitable directions for further investigation.

Conclusions

Systematic studies of solubility have shown that in H_3PO_4, $AlPO_4$ has a negative temperature coefficient of solubility at constant pressure so that growth procedures at constant pressure must be designed to overcome this difficulty. The negative temperature coefficient of solubility may be explained on the basis of the p-v-T behavior of the solvent so that at constant fill, the coefficient may be positive in some regions, although, at least at 80-82% fill, growth experiments at constant density show that the coefficient is negative. In the system SiO_2-H_2O, it was shown that although the temperature coefficient of solubility is negative at constant pressure it is positive at constant density. The solubility of $AlPO_4$ obeys the Van't Hoff relationship giving quite different heats of solution above and below 300°C suggesting that changes in the ortho-meta-pyro phosphoric acid equilibria with temperature may cause differences in the nature of the solvent near 300°. The dependence of solubility on H_3PO_4 concentration gives a ratio $H_3PO_4/AlPO_4$ of ~5 at higher H_3PO_4 concentrations at 170°C suggesting $(Al(H_2PO_4)_3^3$ as a possible species in solution. The solubility dependence on pressure is as might be expected if the dissolving involves the formation of $Al(H_2PO_4)_3$ or related ions.

Techniques for assessing perfection including macroscopic and microscopic examination in an index matching medium, etching, x-ray diffraction linewidth and Lang x-ray topography showed that crevice flawing (dendritic growth), cracks, veils (bubble inclusions), misoriented regions and dislocations all occur in $AlPO_4$. Seed selection and etching to remove seed damage together with growth on orientations other than (0001) especially on Y-cut seeds resulted in considerable improvement in $AlPO_4$ quality.

Acknowledgements

We would like to thank A. J. Caporaso for his assistance with the growth experiments and for discussions, and P. A. Freeland and J. R. Patel for x-ray topographs.

References

1. Y. P. Chang and G. R. Barsch, IEEE Trans. on Sonics and Ultrasonics (1976) 127. See also A. Jhunjhunwala, J. F. Velenio and J. C. Field, J. Appl. Phys. 48, 887 (1977).

2. E. D. Kolb and R. A. Laudise, J. Cryst. Growth, 43, 313 (1978).

3. J. M. Stanley, Ind. Engr. Chem. 46, 1684 (1954).

4. W. R. McBride, Dept. of Navy, Naval Weapons Center, China Lake, California, private communication.

5. Von W. Jahn and E. Kordes, Chem. Erde, 70, 75 (1953).

6. G. W. Morey and P. Niggli, J. Am. Chem. Soc. 35, 1086 (1913)

7. R. L. Barns, R. A. Laudise and R. M. Shields, J. Phys. Chem. 67, 835 (1963). (Al_2O_3 Solubility).

8. R. A. Laudise and E. D. Kolb, Amer. Mineralogist 48, 64 (1963). (ZnO Solubility)

9. R. A. Laudise, E. D. Kolb and J. P. DeNeufville, Amer. Mineralogist 50, 382 (1965). (ZnS Solubility).

10. See R. A. Laudise, Endeavour 28, (Sept. 1969) number 105, p. 114 for a review of hydrothermal solubility and see D. J. Marshall and R. A. Laudise "Crystal Growth, p. 557 Supplement to J. Phys. Chem. Solids, Pergamon Press, New York, 1967 for a discussion of solubility of KTN $[K(Ta_{0.65}Nb_{0.35})O_3]$. See also D. J. Marshall and R. A. Laudise, J. Cryst. Gr. 1, 88 (1967) for solugility of $LiGaO_2$.

11. See R. A. Laudise and J. W. Nielsen, Solid State Physics 12, 149 (1961), Ed. by F. Seitz and D. Turnbull, Academic Press or R. Roy and O. F. Tuttle, Phys. and Chem. Earth 1, 138 (1956).

12. E. Z. Arlidge, V. C. Farmer, B. D. Mitchell and W. A. Mitchell, J. Appl. Chem. 13, 197 (1973).

13. L. H. Cohen and W. Klement, Am. Mineralogist 58, 1086 (1973).

14. G. W. Kennedy, Econ. Geol. 45, 639 (1950).

15. G. W. Kennedy, Am. J. Sci. 248, 530 (1950).

16. R. A. Laudise and A. A. Ballman, J. Phys. Chem. 65, 1396 (1961).

17. See for example, N. V. Sidgwick, "The Chemical Elements and Their Compounds" Vol. I, Clarendon, Oxford, 745 (1950).

18. S. P. Clark, Jr., "Handbook of Physical Constants" published by Geological Society of America (Memoir 97), New York, 1966, p. 401 ff.

19. R. A. Laudise, "The Growth of Single Crystals" Prentice Hall, Englewood Cliffs, N.J. 109 (1970).

20. R. A. Laudise, in "Treatise on Solid State Chemistry" Vol. 5, Ed. by N. B. Hannay, Plenum Press, New York, 435 (1975).

21. R. L. Barns, E. D. Kolb and R. A. Laudise, J. Cryst. Gr. 34, 189 (1976)

22. See for example, E. Roedder in "Data of Geochemistry Chapter JJ", M. Flascher, Editor, U.S. Govt. Printing Office, Washington, 1972.

23. L. A. Gordienko, V. F. Musikov, V. E. Khaoz, L. I. Trinober, Soviet Phys. Cryst. 14 454 (1969).

24. A. R. Lang and V. F. Musikov, J. Appl. Phys. 38, 2477 (1967).

25. R. L. Barns, P. E. Freeland, R. A. Laudise, and J. R. Patel, J. Cryst. Gr. 43, 676 (1978).

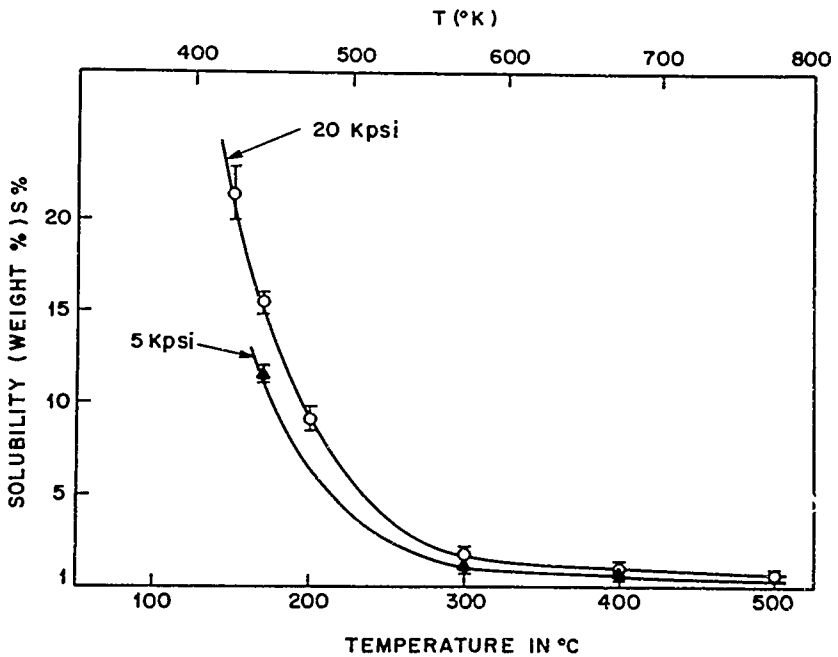

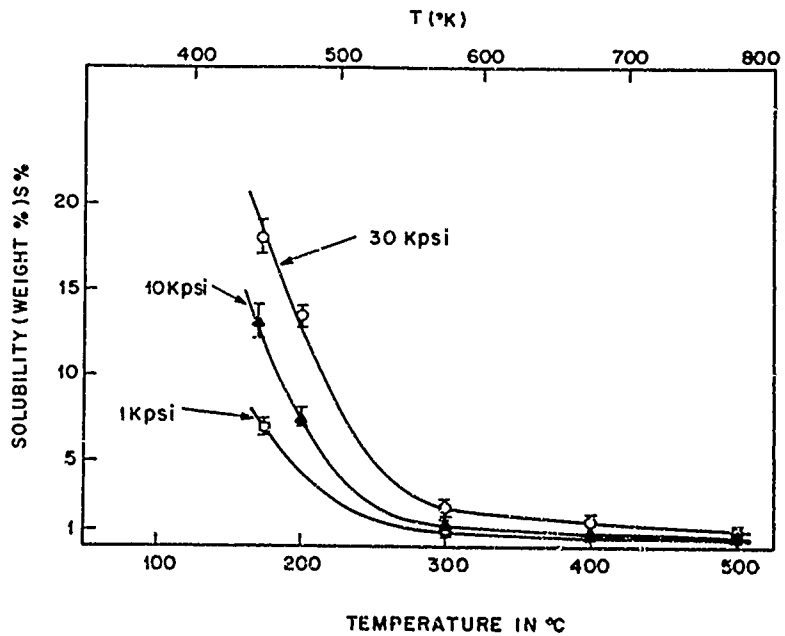

Fig. 1 Weight percent solubility of $AlPO_4$ as a function of temperature in 7.58 m H_3PO_4 (a) 5 and 20 Kpsi, (b) 1,10,30 Kpsi.

FIGURE 1 (a)

FIGURE 1 (B)

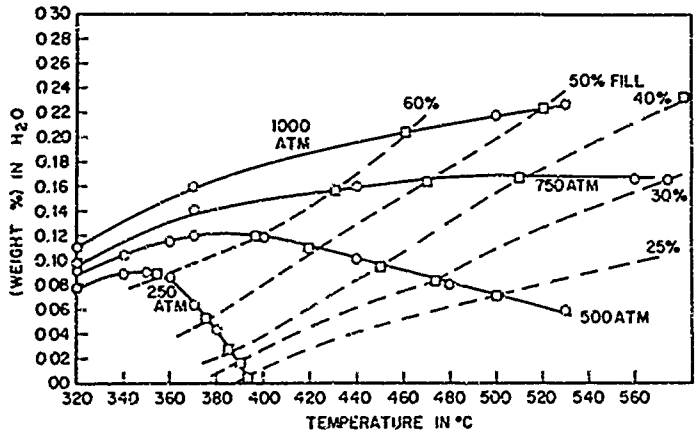

Fig. 2 Solubility of SiO_2 (data of Kennedy)[14] in H_2O as a function of temperature at constant pressure and at constant fill.

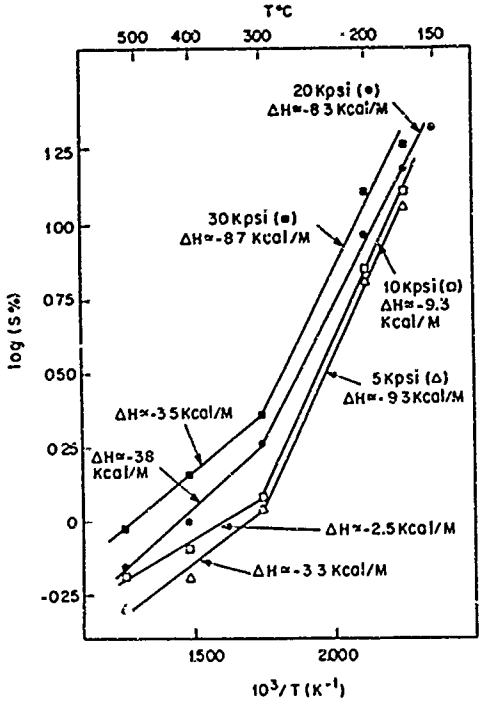

Fig.3 Log solubility of $AlPO_4$ as a function of absolute temperature in 7.58 m H_3PO_4 at several pressures

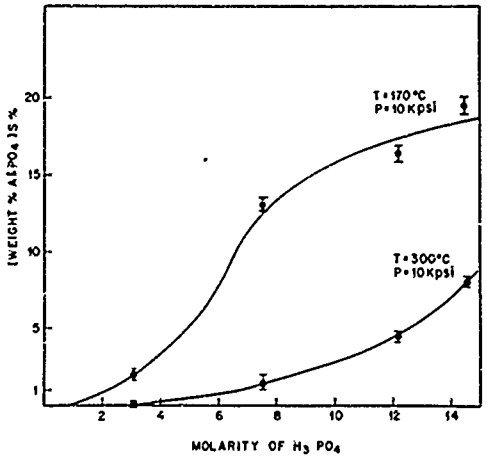

Fig. 4 Solubility of $AlPO_4$ as a function of H_3PO_4 concentration at 170 degrees C and at 300 degrees C at Kpsi

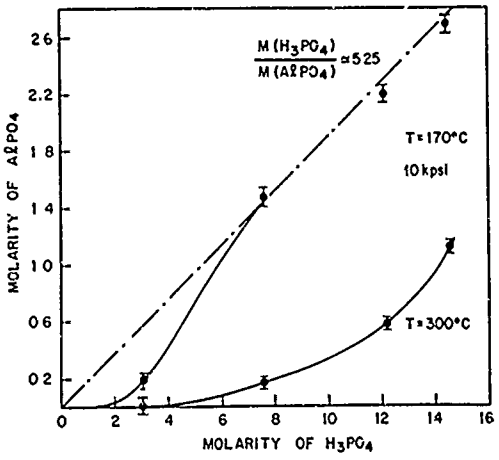

Fig. 5 Molarity of $AlPO_4$ vs. Molarity of H_3PO_4 (from the data of Fig. 4).

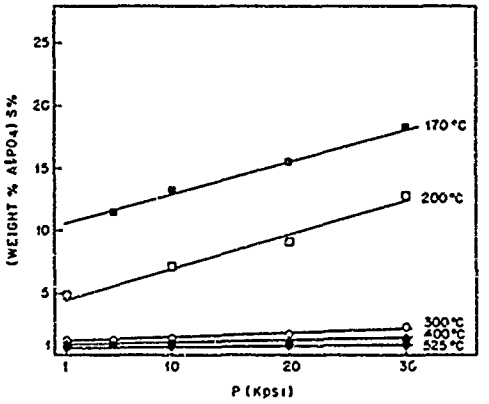

Fig. 6 Solubility of $AlPO_4$ as a function of pressure in 7.58 m H_3PO_4 at several temperatures.

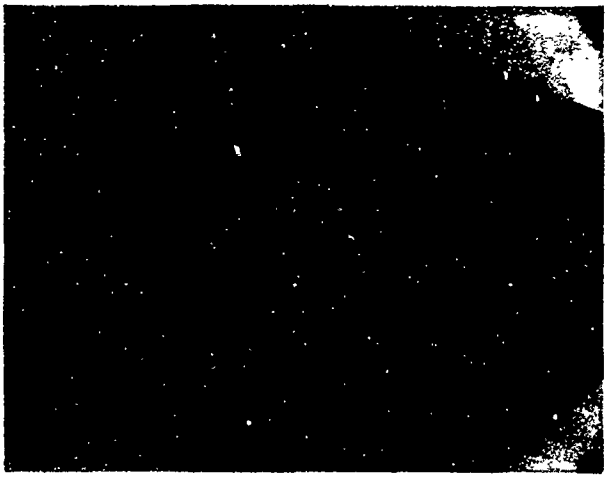

Fig. 8 Cracks in $AlPO_4$ - Growth on $(10\bar{1}1)$ seed, crystal size ∿3 cm max dimension.

Fig. 9 $AlPO_4$ crystal in index matching medium - Growth on (1120) seed, crystal size ∿3 cm.

Fig. 7 Crevice flawing in $AlPO_4$ - Growth on X-cut (11$\bar{2}$0) seed, crystal ∿3 cm max dimension

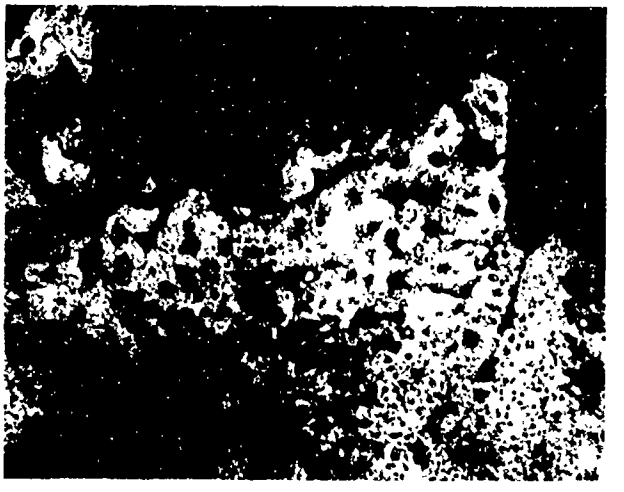

Fig. 10 Bubbles in $AlPO_4$ in index matching medium.

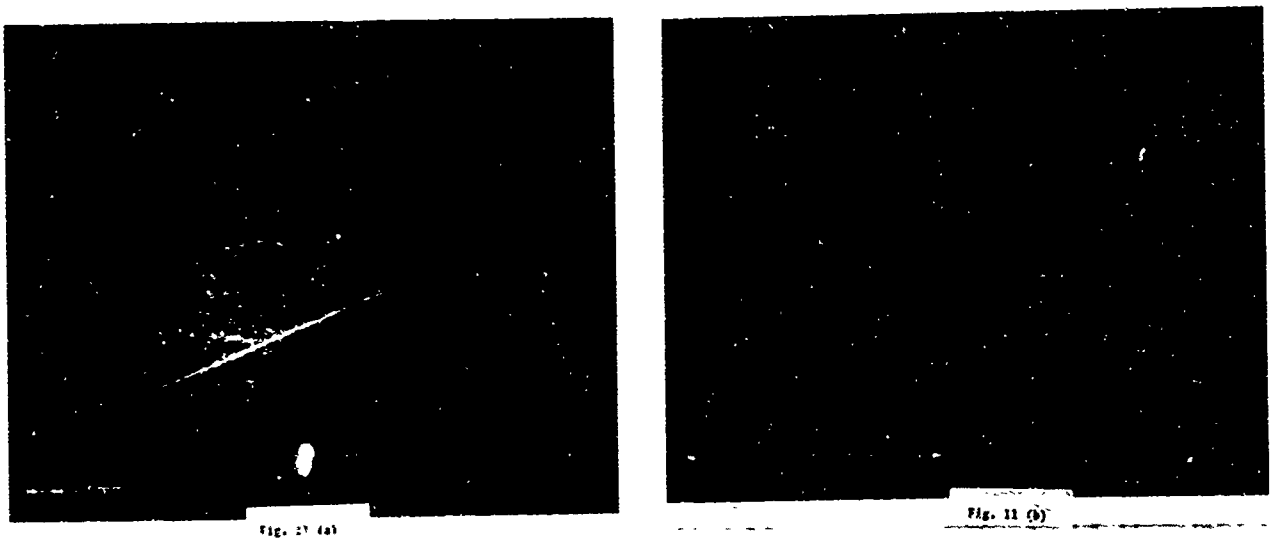

Fig. 11 Etched crystals showing (a) misoriented regions and, (b) growth striae. (a) Growth on X-cut $(11\bar{2}0)$ seed, max. dimension 3 cm, (b) Growth on y-cut $(10\bar{1}0)$ seed, striae width ~0.5 mm.

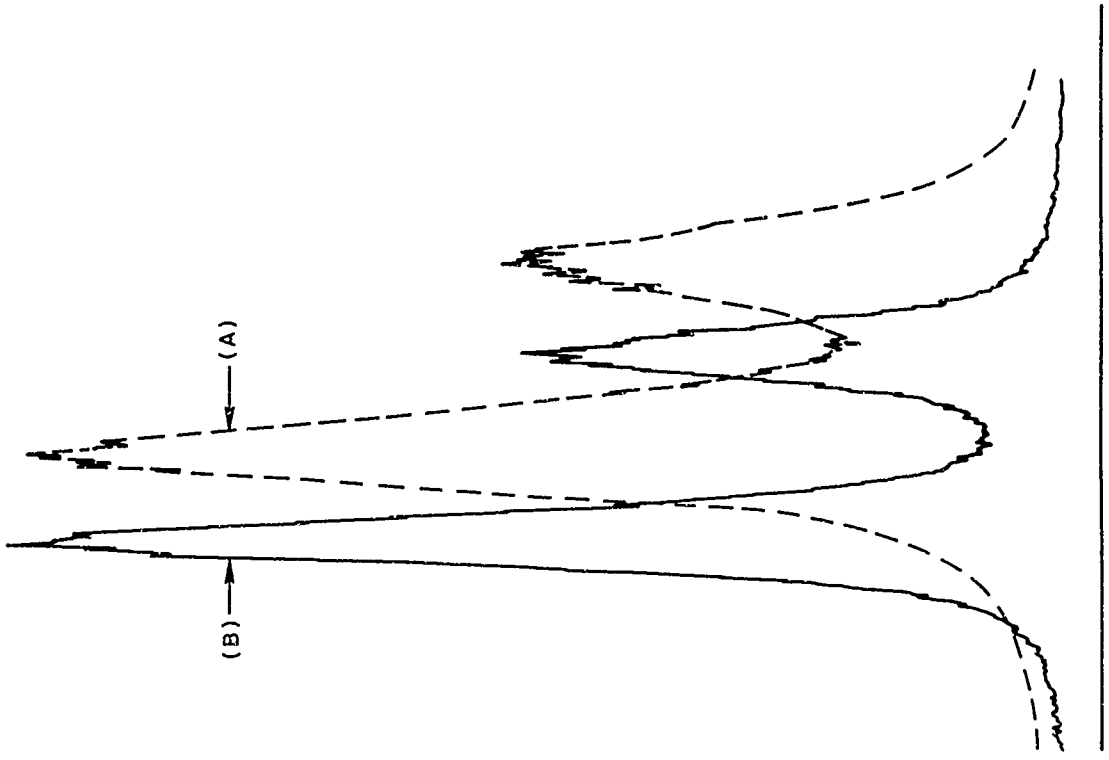

Fig. 12

X-ray diffraction linewidths of $AlPO_4$ crystals. (A) Damaged by surface preparation. (B) Etched (curves offset horizontally for clarity).

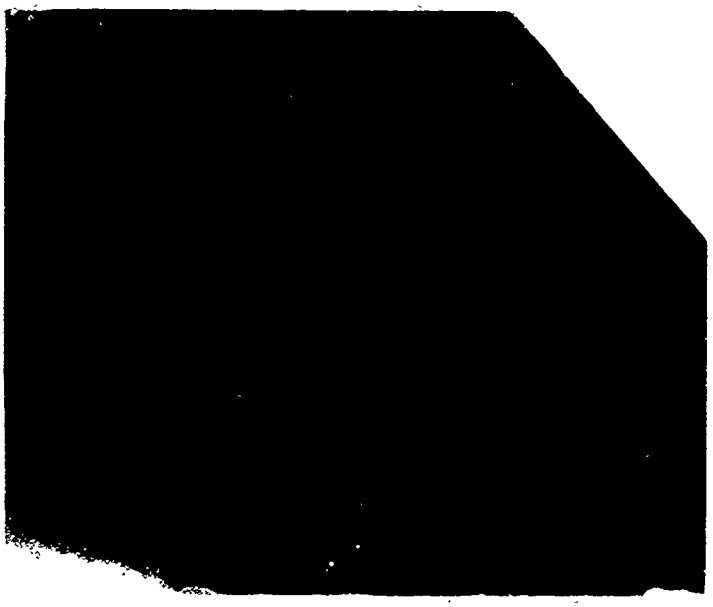

Fig. 13 X-ray topograph of $AlPO_4$ grown on $(10\bar{1}0)$ seed.

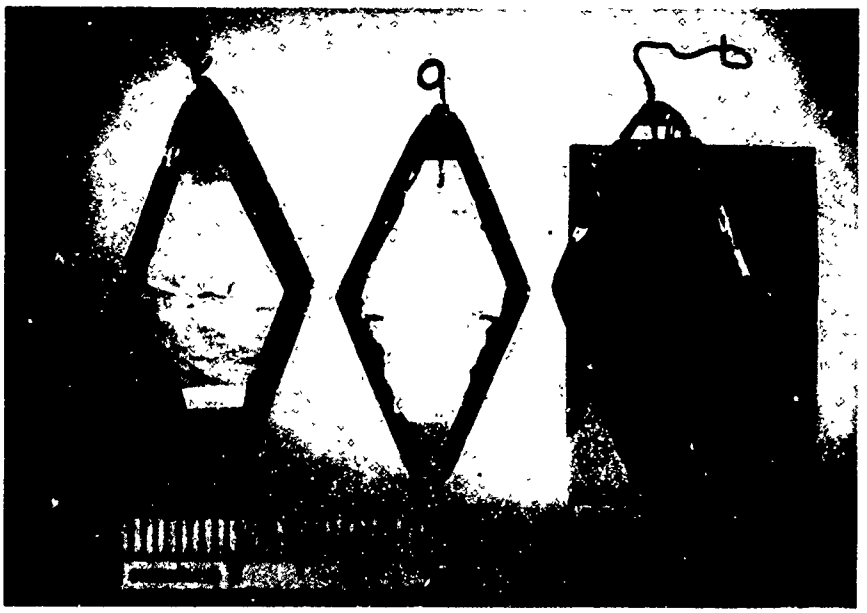

Fig. 14 Good quality $AlPO_4$ crystal, grown on Y-cut $(10\bar{1}0)$ seed at 5 mil/day.

POINT DEFECTS AND RADIATION DAMAGE PROCESSES IN α-QUARTZ

David L. Griscom

Naval Research Laboratory
Washington, D.C. 20375

Abstract

The natures of point defects in α-quartz are briefly reviewed, including the results of a number of very recent electron spin resonance (ESR) studies. Some common impurity-related defects are considered, although emphasis is placed upon those defects encountered in electronic-grade and premium-Q quartz crystals. Only in a few cases have known defect centers been positively correlated with specific optical absorption bands. Transient optical absorption and luminescence have been measured in a field-swept synthetic quartz crystal and in several high purity fused silicas following pulsed irradiation by 500 keV electrons. The results are interpreted as indicating the formation of transient E' centers and perhaps transient oxygen vacancies. Various cathodoluminescence, radioluminescence, and photoluminescence spectra of α-quartz and fused silica are also reviewed. Results found in the literature, together with the present time-resolved data, strongly indicate that a luminescence spectrum peaking near 4.3 eV is due to the recombination of electrons with holes trapped at the sites of isolated oxygen vacancies. A ubiquitous blue luminescence (∿ 2.8 eV) is possibly associated with the formation of transient oxygen vacancy-peroxy linkage intimate pairs. Other possibilities and data are also discussed.

Introduction

It is well known that quartz crystal oscillators are subject to frequency offsets and changes in acoustic loss as a consequence of radiation-induced charge trapping at point defects. An excellent review of this topic has been provided by King and Sander[1], who related both the transient and steady-state frequency offsets to radiation-induced detrapping of positively charged interstitial cations from the sites of one particular impurity-related point defect, the substitutional Al^{3+}. In turn, the many known variants of the so-called "Al center" were comprehensively reviewed by Weil,[2] who emphasized the detailed characterizations that have been possible by means of the technique of electron spin resonance (ESR). Many other important studies have attempted to correlate radiation-induced changes in quartz oscillators with the formation of point defects by making use of other spectroscopic techniques such as optical and infrared spectroscopy[3], radioluminescence[4], and photo conductivity[5] (the literature cited here is exemplary and far from exhaustive). In all of the latter investigations, the respective authors have assumed or attempted to demonstrate correlations between certain measured spectroscopic properties and the presence of specific defect centers previously delineated by ESR. An example of particular relevance has been the association of the radiation-induced A_1 and A_2 optical absorption bands (near 2.0 and 2.6 eV, respectively) with the Al center. Unfortunately, while a large number of studies have repeatedly indicated a connection between the A bands and the Al center, a one-for-one correlation does not seem to exist.[6,7] Moreover, potential correlations between various observed luminescence peaks and any known ESR centers have been regarded as even more tentative.[2,4]

Clearly, the road to a general understanding of the role of point defects in affecting the behavior of quartz oscillators in radiation environments lies in developing further relationships between the various defects characterized by ESR and the other forms of spectroscopic data which are frequently obtained. It is of course evident that the possible influences of defects other than the Al center should be considered. Griscom[8] has recently reviewed a wide range of defect and impurity centers in α-quartz and fused silica, focusing on the ESR characterizations but also listing the very few cases in which firm correlations have been established between these defects and certain well defined optical absorption bands. The present paper seeks to extend, rather than duplicate, the summary of Ref. 8, to which the reader is referred for many important details. In particular, the present work will undertake a critical review of recent radioluminescence[4] and cathodoluminescence[9,10] studies of α-quartz, including the results of transient absorption and and luminescence measurements following pulsed irradiation[11,12] and taking note of very recent discoveries in the areas of ESR[13] and electron microscopy.[14]

Defects and Impurities in α-Quartz

As a minimal background for the following sections, a brief discussion is given of the natures of a few pertinent defect and impurity configurations in α-quartz which can trap charges upon exposure to ionizing radiation. Further details can be found, e.g., in Refs. 2 and 8.

Impurity Centers

The Al Center. The best known impurity center in α-quartz, and perhaps the one of greatest importance to the performance of quartz resonators under radiation conditions, is the Al center. It consists of an electron hole trapped at the site of an "Al^{3+}" substitutional for an "Si^{4+}" in the lattice. Since the substitutional aluminum requires an extra electron to complete all four tetrahedral bonds, it is generally charge compensated in its pre-irradiation state by a monovalent cation (usually, $M^+ = H^+$, Li^+, or Na^+) in a nearby interstitial channel. A shorthand notation has been developed wherein the pre-irradiation state of the substitutional aluminum is designated by $[\,Al/M^+\,]^o$, where the superscript outside the brackets indicates the overall electral charge with respect to a

normal lattice site. Upon irradiation at room temperature, a hole (e^+) is trapped on one of the four oxygens surrounding the aluminum; the interstitial cation, no longer needed for compensation, diffuses away. This "bare" Al center, sometimes designated $[Al_e+]^o$, was originally reported in natural smoky quartz by Griffiths, Owen, and Ward[15] and was interpreted in some detail by O'Brien.[16] O'Brien's model, illustrated in Fig. 1, finds the hole trapped in the non-bonding 2p oxygen orbital perpendicular to the plane defined by Al-O-Si. A body of evidence suggests considerable structural relaxation at the defect site so that the Al-O(hole) bond length becomes substantially longer than the normal Si-O distance in quartz (see Ref. 8 for further discussion); this relaxation may be responsible for the observed positions of the optical A-bands (see below) which are not theoretically explained otherwise.[17]

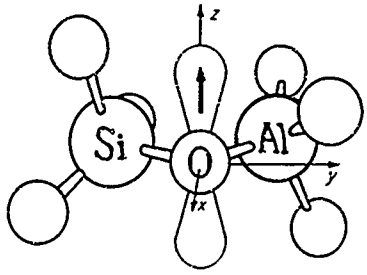

Fig. 1 Steric representation of the $[Al_e^+]^o$ trapped hole center in α-quartz (After Ref. 8.)

As mentioned in the Introduction, a firm correlation between the Al center and the A_1 and A_2 optical bands is lacking. Weeks[6] found a partial correlation between these bands and the $[Al_e^+]^o$ ESR upon γ-irradiation and subsequent thermal decoloration of a synthetic crystal containing 70 ppm Al and 400 ppm Na. However, reirradiation restored the optical bands exactly but gave an $[Al_e^+]^o$ spectrum which was a factor of three larger than after the original irradiation.[6] An explanation of this result is perhaps to be found in the work of Nassau and Prescott,[7] who in performing similar experiments on other synthetic crystals have correlated the $[Al_e^+]^o$ ESR with an optical band at 2.9 eV (which they designated A_3). Since the A_1 and A_2 bands can occur independently of the A_3 band,[17] it is possible e.g., that the latter band was weaker than and obscured by the former in Week's sample. In any event, the origin of the A_1 and A_2 bands should be considered uncertain.

The Ge centers. The most extensively studied extrinsic trapped-electron centers in α-quartz have involved silicon-substituted germanium. Although these have been investigated in synthetic α-quartz deliberately doped with Ge, their influence in electronic grade crystals cannot be ruled out due to the minute numbers of trapped charges concerned (∿ 1 ppm) and the difficulty of analyzing for germanium. In any event, the "Ge center" is a model for a class of defects involving substitutional impurities having the same valence as silicon, but a greater electron affinity. Two types of "bare" Ge centers $[Ge(I,II)_e^-]^{-1}$ have been discussed in the early literature,[18-20] although it has recently been demonstrated that Ge(II) is essentially an excited state of Ge(I).[21] (The shorthand notation has the same meaning as above; e^- stands for a trapped electron and the Roman numerals denote the two variants.) Ge(I) and Ge(II) have been observed only when irradiation was carried out at a cryogenic temperature (e.g., 77K); upon warmup two other germanium-related species, the Ge(A) and Ge(C) centers were observed.[20] The latter were shown to be cation-compensated, charge neutral defects which were denoted $[Ge(A,C)_e^-/M^+]^o$, where $M^+ = Na^+$ or Li^+. Recent work[21] has confirmed the suggestion[20] that $[Ge(A)_e^-/M^+]^o$ results from the capture of a mobile M^+ ion at the site of a $[Ge(II)_e^-]^{-1}$ defect and has shown that the corresponding relationship exists between Ge(C) and Ge(I). It has been demonstrated[22] that the Ge(A,C) centers have optical absorption bands at 4.43 eV.

By x-irradiating alkali- and hydrogen-doped α-quartz samples at 77K, Mackey[20] was able to identify a series of positively charged Al centers still involving the interstitial cation; in the familiar notation, these were denoted $[Al_e^+/M^+]^+$, where $M^+ = Li^+$, Na^+, or H^+. The precursors of these centers in the unirradiated materials were inferred to be the cation-compensated substitutional aluminum $[Al/M^+]^o$. Mackey[20] found that when the samples were warmed to the vicinity of room temperature the holes (and electrons) remained trapped but that the cations diffused away from the aluminum sites and arrived at the sites of Ge(I,II) centers to form the more stable $[Ge(A,C)_e^-/M^+]^o$ defects (see above and Fig. 2). Interestingly, Martin et al.[23] report that $[Al_e^+/M^+]^+$ centers are not formed in electronic grade and premium-Q quartz samples x-irradiated at 77K[23] even though $[Al/M^+]^o$ sites are evidently present. Presumably, this result is related to the extremely low (though unknown) germanium concentration in the latter materials.

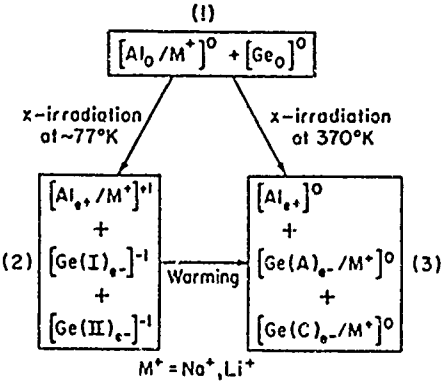

Fig. 2 Kinetic relationships among paramagnetic centers in germanium doped α-quartz. (After Ref. 20.)

Other extrinsic defect centers. Some other defects of conceivable relevance to the quartz oscillator problem are the $GeHLi_2$ centers[24], the nearly analogous GeH_3 centers[25], the so-called β-centers[26] $[Ge_e^-/Na^+, M,N]^o$ where M, N = Na or Li, and the proton-compensated Ti^{3+} centers,[27] In the former two cases, preexisting lithium- or protron-compensated substitutional Ge^{2+} ions are envisioned to capture a radiation-produced hydrogen atom. Correspondingly, the titanium-associated defect appears to result from the capture of a mobile H^o at the site of a substitutional Ti^{4+}. The hydrogen atoms, which have been observed by ESR after irradiation at 77K,[23,27-29] presumably are the result of radiolysis of OH groups and/or $[Al/H^+]^o$ complexes and undoubtedly play an important intermediate role in the radiation

damage process at room temperature. On the other hand, the β-centers are believed to be the result of sequential capture of electrons and mobile alkali ions at the sites of substitutional Ge^{4+} ions. Even though germanium and titanium may be virtually absent from premium-Q quartz crystals, it remains possible that the few impurities of these types present may serve as nuclei for the formation of multiple-cation defects similar to those listed here.

Intrinsic Defect Centers

E′ Centers. E′ is the nomenclature[30-32] which has been applied to a class of defects in α-quartz associated with oxygen vacancies. From the ESR viewpoint, the E′ center consists of an unpaired electron localized in the dangling sp^3 hybrid orbital of a pyramidal SiO_3 unit. In crystal quartz, these dangling orbitals were always found to be parallel to Si-O bond directions, thus giving strong support to the oxygen vacancy model. The fact that the primary ^{29}Si hyperfine interaction of the E′ center showed a localization on one, rather than two silicons, led initially to the suggestion of an Si-O divancancy[32] but has recently been explained in a more satisfactory manner in terms of the asymmetric relaxation shown in Fig 3.[33] While there is no direct evidence that one of the two silicons neighboring the vacancy actually relaxes to planarity, Feigl, Fowler and Yip[33] based their argument to this effect on well-established stereochemical principles coupled with detailed theoretical calculations.[34]

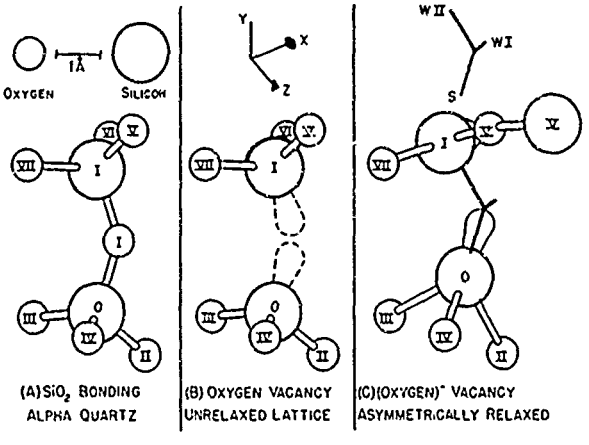

Fig. 3 Asymmetric relaxation model for the formation of the E_1' center in α-quartz. (After Ref. 33.)

Further support for the model of Feigl, Fowler and Yip derives from a study of the analogous boron E′ center in a B_2O_3 - SiO_2 glass,[35] In this glass, boron is known to be planar trigonally coordinated but, as shown by Griscom et al.,[35] upon trapping of an electron the local configuration distorts so that the boron puckers out of the plane of the three oxygens to which it is bonded. Since the ESR hyperfine parameters are directly related to the bond angles at the defect sites, it has been possible to derive distributions of bond angles for E′ centers in glasses, these distributions being consequences of the randomness in the vitreous state.[36] As shown in Fig 4, the apex angle ρ for the Si E′ center has a nearly Gaussian distribution in fused silica, with a mere 0.7° halfwidth;[36] a similar result was noted for the B E′ center.[35] This finding shows that the pyramidal geometry of the SiO_3 unit

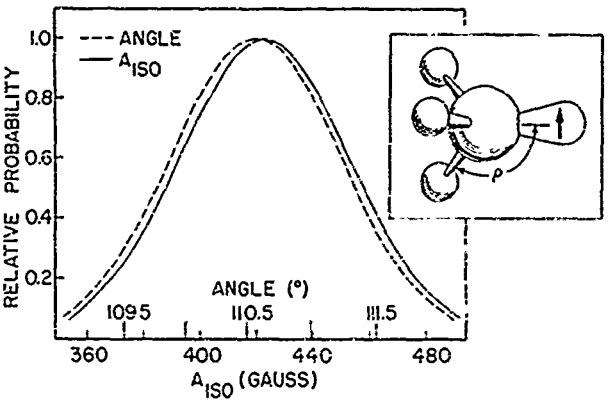

Fig. 4 Distribution in bond angles for the E′ center in glassy silica, as derived from the experimentally determined distribution in ^{29}Si hyperfing coupling. (After Ref. 36.)

retaining the unpaired electron is relatively precisely defined even in the presence of random strain fields.

Several varieties of E′ center have been delineated in α-quartz and these have been distinguished by subscripts. The E_1' center is illustrated in Fig 3; it is believed to result from the trapping a hole e^+ at the site of a neutral oxygen vacancy, i.e., a vacancy initially containing two electrons in the dangling silicon orbitals. The E_1' center has an optical absorption band at ∿ 5.85 eV.[37] The E_2' center finds the unpaired electron trapped on the opposite side of the vacancy in Fig. 3,[32,38] with silicon "0" presumably relaxing into the plane of oxygens II, III, and IV. The E_2' center is weakly associated with a proton[32] and has been shown to have an optical absorption near 5.5 eV.[30,31] A third related defect, the E_4' center, has only recently been fully characterized[39]; it appears to result from the trapping of a radiation-produced hydrogen atom at the site of a neutral oxygen vacancy forming an E′-type defect with a captive H^- ion.[40]

Peroxy Radical Defects. As demonstrated only recently,[13,41] the peroxy radical, or $RO_2\cdot$, is a fundamental defect center in high purity fused silica. It can be produced in low-OH silica by γ-irradiation or by the act of fiber drawing and annealing[41] or in silicas of any OH content by neutron irradiation.[13] The ESR evidence for peroxy radicals in vitreous SiO_2 is summarized in Fig. 5, where the dotted curves represent computer line-shape simulations used to derive g values and hyperfine splittings. Stapelbroek et al.[41] noted that the g tensor for a certain well defined defect in silica (Fig. 5a) was consistent with an O_2^--type center. It then remained for Friebele et al.[13] to demonstrate by ^{17}O-enrichment a hyperfine interaction of this particular defect with two inequivalent ^{17}O nuclei (Fig. 5b), thus proving the peroxy radical model.

The precursor of the peroxy radical in silica is believed[13] to be the peroxy linkage ≡Si-O-O-Si≡ , which is envisioned to be half of a Frenkel pair, the other half being the oxygen vacancy ≡Si-Si≡ . Fig. 6 illustrates how the oxygen vacancy can trap a hole to form an E_1' center while the peroxy linkage can trap a hole to form a peroxy radical.

When low-OH fused silica is γ-irradiated at room temperature, the relatively large induced peroxy radical concentration (∿ 10^{16} cm^{-3} for a dose of 10^8 rad) is found to double upon annealing to 300°C.[41]

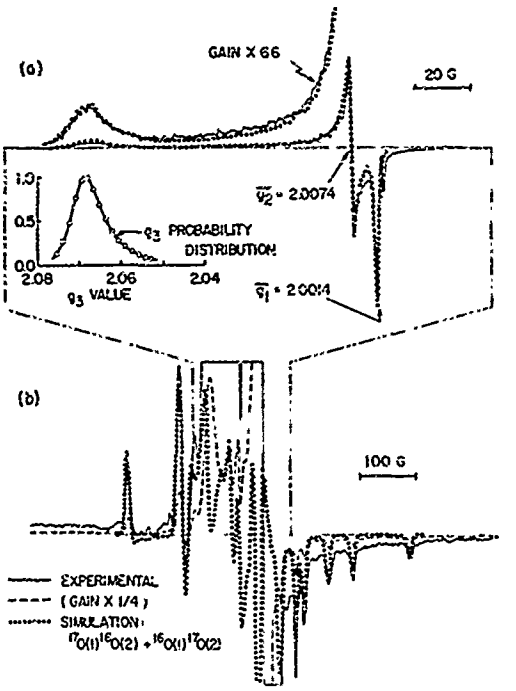

Fig. 5 ESR spectra of the peroxy radical defect in fused silica: (a) Low-OH silica after γ-irradiation and annealing. (b) ^{17}O-enriched silica after neutron irradiation and annealing. (After Refs. 13 and 41.)

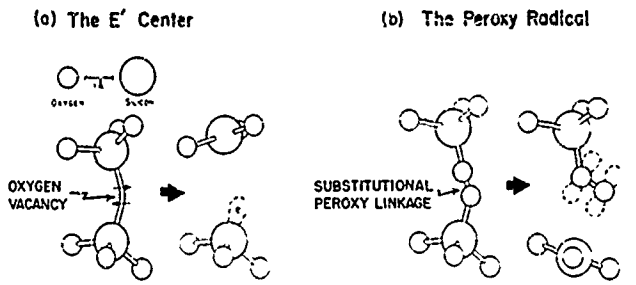

Fig. 6 Formation of intrinsic defect centers in α-quartz and fused silica by hole trapping at the sites of a neutral Frenkel defect pair.

This unexpected behavior was also mirrored by the amplitude of an optical absorption band at 7.6 eV, thereby demonstrating that the peroxy radical has an optical transition at this energy.[41]

While there has been no complete ESR confirmation of the existence of peroxy radicals in irradiated α-quartz, Weeks[6] has reported a γ-ray-induced absorption band at 7.6 eV in a synthetic crystal corresponding to $\gtrsim 10^{16}$ defects cm^{-3} for a dose of $\sim 10^9$ rad. This band increased by a factor of ∿ 1.4 upon annealing to 300°C and a similar behavior was noted for certain unidentified ESR lines having g values of 2.008, 2.016, and 2.021 for the magnetic field parallel to the c-axis. Since these g values lie within the span of the principle axis values for the peroxy radical in silica (see Fig. 5a), a strong argument can be mounted that Weeks has in fact observed the peroxy radical in α-quartz. The observed annealing behavior, coupled with a doubling of the 7.6 eV band upon reirradiation, supports the suggestion[6] that this band has a precursor state which does not absorb visible light but which can be created by irradiation and annealing. It now seems likely that this precursor is the peroxy linkage.

Experimental

Transient optical effects in a variety of fused silicas and one sample of field-swept, X-cut Sawyer quartz were observed following 5-nanosec pulses of 600 keV electrons from a Febetron 706 source.[11,12] Each pulse deposited ∿ 10^5 rad into a zone ∿ 1 mm deep, corresponding to an areal energy deposition of ∿ 2 x 10^{18} eV/cm^2. Samples were in the form of rectangular prisms ∿ 1 x 1.5 x 0.5 cm polished on the front and two end faces. Time-resolved optical absorption was measured by passing monochromatized light into one end face at a slight angle (∿ 15°) to the polished, irradiated front face, resulting in total internal reflection of this probe beam and two oblique passes through the irradiated zone. Upon exiting the third polished face, the probe light entered a double monochromator and was detected by a photomultipier. Transient luminescence was measured in the same geometry by turning off the probe light. Sample temperatures were maintained near 300, 77, or 4.2K by means of a shielded cold finger arrangement in an evaculated chamber.

Other experimental data have been taken from the literature; the reader is referred to the individual sources cited for pertinent experimental details.

Transient Optical Absorption

Pulsed electron irradiation of α-quartz and fused silica samples resulted in transient optical absorption bands which decayed in times of the order of milliseconds or less.[11,12] Fig. 7 presents the induced optical densities at various wavelengths measured at a fixed time (∿ 10μ sec) following electron pulses delivered at 4.2K. In the case of the α-quartz sample (Fig. 7b) the measurement time was much shorter than the single exponential decay constant determined (further discussion of the decay kinetics will be deferred to the following Section).

The data of Fig. 7 were obtained by a point-by-point method and actually represent the averages of individual measurements following 2-6 electron pulses in the case of the glass sample and 1-3 pulses in the case of the quartz sample. Considerable shot-to-shot scatter (up to ± 50%) due to variations in the electron source intensity were encountered; much of this scatter is averaged out in the case of the glass data. It is to be noted that the point-by-point method resulted in each sample receiving an ever-increasing total dose during the course of an experiment. However, no evidence could be found of a systematic dependence of the transient absorption upon accumulated dose. The distinction between transient and permanent damage should be emphasized here. Comparing the present results obtained at 4.2K for Corning 7940 with the "permanent" damage studies of Arnold and Compton[42] at 77K, leads to the ratio (transient absorption per unit dose): (permanent absorption per unit dose) $\gtrsim 10^2$ in the E_1' region of the spectrum (∿ 5.85 eV).

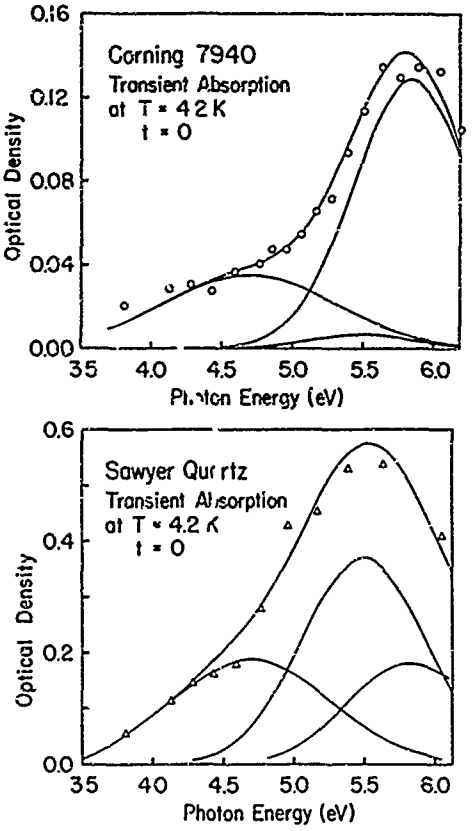

Fig. 7 Transient optical absorption in (a) Corning 7940 fused silica and (b) field-swept Sawyer quartz immediately following pulsed irradiation by 500 keV electrons. (After Ref. 11.)

The two data sets of Fig. 7 have each been fitted by three Gaussian bands constrained to have peak positions of 5.85, 5.5, and 4.7 eV, corresponding respectively to the E_1' and E_2' bands and an unidentified band consistently observed as permanent damage in high purity fused silicas.[43] These fits are certainly not unique, particularly in view of the scatter in the quartz data, but they nevertheless demonstrate that the transient absorption bands are quite possibly identical with well known permanent bands described in the literature. For the sake of discussion, it will be assumed in the remainder of this paper that transient E' centers of some nature are formed in both α -quartz and glassy silica as a result of pulsed electron irradiation.

An estimate of the total number of transient E' centers per electron pulse can be made by means of the expression[37]

$$N = 7.06 \times 10^{15}\, \alpha_{max}\, \Delta E/f, \qquad (1)$$

where α_{max} is the initial absorption coefficient at the peak of the band, ΔE is the full width at half maximum, and f is the oscillator strength of the defect. Assuming values of f for the E_1' and E_2' centers to be[37] 0.14 and 0.28, respectively, and an effective optical path length through the irradiated zone of 0.8 cm, the fitted curves of Fig. 7b in conjunction with eq. (1) yield $N(E_1' + E_2') \approx 2.5 \times 10^{16}$ cm^{-3}. This transient population--induced by a 10^5 rad pulse--is comparable to the density of permanent E_2' centers induced in synthetic quartz crystals by a γ-ray dose of $\sim 2 \times 10^9$ rad[32] and presumably exceeds the number of oxygen vacancies preexisting in the crystals before irradiation. Thus, there are grounds for considering the possible occurrence of radiation-induced transient oxygen vacancies.

Luminescence

The purpose of this section is to summarize and discuss the results of various studies of the light emission from α -quartz or fused silica, primarily as observed during or immediately following exposure to ionizing irradiation or bombardment by energetic particles. The terminology radioluminescence is generally used in the cases of steady state excitation by x-rays or γ-rays; cathodoluminesce implies steady state electron-beam excitation. Short-lived luminescence observed following pulsed irradiation shall be referred to simply as transient luminescence. Some results of photo luminescence, stimulated by visible or UV light, will be mentioned in the context of the other experiments.

Spectral Types

The observed luminescence spectra of α -quartz and fused silica under high-energy stimulation appear to be classifiable into at least three distinct "bands", centered near 2.8 eV (440 nm), 4.3 eV (290 nm), and 6.7 eV (185 nm). In Fig. 8 are compiled a number of cathodoluminescence, radioluminescence, and transient luminescence spectra spanning the spectral range of the two lower energy bands.

The Blue Luminescence. It can be noted in Fig. 8 that the 2.8 eV ("blue") band seems to be ubiquitous to many varieties of α -quartz and fused silica, although its exact position and width is a decided function of temperature and evidently depends as well on impurity content and/or other factors. By contrast, this blue luminescence is apparently much less sensitive to whether the sample is crystalline or glassy.

The temperature dependence of the γ-ray stimulated blue radioluminesce measured by Mattern et al.[4] is illustrated in Fig. 9. These authors showed that the quenching of the luminescence with increasing temperature is consistent with a classical luminescence model involving a thermally activated nonradiative decay mechanism in competition with the radiative channel(s). Mattern et al.[4] argued that the blue luminescence is almost certainly a superposition of several bands, so that the apparent shift to higher energies with increasing temperature would be accounted by lower activation energies for quenching of the lower energy components. Similar shifts and thermal quenching effects were observed by Sigel and Griscom[11,12] for the transient luminescence in field-swept Sawyer quartz (Fig. 8a). Therefore the blue transient luminescence and the blue radioluminescence probably have the same origin. Mattern et al.[4] noted that the blue radioluminescence was a factor of 50 more intense in a synthetic quartz sample than in a specimen of natural Brazilian quartz. The latter fact can not yet be interpreted since the impurity contents of the samples were not determined. Possible origins of the blue luminescence will be considered in later sections.

The UV Luminescence. Several weak e-beam stimulated luminescence bands in the ultra violet region were originally reported in fused silica by Mitchell and Denure[9] (Fig. 8d). Recently, Jones and Embree[10]

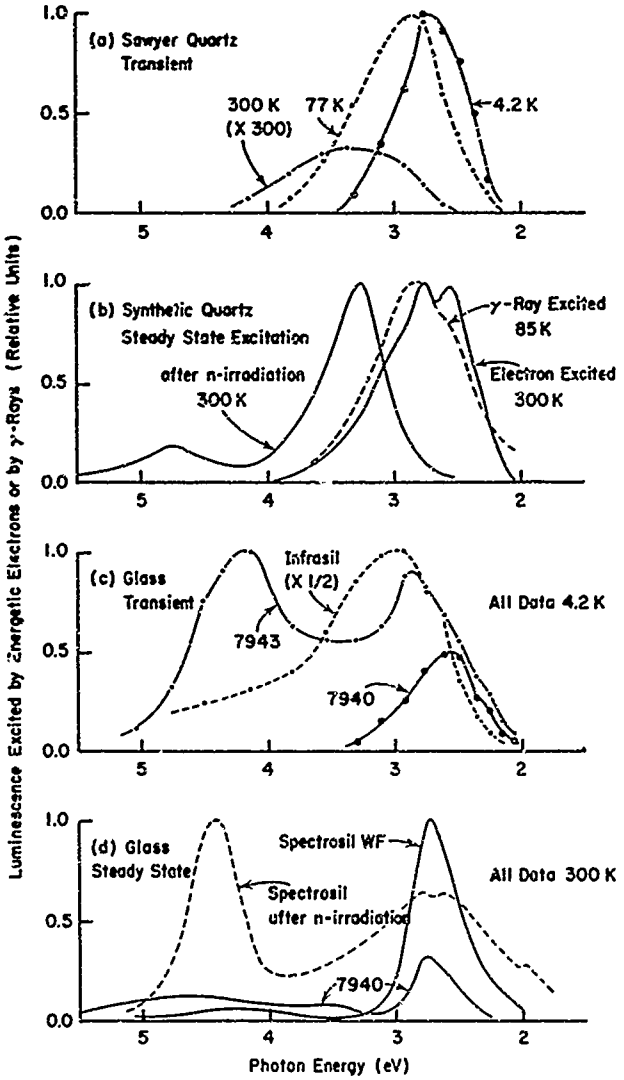

Fig. 8 Luminescence emission in the visible and UV from α -quartz (a,b) and fused silica (c,d) as stimulated by pulsed (A,c) or steady state (b,d) irradiation. (Data of (a) and (c) from Ref. 11 and 12; (b) from Refs. 4 and 10; (d) from Refs. 9 and 10.)

observed a more intense band centered near 4.3 eV in silica glass samples which had been neutron-irradiated to a high fluence ($\sim 10^{18}$ fast neutrons/cm^2) (Fig. 8d). A similar neutron-induced band was found in α -quartz at a slightly higher energy (Fig. 8b). Jones and Embree[10] identified these bands with oxygen vacancies by finding a positive correlation between their intensities and the concentrations of E_1' centers in the irradiated samples and also by establishing a positive correlation between a 4.3 eV band and the degree of chemical reduction in SiO_2 films grown on silicon.

Sigel and Griscom[11] had also observed a transient luminescence band near 4.3 eV (Fig. 8c), but they only observed this UV band in one of the several fused silica samples which they studied. This particular sample was Corning 7943, a low-OH silica which is fired in H_2 on a graphite mandrel in the final stage of

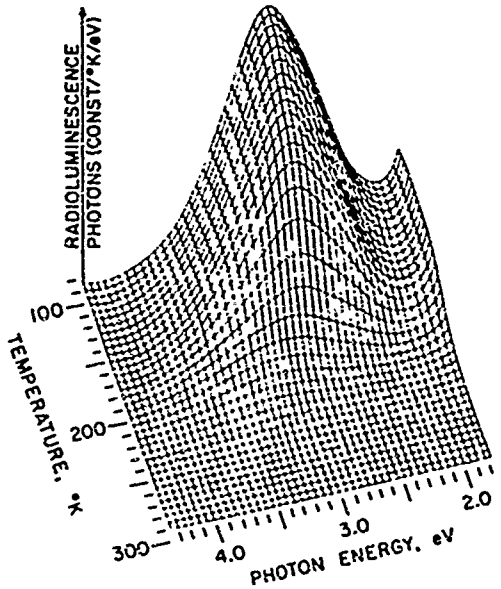

Fig. 9 "3-D" plot of luminescence emission from synthetic α -quartz as stimulated by steady state γ-irradiation. (After Ref. 4.)

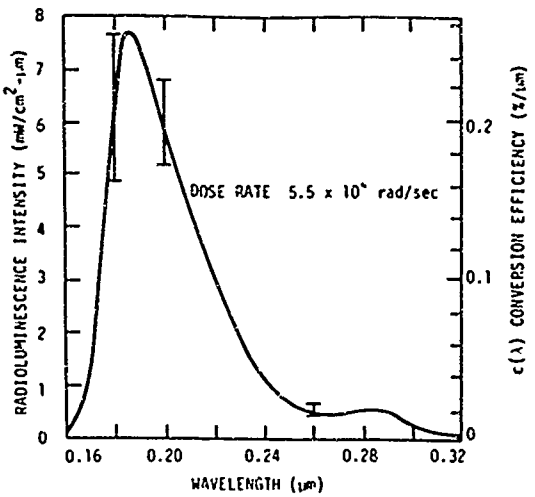

Fig.10 Luminescence emission from α -quartz in the vacuum UV as stimulated by steady state irradiation by 2.5 MeV electrons, (After Ref. 46.)

manufacture.[44] Friebele et al.[45] showed by counting E' center yields that Corning 7943 contains 8-25 times more oxygen vacancies as-manufactured than other commercial silicas. The case for associating the 4.3 eV emission band with oxygen deficiency therefore seems complete.

The Vacuum-UV Luminescence. Treadway et al.[46] studied the cathodoluminescence response of a number of materials including α -quartz and high purity fused silica under irradiation by 2.5 MeV electrons in the dose rate regime 6 x 10^3 - 1.5 x 10^5 rad/sec. They found (Fig. 10) an intense luminescence band at 6.7 eV (185 nm) whose intensity scaled linearly with dose

rate, as well as a much weaker band near 4.3 eV corresponding to the UV-luminescence described above. The efficiency of converting the deposited energy into vacuum-UV luminescence was determined to be 3×10^{-3} for quartz and 9×10^{-4} for silica glass. The lifetime of the 6.7 eV luminescence was less than 1 msec.

Time Resolution

Typical decay curves for the blue luminescence in α-quartz and fused silica following 3-nsec pulses of 500 keV electrons are shown in Fig. 11.[11,12] It can be seen that in α-quartz each decay curve can be reasonably well characterized by a single exponential decay constant τ, which is only weakly dependent on temperature. The relative quantum efficiency is seen to fall off rapidly above 77K, however. By contrast, a wide variety of fused silica samples all exhibit complex decay curves which are evidently due to a wide range of decay times. Relative to quartz, the quantum efficiencies of the glasses are low, even at liquid helium temperature.

In Fig. 11, the curvature exhibited by the plots of log (luminescence intensity) vs. time for the glasses proves to be a distinct advantage when one addresses the problem of attempting to correlate the transient luminescence bands with individual transient absorption bands. The logic is as follows. If the luminescence arises from efficient electron-hole recombination at a given color center then one quantum of luminescence will be emitted for one color center destroyed; in effect, the decay of the luminescence would then be constrained to follow the time derivative of the decay of the absorption. For quartz, where a single decay constant is exhibited, this outcome is trivial: the derivative of a simple exponential is another exponential with the same decay constant. But for the glasses, where the transient absorption decays with approximately the same curvature as the luminescence on the semilog plots,[11,12] the time derivative of the absorption is a dramatically different curve (Fig. 12). On this basis it can immediately be concluded[11,12] that the blue transient luminescence in Corning 7940 and 7943 fused silicas is not the primary result of electron-hole recombination at E′ center sites (the defects giving rise to the absorptions in the range 210-230 nm). The decay of transient E′ centers in these silicas is therefore primarily nonradiative and the blue luminescence is only cryptically related to the disappearence of these centers. On the other hand, the much more rapid decay of the 4.3 eV (300 nm) luminescence in 7943 closely tracks the time derivative of the absorption in the E′ region (see Fig. 12, upper). Whence in 7943--but not in 7940--a large number of E′ centers are decaying radiatively with high quantum efficiency, giving rise to a 4.3 eV emission. Since this UV luminescence (see above) has been well identified with oxygen deficient materials, or with neutron-bombarded materials where oxygens are presumed to have been displaced many lattice spacings, the time resolved data permit the explicit conclusion that the 4.3 eV luminescence results from the annihillation of E′ centers at the sites of isolated oxygen vacancies.

Photoluminescence

Although photoluminescence due to impurities in SiO_2 is well known, there have been few reports of light-stimulated luminescence in high purity quartz and fused silica,[12,47,48] However, unpublished work by Sigel[49] has shown that field-swept Sawyer quartz and all commercially available high purity fused silicas ($\lesssim 1\%$ total cationic impurities) exhibit an intense blue luminescence, essentially identical to

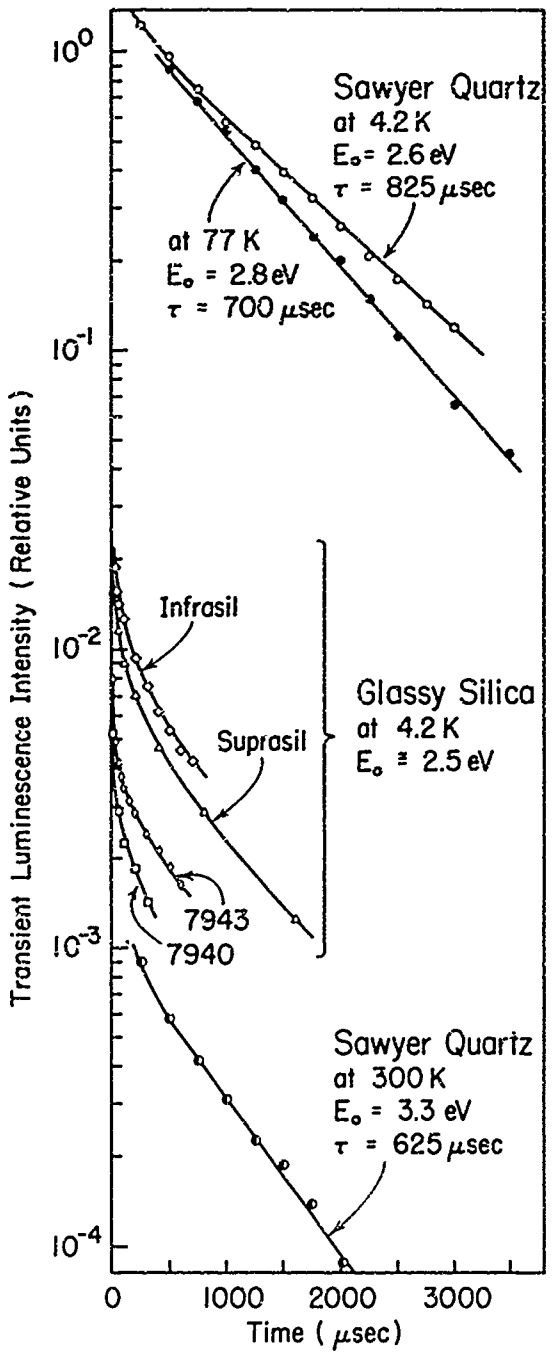

Fig.11 Time decay of transient blue luminescence in α-quartz and fused silica following pulsed irradiation by 500 keV electrons. (After Ref. 11.)

that described above, when stimulated by near ultraviolet light at temperatures $\lesssim 77$ K. The excitation spectrum for this blue luminescence peaks near 4.2 eV.[12] Preliminary indications[49] are that this luminescence is of roughly the same intensity in both α-quartz and fused silica and that this intensity increases steadily with exposure to UV light over time

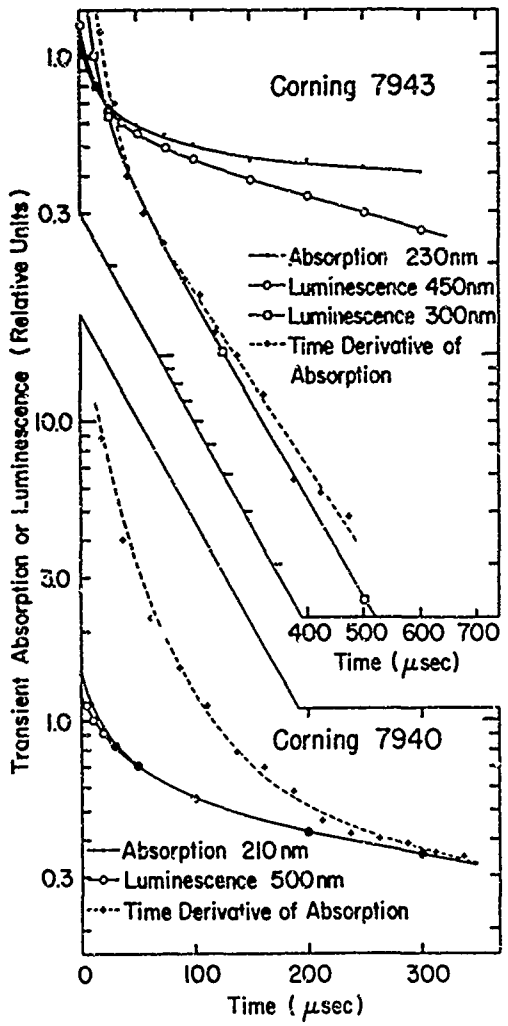

Fig.12 Time decay of transient absorption and luminescence in two different fused silicas following pulsed irradiation by 500 keV electrons. (Note different time scales.) (After Ref. 11.)

periods ∿ 10 hours. The intensity of this blue photoluminescence was not significantly changed in silica samples deliberately doped with alkalis, aluminum, or germanium.[12]

Sigel[12] also described a separate photoluminescence spectrum which could be induced in fused silica by 2 MeV electron bombardment at cryogenic temperatures. The excitation spectrum, centered near 4.9 eV, was broad and somewhat structured, whereas the emission was quite sharp and occurred in the red at 1.9 eV.

Gee and Kastner[48] have very recently discovered an additional photoluminescence, emitting in a broad band peaking near 4.3 eV (but extending below 3eV) in two unirradiated high purity fused silicas, Suprasil 1 having ∿ 1200 ppm OH and Suprasil W1 having ∿ 10 ppm OH. The excitation spectrum fell in the vacuum-ultraviolet, peaking near 7.6 eV. Irradiation by 10^{19} fast neutrons/cm^2 gave rise to a sharp emission band (∿ 0.5 eV full width) near 4.4 eV which was ∿ 20 times more intense than the band in the unirradiated materials. Neutron irradiation broadened the excitation spectrum and caused a slight shift (∿ 0.2 eV) of its center of gravity toward lower energies. Based on the discussion just above, it seems likely that the 4.3 eV luminescence observed by Gee and Kastner in the neutron-irradiated silicas arises from the excitation and radiative recombination of electron-hole pairs at the sites of isolated oxygen vacancies.

Discussion

Previous sections have (1) summarized what is known of the natures of point defects in α -quartz based on ESR studies, (2) presented the results of an investigation of transient optical absorption in α -quartz and fused silica, and (3) reviewed and briefly discussed a wide variety of luminescence data obtained for these materials. It should be evident that the various optical spectroscopic data are at the same time too complex to be explained by any simple theory and yet insufficient to support highly elaborate constructions. Mindful of the difficulties, the present section will endeavor to knit together as best as possible the various results, highlighting those conclusions which seem quite firm and going on to propose a range of possible explanations for the remaining phenomena.

Spectroscopy of Isolated Oxygen Vacancies

The occurrence of the E_1' center, and its associated optical band at ∿ 5.85 eV, has been correlated with the presence of oxygen vacancies in both α -quartz and fused silica (see section on defects). This intrinsic defect and its optical signature can be increased by orders of magnitude by making materials that are oxygen deficient or by displacing atoms by neutron bombardment. As discussed above, a cathodoluminescence band at 4.3 eV has also been correlated with the presence of oxygen vacancies (the fact that this band is particularly intense in oxygen deficient materials shows that it is not associated with the oxygens displaced during neutron irradiation). Moreover, by time resolved spectroscopy (Fig. 12) the 4.3 eV luminescence has been explicitly tied to the radiative recombination of electrons and holes at E' sites. These firm results permit some relatively speculation-free modeling.

The consensus among workers is that the E_1' center results from the trapping of a hole at a neutral oxygen vacancy, as in Fig. 6a. The two electrons initially in the silicon orbitals projecting into the vacancy undoubtedly occupy an energy level in the band gap; it is a reasonable assumption that this level lies within a few eV of the valence band edge (Fig. 13, left) and that there are optical transitions associated with this state. Judging from the vacuum-UV spectrum[49] of Corning 7943, these transitions begin near and above 6 eV. This justifies the very approximate placement of the doubly occupied level in Fig. 13. It is known that when one of the electrons is removed an E_1' center results, with the remaining electron being trapped on just one of the two silicons. The theory of Feigl, Fowler, and Yip,[33,34] now widely accepted, says that the other silicon (labeled II in Fig. 13) relaxes into the plane of the three oxygens to which it is bonded. The state which terminates the 5.85 eV optical transition has never been specified. It is suggested here that this transition is due to charge transfer from Si_I to Si_{II} in Fig. 13. The unfilled silicon 3p orbital on Si_{II} should at any rate have a substantially higher energy than the sp^3 orbital on Si_I, since for the free Si atom the 3s state lies ∿ 5 eV below the 3p.

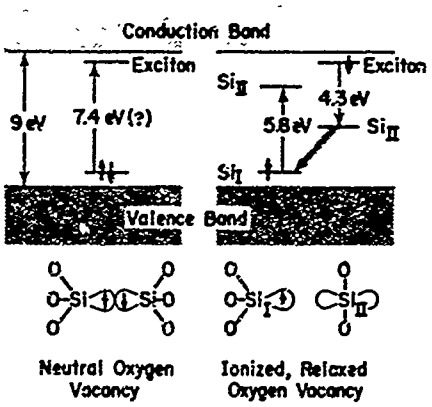

Fig.13 Proposed model for optical absorption and luminescence at the sites of isolated oxygen vacancies in α-quartz and fused silica. Actual placement of the ground-state defect levels within the band gap is uncertain, although the model requires the unfilled state on Si_{II} to fall below the conduction band edge. Note that the steric representation assumes Si_{II} lies at the center of a triangle of oxygens viewed edge-on. Crosshatched arrow represents a radiationless transition.

Sigel[12] has found that illuminating into the 5.85 eV E_1' band produces neither photocurrent nor photoluminescence. Thus it is certain that the state which terminates the 5.85 eV transition is not the same as the state that originates the 4.3 eV luminescence. It is therefore postulated here that the luminescence originates from an exciton state that finds the electron in a diffuse hydrogenic orbit about the trapped hole (E_1' center). Calling next to mind the photoluminescence results of Gee and Kastner[48] for neutron irradiated silica, it is inviting to suggest that the 7.4 eV excitation spectrum is in fact the excitation of an exciton at the site of a neutral oxygen vacancy (Fig. 13, left). The 4.3 eV luminescence would then follow (after structural relaxation in the ground state of the hole) as illustrated to the right of Fig. 13. (Note that the energy of an electron in the dangling 3p orbital of Si_{II} clearly must depend on whether or not there is an electron in the opposing orbital on Si_I, since the two electrons can lower their energy by forming a bond.)

Transient Absorption by E′ Centers

Based on the foregoing discussion, the transient optical absorption induced in the 5.8 eV region can be due to the momentary trapping of holes at isolated oxygen vacancies in materials, such as Corning 7943, which are oxygen deficient. Indeed, the number of preexisting oxygen vacancies in 7943 estimated[37,45] from the yield of permanent E_1' centers after a γ-ray dose of $\sim 10^8$ rad is of the same order as the number density of ionizations per electron pulse ($\sim 5 \times 10^{17}$ cm^{-3}) in the present experiment, assuming with Hughes[5] a figure of ∿ 30 eV per ionization. On the other hand, the estimate made above of the number of transient E′ centers induced per pulse in field-swept Sawyer quartz ($\sim 2.5 \times 10^{16}$ cm^{-3}) is probably well in excess of the number of isolated oxygen vacancies preexisting in this material. Weeks[32] has measured ∿ 10^{16} E_2' centers/cm^3 in synthetic quartz crystals only after a γ-ray dose of $\sim 2 \times 10^9$ rad.

The enormous transient absorption induced in α-quartz and fused silica by pulsed electron bombardment has been previously ascribed to "transient bond breakage".[11,12] However, if one accepts the present model for the mechanism by which the E′ center absorbs light, i.e., the $Si_I \rightarrow Si_{II}$ charge transfer mechanism illustrated in Fig. 13, then the transient E′ centers in in α-quartz must arise not merely from transient bond breakage but from transient oxygen vacancies. While such a suggestion has a decidely ad hoc quality, its plausibility is enhanced by several other recent observations: (1) The peroxy linkage, or substitutional O_2^{2-} unit appears to be a stable neutral defect in SiO_2[13,41] --a defect which is the complement of the neutral oxygen vacancy. (2) It has been found that α-quartz can be completely amorphized by sufficient exposure to 20 keV electrons in an electron microscope[14]--showing that atoms can be rearranged by ionizing processes not sufficiently energetic to actually break bonds. (3) The ubiquitous blue photoluminescence (4.2 eV peak excitation) can be enhanced by prolonged UV irradiation in both crystalline α-quartz and glassy fused silicas of the highest purities.[49] In view of observation (1), the mechanism for (2) and (3) could be a stimulated "tunnelling" of a neutral oxygen from a normal lattice site onto an immediately adjacent O^{2-} site where it would form a metastable O_2^{2-} "crowd ion". This is the specific model of a transient oxygen vacancy envisioned here.

Models for Transient Processes in α-Quartz and Fused Silica

Within the framework of the concepts outlined above, the blue (2.8 eV) luminescence could conceivably arise at the sites of O_2^{2-} peroxy linkages. The electronic structure of O_2^0, O_2^-, and O_2^{2-} is well known and is approximately illustrated in Fig. 14, where the O_2^{2-} and O_2^- species are assumed to be incorporated into SiO_2 as defects. The 7.6 eV optical transition for O_2^- in silica has been directly demonstrated[41] and the 4.7 eV transition has been inferred from ESR data.[41] In Fig. 14, the energy levels for the di-oxygen species have been adjusted with respect to the energy bands of SiO_2 on the simple basis of the observed stability of these species in that medium; this stability constrains the highest filled orbitals of the embedded O_2^{2-} to lie not far above the valence band edge. (Note that the

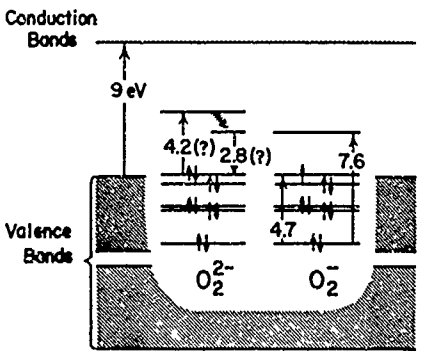

Fig.14 Proposed registration of the electronic energy levels of embedded O_2^{2-} and O_2^- molecular ions with the band structure of silicon dioxide. Assignment of the 2.8 eV photoluminescence to the O_2^{2-} species has not been demonstrated. Crosshatched arrow represents a radiationless transition.

band structure of α-quartz has been reasonably well established; for a review, see Ref. 50.) In the present view, a transient O_2^{2-} population might result from many forms of low energy irradiation, including photons of energies $\gtrsim$ 5 eV.

As of this writing, the origin of the 2.8 eV luminescence must still be regarded as an open question, the model of Fig. 14 being but one possibility. Other models for the blue luminescence and also for the 6.7 eV emission are suggested in Fig. 15. At the left of this figure is a stylized portrayal of the structure of the perfect quartz lattice. Figure 15b represents the ionization of an Si-O-Si bond, leaving a hole in the bonding orbital and a mobile electron high in the conduction band. According the Hughes,[5] these electrons, which give rise to a radiation-induced conductivity (RIC), decay into bound states or traps within ∿ 5-30 nsec. The decay times of this "fast" RIC are evidently related to the impurity contents of the materials.[5] According to the work of Sigel and Griscom,[11,12] there next follows a process or processes with decay times ∿ 1 msec in α-quartz; shorter times ∿ 1-500 μsec observed[11,12] for silica glass may result from the broad distribution of two-level configurational systems which are evidently intrinsic to the glassy state (e.g., Ref 51). The present paper suggests a specific two-level system, the oxygen vacancy-peroxy linkage intimate pair, as possibly being responsible for the transient phenomena which take place in α-quartz on a time scale ∿ 1 msec (Fig. 15c). Alternatively, these "intermediate lifetime" processes may have their rates determined by shallow trapping of electrons at impurity sites (Fig. 15d), the decay of mobile excitons (Fig. 15e), or the diffusion of mobile holes to impurity recombination sites. The fact that the decay time of the blue luminescence in quartz is so weakly dependent on temperature (Fig. 11) tends to argue against a thermally activated hopping mechanism as the rate-determining process, however.

It is of course well known that transient frequency offsets and delayed conductivity phenomena occur in quartz crystal oscillators on a "slow" time scale ∿ 1-1000 sec. The annealing of the induced frequency offset is believed[1] to result from the diffusion-limited recombination of hydrogen atoms at the sites of $[Al_e^+]^o$ traps; this belief receives support from the observation by Flanagan and Wrobel[52] of a transient optical absorption in the A-band region, decaying with a time constant $\gtrsim$ 1 sec. The delayed conductivity in unswept crystals appears to be due to motions of alkali ions in the c-axis channels.[5] A major objective of the present paper has been to shed new light on those radiation-induced processes which take place in α-quartz on the "intermediate" time scale of ∿ 10^{-6} - 10^{-3} sec.

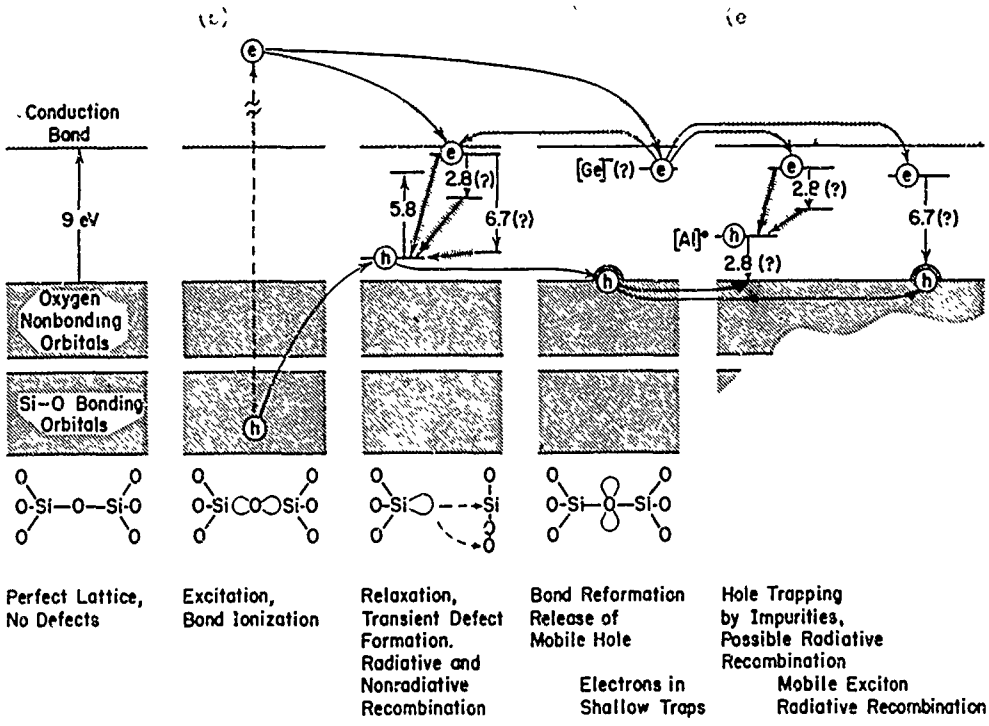

Fig. 15 Proposed models for transient processes in silicon dioxide. Several possible origins for the observed luminescences at 2.8 and 6.7 eV are suggested. Transient E′ center formation envisioned in (c) involves an oxygen vacancy - peroxy linkage intimate pair (see text). Cross-hatched arrows represent radiationless transitions.

References

1. J.C. King and H.H. Sander, Proc. 27th AFCS, June 1973, pp. 113-119; Radiation Effects 26, 203-212 (1975).

2. J.A. Weil, Proc. 27th AFCS, June 1973, pp. 153-156; Radiation Effects 26, 261-265 (1975).

3. G.B. Krefft, Radiation Effects 26, 249-259 (1975).

4. P.L. Mattern, K. Lengweiler, and P.W. Levy, Proc. 27th AFCS, June 1973, pp. 139-152; Radiation Effects 26, 237-248 (1975).

5. R.C. Hughes, Proc. 27th AFCS, June 1973, pp. 128-135; Radiation Effects 26, 225-235 (1975).

6. R.A. Weeks, J. Am. Ceram. Soc. 53, 176-179 (1970).

7. K. Nassau and B.E. Prescott, Phys. State. Sol. (a) 29, 659-663 (1975).

8. D.L. Griscom, The Physics of SiO_2 and its Interfaces, S.T. Pantelides, ed. (Pergamon Press, Elmsford, NY, 1978) pp. 232-252.

9. J.P. Mitchell and D.G. Denure, Solid State Electronics 16, 825-839 (1973).

10. C.E. Jones and D. Embree, J. App. Phys. 47, 5365-5371 (1976).

11. D.L. Griscom and G.H. Sigel, Jr., Bull. Am. Phys. Soc. 13, 1474 (1968); G.H. Sigel, Jr. and D.L. Griscom, Bull. Am. Ceram. Soc. 48, 447 (1969).

12. G.H. Sigel, Jr., J. Non-Cryst. Solids 13, 372-398 (1973/74).

13. E.J. Friebele, D.L. Griscom, M. Stapelbroek, and R.A. Weeks, Phys. Rev. Lettr. 42, 1346-1349 (1979).

14. M.R. Pascucci, EMSA Conf., San Antonio, Texas, Aug. 1979; L.W. Hobbs and M.R. Pascucci, 3rd Europhysics Conf. on Defects in Ionic Crystals, Canterbury, England, Sept. 1979.

15. J.H.E. Griffiths, J. Owen, and I. M. Ward, Defects in Crystalline Solids, Bristol Conf , (Physical Soc., London, 1955). pp. 81-87.

16. M.C.M. O'Brien, Proc. Roy. Soc. (London) A231, 404-414 (1955).

17. O.T. Schirmer, Solid State Commun. 18, 1349-1354 (1976).

18. J.H. Anderson and J.A. Weil, J. Chem. Phys. 31, 427-434 (1959).

19. Y. Haven, A. Kats, and J.S. Van Wieringen, Philips Res. Repts. 21, 446-459 (1966).

20. J.H. Mackey, Jr., J. Chem. Phys. 39, 74-83 (1963).

21. J. Isoya, J.A. Weil, and R.F.C. Claridge, J. Chem. Phys. 69, 4876-4884 (1978).

22. J.H. Anderson, F.J. Feigl, and M. Schlesinger, J. Phys. Chem. Solids 35, 1425-1428 (1974).

23. J.J. Martin, S.P. Doherty, L.E. Halliburton, M. Markes, N. Koumvakalis, W.A. Sibley, R.N. Brown, and A. Armington, Proc. 33rd AFCS, May 1979, these proceedings.

24. J.A. Weil, J. Chem. Phys. 55, 4685-4698 (1971).

25. F.C. Laman and J.A. Weil, The Physics of SiO_2 and its Interfaces, S.T. Pantelides, ed. (Pergamon Press, Elmsford, NY, 1978) pp. 253-257.

26. R.V. Lorenze and F.J. Feigl, Phys. Rev. B 8, 4833-4841 (1973); also unpublished work.

27. H. Rinneberg and J.A. Weil, J. Chem. Phys. 56, 2019-2028 (1972).

28. R.A. Weeks and M. Abraham, J. Chem. Phys. 42, 68-71 (1965).

29. B.D. Perlson and J.A. Weil, J. Magn. Res. 15, 594-595 (1974).

30. R.A. Weeks, J. Appl. Phys. 27, 1376-1381 (1956).

31. C.M. Nelson and R.A. Weeks, J. Am. Ceram. Soc. 43, 396-399 (1960); R.A. Weeks and C.M. Nelson, Ibid, 399-404.

32. R.A. Weeks, Phys. Rev. 130, 570-576 (1963).

33. F.J. Feigl, W.B. Fowler, and K.L. Yip, Sol. State Comm. 14 225-229 (1975).

34. K.L. Yip and W.B. Fowler, Phys. Rev. B 11, 2327-2338 (1975).

35. D.L. Griscom, G.H. Sigel, Jr., and R.J. Ginther, J. Appl. Phys. 47, 960-967 (1976).

36. D.L. Griscom, E.J. Friebele, and G.H. Sigel, Jr., Solid State Commun. 15, 479-483 (1974).

37. R.A. Weeks and E. Sonder, Paramagnetic Resonance, Vol. 2, W. Low, ed. (Academic Press, New York, 1963) pp. 869-879.

38. F.J. Feigl and J.H. Anderson, J. Phys. Chem. Solids 31, 575-596 (1970).

39. L.E. Halliburton, R.D. Perlson, R.A. Weeks, J.A. Weil, and M.C. Wintersgill, Solid State Commun. 30, 575-579 (1979).

40. L.E. Halliburton and J.A. Weil, (private communication, 1979).

41. M. Stapelbroek, D.L. Griscom, E.J. Friebele, and G.H. Sigel, Jr., J. Non-Cryst. Solids 32, 313-326 (1979).

42. G.W. Arnold and W.D. Compton, Phys. Rev. 116, 802-811 (1959).

43. E.J. Friebele, D.L. Griscom, and G.H. Sigel, Jr., Non-Crystalline Solids, G.H. Frischat, ed. (Trans Tech, Aedermannsdorf, 1977) pp. 154-159.

44. H. Rawson, Inorganic Glass-Forming Systems (Academic Press, New York, 1967), (See p. 46.)

45. E.J. Friebele, R.J. Ginther, and G.H. Sigel, Jr., Appl. Phys. Lettr. 24, 412-414 (1974).

46. M.J. Treadway, B.C. Passenheim, and B.D. Kitterer, IEEE Trans. on Nuc. Sci. NS-22, 2253-2258 (1975).

47. G.H. Sigel, Jr., E.J. Friebele, R.J. Ginther, and D.L. Griscom, IEEE Trans, on Nuc. Sci, NS-21, 56-61 (1974).

48. C.M. Gee and M. Kastner, (preprint supplied by authors, 1979).

49. G.H. Sigel, Jr., (private communication, 1979).

50. D.L. Griscom, J. Non-Cryst Solids 24, 155-234 (1977).

51. J.E. Graebner and B. Golding, Phys. Rev. B 19, 964-975 (1978).

52. T.M. Flanagan and T.F. Wrobel, IEEE Trans. on Nuc. Sci. NS-16, 130-137 (1969).

A HIGH-SENSITIVITY AC DILATOMETER FOR THE DIRECT MEASUREMENT OF PIEZOELECTRICITY AND ELECTROSTRICTION

Kenji Uchino and Leslie E. Cross
Materials Research Laboratory, The Pennsylvania State University
University Park, Pennsylvania

Summary

A capacitance type dilatometer has been constructed which is capable of resolving low frequency AC linear displacements of 10^{-13} meters (0.001Å) and can be used for the direct measurement of piezoelectric and electrostrictive deformations.

The sensing element of the dilatometer system is a parallel plate capacitor with sputtered platinum electrodes supported on fused silica optical flats. Changes of plate separation are sensed by the associated change in dielectric capacitance which is monitored by a capacitance bridge. Slow drift in the capacitance due to thermally induced changes in the plate separation are reduced to an equivalent plate separation change of less than ±0.002Å/minute by a DC servo actuated by the bridge unbalance signal which corrects the capacitor plate position through ceramic piezoelectric PZT pushers.

For AC measurement, one plate of the dilatometer is driven along the axis of the capacitor at a frequency of 14 Hz by a standard piezoelectric quartz crystal. The second plate of the sensing capacitor is driven in phase at the same frequency by the piezoelectric or electrostrictor of interest. A narrow band phase locked detector isolates and amplifies the 14 Hz signal detected in the unbalance output of the bridge detector. By adjusting the magnitudes of the AC voltage applied to the standard and the unknown crystals to produce a null response at 14 Hz, the electromechanical constants of the two crystals can be compared with very high precision.

Some examples are given of piezoelectric and electrostrictive crystals and ceramics which have been measured on the instrument.

Introduction

Electrostriction which is the basic electromechanical coupling in all non-piezoelectric solids is at present very poorly understood. There are few reliable data for the separate components of the electrostriction tensor even in simple solids, and there is no theory which is adequate even for alkali halide crystals. Experimentally, the difficulty is clearly associated with the very small magnitude of the electrostrictive strains even at the highest possible field levels in simple low permittivity solids. Theoretically the absence of well authenticated experimental values has certainly been a major disincentive to development and none of the present theories is viable.

The instrument described in this paper has been designed to resolve AC linear displacements of 10^{-13} meters (10^{-3} Å) and to permit the precise measurement of the very small electrostrictive strains in low permittivity solids. (The work is a preliminary part of a larger program in the Materials Research Laboratory which focuses upon both the experimental measurement and the theoretical description of electrostriction.) The AC differential capacitance dilatometer which has been constructed is based upon an early design by Bohatý and Haussühl.[1]

In this paper, the principle of the capacitance dilatometer is described first, the DC servo stabilization of the sensing capacitor which is the key to improved stability and sensitivity discussed, and the experimental arrangement detailed. The development of a unique new AC calibration capacitor is briefly described and finally some examples are given of piezoelectric and electrostrictive crystals and ceramics which have been measured on the instrument.

Design of the Capacitance Dilatometer

The scheme of the dilatometer is shown in Fig.1. The strain sensing capacitor consists of two platinum sputtered fused silica plates (2" diameter). The electrostrictive (or piezoelectric) sample plated with sputtered platinum electrodes is rigidly mechanically connected through an insulating lucite support to the right plate of the sensing capacitor. If the sample crystal is driven electrically, the right plate will be excited mechanically through the electrostrictive (or piezoelectric) strain generated in the crystal. A standard piezoelectric crystal is mounted in a similar manner so that the piezoelectrically generated strain is communicated to the left plate. Since the sensing capacitance C is given by

$$C = \varepsilon \frac{A}{\ell} \qquad (1)$$

where ε is the permittivity of air at atmospheric pressure, A the plate area, and ℓ the separation, the capacitance change ΔC associated with a small change in ℓ ($\Delta\ell$) will be given by

$$\Delta C = \left(-\frac{\varepsilon A}{\ell^2}\right)\Delta\ell = K\Delta\ell \qquad (2)$$

If the electrostrictive and the piezoelectric standard crystals are driven with AC voltages at frequencies of ω and 2ω, both capacitor plates will be excited mechanically at a frequency of 2ω. When the phase and amplitudes of the electric fields of both crystals are suitably chosen, the capacitor plates will vibrate in exact synchronism producing a net zero modulation of the separation and thus of the capacitance at 2ω. Figure 2 shows the crystal deformations in the piezoelectric standard and the electrostrictive sample at the null condition. Clearly, if this null condition can be precisely established, then from the AC voltages applied to both crystals, their known dimensions and the piezoelectric coefficient of the standard crystal (quartz) the unknown electrostrictive coefficient can be calculated. For the piezoelectric sample the situation is slightly different.

A simple block diagram of the full measuring system is given in Fig. 3. The components of the mechanical circuit (a,b,c,d) are identical in principle to those used by Behatý and Haussühl.[1] However, to sense and control the capacitor (b,c) a General Radio 1620 capacitance measuring assembly is used (j,k,l). To obtain maximum sensitivity, the capacitance bridge is operated at a frequency of 5 kHz, the standard piezoelectric crystal is driven at 14 Hz and the electrostrictor under study at 7 Hz. The phase locked detector is locked to the 14 Hz driving oscillator.

DC Servo Stabilization

Obviously the sensitivity constant K in Eq (2) can be made very large if the separation ℓ can be made very small. In a practical system, however, a limiting value of ℓ is set by slow dimension changes due to thermal drift. Even though the mechanical support for the sensing capacitor is made from super invar with a very small thermal expansion coefficient ($\lesssim 0.3 \times 10^{-6}$ deg^{-1}), and the assembly is put into a chamber controlled to ± 0.04°C, thermal dimension changes are still very much larger than the electrostrictive displacements induced at tolerable fields, and would take the bridge detector well out of its linear range. To overcome this problem, a DC output from the phase locked bridge detector is used to operate a Burleigh RC42 servo amplifier which actuates three parallel piezoceramic mechanical actuators made of PZT controlling the static plate separation (ℓ_0).

Instrument Examinations

Servo-Positioner Check

After the system has stabilized for some four hours, the DC servo system is disabled and the intrinsic drift rate of the capacitance determined by measuring the bridge unbalance signal as a function of time (Fig. 4). By rebalancing the bridge periodically the capacitance increment for a given unbalance voltage can be determined, and from the AC a corresponding $\Delta\ell$ can be calculated. It is evident from Fig. 4 that without compensation the drift rate corresponds to a plate separation change of 1 Å/minute. Maintaining the same conditions, the DC servo is now turned on, and at the same gain setting no drift is discernible. Turning the gain up by a factor of 100, however, (Fig. 4, right-hand scale) it is evident that the drift rate now corresponds to a linear dimension change of 0.002Å/minute.

Resolution Check

To check the AC sensitivity the standard quartz crystal was driven by a Wavetek Model 142 oscillator at 14 Hz. With 30 volts rms applied to the bridge, the lock-in output as a function of voltage applied to the quartz crystal is given in Fig. 5. The linear relation expected for a piezoelectric is clearly evident. Right-hand scale shows the actual deformation of the quartz crystal in Å rms, calculated by use of the absolute calibrator that will be discussed later. The experimental error is much smaller than the solid circles and is about ± 0.1 mV, which corresponds to $\pm 10^{-3}$ Å. This value is the smallest resolvable increment at present. Taking the quartz thickness value of $\ell = 5.45$ mm, the resolvable increment corresponds to the resolvable strain $\Delta\ell/\ell = \pm 2.10^{-11}$.

Further Checks

The lock-in output for a fixed value of drive voltage to the quartz standard (10.8 V rms) was recorded as a function of capacitor plate separation (Fig. 6) and of voltage applied to the capacitance bridge (Fig. 7). If the measured signal comes only from the capacitance bridge unbalance, this should scale linearly with the square of capacitance and with the bridge oscillator voltage as is evident in Figs. 6 and 7. A slight anomaly observed at 110 pF in Fig. 6 is caused by the sensitivity dial change of the capacitance bridge.

AC Calibration Capacitor

We have described, so far, a system in which the known piezoelectric coefficient of a standard quartz crystal has been used to calibrate the AC voltage output in terms of a calculated plate separation change. We propose a different way of deriving the sensitivity by using a very small 3-terminal variable air capacitor which can be driven at low AC. Figure 8 shows the principle of the absolute calibrator using an alternating capacitance. When the capacitor plate is driven mechanically by the electromechanically generated strain in the crystal (I), the capacitance bridge output (5 kHz) is modulated at 14 Hz as in the bottom figure. If we use the small alternating capacitance connected in parallel to the sensing capacitor instead of driving the sample (II), the same order of modulated output can be established. If we measure the lock-in output by driving this alternating capacitance, from the known alternating capacitance change and the capacitance of the sensing capacitor, we can calculate the equivalent AC linear deformation using Eq (2). The scheme of the alternating capacitance generator designed is shown in Fig. 9. The capacitance is made in a completely shielded aluminum box. When the central circular aluminum plate is in the vertical position, no electric flux can thread between the needles and the capacitance is almost equal to zero. In the horizontal position the capacitance shows a maximum. By rotating the

aluminum plate with a constant speed motor (Electro-Craft Motomatic System), a sinusoidal capacitance change (3-26 aF) can be obtained as shown in the bottom figure. The reference signal to the phase locked detector is produced by the photodiode and the rotating shutter fixed on the rotating axis.

If we obtain the lock-in output of V_{ACG} mV by driving the alternating capacitance generator under one instrument condition with the sensing capacitor of C pF, the sample crystal deformation in Å rms corresponding to the unit lock-in output in mV can be calculated as follows when measured under the same condition:

$$\left(\frac{\Delta \ell}{V_{ACG}}\right) = \frac{1430}{V_{ACG}\, C^2} \text{ [Å/mV]} \qquad (3)$$

Sample Measurements

To get the unknown piezoelectric or electrostrictive coefficient, there are three different ways of using the present instrument:

1. Absolute Calibration
   (using alternating capacitance generator)
2. Relative Calibration
   (using standard quartz driving)
   A. Separate vibrating method
   B. Null condition method
3. Sign Determination of Electrostrictive Coefficient
   (using electrostrictive standard PMN driving)

Absolute Calibration

By using the output from the alternating capacitance generator, the deformation corresponding to the lock-in output can be calculated. The piezoelectric or electrostrictive coefficient will, therefore, be given as follows:

$$d = \left(\frac{\Delta \ell}{V_{ACG}}\right) \times 10^{-10}\, V_{P,OUT}/V_{P,IN} \text{ [mV}^{-1}\text{]} \qquad (4a)$$

or

$$M = \sqrt{2}\left(\frac{\Delta \ell}{V_{ACG}}\right) \times 10^{-10}\, \ell_E\, V_{E,OUT}/V_{E,IN}^{\,2} \text{ [m}^2\text{V}^{-2}\text{]} \qquad (4b)$$

where V_{OUT} is the lock-in output voltage in mV, V_{IN} is the voltage applied to the sample in V rms and ℓ the thickness of the sample in m. Figure 5 is a good example for the piezoelectric case. We obtained the piezoelectric coefficient of quartz as $d_{11} = 2.27 \pm 0.01 \times 10^{-12}$ mV^{-1} from the data.

Separate Vibrating Method

The lock-in output was recorded separately for the piezoelectric wurtzite and quartz under the optimum condition (Fig. 10). By using the output ratio of wurtzite and quartz at the same applied voltage and the quartz piezoelectric coefficient, the wurtzite piezoelectric coefficient can be calculated as follows:

$$d_S = \frac{V_{S,OUT}}{V_{Q,OUT}}\, d_Q \qquad (5)$$

Null Condition Method

With a fixed value of drive voltage to the wurtzite sample, the lock-in output as a function of voltage applied to the standard quartz crystals was measured (Fig. 11). The null condition is established at the output minimum position. By using the ratio of the voltage applied to the wurtzite and the minimum position voltage and the quartz piezoelectric coefficient, the wurtzite coefficient can also be calculated as follows:

$$d_S = \frac{V_{Q,IN}}{V_{S,IN}}\, d_Q \qquad (6)$$

where crystal driving voltages are treated as root mean square values. Both methods gave the same value of the wurtzite piezoelectric coefficient ($d_{33} = 3.20 \pm 0.02 \times 10^{-12}$ mV^{-1}).

Figures 12 and 13 show the data for the electrostrictive sample $Pb(Mg_{1/3}Nb_{2/3})O_3$ ceramic. Lock-in output was completely proportional to the square of applied voltage (Fig.12). Very clear null condition can also be obtained at about 100 V rms to the standard quartz (Fig. 13). In this case the electrostrictive coefficient is calculated as follows:

$$M_S = \sqrt{2}\, \ell_S d_Q V_{Q,IN}/V_{S,IN}^{\,2} \qquad (7)$$

where $V_{S,IN}$ and $V_{Q,IN}$ are voltages applied to the sample and to quartz standard at the output minimum position, ℓ_S the sample thickness.

It is worth mentioning here that in a practical case, however, the lock-in output minimum is not exactly equal to zero because of a slight phase difference between the vibrations of both crystals. The details are discussed in the appendix.

Sign Determination of Electrostrictive Coefficient

To determine the sign of the unknown electrostrictive coefficient is rather complicated in a system which consists of the piezoelectric standard and the unknown electrostrictor, not only because the electric field frequency applied to the sample is different from the frequency for the standard, but also because the vibrational phase of the piezoelectric has two possibilities (180° difference) due to the crystal setting. We propose to use a known electrostrictor as a standard instead of quartz crystal, since the electrostrictive strain is not affected by 180° setting difference.

$Pb(Mg_{1/3}Nb_{2/3})O_3$ ceramic with perovskite-type structure is one of the best examples, which has a positive electrostrictive coefficient ($M = 1.05 \pm 0.01 \times 10^{-16}$ m^{2}V^{-2}).[2]

Example Data and Discussion

Some example data of piezoelectric and electrostrictive crystals and ceramics measured by the established instrument are listed in Table I, compared with the previous data. Coincidence between the values determined by the present and previous works for quartz and wurtzite indicates the precision of the established instrument. It is worth mentioning that the error is ten times smaller than the ones in the previous works. We emphasize that the resolution of ±0.001Å is equal to the greatest one in the world and corresponds to the resolvable strain $\Delta\ell/\ell \leq \pm 10^{-10}$, the order of which other measurements (e.g. x-ray diffractometer) cannot attain to.

Further measurements about many samples including alkali halide crystals will be made in the near future.

Acknowledgments

This work was sponsored by the Office of Naval Research through Contract N00014-78-C-0291. We also wish to thank our colleague Dr. Barsch at the Materials Research Laboratory for his many samples.

References

1) Bohatý, L. and Haussühl, S. (1977) Acta Cryst. A33, 114.
2) Cross, L.E., Jang, S.J., Newnham, R.E., Nomura, S. and Uchino, K. Ferroelectrics (submitted).
3) Bottom, V.E. (1970) J. Appl. Phys. 41, 3941.
4) Kobyakov, I.B. and Pado, G.S. (1968) Soviet Phys. Solid State 9, 1707.
5) Chang, Z.P. and Barsch, G.R. (1976) IEEE Trans.-Sonics and Ultrasonics 3, 127.

Appendix

Superposition of Two Waves with Different Phases

When a_1 and a_2 are the amplitudes of AC deformations of the sample and the standard crystals respectively and δ the phase difference, the change of the sensing capacitor separation $\Delta\ell$ will be given as follows:

$$\begin{aligned}\Delta\ell &= a_1 \sin\omega t - a_2 \sin(\omega t+\delta) \\ &= (a_1 - a_2\cos\delta)\sin\omega t - a_2 \sin\omega \cos\omega t \\ &= [a_1^2 - 2a_1a_2\cos\delta + a_2^2]^{1/2} \sin(\omega t-\psi) \qquad (8)\end{aligned}$$

where $\tan\psi = a_2 \sin\delta / (a_1 - a_2\cos\delta)$.

$[1-2r\cos\delta+r^2]^{1/2}$ term represents, therefore, the normalized shape of the dilatometer output curve as a function of driving voltage applied to the quartz standard. Figure 14 shows the theoretical calculation of the null condition method for various phase differences.

Table I. Some example data of electromechanical coefficients

Sample	Coefficient	Present	Previous
Quartz <100>	d_{11} ($\times 10^{-12}$ mV^{-1})	+2.27 (±0.01)	+2.27[3]
Wurtzite <001>	d_{33} ($\times 10^{-12}$ mV^{-1})	+3.20 (±0.02)	+3.2 (±0.2)[4]
Berlinite <100>	d_{11} ($\times 10^{-12}$ mV^{-1})	-3.98 (±0.05)	-5.3 (±1.6)[5]
$Pb(Mg_{1/3}Nb_{2/3})O_3$ (ceramic)	M'_{11} ($\times 10^{-16}$ m^2V^{-2})	+1.05 (±0.01)	+1.4 (±0.2)[2]

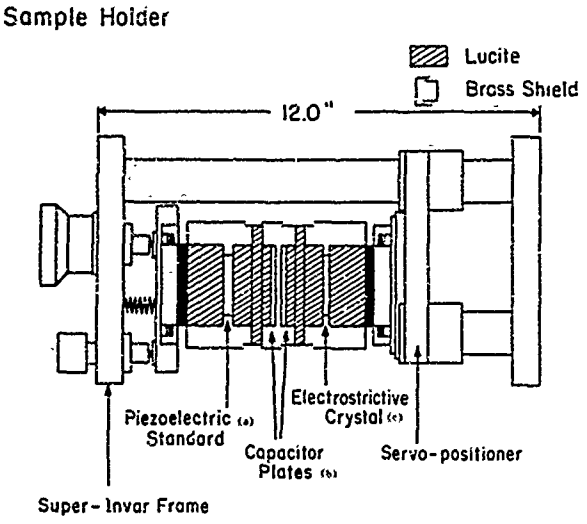

Fig. 1
Schematic of the dilatometer and support structure.

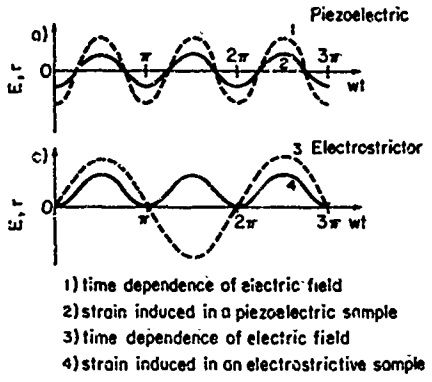

Fig. 2 Crystal deformations induced in the piezoelectric and the electro-strictor at null condition.

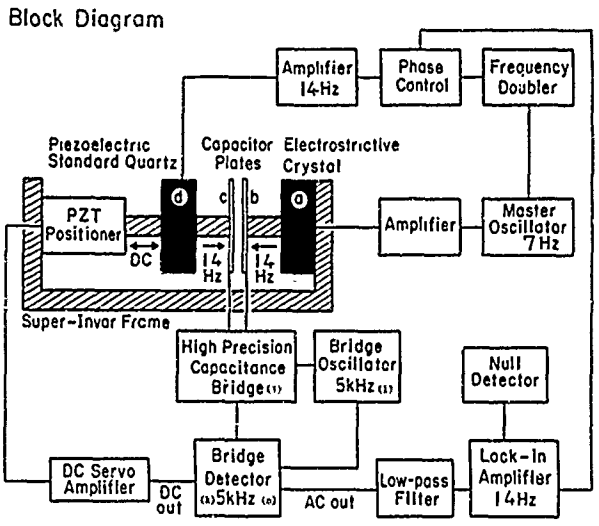

Fig. 3 Schematic diagram of the AC dilatometer.

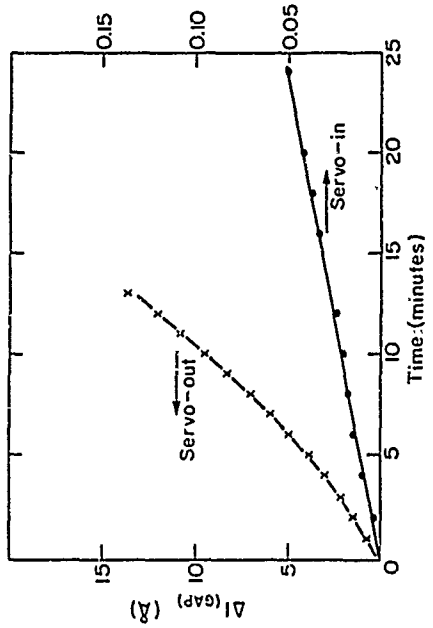

Fig. 4 DC plate separation change $\Delta\ell$ as a function of time with and without the drift compensation Servo amplifier.

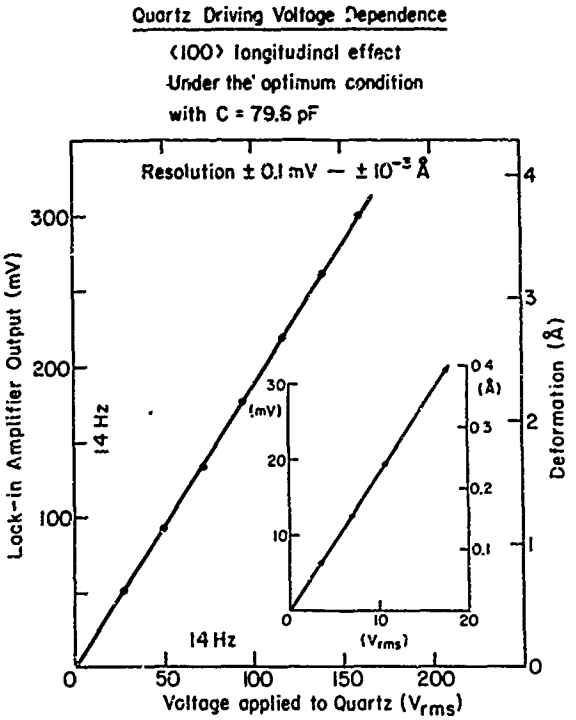

Fig. 5 Dilatometer output and the actual deformation as a function of driving voltage applied to the quartz standard crystal.

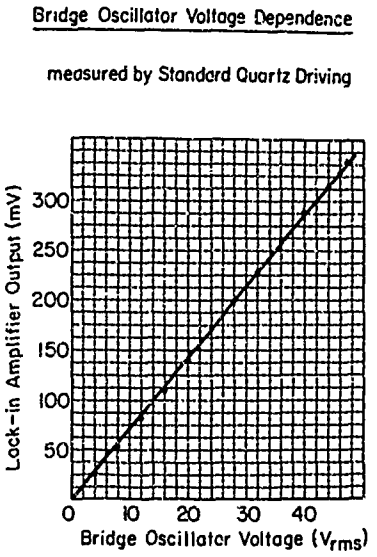

Fig. 7 Dilatometer output as a function of bridge oscillator voltage for fixed 10.8 V rms applied to the quartz crystal.

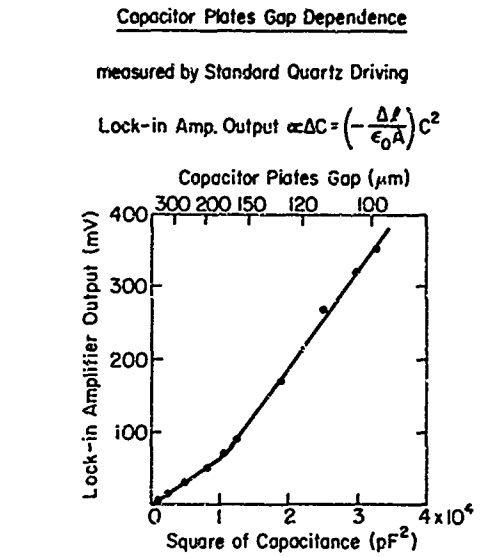

Fig. 6 Dilatometer output as a function of capacitor plate separation.

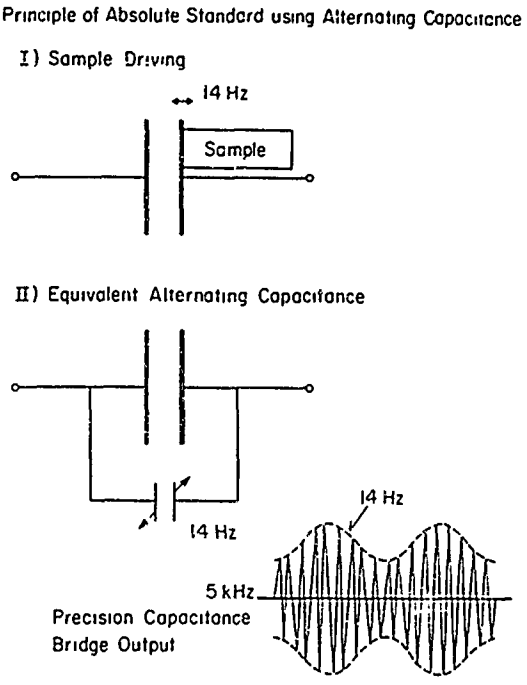

Fig. 8 Principle of the absolute calibrator. (I) sample driving: (II) equivalent alternating capacitance.

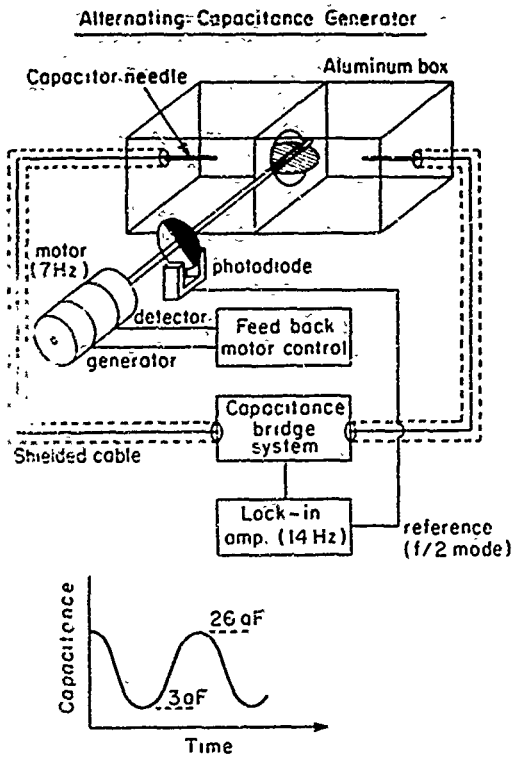

Fig 9 Scheme of the alternating capacitance generator.

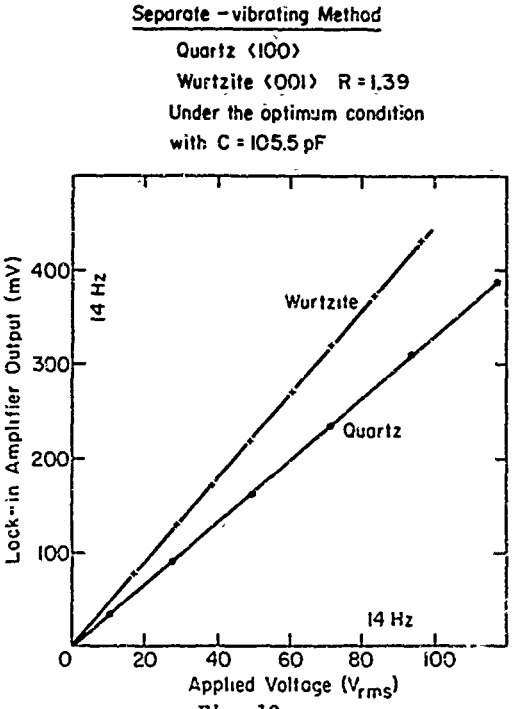

Fig. 10

Separate vibrating method for wurtzite and quartz.

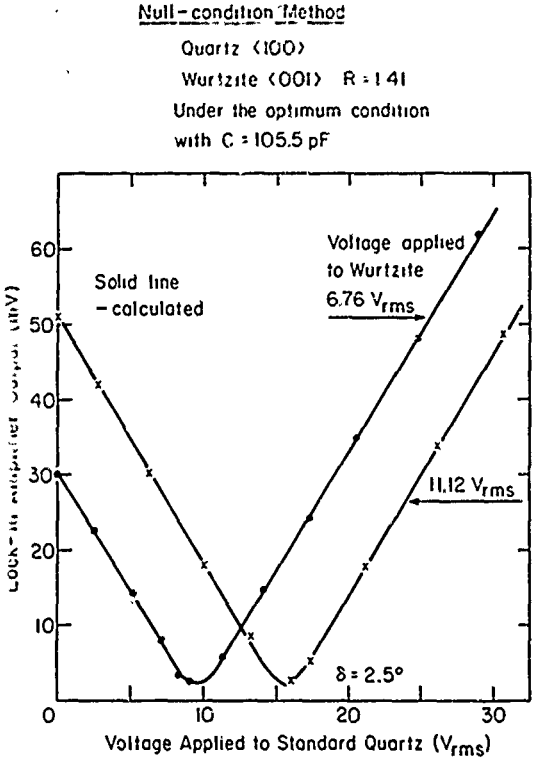

Fig. 11

Null condition method between wurtzite and quartz.

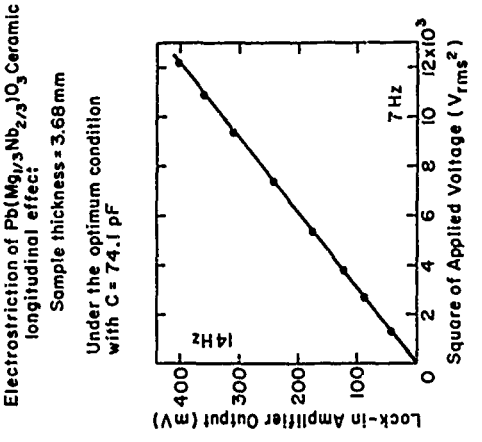

Fig. 12 Dilatometer output as a function of square of driving voltage applied to $Pb(Mg_{1/3}Nb_{2/3})O_3$ ceramic.

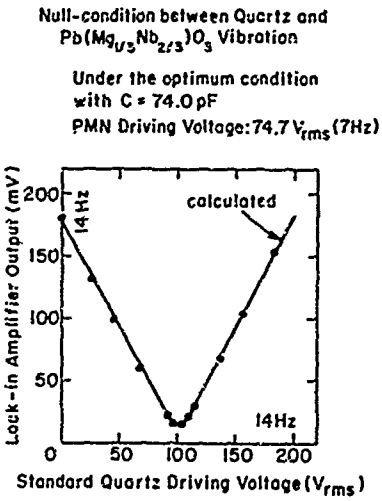

Fig. 13 Null condition method between PMN and quartz.

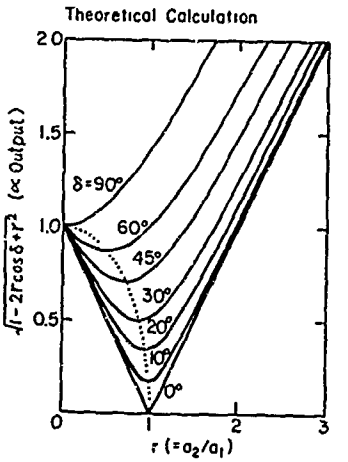

Fig. 14 Theoretical calculation of the null condition method for various phase differences between the sample and the standard vibrations.

RADIATION-INDUCED FREQUENCY TRANSIENTS IN AT, BT AND SC CUT QUARTZ RESONATORS*

D. R. Koehler
Sandia Laboratories, Albuquerque

Abstract

Earlier studies of transient frequency changes in high-purity swept AT quartz resonators led to the conclusion that impurity-induced effects were, if present, small, while the observed changes were qualitatively and quantitatively well characterized in terms of the time changing temperature of the vibrating quartz and its effect on frequency.

In the present work we have prepared 5 MHz, AT cut fifth overtone, and BT and SC cut third overtone resonators from a single stone of Sawyer swept Premium-Q quartz. The resonators were operated in precision ovenized oscillators at or near their turnover temperatures. Pulsed irradiation, at dose levels of the order of 10^4 rads (Si) per pulse, was accomplished at the Sandia Labs' Hermes II facility operating in the Bremsstrahlung mode.

The experimental data display negative frequency transients for the AT cut resonators, positive frequency transients for the BT cut resonators, and very small transient effects for the SC cut resonators. From these experimental results we conclude that: (1) no measurable impurity-induced frequency changes (elastic modulus changes) are being observed in this high-purity, swept-quartz, and that (2) the frequency transients are accurately modelled in terms of transient temperature effects stemming from the thermal characteristics of the resonator structure.

Introduction

In earlier work[1,2] on transient frequency changes in high-purity, swept AT cut quartz resonators, we were led to the conclusion that impurity-induced effects were, if present, small. The observed changes were qualitatively and quantitatively well characterized in terms of the time changing temperature of the vibrating quartz and its effect on frequency. Thermal transient-induced frequency changes in AT cut resonators were observed as early as 1959[3] and described empirically as a function of the time changing ambient.[4] Holland's[5] work on thermal gradient effects in thickness shear resonators led to the TTC cut, which is approximately equivalent to EerNisse's stress compensated, SC cut.[6] Holland's calculations deal with thermal gradients in the thickness direction while, in the present work, the thermal modelling of the resonator structure is concerned with radial heat flow and relates the instantaneous frequency change linearly to the rate of change of temperature at the oscillating boundary.

Some insight into the mechanism responsible for this effect has been offered by Warner.[7] He has shown that parallel field excitation reduces the thermal shock sensitivities associated with changing ambients, and he attributes this reduced sensitivity to the absence of quartz-electrode stresses. This attribution is consistent with the observation of a lack of frequency change in SC cut resonators exposed to time changing temperatures.[8]

For further investigation of these ideas relative to our radiation studies, it was suggested that measurements on BT and SC cut resonators could offer additional clarification of the induced thermal effects as well as offering an enhanced sensitivity to frequency changes stemming from impurities. The TTC cut, or SC cut, is designed to minimize thermal shock induced frequency shifts and should thus allow sensitive measurements of impurity effects (elastic modulus changes) on the resonator frequency, although this notion is dependent upon how the various frequency determining elastic moduli are individually modified by the radiation. The BT cut, on the other hand, has a thermal shock coefficient opposite in sign to the AT cut and one should see positive frequency transients resulting from radiation heating. From an impurity effects perspective, however, King's[9] measurements, as well as earlier experiments by Frondel,[10] showed that in natural quartz BT cut resonators, the radiation-induced steady-state frequency changes were as great as ten times the changes observed in AT cut resonators and of the same sign. If the radiation-induced transient frequency changes followed this steady-state frequency-change behavior, therefore, one should see large negative frequency excursions after pulse irradiation.

*This work was supported by the U.S. Department of Energy.

Experimental Details

In the present work we have prepared 5 MHz, AT cut fifth overtone, and BT and SC cut third overtone resonators* from a single stone of Sawyer+ swept Premium-Q quartz. Except for the quartz blank thickness and the electrode thickness, all the resonator construction details are the same. The resonators were operated in precision oscillators at or near their turnover temperatures in proportionally controlled, double ovens. Pulsed irradiation was accomplished at the Sandia Labs' Hermes II facility which is a 10 Mev, 70 ns pulse width, electron beam source operating in the Bremsstrahlung mode.

Electrical noise and EMP effects were avoided by doubly shielding the oscillator, oven, and signal cables. Although lead collimators were used to minimize exposure to the oscillator and oven control circuitry, some evidence for radiation-induced changes in the oscillator transistor has been seen and will be discussed below. These experimental details and the basic instrumentation shown in Figure 1 have been described before but are mentioned here for easier reference.

Frequency was recorded at 0.1 second intervals from approximately 5 seconds before the radiation pulse to several hundred seconds after with a resolution of approximately two parts in 10^9. At dose levels of the order of 10^4 rads (Si) per pulse, prompt photoconductivity in the oscillator caused momentary (approximately 30 microseconds) shutdown. Temporary oven turnoff also resulted from the significant temperature rise in the oven assembly. The oven heating current as well as the AGC level, which is a measure of resonator resistance, was also monitored.

Experimental Results and Modelling

The AGC measurements showed no resistance changes resulting from the radiation. Resistance-dependent frequency changes were therefore not present.

The physical structure of the resonator pertinent to heating considerations is shown in Figure 2 and was used to construct a thermal model of the resonator. The equivalent electrical circuit of the lumped-element thermal model is shown in Figure 3. For purposes of calculating dynamic and static frequency changes stemming from radiation-induced temperature changes, the various nodes in the model are instantaneously charged to voltage levels equivalent to the nodal radiation doses. The details of such modelling efforts have been presented earlier,[1,2] and for calculations of frequency changes, the voltage and time rate of change of voltage have their equivalent in temperature and time rate of change of temperature. In particular, at the quartz vibrational zone, C_o in Figure 3, the electrical state translates to the instantaneous frequency via Equation 2 in Reference 1, repeated here:

$$\Delta f/f(t) = \beta \frac{dT(t)}{dt} + \gamma(T(t) - T(o)) \quad .$$

The frequency at time t is not only the static function of temperature γ, but depends also on thermal transients, $\beta \frac{dT}{dt}$ (see Reference 4). The coefficient, β, in the transient frequency term has been measured for the AT, BT, and SC cut resonators.[8] However, if the empirical dependence has its basis in a thickness-direction thermal gradient in an electroded resonator, then an acceptable theoretical treatment should demonstrate the relationship between heat flow, occurring either radially or conceivably via a thermal path through the electrodes to the oscillating region, and such a thermal gradient. Warner's[7] results with parallel field excited resonators could be interpreted in this perspective also, although it is not clear whether a thickness-direction temperature-gradient or a quartz-electrode interface stress is the mechanism responsible for the frequency change.

Computer calculations of thermal equilibration, after pulsed radiation deposition, generate the frequency transient curves shown in Figures 4, 5 and 6. The experimental data for the AT resonators of this study are shown in Figure 4 and display the same qualitative and quantitative behavior observed in earlier studies of high-purity, swept-quartz resonators. The correlation with the thermal model suggests very little impurity-induced frequency effects in this high-purity quartz. It should be mentioned, however, that differences in sweeping techniques can produce variations in radiation-induced resonator frequency changes,[11] and therefore further qualification of quartz material and purification processes is usually necessary to demonstrate radiation hardness.

Early-time structure in the frequency transient is associated with heat flow into the oscillating region from the ribbon supports, while later-time structure is associated with cooling followed by oven-controlled heat flow.

The experimental data for the BT and SC cut resonators are shown in Figures 5 and 6. The unstructured transient for the SC resonator in Figure 5 showed a permanent, approximately 2-3 pp 10^8, negative frequency offset which was recovered by replacing the oscillator transistor. Subsequent exposure to the radiation pulse again produced the unstructured, negative frequency offset. Heretofore, the negative frequency transients observed with AT cut resonators have tended to mask this effect. Further experimentation is planned for studying these radiation effects on oscillator transistors.

The raw data for the BT resonator frequency changes also displayed evidence of such a transistor produced offset and, therefore, the BT data shown in Figure 5 have been displaced positively by 3 pp 10^8. The excellent agreement, both qualitative and quantitative, with the thermally-induced changes calculated from the

*Fabricated by Frequency Electronics Inc., New Hyde Park, NY

+Sawyer Research Products, Inc., Eastlake, OH

model, again suggests a predominance of radiation heating effects over impurity-generated frequency changes. No calculations were made for the SC resonator since neither static nor dynamic temperature changes should produce a frequency change detectable on the scale shown.

In Figure 6 we display the frequency transient results from irradiation when operating the SC cut resonator at 14 degrees below turnover. The thermal calculations were performed with a zero-value thermal-transient coefficient and the data have again been translated positively by 2.4 pp 10^8. The agreement between the data as generated in this experiment as well as in the experiment at turnover and the thermal modelling calculations, further supports a description of the induced frequency transients based on radiation heating of the resonator.

Conclusions

Further evidence has been established confirming the conclusion that high-purity, swept-quartz, as represented in this study by SARP Swept Premium-Q material, is sufficiently pure that thermal frequency effects dominate under pulsed irradiation. Transient frequency changes induced in BT, SC and AT cut resonators can be accurately described by thermal modelling of the resonator structure which takes into account both static and dynamic temperature effects arising from radiation heating. The stress compensated SC cut or thermal transient compensated TTC cut, fabricated from high-purity quartz, furthermore, offers an excellent radiation-resistant resonator, since both radiation-induced impurity effects and radiation-induced thermal effects on frequency are minimized.

Acknowledgments

The author wishes to recognize the valuable technical assistance of C. F. Joerg and G. R. Dulleck in carrying out these experiments.

References

1. D. R. Koehler, T. J. Young and R. A. Adams, Ultrasonics Symp. Proc., IEEE No. 77, CH 1264-ISU (1977).

2. T. J. Young, D. R. Koehler and R. A. Adams, "Radiation-Induced Frequency and Resistance Changes in Electrolyzed High-Purity Quartz Resonators" Proceedings of the 32nd Annual Symposium on Frequency Control, U.S. Army Electronics Command, Fort Monmouth, NJ pp. 34-42 (1978), copies available from Electronics Industries Association, 2001 Eye St. NW, Washington, D.C. 20006.

3. A. W. Warner and D. L. White, 11th Interim Report on an Ultra Precise Standard of Frequency, Report No. 27480-J, Signal Corps Contract No. DA36039 SC 73078, July 23, 1959.

4. T. C. Anderson and F. G. Merrill, IRE Trans. on Instrumentation, I-9, 136 (1960).

5. R. Holland, Ultrasonics Symp. Proc., IEEE No. 74, CH 0896-ISU (1974).

6. E. P. EerNisse, "Quartz Resonator Frequency Shifts Arising from Electrode Stress," Proceedings of the 29th Annual Symposium on Frequency Control, U.S. Army Electronics Command, Fort Monmouth, NJ pp. 1-9, (1975).

7. A. W. Warner, "Use of Parallel-Field Excitation in the Design of Quartz Crystal Units," Proceedings of the 17th Annual Symposium on Frequency Control, U.S. Army Electronics Command, Fort Monmouth, NJ pp. 248-266, (1963).

8. J. A. Kusters, Transactions on Sonics and Ultrasonics, SU-23 273 (1976).

9. J. C. King, Bell System Tech. J., 38, 573 (1959).

10. C. Frondel, Amer. Mineral. 30, 432 (1945).

11. J. C. King and H. H. Sander, Radiation Effects, 26, 203 (1975).

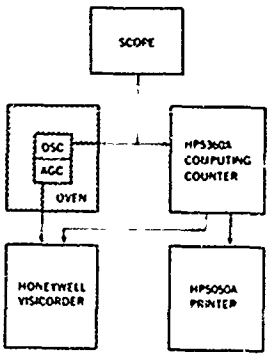

1. Block diagram of data recording system for measuring oscillator frequency and equivalent crystal resistance as a function of time following a short-duration radiation exposure.

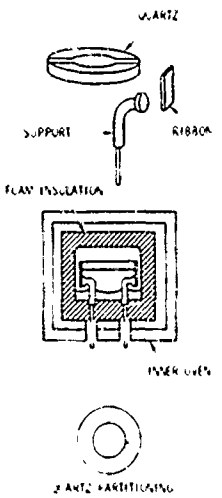

2. Structure of crystal resonator and oven assembly.

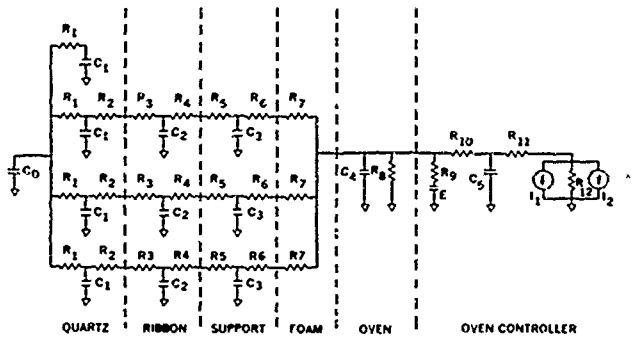

3 Lumped-element thermal-model of resonator and oven structure in equivalent electrical form.

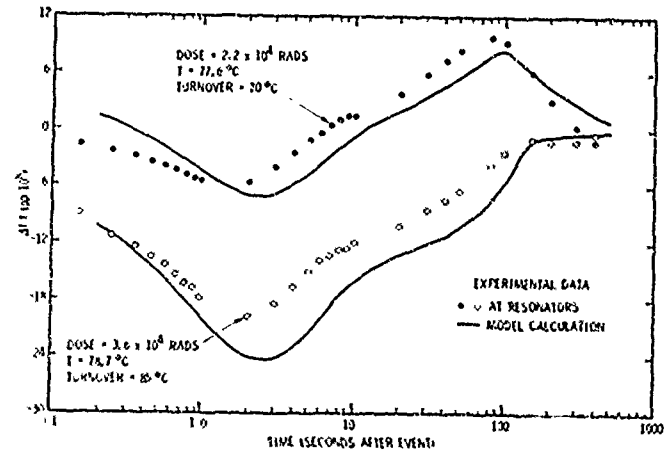

4 Frequency transient following pulse irradiation for AT cut resonators.

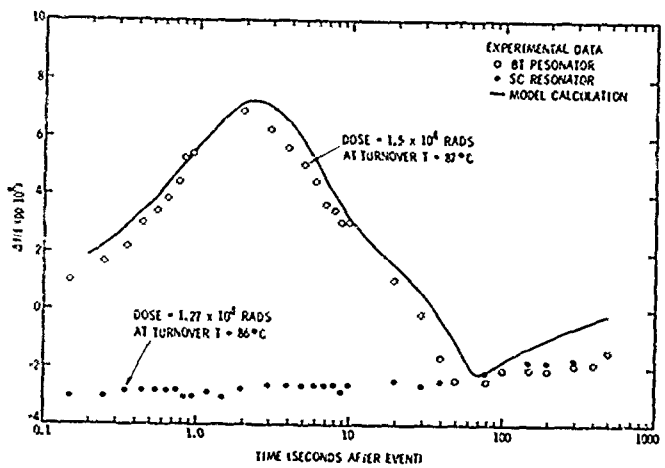

5 Frequency transient following pulse irradiation for BT and SC cut resonators.

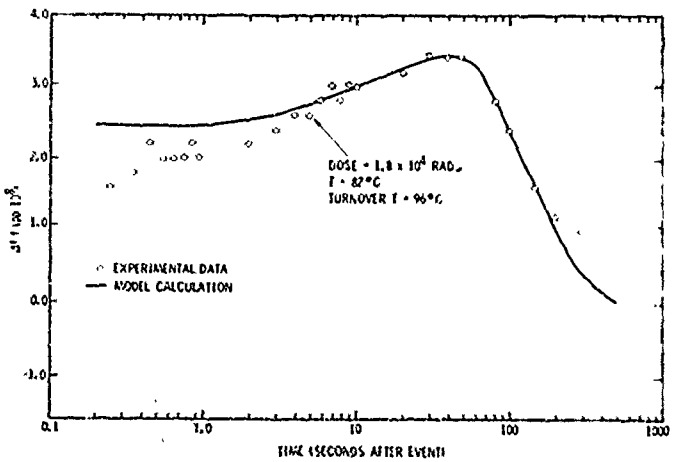

6 Frequency transient following pulse irradiation for SC cut resonator operated below turnover.

RADIATION EFFECTS IN SWEPT PREMIUM-Q QUARTZ MATERIAL, RESONATORS AND OSCILLATORS

Herbert G. Lipson, Ferdinand Euler, and Paul A. Ligor

Rome Air Development Center
Deputy for Electronic Technology
Hanscom AFB, MA 01731

Summary

New results are reported on a continuing evaluation of radiation effects in swept Premium-Q quartz consisting of measurement of low-temperature infrared impurity spectra, determination of resonator Q as function of temperature, and oscillator frequency changes induced by 10 MeV electrons and ^{60}Co gamma rays.

The infrared spectra obtained show two groups of polarization dependent impurity bands, designated s- and e-bands. The strengths of s-bands are related to growth while those of the e-bands depend primarily on electrodiffusion or sweeping. Strong e-bands have also been introduced by ^{60}Co gamma irradiation in unswept Premium-Q quartz. In swept Premium-Q quartz, e_2 band strength behavior with accumulated dose varies from sample to sample, even when swept by the same process. When reduced in strength by irradiation, e-bands can be partially restored by isochronal annealing between 300 and 350°C. A relation between the change in e_2 band strength and the amount of oscillator frequency offset introduced by irradiation is indicated.

Neither the infrared spectra, $Q^{-1}(T)$ nor steady-state oscillator frequency offset data showed any features related to differences between the SARP I and SARP II sweeping processes. 10 MeV electrons and ^{60}Co gamma rays induce similar oscillator frequency offset characteristics. Oscillator AGC voltage shows transient changes of the resonator resistance in the msec time interval after electron irradiation. The effect of these changes dominates the observed short-term frequency transients.

Keywords: Swept Premium-Q Quartz Resonators, Impurity Bands, Infrared Spectra, Acoustic Losses, Oscillators, Radiation Effects.

Introduction

In this paper we present the most recent results of our investigations of the effects of ionizing radiation on crystal resonators and oscillators, and the material utilized in their fabrication. As reported before,[1-3] it is the objective of our ongoing work to assure the commercial availability of consistent high-grade quartz capable of satisfying the stringent military requirements imposed by applications such as satellite-borne frequency standards. For this purpose we determine, measure and evaluate the parameters which may have an important influence on the radiation response of the oscillator. This task is approached on three levels: (1) material growth, sweeping (electrodiffusion), non-destructive physical characterization and low temperature infrared spectroscopy before and after irradiation, (2) resonator evaluation by measurement of Q as function of temperature before and after irradiation and (3) determination of transient and permanent radiation effects on oscillator performance.

During the last year we have expanded our material selection and experimental techniques. We report here data on quartz swept by the current process of Sawyer Research Products, Inc. (SARP II) and on resonators fabricated from this material. We are now using ^{60}Co gamma irradiation and isochronal annealing of quartz samples in combination with the low temperature infrared spectra as additional diagnostic aids. There are indications that some of the observed modifications of the spectra correlate with radiation-induced permanent frequency changes in oscillators. By measurement of the automatic gain control (AGC) voltage of the oscillator as function of time after irradiation, we can now determine transient changes of the resonator resistance in the msec time regime. We have found that the effect of these resistance changes dominates the frequency transients observed during this time interval.

Experimental Procedure

Samples

The results reported in this paper were obtained on SARP grown Premium-Q grade quartz, swept by any of five different processes and on unswept material used for a reference base. These include SARP I and SARP II, sweeping in air or vacuum at Sandia Laboratories,* and sweeping in dried nitrogen ambient at RADC/ES.** Precision made 5 MHz 5th overtone AT cut quartz resonators, widely used in high-precision oven controlled crystal oscillators

---

* under the direction of T. J. Young.

** Solid State Sciences Division of the Deputy for Electronic Technology, Rome Air Development Center.

Table I. Premium-Q quartz sample and resonator identification and characterization.

Autoclave run	crystal and bar	sweeping process	sweeping run	resonator series FEI	Bliley	data presented in this paper Figure	Table
A 6 - 21	-	SARP I	35 d	-	24343	11	V
A 6 - 24	-	SARP I	A4I	B	BE	6, 7, 10	II, III, V
A14 - 23	-	SARP I	C7C	-	24334	11	V
A14 - 27	A 2	SARP I	H1S	-	BB	7	V
D14 - 45	32 b (o)	SARP I	H3S	R	-	2, 5, 12	II, III, IV, V
D14 - 45	40 b	SARP I	H4S	-	-	2	II
A14 - 27	γ 2	SARP II	H5S	-	BC	2, 7, 11, 13	II, III, V
D14 - 45	6 b	SARP II	G14H	-	BF		V
D14 - 45	10 b (o)	SARP II	G18H	N	-		V
D14 - 45	39 b	SARP II	G17H	-	-	2	II
A14 - 27	α 1	Sandia, air	-	E	-	4	III, IV, V
A14-27	μ 2	Sandia, vacuum	-	F	BA	8	V
A14 - 27	μ 1	RADC/ES	-	-	BI	9	V
D14 - 45	1 b (o)	RADC/ES	-	-	BH	9	V
D14 - 45	39 a	unswept	-	G	-	13	
D14 - 45	D h	unswept	-	-	-	3	III

(o) meets SARP optical quality requirements.

(OCXO), were fabricated from these materials by Bliley Electric Company and Frequency Electronics, Inc. (FEI).[2] A few resonators also were obtained that operate at 5.115 MHz.*

These materials and resonators are listed in Table I, by autoclave run, crystal, bar and resonator series identifiers.

Low Temperature Infrared Spectroscopy

Infrared transmission of the quartz samples before and after irradiation was measured at low temperature between 3100 and 3700 cm^{-1} with either of two instruments, a double beam Digilab FTS-14 Fourier spectrophotometer, or a single beam Ebert mounted Perkin-Elmer E-1 grating spectrometer operated in double pass mode, with the resolutions and accuracy values as follows:

Instrument	Resolutions (cm^{-1})	Accuracy (cm^{-1})
FTS-14	1	$\pm$ 0.25
E-1	2 - 4	$\pm$ 1

The details of measurement procedures and cryogenic equipment are described in a previous paper.[1] The transmission of polished samples with faces normal to the X-, Y- and Z-directions was measured with unpolarized radiation with the electric vector E perpendicular to Y or Z. Absorption coefficients were calculated from the double beam transmission after appropriate normalization, using the reflectivity value 0.040 found for quartz in the vicinity of 3700 cm^{-1}. For single beam measurements a reference curve was obtained with the sample removed. By rapidly scanning a specified wavenumber range with the FTS-14 during a very slow temperature rise from 6 to 80K, measurements were made at selected temperatures held to within $\pm$ 1 K. Liquid nitrogen cooling to 85 $\pm$ 5 K was used for other measurements.

The RADC/ES 34 kCurie ^{60}Co source was utilized for gamma irradiation of the quartz samples, with doses ranging from 1 to 21 Mrad. Isochronal annealing was performed by moving the sample gradually into the center of a wire wound quartz tube furnace stabilized at the required temperature value. A thermocouple was kept in contact with the sample. The sample was withdrawn 20 minutes after it reached the desired temperature, found to be constant within $\pm$ 3°C across the sample during this period.

Resonator Q and Oscillator Frequency Measurements

The procedures involved in these two aspects of our investigation have been described before[2] and are briefly summarized here.

Resonator Q was obtained from measurements of the series resonance resistance R_1 as function of temperature T, between 4.5 and 420K. The reactance components C_1 and L_1 of the series branch of the crystal equivalent circuit were determined at room temperature and considered to be independent of temperature.

For oscillator irradiation, we utilized FEI OCXO model 2037B as test bed for the resonators. Their design permits collimated irradiation of the resonator with minimum exposure of the other components. After warm-up to turnover temperature (frequency minimum) and stabilization for at least several days, the resonators were irradiated with 10 MeV electrons at the RADC/ES Linear Accelerator (Linac) facility with a

*by courtesy of D. A. Emmons, Frequency & Time Systems, Inc.

total dose of 1 Mrad, accumulated in approximately 12 logarithmic steps, starting from 200 rads. After each exposure the oscillator frequency was measured continuously, with sampling times increasing from 1 msec to 100 sec. These measurements continued long enough to determine the steady-state (permanent) frequency offset.

Simultaneously, the oscillator output voltage and the AGC voltage V_A was measured by photographic recording of oscilloscope traces. Observed changes in V_A indicate changes in the resonator resistance R. A calibration function $R(V_A)$ was determined without irradiation, using resistors in series with the resonator, at the turnover temperature for each resonator-oscillator combination. In these calibrations, the oscillator frequency f(R) changes[4] as function of the combined resistance of the resonator and resistor.

Irradiation of resonators with comparable doses of ^{60}Co gamma rays was also performed. In this case the resonator was removed from the oscillator and reinserted after exposure. With this mode of irradiation the two hour warm-up of the oscillators precluded the measurement of short term frequency and resistance transients. In the absence of irradiation, the frequency was found to retrace after reinsertion, warm-up and over night stabilization within $\pm$ 3 pp 10^9.

Results and Discussion

Low Temperature Impurity Spectra

Unswept Premium-Q Quartz. This grade of synthetic quartz has relatively low impurity concentrations and impurity band spectra can only be observed at low temperatures. We have reported[1] that below 85 K four principal bands are found in nearly all unswept Premium-Q quartz, with peak positions at 3348, 3396, 3438 and 3581 cm^{-1}. These bands, attributed to the role of H^+ in O-H stretching vibrations,[5] are characteristically found in the spectra of synthetic quartz.[6] We have designated them as s_1, s_2, s_3 and s_4, respectively. While the band peak positions vary only slightly ($\pm$ 1 cm^{-1}),their intensities can exhibit large variation from bar to bar and in some cases between adjacent regions of a bar. The intensities are also polarization dependent with a weaker s_1 band and stronger s_3 and s_4 bands measured with E$\perp$Z than with E$\perp$Y, or E$\perp$X. The impurity bands are superimposed over broad Si-O lattice mode overtone bands centered at approximately 3200, 3300 and 3400 cm^{-1}.

Swept Premium-Q Quartz. Sweeping (electrodiffusion) was found[1] to change the s-band intensity very little, i.e. within the differences due to local growth variations. Sweeping introduces, however, two additional bands with peaks at 3306 and 3366 cm^{-1}, which have been designated e_1 and e_2. The e_1 band can be clearly resolved only in quartz with higher impurity concentrations than Premium-Q, such as Electronic grade. Both e_1 and e_2 show strong polarizability, exhibiting greater strength with E$\perp$Z.

The e-bands are attributed[5,6,7] to O-H vibrations in the vicinity of aluminum ions in silicon sites, Al^{3+}_{Si}, with the H^+ providing charge compensation. These e-bands are rarely found in as-grown synthetic quartz where alkali ions compensate the charge instead of H^+. Sweeping removes the alkali ions and replaces them with H^+ from the water vapor present even in dried ambient gas, thus introducing e-bands. We have found that e-bands are weak in vacuum swept material, apparently for lack of available hydrogen.

The e-bands cannot be introduced by heating alone but require the highly increased ion mobility provided e.g. by an electric field of kV/cm strength. We have observed no e-bands in a Premium-Q sample maintained at 500°C for 3 months without an applied electric field.

The e_2 band peak height decreases strongly with temperature as shown in Fig. 1. This decrease is coupled with an increase in band width. When correction is applied for the instrument resolution of 1 cm^{-1}, band widths of 1.0 to 2.3 cm^{-1} between 6 and 80 K, respectively, are estimated, and the same integrated intensity is found at each temperature. From the latter result, the e_2 peak height above the Si-O lattice band background is a valid measure of band strength if comparisons are made, as in this paper, with the same resolution and temperature.

Some questions have been raised about the influence of differences between the SARP I and II sweeping procedures on quartz quality and radiation response. Comparison of the spectra presented in Fig. 2 and e_2 band peak absorption coefficients derived from these spectra, listed in Table II, show that e_2 band strength alone cannot be used to characterize either process. The wide range of strengths found probably indicates variations in impurity content present in the material before sweeping.

Table II. Peak absorption coefficient of the 3366 cm^{-1} e_2 band at 85 K , with E$\perp$Y, in SARP I and SARP II swept Premium-Q quartz.

Sweeping process	autoclave run	bar	absorption coefficient cm^{-1}
SARP I	A 6 - 24	A4I	0.120
	D14 - 45	32b	0.099
	D14 - 45	40b	0.209
SARP II	A14 - 27	H5S	0.090
	D14 - 45	39b	0.125

Radiation Effects on Impurity Spectra

Unswept Premium-Q Quartz. The e-bands produced by sweeping are also introduced by ^{60}Co gamma irradiation. As with sweeping, the defect transformation Al^{3+}_{Si}-$Na^+ \rightarrow Al^{3+}_{Si}$-$H^+$ can be effected by ionizing radiation at sufficiently high temperatures.[7] Figure 3 shows the spectra of two sections of an unswept Premium-Q bar after 2 Mrad irradiation, displaying e- and s-bands. The bottom and center spectra are for measurements on the same section with E$\perp$Y and E$\perp$Z, respectively. The top spectrum is that of another section cut adjacent to the first, closer to the end of the bar. Even though the s-bands are different in strength for the two sections, the e_2 bands are of essentially equal strength when measured with the same sample orientation, e.g. E$\perp$Z. These findings indicate that the hydrogen distribution shown by the s-bands is different in the two sections. Nevertheless, the alkali distribution after irradiation appears to be similar, according to e_2 band strength.

Swept Premium-Q Quartz. In this material Na^+ and other alkali ions have been removed by the sweeping process and e-bands are observed indicating the presence of $H^+ - Al^{3+}_{Si}$ centers. Changes in the e_2 band strength after ^{60}Co irradiation for samples swept by different procedures can be seen from Figs. 4-6.

Figure 4 shows the 85 K pre- and post-irradiation spectra measured with E$\perp$Y and E$\perp$Z for a sample swept in air by Sandia Laboratories. Similar spectra are shown in Fig. 5 for SARP swept bar 32b. In Fig. 6,

E⊥Y spectra are shown for another SARP I swept sample, from bar A4I, both before and after irradiation, and after annealing between 300 and 350°C.

From these Figures and Table III which lists the e_2 band peak absorption coefficients as a function of radiation dose and annealing temperatures the following observations can be made.

A 20% decrease in e_2 band strength with E⊥Z, and a 50% increase with E⊥Y are found after a 21 Mrad irradiation with the air swept sample. Also with this sample, a decrease in the narrow s_4 band with E⊥Z and an increase with E⊥Y is observed after irradiation. For the SARP I swept sample 32b, a similar dose produces a 20% decrease in e_2 strength with E⊥Z and a 15% increase with E⊥Y. No significant changes (< 5%) are found for the s_4 band.

The e_2 band measured with E⊥Y shows a completely different behavior with irradiation for the other SARP I swept (A6-24) sample. The e_2 band strength is reduced to approximately 25% of its pre-irradiation value with a 1 Mrad dose and to 10% with 11 Mrad. At the same time, two weak bands appear with 1 Mrad at 3420 and 3545 cm^{-1} and grow in strength with additional irradiation. Annealing between 300 and 350°C increases both the e_2 and 3420 cm^{-1} bands and decreases the one at 3545 cm^{-1}. Annealing at 375°C produced no further effects. No s_4 band was present in this sample before and after irradiation or annealing.

Oscillators utilizing resonators fabricated from bars of the air swept and 32b samples, in which relatively small e_2 band changes were observed with irradiation, showed low radiation-induced permanent frequency offset with a 1 Mrad dose. In contrast, those fabricated from bar A4I, for which large e_2 band changes occurred, had a ten times larger frequency offset with the same dose. This relationship between changes in e_2 band strength and frequency offset may possibly be used as guide to select quartz bars for fabrication of resonators with low frequency offset.

The decrease in e_2 band strength with E⊥Z and the increase with E⊥Y after irradiation of the air swept and 32B samples indicates that the corresponding O-H vibrations have become less polarized. In the case of A4I, the strong decrease in the e_2 band and the growth of other bands implies a redistribution of H^+ into other sites.

Acoustic Losses, $Q^{-1}(T)$.

Results of our $Q^{-1}(T)$ measurements are shown in Fig. 7 for SARP swept, in Fig. 8 for vacuum swept and in Fig. 9 for nitrogen swept Premium-Q quartz resonators. The following features are observed from the curves: (1) extremely low losses at liquid helium temperatures ($Q=8\times10^7$ is not unusual), (2) a loss peak near 20 K attributed to phonon-phonon interaction,[8] (3) narrow peaks at various temperatures due to coupled modes, (4) wider and often quite weak peaks attributed to various impurity and defect centers in the quartz. Only a few of these have been identified. The peak near 50 K is due to the Al^{3+}_{Si}-Na^+ center[8] and is found, although sometimes very weak, even in resonators fabricated from swept Premium-Q quartz such as BE-91 and BC-82. The larger 50 K peaks found with BB-76 and BA-75 most likely have a superimposed mode coupling component. The prominent peak found with F-6 near 135 K is characteristic for swept quartz.[8] Ionizing radiation tends to remove this peak and introduces another one near 100 K, as shown in the dashed line in Fig. 8. Although the resonators F-6, F-2 and BA-75 were fabricated from the same bar, they show different 135 K peak strengths; another piece of evidence for variable defect concentration in a given bar. As with the infrared spectra, the $Q^{-1}(T)$ data presented in Fig. 7 also show no features which discriminate between the SARP and II sweeping processes. The curves in Fig. 9 for the nitrogen swept resonators BI-76 and BH-68 show unusually high phonon-phonon interaction, about three times as strong as normally found with swept Premium-Q.

Radiation Effects on Resonators and Oscillators.

Steady-State (Permanent) Frequency Offset. Figure 10 shows a comparison of the steady-state frequency offset produced by irradiation of resonators with 10 MeV electrons and ^{60}Co gamma rays. The shaded area represents the electron irradiation data obtained on six resonators, fabricated from one bar of SARP I swept Premium-Q quartz, while the solid lines for the gamma ray data were obtained from two additional resonators taken from the same bar. Aside from a difference in magnitude, the same general dependence on the accumulated dose is observed for both sets of data, in spite of substantial differences in the experimental conditions. Within the limitations shown by these data, we have utilized both techniques to determine the steady-state frequency offset of resonators after irradiation with doses of about 1 Mrad.

Table III. Effect of ^{60}Co irradiation and of 20 minute isochronal annealing on 3366 cm^{-1} e_2 band strength in Premium-Q quartz, measured at 85 K.

Accum. dose Mrad	annealing temperature °C	peak absorption coefficient (cm^{-1}) unswept (Dh) E⊥Z	E⊥Y	SARP I swept (32b) E⊥Z	E⊥Y	SARP I swept (A4I) E⊥Y	Sandia air swept E⊥Z	E⊥Y
0	-	0	0	0.220 ±.001	0.099 ±.001	0.120	0.201	0.056
1	-	-	-	-	-	0.033	-	-
2	-	0.297 ±.003	0.128 ±.007	-	-	-	-	-
8	-	-	-	0.174 ±.007	0.102 ±.008	-	-	-
11	-	-	-	-	-	0.012	0.160 ±.013	0.060 ±.005
20	-	-	-	0.172 ±.003	0.115 ±.001	-	-	-
21	-	-	-	-	-	-	0.157 ±.012	0.092 ±.007
11	300	-	-	-	-	0.037	-	-
11	325	-	-	-	-	0.055	-	-
11	350	-	-	-	-	0.064	-	-

Results of steady-state frequency offset measurements on resonators fabricated from 12 bars of swept Premium-Q quartz are presented in Table IV.

Table IV. Steady-state frequency offset after irradiation with 1 Mrad accumulated dose.

Sweeping process	Resonator identification	Frequency offset parts per 10^9
SARP I	24343	-40
	B-1...B-16	-270...-470
	24334	-375
	BB-80	-34
	R-48	-20
SARP II	BC-81	-84
	BF-97	-20
	N-169	-12
RADC/ES	BI-76	+8
	BH-68	+12
Sandia, air	E-3, E-1	-30, -40
Sandia, vacuum	F-2, F-6	-8, -20

These data confirm what we have reported before,[2] namely, the incidence of low and high off-set values found for doses exceeding 10^4 rad. With 1 Mrad irradiation, high values between -200 and -500 pp 10^9 are found with resonators fabricated from SARP I swept quartz, while the highest offset found with SARP II sweeping is -84 pp 10^9. All sweeping processes listed here have yielded a number of bars from which resonators with low offset have been fabricated. Incidence of high offset is not characteristic for any of the five sweeping processes studied here, but all resonators fabricated from the same bar usually show similar offset values.

Figure 11 shows one example each for low, intermediate and high frequency offset dose dependence. The three curves show that this offset begins after 10^4 rad. High offset, undesirable for long-term satellite missions, can be alleviated by prophylactic irradiation. We have shown[3] that irradiation with 1 Mrad reduces the effect of further irradiation substantially and that annealing with time is limited to minor changes saturating near 5 pp 10^9 within 2 to 3 months. We also found that a 1 Mrad dose has no effect on the Allen variance of the oscillator.

High offset appears to be associated[2] with decreased acoustic losses between 50 and 70 K. With the intermediate offset type resonator BC-81, the effect is too weak to be seen. It should be emphasized that the quartz utilized in the high-offset resonator series B showed infrared spectra with the e_2 sweeping band abnormally sensitive to irradiation.

Long-Term Transient Changes.

Most resonators listed in Table IV exhibit only moderate overnight transient frequency changes, ranging from -5 to +8 pp 10^9. However, more substantial transients cannot be ruled out, as shown in Fig. 12. Several hours after a 1 Mrad exposure, a strong change was observed which took about 6 days to recover. Anotherresonator, BC-81, as indicated in Fig. 11, shows an overnight frequency increase of 45 pp 10^9, after the last exposure.

Short-Term Transient Changes.

The transient frequency changes observed within 1 sec after 10 MeV electron irradiation were found[3] to depend not only on the resonator but also on the oscillator test bed. Measurements of the AGC voltage showed that these frequency changes are accompanied by changes of resonator resistance. Figure 13 shows several examples of these simultaneous transients. With unswept Premium-Q resonators such as G-1, the maximum of the resistance change is large and occurs between 100 and 300 msec after an electron pulse. With pulses repeating every 200 msec the resistance changes accumulate. Oscillation ceases after 3 or more pulses when the resistance exceeds the AGC limit shown. Some time after the irradiation is completed, oscillation resumes when the resistance has decayed to a value below the AGC limit. With swept Premium-Q resonators, such as BC-81, the maximum resistance change is substantially lower and occurs between 5 and 30 msec after the pulse. Resistance build-up, with multiple pulses, and cessation of oscillation were not observed in this case.

The resistance transient is related to a frequency transient that can be calculated with the calibration function f(R) mentioned in the preceding section on experimental procedures. As shown in Fig. 13 (right) these calculated frequency transients (dashed lines) are close to the observed ones (solid lines). Whereas the resistance transients originate in the quartz material, their effect on the frequency transients is modified by the oscillator circuitry.

Conclusions

From the data presented the following conclusions can be made.

1. Non-uniform impurity concentration across Premium-Q quartz bars has been indicated by variations in the strength of low temperature infrared spectra s-bands and weak impurity peaks in the acoustic losses of resonators.

2. No definite characterization of a specific sweeping process can be made in terms of either the infrared e-band spectra, acoustic losses, or radiation-induced frequency offset.

3. The e-bands produced by the removal of alkali ions from the vicinity of substitutional aluminum and replacement with H^+ in the sweeping process can also be produced in unswept or modified in swept material by ionizing radiation. These modifications are relatively small in some samples of swept Premium-Q quartz and very large in others. These changes in e-band strength appear to be related to differences found in the radiation-induced permanent oscillator frequency offset.

4. The effect of radiation induced transient changes of resonator resistance dominates the short-term transient oscillator frequency changes in the msec time interval after exposure with pulsed 10 MeV electrons.

Acknowledgements

The authors wish to thank the following associates at RADC. C. P. Werner for help with the acoustic loss measurements, L. F. Lowe, D. C. LaPierre and J. Capelli

for irradiation of the samples, A. F. Armington and R. N. Brown for providing samples of swept quartz, and A. Kahan and N. F. Yannoni for continued interest and support. They also wish to express their appreciation to D. Bandes of Parke Mathematical Laboratories for the computer programming and data processing, and to J. C. King of Sandia Laboratories and J. J. Martin of Oklahoma State University for helpful discussions.

References

1. H. G. Lipson, F. Euler and A. F. Armington, "Low Temperature Infrared Absorption of Impurities in High Grade Quartz", Proc. 32nd Annual Symposium on Frequency Control, 11 (1978).

2. F. Euler, P. Ligor, A. Kahan, P. Pellegrini, T. M. Flanagan and T. F. Wrobel, "Steady State Radiation Effects in Precision Quartz Resonators", Proc. 32nd Annual Symposium on Frequency Control, 24 (1978).

3. P. Pellegrini, F. Euler, A. Kahan, T. M. Flanagan and T. F. Wrobel, IEEE Trans. on Nuclear Science, NS25, 1267 (Dec. 1978).

4. T. J. Young, D. R. Koehler and R. A. Adams, "Radiation Induced Frequency Changes in Electrolyzed High Purity Quartz Resonators", Proc. 32nd Annual Symposium on Frequency Control, 34 (1978).

5. A. Kats, Philips Res. Reports, 17, 133 (1962).

6. R. N. Brown and A. Kahan, J. Phys. Chem. Solids, 36, 467, (1975).

7. J. J. Martin, L. E. Halliburton, M. Markes, N. Koumvakalis, W. A. Sibley, R. N. Brown and A. Armington, "Radiation-Induced Mobility of Interstitial Ions in Synthetic Quartz", Proc. 33rd Annual Symposium on Frequency Control, (1979), following paper. Also W. A. Sibley, J. J. Martin, M. C. Wintersgill and J. D. Brown, J. Appl. Physics, to be published.

8. D. B. Fraser, Physical Acoustics, W. P. Mason, editor, Volume V, Academic Press, New York, 1968, pp. 59-110.

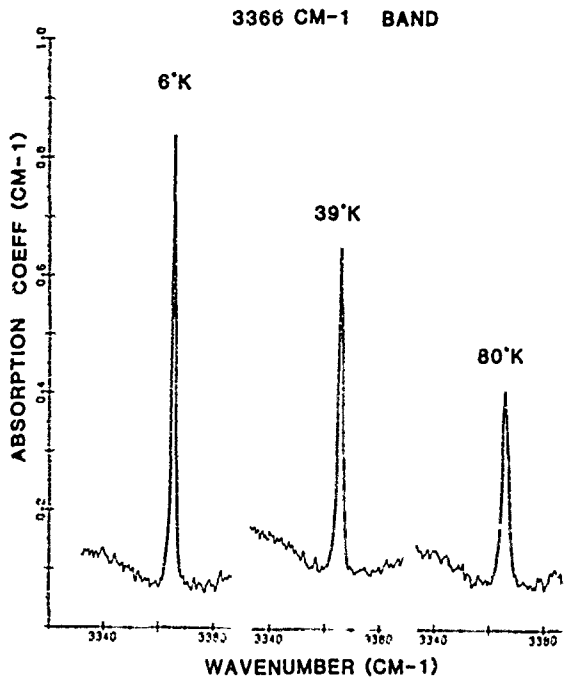

Fig. 1. Temperature dependence of the 3366 cm^{-1} e_2 band absorption, measured with E ⊥ Z.

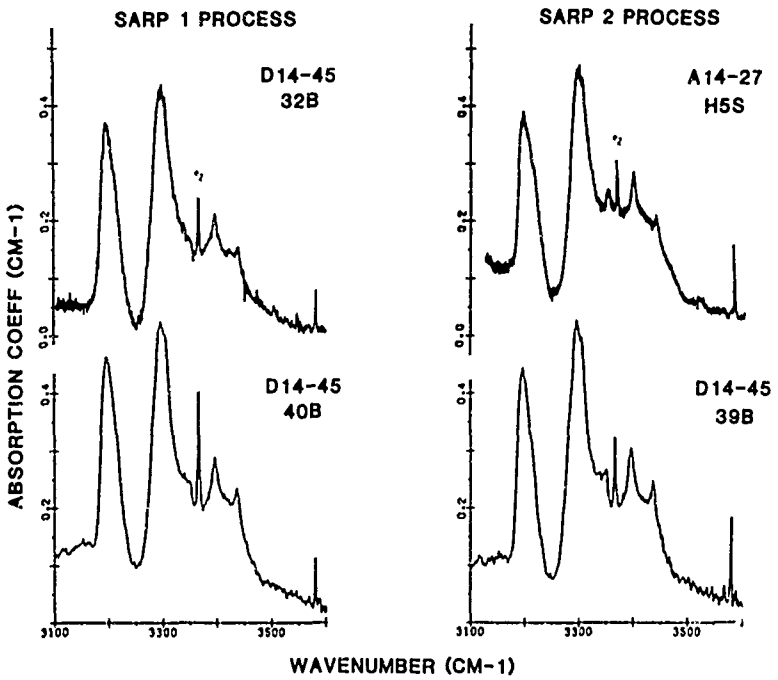

Fig. 2. Absorption spectra of Premium-Q quartz samples swept by SARP processes I and II, taken at 85 K, with E ⊥ Y.

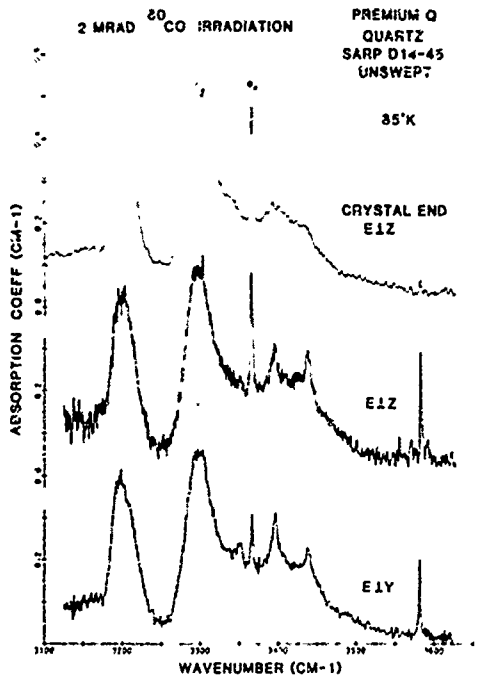

Fig. 3. Absorption of unswept Premium-Q quartz, from autoclave run D14-45, after irradiation; center and bottom spectra for same section, top section for an adjacent section closer to the end of the bar.

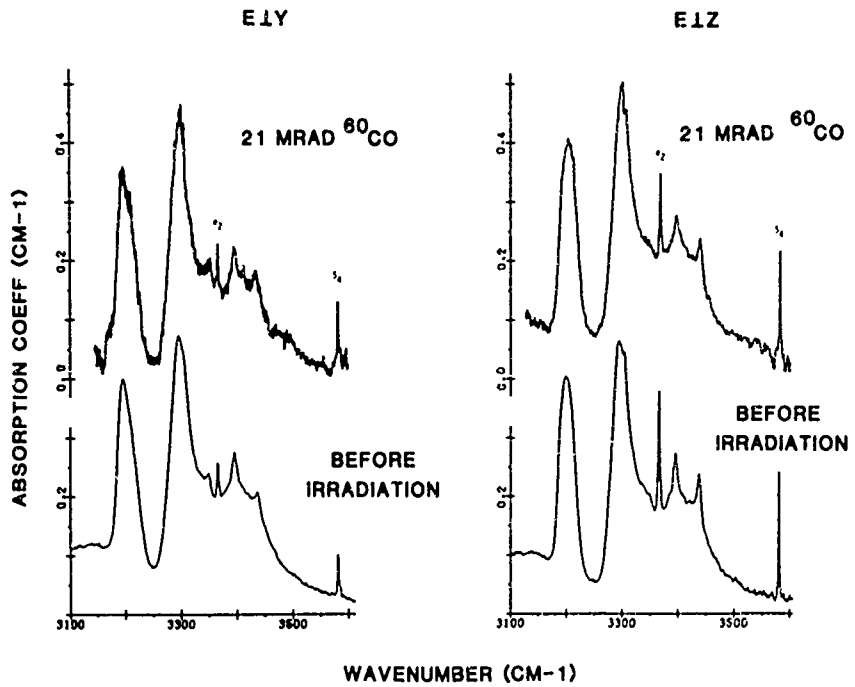

Fig. 4. Absorption spectra of Sandia air swept Premium-Q quartz, from autoclave run A14-27, taken at 85 K, before and after irradiation.

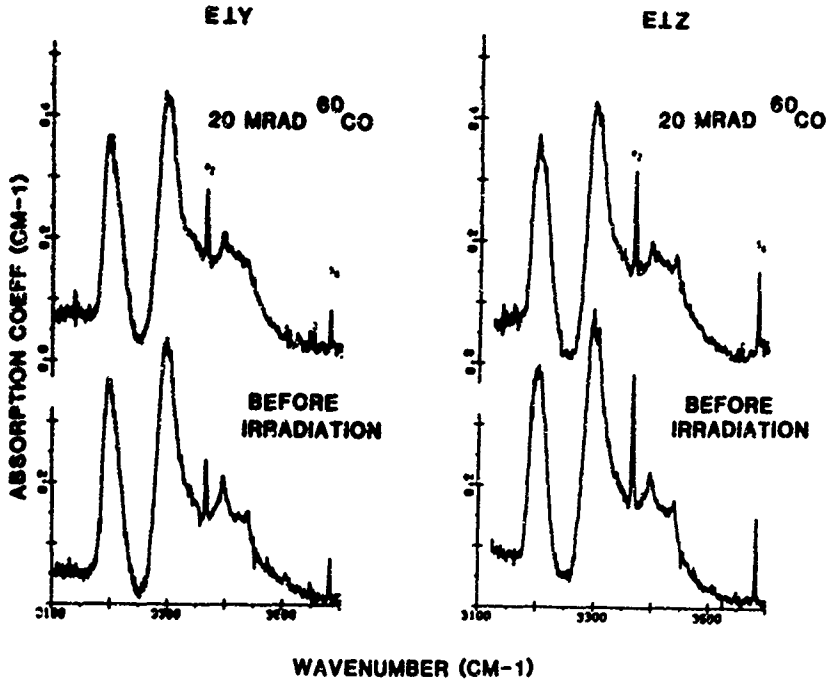

Fig. 5. Absorption spectra of SARP I swept Premium-Q quartz, from autoclave run D14-45, bar 32b-H3S, taken at 85 K, before and after irradiation.

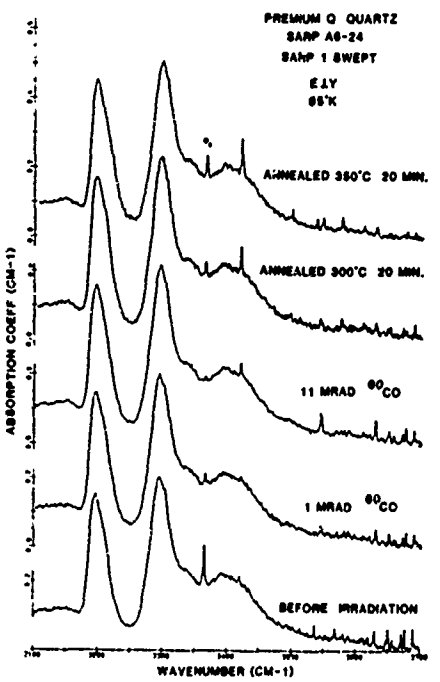

Fig. 6. Absorption spectra of SARP I swept Premium-Q quartz, from autoclave run A6-24, bar A4I, showing effects of irradiation and annealing; note the intensity changes of band e_2.

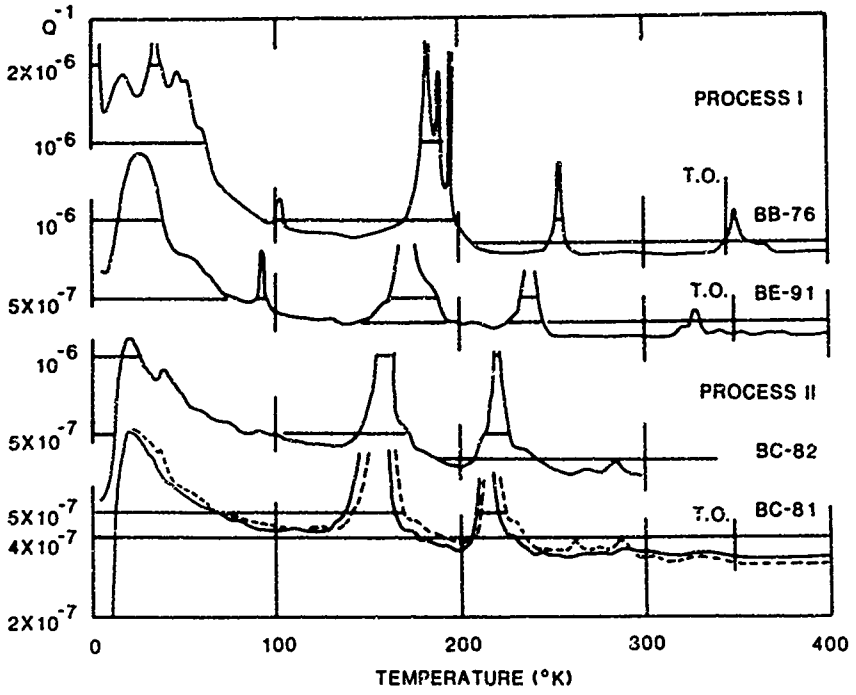

Fig. 7. Acoustic losses, $Q^{-1}(T)$, of SARP I and SARP II swept Premium-Q quartz resonators; T.O.: turnover temperature; solid lines: unirradiated; dashed line: irradiated with 1 Mrad of 10 MeV electrons.

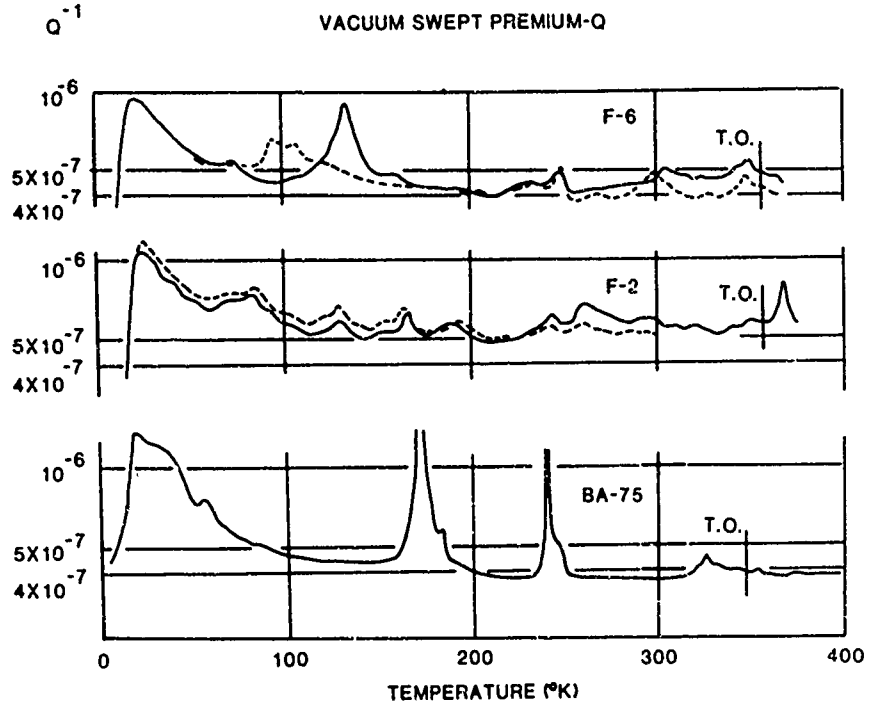

Fig. 8. Acoustic losses, $Q^{-1}(T)$, of Sandia vacuum swept Premium-Q quartz resonators; T.O.: turnover temperature; solid lines: unirradiated; dashed lines: irradiated with 1 Mrad of 10 MeV electrons.

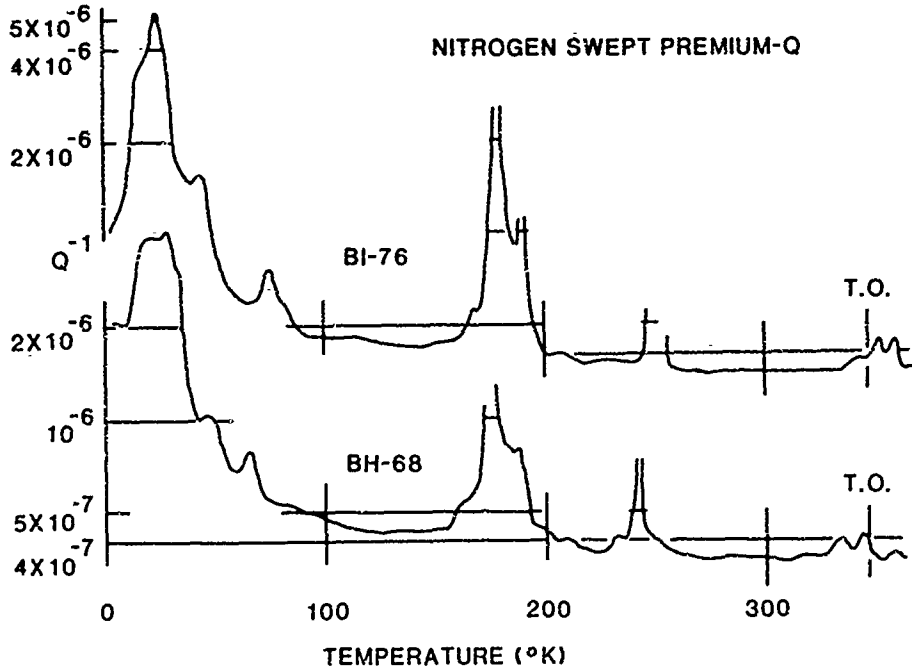

Fig. 9. Acoustic losses, $Q^{-1}(T)$, of nitrogen swept Premium-Q quartz resonators; T.O.: turnover temperature; note high phonon-phonon interaction peaks near 20 K.

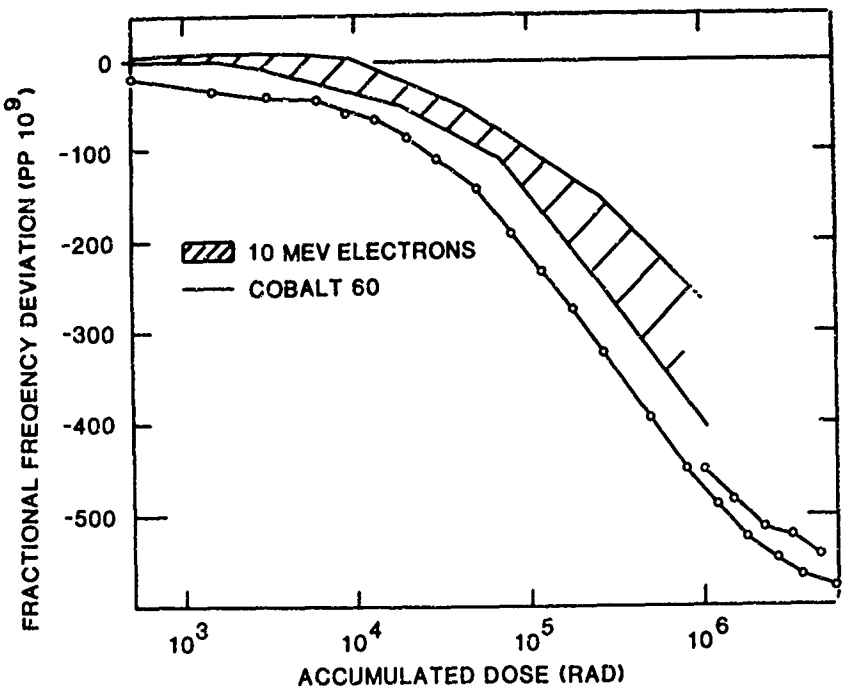

Fig. 10. Steady-state frequency offset induced by irradiation with comparable doses of 10 MeV electrons (data from six resonators) and ^{60}Co gamma rays (data from two resonators) in SARP I swept Premium-Q quartz resonators; material from SARP autoclave run A6-24, bar A4I.

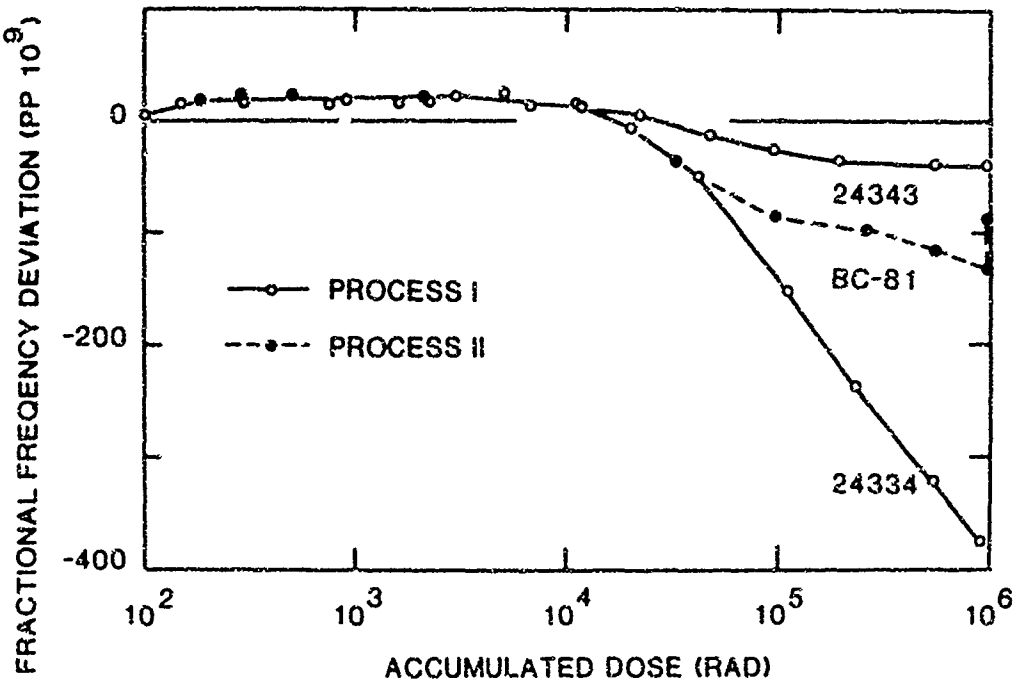

Fig. 11. Steady-state frequency offset induced by 10 MeV electron irradiation in SARP I and SARP II swept Premium-Q quartz resonators; note overnight frequency change after the last exposure of BC-81, near 10^6 rads.

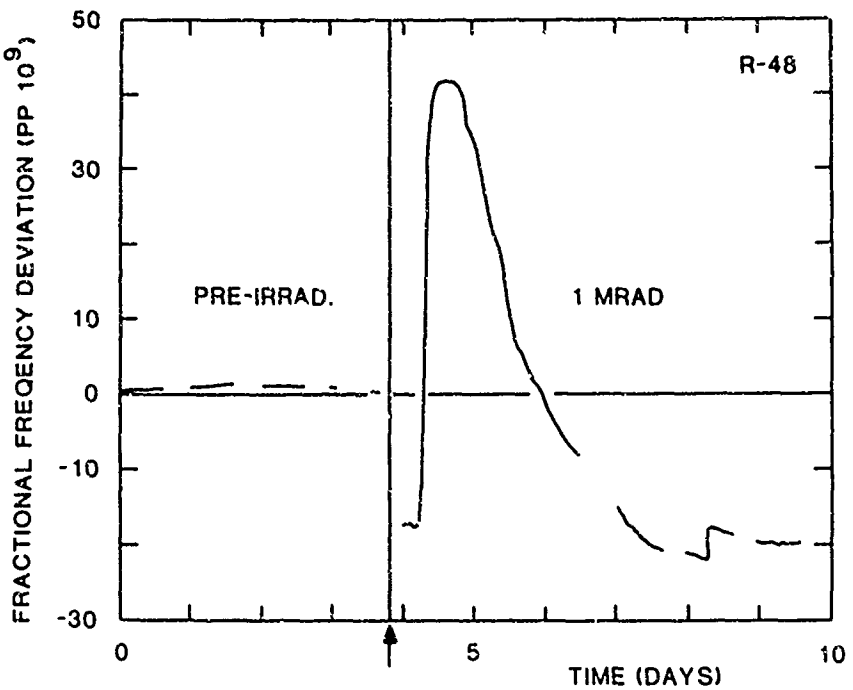

Fig. 12. Long-term transient frequency change after 1 Mrad ^{60}Co irradiation in SARP I swept Premium-Q quartz resonator R-48; arrow indicates start of 18 minute irradiation.

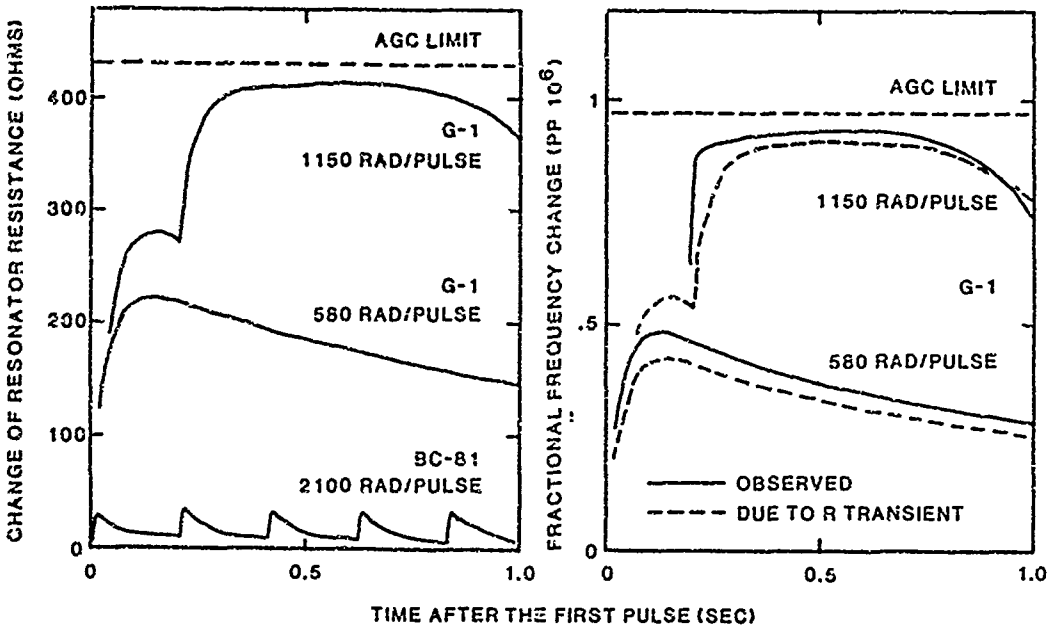

Fig. 13. Short-term transient resistance and frequency changes in one unswept(G-1) and one SARP II swept Premium-Q quartz resonator (BC-81), irradiated with single (center) double (top) and multiple (bottom, left only) pulses of 10 MeV electrons; doses per pulse as indicated; constant signal amplitude is maintained below the shown AGC limit above which oscillator ceases.

RADIATION-INDUCED MOBILITY OF INTERSTITIAL IONS IN SYNTHETIC QUARTZ

J. J. Martin, S. P. Doherty, L. E. Halliburton, M. Markes, N. Koumvakalis and W. A. Sibley
Department of Physics, Oklahoma State University
Stillwater, Oklahoma 74074

and

R. N. Brown and A. Armington
Rome Air Development Center (RADC/ET)
Hanscom AFB, Maryland 01731

Summary

We have used infrared absorption (IR), electron spin resonance (ESR), and acoustic loss (Q^{-1}) measurements on well-characterized Sawyer Premium Q and Electronic Grade quartz to investigate the radiation-induced mobility of interstitial ions. Our IR and ESR results show that under irradiation below 200K hydrogen is the dominant mobile interstitial. For irradiation above 200K, interstitial Na^+ ions become mobile and allow Al-OH^- and $[Al_{e+}]^o$ centers to be formed. The Al-OH^- complex gives rise to the 3367 cm^{-1} and 3306 cm^{-1} infrared bands. The mobility of interstitial Na^+ ions above 200K is further demonstrated by the disappearance of the 50K Na acoustic loss peak in both Na-swept Premium Q and Electronic Grade resonators. The normal sweeping process replaces the interstitial alkali, which charge compensates a substitutional Al^{3+}, with H^+ to form the Al-OH^-complex. Since the Al-OH^-complex is readily converted to $[Al_{e+}]^o$ centers by irradiation at 77K, we propose the following sensitive test for the completeness of the sweeping process: a) irradiate a sample at 77K and measure the $[Al_{e+}]^o$ concentration by ESR, b) irradiate the sample at room temperature and remeasure the $[Al_{e+}]^o$ concentration, c) repeat step a. If the sweeping process is complete, the $[Al_{e+}]^o$ concentration in steps a and c will be the same since step b will not displace any alkalis.

Introduction

Because of its piezoelectric properties, quartz has many applications in electronic instrumentation. Examples range from crystal-controlled oscillators and SAW-devices for use in time keeping and communication links to temperature and mass measuring instruments. In many cases, such as precision oscillators in satellites, the operation of quartz-containing devices can be degraded by radiation.[1-3] Thus, the defect structure of crystalline SiO_2 is a subject of considerable importance.

Direct studies of radiation-induced effects in quartz began with the work of Griffiths et al.[5] on the aluminum associated trapped hole center (now known as the $[Al_{e+}]^o$ center) and the work of Weeks[6] on the oxygen-vacancy-associated trapped electron center (E_1' center). For the $[Al_{e+}]^o$ center, O'Brien[7] successfully interpreted the magnetic resonance data in terms of a model having a hole trapped primarily in a non-bonding orbital of an oxygen ion adjacent to the substitutional aluminum. The comprehensive review by Weil[8] describes additional work on the aluminum-associated hole centers.

All quartz, natural or synthetic, contains aluminum substituting for silicon and thus charge compensators, the most common of which are interstitial H^+, Li^+ and Na^+, are required. It is expected that these interstitials will play a direct role in the response of quartz to radiation and this expectation has been born out by many experiments. The 50K acoustic loss peak observed in 5 MHz 5th overtone AT cut crystals which is attributed to interstitial Na^+ ions is removed by ionizing radiation.[4]

Interstitial H^+ ions are usually associated with a non-bonding oxygen orbital in the form of OH^- molecules. This association gives rise to infrared absorption which is used to routinely evaluate the quality of quartz.[9,10] If the IR measurements are made at cryogenic temperatures, the absorption bands narrow substantially and allow detailed investigations of the role of OH^- molecules.[11-13] Recent work by Sibley, et al.[14] shows that irradiation of a quartz sample held at liquid nitrogen or liquid helium temperatures breaks up the OH^- radicals and thus reduces the OH^- absorption. On the other hand, irradiation of unswept synthetic quartz while it is at room temperatures does not change the total OH^- absorption compared to before irradiation, but does produce two new bands.

Quartz has relatively large Z-axis channels along which the interstitial ions can move. Kats[11] making use of this characteristic, applied an electric field parallel to the Z-axis while holding the sample temperature in the 400 °C to 550 °C range. He succeeded in "sweeping" hydrogen and alkali interstitial ions into and out of the sample. Since charge neutrality must be maintained, if one species is removed it must be replaced by a similarly charged species. This technique of changing the relative concentration of hydrogen and alkali ions by sweeping has been used by many investigators and has proven extremely useful in defect identification studies. More importantly, sweeping prior to fabrication has been reported[15] to increase the radiation hardness of quartz crystals used in precision oscillators.

While the hole and E' centers can be observed

with electron spin resonance (ESR) and the OH^- molecules by infrared measurements, direct observation of the alkali interstitials is more difficult. Their presence is known to affect the Q of crystals and, therefore, the frequency stability of the oscillator. For example, Fraser[16] has shown that the 50K loss peak is due to interstitial Na^+ by sweeping Na into natural quartz.

In the present investigation, we have used parallel IR absorption, ESR, and Q^{-1} studies to obtain information about defect formation and migration during irradiation and thermal annealing in quartz. The samples studied were all commercially-available high-quality quartz, thus making our results directly applicable to device operation. The major portion of the paper is concerned with the radiation-induced mobility of interstitial H^+ and Na^+ ions. We find that the H^+ ions are mobile at all temperatures under irradiation but that the Na^+ ions are only mobile above 200K. As an application of these results, we describe a sensitive testing procedure for measuring the extent to which the interstitial Na^+ ions have been removed by the sweeping process.

Samples

A series of well documented, pure Z-growth, lumbered bars of Electronic Grade, swept Electronic Grade, Premium Q, and swept Premium Q were purchased from Sawyer Research Products. The bars were labeled EG and PQ for Electronic Grade and Premium Q, respectively, and then designated with a third letter to code the individual bar. Samples from each bar were numbered serially. Thus, sample EG-E30 was the 30th sample cut from bar E of the Electronic Grade (EG) material. Several bars had been cut in half by Sawyer and one half of the bar swept with their process, SARP I or SARP II. A number of samples were also swept at OSU and RADC. Several samples from bars EG-E and PQ-E were analyzed for Al, Li, Na, K and Fe by the Analytical Chemistry Division at Oak Ridge National Laboratory. The results are given in Table I.

TABLE I. IMPURITY ANALYSIS IN IMPURITY ATOMS PER MILLION SiO_2

Sample	Al	Li	Na	K	Fe
EG-E37		<9[+]	20	3	
EG-E39	4.5				32
EG-E43*	6.5	<9	<3	<1.5	
PQ-E2	16	<9	9	<1.5	75

[+] < Indicates the limit of detectability.
* Sample EG-E43 was swept at OSU.

The impurity analysis indicates that bar EG-E contains substantially more alkali ions than aluminum. Sample EG-E43, which was swept at OSU, shows a very low Na content as compared to sample EG-E37 which was not swept. Our ESR results suggest that Fe is not an isolated substitutional impurity. A few samples were also taken from the Premium Q bars D14-45 obtained from Sawyer by RADC. Plano convex AT cut 5 MHz 5th overtone resonators were fabricated from Premium Q bar D14-45DC that had been electrodiffused with Na at RADC and from an earlier Electronic Grade bar labeled SEG. Optical samples were also taken from these two bars. Optical and ESR samples were also cut from bars EG-E, PQ-E, and PQ-F for this study.

Results and Discussion

Infrared Absorption

Kats[11] and Lipson et al.[13] have investigated the IR spectrum of OH^- molecules in quartz as a function of various types of sweeping and Brown and Kahan[12] have investigated radiation effects in the IR spectrum. Recently, Sibley et al.[14] have also investigated the effects of ionizing radiation on the IR absorption of OH^- impurities. The upper curves in Fig. 1 show the IR absorption of Electronic Grade sample EG-E30 and of Premium Q sample D14-45-9b. The spectra were taken with the samples cooled to 80K and with the optical electric field perpendicular to the Z-axis. The Electronic Grade sample shows prominant OH^- bands at 3581 cm^{-1}, 3437 cm^{-1}, 3400 cm^{-1}, and 3348 cm^{-1} and intrinsic bands at 3300 cm^{-1} and 3200 cm^{-1}. The area under the OH^- bands corresponds to an OH^- concentration of approximately 15 ppm. The much smaller OH^- bands in the Premium Q^- sample indicate that it contains about 1 ppm OH^-. Hydrogen is expected to act as a charge compensator for various types of defects or impurities. We have not been able to directly correlate these bands with any specific impurity. If the sample is irradiated with 1.75 MeV electrons or with x-rays while it is held at 80K the OH^- bands decrease which indicates that the hydrogen is removed from the IR-active center and forms other types of defects. If the sample is then annealed to room temperature and the IR spectrum rerun after cooling the sample to 80K, we find that the original OH^- bands have been restored. This result indicates that the new hydrogen-related defects are thermally unstable below room temperature.

If the sample is, instead, irradiated to a dose of 2000 Joules/cm^3 while it is held at room temperature, absorption bands at 3367 cm^{-1} and 3306 cm^{-1} are produced as shown in the lower curve of Fig. 1. Kats[11] has suggested that these two bands are due to an isolated Al^{3+}-OH^- complex. In swept material,[11,13] the 3367 cm^{-1} and 3306 cm^{-1} bands are present before irradiation. Under irradiation at 80K, these two new bands are destroyed. Upon warming to 300K the two bands regain their original strength.

Since the 3367 cm^{-1} and 3306 cm^{-1} pair are produced in unswept material by irradiation at 300K, but not by irradiation at 77K, we investigated the effects of irradiation at intermediate temperatures. The sample was mounted in the optical Dewar, warmed to temperature T, irradiated to a dose of 2000 J/cm^3 with 1.75 MeV electrons, and then returned to 80K for the IR scan. Figure 2 shows that the bands do not start to grow under irradiation until the sample is approximately at 200K. Near 240K, the 3306 cm^{-1} band decreases and the 3367 cm^{-1} continues to grow. Similar behavior

was observed upon annealing the sample after 80K irradiation.[14] If we assume that both bands are due to very similar defects, possibly Al^{3+}-OH^- and plot the sum of peak heights for the two bands we get the upper curve shown in Fig. 2. This result shows that the center responsible for the 3367 cm^{-1} and 3306 cm^{-1} bands starts to grow in under irradiation at about 200K and saturates for temperatures above 250K. This center, possibly Al^{3+}-OH^-, when produced by irradiation is stable under isochronal annealing up to about 600K as shown in Fig. 3. For this experiment the sample was first irradiated at 300K, measured at 80K, then heated for 10 minutes at temperature T, quenched in liquid nitrogen and remeasured. When the center is produced by sweeping it is stable up to at least 800K.

Electron Spin Resonance

The ESR spectrometer used in this work was a 9.1 GHz home-built homodyne microwave bridge with a 9-inch Varian Field-dial magnet. The magnetic field was modulated at 100 KHz. All ESR data were taken at 77K. In quartz, many of the electron-like paramagnetic defects are most easily observed with the phase-sensitive detector adjusted "out-of-phase" while hole-like centers are observed with the detector adjusted "in-phase". Curve a of Fig. 4 shows the in-phase response of unswept Electronic Grade sample EG-E37 after an initial electron irradiation at 77K. Curve b of Fig. 4 shows the out-of-phase response of this same sample. No ESR signals were observed in this or any other samples before irradiation. Both curves contain previously unreported ESR spectra. One of these, U-1 in Fig. 1a, is hole-like. This notation is arbitrary and only meant to be used until a model, and thus a more precise label can be assigned. Additional unlabeled and unidentified hole-like spectra, as well as the $[Al_{e+}]^o$ center, are present in curve a. The electron-like spectra U-2, U-3, and U-4 are found in Fig. 4b. The doublet hyperfine splitting of the U-2 and U-3 centers strongly suggests that they are perturbed by a nearby proton. Another signal present in the spectrum, but not shown on this scale, is the widely-split doublet due to atomic hydrogen.[17] All but the U-4 center were destroyed by warming the sample to room temperature. Figure 5 shows the thermal stability of these defects during a series of 5 minute pulse anneals at progressively higher temperatures. The monitoring temperature was 85K. Very few $[Al_{e+}]^o$ centers were produced by the initial low temperature irradiation, and they thermally decayed between 90K and 110K as did the hole-like U-1 center. In this same temperature region the hydrogen atom, H^o, and the U-3 center increased as the U-2 decreased. Between 115K and 135K, the hydrogen atom was thermally destroyed while at the same time the hydrogen-perturbed U-2 and U-3 centers grew. At higher temperatures, all of the centers except the U-4 disappeared. Qualitatively, the production of atomic hydrogen and the hydrogen-related U-2 and U-3 centers by irradiation of the sample at low temperatures correlates very well with the reduction of the OH^- IR absorption described above. Although the recovery of the IR bands upon annealing does not show the detailed structure seen in the decay of the hydrogen-related ESR signals, the IR bands do recover over this same temperature range. These results show that the hydrogen ion is mobile under irradiation even at very low temperatures.

After the initial 77K irradiation, a subsequent identical irradiation at room temperature of this same Electronic Grade sample EG-E37 was made. This irradiation produced a larger $[Al_{e+}]^o$ center signal and the hydrogen-related oxygen-vacancy centers E_2' and E_4'.[18,19,20] Identical spectra have been observed in similar samples that have only been irradiated at room temperature. The sample EG-E37 was then reirradiated at 77K. The "in-phase" (hole-like) spectra for these three irradiations are shown in Fig. 6. The striking feature of this irradiation sequence is the large enhancement of the $[Al_{e+}]^o$ center concentration by the room temperature irradiation and the even larger increase following the second low temperature irradiation. Following the room temperature and subsequent low temperature irradiation, the thermal annealing was repeated. The hydrogen atom center and the U-1, U-2 and U-3 centers showed the same behavior as before. The major new features are the appearance of the E_2' and E_4' centers above 120K and the decrease of the $[Al_{e+}]^o$ center only to the concentration established by the room temperature irradiation.

This complete irradiation sequence was repeated on the swept sample EG-F12. Bar EG-F was a paired bar to bar EG-E so the main difference was that it had been swept by Sawyer. The initial 77K irradiation produced a factor of 25 increase in the $[Al_{e+}]^o$ center concentration over that of the unswept sample EG-E37. The production of $[Al_{e+}]^o$ centers as well as the other centers in the two samples was very similar for the room temperature irradiations.

The enhanced production of $[Al_{e+}]^o$ centers by a 77K irradiation is produced either by an initial room temperature irradiation or by sweeping. In both room temperature irradiated unswept samples and in unirradiated swept samples, the 3367 cm^{-1} and 3306 cm^{-1} infrared bands are present. We have found that if they are not present then a 77K irradiation produces only a small $[Al_{e+}]^o$ center concentration. These results are illustrated by the parallel IR absorption spectra and ESR spectra that were run on unswept Premium Q sample PQ-E5 and swept Premium Q sample PQ-F10. Bars PQ-E and PQ-F were halves of an original Premium Q bar; the half labeled PQ-F was swept by Sawyer. Figure 7 shows the results on PQ-E5. Curve a gives the initial IR spectrum taken at 80K; note the absence of the 3367 cm^{-1} and 3306 cm^{-1} bands. The noisy trace is due to the small sample size since the actual ESR sample (2 x 3 x 8 mm^3) was used for the optical measurements. No ESR signals were observed before irradiation. Curve b on the left shows the IR spectrum after irradiation at 80K, the right hand trace shows the complementary weak $[Al_{e+}]^o$ center ESR signal. Curve c was taken after the sample had been warmed to 300K. The IR trace of curve d shows the 3367 cm^{-1} and 3306 cm^{-1} bands produced by a room temperature irradiation; the ESR trace

shows the complementary $[Al_{e+}]^o$ center spectrum. Curve e shows the complementary IR absorption and $[Al_{e+}]^o$ center spectra taken after a low temperature irradiation; note the large increase in the $[Al_{e+}]^o$ center signal and the disappearance of the 3367 cm^{-1} and 3306 cm^{-1} bands. Figure 8 shows the identical sequence of IR and ESR spectra and irradiations taken on Sawyer-swept sample PQ-F10. Curve a shows the IR absorption, note the presence of the 3367 cm^{-1} and 3306 cm^{-1} bands; no $[Al_{e+}]^o$ center absorption spectrum was observed. Curve b was taken after an initial low temperature irradiation; note the large $[Al_{e+}]^o$ center ESR signal and the absence of the 3367 cm^{-1} and 3306 cm^{-1} bands. Curve c shows the IR absorption after the sample was warmed to 300K; the complementary ESR trace was omitted since it is the same as curve d which was taken after a room temperature irradiation. Curve e is for the final low temperature irradiation; here the $[Al_{e+}]^o$ center concentration is only slightly larger than the concentration following the initial low temperature irradiation.

Further evidence connecting the enhanced production of the $[Al_{e+}]^o$ center after a low temperature irradiation with the presence of the 3367 cm^{-1} and 3306 cm^{-1} bands was found by a series of irradiations at progressively higher temperatures, between 77K and 300K. Following each irradiation the sample was returned to 77K and reirradiated to insure filling all electron traps before measuring the $[Al_{e+}]^o$ center ESR spectrum. The intensity of this 77K-irradiation-produced $[Al_{e+}]^o$ center spectrum is plotted versus the intermediate irradiation temperature for unswept sample EG-E34 in Fig. 9. The onset of the $[Al_{e+}]^o$ center enhancement for unswept samples starts at 200K; this enhancement closely matches the onset of the production of the 3367 cm^{-1} and 3306 cm^{-1} bands during irradiation at intermediate temperatures as shown in Fig. 2.

Figure 10 shows the high temperature anneal characteristics of the $[Al_{e+}]^o$ center enhancement in unswept samples EG-E38. In this run the sample was first irradiated at 300K and then at 77K to establish the base $[Al_{e+}]^o$ concentration. The sample was then annealed for 15 minutes at temperature T, reirradiated at 77K, and then measured. The decay in the enhancement occurs in the 575K to 675K range. This again matches the disappearance of the Al-OH^- center measured by the 3367 cm^{-1} and 3306 cm^{-1} bands in unswept sample EG-E30, as shown in Fig. 10. In swept material the enhanced $[Al_{e+}]^o$ production and the 3367 cm^{-1} and 3306 cm^{-1} bands are stable under high temperature anneal.

Model

The chemical analysis described in the sample section indicates that in our unswept Sawyer Electronic Grade and Premium Q material sodium is the major alkali impurity. Much of the Na probably acts as a charge compensator for Al^{3+} substitutional impurities. When combined with our IR and ESR results, the following picture emerges. Hydrogen is mobile under irradiation at all temperatures. At sufficiently low temperatures it is trapped as the atomic hydrogen center and as several other centers. Upon warming the sample to room temperature hydrogen returns to its original OH^- configuration. If the irradiation is performed at temperatures above 200K the interstitial Na^+ ions (and possibly other alkalis) which were trapped near substitutional Al^{3+} ions becomes mobile. Then, depending upon the availability of electron traps, a hole or an H^+ ion becomes bound to a neighboring oxygen forming either the $[Al_{e+}]^o$ or Al-OH^- center. The latter is most likely responsible for the 3367 cm^{-1} and 3306 cm^{-1} infrared bands. Finally, a subsequent low temperature irradiation fills the shallow electron traps so that the $[Al_{e+}]^o$ center concentration increases. This picture is consistent with the usual sweeping processes in which Na and other alkalis are replaced by hydrogen. For example, sample EG-E43 which was swept at OSU showed a decrease in Na content from approximately 20 ppm to less than 3 ppm after sweeping. The sweeping process replaces the interstitial Na^+ near a Al^{3+} with a H^+; thus, producing the 3367 cm^{-1} and 3306 cm^{-1} bands and causing a large $[Al_{e+}]^o$ center concentration after the first low temperature irradiation.

Sweeping Test

Besides providing a more fundamental understanding of the radiation response of synthetic quartz, the present investigation also has practical application with regard to sweeping. The onset of the radiation-induced mobility of interstitial Na^+ ions above approximately 200K provides a method for evaluating the extent to which these alkali ions have been removed from a crystal by the sweeping process. This evaluation procedure would consist of examining the $[Al_{e+}]^o$ center ESR spectrum after each step of the following sequence of three irradiations; initial 77K irradiation, room temperature irradiation and re-irradiation at 77K. For a sample in which the sweeping process is complete (i.e., all the alkalis have been replaced by hydrogen), the $[Al_{e+}]^o$ center ESR spectrum will have the same intensity after the first 77K irradiation as after the second 77K irradiation. In the case of a partially-swept sample, the ratio of the $[Al_{e+}]^o$ center ESR spectrum intensity after the first 77K irradiation to that after the second 77K irradiation is a sensitive indicator of what fraction of interstitial Na^+ ions have been replaced by hydrogen ions. In this sweeping evaluation procedure, the intermediate room temperature irradiation is, of course, a crucial step. This technique for evaluation of completeness of sweeping has given consistent results for every Sawyer-grown quartz sample we have investigated and we believe it to be valid for any synthetic quartz grown using sodium carbonate as the mineralizer. We cannot yet generalize the result to all quartz since it is not known whether interstitial Li^+ ions will become mobile at the same temperature as the Na^+ ions when the sample is subjected to a radiation field.

Acoustic Loss

Acoustic loss, Q^{-1}, measurements have been made by the log decrement method on several Na-

swept Premium Q resonators and on several unswept Electronic Grade resonators. All resonators were 5 MHz 5th overtone AT cut plano-convex blanks mounted in a gap holder. The holder was attached to a variable temperature cryostat so that Q^{-1} measurements could be made over the 5 to 350K temperature range. A Premium Q bar from Sawyer autoclave run D14-45 was first swept in an Ar atmosphere,[13] then a layer of $NaCO_3$ was vapor deposited, and the sweeping run repeated. Samples from this Na-swept bar are labeled D14-45DC. Infrared studies on an optical sample from this bar show the presence of the 3367 cm^{-1} and 3306 cm^{-1} bands. However, when an optical sample from this bar was irradiated, at room temperature the 3367 cm^{-1} and 3306 cm^{-1} bands showed approximately a 20% increase. This suggests that approximately 20% of the Al^{3+}-OH^- complexes were converted to Al^{3+}-Na^+ complexes during the second sweeping run. The Electronic Grade resonators were fabricated from an earlier batch of Sawyer material labeled SEG. Infrared studies show no major difference between this material and the more recent EG bars.

The solid curve in Fig. 11 shows the as-received 5 MHz Q^{-1} results for Na-swept resonator D14-45DC (2). A number of the peaks are due to interfering modes. The large loss peak near 50K is due to the Al^{3+}-Na^+ complexes.[16] Our own measurements on unswept resonators from Premium Q bar D14-45-9b and those of Euler et al.[3] on swept D14-45 series resonators show no evidence of the 50K Na loss peak. Thus, we can conclude that Na was introduced during the sweeping process. A series of irradiations with 1.75 MeV electrons to a dose of 2000 J/cm^3 each at 77K, 215K and 300K were made on this resonator and the Q^{-1} vs T spectrum was run after each irradiation. The dashed curve in Fig. 11 shows the complete Q^{-1} spectrum after the third irradiation. The Na loss peak is completely gone after this room temperature irradiation. Figure 12 shows the Q^{-1} spectrum at low temperatures for this resonator in the as-received condition, and after each of the three irradiations at progressively higher temperatures. The irradiation at 77K caused no change in the Na loss peak, the 215K irradiation lowered the peak, and the 300K irradiation completely removed it. This behavior is in excellent agreement with our IR and ESR results described above which show that irradiation above 200K moves the Na^+ ion away from the Al^{3+} and replaces it with either a H^+ ion or a hole.

Since unswept Electronic Grade material contains considerable amounts of Na^+, we ran the Q^{-1} spectrum on a Electronic Grade resonator SEG 007(1) in the as-received condition and after irradiations at 180K, 200K, 220K, and 250K. The low temperature results for the unirradiated condition and after the 220K irradiation are shown in Fig. 13. After the 220K irradiation, only a small Na loss peak remains. Figure 14 shows the full spectrum for this Electronic Grade resonator after the 250K irradiation; note that the Na loss peak is completely gone. We have not been able to identify the large loss in the 100K to 170K region. The loss peak near 270K[4] is probably due to OH^-.

Our IR and ESR results indicate that annealing the sample above 700K will restore the unirradiated condition. The Electronic Grade resonator was annealed at 748K and the Q^{-1} spectrum was remeasured. Figure 14 shows that the annealing restored the Na loss peak.

Thus, we see that the behavior of the Al^{3+}-Na^+ complex, as measured by the acoustic loss peak, follows the IR and ESR results. Figure 15 shows the fractional decrease $\Delta Q^{-1}/\Delta Q_o^{-1}$, where ΔQ_o^{-1} is the original height of the Na loss peak, versus irradiation temperature. The open diamonds represent the Na-swept Premium Q resonator and the open squares the Electronic Grade resonator. The Na loss peak disappears under irradiation at the same temperatures for which the Al^{3+}-OH^- complex (measured by the 3367 cm^{-1} and 3306 cm^{-1} infrared bands) as shown by the solid circles in Fig. 15 and by the enhancement under irradiation of the $[Al_{e+}]^o$ center is shown by the solid squares in Fig. 15.

The authors thank Dave Randall of K-W Manufacturing, Prague, OK, for his help in fabricating the resonators. This work was supported in part by the U.S. Air Force, Contract No. F19628-77-C-017.

References

1. J. C. King and H. H. Sander, IEEE Trans. on Nuc. Sci. NS-19, 23 (1972).

2. T. M. Flanagan, IEEE Trans. on Nuc. Sci. NS-21, 390 (1974).

3. F. Euler, P. Ligor, A. Kahan, P. Pellegrini, T. M. Flanagan and T. F. Wrobel, IEEE Trans. on Nuc. Sci. NS-25, 1267 (1978).

4. D. B. Fraser. Physical Acoustics (W. P. Mason, ed.) Vol. III-Part A, pp. 1-42, Academic Press, New York, 1966.

5. J. H. E. Griffiths, J. Owen and I. M. Ward, Defects in Crystalline Solids (London, 1955), Bristol Conference, p. 88, Physical Soc.

6. R. A. Weeks, J. Appl. Phys. 27, 1376 (1956).

7. M. C. M. O'Brien, Proc. Roy. Soc. (London) A231, 404 (1955).

8. J. A. Weil, Rad. Effects 26, 261 (1975) also "A Review of Impurity Atom Defects in α-Quartz as Observed by Electron Paramagnetic Resonance "Proceedings, 27th Annual Symposium on Frequency Control, U.S. Army Electronics Command, Fort Monmouth, New Jersey, p. 153 (1973).

9. D. B. Fraser, D. M. Dodd, D. W. Rudd and W. J. Carroll, Frequency, 4, 18 (1966).

10. B. Sawyer, IEEE Trans. Sus., SU-19, 41 (1972).

11. A. Kats, Phillips Research Reports 17, 133 (1962).

12. R. N. Brown and A. Kahan, J. Phys. Chem. Solids 36, 467 (1975).

13. H. G. Lipson, F. Euler and A. F. Armington, "Low Temperature Infrared Absorption of Impurities in High Grade Quartz" Proceedings, 32nd Annual Symposium on Frequency Control, U.S. Army Electronics Command, Fort Monmouth, New Jersey, pp. 11-23 (1978).

14. W. A. Sibley, J. J. Martin, M. C. Wintersgill and J. D. Brown, J. Appl. Phys. (in press).

15. B. R. Capone, A. Kahan, R. N. Brown and J. R. Buckmelter; IEEE Trans. on Nuc. Sci., NS-17, 217 (1970).

16. D. B. Fraser, J. Appl. Phys. 35, 2913 (1964).

17. R. A. Weeks and M. Abraham, J. Chem. Phys. 42, 68 (1965).

18. R. A. Weeks, Phys. Rev. 130, 570 (1963).

19. R. A. Weeks and C. M. Nelson, J. Am. Ceram. Soc. 43, 399 (1960).

20. L. E. Halliburton, B. D. Perlson, R. A. Weeks, J. A. Weil and M. C. Wintersgill, Solid State Commun. (in press).

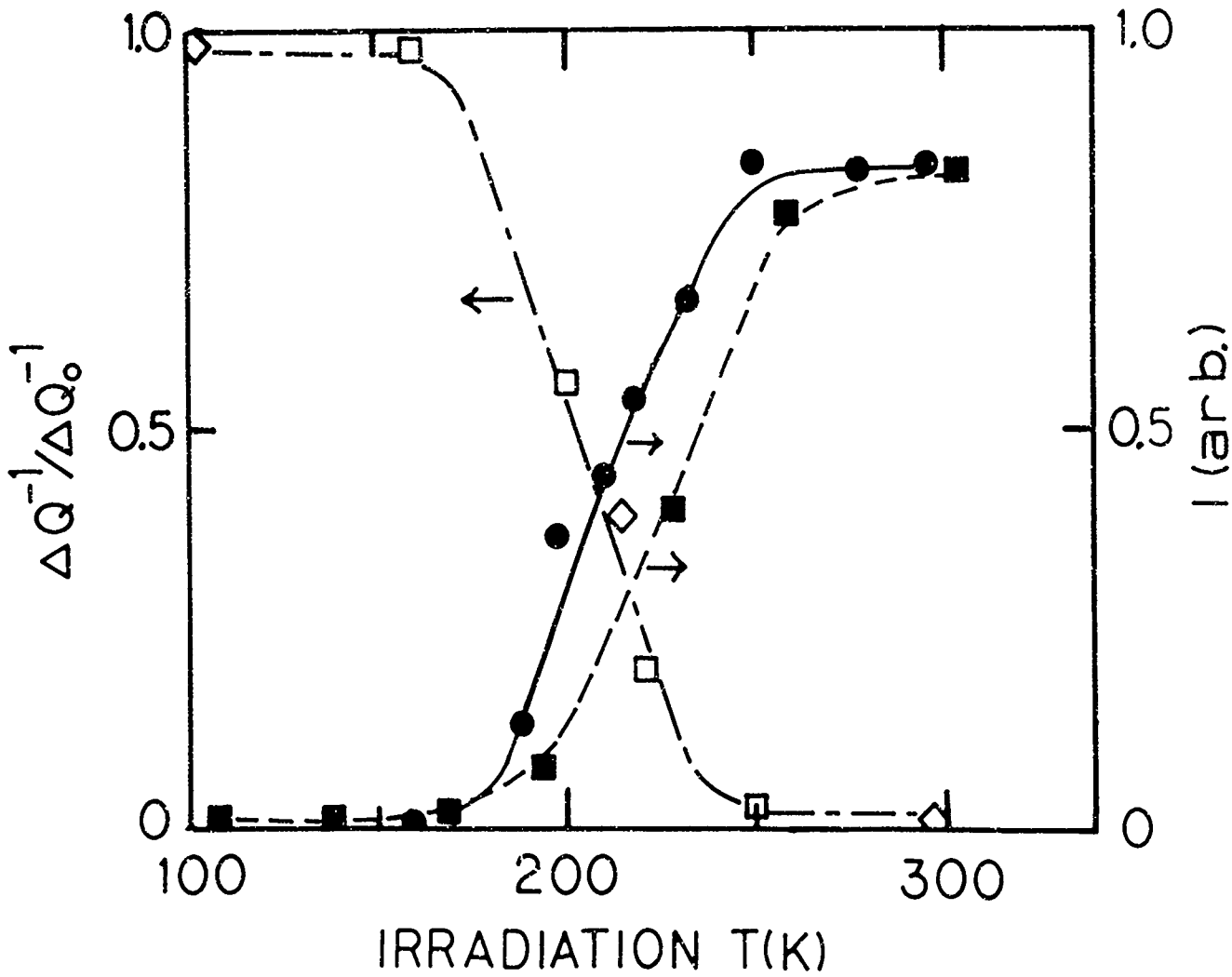

Fig. 15.

The open diamonds and squares give the fractional change in the Na loss peak versus irradiation temperature for the Na-swept Premium Q and unswept Electronic Grade resonators respectively. The closed circles give the total relative concentration for the Al-OH^-centers responsible for the 3367 cm^{-1} and 3306 cm^{-1} infrared bands. These are produced by replacing the interstitial Na^+ with H^+. The closed squares show the enhancement of the $[Al_{e^+}]^o$ concentration as the H^+ replaces the Na^+.

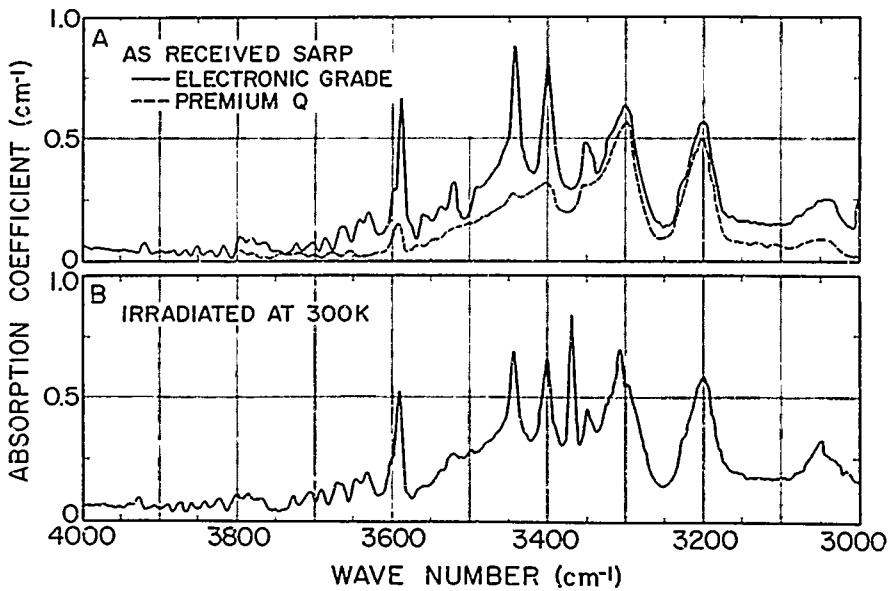

Fig. 1.

In A, the upper solid curve shows the infrared absorption taken at 77K for Electronic Grade sample EG-E30 in the as received condition. The dashed curve shows the results for Premium Q sample D14-45-9b. In B, the infrared absorption in the Electronic Grade Sample after a 300K irradiation to a dose of 2000 J/cm^3 is shown. This irradiation has produced the bands at 3367 cm^{-1} and 3306 cm^{-1}. These two bands are present in swept samples before irradiation.

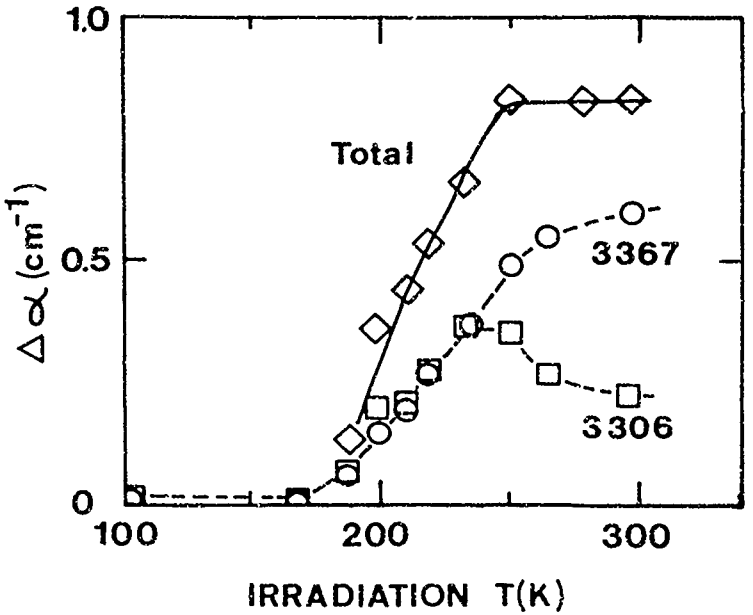

Fig. 2.

The production of the 3367 cm^{-1} and 3306 cm^{-1} bands as a function of sample temperature during irradiation is shown. The sample is unswept Electronic Grade EG-E30. Both bands have the same half-width[14] and if we assume that both are due to Al^{3+}-OH^- the total peak height (upper curve) will describe the total number Al^{3+}-OH^- defects.

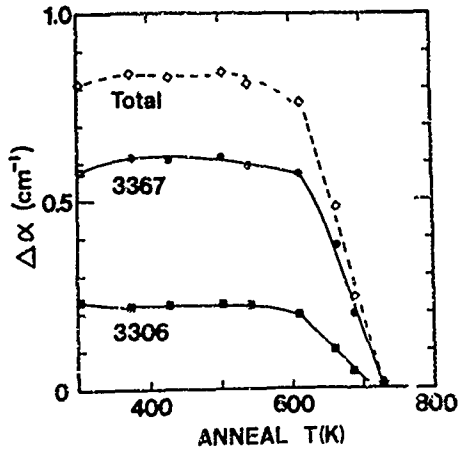

Fig 3.

The high temperature annealing behavior of the center, probably Al^{3+}-OH^-, responsible for the 3367 cm^{-1} and 3306 cm^{-1} bands is shown. In swept material the centers do not anneal out.

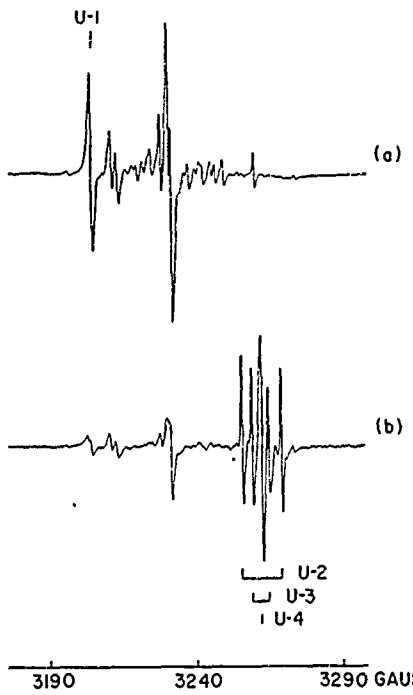

Fig. 4.

Curve a shows the in-phase response of unswept Electronic Grade Sample EG-E37 after an initial electron irradiation at 77K. Center U-1 is a hole like center perturbed by hydrogen. The center curve contains the weak $[Al_{e+}]^o$ signal and several unidentified hole centers. No ESR signals were observed before irradiation in this or any other sample. Curve b shows the out-of-phase response of this same sample. U-2, U-3 and U-4 are electron-like centers with U-2 and U-3 perturbed by hydrogen. The hydrogen atom spectrum was present but was too widely split to show on this diagram.

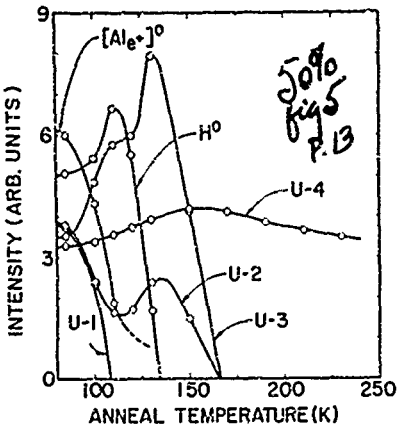

Fig. 5 The Thermal stability of the centers shown in figure 4 is shown. All except the U-4 center decay well before room temperature.

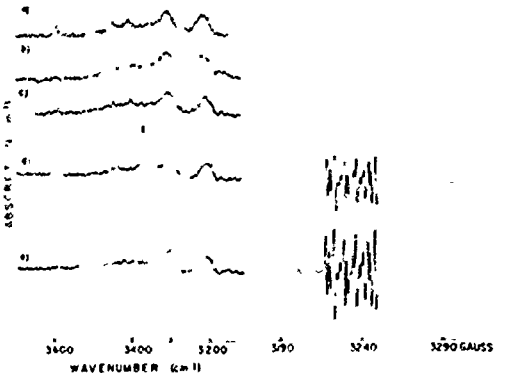

Fig. 7.

The infrared absorption and ESR spectra on unswept Premium Q sample PQ-E5 are shown for a series of irradiations. Curve a is for the as-received sample, no ESR signals were detected. Curve b is for a 80K irradiation, only a small $[Al_{e+}]^{o}$ signal is seen. Curve c is after the sample was warmed to 300K, again no ESR signals were detected. Curve d is after a 300K irradiation, note the large 3367 cm^{-1} and 3306 cm^{-1} bands and the $[Al_{e+}]^{o}$ ESR signal. Curve e is for a subsequent 80K irradiation, the OH^{-} bands have disappeared and the $[Al_{e+}]^{o}$ signal has grown.

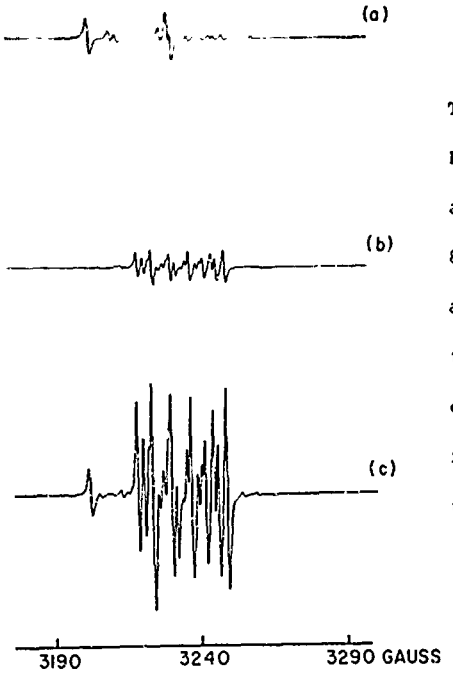

Fig. 6.

Curve a shows the original in-phase (hole-like) ESR spectrum for unswept sample EG-E37 after a 77K irradiation. Curve b shows the in-phase spectrum after a room temperature irradiation and curve c shows the in-phase spectrum after the same was re-irradiated at 77K. Note the very large growth of the $[Al_{e+}]^{o}$ center.

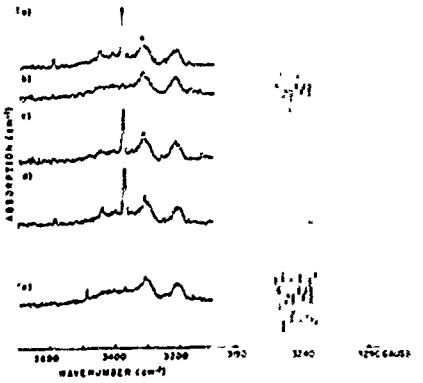

Fig. 8.

A sequence identical to that used in Fig. 7 is shown for the swept Premium Q sample PQ-F10. Note the presence of the 3367 cm^{-1} and 3306 cm^{-1} bands in the as-received condition (curve a) and the large $[Al_{e^+}]^o$ concentration after the first low temperature irradiation.

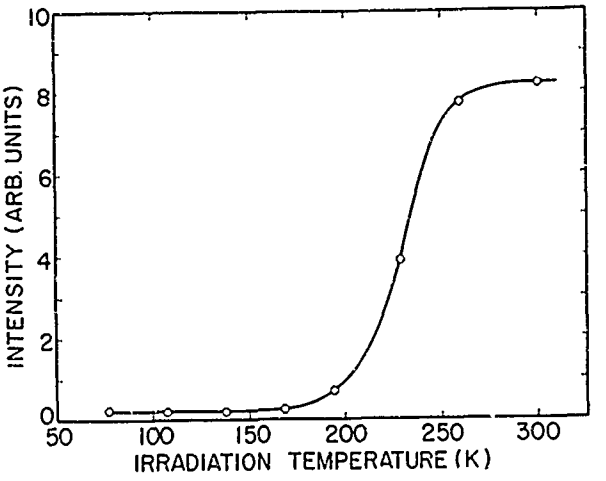

Fig. 9.

The enhancement of the $[Al_{e^+}]^o$ concentration for unswept Electronic Grade sample EG-E34 (measured by ESR) is shown as a function of sample temperature during the initial irradiation. The sample was subsequently irradiated at 77K. The curve matches the production of the 3367 cm^{-1} and 3306 cm^{-1} bands shown in Fig. 2.

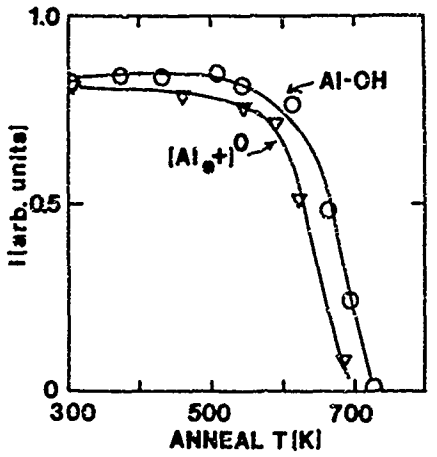

Fig. 10.

The high temperature annealing of the $[Al_{e+}]^{\circ}$ enhancement in unswept Electronic Grade sample EG-E38 is shown. The sample was heated to temperature T then reirradiated at 77K and measured. The decay in enhancement matches the annealing of the $Al\text{-}OH^{-}$ as measured by the 3367 cm^{-1} and 3306 cm^{-1} bands.

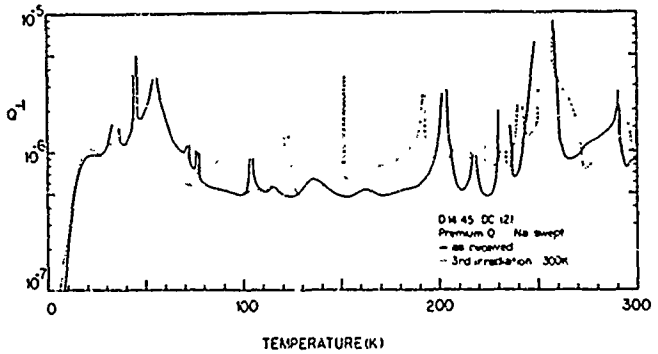

Fig. 11.

The solid curve shows the as-received Q^{-1} vs T spectrum at 5 MHz for a Na-swept Premium Q resonator. The Na loss peak is near 50K. After a 300K irradiation this peak has disappeared as shown by the dashed curve.

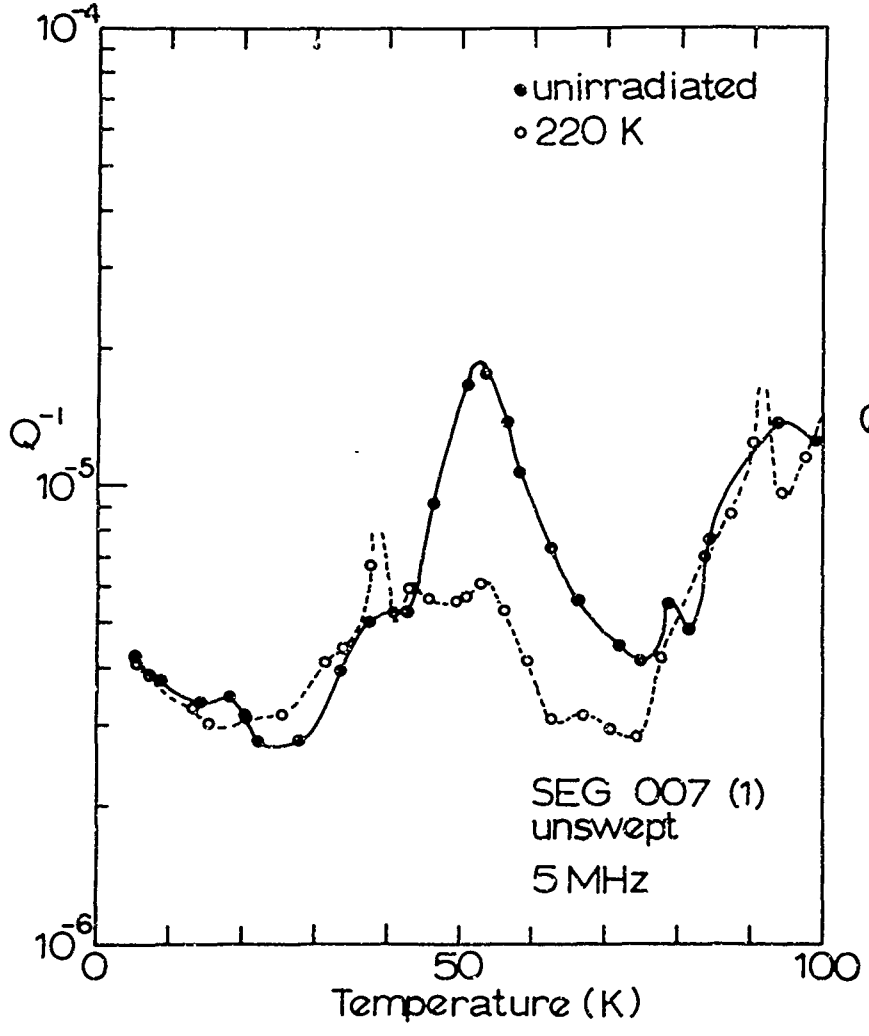

Fig. 13.

The 50K Na loss peak in unswept Electronic Grade material is shown. Only a small portion of the peak remains after an irradiation at 220K.

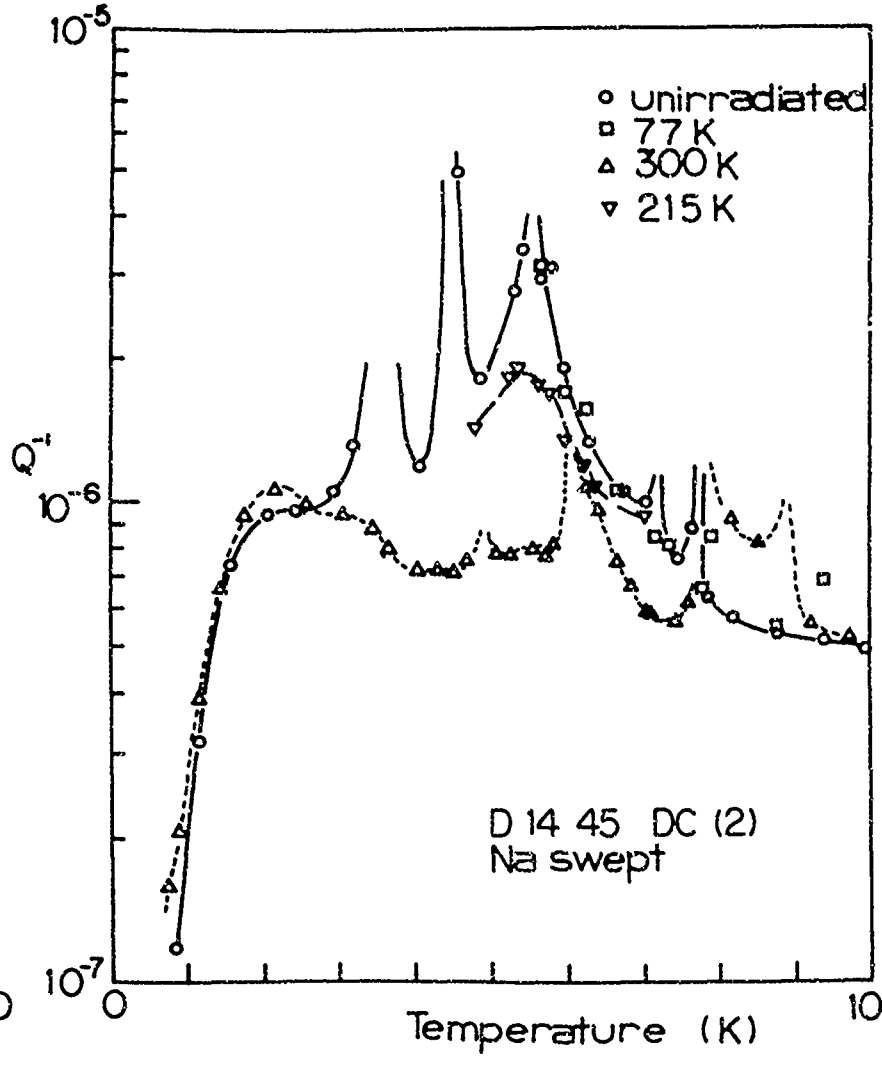

Fig. 12.

The low temperature Q^{-1} spectrum for the Na-swept Premium Q resonator is shown for a series of irradiations. The 77K irradiation produced no change in the 50K Na loss peak, a 215K irradiation substantially reduced it and after a 300K irradiation the Na loss peak is gone.

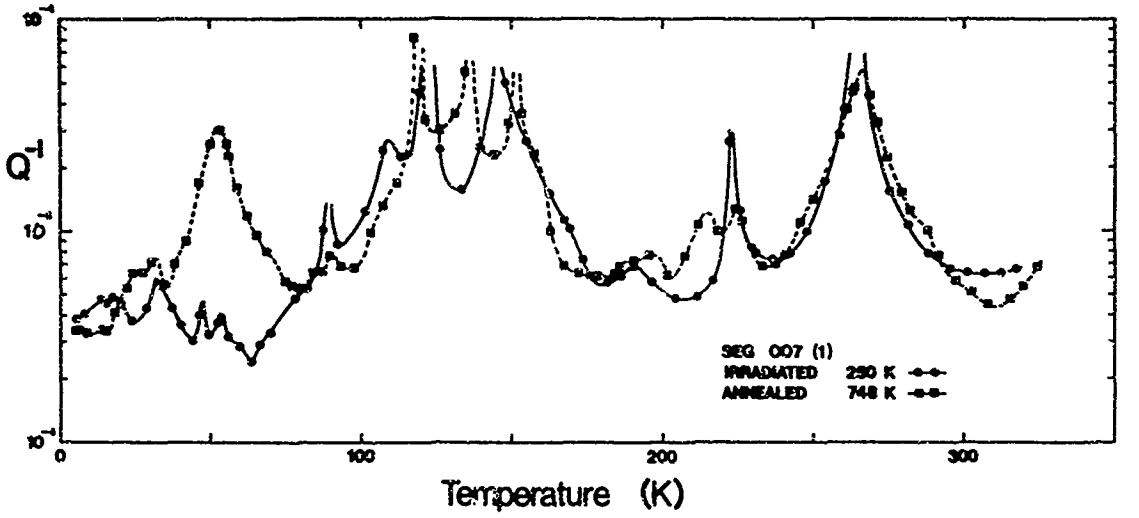

Fig. 14.

The solid curve shows the full Q^{-1} vs T spectrum for the unswept Electronic Grade resonator after a 250K irradiation. The Na loss peak is completely gone. After annealing, the resonator at 748K the loss peak has returned to its original value as shown by the dashed curve.

MONOLITHIC CRYSTAL FILTERS WITH HIGH Q FACTOR AND LOW SPURIOUS LEVEL

René LEFEVRE

C.N.E.T. 38-40 Avenue du Général Leclerc
92131 Issy-les-Moulineaux

Summary

In this paper we describe results obtained on resonators a factors for six pôles monolithic stal structure. Very high Q are obtained at room perature (up to 650000) and their evolution inst the temperature is discussed.

We analyse the activity of the unwanted trap- inharmonic modesand show how it is possible to uce them by optimizing the plate-back of resona- s. For a six-pôles monolithic crystal structure, discuss the influence of its geometrical para- ers on this optimum rejection. Experimental re- ts for two-pôles and six-pôles monolithic crys- structure are presented showing very high re- ator Q-factors and very low spurious level.

Finally we describe the tuning-method for h filters.

Introduction

During the past few years, much progress has n made in the field of monolithic crystal fil- s from both theoretical and practical point of w. With the application of the three-dimensio- equations of linear piezo-electricity to the pôles monolithic filters [1], the analysis of anted modes and their suppression,3,9 the improve- t of tuning procedures, these devices are now iable and are manufactured with economically eptable yields. We contribute to this progress results obtained on six pôles monolithic crys- structures two of them being cascaded to form welve pôles filter. By a careful preparation of tes, a good choice of its geometrical dimensions, ogeneous metallizations and a low stress-suspen- n, we have obtained resonator Q-factor up to 6 000 at 8 MHz. For all the resonators the mean ue is about of 450.000, the lowest value being ically of 350.000. We discuss the evolution of s Q-factor against the temperature.

On the oter hand it is possible to reduce the anted trapped inharmonics modes activity by op- izing the plate-back. In a precedent paper[2], have established the theoretical results for two pôles monolithic filters. We have shown that for end resonators, coupled one side, the antisymmetric modes were, in reality, quasi anti-symmetric modes and piezoelectrically active. But they tend to become purely anti-symmetric when the plate-back increase. It is possible to extend these results to monolithic filters of higher order and obtain, in that case, rejection, of more than 40dB (single plate of 6 resonators), leading to 85 dB rejection for cascaded such plates.

We show experimental results for two pôles and six pôles monolithic crystal filters. We plot the electrical activity of the Q AS_2 and QS_2 modes, versus the trapping factor of resonators, for six pôles monolithic crystal structures and discuss influence of geometrical parameters of the structure. These results allow to keepsufficient value of plate-back in high frequency monolithic crystal filters.

Finally, for their tuning, filters are mounted in their can to include all parasitic capacitances. With a movable slot in front of a mask, the different areas are selected for metallization. A device including reed-relay inside a high vacuum apparatus, permits all possible electrical measures on the filters. As results we present a twelve pôles bilithic filter which satisfy the 1/10eme CCITT specifications.

Q factor

The major result is the high Q factor obtained on rectangular plates of natural quartz at a resonance frequency of 8 MHz. Actually on each plate, at a temperature of 24°C, resonator Q-factor distribution presents a mean value of about 450000 with maximum value of 648000, the lowest value being 361000. On the table I are pointed out the values of Q, motional resistance, Resonant frequency, and motional inductance, of each resonator for some points of temperature.

We see, except for the resonator number two, a very good performance at 10,24,30 and 40°C ; for 20°C the Q of R1 and R4 falls below 200000. At 50°C the Q of R5 and R6 falls below 350000. While the mean value of motional inductance is :

$$Lm = 47.74 \text{ mH}$$

with a standard deviation of $\sigma = 1.39$ mH.

We think that this degradation of Q is du to plate modes, that are overtones of flexural, face-shear and extensional modes. Theses modes are very sensitive with temperature. When resonators frequencies fall between two overtones of theses modes, its Q can be very high only limited by surface morphology, loss in thin film and intrinsec Q of quartz. But when plate modes are coupled to thickness-shear/twist mode the mechanical energy of the latter modes is scattered by the edge of the plate and in the suspension. Heeker 3,4 and al. have recently described a method for calculating plate modes frequencies but it is actually difficult to adjust accurately the dimensions of the plates to obtain that resonators frequencies fall between thoses of plate modes.

Plates are not perfectly polished and are chemically etched to remove the damaged layer caused by the lapping operation. At 8 MHz we obtain a maximum of Q for a removal of about 35 to 40 KHz[5] . This value is slightly smaller than Miller's[6] result. Plates are then cleaned in the boiling Alcohol during about 15 minutes and receive first metallization. They are mounted in their can and again cleaned in boiling alcohol. In its can plate is mounted with a low stress-suspension figure 1 (the plate is not clamped). Electrical leads are wires of aluminium with 50 μm of diameter, and are bonded by ultrasonics waves. Metallizations are made homogeneous by a planetary system and 7000 A on each face seems to be a maximum value of thickness without degradation of Q performance ; For thicker films adhesion is poor and Q decreases.

After a first tuning, plates are cleaned again and the very high Q generally appear at this step and is not modified by further cleanings.

Inharmonic unwanted modes

In a previous paper[2] , we have established that, in a monolithic crystal filter, the unwanted trapped inharmonic modes could be classified in two groups : the quasi-antisymmetric modes (QAS) ant the quasi-symmetric modes (QS).

Here symmetry and anti-symmetry must be reported to an axis normal to the plate and crossing it at the center of one end resonator .QAS modes are piezoelectrically active due to the fact that end resonators are coupled only one side and this is a cause of asymmetry in the behaviour of theses resonators.

The theoretical analysis is made with a bidimensionnal elastic approximation based on a model introduced by Shockley, Curran and Koneval[7]. We assume that Z' is the coupling direction in the filter. Then, with origin of coordinates at the center of one of end resonator, the curve which represents the mechanical displacement u versus the abscissa is not perfectly symmetrical with respect to the ordinate axis. Thus, the electrical current assumed to be proportionnal to the integral of u over area of resonator, is not equal to zero. This asymmetry depends upon the value of the coupling between the end resonator considered and the next resonators. This coupling is a function of so-called trapping factor $\Omega_{z'}$, and interesonators

$$\Omega_{z'} = \frac{\pi}{2} \frac{Lz'}{h} \sqrt{\frac{C66}{\gamma 55}} \sqrt{\frac{Fo^2}{Fr^2} - 1} \quad (1)$$

where :

- Lz' represents the dimension of resonator in the coupling direction
- h is the thickness of the plate
- C_{66} and γ_{55} are the piezoelectrically stiffened values of elastic constants
- F_o is the cut off frequency of the unelectroded plate
- F_r is the cut-off frequency of resonators which take into account lowering effects such as mass loading and electrical boundaries conditions.

spacing which can be traduced eventualy by Ω_{ij} which have the same form that equation (1), when these regions are metallized . i and j varies from 1 to N-1 and 2 to N for a structure with N resonators. We assume all resonators to have the same Ω value. This is not rigorously the case since one of end resonator can be lowered of 1 KHz with respect to the others. But for a structure centered at 8 MHz this produce a variation of .3 percent of its Ω which is negligible.

In figure 2 we have plotted the QAS and QS mode activity of a six resonators structure against Ω. We see the existence of a crest value of this activity at $\Omega \neq \pi$ 2 and a valley value of this activity at $\Omega = \pi$ More exactly we must take into account the third dimension (X) in this analysis and we can approximately define a trapping factor Ω_x,

$$\Omega_x = \Omega_{z'} \frac{Lx}{Lz'} \sqrt{\frac{\gamma 55}{C11}} \quad (2)$$

where L_x is the dimension of resonator in the X direction. In fact, it is false to separate Ω_x and $\Omega_{z'}$ and a powerfull tridimensional model give a more complex value but this approximate fourmula gives good agreements with experimental results. If we assume that $\Omega_z \neq \Omega_x$ and $\Omega = \max(\Omega_x, \Omega_{z'})$, when Ω varies from $\frac{\pi}{2}$ to π values there are 3N QAS modes for a structure with N resonators : $QAS_{z'}$ modes which have two half -wavelenghts in the z' direction, Q AS_x modes which have two half-wavelenghts in the x direction, and QAS x z' modes which have two half-wavelenghts in both direction. But in reality QAS x z'modes are weaker than QAS x and QASz' du to the fact that they are anti-symmetrical in both directions. And in reality they are 2N QAS modes that are piezoelectrically strong modes[8]. In these latter modes QAS x are weaker than QASz' since in the x direction there is not asymmetry. Similarly when Ω is greater than π there are 3N QS modes whose amplitude remains practically constant when Ω increases. There are :

- $QS_{z'}$ modes which have three half-wavelenghts in the z' direction
- QS_x modes which have three half-wavelenghts in the x direction
- $QS_{xz'}$ modes which have three half-wavelenghts in both directions.

The two former are the most piezoelectrically strong modes. There are others modes that we call compounds modes :

$QAS_{z'}$ QS_x modes which have two half-wavelenghts in z' direction and three half-wavelenghts in x direction.

QAS_x $QS_{z'}$ which have the reciprocal configuration.

If we assume that $\Omega_x \neq \Omega_{z'}$ theses modes, since they appear for Ω greater than π, are very weak by their QAS part.

For this reason Ω_x and $\Omega_{z'}$ must be choosen not equal but not very different to prevent the appearance of compound modes before the valley value of QAS modes.

Figures 3 and 4 represents the evolution of this unwanted modes activity for a two pôles monolithic crystal filter centered at 10 MHz. In figure 5 some x ray topograph show the repartition of mechanical displacement under the resonator area. In figure 3b the first QAS modes to appear here is QAS x modes. Then appear the QASz' modes which are more active since the asymmetry is more effective in the z' direction figure 4a. In this figure QS_x modes are already active since $\Omega_x \neq 3.5$. In figure 4b the $QAS_{z'}$ reach their crest

value while QAS_x modes are rejected to 60 dB ; QS_x mode become more active.

The dimensions of each resonator are 2 mm in the z' direction and 3.6 mm in the x direction. Thus $\Omega_x \neq 1.6\ \Omega_{z'}$ This is a very bad choice which show that, in this case, no optimum design can be encountered. Shown in figures 6,7,8 and 9 is the insertion loss versus frequency of a six pôles monolithic crystal filter with Ωas parameter. Here $\Omega_x \neq \Omega_{z'}$ and $\Omega = \max(\Omega_x, \Omega_{z'})$. We see the same evolution of QAS modes and in figure 9, we have a rejection of more 55 dB. At frequencies of FO + 400 KHz we see untrapped inharmonics modes but they have a rejection of 50 dB and are far from the passband of the filter.

In figure 10,11,12 for a six pôles structure we have plotted the evolution of crest values and valley values of the QAS_z modes, when the interesonator-spacing is decreasing from its nominal value (origin of abscissa) to a minimal value by step of .1mm.All unwanted activity is refered to the first main mode. The design possibilities of a filter lay between theses two lines. We see that large values of interesonator-spacing C12 are suitable, while it is more possible varing the others. In the last curve figure 12b where all interesonator-spacings vary simultaneously of the same quantity more possibilities are offered for desigining.

This method of designing allows, in VHF fiters, to keep a sufficient value of plate-back.

Tuning method

From the synthesis of the filter, we generate a mask with adequate dimensions. Then the major part of metallization is deposited in a first high vacuum apparatus by an electron gun. Plates are fitted on a planetary system for homogeneous metallization. Then adjustement of structures, mounted in their can, are made in a second evaporation system which ensures a very clean vacuum (figure 13). In this last step, evaporation are made of gold only.

By means of a movable slot in front of a mask (figure 14) it is possible to select the different areas of the plate for metallization. To control theses adjustements, a system, including reed-relays, and fitted on the can leads of the plate (figure 15) inside the vacuum apparatus permits all possible electrical measures. It is possible to put inductances in parallel to eacl resonator to compensate for the static capacitances.

First, are tuned at the same frequency, resonators. Then the coupling between resonators is adjusted. For these adjustements, we take into account the influence of surroundings resonators. Then we tune the frequencies of end resonators to take into account the static capacitance for one end and the coupling for the other end.

Finally we adjust the center frequency by a slight metallization on all areas. The method of measurement employs a T network with 50 Ωloads associated to a network analyser. This is the more accurate method when values of motional resistances are much smaller than 50 Ω . The system is coupled to a desktop computer.

Choosing as reference for evaluation of relative errors the filter bandwith (ie 4 KHz), the accuracy for the adjusted coupling values is about .5 % and less than .3 % for the resonant-frequencies of resonators.

As result we present in figures 17 and 18 the insertion loss versus frequency of a twelve-pôles. bilithic crystal filter which satisfy the 1/10eme CCITT specification. In fact 13 or 14 resonators would allow far a better margin with respect to the specifications.

Conclusion and furher developments

We have shown that it was possible to obtain very good performances on monolithic crystal filters by way of design optimization : very high Q-factors (up to 650000) and low spurious level. However high Q-factors are not actually stable over a wide range of temperature. Study of the plate-modes frequencies versus temperature both theroretically and practically will indicate if it is possible to prevent catastrophic coupling, in the bandwith of the filter, between thickness-sheart/twist modes and plate modes.

We have shown a method which gives good results to reduce the inharmonic activity and a very effective rejection for the case of bilithic filters. For monolithic filters, in case of tight specifications it will be interesting to combine this method with that described by Pearman and Rennick[9].

The tuning method described above, gives good resuls and a rapid convergence in the case of such narrow-band filters.

Aknowledgments

The author is most grateful to Dr. J. Detaint for X ray topograph work and to MM. L. Jenselme and D. Servajean for their experimental work.

References

1. H.F. TIERSTEN, "An analysis of overtone modes in monolithic crystal filters", Proc. of the 30th Ann. Symp. on Freq.Control pp. 103-108 (1976).
2. A. GLOWINSKI, R. LANCON, R. LEFEVRE, "Effects of asymmetry in trapped-energy piezoelectric resonators" Proc. of 27th Ann. Sym. on freq. control pp. 233-242 (1973).
3. T.R. MEEKER, "X1 and X3 Flexure, Face-shear, Extension, thickness-shear and thickness-twist modes in rectangular rotated Y-cut quartz plates", Proc. of 31th Ann. Symp. on freq. control pp. 35-43 (1977).
4. R.D. MINDLIN and W.J. SPENCER, "Anharmonics Thickness-Txist Overtones of Thickness-shear and flexural vibiations of rectangular AT cut quartz plates", J. Acoust. Soc. Am. 42, pp. 1268-1277 (1967).
5. R.N. CASTELLANO, T.R. MEEKER, R.C. SUNDAHL, "The relationship between quartz surface morphology and the Q of high frequency resonators", proc. of 31thAnn. Symp. on freq. Control pp. 126-130 (1977).
6. A.J. MILLER, "Preparation of quartz crystal plates for monolithic crystal filters", Proc. of 24th Ann. Symp. Control pp. 93-103 (1970).
7. W. SHOCKLEY, D.R. CURRAN, D.J. KONEVAL, "Energy trapping and related suties of Multiple electrode filter crystals", Proc. of 17th Ann. Sym. on freq. control pp. 88-126 (1963).
8. R.D. MINDLIN, D.C. GAZIS, "Strong resonances of rectangular AT cut quartz plates", Proc. 4th U.S. Nat. congress of applied Mechanics pp. 305-310 (1962).
9. G.T. PEARMAN, R.C. RENNICK, "Unwanted modes in monolithic crystal filters", proc. of 31th Ann. Symp. on freq. control pp. 191-196 (1977).

RESONATOR NUMBER	Q * 10^3	MOTIONAL RESISTANCE(Ω)	RESONANT FREQUENCY(KHz)	MOTIONAL INDUCTANCE(mH)	TEMPERATURE °C
R1	363.14	6.68	8004. 113	48.23	
R2	363.35	6.67	8004. 157	48.19	
R3	485.30	5.12	8004. 225	49.41	
R4	412.92	6.02	8004. 227	49.43	10
R5	472.41	4.86	8004. 247	45.65	
R6	423.47	5.66	8003. 491	47.66	
R1	191.24	11.76	8004. 107	44.72	
R2	224.71	11.22	8004. 161	50.13	
R3	423.02	5.67	8004. 213	47.69	
R4	146.15	15.71	8004. 219	45.71	20
R5	470.51	4.91	8004. 239	45.94	
R6	390.18	6.20	8003. 479	48.11	
R1	393.15	6.1	8004. 103	47.61	
R2	361.26	6.77	8004. 155	48.63	
R3	587.85	4.17	8004. 209	48.74	
R4	497.75	4.82	8004. 215	47.70	24
R5	648.02	3.80	8004. 231	48.96	
R6	503.47	4.70	8003. 487	46.96	
R1	536.45	4.56	8004. 101	48.64	
R2	315.54	7.81	8004. 147	49	
R3	594.31	9.07	8004. 201	48.10	
R4	500.33	4.76	8004. 209	47.36	30
R5	611.30	3.81	8004. 225	46.31	
R6	549.22	4.31	8003. 469	47.07	
R1	421.07	5.74	8004. 087	48.06	
R2	319.01	7.60	8004. 135	48.21	
R3	442.40	5.70	8004. 187	50.14	
R4	458.74	5.21	8004. 197	47.52	40
R5	536.46	4.56	8004. 213	46.84	
R6	406.70	5.60	8003 455	45.29	
R1	496.74	4.87	8004. 079	48.10	
R2	336.04	7.34	8004. 129	49.05	
R3	418.90	5.81	8004. 189	48.39	
R4	541.73	4.45	8004. 183	47.93	50
R5	325.14	7.22	8004. 201	46.68	
R6	251.56	8.94	8003. 501	44.72	

Table 1 :

Resonators Q-factors of a typical monolithic crystal structure for some values of temperature.

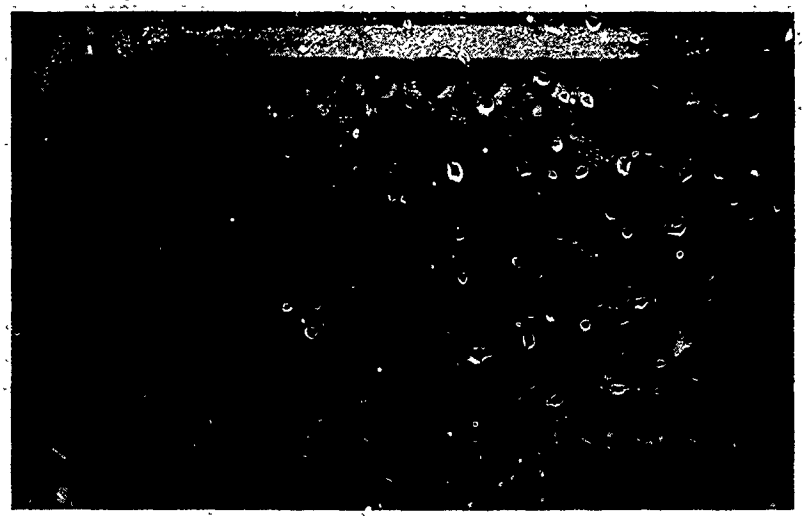

Figure 1

Six pôles monolithic crystal structure mounted on its can with low-stress suspension.

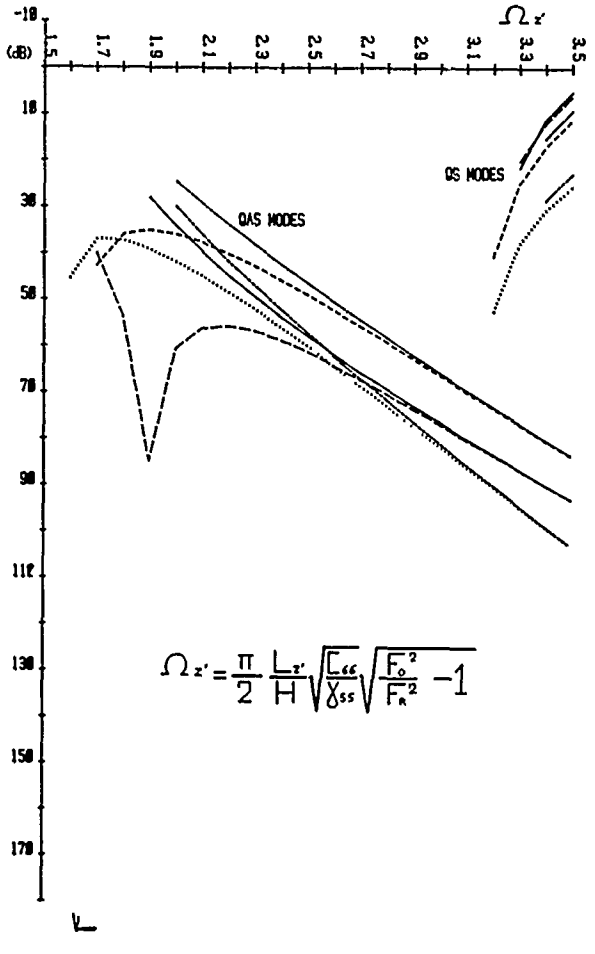

Figure 2

Activity of unwanted inharmonic modes in a six pôles monolithic crystal structure, versus trapping factor (amplitude are refered to the first main mode).

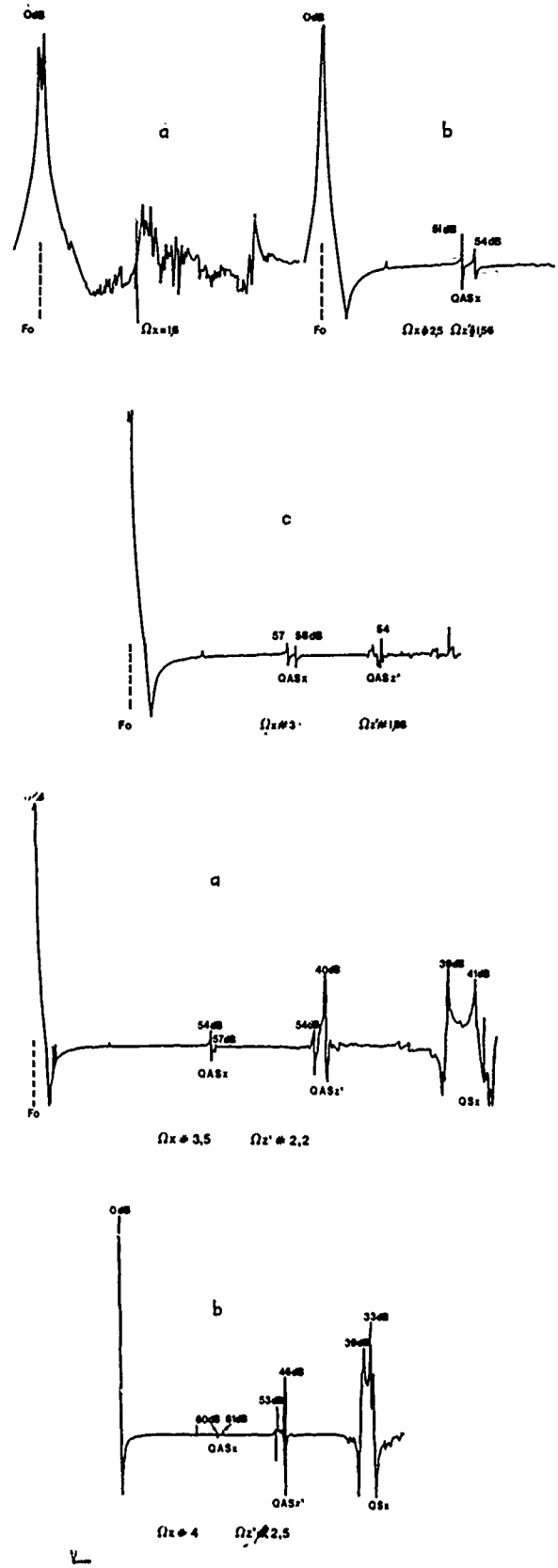

Figures 3 et 4

Insertion loss versus frequency of a two pôles monolithic crystal structure, showing the unwanted mode activity, for various values of Ω_x and $\Omega_{z'}$.

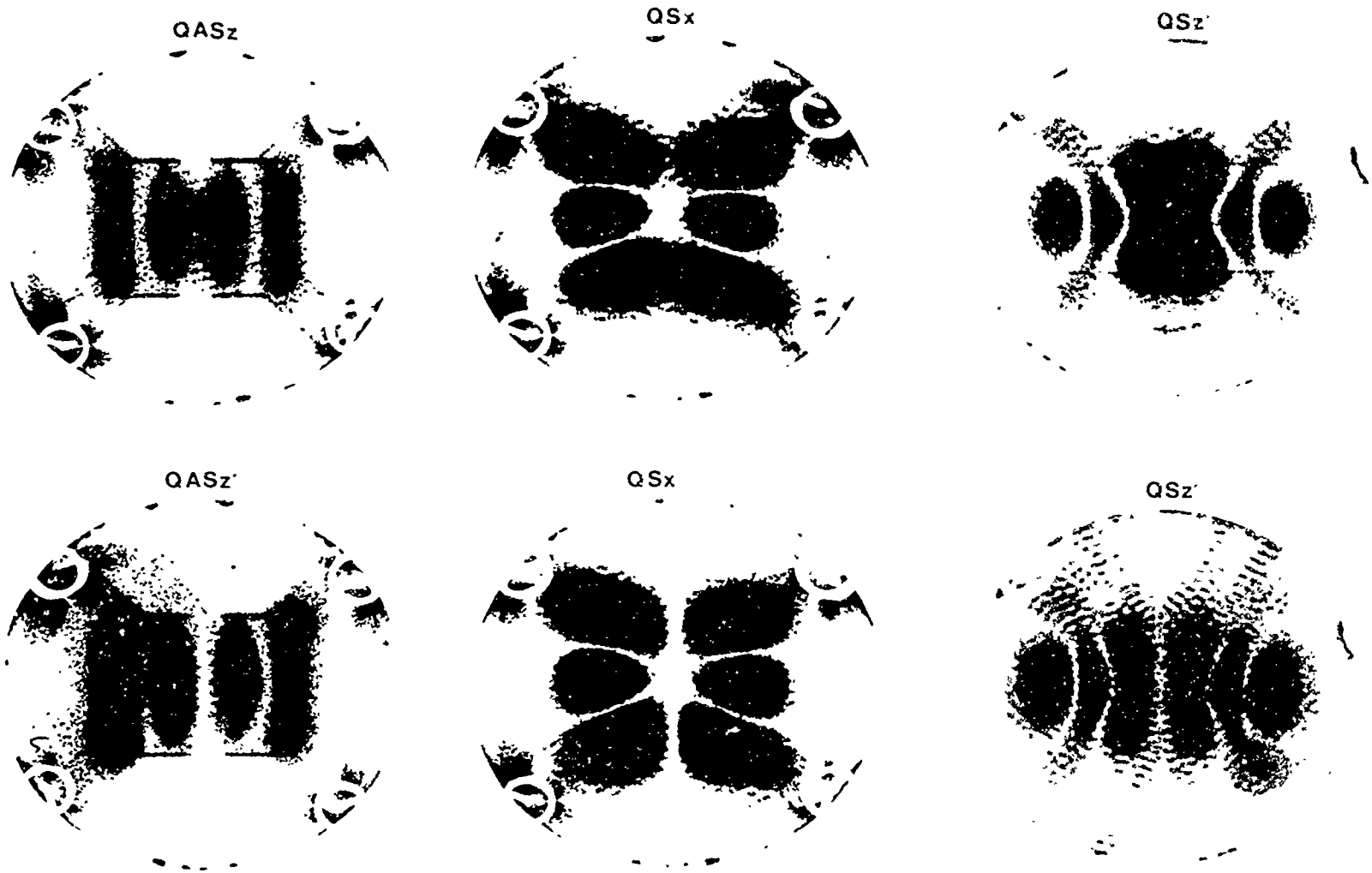

Figure 5

x ray topograph of the two pôles monolithic crystal structure showing the distribution of mechanical energy of some typical unwanted modes.

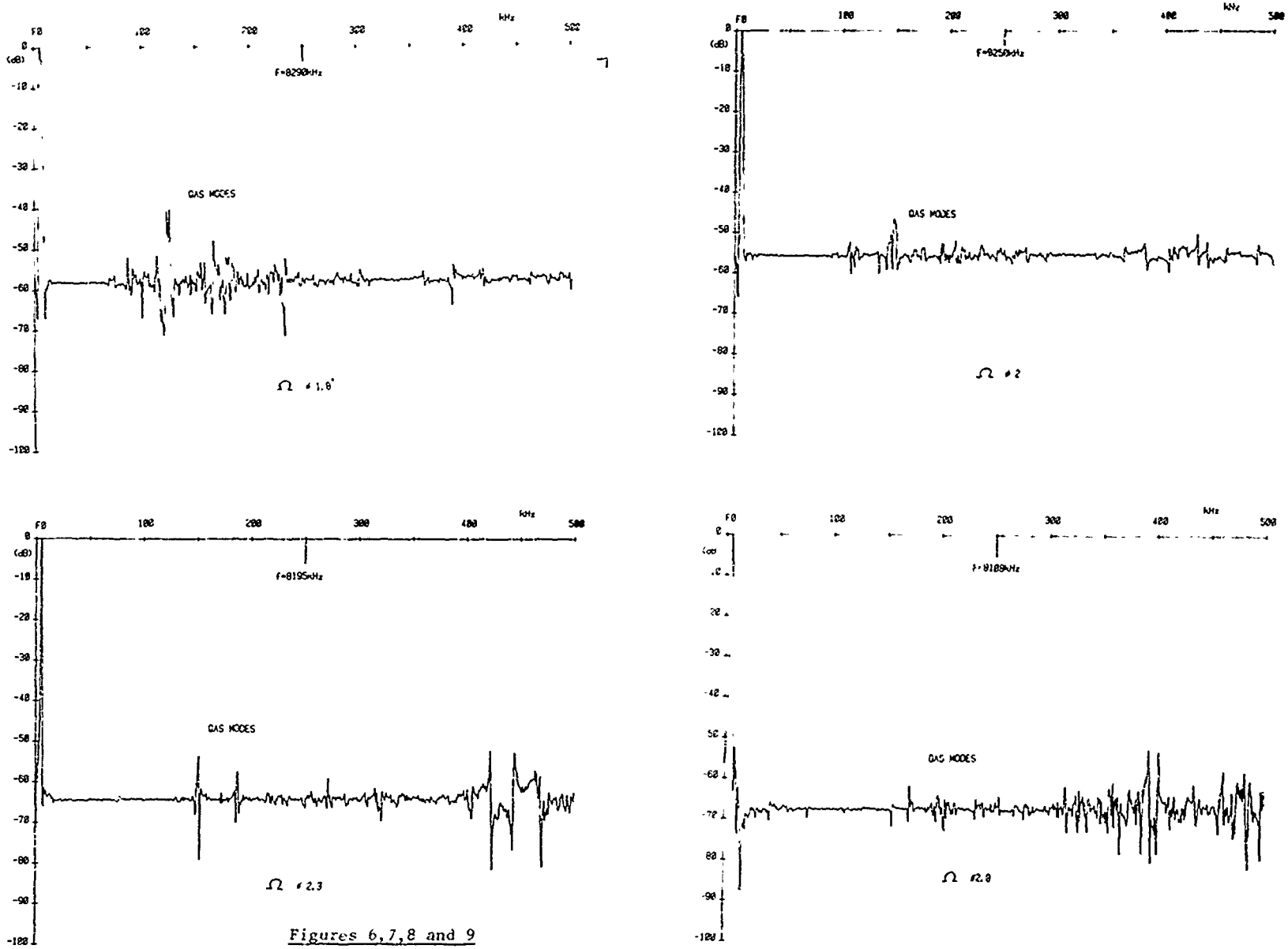

Figures 6,7,8 and 9

Insertion loss versus frequency of a six pôles monolithic crystal structure, showing the unwanted modes activity for various values of $\Omega = \max(\Omega_x, \Omega_{z'})$.

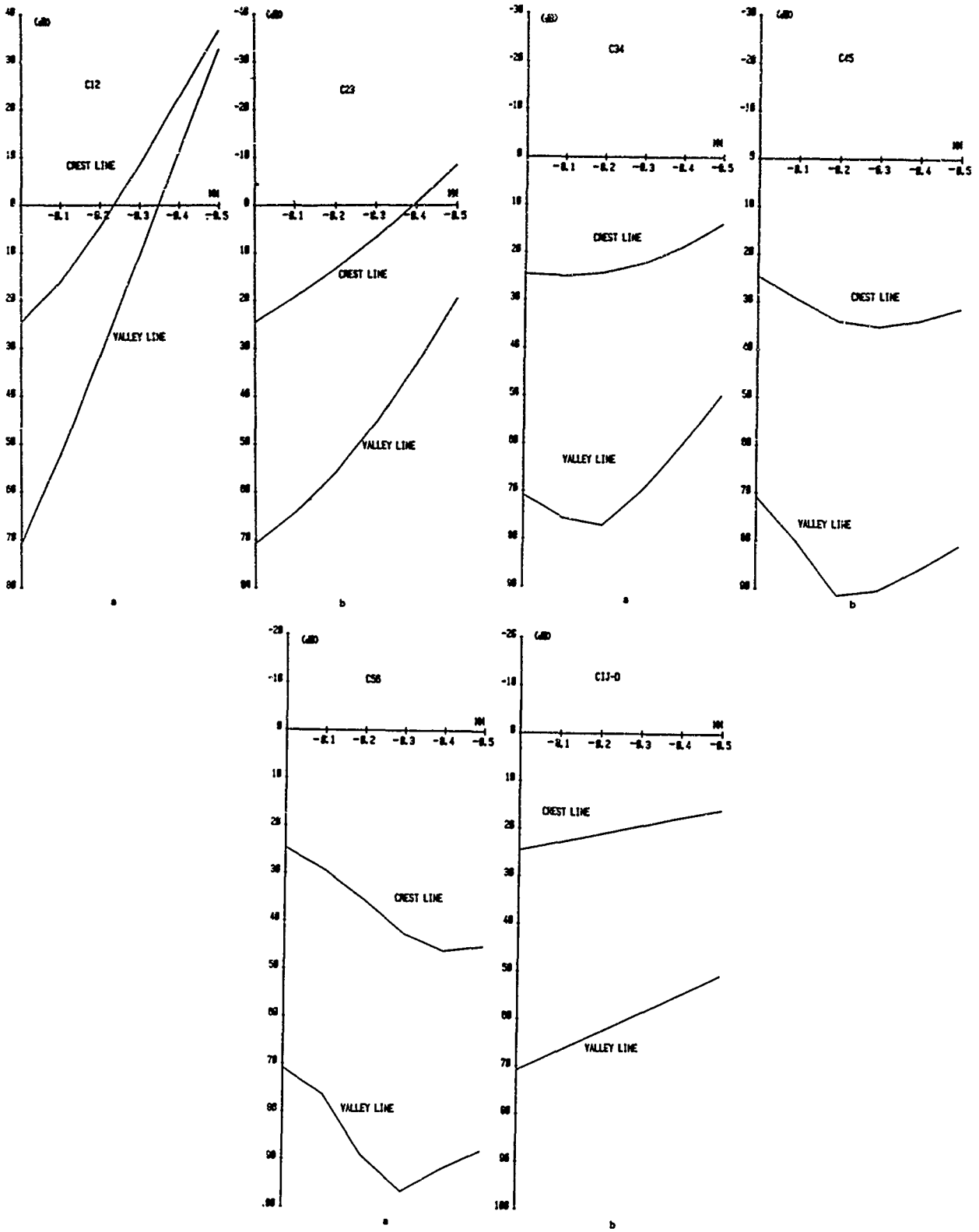

Figures 10,11 and 12

Evolution of crest values and valley values of Q AS_z modes in a six pôles monolithic crystal structure versus interesonator spacing.

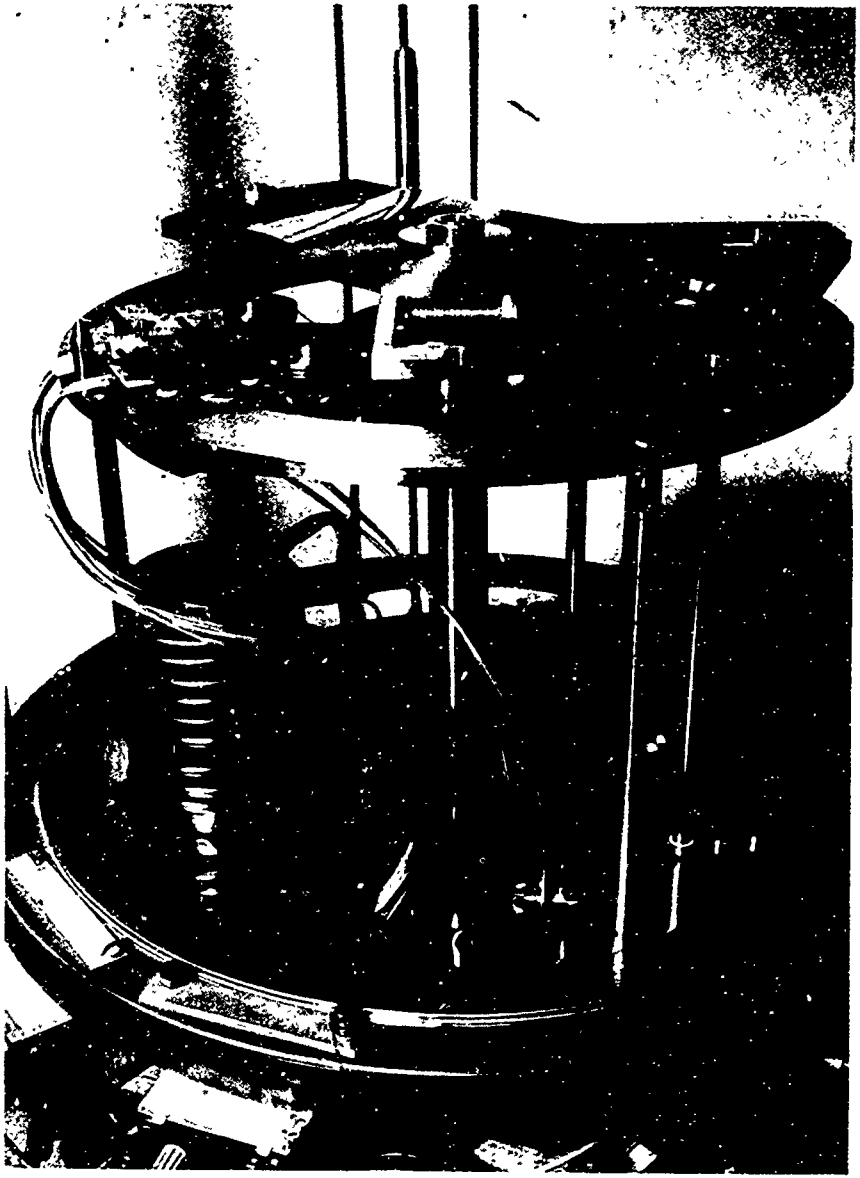

Figure 13

Inside of high vacuum apparatus showing the tuning system.

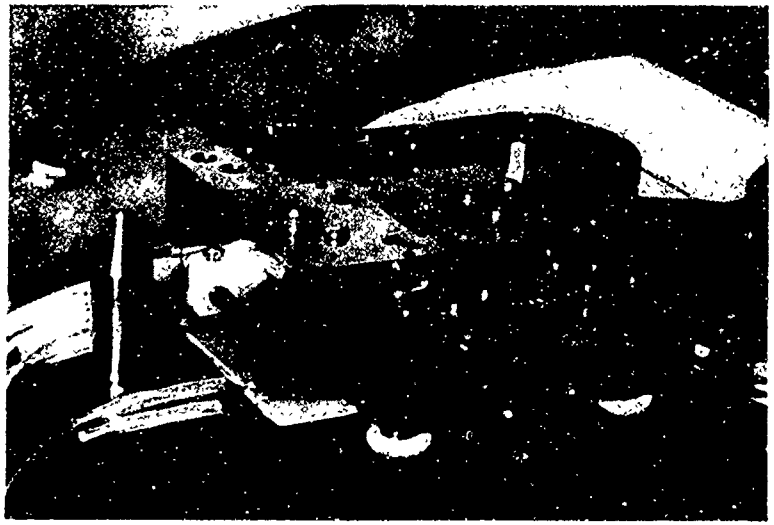

Figure 14

Detail of tuning system showing the movable slot below the mask.

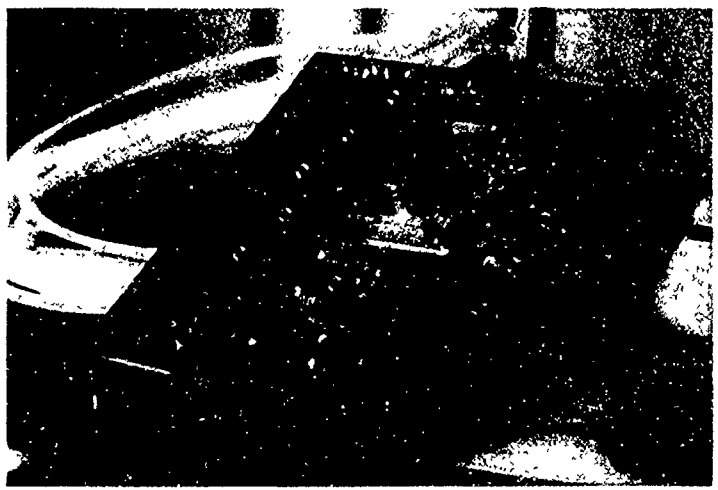

Figure 15

Printed circuit showing the plate mounted on its can and plugged in for electrical measurements. We can see the inductances which compensate for parasitic capacitances of each resonator.

Figure 16

Passband response of the twelve pôles bilithic crystal filter.

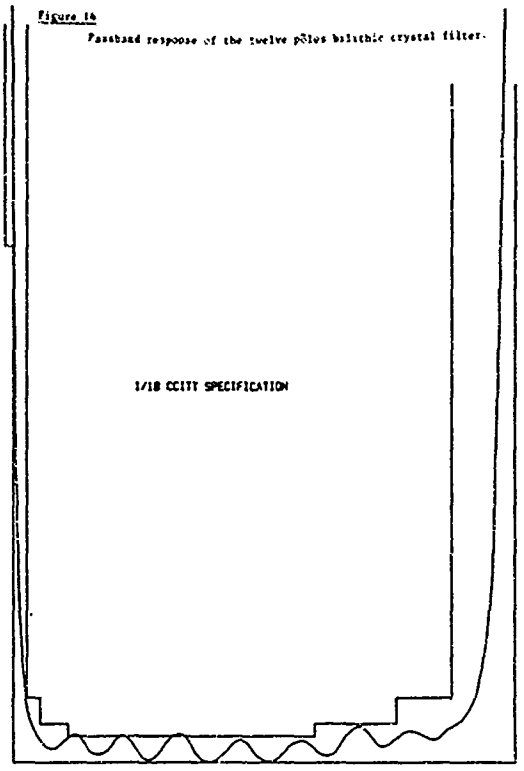

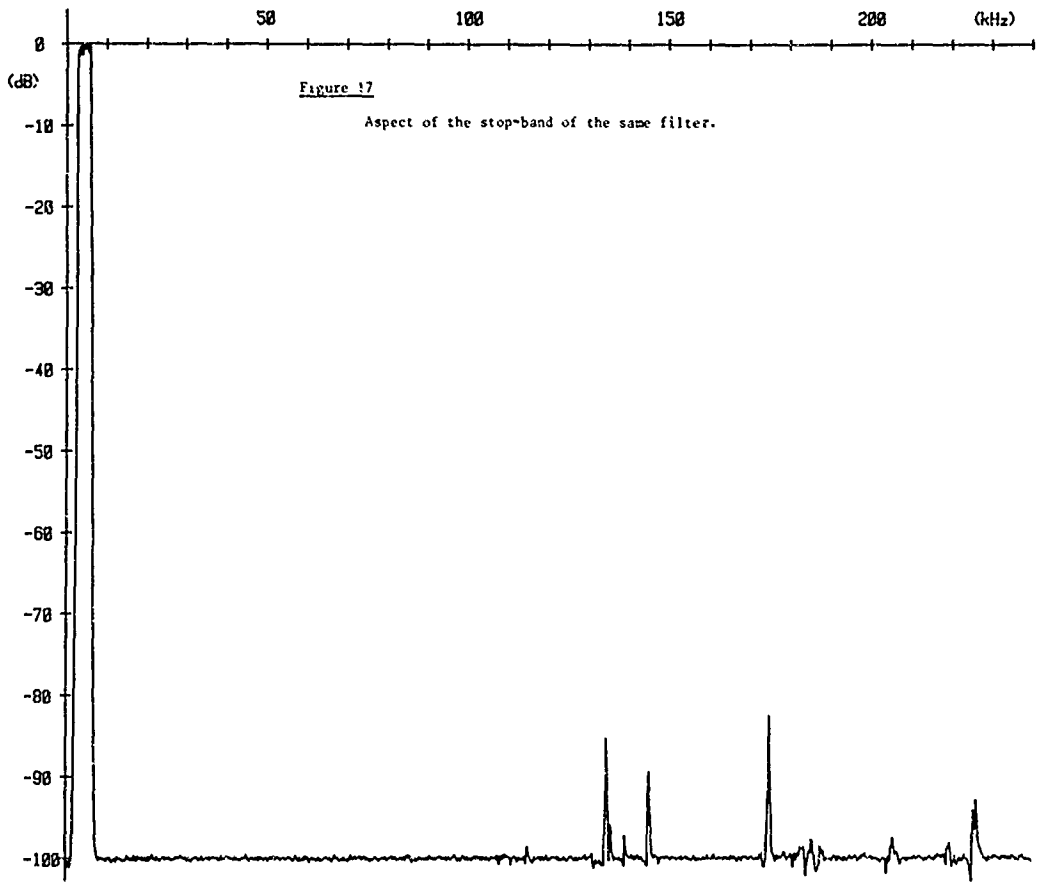

Figure 17

Aspect of the stop-band of the same filter.

A FOUR-FREQUENCY PROCESS FOR ACCURATELY MEASURING COUPLED-DUAL RESONATOR CRYSTALS

G. E. Roberts
General Electric Co.
Lynchburg, Va. 24502

Introduction

In designing coupled-dual crystals for filter and discriminator applications, inductance, resonator frequencies, Q, coupling, and perhaps spurious are usually the major parameters under consideration. In processing a coupled-dual crystal, the major parameters under consideration are resonator frequencies and coupling. If the conventional two-mesh equivalent circuit of a coupled-dual crystal is considered, each resonator ideally could be monitored directly by physically open-circuiting the other mesh since that was done hypothetically in defining the resonator frequencies. In practice, this condition is approximated by placing an external inductance, so called neutralizing inductance, across the static pin-to-pin capacitance C_o in the mesh to be open-circuited and then tuning the parallel combination to the nominal frequency of the resonator to be measured. This method for measuring resonator frequencies is undesirable due to accuracy, repeatability, and calibration problems [1,2].

Another method of monitoring resonator frequency [1] is to leave the resonator not being measured open-circuited. This terminates this resonator with its C_o and mistunes the resonator to be measured. From the equivalent circuit, the nominal frequency of the mistuned resonator to be measured can be calculated. This frequency is referred to as the tuning frequency of that resonator. From a circuit point of view, the tuning frequency of either of the two resonators occurs at the lowest frequency of the two zeros of the input impedance to the resonator in question. The measured tuning frequency of each resonator is then compared to the nominal value to determine if each resonator is at its correct frequency. Although this method is much better than the neutralizing inductance method, tuning frequency is a function of the value of the C_o across the resonator not being measured. Variations in C_o caused by crystal base variations and differences in the measurement fixtures from unit to unit can cause undesirable errors in the measured tuning frequencies.

The value of coupling is normally considered as the frequency difference between the two zeros of the input impedance of one resonator with the C_o of the other resonator short-circuited. Use is often made of the individual positions of these two zeros in handling coupling. If both resonators are on the same frequency, the short-circuit zeros are equally spaced above and below that frequency with the distance between them being the value of coupling. If one resonator frequency is plated below the other, the distance between the short-circuit zeros becomes larger. Although this method of determining coupling is useful, coupling is a function of the resonant frequencies as well as the resonator configuration and plateback. Since the resonators can differ in frequency at a given stage in the process of a coupled-dual, the intrinsic coupling of a crystal, as determined when both resonators are on the same frequency, is unknown.

This intrinsic coupling called synchronous peak separation frequency, in this paper, is defined as the absolute value of the diffrence between the frequencies of the two short-circuit zeros that would occur if the two resonators were tuned to the same resonant frequency. This resonant frequency is given by the geometric mean of the frequencies of the two short-circuit zeros.

In this paper, a new measurement method [3] for accurately determining the two resonator frequencies of a coupled-dual resonator crystal and the synchronous peak separation frequency is discussed along with a brief derivation of the relevant expressions in terms of the four frequencies that are measured. The method itself assumes the conventional mesh equivalent circuit of a coupled-dual crystal. The results are independent of the specific value of the static capacitance of each resonator and independent of the specific value of the mesh inductances. This eliminates the need to tune the test fixture used to measure the crystal. Another advantage of this measurement method is the fact that only one resonator need be monitored to obtain the frequency of both resonators and the synchronous peak separation frequency. This feature causes the measurement method to be easily automated. Since the results of this method are independent of the specific values of static capacitance and mesh inductance, it can be used at any step in the crystal process from baseplate to final frequency. Finally, the most significant feature of this measurement method is its inherent ease of calibration, its accuracy, and its repeatability.

Derivation of Method

The basic problem is to look at the driving-point impedance of the standard capacitive-T equivalent circuit of a coupled-dual shown in Fig. 1 with the output short-circuited. A convenient form of this impedance is given in the following equation

$$1/Z_0 = C_{01}s + \frac{\alpha_{11}s^3 + \alpha_{22}s}{\beta_{11}s + \beta_{22}s + \beta_{33}s}, \qquad (1)$$

where

$$\alpha_{11} = L_2C_1C_2C_{12},$$

$$\alpha_{22} = C_1C_2 + C_{12}C_1$$

$$\beta_{11} = L_1L_2C_1C_2C_{12}$$

$$\beta_{22} = L_1C_1C_2 + L_1C_1C_{12} + L_2C_2C_{12} + L_2C_1C_2$$

$$\beta_{33} = C_1 + C_2 + C_{12}.$$

The actual form of Z_0 is given by the following equations

$$Z_0 = \frac{s^4 + A_{11}s^2 + A_{22}}{C_{01}(s^5 + B_{11}s^3 + B_{22}s)}, \qquad (2a)$$

$$= \frac{(s^2+\omega_1^2)(s^2+\omega_3^2)}{C_{01}s(s^2+\omega_2^2)(s^2+\omega_4^2)}, \qquad (2b)$$

where

$$A_{11} = \omega_1^2 + \omega_3^2,$$

$$A_{22} = \omega_1^2\omega_3^2,$$

$$B_{11} = \omega_2^2 + \omega_4^2,$$

$$B_{22} = \omega_2^2\omega_4^2.$$

Equation (2) is then put in the form of Eq. (1) by using a Cauer expansion

$$1/Z_0 = C_{01}s + \frac{C_{01}(B_{11}-A_{11})(s^3+\gamma s)}{s^4 + A_{11}s^2 + A_{22}}, \qquad (3a)$$

where

$$\gamma = (B_{22}-A_{22})/(B_{11}-A_{11}). \qquad (3b)$$

Like terms are then equated to obtain

$$A_{11} = 1/(L_2C_{12}) + 1/(L_2C_2) + 1/(L_1C_1) + 1/(L_1C_{12}), \qquad (4)$$

$$A_{22} = \frac{C_1+C_2+C_{12}}{L_1L_2C_1C_2C_{12}}, \qquad (5)$$

$$C_{01}(B_{11}-A_{11}) = 1/L_1, \qquad (6)$$

$$C_{01}(B_{22}-A_{22}) = \frac{C_1C_2+C_{12}C_1}{L_1L_2C_1C_2C_{12}}, \qquad (7)$$

$$\frac{B_{22}-A_{22}}{B_{11}-A_{11}} = \frac{C_1C_2+C_{12}C_1}{L_2C_1C_2C_{12}}. \qquad (8)$$

From Eq. (8), it is seen that B-resonator frequency is given by

$$\omega_B^2 = \frac{C_2+C_{12}}{L_2C_{12}C_2} = \frac{B_{22}-A_{22}}{B_{11}-A_{11}} = \frac{\omega_2^2\omega_4^2-\omega_1^2\omega_3^2}{\omega_2^2+\omega_4^2-\omega_1^2-\omega_3^2} \qquad (9)$$

$$f_B^2 = \frac{f_2^2f_4^2-f_1^2f_3^2}{f_2^2+f_4^2-f_1^2-f_3^2} \qquad (10)$$

Combining Eq. (9) and Eq. (4), the A-resonator frequency is obtained as

$$A_{11} - \omega_B^2 = \frac{C_{12}+C_1}{L_1C_1C_{12}} = \omega_a^2 \qquad (11)$$

Therefore,

$$f_a^2 = f_1^2 + f_3^2 - f_B^2 \qquad (12)$$

Looking at Eq. (3), it can be seen that

$$1/Z_0 = C_{01}s + 1/Z_C, \qquad (13)$$

where $Z_C = \frac{L_1(s^4+A_{11}s^2+A_{22})}{s^3 + \omega_B^2 s}$. (14)

If Z_C were expanded in a Cauer Expansion, the circuit would be of the form shown in Fig. 2a, where C_a has the form

$$C_a = \frac{C_1C_x}{C_1+C_x} \qquad (15)$$

as shown to Fig. 2b. Comparing Fig. 2b and Fig. 2c, we see that

$$Z_D = Z_E. \tag{16}$$

By equating corresponding parts, we obtain

$$L_2C_2 = L_pC_p + C_xL_p \tag{17}$$

$$C_{12}C_2L_2 = L_pC_pC_x \tag{18}$$

$$C_{12} + C_2 = C_x \tag{19}$$

We can then find C_{12}, C_2 and C_x in terms of L_p, L_2, C_p as follows

$$C_{12} = C_p(L_p/L_2)^{1/2} \tag{20}$$

$$C_2 = C_{12}^2/(C_p - C_{12}) \tag{21}$$

$$C_x = C_{12} + C_2 \tag{22}$$

It can also be seen from Fig. 2b and 2c that

$$\omega_B^2 = 1/(L_pC_p) = 1/[L_2(C_{12}C_2)/(C_{12}+C_2)] \tag{23}$$

Combining Eqs. (20), and (23), we obtain

$$C_{12} = [L_p/L_2]^{1/2}C_p = [\frac{L_pC_p^2}{L_2}]^{1/2} = [\frac{C_p}{\omega_B^2L_2}]^{1/2} \tag{24}$$

From the Cauer Expansion of Eq. (14), C_p can be obtained as

$$C_p = 1/(L_1[A_{11} - \omega_E^2 - A_{22}/\omega_B^2]). \tag{25}$$

Combining Eqs. (24) and (25), we obtain

$$C_{12} = 1/(L_1L_2\omega_B^2[A_{11} - \omega_B^2 - A_{22}/\omega_B^2])^{1/2} \tag{26}$$

then

$$C_{12}(L_1L_2)^{1/2} = 1/[\omega_B^2(A_{11} - \omega_B^2 - A_{22}/\omega_B^2)]^{1/2} \tag{27}$$

but $\omega_a^2 = A_{11} - \omega_B^2$ from Eq. (11) which produces

$$C_{12}[L_1L_2]^{1/2} = 1/[\omega_a^2\omega_B^2 - A_{22}]^{1/2} \tag{28}$$

Therefore,

$$1/(C_{12}(L_1L_2)^{1/2}) = [\omega_B^2\omega_a^2 - A_{22}]^{1/2} = [\omega_B^2\omega_a^2 - \omega_1^2\omega_3^2]^{1/2} \tag{29}$$

Next we define a frequency ω_L as

$$\omega_L^2 = 1/(C_{12}[L_1L_2]^{1/2}) \tag{30}$$

and synchronous peak separation frequency Δf_n, as

$$\Delta f_n = f_L^2/f_0. \tag{31}$$

The coupling coefficient, k_{12}, is

$$k_{12} = \Delta f_n/f_0. \tag{32}$$

Therefore,

$$\Delta f_n = [f_a^2f_B^2 - f_1^2f_3^2]^{1/2}/f_0. \tag{33}$$

If we define f_0 as

$$f_0 = [f_1f_3]^{1/2}, \tag{34}$$

then

$$\Delta f_n = [f_a^2f_B^2 - f_1^2f_3^2]^{1/2}/[f_1f_3]^{1/2} \tag{35}$$

and

$$k_{12} = \Delta f_n/f_0 = [f_a^2f_B^2 - f_1^2f_3^2]^{1/2}/[f_1f_3] \tag{36}$$

At this point f_a, f_B, Δf_n, and k_{12} are independent of the value of C_{01} and also do not require that the value of L_1 or L_2 be known. No assumption regarding L_1 and L_2 have been made up to this point.

If the B-side in Fig. 1a is short-circuited to ground and the A-side is driven, then the A-side driving-point impedance in Eq. 2 has the following coefficients:

$$A_{11} = 1/(L_2C_{12}) + 1/(L_2C_2) + 1/(L_1C_1) + 1/(L_1C_{12}) \tag{37}$$

$$A_{22} = 1/(L_1L_2C_2C_{12}) + 1/(L_1L_2C_1C_{12}) + 1/(L_1L_2C_1C_2) \tag{38}$$

$$B_{11} = 1/(L_2C_{12}) + 1/(L_2C_2) + 1/(L_1C_1) + 1/(L_1C_{12}) + 1/(L_1C_{01}) \tag{39}$$

$$B_{22} = 1/(L_1L_2C_2C_{12}) + 1/(L_1L_2C_1C_2) + 1/(L_1L_2C_2C_{01}) + 1/(L_1L_2C_{12}C_{01}) \quad (40)$$

However, from Eq. 2

$$A_{11} = (2\pi)^2(f_1^2+f_3^2) \quad (41)$$

$$B_{11} = (2\pi)^2(f_2^2+f_4^2) \quad (42)$$

$$A_{22} = (2\pi)^4(f_1^2f_3^2) \quad (43)$$

$$B_{22} = (2\pi)^4(f_2^2f_4^2) \quad (44)$$

where f_1 and f_3 are the zeros of the short-circuit driving-point impedance, f_2 and f_4 are the poles of the short-circuit driving-point impedance. Equations (10) and (12) hold for f_a and f_B and Equation (35) holds for synchronous peak separation.

Suppose we next look at the numerator coefficients of the A-side driving-point impedance with the B-side open-circuited and the numerator coefficients of the B-side driving point impedance with the A-side short-circuited.

The numerator coefficients of the A-side driving point impedance with the B-side open-circuited is merely (37) and (38) with

$$C'_{20} = (C_2C_{02})/(C_2+C_{02}) \quad (45)$$

replacing C_2. Therefore, we will denote these equations as

$$A'_{11} = 1/(L_2C_{12}) + 1/(L_2C_2) + 1/(L_2C_{02}) + 1/(L_1C_1) + 1/(L_1C_{12}) \quad (46)$$

$$A_{22} = 1/(L_1L_2C_1C_{12}) + 1/(L_1L_2C_{02}C_{12}) + 1/(L_1L_2C_1C_{12}) + 1/(L_1L_2C_1C_2) + 1/(L_1L_2C_1C_{02}) \quad (47)$$

These are also the coefficients of the denominator of the driving point impedance if the B-side were driven and the A-side short-circuited.

The numerator coefficients of the driving-point impedance of the A-side with the B-side short-circuited are already given in (37) and (38). It can be shown in a manner similar to the derivation of Equations (10), (12), and (35) that

$$f_a^2 = (f_2^2f_4^2-f_1^2f_3^2)/(f_2^2+f_4^2 - f_1^2-f_3^2)$$

or

$$f_a = [(f_2^2f_4^2-f_1^2f_3^2)/(f_2^2+f_4^2 - f_1^2-f_3^2)]^{1/2}, \quad (48)$$

$$f_B = [f_1^2+f_3^2-f_a^2]^{1/2} \quad (49)$$

and

$$\Delta f_n = [f_a^2f_B^2 - f_1^2f_3^2]^{1/2}/[f_1f_3]^{1/2} \quad (50)$$

where f_1 and f_3 are the zeros of the A-side driving-point impedance function with the B-side short-circuited, and f_2 and f_4 are now the zeros of the A-side driving-point impedance function with the B-side open-circuited. Without loss of generality, C_{02} may consist of the static pin-to-pin capacitance of the crystal in parallel with an external capacitor which could be used to place f_2 and f_4 in more convenient positions for measurement purposes.

The Measurement Fixture

From Equations (48), (49), and (50), we see that f_a, f_B, and Δf_n can be calculated using the zeros, f_2 and f_4, of the A-side driving-point impedance with the B-side open-circuited and the zeros, f_1 and f_3, of the A-side driving-point impedance with the B-side short-circuited. One simple method of displaying these frequencies is by means of a voltage divider type network shown in Fig. 3 in which the driving-point impedance whose zeros are to be measured is put in the series arm. This results in resonances appearing at f_2 and f_4 when the A-side driving-point impedance is displayed with the B-side open-circuited and f_1 and f_3 when this same impedance is displayed with the B-side short-circuited. A complete fixture is shown in Fig. 4.

A frequency synthesizer is connected to J1 in Fig. 4 and a vector voltmeter's A and B probes are connected to J2 and J3, respectively. When the synthesizer is swept over the frequency range of interest with switch S1 open, the frequencies, f_2 and f_4, occur where the VVM's B-probe voltage is at zero phase in the neighborhood of specific maximum voltage amplitudes shown in Fig. 5b. These relative maxima may or may not have the same magnitude. When S1 is closed, f_1 and f_3 occur where the VVM's B-probe voltage is at zero phase in the neighborhood of specific maximum voltage amplitudes shown in Fig. 5a. As a check, the following inequalities should be valid

$$f_1<f_2<f_3<f_4$$

The values of f_1, f_2, f_3, and f_4 can then be used to calculate f_a, f_B, and Δf_n.

Results and Conclusions

A group of 9 crystals at 21.4 MHz were measured on 3 separate fixtures designated as fixture No. 1, fixture No. 2, and fixture No. 3. The crystals were re-measured four hours later on fixture No. 1. The three fixtures were not tuned or adjusted in any way. A 51-ohm 1/4-watt carbon resistor was used to zero the VVM. The mean and standard deviation of the difference between the f_a's, f_B's, and Δf_n's of the crystals read on fixture No. 1 and the f_a's, f_B's, and Δf_n's of the corresponding crystals read on fixture No. 1 four hours later are shown below. Similar results are shown comparing the values of f_a, f_B, and Δf_n obtained initially from fixture No. 1 with those calculated from data on corresponding crystals on fixture No. 2 and No. 3, respectively.

Comparing results of fixture No. 1 with the results of fixture No. 1 obtained 4 hours later:

	Mean of the Difference (Hz)	Standard Deviation of the Difference (Hz)
f_a	-1.53	18.35
f_B	-9.96	15.59
Δf_n	-2.02	12.07

Comparing the results of fixture No. 1 with the results of fixture No. 2:

	Mean of the Difference (Hz)	Standard Deviation of the Difference (Hz)
f_a	10.02	6.53
f_B	-2.04	9.54
Δf_n	-1.39	4.60

Comparing results of fixture No. 1 with the results of No. 3:

	Mean of the Difference (Hz)	Standard Deviation of the Difference (Hz)
f_a	4.37	6.32
f_B	-3.28	4.58
Δf_n	- .71	12.65

Another group of 30 crystals at 20.2 MHz were measured the same way over a period of several days by different operators using a different fixture No. 3.

Comparing results of fixture No. 1 with the results obtained one day later on fixture No. 1:

	Mean of the Difference (Hz)	Standard Deviation of the Difference (Hz)
f_a	-3.17	18.49
f_B	8.37	19.62
Δf_n	-3.14	9.85

Comparing results of fixture No. 1 with the results of fixture No. 2:

	Mean of the Difference (Hz)	Standard Deviation of the Difference (Hz)
f_a	1.32	20.11
f_B	5.64	21.89
Δf_n	-1.62	9.42

Comparing results of fixture No. 1 with the results of fixture No. 3:

	Mean of the Difference (Hz)	Standard Deviation of the Difference (Hz)
f_a	-3.32	18.85
f_B	5.02	22.45
Δf_n	-3.27	10.28

Therefore, it can be seen that the repeatability among three fixtures is essentially the same as that using one fixture twice. The only calibration consisted of calibrating the phase meter on the VVM. Based on similar data from neutralizing inductance fixtures, this four-frequency method is well over an order of magnitude better. Of course, this four frequency process has the capability of measuring synchronous peak separation frequency as well.

Since the equations of f_a, f_B, and Δf_n are independent of the specific value of the static capacitance and mesh inductance of each resonator, the need to tune this test fixture used to monitor the crystal is eliminated making the measurement process inherently very accurate. Also, it can be seen that the equations and measuring process are valid for measuring coupled-dual resonator crystals at any step in

the crystal process after baseplate. Results at four steps in the process of a sample coupled-dual crystal is shown below:

After Baseplate:

f_1 = 21467718 f_3 = 21479841

f_2 = 21470374 f_4 = 21484657

f_a = 21473738 f_B = 21473822

Δf_n = 12123

After Nickel Plate:

f_1 = 21397690 f_3 = 21407342

f_2 = 21400818 f_4 = 21411839

f_a = 21403494 f_B = 21401539

Δf_n = 9452

After Freq. Plate:

f_1 = 21390347 f_3 = 21399480

f_2 = 21392129 f_4 = 21405274

f_a = 21393858 f_B = 21395970

Δf_n = 8885

After Seal:

f_1 = 21390686 f_3 = 21399805

f_2 = 21392487 f_4 = 21405486

f_a = 21394248 f_B = 21396244

Δf_n = 8898

By being able to monitor each step in the process, a process profile can be developed during the design cycle such that the manufacture of the crystal can be closely controlled by in-line testing. Since only one resonator need be monitored to obtain the two resonator frequencies and the synchronous peak separation frequency, the measurement process is easily automated making it an extremely powerful tool for both Engineering and Manufacturing.

References

1. R. C. Rennick, "An Equivalent Circuit Approach to the Design and Analysis of Monolithic Crystal Filters," *IEEE Trans. on Sonics and Ultrasonics*, Vol. SU-20, No. 4, pp 347-354, October 1973.

2. G. E. Roberts, "Apparatus for Measuring the Resonant Frequency and Coupling Coefficient of a Plurality of Coupled Piezoelectric Resonators," U.S. Patent 3,963,982, June 15, 1976.

3. H. J. Peppiatt and G. E. Roberts, "Method of Measuring Parameters of a Crystal Filter," U.S. Patent 4,093,914, June 6, 1978.

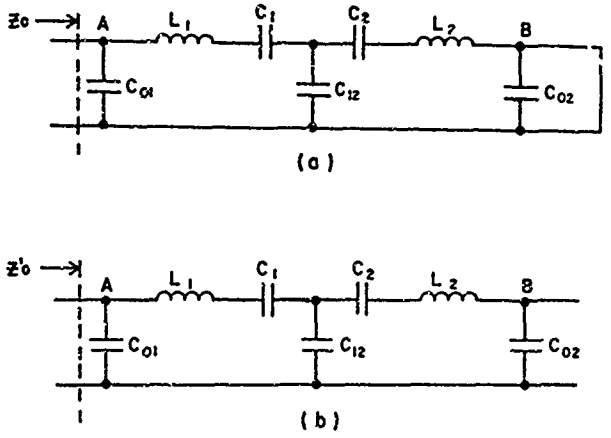

FIG. 1.

CAPACITIVE-T EQUIVALENT CIRCUIT OF A COUPLED-DUAL CRYSTAL (a) WITH THE B-RESONATOR SHORT-CIRCUITED, (b) WITH THE B-RESONATOR OPEN-CIRCUITED.

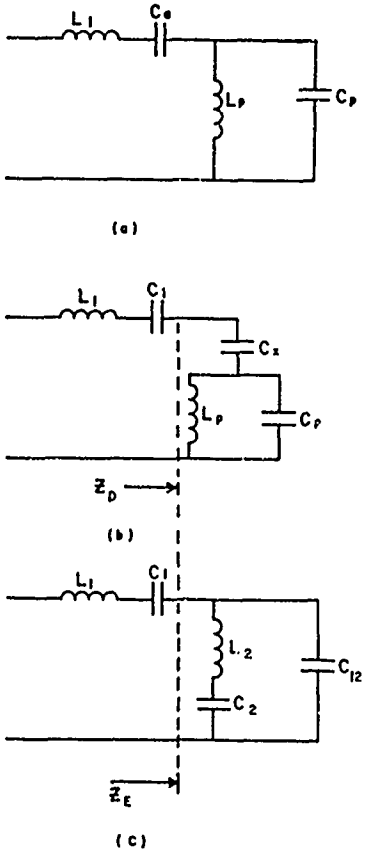

FIG. 2.

TRANSFORMATION FROM A CAUER EXPANSION TO CAPACITIVE-T EQUIVALENT CIRCUITS.

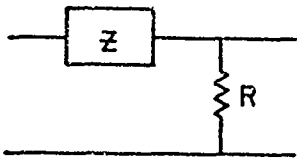

FIG. 3. VOLTAGE-DIVIDER NETWORKS DISPLAYING THE ZEROS OF THE DRIVING-POINT IMPEDANCE.

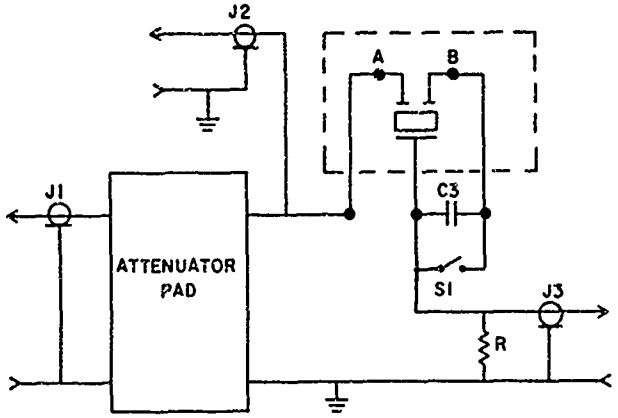

FIG. 4. FIXTURE FOR MEASURING fa, fB, Δfn.

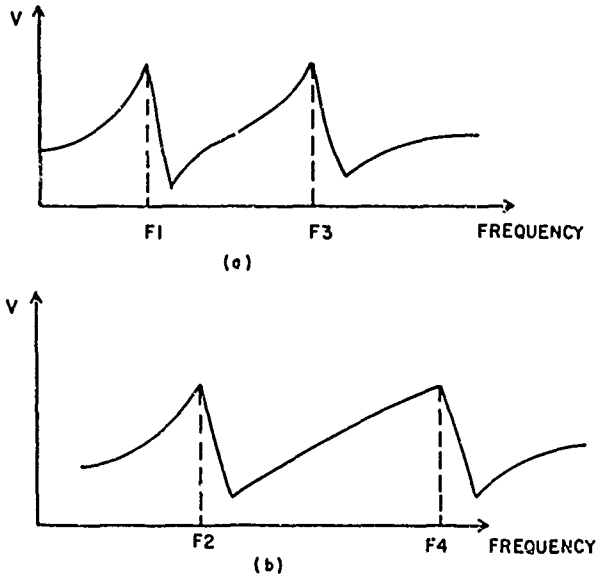

FIG. 5.

TYPICAL RESPONSE OF COUPLED-DUAL CRYSTAL IN TEST FIXTURE WITH (a) SI CLOSED AND (b) SI OPEN.

NEW DISCRETE CRYSTAL FILTERS FOR BELL SYSTEM ANALOG CHANNEL BANKS

by

D. I. McLean and A. F. Graziani
Bell Telephone Laboratories
No. Andover, Massachusetts 01845

and

J. J. Royer
Bell Telephone Laboratories
Allentown, Pennsylvania 18103

Abstract

A new generation of Bell System discrete crystal filters (DCFs) has been developed for use as channel filters. There are three basic designs: two are for domestic Bell System use and the third is for applications where the CCITT requirements must be met.

These three DCF designs are balanced, single-lattice filters with inductor-capacitor end sections. When compared to their predecessors, volume reductions of greater than 10 to 1 and superior electrical characteristics have been achieved.

The lattices are realized with resonator designs consisting of +5° X-cut quartz crystals with divided electrodes covering the frequency range of 60 to 130 kHz. These designs make use of a planar mounting structure wherein each resonator is attached to two rails. The rails mechanically terminate the resonator wires facilitating electrical measurements. The tuned resonators are mounted in carriers which provide both electrical interconnections and protection for the crystal plates.

Results of Monte Carlo statistical analysis are compared with measured filter performance.

Introduction

This paper describes a new generation of Bell System analog channel filters. These filters are a further development of quartz crystal filter technology. The Bell System pioneered the use of quartz crystal resonators in filters and, through continuous development, has kept this technology competitive for channel filters within the Bell System [1]. This latest family of discrete crystal filters (DCFs) has two members for domestic Bell System use and a third member that meets international (CCITT) requirements.

One of the two domestic Bell System DCFs to be described will be used in the Western Electric Company N4 Carrier System [2] which is the latest version of a series of short-haul, analog, carrier systems designated as "N-type." The other domestic Bell System DCF is being used in the Western Electric Company LT-1 connector [3]. The LT-1 Connector is a transmultiplexer that efficiently interfaces L-type, long-haul, analog carrier systems to T-type, digital carrier systems or digital switching systems.

The third DCF to be described is used in applications where the more stringent CCITT requirements must be met; e.g., in the Western Electric Company A7E Channel Bank.

These three, new, DCF designs are balanced, equivalent-lattice filters with inductor-capacitor end sections. Each filter has a single, equivalent-lattice realized with split-electrode, quartz crystal resonators in new miniature mounting structures. These new mounting structures hold multiple resonators in a volume-efficient manner. A differential capacitor is used to

balance the equivalent capaitance bridge of each filter design.

Requirements

Channel filters for frequency division multiplex (FDM) systems provide the band selection needed to multiplex or demultiplex twelve voice channels (200 to 3400 Hz) into or from the 60 to 108 kHz basic group band. See Fig. 1. Single sideband suppressed carrier modulation (lower sideband) using twelve carriers at 4 kHz intervals is the world standard for the basic group band. The N4 and LT-1 equipments use direct modulation into the basic group band and provide for in-band signaling (2600 Hz). The channel filter requirements for this architecture are met by twelve DCF designs with four crystal resonators each. The Western Electric A7E Channel Bank uses two steps to modulate voice channels into the basic group band and provides out-of-band signaling (3825 Hz). The channel filter requirements for this architecture are met by a single DCF design with six crystal resonators.

The Renaissance of an Old Technology

Since 1938 the Bell System has used DCFs as channel filters wherever direct modulation of the twelve voice channels to the 60 to 108 kHz basic group band was appropriate. The newly designed DCFs described in this paper have maintained this trend. They are smaller and have superior response characteristics compared to previous DCFs. However, the monolithic crystal channel filter, or MCF, which was introduced in 1972 and utilizes a second step of modulation at 8 MHz, is still the most compact analog channel filter used in the world today [4].

One of the electrical design techniques that contributed to the successful development of the new DCFs was the application of insertion-loss synthesis methods to the topology of the old DCFs which had been designed on an image parameter basis. This enabled the achievement of superior response characteristics. The Bell Laboratories general purpose synthesis program, which was expanded to include lattice filters, allowed quick analysis of design tradeoffs during the development process.

Another design tool that contributed to the DCF development was a general purpose network analysis program with Monte Carlo statistical analysis capabilities. Computer models of the DCFs were developed to analyze the statistical distributions of the component parameters using Monte Carlo techniques. This increased confidence in meeting all systems requirements, allowed tolerances to be accurately specified and optimum tuning algorithms to be chosen.

Electrical Performance

The schematics of the two types of filters are shown in Fig. 2. At the top is the representation of the N4/LT-1 DCF exhibiting the four split-electrode crystal resonators, Y1 through Y4, the balanced LC end sections and the differential balancing capacitor. Below is the schematic of the A7E DCF. It is similar to the first; the differences being two more resonators and transformer input and output rather than balanced, series inductors.

The discrimination and insertion loss distortion characteristics for an A7E DCF are shown in Fig. 3. These curves are typical of the manufactured product at room temperature. Temperature variation will cause the loss peaks, particularly those farthest from the passband, to move somewhat; but the sharp discrimination skirts and high stopband loss are maintained. Monte Carlo analyses and environmental tests show the filter to be very stable.

Fig. 4 is a representation of the group delay of an A7E DCF. As can be seen, the group delay distortion is well within the CCITT Recommendation G232C.

The insertion loss response characteristic of a typical LT-1 DCF at 25° C is shown in Fig. 5. The stopbands and an expanded representation of the passband are exhibited. The response characteristic of an N4 DCF is not shown, as it is very similar to the LT-1 DCF characteristic in Fig. 5. The stopband loss peak locations are slightly different for the two designs, and the passband of the N4 DCF is approximately 100 Hz wider than the passband of the LT-1 DCF.

The results of a Monte Carlo analysis of the LT-1 DCF design, Figures 6 and 7, show the envelopes of the expected discrimination distribution of 500 random filters. These filters were "constructed" theoretically utilizing the statistics of manufacture and then made to experience temperature variation

and long term aging, also on a statistical basis. This analysis indicates that the design goal of ensuring that 95% of the filters meet their end-of-life objectives was achieved.

Physical Design

Equal in importance to the described electrical design achievements were the breakthroughs in physical design that enabled the great reduction in size compared to previous DCFs.

A significant contribution to the volume reduction was the design of a small, slug-tuned, magnetic component which incorporates the IEC standard RM-5 ferrite cup-core. This inductor has a TCL of +100 PPM/C°. Ceramic temperature compensating capacitors are used in conjunction with these inductors.

The heart of the volume reduction was the repackaging of the crystal assembly. This design work is covered in the next section.

Crystal Resonator Assemblies

The resonator designs consist of +5° X-cut quartz crystals covering the frequency range of 60 to 108 kHz for the N4 and LT-1 Systems and 128 to 132 kHz for the A7E Channel Bank. The inductances of the resonators range between 20 and 300 henries.

The quartz blanks used are finished with a 12 micron abrasive and after cleaning and etching they are metalized with nichrome-gold. Headed mounting wires are soldered directly to this film. The wires are terminated at an odd quarter wavelength by soldering them to metalized epoxy-glass rails. Typical resonator assemblies are shown in Figure 8.

The resonators are adjusted to frequency in this configuration and then tested for frequency, resistance and inductance. The measurement equipment consists of a broadband crystal oscillator, frequency counter and digital voltmeter; all controlled by a programmable calculator. Lot statistics are also computed by the calculator thus permitting close monitoring of the processes which control the crystal parameters.

The resonator assemblies are secured to carriers with conductive epoxy. The result is the crystal networks shown in Figure 9. The conductive epoxy and mounting posts provide the electrical interconnections between the resonators while the carrier affords a measure of protection for the crystal plates during handling.

The crystal networks are then tested electrically. For these tests the selectivity of a remotely programmed frequency synthesizer is required because the resonators are now connected in parallel. Networks that pass are given a final visual and mechanical check prior to filter assembly.

The open mounting of multiple resonators in a plastic, protective carrier allows very dense packaging, while maintaining stable, accurately adjusted crystal parameters. This technique contributed a great deal to the size reduction of these filters compared to previous DCFs.

Conclusion

The new DCFs for Bell System analog channel banks have been described. These DCFs are of two types: a six-resonator design meeting CCITT system requirements and two four-resonator designs meeting Bell System requirements. The electrical and physical design methods and results have been covered. The new crystal assembly designs have been shown. The crystal assemblies and the other components are mounted on a printed circuit board and are enclosed in a can which is designed to mount onto a plug-in printed circuit board. Fig. 10 shows the packages of the two filter designs. The filter on the left is the A7E DCF. The two crystal assemblies of three resonators each can be seen with the capacitors mounted between them. At the ends of the unit are the magnetic components. On the right is a model of the N4/LT-1 DCF. The physical similarities to the A7E DCF are obvious. The exception is the single, four-resonator crystal assembly rather than the pair of three-resonator assemblies. This particular filter is a model of the DCF which passes the 60.6 to 63.8 kHz band; therefore, the crystal resonators are the maximum length of the twelve filter designs.

Acknowledgment

The authors acknowledge with thanks the contributions of the following: F. J. Witt and T. H. Simmonds, Jr., leadership and technical advice; J. H.

Armstrong and K. K. Simpson, crystal design; P. D. Patel and M. R. Randall, physical design; R. C. Rennick and E. D. Walsh, computer aids; R. W. Avery and A. Olsen, magnetic components; and J. E. Murphy and M. Fiore, capacitor evaluation.

References

[1] T. H. Simmonds, Jr., "The Evolution of the Discrete Crystal Single Sideband Selection Filter in the Bell System," IEEE, Proceedings, Vol 67, No. 1, Jan. 1979, pp. 109-115.

[2] C. V. Fanuele, R. E. LeBlanc and L. Y. Levesque, "The New N4 Carrier Terminal," Proceedings - National Telecommunications Conference, December 1978, pp. 21.3.1 - 21.3.8.

[3] W. J. Mitchell, Jr., "The LT-1 - A Conventional Transmultiplexer," Proceedings - National Telecommunications Conference, December 1978, pp. 21.4.1 - 21.4.5.

[4] G. W. Bleisch and W. P. Michaud, "The A6 Channel Bank: Putting New Technologies to Work," Bell Laboratories Record, Vol. 49, No. 8, pp. 251-254, Sept. 1971.

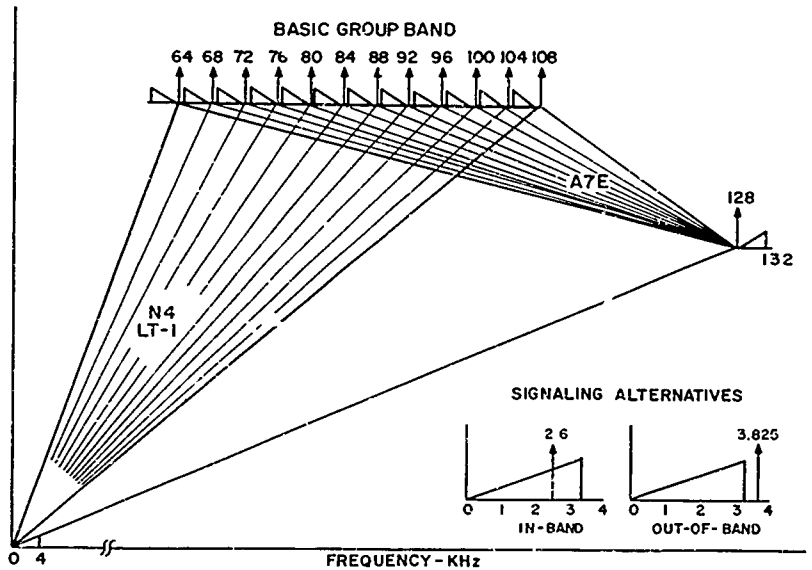

Fig. 1 Frequency Allocations

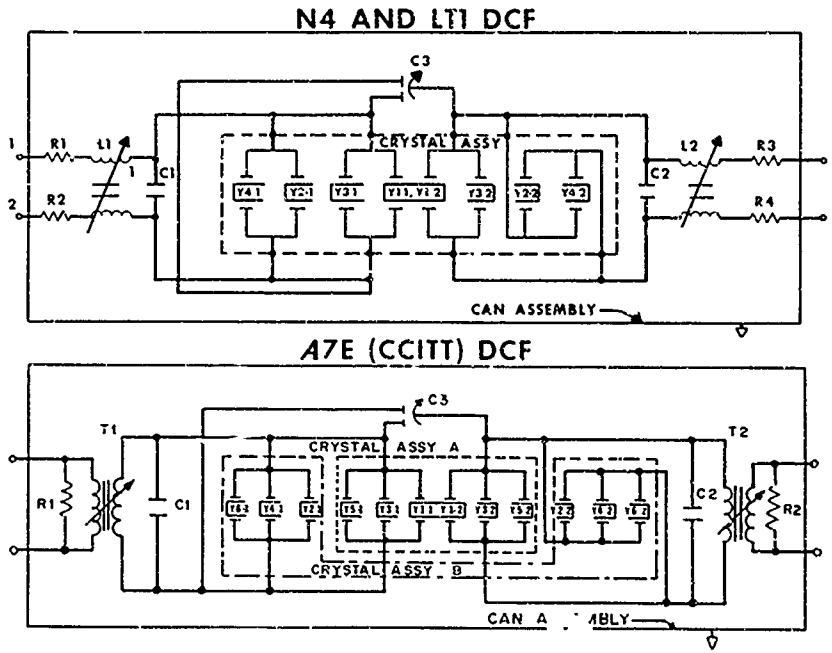

Fig. 2 DCF Schematics

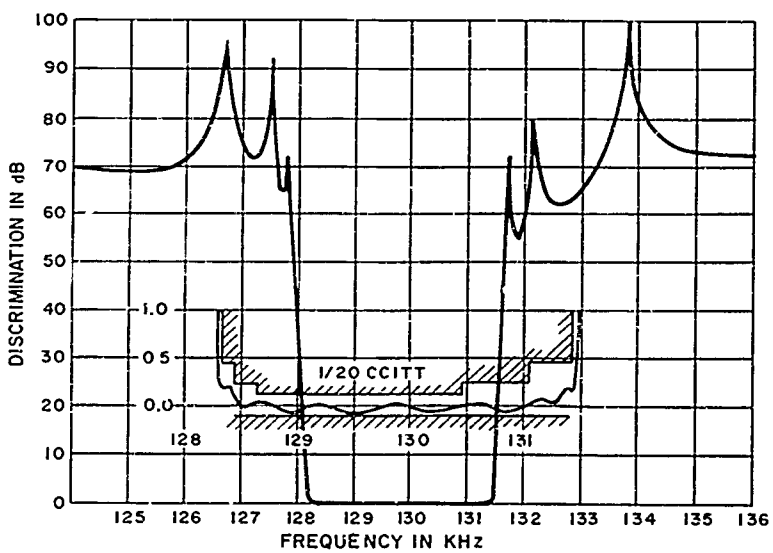

Fig. 3 Discrimination of a Typical A7E DCF at 25°C.

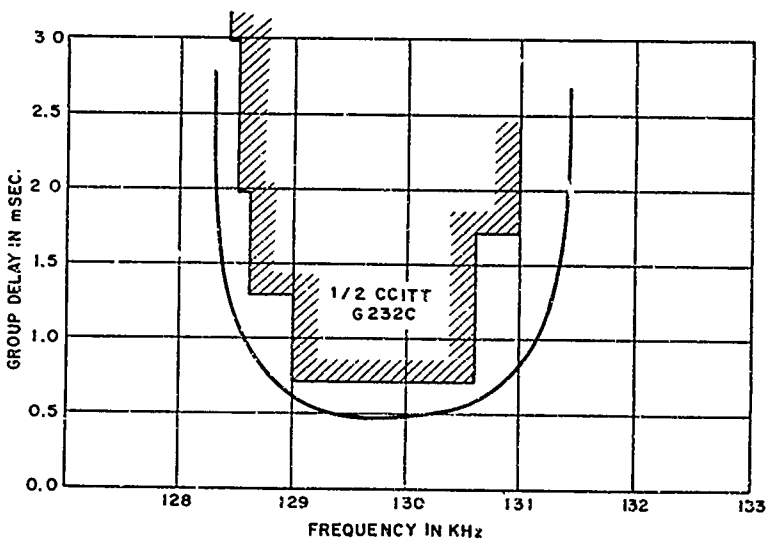

Fig. 4 Delay of an A7E DCF at 25°C.

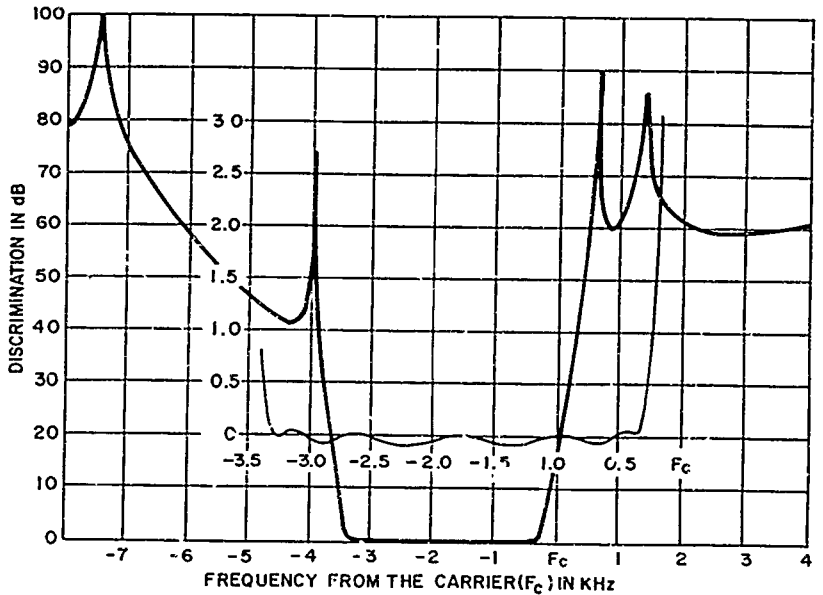

Fig. 5 Discrimination of a Typical LT-1 DCF at 25°C.

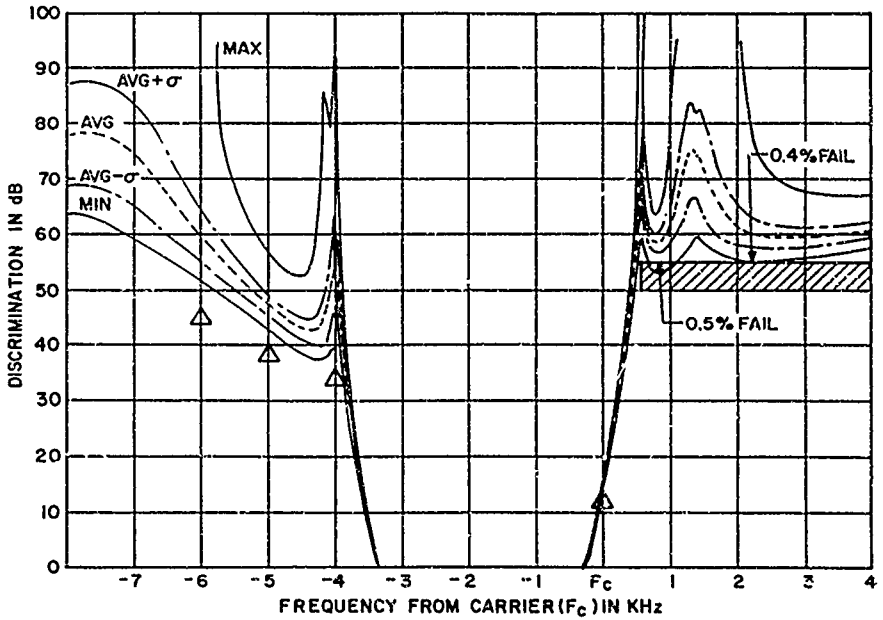

Fig. 6 Predicted Stopband Envelope of an LT-1 DCF at 40+27°C with long term aging.

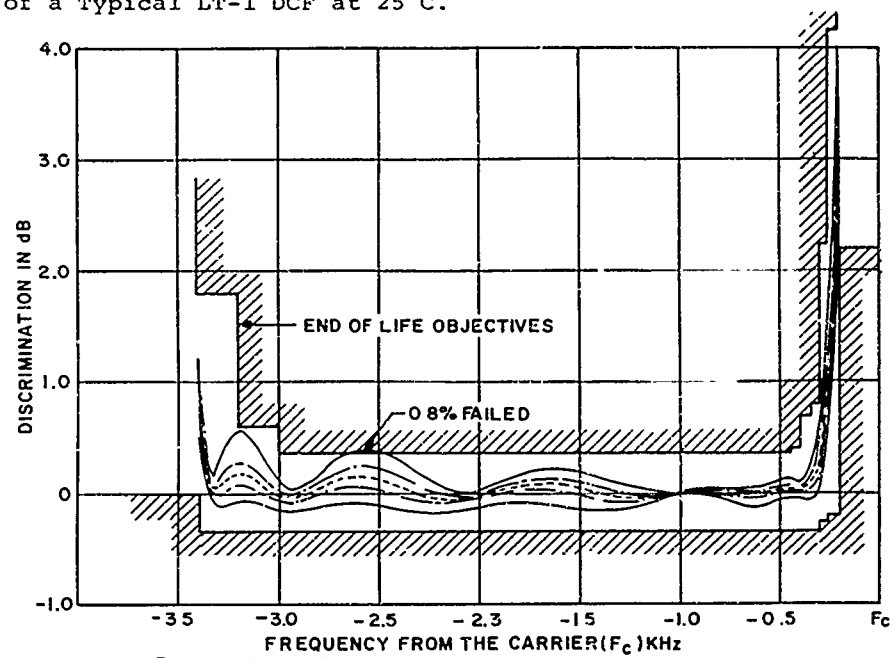

Fig. 7 Predicted Passband Envelope of an LT-1 DCF at 40±27°C with long term aging.

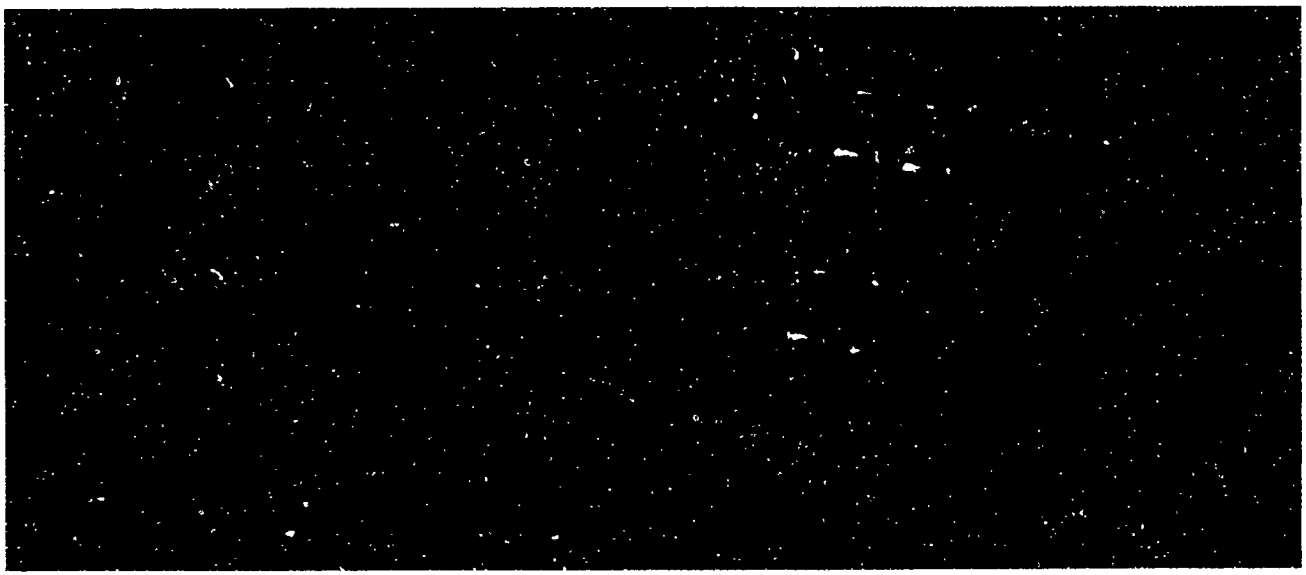

Fig. 8 Resonator Assemblies

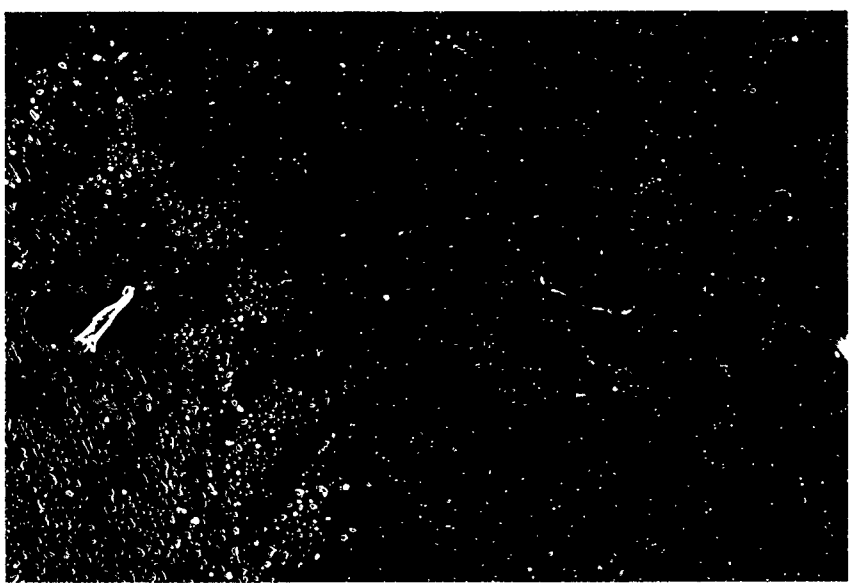

Fig. 9 Crystal Networks

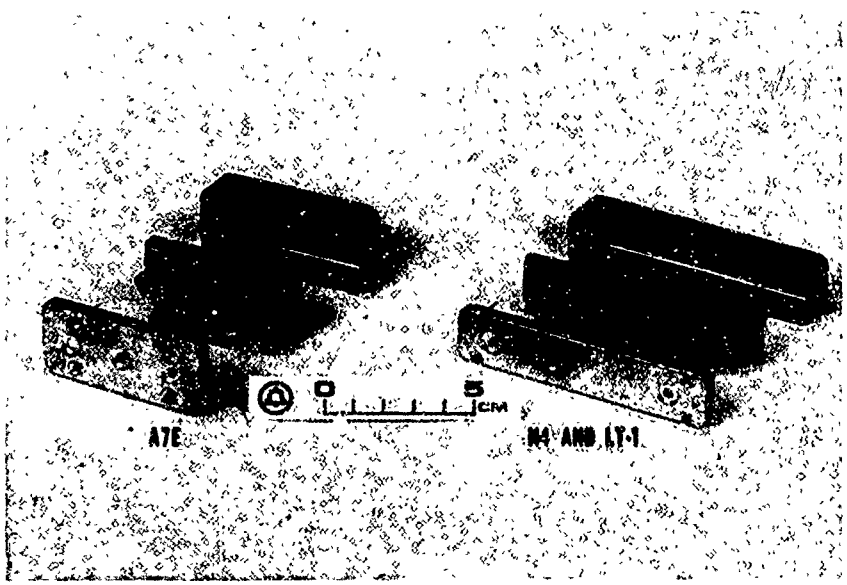

Fig. 10 Bell System Discrete Crystal Filters.

THE DESIGN AND APPLICATION OF ELECTROMECHANICAL SINGLE SILICON BEAM FILTERS

Marija F. Hribšek
Department of Electrical Engineering
University of Belgrade
Belgrade, Yugoslavia

Summary

Principles of operation, design problems and procedure of single silicon beam electromechanical filters design are presented. Using the proposed procedure very selective bandpass filter for 51.825 kHz is designed and its application in multichannel telephony systems is discussed.

Introduction

Recently developed silicon beam filters[1,2] represent the special kind of very selective electromechanical filters suitable for low frequencies and integration. For the selection of the desired frequency range the mechanical resonance of silicon beam is used. This paper will deal with design procedure and application of such filters, but a brief review of the principles of operation is also given to provide better understanding.

Principles of Operation

A single silicon beam filter consists of a thin silicon beam cantilevered over a metal plate, as is shown in Fig. 1.[1] On the top side of the silicon beam at its free end an aluminum film is deposited. The film and the metal plate form the input transducer. The output transducer is the piezoresistive bridge formed by four equal resistors placed at the cantilevered end of the beam. The input signal applied to the input transducer will cause the vibration of the silicon beam. The vibrations are sensed by the piezoresistive bridge which is in balance when the beam does not vibrate. The deflection of the beam and therefore the output voltage of the device is maximal when the frequency of the input signal is equal to the mechanical resonant frequency of the beam. It has been shown[1,2] that the transfer function of the single silicon beam filter has the following form:

$$T(s) = \frac{K}{s^2+s\omega_1/Q+\omega_1^2} \qquad (1)$$

where Q is the Q factor of the silicon beam, and K and ω_1 are the functions of silicon beam dimensions, biasing voltages and physical properties of silicon given by:

$$K=5.32\cdot10^{-15}V_B E_o a^{-2} T^{-2}\omega_1 BC(x_B) \qquad (2)$$

$$B=0.707\left[\sinh(1.875L_1/L)-\sin(1.875L_1/L)\right] - 0.518\left[\cosh(1.875L_1/L)+\cos(1.875L_1/L)\right] \qquad (3)$$

$$C(x_B)=0.707\left[\cosh(1.875x_B/L)+\cos(1.875x_B/L)\right] -0.518\left[\sinh(1.875x_B/L)+\sin(1.875x_B/L)\right] \qquad (4)$$

$$\omega_1 = 2\pi f_1 \qquad (5)$$

where f_1 is the mechanical resonant frequency of the silicon beam given by[1,2,3]

$$f_1=1.125\cdot10^5 T/L^2 \qquad (6)$$

Equation (1) obviously represents the transfer function of a low pass filter. However, since the Q factor of the filter is very high (>1000), as has been shown[1,2], it can be used for very selective band pass filtering around the frequency f_1.

Design of single silicon beam filter

The design procedure consists of several steps in which the dimensions of the filter and the values of biasing voltages are determined. The basic guidelines of the design are:

1. The dimensions of the filter should be as small as possible to achieve higher density and consequently lower cost.
2. The minimal dimensions of the filter are limited by the fabrication technology.
3. All parameters should be determined in such a way to produce minimal losses at the resonant frequency.

The first step in the design procedure is to calculate the length L and the thickness T of the cantelevered silicon beam from the given resonant frequency. From equation (6) is obvious that for given f_1 the lower values of T will give the smaller L. Since the smallest physically obtainable thickness is 10^{-3} cm[1,2] the corresponding length can be calculated as:

$$L = 10.6\, f_1^{-0.5} \qquad (7)$$

From (1) to (6) we can see that they are not the functions of the beam width W. We choose the minimal value for the width which is determined by the dimensions of the piezoresistive bridge and its contact leads. It has been shown[1,2] that the minimal width is 0.035 cm.

The next step is to calculate the length L_1, determining the length of the aluminum film at the top of the beam. It is calculated from the condition that the parameter B is maximal, which gives the minimal attenuation at the resonant frequency. From (3) can be found that the maximal B demands minimal L_1. The minimal L_1 is determined by the dimensions of the piezoresistive bridge and for the minimal dimensions of the bridge L_1 is 0.0175 cm.

The coordinate of the bridge center x_B is determined in the same way as L_1 from the condition that $C(x_B)$ is maximal. The optimal value of x_B is its minimum which is determined by the smallest obtainable bridge dimensions. Since the minimal bridge length is 0.0125 cm[1,2] the optimal value of x_B is 0.00625 cm.

The last dimension which has to be determined is the distance a between the metal plate and the beam. In order to get less attenuation at the resonant frequency a has to be as small as possible but its physical limit is 10^{-3} cm.

Besides the dimensions, the values of bias voltages E_o and V_B should be determined. In order to lessen the attenuation at the resonant frequency the higher values of E_o and V_B should be selected. However, the maximal value of V_B is limited by permissible dissipation of bridge resistors, and the maximal value of E_o is determined from the equilibrium between the D.C. component of the input electrostatic force and the mechanical restoring force of the beam and is given by [1,2]:

$$E_{om} = (2/27)^{1/2}\left[a^3T^3E/L^3(L-L_1)\varepsilon_o\right]^{1/2} \qquad (8)$$

where E is Young's modulus and ε_o is the permitivity of the air. It is not recommended to use for E_o values close to E_{om} because in that case some changes in the elasticity of the beam occur[4] and change the resonant frequency of the filter.

This fact can be used sometimes for the correction of the resonant frequency, but usually when the resonant frequency is correct, the value of E_o should be around 0,1 E_{om}.

Following the presented procedure the single silicon beam filter for the frequency of 51.825 kHz is designed. Assuming that the bridge resistors have values between 0.5 and 1k the following values of the dimensions and voltages are calculated:

$T = 10^{-3}$ cm
$a = 10^{-3}$ cm
$L = 0.04656$ cm
$W_1 = 0.035$ cm
$L_1 = 0.0175$ cm
$x_B = 0.00625$ cm
$V_B = 20V$
$E_o = 50V$

These values give:

$$T(j\omega_1) = 1.471 \cdot 10^{-4} \qquad (9)$$

and the normalized frequency response shown with solid line in Fig.2. With the dashed line in Fig. 2 is shown the normalized frequency response of the Siemens electromechanical filter[5] presently used in multichannel telephon systems.

Discussion

In this paper the design procedure of the single silicon beam filter is presented. It has been shown that many conditions have to be satisfied, but the design procedure is very simple if the limits set up by physical realization are known. The presented design procedure is illustrated by the example of the filter with resonant frequency of 51.825 kHz. It can be seen that the designed filter is competitive with the Siemens filter which is much bigger than the designed filter. The only disadvantage of the designed filter is its attenuation at the resonant frequency which can be avoided by an amplifier integrated in the base of the beam.

References

1 M. Hribšek, "High Q Selective Filters Using Mechanical Resonance of Silicon Beams", Ph. D. Thesis, September 1976.

2 M.Hribšek, R.W. Newcomb, "High Q Selective Filters Using Mechanical Resonance of Silicon Beams", IEEE Trans. Circ. Systems, CAS-25, No.4, April 1978.

3 M.Hribšek, R.W. Newcomb, "Ekvivalentni model prostog silicijumskog filtra", ETAN, 1977, V.1,p229-234.

4 H.C. Nathanson et al. "The Resonant Gate Transistor" IEEE Trans. on El. Devices, Vol. ED- 14, No.3, pp.117-133, March 1967.

5 Technische Daten, Wahlfilter Sendseite, Siemens 1976.

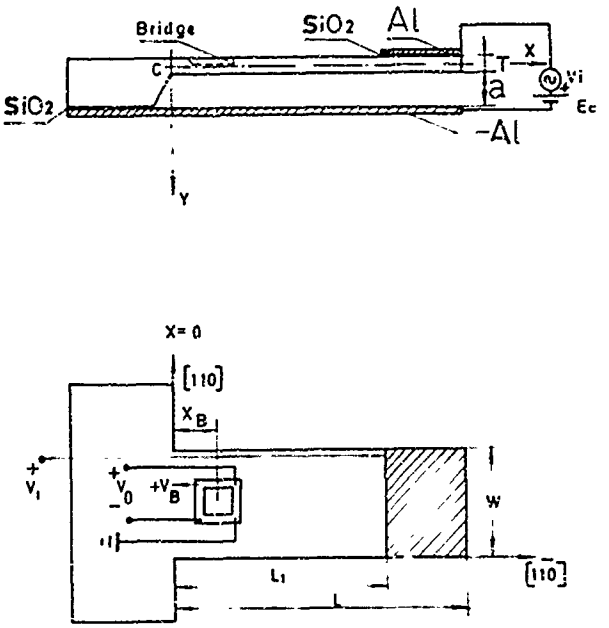

Figure 1.

Single silicon beam filter

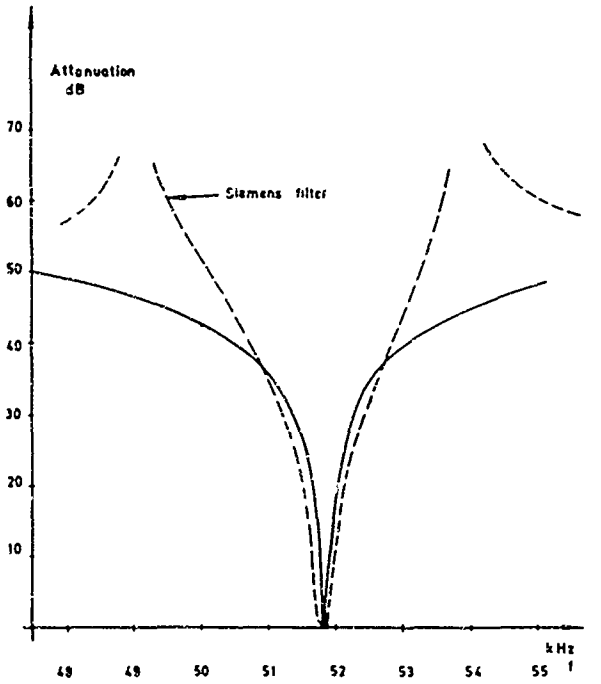

Figure 2.

Frequency responses of the single silicon beam filter and Siemens filter

A REVIEW OF THE NEW IEEE STANDARD ON PIEZOELECTRICITY

Thryqve R. Meeker

Bell Telephone Laboratories, Incorporated
555 Union Boulevard
Allentown, Pennsylvania 18103

Summary

A new standard on piezoelectricity (IEEE Std. 176-1978) has been issued recently by the Institute of Electrical and Electronics Engineers. The contents of this standard are reviewed briefly. Some historical background on piezoelectric standards is discussed. Particular emphasis is placed on changes in the definition of reference plates, and in the signs of coordinate axes, piezoelectric and elastic constants, and angle of rotation for quartz bars and plates.

The role of these changes in the use of published tables of material constants and of various sets of rotation equations in theoretical studies is discussed.

Introduction

The development of standards on piezoelectric crystals and measurements has been the product of considerable work and debate by many people. Early piezoelectric standards were prepared by the Standards Committee of the Institute of Radio Engineers in the mid 1940's. When the Institute of Radio Engineers was merged with the Institute of Electronic and Electrical Engineers, the later issues of the IRE standards were adopted as IEEE standards. Figure 1 lists the titles of these standards, along with the IRE, IEEE, and ANSI (American National Standards Institute) notations. The 1945 IRE reference should probably be called a recommendation and not a standard. In Figure 1 REAFF is the IEEE expression for reaffirm and R is the ANSI equivalent expression.

These standards define terms and measurement techniques and refer to publications for background theory and vibration mode descriptions. The standards committees paid special attention to two technologically important materials--quartz and piezoelectric ceramics.

The complexity of the measurements, the tensor and matrix description of the material constants, and the existence of enantiomorphic crystal forms led to changes in sign conventions from time to time, as the standards committees tried to make the conventions easier to understand and use.

As the theory of the piezoelectric resonator became more systematic and more widely understood, the need for a new standard became clear. Extensive work on new materials, such as lithium niobate and lithium tantalate, also indicated the need for a new standard.

The new standard was jointly sponsored by the Transducers and Resonators Committee of the IEEE Group on Sonics and Ultrasonics and by the Frequency Control and Time Committee of the IEEE Group on Instrumentation and Measurements. Primary authors were A. H. Meitzler (Chairman), H. F. Tiersten, A. W. Warner, D. Berlincourt, G. A. Coquin, and F. S. Welsh, III.

For the new standard (IEEE STD 176-1978) the standards committee decided to:

1. Abandon the use of a separate sign convention for the piezoelectric constants of quartz.
2. Abandon the definition of electromechanical coupling factors based on interaction energies.
3. Add a section on theoretical concepts and mathematical relationships.

4. Revise the material covered in IEEE STDS 176 and 178.

5. Treat enantiomorphic crystal forms in greater detail.

6. Clarify the techniques of piezoelectric determination of the sense of the crystal axes.

7. Clarify the system of notation for designating plates and bars.

8. Include tables useful in theoretical and experimental work.

9. Include a section on modern analyses of plane wave motions and vibrations.

10. Review measurement techniques.

Figure 2 lists the table of contents of IEEE Standard 176-1978. Figure 2 shows the broad scope of the new standard. Section 2 through Section 6 constitute a short but detailed review of the theory and application of piezoelectric crystals. Section 8 contains many important references for the reader interested in a more detailed study.

In this paper some implications of the change in sign of the piezoelectric constants of quartz and of the changes in the sense of the crystallographic axes are discussed. Some of the history of conventions for elastic and piezoelectric properties of crystals is reviewed. The questions discussed in the next section of this paper are summarized in Figure 3, which includes some of the content of a paragraph in the new standard[1].

Conventions for Electric and Piezoelectric Properties of Alpha Quartz

Figure 4 summarizes the historical highlights of some of the sign conventions which have been used for the properties of alpha quartz. Included in this table are the conventions used in the 1945 IRE Recommendations[2], the 1949 IRE Standard[3], and the new 1978 IEEE Standard[1]. Also included are the conventions used by Heising[4], Cady[5], and Mason[6] in their books on piezoelectric crystals and devices. For each property the convention for left quartz is given first, followed by the convention for right quartz, ie. - / -. Figure 4 is not intended to be complete. It is only intended to illustrate some of the important changes in convention that have evolved during the last thirty-five years. Changes in the handedness of the crystal axes, the sign of the angle associated with counterclockwise rotation as observed from the positive end of the rotation axis toward the origin, the AT rotation angle, the sign of the voltage developed for tension along X, and the motion of conoscope rings for clockwise analyzer motion are listed in Figure 4. Figure 4 suggests that the only conventions that have remained the same are the rotation of polarized light (or the handedness assigned to a particular enantiomorphic form of quartz) and the use of a right handed coordinate system for right quartz.

Figure 5 lists historical highlights of some of the sign conventions used for piezoelectric and elastic constants of alpha quartz. Besides the conventions adopted in the three standards, those used in the books by Heising[4], Cady[5], and Mason[6] are also shown in Figure 5, as well as the signs used by Bechmann[7]. Actually the later paper by Bechmann, Ballato, and Lukaszek[8] is the one most often referenced. The later paper refers to the earlier paper for the room temperature values of the constants, but changes e_{14} from -0.0406 coulomb/meter^2 to +0.0403 coulomb/meter^2 without comment. It must be emphasized that the earlier Bechmann values of constants were tabulated for left quartz. The handedness of the quartz used in the subsequent temperature coefficient studies is not emphasized[8]. Figure 5 contains the signs for both left and right alpha quartz as they were defined by Bechmann[7] in accordance with the 1949 standard.

Figure 6 shows crystal rotation equations for Group VII Trigonal Classes 18, 19, 20[9]. Quartz belongs to this group[19]. For this group rotation formulas for selected constants are presented according to Cady[10] and Mason[11]. The formula used by Bechmann, Ballato, and Lukaszek[12] to analyze their temperature coefficient data is also given in Figure 6. In Figure 6 the numbers after the author's names are volume number and page numbers in References 5, 6, and 8. Since the rotation equations were derived by algebraic manipulation of the appropriate tensor rotations, the various sign changes shown in Figure 6 must be understood in terms of the changes in the sign of the rotation angle and the signs of C_{14}, e_{14}, and e_{11}. The examples given in Figure 6 illustrate the only two combinations of factors that occur in the complete set of rotation equations for X_1 axis rotation for Group VII. In the equations giving rotated values for all constants except C_{14} or e_{14}, $\sin\theta$ is either squared or is multiplied by C_{14} or e_{14}. In the equations giving rotated values for C_{14} or e_{14}, $\sin\theta$ appears in one term and C_{14} or e_{14} appear in the other. As a result of this form of the rotation equations, a change in the sign of an angle must be accompanied by a change either in the sign of C_{14} and e_{14} or in the sign of the appropriate terms of the rotation equations. Otherwise the magnitudes of some of rotated elastic and piezoelectric constants depend on the convention used. A footnote in the 1949 IRE standard[13] suggests that the rotation signs and constant signs had been adjusted to keep the Cady rotation equations the same for right and left quartz.

When material constants are determined using a particular set of rotation equations, great care must be exercised to make the rotation equations, the signs of the

constants, and the sign of a counterclockwise rotation consistent. When reporting the results of such work, authors should refer to all conventions and rotation equations used.

Calculations of the frequency or admittance of a plate or bar of a particular orientation are often reported. In the rotations used angles are measured from the reference material coordinate system toward the final system.

Misprints and Errors in IEEE Standard 176-1978

An error[14] in the voltage convention in the new standard caused Equations 79, 82, 90, 96, 107, 111, and 117 to have the wrong sign.

A few typographical errors[15] are mentioned here for reference. On page 46 Table 9, "electrochemical" should be "electromechanical". On page 26 Figure 5, the head of the -51° arrow should extend to the dashed line.

Conclusions

A long history of piezoelectric standards is continuing. The application of the new standard to theoretical work will require that computer programs and tables of material constants be revised. The application of the new standard to production work will require that specifications be revised. The scientific, engineering, and production communities will have to decide whether the required changes in documents are worth the reduced confusion that standardization always yields.

Some misprints and errors in the new standard have been mentioned. It is hoped that the standards committee will issue the necessary corrections.

References

[1] IEEE Standard 176-1978, page 17 (1978)

[2] 1945 IRE Recommendation, see note in W. G. Cady, Dover Publications, New York, Vol. II, page 755 (1964, not 1946)

[3] Standards on Piezoelectric Crystals, 1949, Proceedings of the IRE, Vol. 37, No. 12, pages 1378-1395 (1949)

[4] R. A. Heising, Quartz Crystals for Electrical Circuits , D. Van Nostrand Company, New York (1946)

[5] W. G. Cady, Piezoelectricity , Vol. I and Vol. II, Dover Publications, New York (1964, 1946)

[6] W. P. Mason, Piezoelectric Crystals and Their Application to Ultrasonics , D. Van Nostrand Company, New York (1950)

[7] R. Bechmann, Physical Review, Vol. 110, No. 5, pages 1060-1061 (1958)

[8] R. Bechmann, A. D. Ballato, and T. J. Lukaszek, Proceedings of the IRE, Vol. 50, No. 8, pages 1812-1822 (1962)

[9] Reference 5, Vol. II, page 55

[10] Reference 5, Vol. I, page 76 and page 77

[11] Reference 6, page 94

[12] Reference 8, page 1819

[13] Reference 3, page 1385

[14] Private Communication, H. F. Tiersten

[15] Private Communication, A. D. Ballato

A LIST OF STANDARDS ON PIEZOELECTRIC CRYSTALS AND RESONATORS

A. PIEZOELECTRIC CRYSTALS: RECOMMENDED TERMINOLOGY
1945 IRE

B. PIEZOELECTRIC CRYSTALS
49 IRE 14.S1
IEEE STD 176–1949 (REAFF 1971)
ANSI C83.3–1951 (R 1972)

C. DEFINITIONS AND METHODS OF MEASUREMENT FOR PIEZOELECTRIC VIBRATORS
57 IRE 14.51
IEEE STD 177–1966
ANSI C83.17–1970

D. DETERMINATION OF THE ELASTIC, PIEZOELECTRIC, AND DIELECTRIC CONSTANTS – THE ELECTROMECHANICAL COUPLING
58 IRE 14.S1
IEEE STD 178–1958 (REAFF 1972)
ANSI C83.23–1960 (R 1972)

E. MEASUREMENTS OF PIEZOELECTRIC CERAMICS
IEEE STD 179–1961 (REAFF 1971)
ANSI C83.24–1962 (R 1972)

Figure 1

TABLE OF CONTENTS OF IEEE STD 176-1978

SECTION 1
SCOPE AND UNITS

SECTION 2
LINEAR THEORY OF PIEZOELETRICITY

SECTION 3
CRYSTALLOGRAPHY OF PIEZOELECTIC CRYSTALS

SECTION 4
WAVE AND VIBRATION THEORY

SECTION 5
SIMPLE HOMOGENEOUS STATIC SOLUTIONS

SECTION 6
DETERMINATION OF ELASTIC, PIEZOELECTRIC, AND DIELECTRIC CONSTANTS

SECTION 7
STANDARDS REFERENCES – 7 REFERENCES

SECTION 8
BIBLOGRAPHY - 41 REFERENCES

16 FIGURES

11 TABLES

Figure 2

WORKING WITH PIEZOELECTRIC MATERIALS AND DEVICES

1. A SET OF ELASTIC, PIEZOELECTRIC, AND DIELECTRIC CONSTANTS IS NEEDED
2. CONSISTENT SIGN CONVENTIONS ARE NECESSARY
   a. CONSTANTS
   b. AXES
3. BAR SHAPES AND ORIENTATIONS
   a. SKETCH IS CLEAREST
   b. CONVENTIONS FOR ANGULAR ROTATIONS
4. ROTATIONAL EQUATIONS
   a. CONSISTENT WITH MATERIAL AND COORDINATE SIGN CONVENTIONS

Figure 3

HISTORICAL HIGHLIGHTS OF CONVENTIONS FOR ELASTIC, PIEZOELECTRIC, AND OPTICAL PROPERTIES OF ALPHA QUARTZ

(LEFT/RIGHT)

CONVENTION	HANDEDNESS OF COORDINATE SYSTEM	SIGN OF ANGLE FOR CCW ROTATION + TO 0 ON AXIS	AT ANGLE	SIGN OF VOLTAGE FOR TENSION ALONG X	CONOSCOPE RING MOTION FOR CW ANALYZER MOTION
1945 IRE	(L/R)	(★ ★)	(★ ★)	(★ ★)	(★ ★)
1946 HEISING	(L/R)	(/+)	+35.25	(+/+)	(CONTRACT
1946 CADY	(L/R)	(−/+)	−35.25	(+/+)	(★ ★)
1949 IRE	(R/R)	(/+)	+35.25	(+/−)	(CONTRACT EXPAND)
1950 MASON	(/R)	(★ ★)	+35.25	(★ ★)	(★ ★)
1978 (IEEE)	(R/R)	(/+)	−35.25	(/+)	(CONTRACT EXPAND)

★ ★ NOT DISCUSSED

Figure 4

HISTORICAL HIGHLIGHTS OF SIGN CONVENTIONS FOR ELASTIC AND PIEZOELECTRIC CONSTANTS OF ALPHA QUARTZ

(LEFT/RIGHT)

CONVENTION	SIGN OF e_{11}	SIGN OF e_{14}	SIGN OF C_{14}
1945 IRE	(+ +)	(+ +)	(★ ★)
1946 HEISING	(−)	(−)	(+)
1946 CADY	(+ +)	(+ +)	(+ +)
1949 IRE	(+ −)	(−/+)	(−/−)
1950 MASON	(★ ★)	(★ ★)	(/+)
1958 BECHMANN ★	(+ −)	(− +)	(−/−)
1978 IEEE	(−/+)	(−/+)	(★ ★)

★ SIGN CONVENTIONS WERE REPEATED IN 1962 BY BECHMANN, BALLATO, LUKASZEK EXCEPT THAT SIGN OF e_{14} WAS CHANGED WITHOUT COMMENT. I ASSUME THAT ALL CRYSTALS USED IN THE 1962 STUDIES WERE RIGHT QUARTZ.

★ ★ NOT DISCUSSED

Figure 5

SELECTED ROTATION EQUATIONS (X AXIS) FOR GROUP VII TRIGONAL CLASSES 18, 19, 20

CADY I 77 (1946)

$$C_{14}' = (C^2 - S^2)\,C_{14} - CS\,(C_{12} - C_{13})$$

$$C_{66}' = S^2 C_{44} + C^2 C_{66} + 2\,CS\,C_{14}$$

BECHMANN, BALLATO, LUKASZEK 1819 (1962)

$$C_{66}' = S^2 C_{44} + C^2 C_{66} + 2\,CS\,C_{14}$$

MASON 94 (1950)

$$C_{66}' = S^2 C_{44} + C^2 C_{66} - 2\,CS\,C_{14}$$

CADY I 212 (1946)

$$e_{14}' = CS\,e_{11} + (C^2 - S^2)\,e_{14}$$

$$e_{11}' = e_{11}$$

$C = \cos\theta$

$S = \sin\theta$

Figure 6

TRIM SENSITIVITY
A USEFUL CHARACTERIZATION OF A RESONATOR

John H. Sherman, Jr.

U.S. Mobile Radio Department
General Electric Company
Lynchburg, Virginia 24502

ABSTRACT

Two terms, Trim and Trim Sensitivity are defined and the latter examined in detail. Design equations for Trim Sensitivity are derived. Equations are found for ready measurement of Trim Sensitivity. By these equations the relation with the more familiar motional capacitance and inductance is clarified. Application to two common problems of compensated oscillator production illustrates the utility of the concept of Trim Sensitivity.

Key Words: Trim, Trim Sensitivity, motional parameters, quartz crystal, resonator, compensated oscillator, TCXO, modulated oscillator, VCXO.

Symbols and Units

The following symbols are used in the paper, with definitions and units.

A, the area of an electrode in mm^2.

C_t, the capacitance measured at the external terminals of the resonator, in farads.

C_1, the equivalent motional capacitance posited in the Butterworth-Van Dyke equivalent circuit of the resonator, in farads.

C_s, the capacitance of the electronic circuit to which the resonator is connected, observed at the connection terminals, in farads.

f_a, the antiresonant or inherent self-resonant frequency of the isolated resonator, in hertz.

f_r, the resonating frequency of the resonator and load capacitor, C_ℓ connected, in hertz.

f_s, the series resonant or resonant frequency of the short circuited resonator, in hertz.

L, the equivalent motional inductance posited in the Butterworth-Van Dyke equivalent circuit of the resonator, in henries.

m, the overtone order of operation of the resonator, an odd integer, a numeric.

r, the ratio of C_0 to C_1, a geometric property of the resonator shape invariant underchange of scale, a function of m increasing at a rate faster than m^2, usually written r_c a numeric.

S, Trim Sensitivity, $\frac{-1}{f_r}\frac{d f_r}{d C_\ell}$, in parts per farad. (Commonly used in ppM/pf with a conversion factor of 10^6).

T, Trim, $\frac{-d f_r}{d C_\ell}$ in Hz/f. (Commonly used in Hz/pf with a conversion factor of 10^{12}).

$\gamma(C_\ell)$, the temperature coefficient of the circuit capacitance C_ℓ with the modulating or compensator voltage held constant at nominal value, in parts/K.

$T(f_r)$, the temperature coefficient of the load resonant frequency of the resonator loaded with the capacitance C_ℓ evaluated at reference temperature, in parts/K.

Other quantities used are defined and discussed upon introduction in the text.

Introduction

A substantial literature is developing on the measurement of crystal resonators. For the most part the emphasis is directed toward the improved determination of the values of the element values in an equivalent circuit. There

is no doubt that knowledge with great precision of the values of these parameters will allow the accurate computation of the behavior of the resonator in a circuit of application. In the design of resonators for use in filter networks considerations of impedance matching lead directly to the specification with tolerance of the value of one of the motional arm parameters. It is hard to visualize any other effective means of specifying and characterizing a resonator for filter use than by the actual value of a motional parameter.

In the case of resonators for use in oscillators the case is quite different. Almost never are all of the degrees of design freedom consumed in the specification of an oscillator resonator by performance. That this is true even of resonators intended for use in such stringent applications as temperature compensated or directly modulated oscillators is not commonly appreciated. In a difficult application the first successful resonator design to be found is usually treated as the only acceptable design.

This is advantageous to the original designer, of course, but not to the user. By this approach all other potential suppliers are forced to take on the puzzle of finding that one design out of the continuum of equally valid designs allowed by the laws of nature. Generally the accepted design contains elements of habitual practice of which even the designer is hardly aware. The existence of a successful design is, of course, important knowledge. The insistence that it must be the only one used is to ignore the valid distinction drawn by mathematicians between necessary and sufficient conditions. A solution in hand is, itself, a sufficient condition for a solution to exist. This solution is necessary as well only if it uses all the degrees of freedom.

Strangely, it is easier to illustrate excess degrees of freedom by a first reference to the resonators of a monolithic crystal filter. While considerations of impedance lead directly to the specification of areas of resonator electrodes, the designer still has wide latitude in the choice of aspect ratio of the resonators, whether the array shall be disposed along X or Z, and where in a continuum of interdependent values for either configuration to specify the plateback and resonator separation. A similar look at available options in oscillator resonators will be essayed near the end of the paper.

Frequency "Trimming"

Whenever it is required that the accuracy of frequency be greater than that practical to be built into the resonator, adjustable components are included in the oscillator circuit to allow the adjustment of the frequency of the assemblage. The most commonly used component for this purpose over the years has been a small variable capacitor called, in the vernacular, a "trimmer". It is thus reasonable to call the adjustment of frequency using a trimmer "trimming". Other terms have been used, such as "rubbering". There is no standard terminology. Perhaps this paper may serve to stabilize terminology.

In particular I wish to introduce two terms into our vocabulary. They are:

1) Trim, the negative of the rate of change of frequency with respect to load capacitance. In quartz resonators this commonly lies between 10^{12} and 10^{15} Hz/f or between 1 and 1000 Hz/pf.

$$T = -df_r/dC_\ell \qquad (1)$$

2) Trim Sensitivity, the negative of the logarithmic derivative of frequency with respect to load capacitance. In quartz resonators this commonly lies between 10^5 and 10^8/f or between 0.1 and 100 ppM/pf.

$$S = \frac{-1}{f_r}\ \frac{df_r}{dC_\ell} \qquad (2)$$

These derivatives are quite different from that one examined by Noble [1] who studied the condition for the maximum frequency difference between "trimmer meshed" and "trimmer open" in an oscillator. He found this to occur when the resonator static capacitance value is the geometric mean of the extreme values of the load capacitance.

Ballato [2] [3] has studied a variety of load-capacitance-related phenomena. He has found it convenient to define a parameter or fraction which he has called α :

$$\alpha = C_o/(C_o + C_\ell) \qquad (3)$$

The range of α is from 1 to 0.
It will be convenient for us to employ this term in this paper on occasion. For simplicity's sake, instead of r_c, the ratio of the capacitances in the equivalent circuit, I will use the letter ρ , thus:

$$\rho = r_c = C_o/C_1 \qquad (4)$$

In my experience the quantity Trim has been adequately treated as the product of Trim Sensitivity and frequency. It will be so treated here. The following discussion will bear entirely on Trim Sensitivity.

Design For Trim Sensitivity

The conventional Butterworth-Van Dyke equivalent circuit incorporates an equivalent resonance resistance in the motional arm. A detailed analysis of this finite Q circuit [2] shows that the errors of frequency attendant upon ignoring losses are of the order of $1/Q^2$. Inasmuch as Q in excess of 10^4 may ordinarily be assumed for a practical quartz resonator, the errors in computed frequency will be on the order of parts in 10^8. In the derivations we will, therefore, confidently consider a lossless equivalent circuit.

In the lossless circuit three frequencies are commonly discussed. They are the series resonant frequency

$$f_s = 1 \Big/ 2\pi\sqrt{LC_1} \tag{5}$$

the antiresonant frequency

$$f_a = f_s \sqrt{1 + \frac{C_1}{C_o}} = f_s\sqrt{1 + \frac{1}{\rho}} \tag{6}$$

the load resonant frequency

$$f_r = f_s\sqrt{1 + \frac{C_1}{C_o+C_\ell}} = f_s\sqrt{1 + \frac{\alpha}{\rho}} \tag{7}$$

where the load capacitance C_ℓ is connected either in series or in parallel with the resonator terminals [2]. The load resonant frequency is the actual frequency at which the oscillator operates.

Performing the logarithmic differentiation we get:

$$S = \frac{-1}{f_r}\frac{df_r}{dC_\ell} = \frac{C_1}{2(C_o+C_\ell)^2} \Big/ (1 + \frac{C_1}{C_o+C_\ell}) \tag{8}$$

$$= \frac{C_o}{2\rho(C_o+C_\ell)^2} \Big/ (1 + \frac{C_1}{C_o+C_\ell}) \tag{8a}$$

$$= \frac{\alpha^2}{2C_1\rho^2} \Big/ (1 + \frac{\alpha}{\rho}) \tag{8b}$$

At this point it is desirable to consider the magnitude of the demoninator term $(1 + \alpha/\rho)$. The absolute maximum value of α is unity while for quartz the absolute minimum of ρ is around 100. α/ρ is therefore never greater than 1 percent, and is usually more than an order of magnitude smaller than that. One can with an accuracy of the order of 0.1 percent approximate (8) by:

$$S \approx \frac{\alpha^2}{2C_1\rho^2} = \frac{C_o}{2\rho(C_o+C_\ell)^2} \tag{9}$$

Now if S is treated as a crystal parameter subject to specification, the electrode design follows directly from the solution of (9) for C_o

$$C_o^2 + (2C_\ell - 1/2\rho S)\,C_o + C_\ell^2 = 0 \tag{10}$$

$$C_o = 1/4\rho S - C_\ell - \sqrt{1/16\rho^2S^2 - C_\ell/2\rho S} \tag{11}$$

The negative square root is chosen in order to design the smaller of the two electrode sizes which will satisfy the requirement. I have never seen the case where the larger was to be preferred.

The area of an electrode to satisfy this is readily found [4] :

$$A = mCo \times 10^{20}/2.42f_s \tag{12}$$

Measurement

Quite directly from (7), by squaring and rearranging:

$$C_1 = (C_o+C_\ell)\left(\frac{f_r^2 - f_s^2}{f_s^2}\right) \tag{13}$$

When this is combined with (5) we obtain:

$$L = 1/4\pi^2(C_o+C_\ell)(f_r^2 - f_s^2) \tag{14}$$

Furthermore, from (8)

$$S = \frac{C_1}{2(C_o+C_\ell)^2} \Big/ (1 + \frac{C_1}{C_o+C_\ell}) = \frac{C_1}{2(C_o+C_\ell)^2}\frac{f_s^2}{f_r^2}$$

which combines with (13) to yield:

$$S = \frac{(f_r^2 - f_s^2)}{2(C_o+C_\ell)\,f_r^2} \tag{15}$$

Note that the measurement of C_1, L and S require measurement of the same three measurable quantities, the series resonant frequency f_s, the load resonant frequency f_r and the total static capacitance $C_o + C_\ell$. This makes the three characterizations of the resonator exactly equally accessable. From this viewpoint it is difficult to ascribe any primacy to the characterization by motional parameters. Indeed, the case is exactly the opposite, as the motional parameters are pure fictions, being "equivalent" electrical elements in no sense real, while the trim sensitivity is a property of a real quartz crystal by which the equivalent parameters may be explained or rationalized.

These equations are readily used with computers and programmable calculators as they stand. They can be recast in approximations which are good to better than one percent using only first powers of frequency. By following out the kind of argument used in the development of the design equation one can show that the sum of the errors in calling $(f_s+f_r)/f_s$ and $(f_s+f_r)/f_r$ both equal to 2 is the error found negligible there.

Thus (13) becomes:

$$C_1 \approx 2(C_o+C_\ell)\frac{(f_r - f_s)}{f_s} \tag{13a}$$

(14) becomes:

$$L \approx 1/8\pi^2 f_s(C_o+C_\ell)(f_r - f_s) \tag{14a}$$

and (15) becomes:

$$S \approx \frac{f_r - f_s}{(C_o+C_\ell)f_r} \tag{15a}$$

Applications

It was stated at the beginning of the paper that even the most critically specified and designed oscillator resonators rarely have consumed all the degrees of design freedom available. It was thus implied that alternate and even quite disparate seeming designs could possibly be equally acceptable in an established application. One example will be discussed.

Suppose that a compensated oscillator has been designed around a particular resonator and a certain performance achieved. Then for some reason it becomes necessary to locate an alternate source of resonators. The design of the original resonator belongs to the maker. A similar but far from identical resonator is offered from another vendor. The question is: Can this second resonator be used with the existing compensation scheme, and, if so, how?

The answer is found by consideration of Trim Sensitivity. If the two combinations can be made to have the same trim sensitivity then they will react the same to the compensator. Recalling (9) we write:

$$\frac{\alpha^2}{2C_1\,\rho^2} = \frac{\alpha'^2}{2C_1'\,\rho'^2} \qquad (16)$$

In general the two crystals will differ in static capacitance, motional capacitance and in capacitance ratio. These are properties of the isolated resonators, while α is a property of the combination of the crystal with the circuit. We obtain

$$\alpha' = \frac{\rho'}{\rho}\sqrt{\frac{C_1'}{C_1}}\;\alpha \qquad (17)$$

and from (3)

$$C_\ell' = \frac{(1-\alpha')}{\alpha'}\,C_o' \qquad (18)$$

Thus is a new load capacitance found at which the compensation is valid for the second crystal. If this value represents good circuit practice the crystal can be used by calibrating it at the new value of load capacitance and adding or subtracting zero coefficient (NPO) capacitance in the oscillator circuit to achieve the new value.

Now a complication arises. By changing the load capacitance the inflection temperature slope of the temperature-frequency characteristic has been altered [3] . Commonly one says the apparent angle has been changed. Bechmann [5] obtained the value 0.66×10^{-6}/K for the difference of first order temperature coefficient of frequency between antiresonance and series resonance. The rate of change of that temperature coefficient with angle θ is -5.15×10^{-6}/K deg θ. His value for the equivalent angle difference between series and antiresonance is thus 7.7 minutes. This difference in apparent angle is linear with frequency in the interval between these two limiting frequencies. Changing the load capacitance, by moving the frequency between these extremes, moves the apparent angle.

Two options are open. Angle adjustment in production allows the effect of the change of load capacitance to be cancelled. The other option is explained again by Trim Sensitivity.

The product of Trim Sensitivity and temperature rate of change of capacitance is a temperature coefficient of frequency. The temperature rate of change of load capacitance is the product of load capacitance and temperature coefficient of load capacitance. Therefore:

$$\Delta T(f_r) = -C_\ell\, S\Delta T(C_\ell) \qquad (19)$$

This is an incremental temperature coefficient of frequency. The change in slope of the temperature-frequency characteristic can be compensated by changing the temperature characteristic of C_ℓ. Thus:

$$\Delta T(C_\ell) = -\Delta T(f_r)/C_\ell S \qquad (20)$$

By the use of other than zero coefficient capacitors in establishing the new load capacitance the consequence of the change of load capacitance can be negated.

Note that these are actually two independent applications of the concept of Trim Sensitivity. Of great utility is the fact that the temperature characteristic of the static portion of load capacitance can be adjusted to compensate the effect of cutting tolerances among the crystals of a production, allowing the compensator profile to be standardized. This is much less costly than having the temperature coefficient of the static C_ℓ be standardized and the compensation profile be made peculiar to the individual resonators.

Notes

Capacitance ratio The capacitance ratio is a measure of the electromechanical coupling of the resonator. This is a function not only of the orientation of the plate, but also of its contour, the dimensions of the electroded area and the mass loading. Even very similar appearing resonators of the simplest design made in different shops will display differing values of capacitance ratio because of subtle differences in the parallelism of surfaces resulting from small differences in shop practices. AT-cut resonators built of nominally uncontoured wafers normally display capacitance ratios between about 185 and 210 on the fundamental, while contoured resonators can have ratios to about 1000. Consistent practices will yield consistent results, so monitoring capacitance ratio or Trim Sensitivity provides a convenient way of monitoring Lap Room practices.

Capacitance ratio is found using (7)

$$\rho = \frac{f_s^2 \ \alpha}{f_r^2 - f_s^2} = \frac{f_s^2 \ C_o}{(f_1^2 - f_s^2)(C_o + C_\ell)} \qquad (21)$$

Ideological battles rage over the definition of C_o, whether C_o should be considered to change or to stay constant if the resonator element is repackaged. The question has to do with how one handles the stray holder capacitance. If it is treated as part of the outside world it is included in C_ℓ and one value of C_o (hence ρ) is found. If it is treated as part of the resonator then one finds a different value of C_o and a different value of ρ. I find it easier to think clearly in this question as if the holder is part of the outside world, as the interpretation of the stray capacitance as part of the load is unambiguous, C_o and ρ remaining constant while the grounding of the envelope in the other view causes a change in C_o and ρ. In any case consistency is necessary. Where $(C_o + C_\ell)$ is to be used the result is the same in either case.

Measurement The method of measurement is not of direct interest in the discussion of Trim Sensitivity. The various readings of capacitance and frequency needed to be measured have been measured over the years in a variety of ways. Indeed, to make a very good determination of Trim Sensitivity it is not actually necessary to measure the series resonance and load resonance frequencies at all. One can find the Trim Sensitivity of a resonator at (say) 20 pf by measuring the frequency at 19.5 and 20.5 pf. The difference is the Trim in Hz/pf and the Trim Sensitivity in ppM/pf is just this divided by the frequency in MHz. This has certain attractions in specialized test equipment, though switching exactly 1pf reliably is extremely difficult. The number of measurements needed is the same.

By far the most convenient instrument on which to make all of the measurements required for the approach of this paper is the Saunders Model 100 HF transistorized crystal impedance meter on which all the measurements needed are made in a single setup. With this instrument the crystal envelope should not be grounded. This implies a treatment of C_o different from that described above. Consistency is still possible, however.

Conclusion

The concept of Trim Sensitivity facilitates discussion of resonator behavior under conditions of varying load capacitance. It allows the consideration of design degrees of freedom previously inaccessible and offers conceptual means to simplify complex problems of design of compensated and modulated oscillators. Convenient measurement techniques and design equations make this characterization accessible as well as instructive.

References

[1] F.W. Noble, "Variable Frequency Crystal Oscillators", Proc IEEE, Vol 54, No. 12, pp 1976-78, December 1966.

[2] A. Ballato, "The Effect of Load Capacitors on the Frequency of Quartz Crystals", ECOM-2617, June 1965, AD-621357.

[3] A. Ballato, "Frequency - Temperature-Load Capacitance Behavior of Resonators for TXCO Application" IEEE Trans Sonics and Ultrasonics, Vol SU-25, No. 4 pp 190, 191, July 1978

[4] R.A. Sykes in "Information Bulletin on Quartz Crystal Units" ASESA 52-9, August 1952 Appendix I, p 15.

[5] R. Bechmann, "Influence of the Order of Overtone on the Temperature Coefficient of Frequency of AT-Type Quartz Resonators", Proc IRE Vol 43 No. 11 pp 1667-8, November 1955.

NEW METAL ENCLOSURES FOR RESISTANCE WELDING DEVELOPED TO MEET MIL-SPECIFICATIONS

Dieter Fuchs and Klaus H. Mücke

Jenaer Glaswerk Schott & Gen., Landshut

Abstract

Metal enclosures for resistance welding which are electroless nickel plated do not meet the MIL-Specifications with regard to solderability and corrosion resistance. These problems can be easily solved by tin-plating of the sealed crystal units. A tin-plated crystal unit will withstand both solderability test of the flying leads and salt spray test and can be performed in just one economic barrel tin-plating process.

After long-term aging of tin-plated crystal units at elevated temperatures a relatively high negative frequency shift due to mass loading of the crystal blank has been observed when using common enclosure components. Extensive mass spectrometric investigations have shown a formation of water vapor inside the enclosure after aging. This can be explained by the permeation of hydrogen into the enclosure which is generated during the pickling and plating processes and its reaction with residues of oxygen and / or oxides.

For high reliable crystals adequate enclosures have been developed which prevent the permeation of hydrogen by applying certain metallic layers as a thin overall coating on the metal surfaces of the enclosure components. Enclosures treated this way hardly show any frequency shift after aging.

Introduction

It is a well-known fact, that metal enclosures for resistance welding made out of cold rolled steel which are electroless nickel plated, do not meet the MIL-Specifications with regard to solderability and corrosion resistance. Nickel plated surfaces show a very poor solderability and can be tinned and soldered satisfactorily by using activated fluxes only. Nickel plated steel also tends to corrode and rust when subjected to a salt spray test due to imperfections within the nickel layer. Both problems can be easily solved by tin-plating of the exposed surfaces of the sealed crystal unit. A tin plated crystal unit will withstand both solderability test of the flying leads and salt spray test and can be performed in just one economic barrel tin-plating process. An overall tin-plating of the sealed crystal unit has also the advantage of covering and protecting the weld seam. For this final tin-plating operation dull tin-plating should have priority over a bright tin-plating because dull tin-plating shows, according to our experience, a better solderability especially after long-term exposure at elevated temperatures. Considering the tendency to dentritic growth of tin on the glass bead a dull tin-plating with a tin-lead alloy should have preference.

Since the introduction of resistance weld crystal enclosures some years ago a variety of crystal problems occured, some of them were specific for resistance weld enclosures and this sealing technology. In a close collaboration with several crystal manufacturers all these problems could be solved. One of the most serious problems is the shift of the resonance frequency during and after sealing of the crystal enclosure. Two different kinds of frequency shift can be observed:

1. Positive frequency shift, i.e. an increase of the resonance frequency
2. Negative frequency shift, i.e. a decrease of the resonance frequency

Positive Frequency Shift

The most common reason for a positive frequency shift is the relief of mechanical stresses on the crystal transferred from the crystal mounts during a long-term aging at elevated temperatures. These stresses might be caused either by the mounts or by a deformation of the crystal holder during the welding process. This problem can be easily solved by avoiding any deformation of the crystal holder, by choosing an adequate mount material and mount design. Relatively stiff and rigid crystal mounts should be pre-aged at elevated temperatures for a stress relief prior to the final frequency trimming.

Negative Frequency Shift

Considering the negative frequency shift, normally due to mass loading of the crystal blank, two phenomena have to be considered.

1. Primary frequency shift to observe immediately

after sealing of the crystal enclosure

2. Secondary frequency shift to be observed only after long-term aging at elevated temperatures

Primary Frequency Shift

The primary frequency shift is normally caused by vapor adsorption on the crystal blank. Water vapor might have penetrated leaks in the glass-to-metal seal or in the weld joint between crystal holder and can. However these two possible sources for leaks with a subsequent frequency shift can be neglected if the advanced projection welding technology using a capacitor discharge welding equipment is applied and reliable compression glass-to-metal seals for the crystal holders are used.

A further possible reason for the primary frequency shift can be the condensation of lubricant residues, which are incorporated in the surface especially of the cans during the stamping process. These residues can be liberated and evaporated by the thermal load of the welding process and will be adsorbed on the crystal blank. This effect is considerably diminished by applying the projection welding technology with a reduced thermal impact load. As a further improvement specially degassed enclosure components both bases and cans can be supplied to avoid any evaporation of lubricant residues.

Secondary Frequency Shift

To meet the requirements with regard to solderability and corrosion resistance an overall tin-plating of the sealed crystal unit was recommended in the past. The results have been satisfying in every respect except the stability of the resonance frequency in continous operation and after aging at elevated temperatures. Under these conditions a remarkable negative frequency shift, the so-called secondary frequency shift has been observed.

With a 4 MHz quartz crystal resonator mounted in a resistance welded HC 18 enclosure and tin plated after sealing the resonance frequency decreased by about 20 ppm after aging at a temperature of 105 °C for 150 hours (Fig. 1, curve uncoated). After aging for a longer period the negative frequency shift will even be worse as saturation has not been reached completely after 150 hours. It was suspected first that water vapor penetrated small leaks within the glass-to-metal seal or the weld joint, but leakage tests with an extremely sensitive helium detector and with radioactive tracing gases showed no evidence of leaks. Furthermore unplated crystal units did not show any secondary frequency shift. Also no significant change in the resonance frequency was detected immediately after the tin-plating process. The significant frequency shift only appeared after aging at elevated temperatures. The frequency shift was also reversible when the enclosures were opened in a dry atmosphere. Therefore it was suspected that the composition of the protective gas or vacuum within the tin plated enclosures has been changed during temperature storage.

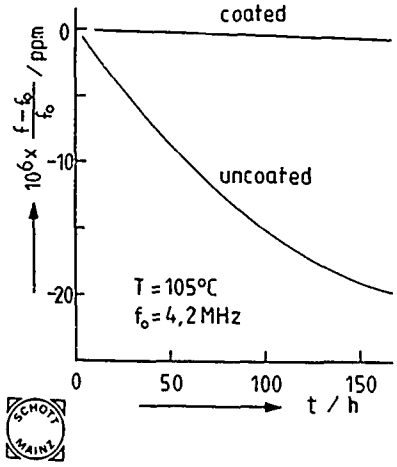

Fig. 1

Extensive investigations by means of a special mass spectrometer have shown significant differences in the composition of the residual gas in the enclosures. The first row of figure 2 represents the gas composition of the protective gas inside a resistance welded crystal unit immediately after sealing.

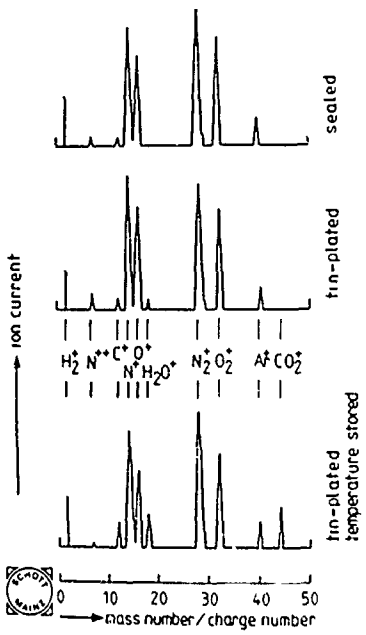

Fig. 2

The major gas components are hydrogen, nitrogen, oxygen and argon (protective gas: dry air). In the second row the analysis of the residual gas after tin-plating shows already a small amount of water. After storage at elevated temperatures, shown in the third row, the composition of the residual gas differs significantly from the original composition of the residual gas. Both the carbon-dioxide and the water vapor content increased considerably which led to a decrease in the oxygen content. As the hydrogen content did not change significantly, hydrogen must have penetrated from the outside of the enclosure or be liberated from the metallic components of the enclosure during the temperature storage. The hydrogen needed to form water vapor may come from the cleaning processes prior to the tin-plating (e.g. pickling in acids or electrolytic degreasing) during which atomic hydrogen is generated which diffuses into the walls of the enclosure. This effect is very pronounced with steel and nickel. Additionally atomic hydrogen is developed during the tin-plating process when the enclosure acts as cathode. This hydrogen will form water causing the negative frequency shift by mass loading due to water vapor adsorption. It is still unknown which process of hydrogen formation dominates and how water vapor is developed. To explain these phenomena the investigations have to be continued.

However the present knowledge is sufficient for basic considerations for the design of an enclosure in which no water vapor is formed which could change the resonance frequency after temperature aging. Extensive investigations have shown that certain nickel based alloys as a thin overall coating of all metallic components of the enclosure prevent both the penetration of hydrogen into the wall of the enclosure as well as its exit from the wall into the interior of the enclosure. This coating is about 50 µm thick and does not interfere the weldability. Figure 1 shows the resonance frequency of a 4 MHz quartz crystal resonator after aging whose enclosure components were coated with the afore mentioned metallic compound prior to tin-plating. The resonance frequency of tin-plated crystal units with coated enclosures hardly show any change in the resonance frequency whereas the resonance frequency drops rapidly with increasing aging time when the enclosures are uncoated before tin-plating. Crystal enclosures with this special metallic coating can be economically barrel tin plated after sealing to protect the enclosures against corrosion and to achieve a perfect solderability of the flying leads without affecting the resonance frequency even after long-term aging. Using these new developed enclosure components the main problems to meet the requirements of the MIL-Specification with crystal units sealed by resistance welding are now solved.

Conclusion

To meet the MIL-Specifications for high reliable crystals the following premises for resistance weld enclosures have to be satisfied:

1. thoroughly degassed enclosure components
2. specially coated metal surfaces of the enclosure components
3. crystal holders with reinforced compression seals
4. adequate crystal mount design and mount material
5. projection welding with a capacitor discharge welding equipment
6. tin plating of the crystal units after sealing, preferable with a tin-lead alloy to avoid tin whiskers on the glass beads.

References

1. D. Fuchs, Proceedings of the 32nd Annual Symposium on Frequency Control, 1978, p. 321 - 325
2. H. Knödler, J.P. Bock and W. Knatz, Glastechnische Berichte 52 (1979) Nr. 2, p. 31 - 42
3. K.H. Mücke, Schott-Information 4/78
4. K.H. Mücke, Solid State Technology, to be published 9/1979

QUARTZ CRYSTAL MEASUREMENTS BY A 'PHASE-AMPLITUDE' METHOD

W.D. Beaver, W.E. Van Loben Sels, M. Wang

Comtec Economation, Inc., Irvine, California

Summary

This paper presents several considerations involved in the development of an automated test system employing the transmission test method recommended by the International Electrotechnical Commission in their Publication 444. It is shown that the method fails when attempting to measure crystals having large values for the ratio of the resistance to the reactance of the total shunt capacitance, which is defined in the paper as α. The paper further details the employment of a capacitance nulling network which is embodied in a completely automatic test system. The automatic test system which employs a microprocessor CPU is discussed and measurement data is presented. Measurement data is shown for crystals measured over the range from 10 MHz to 183 MHz. These measurements show the excellent repeatability of standard deviations on the order of part per 10^8 for frequency and less than 0.5% for motional parameters.

Introduction

Over the past few years a large number of papers have been presented which give different methods for making passive measurements on quartz crystals. These methods include the network analyzers - parameter method[1], the balanced bridge method[2, 3, 4] and the zero phase PI - network technique[5, 6, 7, 8] as described in International Electrotechnical Commission, Publication 444. This paper deals with the zero phase, PI - network method, and its application to higher frequency crystals, and certain aspects of the development of an automatic test system to facilitate the measurement of the resonant frequency and motional parameters of quartz crystals at temperatures defined over a specific temperature range.

The need for precision automatic testing of quartz crystals has become more pressing as the production volume of tight tolerance crystals has increased. In recent years the channel spacing for point to point radio communication has been reduced from 50 KHz to 25 KHz and in 1980 for some requirements to 12.5 KHz. This places rigid constraints upon the allowed tolerances which the crystals must meet. For example, the temperature variation allowed is $\pm$ 5 ppm maximum over the range from - 20°C to + 70°C. Aging is specified at $\pm$ 2 ppm per year, the frequency adjustment is specified at $\pm$ 5 ppm or better, and the motional parameters must be controlled to within $\pm$ 5%. All crystals employed in these applications must therefore be thoroughly tested. The labor involved in performing these tests without an automatic test system is appreciable and requires a reasonably skilled operator to calibrate the measurement system and perform the tests. The automatic test system to be described contains software which automatically self-calibrates the system and performs the tests without operator support after the initial data has been entered.

Some Fundamental Definitions

At frequencies close to the frequency of the mechanical resonance the electrical equivalent circuit is represented by the two terminal network shown in Figure 1[9]. This circuit consists of a capacitance C_1, inductance L_1, and resistance R_1 in series shunted by the parallel capacitance C_0. Figure 1 also shows curves which represent the magnitude of the impedance of the equivalent electric network ($|Z|$), its resistive component (R_e), its reactive component (X_e) and the reactance X_1 of the series branch. Three frequencies f_m, f_s and f_r are also shown. The frequency f_m is defined as the frequency of the minimum impedance; f_s is the resonant frequency of the series arm; and f_r is the frequency of zero reactance nearest to f_s. It is also worth noting that f_m is also known as the frequency of maximum amplitude and f_r is the so-called zero phase frequency.

We should also note that generally the capacitance C_0 is supplemented by additional shunt capacitance C_s from the fixture being employed by the measurement system.

At this point we shall define a parameter "α" to be equal to the ratio of the motional resistance of the equivalent electrical circuit to the reactance of the shunt capacitance at series resonance. The equation is

$$\alpha = R_1 (2\pi f_s) (C_0 + C_s)$$

In later paragraphs we will make reference to α and discuss how the measurements are influenced by its magnitude.

Also, it is important to review Figure 2, which presents both the measuring circuit and the PI - network recommended in the International Electrotechnical Commission, Publication 444. The zero phase method recommended in that publication has been discussed in many papers including those referenced and needs not to be repeated in this article. The method is recommended for use at frequencies up to 125 MHz, but it is at these higher frequencies that considerable care must be exercised in the interpretation of the measurement data. This is largely because of the larger value of α for higher overtone crystals at higher frequencies.

Use of Transmission Method at Higher Frequencies

Difficulties are readily apparent when the recommended method is employed and higher frequencies under conditions when the value of α is large. If we analyze the PI - network containing the quartz resonator and express the transmission amplitude and phase in terms of α we can then plot the amplitude and phase as a function of frequency for different values of α.

Figure 3 shows the relative amplitude of the transmitted signal about the series resonant frequency. In this plot the abscissa is frequency dimensioned in half - 3dB bandwidths and the ordinate is normalized amplitude. Five plots are shown for values of α ranging from 0 to .8. The curves have been normalized so that the maximum amplitude of each curve is 100. The important thing to note is that the frequency of maximum amplitude is decreasing and the shape of the resonance curves becomes more dissymmetrical as the value of α increases.

Figure 4 shows six plots of the transmission phase as a function of frequency for values of α ranging from 0 to 1. In this figure the abscissa is frequency dimensioned in half - 3dB bandwidths and the ordinate is in degrees of phase. Several things are illustrated in this figure. First, we see that for small values of α the frequency where the phase is zero is increasing for increasing values of α. Also, we see that for certain values of α the transmission phase no longer has a zero phase frequency within the 3dB bandwidth of the series resonant frequency. With the PI - network shown in Figure 2, the limiting value of α is 0.5. For values of α above this, no zero phase frequency will occur.

Several examples serve to put this into perspective. For example, a 15 MHz crystal with a 12 Ω resistance and a $C_0 + C_s$ of 5 pf will have an α of .0057 for the fundamental mode resonance, whereas the same crystal measured on 7th overtone mode has an α of .142. Another example is that of a filter crystal having a series resistance of 156 Ω on 5th overtone at 120 MHz and a total parallel capacitance of 4.6 pf. This crystal has an α of about 0.55 and would therefore not exhibit a zero phase frequency, even though it is well within the applicable frequency range of the recommended method.

It is also obvious, that for smaller values of α, considerable interpretation is necessary to effectively use the measured data and that the method must be augmented in some way if it is to be applied to measure crystals for which α is greater than 0.2.

Means of Using the IEC Zero Phase Measurement Method for Higher Frequency Crystals

Two ways of utilizing the IEC method to allow for the determination of the series resonant frequency and the motional parameters involve on one hand computing the parameters after certain frequency and amplitude measurements are made and on the other hand minimizing the value of α by employing a capacitance nulling circuit across the crystal.

Figure 5 presents an algorithm which can be employed for values of $\alpha \leq .2$. The steps consist of measuring the zero phase frequency, the value of the maximum amplitude, measuring the frequencies of the upper and lower - 3dB level on the amplitude response. From these measurements the constant K is computed and then α. Once α is computed F_s, R_1 and L_1 may be computed from the equations shown in Figure 5.

As mentioned as an alternative to this is the incorporation of a network to null out the capacitance which shunts the series motional arm of the equivalent circuit[10]. This is accomplished by employing the network shown in Figure 6. The inductance is placed directly across the crystal resonator and tuning is performed by biasing the varacter diodes. As this effective parallel capacitance is decreased, the values of f_m and f_r converge to f_s. In this case, the measurement of the zero phase frequency suffices.

For example, for the 183.2 MHz crystal whose measurement data is shown in Figure 11, the effective parallel capacitance is reduced by the nulling circuit to about 0.03 pf which results in an α of 0.0028. The difference frequency between f_s and f_r related to this small α value is 15.12 Hz or 8.26 pp 10^8.

Application of Microprocessor Control Techniques to the Measurement Process

For several reasons the passive zero phase measurement method lends itself to computer implementation. The block diagram of such an embodiment is shown in Figure 7. This system, Comtec Model 770204-VHF, consists of the following components:

Microprocessor - CPU with PROM and RAM Memory, Data I/O Interface,
Keyboard for data entry,
CRT Display for system - operator interaction,
Magnetic Disc Unit,
Printer,
RS-232 Interface Output Buss,
2 Frequency Synthesizers,
Measurement Unit, and
2 Ambient Temperature Test Chambers with Mechanical Transport Fixtures and Temperature Controls

Figure 8 shows the block diagram of the measurement unit for Model 770204-VHF. The two frequency synthesizer units employ the same frequency standard which is controlled by the computer via a BCD programmable interface. One frequency synthesizer unit drives the PI - network containing the crystal being tested, and the other frequency synthesizer unit serves as a tracking reference frequency used to establish a 25 KHz intermediate frequency.

The test and reference signals are processed by squaring amplifiers and trigger circuits and applied to a phase to voltage converter. The purpose of this circuit is to convert the phase difference between the reference signal and the test signal into a voltage proportional to the magnitude of the phase difference. This difference is returned to the computer in BCD.

The amplitude of the test signal is also monitored and converted to DC before it is fed to the computer in binary code.

The computer also controls the biasing of the varacter diodes in the capacitance nulling circuits. The nulling is performed at a frequency which is 100 KHz below the nominal crystal frequency. The varacters are tuned for a minimum of the test signal.

The major steps in the Automatic Test Sequence are shown in Figure 9. The steps shown allow for the measurement of frequency, R_1, L_1 or C_1 and C_0. The operator can specify which of the parameters are to be measured.

System Calibration

As mentioned earlier, the system is self-calibrating with the calibration taking place at each temperature so that variations with temperature are compensated for. The initial calibration takes place with the crystal holder in the "home position". In this arrangement the measurement head is in an open circuit condition. The computer proceeds to null out the capacitance at the nominal frequencies of each frequency group of crystals which are to be measured. The related data is stored in memory. The crystal holder is then positioned so that the shorting bar located in the 00 position of the crystal holder is across the jaws of the measurement head, thus establishing a short circuit condition. Under this condition the "zero phase" condition and the reference amplitude is determined for each frequency group and these are stored in memory. The crystal holder is then indexed sequentially from crystal to crystal and the value of the pre-nulled amplitude is measured and stored. The frequency is then off-set to 100 KHz below the nominal frequency of each group and the biasing voltage equivalent to the nulled condition is determined and stored. By utilizing this type of calibration many system variables can be compensated for to allow for very precise crystal measurements.

Examples of Measurement Data

Figures 10 and 11 show tabulations of data for crystals ranging from 10 MHz to 183 MHz.

In Figure 10 is shown the printout from a test run in which crystals having frequencies ranging from 10 MHz to 90.42 MHz were tested. A major advantage of this test system is that lots of crystals having widely different frequencies may be tested simultaneously.

The input data is shown at the top of the listing. This includes the date, the shift, an operator identification, the desired print-out mode, the oven which is being used, the temperature profile desired (up to 100 sets of temperatures may be stored on magnetic disk), the test mode (designates which parameters are to be measured), the frequency range, and the crystal code (up to 1,000 different sets of crystal specifications may be stored on the magnetic disk). The operator then inputs the nominal frequency of each frequency group entering the location (1 to 99) of the last unit for each group. The print-out of data shows the entered nominal frequency, the measured frequency, the resistance and the motional inductance.

In Figure 11 is shown the repeated measurement of four different frequency crystals having frequencies of 110 MHz, 154 MHz, 176 MHz and 183 MHz. An analysis of this data to determine the mean of each set of measurements and the standard deviation is given below. The standard deviation is also given in parts per 10^8 for frequency as well as in Hz and percent for both resistance and inductance as well as ohms and milli Henries respectively.

Data Analysis

Unit	Mean Frequency (Hz)	Standard Deviation (Hz)	Standard Deviation ($pp10^8$)
A	110,002,093.8	2.48	2.26
B	154,001,324.3	3.89	2.52
C	176,797,950.8	13.02	7.36
D	183,199,435.9	8.93	4.87

Unit	Mean Resistance (Ω)	Standard Deviation (Ω)	Standard Deviation (%)
A	39.32	.063	0.16
B	77.17	.094	0.12
C	207.88	.162	0.08
D	80.90	.17	0.21

Unit	Mean Inductance (mH)	Standard Deviation (mH)	Standard Deviation (%)
A	4.197	.0067	0.16
B	4.847	.0094	0.19
C	1.829	.0057	0.31
D	2.514	.005	0.20

An interesting point is that the 176 MHz crystal has a Q of only 10,000 and an α of about 1.1. This crystal would not have a zero phase frequency within the 3dB bandwidth of the series resonant frequency. It is only possible to measure such crystals when the shunt capacity is nu'led out, which is accomplished automatically with this system.

Mechanical Construction

An important part of any test system is the mechanical construction, which in this system includes the automatic positioning of the crystals and the construction of the measurement head. In the development of this automatic test system the early measurement heads were produced employing the rod and disk resistors referred to in the IEC Publication 444. However, these were found to be less than satisfactory. The major problem was that the parts would not remain stable after repeated temperature cycling. The rod and disk resistor were fitted into the heads using a variety of methods employing solder and a number of different types of conductive epoxies. None of these methods proved to be successful in achieving the desired results. For this reason, Comtec developed a thickfilm PI - network. The three resistor disk - rod - disk arrangement is replaced by a symmetrical thickfilm arrangement of five resistors on a ceramic substrate. When the circuits are placed into the heads, their values coincide with those of the rod and disk version.

The construction of the measurement head is shown in Figure 12 in three photographs. Figure 12-A shows a breakdown of it into its different components. The knife - edge contacts are attached directly to the ceramic substrate. This results in a very short path length from the contact to the crystal to each PI section. Figure 12-C shows the head with the capacitance nulling head in place. Figure 13 shows a diagram of how the contact to the crystal is made. The crystals are placed into a holder whose construction is shown in Figure 14. This holder will accommodate 99 crystals. The 0 position is reserved for either a shorting bar or a reference calibration resistor. However, the system, Model 770204-VHF, can test 198 crystals simultanecusly since it comes with two test chambers. While one chamber is stabilizing at a temperature, the system is making measurements on crystals in the other chamber.

Figure 15 shows a photograph of the test chamber door containing the transport fixturing, the head mechanism and the crystal holder. Rigid coaxial cable is employed between the measuring head and the hetrodyne circuitry mounted on the outside of the door. Figure 16 shows a close-up of the measurement head making contact to the crystals.

Conclusion

A development program has been carried out to explore and overcome the difficulties in the application of the transmission measurement technique and extend its range to frequencies at and above 200 MHz.

Comtec has completed the development of a completely automatic test system capable of measuring the frequency and the parameters of the equivalent electrical circuit, both at room temperatures and at temperatures over a broad range. The total operational system has been developed and system computers have been in field operation for more than one year. Preliminary lower limit estimates of the absolute accuracy of the resonance frequency, resistance and motional inductance are $\pm$ 2 $pp10^7$ in the range up to 50 MHz, $\pm$ 5 $pp10^7$ up to 100 MHz, $\pm$ 1 ppm up to 200 MHz and $\pm$ 2% up to 100 MHz and $\pm$ 4% up to 200 MHz for the motional parameters.

The authors wish also to thank Mr. H.O. Lewis and Mr. M.S. Voelker for their contributions to the development and design effort.

References

1. Pustarfi, H.S. and W.L. Smith, "An Automatic Crystal Measurement System", Proc. 27th Freq. Control Symposium, U.S.A.E.C., pp 63-72, 1973.

2. Ballato, A., P. Blomster and E. Hafner, "Quartz Crystal Measurements", R. & D. Technical Report ECOM-3374, U.S.A.E.C., December 1970.

3. Hafner, E. and W.J. Riley, "Implementation of Bridge Measurement Techniques for Quartz

Crystal Parameters", Proc. 30th Freq. Control Symposium, pp 92-102, May 1976.

4. Malinowski, G. and E. Hafner, "Automatic Microcircuit Bridge for Measurement on Quartz Crystal Units", Proc. 32nd Freq. Control Symposium, pp 354-364, 1978.

5. Grenier, R. P., "Technique for Crystal Resonance Measurements based on Phase Detection in a Transmission Type Measurement System", Proc. 22nd Annual Symposium on Freq. Control, pp 259-268, 1968.

6. Frerking, M. E., "Vector Voltmeter Crystal Measurement System", Proc. 23rd Annual Symposium on Freq. Control, pp 93-101, 1969.

7. Franx, C., "On Precision Measurements of Frequency and Resistance of Quartz Crystal Units", Proc. 23rd Annual Symposium on Freq. Control, pp 102-110, 1969.

8. Franx, C., "A Report on I.E.C. Technical Committee TC 49", Proc. 24th Annual Symposium on Freq. Control, pp 172-176, 1970.

9. "Standard Definitions and Methods of Measurement for Piezoelectric Vibrator", IEEE Std. No. 177, May 1966.

10. Fischer, R. and L. Schulzke, "Extending the Frequency Range of the Transmission Line Method for the Measurement of Quartz Crystals up to 250 MHz", Proc. 31st Freq. Control Symposium, pp 96-101, 1977.

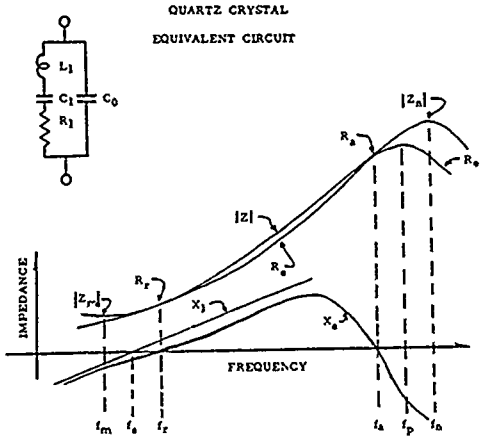

f_m = frequency at minimum impedance Z_m
f_e = series resonant frequency ($X_j = 0$)
f_r = frequency of zero reactance
R_r = Resistance at f_r
f_a = Anti-resonant frequency (zero susceptance)
f_p = Parallel resonant frequency
f_n = frequency at maximum impedance (Z_n)
R_a = Resistance at f_a

FIGURE 1

IEC Recommended Measuring Circuit and PI - Network

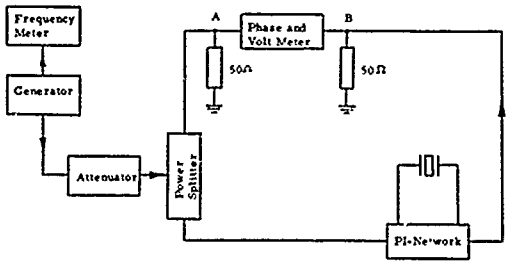

(a) IEC RECOMMENDED MEASURING CIRCUIT

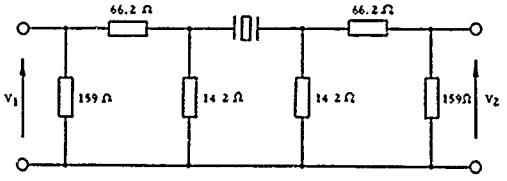

(b) IEC RECOMMENDED PI-NETWORK

FIGURE 2

Transmission Amplitude versus Frequency for PI - Network Containing Crystals

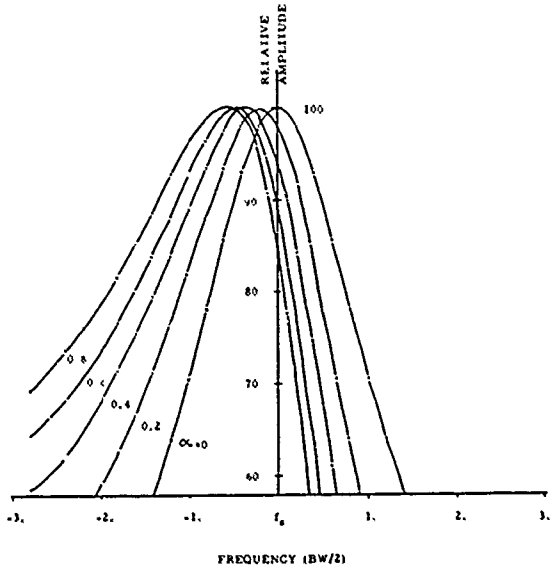

FIGURE 3

Transmission Phase versus Frequency for PI - Network Containing Crystals

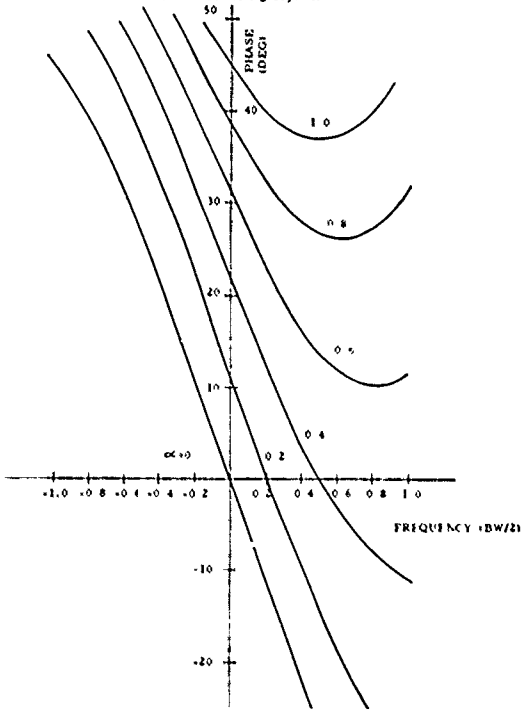

FIGURE 4

Algorithm Involving α for Computing Crystal Parameters

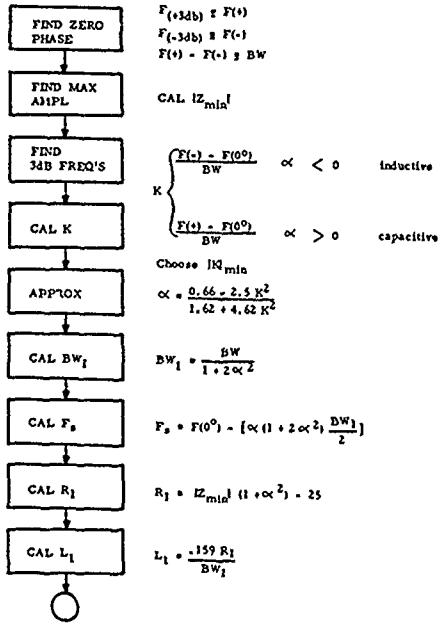

FIGURE 5

Capacitance Nulling Network with Performance Data

Crystal and PI - Network

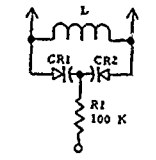

CR1 + CR2: 10 - 40 pf

L (100 - 160 MHz): 0.1 uh

L (140 - 200 MHz) .05 uh

PERFORMANCE OF NULLING NETWORK

Frequency (MHz)	Ref. Level (Volt)	Null Level (Volt)	Ratio	Equiv. R (Ω)	Ratio to 100Ω	Max. Null (dB)
100	3.55	.025	140	3,500	35	30
120	3.53	.016	220	5,500	35	35
140	3.49	.015	230	5,700	57	35
150	3.51	.008	440	11,000	110	41
160	4.31	.005	860	21,000	210	46
180	4.92	.005	980	25,000	250	48
200	4.39	.015	290	7,300	73	37

FIGURE 6

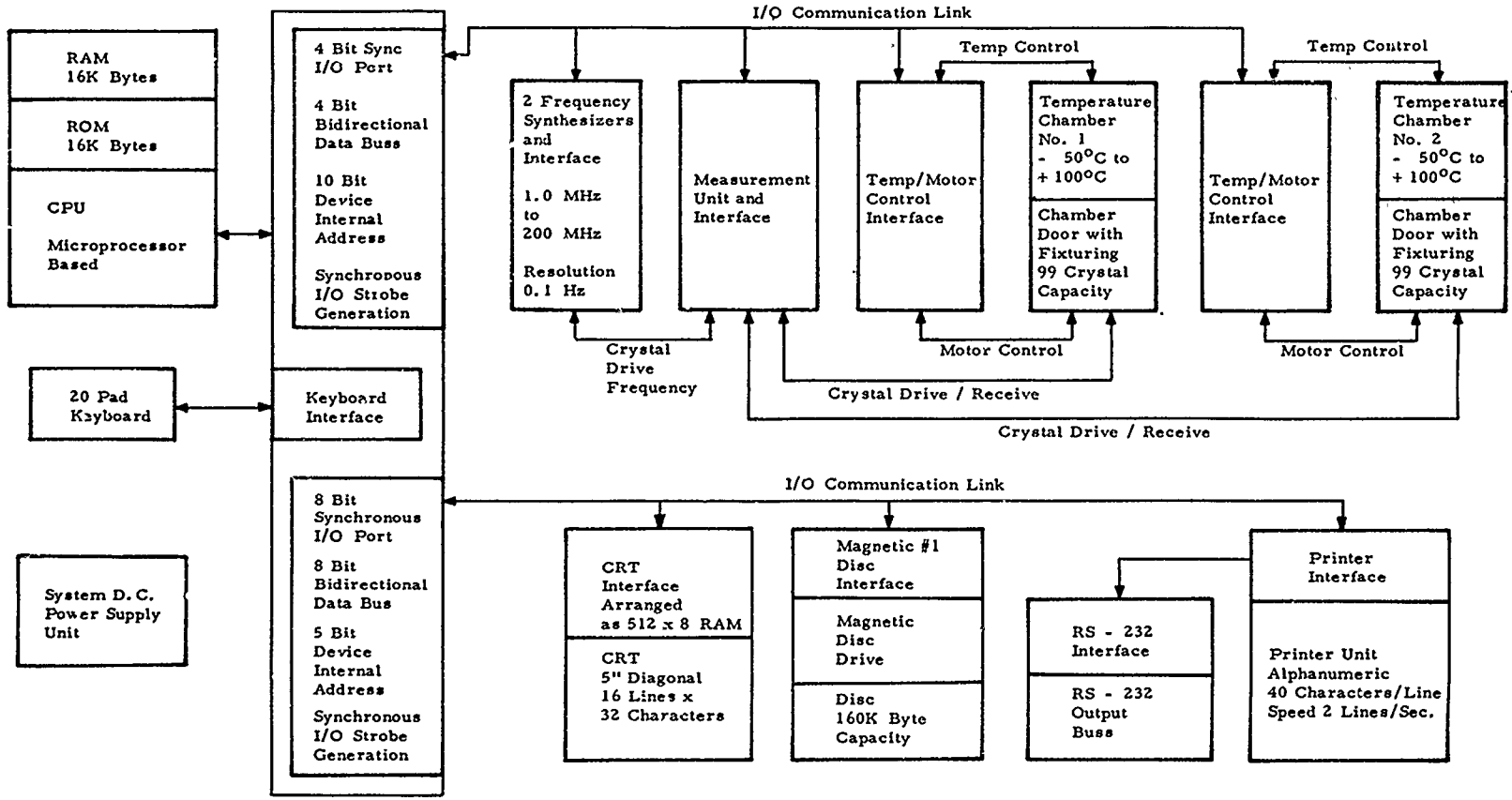

BLOCK DIAGRAM

QUARTZ CRYSTAL TEST SYSTEM

COMTEC MODEL 770204-VHF

FIGURE 7

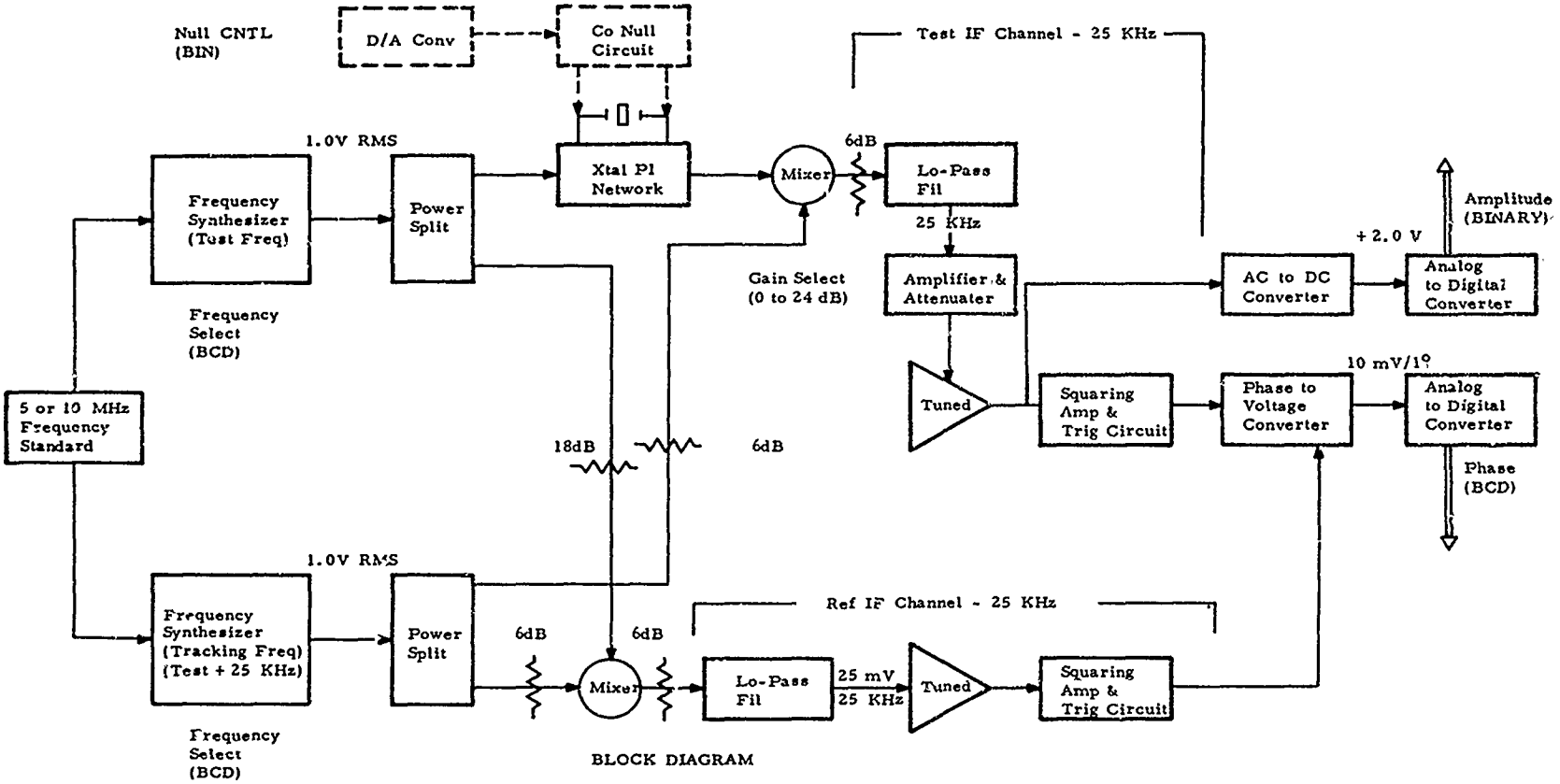

BLOCK DIAGRAM

MEASUREMENT UNIT

COMTEC MODEL 770204-VHF

FIGURE 8

MAJOR STEPS IN

AUTOMATIC TEST SEQUENCE

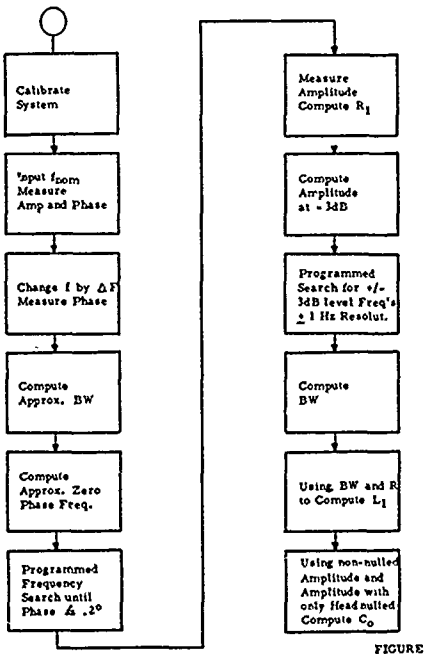

FIGURE 9

MEASUREMENT DATA

```
DATE 52179
SHFT 1              OVEN CODE END
OPER B                        UNIT
PRNT 2               1    101  09
OVEN 1
PRFL 01
MODE 3 RANGE 2

RANGE:1=1-10
MHZ   2=8-160
      3=150-200


 10000000  01
 19575000  02
 44000000  03
 90420000  04
 55000000  05
 51000000  06
 82000000  07
 53000000  08
 66000000  09


52179 +90 1
101    FN-HZ       FX-HZ   R-OHM  L-MHY S
:01 010000000  009995071 +008.6  08.59
02 019575000  019575153 +002.6  02.12
03 044000000  044000035 +017.6  05.50
04 090420000  090419806 +040.8  04.16
05 055000000  054999901 +009.8  03.07
06 051000000  050999549 +013.8  04.43
07 082000000  081998381 +035.5  04.33
08 053000000  052999770 +007.3  15.45
09 066000000  065999840 +032.8  08.37
52179 +25 1
```

FIGURE 10

```
DATE 52179
SHFT 1          OVEN CODE END
OPER A                    UNIT
PRNT 2           1    102  20
OVEN 1
PRFL 01
MODE 3 RANGE 2

RANGE:1=1-10
MHZ   2=8-160
      3=150-200


110000000  10
154000000  20
```

```
52179 +90 1
 02    FN-HZ       FX-HZ  R-OHM  L-MH\ S
:01 110000000  110002051 +037.1  04.85
02 110000000  110002094 +039.4  04.19
03 110000000  110002095 +039.3  04.20
04 110000000  110002095 +039.3  04.20
05 110000000  110002099 +039.3  04.21
06 110000000  110002092 +039.3  04.20
07 110000000  110002094 +039.4  04.19
08 110000000  110002097 +039.3  04.20
09 110000000  110002097 +039.4  04.19
10 110000000  110002090 +039.2  04.19
11 154000000  154001329 +077.1  04.83
12 154000000  154001320 +077.1  04.85
13 154000000  154001320 +077.3  04.84
14 154000000  154001320 +077.1  04.86
15 154000000  154001327 +077.1  04.86
16 154000000  154001322 +077.1  04.85
17 154000000  154001[illegible] +077.3  04.84
18 154000000  154001329 +077.3  04.84
19 154000000  154001323 +077.1  04.85
20 154000000  154001329 +077.3  04.84
52179 +25 1
```

```
DATE 52179
SHFT 1          OVEN CODE END
OPER A                    UNIT
PRNT 2           1    102  20
OVEN 1
PRFL 01
MODE 3 RANGE 3

RANGE:1=1-10
MHZ   2=8-160
      3=150-200


 76800000  10
 83200000  20
```

```
52179 +90 1
10     FN-HZ       FX-HZ  R-OHM  L-MH\ S
:01 176800000  176797946 +207.5  01.82
02 176800000  176797918 +207.8  01.82
03 176800000  176797960 +207.8  01.83
04 176800000  176797939 +207.8  01.83
05 176800000  176797951 +208.0  01.83
06 176800000  176797958 +208.0  01.83
07 176800000  176797962 +208.0  01.83
08 176800000  176797950 +208.0  01.83
09 176800000  176797960 +208.0  01.84
10 176800000  176797962 +208.0  01.84
11 183200000  183199457 +080.7  02.51
12 183200000  183199445 +081.2  02.51
13 183200000  183199[illegible] +080.9  02.52
14 183200000  183199[illegible] +081.2  02.51
15 183200000  183199439 +080.9  02.52
16 183200000  183199427 +080.8  02.52
17 183200000  183199432 +080.8  02.51
18 183200000  183199428 +080.8  02.52
19 183200000  183199[illegible] +080.8  02.51
20 183200000  183199435 +080.8  02.52
52179 +25 1
```

MEASUREMENT DATA

FIGURE 11

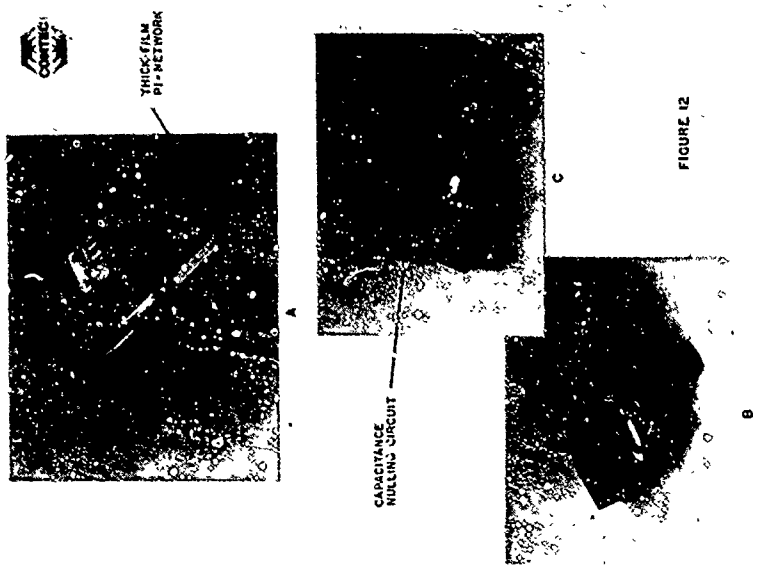

COMTEC MODEL 770204-VHF
MEASUREMENT HEAD

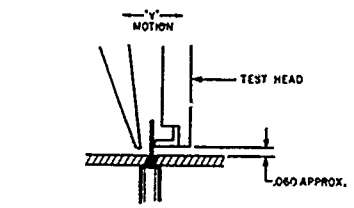

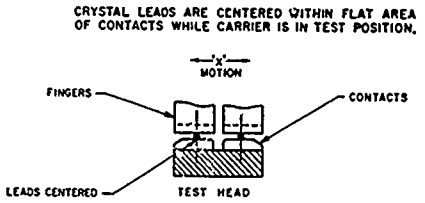

FIGURE 13

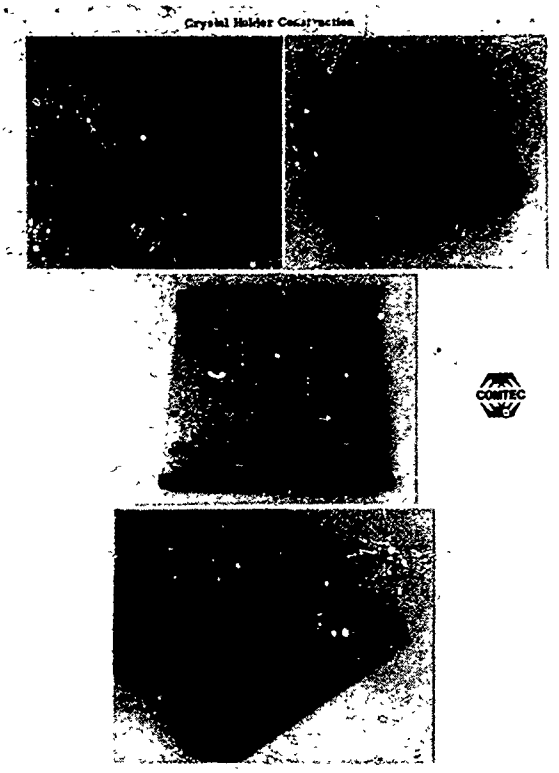

FIGURE 14

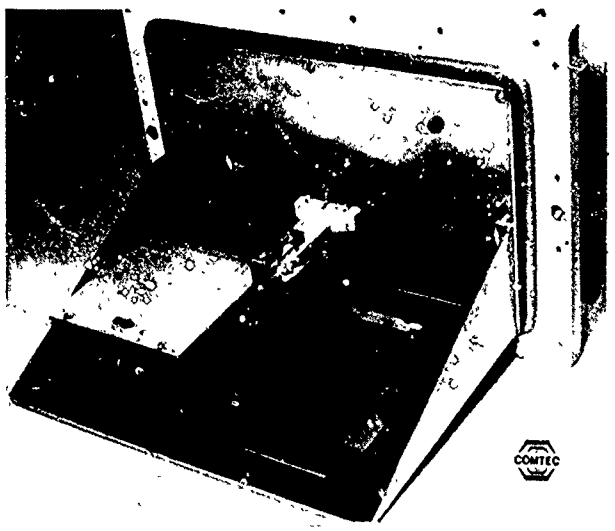

FIGURE 15

Mechanical Arrangement of the Test Fixturing

FIGURE 16

Mechanical Arrangement of the Test Fixturing

AUTOMATIC MEASUREMENT OF PARAMETERS OF VHF QUARTZ CRYSTAL RESONATORS

Y. Tsuzuki, M. Toki, T. Adachi and H. Yanagi

Yokohama National University
Hodogaya-ku, Yokohama 240
Japan

Summary

An automatic precise measurement method of all parameters of VHF quartz crystal units is described. Whole measuring system, including a minicomputer for data processing, has been arranged, and measurements were made on 125MHz and 175MHz crystal units. The results suggest that the system can be a precise measuring method of all parameters of a VHF crystal unit.

Introduction

As VHF quartz crystal resonators take more and more important roles in communication techniques, precise measurement of resonator parameters in VHF range becomes important and efforts have been made in many places.

Electrical characteristics of a resonator in the vicinity of its resonance frequency can usually be represented by equivalent circuit, consisting of $R_1L_1C_1$ series resonance circuit with equivalent parallel capacitance C_0, as shown in Fig. 1. Instead of a set of four parameters: R_1, L_1, C_1 and C_0, another set of parameters is usually used. These are the series resonance frequency f_s, the motional resistance R_1, the motional inductance L_1 and the capacitance ratio $r = C_0/C_1$. In these parameters, f_s is the most important, and R_1 the next. However, as we cannot measure f_s and R_1 directly, zero susceptance frequency f_r and the equivalent resistance R_r at f_r are frequently used as the substitutes. The differences between these parameters are negligibly small when the frequency is relatively low, say, lower than 100MHz. As the relating parameters, quality factor Q and figure of merit $M = Q/r$ are also important. The figure of merit M is relatively small in VHF range, say less than 10 in the frequency range higher than 100MHz. This makes the difference between f_s and f_r, and the difference between R_1 and R_r considerably large.

As measurement methods in VHF range, CI-meter and π-network method are widely in use[1]. These methods are mainly for f_r and R_r measurements. The reference resistor is used as the pure resistance element even in VHF range. It seems that it is very difficult to obtain pure resistance elements in VHF range, and it is, therefore, difficult to evaluate absolute errors of the measurement. However, the reproducibility of the measurement has been established and the methods are useful in manufacturing and inspection processes.

Features of the method in this paper are:

(1) All parameters can be measured without use of reference resistors.

(2) Accuracy as well as reproducibility can be evaluated.

Principle of measurement

This method is basically a kind of transmission method. (Fig. 1)

First, the frequency characteristics of the voltage ratio $A = |V_2/V_1|$ are measured automatically with the equal frequency separation in the vicinity of the resonance frequency. If the effect of the residual susceptance B_L in the load circuit is negligibly small, all parameters of a crystal unit can be determined from the frequency characteristics of the voltage ratio. In VHF range, however, we must take the effect of the residual susceptance into consideration. Therefore, next, the frequency characteristics of the phase difference between V_1 and V_2 are measured around the zero phase frequency with an equal frequency separation, in order to determine the zero phase frequency precisely. The values of crystal parameters and the residual susceptance are determined so that the frequency characteristics calculated from these values give the best agreement with the measured data. Once the evaluation of the residual susceptance is carefully made with several resonators having good performance, the phase difference measurement is not necessary thereafter.

Data processing

The procedure of the data processing method is as follows. First, a set of initial approximate values of the four parameters are determined in a simple manner--by equating f_s to the maximum voltage ratio frequency f_m in Fig. 3, for instance. approximate values of the voltage ratio A are calculated from these initial parameter values and the differences δA between the calculated values of the volt-

age ratio A from the measured data are obtained. Then, correction is made on each parameter so as to reduce the differences δA throughout the frequency range of the data processing. This correction process is repeated until the correction terms of each parameter become satsfactorily small.

The equation for the calculation of the correction terms are derived in the following manner. Let δf_s, δR_1, δL_1 and δr be the correction terms of the initial approximate values of the parameters. If the correction terms are small, the following first order approximation can be used.

$$\delta A \simeq (\partial A/\partial f_s)\delta f_s + (\partial A/\partial R_1)\delta R_1 + (\partial A/\partial L_1)\delta L_1 + (\partial A/\partial r)\delta r \qquad (1)$$

On the basis of the Least Square Method, correction terms, which reduce the differences δA throughout the frequency range of the data processing, are determined so as to minimize the square sum of the resultant deviation in (1):

$$S = \sum_{i=1}^{N} [\, \delta A - (\partial A/\partial f_s)\delta f_s - (\partial A/\partial R_1)\delta R_1 - (\partial A/\partial L_1)\delta L_1 - (\partial A/\partial r)\delta r \,]_i^2, \qquad (2)$$

where N is the number of data used in the data processing. This procedure gives the following equation for the correction terms.

$$\begin{bmatrix} \delta f_s \\ \delta R_1 \\ \delta L_1 \\ \delta r \end{bmatrix} = \begin{bmatrix} \Sigma (\frac{\partial A}{\partial f_s})^2 & \Sigma \frac{\partial A}{\partial f_s}\frac{\partial A}{\partial R_1} & \Sigma \frac{\partial A}{\partial f_s}\frac{\partial A}{\partial L_1} & \Sigma \frac{\partial A}{\partial f_s}\frac{\partial A}{\partial r} \\ \Sigma \frac{\partial A}{\partial R_1}\frac{\partial A}{\partial f_s} & \Sigma (\frac{\partial A}{\partial R_1})^2 & \Sigma \frac{\partial A}{\partial R_1}\frac{\partial A}{\partial L_1} & \Sigma \frac{\partial A}{\partial R_1}\frac{\partial A}{\partial r} \\ \Sigma \frac{\partial A}{\partial L_1}\frac{\partial A}{\partial f_s} & \Sigma \frac{\partial A}{\partial L_1}\frac{\partial A}{\partial R_1} & \Sigma (\frac{\partial A}{\partial L_1})^2 & \Sigma \frac{\partial A}{\partial L_1}\frac{\partial A}{\partial r} \\ \Sigma \frac{\partial A}{\partial r}\frac{\partial A}{\partial f_s} & \Sigma \frac{\partial A}{\partial r}\frac{\partial A}{\partial R_1} & \Sigma \frac{\partial A}{\partial r}\frac{\partial A}{\partial L_1} & \Sigma (\frac{\partial A}{\partial r})^2 \end{bmatrix}^{-1}$$

$$\times \begin{bmatrix} \Sigma\, \delta A \frac{\partial A}{\partial f_s} \\ \Sigma\, \delta A \frac{\partial A}{\partial R_1} \\ \Sigma\, \delta A \frac{\partial A}{\partial L_1} \\ \Sigma\, \delta A \frac{\partial A}{\partial r} \end{bmatrix}, \qquad (3)$$

where the summations are over the whole data used in the data processing. In the frequency range lower than 100MHz, where the figure of merit of a resonator is usually larger than 10, the equations for the correction terms become much simpler[2].

By using the equation (3), the evaluation of the residual susceptance B_L and the determination of all parameter values are made in the following manner. At first, the values of the parameters are determined from the measured voltage ratio characteristics by assuming that the load circuit is a pure resistance element. Then, the zero phase frequency of (V_2/V_1) can be calculated from these parameter values. This frequency differs more or less from the measured one because of the neglect of the residual susceptance in the load circuit. The residual susceptance B_L can be evaluated from the difference between the two frequencies, and all parameter values are re-calculated by taking the existence of B_L into consideration.

Automatic measuring system

Figure 4 shows the diagram of the whole measuring system, including minicomputer for data processing.

The measurement of the voltage transfer ratio is carried out under the control of the System Controller (utilizing microcomputer). The output signal of a Frequency Synthesizer goes through a Low Pass Filter and an Attenuator, and reaches the input of the Transmission Circuit. The input and output voltages go to the Vector Voltmeter, and are converted to 20kHz IF outputs. Then, these 20kHz signals are converted to digital signals by the Digital Level Meter, and stored in a memory in the system controller. For the phase angle measurement, the d.c. output of the phase angle from the vector voltmeter is converted to digital signal, and also stored in the memory. During the entire measurement, the output voltage of the transmission circuit is kept constant by an Automatic Attenuator, that is, the crystal current is kept constant during the measurement to avoid the effect of drive level dependency. After the data measurement, the whole data are transfered to the Minicomputer for data processing. The values of the parameters and other relating informations, such as r.m.s. deviation in simulation, are typed out from the Teletypewriter. In the voltage ratio measurement, the initial calibration of the system is made by using precision attenuators so that the systematic errors produced by the vector voltmeter and the digital level meter becomes as small as possible.

The operation of the system is rather simple. As the initial setting, nominal frequency of the crystal unit is put into the controller from the keyboard. Then, the system controller makes a survey of the resonance curve, and decides the starting frequency and the frequency increment, and automatically starts the measurement.

The transmission circuit used is originally designed by Dr. Koga, and is in wide use in Japan as the precise measuring circuit. The crystal sockets are directly connected to the receptacles for the probe tips of the vector voltmeter. A slight modification was made on the load circuit. That is, an originally attached carbon resistor and a compensating capacitor were replaced by a metal film tip resistor. This load resistor is connected between the output side crystal socket and the grounding metal sheath for the voltmeter probe in the shortest distance so as to make parasitic reactance as small as possible.

Experimental results

Figure 5 shows an example of the printed output of the measuring system. All informations, including measured data and processed results, are listed in it. Important portions of the above results are extracted and shown in Fig. 6. The measured voltage ratio characteristics of a 5th overtone 125MHz crystal unit are shown in (a). The number of actually measured data is twice of the number of points in the figure, and only the even numbered points are plotted in the figure. The data near the parallel resonance frequency, that is, the data on the right side of the vertical broken line in the figure were not used in the data processing. The obtained values of the parameters and also the evaluated value of the residual susceptance in the load impedance in the form of the phase angle are shown in (b). This phase angle is equivalent to the existence of 0.24pF of resultant stray capacitance C_L in parallel with the load resistance R_L, and is a negligibly small value. The distribution of the residual differences between the measured voltage ratio characteristics data and the calculated ones, calculated by using the obtained parameter values, are shown in (c). The r.m.s. deviation σ_A is merely 0.4% and the agreement is very well. This means that the crystal parameters were measured precisely.

Table I shows the measured results on three different crystal units having the resonance frequencies of 125MHz in 5th overtone and 175MHz in 7th overtone. The r.m.s. deviation σ_A of the voltage ratio is less than 0.5% for all resonators. The phase angle of the load impedance were evaluated to be less than about 1 degree for all resonators. From these experimental results up to 175MHz, the measurement errors are less than 1×10^{-7} in f_s and less than 2% in R_1, L_1 and r.

Conclusion

An automatic precise measuring method of all equivalent circuit parameters: f_s, R_1, L_1 and r, and relating parameters such as Q and M of VHF quartz crystal resonators has been developed. Whole measuring system, including a minicomputer for data processing, has been arranged. Experimental results of measurements on 125MHz and 175MHz crystal units suggest the estimated errors are less than 1×10^{-7} in f_s and less than 2% in R_1, L_1 and r.

This method can be used for the measurement in the frequency range higher than 175MHz. However, it is necessary to prepare crystal units having good performances in order to estimate the accuracy of the measurement.

Acknowledgment

The authors wish to acknowledge Fujitsu Limited for the offer of 6800 Microcomputer system for the system controller.

References

[1] E. A. Gerber and R. A. Sykes, "A Quarter Century of Progress in The Theory and Development of Crystals for Frequency Control and Selection", in Proc. 25th Frequency Control Symp., U.S. Army Electronics Command, Fort Monmoth, NJ, 1971, pp. 1 - 45.

[2] Y. Tsuzuki and M. Toki, "Precise Determination of Equivalent Circuit Parameters of Quartz Crystal Resonators", Proc. IEEE, p. 1249 (Proc. Letters), Aug. 1976.

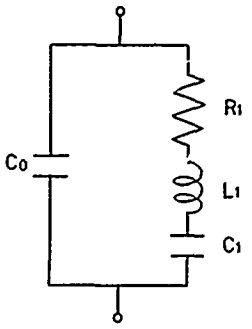

Fig.1 Equivalent Circuit

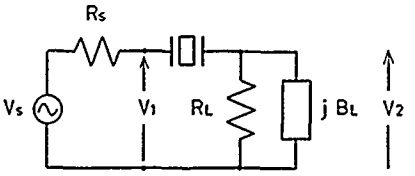

Fig.2 Measuring Circuit

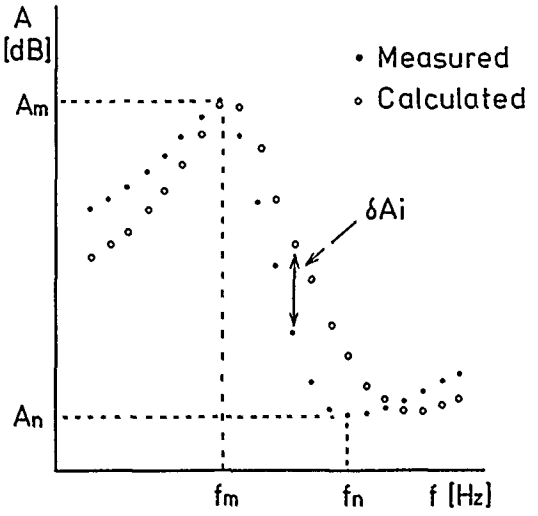

Fig.3 Frequency Characteristics of Voltage Transfer Ratio

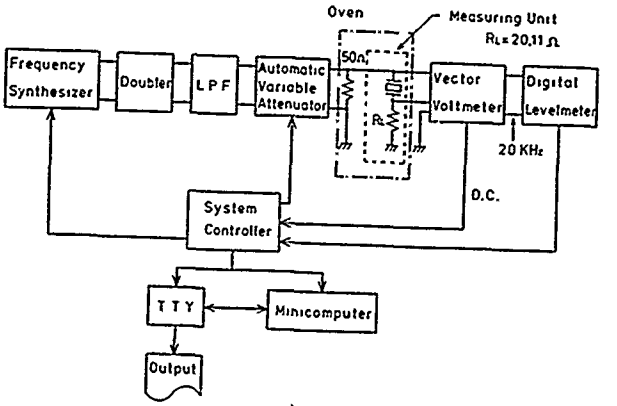

Fig.4 Automatic Measurement System of VHF Quartz Crystal Resonators

```
      *** PRECISE DETERMINATION OF VHF QUARTZ PARAMETERS ***      PDVQ-LSM4

*** CALICRATION-DATA-IDENTIFICATION...MOCH7700
*** PLEASE KEY IN FOLLOWING DATA ***
   YYMM    DDIT    FREQ.   QUARTZ  NUMBER   A.S.M OBSERVER FR-METER ANY-COMMENT
   1979    5/14    125M                              T.A.K  YTL0

*** PLEASE KEY IN ***      FR                          RL
                        62500349.0                    20.11

*** PLEASE START AUTO DATA LOGGER ***
        START-FREQ= 6249700      DELTA-F= 10      DATA-NO=   78
  1471 1440 1447 1434 1421 1406 1391 1376 1358 1341 1323 1305 1286 1264 1241
  1219 1199 1173 1147 1117 1086 1054 1021  986  950  913  876  839  804  774
   750  736  734  747  778  824  886  958 1041 1129 1216 1308 1403 1499 1594
  1688 1778 1871 1967 2065 2163 2251 2350 2457 2564 2670 2780 2892 3008 3126
  3236 3352 3460 3551 3614 3641 3632 3593 3536  760
*** INITIAL-VALUE OF EQUIVARENT-CIRCUIT ***
 0.785400678E+09 0.276882461E+02 0.235067395E-02 0 946973255E+04 0.785442147E+09
 0.653074572E-11 0.489644158E-15 0.137276484E+04 0.666769201E+05 0.704125695E+01

          BAND-BEGN=  1          BAND-END=  59

*** SIGMA OF A-CALCULATED ***   (UNIT %)
   9.4112(*****)    .8931(-21.9)    .3891(   .7)    .3601(   .1)    .3600(   .1)
  CL= 0.000E+00 FRM= 125000703.8    .4491( +9.3)    .3674(   .2)    .3590(   .2)
  CL= 0.100E-11 FRM= 125000679.8    .4180   7.4)    .3544(   .2)    .3597(   .1)
  CL= 0.23?E-12 FRM= 125000698.3

*** GRAPH CHART OF A-MEASURED AND DA/A ***
          (*)-DATA.MEASURED  (+)-DA/A  (X)=10TIMES OF .DA/A

 NO  FREQ    AV.AM    -2.0      -1.0       0.0       1.0       2.000     AC-AM
  2 994.1  .1783  .     .      .  +X      .         .         .         .0110
  4 994.5  .1835  .     .      .  +X      .         .         .         .0048
  6 994.9  .1893  .     .      .  +X      .         .         .         .0122
  8 995.3  .1955  .     .      .  * .X    .         .         .         .0291
 10 995.7  .2033  .     .      .  *+X     .         .         .         .0141
 12 996.1  .2118  .     .      .  * X     .         .         .         .0243
 14 996.5  .2226  .     .      .  X +*    .         .         .         =.0159
 16 996.9  .2344  .     .      .  X * *   .         .         .         =.0244
 18 997.3  .2480  .     .      .  X+ *.   .         .         .         =.0136
 20 997.7  .2639  .     .      .  X+ .*   .         .         .         =.0060
 22 998.1  .2841  .     .      .  X  +    .  *      .         .         =.0290
 24 998.5  .3046  .     .      .  X  +    .  .*     .         .         =.0157
 26 998.9  .3329  .     .      .    * X   .    .*.  .         .         .0145
 28 999.3  .3637  .     .      .    +     .      * .         .         .0049
 30 999.7  .3943  .     .      .    +X    .         .*        .         .0107
 32    .1  .4164  .     .      .    +X    .         .         .*        .0100
 34    .5  .4176  .     .      .   X+     .         .         .*        =.0063
 36    .9  .3889  .     .      .   X+     .         .         .*        =.0100
 38   1.3  .3374  .     .      .   X+     .         .  *      .         =.0076
 40   1.7  .2793  .     .      .   X+     .  *      .         .         =.0111
 42   2.1  .2257  .     .      .  +*X     .         .         .         .0243
 44   2.5  .1816  .     .      .  .* X    .         .         .         .0191
 46   2.9  .1458  .     .      .    * X   .         .         .         .0301
 48   3.3  .1181  .     .   *. .  X  +.   .         .         .         =.0507
 50   3.7  .0950  .     .*  .  X    *    .         .         .         =.0355
 52   4.1  .0764  .   *.  X .         *   .         .         .         =.1206
 54   4.5  .0604  .  *    .  .         *   X         .         .         .0402
 56   4.9  .0472  .  *    .  .         .*    X       .         .         .0802
 58   5.3  .0367  .*--*---.--.---*----*---*---*X----*---*---*---*---*   .0748
 60   5.7  .0292  . *     .  .      X  *   .   .     .         .         =.0478
 62   6.1  .0216  X *     .  .      .  *   .   .     .         .         =.2577
 64   6.5  .0168  X *     .  .*     .  .   .   .     .         .         =.7916
 66   6.9  .0146  X*      .  .      .  .   .   .     .         .         =1.5233
 68   7.3  .0149  X*      .  .      .  .   .   .     .         .         =1 9119
 70   7.7  .2123  *       .  .      .  *   .   .     .         .         =29.1588

*** DETERMINED PARAMETERS ***
   FS=  125[illegible].87                  R1=  28.709
   L1=  .0024711                           C0=  9448
   FP= 125007044. C0= 0.58540E-11 C1= 0.40479DE-15          Q=  73074.  M=  7.57

   DAMAX=29.1
   FR-CALCULATED=  125000701.5 HZ      RR=  29.22 OHM
   FR-MEASURED   =  125000698.0 HZ     PHASE-ERROR=  .21 DEG   (CL= 0.239E-12)
```

Fig 5 Example of Teletypewriter Printout

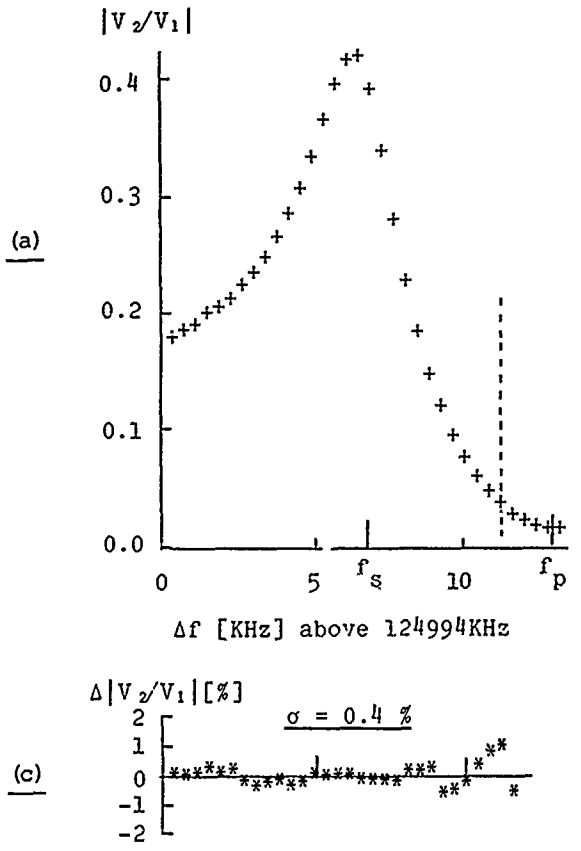

(b)

f_s = 125000587 [Hz]

R_1 = 28.71 [ohm]

L_1 = 2.671 [mH]

r = 9.648 x 10^3

Q = 7.31 x 10^4

M = 7.6

ϕ_L = 0.2 [Deg]

C_L = 0.24 [pF]

Fig. 6. Example of Measurement on 125MHz Resonator

Table 1 Measured Results of Three Resonators

(a) 125 MHz

NO.	f_s [Hz]	R_1 [Ω]	L_1 [mH]	r	Q	M	σ_f [%]	f_r(det.) [Hz]	f_r(meas.) [Hz]	ϕ_L [deg]
1	125000587	28.71	2.671	9.648×10^3	7.31×10^4	7.6	0.4	125000702	125000698	0.2
2	125000092	21.34	2.161	1.095×10^4	7.95×10^4	7.3	0.4	125000203	125000202	0.0
3	124999305	28.46	2.359	8.440×10^3	6.51×10^4	7.7	0.4	124999432	124999424	0.5

(b) 175 MHz

NO.	f_s [Hz]	R_1 [Ω]	L_1 [mH]	r	Q	M	σ_f [%]	f_r(det.) [Hz]	f_r(meas) [Hz]	ϕ_L [deg]
1	175003300	59.59	3.195	2.431×10^4	5.90×10^4	2.4	0.3	175004082	175004086	-0.1
2	175016517	42.78	2.456	2.650×10^4	6.31×10^4	2.4	0.3	175017271	175017224	1.1
3	175002705	55.29	2.646	2.007×10^4	5.26×10^4	2.6	0.3	175003475	175003456	0.4

Crystal Current 0.09 mA

Temperature 25.3 C

DIGITAL FILTERS - AN OVERVIEW

F. J. Witt

Bell Telephone Laboratories
No. Andover, MA 01845

In my remarks I will attempt to set digital filters in the proper perspective relative to the other filter technologies which are being discussed during this session. First, some clarification of what is meant by digital filters is in order. I like to think of digital filters as a subset of two more general categories - digital signal processors and sampled-data filters.

By digital signal processing is meant the manipulation of signals which are represented in digital form. Such processes as modulation, amplification, limiting, detection, multiplexing and filtering may be performed on signals which are represented in digital, usually binary, form. In most hardware implementations of digital filters, some of these other processes are usually also being performed. In fact, it is rare to see a stand-alone digital filter in a system application. Even more rare is a digital filter in an analog signal processing environment, where, of course, suitable A/D and D/A converters would be required before and after the digital filter. Digital filters more often find application in systems where the signals appear in a digital representation, rather than in an analog format. The term digital filtering is also applied to nonhardware applications, such as the processing of noisy images with the aid of a digital computer to improve resolution.

The other more general category, sampled-data filters, applies to filters which act on signals which have been sampled, in contrast to the more traditional concept of a filter, which processes a continuous representation of the signal. This distinction has some very important ramifications which significantly influence the way in which digital filters are applied. The digital filter is a sampled-data filter for which the amplitude levels have been quantized so that a digital, again usually binary, representation of the individual samples may be used.

In Figure 1 we see a comparison of four ways of realizing roughly comparable filter characteristics. These are an LC passive filter, an RC active filter, a switched capacitor active filter and a digital filter. This session has slighted the LC passive filter, but I'm sure most of you realize that it still plays an important role in modern telecommunications equipment. The RC active filter has supplanted the LC passive filter in many low frequency (<50 kHz) applications. In the last few years, the switched capacitor filter has emerged as a best choice in some low frequency applications. This technology has the advantage that it permits the realization of fairly complex precision filters on a single chip of silicon and, most importantly, it provides a filter realization approach which requires no tuning. In the digital filter, we see that the building blocks are multipliers, adders and delay elements, the latter playing the memory role of the L and C elements used in the other approaches. The delay elements are usually realized as shift registers.

In Figure 1 we see a particular digital filter topology. Note that there are feed back paths in the filter. Such a filter is referred to as a "recursive" digital filter. It has also been called an "infinite impulse response" or IIR filter. We may also derive a digital filter from a transversal or "tapped delay line" filter. In this case, weighted signals from the individual taps are combined to realize the desired filter characteristic. Here, there is no feedback, and the filter is referred to as a "nonrecursive" digital filter. Also, since an input signal of limited duration will eventually pass through the filter, such filters are often

called "finite impulse response" or FIR filters. So much for the jargon, but I do wish to make the point that there are many (more than I have discussed) digital filter topologies which must be considered.

A related issue also concerns filter architecture. A key building block in a digital filter is the multiplier. Suppose I wish to multiply a binary number by a constant. I have several choices. One common approach, which is similar to the way we manually multiply two numbers together, is to add, shift, add, shift, etc. Such an approach is readily realized with digital logic elements. On the other hand, I can achieve the same result by storing a set of products in a memory and using the incoming data, i.e., the variable multiplicand, as an address. Clearly, the approach chosen will be strongly related to the capabilities of the device technologies I have available to me, and it will ultimately become an economic decision.

One should realize that digital filters require power. There are applications for which feasibility using a digital signal processing approach has been demonstrated, but which were implemented using more conventional means, primarily because of power considerations. This situation is changing rapidly, however, as VLSI advances are applied to digital signal processing applications.

An important feature of digital filters, which is not available with the other approaches shown in Figure 1, is that of multiplexing capability. Digital filtering consists of the manipulation of samples, represented by a sequence of ones and zeros. These samples are distinct and march through the filter in sequence. It is possible to interleave samples from several different signals and process them without any interference between signals. In fact, it is possible to pass a signal through a digital filter and to reintroduce it to the same digital filter, but with a different set of filter parameters than was used during the first pass. Thus, a second-order filter may be used as a 2nth order filter. The delay element which is used for memory, the shift register, does not mix the signals, as would occur if an LC or RC filter were used in a similar way. Of course, the price paid for multiplexing is the need for higher speed logic, which implies higher power requirements, and, of course, delay blocks with more bit capacity.

A digital signal processor is basically a custom designed digital computer working in real time. When one examines the implications of this fact, it becomes clear that present speed and power limitations restrict all but the simplest processing to relatively low frequencies, say equivalent analog signal processing frequencies less than 0.5 MHz. So, as with RC active filters, digital filters are restricted in their upper frequency range.

Figure 2 shows an example of a device used for digital signal processing. It is a 12xn-bit serial multiplier capable of speeds up to 20 Mbit/sec and dissipating only 0.7 watt. This device and similar devices have been used in the two circuit boards shown in Figure 3. On the left is a code converter which converts μ-law representation of a signal sample to a linear representation of that same sample and vice versa. Today we have a single chip, two of which will perform the function performed by this entire board.

The circuit board on the right contains, among other things, a digital filter which is only one second-order section. However, this single section is multiplexed to realize a fourth-order bandpass filter, a fourth-order band-elimination filter and, to top it off, further multiplexing is incorporated to handle 16 channels. The bit rate through the second-order section is 6 MHz even though only voice frequencies are being processed. This filter is imbedded in a time division switching system where all of the signals exist in a digital format. Without digital signal processing, it would have been necessary to convert to the analog format, pass the signals through 16 analog signal processors (including filters) and convert back to the digital format.

I have attempted to briefly describe some aspects of digital filters, including their unique features and their limitations. It is clear that they will be playing an increasingly important role in future systems design.

FIGURE 1 - Several filter technologies

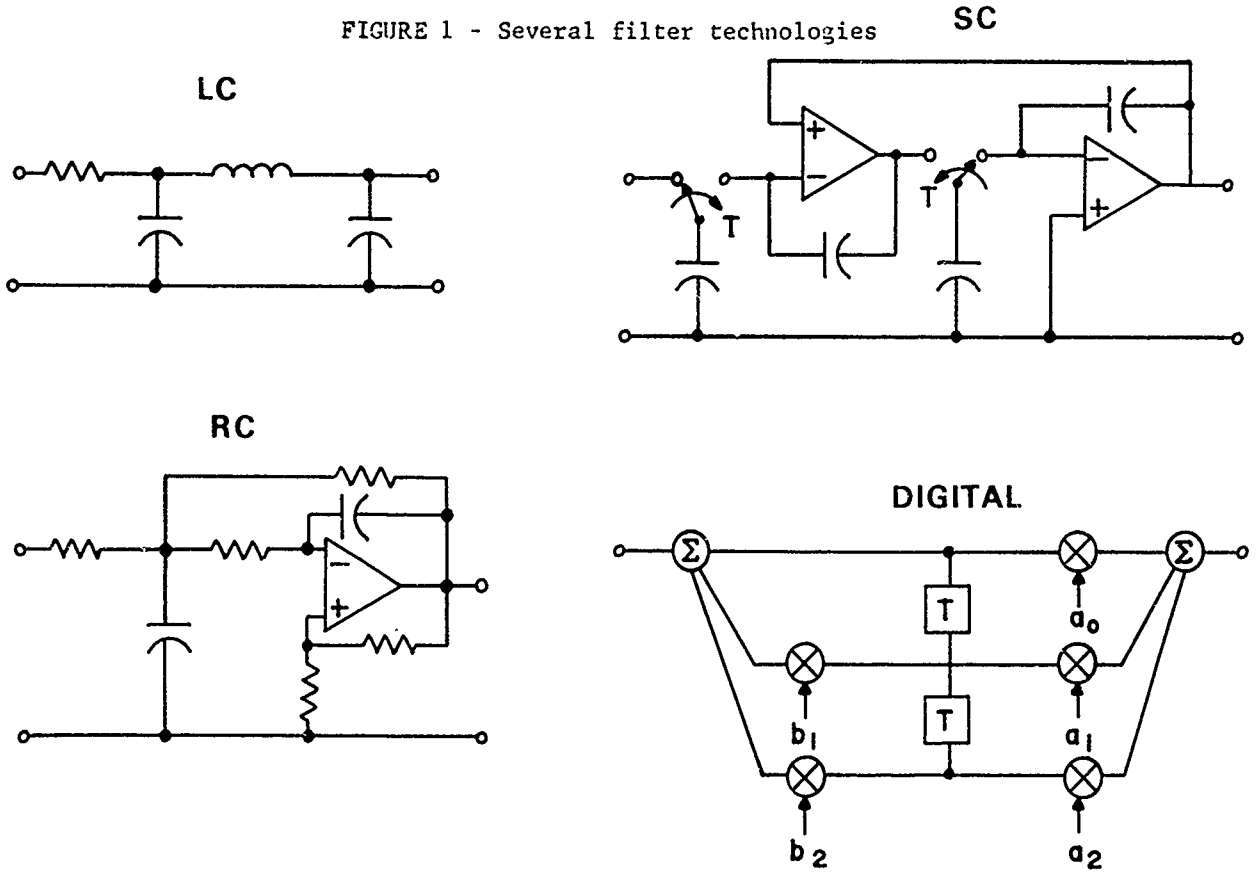

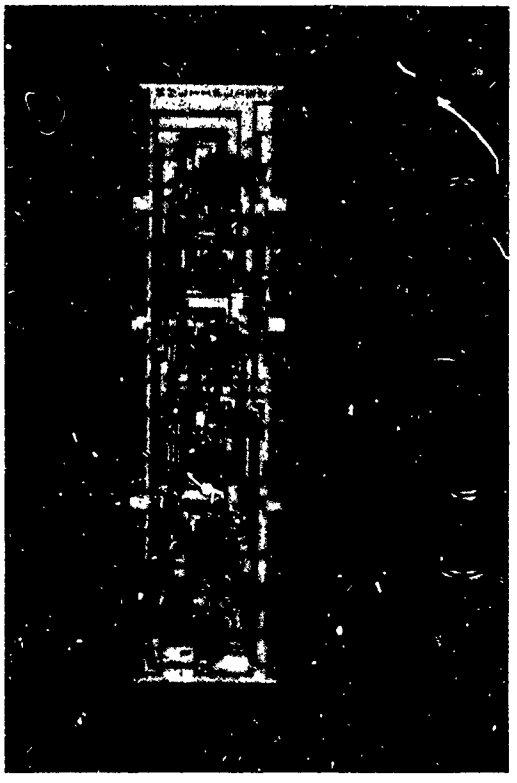

FIGURE 2 - 16 x n serial multiplier

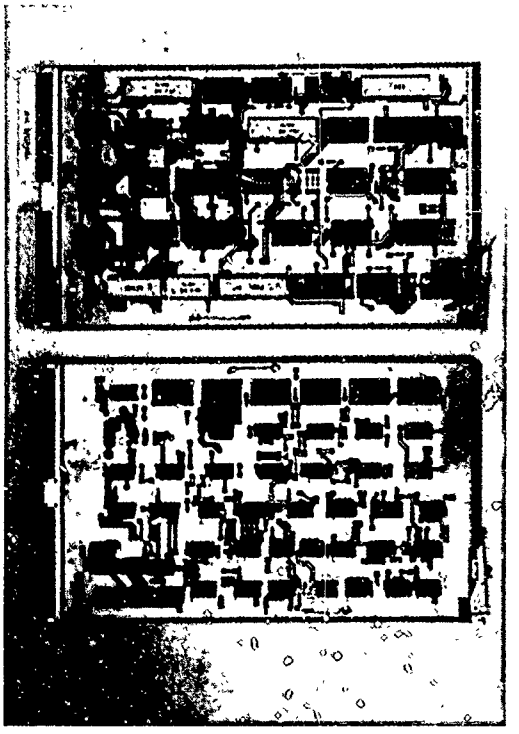

FIGURE 3 - Circuit packs from a digital signal processor

MODERN CRYSTAL FILTERS

R. C. Smythe

Piezo Techonolgy Inc.
Orlando, Florida 32804

SUMMARY

Crystal filters are currently available from roughly 10 kHz. to 300 MHz., with most new applications lying above 4.5 MHz. at bandwidths of 0.3 % or less, in order to take advantages of integrated crystal filter technology. The performance and applications of conventional and integrated crystal filters are discussed and illustrated by examples. Some future trends are indicated.

INTRODUCTION

This paper attempts to summarize, and illustrate by examples, the current status of crystal filter technology, and o indicate some areas of development. The emphasis is on performance and applications, rather than on details of design or construction, which are treated elsewhere[1, 2, 3].

Crystal filters using single-mode resonators (conventional or discrete-resonator crystal filters) have been in use since the 30's[4]. Until the late 50's, applications were primarily within the telephone system. Since then, other applications have gradually become important. In particular, crystal filters and frequency demodulators are widely used in mobile radios. The use of crystal filters in these and other fields was greatly accelerated by the development in the 60's of integrated crystal filters - monolithic and tandem monolithic filters, using acoustically-coupled thickness shear resonators (a type of multi-mode resonator), and hybrid monolithic filters, which use both acoustically-coupled resonators and single resonators.

RANGE OF FREQUENCY AND BANDWIDTH

As shown in Figure 1, crystal filters claim a domain that runs from 10 kHz. or less to about 300 MHz. with fractional bandwidths from .01% to as much as 10%. Integrated crystal filters claim only the portion from about 4.5 MHz. upward and below roughly .3% bandwidth*. Nevertheless, for reasons of cost and size, it would appear that the majority of crystal filters now being manufactured are integrated crystal filters**. Where system considerations dictate lower frequencies or substantially greater fractional bandwidths, conventional crystal filters are still used. Through most of the VHF range, conventional crystal filters compete only feebly with monolithic and tandem monolithic filters. From 4.5 or 5 MHz. to 30 or 35 MHz. at bandwidths up to 0.3%, integrated and conventional filters compete on the basis of cost, size, and performance.

APPLICATIONS AND EXAMPLES

Principal areas of application for crystal filters are listed in Table I. Of greatest importance by far is the area of communications, especially telecommunications and mobile communications.

In telecommunications, conventional, hybrid, and monolithic crystal filters are extensively employed as single-channel sideband bandpass filters in frequency-diversity multiplex transmission systems[4]. Modern examples include the 9-pole hybrid monolithic GTE Lenkurt channel filter[5] and the 8-pole Western Electric monolithic channel filter[6], both in the 8 MHz. range, and the newly designed Western Electric discrete-resonator channel filters operating at 60 to 108 kHz. [4, 7].

In mobile communications, tandem monolithic crystal filters are used as i-f filters in both single and double conversion receivers. Two-pole monolithic filters are used in frequency demodulation circuits in narrow-band fm land mobile receivers. In paging receivers, and as field-installed options in land and aeronautical mobile service, VHF monolithic and tandem monolithic filters are used as front-end preselectors.

Examples illustrating performance and applications of a variety of modern crystal filters are presented in Table II and Figures 2 through 9.

* In common with most such frequency-bandwidth maps, Fig. 1 is a rough guide, and should only be used as such.

** Production statistics for the industry are not available.

The first two examples in Table II represent single-sideband filters designed using insertion parameter methods. While the use of single-sideband and other general types of crystal filter response functions are of increasing importance, for the great majority of applications Tchebycheff designs, which combine favorable element values with low component sensitivities, remain the most cost-effective solution. The remaining examples of Table II are representative.

AREAS FOR FUTURE DEVELOPMENT

From the introductory remarks it may be seen that while crystal filters have been in use for over 4 decades, the crystal filter industry, outside of the telephone industry, is scarcely more than 20 years old. Driven by expanding markets, innovations and improvements continue to be made. In particular, current development efforts are being focused on manufacturing cost reductions, specialized types of filter response, frequency range extension, and new piezoelectric materials.

Manufacturing cost reductions involve 1) process improvement, to obtain better yield, and 2) reduction of labor content through product design, process innovation and automation. These efforts, made possible by increased manufacturing volume, are being carried out almost entirely on a proprietary basis by a number of companies and are beyond the scope of this paper.

Increases in single-sideband transmission and in data transmission are expected to lead to further developments in sideband crystal filters in the 5 to 9 MHz. frequency range and in filters with controlled group delay or phase response. With regard to the latter, specifications by communications systems and equipment designers are expected to become more realistic as the relationships between group delay or phase response and bit error rates become better understood.

The frequency range of resonators and crystal filters is being extended upward by new and improved methods of wafer fabrication. In particular, the chemical etching techniques of Vig[8] are promising. Berte and Hartemann[9] have had great success in fabricating wafers only a few micrometers in thickness using ion milling. They have succesfully fabricated AT-cut quartz resonators with fundamental resonance frequencies up to 525 MHz.[10] and lithium tantalate two-pole monolithic filters up to 230 MHz. with bandwidths approaching 2%[9].

Spurred in part by acoustic surface wave filter requirements, new piezoelectric materials are being investigated more intensively than at any time in the past. Practical application to crystal filters appears to be some years away, but the long range potential of aluminum orthophosphate (berlinite)[11-13] appears to be excellent. For crystal filter applications, thickness-shear modes with good frequency-temperature characteristics and piezoelectric coupling (and hence fractional bandwidths) greater than AT-cut quartz are believed to exist.

REFERENCES

1. Sheahan, D. F., & R. A. Johnson, Editors, "Modern Crystal and Mechanical Filters", IEEE Press, New York; 1977.

2. Smythe, R. C., "Communications Systems Benefit from Monolithic Crystal Filters", Electronics, v. 45, No. 3, pp. 48-51; Jan. 31, 1972.

3. Smythe, R. C., "Some Recent Advances in Integrated Crystal Filters", Proc. IEEE, v. 67, No. 1, pp. 119-129; Jan., 1979.

4. Simmonds, Thomas H., Jr., "The Evolution of the Discrete Crystal Single-Sideband Selection Filter in the Bell System", Proc. IEEE, v 67, No.1, pp. 109-115; Jan. 1979.

5. Sheahan, D. F., "Polylithic Crystal Filters", Proc. 29th Annual Symposium on Frequency Control, pp. 120-127; 1975.

6. Pearman, G. T., & R. C. Rennick, "Unwanted Modes in Monolithic Crystal Filters", Proc. 31st Annual Symposium on Frequency Control, pp. 191-196; 1977.

7. McLean, D.I., A. F. Greaziani, and J.J. Royer, "New Discrete Crystal Filters for Bell System Analog Channel Banks", these Proceedings.

8. Vig, J.R., J.W. LeBus, and R. L. Filler, "Chemically Polished Quartz", Proc. 31st Annual Symposium on Frequency Control, pp. 131-143; 1977.

9. Berte, Marc, "Acoustic Bulk Wave Resonators & Filters Operating in the Fundamental Mode at Frequencies Greater than 100 MHz"., Proc. 31st Annual Symposium on Frequency Control, pp. 122-125; 1977.

10. Berte, M., & P. Hartemann, "Resonateurs en Quartz Fonctionnant a des Frequencies Fondementales Superieures A 100 MHz."., L'Onde Electrique; to appear.

11. Chang, Z.P., and G.R. Barsch, "Elastic Constants and Thermal Expansion of Berlinite", IEEE Trans., v. SU-23, No. 2, pp. 127-135; March 1976.

12. Detaint, J. et al, "Bulk and Surface Acoustic Wave Propagation in Berlinite", these Proceedings.

13. Ozimek, E.J. and Chai, B.H.T., "Piezoelectric Properties of Single-Crystal Berlinite", these Proceedings.

TABLE 1

CRYSTAL FILTER APPLICATION AREAS

I. COMMUNICATIONS
   - A. Telecommunications
   - B. Mobile Communications
     1. Land Mobile Receivers (VHF, UHF)
        - a. IF Filters
        - b. Frequency Demodulators
        - c. Front-end Filters
     2. Aeronautical Mobile (VHF, UHF)
        - a. IF Filters
        - b. Front-end Filters
     3. Marine Mobile (VHF)
        - a. IF Filters
        - b. Frequency Demodulators
     4. Paging Receivers (VHF)
        - a. IF Filters
        - b. Front-end Filters
   - C. H-F Communications
   - D. Satellite Communications

II. NAVIGATION AIDS
   - A. Conventional
   - B. Satellite Based

III. OTHER
   - A. Frequency Synthesis

TABLE II

EXAMPLES, WITH APPLICATIONS

Fig.	Freq. (MHz.)	BW (kHz.)	No. Poles	No. Wafers	Overtone	Application (Ref. Table I)	Configuration
*	.064-.108	3.4	6	4	1	I.A.	Conventional
**	8.14	3.4	9	5	1	I.A.	Hybrid Monolithic
2	10.7	± 7.5	4	2	1	I.B.1.a.	Tandem Monolithic
3	21.4	± 7.5	8	4	1	I.B.1.a.	Tandem Monolithic
4	30.112	± 11	10	5	1	I.B.2.a.	
5	45	± 6.5	4	1	3	I.B.1.a.	Monolithic (2 two-pole sections on single wafer)
6	75	± 13	4	1	3	II.A.	
7	154	± 6.5	4	2	5	I.B.1.c.	Tandem Monolithic
8	243	± 7.5	2	1	7	II.A., III.A	Monolithic
9	21.4	± 5	2	1	1	I.B.1.b.	Tandem Monolithic

* See Ref. 4,7
** See Ref. 5, Fig. 12

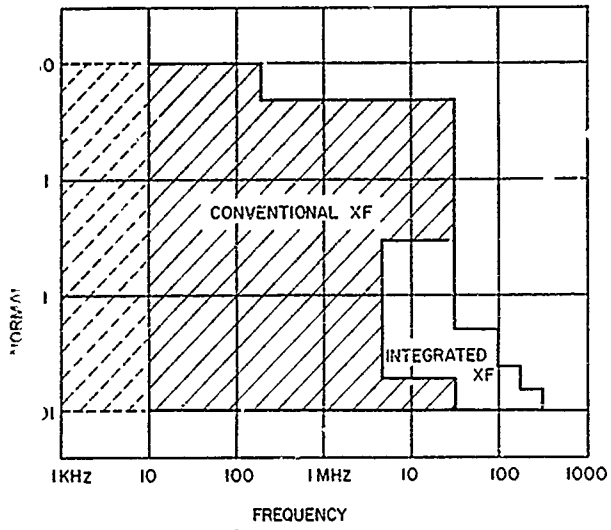

Fig. 1. Bandwidth - Frequency Domain For Conventional and Integrated Crystal Filters.

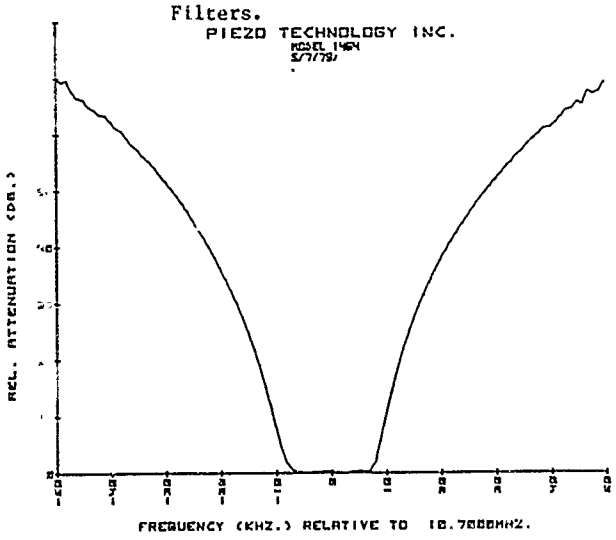

Fig. 2 4-Pole Tandem Monolithic Filter Attenuation Characteristic fo = 10.7 MHz., B_3= ± 7.5 kHz.

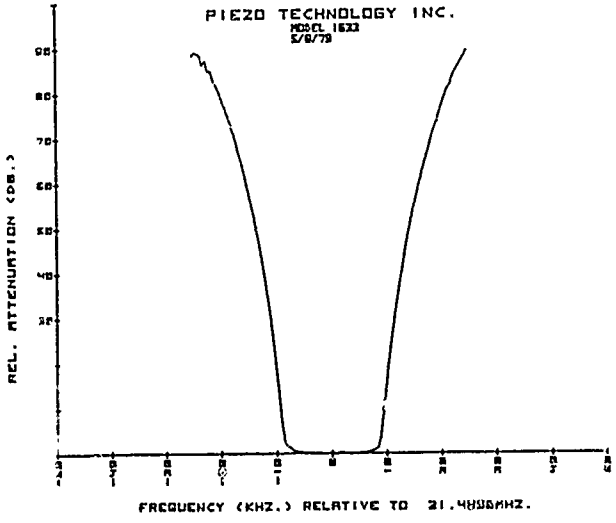

Fig. 3 8-Pole Tandem Monolithic Filter Attenuation Characteristic fo = 21.4 MHz., B_6= ± 7.5 kHz.

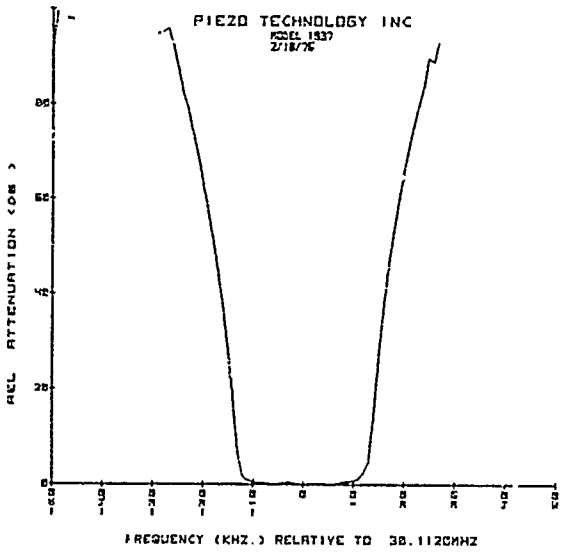

Fig. 4 10-Pole Tandem Monolithic Filter Attenuation Characteristic fo = 30.112 MHz., B_6= ± 11 kHz.

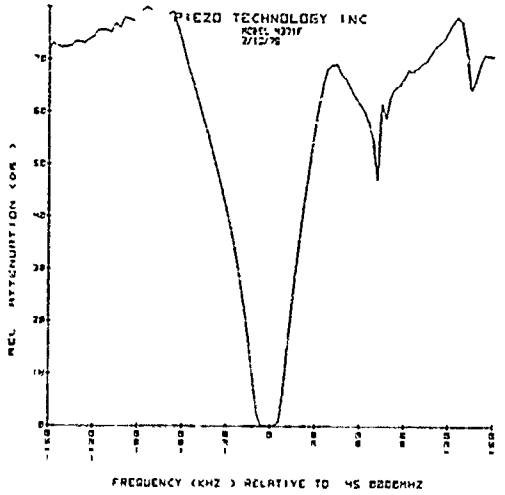

Fig. 5 4-Pole Monolithic Filter Attenuation Characteristic
fo = 45 MHz., B_3= ± 7.5 kHz;
a) Overall Response

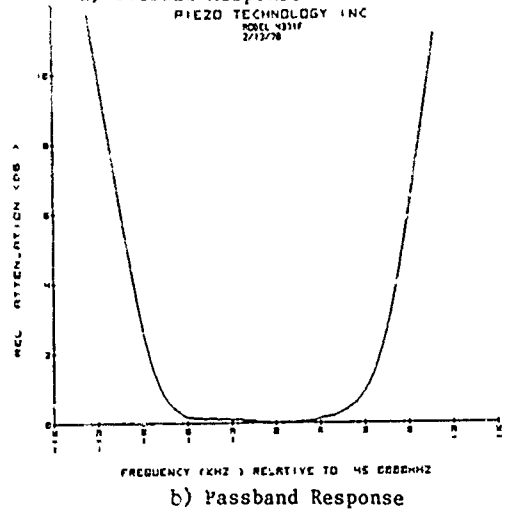

b) Passband Response

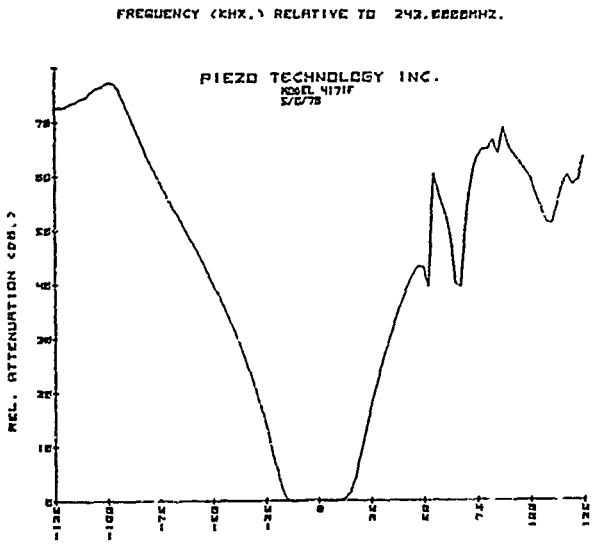

Fig. 6 4-Pole Monolithic Filter Attenuation Characteristic
fo= 75 MHz., B_6= ± 13 kHz.

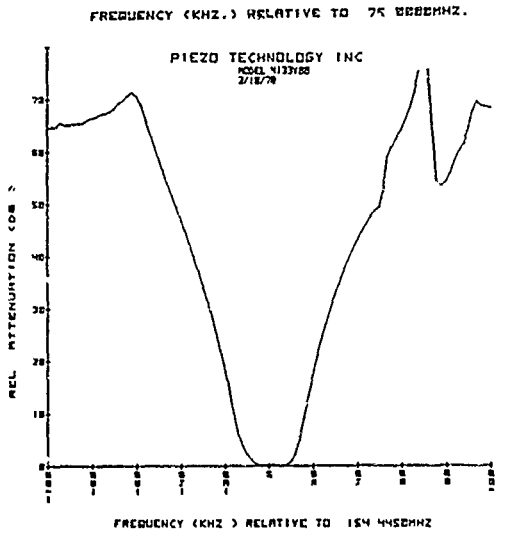

Fig. 7 4-Pole Tandem Monolithic Filter Attenuation Characteristic
fo = 154.445 MHz., B_3= ± 6.75 kHz.

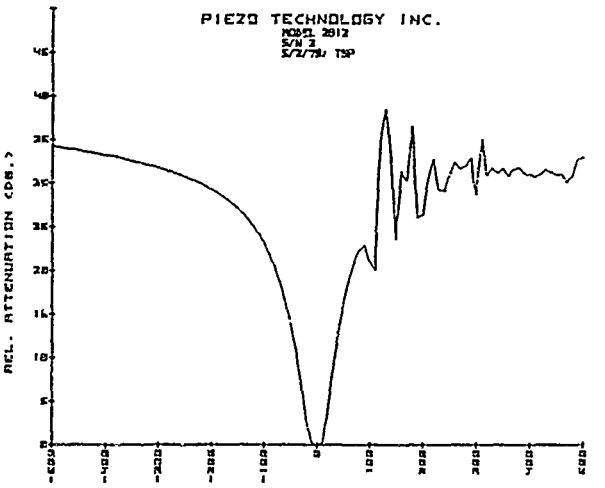

Fig. 8 2-Pole Monolithic Filter Atenuation Characteristic
fo = 243 MHz., B_6= ± 5 kHz.

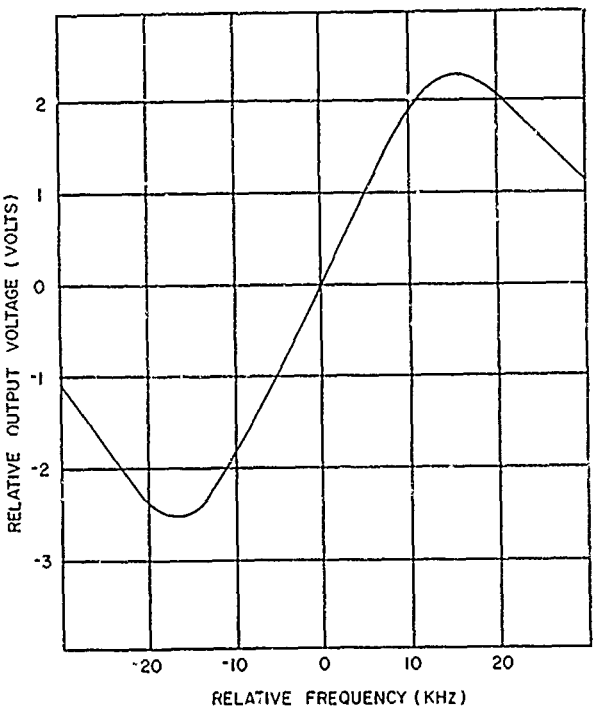

Fig. 9 Frequency Discriminator Characteristic Using 2-Pole Monolithic Filter and IC Phase Detector; fo = 10.7 MHz.

CCD AND SWITCHED CAPACITOR FILTERS

C. R. Hewes

Texas Instruments Incorporated
P. O. Box 225936
Dallas, Texas 75222

Abstract

CCDs and switched capacitor filters offer the system designer highly integrated functions on a single IC. CCD and switched capacitor filter techniques are briefly reviewed and a number of applications are described.

Introduction

Charge coupled devices (CCDs) are inherently analog and as such they are ideally suited to a number of sample data filtering functions.[1,2,3] As soon as the principles of CCD filters were demonstrated,[4] it became evident that a considerable amount of support circuitry is required to operate the devices and to facilitate the interface of CCD filters to the rest of any realistic system. This has led to the incorporation of clock circuits, amplifiers, multipliers, A/D and D/A circuits, and other functions on the same chip with CCDs. Recently switched capacitor filters[5] have also been realized in monolithic form, and these devices have proven to be complimentary to CCDs and their capabilities and, at the same time, compatible in the fabrication technology. Both switched capacitor and CCD filters are being exploited in recent IC designs as will be reviewed in this paper. We find that in some filter applications CCDs offer both area and power savings in comparison to switched capacitor filters, while in other functions the opposite is true. The two filtering applications are related in that both CCDs and switched capacitor filters accomplish their filtering functions by manipulating charge packets representing analog signals. Both approaches utilize the basic capability of MOS technology for precision ratioed capacitances to perform these manipulations and also to store the analog signals.

CCD Transversal Filters

Although both transversal filters and recursive filters have been constructed with CCDs, most work to date has involved the use of the CCD transversal filter. Two general types of transversal filters have been utilized. The first being the so-called split-electrode filter[4] and the second a parallel input CCD filter. A diagram of an N-stage transversal filter structure is shown in Figure 1. It consists of some means for delaying and storing the last N values of an input signal, multiplying these values by the weighting coefficients h_N and summing these products to obtain the output. The expression which describes these operations is

$$v_{out}(nT_c) = \sum_{m=0}^{N-1} h_m v_{in}\left[(n-m)T_c\right] \qquad (1)$$

where $v_{out}(nT_c)$ and $v_{in}(n-m)T_c$ are the n^{th} and $(n-m)^{th}$ time sample of the output and input signal respectively, and T_c is the sampling period. By taking the Fourier transform of this expression the transfer function, $H(\omega) = V_{out}(\omega)/V_{in}(\omega)$ is found to be

$$H(\omega) = \sum_{h=0}^{N-1} h_n e^{-j\omega nT_c} \qquad (2)$$

As can be determined from Equation 2, since this is a sampled data filter, the frequency response has a periodicity equal to the reciprocal of the sample rate which requires that the input signal must be band limited to prevent aliasing. The design problem of determining the best set of coefficients which provides the closest approximation to the desired frequency response has basically been solved. There are several computer programs that are generally available which can very efficiently perform this task.[6,7] The commonly used technique for constructing CCD transversal filters has been the split-electrode approach which is shown in Figure 2. The basic structure is a CCD delay line which has one of the electrodes in each stage split in two parts. In Figure 2a the signal charges are sensed on ϕ_3 sense electrodes which are unclocked. As charge transfers from the ϕ_2 electrode to the ϕ_3 sense electrode, the current which flows into the K^{th} sensing line consists of a part which would flow if no signal charge were present plus a part approximately equal to the signal charge. Therefore, the signal charge can be determined by integrating the current flowing to the ϕ_3 electrode during the charge transfer. Weighting is performed by splitting the ϕ_3 electrode and integrating separately the current flowing into each portion. A weighting coefficient of zero corresponds to a split in the center of the electrode while positive and negative h_N are achieved by appropriately proportioning the charge between the ϕ_3^+ and ϕ_3^-. The summation is achieved

by connecting together the ϕ_3^+ and the ϕ_3^- electrodes as shown in Figure 2b and the filter output is obtained by integrating the difference in the ϕ_3^+ and ϕ_3^- sense clock line currents in the output amplifier as shown. The split-electrode technique was first developed for use in bucket-brigade devices (BBDs)[8] and has been widely used for both CCD and BBD filters. Design techniques are further described in references 9 and 10.

The capabilities of CCDs are well matched to many low pass and band pass filtering applications. In these cases it is often very desirable to have a combination of linear phase, very sharp transitions between pass band and stop bands and high precision in the frequency response. The added feature of precise tunability by means of a clock signal makes functions possible with CCD filters which are very difficult with conventional filter technologies. Below we describe a CCD filter which could be used as an IF filter for a communications receiver.

An IF filter for receiver applications must meet several difficult requirements, among these are high dynamic range, very narrow transition bands for good adjacent channel rejections, reasonably flat in-band response, very high stop band rejection and very accurate band edge frequencies. A prototype filter for use in single side band selection as part of a receiver has been fabricated. This completely self-contained filter IC comprises two cascaded CCD filters, each having 300 weighting coefficients. All clock circuits, amplifiers, and internal biasing are built-in. Each filter is designed for approximately 38 dB stop band rejection and the two devices are cascaded to achieve approximately 76 dB stop band rejection with a pass band of 2.2 KHz at a band center of 25 KHz when the CCDs are clocked at 100 KHz. The transition bandwidth from pass band to stop band is 600 Hz. A photograph of the frequency response to the device is shown in Figure 3. The dynamic range (defined as the ratio of the 1% intermodulation level for a two-tone test to the noise level of the device) is typically 70 dB.

The split electrode CCD filter technique described above has limitations in frequency at around 1-5 MHz sampling rates. This is primarily due to the limitations of the operation amplifier used in the output circuit for the device. CCD transversal filters can be restructured so that the weighting is applied at the input rather than the output as illustrated in Figure 4. This filter has the same transfer function (Equations 1 and 2) as the more conventional output weighted device. The simplified CCD structure is shown schematically in Figure 4b. In this type of transversal CCD filter, the weighting is achieved by varying the size of the charge metering wells at separate inputs distributed along CCD delay lines. Each stage of the CCD adds the charge from its corresponding input to the accumulated charge packets from preceding stages. As illustrated, the CCD channel width grows towards the output end in order to accomodate the increasing charge. Although the diagram illustrates only positive weighting coefficients the negative weights can be obtained by adding a parallel channel and differencing the output signals.

The primary advantage of this input weighted device is a simplified output circuit and the capability of high speed operation. The output weighted device of Figure 2 required an operational amplifier using an integrator which is typically operating at a high gain mode due to large parasitic capacitances on the split electrode sense lines. In the input weighted device, however, the output mode capacitance is quite small and can be used directly to perform the charge to voltage conversion. A simple source follower is then used for the output buffer and it has inherently higher bandwidth and lower noise than practical on-chip operational amplifiers. Sampling rates of 10-30 MHz are possible with this structure. The primary disadvantage of the input weighted CCD is that the CCD area is larger for a given transfer function than the corresponding output weighted device.

Switched Capacitor Recursive Filters

Transversal filters which have only zeros of transmission in their transfer function are relatively inefficient in their use of silicon area for certain types of frequency responses such as narrow band and band pass filters. For these cases a recursive filter (i.e., one which has feedback) that implements poles would be more appropriate. However, CCD recursive filters have several disadvantages. First, in order to implement a stable, accurate recursive filter using CCDs, it is necessary to perform charge to voltage and voltage to charge conversions with high precision and accuracy. Second, the recursive filter most compatible with CCD implementation is the so-called direct form filter but the direct form architecture is known to have very high sensitivity to coefficient accuracy. Thus, it is difficult to achieve sufficient accuracy in CCD recursive filters, especially for filters with high Q poles. Another approach to realization of recursive filters is the use of switched capacitor filters which are described in more detail in references 5, 11 and 12.

Switched capacitor filters rely on the use of switches, precision ratioed capacitors, and operational amplifiers used as integrators. The basic building blocks such filters as the sample data integrator shown in Figure 5 and described in more detail below. The advantage of using switched capacitor recursive filters is that they are compatible with architecture such as ladder filters, which have a very low coefficient sensitivity. The integrator forms the basis of a second order filter section as shown in Figure 6. The two integrators can be seen in this figure. One is formed with the capacitors $\alpha_L C_L$ and C_L and the other by $\alpha_C C_C$ and C_C. A sign inversion is accomplished by adding a second switch to the bottom plate of capacitors so that the polarity can be reversed when discharging this capacitor into its corresponding integrator. The Z-transform of this circuit can be written as

$$\frac{V_{out}(z)}{V_{in}(z)} = \frac{-\alpha_i\alpha_c\ (z-1)}{z^2 - (2-\alpha_c\alpha_T-\alpha_c\alpha_L)z+(1-\alpha_c\alpha_T)} \qquad (3)$$

We can see from the Z-transform that the frequency response is independent of the absolute values of either C_L or C_C but depends only on the ratios α_C,α_L and α_T. MOS fabrication techniques allow the control of such capacitor ratios to a precision on the order of 0.1% which is adequate for many filtering problems.

CCD Chirp Z-Transform

As discussed above the CCD is ideally suited for any operations which can be cast in the form of a transversal filtering operation. In seeking CCD applications, algorithms which utilize transversal filters are important. The chirp Z-transform (CZT) is an algorithm for performing the discrete Fourier transform (DFT) in which the bulk of the computation is performed in a chirp transversal filter, and for this reason it is particularly attractive for CCD implementation.[13-16] When implemented digitally, the CZT has no advantages over the conventional fast Fourier transform algorithm. However, the algorithm lends itself naturally to implementation with charge coupled device transversal filters. The CZT gets its name from the fact that it is implemented in an analog manner by (1) premultiplying the time signal with a chirp (linear FM waveform), (2) filtering in a chirp convolution filter and (3) post multiplying with a chirp waveform. A block diagram is shown schematically in Figure 7. After some early work using 500 stage CCD transversal filters for 500 point CZTs,[10,15] more recent developments have integrated the transform in a 512 point CZT[17] and a 32 point CZT[18] in monolithic form. These monolithic chips include the premultiplying D/A converters, the ROMs for storing the chirp waveforms, the CCD convolution filters, input amplifiers, output amplifiers, and the clock circuits and logic to operate the IC.

Speech Processing

Speech signals are well matched to the capabilities of both CCDs and switched capacitor filters. The applications of speech processing signals are presently expanding very rapidly and they range from vocoders to speaker verification systems to word recognition and to a variety of speech synthesis applications. The capability of CCD and switched capacitor filters with large scale integration promises to have significant impact on lowering the cost and complexity of such speech systems.

One application is the vocoder described below. The function of this vocoder system is to reduce the data rate of speech transmission to 2.4 Kbit/sec while maintaining high quality and intelligibility in the reconstructed speech signal at the receiver. The block diagram of the channel vocoder is depicted in Figure 8. The integrated system is based on the system and algorithm developed in the UK.[18] Two portions of the system which are enclosed in the dashed lines in Figure 8 are being implemented with two custom designed CCD/NMOS integrated circuits, while the remaining functions are implemented with a few simple analog components and microcomputer circuits. One of these two special circuits is used for speech analysis and the other for synthesis.

Programmable CCD Filters

Perhaps one of the most intriguing of CCD filters is that of an electrically programmable device. Both digitally programmable transversal filters and analog/analog correlator devices have been reported. These types of devices offer the eventual possibility of universal devices which the user programs for his own purposes. Also such devices can be used in adaptive filtering applications where the filter characteristics continually change under the control of some digital computer algorithm. Such devices could be used for matched filters for pn sequence codes which periodically change. Programmable transversal filters can be built up from the basic elements shown in Figure 9. This diagram is simply that of a transversal filter in which each of the weighting coefficients has the value of either 1 or 0. In addition, each of the weighting coefficients can be programmed by means of information in a digital chip register constructed physically in parallel with the CCD which has one delay stage corresponding to each delay stage of the CCD. The filter shown in Figure 8 then is capable of convolving at sequence of analog samples with a programmable sequence of 1's and 0's. A laboratory demonstration of the CCD device operating in this manner has been fabricated having 32 4-bit weighting coefficients in each CCD. Two such CCDs were operated in parallel to construct a programmable transversal filter having 32 stages with each stage having an 8-bit programmable weighting coefficients. A band pass filter response obtained from the device is shown in Figure 9. This device was also reprogrammed to form other band pass functions and low pass functions by simply changing the electrical signals inputted to the digital shift register. This device has been successfully coupled to a microprocessor to implement an adaptive filter.

Conclusions

MOS sample data filters of CCDs and switched capacitors are not expected to replace digital filters or any other filter technologies in all signal processing applications. Analog sampled data filters have performance limitations with respect to other filters in the area of speed, time delay, time-bandwidth product, dynamic range, accuracy and linearity. Furthermore, sampled data analog filters have limited flexibility compared with other digital techniques and most analog designs are customized to a particular application. However, CCDs and switched capacitors are expected to make significant impact on those signal processing functions which fulfill the twin requirements of relatively modest performance and

sufficiently high volume that low cost is a principle design goal.

In the general way it can be said that CCD split electrode filters are usually limited to applications where the sampling rate is below 1-5 MHz, and where the number of weighting coefficients is below 1000. Switched capacitor filters are also iimited to relatively low frequency sampling rates on the rates on the order of 1 MHz or less and filtering in the audio (< 100 KHz) frequency range. We may see some improvements in the speed area as photolithography allows the fabrication of smaller geometries in the MOS circuits but these figures are not expected to change too dramatically. The CCD transversal filter having parallel input structure is capable of operating at sampling rates much higher, in the tens of MHz and is probably the architecture which would be used in higher frequency applications of the technology.

Besides the areas mentioned previously in this paper, other application areas include Doppler processing in moving target radar, telecommunications, IR imaging processing, matched filtering and spread spectrum communications, adaptive filtering, and video bandwidth reduction.

References

1. C.H. Sequin and M.F. Tompsett, Charge Transfer Devices, Advances in Electronics and Electron Physics, Supplement 8, Academic Press, 1 1975.

2. M.J. Howes and D.V. Morgan, Ed. Solid-State Devices and Circuits, Vol. 11. Charge-Coupled Devices, Wiley, to be published Chapter V.

3. Charge-Coupled Devices: Technology and Application, Edited by R. Melen and D.D. Buss, IEEE Press, N.Y. 1977, Part V.

4. D.D. Buss, D.R. Collins, W.H. Bailey, and C.R. Reeves, "Transversal Filtering Using Charge-Transfer Devices," IEEE Journal of Solid State Circuits SC-8, April 1973, pp 131-136.

5. R.W. Brodersen, P.R. Gray, D.A. Hodges, "MOS Switched Capacitor Filters," this issue.

6. J.H. McClellan and T.W. Parks and L.R. Rabiner, "A Computer Program for Designing Optional FIR Linear Phase Digital Filters," IEEE Transactions of Audio and Electroacoustics, AU-21, 506 (1973).

7. M.T. McCallig, Linear and Nonlinear Phase Nonrecursive Digital Filter Design," Proceedings 1967 International Symposium on Circuits and Systems, Phoenix. 1977, pp 478-481.

8. F.L.J. Sangster, "The Bucket-Brigade Delay Line, A Shift Register for Analogue Signals," Phillips Technical Review, 31, pp 97-110,1970.

9. R.D. Baertsch, W.H. Engeler, H.S. Goldberg C.M. Puckette, and J.J. Tiemann, "The Desig and Operation of Practical Charge-Transfer Transversal Filters," IEEE J. Solid-State Circuits SC-11, Feb. 1976, pp 65-74.

10. R.W. Brodersen, C.R. Hewes and D.D. Buss, "A 500-Stage CCD Transversal Filter for Spectr Analysis," J. Solid-State Circuits, SC-11, February 1976, pp 75-83.

11. B.J. Hosticka, R.W. Brodersen, and P.R. Gra "MOS Sampled Data Filters Using Switched Capacitor Integrators," IEEE J. Solid-State Circuits, SC-12, (1977) pp 600-608.

12. J.T. Caves, M.A. Copeland, C.F. Rahim, and S.D. Rosenbaum, "Sampled Analog Filtering Using Switched Capacitors as Resistor Equivalents," IEEE J. Solid State Circuits, SC-(1977), pp 591-600.

13. L.R. Rabiner, R.W. Schafer, and C.M. Rader, "The Chirp Z-Transform Algorithm," IEEE Trans. Audio Electroacoust., Vol. AU-17, pp 86-92, June 1969.

14. H.J. Whitehouse, J.M Speiser, and R.W. Mear "High Speed Serial Access Linear Transform Implementations," presented at the All Applications Digital Computer Symposium, Orlando. FL, Jan. 1973, paper NUC TN 1026.

15. R.W. Brodersen, H.S. Fu, R.C. Frye, and D.D Buss, "A 500-Point Fourier Transform Using Charge-Coupled Devices," in 1975 Int. Solid-State Circuits Conf. Digest of Tech. Papers. Philadelphia, Feb. 1975, pp 144-145.

16. D.D. Buss, R.L. Veenkant, R.W. Brodersen, an C.R. Hewes, "Comparison Between the CCD CZT and and the Digital FFT," Proc. Int. Conf. Applications of Charge-Coupled Devices, San Diego, Oct. 1975, pp 267-281.

18 W.C. Eversole, D.J. Mayer, P.W. Boschart, M. de Wit, C.R. Hewes, and D.D. Buss, "A Completely Integrated 32-Point Chirp Z-Transform IEEE J. Solid-State Circuits, Dec. 1978, pp 822-831.

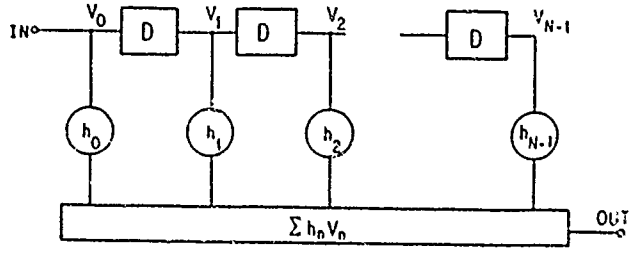

Figure 1. Block diagram of a transversal filter showing delay stages D and weighting coefficients h_n, n = o, N-1.

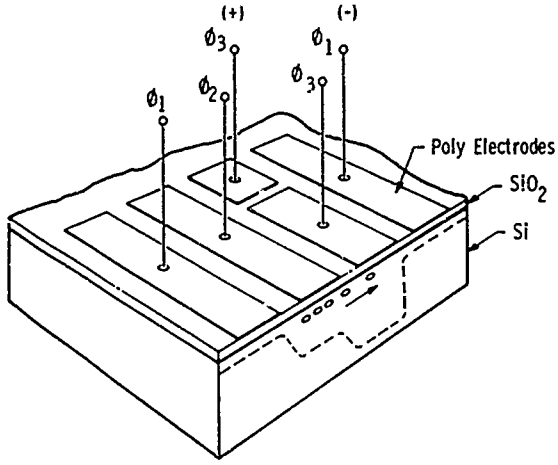

(a)

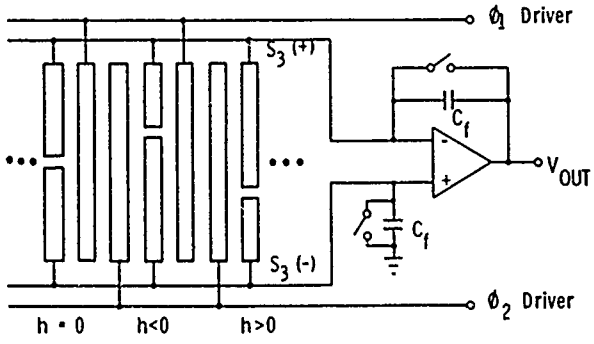

(b)

Figure 2. Schematic diagram of a CCD split electrode filter. In a) the structure is indicated, and in b) the charge sensing is illustrated.

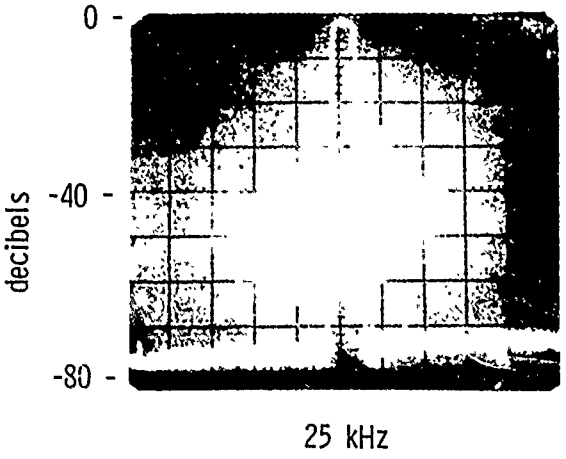

Figure 3. Filter response of a CCD filter IC containing two cascaded 300 stage CCD filters and all associated clocks and amplifiers.

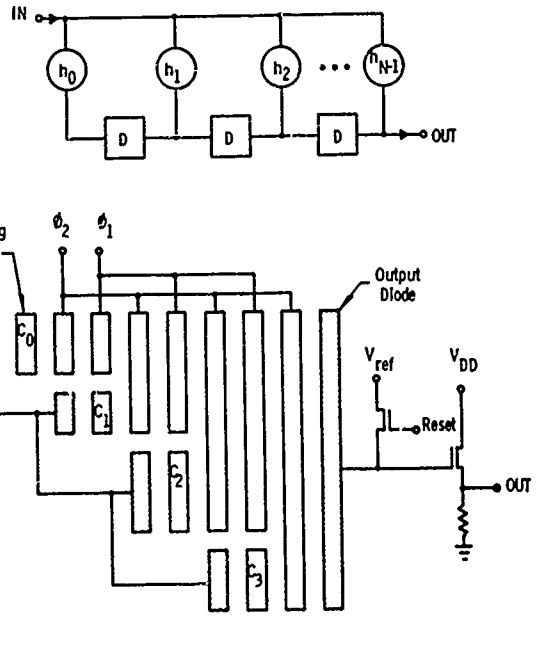

Figure 4. a) Block diagram of the transversal input filter structure and b) schematic of a 4-stage CCD transversal input CCD filter. For simplicity, much of the circuitry is omitted. Charge transfers from each input to the right and is added together before reaching the output diode.

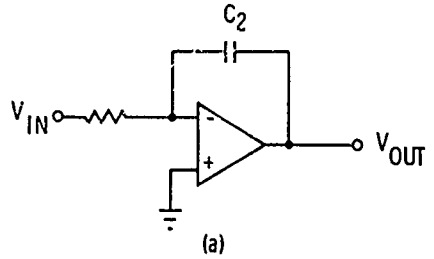

(a)

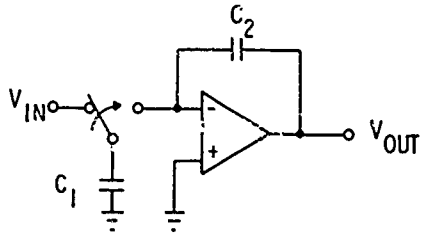

(b)

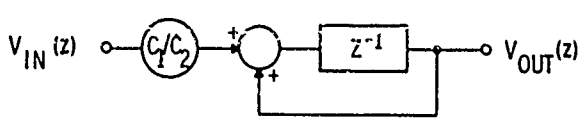

(c)

Figure 5. a) Conventional RF integrator, b) Sampled data integrator, c) Z-transform of integrator in (b)

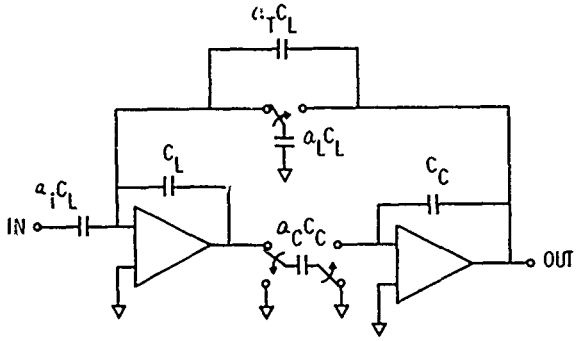

Figure 6. Two pole bandpass filter using switched capacitor integrators.

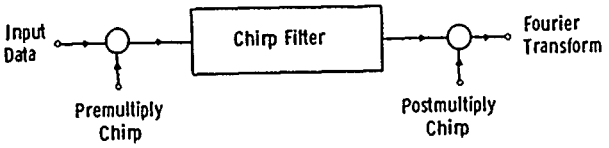

Figure 7. a) Simplified block diagram of the CZT algorithm. b) Block diagram of the compiex arithmetic of the CZT. The CCD transversal filters are designated by SIN and COS. The real and imaginary parts of the input (f_n) and output (F_K) are indicated with the superscripts I and R.

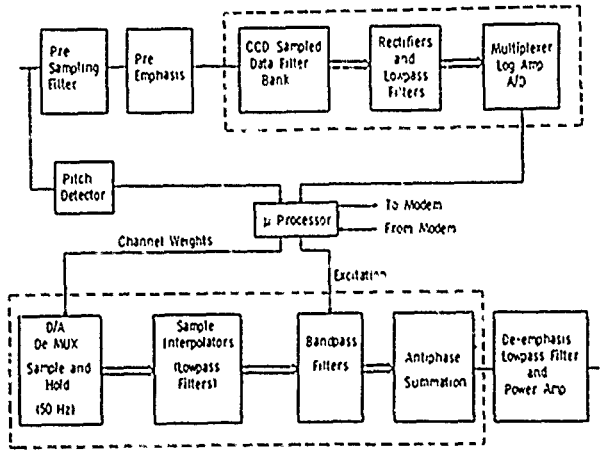

Figure 8. Block diagram of a channel vocoder based on two custom IC functions enclosed in dashed lines.

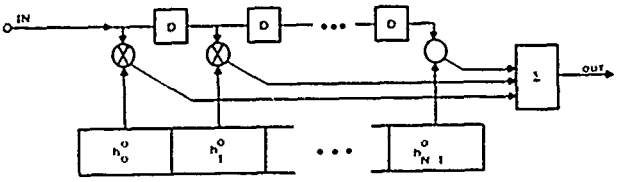

Figure 9. Block diagram of a one bit digital analog programmable filter.

SURFACE ACOUSTIC WAVE (SAW) BANDPASS FILTER REVIEW

R.C. Rosenfeld

Sawtek Incorporated
Orlando, Florida 32804

Summary

This paper briefly reviews the capabilities, applications, and advantages of SAW bandpass filters. Surface acoustic wave devices have been in systems for nearly 10 years and now offer a broad range of signal processing functions from delay lines to acousto-electric convolvers. However, this paper is limited to transversal bandpass filters and resonator filters. A typical SAW bandpass filter response is illustrated.

Advantages

Many of the SAW filter advantages are due to its physical structure. SAW filters are rugged and reliable. Because their operating frequencies are set by photolithographic processes, they do not require tuning nor become detuned in the field. Semiconductor type wafer processing which is used in SAW filter fabrication allows large volume production of economical and reproducible devices. Also, their performance capabilities are achieved with relatively small size and weight.

Transversal Bandpass Filter Capabilities

Table I lists transversal bandpass filter capabilities. SAW bandpass filters typically operate from 10 MHz to 1500 MHz. The low end is limited by the large size of the filters and the high end by the submicron resolution required for the electrode geometry. Presently, the majority of SAW filters are in the 20 to 400 MHz range. Above 1 GHz, electron-beam pattern generators are required for photomask construction; however, there are devices in production around 1.5 GHz.

Fractional bandwidths from 0.2% to 67% are available. The lower end is limited by the number of acoustic wavelengths that can be realized in a practical transducer length and the upper end by bulk wave interference and insertion loss. "Dispersive transducers" are used in the broad band filters.

Insertion loss varies from 2 dB to 6 dB in "low-loss" types of SAW filters and from 6 dB to 30 dB in conventional SAW filters. Conventional SAW filters are commonly mismatched to reduce the "triple-transit" spurious signal peculiar to SAW technology.

Sidelobe and spurious rejection of 40 to 70 dB can be achieved although 40 to 60 dB is common in lower shape-factor filters or very broad band filters. Bulk modes, diffraction, electromagnetic feedthrough, and other second-order affects limit rejection.

A most important capability of SAW filters is their excellent selectivity. Filters with shape factors as low as 1.15 have been in production for several years, although the majority of filters have 1.3 to 4.0 shape factors. Minimum achievable shape factor is limited by diffraction and other second-order affects.

Passband amplitude and phase ripple are typically 0.1 to 2 dB and 1 to 15 degrees, respectively. Triple transit, and in some cases, electromagnetic feedthrough are the primary cause of a fast ripple, while the matching network introduces a slow amplitude variation.

Triple transit and electromagnetic feedthrough are also the primary cause of group delay deviation across the passband. Deviation as low as 1 nsec has been achieved although 10 to 50 nsec is common in filters designed for precise group delay. Group delay deviation may be much higher in filters where it is not an important consideration.

Temperature dependence of the two most commonly used substrates are shown. Lithium niobate is used for wide band filters in which the 94 ppm/°C temperature coefficient is acceptable. Narrowband filters usually employ ST-Quartz which has a parabolic temperature dependence with a turnover point at room temperature. For example, at $\pm$ 50°C, the center frequency of a ST-Quartz filter would be changed 80 ppm.

Crystal length for a filter constructed from two equal length transducers is given in inches by approximatly 1/(2XTW) where the transition width (TW) is in MHz. Or, vice versa, this relation gives a minimum practical transition width of approximately 150 kHz for a 3.0 inch long crystal. As with all filter technologies, it is not possible to optimize all parameters simultaneously in one filter due to the interdependency of parameters

Transversal Filter Characteristics

To illustrate filter characteristics, the spectrum of a bandpass filter manufactured at Sawtek is shown in Figure 1. The filter is on ST-Quartz and is matched to 17 dB insertion loss by a series inductor at each port. The 3 dB fractional bandwidth is 4.5% and the rejection is 60 dB. The 60 dB to 3 dB shape factor is 1.9. Minimum rejection on the high side is limited to 60 dB by bulk modes.

The 3 dB bandwidth spectrum (Fig. 2) shows an amplitude ripple of 0.2 dB peak-to-peak, phase ripple of approximately 1.5 degrees with a 4.5 degree slow variation, and group delay ripple of 160 nsec. As mentioned before, this ripple is caused by triple-transit.

Filter Applications

The majority of SAW bandpass filter applications have been IF filters in government systems. A list of government systems that have employed SAW filters is given in Ref. 1. Included in that list is the Mariner satellite, now called Voyager I & II, that was launched in 1977 with a SAW bandpass filter on board. This filter has recently passed Jupiter and is now on its way to Saturn.

Commercial applications that employ SAW filters in production or prototype systems include the well-known TV IF filter, CATV filters, IF filters for satellite and earth microwave communications, avionics communication and distance measuring equipment, electrical instrumentation, and low-cost transceivers for energy management systems.

Resonator Bandpass Filters

SAW transversal filters can achieve fractional bandwidths as low as 0.2%. A relatively new SAW device, the SAW resonator filter can provide bandwidths from 0.2% down to 0.002%. The SAW resonator's electrical characteristics are similar to the crystal resonator, but the fabrication is similar to SAW transversal filter fabrication. Thus, it has the usual SAW advantages such as planar wafer processing, rugged and reliable construction and packaging, and small size. However, frequency trimming is necessary just as in crystal resonators.

Resonator Filter Characteristics

Table II lists resonator filter characteristics. The SAW resonator operates through the VHF and lower UHF frequency ranges and achieves losses as low as a few dB and rejection as high as 80 dB. Impedances are similar to those achieved in third overtone crystals: a minimum C_0/C_1 ratio of approximately 1,500 and motional inductance from 1000 to 100 uh. Its temperature stability, unfortunately, is not as good as the crystal resonator AT-cut quartz, as shown by two points on its parabolic temperature curve in Table II. However, the temperature stability is adequate for many narrowband filter applications. Aging has been demonstrated under 1 ppm/year, but is typically in the 1 to 10 ppm range, at this time.

State-of-the-art SAW resonator filter characteristics have been demonstrated in a paper by L.A. Coldren and R.L. Rosenburg. A 4-pole filter response derived by cascading two 2-section resonators at a center frequency of 75.14 MHz achieved spurious rejection of almost 80 dB. Applications for filters with these characteristics include higher frequency IF filter and low-loss front-end filters. In narrowband receivers, possibly all of the filtering could be achieved at the front end.

Future Developments

In conclusion, important future developments in SAW bandpass filter technology are widespread application of SAW resonator filters, volume production of low-loss transversal filters, increased use of multiple bandwidth and multiple frequency filter banks, 1 to 2 GHz filters including shallow-bulk acoustic wave filters, and resonator and delay line UHF oscillators. (Several of these topics are covered in the SAW session of this symposium). Finally, an important breakthrough for SAW technology, especially for resonators, would be the discovery of a new temperature stable orientation of quartz.

Acknowledgement

The author is grateful to L.A. Coldren and R.L. Rosenburg of Bell Labs for providing a slide of their 4-pole resonator filter that was used in the panel presentation and to his colleagues at Sawtek for their suggestions and help in preparing this paper.

References

1. R.C. Williamson, "Case Studies of Successful Surface Acoustic Wave Devices," 1977 Ultrasonics Symposium Proc., IEEE CAT. #77CH1264-ISU, pp. 460-468.

2. Larry A. Coldren and Robert L. Rosenberg, "Surface Acoustic Wave Resonator Filters," Proc. IEEE (Special Issue on Miniaturized Filters), Vol. 67, pp. 147-158, Jan. 1979.

Table I

SAW Transversal Bandpass Filter Capabilities

Frequency	10 - 1500	MHz
Fractional Bandwidth	0.2 - 67	%
Insertion Loss	2 - 30	dB
Rejection	40 - 70	dB
Shape Factor	1.15 - 4	40 dB/3 dB
Passband Ripple	0.1 - 2	dB
Phase Ripple	1 - 15	degrees
Group Delay Deviation	1 - 500	nsec.
Temperature Dependence	94 ppm/°C -80 ppm/±50°C	$LiNbO_3$ ST-Quartz
Crystal Length	1/(2xTW)	inches

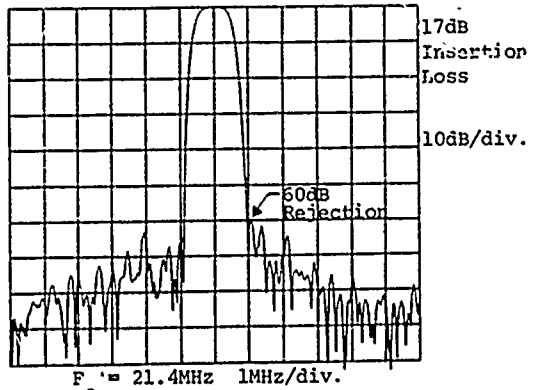

Fig. 1. SAW Transversal Bandpass Filter Frequency Response

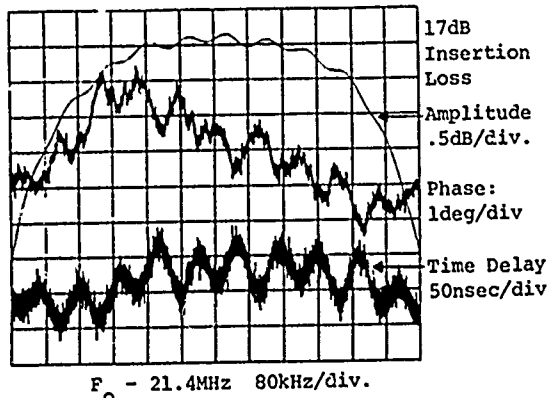

Fig. 2 SAW Transversal Bandpass Filter Spectral Response over 3dB Bandwidth

Table II.

SAW Resonator Bandpass Filter Capabilities

Frequency	40 - 1000 MHz
Fractional Bandwidth	0.002 - 0.2%
Insertion Loss	1 - 20 dB
Rejection	20 - 80 dB
Impedance	Similar to 3rd Overtone Crystal Filters
Temperature Dependence	-20 ppm/±25°C -80 ppm/±50°C
Aging	1 - 10 ppm/year

MECHANICAL FILTERS

E. M. Frymoyer, Ph.D.

Rockwell International
Electronic Devices Division
Newport Beach, California

Summary

Mechanical Filters have been an industry standard for single sideband selectivity for 28 years. Recent advances in production technology and in construction techniques have contributed to make the Mechanical Filter a cost and size effective and reliable technology for HF communications, control systems and telephone analog multiplex systems. New developments are resulting in tight delay control for applications in HF networks carrying high density data traffic.

The Collins Disc-Wire Mechanical Filter was developed in 1950 and became a production device in 1952. The disc-wire filter was applied to the 12-channel, 60-108KHz Frequency Division Multiplex System in 1957 and in the same year, other Mechanical Filters by Telefunken and Kokusai. In 1972, the single filter premodulated FDM system was placed in production by Rockwell-Collins with disc-wire filters (Fig. 1) and Siemens with bar-flexure mechanical filters. In 1978, Fujitsu and NEC applied torsional mode premodulation mechanical filters at 128KHz to the FDM Service. These dates are summarized in Table I.

Acoustic bandpass Filter technologies span the center frequency range from 500Hz to 600MHz in commercially available technologies outlined in Fig. 2. These include Mechanical Tuning Fork, Bar Flexure, Torsional and Disc Wire through Quartz Crystal Filters in various forms to the relatively new production Surface Acoustic Wave technologies.

The Disc Wire Filter achieves a highly stable and repeatable ladder filter by coupling discs fabricated from specially formulated nickel-iron alloys by means of similar composition wires welded to the disc. This achieves the acoustic analog of the electrical network as shown in Fig. 3. The low frequency technology is achieved by coupling thickness flexure bars with coupling wires in torsion at the flexural nodal points. The range of application as bandwidth percent over center frequency range is also shown.

A principal current application of the disc wire technology is to the Frequency Division Multiplex System premodulation modem shown in Fig. 4.[1] Here a single filter is employed with a 256KHz carrier frequency in a premodulation method used so that a single filter rather than 12 separate channel filters may be manufactured.

For in-band signaling, a lower sideband 6-pole, two zero realization is used as shown in Fig. 5. The finite zeros are produced by the bridging wires. The response is shown in Fig. 6 as the solid curve. The low pass filter at audio frequency supplies the sharp lower (after reflection) cut-off of the filter. This allows tight, extremely reproducible and cost effective channel modems to be manufactured. An added benefit is that delay equalization may be added at the audio frequency resulting in extremely tight delay control. For the out-of-band signaling case, a 7-pole, two zero bridge filter is used as shown in Fig. 7. The main effect is a sharper cut-off. In both cases, in-band ripple is ±0.2dB. To date, more than 250,000 of these filters have been produced.

Performance

The stability of the mechanical filter with temperature is controlled by the temperature coefficient of the heat treated nickel-iron alloy material shown in Fig. 8. The nominal shift is shown as the solid lines with data points superimposed. The range of the shift is 70Hz positive over -55°C to +100°C. Over the range -30°C to +50°C, 30 to 40Hz is a more typical shift. The curve may be modified by cold working and heat treating to be optimum for a specific temperature range.

The manufacturing process variations are superimposed on this basic material behavior. In the accompanying Table II, this is shown for measurements made over several thousand of commercial 455KHz single sideband filters. The filters employed ferrite transducers. Shown are the average values at room temperature, the shift maximum and minimum over the temperature range and the maximum shift of any filter of the sample from that at 25°C. The lower 3dB point stability shows the basic material characteristics and the remaining values, especially the small change in response

variation demonstrates the stability of the high production manufacturing processes which are largely computer controlled.

Low Frequency Filters

In addition to the 3825Hz telephone signaling application, large numbers of these low frequency bar-flexure filters are used by many equipment manufacturers for Omega Navigation receivers. The excellent temperature stability, low aging and dynamic range, allow very selective, yet low loss front-end filters to be fabricated. Fig. 9 and Fig. 10 show the temperature stability both of the stop and passbands of these filters.

Delay Correction

Many analog voice channel communications systems today are being used to carry data traffic. Here the desired sharp cut-off achievable with high Q resonators using mechanical resonant elements cause delay distortion. Chebyshev and other finite pole realizations have in any case significant delay distortion. This can be greatly reduced economically if a mechanical single sideband filter such as the channel filter discussed above is used together with a easily reproducible low pass filter at audio. The stability and repeatability of this combination allows an audio delay equalizer made from active RC technology to be cascaded with it. The tight, low ripple, rapid cut-off of the combination is shown in Fig. 11 as the equivalent response at the intermediate frequency. The 6-section active RC equalizer in cascade reduces differential delay variation from 1000ms to ±100ms over the equivalent audio band 200 to 3200Hz.

References

1. Johnson, R.A., and Winget, W.A., "FDM Equipment Using Mechanical Filters," Proc. 1974 IEEE ISCAS, San Francisco, CA, April 1974, pp. 127-131.

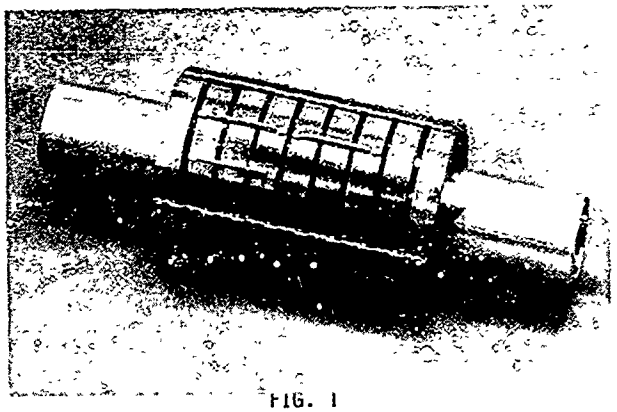

FIG. 1

DISC WIRE MECHANICAL FILTER FOR ROCKWELL-COLLINS MX-108 FREQUENCY DIVISION MULTIPLEX

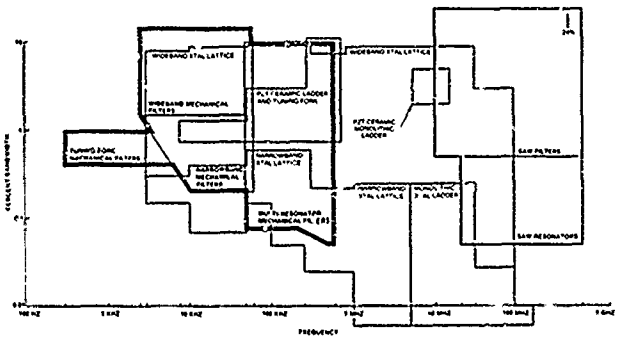

FIG. 2

ACOUSTIC FILTERS SPAN THE FREQUENCY BANDWIDTH SPACE

- 1952 • ROCKWELL-COLLINS HF RADIO MECHANICAL FILTERS
- 1957 • ROCKWELL-COLLINS TELEPHONE CHANNEL FILTERS
- 1957 • KOKUSAI AND TELEFUNKEN FILTERS
- 1972 • ROCKWELL-COLLINS MX-108 PREMODULATION CHANNEL FILTERS
- 1972 • SIEMENS 48 KHZ PREMODULATION CHANNEL FILTERS
- 1978 • NEC AND FUJITSU 128 KHZ CHANNEL FILTERS

TABLE I MECHANICAL FILTER PRODUCTION MILESTONES

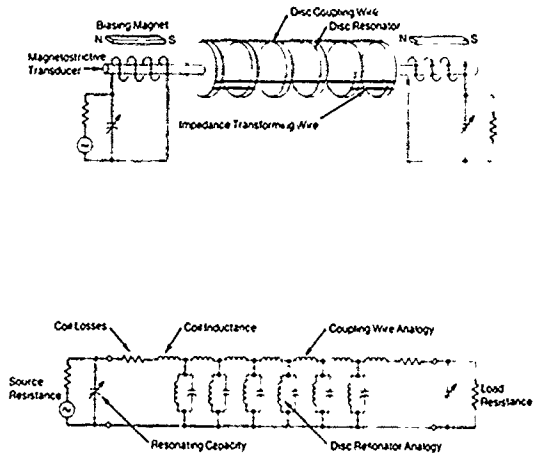

FIG. 3 MECHANICAL FILTER ACOUSTICAL ANALOGY

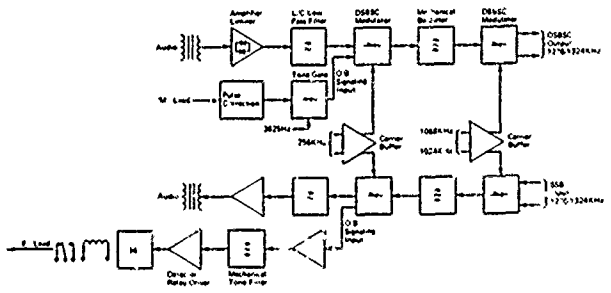

FIG. 4 FDM PREMODULATION SCHEME

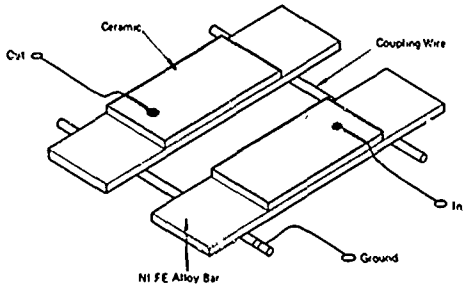

FIG. 3A LOW FREQUENCY PHYSICAL STRUCTURE

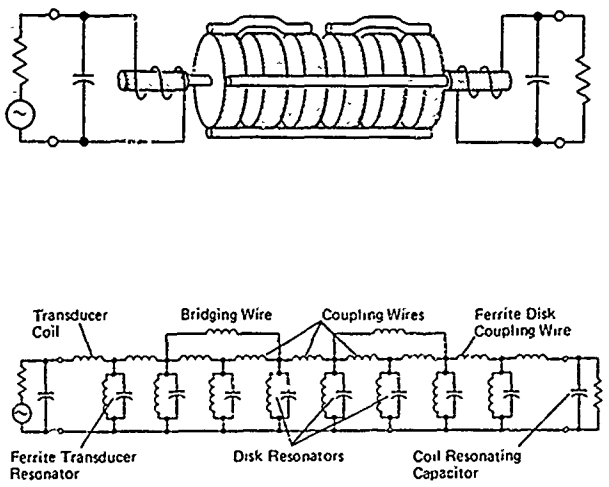

FIG. 5 6-POLE, 2 ZERO FDM MECHANICAL FILTER

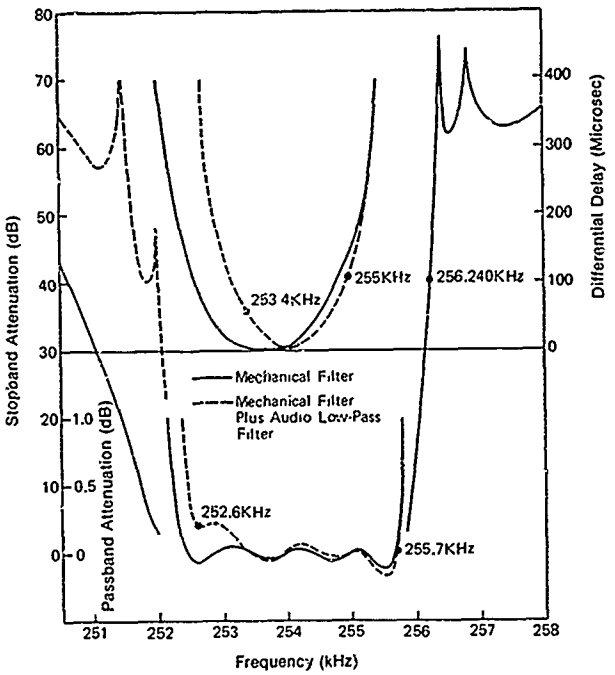

FIG. 6
RESPONSE OF FDM MODEM IN ADVANCED SIGNALING CASE

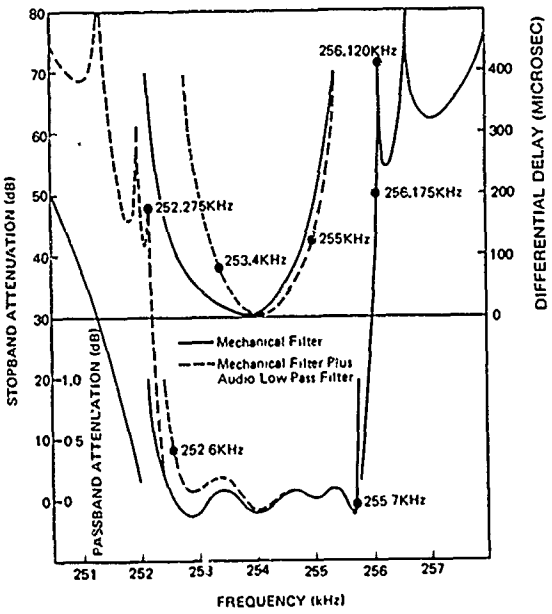

FIG. 7
RESPONSE OF FDM MODEM IN OUT-OF-BAND SIGNALING CASE

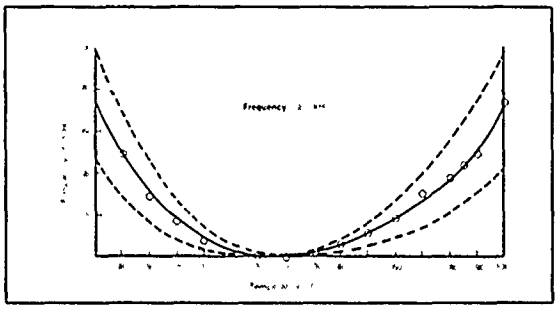

FIG. 8
DISC RESONATOR FREQUENCY SHIFT CHARACTERISTICS

Parameter	+25°C	-30°C to +50°C		Maximum Δ from 25°C
	Average Value	Minimum Value	Maximum Value	
Response Variation in dB	0.88	0.4	2.1	1.22
Insertion Loss in dB	2.7	2.4	4.1	1.40
3 dB Bandwidth in Hz	2152	2070	2230	82
60 dB Bandwidth in Hz	4342	4210	4480	138
Frequency in kHz of Low Side 3 dB Point	455.392	455.350	455.450	58
Frequency in kHz of High Side 3 dB Point	457.541	457.450	457.640	99
Frequency in kHz of Low Side 60 dB Point	454.305	454.170	454.400	135
Frequency in kHz of High Side 60 dB Point	458.624	458.480	458.770	146

TABLE II

TYPICAL COMMERCIAL TEMPERATURE VARIATIONS FOR DISC WIRE MECHANICAL FILTERS - ACTUAL PRODUCTION AVERAGES

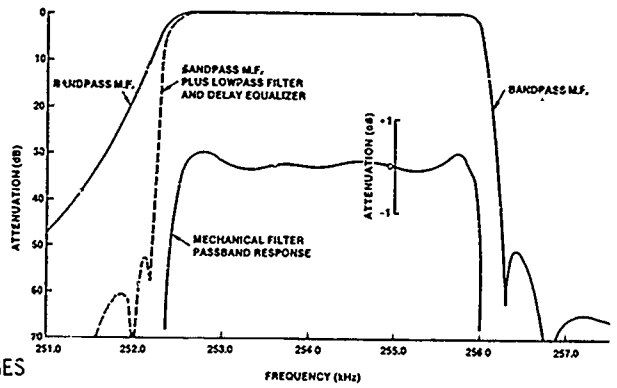

FIG. 11

AMPLITUDE RESPONSE OF DELAY CONTROLLED MODEM USING MECHANICAL FILTER LOW PASS FILTER AND 6-SECTION ACTIVE EQUALIZER

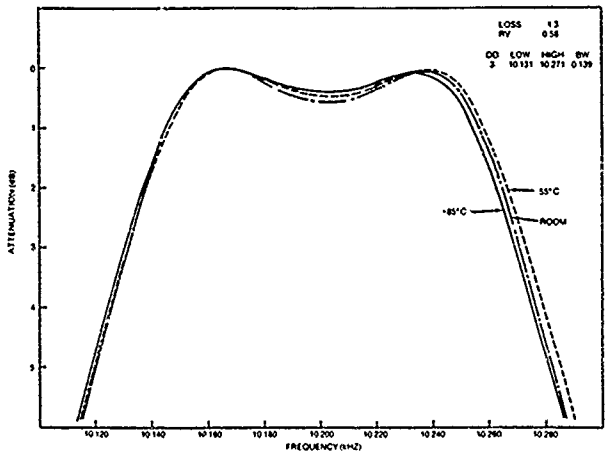

FIG. 9

LINEAR PLOT OF TEMPERATURE VARIATION OF OMEGA LOW FREQUENCY MECHANICAL FILTERS - PASSBAND

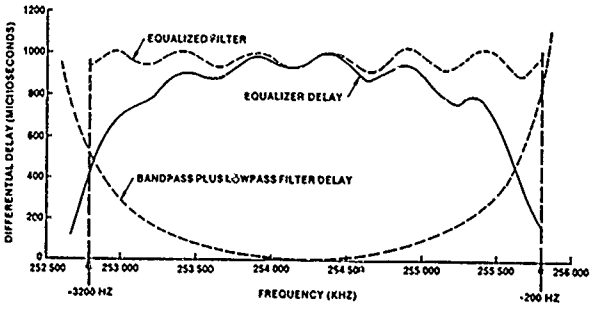

FIG. 12

DELAY RESPONSE OF DELAY CONTROLLED MODEM USING MECHANICAL FILTER LOW PASS FILTER AND 6-SECTION ACTIVE EQUALIZER

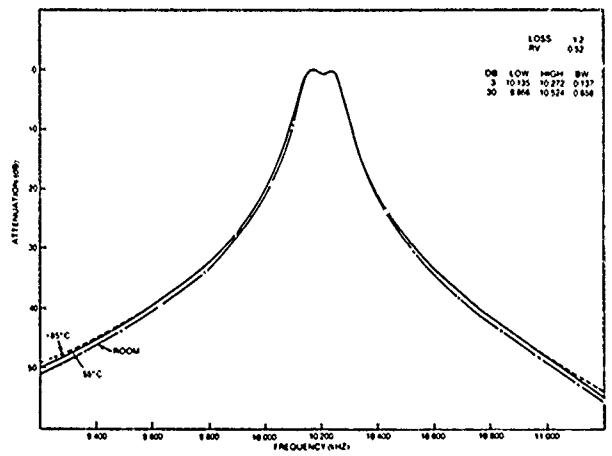

FIG. 10

LOGARITHMIC STOPBAND PLOT OF TEMPERATURE VARIATION OF OF OMEGA LOW FREQUENCY MECHANICAL FILTERS

TEMPERATURE INDUCED FREQUENCY CHANGES IN ELECTRODED CONTOURED QUARTZ CRYSTAL RESONATORS

B.K. Sinha and H.F. Tiersten

Department of Mechanical Engineering, Aeronautical Engineering & Mechanics
Rensselaer Polytechnic Institute, Troy, New York 12181

Abstract

A system of approximate equations recently obtained for the determination of thermal stresses in electroded piezoelectric plates is applied to contoured AT-cut quartz crystal resonators. The changes in resonant frequency resulting from the thermally induced biasing stresses and strains are determined from an equation for the first perturbation of the eigenvalue of the piezoelectric solution due to a bias. The changes in resonant frequency with temperature are calculated for the fundamental and some of the anharmonic overtones of the fundamental and some of the harmonic overtone thickness modes, which were obtained in a recent analysis of overtone modes in contoured crystal resonators.

1. Introduction

A perturbation analysis of the linear electroelastic equations for small fields superposed on a bias has been performed[1]. The change in resonant frequency due to any bias such as, e.g., a residual stress may readily be obtained from the resulting equation for the first perturbation of the eigenvalue if the bias is known. In addition, a system of approximate plate equations for the determination of thermal stresses in thin piezoelectric plates coated with large much thinner films was derived[2]. The resulting approximate equations simplify the treatment of many thermal stress problems considerably, and the three-dimensional detail not included in the approximate description is not deemed to be important for our purposes. Furthermore, an analysis of contoured AT-cut quartz crystal resonators vibrating in the usual coupled thickness-shear and thickness-twist modes has been performed[3,4], and it has been shown[3,4] that the calculations of the fundamental and the anharmonic overtones of the fundamental and each harmonic overtone thickness mode agree extremely well with experiment.

In this paper the aforementioned system of approximate static thermoelastic plate equations for the anisotropic plated crystal plate is applied to contoured AT-cut quartz plates with large circular electrodes. As in the earlier work[3], the simple solution of the approximate plate equations for the thermally induced deformation field holds for large electrodes of essentially arbitrary shape. The approximate three-dimensional displacement field resulting from the solution of the plate equations is readily determined from the description. The substitution of this three-dimensional displacement field into the above mentioned equation for the first perturbation of the eigenvalue[1] along with the recently obtained solution[3,4] for the vibrating modes in contoured quartz crystal resonators enables the calculation of the temperature dependence of the resonant frequencies of electroded contoured AT-cut quartz crystal resonators due to the thermally induced biasing deformation. The change in frequency with temperature resulting from the newly defined temperature derivatives of the fundamental elastic constants of quartz[5,6] is calculated from the equation for the frequency of the modes in contoured resonators[3,4]. The combination of the two changes yields the actual change in frequency with temperature of the contoured resonator. The results of calculations for gold electrodes on contoured AT-cut quartz resonators for various harmonic and anharmonic modes, different film thickness and different curvatures are presented. Among other things, the apparent shift in angle of the zero temperature cut for the contoured resonator is calculated for the first, third and fifth harmonic.

2. Perturbation Equations

For purely elastic nonlinearities the equation for the first perturbation of the eigenvalue obtained from the perturbation analysis[1] mentioned in the Introduction may be written in the form

$$\Delta_\mu = H_\mu/2\omega_\mu, \quad \omega = \omega_\mu - \Delta_\mu, \tag{2.1}$$

where ω_μ and ω are the unperturbed and perturbed eigenfrequencies, respectively, and

$$H_\mu = -\int_V \tilde{K}^n_{L\gamma} g^\mu_{\gamma,L}\, dV, \tag{2.2}$$

where V is the undeformed volume of the piezoelectric plate at the reference temperature T_0. In (2.2) g^μ_γ denotes the normalized mechanical displacement vector, and $\tilde{K}^n_{L\gamma}$ denotes the portion of the Piola-Kirchhoff stress tensor resulting from the biasing state in the presence of the g^μ_γ, and is given by

$$\tilde{K}^n_{L\gamma} = \hat{c}_{L\gamma M\alpha}\, g^\mu_{\alpha,M}, \tag{2.3}$$

where

$$\hat{c}_{L\gamma M\alpha} = T^1_{LM}\delta_{\gamma\delta} + c_{3L\gamma M\alpha AB}E^1_{AB} + c_{2L\gamma KM}w_{\alpha,K} + c_{2LKM\alpha}w_{\gamma,K}\,, \tag{2.4}$$

and

$$T^1_{LM} = c_{2LMKN}E^1_{KN} - \nu_{LM}(T-T_o)\,,$$
$$E^1_{KN} = \frac{1}{2}\,(w_{K,N} + w_{N,K})\,. \tag{2.5}$$

The quantities T^1_{LM}, E^1_{AB} and w_K denote the static biasing stress, strain and displacement field, respectively. Thus, in this description the present position $\underset{\sim}{x}$ is related to the reference position $\underset{\sim}{X}$ by

$$\underset{\sim}{x}(X_L,t) = \underset{\sim}{X} + \underset{\sim}{w}(X_L) + \underset{\sim}{u}(X_L,t)\,. \tag{2.6}$$

The coefficients c_{LMKN} and $c_{3L\gamma M\alpha AB}$ denote the second and third order elastic constants, respectively, ν_{LM} denotes the thermoelastic coupling coefficients and T denotes the present temperature.

The normalized eigensolution g^μ_γ and $\hat{f}^\mu$ is defined by

$$g^\mu_\gamma = \frac{u^\mu_\gamma}{N_\mu}\,,\quad \hat{f}^\mu = \frac{\tilde{\varphi}^\mu}{N_\mu}\,,\quad N^2_\mu = \int_V \rho u^\mu_\gamma u^\mu_\gamma\,dV\,, \tag{2.7}$$

where u^μ_γ and $\hat{\varphi}^\mu$ are the mechanical displacement and electric potential, respectively, which satisfy the equations of linear piezoelectricity

$$\tilde{K}^\ell_{L\gamma} = c_{2L\gamma M\alpha}u_{\alpha,M} + e_{ML\gamma}\tilde{\varphi}_{,M}\,,$$
$$\tilde{D}^\ell_L = e_{LM\gamma}u_{\gamma,M} - \epsilon_{LM}\tilde{\varphi}_{,M}\,, \tag{2.8}$$
$$\tilde{K}^\ell_{L\gamma,L} = \rho\ddot{u}_\gamma\,,\quad \tilde{D}^\ell_{L,L} = 0\,, \tag{2.9}$$

subject to the appropriate boundary conditions, and ρ is the mass density. Equations (2.8) are the linear piezoelectric constitutive relations and (2.9) are the stress equations of motion and charge equation of electrostatics, respectively. The upper cycle notation for many dynamic variables and the capital Latin and lower case Greek index notation is being employed for consistency with Ref.1, as is the remainder of the notation in this section.

3. Temperature Induced Biasing State

A schematic diagram of the electroded contoured crystal plate is shown in Fig.1 along with the associated coordinate system. It has been shown[2] that referred to this coordinate system the static purely extensional thermoelastic plate equations for the plated crystal plate may be written in the form

$$\mathcal{N}^{(0)}_{AB,A} = 0\,,\quad \mathcal{N}^{(2)}_{AB,A} = 0\,, \tag{3.1}$$

where A, B, C, D take the values 1 and 3 and skip 2 and $\mathcal{N}^{(0)}_{AB}$ and $\mathcal{N}^{(2)}_{AB}$ are the zero and second order plate stress resultants, respectively, for the electroded crystal plate. For homogeneous temperature states and identical electrodes on the upper and lower surfaces the extensional constitutive equations may be written in the form

$$\mathcal{N}^{(0)}_{AB} = 2h\Big(\gamma_{ABCD} + \frac{2h'}{h}\,\gamma'_{ABCD}\Big)E^{(0)}_{CD} + 2h^3\Big(\frac{1}{3}\,\gamma_{ABCD} + \frac{2h'}{h}\,\gamma'_{ABCD}\Big)E^{(2)}_{CD} - 2h\Big(\beta_{AB} + \frac{2h'}{h}\,\nu^{*\prime}_{AB}\Big)(T-T_o)\,,$$
$$\mathcal{N}^{(2)}_{AB} = \frac{2}{3}\,h^3\Big(\gamma_{ABCD} + \frac{6h'}{h}\,\gamma'_{ABCD}\Big)E^{(0)}_{CD} + \frac{2}{5}\,h^5\Big(\gamma_{ABCD} + \frac{10h'}{h}\,\gamma'_{ABCD}\Big)E^{(2)}_{CD} - \frac{2}{3}\,h^3\Big(\beta_{AB} + \frac{6h'}{h}\,\nu^{*\prime}_{AB}\Big)(T-T_o)\,, \tag{3.2}$$

where

$$k_{WS} = c^{-1}_{WV}c_{VS}\,,\quad \zeta_W = c^{-1}_{WV}\nu_V\,, \tag{3.3}$$

in the compressed notation and we have introduced the usual compressed matrix notation[7] for tensor indices according to the scheme

$$R,S = 1,3,5\,;\quad W,V = 2,4,6\,, \tag{3.4}$$

and

$$\gamma_{RS} = c_{RS} - c_{RW}c^{-1}_{WV}c_{VS}\,,\quad \beta_R = \nu_R - c_{RW}c^{-1}_{WV}\nu_V\,. \tag{3.5}$$

The γ_{RS} are Voigts' anisotropic plate elastic constants and the β_R are the associated anisotropic plate thermoelastic constants. For the case of anisotropic extension considered here the three-dimensional strains E_{KL}, which are needed in the perturbation equation, are related to the plate strains by

$$E_{KL} = \frac{1}{2}\,(w_{K,L} + w_{L,K}) = E^{(0)}_{KL} + X_2E^{(2)}_{KL}\,. \tag{3.6}$$

The plate strains $E^{(n)}_{AB}$ $(n = 0,2)$, which occur in (3.2), are given by

$$E^{(n)}_{AB} = \frac{1}{2}\,(w^{(n)}_{A,B} + w^{(n)}_{B,A})\,, \tag{3.7}$$

and the remaining plate strains, which are needed in (3.6) as well, may be obtained from

$$E^{(0)}_W = -\,c^{-1}_{WV}c_{VS}E^{(0)}_S + c^{-1}_{WV}\nu_V(T-T_o)\,,$$
$$E^{(2)}_W = -\,c^{-1}_{WV}c_{VS}E^{(2)}_S\,. \tag{3.8}$$

In Fig.1, the X_2-coordinate axis is normal to the flat major surface of the plate at $T = T_o$. Since the outside edges of the plate are traction free, we have

$$\hat{N}_A\mathcal{N}^{(0)}_{AB} = 0\,,\quad \hat{N}_A\mathcal{N}^{(2)}_{AB} = 0 \quad \text{on outside edges,} \tag{3.9}$$

where $\hat{N}_A$ denotes the outwardly directed unit normal to the edge of the plate at $T = T_o$. From (3.1) and (3.9) we have

$$\mathcal{N}^{(0)}_{AB} = 0\,,\quad \mathcal{N}^{(2)}_{AB} = 0\,, \tag{3.10}$$

for the unelectroded portion of the plate. Since at the junction between the electroded and unelectroded regions of the plate we have the continuity of

$$N_A\mathcal{N}^{(0)}_{AB}\,,\quad N_A\mathcal{N}^{(2)}_{AB}\,, \tag{3.11}$$

where N_A denotes the outwardly directed unit normal to the edge of the electrode at $T = T_o$, the solution satisfying (3.11), (3.10) and (3.1) takes the form

$$\chi_{AB}^{(0)} = 0, \quad \chi_{AB}^{(2)} = 0 \text{ everywhere.} \tag{3.12}$$

This solution is unique to within static homogeneous plate rotations of zero and second order. Substituting from (3.2) into (3.12), we obtain

$$\left(\gamma_{RS} + \frac{2h'}{h}\gamma'_{RS}\right)E_S^{(0)} + h^2\left(\frac{\gamma_{RS}}{3} + \frac{2h'}{h}\gamma'_{RS}\right)E_S^{(2)} = \left(\beta_R + \frac{2h'}{h}\nu_R^{*\prime}\right)(T - T_o),$$

$$\left(\gamma_{RS} + \frac{6h'}{h}\gamma'_{RS}\right)E_S^{(0)} + h^2\left(\frac{3}{5}\gamma_{RS} + \frac{6h'}{h}\gamma'_{RS}\right)E_S^{(2)} = \left(\beta_R + \frac{6h'}{h}\nu_R^{*\prime}\right)(T - T_o). \tag{3.13}$$

Equations (3.13) constitute six homogeneous linear equations which may readily be solved for the six plate strains $E_S^{(0)}$ and $E_S^{(2)}$. Note that Eq. (3.13) holds for the slowly varying h of the contoured resonator. When $E_S^{(0)}$ and $E_S^{(2)}$ have been determined from (3.13), $E_W^{(0)}$ and $E_W^{(2)}$ are readily determined from (3.8). Then the three-dimensional biasing strain can be obtained from (3.6), which is for anisotropic extension, and the curvature of the contoured crystal is assumed to be sufficiently small that flexural biasing deformations can be neglected for the plano-convex resonator with identical electrodes subject to a homogeneous temperature change $(T - T_o)$.

It is well known that in static linear elasticity the solution to a boundary value problem is unique only to within a static homogeneous (global) infinitesimal rigid rotation[8]. In addition, the change in frequency due to a homogeneous infinitesimal rigid rotation has been shown to vanish[2]. Consequently, without any loss in generality, we may select the homogeneous rigid rotation to take any value that is convenient and in particular to vanish. Accordingly, we take

$$\Omega_{KL}^1 = \frac{1}{2}(w_{L,K} - w_{K,L}) = 0, \tag{3.14}$$

which with (3.6) yields

$$w_{L,K} = E_{KL} = E_{KL}^{(0)} + X_2^2 E_{KL}^{(2)}, \tag{3.15}$$

which provides the biasing displacement gradients $w_{K,N}$ as a known linear function of $(T - T_o)$. Thus, we may now obtain $\hat{c}_{LYMQ}$ in (2.4) as a known linear function of $(T - T_o)$.

4. Eigenmodes in Contoured Resonators

Referred to the coordinate system in Fig. 1, it has been shown[3,4] that the eigensolutions for coupled thickness-shear and thickness-twist vibrations in contoured rotated Y-cut quartz resonators can be written in the form

$$u_{1nmp} = \sin\frac{n\pi X_2}{2h}\, u_{nmp} e^{i\omega_{nmp}t}, \tag{4.1}$$

where

$$u_{nmp} = A^{nmp}\, e^{-\alpha_n \frac{X_1^2}{2}} H_m(\sqrt{\alpha_n}X_1) e^{-\beta_n \frac{X_3^2}{2}} H_p(\sqrt{\beta_n}X_3), \tag{4.2}$$

and along with u_1 we have

$$\varphi = \frac{e_{26}}{\epsilon_{22}} u_{nmp}\left(\sin\frac{n\pi X_2}{2h} - (-1)^{\frac{n-1}{2}}\frac{X_2}{h}\right)e^{i\omega_{nmp}t}, \tag{4.3}$$

where for the modes of interest[3,4]

$$n = 1,3,5, \ldots; \quad m,p = 0,2,4 \ldots\ldots. \tag{4.4}$$

In (4.2) H_m and H_p are Hermite polynomials and

$$\alpha_n^2 = \frac{n^2\pi^2\hat{c}_{66}}{8Rh_o^3 M_n}, \quad \beta_n^2 = \frac{n^2\pi^2\hat{c}_{66}}{8Rh_o^3 c_{55}}, \tag{4.5}$$

where

$$M_n = c_{11} + (c_{12} + c_{66})\, r + 4\,\frac{(r\bar{c}_{66} - c_{66})(c_{22}r + c_{12})\cot\kappa n\pi/2}{c_{22}n\pi\kappa},$$

$$\bar{c}_{66} = c_{66} + \frac{e_{66}^2}{\epsilon_{22}}, \quad \hat{c}_{66} = \bar{c}_{66}\left(1 - \frac{8k_{26}^2}{n^2\pi^2} - 2\hat{R}\right), \tag{4.6}$$

$$k_{25}^2 = \frac{e_{26}^2}{\bar{c}_{66}\epsilon_{22}}, \quad \hat{R} = \frac{2\rho' h'}{\rho h}, \quad \kappa = \sqrt{\frac{\bar{c}_{66}}{c_{22}}}, \quad r = \frac{c_{12} + c_{66}}{\bar{c}_{66} - c_{22}},$$

and ρ and ρ' are the mass densities of the quartz and the electrodes, respectively, and c_{11}, c_{12}, c_{66}, c_{22}, e_{26} and ϵ_{22} are elastic, piezoelectric and dielectric constants, respectively. The eigenfrequencies corresponding to the eigensolutions in (4.1) with (4.2) are given by[3,4]

$$\omega_{nmp}^2 = \frac{n^2\pi^2\hat{c}_{66}}{4h_o^2\rho}\left[1 + \frac{1}{n\pi}\sqrt{\frac{2h_o}{R}}\left(\sqrt{\frac{M_n}{\hat{c}_{66}}}(2m+1) + \sqrt{\frac{c_{55}}{\hat{c}_{66}}}(2p+1)\right)\right]. \tag{4.7}$$

In addition to u_{1nmp} given in (4.1) there is a u_{2nmp}[3,4], which is derived[9] from u_{1nmp} and is an order of magnitude smaller than u_{1nmp} but is required in this work anyway. However, since the discussion of the relation of u_{2nmp} is unusually cumbersome, it is being omitted from this work[10].

From this unperturbed eigensolution for the contoured crystal plate we can determine the normalized eigensolution we need for the perturbation formulation in Sec. 2 simply by writing

$$q_1 = u_1/N, \quad f = \varphi/N, \tag{4.8}$$

where, for $A^{nmp} = 1$, we obtain[9]

$$N^2 = \rho\pi h_o 2^m m!\; 2^p p!/\sqrt{\alpha_n}\sqrt{\beta_n}. \tag{4.9}$$

In obtaining Eq. (4.9) we have replaced 2h by $2h_o$ since the eigensolutions are sharply confined in the vicinity of the center of the contoured plate and

have negligible amplitudes at relatively small values of X_1 and X_3.

5. Temperature Dependence of Resonant Frequency

The change in the resonant frequency with temperature of any electroded contoured rotated Y-cut quartz plate resulting from the thermally induced biasing deformation may now be determined from (2.1), which we rewrite here for any one mode in the form

$$\Delta_M = H_M/2\omega_M, \quad \omega = \omega_M - \Delta, \tag{5.1}$$

where for the case of coupled thickness-shear and thickness-twist vibrations of contoured resonators considered here we have[9]

$$H_M = -\int_{-\ell}^{\ell} dX_1 \int_{-\ell}^{\ell} dX_3 \int_{-h}^{h} dX_2 (\tilde{K}^n_{L1} g^n_{1,L} + \tilde{K}^n_{22} g^n_{2,2}), \tag{5.2}$$

since $g_{3,L}$ and $g_{2,1}$ and $g_{2,3}$ are negligible[9]. From (2.3) for the mode being perturbed here, we have

$$\tilde{K}^n_{L1} = \hat{c}_{L1K1} g^M_{1,K} + \hat{c}_{L122} g^M_{2,2},$$
$$\tilde{K}^n_{22} = \hat{c}_{22K1} g^M_{1,k} + \hat{c}_{2222} g^M_{2,2}; \tag{5.3}$$

where $\hat{c}_{L\gamma K\alpha}$ is known as a linear expression in $(T - T_0)$ from the analysis in Sec.3. Although the change in the elastic constants with temperature,

$$\Delta c_{2L\gamma K\alpha} = (dc_{2L\gamma K\alpha}/dT)(T - T_0), \tag{5.4}$$

can in principle be included in the perturbation integral (5.2) simply by including them in (5.3), it is not at all purposeful to do this[9] because of the nature of the procedure employed[3,4,11,12] in obtaining the approximate solution for the vibrational modes in the contoured resonator. Instead, it is more profitable to obtain the change in frequency $\delta\omega$ with temperature due to the change in the elastic constants with temperature simply by differentiating (4.7) with respect to temperature[9]. The $\delta\omega$ thus determined must be subtracted[9] from the Δ_M obtained from (5.1) in order to obtain the total change in resonant frequency $\Delta\omega$ with temperature of the electroded contoured rotated Y-cut quartz plate. The $dc_{2L\gamma K\alpha}/dT$ are obtained from the first temperature derivatives of the fundamental elastic constants of quartz[5,6] $d\tilde{c}_{0EFG}/dT$ referred to the principal axes by the tensor transformation relation

$$\frac{d}{dT} c_{2L\gamma K\alpha} = a_{LD} a_{\gamma E} a_{KF} a_{\alpha G} \frac{d}{dT} \tilde{c}_{2DEFG}, \tag{5.5}$$

where the $a_{\gamma\varepsilon}$ are the matrix of direction cosines for the transformation from the principal axes to the coordinate system containing the axes referred to the contoured plate. When the conventional IEEE notation[13] for doubly-rotated plates is written in the form $(Y,X,w,\ell)\varphi,\theta$, where $\psi = 0$, the rotation angles φ and θ are the first two Euler angles, and for the AT-cut[14], $\varphi = 0°$ and $\theta = 35.25°$, from which the $a_{\alpha G}$ can be determined. Clearly, the transformation relations for the second and third order elastic, piezoelectric and dielectric constants, and coefficients of linear expansion may be written in the respective forms

$$c_{2KLMN} = a_{KD} a_{LE} a_{MF} a_{NG} \tilde{c}_{2DEFG}$$
$$c_{3KLMNAB} = a_{KD} a_{LE} a_{MF} a_{NG} a_{AH} a_{BI} \tilde{c}_{3DEFGHI},$$
$$e_{KLM} = a_{KD} a_{LE} a_{MF} \tilde{e}_{DEF}$$
$$\epsilon_{KL} = a_{KM} a_{LN} \tilde{\epsilon}_{MN}, \quad \alpha_{KL} = a_{KM} a_{LN} \tilde{\alpha}_{MN}, \tag{5.6}$$

where the tensor quantities with the upper cycle are referred to the principal axes of the crystal.

The resonant frequency, called ω_M here, for the particular unperturbed mode of interest is calculated from (4.7), and the associated mode shape shape[9,10] is obtained from (4.1) and (4.2), with (4.4) and (4.5). Then the perturbation integral H_M is evaluated by employing (5.3) and $(4.8)_1$ in (5.2) and performing the integrations[9], after which $\delta\omega$ is obtained from (4.7). Then the actual change in frequency with temperature $\Delta\omega$ is obtained from the relation[9]

$$\Delta\omega = \Delta_M - \delta\omega. \tag{5.7}$$

Calculations have been performed using the known values of the second order elastic, piezoelectric and dielectric constants of quartz[15], the third order elastic[16] and thermoelastic[17] constants of quartz and the recently obtained[5,6] temperature derivatives of the fundamental elastic constants of quartz. The results of the calculations are presented in Figs.2 - 5 and Table I. Figure 2 shows the actual rotation angle for the zero temperature coefficient of frequency AT-cut as a function of the radius of curvature for the first, third and fifth harmonics for a center thickness $2h_0$ of 2.4772 mm. The results are independent of the thickness of the electrode because the influence of the electrode is about two orders of magnitude smaller than the scale shown in the figure. Note that all curves are asymptotic to the line corresponding to $\theta = 35.25°$ for the flat plate as R becomes large. Figure 3 shows log-log plots of the change in rotation angle for the zero temperature cut from $\theta = 35.25°$ for the flat plate as a function of $2h_0/R$ for the first, third and fifth harmonics for two different values of $2h_0$. The solid curves are for $2h_0 = 2.4772$ mm and the dotted curves are for $2h_0 = 1.6515$ mm. Again, and for the same reasons, these results are independent of the electrode thickness. These calculated results are in substantial agreement with known measured design curves[9]. Figure 4 shows the calculated change in frequency with temperature of the AT-cut ($\theta = 35.25°$) as a function of the radius of curvature for the first, third and fifth harmonics for a center thickness of $2h_0 = 1.6515$ mm. Note that all curves are asymptotic to zero for large R. Figure 5 shows the change in frequency due to the presence of the electrodes for a particular contoured resonator and angle of cut as a function of the electrode thickness for the first, third and fifth harmonics and a number of the anharmonics of each harmonic. The contoured resonator is plano-convex with a center thickness $2h_0 = 1.6515$ mm, a radius of

curvature R = 5.08 cm, an electrode radius ℓ = .475 cm and a cut angle $\theta = 35.08^{\circ}$, which corresponds to the zero temperature cut for the fundamental mode (n = 1, m = p = 0) for this particular contoured resonator. The dotted lines are for the first, third and fifth harmonic thickness mode for the flat plate with the same cut angle. Table I shows the calculated differences in the change in frequency with temperature due to the electrodes between a few of the lowest anharmonics of a given harmonic and that harmonic for the first, third and fifth harmonics. These well-defined differences in the change in frequency with temperature between the anharmonic modes of a contoured resonator can in principle, and may conceivably in practice, afford a means of evaluating the intrinsic stress in the electrodes from resonance measurements.

Acknowledgements

We wish to thank D. Stevens of Rensselaer Polytechnic Institute for help with the calculations.

This work was supported in part by the Army Research Office under Grant No. DAAG 29-76-G-0173, the Office of Naval Research under Contract No. N00014-76-C-0368 and the National Science Foundation under Grant No. ENG 72-04223.

References

1. H.F. Tiersten, J. Acoust. Soc. Am., 64, 832 (1978).
2. H.F. Tiersten and B.K. Sinha, "Temperature Dependence of the Resonant Frequency of Electroded Doubly-Rotated Quartz Thickness-Mode Resonators," to be published in the J. Appl. Phys.
3. H.F. Tiersten and R.C. Smythe, "An Analysis of Overtone Modes in Contoured Crystal Resonators," Proceedings of the 31st Annual Symposium on Frequency Control, U.S. Army Electronics Command, Fort Monmouth, New Jersey, 44 (1977).
4. H.F. Tiersten and R.C. Smythe, "An Analysis of Contoured Crystal Resonators Operating in Overtones of Coupled Thickness-Shear and Thickness-Twist," to be published in the J. Acoust. Soc. Am.
5. B.K. Sinha and H.F. Tiersten, "Temperature Derivatives of the Fundamental Elastic Constants of Quartz," Proceedings of the 32nd Annual Symposium on Frequency Control, U.S. Army Electronics Research and Development Command, Fort Monmouth, New Jersey, 150 (1978).
6. B.K. Sinha and H.F. Tiersten, J. Appl. Phys., 50, 2732 (1979).
7. H.F. Tiersten, Linear Piezoelectric Plate Vibrations (Plenum, New York, 1969), Chap.7, Sec.1.
8. A.E.H. Love, A Treatise on the Mathematical Theory of Elasticity, 4th ed. (Cambridge University Press, Cambridge, 1927) also (Dover, New York, 1944) Secs.18 and 118.
9. For more detail see B.K. Sinha and H.F. Tiersten, "Temperature Dependence of the Resonant Frequency of Electroded Contoured AT-cut Quartz Crystal Resonators," to be issued as a technical report, Rensselaer Polytechnic Institute, Troy, NY 12181.
10. The rather involved detailed discussion of the relation between $u_{2n=p}$ and $u_{1n=p}$ for the modes in the contoured resonator is included in Ref.9.
11. H.F. Tiersten, "Analysis of Intermodulation in Thickness-Shear and Trapped Energy Resonators," J. Acoust. Soc. Am., 57, 667 (1975).
12. H.F. Tiersten, "Analysis of Trapped Energy Resonators Operating in Overtones of Coupled Thickness-Shear and Thickness-Twist," J. Acoust. Soc. Am., 59, 879 (1976).
13. "Standards on Piezoelectric Crystals, 1949," Proc. IRE, 37, 1378 (1949). Since the transformation programs were written before the new IEEE Standard on Piezoelectricity - IEEE Std 176-1978 - was issued, it was more convenient to use the crystallographic conventions based on the old 1949 Standards.
14. The angle quoted is for the flat plate. For the contoured resonator the angle θ changes in accordance with the discussion in Sec.5.
15. R. Bechmann, "Elastic and Piezoelectric Constants of Alpha-Quartz," Phys. Rev., 110, 1060 (1958).
16. R.N. Thurston, H.J. McSkimin and P. Andreatch, Jr., "Third Order Elastic Constants of Quartz," J. Appl. Phys., 37, 267 (1966).
17. F. Kohlrausch, Lehrbuch der prakt. Physik, 16. aufl. 5. 158 (1930). Constants employed in Ref.18.
18. R. Bechmann, A.D. Ballato and T.J. Lukaszek, "Higher Order Temperature Coefficients of the Elastic Stiffnesses and Compliances of Alpha-Quartz," Proc. IRE, 50, 1812 (1962).

TABLE I

Difference in the Temperature Induced Frequency Change due to the Electrodes for the Lowest Three Harmonic Modes and the Lowest Lateral Overtones of Each Harmonic at 25°C
($2h_o$ = 1.6515 mm, 2h' = 1000 Å, R = 5.08 cm, 2ℓ = 0.95 cm, $\theta = 35.08^{\circ}$)

Mode (n,0,0) - (n,m,p)	Difference in Electrode Induced Frequency Change $\Delta f/f(T-T_o)$ (PPM/K)
(1,0,0) - (1,0,2)	-3.29×10^{-3}
(1,0,0) - (1,2,0)	- 3.60
(1,0,0) - (1,2,2)	- 5.18
(3,0,0) - (3,0,2)	- 0.47
(3,0,0) - (3,2,0)	- 1.38
(3,0,0) - (3,2,2)	- 1.53
(5,0,0) - (5,0,2)	- 0.36
(5,0,0) - (5,2,0)	- 0.97
(5,0,0) - (5,2,2)	- 1.18

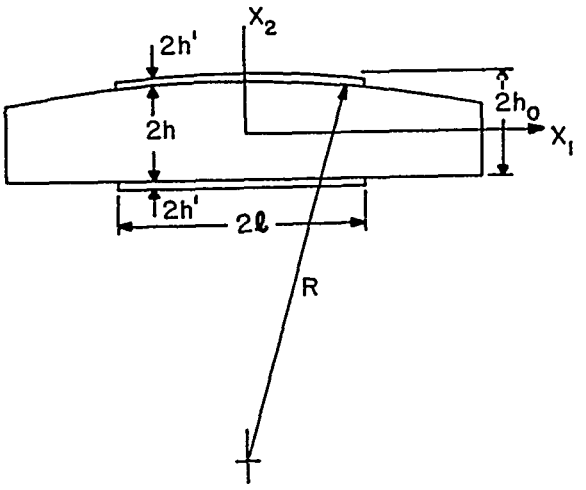

Figure 1 Plano-convex Resonator

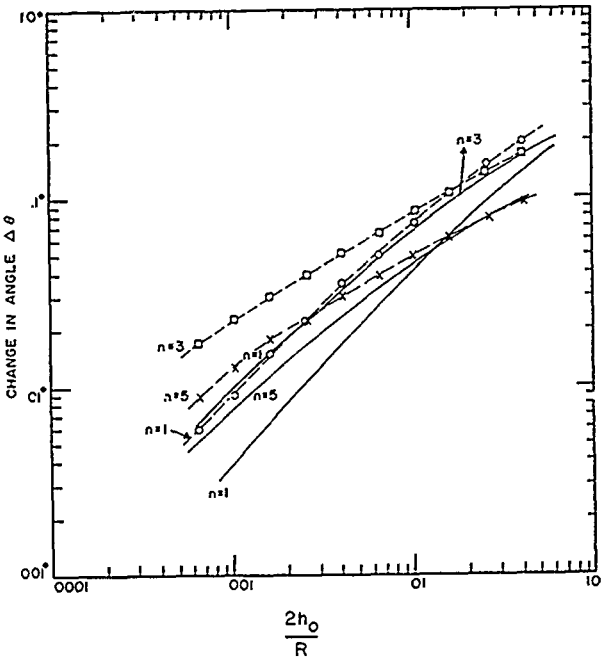

Figure 3

Change in the Rotation Angle $\Delta\theta$ from $\theta = 35.25°$ for the Zero Temperature Cut as a Function of $2h_o/R$ for the Three Lowest Harmonic Modes. The solid curves are for $2h_o$ = 2.4772 mm and the dotted curves are for $2h_o = 1.6515$ mm.

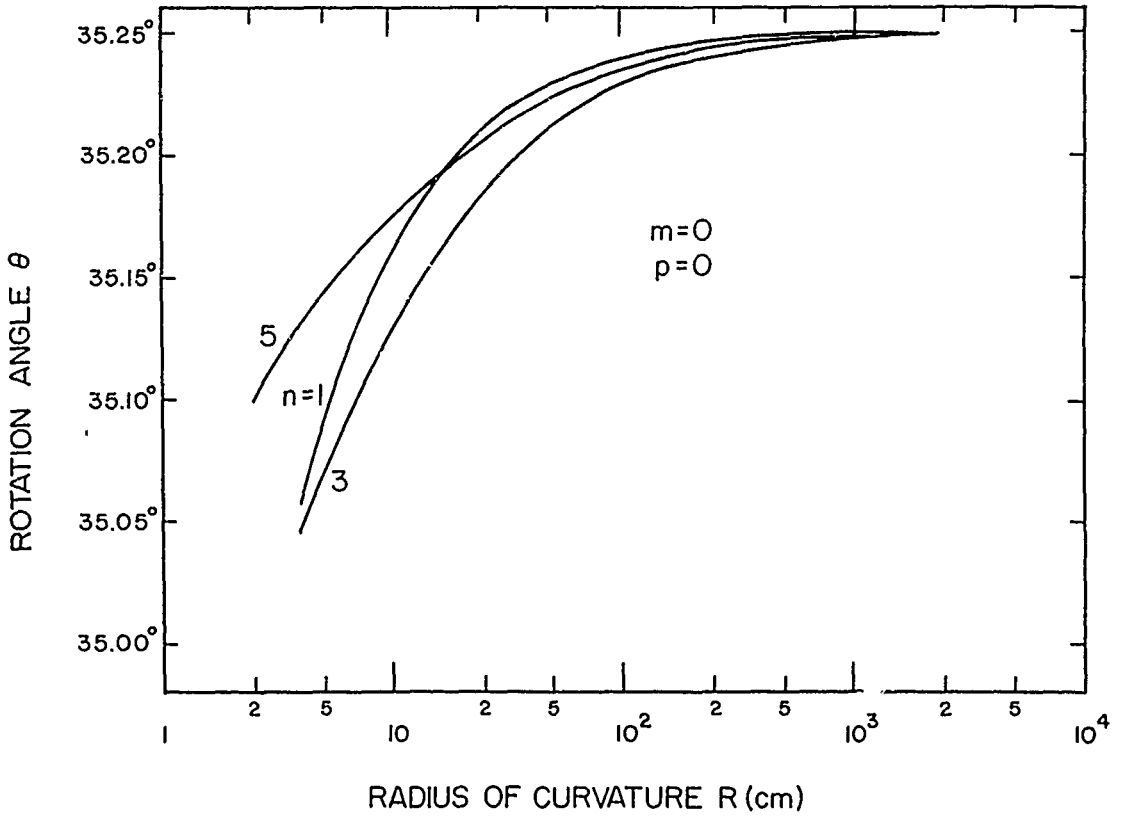

Figure 2 Rotation Angle θ for the Zero Temperature Coefficient of Frequency AT-cut as a Function of the Radius of Curvature R for Some Harmonic Modes. The center thickness $2h_o = 2.4772$ mm.

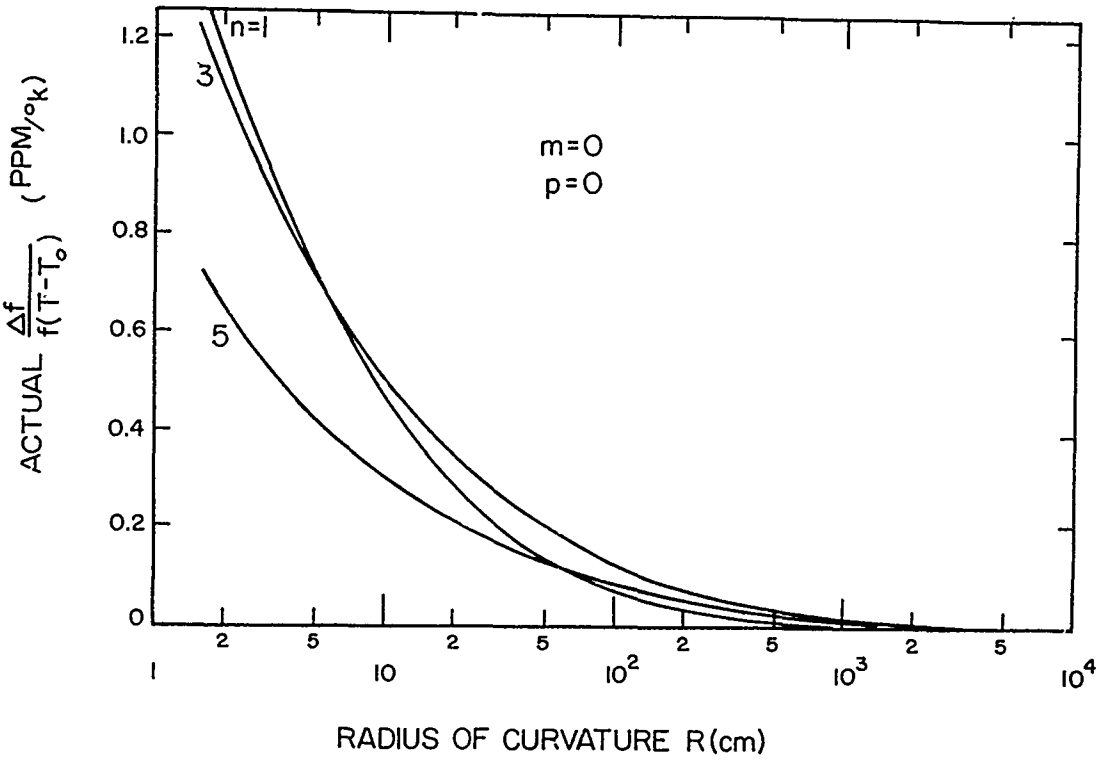

Figure 4

Relative Change in the Resonant Frequency per °K for a Plano-convex AT-cut ($\theta = 35.25^\circ$) Resonator as a Function of the Radius of Curvature for the Three Lowest Harmonic Modes. The center thickness $2h_o$ = 1.6515 mm.

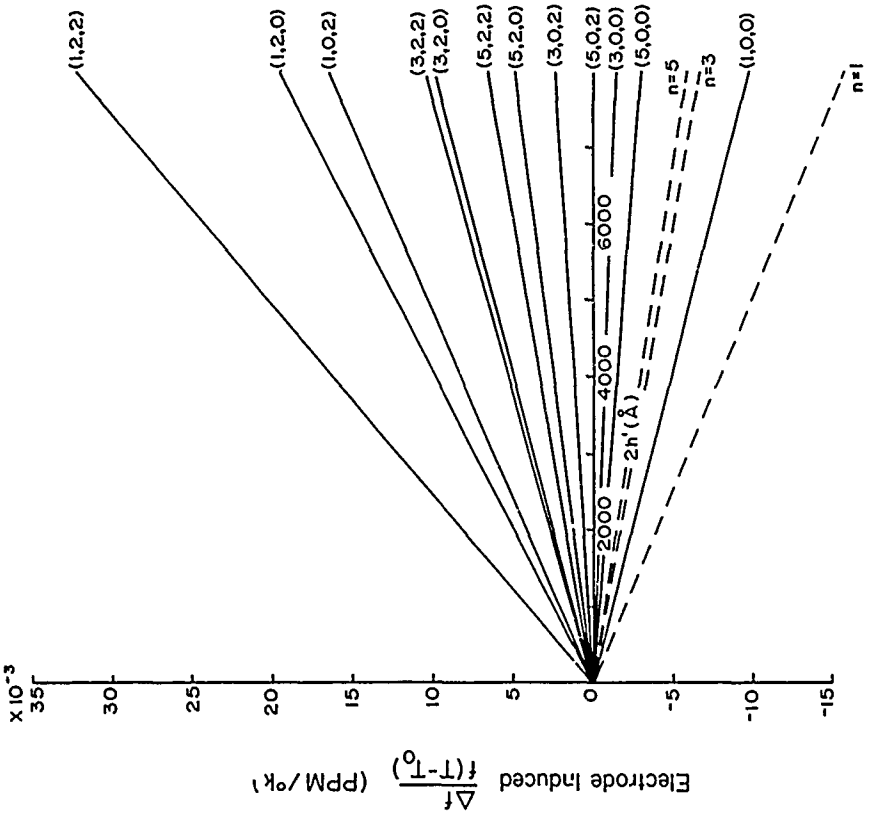

Figure 5

Relative Change in the Resonant Frequency Shifts per °K due to the Electrodes for a Plano-convex resonator with $2h_o$ = 1.6515 mm, R = 5.08 cm, $2h_o$ = 0.95 cm and $\theta = 35.08^\circ$ as a Function of the Electrode Thickness for the Lowest Three Harmonic Modes and the Lowest Anharmonic overtones of each Harmonic. The dotted lines are for a flat plate resonator with $\theta = 35.08^\circ$

FREQUENCY RESPONSE OF A QUARTZ OSCILLATOR TO TEMPERATURE FLUCTUATION

Yasuaki Teramachi, Mutsuhiko Horie, Hideki Kataoka and Toshimitsu Musha

Department of Applied Electronics, Tokyo Institute of Technology
4259 Nagatsuta, Midoriku, Yokohama 227, JAPAN

Summary

Frequency fluctuations of the quartz oscillator was measured by periodically varying the oven temperature, and the transfer function of the frequency variation for the temperature variation was derived such that it best fits the observation. The transfer function contains heat effects of the housing, supports, and the temperature sensor in addition to the resonator itself. Frequency fluctuations of the oscillator were compared with the spontaneous temperature fluctuation of the temperature-stabilized oven. They partly obey the transfer function but partly stochastic independent of each other.

Introduction

Frequency of a quartz oscillator is influenced by a temperature fluctuation even at a turn-over temperature because the frequency fluctuation depends on a time rate of change of the temperature as well as a temperature itself. The frequency responses to a triangular temperature increase[1] and to a step temperature increase[2] were already measured. Ballad and Vig proposed a formula for static and dynamic responses which is nonlinear in a temperature increase.[3] Practically a quartz oscillator is placed in a temperature-controlled oven and hence the temperature fluctuation is very small. For such a small temperature fluctuation a relationship between the frequency fluctuation and temperature fluctuation must be linear as far as one is the result of the other.

We have analyzed their mutual relation in terms of a concept of the transfer function. From the functional form of the transfer function which simulates observations, speculations were made about physical processes involved. It has been found that the frequency fluctuation is not completely connected to the temperature fluctuation; their relationship is partly causal and partly stochastic.

Method

Temperature was measured with a platinum resistor which composed a branch of a bridge circuit. This temperature sensor was placed in a cavity made in a copper block. The response time of the sensor is 50 sec and the minimum detectable temperature variation is about 1 mdeg.

Specimen was a 5-MHz 5th overtone AT-cut plano-convex quartz crystal resonator mounted in an HC-6U housing. The specimen was placed in another cavity made in the same copper block; a large mass and a large thermal conductivity of the copper block assure that the specimen was at as close a temperature to that of the temperature sensor as possible. A small temperature fluctuation was able to be externally given to the oven.

Difference voltages of the bridge were amplified 1000 times with an instrumentation amplifier which was mounted in the oven to avoid thermoelectric effect. These analog signals proportional to temperature fluctuation were passed through a low-pass filter to minimize aliasing after digital data processing and converted into 12-bit digital signals; they are punched out on a paper tape which was controlled by a CPU 8080A.

The frequency of the oscillator under measurement was mixed with the frequency of a reference quartz crystal oscillator which was placed within a double oven of which temperature was better controlled. The period of their beat signal was measured with a counter and the data were also punched out on the same paper tape together with the temperature data. The period of the beat signal was averaged over 100 periods to reduce the aliasing. A block diagram of the whole system is shown in Fig. 1.

Temperature variation and frequency variation

A periodic temperature variation was given to the oven; Fig. 2a shows a waveform of a temperature variation where the period is 22 minutes and the amplitude is 5 mdeg. The frequency fluctuation at four temperatures are plotted in (b) through (e); the turn-over temperature is 75.5°C. Dashed lines indicate frequency fluctuations expected from the static temperature frequency response; the discrepancies between this and observation are approximately proportional the time rate of temperature.

We have tentatively derived a transfer function which consists of two terms; one is equal to the temperature coefficient of the frequency times the temperature variation and the other is proportional to the time rate of change of the temperature of which proportionality coefficient has been determined such that results best fit the observation. The gain and the phase of the transfer function thus derived are shown by dashed lines in Fig. 3. There still remains some amount of discrepancy from the observation.

Transfer function

To eliminate discrepancies between the observed frequency fluctuation and the expected frequency fluctuation calculated with the aid of the transfer function as a result of the artificially applied periodic temperature variation, some terms have been added to the original transfer function. Solid lines in Fig.3 were calculated with this new transfer function $\tilde{H}(\omega)$ which is

$$\tilde{H}(\omega) = H(\omega)A(\omega)/B(\omega) \quad (1)$$

where

$$H(\omega) = \alpha(T) + j\omega\beta \quad (2)$$

$$A(\omega) = 1/(1 + j\omega\tau_1)(1 + j\omega\tau_2) \quad (3)$$

$$B(\omega) = 1/(1 + j\omega\tau_3) \quad (4)$$

and

$$\beta = -120\ /\text{deg},\ \tau_1 = 10\ \text{s},\ \tau_2 = 110\ \text{s}$$

$$\tau_3 = 50\ \text{s}.$$

$H(\omega)$ represents a transfer function of the quartz resonator itself, where α is a temperature coefficient of the resonant frequency variation which strongly depends on the temprature and $j\beta\omega$ stands for the effect of the time rate of change of the temperature, the value of β being constant over temperatures we investigated(57 °C to 77.6 °C). $A(\omega)$ is a transfer function of the supports and housing of the resonator. Term $1 + j\omega\tau$ is a transfer function for a simple relaxation process with relaxation time τ; therefore, $A(\omega)$ is concerned with two relaxation processes, one occuring after another. $B(\omega)$ refers to a single relaxation process probably of heat conduction of the temperature sensor. The block diagram of this structure is shown in Fig.4. T_1 is a temperture on the surface of the resonator, T_2 is a temperature of the sensor, T_N is circuit noise, F_N is partly circuit noise and partly spontaneous fluctuation of the resonant frequency, and $\tilde{F}$ and $\tilde{T}$ are frequency and temperature outputs.

Conclusions

Causal relationship between frequency fluctuations of a quartz oscillator and fluctuations of an oven has been investigated in terms of the transfer function. The following is found

1) The transfer function contains thermal effect of the housing of a quartz resonator, and another thermal effect of a temperature sensor.
2) The thermal effect of the housing is represented by two relaxation processes with different time constants, they occurring one after another.
3) The thermal effect of the temperature sensor is represented by a single relaxation process.
4) Relatively large spontaneous frequency fluctuations are taking place at fluctuation frequencies above 10^{-3} Hz, under spontaneous temperature fluctuations of standard deviation 1 mdeg.

Acknowledgement

The authors wish to acknowledge helpful discussions with Prof. H. Fukuyo of the Chiba University and Prof. N. Ohura of the Tokyo Institute of Technology.

This work was supported by the Grant-in-Aid for Scientific Research.

References

1. J. A. Kusters, "Transient Thermal Compensation for Quartz Resonators", IEEE Trans. Sonics Ultrason., Vol. SU-23, No. 4, July 1976, pp. 273-276.

2 A. W. Warner, "Use of Parallel-field Excitation in the Design of Quartz Crystal Units", Proc. 17th AFCS, May 1963, pp. 248-266.

3 A. Ballato and J. R. Vig, "Static and Dynamic Frequency-Temperature Behavior of Singly and Doubly Rotated, Oven-controlled Quartz Resonators", Proc. 32th AFCS, May 1978, pp. 180-188.

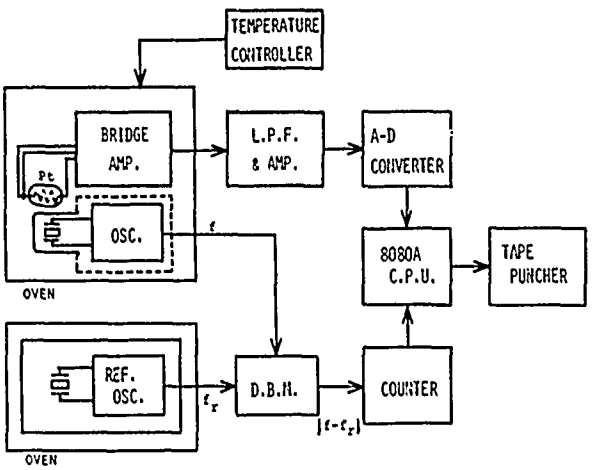

Fig.1 Block diagram of the experimental setup for measuring frequency fluctuation of a quartz crystal oscillator. The quartz resonator to be measured is mounted in the upper oven, of which temperature is detected by a Pt resistor composing a branch of a bridge circuit. The frequency is compared with a frequency of a reference quartz oscillator.

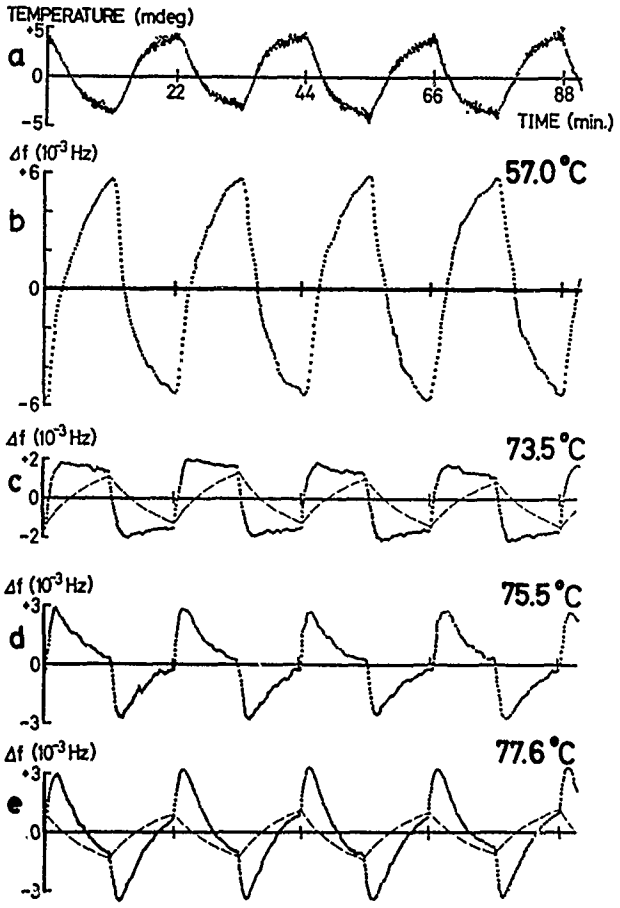

Fig.2 Periodic temperature variation (a) which is artificially generated and frequency variations (b, c,d,e) at temperatures listed in the figure. The turn-over temperature is 75.5 °C. Dashed lines indicate frequency variations expected from the temperature coefficient of the resonant frequency.

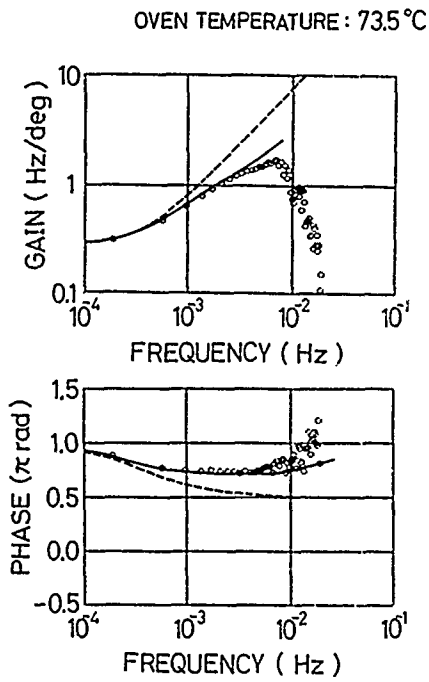

Fig.3 The transfer functions of the frequency fluctuation which was derived by applying periodic temperature variations(0.03 deg). Dashed line refers to when the transfer function consists only of terms proportional to temperature variation and to its time rate of change. More terms are needed to better approximate the observation.

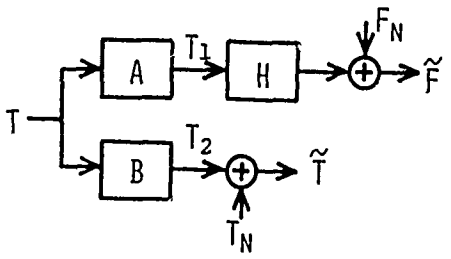

Fig.4 A physical model for the transfer function we used. $\tilde{F}$ and $\tilde{T}$ are outputs of frequency and temperature fluctuations. F_N stands for circuit noise and spontaneous frequency fluctuation. T_N is circuit noise. A and B are temperature transfer functions of a housing of the quartz resonator and the temperature sensor. T is the temperature of copper block in which the resonator and the temperature sensor are mounted.

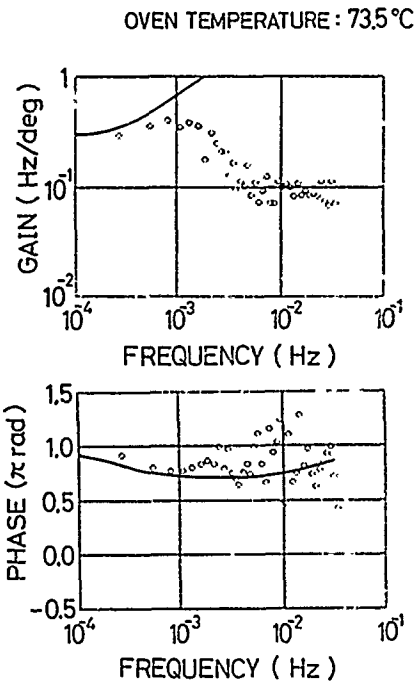

Fig.5 Observed values of the transfer function as a function of the spontaneous temperature fluctuation of the oven. Solid lines are caliculated from eq.(1).

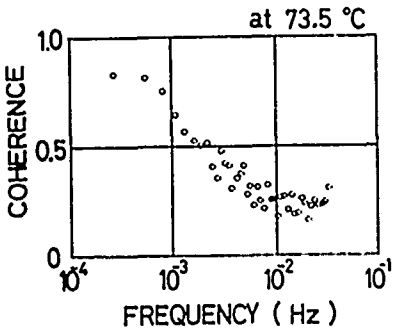

Fig. 6 Coherence spectrum between temperature fluctuation and frequency fluctuation where the artificial temperature variation is not applied.

DYNAMIC THERMAL BEHAVIOR OF QUARTZ RESONATORS

G. Théobald, G. Marianneau, R. Prétot, J.J. Gagnepain

Laboratoire de Physique et Métrologie des Oscillateurs du C.N.R.S.
associé à l'Université de Franche-Comté-Besançon
32 avenue de l'Observatoire 25000 Besançon France

Summary

The regular model of the thermal properties of quartz crystal resonators consisting of a third order polynomial representation versus temperature can be used to determine frequency shifts only for very slow temperature changes, i.e. when the temperature distribution is uniform and no thermal gradients occur. In fact this condition rarely is satisfied and it is necessary to take into account the spatial temperature distribution resulting from external fluctuations and heat diffusion along the connecting wires, the mounting, the electrodes and the crystal itself. Those mechanisms are described and it is shown that the resulting frequency changes generally are proportionnal to the time derivative of the external temperature. This simulation enables to calculate the relative magnitude of the dynamic thermal sensitivity of singly and doubly-rotated cuts with respect to AT-cut. It can be used either for small or large amplitude temperature variations.

The predicted values are compared with experimental data for AT and SC cuts, and it is confirmed that the SC cut exhibits a thermal transient effect lowered by a factor 50.

Temperature variations can be step, ramp, or sinusoïdal functions produced by a digital temperature controlled oven.

The temperature stability required for very stable oscillators can be deduced from this study by means of the dynamic temperature coefficient. By using a quartz sensor for temperature measurement and a digital servo-system, the accuracy in temperature control can be greatly improved.

Introduction

Operating a quartz crystal resonator at the turn-over point of its static frequency-temperature curve does not cancell out the all frequency shifts related with temperature variations. Only the very slow one can be eliminated. In fact any external temperature variation is followed by heat diffusion, between the surrounding medium and the crystal itself, along the connecting wires, the supports and the electrodes. Consequently temperature within the crystal has a spatial distribution and the thermal behavior includes at the same time spatial and temporel gradients. It follows that thermal stresses and strains take place and induce frequency shifts by non linear coupling with the high frequency wave.

This dynamic thermal behavior lead to frequency fluctuations much larger than would be expected from the static one as it has been shown by Ballato[1] who proposed a phenomenological model by introducing an additional term, time dependant, in the first order temperature coefficient of the static f-T effect. This model was the first one easily usable for describing the dynamic behavior of quartz resonators and is in good agreement with experimental results for small amplitude temperature variations. It is also interesting to relate the dynamic temperature coefficient to the crystal fundamental constants as it has been done by Holland[2,3] in the case of an initial heat distribution along the thickness. Such a calculation determines the relative amplitude of the effect whatever the crystal orientation is and enables to desensitize the resonator in the vicinity of TS and SC cuts.

The purpose of this paper is to build up a model equivalent to Ballato's model by starting from the crystal fundamental constants and using Holland's calculation. The temperature distribution along the crystal thickness is to be determined as a function of the surrounding medium fluctuation and the support and mounting configuration. The guideline being to demonstrate that the relative frequency fluctuations directly are proportionnal to the time derivative of external temperature.

Frequency variations

A one-dimensional model is used consisting in a crystal plate of thickness 2h, of infinite lateral sizes along x_1 and x_3 and uniformly plated on its two faces. The plate is linked with the surrounding medium by two equivalent symmetrical wires. Let T(t) be the external temperature , $\Phi(t)$ the temperature on the plate faces and $\theta(x_2,t)$ the temperature within the crystal as shown on fig. 1.

The $\theta(x_2,t)$ temperature can be splitted into two terms

$$\theta(x_2,t) = \overline{f}(t) + f(x_2,t) \qquad (1)$$

the first one $\overline{f}$ being independant of the spatial

variable x_2 and corresponding to some average along the plate thickness ; the second one $f(x_2,t)$ is a complementary function representative of the temperature gradients.

Under a temperature variation an adiabatic deformation takes place and the medium becomes inhomogeneous. Therefore the wave propagation condition is modified. If one refers to a natural state coordinate system the non linear propagation equation is

$$\rho_o \ddot{u}_i = \left(\overline{A_{iskr}}\, u_{k,r}\right)_{,s} \tag{2}$$

where $\overline{A_{iskr}}$ is the modified elastic constant which can be written following the form

$$\overline{A_{iskr}} = C_{iskr} + \overline{H_{iskr}} \tag{3}$$

C_{iskr} are the regular second order elastic constants and $\overline{H_{iskr}}$ the perturbation terms which are related to the thermal stresses and strains. Let u_i° be the mechanical vibration amplitude components of the wave when propagating in the unperturbated medium and $u_i^{\circ *}$ the complex conjugate. By using a perturbation method the relative frequency shift $\Delta\omega/\omega_o$ can be calculated

$$\Delta\omega/\omega_o = \frac{\int_v u_{i,s}^{\circ *}\, \overline{H_{iskr}}\, u_{k,r}^{\circ}\, dv}{2\rho_o \omega_o^2 \int_v u_i^\circ\, u_i^{\circ *}\, dv} \tag{4}$$

ρ_o being the specific mass and V_o the wave velocity of the unstrained crystal.

If one considers a pure thickness shear vibration mode

$$u_1^\circ = a_1\, e^{j\omega t}\, \sin\frac{\omega x_2}{V_o} \tag{5}$$

relation (4) takes the simple form

$$\Delta\omega/\omega_o = \frac{1}{2\rho_o V_o^2 h} \int_{-h}^{+h} \overline{H_{1212}}\, \cos^2\frac{\omega x_2}{V_o}\, dx_2 \tag{6}$$

with

$$\overline{H_{1212}} = \overline{T_{22}} + (C_{121211} + 2C_{1212})\overline{\eta_{11}} + C_{121222}\overline{\eta_{22}} + C_{121233}\overline{\eta_{33}} + C_{121223}\overline{\eta_{23}} + C_{1212}\alpha_{C_{1212}}\,\Theta \tag{7}$$

The $\overline{T_{ij}}$ and $\overline{\eta_{k\ell}}$ quantities correspond to the thermal stresses and strains ; the $C_{ijk\ell mnpq}$'s are the non linear 3rd order elastic constants and $\alpha_{C_{1212}}$ is the true temperature coefficient of the C_{1212} elastic constant[4]. The determination of the predeformation will therefore lead to the frequency shifts by using relations (6) and (7).

Determination of the thermal strains and stresses

Let us consider a free plate with negligible edge effects as presented on fig. 1. (In fact a more accurate model must take into account the influence of the mounting, i.e. the reaction forces at the fixation points under the crystal dilatation). By following Holland[2] the adiabatic deformation η_{ij} which takes place immediately after an external temperature change Φ is given by

$$\begin{aligned}
\overline{\eta_{11}} &= \alpha_{11}\,\overline{\Theta} \\
\overline{\eta_{22}} &= \alpha_{22}\,\overline{\Theta} \\
\overline{\eta_{33}} &= \alpha'_{33}\,\Theta - (C'_{1133}\,\alpha_{11} + C'_{2233}\,\alpha_{22})\,\overline{\Theta} \\
\overline{\eta_{23}} &= \alpha'_{23}\,\Theta - (C'_{1123}\,\alpha_{11} + C'_{2223}\,\alpha_{22})\,\overline{\Theta} \\
\overline{\eta_{13}} &= 0 \\
\overline{\eta_{12}} &= 0
\end{aligned} \tag{8}$$

where the α_{ij} are the thermal expansion coefficients. The $C'_{ijk\ell}$ and α'_{ij} can be easily found in the paper of ref. 2. $\overline{\Theta}$ is the average of the temperature on the plate thickness.

$$\overline{\Theta} = \frac{1}{2h}\int_{-h}^{+h} \Theta\,(x_2,t)\, dx_2 \tag{9}$$

The corresponding stresses directly follow by the use of the stress-strain relations. With equations (7), (8), (9) and (1) in (6) and by using single-subscript notation the relative frequency shift is written

$$\Delta\omega/\omega_o = \frac{\overline{h_{66}}+\overline{k_{66}}}{2\rho_o V_o^2}\,\overline{\Theta} + \frac{\overline{k_{66}}}{4h\rho_o V_o^2}\int_{-h}^{+h} f(x_2,t)\cos\frac{2\omega_o x_2}{V_o}\, dx_2 \tag{10}$$

where

$$\overline{h_{66}} = C_{661}\alpha_1 + C_{663}\alpha_3 - C_{662}C'_{2\mu}\alpha_\mu - C_{664}C'_4\alpha_\mu \tag{11}$$

$$\overline{k_{66}} = C_{662}\,\alpha'_2 + C_{664}\,\alpha'_4 + \alpha_{C_{66}}\,C_{66} \tag{12}$$

The quantity $(1/2)(\overline{h66} + \overline{k66})$ corresponds to the static temperature derivative a_o of the resonator resonance frequency[4]. Therefore

$$\Delta\omega/\omega_o = a_o\overline{\Theta} + \frac{\overline{k_{66}}}{4hC_{66}}\int_{-h}^{+h} f(x_2,t)\cos\frac{2\omega_o x_2}{V_o}\, dx_2 \tag{13}$$

It can be observed that the relative frequency variations is composed of two terms. The first one corresponds to the static thermal behavior and is related to the mean value of the temperature. The second one is the dynamic effect. In order to decrease the dynamic sensitivity a doubly-rotated cut can be used which at the same time enables to keep a_o at zero and minimize the $\overline{k_{66}}$ coefficient. Such a research leads to desensitized cuts located in the vicinity of the TS and SC cuts as shown by the data presented on table I.

Crystal cut	AT	Y	BT	ϕ=22°5 θ=34°3	ϕ=22°8 θ=34°3	ϕ=21°9 θ=33°9
$\frac{\overline{k_{66}}}{\overline{k_{66_{AT}}}}$	1	2,7	-1.8	-1.9×10^{-2}	-1.8×10^{-2}	8.4×10^{-2}

Table I

Values of the coefficient k_{66} representative of the dynamic thermal behavior for various crystal orientations. The coefficient is normalized with respect to the AT cut.

Temperature distribution

In the case of the one-dimensionnal model the temperature $\theta(x_2,t)$ can easily be given in a general form as a function of the boundary temperature $\phi(t)$[5]

$$\theta(x_2,t) = \sum_{\substack{n=1 \\ n \text{ odd}}}^{\infty} \frac{n\pi\kappa}{2h^2} \exp\left(-\frac{n^2\pi^2\kappa t}{4h^2}\right) \sin\left(\frac{n\pi x_2}{2h}\right) I(t) \quad (14)$$

with $$I(t) = \int_0^t \exp\left(\frac{n^2\pi^2\kappa}{4h^2}\tau\right) \phi(\tau)\, d\tau$$

where κ is the thermal diffusivity constant of the material. If $\phi(t)$ is a slowly variable function of time the integration in relation (14) can be performed by parts and derivatives higher than the 1rst order one are neglected. Thus a simple relation is obtained

$$\theta(x_2,t) = \phi(t) + \frac{1}{2\kappa}\left(x_2^2 - \frac{h^2}{4}\right)\dot{\phi}(t) \quad (15)$$

with $\dot{\phi}(t) = d\phi/dt$. By comparison with relation (1) it follows

$$\overline{f}(t) = \phi(t) - \frac{h^2}{8\kappa}\dot{\phi}(t) \quad (16)$$

$$f(x_2,t) = \frac{x_2^2}{2\kappa}\dot{\phi}(t) \quad (17)$$

As it has been shown above, the corresponding frequency variations can be divided into the static and the dynamic ones. Generally the first ones are cancelled out by using the appropriate cut. The dynamic remaining term only depends on the complementary function $f(x_2,t)$ and therefore is proportionnal the $\dot{\phi}(t)$. This confirms the phenomenological model given by Ballato[1].

A one-dimensionnel model is not very satisfactory, because it does not represent a real resonator. If the main faces are not entirely covered by electrodes with a thermal conductivity higher than the conductivity of the crystal, transverse thermal diffusion will occur and modify the temperature gradient distribution. In fact the electrodes are deposited at the center of the plate and the thermal conductivity of the crystal and the plating are comparable. Then it would be necessary to take into account the functionnal dependance of the temperature along the x_1 and x_3 axis. An other way is not to use the true value of κ but to consider it as a correcting factor to be adjusted.

By the use of equation (17) into (13) the frequency variation as a function of $\phi(t)$ and $\dot{\phi}(t)$ is obtained

$$\Delta\omega/\omega_o = a_o\left(\phi - \frac{h^2}{3\kappa}\dot{\phi}\right) + \tilde{a}\,\dot{\phi} \quad (18)$$

The first term depends upon the regular 1st order static temperature coefficient a_o and can be neglected, a_o being made small by adjusting the cut angles. $\tilde{a}$ is the dynamic temperature coefficient of frequency and is directly proportionnal to k_{66}. Its absolute value can be calculated but because of the preceding remarks it does not fit with the experimental data for resonators vibrating on overtones and a phenomenological determination is preferable directly or by means of κ.

The higher order static temperature coefficients can be added in equation (18). If the crystal thickness is small so that $h^2/3\kappa$ is smaller than the relaxation time of the temperature, the final form is

$$\Delta\omega/\omega_o = \tilde{a}\, d\phi/dt + a_o(\phi-\phi_o) + b_o(\phi-\phi_o)^2 + c_o(\phi-\phi_o)^3 \quad (19)$$

where ϕ_o is the reference temperature.

Remark : The heat exchanges between the crystal boundaries at temperature $\phi(t)$ and the surrounding medium at T(t) take place through the connecting wires and the supports represented on fig. 1 by two equivalent wires of length ℓ and diffusivity constant ξ. Temperature $\phi(X_2,t)$ at any point of the rod[5] of coordinate X_2 (X_2 being measured from its outer end) is given by

$$\phi(X_2,t) = \frac{X_2}{2\sqrt{\pi}\,\xi}\int_0^t \frac{T(t)}{(t-\tau)^{3/2}} \exp\left(-X_2^2/4\xi(t-\tau)\right) d\tau \quad (20)$$

In the case of a general function T(t) this integration must be performed with a computer. In the simplest case of sinusoïdal temperature variations of amplitude ΔT_o the solution is easily obtained

$$\phi(X_2,t) = \phi_o \sin(\Omega t + \psi) \quad (21)$$

with the amplitude and the phase difference

$$\phi_o/\Delta T_o = \exp\left(-\left(\frac{\Omega}{2\xi}\right)^{1/2}\ell\right), \quad \psi = \left(\frac{\Omega}{2\xi}\right)^{1/2}\ell \quad (22)$$

This corresponds to an equivalent cut-off frequency of the order of 10^3 Hz.

Experimental results

Regular AT cut 5th overtone 5 MHz resonators were submitted to temperature cyclings by using a temperature controlled oven, the schematic diagram of which is represented on fig. 2. Two resonators are in the oven. One is the resonator under test, the other one is an LC cut unit with high

temperature sensitivity used as temperature probe. Each of these resonators drives an oscillator (at 5 MHz and 28 MHz respectively), the frequency of which is measured on a counter through an electronic switch. A computer drives the oven by comparing the measured temperature with a reference temperature. This temperature follows a variation law given by a program included in the computer. Sinusoïdal temperature cyclings can be realized between 30°C and +120°C with a basic accuracy of 0.001°C.

Fig. 3a shows the experimental curves obtained by sweeping temperature over a large scale (from 5°C to +65°C about 30°C) - curve 1 : static f-T characteristic - curve 2 : sweep frequency of 2.3×10^{-4} Hz. Fig. 3b presents the corresponding theoretical curves obtained by using a $\tilde{a}$ value of 1.3×10^{-5} s/°C. The model fits with the experimental data even for very large temperature fluctuations.

On fig. 4a and 4b are presented the same types of experimental and theoretical f-T curves for temperature cyclings betwwen 61°C and 69°C about the turn-over point located at 65°C.

Fig. 5a and 5b present temperature cyclings of the same amplitude as on fig. 4a and 4b but centered at the left hand side of the turn-over point, at 27°C.

Temperature cyclings with a very small amplitude (± 0.05°C) about the turn-over point (65°C) are shown on fig. 6a and 6b. It can be observed the model is convenient whatever the temperature variation amplitudes are, large or small.

The same measurements and simulations were performed with an SC cut -3rd overtone- 5 MHz resonator as shown on fig. 7a and 7b. The temperature range was ± 4°C about the turn-over point at 60°C. For the SC cut the $\tilde{a}$ coefficient is equal to 3.10^{-7} s/°C and is about 50 times lower than for the AT cut, with an inverse sign.

Thermal perturbation in quartz oscillators

The previous measurements were performed for slow temperature variations (frequencies of the order of a few 10^{-4} Hz) and therefore the temperature on the crystal boundaries can be considered to be similar to the external temperature. But for faster variations the diffusion in the connecting wires are to be taken into account. This is equivalent to a low pass filter, therefore when looking at Fourier frequencies within the linewidth of this equivalent filter the temperature fluctuations are not modified, but outside the linewidth those fluctuations are integrated. Thus there are two effects : an integration effect due to the connections followed by a derivation effect due to the crystal itself.

Therefore the frequency fluctuations can be directly proportionnal to the external temperature fluctuations but with a different sign, $\tilde{a}$ being negative for AT cut. This is illustrated by fig. 8 where frequency and temperature fluctuations of an oscillator using AT cut resonator simultaneously were recorded.

Frequency control in quartz oscillators is mainly limited by the dynamic thermal behavior of the resonator, caracterized by the coefficient $\tilde{a}$ which is of the order of 10^{-9} °C/s for AT cut resonators and a few parts in 10^{-7} °C/s for SC cut resonators. To achieve a frequency stability of 1×10^{-13} it is necessary to control temperature fluctuations at a level lower than 10^{-8} °C/s if an AT cut resonator is used. Variations as small as 0.01 µ°C/s or 1 µ°C/100s are not easy to control and this needs a very accurate thermostat, and also thermal filters around the crystal, and thermal shunts between the inner part of the oven and the external medium. Both problems can be splited :

accurate temperature control mainly is a problem of temperature sensor and servo system electronics;

thermal filter is a problem of oven configuration and material choice. A solution can be proposed for the first one. A quartz resonator with a high Irst order temperature coefficient is used as temperature sensor and is strongly coupled with the second resonator. After several steps of frequency multiplication and mixing, for increasing the sensitivity, the frequency representative of temperature is compared to a stable 5 MHz reference frequency and the difference is calculated by a microprocessor which drives the oven heater. All the adequate corrections for the servo loop can be included in the processor program. This is a powerful possibility of such a system. Fig. 9 shows temperature stability over several days obtained by following this principle. It is important to remark that the oven itself was just an aluminum cylinder containing a copper block with both resonators, but without any thermal shunt. Therefore the thermal conditions were not the best ones. The mean stability per day is of the order of 0.0001°C and corresponds to the actual frequency resolution of this system, which can still be improved. It does not seem to be unreasonable to expect temperature stability as good as 10µ °C at short term as well as at long term with a single oven thermostat.

References

(1) A. Ballato, J. Vig.,"Static and dynamic frequency-temperature behavior of singly and doubly rotated, oven-controlled quartz resonators", Proc. 32nd Ann. Frequency Control, Fort Monmouth (1978).

(2) R. Holland, "Non uniformly heated anisotropic plates : I Mechanical distorsion and relaxation", IEEE Trans. Sonics and Ultrasonics, vol. SU-21, n° 3, (July 1974).

(3) R. Holland, "Non uniformly heated anisotropic plates : II Frequency transients in AT and BT quartz plates", Ultrasonics Symp. Proc. IEEE Cat. # 74 CHO 896-1SU (1974).

(4) B. Sinha, H. Tiersten, "Temperature derivatives of the fundamental elastic constants of quartz", Proc. 32nd Ann. Frequency Control Symp., Fort Monmouth (1978)

(5) H. Carslaw, J. Jaeger, "Conduction of heat in solids", Oxford University Press, London (1959).

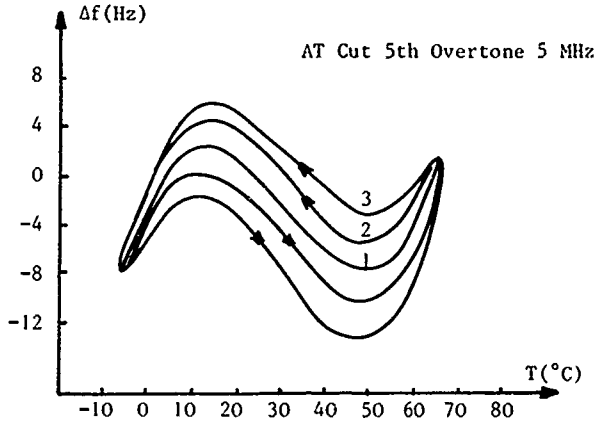

Fig. 3a : Experimental sinusoïdal temperature cycling
curve 1 : static f-T behavior
curve 2 : sweep frequency : 2.3 10^{-4} Hz
curve 3 : 4.6 10^{-4} Hz
temperature range ΔT = ± 35°C about 30°C

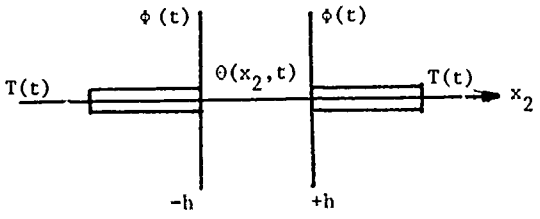

Fig. 1 : One-dimensionnal thermal diffusion model of a thickness shear vibrating quartz resonator

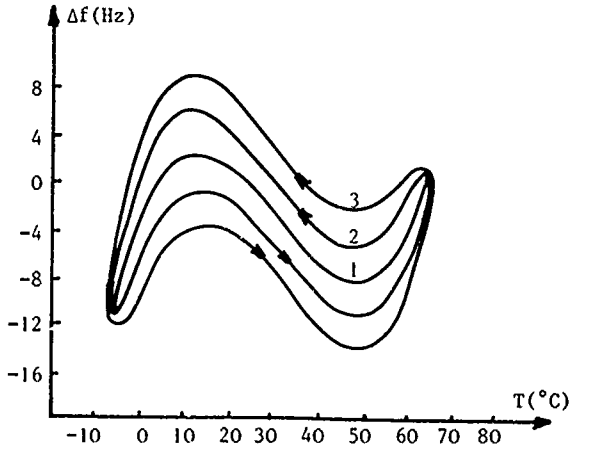

Fig. 3b : Theoretical curves

a_o = -8.2 10^{-8}/°C ; b_o = -1.7 10^{-9}/°C²

c_o = 10^{-10}/°C³ ; $\tilde{a}$ = -1.3 10^{-5} s/°C

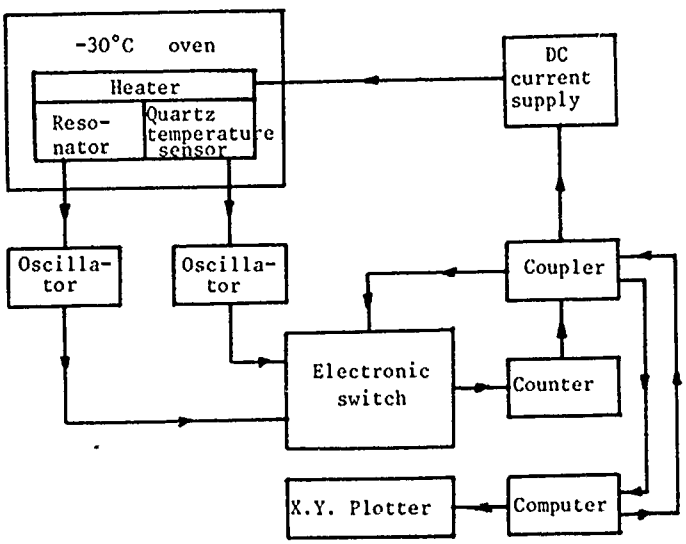

Fig. 2 : Schematic diagram of the temperature controlled oven used for temperature cyclings

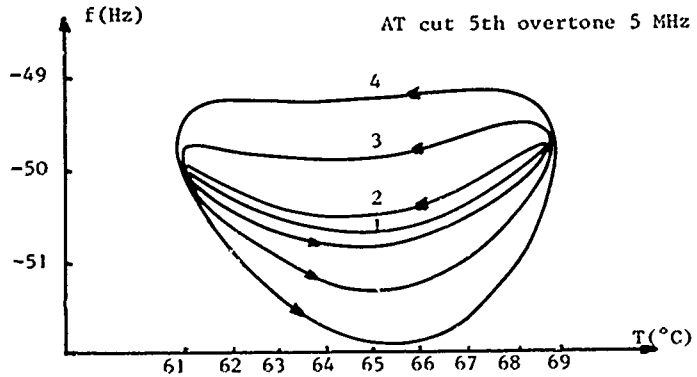

Fig. 4a - Experimental sinusoïdal temperature cycling

curve 1 : static f-T behavior ; curve 2 : sweep frequency 9.2 10^{-5} Hz ;
curve 3 : 3.7 10^{-4} Hz ; curve 4 : 7.4 10^{-4} Hz.
temperature range ΔT = + 4°C about 65°C

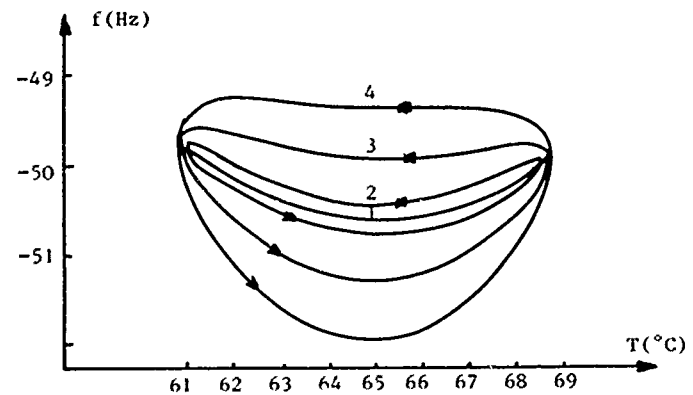

Fig. 4b : Theoretical curves

$a_o = -8.2\ 10^{-8}/°C$; $b_o = -1.7\ 10^{-9}/°C^2$
$c_o = 10^{-10}\ /°C^3$; $\tilde{a} = -1.3\ 10^{-5}$ s/°C

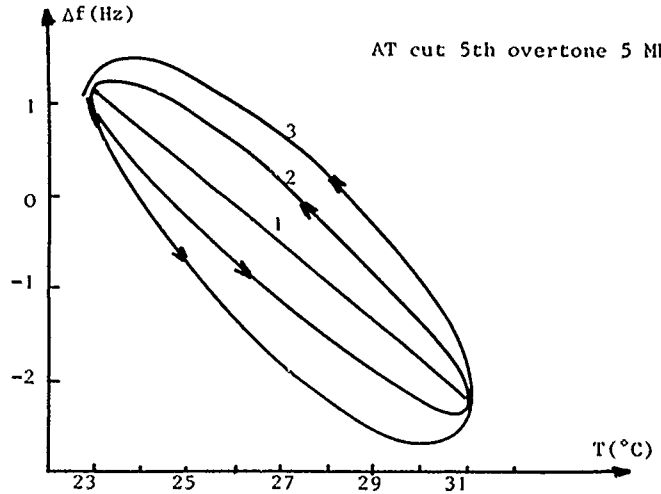

Fig. 5a : Experimental sinusoïdal temperature cycling

curve 1 : static f-T behavior
curve 2 : 4.6 10^{-4} Hz ; curve 3 : 9.3 10^{-4} Hz
temperature range ΔT = + 4°C about 27°C

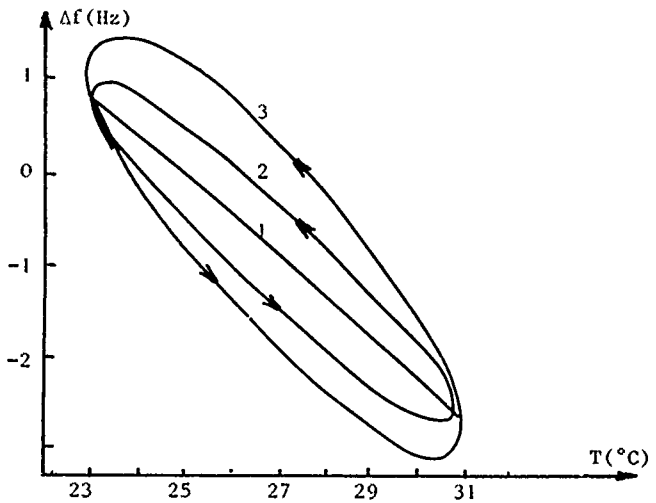

Fig. 5b : Theoretical curves

$a_o = -8.2\ 10^{-8}/°C$; $b_o = -1.7\ 10^{-9}/°C^2$
$c_o = 10^{-10}\ /°C^3$; $\tilde{a} = -1.3\ 10^{-5}$ s/°C

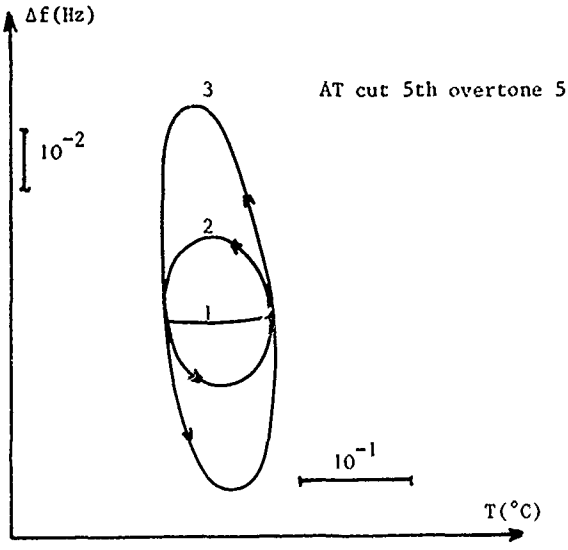

Fig. 6a : Experimental sinusoïdal temperature cycling

curve 1 : static f-T behavior
curve 2 : 5.5 10^{-4} Hz ; curve 3 : 1.6 10^{-3} Hz
temperature range ΔT = ± 0.05°C about the turn-over point at 65°C.

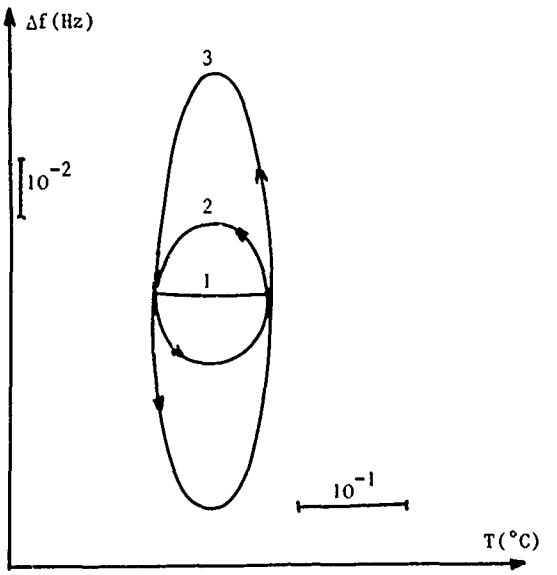

Fig. 6b : Theoretical curves

a_o = -8.2 10^{-8}/°C ; b_o = -1.7 10^{-9}/°C²
c_o = 10^{-10} /°C³ ; $\hat{a}$ = -1.3 10^{-5} s/°C

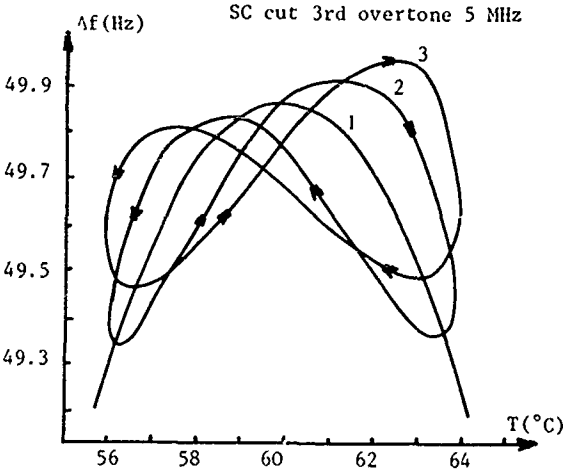

Fig. 7a : Experimental sinusoïdal temperature cycling

curve 1 : static f-T behavior
curve 2 : 9.1 10^{-4} Hz ; curve 3 : 1.8 10^{-3} Hz
temperature range ± 4°C about the turn-over point at 60°C

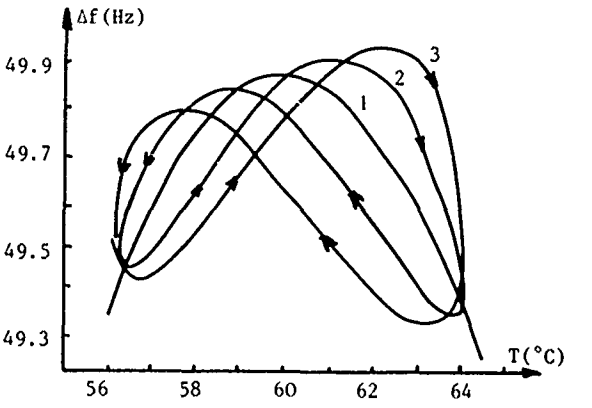

Fig. 7b : Theoretical curves

a_o = 6.4 10^{-7}/°C ; b_o = -1.2 10^{-8}/°C²
c_o = 6 10^{-11}/°C³ ; $\hat{a}$ = 3.10^{-7} s/°C

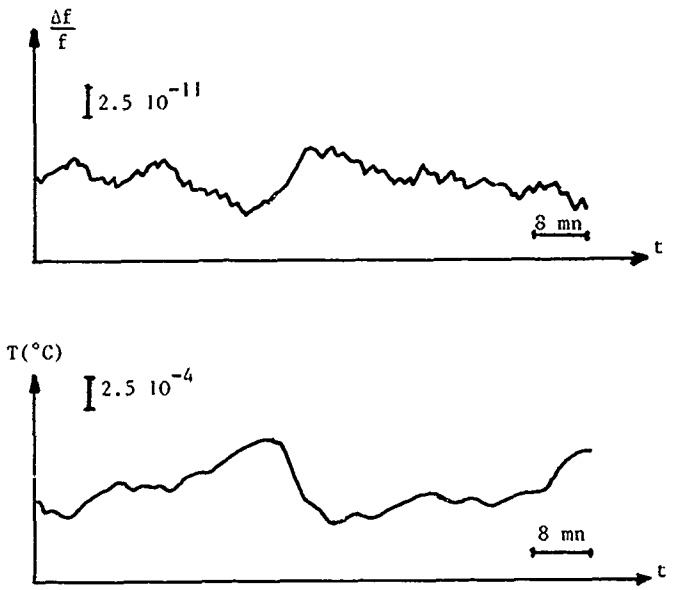

Fig. 8 : Frequency and Temperature fluctuations of a 5 MHz AT cut oscillator

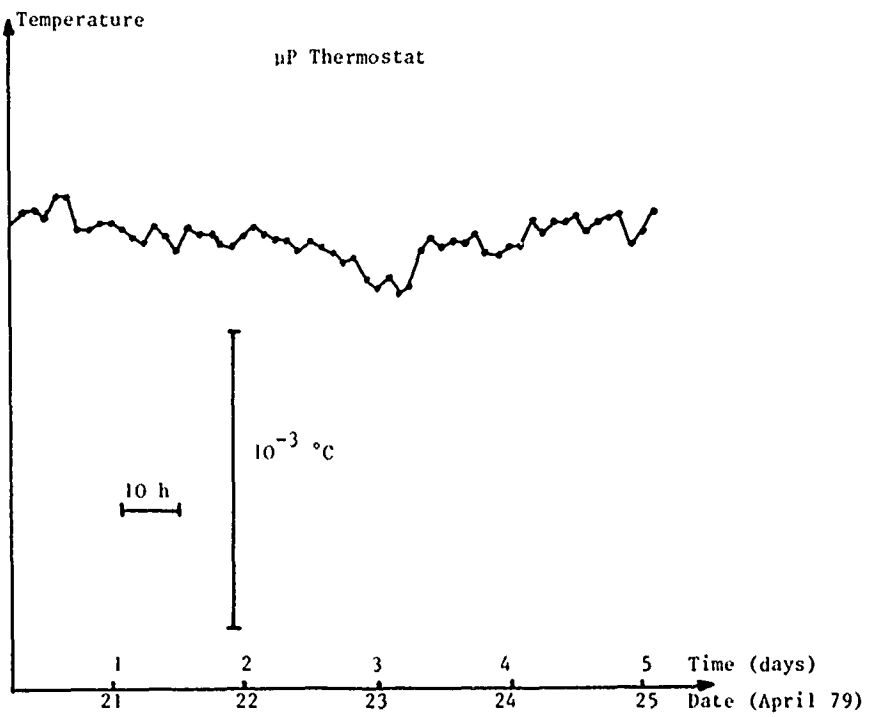

Fig. 9 : Temperature stability of a digital thermostat

NEW QUARTZ TUNING FORK WITH VERY LOW TEMPERATURE COEFFICIENT

Eishi Momosaki, Shigeru Kogure, Minoru Inoue and Tetsumi Sonoda

Suwa Seikosha Co., Ltd.
Suwa Japan

Summary

We have developed a new quartz tuning fork cut at new angles, which are designated M-cuts (M_1-, M_2-, M_3- and M_4-cuts). The resonant frequency of this quartz tuning fork does not change by about one part in a million over a 70-degree centigrade range of temperature. This quartz tuning fork obtains its very excellent frequency-temperature characteristics from the fact that both the 1st- and 2nd- order temperature coefficients are zero. The frequency-temperature characteristics of this new quartz tuning fork is comparable to that of the AT-cut or GT-cut resonators.

Introduction

Today quartz resonators used in watches are mainly 5°X-cut quartz tuning forks, which feature a variety of advantages in watch application. However, the ever increasing demand for higher accuracy of the watch has required us to find ways to improve the frequency-temperature characteristics of the quartz tuning fork.

The ways so far devised for improved frequency-temperature characteristics of the rosonators are as follows :

1. Compensation of temperature characteristics by means of a temperature sensor (barium titanate capacitor, thermistor)
2. Compensation of temperature characteristics by means of additional quartz resonators.
3. Use of a quartz resonator (AT-cut or GT-cut crystal resonator) with good temperature characteristics.

These methods, however, are no exception in having their own drawbacks. We have thus started out from a completely innovative viewpoint and successfully developed a new version of quartz tuning fork with very excellent temperature characteristics and with every advantage of current tuning fork type quartz crystal resonators.

Our attempt to improve the frequency-temperature characteristics of a flexural mode consists of taking into account the coupling with a torsional mode. We have studied the resonant frequency-temperature characteristics of a coupled flexural mode with a torsional mode in a quartz tuning fork.

Analysis

Influence of coupling

First of all, we are concerned with how to improve the frequency-temperature characteristics by means of coupling between modes. Let us now analyze the frequency-temperature characteristics of a flexural mode of vibration without coupling with other modes. The resonant frequency f(T) of the flexural mode at a given temperature can be expressed with the room temperature (20°C) as the reference temperature as

$$f(T)=f(20)\left(1+\alpha(T-20)+\beta(T-20)^2+\gamma(T-20)^3\right) \qquad (1)$$

where α : 1st-order temperature coefficient
β : 2nd-order temperature coefficient
γ : 3rd-order temperature coefficient
T : temperature.

On the other hand, the resonant frequency f(T) of the flexural mode at a given temperature T(°C) can be expanded approximately around the turnover temperature Tp(°C) as the followings :

$$f(T)=f(Tp)\left(1+\beta(T-Tp)^2+\gamma(T-Tp)^3\right) \qquad (2)$$

where β : 2nd-order temperature coefficient
γ : 3rd-order temperature coefficient
Tp : turnover temperature.

In Fig. 10, the broken line shows β in Eq. (2) plotted against the angle ϕ of cut in Fig. 3. These values are obtained by solving two dimentional vibrational equations for a flexural beam[3]. In this figure, we know $\beta=0$ as the angles $\phi=-3$(deg.) and $\phi=17$(deg.). In these conditions the values of Tp are negative. Hence, we predicted that we could obtain a quartz tuning fork with β vanishing at the room temperature if we made Tp to be the room temperature. Making Tp to be the room temperature(20°C) means that $\alpha=0$ in Eq. (1). The value of α may be primarily influenced by coupling between modes. The value of β may be, therefore, a little changed when Tp is changed, i.e. α is changed, by coupling between modes. Hence, it is considered that the curve of β at Tp is similar to the curve of the broken line in Fig. 10 when Tp is changed to be the room temperature by coupling between modes. Taking the coupling between modes into consideretion, the curve of β at 20°C of the coupled flexural mode has been exactly calculated by using the computer program of the finite element method called NASTRAN. This calculational procedure is mentioned later in the appendix.

As mentioned above, we have attempted to make both the values of α and β to vanish at the room temperature by elastically coupling the flexural mode of vibration with a torsional mode.

Investigation of new angles of cut

We contemplated coupling elastically the main mode of vibration with another in order to improve the frequency-temperature characteristics of the conventional quartz tuning fork as mentioned above[4].

Our attention was paid to the flexural and torsional modes of vibration from among the various modes of vibration inherent in the tuning fork type quartz rosonator. Fig. 5 shows frequency spectrum of a quartz tuning fork of d=1340(μm) and l=3675(μm) (Fig. 2), computed by means of the program at the temperature of 20°C referred in the appendix. In Fig. 5, F_0 is the flexural vibration which has been used conventionally and T_0 the torsional vibration of the tuning fork tine. Fig. 6 and Fig. 7 show respectively the displacement of the F_0 mode and T_0 mode of vibration. The displacement in these figures represent those on the line AB on the mid-plane of the quartz resonator as illustrated below each figure. U_X is the displacement in the X direction and U_T the torsional displacement about the Y-axis(the line AB). The appearance of vibrational displacement distribution as viewed from the top of the quartz tuning fork is also shown with each figure. The T_0 mode is the torsional vibration whose twist directions are opposite each other for the right and left tines of the tuning fork.

In Fig. 5, the T_0 mode, as it gets closer to the F_0 mode, will affect the F_0 mode. This effect may be evident in frequency spectrum of Fig. 5, where increasing the thickness t from a lower level up toward t_o will result in the F_0 mode frequency gradually rising and finally reaching the T_0 mode. Now let us define

$$\delta f=f_F-f_T \tag{3}$$

where f_F is the F_0 mode frequency, and f_T the T_0 mode frequency. This expression suggests that the maximum coupling between the two modes of vibration occures when the frequencies f_F and f_T are the closest to each other, that is, when δf is minimum. It takes place when the thickness t in Fig. 5 is t_o. How far the two modes of vibration can couple with each other may be determined by the frequency difference δf_o at this thickness of maximum coupling. When the two vibrations do not couple but degenerate to have the same frequency, then $\delta f_o=0$. The extent to which the two modes couple with each other can be estimated by δf or the thickness t.

Let us now analyze how the frequency-temperature characteristics of the F_0 mode of vibration is affected by its coupling with the T_0 mode of vibration. If the angles ϕ , θ , ψ of cut in Fig. 3 are given, the frequency-temperature characteristics of a quartz tunig fork can be generally shown in a parabolic curve with its convex facing upward, which takes the form of curve (A) in Fig. 8. With the thickness t of this resonator increased toward t_o, the curve (A) will change to be the curve (B). For the curve (B), α is zero in the equation (1), meaning the turnover temperature is 20(°C). Therefore α can be easily changed by the coupling of two vibrations. This process can be computed in detail using the NASTRAN program mentioned in the appendix. Values of f_F, which can be calculated for given angles of cut, form (shape or dimension) and temperature, were first computed for several temperatures, and then the temperature coefficients of coupled f_F in the expression (1) were derived by means of the least square method. Fig. 9 shows the temperature coefficients for the angles $\phi=-11$, $\theta=0$ and $\psi=0$, while the curve (A) and the curve (B) in Fig. 8 represent the temperature characteristics for thickness t less than 88(um) and thickness t=88(um) respectively. Fig. 9, accordingly, shows the relationship between α and β for these thicknesses t, where t_{opt}= 88(um).

In Fig. 10 the solid line shows β values plotted against the angle ϕ where the thickness t was controlled so as to constantly produce $\alpha = 0$. It is predicted from Fig. 10 that $\beta = 0$, in addition to $\alpha = 0$, in the vicinity of $\phi = -10°$ and $\phi = 25°$ (named M_1-cut and M_2-cut respectively). For these new angles of cut, therefore, the frequency-temperature characteristics of the quartz tuning fork depend only on r in the expression (1) and are given in a cubic curve. The frequency-temperature characteristics thus predicted of M_1-cut are shown in Fig. 11. They can favourably compare with the excellent characteristics of the well-known AT-cut quartz oscillator.

The above discussion only deals with the quartz tuning fork rotated by ϕ about the x-axis (See Fig. 3.). But the same analysis in applicable to the tuning fork rotated by θ about the y-axis. Fig. 12 shows the result of such analysis, which allows us to predict the presence of new angles of cut where $\alpha = \beta = 0$ for certain θ's (for negative θ named M_3-cut and for positive θ M_4-cut). In this figure the broken line shows the values of β at Tp without coupling and the solid line shows the values of β at 20°C of coupled f_F.

Experimental

We produced actually the quartz tuning fork predicted by the calculation described above. The angle ϕ of cut was about -10° (M_1-cut) as predicted in the analysis whereas the external dimensions were the same as those used in the above-mentioned calculation. The shape and electrode pattern were formed by the photo-lithographic process[5]. Fig. 13 and Fig. 14 show respectively the F_0 mode and the T_0 mode of vibration observed and confirmed by laser-holography. These vibrational displacement distributions are both in a good agreement with the results of computation with NASTRAN shown in Figs. 6 and 7.

Fig. 15 shows the temperature characteristics of f_F for the angle $\phi = -9.5$(deg.). When $\delta f = 4.4$ (kHz), α is negative and therefore the turnover temperature is lower than the room temperature. But when δf is decreased to be 3.3 (kHz), the turnover temperature is higher than the room temperature. Fig. 16 shows the change in the frequency-temperature characteristics represented by α and β in the expression (1). The abscissa stands for δf, which can be converted into t by using Fig. 5. When $\delta f = 4$ (kHz), $\alpha = 0$.

We made experiments with varying angles of ϕ, thickness, and therefore δf. Fig. 17 shows β values plotted against ϕ when $\alpha = 0$. The solid line in the figure represents the result of computation with NASTRAN (Fig. 10), indicating an excellent agreement between the results of calculation and experiment. Thus, when the angle ϕ is in the vicinity of -10°, we get $\alpha = 0$ and $\beta = 0$. Measurements of frequency-temperature characteristics of M_1-cut under the above conditions are shown in Fig. 18. Thus, quite an innovative quartz tuning fork was developed which has cubic temperature characteristics. Fig. 19 shows the new quartz tuning fork with a very low temperature coefficient.

Characteristics

We have successfully developed a new quartz tuning fork which features the following advantages over the conventional quartz resonators :

(1) Excellent frequency-temperature characteristics

The resonant frequency does not change by about one part in a million over a 70-degree centigrade range of temperature, because both the 1st and 2nd derivatives of the frequency by the temperature are zero.

(2) Low power consumption

This quartz resonator can be designed to have any resonant frequency in the range of 50 kHz to 200 kHz. The quartz tuning fork with a lower frequency, especially, is desirable for portable time standard equipments, for which the power consumption is to be lowered.

(3) Simplicity

This quartz tuning fork does not need any additional temperature compensating devices or circuits.

(4) Low impedance and high quality factor

The crystal impedance is low on account of the high efficiency of electric field with the optimal electrodes configuration. Standard specifications are as follows :

Oscillation frequency	100 kHz
Series resonance resistance	10 kΩ
Quality factor	20×10^4
Series capacitance	1.0×10^{-3}pF
Parallel capacitance	1.0pF

(5) Miniature size and adaptability to mass production

The lithographic manufacture of this resonator promises dimensional precision as well as miniaturization. In fact, our standard resonator is currently mounted in a miniature case of 2.0 mm in dia. and 6.0 mm

in length. These resonators are almost uniform in size as they are formed lithographically, and they are suited to mass production owing to batch treatment.

(6) High resistance to shock

This resonator withstands shocks of drops well thanks to its small size and mass. Frequency variation of this resonator is small when it is dropped from a height of one meter.

(7) Free from gravity

The resonant frequency is little affected by gravity if the quartz tuning fork is designed to have a higher frequency. Frequency deviation of the 100 kHz quartz tuning fork due to gravity is one third of the conventional quartz tuning fork.

Conclusions

We have investigated new angles of cut, named M-cuts (M_1-, M_2-, M_3- and M_4-cuts) and successfully developed new quartz tuning fork with very low temperature coefficient.

Based on the knowledge accumulated through our analysis and experiment discussed in this paper, we are making further efforts to investigate the quartz tuning fork with more advantages in every possible way.

Acknowledgements

The authors wish to express their heartfelt appreciation to the co-workers of Suwa Seikosha Co., Ltd., and those of Matsushima Kogyo Co., Ltd., for their direct cooperation in this work.

Particular thanks are due to Mr. M. Imai, Mr. K. Miyasaka and other members of the Data Processing Department for their valuable advice and cooperation in our use of computer.

The authors are also indebted to Mr. K. Yamamura, Mr. T. Saito and Mr. S. Kusama for their encouragement throughout the course of this work.

References

1. M. Ariga, Bull. Tokyo Inst. Tech. A-No. 2, 1956
2. M. Nakazawa, Paper of T. G. US 76-6, p. 7 (1978-03), IECE Japan
3. M. Takagi, Technical Report of Suwa Seikosha Co., Ltd. (unpublished)
4. W. P. Mason, Proc. of the I. R. E., p. 220 May, 1940
5. K. Oguchi and E. Momosaki, Proc. of 32nd Annual Symposium on Frequency Control, p. 277, 1978

Appendix

Calculational procedure

In an effort to develop a new quartz tuning fork, we used the finite element method to calculate the resonant frequencies and the associated vibrational modes. The computer program used was NASTRAN, and the element used was a solid element. Fig. 1 shows this solid isoparametric element. The system of coordinates used in the analysis is shown in Fig. 3, where the x-axis, y-axis and z-axis represent the electrical axis, the mechanical axis and the optical axis of quartz crystal, respectively. The new coordinate system of X-axis, Y-axis and Z-axis was assumed by rotating counterclockwise about the x-axis by Φ, the y-axis by θ, the z-axis by ψ in turn. The X-, Y- and Z-axes in Fig. 2 represent a new coordinate system thus defined.

In the analysis, the model was assumed to be anisotropic, and the following values relative to the temperature after angular transformation of axes were calculated using a computer[1,2]. The data thus obtained were used then to calculate the eigen values and associated modes with NASTRAN.

At temperature T for a new coordinate system of (ϕ, θ, ψ), the data are given by the following :

Elastic constant matrix : Cij(T)

$$Cij(T) = \begin{pmatrix} C_{11} & C_{12} & \cdots & C_{16} \\ \vdots & \vdots & & \vdots \\ C_{61} & C_{62} & \cdots & C_{66} \end{pmatrix}$$

Density : $\rho(T)$

Coordinates of each grid : G(k, T)

T ; temperature

k ; node number

The details on procedures of the calculation and the program will not be discussed in this paper.

With this method, we can calculate the frequency-temperature characteristics of any mode for any shape or contour and any orientation of a quartz tuning fork. For instance, we computed the frequency-temperature characteristics of a quartz tuning fork currently used in a watch. The dimensions in Fig. 2 used were : d=900 (μm), l=4700 (μm), t=100 (μm). In Fig. 4 the broken line represents, as a reference[3], the temperature characteristics for the pure flexural vibration obtained by solving

approximately two dimensional equations for a flexural beam without NASTRAN. Open circular points represent experimental values.

As a result, we found that the temperature characteristics of a quartz tuning fork could be computed fairly accurately by means of NASTRAN through the use of a model as shown in Fig. 2 and an anisotropic solid element.

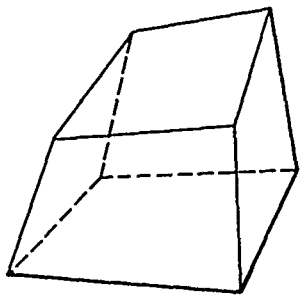

Fig.1 Solid isoparametric element

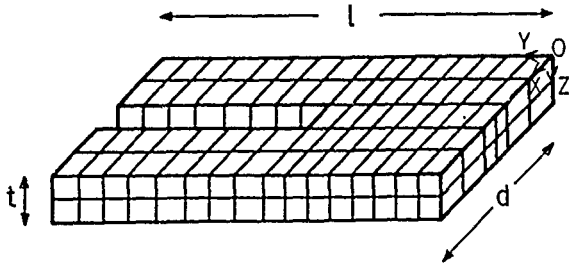

Fig.2 Model of a tuning fork

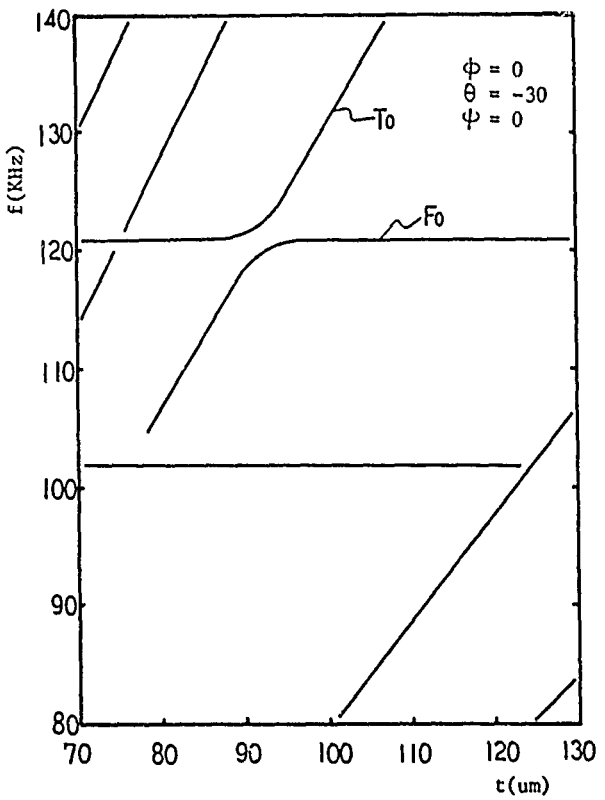

Fig.5 Frequency spectrum of a M_3-cut tuning fork

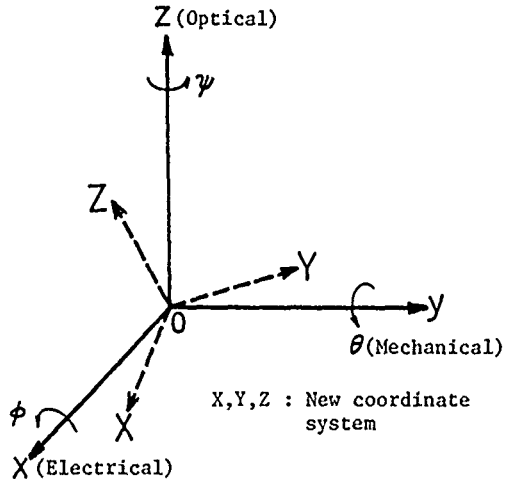

Fig.3 Coordinate system

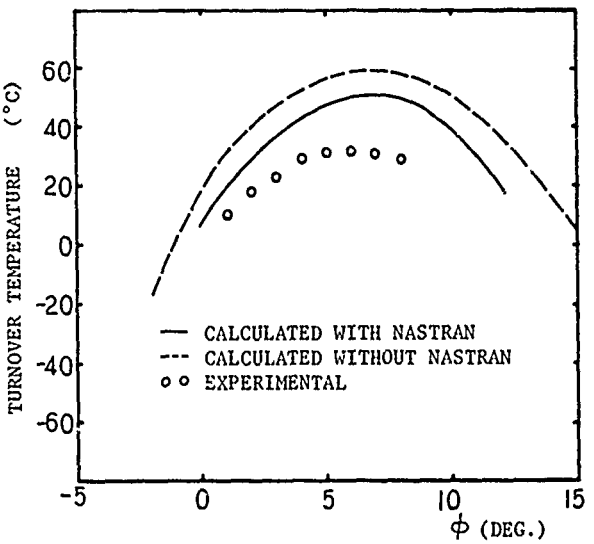

Fig.4 Turnover temperature of a current tuning fork vs. angles of cut

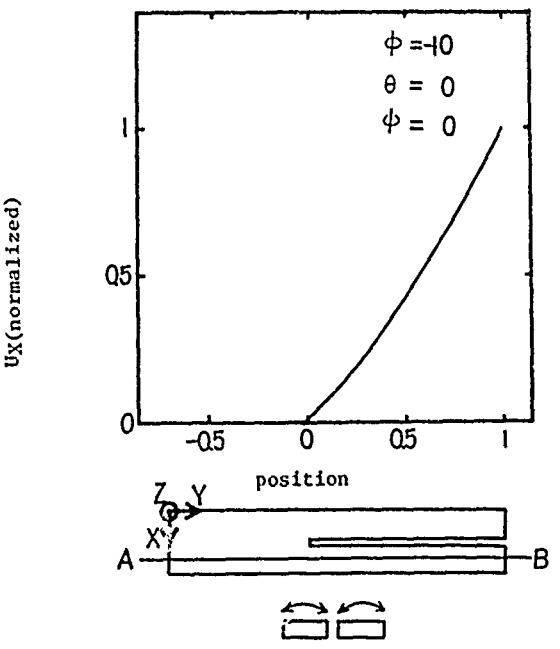

Fig.6 Displacement of Fo mode(calculated)

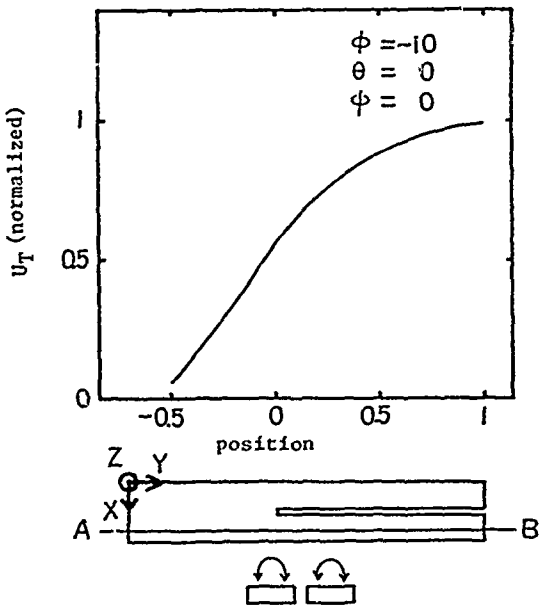

Fig.7 Displacement of To mode(calculated)

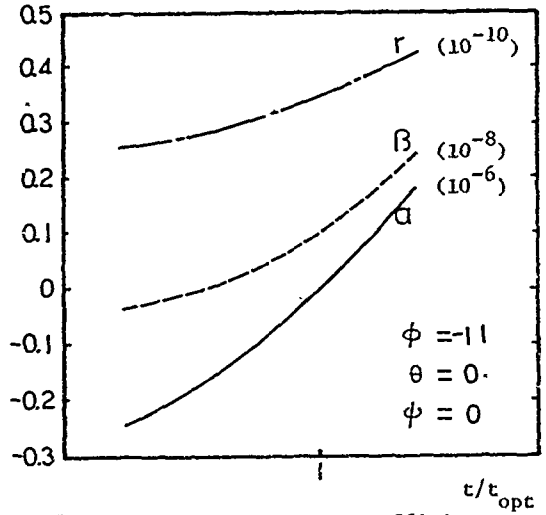

Fig.9 Frequency-temperature coefficients vs. t/t_{opt}

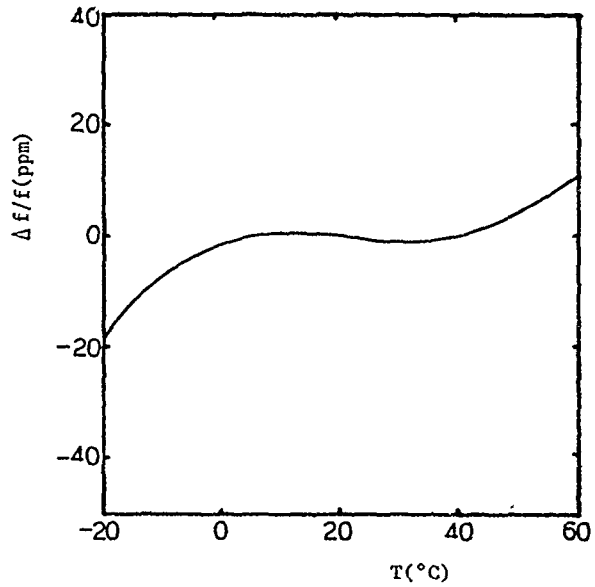

Fig.11 Frequency-temperature characteristics of a predicted M_1-cut quartz tuning fork.

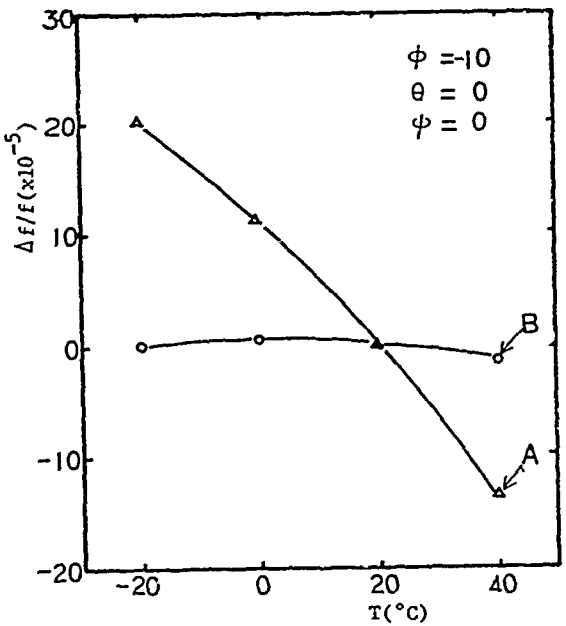

Fig.8 Dependence of frequency-temperature characterisitics on thickness

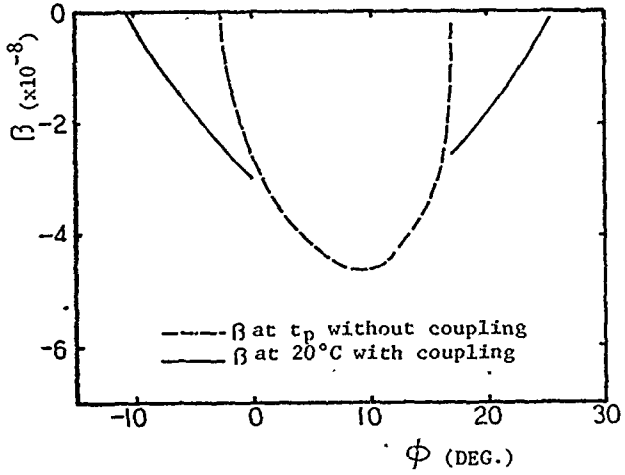

Fig.10 2nd-order temperature coefficient vs.φ

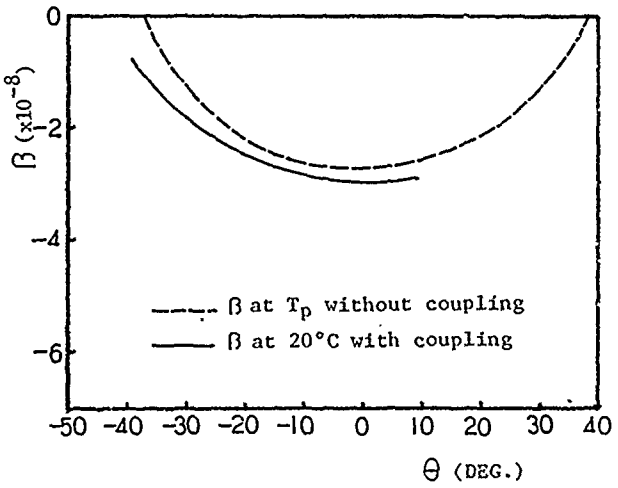

Fig.12 2nd-order temperature coefficient vs.θ

Holographic image

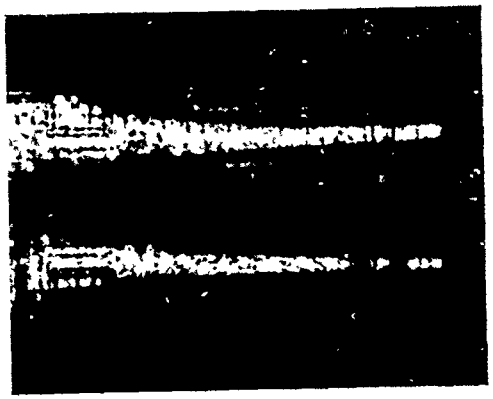

Holographic image

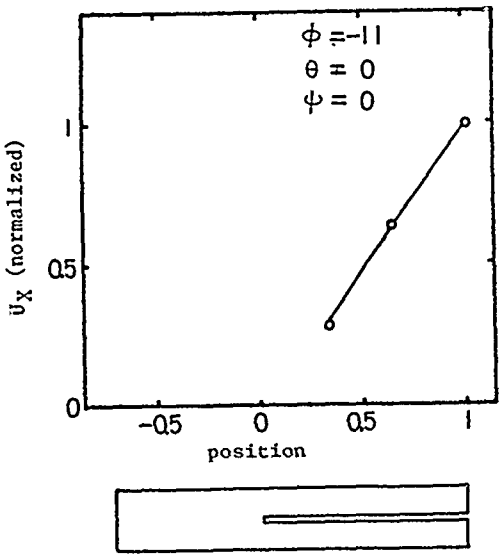

Fig.13 Displacement of Fo mode(experimental)

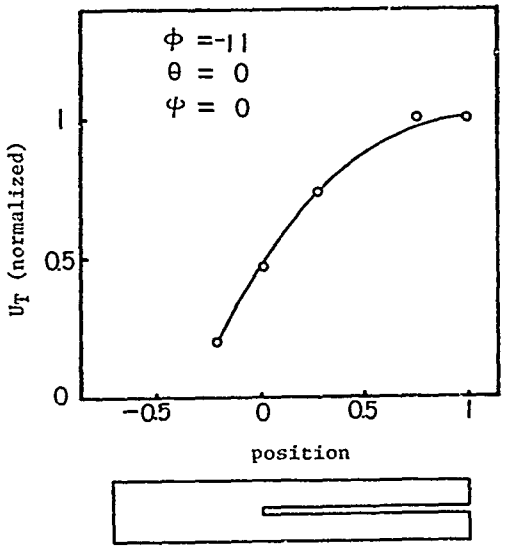

Fig.14 Displacement of T_0 mode (experimental)

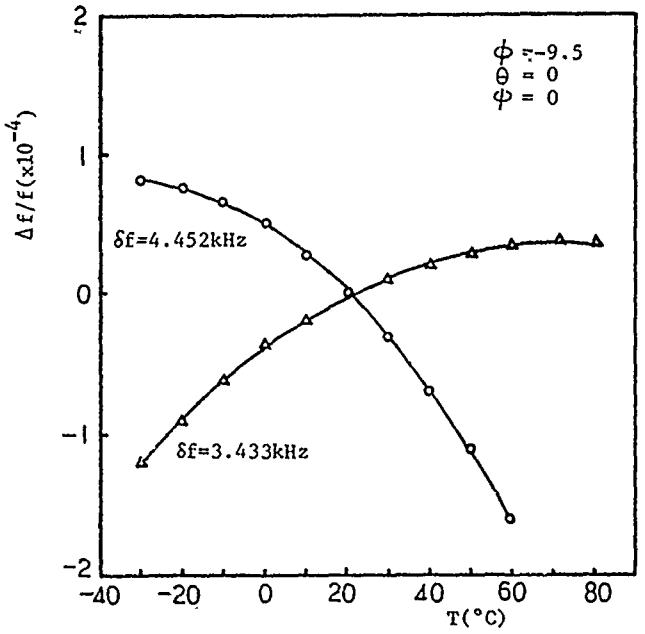

Fig.15 Frequency-temperature characteristics

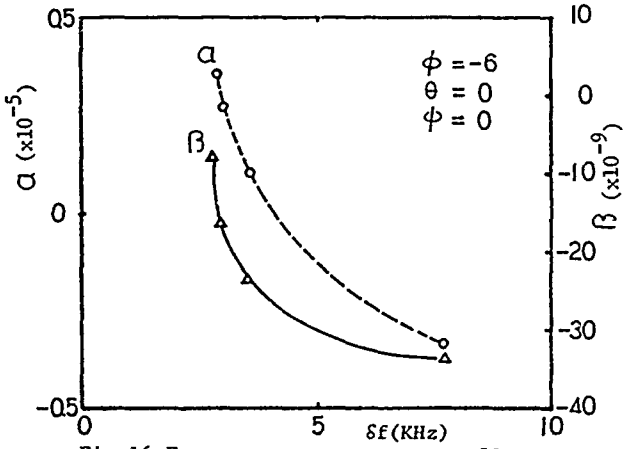

Fig.16 Frequency-temperature coefficient vs. δf

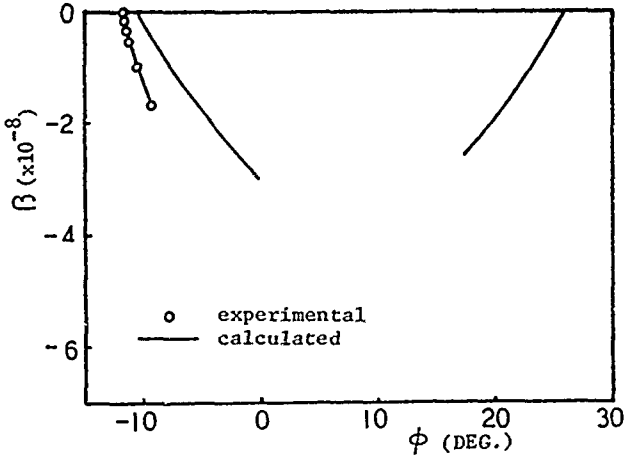

Fig.17 2nd-order temperature coefficient vs. φ

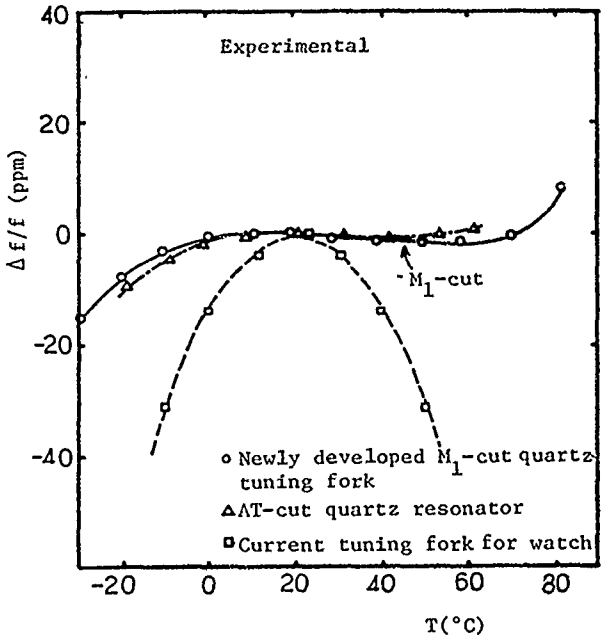

Fig.18 Frequency-temperature characteristics

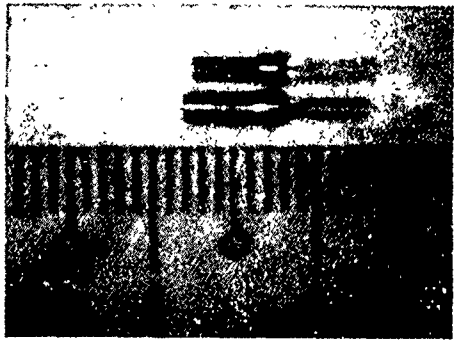

Fig.19 Newly developed quartz tuning fork produced by photolithographic process

A NEW QUARTZ CRYSTAL CUT FOR CONTOUR MODE RESONATORS

J. Hermann and C. Bourgeois

Centre Electronique Horloger S.A.
Neuchâtel, Switzerland

Summary

A computer procedure, based on variational techniques, has been developped to determine the frequency, the temperature behavior and the piezoelectric coupling of rectangular contour mode resonators of any crystallographic orientation.

This program has been instrumental in the discovery of a new quartz crystal cut, derived from a Z cut plate by a rotation about the Y axis, followed by a second rotation about the Z' axis. The first-order frequency-temperature coefficient of rectangular resonators, vibrating in extension along the Y' axis of this new plate, is very nearly independent of the width to length ratio. For a suitable choice of this dimensional ratio, the frequency-temperature curve exhibits a cubic behavior with a third-order coefficient of about $50 \times 10^{-12}/K^3$. The metallization pattern, which combines both in-plane and out-of-plane components of the electric field, has been devised so as to minimize the coupling to the unwanted modes.

Introduction

Since 1937, when Hight and Willard described the CT- and DT-cut resonators, a great deal of work has been devoted to contour mode resonators. The GT-cut, found in 1940 by W.P. Mason, is an outstanding member of this group, its frequency-temperature behavior being the best of all known crystal resonators. The purpose of this paper is to describe a new contour mode resonator characterized by a good temperature behavior, but devoid of the drawback of the GT-cut resonator, namely its high sensitivity to the width to length ratio.

It is well known that variational calculus, more precisely the Rayleigh-Ritz techniques, can be applied to approximate the normal modes of elastic structures. By giving due consideration to several programming details, it has been possible to refine this technique so as to use it for the determination of the frequency-temperature behavior of contour mode quartz resonators. This method, in conjunction with a somewhat arbitrary search procedure, has yielded a new quartz crystal cut suitable for width-extensional resonators.

Variational Calculation of the Frequency-Temperature Behavior

Eer Nisse and Holland [1, 2] used variational calculus to compute the frequencies of isotropic rectangular plates vibrating in contour modes. They expanded the displacements in a linear combination of trial functions, which they chose to be orthogonal circular functions. One can however show that, for a given number of trial functions, a power series expansion yields more exact frequencies in almost all cases, with the exception of very simple modes. The matrices representing the elastic and kinetic energies are then similar to Hilbert matrices, so that special techniques have to be devised to find the eigenvalues.

In order to apply this variational technique to the determination of the frequency-temperature behavior, one has to compute the frequencies at different temperatures, taking into account the temperature coefficients of all constants involved. It is then important to ensure that the difference between computed and exact frequencies be very nearly independent of the reference temperature. This can be achieved by memorizing the schemes used for the various matrix operations at one temperature, and by imposing these same schemes at the other temperatures required to determine the frequency-temperature coefficients. This procedure precludes the use of iterative methods to compute the eigenvalues.

The temperature behavior of various quartz contour mode resonators has been computed and checked against published values. The agreement is generally quite good, the discrepancies depending essentially upon the choice of the temperature coefficients of the elastic constants.

For the sake of illustration, the frequency-temperature behavior of GT-cut resonators has been determined. Figure 1 gives the first-, second- and third-order temperature coefficients, computed at 25°C, as a function of the width to length ratio. The curves correspond to the

extensional mode along the Z' axis, which is a width-extension in the left part of the figure, resp. a length-extension in the right part. This set of curves shows two noteworthy features:

(i) For a dimensional ratio of about 0.86 all three temperature coefficients are almost zero, yielding an extremely good temperature behavior.

(ii) Changing the width to length ratio by 1% around this value produces a shift of $2.5 \times 10^{-6}/K$ in the first-order temperature coefficient. This high sensitivity is due to an elastic coupling between both extensional modes, which is responsible for the very large variation of the temperature coefficients of a nearly square plate.

Search for a New Quartz Crystal Cut

In order to find a resonator whose first-order temperature coefficient of frequency is independent of the dimensional ratio, a pure extensional mode has been selected. This restrictive -and somewhat arbitrary- choice requires that both elastic constants responsible for the coupling with the surface shear mode, respectively with the other extensional mode, be negligibly small. The desired mode should then be devoid of coupling effects, whatever its width to length ratio. A further condition is that the first-order frequency-temperature coefficient of the chosen mode, denoted Tf (1), be zero. It turns out that all three requirements can be met by using a Z cut plate, first rotated about the Y axis and then about the Z' axis, as shown in figure 2.

For the selected mode to consist of a pure extension along the Y' axis, it is sufficient that $s'_{21} = 0 = s'_{26}$. Figure 3 represents both loci in the $\varphi - \theta$ plane. The first-order frequency-temperature coefficient of a hypothetical crystal, satisfying the above conditions everywhere in the $\varphi - \theta$ plane, can be computed. The locus corresponding to a zero of this coefficient, which is independent of the width to length ratio, is shown by a dashed line in the same figure. Two significant features are to be noted:

(i) All three curves intersect approximately at a single point, which defines a new cut.

(ii) The curve $Tf(1) = 0$ also passes through that same point, at which it has the same tangent as the dashed curve. This tangent is approximately parallel to the θ axis, which means that the first-order temperature coefficient of frequency is very nearly independent of the rotation about the normal of the plate. Consequently this coefficient is essentially controlled by the substrate angle φ.

The frequency-temperature behavior of resonators corresponding to this new cut has been computed using the variational method described above. Figure 4 shows the first-, second- and third-order frequency temperature coefficients of the extensional mode along the Y' axis, computed at 25°C, as a function of the width to length ratio. To the left of the vertical dashed line this mode has a higher frequency than the extensional mode along the X' axis. This figure calls for the following remarks:

(i) As expected the first-order temperature coefficient of frequency is quite independent of the width to length ratio, and is almost zero.

(ii) Higher order temperature coefficients do show coupling effects, which are at a maximum for a width to length ratio of about 0.87. This is due to the temperature dependency of both curves $s'_{21} = 0$ and $s'_{26} = 0$ in the $\varphi - \theta$ plane.

(iii) For a dimensional ratio of about 2/3, the first- and second-order temperature coefficients are both zero, which means that the frequency-temperature curve exhibits a cubic variation. The inflection point lies near room temperature, and the third-order coefficient is about $50 \times 10^{-12}/K^3$.

To precisely annul the first-order temperature coefficient of frequency requires a slight increase in the substrate angle φ. The corresponding cut is then (ZXwt) $26\,1/2^\circ/20^\circ$. It is suggested that this orientation be designated ZT-cut, to stress the fact that it is relatively simply oriented with respect to a Z cut plate.

Properties of "ZT-cut" resonators

The main properties of a resonator designed for use at room temperature are the following:

orientation. (ZXwt) φ/θ with $\varphi = 26\,1/2^\circ$ and $\theta = 20^\circ$

mode of motion: width-extension (see fig. 5)

frequency constant: 2823 kHz · mm

dimensional ratio : $w/l = 0.67$

frequency-temperature curve: cubic

inflection temperature : $\sim 20^\circ C$

temp. coeff. at 20°C: $\begin{cases} Tf(1) \lessapprox \pm 0.1 \times 10^{-6}/K \\ Tf(3) \sim 50 \times 10^{-12}/K^3 \end{cases}$

The following computed sensitivities show that the first-order temperature coefficient is essentially controlled by the substrate angle φ.

$$\frac{\partial Tf(1)}{\partial \varphi} = 1.9 \times 10^{-6}/K \cdot deg$$

$$\frac{\partial Tf(1)}{\partial \theta} = 0.1 \text{ to } 0.2 \times 10^{-6}/K \cdot deg$$

$$\frac{\partial Tf(1)}{\partial (\frac{w}{l})} = 0.05 \text{ to } 0.1 \times 10^{-6}/K \cdot \%$$

Decreasing the width to length ratio to 0.64 increases the inflection temperature to about 65°C, whereas the third-order temperature coefficient slightly decreases to about $40 \times 10^{-12}/K^3$.

Due to coupling effects with the second surface shear and with the third flexure modes, there exist a forbidden range for the width to length ratio. This range has not yet been investigated experimentally, so that only theoretical limits are known. If these values are correct, the inflection temperature cannot be chosen between 25°C and 40°C. This appears to be the only limitation in an otherwise large range.

Piezoelectric coupling

The fact that this new resonator uses a doubly rotated substrate implies that several modes are piezoelectrically coupled. The only troublesome modes are in fact the fundamental surface shear and the length-extension, which are shown in figures 6 and 7. In order to ensure that the right mode be selected by a Pierce oscillator, it can be proved that the following relation must hold:

$$\frac{QC}{\omega}\Big|_{\text{desired mode}} > \frac{QC}{\omega}\Big|_{\text{unwanted modes}}$$

with Q : quality factor

C : motional capacitance

Since there is not much one can do to lower the Q factors of the unwanted modes, it is necessary to minimize the following ratios:

$$r_s = \frac{\frac{C}{\omega}\Big|_{\text{shear}}}{\frac{C}{\omega}\Big|_{\text{width-extension}}} \qquad r_l = \frac{\frac{C}{\omega}\Big|_{\text{length-extension}}}{\frac{C}{\omega}\Big|_{\text{width-extension}}}$$

This goal is achieved by choosing the metallization pattern shown in figure 8, which combines both in-plane and out-of-plane components of the electric field. The motional capacitances of the three modes involved can be determined by a procedure based on conformal transformations of the cross section of the plate. This method is quite similar to that used for flexural and length-extensional resonators [3]. The computation takes into account 6 piezoelectric constants, namely: d_{21}, d_{22}, d_{26}, d_{31}, d_{32} and d_{36}; it assumes the crystal to be electrically isotropic, so that only one dielectric constant is considered.

Figure 9 represents the dimensionless quantities r_s and r_l, computed for a thickness to width ratio of 8%, as a function of the metallization ratio m/w. Also shown in this figure is k^2, the square of the electromechanical coupling factor. It is apparent that for a fully metallized plate ($m = w$) the shear mode would be the one driven by the oscillator. The most convenient metallization ratio is $\frac{m}{w} = 0.25$, which corresponds to a minimum of r_l.

Experimental results

Our experimental work has been centered on the realization of a small size resonator, suitable for wrist watch applications. The mounting system consists of two chemically etched wires soldered to the center of the plate. The plate thickness has been chosen so as to avoid any coupling to out-of-plane modes of motion. The main characteristics of this design are summarized as follows:

frequency : 2^{20} Hz ≈ 1,05 MHz

crystal dimensions : thickness : 0.2 mm; width : 2.7 mm; length : 4.0 mm

quality factor : 200 to 300×10^3

motional capacitance : 1.2 fF

inflection temperature : 20 ± 5°C

third-order temperature coefficient : $Tf(3) = 50 \pm 5 \times 10^{12}/K^3$

The temperature behavior, as well as the motional capacitance, are in good agreement with theoretical values.

Conclusions

The new cut described in this paper has been found by purely theoretical means. It is suitable for width-extensional resonators having a cubic frequency-temperature behavior, with a third-order temperature coefficient about two times lower than that of an AT-cut resonator. The low sensitivity of the first-order temperature coefficient of frequency to the width to length ratio eliminates the need for any adjustment.

This resonator seems attractive for wrist watch applications, but could be useful for other purposes as well.

References

1. E.P. EerNisse, "Coupled-Mode Approach to Elastic-Vibration Analysis", J. Acoust. Soc. Am., Vol.40, pp. 1045-1050, November 1966.

2. R. Holland, "Contour Extensional Resonant Properties of Rectangular Piezoelectric Plates", IEEE Trans. Sonics and Ultrasonics, SU-15, pp. 97-105, April 1968.

3. J. Hermann, "Determination of the Electro-mechanical Coupling Factor of Quartz Bars Vibrating in Flexure or Length-extension", Proceedings 29th Annual Symposium on Frequency Control, pp. 26-34, May 1975.

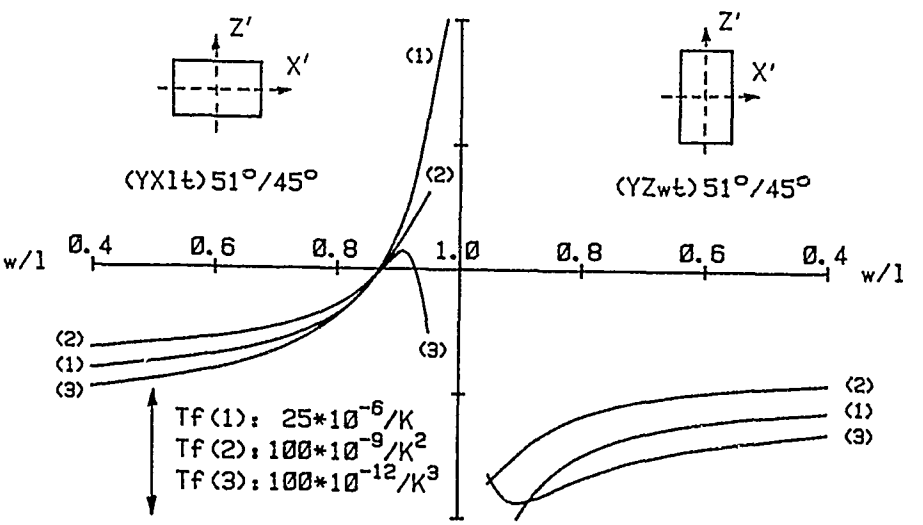

Fig. 1 GT-Cut : Frequency-Temperature Coefficients

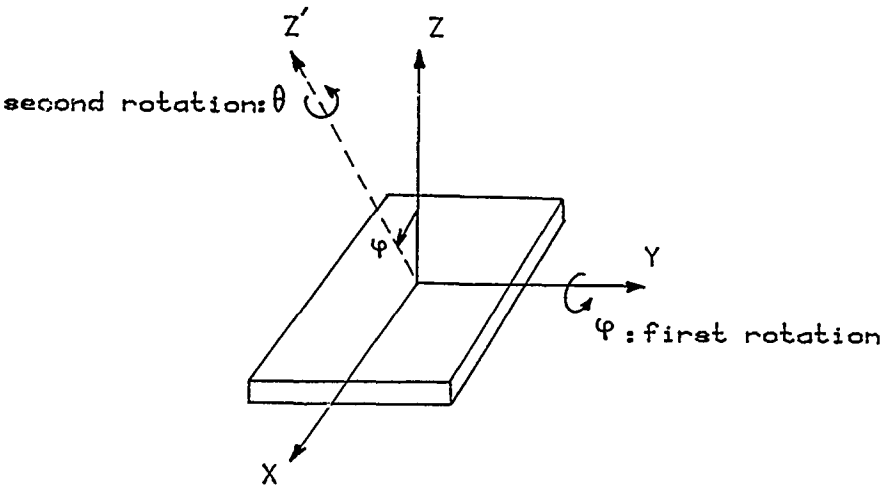

Fig. 2 Doubly Rotated Z-Cut Plate

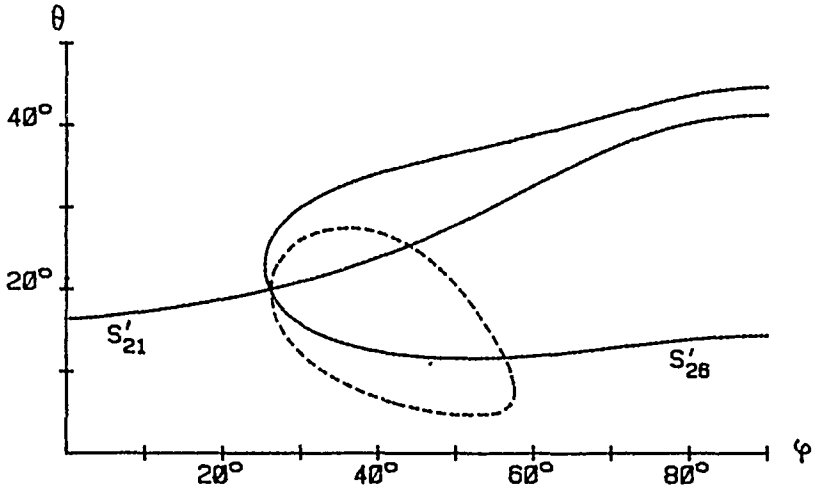

Fig. 3 Loci of $S'_{21} = 0 = S'_{26}$

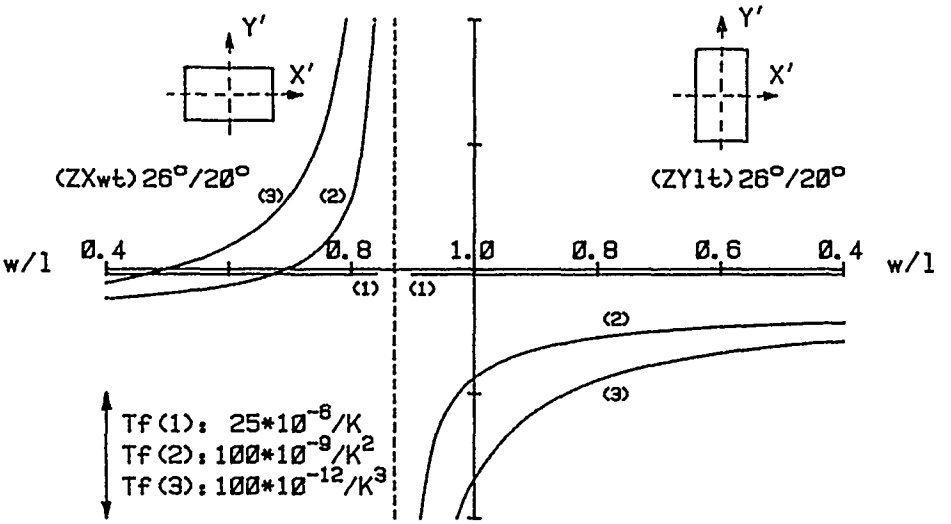

Fig. 4 New Cut : Frequenoy-Temperature Coeffioients

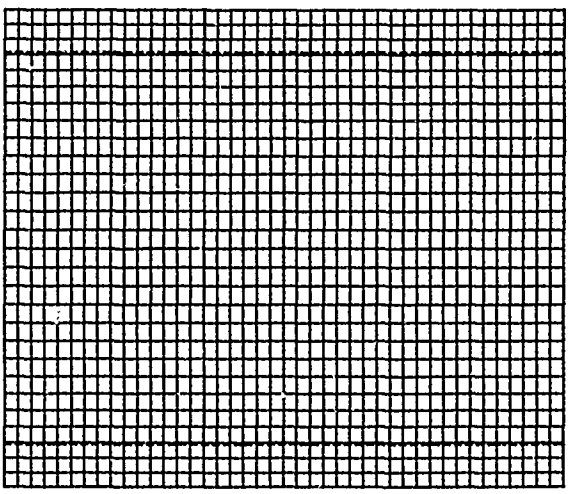

Fig. 5 New Cut : Width-Extensional Mode

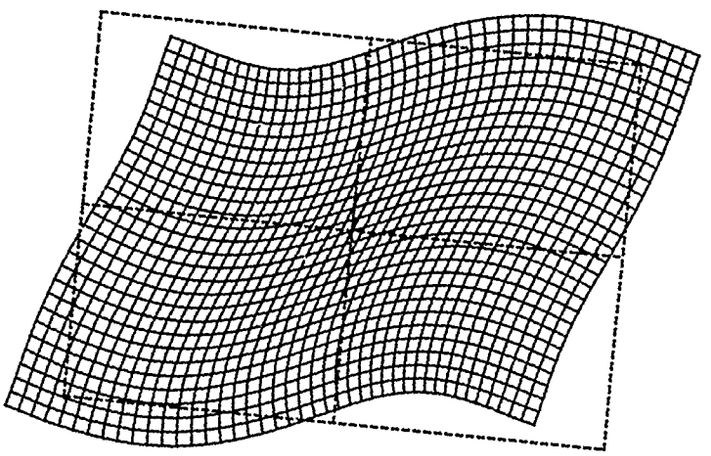

Fig. 6 New Cut : Surface Shear Mode

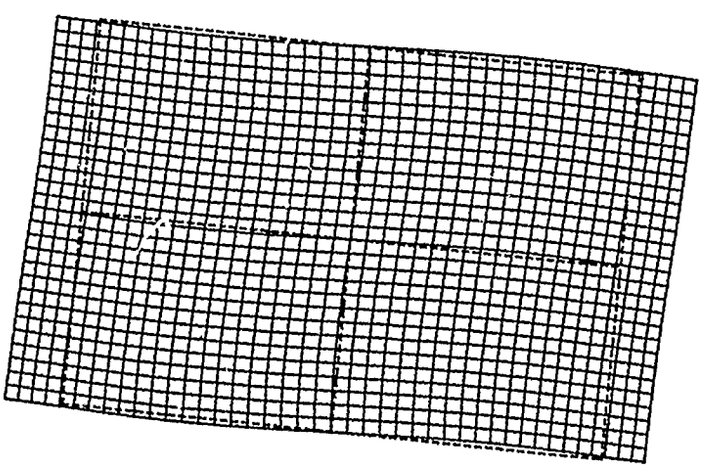

Fig. 7 New Cut : Length-Extensional Mode

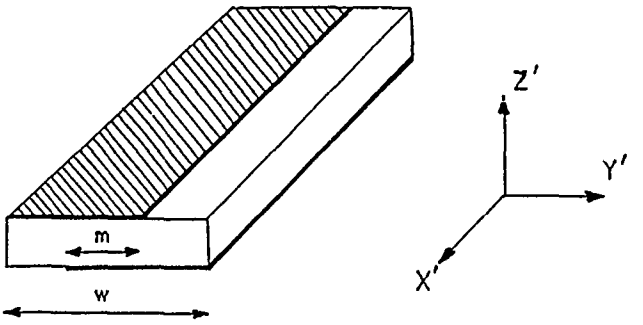

Fig. 8 Metallization Pattern

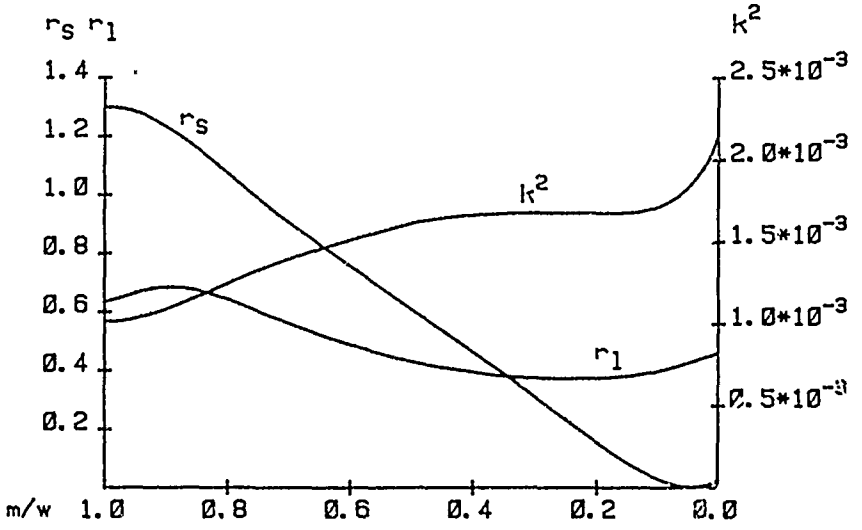

Fig. 9 r_s , r_l and k^2 versus Metallization Width

THREE-DIMENSIONAL VARIATIONAL ANALYSIS OF SMALL CRYSTAL RESONATORS

R.F. Milsom

Philips Research Laboratories
Redhill, Surrey, RH1 5HA, England

Abstract

A variational theory for the three-dimensional analysis of small crystal resonators is described. The theory is particularly applicable to the latest designs of miniature resonators which have a width dimension comparable to the thickness. The method is based on the theory of EerNisse and Holland but uses a particular choice of trial functions each of which is constrained to satisfy the differential equations. This choice is shown to have a number of advantages. The full effects of piezoelectric coupling and the mass-loading of the electrodes are included in the model. The analysis is applied to the AT-cut bar-type resonator elongated in the Z'-direction whose energy-trapping property has been unexplained theoretically. The results of plate equation analysis were used to further narrow the choice of trial functions.

Introduction

AT-cut quartz plates have been employed for frequency control applications for many years. More recently however, smaller bar-type resonators have been described. This follows the general trend towards miniaturization of all electronic components, and it is confidently expected that still smaller resonator designs will be proposed. Principal examples of the new smaller designs are those described by Onoe[1] and Zumsteg[2]. These are both AT-cut quartz bars, the former elongated in the X-direction and the latter in the Z'-direction (see Fig. 1). The Zumsteg design is of particular interest because very good energy trapping is achieved with modest metallisation and no contouring of the crystal faces. A quality factor of 500,000 has been reported. Good temperature stability is also observed. Current theory, employing the plate theory of Mindlin[3] and an energy trapping theory analogous to that of Shockley[4] gives poor agreement with the measured spatial distribution of energy. Indeed the exponential decay measured in the unmetallised region is some 4 times stronger than that predicted.[5] On the other hand the eigen-frequencies are accurately predicted as shown in Fig. 2.[2] The philosophy of the plate equation approach is that of finding an exact solution to a set of approximate equations. The basis of the approximation is that the solution can be expanded in a power series in the thickness co-ordinate, and because the thickness is significantly smaller than the other dimensions this series can be truncated, usually after the first order term or at worst after the second order term.[6] However if one of the other dimensions is comparable to the thickness, higher order terms could be significant. The inclusion of such terms would lead to a much larger set of somewhat unwieldy equations. Zumsteg included only first order terms[5] and this is almost certainly inadequate for a width-to-thickness ratio of approximately 3. However. if a solution including higher order terms was attempted it is difficult to see how Shockley's technique of matching the stress and displacement associated with evanescent and propagating modes in the unmetallised and metallised regions respectively could be satisfactorily applied. Alternative theory must be considered.

The method described here is an extension of the variational solution due to Eernisse and Holland.[7] The loading effect of electrodes is included in the analysis in a more rigourous way than in Shockley's theory and we may therefore expect improved accuracy for the energy trapping. Piezoelectricity is included in the analysis to give a fully self-consistent solution. This is not strictly necessary for weakly piezoelectric materials such as quartz, but there is a growing interest in more strongly piezoelectric materials for possible frequency control applications.[8] The model is therefore being developed to include cases where piezoelectricity is a first-order rather than second-order effect.

Differential Equations

Consider the arbitarily shaped piezoelectric body in Fig. 3. Parts of the surface denoted by S_e are coated with metal electrodes but are otherwise mechanically free. Other parts denoted by S_c are mechanically clamped but electrically free and the remaining surface area denoted by S_f is both electrically and mechanically free. Solutions are required for the electrical and mechanical fields when voltages sinusoidally varying with time are applied to the electrodes. The solution must satisfy the following differential equations within the solid,

$$T_{ij,j} - \rho\ddot{u}_i = 0 \quad \text{(Newton's Law)} \qquad (1)$$

and $D_{i,i} = 0$ (Gauss'Law) (2)

where T, ρ, u and D are respectively stress, density, particle displacement and electric flux density. The normal tensor notation is used so that comma denotes differentiation with respect to spatial co-ordinates and dot denotes differentiation with respect to time. Body forces are assumed to be zero and have been omitted from equation (1) and free charge within the solid has similarly been omitted from equation (2) because the solid is a perfect insulator. Equations (1) and (2) are coupled by the piezoelectric equations of state.

$$T_{ij} = c^E_{ijkl}S_{kl} - e_{kij}E_k \quad (3)$$

$$D_i = e_{ikl}S_{kl} + \varepsilon^s_{ik}E_k \quad (4)$$

where S, E, c^E, e, ε^s are respectively strain, electric field, and the stiffness, piezoelectric and permittivity tensors of the solid. In addition,

$$S_{ij} = \tfrac{1}{2}(u_{i,j} + u_{j,i}) \quad (5)$$

and $E_i = -\phi_{,i}$ (6)

where ϕ is electric potential. Substituting equations (5) and (6) into (3) and (4) and hence into (1) and (2) gives the differential equations in their most useful form,

$$-\rho\ddot{u}_j + c^E_{ijkl}u_{k,li} + e_{kij}\phi_{,ki} = 0 \quad (j=1,2,3) \quad (7)$$

$$e_{ikl}u_{k,li} - \varepsilon^s_{ik}\phi_{,ki} = 0 \quad (8)$$

Boundary conditions

Before describing the boundary conditions that the above equations must satisfy a number of assumptions are made. Firstly the electric field outside the solid is assumed to be negligible. Secondly the electrodes are negligibly thin but are assumed to have a finite mass m per unit area, and thirdly the electrodes have zero resistance. The unit outward normal at the surface is denoted by N_j. The boundary conditions are then as follows.

$$u_i = 0 \quad \text{on } S_c \quad (9)$$

$$N_jT_{ij} = 0 \quad \text{on } S_f \quad (10)$$

$$-N_jT_{ij} = m\ddot{u}_i \quad \text{on } S_e \quad (11)$$

$$N_jD_j = 0 \quad \text{on } S_c \text{ and } S_f \quad (12)$$

$$\phi = V_p\exp(j\omega t) \quad \text{on } S_e \quad (13)$$

where $V_p\exp(j\omega t)$ is the voltage applied to the p^{th} electrode, with angular frequency ω. The exponential time dependence $\exp(j\omega t)$ is common to all field variables and is omitted henceforth.

Variational formalism

The problem may be described in terms of the above differential equations and boundary conditions. An alternative description is possible using variational calculus. This involves finding a Lagrangian which is stationary with respect to arbitrary variations if and only if the differential equations and boundary conditions are satisfied. Eernisse and Holland have shown that the appropriate Lagrangian is (Ref.7, p.131)

$$L = \tfrac{1}{2}\iiint_V (S_{ij}T_{ij} + \rho\dot{u}_i\dot{u}_i - D_iE_i)dV - \iint_{S_c} u_iN_jT_{ij}\,dA - \sum_p \iint_{S_e} (\phi - V_p)N_jD_i\,dA \quad (14)$$

where V is the volume of the solid including the electrodes.

Now consider arbitrary infinitessimal first variations $\delta\phi$ and δu_i to the independent field variables ϕ and u_i. The corresponding variations δD_i and δT_{ij} to the dependent field variables D_i and T_{ij} are given by the equations (3) (4) (5) and (6). Using the divergence theorem it may be shown that the first variation of L is

$$\delta L = -\iiint_V \delta u_i[T_{ij,j} - \rho\ddot{u}_i]dV - \iiint_V \delta\phi D_{i,i}\,dV - \iint_{S_c} u_iN_j\delta T_{ij}dA - \iint_{S_e} (\phi - V_p)N_j\delta D_j dA + \iint_{S_e+S_f} \delta u_iN_jT_{ij}\,dA + \iint_{S_f} \delta\phi N_jD_j\,dA \quad (15)$$

Using the assumption that the electrodes are infinitessimally thin but have finite mass m per unit area, it follows that the only contribution to the two volume integrals from the electrodes reduces to a single surface integral,

$$\iint_{S_e} \delta u_i m\ddot{u}_i\,dA$$

then, $\delta L = -\iiint_V \delta u_i [T_{ij,j} - \rho \ddot{u}_i] dV - \iiint_V \delta\phi D_{i,i}\, dV$

$$-\iint_{S_c} u_i N_i \delta T_{ij}\, dA - \iint_{S_e} (\phi - V_p) N_i \delta D_j\, dA$$

$$+\iint_{S_e} \delta u_i N_j T_{ij}\, dA + \iint_{S_e} \delta u_i (N_j T_{ij} + m\ddot{u}_i) dA$$

$$+\iint_{S_f} \delta\phi N_j D_j\, dA \qquad (16)$$

where the two volume integrals are taken over the piezoelectric solid only. Inspection of each term of equation (16) and comparison with equations (1) (2) (9) (10) (11) (12) and (13) verifies that δL vanishes for arbitray variations, so the Lagrangian is indeed stationary. This stationary property is used to obtain the solution. In general the variational solution for the independent field variables is expanded in a set of trial functions f_{in} with unknown amplitudes A_{in}.

Thus,

$$u_i = \sum_n A_{in} f_{in}(x_1, x_2, x_3) \quad (i = 1,2,3,4) \qquad (17)$$

where ϕ has been rewritten as u_4 for convenience. Arbitrary variations are achieved by varying each of the A_{in} in turn by δA_{in}. Thus

$$\delta u_i = \delta A_{in}\, f_{in}(x_1, x_2, x_3) \qquad (18)$$

Substitution of equations (17) and (18) into (16) yields a system of linear equations,

$$\frac{\delta L}{\delta A_{in}} = 0 \qquad (19)$$

which are solved for the A_{in}. This general method is sometimes referred to as the Rayleigh-Ritz technique.

Choice of trial functions

Eernisse and Holland chose for their trial functions Fourier expansions in the spatial coordinates. Others have used more sophisticated trial functions which obey the differential equations and some of the boundary conditions.[9] In this work trial functions obeying only the differential equations but none of the boundary conditions are used. This form of trial solution has certain advantages over the simple Fourier expansions but the extra sophistication of satisfying boundary conditions has been rejected for three reasons. Firstly finding each such trial solution may be a lengthy computing exercise in its own right, secondly such solutions may be too restrictive because the model is to be applicable to a variety of geometries involving inhomogeneous boundary conditions due to partial metallisation of surfaces, and thirdly there are doubts about the completeness of such sets of solutions.

Here the solutions are expanded in Fourier series in two spatial coordinates say x_1 and x_3. Thus making no assumptions concerning the symmetry of the solution,

$$u_i = \sum_r [A_{ir}^{(1)} \sin(k_{1r}x_1)\sin(k_{3r}x_3)\, f_r^{(1)}(x_2)$$

$$+A_{ir}^{(2)} \sin(k_{1r}x_1)\cos(k_{3r}x_3)\, f_r^{(2)}(x_2)$$

$$+A_{ir}^{(3)} \cos(k_{1r}x_1)\sin(k_{3r}x_3) f_r^{(3)}(x_2)$$

$$+A_{ir}^{(4)} \cos(k_{1r}x_1)\cos(k_{3r}x_3) f_r^{(4)}(x_2)] \qquad (20)$$

The functions $f_r^{(j)}(x_2)$ must be chosen so that equation (20) satisfies the differential equations (7) and (8). k_{1r} and k_{3r} are the spatial harmonic wave numbers in the x_1 and x_3 directions which are defined in detail later. Equation (20) may be written much more concisely in complex form. Thus

$$u_i = \sum_r A_{ir} \exp(jk_{1r}x_1 + jk_{3r}x_3) . f_r(x_2) \qquad (21)$$

where k_{1r} and k_{3r} take both positive and negative values and the A_{ir} are in general complex. It is now assumed that

$$f_r(x_2) = \exp(jk_2x_2) \qquad (22)$$

so that values of k_2 which satisfy the differential equations must be found. Substituting equation (22) into equations (7) and (8) yields

$$H_{ji}A_{ir} = 0 \quad (j = 1, 2, 3, 4) \qquad (23)$$

where

$$H_{ji} = \rho\omega^2\delta_{ji} - k_{1r}k_{kr}c^E_{kjil} \quad (i,j = 1,2,3)$$

$$H_{j4} = H_{4j} = k_{1r}k_{kr}e_{kj1} \quad (j = 1,2,3)$$

and $H_{44} = k_{1r}k_{kr}\varepsilon^S_{1k} \qquad (24)$

For a non-trivial solution to equation (23)

$$|H_{ji}| = 0 \qquad (25)$$

In general the determinant of H is an eighth order polynomial in k_2. Thus

$$\sum_{i=0}^{8} D_i \, k_2^{\,i} = 0 \qquad (26)$$

where $D_i = \sum_{k=1}^{4} \sum_{j=0}^{2k-i} G_{kij} \, \omega^{8-2k} k_{1r}^{\,j} k_{3r}^{\,2k-i-j}$

and where the constants G_{kij} are piezoelectrically generalised Christoffel constants of the solid. There are therefore eight possible values of k_2 for each choice of ω, k_{1r}, k_{3r} which are readily obtained by solving equation (26). for each value of k_2 there is a corresponding solution to equation (23) for the ratio A_{ir}/A_{4r} ($=a_{ir}$ say) so equation (21) may now be rewritten

$$u_i = \Sigma_t B_t a_{it} \exp(jk_{1t}x_1) \quad (i = 1,2,3,4) \qquad (28)$$

where the B_t are the unknown amplitudes, the term in the brackets is summed over 1 = 1, 2 and 3, and the summation over t includes all eight possible values of k_{2t} for each choice of k_{1t} and k_{3t}. Because the trial function in equation (28) is an exact solution of equations (7) and (8) the first two integrals in equation (16) vanish. Furthermore since the variational parameters B_t are complex, complex variations are possible, and equation (16) can be written

$$\delta L = -\iint_{S_c} u_i N_j \delta T_{ij}^{*} dA - \iint_{S_e} (\phi - V_p) N_j \delta D_j^{*} \, dA$$

$$+ \iint_{S_f} \delta u_i^{*} N_j T_{ij} \, dA + \iint_{S_e} -\delta u_i^{*} (N_j T_{ij} + m\ddot{u}_i) \, dA$$

$$+ \iint_{S_f} \delta\phi^{*} N_j D_j \, dA \qquad (29)$$

It remains to substitute equation (28) and the variation $\delta u_i = \delta B_t a_{it} \exp(jk_{1t}x_1)$ for all values of t into equation (29) to give the linear equations in B_t. These will in general have the form

$$\sum_{t=1}^{R} \mu_{rt} B_t = \upsilon_r \quad (r = 1..T) \qquad (30)$$

where μ_{rt}, υ_r are complex. The integrations in the evaluation of μ_{rt} and υ_r can be made particularly simple by rotating the concise expressions in equation (28) to new sets of coordinate axes for each crystal face, such that one of the new axes is normal to that face and one or both of the other axes are aligned with crystal edges. To find the short circuit resonant frequencies the applied voltages V_p are set equal to zero which makes the column vector υ_r zero. The resonances are then given by the zeros of the determinant of μ_{rt}.

The advantages of finding trial solutions that obey the differential equations are now apparent. Firstly, the volume integrals vanish identically. Secondly, the number of unknown variational parameters B_t has been reduced by a factor of 4 because there is a fixed relationship between u_1, u_2, u_3 and ϕ for each t. Thirdly, at most 8 values of k_2 are required for a complete expansion in the x_2 direction. And finally rapid convergence can be expected because part of the problem has been solved before the variational technique is employed. One disadvantage is that the trial functions must be computed at each frequency, unlike the frequency independent functions used by Eernisse and Holland. Therefore, although fewer functions will in general be required for a given accuracy the computations may be more time-consuming.

Application of analysis to Zumsteg resonator

The above analysis is completely general. It will now be applied to the particular bar-type resonator described by Zumsteg.[2,5] This is shown in Fig. 1. Measurements of the distribution of vibration amplitude were reported for a resonator with dimensions L_1 = 1.25 mm, L_2 = 0.4 mm L_3 = 10 mm and W = 3 mm and with a metallisation of 2350 Å gold equivalent. The solution is here expanded in a Fourier series in the length or x_3-direction. Thus k_{3r} takes the 2N values

$$k_{3r} = -\frac{N\pi}{L_3}, -\frac{(N-1)\pi}{L_3} \ldots -\frac{\pi}{L_3}, \frac{\pi}{L_3} \ldots \frac{(N-1)\pi}{L_3}, \frac{N\pi}{L_3} \qquad (31)$$

The solution could also be expanded in a complete Fourier series in the width or x_1 direction, but using the results of Mindlin's theory[3] for AT-plates of finite width it is possible to be more selective in the choice of values for k_{1r}. These results, illustrated in Fig. 2 suggest that the operating mode is thickness shear coupled to flexure. The flexure is essentially forced by the thickness shear through coupling at the width faces. The fundamental frequency of the shear mode for an infinite plate

$$f_o = \left(\sqrt{c_{66}^{E}/\rho} \right) / \left(2L_2 \right)$$

is 4.13 MHz. The operating frequency f is measured at 4.2 MHz.[5] Fig. 2 shows clearly that for a width/thickness ratio of 3.125 the ratio f/f_o can only be close to unity for 4th harmonic flexure (i.e. m = 4). Although the mode of interest is trapped in the x_3-direction whereas Mindlin's theory gives solutions independent of x_3, it is reasonable to assume that the mode

remains essentially thickness shear coupled to 4th harmonic flexure. For the purpose of this calculation it is assumed that the width to thickness ratio is equal to 3.2. Then from Ref. 3 k_{1r} takes only the values,

$$k_{1r} = 0, \quad -\frac{4\pi}{L_1}, \quad \frac{4\pi}{L_1} \qquad (32)$$

Other width to thickness ratios would require different values. The trial functions given by $k_{1r} = 0$ (i.e. those independent of x_1) are essentially thickness shear. Bearing in mind that there are 8 values of k_{2r} for each combination of k_{1r}, k_{3r} there is a total of 3 x 8 x 2N (=48N) independent trial functions.

The limited choice of harmonic components in equation (32) calls for a modification to the theory. The integral over the faces at $x_1=\pm L_1/2$ vanishes identically for all solutions (i.e. not if and only if the boundary conditions are satisfied), because the contributions are equal and opposite. This modification which is based on the Mindlin theory will not be described in detail here.

A number of calculations have been made for the above resonator dimensions, using the quartz data published by Bechmann.[10] The value of N was 3 which gives 144 terms in the expansion. The resonant frequency is found to be 4.15 MHz compared to the measured value of 4.2 MHz.[5] The displacement associated with the resonant mode is illustrated in Figs. 4 and 5. Fig. 4 shows the predicted vibration pattern in planes normal to x_3 at $x_3 = 0, \pm 3L_3/20$ and $\pm L_3/2$. These confirm that the mode type is thickness shear coupled to flexure. Fig. 5 shows the predicted vibration pattern in planes normal to x_1 at $x_1 = 0, \pm L_1/8$ and $\pm L_1/4$. The pattern is periodic in x_1, repeating itself at intervals of $L_1/2$. The strong attenuation of the displacement amplitude in the x_3-direction is clearly shown in both sets of diagrams. Normallised displacement u_2 at the surface $x_2 = L_2/2$ is shown as a function of x_3 in Fig. 6(c). The value of N was increased to 4 for the field calculations at the resonant frequency. The small ripple is a consequence of taking a finite number of terms in the expansion in x_3. The variational solution is compared with Zumsteg's measurements and his own predictions,[5] Figs. 6(b) and 6(a). The agreement between theory and experiment has clearly been greatly improved. In particular the variational theory predicts an amplitude ratio between electrode edge and electrode centre of 46%. This compares with a measured value of 45% and Zumsteg's original predicted value of 74% (implied by the value of 0.088 of normallised decay coefficient given). Further confirmation of the predicted mode-shape is given by the qualitative intensity of $|\partial^2 u_1/\partial x_2^2|$ and $|\partial^2 u_2/\partial x_1^2|$ in planes normal to x_2 measured by X-ray diffraction as shown in Fig.7. The predicted distribution of these quantities in the x_1 direction is shown in Fig. 8 for comparison. The solution for the mode shape observed in the x_3-direction is also compared to finite element calculations using the ASKA program.[11] These are illustrated in Fig. 9. The calculations are two-dimensional, assuming zero variation with x_3. The first ten modes are shown, mode number 8 being the one of interest here. There is close agreement with the 3-dimensional variational solution in Fig. 4, disregarding the x_3-variation. A full 3-dimensional solution using ASKA would have required excessive computer store. The frequency difference between the two solutions is mainly due to the slightly different width dimensions used, and also the fact that one solution is 2-dimensional and the other 3-dimensional.

Conclusion

A powerful method for analysing resonators has been described. This method is completely general but here has been addressed to the analysis of the new class of miniaturized resonators whose energy-trapping property had not hitherto been understood theoretically. Although results have only been presented for the Zumsteg design, the method is readily applicable to the Onoe design with contouring and tilting of the faces. Prediction of spurious modes would be possible by taking a complete Fourier expansion in the x_1-direction rather than selecting terms appropriate only for the mode of interest. This would however require excessive computer storage at present. Nevertheless, the three-dimensional modelling of the principal mode demands less storage than would be required by the finite element method for similar accuracy. The efficiency of the computer program is currently rather poor and this is now being improved before the program is run extensively to predict other resonator parameters. The accurate prediction of energy-trapping suggests that the method could be used to analyse monolithic filters on similar bar-type structures.

The author gratefully acknowledges the help of Daniel Vangheluwe of Philips Elcoma for providing the X-ray measurements and ASKA results and also for many useful discussions.

References

1. M. Onoe and M. Okazaki, Proc. 29th ASFC, pp.42-48, 1975.

2. A.E. Zumsteg and P. Suda, Proc. 30th ASFC, pp.196-201, 1976.

3. R.D. Mindlin, J. Appl. Phys., 22, pp.316-323 1951.

4. W. Shockley, D.R. Curran and D.J. Koneval, J. Acoust. Soc. Am., 41, p.981, 1967.

5. A.E. Zumsteg, P. Suda and W. Zingg, Proc. 32nd, ASFC, pp.260-266, 1978.

6. H.F. Tiersten, "Linear Piezoelectric Plate Vibrations", Chap. 13, Plenum Press, 1969.

7. R. Holland and E.P. EerNisse, "Design of Resonant Piezoelectric Devices", Chaps. 3 and 4, M.I.T. Press, 1969.

8. R.M. O'Connell and P.H. Carr, Proc. 32nd, ASFC, pp.189-195, 1978.

9. M. Onoe, J. Acoust. Soc. Am., 30, pp.1159-1162.

10. R. Bechmann, A.D. Ballato and T.J. Lukaszek, Proc. IRE, 50, p.1812, 1962.

11. D.C.L. Vangheluwe, Proc. 32nd, ASFC., pp. 134-141, 1978.

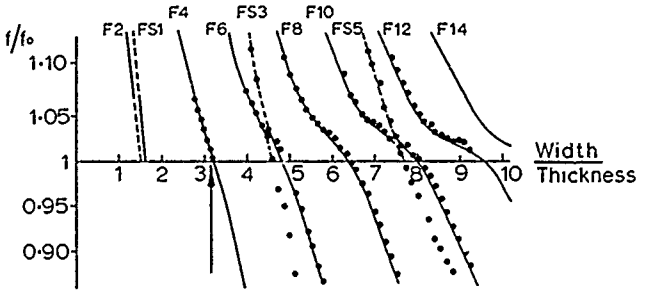

Fig.2 Eigen-frequencies of rectangular AT-cut resonators versus ratio of width (x dimension) to thickness (y'dimension)

——— } Mindlin theory (Ref.3)
- - - - }

..... Zumsteg's measurements (Ref.2)

(Arrow indicates mode of interest)

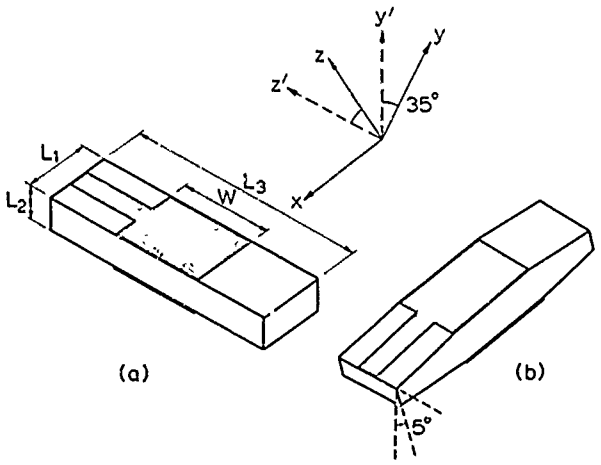

Fig.1 Bar-type AT-cut quartz resonators

(a) Zumsteg design (b) Onoe design

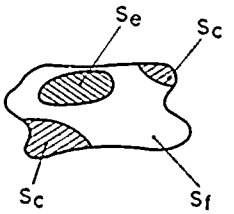

Fig.3 Arbitrarily-shaped piezoelectric body

S_e : Metallised surfaces

S_c : Mechanically clamped surfaces

S_f : Mechanically and electrically free surfaces

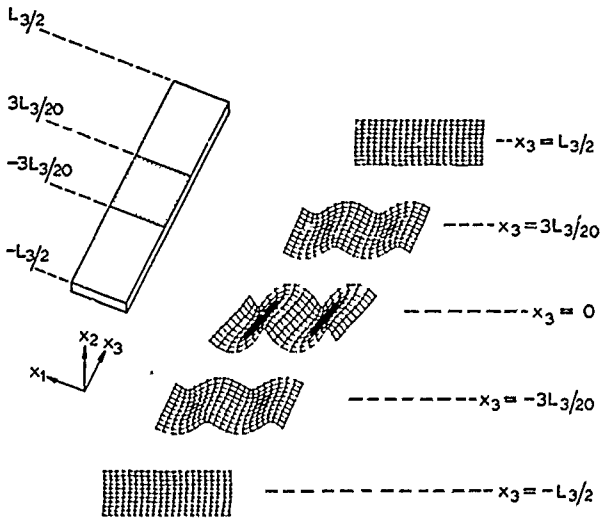

Fig.4 Computed vibration pattern of main resonance at planes normal to x_3

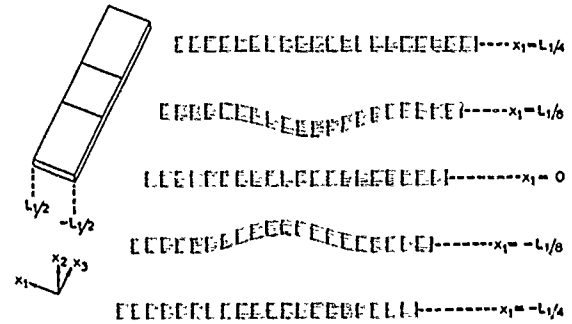

Fig.5 Computed vibration pattern of main resonance at planes normal to x_1

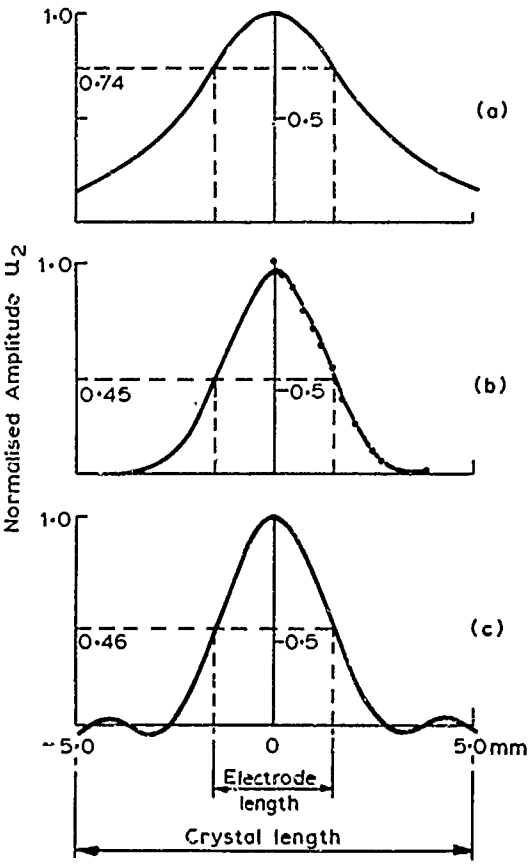

Fig.6 Amplitude of vibration component u_2 vs.x_3

($x_1 = L_1/8$, $x_2 = L_2/2$)

(a) Zumsteg theory
(b) Zumsteg measurements
(c) Variational theory

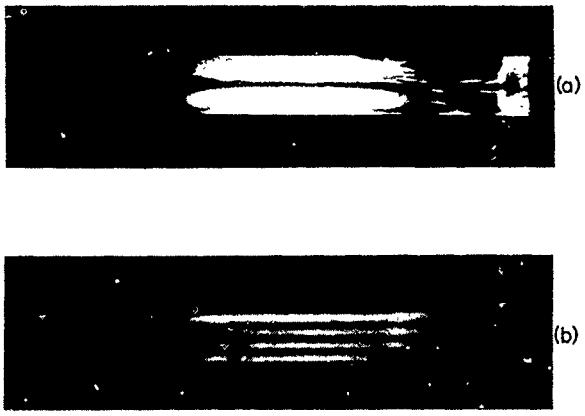

Fig.7 X-ray topographs of vibration intensity in plane normal to x_2

(a) $|\partial^2 u_1/\partial x_2^2|$

(b) $|\partial^2 u_2/\partial x_1^2|$

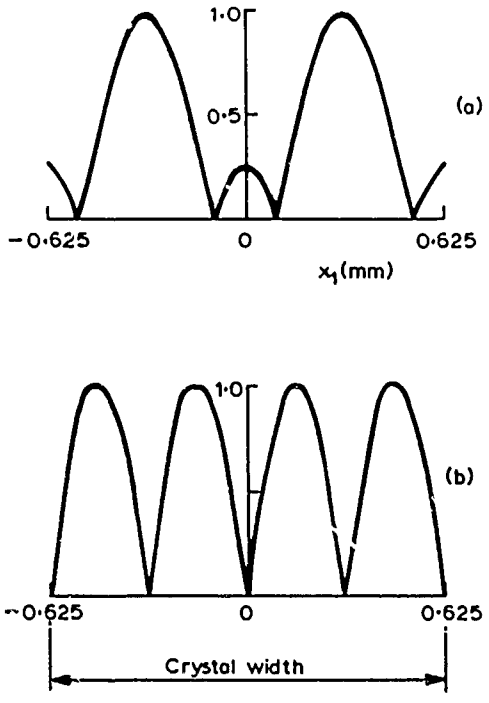

Fig.8 Computed vibration intensity vs. x_1

($x_2 = L_2/2$, $x_3 = 0$)

(a) $|\partial^2 u_1/\partial x_2^2|$

(b) $|\partial^2 u_2/\partial x_1^2|$

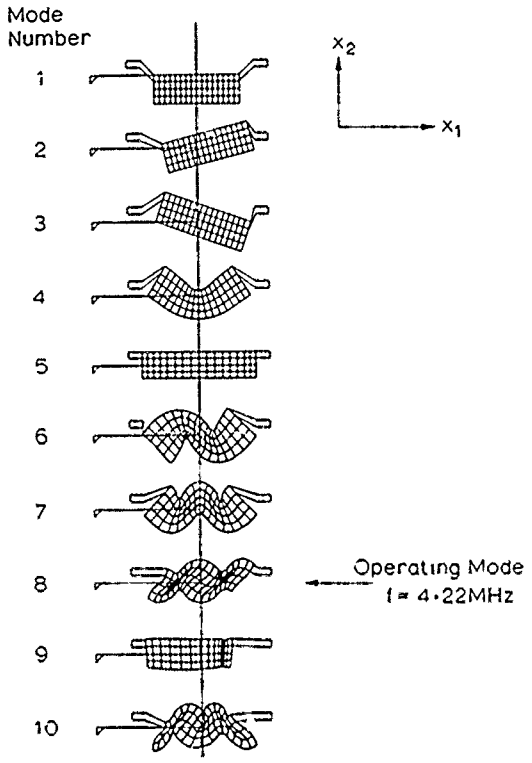

Fig.9 Vibration patterns of first 10 eigen modes found by two-dimensional finite-element analysis using ASKA program (L_1 = 1.2 mm, L_2 = 0.4 mm. Calculations independent of x_3)

FREQUENCY TEMPERATURE CHARACTERISTICS OF RECTANGULAR AT-CUT QUARTZ PLATES

Toshitake Kato and Hiromi Ueda
Citizen Watch Co., Ltd.
Technical Laboratory

Summary

In this paper the resonant frequency-temperature characteristics of coupled fundamental thickness-shear mode of rectangular AT-cut quartz plates with all four edges free are studied.

A resonant frequency formula is proposed to obtain the resonant frequencies of a finite rectangular quartz plate from those of an infinite plates. Mindlin's frequency equations are solved in two cases; in one case, the Z'-dimension is infinite, and in the other case, the X-dimension is infinite. In both cases the piezoelectric terms are taken into account.

Using the approximate resonant frequency formula, frequency temperature coefficients for rectangular AT-cut quartz plates with various X- and Z'-dimensions are numerically calculated.

The method obtained seems to be useful for design and fabrication of rectangular quartz resonators.

Introduction

Rectangular AT-cut quartz resonators have moved into an important position as an electrical part of electric watches and other small electric instruments. Increasing requirements concerning the temperature dependence of the resonant frequency of these resonators make it necessary to know in detail the influence of various parameters on the resonant frequency, such as the shape and dimensions of the resonator and the electrode.

One of the most recent attempts to obtain theoretically the temperature dependence of the resonant frequency of AT-cut quartz plates is that done by Zelenka.[1] In his paper the piezoelectric stiffening was taken into account by substituting C_{66}^{D} for C_{66}. But it seems to be difficult to predict with practical accuracy the temperature dependence of the resonant frequency by this method. The reasons why this cannot be done are that consideration of piezoelectricity is insufficient and that the method considers only the thickness-twist mode and does not consider face-shear mode.

In the case of low width-to-thickness ratios, the resonant frequency of the thickness-twist overtones are more than 10% higher than those of the fundamental thickness-shear mode, and the coupling between these modes is very small. Hence, in this paper, the thickness-twist modes are omitted and the face-shear mode is considered. Piezoelectricity is also taken into account, by using Mindlin's equation [2,3].

It is very difficult to obtain a strict resolution about vibration of rectangular plates with all four edges free considering piezoelectricity. Therefore, in this paper, a resonant frequency formula is proposed to obtain the resonant frequencies of a finite rectangular quartz plate from those of an infinite plates. Then two-dimensional equations are solved for two quartz plates which have infinite length in one direction and finite length in the other direction, considering piezoelectricity. The results are combined by using the above mentioned frequency formula to obtain resonant frequencies of a quartz plate which has finite length in both x and z'.

Principle

The combination frequency formula to obtain the resonant frequencies of a finite plate can be derived as follows. As shown in Fig. 1, let dimensions of a finite quartz plate be l in x-axis, w in z'-axis and h in thickness, and the resonant frequency be ω, and let a resonant frequency of a quartz plate which is infinite in x-axis and has finite length w in z'-axis be ωz. To obtain ω, it is enough to know the ratio

$$\frac{\omega}{\omega z} = e \qquad (1)$$

e seems to be represented by a complex function of length, width, thickness, cut angle, etc. But in this paper, it is assumed that e can be approximated by the following value.

As shown in Fig. 2, when a resonant frequency of a quartz plate which is infinite in both x and z'-axes is ωl, and a resonant frequency of a quartz plate which has a length of l in x-axis and infinite length in z'-axis is ωx, the ratio

$$\frac{\omega x}{\omega l} = e_1 \qquad (2)$$

can be obtained by means of several analysis methods.

Both e and e_1 give the ratios of resonant frequencies of quartz plates which have finite length in x-axis. The only difference is the length in z'-axis. Considering that dependence of the length in z'-axis upon resonant frequency is small, an assumption of e=e1 may be proper. Therefore, from (1) and (2),

$$\frac{\omega}{\omega_z} = \frac{\omega_x}{\omega_1}$$

$$\omega = \frac{\omega_z}{\omega_1}\omega_x \qquad (3)$$

Both ω_z/ω_1 and ω_x can be obtained by means of appropriate analytical method. Therefore, a resonant frequency of a finite quartz plate can be obtained from equ. (3).

Frequency formula for a quartz plate with finite length along X axis

In this section we determine resonant frequency ω_x of a quartz plate with finite length ℓ along X axis and infinite length along Z' axis. To do this, we start with formulas (30), (31) and (32) given by Mindlin [2]. (Fig.3)
Substituting $\xi=2b\psi_1, \eta=u_2$, and h=2b into the above equations and cancelling ϕ give:

$$Mx=D_1(1+J).2b\psi_1'$$

$$Qx=D_6.2b(u_2'+(1+N)\psi_1)+F_6\phi_0$$

$$D_6(u_2''+(1+N)\psi_1')+\rho\omega^2u_2=0$$

$$\frac{D_1}{R}(1+J)\psi_1''-\frac{D_6}{R}(u_2'+(1+N)\psi_1)+\rho\omega^2\psi_1=\frac{3}{2}b^{-3}F_6\phi_0$$

where

$$J=\frac{(e_{11}-e_{12}C_{12}/C_{22})^2}{(C_{11}-C_{12}^2/C_{22})(K_1+e_{12}^2/C_{22})}$$

$$N=\frac{e_{26}(e_{11}-e_{12}C_{12}/C_{22})}{C_{66}(K_1+e_{12}^2/C_{22})}$$

Symbols used in the above equations with no commentary are the same as those used in the Mindlin's report.[2]
We now make another substitution for the above equations as follows:

$$\hat{\psi}_1=\psi_1(1+N) \qquad \bar{\hat{\psi}}=\bar{\psi}_1(1+N)$$

$$\gamma_{11}'=(C_{11}-C_{12}^2/C_{22})\frac{1+J}{1+N} \qquad \bar{k}_1^2=k_1^2\cdot\frac{1+3R}{(1+R)^2}$$

$$k_1^2=\frac{\alpha_1^2}{3}(1+e_{26}^2/C_{66}K_2) \qquad R=\frac{\rho'b'}{\rho b} \qquad (4)$$

α_1: The first root of

$$\tan\alpha_n=\alpha_n\left(1+\frac{C_{66}K_2}{e_{26}^2}\right)$$

where barred symbols apply to the plated part, k_1, $\bar{k}_1$ are the shear correction factors and R is the ratio of the mass per unit area of both electrodes to the mass per unit area of the plate. Then we may write down the equations of motion as follows:

For unplated portion:

$$k_1C_{66}(u_{2,11}+\hat{\psi}_{1,1})+\rho\omega^2u_2=0$$

$$\gamma_{11}'\hat{\psi}_{1,11}-3b^{-2}k_1^2C_{66}(u_{2,1}+\hat{\psi}_1)+\frac{\rho\omega^2}{1+N}\hat{\psi}_1=0$$

$$M_1=Mx=\frac{2}{3}b^3\gamma_{11}'\hat{\psi}_{1,1} \qquad (5)$$

$$Q_1=Qx=2bk_1^2C_{66}(u_{2,1}+\hat{\psi}_1)$$

For plated portion (the quantities are marked with prime expressed by barred symbols.)

$$\bar{k}_1^2c_{66}(\bar{u}_{2,11}+\hat{\bar{\psi}}_{1,1})+\rho(1+R)\omega^2\bar{u}_2=0$$

$$\gamma_{11}'\hat{\bar{\psi}}_{1,11}-3b^{-2}\bar{k}_1^2{}_{66}(\bar{u}_{2,1}+\hat{\bar{\psi}}_1)+\frac{\rho\omega^2(1+3R)}{1+N}\hat{\bar{\psi}}_1=$$

$$\frac{2}{3}b^3F_6\phi_0 \qquad (6)$$

$$\bar{M}_1=\frac{2}{3}b^3\gamma_{11}'\hat{\bar{\psi}}_{1,1}$$

$$\bar{Q}_1=2b\bar{k}_1^2C_{66}(\bar{u}_{2,1}+\hat{\bar{\psi}}_1)+F_6\phi_0$$

The above equations have almost the same forms as equations (1), (3), (4), and (6) given by Lee and Spencer.[4]

For the plated portion of the plate, therefore, we may assume the solution of equation (6) as:

$$\bar{u}_2=\bar{A}_1b\sin\bar{\xi}_1x_1+\bar{A}_2b\sin\bar{\xi}_2x_1$$

$$\hat{\bar{\psi}}_1=\Sigma\bar{B}_i\cos\bar{\xi}_ix_1+C \qquad (i=1,2)$$

$$C=\frac{2}{3}b^3F_6\phi_0/\left(\frac{\rho\omega^2}{1+N}(1+3R)-3b^{-2}k_1^2C_{66}\right)$$

Also for the unplated portion of the plate we may assume the solution of equation (5) as:

$$u_2=\Sigma A_{i1}b\sin\xi_i(x_1-a)+\Sigma A_{i2}b\cos\xi_i(x_1-a)$$

$$\hat{\psi}_1=\Sigma B_{i1}\cos\xi_i(x_1-a)+\Sigma B_{i2}\sin\xi_i(x_1-a),$$

$$(i=1,2)$$

By substituting the above equations into eqs. (5) and (6), and into the boundary conditions Ml=0, Ql=0 at $x1=\pm\frac{\ell}{2}$, $u_2=\bar{u}_2$ $\hat{\psi}=\hat{\bar{\psi}}_1$, Ml=Ml, Ql=Ql at x1=±a, and also determining the condition that may give non-trivial solutions of simultaneous equations of Aij and Bij comprised of those equations, we can obtain the object frequency formula of ω_x.
The frequency equation may be written in the same form as that given in Lee and Spencer's paper [4] as:

$$|a|=\begin{vmatrix} a_{11} & a_{12} & 0 & \phi_1 & 0 & \phi_2 \\ a_{21} & a_{11} & 1 & 0 & 1 & 0 \\ a_{31} & a_{32} & \sigma_1 & 0 & \sigma_2 & 0 \\ a_{41} & a_{42} & 0 & -\alpha_1 & 0 & -\alpha_1 \\ 0 & 0 & a_{53} & a_{54} & a_{55} & a_{56} \\ 0 & 0 & a_{63} & a_{64} & a_{65} & a_{66} \end{vmatrix} = 0 \qquad (7)$$

The relations for the calculation of the components of the frequency equation (7) are almost same as those given in paper [4], but for the calculation of the quantities given below it is necessary to use the following relations.

$$\begin{aligned} &\bar{x}=x=0 && \hat{\gamma}_{11}=\gamma'_{11}/3k_1^2C_{66} \\ &\bar{\gamma}_{11}=\gamma'_{11}/3k_1^2{}_{66} && B=(\frac{1}{1+N}+3\hat{\gamma}_{11})\Omega^2 \\ &\bar{B}=(\frac{1}{1+N}+3r\bar{\gamma}_{11})\bar{\Omega}^2 && C=3(1-\frac{\Omega^2}{1+N})\Omega^2 \\ &\bar{C}=3r(1-\frac{\bar{\Omega}^2}{1+N})\bar{\Omega}^2 && d^*=(\frac{\ell}{2}-a)/b \end{aligned} \qquad (8)$$

Determining $\omega z/\omega_1$

We then determine the frequency equation for a quartz plate with infinite length along X axis and finite length along Z' axis with its piezoelectrical characteristics taken into account. In eqs. (26) through (32) given in Mindlin's paper 3 we assume the displacement and potential as follows:

$$\begin{aligned} &u_1{}^{(0)}=\bar{u}_1=B_1 b\sin\zeta x_3 \\ &u_1{}^{(1)}=\psi_1=B_4\cos\zeta x_3 \\ &\phi^{(0)}=C_1 b\sin\zeta x_3 \\ &u_2{}^{(0)}=\bar{u}_2=0, \qquad u_3{}^{(0)}=\bar{u}_3=0 \\ &u_3{}^{(1)}=\psi_3=0 \qquad \phi^{(1)}=0 \end{aligned}$$

We then substitute the above equations into eqs. (26) through (32). (The above assumption is based on a process in which the thickness-twist mode is omitted, face-shear mode is taken into account, and potential component $\phi^{(1)}$ in regard to the thickness-twist mode is omitted.) According to the assumption that the obtained equation has a non-trivial solution in regard to B1, B4, and C1, we obtain:

$$\begin{vmatrix} \hat{C}_{55}\bar{\zeta}^2-3\Omega^2 & \hat{C}_{56}\bar{\zeta} & \hat{e}_{35}\bar{\zeta} \\ \hat{C}_{56}\bar{\zeta} & \hat{\gamma}_{55}\bar{\zeta}+1-\Omega^2 & \hat{e}_{36} \\ \hat{e}_{35}\bar{\zeta} & \hat{e}_{36} & -\hat{e}_{33} \end{vmatrix} = 0 \qquad (9)$$

where

$$\begin{aligned} &\hat{C}_{55}=C_{55}/k_1^2C_{66} && \bar{\zeta}=b\zeta \\ &\hat{C}_{56}=C_{56}/k_1C_{66} && \Omega^2=\frac{\omega z^2}{(\frac{3k_1^2C_{66}}{\rho b^2})}=\frac{\omega z^2}{\omega_1{}^2} \\ &\hat{\gamma}_{55}=\gamma_{55}/3k_1^2C_{66} && \hat{e}_{36}=e_{36}/k_1C_{66} \\ &\hat{e}_{35}=e_{35}/k_1^2C_{66} && \hat{\varepsilon}_{33}=\varepsilon_{33}/k_1^2C_{66} \end{aligned} \qquad (10)$$

when we assume the roots of eq.(9) as $\bar{\zeta}_1$ and $\bar{\zeta}_2$, we obtain the following equation from that assumption which would satisfy the boundary conditions at $x3=\pm\frac{\omega}{2}$:

$$(\hat{C}_{55}{}^*\bar{\zeta}_1\beta_1+\hat{C}_{56}{}^*)\bar{\zeta}_2\cos\frac{\zeta_1 w}{2}\sin\frac{\zeta_2 w}{2} + (\hat{C}_{55}{}^*\bar{\zeta}_2\beta_2+\hat{C}_{56}{}^*)\sin\frac{\zeta_1 w}{2}\cos\frac{\zeta_2 w}{2}=0 \qquad (11)$$

where

$$\beta_1=-(\hat{\gamma}_{55}\bar{\zeta}_1^2+1+\frac{\hat{e}_{36}^2}{\hat{\varepsilon}_{33}}-\Omega^2)/\hat{C}_{56}{}^*\bar{\zeta}_1$$

$$\beta_2=-(\hat{\gamma}_{55}\bar{\zeta}_2^2+1+\frac{\hat{e}_{36}^2}{\hat{\varepsilon}_{33}}-\Omega^2)/\hat{C}_{56}{}^*\bar{\zeta}_2$$

$$\hat{C}_{55}{}^*=\hat{C}_{55}+\frac{\hat{e}_{35}^2}{\hat{\varepsilon}_{33}}, \qquad \hat{C}_{56}{}^*=\hat{C}_{56}+\frac{\hat{e}_{35}\hat{e}_{36}}{\hat{\varepsilon}_{33}}$$

According to the definition, the root Ω of the equation (11) is equal to $\omega z/\omega_1$.

Application to Temperature Characteristics

Combining the solutions of the above two different frequency equations into one by using eq.(3) gives the resonant frequency of the quartz plate with finite lengths along both X and Z' axis, and having an arbitrary electrode size. (Fig.4) As one of the applications of this frequency formula, we can determine the temperature coefficient of finite quartz plates. We computed the mean temperature coefficient of the resonant frequency over 25°C to 40°C using the same dimensions as in the experiment of Royer 7, and compared it with the experimental results by Royer. The values of the elastic stiffnesses and their temperature coefficients, etc. used in the calculation were taken from papers [1,5,6].

The curved line in Fig. 5 shows the calculated result, which agrees with the experimental result indicated by black dots.

Figure 6 shows the calculated and measured loci of zero temperature coefficients of the resonant frequency. As can be seen in the figure, both calculation and experiment agree with each other, which indicates the propriety of frequency formula (3).

Experimental Results

To examine the accuracy of the frequency formula, we experimentally obtained the resonant frequency variations as measured by changing the w/h of a quartz plate with ℓ/h=31.25 over 3.4 to 6.4. The result of the measurement is shown by black dots in Fig. 7. As seen in the figure, the resonant frequency variation accompanied with width-dimension variation agrees with the calculated result which is shown by the solid line.

Figure 8 and 9 show mean temperature-coefficient variation over 20°C to 30°C with respect to width to thickness ratio Z'/Y', cut angles θ=35°03', 35°24', length to thickness ratio X/Y'=15, and electrode ratio 2a/ℓ=1.0.
An agreement is seen between the measured result shown by black dots and the calculated result shown by the solid line.

However, the measured value tends to be lessened around 2 to 3 ppm/deg in the neighborhood of Z'/Y'=3.75 as compared with the calculated value. This seems to be due to the fact that the extension mode along Z' axis is omitted from the theoretical equation mentioned earlier.
The improvement of this equation by taking this point into account will be our future thesis.

Conclusion

A frequency formula valid for rectangular quartz plates with finite lengths along both X and Z' axis has been obtained with the piezoelectric terms taken into account.
As a result of calculations, using this frequency formula on the frequency-temperature characteristics of rectangular AT-cut quartz plates, it has been revealed that the temperature characteristics of a quartz plate with a specified shape can be foreseen with considerable precision.
The formula obtained seems to be quite useful for the design of rectangular quartz resonator.
Also the measured value was considerably lessened with respect to the theoretical value at around Z'/Y'=3.75.
This will be elucidated in our future discussions.

References

(1) J. Zelenka, The influence of electrodes on the resonance frequency of AT-cut quartz plates. Int. J. Solids Struct. 11, 871-876 (1975)

(2) R. D. Mindlin, Forced Thickness-Shear and Flexural Vibrations of Piezoelectric Crystal plates, J. Appl. Phys. 23, 83-88 (1952)

(3) R. D. Mindlin, High Frequency Vibrations of Piezoelectric Crystal Plates, Int. J. Solids Struct. 8, 895-906 (1972)

(4) P. C. Y. Lee and W. J. Spencer, Shear-Flexure-Twist Vibrations in Rectangular AT-cut Quartz Plates with Partial Electrodes, J. Acoust. Soc. Amer. 45, 637-645 (1968)

(5) R. Bechmann, Numerical data and Functional relationships in science and technology, Landolt-Börnstein Series (Edited by K. H. Hellwege), Vol. 1, Springer, Berlin (1966)

(6) R. Bechmann et al. Proc. IRE 50, 1812-1822 (1962)

(7) J. J. Royer, Rectangular AT-cut resonators, Proc. 27th Freq. Control Symp., 30-34 (1973)

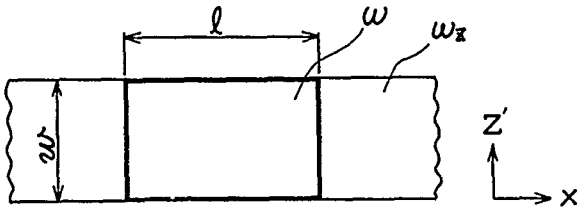

Fig. 1 Quartz plates, one of which is infinite in x-dimension and the other is finite both in x and z'-dimension.

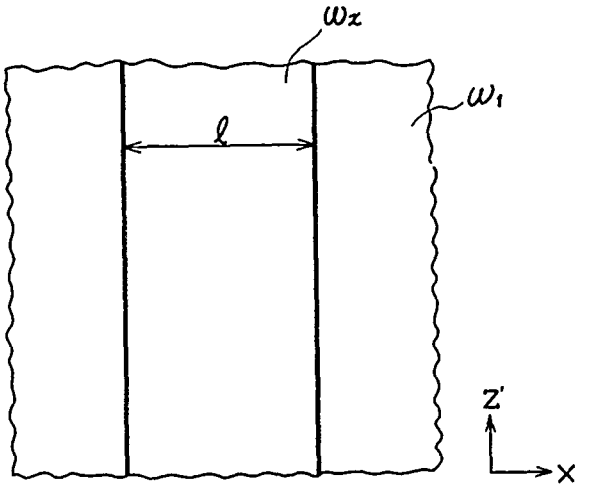

Fig. 2 Quartz plates, one of which is infinite in z'-dimension and the other is finite both in x and z'-dimension.

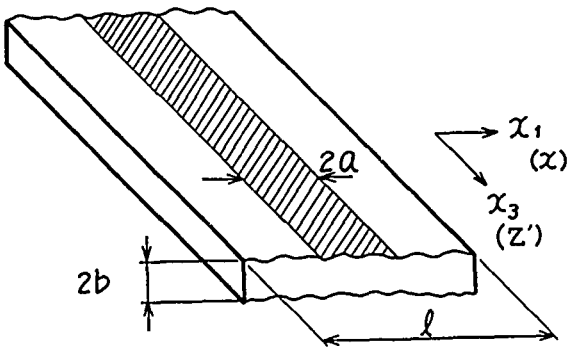

Fig. 3 Quartz plates with electrode. z'-dimension is infinite.

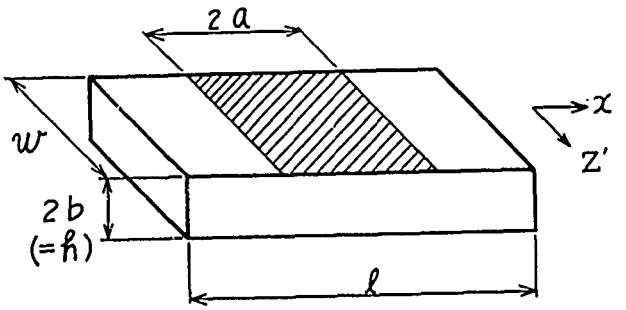

Fig. 4 Quartz plates with electrode. Both x and z'-dimension are finite.

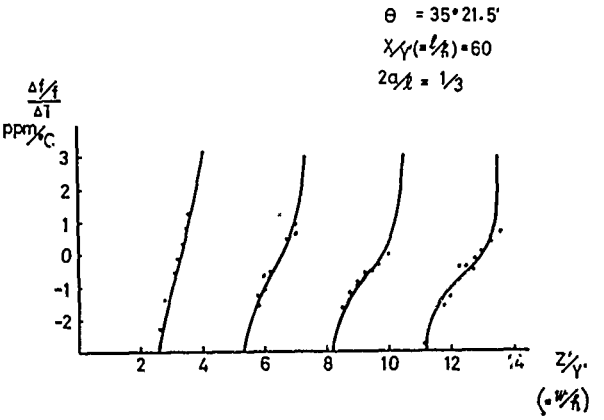

Fig. 5 Mean frequency-temperature coefficient between 25°C & 40°C, calculated and measured.

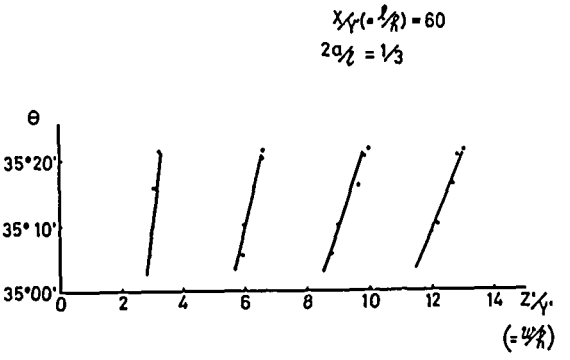

Fig. 6 Loci of zero temperature coefficients of frequency.

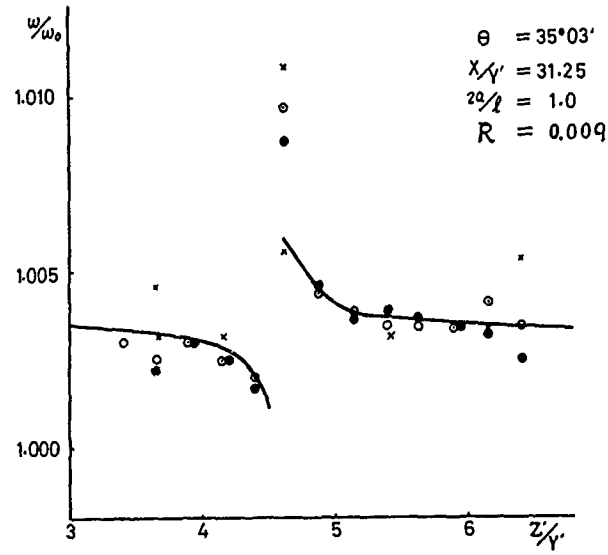

Fig. 7 Resonant frequency change as a function of z'/y'.

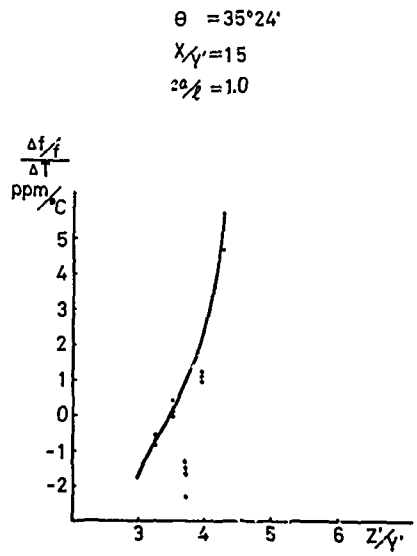

Fig. 8 Frequency-temperature coefficient between 20 & 30°C. θ=35°24'.

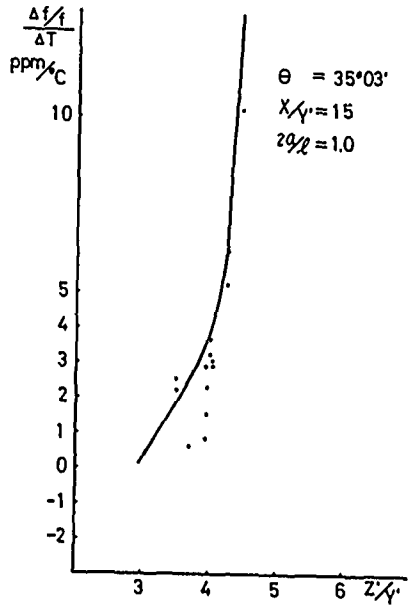

Fig. 9 Frequency-temperature coefficient between 20 & 30°C. θ=35°3'.

NEW FREQUENCY-TEMPERATURE CHARACTERISTICS OF 4.19MHz BEVELED RECTANGULAR AT-CUT QUARTZ RESONATOR

Shiro Yamashita, Shunichi Motte, Kunihiro Takahashi
Naoyuki Echigo, Akira Watanabe, Koji Kubota

DAINI SEIKOSHA CO., LTD.
6-31-1 Kameido, Koto-ku, Tokyo 136, Japan

Summary

At the last Frequency Control Symposium, we reported the experimental results of the unwanted mode for the beveled rectangular AT-cut quartz resonator with a view to its miniaturization. Detailed investigations were made, where ℓ/t=15.7 approximately, w/t=2.8 to 3.4, ℓ=length along X-axis, w=width along Z'-axis, and t=thickness of the resonator.

We have extended the previous range of detailed investigations of ℓ/t and w/t. Over the range of w/t=1.50 to 4.75, the variations of unwanted mode and of frequency-temperature characteristics of thickness-shear mode have been reinvestigated in detail.

Further, with Monte Carlo method, we investigated to simulate the carrying accuracy of the quartz watches using our quartz resonators which have various inflection point temperature.

Some of the results are as follows:

(1) In the three ranges of the dimensional ratio of w/t=2.1~2.9, 3.2~3.5 and 3.88~4.35, the frequency-temperature characteristic of the cubic curve can be practically effectuated in the vicinity of the normal temperature.

(2) In the range where w/t is 2.1~2.9, the inflection point temperature of the frequency-temperature characteristic curve shows a tendency different from what has so far been reported, namely, the inflection point temperature decreases as w/t decreases and can be made lower than the theoretical value of an infinite AT-cut quartz plate: i.e. this inflection point temperature can be varied continuously over the wide range of -20°C to +35°C.

(3) According to the carrying accuracy simulation of the watches by the Monte Carlo method, the AT-cut quartz resonator having the inflection point temperature of 20°C is expedient for the highly accurate watch among AT-cut quartz resonators having the inflection point temperatures of 11°C, 20°C and 35°C.

Introduction

At the last Frequency Control Symposium, we reported research results of miniaturization of the beveled rectangular AT-cut quartz resonators.[1] It was revealed then that, taking the lengthwise direction of the resonator as X-axis direction of quartz crystal coordinate, the frequency-temperature curve takes a similar profile with that for the infinite AT-cut plate in the vicinity of ℓ/t=15.7 and w/t=3.3 (where ℓ is the length, w is the width and t is the thickness of the resonator respectively) and that we could mass-produce those resonators which have the inflection point temperature higher by about 5°C than that of infinite plate.

This resonator which measures 6.2 x 1.3 x 0.4 mm at 4.19MHz could fully take the place of the conventional resonators for watches and was found by far superior to former quartz resonators for watches in the field of vibration characteristics. Judging from this point of view, it can be said that this type of resonator can satisfactorily be put to practical use for highly accuracte watches.

If we are allowed to hope more, however, the frequency variation due to the temperature variation in the range of less than 10°C can not be sufficiently small as in the case of even the infinite AT-cut plate. If this point can be improved, a marked improvement will be made in the branch of devices used in the range of temperature centering around the room temperature such as, for example, watches, clocks and other electronic devices.

It has so far been reported that the inflection point temperature of the frequency-temperature characteristic curve increases compared with that of the infinite AT-cut plate (namely 28°C at the curve giving zero temperature coefficient: M. Ariga)[1),2),3)] when the AT-cut quartz resonator has been miniaturized. The dimensional ratio range showing the above tendency was also confirmed through our experiments with the long-X rectangular AT-cut quartz resonator. However, the same tendency could not always be observed during the experiments over the wide range of the dimensional ratio. Moreover, it was assumed that there was a possibility of deviating from the former tendency in the comparatively small range of the dimensional ratio.

We have therfore carried on our research about the inflection point temperature of the frequency-temperature characteristic curve for manufacturing AT-cut quartz resonators, under the most suitable conditions for mass-production and yet smaller in size as compared with the conventional ones, for electronic apparatus, for instance, watches, clocks or communications apparatus mainly used in the room temperature. As the result of

the research, we have succeeded in believing that the inflection point temperature can be variedfrom at least -20°C to +35°C in the range of miniaturized dimension which can meet requirements to be used for even 4MHz watches. As we have not seen any report concerning the AT-cut quartz resonator giving the inflection point temperature lower than that of the infinite AT-cut plate, we have carried on the research in details from various angles with a special emphasis. As the result, it has been ascertained that we have been able to produce the AT-cut quartz resonator which has enough reproducibility, is excellent in characteristics of a resonator and is suitable for mass-production in smaller size than those resonators so far having been used.

When the inflection point temperature for the frequency-temperature characteristic curve is lowered than that for the infinite AT-cut plate, the flat range (less variation against the temperature) of the curve shifts to the lower-temperature side and accordingly it is considered that this is desirable characteristics for electronic apparatus much used in the vicinity of the room temperature. In order to corroborate the abovementioned fact, we have carried out the carrying accuracy simulation of the watches for the AT-cut quartz resonators with the inflection point temperature of 11°C, 20°C and 35°C by means of the Monte Carlo method. The results shows that the inflection point temperature of 20°C is the most desirable for the watch.

In the following, we will report a part of the results of the research about the rectangular AT-cut quartz resonator which is long in the direction of the X axis placing the focus on the frequency spectrum concerning width dimension and on the relation between the width dimension and the inflection point temperature. Further, we will make a partial report of the carrying accuracy simulation by means of the Monte Carlo method when the above mentioned resonator has been used to a watch.

Frequency Spectrum Concerning Width Dimension

In order to improve the frequency-temperature characteristics and the mass productivity of the beveled rectangular AT-cut quartz resonator which is long in the direction of the X axis, we made a study of the frequency spectrum including both sides of the region of the w/t which we made a report of at the last Frequency Control Symposium.[11]

Fig.1 shows the cutting angle of the quartz resonator.

Fig.2 shows the symbols of the quartz resonator used in the experiment performed by us.

Fig.3 shows the frequency spectrum measured every time when the width dimension of a specimen of a rectangular AT-cut of $\ell/t \fallingdotseq 15.5$, $\ell_0/t \fallingdotseq 3.5$ and $w/t \fallingdotseq 4.75$ was shaved by $\Delta(w/t) \fallingdotseq 0.05$ to $w/t = 3.00$.

Fig.4 shows the slopes of the frequency-temperature curve in the vicinity of about 20°C by means of measuring the frequency-temperature characteristics of the fundamental thickness-shear vibration every time when the same specimen as that used in the case of Fig.3 was shaved by as much as $\Delta(w/t)=0.125$. The cut angle θ of the specimen of the data shown in this figure is about 35°22'.

In Fig.3, the mark of X in the vicinity of the frequency constant $f \cdot t = 1680$kHz·mm shows the thickness-shear vibration while the black round marks show various spurious (unwanted) vibration. It is worthy of special mention here that there exist two kinds of unwanted modes showing by nearly straight lines connecting S and S', and T and T'. These unwanted modes are assumed respectively to be the tertiary overtone of the width-shear mode and the secondary overtone of the width-extensional mode , however, more accurately, it should be probed by Fukuyo's probe method.[10]

In Fig.4, the frequency-temperature coefficient of the thickness-shear mode in the vicinity of the normal temperature shows a large negative value with $w/t \fallingdotseq 4.7$ and 3.63 where the thickness-shear mode is strongly effected by the above-mentioned modes. It is therefore advisable to avoid these modes in designing the resonator.

Also as shown in Fig.4, in the two ranges for the dimensional ratio of $w/t \fallingdotseq 3.88$ to 4.35 and $w/t \fallingdotseq 3.2$ to 3.5, the frequency-temperature characteristics of the thickness-shear mode becomes almost zero temperature coefficient. Accordingly, in these two ranges of the dimensional ratio in Fig.4, it becomes possible to obtain the beveled rectangular AT-cut quartz resonator showing excellent frequency-temperature characteristic which is the essential characteristic of the AT-cut quartz resonator by means of properly selecting the width dimension after evading any adverse effects to the thickness-shear mode due to a fine unwanted mode. At the last Frequency Control Symposium, we reported the experimental results of the unwanted mode for the beveled rectangular AT-cut quartz resonator for the range of $w/t = 3.2 \sim 3.5$.

We will now show the research results executed in the range of the smaller value than that in the range as shown in Fig.4.

The curve A in Fig.5 shows plotted slopes $\frac{\partial}{\partial T}\left(\frac{\Delta f}{f}\right)$ in the vicinity of 20°C obtained every time by means of measuring the frequency-temperature characteristics for the fundamental thickness-shear mode when the width of the beveled rectangular AT-cut quartz resonator having $w/t \fallingdotseq 4.75$ was shaved little by little where ℓ/t is 15.5, ℓ_0/t is 3.5 approximately. Here the cut angle of the resonator is about 35°24'. It is observed in this curve that the frequency-temperature coefficient of the thickness-shear mode shows a large negative value as the value of w/t becomes smaller toward about 3.0, while the coefficient approaches to zero when the value of w/t passed through about 3.0 and it will show gradual larger negative values again as w/t becomes further smaller. The former is considered that the thickness-shear mode is under the influence of the secondary overtone of the width-shear mode when the value of w/t is approximately 3.0 and the latter is considered to have been brought on by the fact that the thickness-shear mode has heavily been affected by the fundamental width-shear mode because of agreement of the frequency of the fundamental thickness-shear mode with that of the fundamental width-shear mode when the value of w/t is approximately 1.5.

Further, the frequency-temperature coefficient of the thickness-shear mode shows the value close to zero in the range of w/t=2.1 ~ 2.9. In this range, the frequency-temperature characteristics having the zero temperature coefficient can be obtained by means of selecting the cut angle properly. Fig.6 shows the optimum cut angles for all the dimensions which have been obtained from calculations.

R.D. Mindlin[4] pointed out that in the case of the rectangular AT-cut quartz resonator with finite width dimension, the vibration mode of the thickness-shear mode became to have a quite simple mode when, as shown in Fig.7, the side planes, the X-Y' planes, were cut with the positive direction of the X axis directed toward you and by means of tilting it about 6°($\psi \fallingdotseq 6°$) counterclockwise.

In Fig.5, the curve B shows the plotted slopes $\frac{\partial}{\partial T}(\frac{\Delta f}{f})$ in the vicinity of 20°C of the frequency-temperature curves of the thickness-shear mode when the side planes of the beveled rectangular AT-cut quartz resonator were tilted by $\psi \fallingdotseq 6°$ as shown in Fig.7 and the width dimension w was decreased by means of shaving little by little, where $\ell/t \fallingdotseq 15.5$. As is shown by the curve B in Fig.5, the variation of the frequency-temperature characteristics of the thickness-shear mode caused by the change of the width dimension is far smaller than that when the side planes have not been tilted when tilted by about 6°. This tendency can be explaned that the influence of the width-shear mode on the thickness-shear mode has been lightened as the result of uncoupling between the thickness-shear mode and the width-shear mode due to that the side planes have been tilted by about 6°. From this fact, it may be said that the resonator with smaller dispersion of the frequency-temperature characteristics can be obtained in mass-production when the side planes are tilted properly.

On the other hand, tilting the side planes involves increased manufacturing process which requires high manufacturing technology. It is therefore difficult to say that this process can be suitable for mass-production without reserve.

Inflection Point Temperature

The effect of the width dimension on the frequency-temperature characteristics of the rectangular AT-cut quartz resonator was studied by J.J. Royer[5]. He studied the frequency-temperature characteristics of the rectangular AT-cut quartz resonator having $\ell/t=60$ and $\ell_0/t=0$ covering the range from w/t=30 to w/t=2.5. He reported that the inflection point temperature was about 40°C in the case of w/t=3.0 when the frequency-temperature curve showed zero temperature coefficient.

He also reports about the region of w/t<1, namely the New DT-cut, where the dimension of the Z' axis was made smaller than that of the Y' axis.[6] There is no detailed report available concerning the case where the value of w/t lies in between (namely, 1<w/t<2.5).

As is shown by curve A in Fig.5, however, our research revealed that the frequency-temperature coefficients are close to zero in the vicinity of the normal temperature when the value of w/t lies between about 2.1 and 2.9. Based on this finding, we made further experiments with w/t value limited in the above region. As the result, we could obtain the cubic curve of the frequency-temperature characteristic about the fundamental thickness-shear mode as shown in Fig.8. In the figure, the curve C-C' is for $w/t \fallingdotseq 2.3$, the curve D-D' is for the case where $w/t \fallingdotseq 2.5$ and the curve E-E' is for the case where $w/t \fallingdotseq 2.75$ respectively. Needless to say, the cut angle θ giving the optimum frequency temperature characteristics in each of these values of w/t differs from each other.

Each inflection point temperature T_1 for the frequency-temperature curves shown by C-C', D-D' and E-E' in Fig.8 is 5°C, 20°C and 28°C respectively. Here T_1 is the temperature where the value of the secondary differential coefficient $\frac{\partial^2}{\partial T^2}(\frac{\Delta f}{f})$ becomes zero. According to the theory by I. Koga and M. Ariga concerning the infinite AT-cut plate,[7] the inflection point temperature is about 28°C when the frequency-temperature curve gives zero temperature coefficient. According to the results of our experiments, however, the inflection point temperature when the frequency-temperature curve gives zero temperature coefficient can be lower than the theoretical value for the infinite AT-cut plate in the region of w/t<3.0 as mentioned above. It was also made clear, moreover, that the inflection point temperature T_1 can, as shown in Fig.9, be selected over a fairly wide extent by means of changing w/t.

Method of Measurement

The measurement of the characteristics of the resonator was carried out using the supporting method as shown in Photo 1. Through this method, many unwanted modes could be measured highly sensitively and the Q value for the thickness-shear mode could be kept in high value.

Estimation of Carrying Accuracy of Watch by Monte Carlo Method

As mentioned above, the inflection point temperature of the frequency-temperature curve for the thickness-shear mode of the beveled rectangular AT-cut quartz resonator can be made lower than that of the infinite AT-cut plate and moreover it was made clear that it could be selected optionally over the definite extent. Accordingly we studied what meaning such a resonator had for the environmental conditions where it was used.

As an example, we would like to mention about the case where the carrying accuracy of the watches using above mentioned resonator was estimated by help of the simulation using the Monte Carlo method.[8),9)]

The accuracy or a watch is determined by the frequency of a resonator. Also the frequency of a quartz resonator changes, for example, by temperature. The carrying accuracy of a quartz watch can therefore be obtained when the frequency temperature characteristics of a quartz resonator used and the environmental temperature where the watch is placed as well as the duration of time in which the watch is placed in each of the above-mentioned environmental temperatures are made known.

For executing the simulation for estimating

the carrying accuracy here, the temperature of the watch shall be assumed to be 29.5°C on an average when it is worn and to be the room temperature when it is not worn. As the room temperature, we divided one year into 12 months and used the modified values of average temperature of every month. As the atmospheric temperature differ from each other from one district to another, we have divided whole Japan into 80 towns and cities and monthly average temperature for each city was used.

The contents of the simulation for the carrying accuracy is shown in Fig.10.

1. Selection of Cut Angle:
   To select a certain value from among the cut angles having dispersion in the neighborhood of the central value, θ_0.
2. Selection of Adjusted Frequency:
   To adjust the frequency of quartz resonator at the temperature of 24°C. A certain value shall be selected from among the adjusted frequency having dispersion in the vicinity of the central value of f_0.
3. Selection of Frequency Aging:
   To select a certain value from among the amounts of the frequency aging having dispersion in the vicinity of the central value of A_0.
4. Selection of Starting Month of Carrying:
   To select a certain month from 12 months of a year.
5. Selection of Towns and Cities:
   To select one city or town from among the 80 cities and towns. By this the average temperature of the watch when it is not wore every month, T_{R_0} is determined.
6. Selection of Average Carrying Duration:
   Daily average carrying duration, H_{W_0} shall be selected. The distribution shown in the figure is what has been obtained from the actual investigation.
7. Designation of Carrying Duration:
   The carrying duration H_w is supposed to have dispersion in the vicinity of the average carrying duration. The carrying duration for simulation shall be selected from it.
8. Designation of Carrying Temperature:
   The temperature of the watch when it is worn, T_w is supposed to have dispersion in the vicinity of the average temperature of 29.5°C. The carrying temperature shall be selected from this dispersion.
9. Designation of Room Temperature:
   The temperature of a watch when it is not worn, T_R is supposed to have dispersion in the neighborhood of the average room temperature T_{R_0}. The room temperature shall be selected from the dispersion.
10. Calculation of Daily Error:
    The daily error, t_d shall be obtained from the following formula:

$$t_d = \frac{\{f_{T_W} \times H_W + f_{T_R}(24 - H_W)\} \times 3600}{86400 \times 2^m}$$

    where f_{TW}, f_{TR} = frequency at T_W, T_R, respectively
    2^m is the frequency designed to be used.
11. Calculation of Monthly Error:
    The monthly error, t_m shall be calculated by multiplying the average obtained by repeating n times the procedures 7. to 10. above by 30.

$$t_m = \left(\sum_{k=1}^{n} t_{dk}\right)/n \times 30$$

12. Calculation of Yearly Error:
    The yearly error, t_y shall be calculated by means of adding up the monthly error of 12 months which shall begin with the starting month of carrying.

$$t_y = \left(\sum_{\ell=1}^{12} t_{m\ell}\right)$$

    where ℓ=1 means the starting month of carrying.
    The simulation shall be brought to a close after we have repeated N times the procedures mentioned in 1. to 12. above.
    The cpu time for this simulation is about 15 minutes under the conditions that N=1000 and n=50.

The distinctive feature of the Monte Carlo method lies in the fact that, in the operation of 1. to 9. mentioned above, the method make use of random numbers in selecting appropriative value, month and city. By help of this simulation for estimation of the carrying accuracy, it is possible for us to know how big an extent of error many quartz watches having the characteristic of 1. to 3. mentioned above have on an average of 12 months and also what percent of these wathces can stand the test for a certain indicated yearly error.

We have carried out the estimation of the carrying accuracy for the three cases of the inflection point temperatures of 35°C, 20°C and 11°C when the frequency-temperature characteristic give zero temperature coefficient. In using the AT-cut quartz resonators having these inflection point temperatures for the watches, it is necessary for us to find out the optimum conditions for the cut angle and adjusted frequency which can highten the carrying accuracy to the maximum. The optimum values for the adjusted frequency at 24°C are as follows in their inflection point temperatures in the case where the frequency is 4.19MHz.

= 4194304.1Hz at 24°C for T_i = 11°C
= 4194304.3Hz " " T_i = 20°C
= 4194304.6Hz " " T_i = 35°C

The above correspond to 2.06×10^{-3} sec/day, 6.18×10^{-3} sec/day and 12.36×10^{-3} sec/day respectively.

Fig.11 shows the frequency-temperature characteristics of three resonators with the optimum adjusted frequency and the optimum cut angle at respective inflection point temperatures.

Table 1 shows the rate of acceptance of the watches which can satisfy the requirement of yearly error within 3 seconds among many those having the resonators of each three kinds of inflection point temperatures in the case where the frequency at 24° C is adjusted in the vicinity of the optimum adjusted frequency within the extent of ±0.024ppm and the cut angle for the resonators is made ±15" around the optimum cut angle and moreover it is supposed that the aging amount of the frequency of the resonator is zero throughout one year.

It is understood from Table 1 that the highest accuracy can be obtained when T_i is 20°C among the three kinds of inflection point temperatures.

Next we would like to state about the carrying accuracy taking the aging of the frequency into

consideration in the case where AT-cut quartz with the inflection point temperature of 20°C.

First, the cut angle of each resonator shall, as shown in Fig.12, be placed in the range of ±30" in the vicinity of the optimum cut angle. Figs. 13 and 14 show the rate of acceptance of the watches satisfying the yearly error within 5 seconds among many watches whose adjustment frequency at 24°C has been adjusted within ±0.00206 sec/day and ±0.00512 sec/day respectively.

From Figs. 13 and 14, the following two cases may be considered as examples of the conditions satisfying the rate of 90% when the AT-cut quartz resonators are used.

1. Cut angle: ±30"
   Adjustment accuracy: ±0.00206 sec/day
   Frequency aging amount: within 0.2ppm/year
2. Cut angle: ±30"
   Adjustment accuracy: ±0.00512 sec/day
   Frequency aging amount: within 0.1ppm/year

The above is the description about the watch and it is presumed that, in the case of clocks, the improvement of accuracy is made possible still more.

Trial Production of Beveled Rectangular AT-cut Quartz Resonator

As the results of the research mentioned in the preceding section, one having the inflection point temperature of 20°C was found most desirable for making highly accurate watches as the resonator for watches among the AT-cut quartz resonators having the inflection point temperature of 11°C, 20°C and 35°C.

Then as the results of having strictly selected the dimensional ratio, we performed trial production and obtained the resonators having the excellent temperature characteristics of frequency and equivalent resistance as shown in Fig.15. The frequency-temperature characteristic shown in the said figure has the inflection point temperature of about 18.8°C. The dimension of this resonator is: $\ell/t \fallingdotseq 15.1$, $w/t \fallingdotseq 2.5$ and $\ell_0/t \fallingdotseq 3.45$. The frequency-temperature curve shown in the said figure is quite the same as the curve according to the theoretical equation by Ariga except for the inflection point, namely the shape of the curve is precisely in accord with the theoretical one although the inflection point temperature is lower than that of the theoretical value by 9°C approximately.

As shown in the figure, the equivalent resistance of this resonator is about 40Ω in the range of temperatures of -20°C to 70°C.

In Fig.16, the straight line B shows the change of the inclination of the frequency-temperature curve at the inflection point temperature when the experimental cut angle θ is changed. The straight line A is according to the theory of the infinite AT-cut plate. The straight lines A and B is nearly in parallel and, accordingly, the variation of the frequency-temperature coefficient at the inflection point temperature due to the variation of the cut angle can also be said to have the nearly same value.

Furthermore, this resonator has the excellent mass-productivity and the yield rate of our trial production of many resonators was considerably high. The production tolerance of this resonator is in no way inferior to the resonator reported at the last Frequency Control Symposium[10] and is also promising in the aspect of mass-production.

It should also be noted that, as the results of the shock test for the resonators which housed in the case for watches, the anti-impact characteristics of this resonator was found by no means inferior with our data reported at the last Frequency Control Symposium.[11]

Conclusion

In the range of $w/t=1.5 \sim 4.75$, there is a plural number of ranges of w/t where the frequency-temperature curve of the miniaturized beveled rectangular AT-cut quartz resonator is the cubic curve in the vicinity of the normal temperature. At least, it is possible to realize practically the cubic frequency-temperature curve in the three ranges where $w/t=3.88 \sim 4.35$, $w/t=3.2 \sim 3.5$ and $w/t=2.1 \sim 2.9$.

When w/t is larger than 3.0, as reported up to now, in the region of the w/t mentioned above, the inflection point temperature of the frequency-temperature curve is higher than that of the infinite AT-cut plate due to the miniaturization. However, in the case where w/t is in the range of less than 3.0, a new theoretical rule can be observed to exist: that is, the inflection point temperature of the frequency-temperature curve can be changed continuously in the range of -20°C to +35°C at least as the w/t changes. The last mentioned frequency-temperature characteristics are considered as the new frequency-temperature characteristics for the AT-cut quartz resonator.

For the resonator having these new frequency-temperature characteristics, the inflection point temperature can be designed most properly to meet the requirements for the working temperature of the apparatus in which the resonator is used. According to the research results by means of the Monte Carlo method, it is possible for us to produce watches of higher accuracy mainly used in Japan than those using the conventional AT-cut quartz resonators by providing the resonator with the inflection point temperature of 20°C or thereabout.

Acknowledgement

The authors would like to thank Mr. Tsuneo Kuwabara for skillful contributions and Mr. Yasukazu Kawamura for useful advice and kind encouragement. We would also like to acknowledge the considerable assistance of the persons in charge of trial production.

References

1) M. Ariga: "The elastic constants of quartz and their temperature characteristics", Bull. Tokyo Inst. Teck. A-No.2, 1956 (in Japanese)
2) J.J. Royer: "Rectangular AT-cut resonators", Proc. 27th Ann. Symp. on Freq. Control, PP30 ~ 34, 1973

3) M. Onoe, M. Okazaki: "Miniature AT-cut strip resonators with tilted edges", Proc. 29th Ann. Symp. on Freq. Control, PP42 ~ 48, 1975
4) R.D. Mindlin: "Thickness-twist vibrations of a quartz strip", Proc. 24th Ann. Symp. on Freq. Control, PP17 ~ 20, 1970
5) J.J. Royer: the same as reference 2)
6) J.J. Royer: "A new DT quartz resonator", IEEE. Trans. Sonics and Ultrasonics, Vol SU-17, No.1 Jan. PP18~22, 1970
7) I. Koga, M. Aruga: "Theory of plane elastic waves in a piezoelectric crystalline medium and determination of elastic and piezoelectric constants of quartz", Phys. Rev. Vol. 109, No.5 March 1, PP1467 ~ 1473, 1958
8) Y. Ikehata: "Accuracy estimation of quartz crystal watch under normal wearing conditions", J. of the Horological Institute of Japan No.73, 1975 (in Japanese)
9) S. Komaki, H. Hanyuda: "Accuracy estimation of quartz crystal watch under normal wearing conditions (No.2)", J. of the Horological Institute of Japan No.80, 1977 (in Japanese)
10) H. Fukuyo: "Researches in modes of vibrations of quartz crystal resonators by means of the Probe Method", Bull. Tokyo Inst. Tech., A-No.1, 1955 (in Japanese)
11) S. Yamashita, N. Echigo et al.: "A 4.19MHz beveled miniature rectangular At-cut quartz resonator", 32nd Ann. Symp. on Freq. Control, PP267~276, 1978

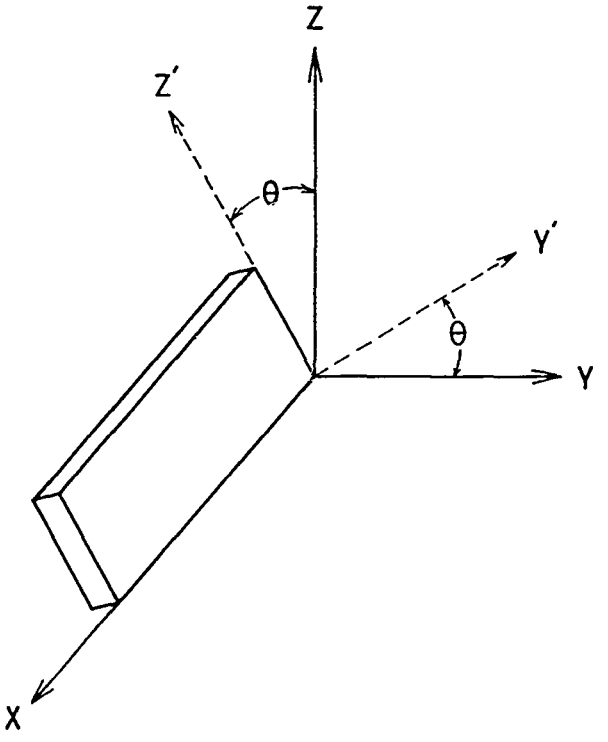

Fig. 1. Long-X rectangular AT-cut resonator.

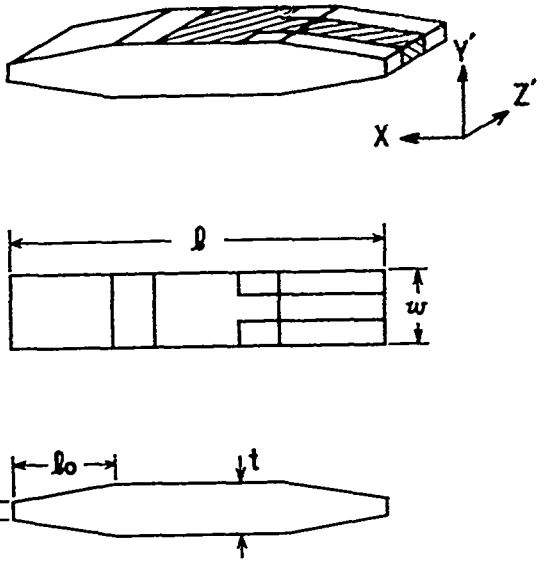

Fig. 2.

Partially electroded rectangular AT-cut resonator

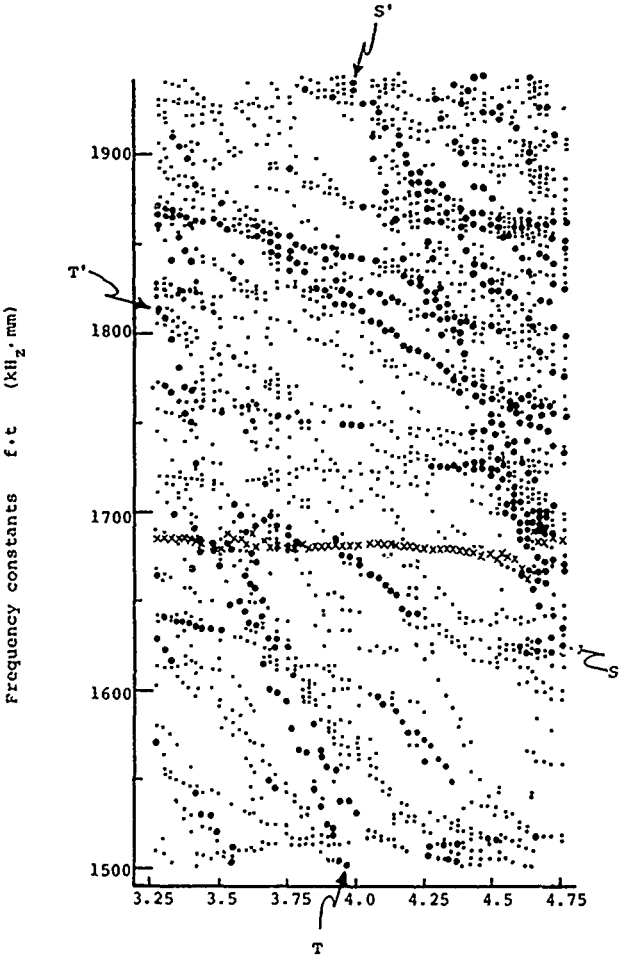

Fig. 3.

Frequency spectrum for beveled rectangular resonators

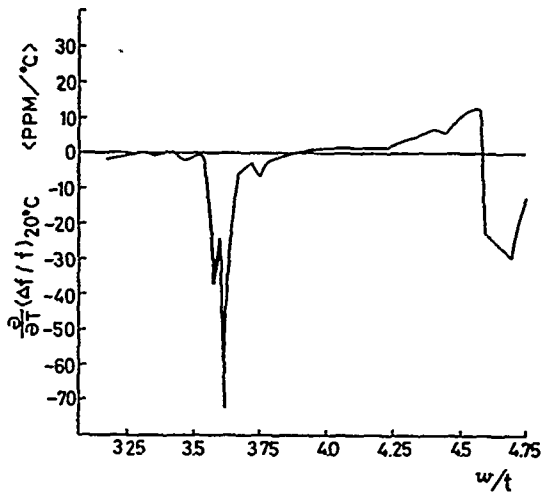

Fig. 4. Measured frequency-temperature coefficient vs. w/t.

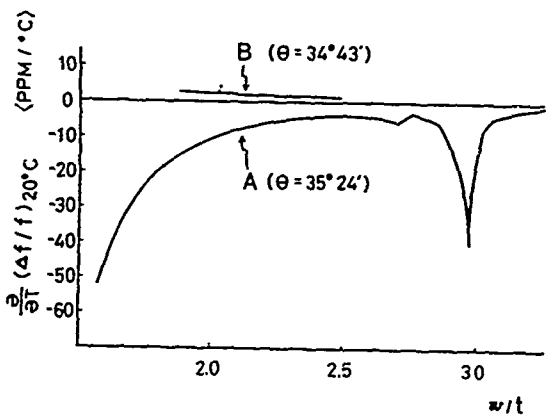

Fig. 5. Measured frequency-temperature coefficient vs. w/t.

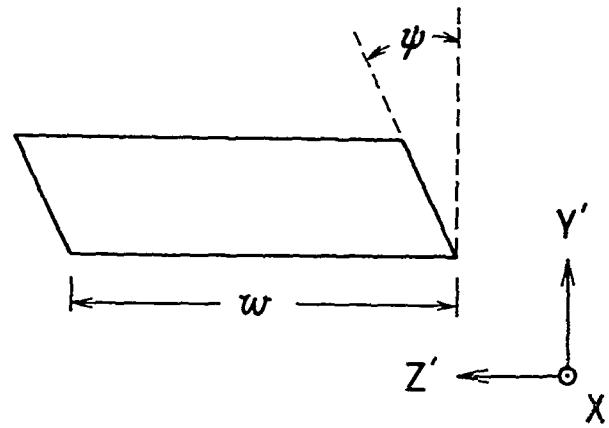

Fig. 7. Inclination of edge cuts.

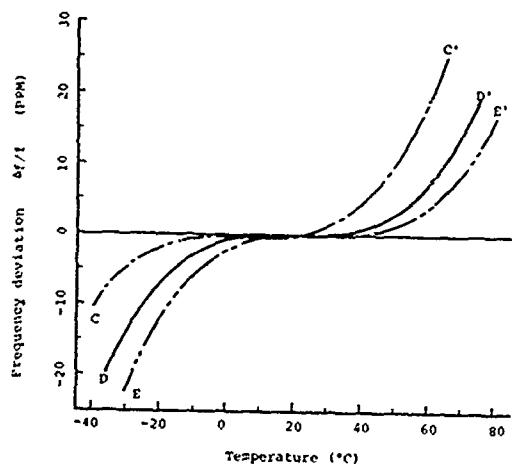

Fig. 8.
Frequency temperature curves for three different values of w/t.

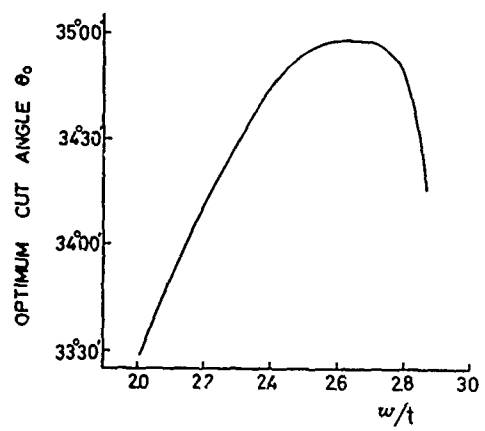

Fig. 6. Optimum cut angle vs. w/t.

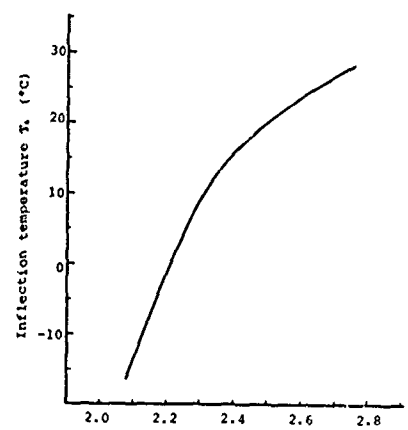

Fig. 9. Inflection temperature

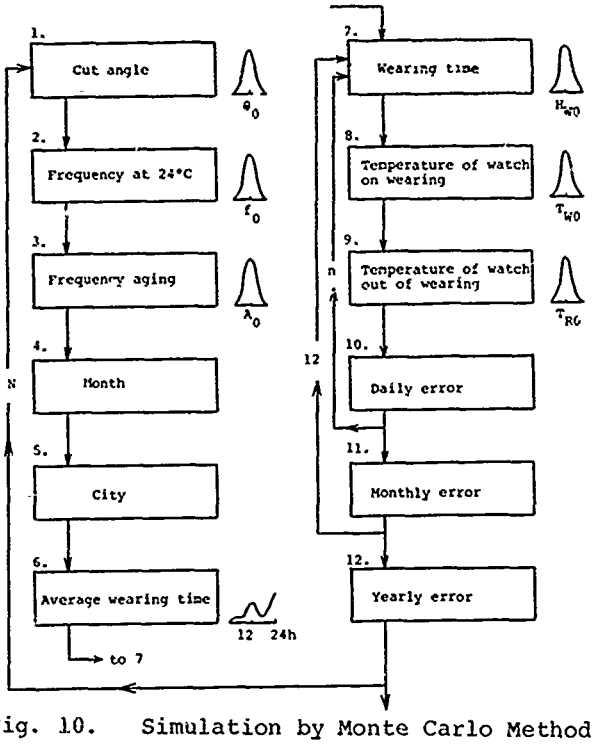

Fig. 10. Simulation by Monte Carlo Method

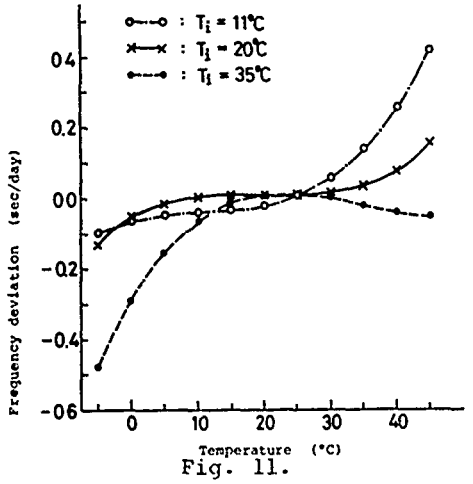

Fig. 11.

Optimum frequency-temperature curves for three T_i.

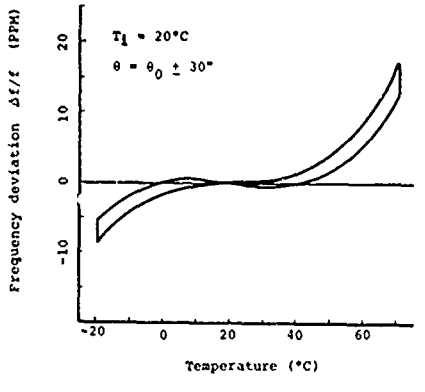

Fig. 12. Range of the frequency temperature curves used on the simulation

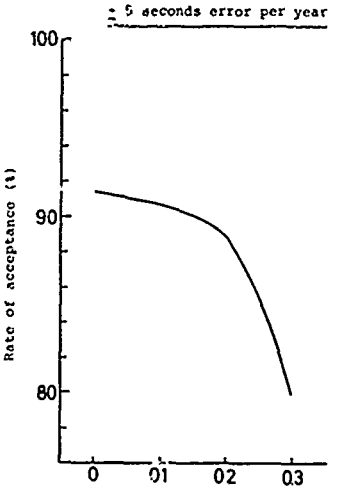

Fig. 13. Rate of acceptance vs. frequency aging.

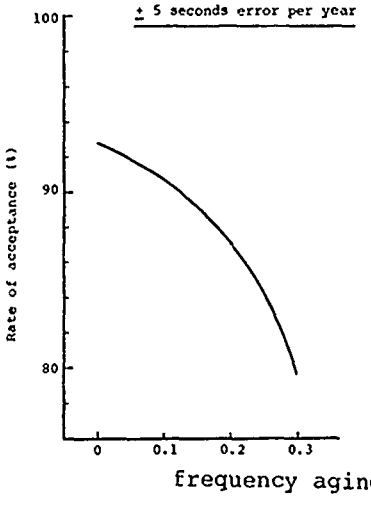

Fig. 14. Rate of acceptance vs. frequency aging.

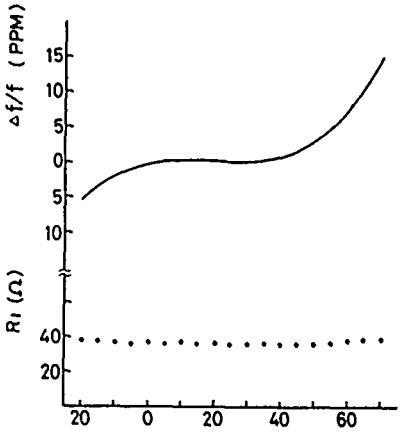

Fig. 15.
Temperature characteristics of $\Delta f/f$ and R_1.

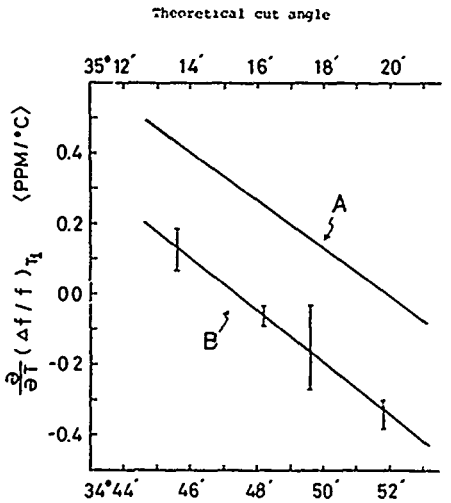

Experimental cut angle for rectangular AT-cut resonator

Fig. 16. Comparison of theoretical and experimental results.

T_i	Rate of Acceptance
35°C	77.7 %
20°C	92.4 %
11°C	82.8 %

Table 1. Rate of Acceptance
(± 3 seconds error per year)

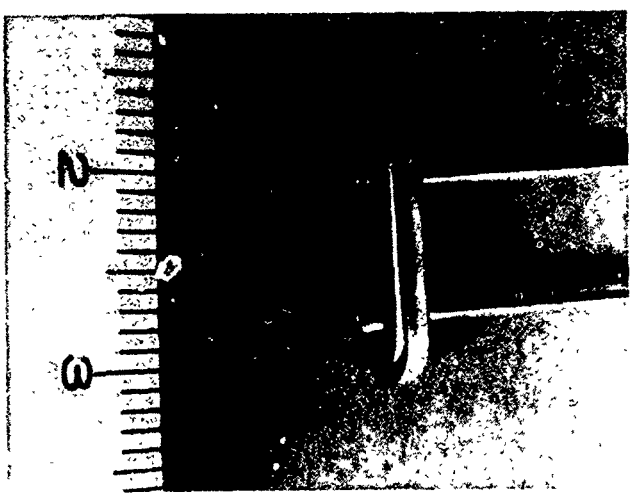

Photo 1. Quartz resonator supported by elastic pins.

EXTENSION, FLEXURE, AND SHEAR MODES IN ROTATED X-CUT QUARTZ RECTANGULAR BARS

T. R. Meeker

Bell Telephone Laboratories, Incorporated
555 Union Boulevard
Allentown, Pennsylvania

Abstract

Lee's theory of extension, flexure, and shear modes in bars is discussed. Lee's bar constants are tabulated versus the crystal angle for a rotated X-cut quartz bar. The dispersion relations are plotted for all five modes for a -5 degree X-cut quartz bar. Wavenumber approximations are used to convert the dispersion relations into frequency equations.

Approximate inharmonic frequencies of all five modes are calculated. These types of inharmonic modes do not appear to have been discussed before. These inharmonic modes have phase reversals through the width of the bar. Since several inharmonics on each overtone of the five modes are generally possible, a very large number of unwanted modes in extensional and flexural crystal resonators can be understood in terms of Lee's model as extended to include the inharmonics. The dependence of the frequency of these modes on bar width and length is discussed.

Introduction

A Mindlin type theory of extension, width length flexure, width shear, transverse shear, and width twist in 5° X-cut quartz bars*[1,2] has already been reported.[3] For a bar with equal thickness electrodes the dispersion relations for this theory separate into two dispersion relations: one set for coupled extension, width length flexure, and width shear and a second set for coupled transverse shear and width twist. The boundary value solution of the coupled extension, width length flexure, and width shear has been reported in detail.[3] The resonant frequencies calculated from this boundary value solution agree very well with experimental frequencies of 5° X-cut quartz bars.[3]

In this paper both sets of dispersion relations are plotted. Instead of solving the boundary value problem, the dispersion relations are converted into frequency equations by a pair of wave number approximations,[4] one for extension, width shear, transverse shear, and width twist and a second for the width length flexure. These approximate frequency equations are cubic and quadratic functions of frequency and can therefore be solved without root searches. For many purposes, such as a general design search or the location and identification of unwanted modes, the present approximation is adequate. For these purposes the reduced cost of the computation without root searches may be significant.

The Bar Constants

The five coupled plate differential equations and the eight plate stress components developed by Mindlin[5] are expressed in terms of the zeroth order and first order dependence of elastic displacement on plate thickness. In the Lee bar theory the bar is a slice of the Mindlin plate. The plate thickness becomes the bar width. The plate equations are integrated through the bar thickness (parallel to the plane of the plate) to zeroth order only. Forces on the faces normal to the bar thickness are included so that electrode effects can be included in the theory.

The bar geometry and coordinate system are shown in Figure 1. The bar length is along x_3, the bar width is along x_2, and the bar thickness is along x_1.

The plate from which the bar is sliced is indicated by the dotted lines parallel to the x_1 axis in Figure 1. This orientation of the bar was used so that the bar electrodes would be on the natural electrical faces of the quartz and so that the plate equations developed by Mindlin[5] could be used in the derivation without revision. This choice of orientation, however, makes a -5° X-cut bar into a -95° X-cut bar. In the rest of this paper the rotation angles will be shifted by 90° to preserve the usual notation for the -5° and + 18.5° X-cut bars.

By setting

*This cut has been called +5° or -5° by various authors. -5° is consistent with the Cady diagram[1] and the new IEEE standard.[2]

$$T_{11}^{(0)} = 0$$

$$T_{11}^{(1)} = 0 \qquad (1)$$

at all points in the plate and by setting

$$T_{12}^{(0)} = 0 \quad ,$$

$$T_{13}^{(0)} = 0 \quad , \qquad (2)$$

and

$$T_{13}^{(1)} = 0$$

on x_1 faces at $\frac{T}{2}$ and $+\frac{T}{2}$, the following bar constants can be defined for quartz and electrode bars:

$$C_{ij}^{*m} = C_{ij}^{sm} - \frac{C_{1i}^{sm} \times C_{1j}^{sm}}{C_{11}^{sm}} \quad ,$$

$$i = 3 \text{ or } 4$$
$$j = 3 \text{ or } 4$$

$$C_{ij}^{*m} = C_{ij}^{sm} \quad , \qquad (3)$$

$$i = 5 \text{ or } 6$$
$$j = 5 \text{ or } 6$$

$$\gamma_{33}^{*m} = \gamma_{33}^{sm} - \frac{\gamma_{13}^{sm} \times \gamma_{13}^{sm}}{\gamma_{11}^{sm}} \quad ,$$

and

$$\gamma_{55}^{*m} = \gamma_{55}^{sm} \quad ,$$

where m = q for quartz or e for electrode.

In Equation (3) the starred constants are constants for bar material (m=q) and electrode material (m=e) and the constants with superscript "s" are the Mindlin plate constants. A matrix technique for calculating the C_{ij}^{s} and the γ_{ij}^{s} has already been reported.[6]

When the electrode bars are attached to the x_1 faces of the quartz bar, matching of stress and displacement components may be expressed as changes in the bar constants (electrode stiffening) and in the bar density (electrode mass). The bar constants including electrode stiffening and mass are:

$$C_{ij}^{b} = K_i^q K_j^q C_{ij}^{*q} + 2\frac{t}{T} K_i^e K_j^e C_{ij}^{*e} \quad ,$$

$$\gamma_{ij}^{b} = \gamma_{ij}^{*q} + 2\frac{t}{T}\gamma_{ij}^{*e} \quad , \qquad (4)$$

and

$$\rho^{b} = \rho^{q} + 2\frac{t}{T}\rho^{e} \quad ,$$

where ρ^q is the density of quartz, t is the thickness of one electrode and T is the quartz thickness. In Equation 4 the K_i^m and K_j^m are the Mindlin plate constant corrections to make the approximate plate theory exact for long wavelength plate solutions.[5,7] For this paper the K_i^m and K_j^m for the quartz bar and for the electrode bar are:

$$K_1^m = K_2^m = K_3 = K_5^m = 1$$

$$m = \text{quartz (q) or electrode (e)}$$

$$(K_4^q)^2 = \frac{\pi^2}{24}\left\{\frac{C_{22}^E + C_{44}^E - \left[(C_{22}^E - C_{44}^E)^2 + 4(C_{24}^E)^2\right]^{1/2}}{C_{44}^{*q}}\right\}$$

$$(K_6^q)^2 = \frac{\pi^2}{12} \qquad (5)$$

$$(K_4^e)^2 = \frac{\pi^2}{12}$$

$$(K_6^e)^2 = \frac{\pi^2}{12} \quad ,$$

where the C_{ij}^E are the constant electric field stiffnesses of the quartz bar. The bar constants just defined result from removing the dependence of $\mu_1^{(0)}$ and $\mu_1^{(1)}$ on x_1 from the stress equations for the plate. $\mu_1^{(0)}$ and $\mu_1^{(1)}$ are retained in this theory as independent of x_1. Figure 2 and Figure 3 show how the eight bar constants of the Lee theory depend on the orientation of the quartz in the bar.

As mentioned earlier the value of θ used in Figure 2 and Figure 3 is not the same as that defined in Figure 1. The 90° difference is to make the notation for the two common extensional mode bars consistent with current practice. To clarify this change the angles corresponding to length (Z) along X_3 or X_2 are marked on Figure 2 and Figure 3.

The Characteristic Equation For The Bar

The zeroth order and first order bar displacement components shown in Figure 4 are solutions to the five coupled bar differential equations[3] if the following set of homogeneous equations are satisfied simultaneously:

$$\begin{bmatrix} [\rho(1+R)\omega^2 b^2 + D_{11}] & 0 & 0 & [D_{14}] & 0 \\ 0 & [\rho(1+R)\omega^2 b^2 + D_{22}] & [D_{23}] & 0 & [D_{25}] \\ 0 & [D_{23}] & [\rho(1+R)\omega^2 b^2 + D_{33}] & 0 & [D_{35}] \\ [D_{14}] & 0 & 0 & [\rho(\tfrac{1+R}{3})\omega^2 b^2 + D_{44}] & 0 \\ 0 & [D_{25}] & [D_{35}] & 0 & [\rho(\tfrac{1+R}{3})\omega^2 b^2 + D_{55}] \end{bmatrix} \begin{bmatrix} u_{10}^{(0)} \\ u_{20}^{(0)} \\ u_{30}^{(0)} \\ u_{10}^{(1)} \\ u_{30}^{(1)} \end{bmatrix} = 0 \qquad (6)$$

where ρ is the density of quartz and $R = 2\frac{t}{T}\frac{\rho^e}{\rho^q}$. Sketches of the approximate shapes of the five displacement components[3] are shown in Figure 5. In Equation (5) the D_{ij} (for real k_e) are defined as follows:

$$D_{11} = -k_3^2 b^2 C_{55}^b$$

$$D_{14} = -k_3 \; b \; C_{56}^b$$

$$D_{22} = -k_3^2 b^2 C_{44}^b$$

$$D_{23} = -k_3^2 b^2 C_{34}^b$$

$$D_{25} = -k_3 \; b \; C_{44}^b \qquad (7)$$

$$D_{33} = -k_3^2 b^2 C_{33}^b$$

$$D_{35} = -k_3 \; b \; C_{34}^b$$

$$D_{44} = -k_3^2 b^2 \frac{\gamma_{55}^b}{3} - C_{66}^b$$

$$D_{55} = -k_3^2 b^2 \frac{\gamma_{33}^b}{3} - C_{44}^b$$

The D_{ij} in Equation (6) are written in terms of the bar constants described in the preceding section. Equation (6) therefore includes the effects of electrode stiffening and mass. In Equation (6) k_3 is the wavenumber for waves traveling in the x_3 direction (along the length of the bar) and $b=W/2$.

The zero values of coefficients in Equation (6) result from using electrodes of equal thicknesses on the x_1 faces of the bar. Unequal electrode thicknesses produce nonzero coefficients and couple all five mode types together.

The Dispersion Relations

The determinant condition for a solution to the cubic part of Equation (6) may be written as

$$\begin{vmatrix} [\rho(1+R)\omega^2 b^2 + D_{22}] & [D_{23}] & [D_{25}] \\ [D_{23}] & [\rho(1+R)\omega^2 b^2 + D_{33}] & [D_{35}] \\ [D_{25}] & [D_{35}] & [\rho(\tfrac{1+R}{3})\omega^2 b^2 + D_{55}] \end{vmatrix} = 0 \qquad (8)$$

Equation (8) may be expanded into a cubic equation in $(\omega b)^2$. For real k_3 this cubic can be solved by the trigonometric method[8] for three positive real values of $(\omega b)^2$.

If the cubic expansion of Equation (8) is

$$(\omega b)^6 + B(\omega b)^4 + C(\omega b)^2 + D = 0 \qquad (9)$$

and k_3 is real,

$$B = \frac{1}{\rho}(3 D_{55} + D_{22} + D_{33})$$

$$C = \frac{1}{\rho^2}(3 D_{33} D_{55} + D_{33} D_{22} + 3 D_{22} D_{55} - 3 D_{35} D_{35} - D_{23} D_{23} - 3 D_{25} D_{25}) \qquad (10)$$

and $$D = \frac{3}{\rho^3}(D_{22} D_{33} D_{55} - D_{22} D_{35} D_{35} - D_{23} D_{23} D_{55} + D_{23} D_{35} D_{25} + D_{25} D_{23} D_{35} - D_{25} D_{25} D_{33})$$

The determinant condition for a solution to the quadratic part of Equation (6) may be written as

$$\begin{vmatrix} [\rho(1+R)\omega^2 b^2 + D_{11}] & [D_{14}] \\ [D_{14}] & [\rho(\tfrac{1+R}{3})\omega^2 b^2 + D_{44}] \end{vmatrix} = 0 \qquad (11)$$

If the quadratic expansion of equation 11 is

$$E(\omega b)^4 + G(\omega b)^2 + H = 0 \qquad (12)$$

and k_3 is real,

$$E = \frac{1}{3}\rho^2$$

$$G = \frac{1}{3}\rho(3D_{44} + D_{11}) \qquad (13)$$

and $$H = D_{11} D_{44} - D_{14} D_{14}$$

Equation 12 is quadratic in $(\omega b)^2$ and can be solved by the ordinary quadratic formula.

Although some of the D_{ij} become imaginary for imaginary wave number, the cubic and quadratic coefficients (Equation (10) and Equation (13)) remain real; the signs of some of the coefficients change when jk_{3i} is substituted for k_3 in the equations. For the case of imaginary k_3, $(k_3 = jk_{3i})$ the cubic coefficients become

$$B' = \frac{1}{\rho}(3 D_{55}' + D_{22} + D_{33})$$

$$C' = \frac{1}{\rho^2}(3 D_{33} D_{55}' + D_{33} D_{22} + 3 D_{22} D_{55}' + 3 D_{35} D_{35} - D_{23} D_{23} + 3 D_{25} D_{25}) \qquad (14)$$

and $$D' = \frac{3}{\rho^3}(D_{22} D_{33} D_{55}' + D_{22} D_{35} D_{35} - D_{23} D_{23} D_{55}' - D_{23} D_{35} D_{25} - D_{25} D_{23} D_{35} + D_{25} D_{25} D_{33})$$

where

$$D_{55}' = -C_{44}^b + \frac{1}{3} b^2 k_{3i}^2 \gamma_{55}^b$$

For $k_3 = {}_j k_{3i}$ the quadratic coefficients become

$$E' = \tfrac{1}{3}\rho^2$$

$$G' = \tfrac{1}{3}\rho(3D_{44}' - D_{11}) \qquad (15)$$

and $$H' = -D_{11}D_{44}' - D_{14}D_{14}$$

where $$D_{44}' = -C_{66}{}^b + \tfrac{1}{3}b^2 k_{3i}{}^2 \gamma_{55}{}^b$$

The dependence of ω on k_3 has already been reported for the extensional, width length flexure, and width shear bar modes.[3] Figure 6 shows the dispersion relations for all five modes of this theory.

Width shear and width twist have branches with imaginary wave number and have cut off frequencies. These are high frequency bar modes. The other three modes have branches that have zero frequency at zero wavenumber. Extension and transverse shear have linear dispersion curves, while the width length flexure has a shallow positive curvature and the frequency approaches zero with zero dependence on the wavenumber. Five real frequency solutions exist for all real values of k_3. For imaginary k_3 near zero, there are three real frequency solutions and two complex frequency solutions. For larger values of imaginary k_3, there is one real frequency solution and four complex frequency solutions.[9] A discussion of the significance of these complex frequency solutions is beyond the scope of this paper.

The Wave Number Approximations

The dispersion relations can be converted into approximate frequency equations by assuming that the length of the bar is an odd number of half wavelengths. This approximation amounts to solving the boundary conditions on the bar ends for one stress or displacement component. The other stress components are ignored in this approximation.

The wave number approximation consists in setting

$$k_3 = \frac{2\pi}{\lambda} = \frac{n_3\pi}{L} \qquad (16)$$

in the dispersion relations,[4] and then solving for the five frequencies. In Equation (16) n_3 is the number of half wavelengths along x_3 and L is the bar length. The frequencies of extension, transverse shear, width shear, and width twist are taken from this calculation. The frequency of the flexure is not given correctly by this calculation because the boundary condition for flexure is more complex than that for the other modes.[11] A wave number approximation for the bar flexure has been reported.[3,10] For large wavenumber this approximation may be given by

$$k_3 = \frac{(n_3 + 0.5)\pi}{L} \qquad (17)$$

A more accurate wavenumber solution can be obtained by using the Mason number in place of $(n_3 + \frac{1}{2})\pi$. In this paper the flexural frequency is obtained by using the wavenumber approximation as

$$k_3 = \frac{M(n_3, W/L)}{L} \qquad (18)$$

where $M(n_3, W/L)$ is the root of a transcendental equation described earlier.[10] $M(n_3, W/L)$ also depends on the width length ratio of the bar. For the four nonflexures, k_3 from Equation 16 is substituted into the D_{ij} (Equation (7)) and five frequencies are calculated from the cubic and quadratic equations (Equation (9) and Equation (12)). The flexure frequency from this set is discarded. For the flexure calculation, k_3 from Equation 18 is substituted into the D_{ij} and three frequencies are calculated from the cubic equation (Equation (9)). The flexure from this set is retained.

Results

Figure 7 shows the calculated dependence of the frequencies of the three low frequency modes on the ratio of bar width to bar length. The extensional frequency in this theory agrees with experiment within 1 Hz at 10^5 Hz. Overtones of each mode type involve more than one half wavelength along the bar length. Since the frequencies of all these modes depend on the bar width as well as on the bar length, inharmonic modes of each type (corresponding to integral numbers of half wavelengths along the bar width) should also be observed.* Figure 8 shows how the width length flexure with two half wavelengths along the width and five half wavelengths along the length should have the same frequency as the extension when the bar has a width length ratio of 0.08. The use of proper dimensional ratios to avoid the frequency coincidences between extension and overtones of width length flexure is well known.[3,12] A width length ratio of 0.08 satisfies the usual design rule. With the inharmonic width length flexure present, the design rule must be changed or the activity of the unwanted mode must be suppressed.

Frequencies of inharmonic modes of thickness shear and thickness twist are all higher than the fundamental width or length mode.[13] This is due to the fact that these modes have higher frequencies for smaller width and length. As shown above the inharmonic frequencies of width length flexure occur at frequencies lower than the fundamental

*These inharmonics of low frequency modes have not been discussed before.

width frequency. The different behaviour of the flexural inharmonics is due to the fact that the flexure has a lower frequency for a smaller width.

The extensional mode frequency drops slightly with increasing bar width,[14] so that the extensional width inharmonics should be above the fundamental.

The width inharmonics and length overtones produce a very large number of unwanted modes in bars, all of which must be understood and controlled by the resonator designer. Figure 9 shows all the mode frequencies within ±10 kHz of the fundamental extensional mode for a -5° X-cut quartz bar 0.08 inches wide and 1.0 inch long.

The activities of these width dependent bar modes should be strongly affected by the method of lead attachment and by the bar symmetry.

Other low frequency modes that are not discussed in this paper also appear as unwanted modes in bars. These include length torsion and length thickness flexure. Although a discussion of these unwanted modes is beyond the scope of this paper, it is worth mentioning that these modes should also have inharmonics corresponding to multiple phase reversals along the bar width.

Conclusions

The bar equations developed by Lee have been studied for X-cut quartz. The eight bar constants of this theory are plotted versus the orientation of the quartz. Dispersion relations for all five modes are plotted. Width shear and width twist are high frequency width modes and have cutoff frequencies and frequencies with imaginary wavenumber along the bar length. Extension and transverse shear are low frequency length modes with a linear dependence of frequency on real wavenumber. The zero frequency for zero wavenumber (long wavelength) means that these modes have low frequencies. The width length flexure also has zero frequency for zero wavenumber, but it has a shallow positive curvature. The dispersion relation for this mode approaches zero wavenumber with zero slope. Thus the width length flexure has the lowest frequency of the five modes considered.

Inharmonic modes of the low frequency modes have been described for the first time. For the width length flexure these modes occur at frequencies below the corresponding length mode and have multiple phase reversals along the bar width.

Many of the length overtones and width inharmonics of the low frequency modes are unwanted modes in bars. The activities and frequencies of these modes must be controlled by the designer of low frequency resonators.

Acknowledgements

Discussions with S. Kaufman, J. J. Royer, G. T. Pearman, and F. S. Welsh, III have been very helpful.

References

1. W. G. Cady, Piezoelectricity, Vol. II, Dover Publication s, New York, p. 459 (1964).
2. IEEE Standard on Piezoelectricity, 176-1978 (1978).
3. P. C. Y. Lee, Journal of Applied Physics, Vol. 42, No. 11, October, pps. 41394144 (1971).
4. T. R. Meeker, Proceedings of the 31st Annual Symposium on Frequency Control, U.S. Army Electronics Command, Fort Monmouth, N.J., pps. 35-43 (1977).
5. R. D. Mindlin, Quart Applied Math. 19, pps. 51-61 (1961).
6. T. R. Meeker, Proceedings of the 29th Annual Symposium on Frequency Control, U.S. Army Electronics Command, Fort Monmouth, N.J., pps. 54-64 (1975).
7. R. D. Mindlin and W. J. Spencer, Journal of the Acoustical Society of America, Vol. 42, No. 6, pps. 1268-1277 (1967).
8. W. S. Burnside and A. W. Panton, Theory of Equations, Vol I, Dover Publications, New York, pps. 108-111 (1960, 1912).
9. Reference 8, pps 26 - 27
10. H. Lamb, The Dynamical Theory of Sound, Second Edition Dover, New York, page 120 (1960, 1925).
11. W. P. Mason, Journal of the Acoustical Society of America, Vol. VI, pps. 246-249 (1935).
12. R. A. Heising, Quartz Crystal for Electrical Circuits, D. Van Nostrand Company, New York, pps 221-226 (1946).
13. G. T. Pearman and R. C. Rennick, Proceedings of the 31st Annual Symposium on Frequency Control, U.S. Army Electronics Command, Fort Monmouth, N. J., pps. 191-196 (1977).
14. A. E. H. Lover, Mathematical Theory of Elasticity , Fourth Edition, Dover Publication, New York, p. 428 (1944, 1929).

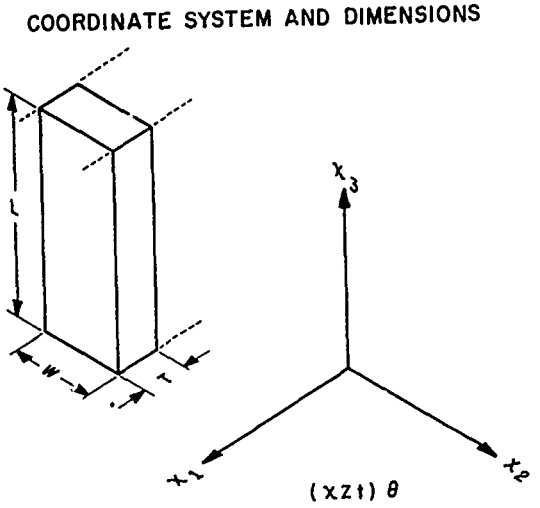

Figure 1 - Bar Geometry and Coordinate System

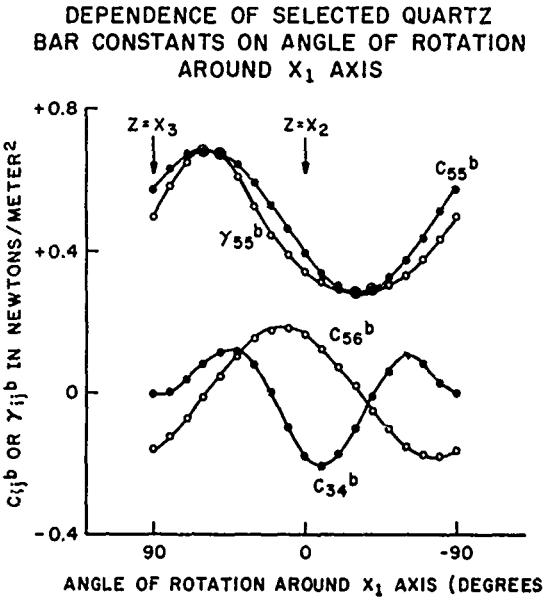

Figure 2 - Dependence of Selected Bar Constants on the Orientation of the Bar.

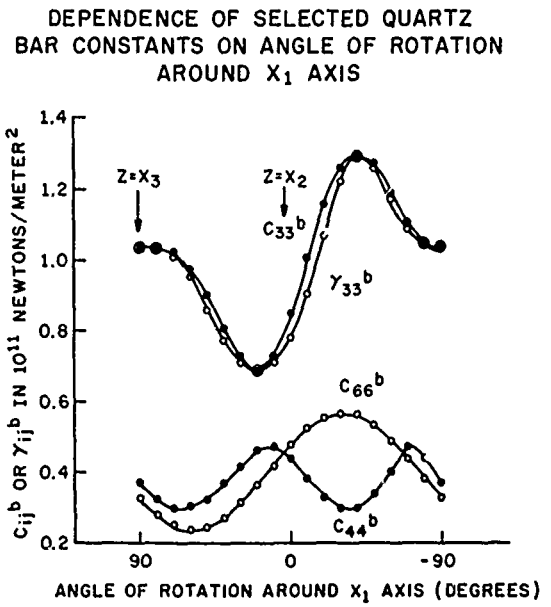

Figure 3 - Dependence of Selected Bar Constants on the Orientation of the Bar.

$$u_1^{(0)} = b\,u_{10}^{(0)}\; e^{jk_3x_3}\; e^{jwt}$$

$$u_2^{(0)} = b\,u_{20}^{(0)}\; e^{jk_3x_3}\; e^{jwt}$$

$$u_3^{(0)} = b\,u_{30}^{(0)}\; e^{jk_3x_3}\; e^{jwt}$$

$$u_1^{(1)} = j\,u_{10}^{(1)}\; e^{jk_3x_3}\; e^{jwt}$$

$$u_3^{(1)} = j\,u_{30}^{(1)}\; e^{jk_3x_3}\; e^{jwt}$$

Figure 4 - Bar Displacement Components.

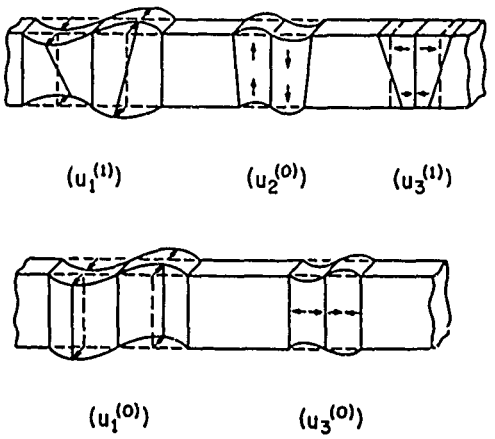

Figure 5 - Bar Displacement Component Shapes.

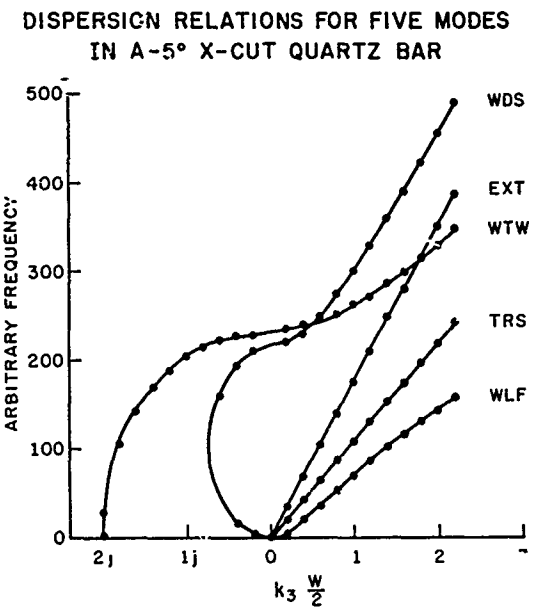

Figure 6 - Five Dispersion Relations for -5° X-cut Quartz Bar. WDS = Width Shear; EXT = Extension; WTW = Width Twist; TRS = Transverse Shear; WLF = Width Length Flexure

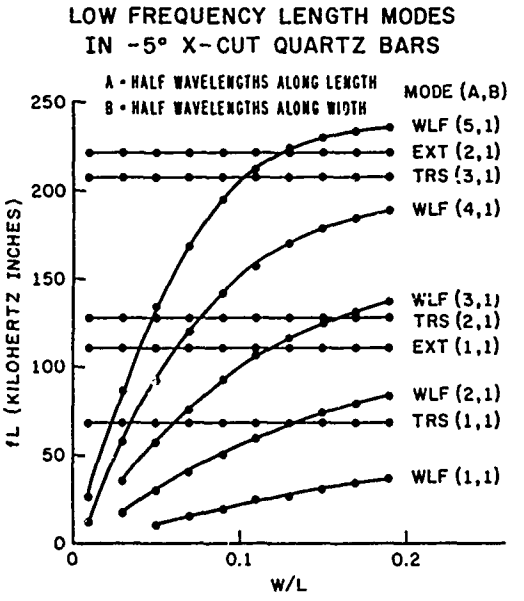

Figure 7 - Calculated Dependence of the Frequencies of Three Low Frequency Bar Modes on the Ratio of Width to Length. WLF = Width Length Flexure; EXT = Extension; TRS = Transverse Shear

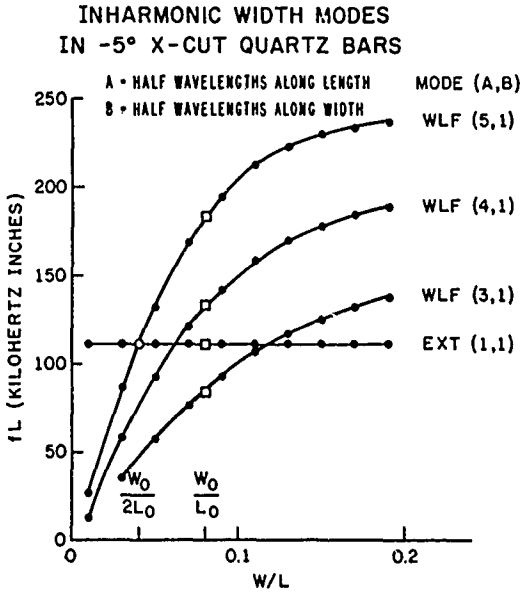

Figure 8

An Inharmonic Width Length Flexure for a -5° X-cut Quartz Bar. WLF = Width Length Flexure; EXT = Extension

MODES IN a-5° x-CUT QUARTZ BAR

LENGTH = 1.0 INCHES (x_2')
WIDTH = 0.08 INCHES (x_3')
THICKNESS = 0.02 INCHES (x_1)

MODES WITH FREQUENCIES WITHIN ±10kHz OF E(1,1)

FREQUENCY (Hz)	MODE (A,B)
110695	EXT(1,1)
110776	EXT(1,2)
110887	EXT(1,3)
111460	EXT(1,4)
113244	EXT(1,5)
116988	EXT(1,6)
119010	EXT(1,7)
111531	WLF(5,2)
107153	WLF(6,3)
108434	WLF(7,4)
112167	WLF(8,5)
117245	WLF(9,6)

A = HALF WAVELENGTHS ALONG LENGTH

B = HALF WAVELENGTHS ALONG WIDTH

Figure 9

Unwanted Mode Frequencies near the Extensional Mode of a -5° X-cut Quartz Bar.
EXT = Extension; WLF = Width Length Flexure

NONLINEAR VIBRATIONS OF QUARTZ RODS

H.F. Tiersten
Department of Mechanical Engineering, Aeronautical Engineering & Mechanics
Rensselaer Polytechnic Institute, Troy, N.Y. 12181

A. Ballato
U.S. Army Electronics Technology and Devices Laboratory
USERADCOM, Fort Monmouth, N.J. 07703

Abstract

A one-dimensional scalar nonlinear differential equation describing the extensional motion of thin piezoelectric rods oriented in an arbitrary direction with respect to the principal axes of the crystal is obtained from the general nonlinear three-dimensional equations of electroelasticity. Only the elastic nonlinearities are included in the description. The electrical behavior is taken to be linear since quartz has small piezoelectric coupling. The treatment provides the relation between the quadratic and cubic nonlinear extensional coefficients of the rod and the fundamental anisotropic elastic constants of second, third and fourth order, along with the well-known relation between Young's modulus and the fundamental second order elastic constants. The quadratic rod coefficients are calculated for various orientations of quartz rods with respect to the principal axes of the quartz crystal. Such calculations cannot be performed for the cubic rod coefficients because the fourth order elastic constants of quartz, on which the cubic coefficients depend, are not presently known. The nonlinear extensional equation is applied in the analysis of intermodulation in quartz rods. A lumped parameter representation of the solution, which is valid in the vicinity of a resonance, is obtained and the influence of the external circuitry is included in the treatment. In particular, the results of this analysis can be used along with measurements to evaluate the cubic rod coefficients for the practical 5° X-cut quartz rod.

1. Introduction

The one-dimensional scalar differential equation describing the extensional motion of thin piezoelectric rods is obtained from the general[1] nonlinear three-dimensional description by means of an iterative procedure. Only the elastic nonlinearities are considered. The relation between the quadratic and cubic coefficients of the rod and the fundamental anisotropic elastic constants of various orders is derived. The quadratic rod coefficients are calculated for various orientations of quartz rods with respect to the principal axes of the crystal but not the cubic rod coefficients because the fundamental elastic constants of fourth order, which are required for the calculation, are not presently known.

The steady state solution of the nonlinear system is determined at an intermodulation frequency by straight-forward iteration from the linear solution. The intermodulation current-voltage relation, which is valid in the vicinity of a resonance, is obtained and the crystal is incorporated in the test circuit and the relation between the intermodulation and driving voltages is determined. This relation and the calculated quadratic rod coefficients can be used along with measurements to determine the cubic rod coefficients for any desired orientation of quartz rod, including, of course, the practical 5°-X-cut.

It should be carefully noted that the coupling between extension and flexure, which can exist in an anisotropic rod, is not included in this description. However, since the coupling of a high overtone of flexure with a low extensional mode occurs only for certain well separated geometries[2], the equation for the anisotropic rod presented here is valid for all other geometric ratios. This means that the equation is valid for almost all geometries and certainly for all practical cases.

2. Nonlinear Equations

The stress equations of motion and charge equation of electrostatics for an electroelastic solid with small piezoelectric coupling may be written in the form[1]

$$K_{LM,L} = \rho^{\circ}\ddot{u}_M, \tag{2.1}$$

$$D_{L,L} = 0. \tag{2.2}$$

The symbols ρ°, u_M, K_{LM} and D_L, respectively, denote the reference mass density, the mechanical displacement, the Piola-Kirchhoff stress tensor and the electric displacement vector. For purposes of this treatment, the constitutive equations for K_{LM} and D_L along with the electric field-electric potential relations may be written in the form[1]

$$K_{LM} = c^{E}_{2LMRS} u_{R,S} - e_{RLM} E_R + \frac{1}{2} c^{E}_{2LMRS} u_{K,R} u_{K,S}$$

$$+ c^{E}_{2LKRS} u_{M,K} u_{R,S} + \frac{1}{2} c^{E}_{3LMKNRS} u_{K,N} u_{R,S}$$

$$+ \frac{1}{2} c^{E}_{2LNRS} u_{M,N} u_{K,R} u_{K,S} + \frac{1}{2} c_{3LKRSNJ} u_{M,K} u_{R,S} u_{N,J}$$

$$+ \frac{1}{2} c_{3LMRSNJ} u_{R,S} u_{K,N} u_{K,J} + \frac{1}{6} c_{4LMRSNKIJ} u_{R,S} u_{N,K} u_{I,J}, \tag{2.3}$$

$$D_L = e_{LNK} u_{N,K} + \epsilon^{S}_{LK} E_K, \quad E_K = -\varphi_{,K}, \tag{2.4}$$

where, in view of the small piezoelectric coupling in quartz, we have included nonlinear elastic terms only and kept the electric and electroelastic terms linear, in accordance with the discussion in the Introduction. In (2.3) and (2.4) φ is the electric scalar potential and c^{E}_{2LMRS}, $c^{E}_{3LMKNRS}$, $c^{E}_{4LMRSNKIJ}$, and ϵ^{S}_{LK} are the second-order elastic, third-order elastic, fourth-order elastic, piezoelectric and dielectric constants, respectively. The associated boundary conditions at the surface of the piezoelectric solid are on $N_L K_{LM}$ or u_M and $N_L D_L$ or φ, where N_L denotes the unit normal to the undeformed surface.

A schematic diagram of the piezoelectric rod is given in Fig. 1, where $2\ell \gg 2w > 2H$ and the surfaces normal to X_3 are fully electroded. Since we are interested in solutions which vary slowly compared with 2h, to lowest order the electrical variables may be written in the form[3,4]

$$E_1 = E_2 = 0, \quad E_3 = -V/2h, \quad D_3 = D_3(X_1, X_2, t), \tag{2.5}$$

where V is the voltage across the electrodes, and D_1 and D_2 are negligible to this order as are deviations from what is shown in (2.5). Since the electrical behavior is linear and the linear electric constitutive equation adjusted for the rod is well known[4], it is convenient to omit the electric field E_K from (2.3) while obtaining the nonlinear rod equation and then introduce the known electric quantities suitably adjusted for the rod.

Since we are interested in wavelengths of the order of ℓ and, hence, solutions varying slowly compared with h (and w), both the inertia and stiffness of the electrodes are negligible and with the rod axis along X_1 we have the boundary conditions

$$K_{2M} = 0 \text{ at } X_2 = \pm w, \quad K_{3M} = 0 \text{ at } X_3 = \pm h. \tag{2.6}$$

Since for the low frequencies of interest the solution varies slowly compared to the cross-sectional dimensions and flexure is uncoupled from extension, which we are considering, we have[5]

$$\ddot{u}_2 \approx 0, \quad \ddot{u}_3 \approx 0, \tag{2.7}$$

but it must be remembered that all $u_{K,M}$ exist. In addition, on account of (2.6), (2.7) and the aforementioned slow variation, from (2.1) we see that we should take[5] all $K_{LM} = 0$ except K_{11}. Under these circumstances all that remains of Eqs. (2.1) is

$$K_{11,1} = \rho \overset{o}{\ddot{u}}_1, \tag{2.8}$$

which is the basic differential equation for the anisotropic rod. We must now find the nonlinear relation between K_{11} and $u_{1,1}$. This is done in the next section.

3. Nonlinear Anisotropic Rod Equations

Since all Piola-Kirchhoff stress components have been taken to vanish except K_{11}, Eq. (2.3) can be put in a more useful form by operating[5] with the reciprocal of the second order elastic constants c^{-1}_{2ABCD}, which are the elastic compliances s_{ABCD}, to obtain

$$s_{AB11} K_{11} = u_{A,B} + \frac{1}{2} u_{K,A} u_{K,B} + s_{ABLM} H_{LM}, \tag{3.1}$$

where

$$H_{LM} = c_{2LKRS} u_{M,K} u_{R,S} + \frac{1}{2} c_{3LMKNRS} u_{K,N} u_{R,S} +$$

$$\frac{1}{2} c_{2LNRS} u_{M,N} u_{K,R} u_{K,S} + \frac{1}{2} c_{3LKRSNJ} u_{M,K} u_{R,S} u_{N,J} +$$

$$\frac{1}{2} c_{3LMRSNJ} u_{R,S} u_{K,N} u_{K,J} + \frac{1}{6} c_{4LMRSNKIJ} u_{R,S} u_{N,K} u_{I,J}. \tag{3.2}$$

For purposes of this work it is convenient to write the nine equations in (3.1) as two separate equations, one for A = B = 1 and the other eight for $AB \neq 11$, thus

$$K_{11} = \frac{1}{s_{1111}} u_{1,1} + \frac{1}{2 s_{1111}} u_{K,1} u_{K,1} + \frac{s_{11LM}}{s_{1111}} H_{LM}, \tag{3.3}$$

$$u_{A,B} = s_{AB11} K_{11} - \frac{1}{2} u_{K,A} u_{K,B} - s_{ABLM} H_{LM}, \quad AB \neq 11. \tag{3.4}$$

The iterative procedure consists of first solving the linear portion of (3.3) for ${}_0K_{11}$, where the zero denotes the order of the iterate, and then substituting into the linear portion of (3.4) to obtain ${}_0u_{A,B}$. Then the ${}_0u_{A,B}$ is substituted into the quadratic terms in (3.3), with (3.2), to obtain ${}_1K_{11}$, which is then substituted into (3.4) along with the substitution of ${}_0u_{A,B}$ into the quadratic terms to obtain ${}_1u_{A,B}$. Finally, the ${}_1u_{A,B}$ is substituted into both the quadratic and cubic terms in (3.3), with (3.2), and only quadratic and cubic terms in $u_{1,1}$ are retained to obtain ${}_2K_{11}$. Accordingly, the zeroth iterate takes the form

$${}_o K_{11} = \frac{u_{1,1}}{s_{1111}}, \quad {}_o u_{A,B} = \frac{s_{AB11}}{s_{1111}} u_{1,1}, \tag{3.5}$$

and we note that in the linear limit the relaxation of stresses results in inhomogeneous strains and zero inhomogeneous rotations[5], so that we have

$${}_o u_{A,B} = {}_o u_{B,A}. \tag{3.6}$$

We further note that although $AB \neq 11$, the form of $(3.5)_2$ reveals that for the zeroth iterate we may allow $AB = 11$. The first iterate takes the form

$$ {}^1K_{11} = \frac{1}{s_{1111}} u_{1,1} + \beta (u_{1,1})^2 , \tag{3.7} $$

$$ {}^1u_{A,B} = \frac{s_{AB11}}{s_{1111}} u_{1,1} + g_{\hat{A}\hat{B}} (u_{1,1})^2 , \tag{3.8} $$

where

$$ \beta = \frac{1}{s_{1111}^3} \left[\frac{1}{2} s_{K111} s_{K111} + s_{11LM} c_{2LKRS} s_{MK11} s_{RS11} + \frac{1}{2} s_{11LM} c_{3LMKNRS} s_{KN11} s_{RS11} \right] , \quad g_{\hat{A}\hat{B}} = s_{\hat{A}\hat{B}11} \beta - \frac{1}{s_{1111}^2} \left[\frac{1}{2} s_{K\hat{A}11} s_{K\hat{B}11} + s_{\hat{A}\hat{B}LM} c_{2LKRS} s_{MK11} s_{RS11} + \frac{1}{2} s_{\hat{A}\hat{B}LM} c_{3LMKNRS} s_{KN11} s_{RS11} \right] , \tag{3.9)-(3.10} $$

and the carets over the indices indicate[5] that both indices cannot simultaneously take the value 1. The second iterate takes the form

$$ {}^2K_{11} = c u_{1,1} + \beta (u_{1,1})^2 + \gamma (u_{1,1})^3 , \tag{3.11} $$

where

$$ c = \frac{1}{s_{1111}} , \quad \gamma = \frac{1}{s_{1111}} \left[s_{K111} g_{\hat{K}1} + s_{11LM} c_{2LKRS} \left(\frac{s_{MK11}}{s_{1111}} g_{\hat{R}\hat{S}} + \frac{s_{RS11}}{s_{1111}} g_{\hat{M}\hat{K}} \right) + s_{11LM} c_{3LMKNRS} \frac{s_{KN11}}{s_{1111}} g_{\hat{R}\hat{S}} + \frac{s_{11LM}}{2 s_{1111}^3} \left(c_{2LNRS} s_{MN11} s_{KR11} s_{KS11} + c_{3LKRSNJ} s_{MK11} s_{RS11} s_{NJ11} + c_{3LMRSNJ} s_{RS11} s_{KN11} s_{KJ11} + \frac{1}{3} c_{4LMRSNKIJ} s_{RS11} s_{NK11} s_{IJ11} \right) \right] , \tag{3.12)-(3.13} $$

and β is given in (3.9). By virtue of the meaning of the carets discussed earlier, we have the convention

$$ g_{\hat{M}\hat{K}} = 0 \text{ for } \hat{M}\hat{K} = 11 . \tag{3.14} $$

Equation (3.11), with (3.9), (3.12) and (3.13), gives the relation between K_{11} and $u_{1,1}$ we have been after.

In accordance with the discussion in Sec.2 we now write the constitutive equations for the anisotropic piezoelectric rod by introducing the known results[4,5] for the linear piezoelectric rod, which with (3.11) enables us to write

$$ K_{11} = c u_{1,1} + \beta (u_{1,1})^2 + \gamma (u_{1,1})^3 - \frac{d_{311}}{s_{1111}} E_3 , \tag{3.15} $$

$$ D_3 = \frac{d_{311}}{s_{1111}} u_{1,1} + \left(\epsilon_{33}^T - \frac{d_{311}^2}{s_{1111}} \right) E_3 . \tag{3.16} $$

The substitution of Eq. (3.15) in (2.8) yields the differential equation of motion of the anisotropic rod and the boundary conditions consist of the specification of K_{11} or u_1 at the ends of the rods $X_1 = \pm \ell$. After a solution has been obtained, the current I can be calculated from the relation

$$ I = 2w \int_{-\ell}^{\ell} \dot{D}_3 \, dX_1 , \tag{3.17} $$

where E_3 in (3.15) and (3.16) is related to the driving voltage V by $(2.5)_2$.

The quadratic rod coefficient β has been calculated from (3.9) for a number of orientations of quartz rods and the results are plotted in Figs.2-4. The ordinary rod constant c is plotted along with $-\beta$ in each figure. The quadratic rod coefficient β is always negative and ranges in value from about $-c$ to about $-5c$. Figure 2 is for the rotated X-cuts with $\theta = 0^\circ$ corresponding to the rod axis along the crystallographic Y-direction. The locations of the $+5^\circ$ - MT- and -18.5° - X-cuts are shown in the figure. Figure 3 is for the rotated Y-cuts with $\theta = 0^\circ$ corresponding to the rod axis along the crystallographic X-direction. This figure exhibits the 2-fold symmetry of quartz with X the digonal axis. Figure 4 is for doubly rotated cuts with $\theta = 0^\circ$ corresponding to the rod in the X-Y plane at $+45^\circ$ from the X-axis. In Figs.2-4 $\theta = \pm 90^\circ$ corresponds to the rod axis along the crystallographic Z-direction.

4. Intermodulation in Rods

In this section we briefly[5] consider the problem of intermodulation in piezoelectric rods. For clarity we reproduce certain of the pertinent equations obtained in Secs.2 and 3 here. The stress equation of motion and charge equation of electrostatics for the piezoelectric rod take the form

$$ K_{11,1} = \rho^0 \ddot{u}_1 , \quad D_{3,3} = 0 , \tag{4.1} $$

where[8]

$$ K_{11} = c u_{1,1} + \beta (u_{1,1})^2 + \gamma (u_{1,1})^3 - \frac{d_{31}}{s_{11}} E_3 , \tag{4.2} $$

$$ D_3 = \frac{d_{31}}{s_{11}} u_{1,1} + \left(\epsilon_{33}^T - \frac{d_{31}^2}{s_{11}} \right) E_3 , \tag{4.3} $$

and c, β and γ are given in (3.12), (3.9) and (3.13). From $(2.5)_2$ we have

$$ E_3 = - \frac{V}{2h} e^{i\omega t} , \tag{4.4} $$

where V is the magnitude of the applied voltage and ω is the steady driving frequency. For a rod free at both ends the boundary conditions are

$$ K_{11} = 0 \text{ at } X_1 = \pm \ell . \tag{4.5} $$

Since the asymptotic solution to the nonlinear problem is obtained by iteration from the solution of the appropriate linear problem, we begin the analysis with a brief[5] presentation of the solution of the associated linear problem. As a solution of the linear problem, i.e., Eqs. $(4.1)_1$ and (4.5), with (4.2) in the absence of β and γ, we write

$$ {}_{o}u_1 = \left({}_{o}u - \frac{d_{31}}{2h} V X_1 \right) e^{i\omega t}, \tag{4.6} $$

the substitution of which in $(4.1)_1$ and (4.5) yields

$$ c\, {}_{o}u_{,11} + \rho^{o}\omega^2\, {}_{o}u = \rho^{o}\omega^2 \frac{d_{31}}{2h} V X_1, \tag{4.7} $$

$$ {}_{o}u_{,1} = 0 \text{ at } X_1 = \pm \ell. \tag{4.8} $$

The eigensolutions of the homogeneous form of (4.7) and (4.8) may be written in the form

$$ u_{1n} = u_n e^{i\omega_n t}, \quad u_n = a_n \sin \eta_n X_1, \tag{4.9} $$

provided[5]

$$ \rho^{o}\omega_n^2 = c\eta_n^2, \quad \eta_n = \frac{n\pi}{2\ell}, \quad n \text{ odd}. \tag{4.10} $$

We write the solution of the forced vibration problem in the form

$$ {}_{o}u = \sum_n A_n \sin \eta_n X_1, \tag{4.11} $$

the substitution of which in (4.7) yields[5]

$$ A_n = - \frac{8\ell(-1)^{\frac{n-1}{2}} d_{31} V}{[(\omega_n^2/\omega^2) - 1] n^2 \pi^2 2h}, \tag{4.12} $$

on account of the orthogonality of $(4.9)_2$ and $(4.10)_2$. Since (4.12) has a resonance denominator, in the vicinity of a resonance, say the Nth, one term in the series in (4.11) dominates and with (4.6) we have

$$ {}_{o}u_1 = \left[{}_{1}A_n \sin \frac{N\pi X_1}{2\ell} - \frac{d_{31} V_{\omega_1}}{2h} X_1 \right] e^{i\omega_1 t}, \tag{4.13} $$

where we have introduced the notation ω_1, V_{ω_1} and ${}_{1}A_N$ to denote the quantities at driving frequency ω_1. Substituting from (4.13) and (4.4) at ω_1 into (4.3), which is then substituted into (3.17), we obtain

$$ I_{\omega_1} = 4w\ell i\omega_1 \frac{\epsilon_{33}^T}{2h} \left[1 + \frac{8(k_{31}^{\ell})^2}{\pi^2 N^2 [(\hat{\omega}_N^2/\omega_1^2) - 1]} \right] V_{\omega_1}, \tag{4.14} $$

where we have made the identification $I_{\omega_1} = -I$ at ω_1 since at ω_1 the crystal is passive[6] and

$$ (k_{31}^{\ell})^2 = d_{31}^2 / s_{11}^E \epsilon_{33}^T, \tag{4.15} $$

and we have replaced ω_N by $\hat{\omega}_N$ where

$$ \hat{\omega}_N = \omega_N + i\omega_N / 2Q_N, \tag{4.16} $$

in which Q_i is the unloaded quality factor of the resonator in that mode, and serves to prevent the resonant denominator from vanishing at $\omega = \omega_N$.

Since we are interested in intermodulation due to the simultaneous application of test tones to the resonator at two nearby frequencies ω_1 and ω_2, both of which are in the neighborhood of ω_N, we consider the steady-state linear solution to the vibration problem already presented in this section to be at the frequencies ω_1 and ω_2. Moreover, since we are interested only in the situation in which the intermodulation frequency Ω is in the vicinity of ω_N, only certain combinations of the nonlinear frequency products are significant. An examination[5] of the form of (4.2) along with a consideration of the foregoing statements and previous experience[6] reveals that only the frequencies of $(2\omega_1 - \omega_2)$ and $(2\omega_2 - \omega_1)$ are of interest in our intermodulation study. Furthermore, it is sufficient for our purposes to determine the response at $(2\omega_1 - \omega_2)$ only because the response at $(2\omega_2 - \omega_1)$ can then be obtained simply by an interchange of the subscripts 1 and 2.

Since we are interested in the response at $(2\omega_1 - \omega_2)$ only, the form of (4.2) reveals[5] that we need determine the first iterate solution ${}_{1}u_1$ due to the quadratic nonlinearity only at $2\omega_1$ and $(\omega_1 - \omega_2)$. Furthermore, in the interest of brevity we obtain ${}_{1}u_1$ at $2\omega_1$ only and simply present the changes in the result at $(\omega_1 - \omega_2)$. The first iterate equation at $2\omega_1$ is obtained by substituting[5] ${}_{o}u_1$ in (4.13) in the quadratic term in $(4.1)_1$, with (4.2), while ignoring the constant term and neglecting the term without a resonant denominator[5] to obtain

$$ c\, {}_{1}u_{1,11} - \rho^{o}\, {}_{1}\ddot{u}_1 = \beta_1 A_N^2 \eta_N^2 \frac{\sin 2\eta_N X_1}{2} e^{i2\omega_1 t}. \tag{4.17} $$

Since the boundary condition is given by (4.5), by virtue of (4.10) the solution for ${}_{1}u_1$ takes the form

$$ {}_{1}u_1 = \left[\sum_m B_m \sin \eta_m X_1 - \frac{d_{31} V_{2\omega_1}}{2h} X_1 \right] e^{i2\omega_1 t}, \tag{4.18} $$

where the B_m are obtained from the orthogonality of the $\sin \eta_m X_1$. Including only one term[5,7], say the Mth, in the series in (4.18), we have

$$ B_M = \frac{\beta_1 A_N^2 \eta_N^3 p_{NM}}{2\ell\rho^{o}(4\omega_1^2 - \hat{\omega}_M^2)} - \frac{8\ell(-1)^{\frac{M-1}{2}} d_{31} V_{2\omega_1}}{[(\hat{\omega}_M^2/4\omega_1^2) - 1] M^2 \pi^2 2h}, \tag{4.19} $$

where

$$ p_{NM} = \frac{2\ell}{\pi} \left[\frac{\sin(2N - M)\pi/2}{2N - M} - \frac{\sin(2N + M)\pi/2}{2N + M} \right]. \tag{4.20} $$

Substituting from (4.18) and (4.4) at $2\omega_1$ into (4.3), which is then substituted into (3.17), we obtain

$$I_{2\omega_1} = -4w\ell i 2\omega_1 \frac{\epsilon_{33}^T}{2h}\left[1 + \frac{8(k_{31}^\ell)^2}{\pi^2 M^2[(\hat{\omega}_M^2/4\omega_1^2) - 1]}\right] V_{2\omega_1}$$
$$+ i2\omega_1 2w \frac{d_{31}}{s_{11}} \frac{\beta_1 A_N {}_2A_N^* \eta_N^3 p_{NM}}{\ell\rho^o(4\omega_1^2 - \hat{\omega}_M^2)}, \quad (4.21)$$

where we have made the identification $I_{2\omega_1} = I$ at $2\omega_1$ since at $2\omega_1$ the crystal is active[5]. In a similar way, including only the Mth term[5,7], at $(\omega_1 - \omega_2) = \alpha$, we obtain

$${}_1u_1 = \left[C_M \sin \eta_M X_1 - \frac{d_{31} V_\alpha}{2h} X_1\right] e^{i\alpha t} \quad (4.22)$$

with

$$C_M = \frac{\beta_1 A_N {}_2A_N^* \eta_N^3 p_{NM}}{2\ell\rho^o(\alpha^2 - \hat{\omega}_M^2)} - \frac{8\ell(-1)^{\frac{M-1}{2}} d_{31} V_\alpha}{[(\hat{\omega}_M^2/\alpha^2) - 1] M^2\pi^2 2h}, \quad (4.23)$$

$$I_\alpha = -4w\ell i\alpha \frac{\epsilon_{33}^T}{2h}\left[1 + \frac{8(k_{31}^\ell)^2}{\pi^2 M^2[(\hat{\omega}_M^2/\alpha^2) - 1]}\right] V_\alpha$$
$$+ i\alpha 2w \frac{d_{31}}{s_{11}} \frac{\beta_1 A_N {}_2A_N^* \eta_N^3 p_{NM}}{\ell\rho^o(\alpha^2 - \hat{\omega}_M^2)}, \quad (4.24)$$

where * denotes complex conjugate.

The second iterate equation at $\Omega = (2\omega_1 - \omega_2)$ is obtained by substituting the appropriate expression[5] for ${}_1u_1$, i.e., a linear combination of the first iterate solution functions at ω_1, ω_2, $2\omega_1$ and α, in both the quadratic and cubic terms in $(4.1)_1$ with (4.2), neglecting terms without resonance denominators compared to terms with resonance denominators and retaining[6] all terms of order ${}_1A_N^2 {}_2A_N^*$ and proportional to $e^{i\Omega t}$ with the result

$$c\,{}_2u_{1,11} - \rho^o\,{}_2\ddot{u}_1 = \frac{\beta}{2}\Big[({}_1A_N^* B_M +$$
$$+ {}_1A_N C_M)\eta_N\eta_M(\eta_N \sin \eta_N X_1 \cos \eta_M X_1$$
$$+ \eta_M \sin \eta_M X_1 \cos \eta_N X_1) - \eta_N^2 \frac{d_{31}}{2h}({}_2A_N^* V_{2\omega_1}$$
$$+ {}_1A_N V_\alpha) \sin \eta_N X_1\Big] e^{i\Omega t}$$
$$+ \frac{9}{4}\gamma\, {}_1A_N^2\, {}_2A_N^* \eta_N^4 \cos^2 \eta_N X_1 \sin \eta_N X_1 e^{i\Omega t}. \quad (4.25)$$

Retaining the one dominant term in the series solution for ${}_2u_1$, we have[5]

$${}_2u_1 = \left[G_N \sin \eta_N X_1 - \frac{d_{31}}{2h} V_\Omega X_1\right] e^{i\Omega t}, \quad (4.26)$$

and with the aid of the orthogonality of the $\sin \eta_N X_1$, we find

$$G_N = -\frac{8\ell(-1)^{\frac{N-1}{2}} d_{31} V_\Omega}{[(\hat{\omega}_N^2/\Omega^2) - 1] N^2\pi^2 2h} + \frac{\beta}{2\ell\rho^o}({}_2A_N^* B_M$$
$$+ {}_1A_N C_M)\eta_N\eta_M\left(\eta_N q_{NM} + \frac{\eta_M p_{NM}}{2}\right) -$$
$$\frac{\beta d_{31}}{4h} \frac{\eta_N^2({}_2A_N^* V_{2\omega_1} + {}_1A_N V_\alpha)}{\rho^o(\Omega^2 - \hat{\omega}_N^2)} + \frac{9}{16}\frac{\gamma\, {}_1A_N^2\, {}_2A_N^* \eta_N^4}{\rho^o(\Omega^2 - \hat{\omega}_N^2)}, \quad (4.27)$$

where

$$q_{NM} = \frac{\sin \eta_M \ell}{\eta_M} - \frac{1}{2}\left[\frac{\sin(2\eta_N + \eta_M)\ell}{2\eta_N + \eta_M} + \frac{\sin(2\eta_N - \eta_M)\ell}{2\eta_N - \eta_M}\right].$$

Substituting from (4.26) and (4.4) at Ω into (4.3), which is then substituted into (3.17), we obtain

$$I_\Omega = -4w\ell i\Omega \frac{\epsilon_{33}^T}{2h}\left[1 + \frac{8(k_{31}^\ell)^2}{\pi^2 N^2[(\hat{\omega}_N^2/\Omega^2) - 1]}\right] V_\Omega$$
$$+ i\Omega 2w \frac{d_{31}}{s_{11}} \frac{\beta(-1)^{\frac{N-1}{2}}}{\rho^o\hat{\omega}_N^2[(\Omega^2/\hat{\omega}_N^2) - 1]}\Big[({}_2A_N^* B_M$$
$$+ {}_1A_N C_M)\eta_N\eta_M \frac{r_{NM}}{\ell} - \frac{d_{31}\eta_N^2}{2h}({}_2A_N^* V_{2\omega_1} + {}_1A_N V_\alpha)\Big]$$
$$- i\Omega 2w \frac{d_{31}}{s_{11}} \frac{18}{16} \frac{\gamma}{\rho^o\hat{\omega}_N^2} \frac{{}_1A_N^2\, {}_2A_N^* \eta_N^4 (-1)^{\frac{N-1}{2}}}{[(\Omega^2/\hat{\omega}_N^2) - 1]}, \quad (4.28)$$

where we have made the identification $I_\Omega = I$ at Ω since the crystal is active[5] at Ω and

$$r_{NM} = \eta_N q_{NM} + \frac{\eta_M p_{NM}}{2}. \quad (4.29)$$

A schematic diagram of the circuit, which is driven at the two-test tone frequencies ω_1 and ω_2, is shown in Fig.5, where V_g is the driving voltage, R_g the generator resistance and R_L the load resistance. Application of Kirchhoff's voltage equation to the circuit shown in Fig.5 at ω_1 and ω_2 yields the two equations

$${}_1V_g + I_{\omega_1}(R_g + R_L) + V_{\omega_1} = 0,$$
$${}_2V_g + I_{\omega_2}(R_g + R_L) + V_{\omega_2} = 0, \quad (4.30)$$

which with (4.14) for ω_1 and the equivalent for ω_2 enables the determination of V_{ω_1} and V_{ω_2} in terms of ${}_1V_g$ and ${}_2V_g$, respectively, from which ${}_1A_N$ and ${}_2A_N$ can be obtained[5] in terms of ${}_1V_g$ and ${}_2V_g$, respectively. The application of Kirchhoff's voltage equation to the circuit shown in Fig.2 at $2\omega_1$, α and Ω yields

$$I_\kappa(R_g + R_L) + V_\kappa = 0, \quad \kappa = 2\omega_1, \ \alpha, \ \Omega, \quad (4.31)$$

since at these frequencies $V_g = 0$. From (4.31) with $\kappa = 2\omega_1$ and $\kappa = \alpha$, respectively, and (4.21) and (4.24), $V_{2\omega_1}$ and V_α may readily be determined in terms of ${}_1V_g$ and ${}_2V_g$. Finally, from (4.31) with $\kappa = \Omega$ and $(4.28)_1$, V_Ω can readily be determined in terms of ${}_1V_g^2\, {}_2V_g^*$ if γ is known. However, since actually γ

is the only unknown quantity, a measurement of the load voltage I_0R_L enables the determination of I_0 and V_0 from (4.31), from which γ can be evaluated from (4.28) for any desired orientation, and in particular, for the practical 5° - X-cut.

Acknowledgements

The work of one of the authors (HFT) was supported in part by the Army Research Office under Grant No. DAAG29-76-G-0173, the Office of Naval Research under Contract No. N00014-76-C-0368 and the National Science Foundation under Grant No. ENG 72-04223.

References

1. H.F. Tiersten, "Analysis of Intermodulation in Thickness-Shear and Trapped Energy Resonators," J. Acoust. Soc. Am., 57, 667 (1975).
2. T.R. Meeker, "Extension, Flexure and Shear Modes in Rotated X-Cut Quartz Rectangular Bars," Proceedings of the 33rd Annual Symposium on Frequency Control, U.S. Army Electronics Research and Development Command, Fort Monmouth, New Jersey, These Proceedings (1979).
3. H.F. Tiersten, Linear Piezoelectric Plate Vibrations (Plenum, New York, 1969), Chap.13.
4. IEEE Standard on Piezoelectricity - IEEE Std. 176 - 1978, Institute of Electrical and Electronics Engineers, New York, New York (1978). Sec.4.5.
5. For more detail see H.F. Tiersten and A. Ballato, "Nonlinear Extensional Vibrations of Quartz Rods," to be issued as a technical report, Rensselaer Polytechnic Institute, Troy, New York 12181.
6. The other frequency combinations that are produced by the products of the nonlinear terms are not of interest in intermodulation studies.
7. Only one term is retained because only the largest term is considered to be of any potential importance. If more are thought to be required, they may be included without difficulty. See Ref.5.
8. In Sec.4 d_{311} is written in the compressed notation d_{31}.

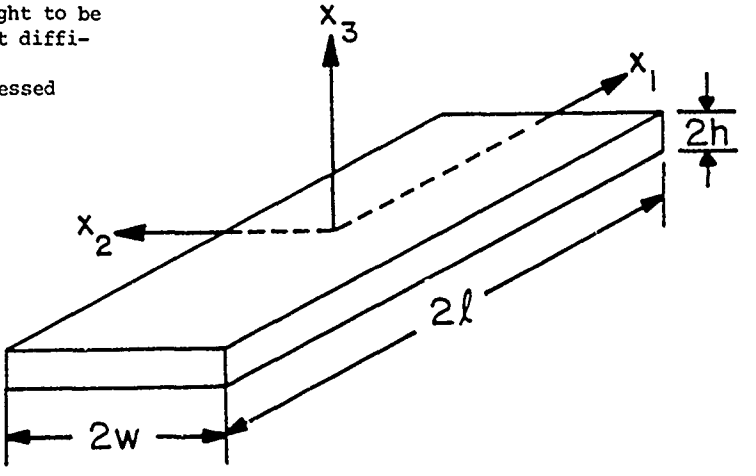

Figure 1 Schematic Diagram of the Electroded Piezoelectric Rod

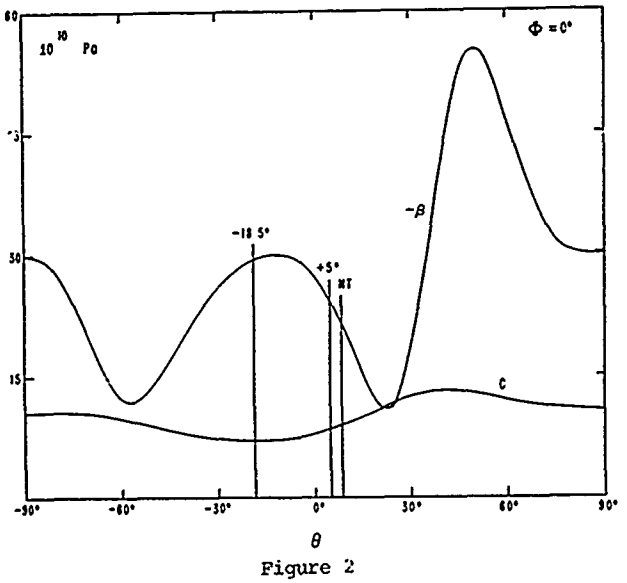

Figure 2

Linear and Quadratic Elastic Constants for Rotated X-cut Quartz Rods

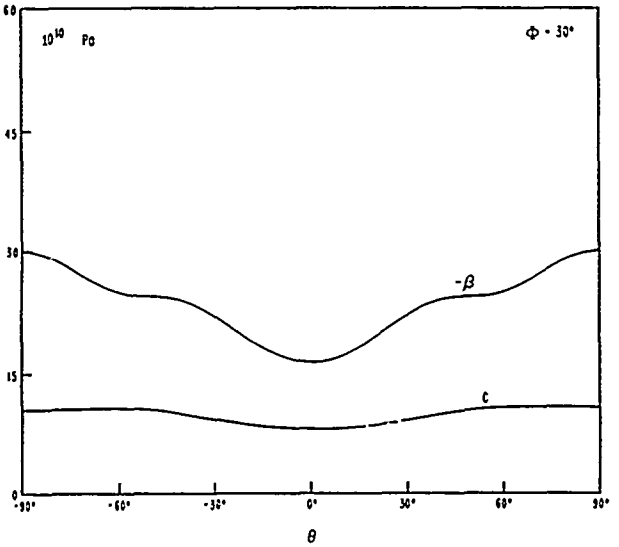

Figure 3

Linear and Quadratic Elastic Constants for Rotated Y-cut Quartz Rods

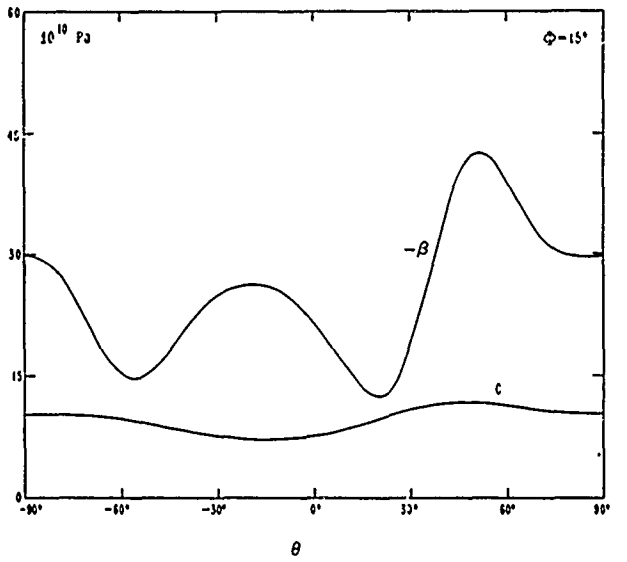

Figure 4

Linear and Quadratic Elastic Constants for a Family of Doubly Rotated Quartz Rods

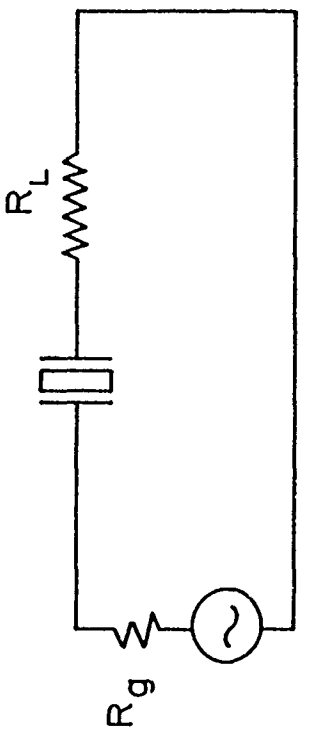

Figure 5 Schematic Diagram of the Reduced Test Circuit

TEMPERATURE DEPENDENCE OF THE FORCE FREQUENCY EFFECT FOR THE ROTATED X-CUT*

Errol P. EerNisse

Sandia Laboratories†
Albuquerque, NM 87185

Summary

The temperature dependence of the force-frequency effect coefficient K_f has been measured for the rotated X-cut quartz resonator from 24 to 300°C. Two choices of azimuthal angle exist for zero temperature dependence of K_f. The magnitude of K_f at these angles is large, thus the rotated X-cut is a viable force transducer. A linear superposition theory using the force-frequency effect as a source term has been derived for calculating resonator frequency shifts, and their temperature dependences, arising from arbitrary force distributions around the resonator perimeter. The theory is confirmed with measurements on a rotated X-cut pressure transducer operating from 24 to 300°C.

Introduction

The force-frequency effect is the shift in resonant frequency of circular, thickness shear-mode resonators caused by diametrically opposed point forces applied on the perimeter in the plane of the resonator blank. The effect arises from nonlinear elastic effects which couple the initial stress of the applied forces to the resonant vibrations. It has been studied extensively around room temperature for frequency control applications where the effect causes undesirable frequency drift and instability.[1-6] The effect can also be used for transducing force to frequency either with point forces or with a uniform perimeter force and is attractive as an inherently digital transducer.[7-9] The transducer effect is dependent on temperature and this can cause not only changes in scale factor but also a shift in the frequency-temperature characteristic which complicates either operation at turnover or compensation with matching crystals.[8,10-12] Several choices for resonator crystallographic orientation have been found for zero temperature dependence of the force-frequency effect[8,11,12] but only one viable choice exists for the uniform perimeter force case.[9,10]

Recent need for a high temperature pressure transducer for geothermal well logging at temperatures as high as 300°C has stimulated work on the rotated X-cut which has frequency-temperature turnovers up to 300°C with small curvatures at turnover.[13] It is the purpose of the present work to present measurements of the force-frequency effect for circular rotated X-cut resonators as a function of temperature from 24°C up to 300°C. The results can be used for designing high temperature transducers based on the force-frequency effect in rotated X-cut resonators.

In addition, the present work includes a formulation of how the force-frequency effect results can be used to construct, by linear superposition, the frequency response, and its temperature dependence, of a resonator to an arbitrary force distribution around the resonator perimeter. This approach is used with the experimental force-frequency results to calculate the temperature dependence of scale factor for a rotated X-cut pressure transducer based on a uniform perimeter force. The model calculations are confirmed by measurements made with an actual rotated X-cut pressure transducer operating between 24°C and 300°C.

Experimental Techniques

Conventionally, the force frequency coefficient, K_f (in m.s/N), is defined as

$$\frac{\Delta f}{f} = K_f \frac{FN_o}{d\tau} \qquad (1)$$

where $\Delta f/f$ is fractional frequency shift, F is the force (in N), N_o is the frequency constant (in m/sec), d is resonator blank diameter (in m) and τ is resonator thickness (in m). The force-frequency effect for a given resonator cut is dependent upon where on the perimeter the forces are applied. For the general class of thickness shear mode orientations $(yxw\ell)\phi,\theta$ in IRE notation,[14] this is usually expressed in terms of the azimuthal angle ψ measured between the x" resonator axis and the point of force application.[6] Positive angle ψ is meas-

*This work was supported by the United States Department of Energy (DOE) under contract number DE-AC04-76-DP00789.

†A United States Department of Energy Facility.

ured counterclockwise about the y" resonator axis.

Measurement of K_f as a function of ψ requires a means of applying a repeatable force at known values of ψ. In the past this has been done by a fixture which allows weights to contact a resonator blank on its perimeter.[1,3,5,12] The blank is rotated to change ψ in these fixtures. For extensive measurements as a function of both ψ and temperature, such approaches are too time consuming. An alternate method for measuring K_f vs ψ without having to rotate the crystal has been devised.[13]

The resonator plate is held by 20 lightly spring-loaded pivoting fingers spaced equally around the perimeter as seen in Fig. 1. Any diametrically opposed pair of fingers can be pushed on periodically with 145 gm of force at 2 Hz with push rods driven by a motor cam-shaft and spring arrangement. The overall arrangement is seen in Fig. 2 with the motor and push rods visible. As seen in Fig. 2, the shape of the overall apparatus is designed to fit into a tube furnace so that the temperature at the resonator end can be controlled.

Measurement of the frequency shift caused by the 2 Hz periodic squeezing is made as shown in Fig. 3. The crystal is incorporated into an oscillator circuit located outside the furnace. The oscillator signal is mixed with a local oscillator signal (obtained from a frequency synthesizer) and the difference frequency is frequency discriminated. The output of the discriminator is measured with a phase locked amplifier locked to the 2 Hz motor-cam by a photoelectric cell signal. The measurements are stable since frequency fluctuations due to any other causes are rejected by the phase locked amplifier. Both magnitude and phase are measured to obtain the magnitude and sign of K_f. Measurements of all 10 pairs of figures takes less than 5 minutes and is accomplished by setting the motor cam arrangement to the desired push rod pair. Repeatability is better than 5%. Calibration was done by using a calibrated spring and a calibrated discriminator output. Also, the results from our apparatus when used with an AT-cut crystal compare within 3% at $\psi = 0$ to the average of data taken in earlier works.[1,3,12] Total error is taken as 5% or less.

Results

Values for K_f vs ψ are shown in Fig. 4 for 24°C and 275°C. Smoothing lines are added to the data for visual purposes. Sizeable changes with temperature are noted.

In Fig. 5, K_f is plotted vs temperature T for selected values of ψ to illustrate the scatter in data and the near linear response of K_f to temperature.

Since the data in Fig. 5 suggest a linear response, values for dK_f/dT obtained from least squared error fits of a straight line to the data for our 10 values of ψ are plotted in Fig. 6 vs ψ. A smooth line has been added for visual purposes. Also included in Fig. 6 is a repeat of the 24°C K_f data for comparison.

It is clear from Fig. 6 that two choices for ψ exist where dK_f/dT are zero, $\psi = 38°$ and $\psi = 133°$. It is of importance to note also in Fig. 6 that these two values of ψ correspond to K_f values very near the maximum available amplitudes of K_f. The AT-cut exhibits the largest maximum K_f seen for the $(yxw\ell)\phi,\theta$ family, but at ψ values where the AT-cut has dK_f/dT equal to zero (ψ values of 40° and 140°), K_f is much smaller than the maximum. Thus the rotated X-cut has a larger magnitude K_f available for $dK_f/dT = 0$ than does the AT-cut (22×10^{-15} vs 18.5×10^{-15} m.s/N). Also, the slope of dK_f/dT vs ψ at the zeros of dK_f/dT is less for the rotated X-cut so the tolerances on ψ location are less stringent.

In addition to the above force frequency coefficient measurements, which are related to point forces acting on the perimeter, measurements have been made on the rotated X-cut of the planar coefficient[15] effect which relates frequency shift to a uniform perimeter force, i.e., a uniform planar stress. The measurements were made using a pressure transducer configuration shown in Fig. 7. The general design is the same as published by others;[9,10] that is, a disc resonator compressed radially inwards by hydrostatic pressure acting on the cylindrical walls, as seen in Fig. 7. Details of the pressure transducer design, which is under development for geothermal well logging, are reported elsewhere.[16] Pressure measurements have been made at temperatures ranging from 24°C to 300°C. The frequency scale factors for the particular geometry used in the experiments are -0.542 ppm/psi at 24°C and -0.690 ppm/psi at 275°C. Repeatability at 1000 psia full scale has been 0.1 psi or better. These uniform planar stress effects on frequency can be related quantitatively to the force-frequency results as shown in the following section.

Application of Results for a Generalized Transducer

Based on the data of Fig. 6, application of the rotated X-cut in a transducer where the force-frequency effect with a point force is used is practical. It is possible also to assign more general importance to the data in Fig. 6 by using the data to construct a general representation for an arbitrary force distribution around the plate perimeter. The representation is general, of course, in that any crystal cut can be used if K_f vs ψ and dK_f/dT vs ψ are known. The use of linear superposition was treated earlier for the case of a

uniform force distribution.[15] The concept can be generalized for a K_{eff} coefficient for a given distribution of force/length on the perimeter. Let the force/length be described by $FL(\psi)$, where $L(\psi)$ is a distribution function normalized to unity. An incremental contribution to $\frac{\Delta f}{f}$, $\delta \frac{\Delta f}{f}$, is caused by $FL(\psi)$ acting over an incremental portion of the perimeter $(d/2)d\psi$:

$$\delta \frac{\Delta f}{f} = \frac{N_o F}{2\tau} K_f(\psi) L(\psi) d\psi \qquad (2)$$

Summing by integration,

$$\frac{\Delta f}{f} = \frac{N_o F}{2\tau} \int_o^\pi K_f(\psi)\ L(\psi) d\psi \ . \qquad (3)$$

If K_{eff} is defined similarly to the planar coefficient[15]

$$\frac{\Delta f}{f} = K_{eff} \frac{F}{\tau} \ , \qquad (4)$$

then

$$K_{eff} = \frac{N_o}{2} \int_o^\pi K_f(\psi)\ L(\psi) d\psi \ . \qquad (5)$$

In a similar manner, one can construct an expression for dK_{eff}/dT,

$$\frac{dK_{eff}}{dT} = \frac{N_o}{2} \int_o^\pi \frac{dK_f(\psi)}{dT} L(\psi) d\psi \ . \qquad (6)$$

Although $K_f(\psi)$ and $dK_f(\psi)/dT$ are not known analytically, numerical techniques or an analytical expression fitted to Fig. 6 could be used to solve Eqs. 5 and 6 for K_{eff} and dK_{eff}/dT.

As an example of the application of Eqs. 5 and 6, assume $L = 1$. This is the uniform perimeter force case of our pressure transducer in Fig. 7. Numerical integration of the curves in Fig. 6 give $K_{eff} = 1.08 \times 10^{-11}$ m^2/N and $dK_{eff}/dT = 1.05 \times 10^{-14}$ m^2/N °C. It is impractical to directly compare these numbers to the pressure transducer results because the pressure gauge structure has a mechanical advantage (stress in resonator larger than outside pressure) which is not known accurately. However, the fractional change in K_{eff} can be compared. The value for $(1/K_{eff})\cdot(dK_{eff}/dT)$ as calculated by numerically integrating the Fig. 6 data is 0.97×10^{-3}. The same ratio for the pressure transducer calculated with the measured values in the previous section is $(-0.690 + 0.542)/(-0.542 \times 251) = 1.09 \times 10^{-3}$. The agreement is excellent considering the numerical integration and confirms the linear superposition approach taken to derive Eqs. 5 and 6.

Conclusions

The temperature dependence of the force-frequency effect coefficient K_f has been measured for the rotated X-cut from 24°C to 300°C. Two azimuthal angles exist for which the derivative with temperature dK_f/dT has zero values, $\psi = 38°$ and $\psi = 133°$. The magnitudes for K_f at these ψ values are nearly the maximum attainable with the rotated X-cut and are larger than the zero temperature effect values for K_f attainable with the AT-cut.

A linear superposition model has been derived that uses the measured K_f vs ψ and dK_f/dT vs ψ behavior as source terms to construct an effective frequency shift coefficient K_{eff} and its temperature dependence dK_{eff}/dT for an arbitrary distribution of forces around the resonator perimeter. The model is confirmed with measurements from a quartz resonator pressure gauge operated between 24°C and 300°C which utilizes a uniform perimeter force configuration.

The rotated X-cut has been shown to be a viable force transducer for applications where a point force is applied to the resonator perimeter (force-frequency effect). The temperature dependence results show that transducers based on a uniform perimeter force distribution, such as the pressure gauge tested, have a strong temperature dependence of scale factor ($dK_{eff}/dT \neq 0$). This effect can be a problem if matched crystals are used for temperature compensation or if a single crystal is used in an oven at turnover because the turnover will shift with pressure. Solution of this problem rests in the linear superposition model and choice of a perimeter force distribution that minimizes the temperature dependence of the effective coefficient K_{eff}. Such studies are under way using slotted resonator plates.

References

[1] A. D. Ballato, "Effects of Initial Stress on Quartz Plates Vibrating in Thickness Modes," in Proc. 14th Annu. Frequency Control Symposium, May-June 1960, p. 89.

[2] R. W. Keyes and F. W. Blair, "Stress Dependence of the Frequency of Quartz Plates," Proc. IEEE, Vol. 55, No. 4, Apr. 1967, p. 565.

[3] J. M. Ratajski, "Force-Frequency Coefficient of Singly-Rotated Vibrating Quartz Crystals," IBM J. Res. Dev., Vol. 12, No. 1, Jan. 1968, p. 92.

[4]P. C. Y. Lee, Y. S. Wang, and X. Markenscoff, "Elastic Waves and Vibrations in Deformed Crystal Plates," in Proc. 27th Annu. Frequency Control Symposium, June 1973, p. 1.

[5]A. Ballato, E. P. EerNisse, and T. Lukaszek, "Force-Frequency Effect in Doubly Rotated Quartz Resonators," in Proc. 31st Annu. Frequency Control Symposium, June 1977, p. 8.

[6]E. P. EerNisse, T. J. Lukaszek, and A. Ballato, "Variational Calculation of Force-Frequency Constants of Doubly Rotated Quartz Resonators," IEEE Trans. on Sonics and Ultrasonics, Vol. SU-25, No. 3, May 1978, p. 132.

[7]R. A. Watson, "Digital Accelerometer Built Around Crystals," Space and Aeronautics, June 1967, p. 111.

[8]M. Onoe, et. al., "Quartz Crystal Accelerometer Insensitive to Temperature Variations," in Proc. 31st Annu. Frequency Control Symposium, June 1-3, 1977, p. 62.

[9]D. L. Hammond and A. Benjaminson, "The Crystal Resonator-A Digital Transducer," IEEE Spectrum, Vol. 6, April 1969, p. 53.

[10]H. E. Karrer and J. Leach, "A Quartz Resonator Pressure Transducer," IEEE Trans. on Indus. Electronics and Control Instrumentation, Vol. IECI-16, July, 1969, p. 44.

[11]H. E. Karrer and R. Ward, "A Low Range Quartz Resonator Pressure Transducer," ISA Trans., Feb., 1977, p. 90.

[12]C. R. Dauwalter, "The Temperature Dependence of the Force Sensitivity of AT-cut Quartz Crystals," in Proc. 26th Annu. Frequency Control Symposium, 1972, p. 108.

[13]E. P. EerNisse, "Rotated X-cut Quartz Resonators for High Temperature Applications," in Proc. 32nd Annu. Frequency Control Symposium, May 31-June 2, 1978, p. 255.

[14]"Standards on Piezoelectric Crystals, 1949," Proc. IRE, Vol. 37, No. 12, pp. 1378-1395, Dec. 1949. (IEEE Standard No. 176).

[15]A. Ballato, E. P. EerNisse, and T. J. Lukaszek, "Experimental Verification of Stress Compensation in the SC-cut," in Proc. of the 1978 Ultrasonics Symposium, IEEE Cat. #78CH 1344-ISU.

[16]E. P. EerNisse, "Quartz Resonator Pressure Gauge: Design and Fabrication Technology," Sandia Laboratories Report SAND78-2264, January, 1979.

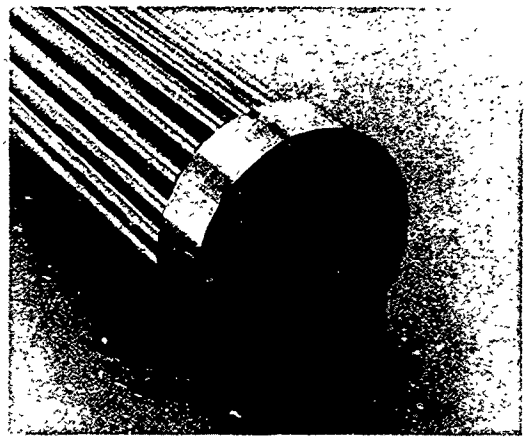

Fig. 1. Photograph of a circular resonator supported on its perimeter by 20 pivoting fingers for force-frequency coefficient measurements. Push rods for applying a periodic force to the pivoting fingers are seen coming in from the upper left.

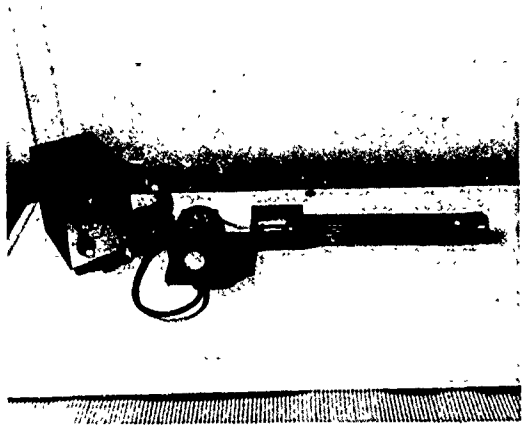

Fig. 2. Overall view of the test apparatus showing the motor and spring arrangement for applying a periodic force to the push rods. Figure 1 is a view of the apparatus from the right hand side.

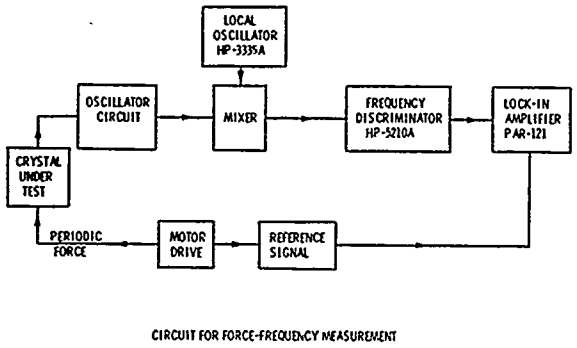

CIRCUIT FOR FORCE-FREQUENCY MEASUREMENT

Fig. 3. Block diagram of circuit used with the apparatus in Fig. 2 to measure the force-frequency coefficient values.

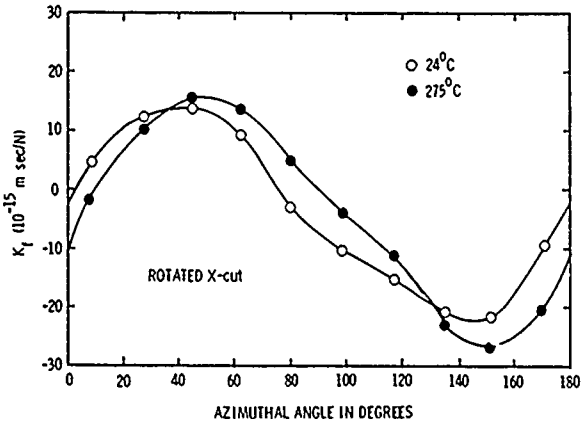

Fig. 4. Force-frequency coefficient for the rotated X-cut at 24°C and 275°C vs azimuthal angle ψ. Lines are added as visual aids.

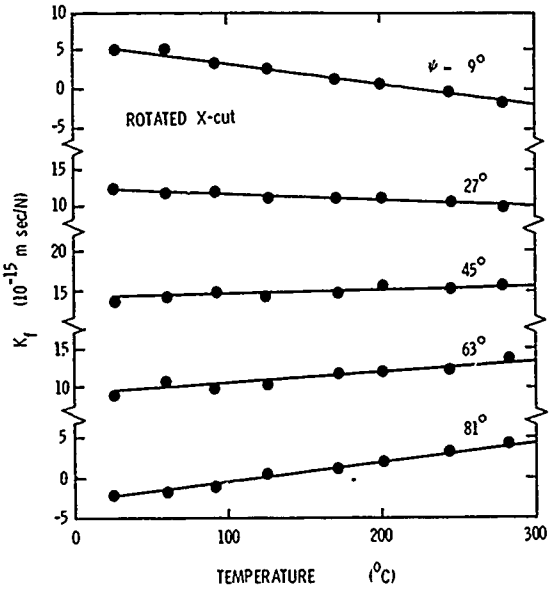

Fig. 5. Force-frequency effect for the rotated X-cut vs temperature from 24°C to 300°C for selected values of azimuthal angle ψ. Lines are least squared error fits of a straight line.

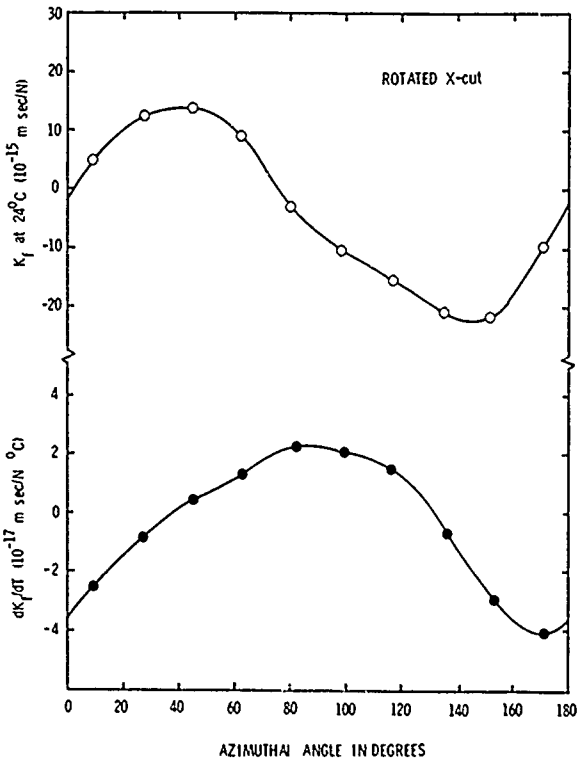

Fig. 6. Force-frequency effect for the rotated X-cut at 24°C and its temperature derivative vs azimuthal angle ψ.

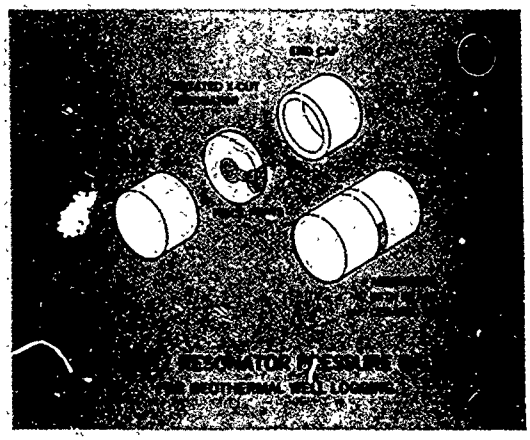

Fig. 7. Exploded view of the rotated X-cut quartz resonator pressure gauge used in the present work to apply uniform perimeter forces to the circular resonator plate.

LOW "g" SENSITIVITY CRYSTAL UNITS AND THEIR TESTING

A. Warner, B. Goldfrank, M. Meirs and M. Rosenfeld

Frequency Electronics, Inc.
New Hyde Park, New York

Summary

The increased use of the doubly oriented AT type crystal units, SC, TTC, FC, etc, has opened the way to the manufacture of crystal units much less affected by a variety of thermally and physically induced stresses. Such units will have faster warm-up, lower aging, less sensitivity to amplitude of vibration, and a lower "g" sensitivity. The manufacturing challenges have been met by improved cutting and x-ray methods as well as careful and exact fabrication techniques. Tests for "g" sensitivity that formerly required temperature controlled ovens mounted on a centrifuge can now be carried out more simply by use of a vibration table and side-band detection, without temperature control. The yield of crystal units having "g" sensitivities less than $2PP10^{10}$ per g in all directions is apparently 75%.

Introduction

It may be of some significance that this is the 20th anniversary of the first talk on the subject of frequency change with acceleration by one of the authors (A. Warner), given at the 13th Annual Symposium on Frequency Control. Figure 1 shows data on one carefully made AT cut unit of that period, and the tests were performed using a centrifuge and temperature controlled oven. These crystal units made in 1959 were not reproducible, and it was stated at that time, "Apparently in practice the sine wave characteristic can change in amplitude, phase, and position." The same thing is still true, except that with the introduction of the SC cut units and better processing techniques we find that the good crystal units are more easily and more consistently produced.

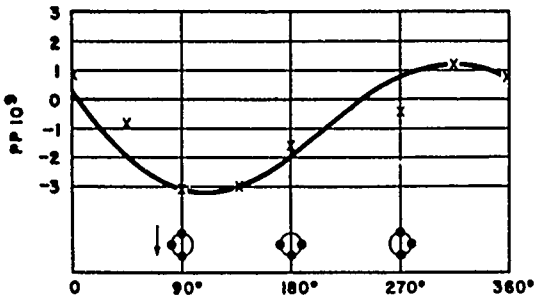

FIGURE 1
Frequency Change Due to 15g acceleration at Various Orientations in the Plane of the Crystal Plate

SC Crystal Units

Other authors in these preceedings have done more than we have in developing the SC cut, and in theoretical studies of acceleration effects in general. However, a few words about the SC cut may be in order. When we started on this SC project two years ago, it was thought that because of the complexity of design and likelihood of increased coupling to unwanted modes, the SC cut would be used only for highly specialized applications. These fears have not materialized. The SC cut is well behaved, and we consider it one of the more significant happenings in our business. The SC is about 10 times less sensitive to amplitude of vibration. Due to its insensitivity to stress the normal thermal transient effects and force-frequency effects are much reduced. Consequently that aging which is due to stress relaxation is also improved. Such units are characterized by faster warm-up, more rapid stabilization, and improved performance under acceleration. Whatever aging remains is more understandable, because it is likely to be a simple first order rate process due to mass transfer.

The question remains, is it practical to manufacture? We think so. It is more difficult to orient by x-ray, but it can be done using only the principal X and Z planes and the normal AT (01 1) reference plane as with the AT cut. Furthermore with improved cutting methods there is less x-ray work needed. Also there is a strong unwanted B mode, 8% higher in frequency than the normal C mode. However it is amenable to circuit design and in addition the B mode is very useful as an exact temperature indicator. What may be less known is that the B mode can be used as a check on the angular orientation of the quartz blank, since the B-C Δf is a function of the angle ϕ.

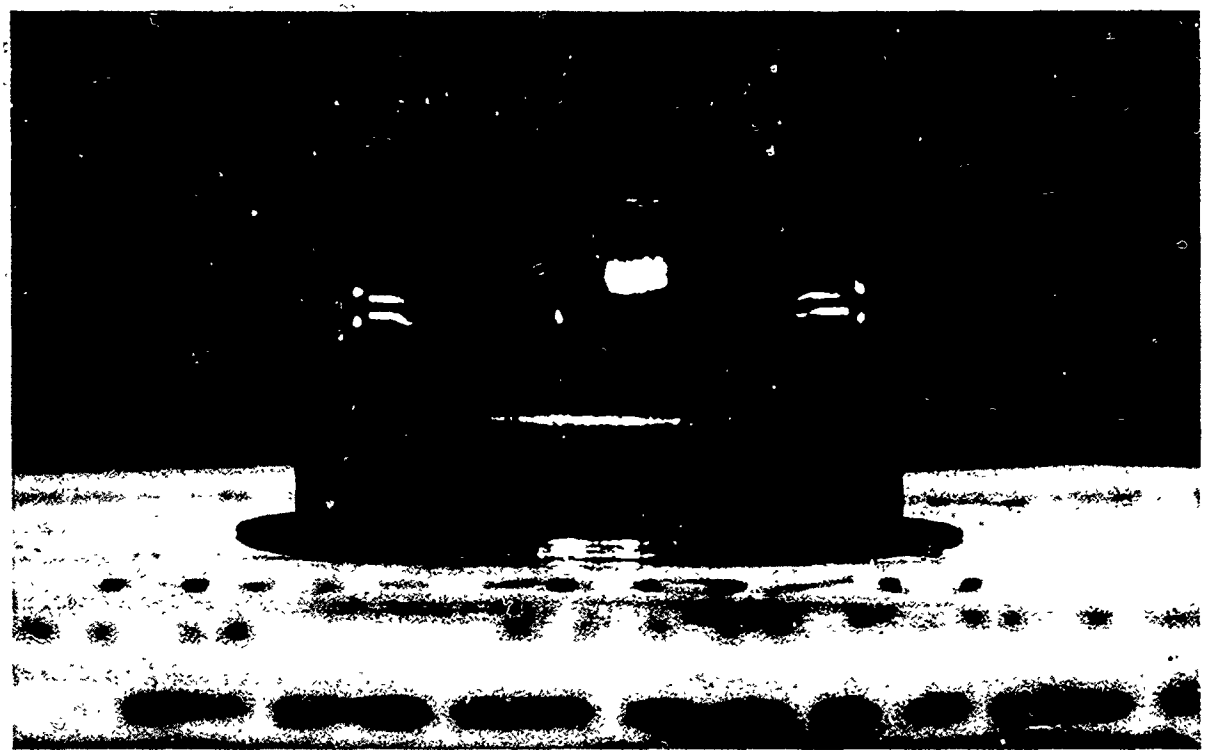

FIGURE 2
5 MHz, 5th Overtone, SC Crystal

We have made a number of 5 MHz 5th overtone SC units, shown in Figure 2 with cover removed. They are bonded at three specially selected points with "g" sensitivity approaching $1PP10^{10}$ per g in all directions. We did move the temperature inflection point from the usual 95°Cto 110°C, in order to give a little more leeway in the matter of angular tolerance for a 70°C zero temperature coefficient. This now compares with the AT cut at 70°C. Since all the advantages of the SC cut do not occur at the same ϕ angle, there is room for such a compromise.

The SC cut is 3 or 4 times higher in impedance than the AT, and consequently a smaller frequency tolerance is needed. This is accomplished by making the frequency adjustment at or near the zero temperature coefficient temperature. Figure 3 shows the C mode frequency vs temperature characteristic at a 70°C turnover, and both the B and C mode resistance. The Q at 260 ohms is 2.8 million. Note that the curve is the inverse of an AT.

Fabrication Procedures

Low "g" sensitivity 'SC' cut quartz crystals are processed in the cleanest possible environment. Frequency Electronics, Inc. has installed a precision processing laboratory, free of organic contaminants.

The crystal blanks are cut from premium Q swept quartz bars using a double sine bar. The crystal blanks are then x-rayed to verify the angle of cut. New Equipment has recently been installed to make angle corrections on raw quartz should the need arise.

The crystal blanks are lapped, contoured, polished and etched. The blanks are cleaned to insure that no contamination remains on the surface of the quartz. Immediately upon completion of cleaning, the crystals are loaded in a stainless mask, the mask is put in to a cryogenic evaporation system and chrome and gold are deposited on the edges of the crystals. The crystals are removed, a sample

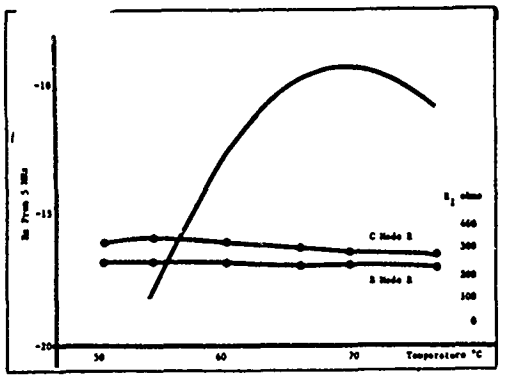

FIGURE 3
Frequency Vs Temperature Curve
SC Cut Crystal - 5 MHz, 5th Overtone

pull test performed and the crystals re-cleaned. The crystals are immediately loaded into a second stainless steel mask and put into a cryogenic vacuum system for gold deposition by evaporation. Each crystal is then thermocompression bonded to a base using an aluminum clad nickel ribbon. The upper turnover temperature is determined for each crystal and the crystal is tuned to frequency. Each crystal and its cover are individually hydrogen fired to remove any oxides, contamination and absorbed gases and loaded into a sealing die. The sealing die and crystal are evacuated using a combination of cryogenic and ion pumping. All crystals are sealed when the vacuum reaches 5×10^{-8} torr or better. Figures 4, 5 and 6 show the vacuum plating apparatus, the x-ray table good to 2 seconds of arc, and some vacuum baking and sealing equipment.

Testing Low "g" Sensitivity Crystal Units

After the crystal unit has been sealed, and before it is assembled in its oscillator-oven, it is very desirable to test for "g" sensitivity. If the crystal unit is out of limits, we want to know this before spending time assembling the crystal in its oven, adjusting the temperature control point, and going through warmup and initial aging.

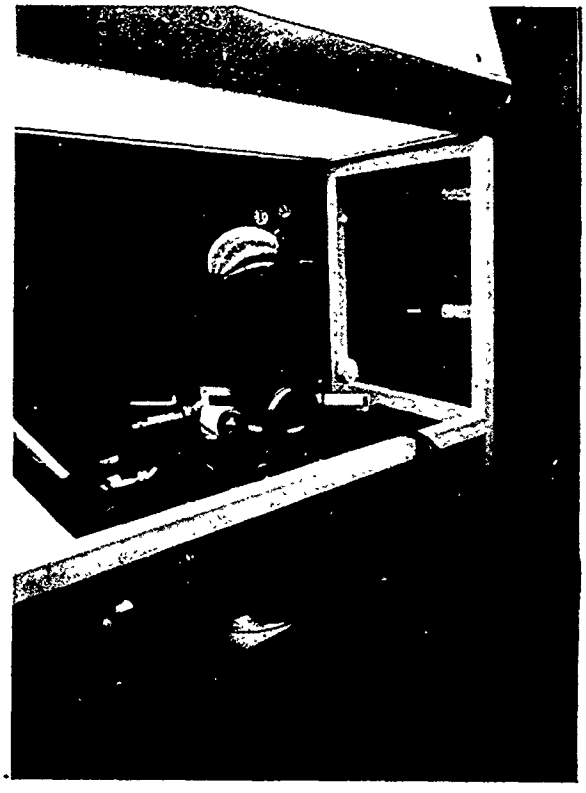

FIGURE 4
Vacuum Plating Facility

FIGURE 5
X-Ray Facility

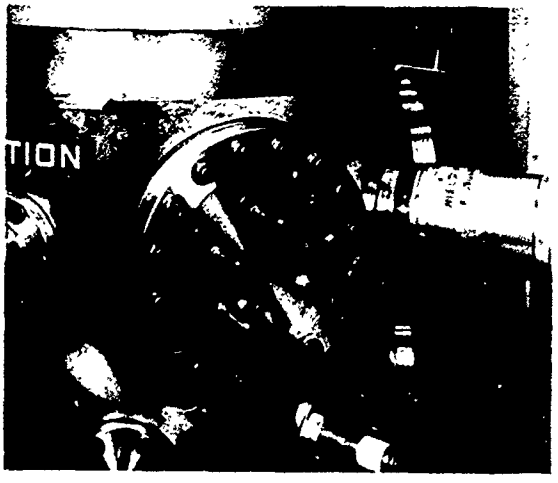

FIGURE 6
Evacuation and Sealing Assembly

A method has been devised to use a vibration method of testing, reasoning that an instantaneous frequency shift due to peak acceleration during vibration can be detected as an FM sideband. The method is as follows: referring to Figure 7, the output of the unit under test is mixed with a synthesizer to produce a carrier frequency of about 2 kHz. The carrier signal is connected to a spectrum analyzer and with the table energized the spectrum is plotted on

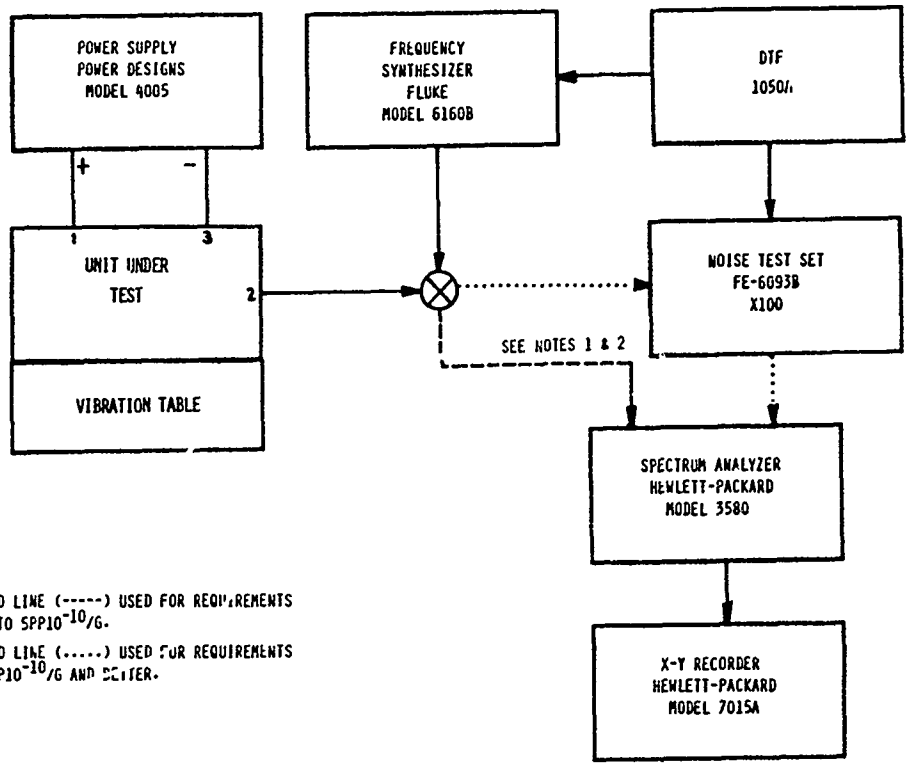

1) DASHED LINE (-----) USED FOR REQUIREMENTS DOWN TO $5PP10^{-10}/G$.

2) DOTTED LINE (.....) USED FOR REQUIREMENTS OF $5PP10^{-10}/G$ AND BETTER.

FIGURE 7
Test Set Up, Vibration Stability Factor

an X-Y recorder. The crystal is mounted to a printed circuit board containing oscillator circuitry and placed in a test fixture. The fixture is designed such that all the input energy from the vibration table should be transmitted directly to the crystal. The fixture is capable of being mounted in three different axes.

A side band will appear on the X-Y plot at a frequency displaced by the vibration frequency from the carrier. The magnitude of the side band is mathematically related to the "g" sensitivity of the crystal by the formulae as shown. The sideband to carrier amplitude ratio equals the proportional frequency shift of the crystal times the carrier frequency over two times the vibration frequency. Three vibration frequencies were used; 50, 200 and 500 Hz. Their amplitudes are adjusted to give the same side-band amplitude vs g sensitivity, so the calibration will be the same. This is 28 g's at 500 Hz, 11.2 g's at 200 Hz and 2.8 g's at 50 Hz. A sideband 90 db down from the carrier corresponds to 2PP in $10^{10}/g$. Six dB lower, or -96 dB, corresponds to half that or 1 PP in $10^{10}/g$. Provisions were made to obtain a 40 dB enhancement by multiplying by 100 when required.

I. Formula for frequency modulated carrier

$$y(t) = A\left(\cos \omega_0 t + \frac{\Delta\theta}{2}(\omega_0 + \omega_m)t + \ldots\right)$$

A = signal amplitude — $\Delta\theta$ = phase modulation

$\frac{\Delta\theta}{2} A$ = sideband amplitude — $\Delta\theta = \frac{\Delta f}{f_m}$

ω_0 = carrier frequency — Δf = peak frequency

ω_m = modulation frequency — f_m = modulation frequency

II. Sideband to carrier ratio $X = \frac{(\Delta\theta/2)(A)}{A} = \frac{\Delta\theta}{2} = \frac{\Delta f}{2f_m}$

$\Delta f = Sf_0 g$

S = vibration sensitivity = $\frac{\Delta f_0}{f_0}$ per g

f_0 = carrier frequency

g = applied vibration level

$$X = \frac{Sf_0 g}{2f_m}$$

$$S = \frac{2f_m X}{f_0 g}$$

DATA COMPARISON SIDEBAND VIBRATION TESTING, AT VS FC VS SC CUT CRYSTALS

Type Cut	⊥ To Blank			Through Active Leads			∥ To Active Leads		
	50 Hz Sideband (dB)	200 Hz Sideband (dB)	500 Hz Sideband (dB)	50 Hz Sideband (dB)	200 Hz Sideband (dB)	500 Hz Sideband (dB)	50 Hz Sideband (dB)	200 Hz Sideband (dB)	500 Hz Sideband (dB)
AT, 3rd O.T.	-81	-70	-82	-70	-66	-75	-85	-72	-90
AT, 3rd O.T.	-98	-88	-90	-77	-79	-83	-84	-89	-90
FC, 3rd O.T.	-84	-84	-88	<-90	-85	<-90	-80	-90	-89
FC, 3rd O.T.	-75	-84	-86	-90	-86	-89	-76	-76	-84
SC, 5th O.T.	-115	-96	-94	-120	-100	-96	-120	-110	-110
SC, 5th O.T.	-99	-99	-89	-105	-100	-98	-93	-92	-92

FIGURE 9
Data Comparison Sideband Vibration Testing, AT Vs FC Vs Sc Cut Crystals

Figure 9 shows the results of testing various crystal units. For each crystal there are three vibration frequencies as well as three mutually perpendicular directions giving 9 opportunities to spot trouble. We must either accept the worst reading or be prepared to explain why not. The results are somewhat non-linear with vibration frequency, and this may be due to the wax used to imbed the crystal and cricuit on the vibration table. In some cases it would appear that not all the vibration energy gets to the crystal can at 500 Hz. Also any departure from a sine wave in the vibration table would alter the equations. The two SC units, one average and one quite good are about 10 to 15 dB lower or 3 to 6 times better for frequency change with acceleration than the other two designs. The next three figures, 10, 11 and 12, show the X-Y plots for one AT, one FC and one SC - all at 200 Hz and perpendicular to the active leads of the crystal mount. The AT is at -72 dB, 200 Hz from the carrier. The FC is at -88 dB, corresponding to 3 PP in 10^{10} per g at this orientation. Note that in these two plots that the background level is at -93 dB. In the plot for the SC unit the background is shifted to -130 dB by addition of the X100 noise test set. Now we see a peak of -112 dB corresponding to a few parts in 10^{11} per g in this direction, with a capability of the apparatus to detect 3 PP in 10^{12} per g.

Figure 13 shows a comparison of the vibration method of g sensitivity testing and the turn-over test for a lot of eight SC cut crystal units. Turning an entire oscillator-oven unit 180° in the vertical plane, of course, effects a 2 g change in acceleration and is pretty fool-proof. The frequency change divided by 2 gives the parts per g at the 2 g level and this is compared with the previous dB

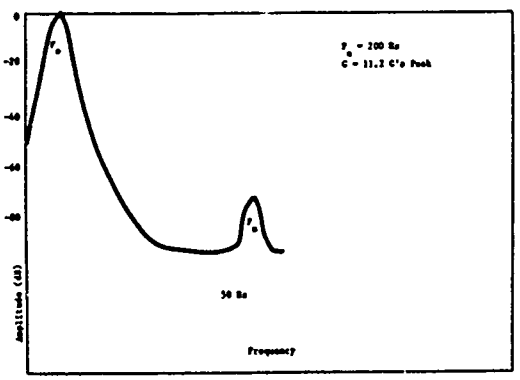

FIGURE 10
AT Cut Crystal Sideband Measurements

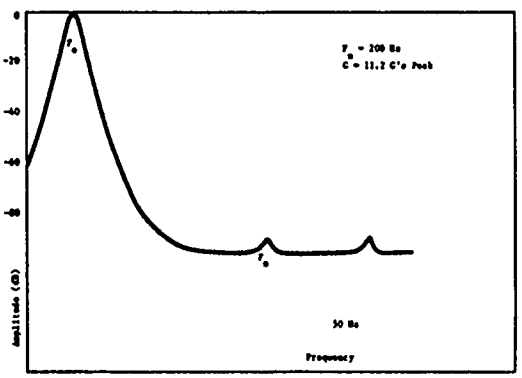

FIGURE 11
FC Cut Crystal Sideband Measurements

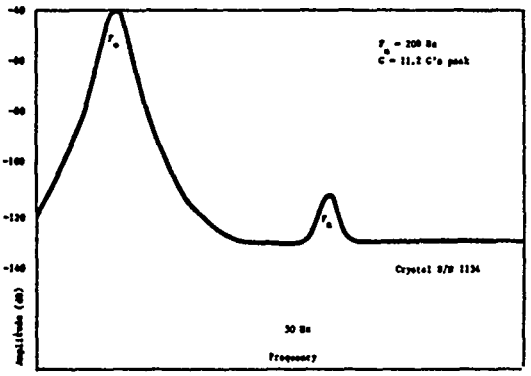

FIGURE 12
SC Cut Crystal Sideband Measurement

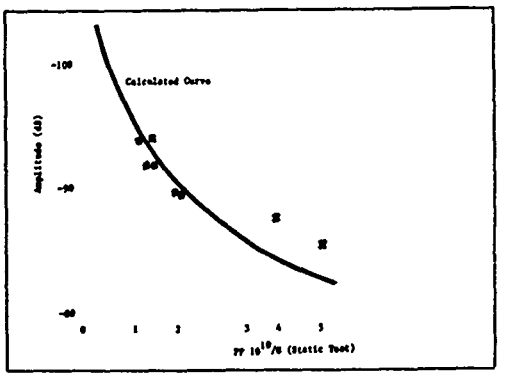

FIGURE 13
G Sensitivity - Static Vs Dynamic Testing
For 8 SC Cut 5 MHz Units

readings for the same crystals in a vibration test. The heavy curve is that calculted by the mathematics shown above on Figure 8. The data points are worst case, so this represents about the worst that would occur for acceleration in any direction. Six of the eight units are 2 PP 10^{10} per g or better.

Hopefully, with more study and greater precision of mounting, we can further improve sensitivity and yield of this and similar designs.

Acknowledgments

We would like to acknowledge the encouragement and support of Dr. Jim Adair and Charlie Friend of Wright Patterson, of conversations with Dr. Harry Tiersten of Rensselaer, Dr. Peter Lee of Princeton, Dr. Art Balato and others at ERADCOM, and help from the entire crystal group at Frequency Electronics.

RESONATORS FOR SEVERE ENVIRONMENTS

T.J. Lukaszek and A. Ballato

US Army Electronics Technology & Devices Laboratory
USAERADCOM, Fort Monmouth, NJ 07703

Abstract

Singly rotated AT cut plates are most often used for frequency control in applications where moderate and high precision is required, but recent developments point to a greatly expanded role for doubly rotated cuts. Virtually all of these thickness mode cuts are of the form of thin circular discs mounted on their edges. Any forces communicated between the mounting supports and the quartz plate produce high stresses and stress-gradients resulting in significant frequency perturbations. This paper describes crystal plate designs having a prescribed lateral contour for singly and doubly rotated plates. These designs provide a relatively large portion of the periphery for mounting, such that mounting stresses are greatly reduced with no detriment to the force immunity of the older-type mounts.

Key Words
Resonators, Frequency Control, Acoustic Waves, Quartz Crystals, Doubly Rotated Cuts, Bulk Acoustic Waves, Force-frequency Effects, Piezoelectric Crystals.

Introduction

Almost all modern resonators used for frequency control in moderate and high precision applications are of quartz, and operate using bulk acoustic waves of the thickness shear variety. At present, the singly rotated AT cut is most often used, but recent developments point to a greatly expanded role for doubly rotated cuts. Furthermore, virtually all of the thickness mode cuts are in the form of thin circular discs. When these are mounted, the mounting clips cover relatively little of the available edge of the crystal plate and any forces communicated between the mounting supports and the quartz plate produce high stresses and stress-gradients in the vicinity of the mounting positions.

The subject of frequency perturbations in quartz vibrators produced by such external forces has received both theoretical and experimental attention previously[1-27]. Those investigations related the initial stress produced by mounting supports to resonance frequency changes, the contribution to long term aging, and the relation to frequency excursions produced in shock and vibration environments. Two-and four-point mount locations with respect to the plate crystallographic axes have been identified which have the potential to produce minimal frequency shifts for in-plane forces. These were identified by azimuth angles ψ in the plane of the plate for which the force-frequency coefficient $K_f(\Psi)$ equals zero. Unfortunately, in practice, it has been found very difficult to position the mounting clips at the precise locations required. Mispositioning and/or increasing the area of the contact points over a larger area has been found to result in substantial frequency shifts.

This paper describes in detail a design for resonator plates having a prescribed lateral contour, with mounting surfaces provided along a relatively large portion of the periphery, so that mounting stresses are greatly reduced in size, with no detriment to the force-immunity of the older type of mounting. A different lateral contour, of rhomboid configuration, for each and every member of the doubly rotated family of quartz cuts located on the zero temperature coefficient locus extending from the AT-cut to the rotated-X-cut is provided. Other advantages of this new scheme are also described.

Singly and Doubly Rotated Cuts of Quartz

"Singly rotated" and "doubly rotated" refer to cuts oriented with respect to the crystallographic axes. The rotation(s) is/are made primarily for reasons of frequency-temperature behavior. Definitions of axes and angles involved in the specification of a cut are shown in Figure 1. Further details are given in Reference 23. When the angle ϕ is zero, the result is the singly rotated Y-cut. The angle ϕ may take on values from 0° to 30° for quartz; any other angle is equivalent to some angle in this range because of crystal symmetry. Although other doubly rotated cuts having zero temperature coefficient of frequency exist, we shall concentrate on the branch of the first order zero temperature coefficient locus where $\theta = +34^\circ$ to $+35^\circ$, and give specific results for the orientations listed in Table 1.

Effects of In-Plane Diametric Force Pairs

Consider a circular plate vibrator as shown in Figure 2. Two force-pairs are shown, F_1 and F_2. These are point-forces. If one set of forces, say F_2 is set to zero, and the other is applied at an azimuth ψ_1 as shown, then the crystal frequency

TABLE 1. ZERO TEMPERATURE COEFFICIENT CUTS

ϕ (degrees)	Cut
0	AT
10	10^{o} V-Cut
15	FC
19.1	IT
21.9 to 22.4	SC; TTC; TS
30	30^{o} V-Cut

will change in direct proportion to the size of the force applied at F_1 . Further, the frequency change Δf is also a function of the angle ψ of the applied force. For a given plate, the quantity Δf is directly proportional to a number $K_f(\psi)$, called the force-frequency coefficient. A polar plot of $K_f(\psi)$ versus ψ is shown in Figure 3 for the AT cut. An important property of the force-frequency effect for diametric force-pairs is that of Superposition. That is, the resultant Δf produced by F_1 and F_2 , from Figure 2, acting simultaneously at any two angles, as shown, is the algebraic sum of the individual Δf's acting alone at those angles. For the AT cut, the optimum mounting location points which produced zero frequency change were determined, and are marked "A", "B", "C", and "D" in Figure 3. For doubly rotated cuts the four-point optimum mounting locations will not be symmetrically disposed about the crystal axes as shown in this figure; this only happens for the AT cut ($\phi=0^0$) because then the two-fold symmetry axis of quartz happens to lie in the plane of the plate.

TABLE 2. OPTIMUM FOUR-POINT MOUNTING LOCATIONS

ϕ (degrees)	ψ (degrees)
0	62.0, 118.0
10	68.5, 125.2
15	74.8, 148.8
19.1	79.3, 163.1
21.9 to 22.4	81.6, 171.9
30	79.3, 184.3

Table 2 gives the optimum four-point mounting locations, (corresponding to points "A", "B", "C" and "D" in Figure 3), which coincide with the angles at which $K_f(\psi)$ equals zero, not only for the AT cut, but for the family of cuts that are of interest here.

The ψ angles given for each ϕ angle are to be supplemented by two more values, obtained by adding 180^0 to the ψ values in the table above. Radial forces acting at these ψ azimuths produce no frequency changes in the quartz resonator. The angles given in Table 2 were obtained from plots[24] of $K_f(\psi)$ versus ψ , shown in Figure 4. In addition to the specific ψ values given in Table 2, the ψ values corresponding to any value of ϕ may be read approximately from the graph provided in Figure 5.

Figure 6 shows the experimental apparatus with which the data were taken. Included are, clockwise from the left, proof masses for establishment of the force levels, crystal oscillator (CI Meter), vacuum pump for holding specimen on sample chuck, and mounting jig apparatus. Further details are given in Reference 22.

Studies to Minimize Frequency Perturbations Due to $K_f(\psi)$.

From the foregoing, one sees that circular quartz plate vibrators do possess points where radial stresses will not produce frequency changes. These are at the azimuths ψ for which the force-frequency coefficient $K_f(\psi)$ equals zero as given in Table 2. Unfortunately, in practice, it is very difficult to design a pin-point mount and to position this mounting clip accurately at the precise ψ location specified. Mispositioning and/or increasing the area of the contact points over a larger area will in general result in a substantial frequency shift. Even if pin-point mounts were achievable, they would give rise to extremely large stress effects at the contact points. As an exam-

TABLE 3. FREQUENCY CHANGE VERSUS ANGLE ψ FOR ROUND AT CUT CRYSTAL.

ψ (degrees)	$\frac{\Delta f}{f}$ (10^{-6})
57	+2.5
58	+2.0
59	+1.5
60	+1.0
61	+ .5
62	0
63	- .5
64	-1.0
65	-1.5
66	-2.0
67	-2.5

ple of mispositioning, consider an AT-cut plate of 14 mm diameter. Table 3 provides measured data on frequency sensitivity vs applied force for a two-point mount repositioned over a ψ angle range of 10^0 in the vicinity of $\psi = 62^0$, the zero force coefficient angle.

These data show a frequency shift of $\pm$ 2.5 x 10^{-6} as the azimuth angle ψ of the applied force is changed by only $\pm$ 5 degrees. As mentioned previously, the size of the frequency change is not only a result of an azimuth angle change, but is a function of the applied force as well. In this case a mass of only 130 grams was applied. Another, and possibly the most compelling reason to improve on current mounting practices, is that the frequency change experienced due to these stress-induced causes will change as the stresses gradually relax with time. This is undesirable for applications where frequency stability due to long term aging effects are to be minimized. From the foregoing one sees that circular quartz plate vibrators do possess points where radial stresses do not affect their frequency. These are the azimuths ψ for which the force-frequency coefficient $K_f(\psi)$ equals zero. But in practice, it is, in fact, extremely difficult to mount a crystal plate at these precise locations and misalignment can cause significant frequency shifts.

Studies to minimize frequency change with respect to increasing the area of contact and/or mispositioning resulted in a geometry which allows the application of collinear forces through the crystal plate in the vicinity where $K_f(\psi)$ is zero, with minimal frequency change. Plate configurations to achieve the desired results are obtained by cutting flats tangent to the zero force coefficient points. One such plate, for an AT-cut, is shown schematically in Figure 7. This figure shows a plate, initially round in outline, on to which four flats were ground on the perimeter. The flats are arranged to be parallel in pairs, and their normals make angles of $\psi = 62^0$ and 118^0 with respect to the X_1 axis. These angles are those of $K_f(\psi) = 0$ mentioned previously. The numbers in parentheses represent six pairs of points, evenly spaced along the flat portions, where opposing forces F were applied; a force-pair F is shown at position (1). Once again, the plates were 14 mm in diameter, and the flats (chords of the circle) were about 6.5 mm. A chord of this length spans an angle $\Delta\psi$ of 55^0. Tests disclosed that, providing the applied forces F were collinear, it did not matter if the forces were at positions (1), (2), or (3); the frequency measured in each case was nearly the same, that is, the change was virtually zero. Likewise, it did not matter (as long as the forces were collinear) whether F was applied at positions (4), (5), or (6); again the change in frequency was small. The angles of the normals to the flat portions were selected with just this end in mind. Table 4 gives typical results in which the force pair applied at each point was due to a 130 gram mass.

Table 5 provides data obtained in a similar-type investigation, except, in this case, the experiment was repeated three times with a different force applied in each run and the measurements were taken at more closely spaced intervals.

As a result of these experiments we may conclude that if a distribution of forces along the flat edges of the crystal plate, acting along the normal to these edges, is applied to the crystal, the net frequency change will be minimal. This means that the flat edges can become the mounting surfaces, and that instead of a "two-point", or "four-point" mount, one can have instead "two-edge", or "four-edge" mounts. In addition, these mounts can span a considerable length, as shown for the above case in which the flat was 6.5 mm. The case of "four-edge" mounts follows directly from the "two-edge" case inasmuch as superposition of forces is known to hold, so it will not be expressly mentioned further.

Specific Configurations for Select Orientations

The lateral contour shown in Figure 7 is for the AT cut; the ψ angles that fix the positions of the flat edges along which the mountings are to be made come from Table 2 or from Figure 5. For cuts other than the AT cut, the ψ values will be different, and the resulting outline of the crystal plate will likewise change with ϕ angle. The portion of the plate shown with circular outline in Figure 7 for the AT plate could be fashioned so that all edges are straight; likewise for the corresponding doubly rotated cuts. In the following, no circular portions are shown; the main feature of this geometry, i.e., the zero-frequency-shift edge mounting contour, is not affected by these unused portions. These edges may be useful for other purposes as will be described later.

The outlines generated for the six cases given in Table 2 are shown in Figures 8 to 13. The full outline determined by the ψ angles is the rhomboid shown for each case, including the dotted lines; the solid-lined figure is arrived at in a manner described below, and represents a preferred configuration. The orientations of the rhomboids with respect to the crystal axes (X, Z' or X", Z") shown, as well as the angle of the rhomboids, are of paramount importance to the proper functioning of these resonators. The inclinations are discussed at the end of this section.

In Figures 8 to 13, all opposite edges are parallel; the two angles given in each figure serve to determine the shape of the plates when taken with another criterion to be discussed below. Since the edges forces must be collinear, the extent of the mounting edges is governed by the necessity of having opposing edges not only parallel, but abreast. Another way of stating this criterion is to say that when the ends of the opposing mounting edges are joined together by two parallel lines, the resultant figure is a rectangle. An example is given in Figure 14, and the construction proceeds as follows. The crystallographic axes are X" and Z"; from X" lines are drawn through the origin at angles ψ_1 , and ψ_2 . (These ψ values are obtained from Table 2; in the case used here, $\phi = 10^0$, so $\psi \approx 69^0$ and $\psi \approx 125^0$). Then, at a con-

TABLE 4. FREQUENCY CHANGE VERSUS FORCE POSITION FOR RHOMBOID AT CUT CRYSTAL

Force pair position	Measured Frequency (MHz)	Frequency change along chord ($\Delta f/f$)
1*	4.998878	
2	4.998879	$\pm$1Hz($\pm 2 \times 10^{-7}$)
3*	4.998880	
4*	4.998874	
5	4.998875	-1Hz(-2×10^{-7})
6*	4.998875	

* Equivalent to mispositioning ψ by $\pm$ 27.5^{0} about the $K_f(\psi) = 0$ points.

TABLE 5. FREQUENCY CHANGE VERSUS FORCE MAGNITUDE FOR RHOMBOID AT CUT CRYSTAL

Force-pair position	Frequency* Hz	($\Delta f/f$) 10^{-7}	Frequency* Hz	($\Delta f/f$) 10^{-7}	Frequency* Hz	($\Delta f/f$) 10^{-7}
	130 grams		230 grams		330 grams	
1.0	884		881		882	
1.5	883		883		881	
2.0	881	$\pm$3 Hz (6.0)	881	$\pm$3 Hz (6.0)	881	$\pm$2 Hz (4.0)
2.5	881		881		882	
3.0	884		884		884	
4.0	884		888		886	
4.5	885		884		885	
5.0	885	-1 Hz (2.0)	886	$\pm$2 Hz (4.0)	887	$\pm$ 2 Hz (4.0)
5.5	885		887		887	
6.0	884		884		883	

* Frequency in hertz above 4.998 MHz; measured values.

venient distance from the origin, along the Z" axis, the point "a" is marked. From "a", a line "a-b" is drawn perpendicular to the line at angle ψ_1; also from "a" a second line "a-c" is drawn perpendicular to the line at angle ψ_2. In the drawing, point "c" is located on the X" axis; this is a convenience, but is not necessary. Next, lines "c-d" and "d-e" are drawn to be parallel to lines "a-b" and "a-c", respectively. The plate can be left in the rhomboid form "a-e-d-c", and there is an advantage to leaving some of the tabs "c-h-f" and "g-e-i" intact. However, considering only the mounting aspect of the problem now, it will be explained how the lines "g-i" and "f-h" arise and what they mean.

Since the edge forces must be collinear, forces applied to the edge "a-e" at an azimuth angle ψ_1, cannot be met by an opposing set of forces acting along edge "c-d" unless the forces in question act only along "a-g" and "d-f". Similarly, for the other edges, the forces can act only along the portions "a-h" and "d-i". Point "f" is found by dropping a perpendicular from "a"; "g" is found from "d"; "h" is found from "d"; "i" is found from "a". Dotted lines "f-h" and "g-i" indicate where the rhomboid outline can be trimmed to produce the hexoid shown in solid lines in Figure 9.

A similar construction follows for the other ϕ values. For the SC cut, shown in Figure 12, the value of $(\psi_2-\psi_1)$ turns out (by accident) to be nearly 90°, and the construction yields a rectangular (or square) plate. The edges of this plate are at an angle to the X" and Z" crystal axis though; the plate is inclined to the X" axis by 36.8°.

The angles can be found analytically as follows: With ψ_1 and ψ_2 the two given angles where $K_f(\psi)$ is zero, then let $A=\cos(\psi_2-\psi_1)$ and $B=(\sin\psi_2/\sin\psi_1)$. Then find θ from $\cos\theta = \{(1-A)/\sqrt{1-2A+B^2}\}$. The angle between the mounting edges is then $\pi(\psi_2-\psi_1)$; the angle between the mounting edge and the edge perpendicular to the ψ_1 line is $(\pi-\theta)$; the angle between the mounting edge and the edge perpendicular to the ψ_2 line is $\{\theta+(\psi_2-\psi_1)\}$. In some cases the supplementary angle must be taken.

The angle between the line joining the dotted vertices in Figures 8 to 13 and the X_1'' axis specifies the inclination of the plate and is denoted α. Values of this angle for the orientations shown in Figures 8 to 13 are given in Table 6. The angle α is equal to $(\psi_2+\psi_1)/2 - \pi/2$.

Additional Considerations

The main feature of this geometry is the use of flat edges on a crystal plate vibrator (singly or doubly rotated), located so that mounting forces acting at the edges do not produce frequency changes. The forces can, and usually do, come about due to shocks and accelerations arising from external sources such as vehicular motion. In addition, long-term frequency shifts, as might be caused by the slow relaxation of the mounting clips and supports, are also prevented. The crystal outlines depend on the ϕ angle of cut; some of these are shown in Figures 8 to 13.

TABLE 6. INCLINATION OF RHOMBOIDS TO CRYSTALLOGRAPHIC X_1'' AXIS.

ϕ (degrees)	α (degrees)
0	0
10	6.9
15	21.8
19.1	31.2
21.9 to 22.4	36.8
30	-48.2

Because of the presence of relatively long, straight edges for mounting, the mounting stresses will be lower than for point-mounts, and the susceptibility to breaking is also reduced. This increased ruggedness is an additional advantage of the new shapes. If, for some reason, point clips are used for mounting, the new shapes have the further advantage that frequency changes due to collinear forces are reduced to zero regardless of where the mounts are positioned along the edge; exact placement of the crystal at the proper place in the mount is not required (cf. Table 5). If, as will usually be the case, the crystal is mounted by clips extending over a portion of the mounting edges, then placement of the crystal in the mount is very easily and rapidly accomplished, since it is unnecessary to orient the crystal with respect to the mounting clips as in present designs. This is because the edges have been designed with the proper orientation already.

In the above description the plates were provided with four flat portions, while the remaining portions of the periphery were left circular (as in Figure 7), were trimmed off to make hexoid shapes (as in Figures 8 to 13) or were left as rhomboid shapes (dotted lines in Figures 8 to 13). There are at least two reasons for modifying the non-mounting edges further; (1) mode spectrum control, and (2) placement of electrode tabs.

(1) Mode spectrum control - A plot of the crystal resonator admittance versus frequency is called the mode spectrum. For oscillator, and more particularly, filter applications, it is desirable that the resonator have a spectrum that contains as few extra resonances as possible. The mode spectra of acceptable and non-acceptable crystals in this regard are shown in Figure 15. Production of good filter crystals depends upon a number of factors, derived from theoretical considerations that collectively go under the name "energy trapping". Several important factors that contribute to energy trapping are:

- plate size and shape, and edge bevel
- electrode size and shape
- electrode thickness
- position of the electrode tabs

Without going into details at this time, it may be very advantageous to have the clipped-off portions of the rhomboid extend beyond the dotted lines in Figure 14. These dotted lines were determined by considerations of collinear edges forces, and it was pointed out that the edges "h-c", "c-f", "i-e", and "e-g" were of no use in this regard. For the purposes of energy trapping, it may be advisable to clip off the non-mounting edges so that they are parallel to "f-h" and "i-g", but at locations closer to points "c" and "e", respectively. This is shown in Figure 16 for the case of the AT cut, although the feature is generic to all the cuts from $\phi=0^{o}$ to $\phi=30^{o}$. Instead of cutting along "f-h" and "i-g", the cuts would be made along the primed, or double-primed lines. Mounting clips would only extend over those portions of the mounting edges where the force-arrows are shown in Figure 16.

(2) Placement of electrode tabs - Electrodes are usually deposited on the crystal surface in a "keyhole" pattern, with overlapping central portions and "tabs" that do not overlap; (see Figure 17). The azimuth angle of the electrode tabs is important in at least two ways: (1) mode spectrum control and (2) temperature gradient compensation. The azimuth angle is the acute angle between the tabs and the crystal X_1'' axis. This angle plays a role in controlling the spectrum of a resonator, although for doubly rotated crystals this is not very well understood yet.

Temperature gradients in the thickness direction of a vibrator produce frequency changes as large as those produced by external forces and accelerations[23] . For the doubly rotated cut at $\phi=21.9^{o}$ to 22.4^{o} this effect vanishes, and permits thermal-transient-compensated crystals for fast warmup oscillators and advanced frequency standards. For these crystals, however, thermal gradients in the lateral direction are not compensated, and do produce frequency shifts. Orienting the electrode tabs in azimuth may minimize this. The tabs would then extend into the lengthened portion of the hexoid crystals as seen in Figure 17, where they may conveniently be connected to the external circuit. If the tabs can be brought out to the mounting portions of the mounting edges, then the mounts can be used for the electrical connections, as is usual for resonators.

Conclusions

This paper describes in detail a design for resonator plates having a prescribed lateral contour, with mounting surfaces provided along relatively large portions of the periphery, so that mounting stresses are greatly reduced in size with no detriment to the force immunity of the older type of mounting. A different lateral contour, of rhomboid configuration, for each and every member of the doubly rotated family of quartz cuts located on the zero temperature coefficient locus extending from the AT-cut to the rotated-X-cut is provided. It is shown that a crystal of 14mm diameter, with this configuration, can be bonded along a 6.5 mm edge (effective $\Delta\psi$ of 55^{0}), which, when subjected to an increased force of 300 per cent, still exhibits less frequency change than the older type mounts even when $\Delta\psi$ is kept less than $\pm 5^{0}$. Finally, the effects of truncating the plates edges on the mode spectrum, and for thermal gradient compensation of the quartz plate, are considered.

References*

1. V.E. Bottom, "Note on the Anomalous Thermal Effect in Quartz Oscillator Plates", American Mineralogist, Vol. 32, Nos. 9 and 10, September-October 1947, pp. 590-591.

2. E.A. Gerber, "Precision Frequency Control for Guided Missiles", Proc. 1st IRE National Convention on Military Electronics, Session 6, June 1957,pp. 91-98.

3. E.A. Gerber, "Reduction of Frequency-Temperature Shift of Piezoelectric Crystals by Application of Temperature-Dependent Pressure", Proc. IRE, Vol. 48, No. 2, February 1960, pp. 244-245.

4. A.D. Ballato and R. Bechmann, "Effect of Initial Stress in Vibrating Quartz Plates", Proc. IRE, Vol. 48, No. 2, February 1960, pp. 261-262.

5. A.D. Ballato, "Effects of Initial Stress on Quartz Plates Vibrating in Thickness Modes", Proc. 14th AFCS, May-June 1960, pp. 89-114.

6. E.A. Gerber and M.H. Miles, "Temperature Compensation of Piezoelectric Resonators by Mechanical Stress", Proc. 15th AFCS, May-Jun 1961, pp. 49-65.

7. E.A. Gerber and M.H. Miles, "Reduction of the Frequency-Temperature Shift of Piezoelectric Resonators by Mechanical Stress", Proc. IRE, Vol. 49, No. 11, November 1961, pp. 1650-1654.

8. C.R. Mingins, R.W. Perry, and L.C. Barcus, "Effects of External Forces (Transient and Permanent)", Quarterly Report No.1 on Contract No. DA28-043-AMC-01240(E), 1 May to 31 July 1965, US Army Electronics Command, Fort Monmouth, NJ 07703.

9. C.R. Mingins, R.W. Perry, and L.C. Barcus, "Effects of External Forces (Transient and Permanent)", Quarterly Report No. 2 on Contract No. DA28-043-AMC-01240(E), 1 August to 31 October 1965, US Army Electronics Command, Fort Monmouth, NJ 07703.

10. C.R. Mingins, R.W. Perry, and L.C. Barcus, "Effects of External Forces (Transient and Permanent)", Quarterly Report No. 3 on Contract No. DA28-043-AMC-01240(E), 1 November 1965 to 31 January 1966, US Army Electronics Command, Fort Monmouth, NJ 07703.

11. C.R. Mingins, R.W. Perry, and L.C. Barcus, "Effects of External Forces (Transient and Permanent)" Final Report on Contract DA28-043-AMC-01240(E), 3 May 1965 to 2 May 1966, US Army Electronics Command, Fort Monmouth, NJ, 07703; "Transient Reactions to Stress Changes in Vibrating Crystal Plates", Proc. 20th AFCS, April 1966, pp.50-69.

12. J.M. Ratajski, "The Force Sensitivity of AT-Cut Quartz Crystals", Proc. 20th AFCS, April 1966, pp. 33-49.

13. R.W. Keyes and F.W. Blair, "Stress Dependence of the Frequency of Quartz Plates", Proc. IEEE, Vol. 55, No. 4, April 1967, pp. 565-566.

14. J.M. Ratajski, "Force-Frequency Coefficient of Singly-Rotated Vibrating Quartz Crystals," IBM J. Res. Dev., Vol. 12, No.1, January 1968, pp. 92-99.

15. P.C.Y. Lee, Y.S. Wang, and X. Markenscoff, "Elastic Waves and Vibrations in Deformed Crystal Plates", Proc. 27th AFCS, June 1973, pp. 1-6.

16. P.C.Y. Lee, Y.S. Wang, and X. Markenscoff, "Effects of Initial Bending on the Resonance Frequencies of Crystal Plates", Proc. 28th AFCS, May 1974, pp. 14-18.

17. P.C.Y. Lee and D.W. Haines, "Piezoelectric Crystals and Electroelasticity", in R.D. Mindlin and Applied Mechanics, (G. Herrmann, ed.) Pergamon Press, New York, 1974, pp. 227-253.

18. P.C.Y. Lee, Y.S. Wang, and X. Markenscoff, "High Frequency Vibrations of Crystal Plates under Initial Stresses", J. Acoust. Soc. Amer., Vol. 57, No.1, Jan 1975, pp. 95-105.

19. P.C.Y. Lee, Y.S. Wang, and X. Markenscoff, "Nonlinear Effects of Initial Bending on the Vibrations of Crystal Plates", J. Acoust. Soc. Am., Vol. 59, No.1, Jan 1976, pp. 90-96.

20. P.C.Y. Lee, "Some Problems in Vibrations of Piezoelectric Crystal Plates", Report on the Workshop on Application of Elastic Waves in Electrical Devices, Non-Destructive Testing and Seismology, (J.D. Achenbach, Y.H. Pao, and H.F. Tiersten, eds.), Northwestern University, Evanston, Illinois 60201, May 1976.pp.442-489.

21. A. Ballato, E.P. EerNisse, and T. Lukaszek, "The Force-Frequency Effect in Doubly Rotated Quartz Resonators",Proc.31st AFCS, June 1977, pp. 8-16.

22. A. Ballato, E.P. EerNisse, and T. Lukaszek, "Force-Frequency and Other Effects in Doubly Rotated Vibrators", Technical Report ECOM-4536, US Army Electronics Command, Fort Monmouth, NJ 07703, September 1977, 45 pp.

23. A. Ballato, "Doubly Rotated Thickness Mode Plate Vibrators", in Physical Acoustics: Principles and Methods, (W.P. Mason and R.N. Thurston, eds.), Vol. 13, Chap. 5. Academic Press, New York, 1977, pp. 115-181.

24. E.P. EerNisse, T. Lukaszek, and A. Ballato, "Variational Calculation of Force-Frequency Constants of Doubly Rotated Quartz Resonators" IEEE Trans. Sonics Ultrason., Vol. SU-25, No.3, May 1978, pp. 132-138.

25. D. Janiaud, L. Nissim, and J.-J. Gagnepain, "Analytical Calculation of Initial Stress Effects on Anisotropic Crystals: Application to Quartz Resonators", Proc. 32nd AFCS, May-June 1978, pp. 169-179.

26. E.P. EerNisse, "Rotated X-Cut Quartz Resonators for High Temperature Applications", Proc. 32nd AFCS, May-June 1978, pp. 255-259.

27. A. Ballato, "Force-Frequency Compensation Applied to Four-Point Mounting of AT-Cut Resonators", IEEE Trans. Sonics Ultrason., Vol. SU-25, No. 4, July 1978, pp. 223-226.

---

* AFCS: Annual Frequency Control Symposium, U.S. Army ERADCOM, Ft Monmouth, NJ.

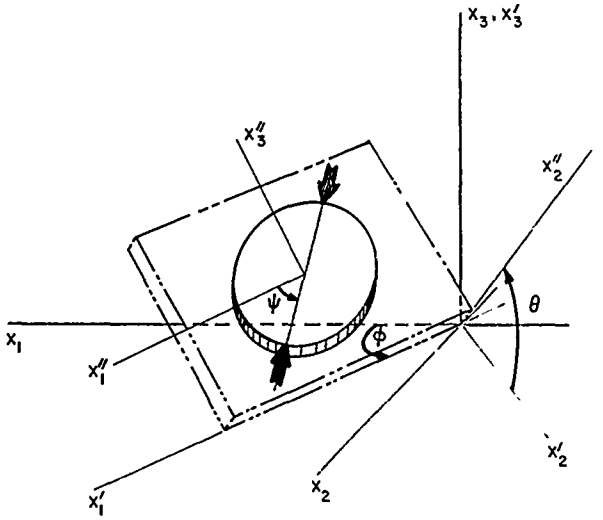

1. Convention for Specifying Plate and Force Angles.

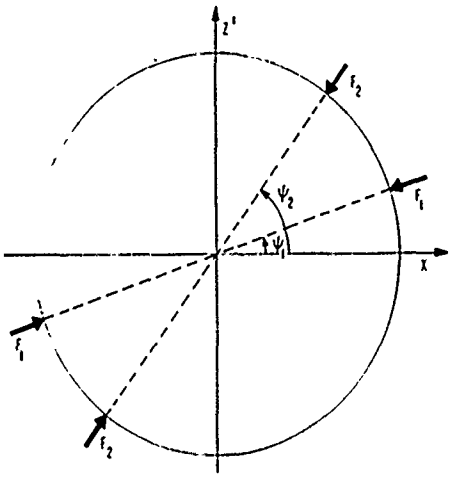

2. Definition of Mounting Angles with Respect to Crystal Axes.

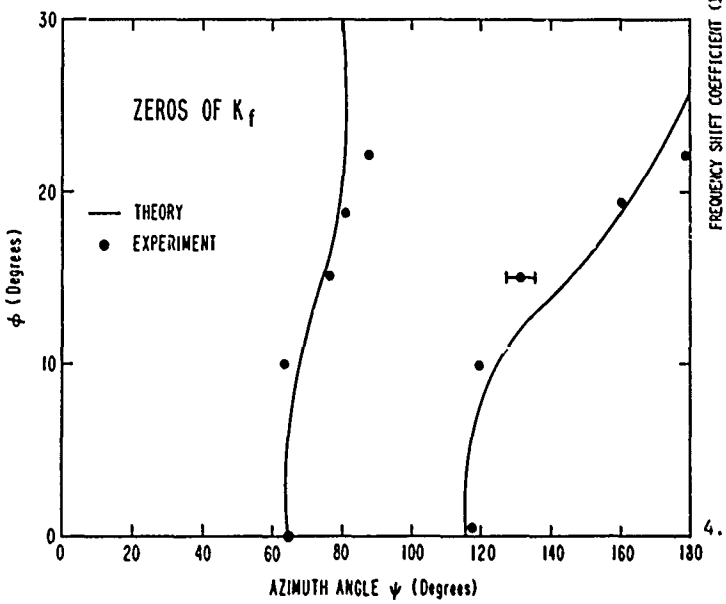

5. Loci in Ø, ψ Plane of Zeros of Coefficient $K_f(\psi)$.

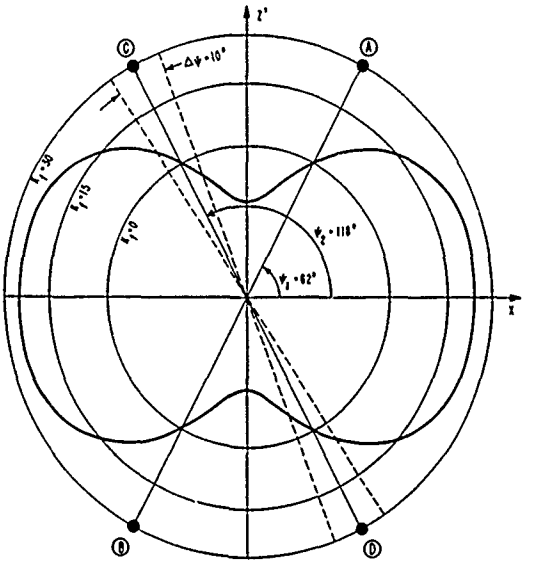

3. Polar Plot of $K_f(\psi)$ versus Angle ψ.

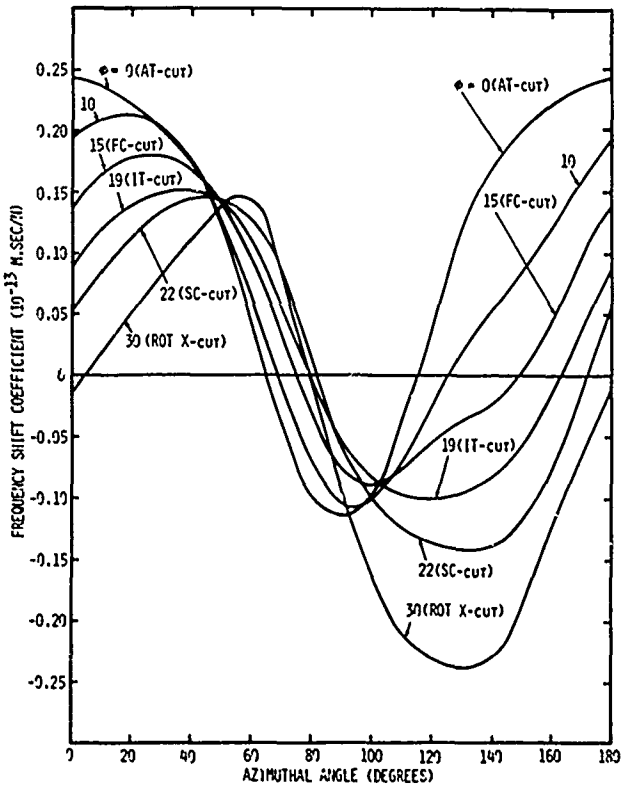

4. Calculated $K_f(\psi)$ for Select Doubly Rotated Cuts.

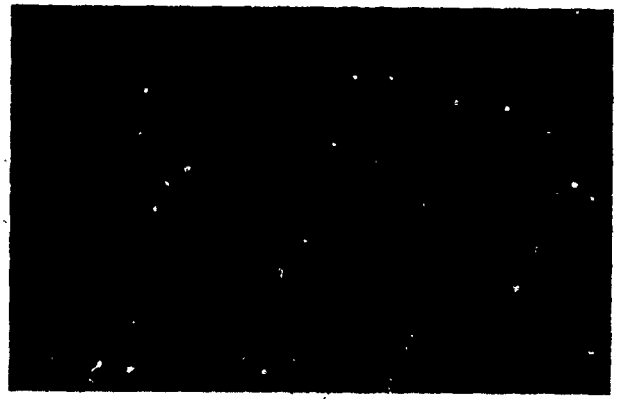

6. Experimental Apparatus for Determining Force-Frequency Effect.

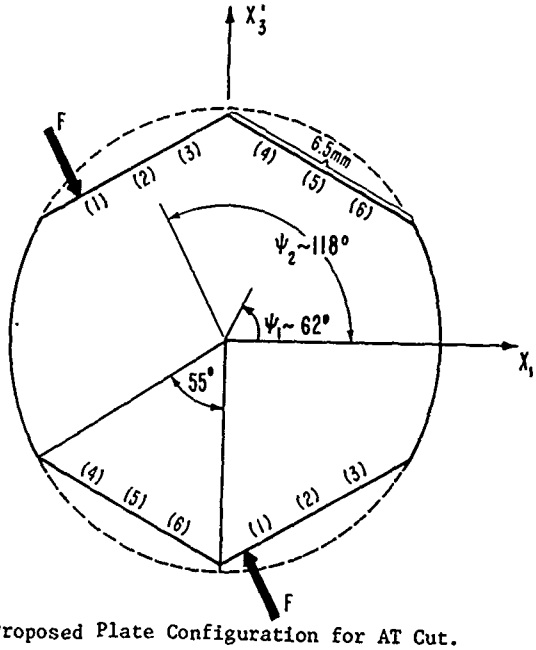

7. Proposed Plate Configuration for AT Cut.

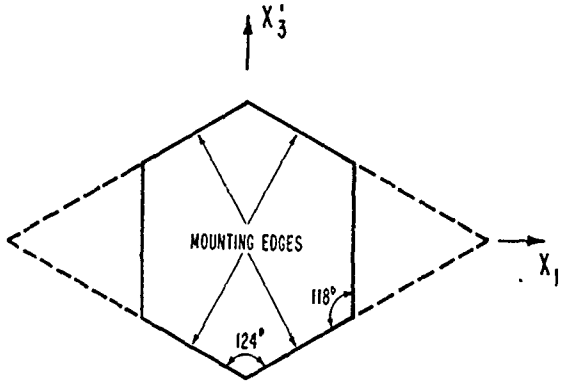

AT CUT (ϕ =0°)

8. Plate Geometry for Minimum Force-Frequency Effect; Ø=0° (AT Cut).

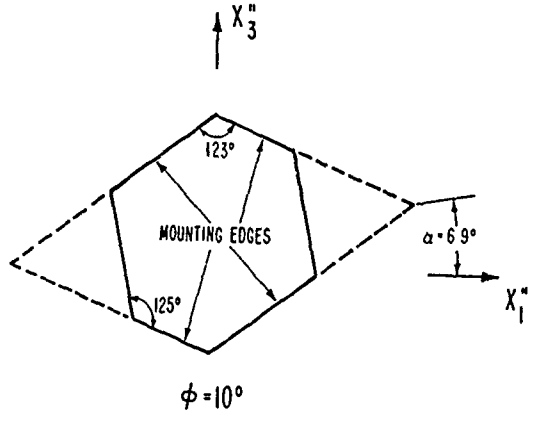

ϕ =10°

9. Plate Geometry for Minimum Force-Frequency Effect; Ø=10°.

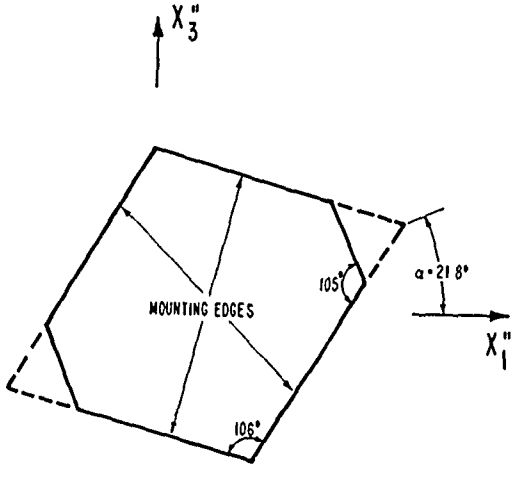

FC CUT (ϕ =15°)

10. Plate Geometry for Minimum Force-Frequency Effect; Ø=15° (FC Cut).

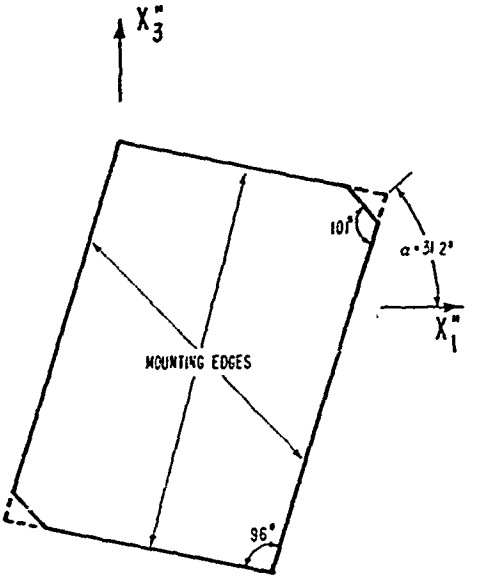

IT CUT (ϕ = 19.1°)

11. Plate Geometry for Minimum Force-Frequency Effect; ϕ=19.1° (IT Cut).

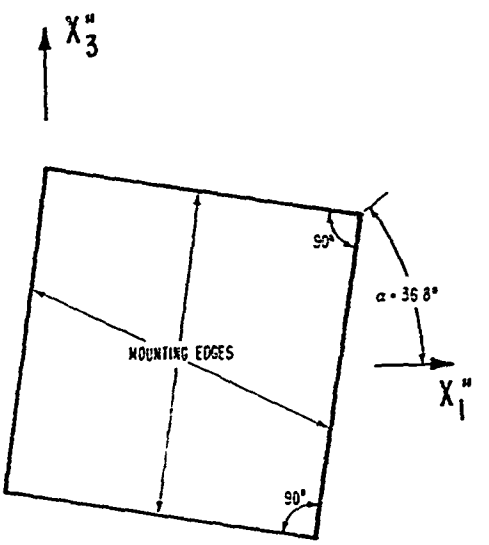

SC CUT (ϕ = 21.9°)

12. Plate Geometry for Minimum Force-Frequency Effect; ϕ=21.9° (SC Cut).

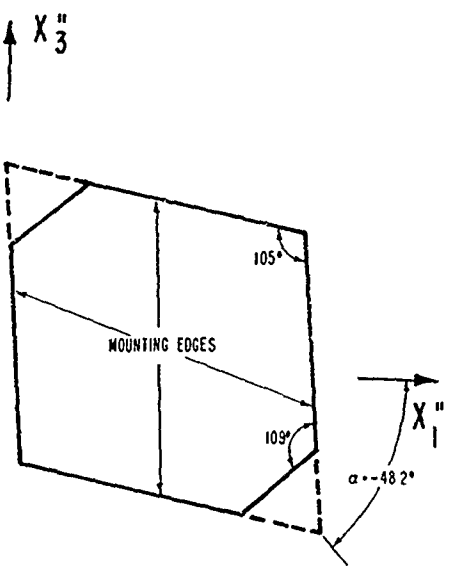

ϕ = 30°

13. Plate Geometry for Minimum Force-Frequency Effect; ϕ=30°.

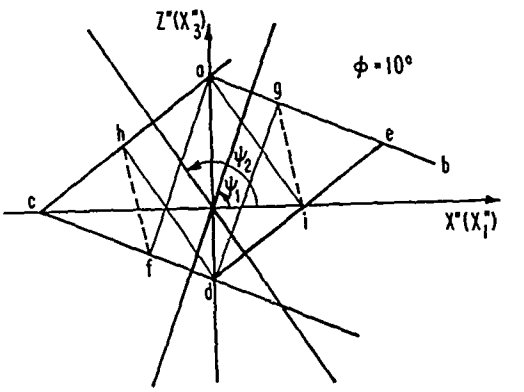

14. Generalized Construction Procedure Applied to ϕ=10° Plate.

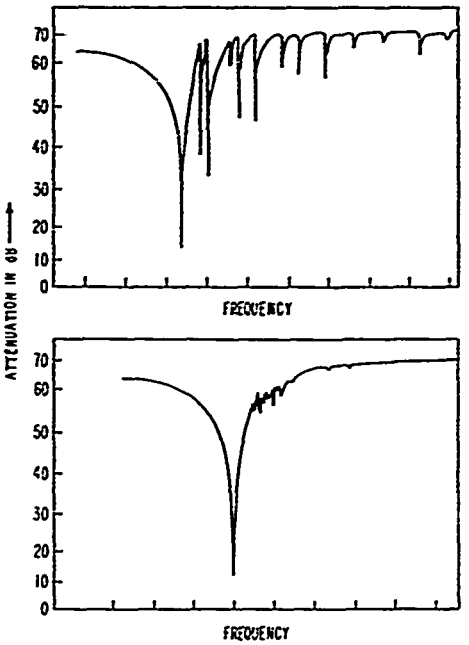

15. Mode Spectrograph Comparison.

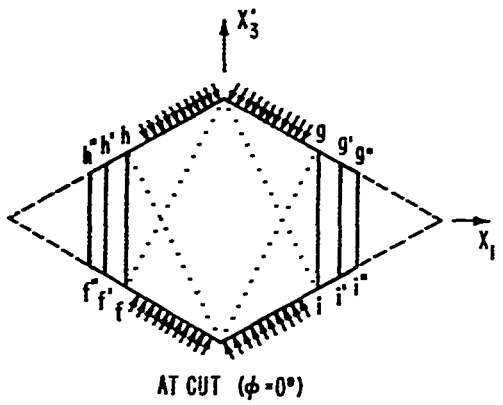

16. Modification of Geometry for Energy Trapping Purposes.

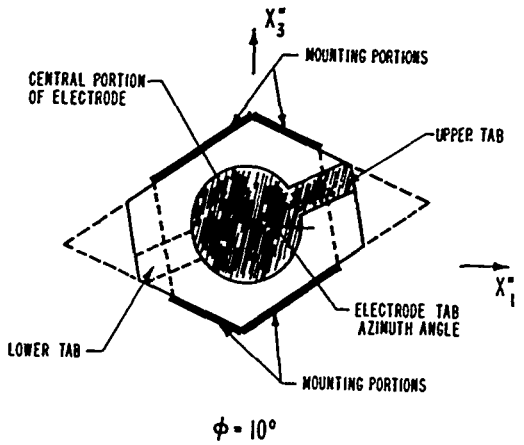

17. Hexoid Resonator with Off-Axis Electrode Tabs.

RESONATORS COMPENSATED FOR ACCELERATION FIELDS

Arthur Ballato

US Army Electronics Technology & Devices Laboratory
USAERADCOM, Fort Monmouth, NJ 07703

Summary

This paper describes resonator configurations that are compensated for arbitrary directions of the acceleration field, and that require no additional electronics other than the oscillator circuitry normally used. This approach produces compensation with no changes in size, weight, and power, and applies to any crystal reference oscillator in any shock/vibration environment whatsoever.

Key Words
Resonators, Frequency Control, Acoustic Waves, Quartz Crystals, Doubly Rotated Cuts, Bulk Acoustic Waves, Force-Frequency Effects, Piezoelectric Crystals, Acceleration Effects, Enantiomorphism, Composite Resonators, Stacked Crystals, Equivalent Networks.

Introduction

Frequency perturbations are produced in crystal resonators by acceleration-induced body forces. These forces are distributed throughout the resonator volume and vary with the acceleration direction. For specific acceleration directions the effect can be sharply reduced by changing the points of application of the mounting supports. Even doubly rotated cuts may be accomodated, (although the mounting design varies with cut), and for some of these cuts the effect is further reduced below the value found for the AT cut. When the acceleration direction is known in advance, positioning the resonator with respect to this direction minimizes the problem.

In high shock and vibration environments such as helicopters, tanks, and other vehicles, and the more moderate environment of manpack use, accelerations occur in arbitrary directions with ensuing large frequency shifts in the crystal resonance frequency. Wher the acceleration is arbitrarily oriented with respect to the resonator, no crystal cut and/or combination of mounting supports can by themselves produce cancellations of the frequency perturbations to the extent required by secure systems. However, by taking advantage of the experimental fact that the resonance frequency shift changes sign with reversal of the acceleration direction and the fortunate happenstance that quartz occurs in right-and left-handed pairs, composite resonators of either discrete or stacked varieties may be fashioned having vastly decreased acceleration sensitivity, whatever the acceleration direction may be, with no concomitant degradation of any of the desirable resonator properties. The approach is applicable to doubly rotated crystals as well as singly, so that the additional nonlinear compensation of thermal transients, etc., that occurs for these cuts can be had along with acceleration hardening.

Acceleration Effects

In the static force-frequency effect,[1–31] forces and moments acting on the peripheral boundary of a crystal resonator serve to produce frequency changes in the resonator. Accelerations of the crystal plate, on the other hand, produce distributed body forces throughout the resonator volume that are communicated at the crystal boundary to the mounting supports. The stress distribution within the crystal depends not only upon the mounting points, but also on the direction of the acceleration. In general the static and dynamic effects will produce different states within the vibrator, and different frequency shifts.[32–53] Some applications of the effect to realize accelerometers have been made,[36,43] but much more often the effect is highly undesirable, and efforts to reduce the effect have continued for the past twenty years.[32,52]

Within the past five years the problem has become particularly acute, due to exacting requirements arising from the present and projected secure digital systems for communication, command, and control, and for navigation/position location. Fortunately, during this interval a number of advances have come about that in combination promise a significant reduction in the acceleration sensitivity of crystal resonators. One of these developments is the introduction of doubly rotated cuts. (References 21-23, 54). Another is the use of new support configurations.[53,55] Additional developments will be detailed in ensuing sections.

Concurrent with these developments, a nonlinear theory has been fashioned by Lee and his co-workers that describes the force-frequency effect,[15–20] and acceleration effects in singly rotated, rotated-Y-cut quartz plates.[40,46,49] A plate theory has also been developed for doubly rotated quartz cuts.[56] Such a theory will provide a necessary understanding of the mounting support problem as applied to acceleration-compensated resonators.

Acceleration Compensation

One of the most recent acceleration compensation schemes is the systems approach of Przyjemski. (References 45,48,51). In it, ancillary accelerometers sense the applied acceleration components along three orthogonal directions and this information is used to feed back a compensation signal to correct the crystal frequency. This arrangement provides improvements of a factor twenty or so over an uncompensated resonator, and works for arbitrary directions of applied acceleration.

Another acceleration compensation scheme is that of Gagnepain and Walls.[41,53,55] In this arrangement, two quartz vibrators are connected electrically in series, in the manner used long ago by Koga[57,58] to effect temperature compensation. Now, however, the crystals are oriented so that the axes along which the acceleration-frequency effect is greatest are antiparallel in pairs. According to the measurements of Valdois,[37-39] for AT cut discs supported along the Z' axis, the directions of greatest acceleration sensitivity are for acceleration fields along the Y' axis, which coincides with the disc thickness, and for fields along the Z' axis. Because the sensitivity is least for X-directed fields, the discs are oriented so that the X axes of both discs are parallel, and the Y' and Z' axes are antiparallel. Then compensation is achieved for directions of acceleration lying in the plane normal to the common X axis. The experimental arrangement and results of Valdois[37-39] are shown in Figure 1.

A configuration alternative to that of Gagnepain and Walls was proposed by Vig,[59] wherein the two paired resonators are mated in the fashion of a two-layer stacked crystal filter.[60-64] In this case the angle ψ between the X axes of both crystals would be zero. The acceleration-frequency behavior would be similar to that of the discrete configuration, but the stack would be more robust and occupy less room than two separate vibrators.

Enantiomorphous Crystals

Two identical crystal resonators can only be manipulated so that an even number of their respective crystal axes are antiparallel. Reversal of an odd number requires an improper rotation. Fortunately, just such an operation is possible with quartz! The operation changes the handedness of the crystal. When two crystal resonators, identical except for their handedness, are used as a pair, they may be oriented as shown in Figure 2 with corresponding axes antiparallel. Then, from the results shown in Figure 1, where the frequency change reverses sign with reversal of acceleration direction, paired resonators will suffer no frequency shift for any direction of the acceleration field. This statement holds for pairs configured as discrete vibrators, or as a composite stack.

Quartz is not the only enantiomorphous crystal, of course. Any representative of the eleven crystal classes given in Figure 3 exhibits this property. These are the classes without a plane of symmetry. The enantiomorphs bear a mirror image relationship to each other; all are noncentrosymmetric, and hence (with the exception of class 432) are piezoelectric. There is at least one representative from each of the seven crystal systems. Figure 3 also gives the number of second and third order elastic coefficients, followed by the number of respective coefficients that are independent. Berlinite (class 32) is enantiomorphous, lithium tantalate and lithium niobate (class 3m) are not.

Paired enantiomorphs of idealized crystals of quartz are given in Figures 4 to 7. In each case the left- hand type is on the left and the right-hand type is on the right. In the figures, and for the rest of the paper it will be convenient to work with coordinate systems having the same chirality as the type of quartz: left for left-quartz, right for right- quartz. This convention was first proposed by Koga[65] in 1929 and adopted in a 1945 report by the IRE, following upon a paper by Cady and Van Dyke.[66] It is also used in Cady's book.[67] The 1949 IRE standard adopted a right-hand coordinate system for both forms, and the latest IEEE standard has continued the convention of its predecessor.[69] A recent paper by Donnay and LePage[70] lucidly sets forth reasons for using two coordinate systems for enantiomorphs. Incidentally, morphological enantiomorphism appears first to have been explicitly recognized by Louis Pasteur; the usual attribution is to Haüy who illustrated both types of quartz, but his writings do not show that he recognized the difference.[71] The question is still very much an open one.[72,73]

The enantiomorphs discussed here correspond to what is called Brazil, or optical, twinning in natural quartz. The other category of twinning often present in natural quartz is Dauphiné, or electrical, twinning, where the two forms are rotated, with respect to each other, about the Z (or optic) axis so that the X axes are in opposite (antiparallel) directions, but the handedness is unaffected. Dauphiné twinning may be brought about relatively easily and involves small changes in atomic positions, whereas Brazil twinning requires the breaking of atomic bonds and a significant expenditure of energy.[74,75] Yoda proposed the use of electrically and optically twinned quartz for crystal vibrators before cultured bars attained the degree of use that they enjoy today.[76]

Right- and left- handed cultured quartz bars ("Y-bars") are shown as line drawings in Figures 8 and 9, respectively;[77] also indicated are the natural "r", "m", and "z" faces, and the orientation of the AT cut. If a left- and a right- handed AT cut are oriented so that their axes are respectively antiparallel, as shown in Figure 2, and connected electrically in series or in parallel, then the combination becomes insensitive to acceleration fields of arbitrary orientation, provided that the symmetry of the mountings is maintained.[53,55] This is the discrete configuration, where the crystal plates are physically unjoined.

Stacked Crystal Structures

The stacked-crystal configuration came about originally for filters[60-64] when used in the multimode configuration. Layered structures utilizing a single mode have been more commonly used.[78-92] Here we discuss the stacking of two enantiomorphous pairs with respective axes antiparallel (as in Figure 2), and operated as a single resonator of composite form. Both crystals are of identical design; that is, they have identical individual frequencies, electrode patterns, etc. Figure 10 gives the four possible two-crystal structures. The two on the left in the figure are connected electrically in series; the two on the right are in parallel electrically. The upper two are arranged so that the electric fields in the two crystal plates are antiparallel; the bottom two structures have electric fields that are parallel in the two crystals. For the upper structures, the odd harmonics (of the composite taken as a whole) are driven, while the even harmonics are driven in the two lower structures. In the upper left and lower right configurations, an insulating film or layer between the crystals is necessary for operation, and large values of capacitance would be associated therewith, to the detriment of the composite. This leaves the two configurations of Figure 11 as the simplest and most practical stacked crystal resonators for acceleration immunity. The structure on the left of the figure consists of two crystal plates connected electrically in parallel, using a common central electrode. It operates at odd harmonics of the fundamental frequency of the composite, i.e., at one half, three halves, etc., of the frequency of each crystal plate operated separately.

The structure on the right side of Figure 11 is the series version of the stack, and operates at even harmonics. A central electrode is not even necessary in this configuration. Provided the plates to be joined have parallel mating surfaces and are sufficiently clean of contaminants, they will adhere. An apparatus that can be used for this purpose is nearing completion.[93]

Implicit in the discussion above have been assumptions that the stacked crystal composite vibrator consists of two crystal twins that each operate in a single mode, and that when the two vibrators are joined, the composite continues to operate in this manner. For the singly rotated cuts (YXℓ) θ of quartz, including the AT and BT cuts, it is easy to see that this will be the case, since each vibrator is driven in the slow shear mode by a thickness-directed electric field. This mode has particle motion strictly along the X axis, so that when the two plates are joined, the composite will also have motions along X; the phase of the motions in the two component plates will depend on how the electrodes are connected, and hence, on whether the electric fields in the two plates are parallel or antiparallel. The phase will dictate whether even or odd harmonics of the composite are driven.

The most important recent development in the area of high precision frequency control has been the introduction of doubly rotated cuts of quartz having compensation of certain nonlinear elastic effects that otherwise cause very undesirable stress-frequency[94,95] and thermal transient/thermal gradient- frequency effects.[96-101] For these crystal cuts the three piezoelectrically driven modes all have particle motion that is neither parallel to, nor perpendicular to, the plate normal. It is not clear, therefore, that such plates can be used in the stacked configuration for acceleration compensation in the manner described above. This will now be demonstrated.

Doubly Rotated Enantiomorphs

Both singly and doubly rotated enantiomorphs are shown in Figure 12. It is seen that the mirror-image property holds for any orientation. Assume that a doubly rotated cut, e.g., the SC cut, has been fashioned in both right- and left- handed forms; also assume that the corresponding plate axes have been simply labeled X,Y and Z (instead of double-prime axes). Now suppose that a portion of each plate is considered to have dimensions such that the eigenvector corresponding to the mode under question points in the direction from an origin "O" along the major hypotenuse of the parallelepiped, as seen in Figure 13. On the left is the left-handed plate (or portion thereof), with particle motion along "OA"; the motion thus has components both along and perpendicular to the major plate surfaces. The mirror image right-handed plate seen in the center of Figure 13 has particle motion along "OB", because "OB" is the mirror image of "AO". In order to orient the right-handed plate so that its axes are antiparallel to those of the left-handed plate, and thereby achieve the configuration for acceleration compensation, it is only necessary to rotate the center drawing in Figure 13 about the Y axis until the rightmost drawing is reached. Then the line "OB", seen in the right portion of the figure is exactly in line with "OA" seen in the left portion of the figure. The stacking thus can take place without any difficulty; the argument holds for all three plate thickness modes, with the conclusion that doubly rotated plates may be stacked as readily as singly rotated plates, and no problem of introducing additional mode coupling will arise, provided the corresponding axes are either all parallel (two plates of the same handedness) or all antiparallel (two plates of opposite handedness).

Realization of acceleration compensation in the manner set forth in this paper requires the availability of quartz bars of both handednesses. Almost all of the cultured quartz Y-bars produced today are right-handed, although left-handed bars can be obtained on special order. Moreover, production has begun of bars ("SC-cut bars") grown for the purpose of making doubly rotated SC cuts.[102,103] These have been right-handed to date. In order to speed the introduction and use of doubly rotated cuts in general, and doubly rotated enantiomorphs in particular, we reproduce in Figures 14 to 17 photographs of an SC-bar.[102] The right-handed original is shown in the lower portion of each figure, and the left-handed print, made by reversing the negative of the original, is shown in the upper portion of each figure. Cor-

responding line drawings, with axes and identification of faces are given in Figures 18 to 25. The correspondences are as follows:

Figure 18 corresponds to Figure 14 (top)
Figure 19 corresponds to Figure 14 (bottom)
Figure 20 corresponds to Figure 15 (top)
Figure 21 corresponds to Figure 15 (bottom)
Figure 22 corresponds to Figure 16 (top)
Figure 23 corresponds to Figure 16 (bottom)
Figure 24 corresponds to Figure 17 (top)
Figure 25 corresponds to Figure 17 (bottom)

Figure 26 depicts the end faces of SC-bars.

In the foregoing we have seen how it is necessary for the corresponding axes of the quartz plates to be properly identified. In particular, it is advantageous to have a simple method of determining the positive and negative X axes of blanks. One practical and simple method is to use chemical etching.[104],[105] For doubly rotated SC cuts it has been shown to be a readily applicable and practical method.[105]

Equivalent Networks

The usual equivalent circuits used for crystals are inappropriate here because they do not take into account the piezoelectric polarities explicitly. Figure 27 shows the analog equivalent network[63] of a crystal wherein a single mode is piezoelectrically driven. The placement of the piezo-transformer dots and the coordinate axes identify the network as representing a right-handed crystal. The corresponding network for a left-handed crystal is given in Figure 28.

In Figure 29, the crystals of Figures 27 and 28 (schematized as boxes), are shown on either side of the central mirror plane of symmetry. The network representation of the reversal of the crystal axes by rotation of one of the plates about the thickness axis is depicted in Figure 30. Attachment of the crystals may now be made to realize either the discrete or the stacked configuration. If the discrete configuration is to be realized, then the following ports are shorted to indicate traction-free mechanical boundary conditions: CD, EF, IJ, and KL. Ports AB and GH are then connected electrically in series or parallel as indicated in the discussion of Figures 10 and 11.

Realization of the stacked configuration requires, in Figure 30, the direct connection of mechanical ports CD and IJ to each other, and shorting of ports EF and KL. The electrical ports are treated as above.

The case of a stacked, doubly rotated pair of plates is shown in Figure 31. Here all three thickness modes are excited in each plate. The rotation of one plate about the thickness axis required for acceleration compensation is represented by the mechanical transformers in the center if we select minus one as the turns ratio. When two of the thickness modes can be neglected compared to the third, then the resulting network appears as in Figure 32 with the minus one ratio chosen. The inductances labeled L are equivalents of electrode mass.[54] Connection of terminals A to D and B to C in Figure 32 produces the parallel connection seen on the left side of Figure 11.

In order for the networks shown to simulate the effects of an acceleration field, the individual parameters must be made functions of the acceleration; this can be done without any great difficulty. In the configurations where compensation takes place, the net frequency deviation will be zero provided the resonators forming the composite are identical in design, in reference frequency and in mounting. The compensation described in this paper arises from geometrical considerations regarding the crystals; it is assumed that the boundary conditions are likewise identical; any departure from symmetry in this regard could be expected to produce deteriorated performance. Any misorientations due to manufacturing deviations resulting in slight relative rotations of the plate about the common thickness (Y) direction will couple all three thickness modes together via a mechanical interface transformer[63] with turns ratios that depart from zero as sin ψ where ψ is the small angular error, and from one as cos ψ.

Racemic Structures:

Advantages - Disadvantages

Insofar as a balanced mixture of right- and left-rotating molecules is called a "racemic" state, the balanced structures introduced in this paper might also be referred to as racemic. We outline below certain of the pros and cons of the racemic structures considered:

Advantages - Permit use of

- Arbitrary acceleration directions
- Discrete or stacked configurations
- Singly or doubly rotated cuts
- Special mounting systems
  - BVA[53],[55]
  - Rhomboid [31]
- Any enantiomorphous crystal class or material
- Plano - convex plates
- Any type of mode for which reversal of the acceleration direction is found to reverse the frequency shift in a single resonator
  - thickness BAW
  - contour BAW
  - flexure BAW
  - SBAW or SSBW
  - SAW
- Any of the above in combination

Disadvantages -

- Bonding or joining plates in stacked structure (But see Ref. 93)
- Edge mounts sensitive to small errors[46],[49]
- Stacking misorientation errors couple modes[63]

Acknowledgment

The author would like to acknowledge helpful discussions with Dr. John Vig, Ted Lukaszek, and John Gualtieri of USAERADCOM, Ft. Monmouth. He also wishes to thank Profs. C.J. Schneer, U. New Hampshire; J. D.H. Donnay, McGill U.; M.J. Buerger and C. Frondel, Harvard U. The author also wishes to cite his twinned friends depicted in Figure 33!

REFERENCES*

1. V.E. Bottom, "Note on the Anomalous Thermal Effect in Quartz Oscillator Plates", American Mineralogist, Vol. 32, September-October 1947, pp. 590-591.

2. E.A. Gerber, "Precision Frequency Control for Guided Missiles", Proc. 1st IRE National Convention on Military Electronics, Session 6, June 1957, pp. 91-98.

3. E.A. Gerber, "Reduction of Frequency-Temperature Shift of Piezoelectric Crystals by Application of Temperature-Dependent Pressure", Proc. IRE, Vol. 48, February 1960, pp. 244-245.

4. A.D. Ballato and R. Bechmann, "Effect of Initial Stress in Vibrating Quartz Plates", Proc. IRE, Vol. 48, February 1960, pp. 261-262.

5. A.D. Ballato, "Effects of Initial Stress on Quartz Plates Vibrating in Thickness Modes", Proc. 14th AFCS, May-June 1960, pp. 89-114.

6. E.A. Gerber and M.H. Miles, "Temperature Compensation of Piezoelectric Resonators by Mechanical Stress", Proc. 15th AFCS, May-June 1961, pp. 49-65.

7. E.A. Gerber and M.H. Miles, "Reduction of the Frequency-Temperature Shift of Piezoelectric Resonators by Mechanical Stress", Proc. IRE, Vol. 49, November 1961, pp. 1650-1654.

8. C.R. Mingins, R.W. Perry, and L.C. Barcus, "Effects of External Forces (Transient and Permanent)", Quarterly Report No. 1 on Contract No. DA28-043-AMC-01240(E), 1 May to 31 July 1965, US Army Electronics Command, Fort Monmouth, NJ 07703.

9. C.R. Mingins R.W. Perry, and L.C. Barcus, "Effects of External Forces (Transient and Permanent)", Quarterly Report No. 2 on Contract No. DA28-043-AMC-01240(E), 1 August to 31 October 1965, US Army Electronics Command, Ft Monmouth, NJ 07703.

10. C.R. Mingins, R.W. Perry, and L.C. Barcus, "Effects of External Forces (Transient and Permanent)", Quarterly Report No. 3 on Contract No. DA28-043-AMC-01240(E), 1 November 1965 to 31 January 1966, US Army Electronics Command, Fort Monmouth, NJ 07703.

11. C.R. Mingins, R.W. Perry, and L.C. Barcus, "Effects of External Forces (Transient and Permanent)", Final Report on Contract DA28-043-AMC-01240(E), 3 May 1965 to 2 May 1966, US Army Electronics Command, Fort Monmouth, NJ 07703; "Transient Reactions to Stress Changes in Vibrating Crystal Plates", Proc. 20th AFCS, April 1966, pp. 50-69.

12. J.M. Ratajski, "The Force Sensitivity of AT-Cut Quartz Crystals", Proc. 20th AFCS, April 1966, pp. 33-49.

13. R.W. Keyes and F.W. Blair, "Stress Dependence of the Frequency of Quartz Plates", Proc. IEEE Vol. 55, April 1967, pp. 565-566.

14. J.M. Ratajski, "Force-Frequency Coefficient of Singly-Rotated Vibrating Quartz Crystals", IBM J. Res. Dev., Vol. 12, January 1968, pp. 92-99.

15. P.C.Y. Lee, Y.S. Wang, and X. Markenscoff, "Elastic Waves and Vibrations in Deformed Crystal Plates", Proc. 27th AFCS, June 1973, pp. 1-6.

16. P.C. Y. Lee, Y.S. Wang, and X. Markenscoff, "Effects of Initial Bending on the Resonance Frequencies of Crystal Plates", Proc. 28th AFCS, May 1974, pp. 14-18.

17. P.C.Y. Lee and D.W. Haines, "Piezoelectric Crystals and Electroelasticity", in R.D.Mindlin and Applied Mechanics, (G. Herrmann, ed.) Pergamon Press, New York, 1974, pp. 227-253.

18. P.C.Y. Lee, Y.S. Wang, and X. Markenscoff, "High Frequency Vibrations of Crystal Plates under Initial Stresses", J. Acoust. Soc. Amer., Vol. 57, Jan 1975, pp. 95-105.

19. P.C.Y. Lee, Y.S. Wang, and X. Markenscoff, "Nonlinear Effects of Initial Bending on the Vibrations of Crystal Plates", J. Acoust. Soc. Am., Vol. 59, Jan 1976, pp. 90-96.

20. P.C.Y. Lee, "Some Problems in Vibrations of Piezoelectric Crystal Plates", Report on the Workshop on Application of Elastic Waves in Electrical Devices, Non-Destructive Testing and Seismology, (J.D. Achenbach, Y.H. Pao, and H.F. Tiersten, eds.), Northwestern University, Evanston, Illinois 60201, May 1976, pp. 442-489.

21. A. Ballato, E.P. EerNisse, and T. Lukaszek, "The Force-Frequency Effect in Doubly Rotated Quartz Resonators", Proc. 31st AFCS, June 1977, pp. 8-16.

22. A. Ballato, T. Lukaszek, and E.P. EerNisse, "Force-Frequency and Other Effects in Doubly Rotated Vibrators", Technical Report ECOM-4536, US Army Electronics Command, Fort Monmouth, NJ 07703, September 1977, 45 pp.

23. E.P. EerNisse, T. Lukaszek, and A. Ballato, "Variational Calculation of Force-Frequency Constants of Doubly Rotated Quartz Resonators", IEEE Trans. Sonics Ultrason., Vol. SU-25, May 1978,pp. 132-138.

24. D. Janiaud, L. Nissim, and J.-J. Gagnepain, "Analytical Calculation of Initial Stress Effects on Anisotropic Crystals: Application to Quartz Resonators", Proc. 32nd AFCS, May-June 1978, pp. 169-179.

25. E.P. EerNisse, "Rotated X-Cut Quartz Resonators for High Temperature Applications", Proc. 32nd AFCS, May-June 1978, pp. 255-259.

26. A. Ballato, "Four-Point Mounting Configuration for Resonators Subjected to Severe Environments", Technical Report ECOM-4544, US Army Electronics Command, Fort Monmouth, NJ 07703, November 1977, 14 pp.

27. A. Ballato, "Force-Frequency Compensation Applied to Four-Point Mounting of AT-Cut Resonators", IEEE Trans. Sonics Ultrason., Vol. SU-25, July 1978, pp. 223-226.

28. T. Lukaszek and A. Ballato, "Resonators for Acceleration Environments", Technical Report DELET-TR-79-10, US Army Electronics R&D Command, Fort Monmouth, NJ 07703, June 1979, 33 pp.

29. E.P. EerNisse, "Temperature Dependence of the Force Frequency Effect for the Rotated X-Cut", these proceedings.

30. E.D. Fletcher and A.J. Douglas, "A Comparison of the Effects of Bending Moments on the Vibrations of AT and SC (or TTC) Cuts of Quartz", these proceedings.

31. T.J. Lukaszek and A. Ballato, "Resonators for Severe Environments", these proceedings.

32. A.W. Warner and D.L. White, "An Ultra-Precise Standard of Frequency", Eleventh Interim Report on Contract DA 36-039 SC-73078 to US Army Signal R&D Laboratory, Fort Monmouth, NJ, July 1959, 42 pp.

33. A.W. Warner, "Design and Performance of Ultraprecise 2.5-mc Quartz Crystal Units", Bell Syst. Tech. J., Vol.39, September 1960,pp.1193-1217.

34. D.L. Hammond, "Precision Quartz Resonators", Proc. 15th AFCS, May-June 1961, pp.125-138.

35. W.J. Spencer and W.L. Smith, "Precision Crystal Frequency Standards", Proc. 15th AFCS, May-June 1961, pp. 139-155.

36. E.A. Gerber, "Piezoelectric Accelerometer", US Patent No. 3,348,076, October 17, 1967.

37. M. Valdois, J. Besson, and J.-J. Gagnepain, "Influence of Environment Conditions on a Quartz Resonator", Proc. 28th AFCS, May 1974,pp. 19-32.

38. M. Valdois, "Étude de l'Influence d'Accélérations sur les Propriétés des Résonateurs à Quartz", Thèse, Universite' de Besançon, June 1974, 73 pp.

39. M. Valdois, "Influence des Conditions d'Environnement sur un Résonateur à Quartz", ONERA Note Technique No. 225, Châtillon, France, 1974, 75 pp.

40. P.C.Y. Lee and K.-M. Wu, "Effects of Acceleration on the Resonance Frequencies of Crystal Plates", Proc. 30th AFCS, June 1976, pp. 1-7.

41. J.-J. Gagnepain and F.L. Walls, "Quartz Crystal Oscillators with Low Acceleration Sensitivity", Technical Report NBSIR 77 - 855, National Bureau of Standards, Washington, DC 20234, March 1977, 15 pp.

42. J.A. Kusters, C.A. Adams, H. Yoshida, and J.G. Leach, "TTC's - Further Developmental Results", Proc. 31st AFCS, June 1977, pp. 3-7.

43. M. Onoe, K. Furusawa, S. Ishigami, T. Sase, and M. Sato, "Quartz Crystal Accelerometer Insensitive to Temperature Variation", Proc. 31st AFCS, June 1977, pp. 62-70.

44. D. Janiaud, "Influence du Support sur la Sensibilite' aux Accélérations d'un Résonateur à Quartz", C.R. Acad. Sc. Paris, t.285, Series B, 12 Sep 1977, pp. 69-72.

45. J.M. Przyjemski, "A Compensation Technique for Acceleration-Induced Frequency Changes in Crystal Oscillators", Technical Report P-606, The Charles Stark Draper Laboratory, Inc., Cambridge, MA 02139, February 1978, 6 pp.

46. P.C.Y. Lee, K.-M. Wu, and Y.S. Wang, "Effects of Acceleration on the Resonance Frequencies of Crystal Plates", J. Acoust. Soc. Am., Vol. 63, April 1978, pp. 1039-1047.

47. R. Allison and S.J. Goldman, "Vibration Effects on Close-In Phase Noise of a 300 MHz Surface Wave Resonator Oscillator", Proc. 32nd AFCS, May-June 1978, pp. 66-73.

48. J.M. Przyjemski, "Improvement in System Performance Using a Crystal Oscillator Compensated for Acceleration Sensitivity", Proc. 32nd AFCS, May June 1978, pp. 426-431.

49. P.C.Y. Lee and K.-M. Wu, "The Influence of Support-Configuration on the Acceleration Sensitivity of Quartz Resonator Plates", IEEE Trans. Sonics Ultrason., Vol. SU-25, July 1978, pp. 220-223.

50. M.M. Valdois and A.B. Dupuy, "Crystal Oscillator Compensated against Frequency Shift Due to Acceleration", U.S. Patent No. 4,100,512, July 11, 1978.

51. D.A. Emmons, "Acceleration Sensitivity Compensation in High Performance Crystal Oscillators", Proc. 10th PTTI, NASA Technical Memorandum 80250, Greenbelt, MD 20771, November 1978, pp. 55-82.

52. A. Warner, B. Goldfrank, M. Meirs, and M. Rosenfeld, "Low 'g' Sensitivity Crystal Units and their Testing", these proceedings.

53. R. Besson, J.-J. Gagnepain, D. Janiaud, and M. Valdois, "Design of a Bulk Wave Quartz Resonator Insensitive to Acceleration", these proceedings.

54. A. Ballato, "Doubly Rotated Thickness Mode Plate Vibrators", in Physical Acoustics: Principles and Methods, (W.P. Mason and R.N. Thurston, eds.) Vol.13, Chap.5. Academic Press, NY, 1977, pp. 115-181.

55. R.J. Besson, "Quartz Crystal and Superconductive Resonators and Oscillators", Proc. 10th PTTI, NASA Technical Memorandum 80250, Greenbelt, MD 20771, November 1978, pp. 101-128.

56. P.C.Y. Lee and K.-M. Wu, "Coupled Resonances in Doubly Rotated Crystal Plates", these proceedings.

57. I. Koga, "Notes on Piezoelectric Quartz Crystals", Proc. IRE, Vol. 24, March 1936, pp. 510-531.

58. D.A. Venn and G.W. Arnold, Jr., "Dual-Crystal Operation for Improved Frequency Stability with Varying Temperature", NRL Report 3892, Naval Research Laboratory, Washington, DC, November 1951, 10 pp.

59. J. Vig, USAERADCOM, Fort Monmouth, NJ 07703, private communication, January 1978.

60. A. Ballato, "Transmission-Line Analogs for Stacked Piezoelectric Crystal Devices", Proc. 26th AFCS, June 1972, pp. 86-91.

61. A. Ballato and T. Lukaszek, "A Novel Frequency Selective Device: The Stacked-Crystal Filter", Proc. 27th AFCS, June 1973, pp. 262-269.

62. A. Ballato and T. Lukaszek, "Stacked-Crystal Filters", Proc. IEEE, Vol. 61, October 1973, pp. 1495-1496.

63. A. Ballato, H.L. Bertoni, and T. Tamir, "Systematic Design of Stacked-Crystal Filters by Microwave Network Methods", IEEE Trans. Microwave Theory Tech., Vol. MTT-22, January 1974, pp. 14-25.

64. C.M. Stearns, S. Wanuga, S. W. Tehon, and A. Kachelmyer, " Multi- Mode Stacked Crystal Filter", Proc. 31st AFCS, June 1977, pp. 197-206.

65. I. Koga, "Piezoelectricity and its Applications", J. Inst. Electr. Eng. Jpn, July 1929,pp. 49-92.

66. W.G. Cady and K.S. Van Dyke, "Proposed Standard Conventions for Expressing the Elastic and Piezoelectric Properties of Right- and Left-Quartz", Proc. IRE, Vol. 30, November 1942, pp. 495-499.

67. W.G. Cady, Piezoelectricity, McGraw-Hill, New York, 1946; Dover, New York, 1964.

68. "Standards on Piezoelectric Crystals, 1949", Proc. IRE, Vol. 37, No. 12, Dec. 1949, pp. 1378-1395.

69. "IEEE Standard on Piezoelectricity", Standard 176-1978, IEEE, New York, September 1978, 55 pp.

70. J.D.H. Donnay and Y. Le Page, "The Vicissitudes of the Low- Quartz Crystal Setting or the Pitfalls of Enantiomorphism", Acta Cryst., Vol. A34, 1 July 1978, pp. 584-594.

71. J.D.H. Donnay, McGill Univ., Montreal, PQ, Canada H3A 2A7, private communication, December 1978.

72. M.J. Buerger, Harvard Univ., Cambridge, MA 02138, private communication, December 1978.

73. C.J. Schneer, Univ. New Hampshire, Durham, NH 03824, private communication, January 1979.

74. R.E. Newnham and L.E. Cross, "Tailored Domains in Quartz and Other Piezoelectrics", Proc. 30th AFCS, June 1976, pp. 71-77.

75. T.L. Anderson, R.E. Newnham, and L.E. Cross, "Coercive Stress for Ferrobielastic Twinning in Quartz", Proc. 31st AFCS, June 1977, pp. 171-177.

76. H. Yoda, "Quartz Crystal Units Utilizing Twinned Natural Raw Quartz", Presented at 15th AFCS, May-June 1961, printed separately, 8 pp.

77. C.B. Sawyer, "Progress in Engineering Cultured Quartz for Use by the Crystal Industry", Proc. 13th AFCS,May 1959, pp. 462-476.

78. W.E. Newell, "Face-Mounted Piezoelectric Resonators", Proc. IEEE, Vol. 53, June 1965, pp. 575-581.

79. W.E. Newell, "Ultrasonics in Integrated Electronics", Proc. IEEE, Vol. 53, Oct. 1965, pp. 1305-1309.

80. Clevite Corporation Staff, Piezoelectric Technology Data for Engineers, Piezoelectric Division, Clevite Corporation, Bedford,Ohio 44146, 1965, 45 pp.

81. J. van Randeraat, Ed., Piezoelectric Ceramics, Electronic Components and Materials Division, N. V. Philips' Gloeilampenfabrieken, Einhoven, The Netherlands, June 1968, 118 pp.

82. T.F. Hueter and R.H. Bolt, Sonics, (Wiley, New York, 1955), Sec. 4.12, pp. 136-146.

83. R. Holland, "The Linear Theory of Multielectrode Piezoelectric Plates", 1966 WESCON Convention Record, Vol. 10, part 3, paper 3/3, 15 pp.

84. E.P. EerNisse, "Resonances of One-Dimensional Composite Piezoelectric and Elastic Structures", IEEE Trans. on Sonics and Ultrasonics, Vol. SU-14, April 1967, pp. 59-67.

85. E.K. Sittig, "Transmission Parameters of Thickness-Driven Piezoelectric Transducers Arranged in Multilayer Configurations", IEEE Trans. on Sonics and Ultrasonics, Vol. SU-14, Oct. 1967, pp. 167-174.

86. E.K. Sittig, A.W. Warner, and H.D. Cook, "Bonded Piezoelectric Transducers for Frequencies Beyond 100 MHz", Ultrasonics, Vol. 7, April 1969, pp. 108-112.

87. O.M. Stuetzer, "Piezoelectric Pulse and Code

Generators", IEEE Trans. on Sonics and Ultrasonics, Vol. SU-14, April 1967, pp. 75-88.

88. R.F. Mitchell and M. Redwood, "Frequency Response of a Distributed Piezoelectric Source of Sound", Electron. Lett., Vol. 4, Mar. 1968 pp. 107-109.

89. R. Holland and E.P. EerNisse, Design of Resonant Piezoelectric Devices, (M.I.T. Press, Cambridge, Mass., 1969), Sec. 2.4, pp. 89-95.

90. D.I. Bolef and M. Menes, "Measurement of Elastic Constants of RbBr, RbI, CsBr, and CsI by an Ultrasonic cw Resonance Technique", J. Appl. Phys., Vol. 11, June 1960, pp. 1010-1017.

91. T.R. Sliker and D.A. Roberts, "A Thin-Film CdS-Quartz Composite Resonator", J. Appl. Phys., Vol. 38, April 1967, pp. 2350-2358.

92. D.A. Roberts, D.J. Koneval and T.R. Sliker, "Alternate Approaches to High Frequency Filter Crystals", Proc. 21st AFCS, April 1967, pp. 83-114.

93. R.J. Ney and E. Hafner, "Continuous Vacuum Processing System for Precision Quartz Crystal Units", these proceedings.

94. E.P. EerNisse, "Quartz Resonator Frequency Shifts Arising from Electrode Stress", Proc. 29th AFCS, May 1975, pp. 1-4.

95. E.P. EerNisse, "Calculations on the Stress Compensated (SC-cut) Quartz Resonator", Proc. 30th AFCS, June 1976, pp. 8-11.

96. R. Holland, "Nonuniformly Heated Anisotropic Plates: II. Frequency Transients in AT and BT Quartz Plates", Proc. IEEE Ultrason. Symp., November 1974, pp. 592-598.

97. J.A. Kusters, "Transient Thermal Compensation for Quartz Resonators", IEEE Trans. Sonics Ultrason., Vol. SU-23, July 1976, pp. 273-276.

98. J.A. Kusters and J.G. Leach, "Further Experimental Data on Stress and Thermal Gradient Compensated Crystals", Proc. IEEE, Vol. 65, February 1977, pp. 282-284.

99. A. Ballato and J.R. Vig, "Static and Dynamic Frequency-Temperature Behavior of Singly and Doubly Rotated, Oven Controlled Quartz Resonators", Proc. 32nd AFCS, May-June 1978, pp. 180-188.

100. A. Ballato, "Static and Dynamic Frequency-Temperature Characteristics of Quartz Vibrators", Technical Report DELET-TR-79-8, US Army Electronics R&D Command, Fort Monmouth, NJ 07703, April 1979, 28 pp.

101. A. Ballato, "Static and Dynamic Behavior of Quartz Resonators", IEEE Trans. Sonics Ultrason., Vol. SU-26, July 1979, in press.

102. D.R. Kinloch, Sawyer Research Products Inc., Eastlake, OH 44094, private communication, January 1977.

103. N.C. Lias, Motorola Inc., Carlisle, PA 17013, private communication, November 1978.

104. P. Suda, A.E. Zumsteg, and W. Zingg, "Anisotropy of Etching Rate for Quartz in Ammonium Bifluoride", these proceedings.

105. R. Brandmayr, R. Filler, and J. Vig, "Etching Studies on Quartz", these proceedings.

---

*AFCS: Annual Frequency Control Symposium, US Army Electronics R&D Command, Fort Monmouth, NJ 07703.

Note added:

R. Ward[106] has pointed out that Y-bars of cultured quartz (Figure 8) can be cut in such a fashion that SC cuts are produced with a yield approximately 30% better than if an SC-bar (Figure 25) is used directly. This possibility is brought about by the three-fold symmetry existing about the Z axis in quartz. Referring to Figure 8, a Y-cut, for example, could be made by cutting perpendicular to the X_2 axis shown. It could also be made by cutting perpendicular to either of the two other X_2 axes spaced around the X_3 axis at intervals of 120^0. In either of the latter cases the area of the slices would be larger than that in the first case. In like manner, to produce SC cuts one could either rotate first around X_3 from X_1 toward X_2 by approximately 22^0, and then make the second rotation about the new X_1' axis, or one could rotate $120^0 + 22^0$, or $240^0 + 22^0$ for the first rotation about X_3 . The second choice, namely $\phi \simeq 262^0$ produces a rotation that leaves the new X_1' axis only about 8^0 (270^0-262^0) from the original $-X_2$ axis. One is then nearly rotating about the length of the Y-bar for the second (θ) rotation. (Because the $-X_2$ axis is involved, the sense of the θ rotation is reversed). Cutting in this fashion is thus nearly as efficient as cutting ATs; one wants, however, to have the X_1 dimension as long as possible. At present, approximately 40 mm along X_3 is standard, and 75 to 100 mm along X_1 can be readily made.

---

106. R. Ward, Colorado Crystal Corp., Loveland, CO 80537, private communication, July 1979.

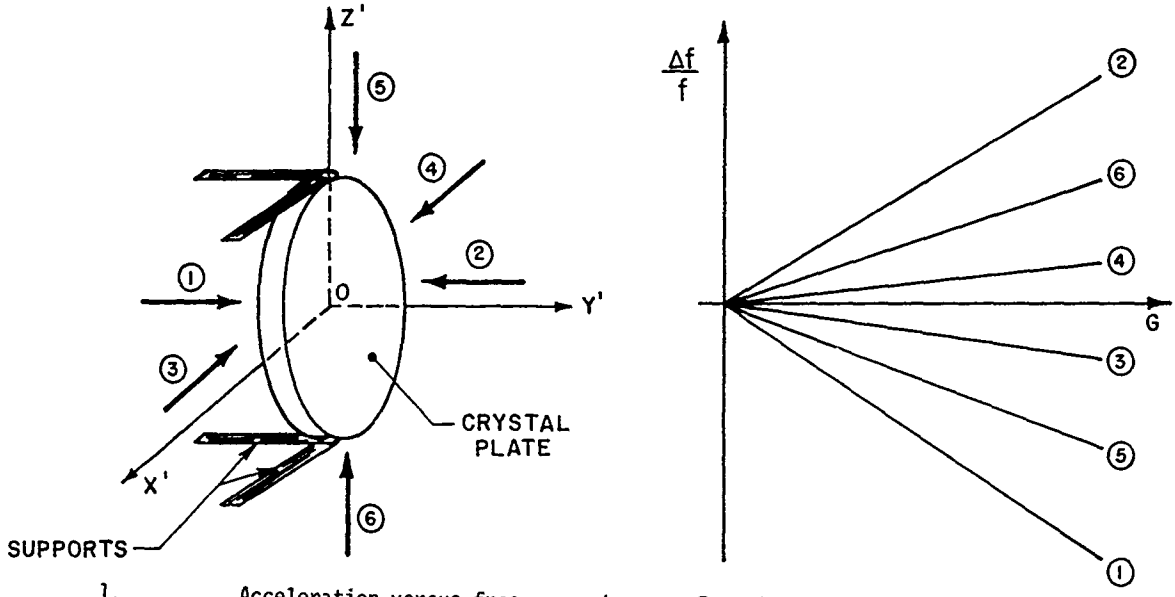

1. Acceleration versus frequency change. Experimental results for AT cut quartz in two-poirt mount. After Valdois [38].

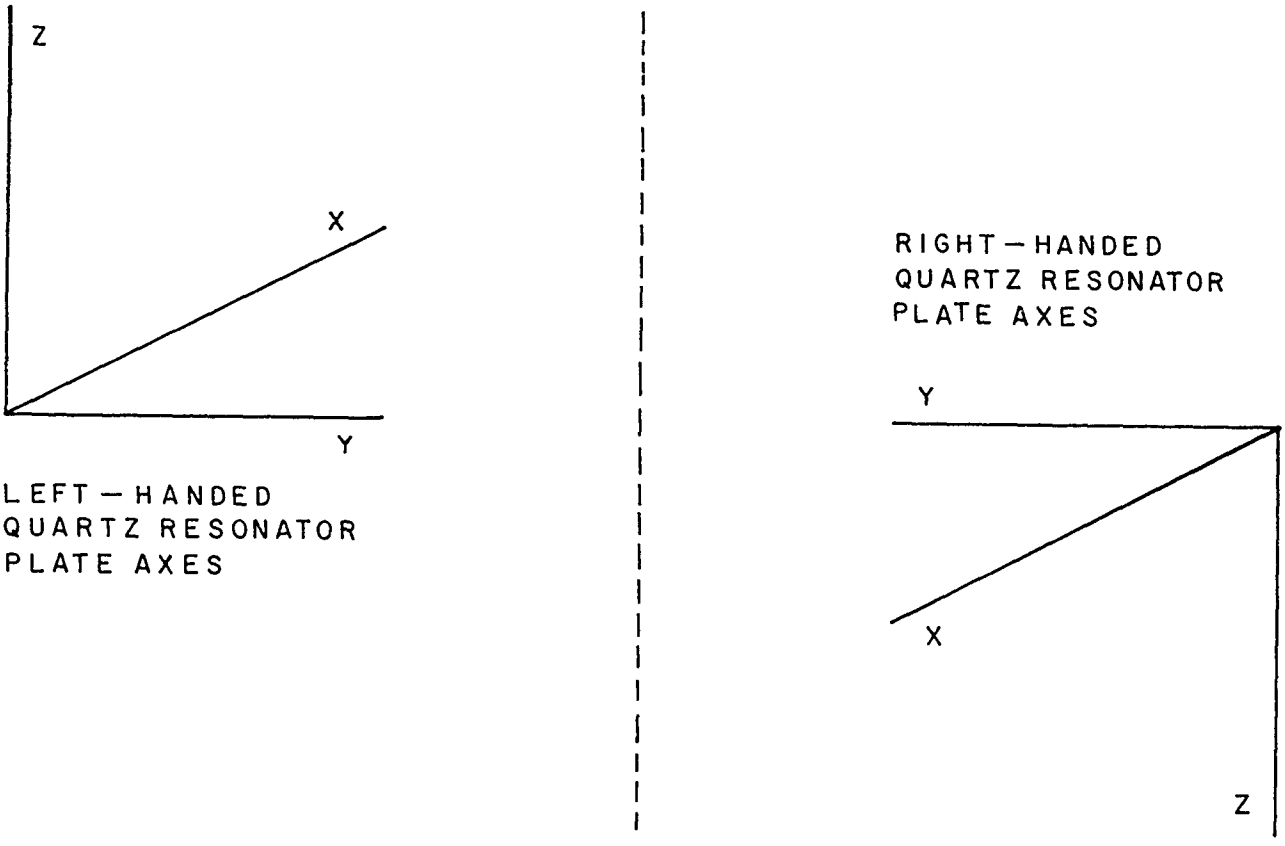

2. Antiparallel axes of enantiomorphs.

	CRYSTAL SYSTEM	CLASS NUMBER	HERMANN-MAUGUIN - SYMBOL	NUMBER OF ELASTIC COEFFICIENTS	
				SECOND ORDER	THIRD ORDER
I	TRIGONAL	1	1	21	56
II	MONOCLINIC	3	2	13	32
III	ORTHORHOMBIC	6	222	9	20
IV a	TETRAGONAL	9	4	11/7	28/16
IV b		12	422	9/6	20/12
V a	TRIGONAL	16	3	15/7	50/20
V b		18	32	12/6	31/14
VI a	HEXAGONAL	21	6	9/5	28/12
VI b		24	622	9/5	20/10
VII a	CUBIC	28	23	9/3	20/8
VII b		30	432	9/3	20/6

3. The eleven enantiomorphous crystal classes.

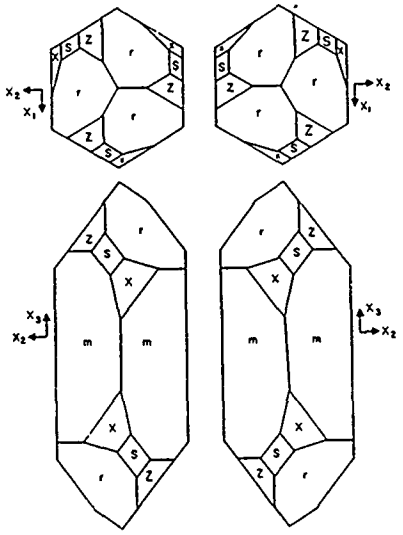

4. Quartz pairs. Looking down $+X_3$(top), and down $+X_1$ (bottom) axes.

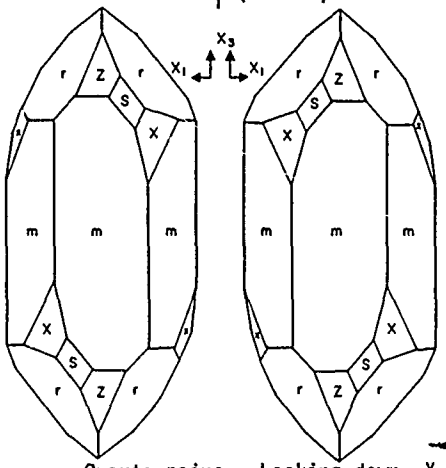

5. Quartz pairs. Looking down $-X_2$ axis.

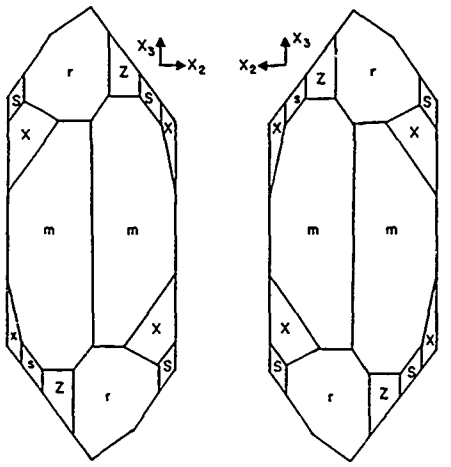

6. Quartz pairs. Looking down $-X_1$ axis.

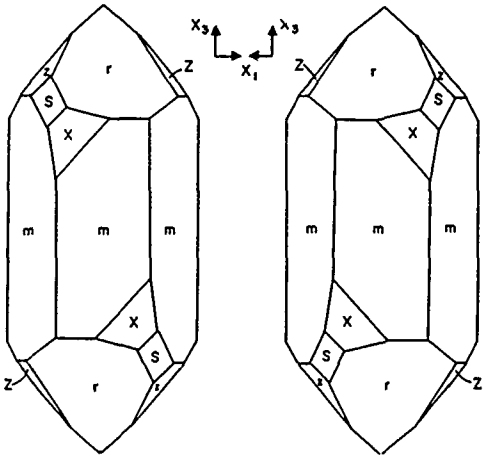

7. Quartz pairs. Looking down $+X_2$ axis.

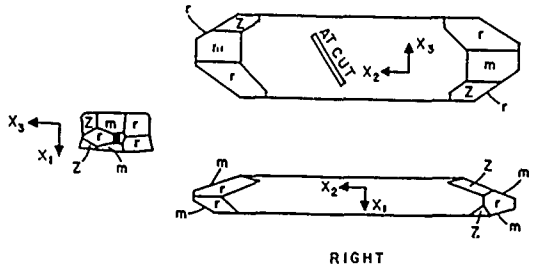

8. Cultured quartz bar, right-handed.

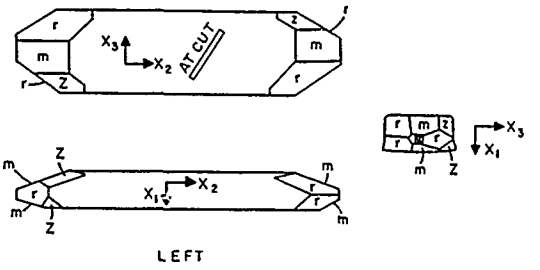

9. Cultured quartz bar, left-handed.

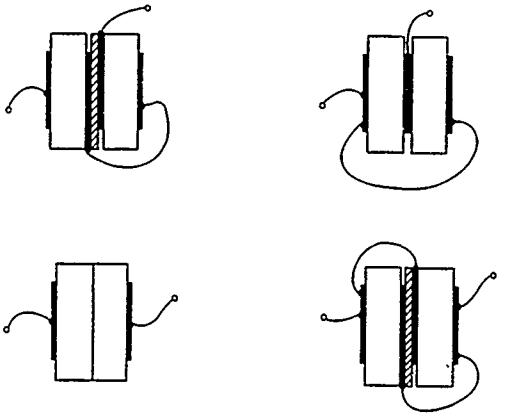

10. Stacked crystal vibrator configurations.

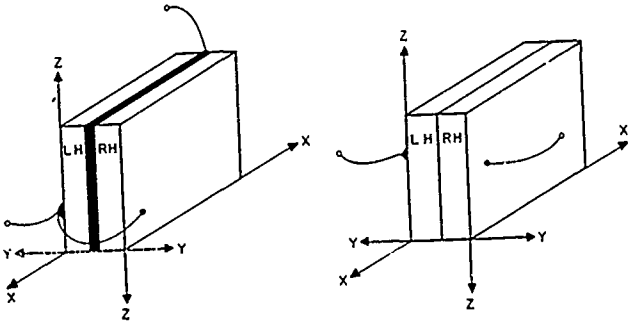

11. Simplest stacked crystal vibrators.

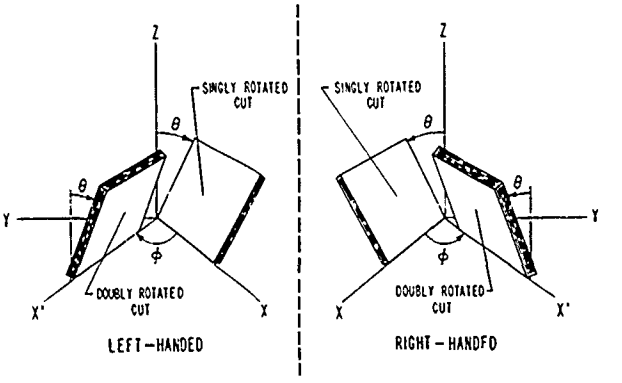

12. Singly and doubly rotated enantiomorphs.

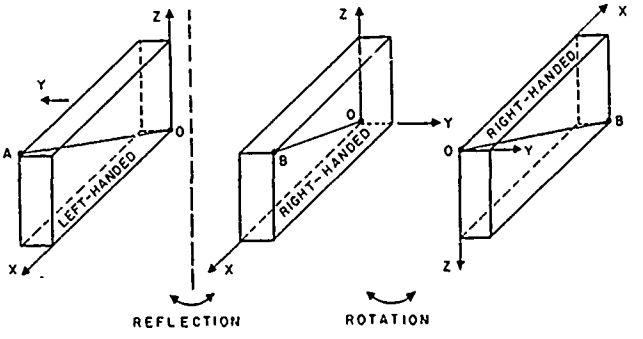

13. Demonstration of parallel displacements in doubly rotated enantiomorphs.

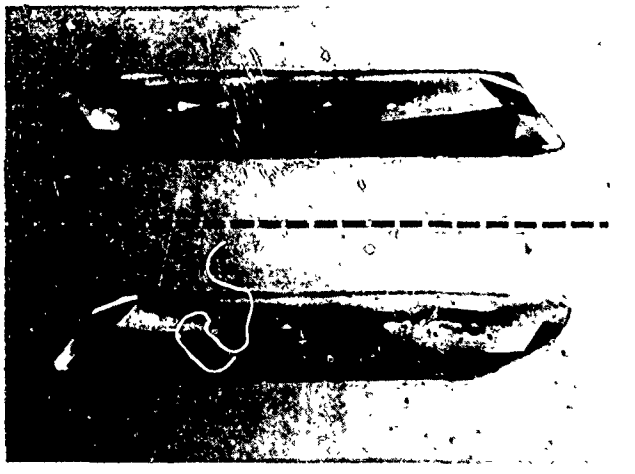

14. Left-handed (top) and right-handed cultured quartz SC-bars, seen looking down $+X_3$ axes.

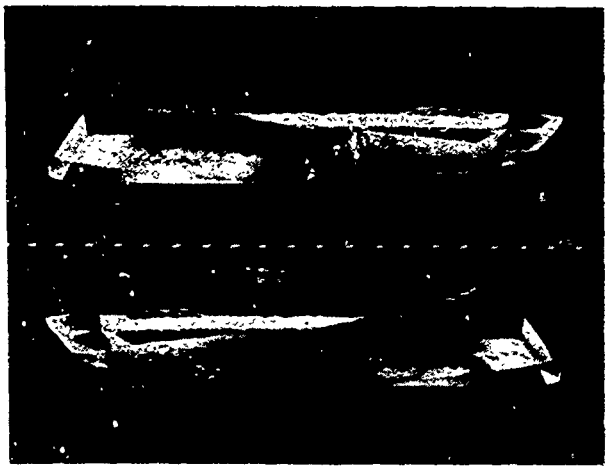

15. Left-handed (top) and right-handed cultured quartz SC-bars, seen looking down $-X_3$ axes.

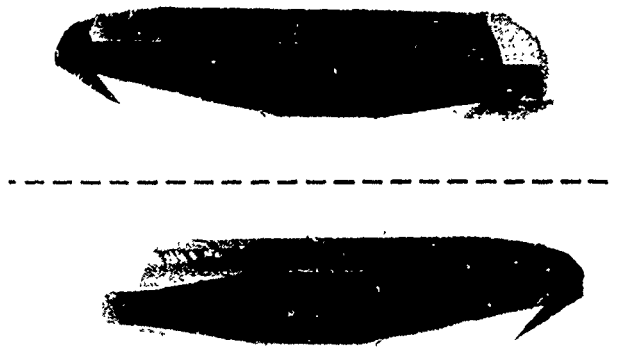

16. Left-handed (top) and right-handed cultured quartz SC-bars, seen looking down $-X_1$ axes.

17. Left-handed (top) and right-handed cultured quartz SC-bars, seen looking down $+X_1$ axes.

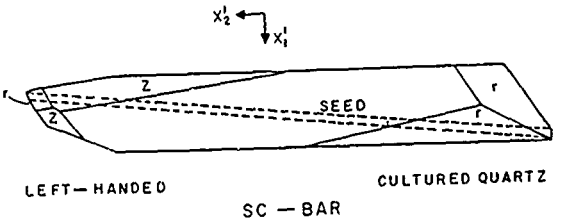

18. Line drawing of Figure 14 (top).

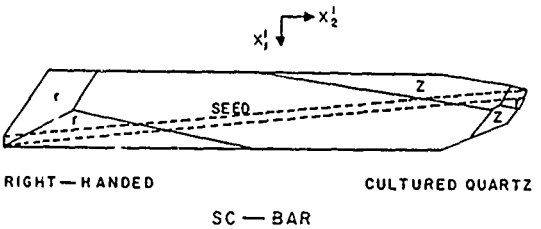

19. Line drawing of Figure 14 (bottom).

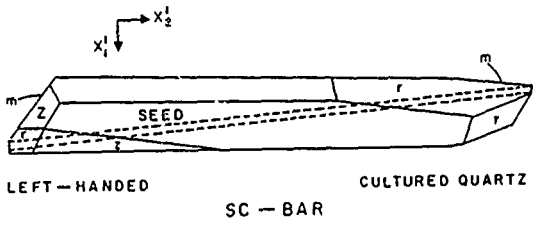

20. Line drawing of Figure 15 (top).

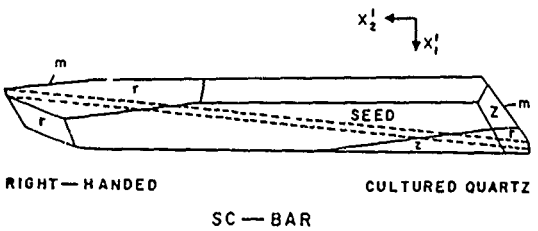

21. Line drawing of Figure 15 (bottom).

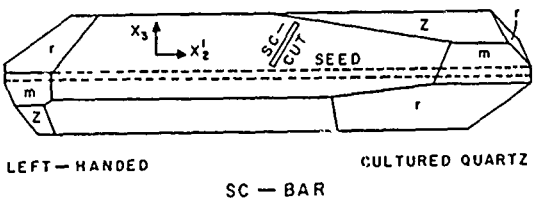

22. Line drawing of Figure 16 (top).

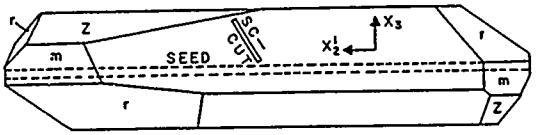

RIGHT—HANDED CULTURED QUARTZ

SC—BAR

23. Line drawing of Figure 16 (bottom).

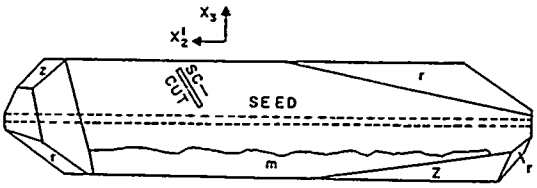

LEFT—HANDED CULTURED QUARTZ

SC—BAR

24. Line drawing of Figure 17 (top).

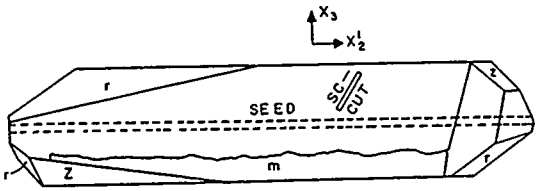

RIGHT—HANDED CULTURED QUARTZ

SC—BAR

25. Line drawing of Figure 17 (bottom).

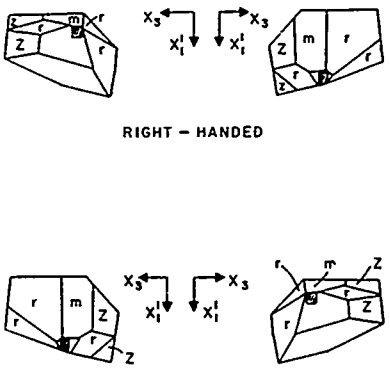

SC—BAR CULTURED QUARTZ

26. Line drawing of left- and right-handed cultured quartz SC-bars, seen looking down the $+X_2$ and $-X_2$ axes.

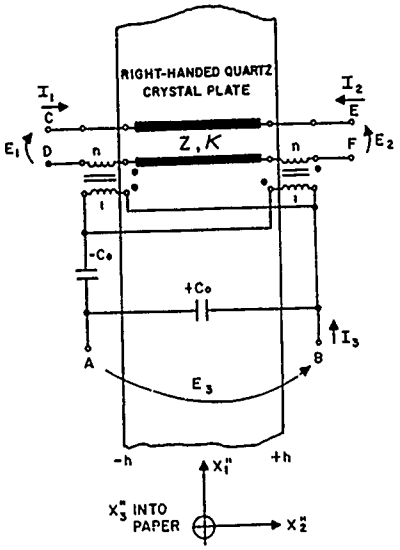

27. Analog equivalent network for right-handed quartz crystal plate with one thickness mode piezoelectrically driven.

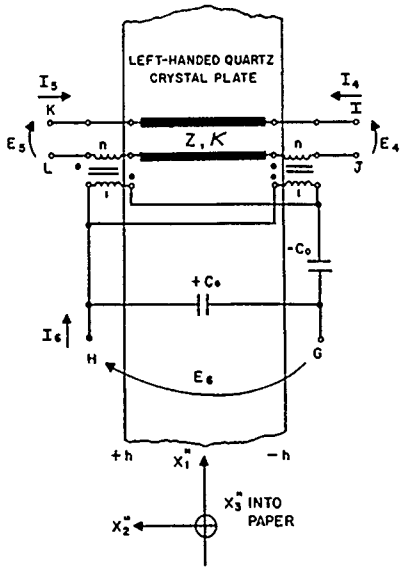

28. Analog equivalent network for left-handed quartz crystal plate with one thickness mode piezoelectrically driven.

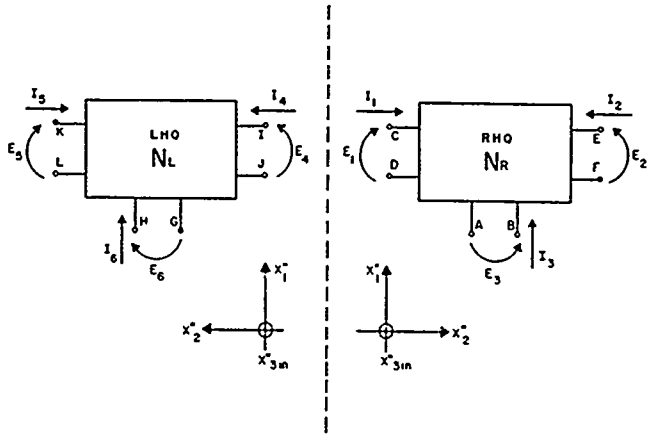

29. Networks of Figures 27 and 28 regarded as mirror images.

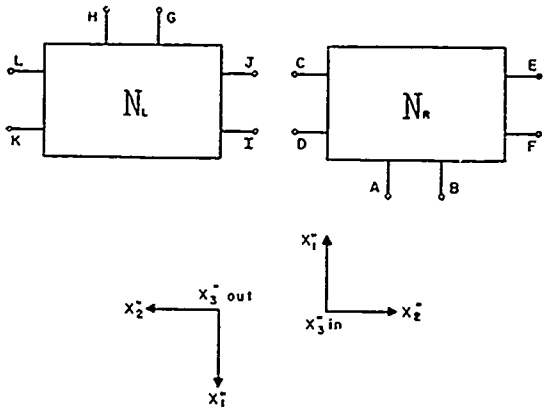

30. Networks of Figure 29 arranged with crystal axes antiparallel.

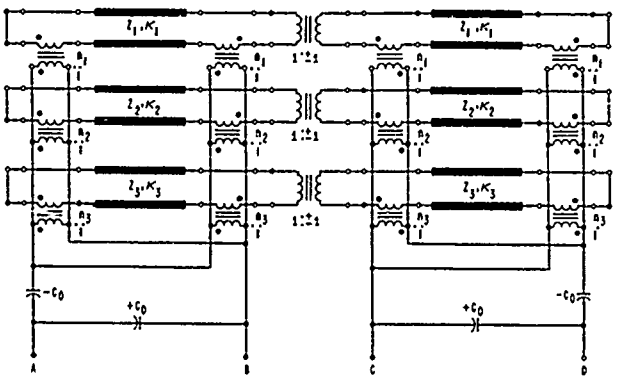

31. Analog equivalent network for two stacked quartz plates with all three thickness modes piezoelectrically excited in each plate, as is the case for doubly rotated cuts.

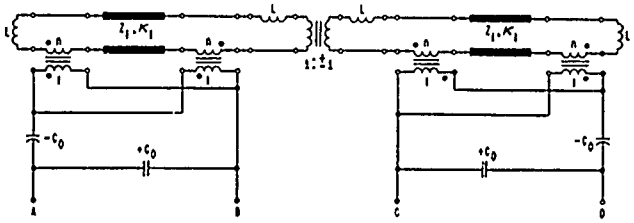

32. Analog equivalent network for two stacked quartz plates with only one thickness mode piezoelectrically excited.

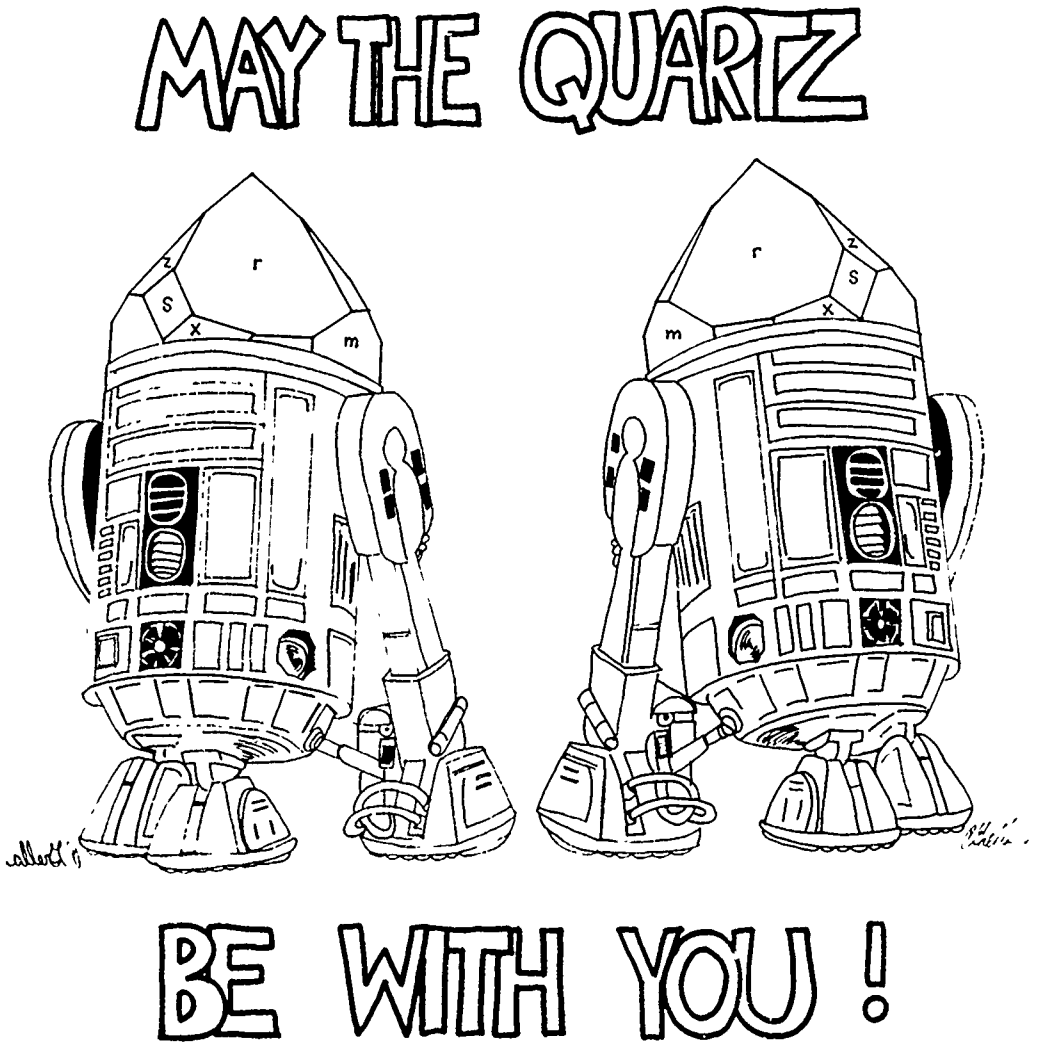

33. Mr. R2D2 (right-rechts-dexter-droit) and Mr. L2SG, enantiomorphs.

DESIGN OF A BULK WAVE QUARTZ RESONATOR INSENSITIVE TO ACCELERATION

R. Besson[+], J.J. Gagnepain[++], D. Laniaud[+++], M. Valdois[+++]

+ Ecole Nationale Supérieure de Mécanique et des Microtechniques Besançon France
++ Laboratoire de Physique et Métrologie des Oscillateurs du C.N.R.S. Besançon France
+++ Office National d'Etudes et de Recherches Aérospatiales 92320 Chatillon France

Summary

Regular thickness shear vibrating AT cut quartz crystal resonators at 5 MHz usually have a G-frequency sensitivity in the order of a few 10^{-9}/G.

Previous theoretical works shown the influence of the angular position of the fixation points on the edges of the resonators. This does not completely explain the experimental behaviour observed in ONERA. Then, a more precise theoretical model is proposed ; it shows that the principal influence is due to the dissymmetry of the total device constituted by the crystal and its supports, with respect to the middle nodal plane of the vibration.

By calculating the static predeformation which is caused by the dissymmetry it is shown that a transverse shear, and its functionnal dependance, along the thickness, are mainly responsible of the phenomena. The frequency variation is taking into account energy trapping.

This theoretical model gives a very close account of the results with regular units and has been confirmed by the achievement of a symmetrical resonator prototype.

The B.V.A. technique is very suitable for such a symmetrical configuration. Resonators of industrial type have been achieved. Details are given about several types of design which were successfully used. They present a sensitivity in the order of 10^{-10}/G for AT cut units and therefore an improvement by a factor of a least 10 compared to regular units. A dual B.V.A. resonator configuration is also described which still allows additional G sensitivity reduction.

Introduction

It is well known that application of acceleration fields on quartz resonators changes the resonant frequency. Also the resulting frequency variation depends on the resonator features and on the acceleration amplitude and direction with respect to the resonator axis[1].

Measurements performed in ONERA on regular AT cut 5 MHz thickness shear vibrating industrial units exhibited maximum sensitivities between 3 and 4 x 10^{-9}/G.

A previous theoretical work[2] explained these phenomena through angular imperfections of the support configuration.

But a resonator for which the support configuration especially is excellent from the angular imperfection point of view was constructed, and nevertheless the G-sensitivity is still some 10^{-9}/G.

Further theoretical studies were undertaken and lead to a different model since it is found that the main reason for the G-sensitivity sits in a configuration dissymmetry in the whole device constituted by the crystal and its supports[3].

In a first step a simplified model will be presented. The supports are only represented by their fixation points on the crystal. Then a more complete model, which takes into account the geometry and support configuration, will be proposed. This last model will exhibit the important part played by the configuration of the total device.

Simplified model of the resonator

A circular thickness shear vibrating plate is supported in two diametric points and submitted to an acceleration Γ parallel to the plate plane as shown on fig. 1. The supports are positionned along the projected x_3 axis. Γ being parallel to the plate plane and the thickness being small, a plane stress distribution can be assumed.

Since the main faces $x_2 = \pm h/2$ are stress free, the stresses T_2, T_4, T_6 equal zero on those faces and therefore can also be considered to be zero in the all plate thickness.

At first the three other stresses T_1, T_3, T_5 were analitycally determined in the case of an isotropic body. Then a more accurate solution has been found for anisotropic bodies and applied to quartz crystal[4]. Thus it has been shown that all stresses at the plate center are zero. But the central part of the resonator is mainly where energy is trapped. Therefore this simplified model is unable to give account of the acceleration sensitivity.

Influence of the support configuration

The industrial units that have been studied generally are constituted by a quartz plate and its supports, those last ones being perpendicular to the main planes of the plate, as shown on fig. 2. The supports are constituted by ribbons which has been folded in three equal parts.

Acceleration parallel to x_3 axis

A bidimensional model is used in the transverse x_2x_3 plane of the resonator. When an acceleration component Γ_3 is applied the crystal is submitted from its supports to axial and shear forces F and to moments M (fig. 3). A trivial calculation yields :

$$F_3 = \frac{Dh}{2} \rho \Gamma_3 \qquad (1)$$

$$F_{2A} = F_{2B} = \frac{\ell}{D - \frac{\ell}{2}} F_3 \qquad (2)$$

$$M = \frac{D}{D - \frac{\ell}{2}} \cdot \frac{\ell}{2} \cdot F_3 \qquad (3)$$

It appears a static shear of the crystal on the lateral sides $x_3 = \pm \frac{D}{2}$ due to the forces F_{2A} and F_{2B}.

The in-plane static stresses resulting of the combination of the body and reaction forces are calculated for an isotropic body[3]. The medium anisotropy will be later introduced by means of the strain-stress relations. Those stresses can be expressed as

$$T_2 = 0 \qquad (4)$$

$$T_3 = -\rho \Gamma_3 x_3 + \frac{6\ell}{h^2} \frac{D}{D - \frac{\ell}{2}} \rho \Gamma_3 x_2 x_3 \qquad (5)$$

$$T_4 = -\frac{3\ell}{h^2} \frac{D}{D - \frac{\ell}{2}} \rho \Gamma_3 \left(x_2^2 - \frac{h^2}{4}\right) \qquad (6)$$

By consideration of energy trapping it can be shown that it is sufficient to consider the stresses at the plate center. In this case, only T_4 is different from zero and its average value $\langle T_4 \rangle$ is

$$\langle T_4 \rangle = \frac{\ell}{2} \frac{D}{D - \frac{\ell}{2}} \rho \Gamma_3 \qquad (7)$$

By using Thurston's non linear equations[5] and by applying a perturbation method the relative frequency deviation can be expressed as

$$\frac{\Delta f}{f} = \lambda \langle T_4 \rangle$$

where

$$\lambda = \frac{1}{2C_{66}} \left((C_{661} + 2C_{66}) s_{14} + C_{662}\, s_{24} + C_{663}\, s_{34} + C_{664}\, s_{44}\right) \qquad (8)$$

The variations of λ as a function of the angle θ (rotation around the x_1 axis) is given by fig. 4. It can be seen that λ vanishes for four values of θ between 0° and 180°. As a consequence the theoretical Γ_3 sensitivity of the resonator also vanishes for those orientations. For an AT cut $\lambda = 3.5 \times 10^{-11}$ m²/N.

These results are applied to the practicle case of regular AT cut units (where the support lengths ℓ = 5 mm). Their corresponding Γ_3 sensitivity is found to be

$$\frac{\Delta f}{f} = 2.7 \times 10^{-9}/G$$

It can be pointed out that the frequency deviation being due to the action of the tangential forces F_{2A} and F_{2B}, the support dissymetry with respect to the crystal x_1x_2 median plane is the main cause of the Γ_3 sensitivity.

Under those conditions in order to symmetrize the resonator and to cancell out F_{2A} and F_{2B} other supports, symmetric of the previous ones with respect to median x_1x_3 plane, are to be added as shown on fig. 5a and fig. 5b, whatever their original shape is.

Remark : The sign of the frequency shift depends if the acceleration is applied in the positive direction or in the negative direction of the x_3 axis. For the units manufactered outside the laboratory it was not possible to know the positive (or negative) direction of the axis. Therefore for the experimental results the sign associated with the frequency shifts are arbitrary.

Acceleration parallel to x_2 axis

When an acceleration component Γ_2 is applied on the resonator the crystal is submitted to the reaction forces and moments as shown on fig. 6. The same calculation as previously gives

$$F_2 = \frac{\pi h D^2}{8} \rho \Gamma_2 \qquad (9)$$

$$F_{3A} = F_{3B} = \frac{3}{4} F_2 \qquad (10)$$

$$M = \frac{\ell}{8} F_2 \qquad (11)$$

The tangential force F_2 does not induce any shear deformation in the crystal and the longitudinal and shear stresses due to the moments M_A and M_B are in average null in the crystal and equally null at its center ($x_3 = 0$).

Nevertheless F_{3A} and F_{3B} generate a compressive stress in the crystal, whose influence already has been presented[4]. By using those results the theoretical frequency shift is calculated for a AT cut resonator

$$\frac{\Delta f}{f} = -3 \times 10^{-9}/G$$

It must be pointed out that the forces F_{3A} and F_{3B} which are responsible of the frequency deviation would be zero if the support ribbons were not folded. The conclusion would be the same, whatever the shape of the support ribbons is, if the resonator was symmetrical with respect to the median plane x_1x_3 as shown on fig. 5a and 5b.

As a result of the previous calculations it is now possible to obtain the frequency deviation versus the acceleration orientation in the x_2x_3 plane.

This theoretical curve is obtained by adding the effects of Γ_2 and Γ_3 accelerations.

Since it is difficult to know the positive direction (or negative) of x_3 axis for an actual industrial unit, an uncertainty remains and it was necessary to draw two sets of theoretical curves, corresponding to the possible combinations, for comparison with experimental data. This comparison is presented by fig. 7, with a satisfactory agreement, in the case of four industrial resonators of the type previously described. (Q_1, Q_2, Q_3 and Q_4).

The experimental frequency deviations were recorded for an azimuthal angle varying from 0° to 360° by 10° step.

Resonators of special configuration

Particular support configurations also have been studied. The first one is represented by the scheme of fig. 8 and is constituted of four supports ribbons perpendicular to the plate plane and positionned at 45° of x_1 and x_3 axis. As the previous ones, this resonator is dissymmetric with respect to the x_1x_3 plane. Fig. 9 represents a resonator supported at to diametric points along the x_3 axis by in-plane ribbons, which are not parallel but form an angle of about 15°. The dissymmetry is now with respect to the transverse plane x_2x_3.

By using the previous model a comparison between experimental and theoretical data was performed and is shown on fig. 10 and 11 for the four support resonator (30 G acceleration was used).

Fig. 12 shows the comparison in the case of the two support configuration.

Design of B.V.A. units with very low G-sensitivity

The B.V.A. technique has already been presented[6,7]. It can easily be seen that the $B.V.A_n$ types, with n even, are suitable for a very symmetrical configuration. Indeed, as it has already been pointed out, the fixation consists of quartz bridges of given shape, length and thickness which are left between the external dormant part (usually a ring) and the internal vibrating part of the crystal. Those bridges, when the technique is mastered, can be evaluated and located with a high degree of accuracy. Especially, the bridges can be very precisely located by respect to the thickness of the crystal (accuracy of the location ± 5 μ if necessary). Since the shape of the bridges can also be evaluated with precision, a high degree of symmetry by respect to the central nodal plane (plane x_1x_3) can be achieved. In addition, in this type of fixation, stresses can be avoided (stresses could be dissymetrical) and there are no discontinuities (which could, in particular cause stresses). As a side consequence no residual frequency deviation is observed in B.V.A. units when the acceleration is suppressed. Also, the angular position of the bridges can be accurately achieved and known. Under those conditions, such B.V.A. units have a very low G-sensitivity provided the external dormant is, itself, symmetrically connected to the mechanical reference by respect of the central nodal plane x_1x_3. Also biconvex units are found to exhibit lower G-sensitivity. Of course, the G-sensitivity does not depend on the fact the unit is coated or electrodeless. This detail will then be neglected on the following schemes.

The final design we adopted is outlined on schemes of fig. 13. The supports s are attached to the external ring in two points A, B (or four points A A' B B' as represented) in such a way that the connections to the mechanical reference R are symmetrical by respect to the central nodal plane (espacially AP = AM). In addition, the attachment points A A' B B' are located on the external ring[8] outside the bridge area and symmetrically by respect to the bridges and the axis of the plate, at least for singly rotated cuts. In addition to the symmetry properties, this special location provides a reduction of the stresses to be transmitted through the bridges from the attachment to the vibrating plate. A maximum sensitivity in the order of 10^{-10}/G can be achieved in the case of AT cut units. In the case of SC cuts, the bridges are differently located but the supports are still symmetrical by respect to the bridges. A sensitivity lower than $5\ 10^{-11}$/G is obtained.

A B.V.A. dual resonator configuration has also been proposed and tested. The scheme of fig. 14 shows this design comprising basically[9] two B.V.A. resonators R_1 and R_2. If the axis are respectively oriented as indicated on fig. 14 (drawn for the AT cut case) very low G sensitivity is obtained, by a compensation process, for the total device. An additionnal reduction factor ranging from 2 to 5 can actually be obtained. R_1 and R_2 can obviously be used in parallel or in series. Also their frequencies can be identical or different. When R_1 and R_2 are used in a parallel configuration, their frequency difference basically does not depend on temperature[10] if the temperature dependances of R_1 and R_2 are similar enough. Among other advantages this new B.V.A. structure gives R_1 a very precise orientation by respect to R_2 and places R_1 and R_2 in very similar thermal conditions.

References

(1) M. Valdois, J.J. Gagnepain, J. Besson, "Influence on environment conditions on a quartz resonator", 28th Ann. Freq. Cont. Symp. (1974).

(2) P.C.Y. Lee, Kuang-Ming-Wu, "Effects of acceleration on the resonance frequencies of crystal plates", 30th Ann. Freq. Cont. Symp. Fort Monmouth (1976).

(3) D. Janiaud, "Modélisation de l'influence d'une accélération sur la fréquence des résonateurs à quartz", Thèse de Docteur-Ingénieur, Besançon (1978).

(4) D. Janiaud, L. Nissim, J.J. Gagnepain, "Analytical calculation of initial stress effects on anisotropic crystals : application to quartz resonators", 32nd Ann. Freq. Cont. Symp., Fort Monmouth (1978).

(5) R.N. Thurston, "Wave propagation in fluids and normal solids", Physical Acoustics, vol. 1, part. A, Academic Press (1966).

R.N. Thurston, J.H. Mac Skimmin, P. Andreatch, "Third-order elastic coefficients of quartz", Journal of Appl. Phys., vol. 37, n° 1, 267-275, (jan. 1966).

(6) R.J. Besson, "A new piezoelectric resonator design", 30th Ann. Freq. Cont. Symp., Fort Monmouth, (1977).

(7) R.J. Besson, "Quartz crystal and superconductive resonators and oscillators", Tutorial 10th PTTI, Washington, (nov. 1978).

(8) Patent pending

(9) R.J. Besson, French Patent, n° 7828728.

(10) R.J. Besson, M. Decailliot, C.R. Acad. Sc. Paris, 288, B57, (22-1-1979).

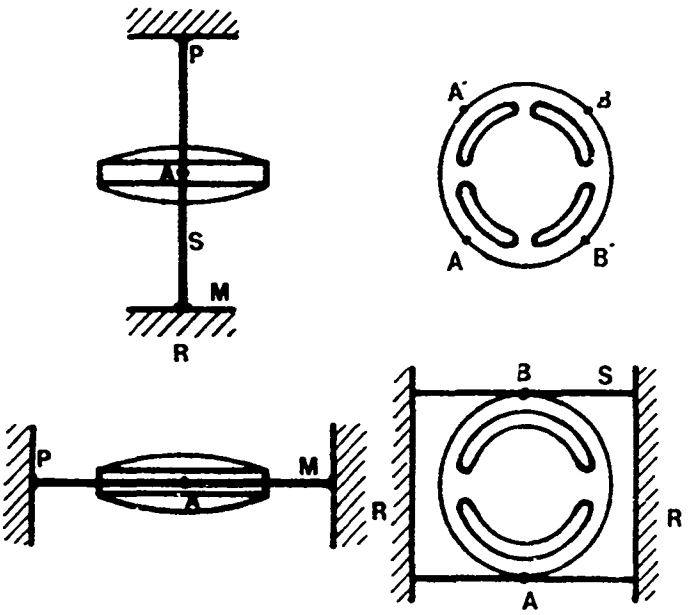

Fig. 13 : BVA design with low G sensitivity

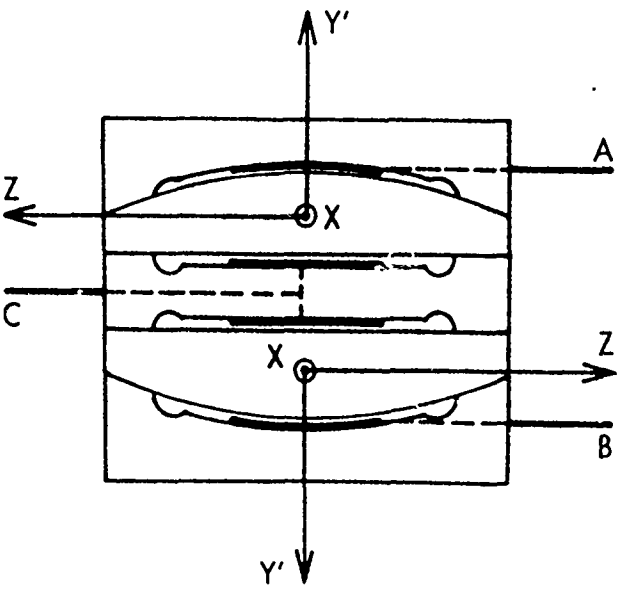

Fig. 14 : BVA dual resonator configuration

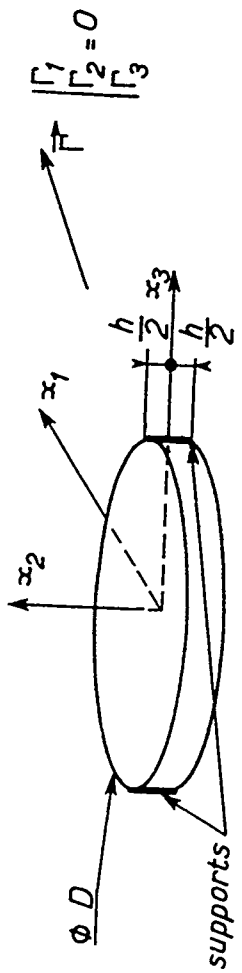

Fig. 1 : 5 MHz 5th overtone resonator. D = 15 mm h ~ 1.65 mm

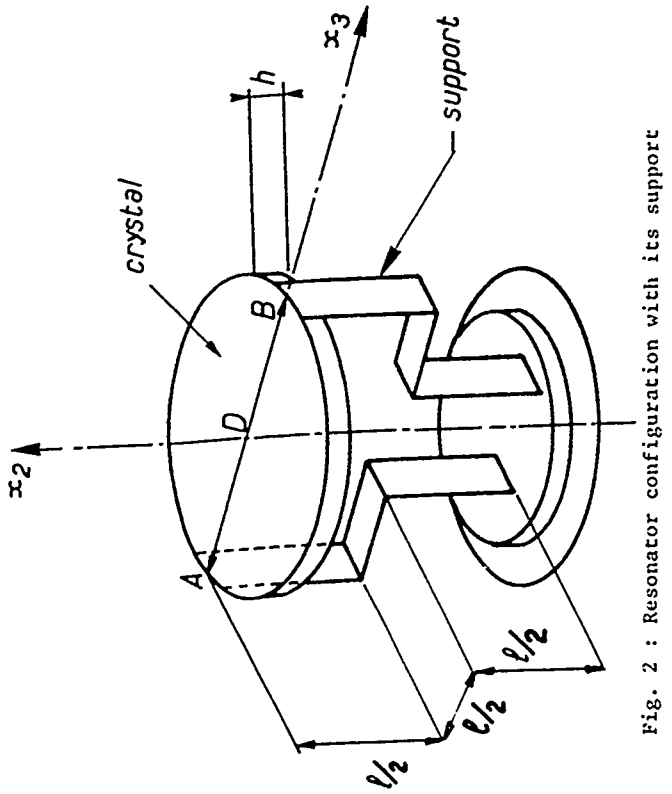

Fig. 2 : Resonator configuration with its support

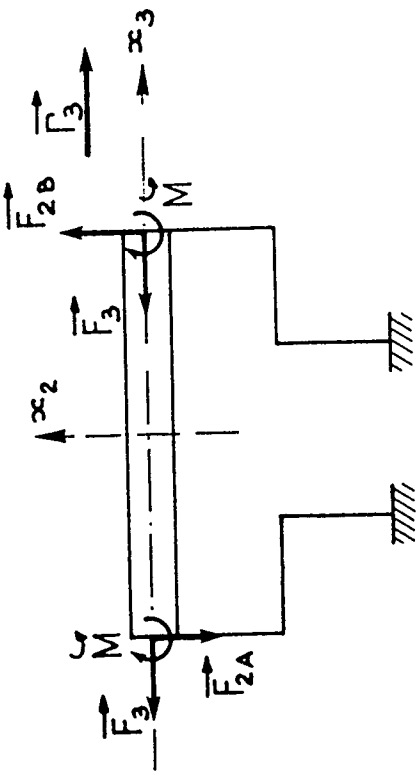

Fig. 3 : Static stress system when the resonator is submitted to an acceleration Γ_3

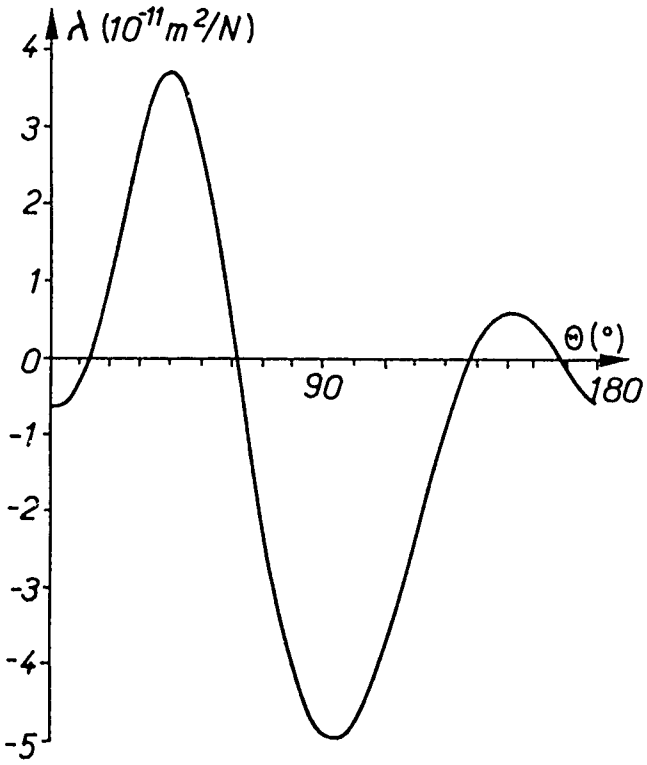

Fig. 4 : Sensitivity coefficient λ for an acceleration Γ_3 as a function of the cut angle Θ

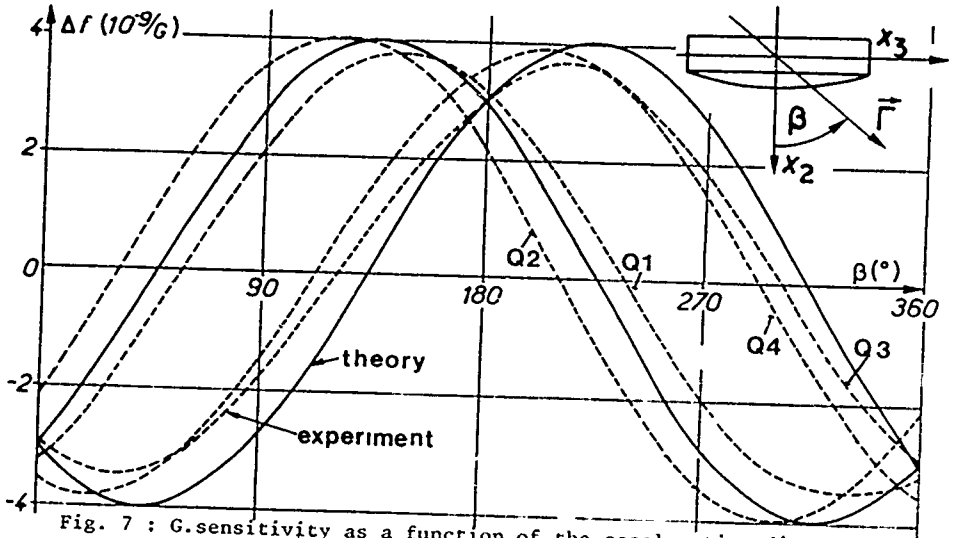

Fig. 7 : G.sensitivity as a function of the acceleration direction in the x_2x_3 plane

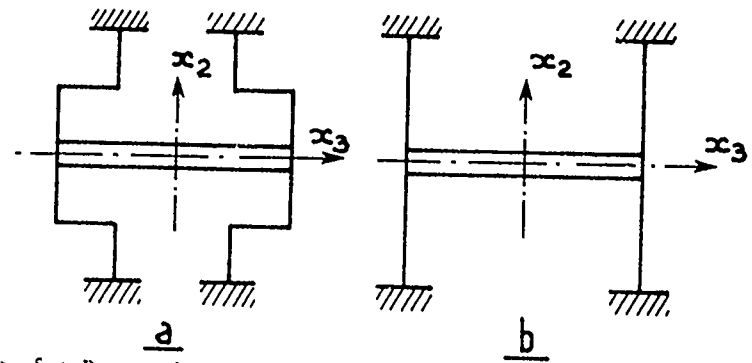

Fig. 5 : Proposed support configuration in order to desensitize the resonator to Γ_3

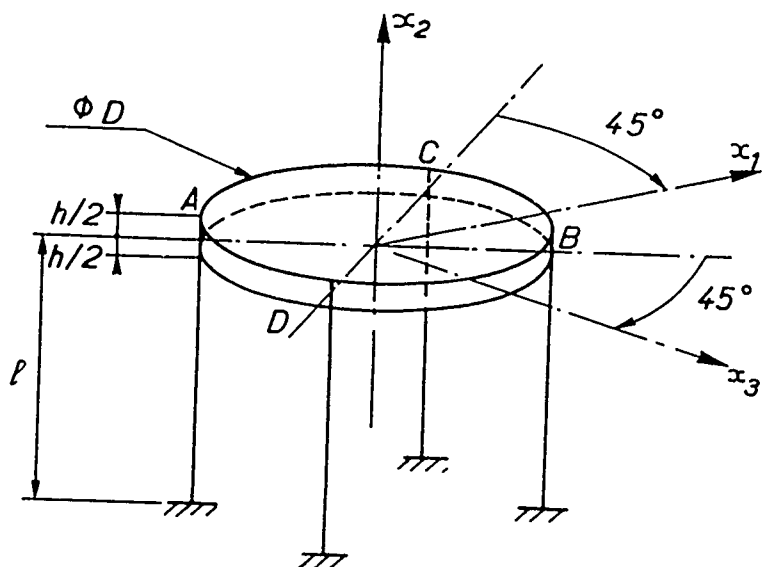

Fig. 8 : Configuration of a resonator with four supports

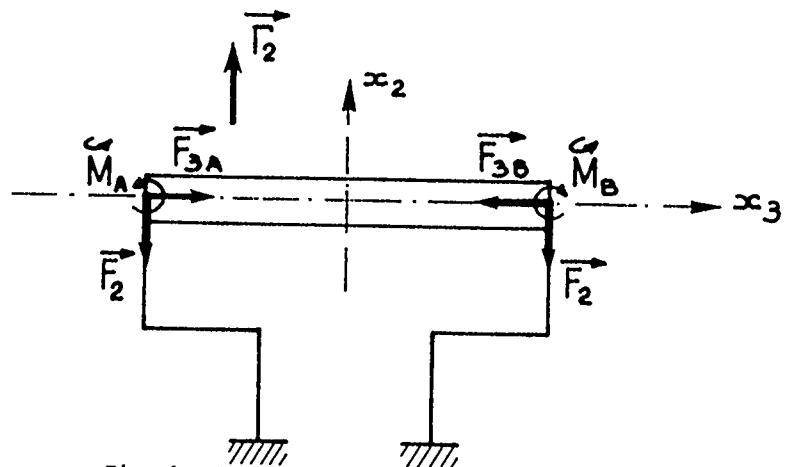

Fig. 6 : Static stress system when the resonator is submitted to an acceleration Γ_2

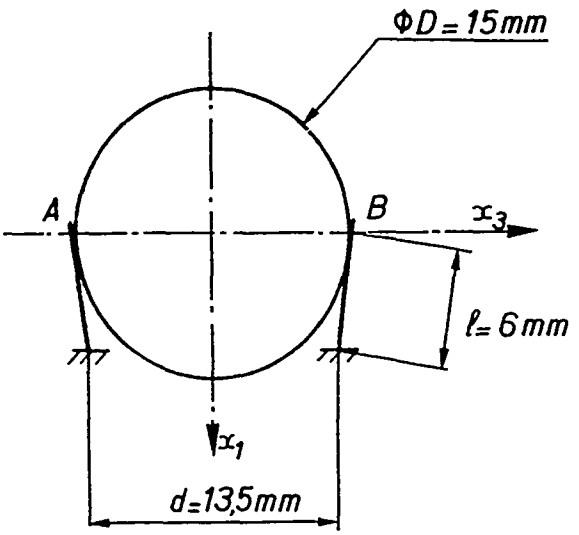

Fig. 9 : Configuration of a resonator with two non parallel supports

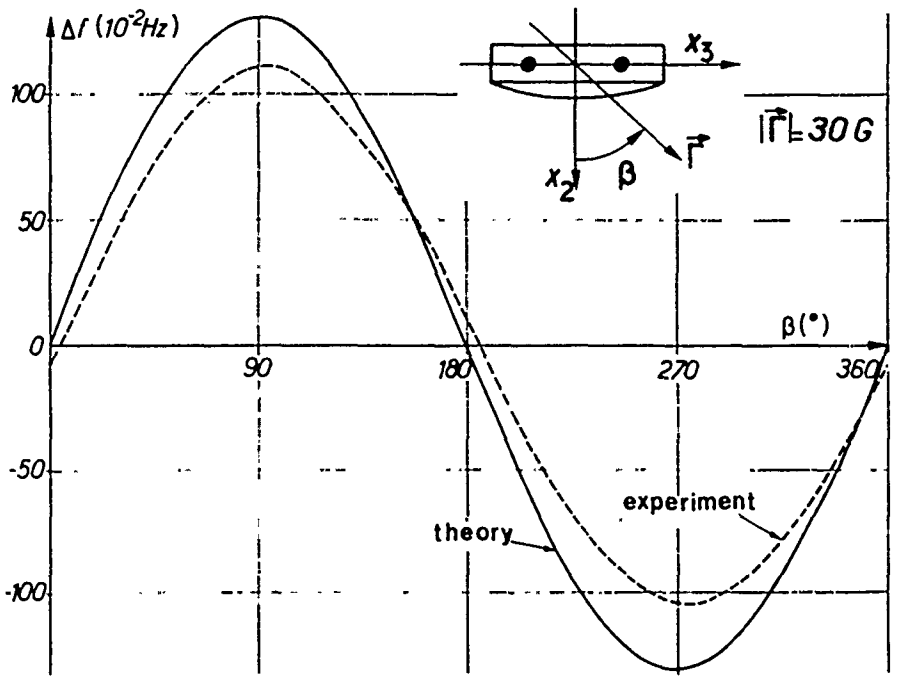

Fig. 10 : G.sensitivity in the x_2x_3 plane of the four support resonator

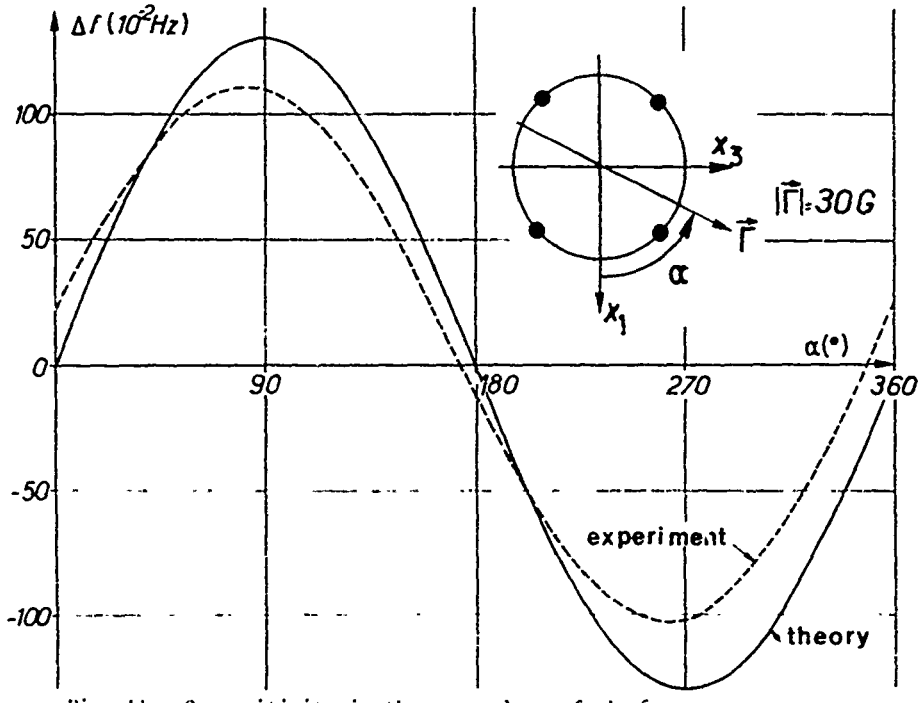

Fig. 11 : G.sensitivity in the x_1x_3 plane of the four support resonator

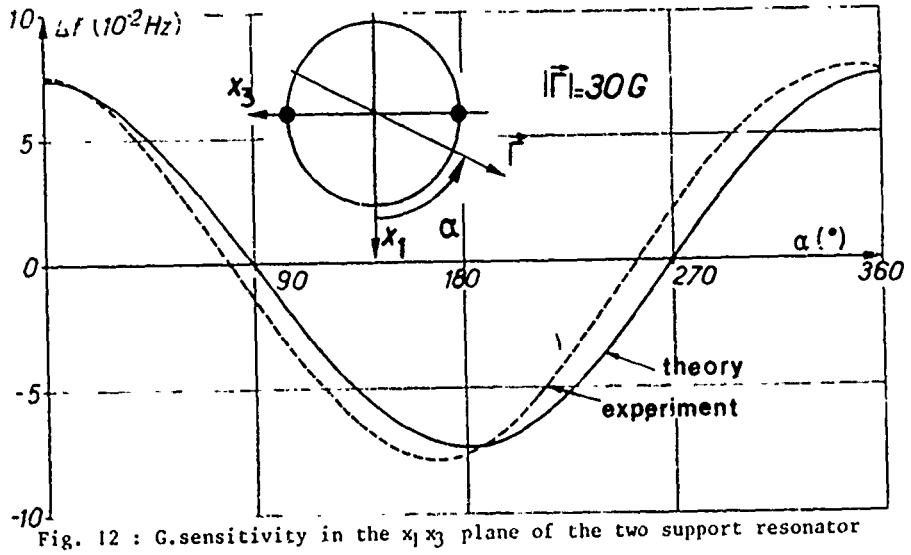

Fig. 12 : G.sensitivity in the x_1x_3 plane of the two support resonator

A COMPARISON OF THE EFFECTS OF BENDING MOMENTS ON THE VIBRATIONS OF AT AND SC (OR TTC) CUTS OF QUARTZ

E.D. Fletcher and A.J. Douglas

Philips Research Laboratories,
Redhill, Surrey RH1 5HA, England

Summary

The effects of bending moments on the frequency of 10 MHz fundamental crystals using AT and SC cuts of quartz has been studied. The bending was applied in two different configurations, one a cantilever and the other a symmetrical arrangement with bending about a diameter defined by a knife edge with the central part removed.

The effects obtained with the cantilever mounting of the AT crystal can be split into two components, one antisymmetrical centred at $\psi = 180^{o}$ with a periodicity of 360^{o} (in ψ) and the other with a periodicity of 90^{o}. The second component is absent in the results obtained on the SC cut.

The symmetrical bending results show that the SC cut is considerably less sensitive than the AT cut. The observations are consistent with the proposition that the frequency changes for symmetrical bending of AT cut crystals are due to the higher order effects (approximately square law with stress) which are also responsible for the component with 90^{o} periodicity found in the cantilever case.

It is expected that the SC cut should have distinct advantages over the AT cut when considering frequency stability in the presence of forces perpendicular to the plane of the crystal especially when these forces are large.

Introduction

In many applications it is important to consider the influence of mechanical forces on the frequency of a quartz crystal resonator. Such forces may arise from accelerations, including vibrations, or they may be imposed statically by the mounts. In the latter case any change with time of the mounting force could be a factor in determining the long term frequency stability.

Static experiments offer the advantage of permitting the investigation of many mounting positions in a relatively short time. They should be considered in general to be complementary to investigations on complete devices using dynamic methods such as vibration tables and centrifuges or the simple '2G' turnover test.

In this paper we consider the effects of static bending stresses on both AT and SC cuts of quartz. We use SC to cover the general region of stress and thermal transient compensated doubly rotated cuts[1]. The results are directly related to the case of two-point mounting across the diameter of a circular device.

Similar experiments on the AT cut have been reported by Mingins, Barcus and Perry[2] and a theoretical study for the case of initial bending in a cantilever mounted resonator has been made by Lee, Wang and Markenscoff[2] who obtained an expression for frequency changes in terms of the second and third order elastic constants, zero order strains and first order strain gradients. Although there is quite good general agreement between the results from these two studies there are also some differences which amount to as much as 50 per cent of the maximum measured frequency deviations. Our results therefore supplement these published ones and introduce new data on the stress compensated (SC) cut.

Experimental Details

We have used crystals 12 mm diameter in both cases with plane parallel lapped and etched faces having a fundamental thickness shear frequency (c-mode) of 10 MHz (within 2%). Electrodes were 4 mm diameter of silver with a thickness giving a relative frequency change due to mass loading of 0.5%. This proved to give efficient energy trapping. We are therefore able to make a direct comparison between the two cuts at the same frequency.

The crystals were supplied by Cathodeon Crystals Ltd, Linton, Cambridge. The doubly rotated cuts have $\phi = 21.9^{o} \pm 0.2^{o}$, $\theta = 33.9^{o} \pm 0.2^{o}$. It is not expected that the stress sensitivity is a rapid function of the angle. The AT cuts have $\phi = 0^{o}$, $\theta = 35.25^{o} \pm 0.02^{o}$.

The apparatus is shown in Fig. 1. The crystal was held in the appropriate support and forces applied through a lever by the direct application of standard masses to a scale pan. The deflection could be measured with an optical lever.

More details of the mounting arrangement are given in Fig. 2. Contact to the crystals was made to short tabs on the electrodes using conducting epoxy cement and thin multistrand wire for flexibility.

For the cantilever mounting (Fig. 2a) the crystal was held at one end by a cylindrical support having a distance between the edges of the top and bottom support points of 1 mm. For reproducible results there should be no significant clamping pressure. In practice the lever was always biased by a relatively small force. This made handling of the crystal easier when using a loose clamp.

Crystals in cantilever mounts do not normally occur in practical devices with the exception of accelerometers but the results can be of use when considering mounts and orientations to minimise effects of bending stresses.

Fig. 2b shows the arrangement for symmetrical bending about a diameter. This should give a more direct indication of the effects on frequency by bending due to forces imposed directly by two similar diametrically opposite mounts or alternatively by accelerations normal to the plate when held in such mounts.

The frequency and equivalent series resistance (ESR) were measured using the phase-zero transmission method (IEC Publication 444). Both parameters were monitored throughout the experiments. Some frequency measurements were made by direct counting but for others the signal was mixed with a reference and the period average of the difference frequency measured. This can increase the accuracy of measurement for the same averaging time.

Measurements were made as a function of the angle ψ, the angle between the mounting axis and the X' axis as defined in Fig. 3. Applied loads of 2 grammes force were commonly used for the cantilever mount and 5 grammes force for the symmetrical mount.

Results

Fig. 4 shows a typical result for an AT crystal in the cantilever support. In general appearance this agrees with those obtained by Mingins et al[1] and only partially with the calculations of Lee et al[2]. These calculations lead to an antisymmetrical function of approximate sine wave appearance centred at 180° and with a period of 360° in ψ. It appears that there is an additional term with a periodicity of 90° in the experimental results. Also shown in Fig. 4 is a sine wave representing this additional term and a curve drawn from the empirical expression $\Delta f \approx 11 \sin(\psi-180) + 2 \sin(4\psi+170)$. We shall discuss later how these results may be used to estimate the behaviour under symmetrical bending conditions.

For the SC cut in the cantilever support (Fig. 5) we get a much smoother antisymmetric curve but the magnitude of the deviations is similar for both cuts.

Fig. 6 shows results for the AT cut in the symmetrical bending support. It is interesting to note that there is no angle of mounting which gives a zero effect and the ratio of maximum to minimum frequency change approaches 5. These results are also basically similar to those given by Mingins et al.

The SC cut on the other hand (Fig. 7) shows orientations giving zero effect and the maximum deviation observed is several times smaller than for the AT cut. In this case we believe that we are observing only residual effects since several crystals have been examined but a consistent pattern of frequency change with orientation has not been established. It is believed that the differences are caused by secondary effects such as those associated with the exact positioning of the electrodes and perhaps the electrode tags.

When considering symmetrical bending it is possible to argue that frequency changes can be estimated by summing the effects from two similar cantilevers (arranged back to back at the axis of bending with effective orientations differing by 180°). Although the stress distribution in the electrode region is not the same in this case as for our experimental situation we might still expect the same general behaviour with orientation. Applying this argument brings our two sets of experimental results into reasonable agreement. Using the cantilever bending results of the AT cut we would expect the component with 360° periodicity to cancel out whilst the component with 90° periodicity should add. This would explain the 90° periodicity found in the experimental results for the symmetrical bending case.

Linearity

The linearity of the frequency change with applied force is of interest both from a fundamental point of view and also when considering the superposition of force-frequency effects.

Fig. 8 shows results obtained for the two bending configurations. We see that for cantilever bending the AT cut can vary from an essentially linear characteristic to a highly non linear one involving a change of sign. The observations are consistent with the proposition that the main antisymmetrical component is linear with stress but that the component with 90 degree periodicity has a higher order dependency. For symmetrical bending the AT cut gives a nonlinear behaviour approaching a square law.

For the SC cut fairly good linearity is maintained in both cases.

Mode Structure

We have also examined the effects of the bending forces on the mode structure, in particular the relative strengths of the b and c modes for the SC cut crystals.

In all cases the bending forces have had very little effect on the ESR's of any of the modes, certainly less than 1 per cent.

Mounting

Valdois, Besson and Gagnepain[4] have studied the effects of accelerations on AT cut crystals and showed that for two support mounting the maximum frequency change resulted from accelerations perpendicular to the plane of the crystal.

Our static results for symmetrical bending should give an indication of the frequency changes to be expected from such accelerations and also indicate optimum mounting angles. With an applied load of 5 grammes force the force applied to the centre of the crystal is 200 times its mass. We therefore expect similar behaviour to that due to an acceleration of 200 'G'.

We expect that the SC cut should offer significant advantages over the AT cut in these circumstances. This will be emphasised at even higher forces due to the power law dependence observed for the AT cut.

In practice other factors may need to be considered. Forces in the plane of the crystal pose a different problem on which considerable work has been done[5,6,7] and Kusters and Leach[8] have shown that the mounting angle can also affect thermal transient effects. The final compromise solution will depend on the particular application.

Conclusions

We have shown that for bending about a diameter SC cut crystals show much smaller frequency changes than AT cut and should therefore be much less sensitive to any forces (due to accelerations or other causes) perpendicular to the plane of the crystal when mounted in two diametrically opposite supports. Frequency changes for the AT crystal also show a higher order dependence on stress in this configuration so that these differences will be emphasized at high levels of stress.

Observations have also been made of the effects of bending in a cantilever support. In this case the two cuts exhibit frequency changes of a similar magnitude. In the AT case however the variation with mounting angle shows a combination of two components with different periodicities in angular dependence. For symmetrical bending one of these is expected to cancel out leaving effects only due to the second component which has a periodicity of 90° and appears to be nonlinear. This assumption permits the results obtained for the two sets of results to be reconciled in a qualitative manner.

Acknowledgements

We should like to acknowledge helpful discussion with and assistance from Messrs J. Dowsett and W.S. Metcalf of Cathodeon Crystals Ltd and Dr J.C. Brice of our laboratories.

This work was partially supported by the Ministry of Defence, Procurement Executive, Directorate of Components, Valves and Devices.

References

1 A good survey is given by Ballato, A., Physical Acoustics Vol. 13 p115-181 Ed. W.P. Mason and R.N. Thurston, Academic Press 1977.

2 Mingins, C.R., Barcus, L.C. and Perry, R.W., Proc. 17th Ann. Freq. Cont. Symp. p51 1963.

3 Lee, P.C.Y., Wang, Y.S. and Markenscoff, X., J. Acoust. Soc. Amer. 59, 90, 1976.

4 Valdois, M., Besson J. and Gagnepain, J-J., Proc. 28th Ann. Freq. Cont. Symp. p19 1974.

5 EerNisse, E.P., Lukaszek, T.J. and Ballato, A., IEEE Trans. Sonics and Ultrasonics SU-25 p132 1978.

6 Lee, P.C.Y. and Kuang-Ming, Wu., IEEE Trans. Sonics & Ultrasonics, SU 25, 220, 1978.

7 Ballato, A., IEEE Trans. Sonics & Ultrasonics, SU 25, p223, 1978.

8 Kusters, J.A. and Leach, J.G., Proc. 31st Ann. Freq. Cont. Symp. p3 1977.

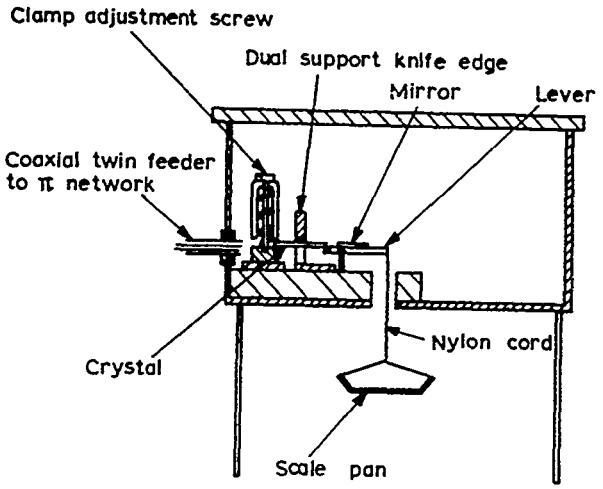

Fig.1. Apparatus for applying bending forces to a crystal.

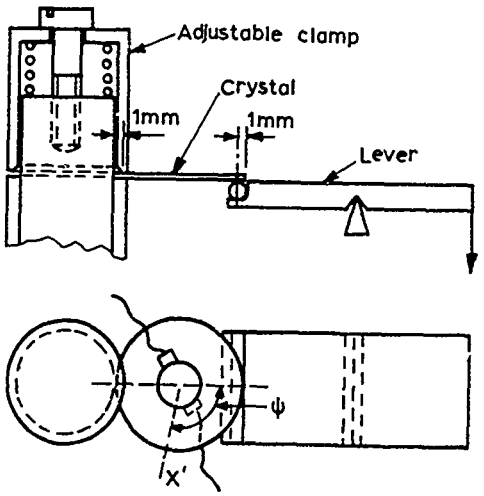

(a) For cantilever bending

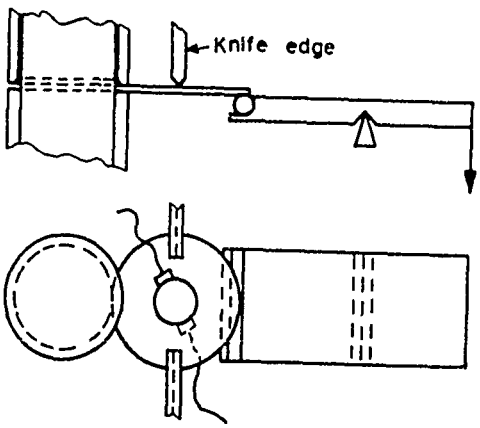

(b) For symmetrical bending

Fig. 2. Details of crystal mounts for bending.

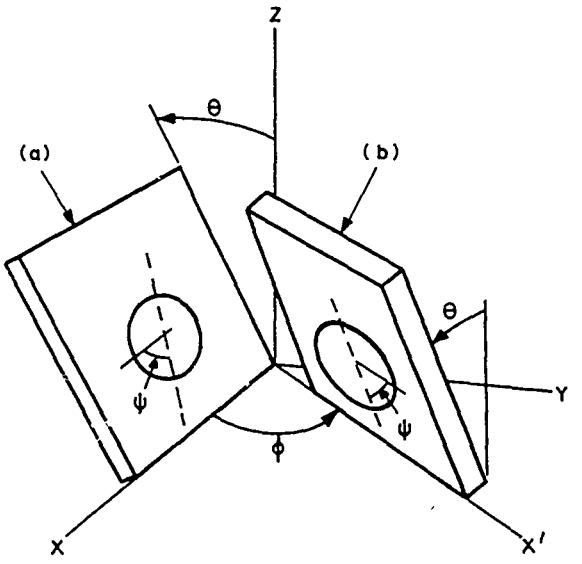

Fig. 3.(a) Singly and (b) doubly rotated crystal plates

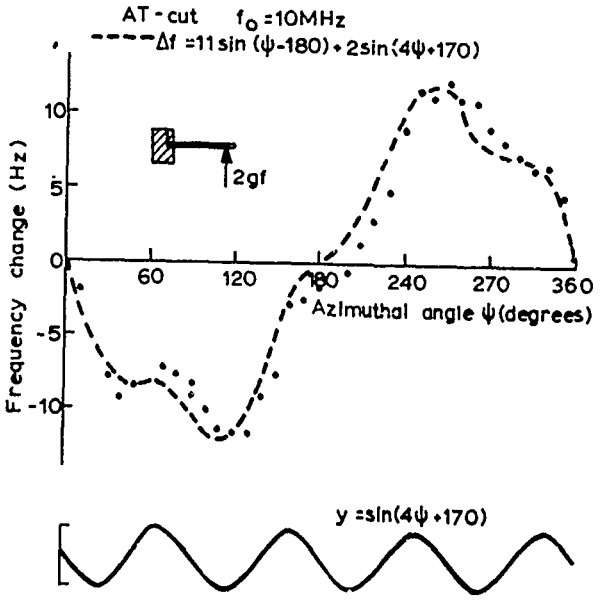

Fig. 4. Frequency change for cantilever bending. AT-cut crystal.

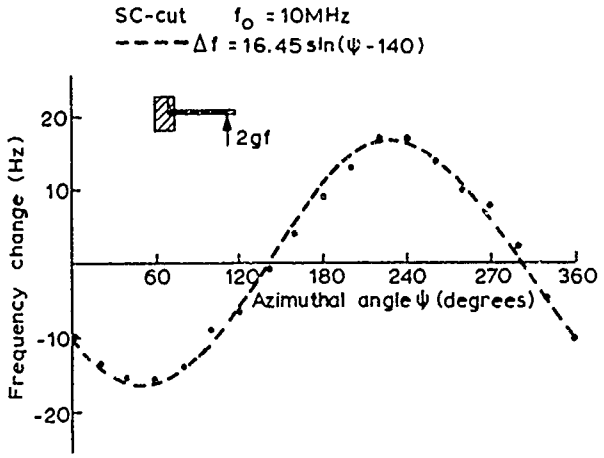

Fig.5 Frequency change for cantilever bending. SC-cut crystal

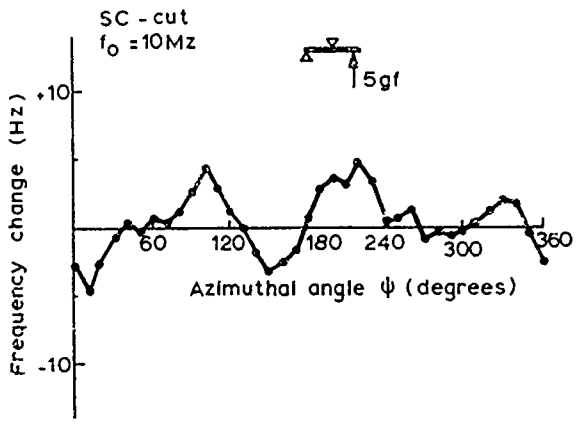

Fig.7. Frequency change for symmetrical bending. SC-cut crystal.

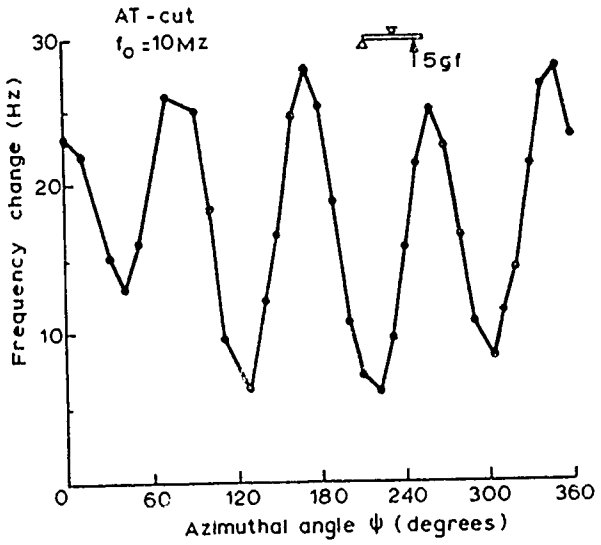

Fig. 6 Frequency change for symmetrical bending AT-cut crystal

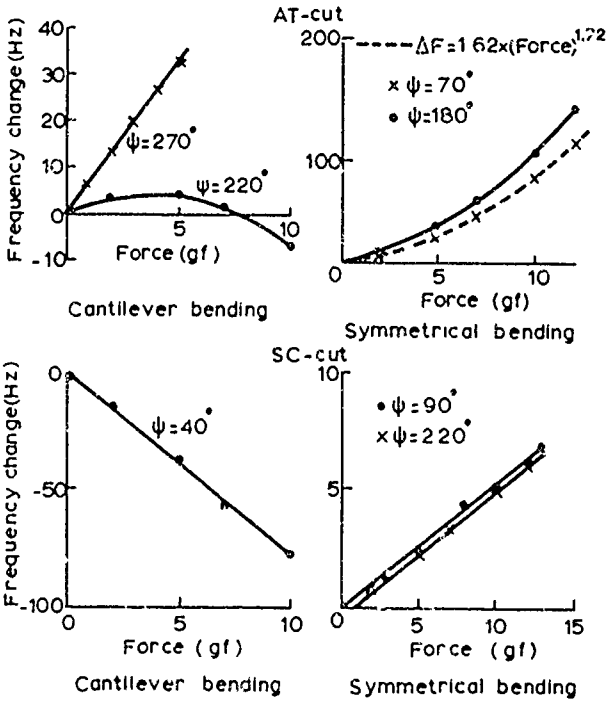

Fig. 8 Linearity of frequency change with applied force.

ETCHING STUDIES ON SINGLY AND DOUBLY ROTATED QUARTZ PLATES

John R. Vig, Ronald J. Brandmayr and Raymond L. Filler

US Army Electronics Technology and Devices Laboratory (ERADCOM)
Fort Monmouth, NJ 07703

Summary

It has been shown previously[1] that when lapped AT-cut quartz plates are etched in a saturated solution of ammonium bifluoride ($NH_4F.HF$), the surface roughness decreases with increasing depth of etching, i.e. the plates are chemically polished. Experiments on other cuts of quartz have shown that etching in a saturated solution of ammonium bifluoride can also polish the (singly rotated) BT and ST-cuts, but not the (doubly rotated) 10°V, FC, IT and SC-cuts. The surfaces of these doubly rotated cuts become rougher with increasing depth of etching in ammonium bifluoride.

Experiments aimed at finding a chemical polish for the SC-cut have been performed with a variety of etchants. The surface morphologies of etched SC-cut plates depend strongly on the compositions of the etching solutions. Some of the solutions evaluated did not produce chemical polishing on either side of SC-cut plates, some produced chemical polishing on one side but not the other, and some were able to chemically polish both sides.

Chemically polished ($\Delta f/f_o f_f = 15$) AT-cut 5 MHz 5th overtone biconvex resonators have exhibited Q's as high as 2.7 million, the Q of 10 MHz 3rd overtone plano-convex chemically polished AT-cut resonators was 0.98 million, and the Q's of 5.3 MHz fundamental mode chemically polished SC-cut resonators ranged up to 1.2 million. Thus, at least up to 10 MHz, the chemical polishing does not produce a significant Q-degradation. Etching conditions that can lead to activity anomalies will also be described.

Key Words. Etching, Polishing, Chemical Polishing, Quartz Crystals, Quartz Resonators, SC-cut.

Introduction

At the 31st Annual Symposium on Frequency Control, we reported that when lapped AT-cut plates are etched in a saturated solution of ammonium bifluoride ($NH_4F.HF$), the surface roughness decreases with increasing depth of etching, i.e. the plates are chemically polished. Etching a 3μm lapped surface to a depth of $\Delta f = 15\ f_o f_f$, where f_o and f_f are the initial and final frequencies, respectively, in MHz, and Δf is the difference between the two frequencies, in kHz, results in a surface roughness of 0.15μm and a roughness angle of 1.3°. Chemically polished AT-cut surfaces are atomically smooth but microscopically undulating, as shown in the scanning electron micrograph of Figure 1.

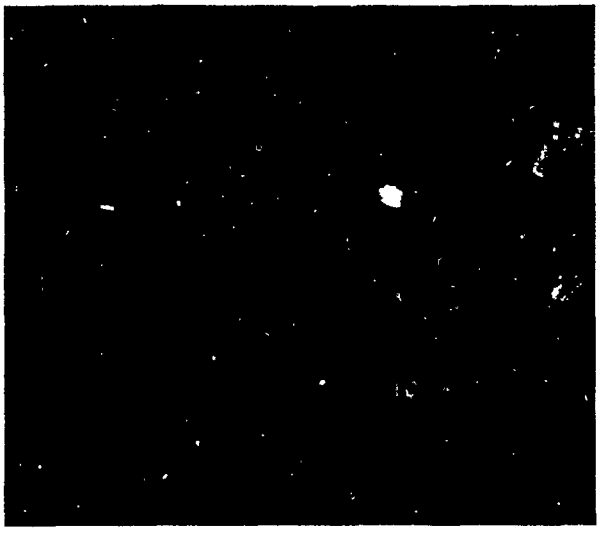

Figure 1 - Chemically Polished AT-Cut Surface

The objectives of the experiments reported in this paper were to determine if other cuts of quartz, particularly the SC-cut, can be similarly chemically polished, and to answer the question of whether or not the chemical polishing produces an inherent Q degradation.

Experimental Methods

The experiments were performed mostly on natural quartz plates lapped with 1μm or 3μm MICROGRIT[2] aluminum oxide abrasives. The main exceptions were the ST-cut plates, which were cultured quartz. The reason natural quartz was used in most of the experiments is that, as we had shown previously, when cultured quartz plates are etched deeply, the results can vary greatly. In most commercially available cultured quartz, the deep etching produces large numbers of etch channels and etch pits which can interfere with

the evaluation of the surface topography.

The etching was performed in directly heated Teflon beakers[3]. The temperature was controlled to within about ± 2°C, and was measured with a Teflon coated thermometer[4]. The carefully cleaned quartz plates were held in Teflon fixtures, and were agitated during etching.

The surface topographies were evaluated by scanning electron microscopy (SEM) and a profile meter, as described previously[1]. All SEM micrographs were taken at a 60° observation angle, with the Z-directions being along the top to bottom direction in each micrograph.

The $NH_4F.HF$ solutions were prepared from $NH_4F.HF$ flakes[5]. The ammonium fluoride (NH_4F) containing solutions were prepared from premixed 40% solutions[6]. The HF containing solutions were prepared from 49% HF solutions[6;7] The concentrations in the various mixtures used in our experiments were deduced from the relative volumes used to prepare the solutions. The concentrations were not measured independently.

Etching BT, ST, 10°V, FC, IT and SC-cut Plates

Etching in a saturated solution of ammonium bifluoride produced chemical polishing on (the singly rotated) BT and ST-cut plates, but not on (the doubly rotated) 10°V, FC, IT and SC-cut plates.

a. BT-cut Plates

When lapped BT-cut plates were etched in a saturated solution of ammonium bifluoride, the surfaces became smoother and smoother with increasing depth of etching. Figure 2 shows an SEM micrograph of the surface of a BT-cut plate which had been etched for 2 hours at 70°C. On cerium oxide polished BT-cut plates that were deeply etched, the surfaces did not develop the striations observable in Figure 2. The surfaces remained featureless, except at defects (such as scratch marks) which are attacked preferentially by the etchant. The BT-cut plates' etch rate was six times slower (in units of $f_o f_f$) than the AT-cut plates' rate.

b. ST-cut Plates

ST-cut cultured quartz plates, which had been Syton polished on one side and rough ground on the other, were etched deeply in a saturated solution of ammonium bifluoride, at 75°C. Figure 3 shows that the rough ground side became chemically polished. The surface topography is similar to the AT-cuts'. Figure 4 shows that the polished side remained polished. The surface topography is featureless, except at crystallographic defects which are attacked preferentially by the etchant. Both Figures also show the presence of etch channels.

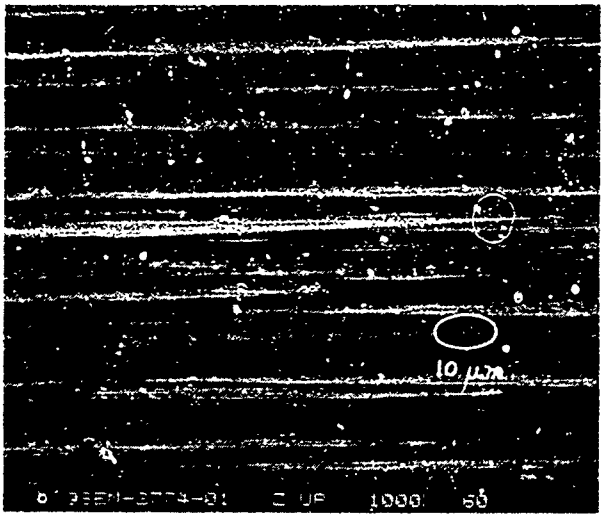

Figure 2 - Chemically Polished BT-cut Surface

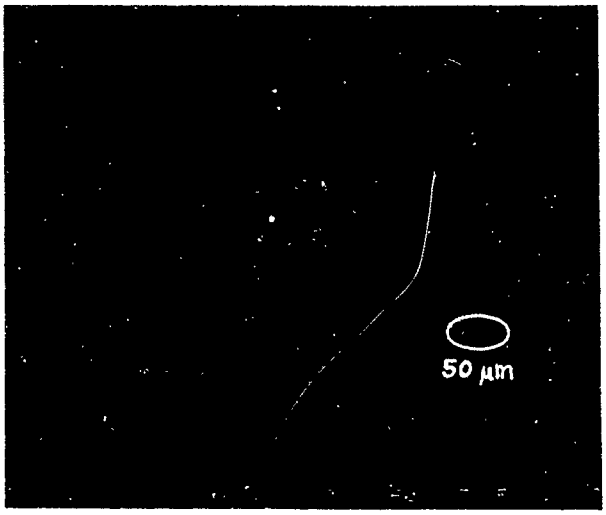

Figure 3 - Chemically Polished ST-cut Surface
Rough Ground Side

Figure 4 - Chemically Polished ST-cut Surface
Polished Side

c. 10°V, FC, IT and SC-cut Plates

When the etching procedure that chemically polished the AT, BT and ST-cuts was attempted on the (doubly rotated) 10°V, FC, IT and SC-cuts, the surfaces did not become smoother and smoother with increasing depth of etching, but remained lusterless in appearance. SEM and Talysurf examinations revealed that as the etching progressed, the surfaces became rougher.

Figures 5 - 7 show examples of the surface topographies of doubly rotated cuts after deep etching in a saturated solution of ammonium bifluoride.

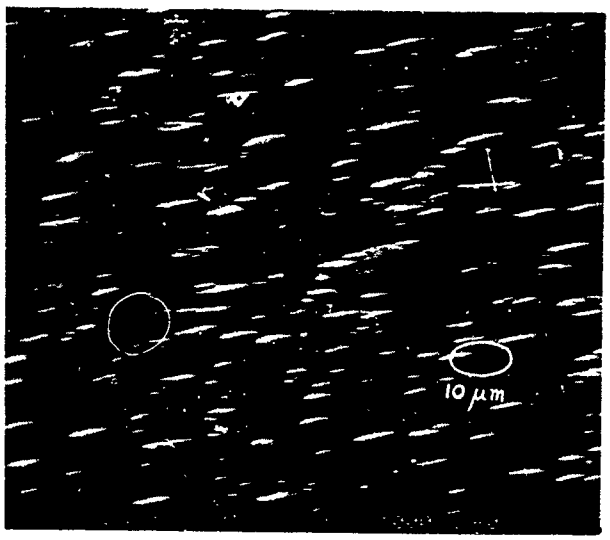

Figure 5 - Deeply Etched 10°V-cut Plate ($NH_4F.HF$)

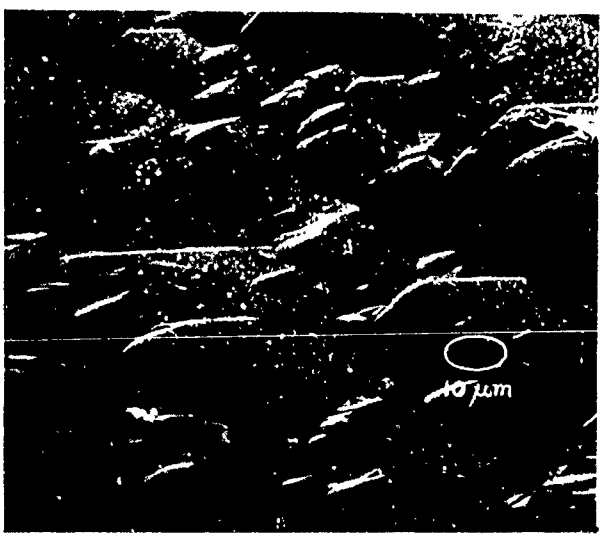

Figure 6 - Deeply Etched FC-cut Plate ($NH_4F.HF$)

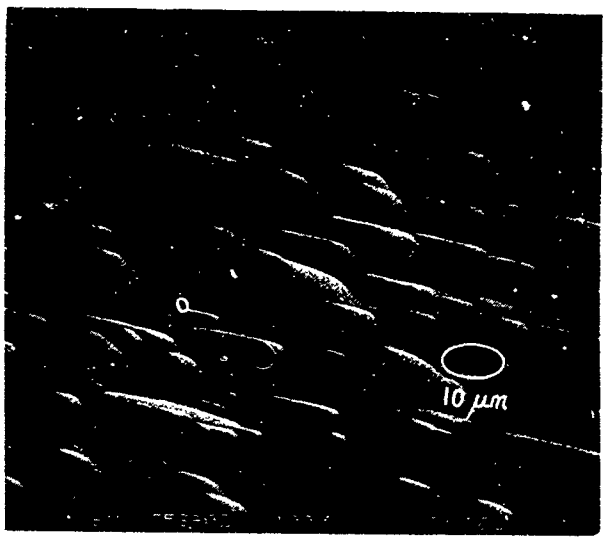

Figure 7 - Deeply Etched SC-cut Plate ($NH_4F.HF$)

Chemical Polishing SC-cut Plates

As discussed previously[1], etching will produce chemical polishing when the etching process is diffusion controlled. Since the chemistry of etching quartz is not fully understood[8], and since the rates of diffusion, adsorption and desorption are also unknown, it was not possible to predict the etching processes that could produce chemically polished SC-cut surfaces.

A series of etchants were therefore evaluated. These etchants were of three categories: 1. hydrofluoric acid (HF) in various concentrations; 2. ammonium bifluoride ($NH_4F.HF$) in various concentrations, and 3. mixtures of 40% ammonium fluoride (NH_4F) with 49% HF, in various ratios. Mixtures of such " buffered fluoride" solutions of NH_4F and HF are used in the semiconductor industry, and are commonly referred to by the ratios of the two components. For example, a "5:1 solution" is a mixture of five parts (by volume) of 40% NH_4F with one part of 49% HF.

Etching SC-cut plates in a concentrated 49% HF solution at 40°C produced surfaces which were lusterless in appearance. Examination of the surfaces by SEM indicated, however, that the surface topographies of these deeply etched ($\Delta f = 26\ f_o f_f$) SC-cut plates differed considerably from the topographies of plates etched to the same depth in the saturated solution of $NH_4F.HF$ at 70°C. Moreover, although both sides of the plates were rough, the topographies of the two sides were different, as is illustrated in Figure 8. Differences between the two sides of the plates etched in saturated $NH_4F.HF$ were also noticable, but were much less obvious.

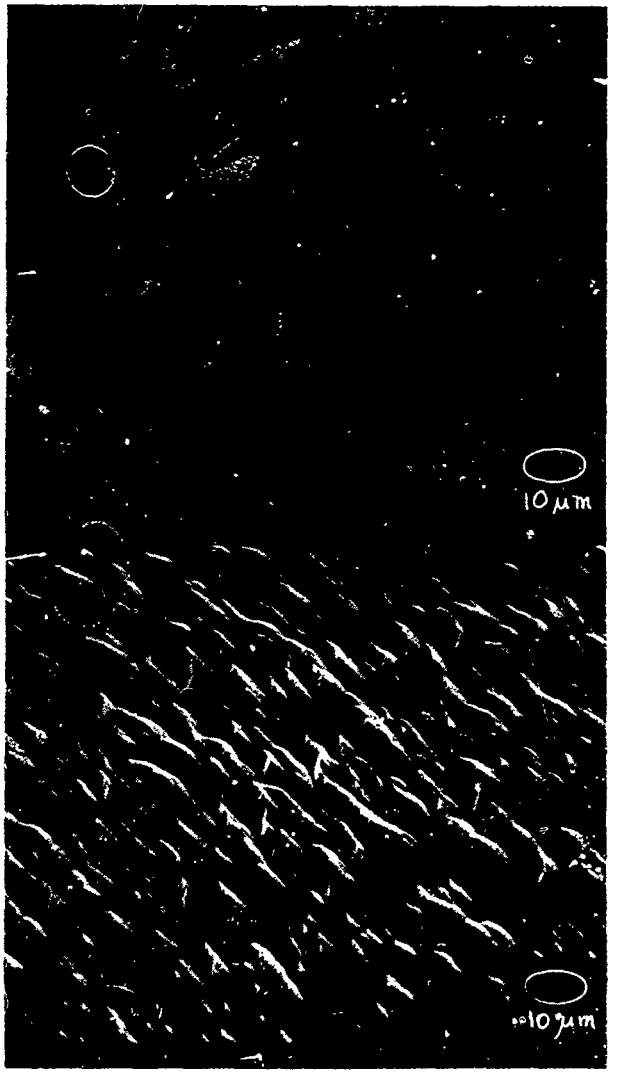

Figure 8 - Two Sides of an SC-cut Plate Deeply Etched in 49% HF

One can explain the different topographies on the two sides of SC-cut (and other doubly rotated) plates by reviewing the etching studies performed by Bond and others[9] between 1889 and 1940, or the paper by Suda et. al. in these Proceedings. In the early experiments, it was found that polished quartz spheres, when etched in concentrated HF, dissolved in a highly anisotropic manner. The dissolving spheres took on a "triangular, lenticular appearance", as shown in Figure 9.

Since the etching progresses much faster along the +X direction than along the -X, and since the thickness direction of doubly rotated plates have a component along the X-direction, the two sides of doubly rotated plates will etch differently. For example, dramatic variations in surface topographies were observed for SC-cut plates etched to the same depth in different solutions. In Figure 8, the topographies consist of arrays of pyramid-like features. As the HF solution was diluted with the NH_4F solution, the pyramids became dome-like features which became flatter and flatter as the HF concentration decreased. Eventually, the plates became chemically polished on one side. As the HF was further diluted, the plates became chemically polished on both sides. The transitions from the rough/rough to the rough/shiny to the shiny/shiny surface topographies could be readily observed with the unaided eye. Plates etched in the 1:3, 1:1, 2:1 and 3:1 solutions at 75°C became polished on one side only. Those which were etched at 75°C in the 4:1, 5:1 and 10:1 solutions became polished on both sides.

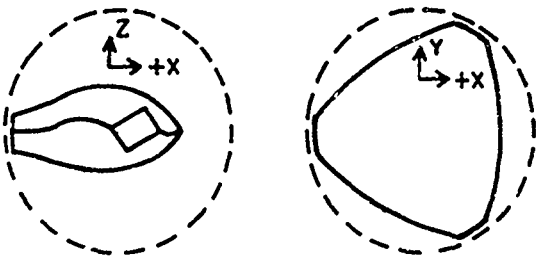

Figure 9 - Deeply Dissolved Quartz Sphere

Figure 10 shows SEM micrographs of the two sides of an SC-cut plate etched in the 2:1 solution ($\Delta f = 16\ f_o f_f$). Figure 11 shows the two sides of an SC-cut plate etched in the 4:1 solution ($\Delta f = 16\ f_o f_f$). The surface roughness of the smoother side is 0.04μm, the rougher side's is 0.08μm. These surfaces are therefore smoother than the surfaces of AT-cut plates chemically polished to the same depth in saturated $NH_4F.HF$.

According to Judge[8], in dilute buffered fluoride solutions the species determining the etching rate of SiO_2 are primarily HF_2^- and HF (but not the free fluoride ion). Since the concentration of these species vary with pH, one might expect that by diluting the HF with water instead of the NH_4F solution, the etching kinetics would change significantly.

When the HF was diluted by four parts water instead of the NH_4F, the resultant 11% HF solution at 75°C was also able to chemically polish both sides of SC-cut plates, as can be seen in Figure 12 ($\Delta f = 15.4\ f_o f_f$). The surface roughnesses of the two sides are 0.04μm and 0.07μm. The etching times were also comparable, 2 hours for the 4:1 solution vs. 2.5 hours for the 11% HF. However, when the same HF concentration was prepared by diluting the HF with two parts NH_4F plus two parts H_2O, the resultant solution produced chemical polishing on one side only.

A dilute $NH_4F.HF$ solution, prepared by mixing one part by weight of $NH_4F.HF$ flakes with five parts H_2O, was also able to chemically polish both sides of SC-cut plates, as shown in Figure 13. The etching time to $\Delta f = 15\ f_o f_f$, at 75°C, was approximately 3 hours, vs. 30 minutes to etch an AT-cut plate to $\Delta f = 15\ f_o f_f$ in saturated $NH_4F.HF$.

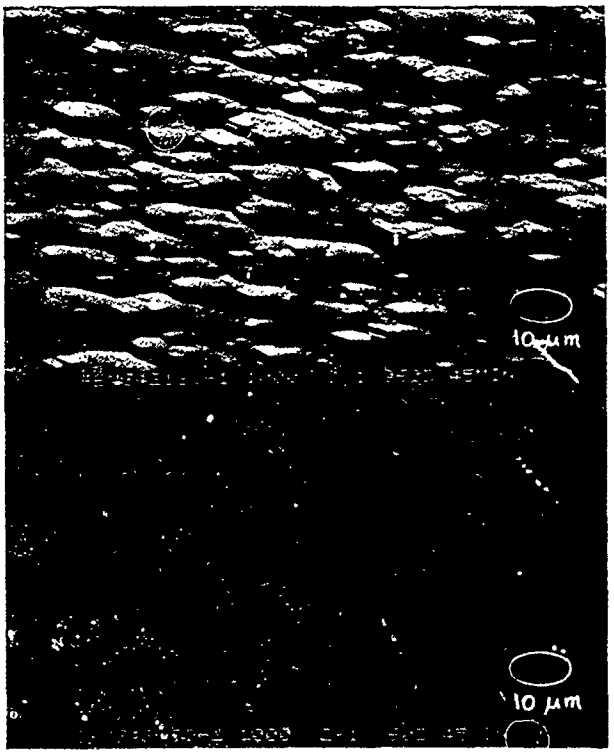

Figure 10 - Two Sides of an SC-cut Plate Deeply Etched in a 2:1 Solution

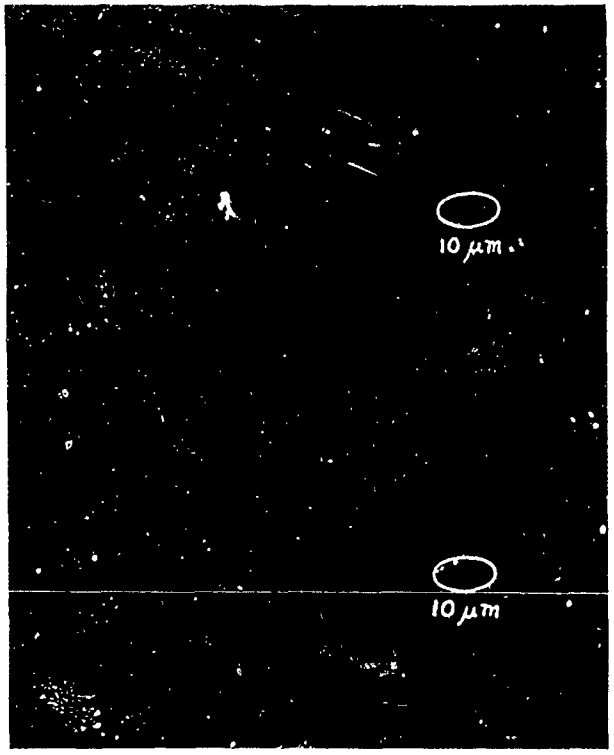

Figure 11 - Two Sides of an SC-cut Plate Deeply Etched in a 4:1 Solution

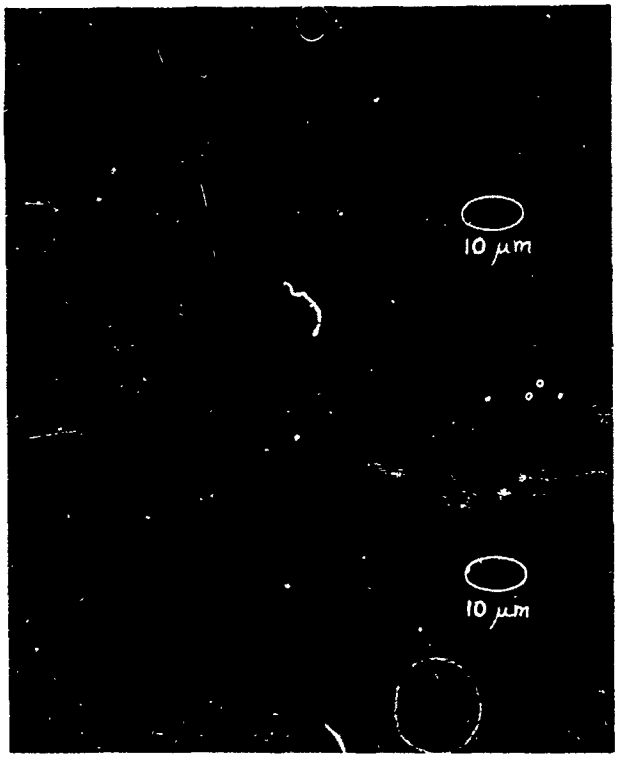

Figure 12 - Two Sides of an SC-cut Plate Deeply Etched in 11% HF

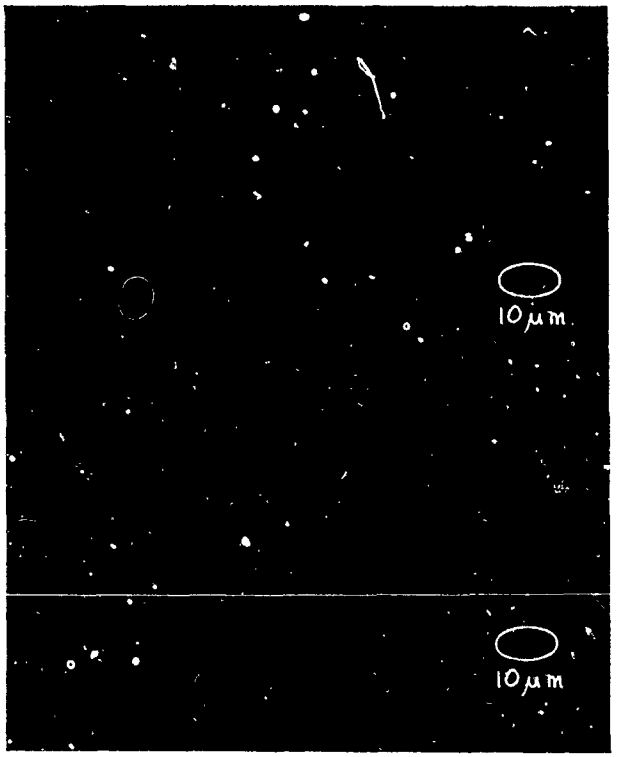

Figure 13 - Two Sides of an SC-cut Plate Deeply Etched in Dilute $NH_4F.HF$

The etching rates were slower for the more dilute solutions. It is more difficult to determine the etching rates for the chemical polishing solutions of the SC-cut than it was for the saturated $NH_4F.HF$. Since the SC-cut's polishing solutions are not saturated, the concentrations change more rapidly during etching, due both to the etching and to evaporation.

The Effects of Chemical Polishing on Resonator Q

a. AT-cut Resonators

To answer the question of whether or not chemical polishing produces an inherent Q degradation, a group of biconvex 5 MHz 5th overtone AT-cut plates were etched in a saturated solution of $NH_4F.HF$, at 75°C, to $\Delta f = 15\ f_o f_f$. Three of the resonators were fabricated and evaluated at Frequency Electronics Inc. (FEI), three were fabricated and evaluated at the General Electric Neutron Devices Dept. (GEND) and three were fabricated and evaluated by the authors. Some of the blanks were Premium Q swept, some were natural quartz. FEI measured Q's of 2.7×10^6, 2.5×10^6 and 2.1×10^6, about the same as the Q's of similarly fabricated resonators made with cerium oxide polished blanks. GEND measured Q's of 2.1×10^6, 2.1×10^6 and 1.2×10^6, and the authors measured 2.6×10^6, 2.4×10^6 and 0.7×10^6.

An attempt was made to determine the cause of the low Q for the resonator with the Q of 0.7×10^6. An SEM examination of the blank surfaces, Figure 14, revealed an approximately 300um gouge near the center of one of the electrodes, plus several smaller defects, a few of which are also shown in Figure 14. It is not certain, however, that these defects produced the Q degradation, because when the blank of the resonator with a Q of 2.6×10^6 was similarly examined, several less deep, but similarly prominent defects were revealed as can be seen in Figure 15.

More work needs to be done to define the relationship between blank defects and Q degradation. However, the fact that Q's as high as 2.7×10^6 could be measured indicates that the chemical polishing does not produce an inherent Q degradation, at least not at 5 MHz.

Q's as high as 980,000 have also been measured for 10 MHz 3rd overtone resonators made with chemically polished ($\Delta f = 15\ f_o f_f$), 14mm diameter, 0.37 diopter plano-convex blanks. This Q is comparable to the highest Q achievable for the blank geometry selected. (The 0.37 diopter contour provides the minimum resistance, not the highest Q.[10])

b. SC-cut Resonators

A group of four 5.3 MHz, fundamental mode, plano-convex 14mm diameter chemically polished SC-cut resonators were fabricated. The contours were 1.0 diopter for two of the blanks, 2.5 diopter for the other two. The blanks were etched $\Delta f = 15\ f_o f_f$ in a 5:1 solution, at 75°C. The c-mode Q's were 1.2×10^6, 1.1×10^6, 1.0×10^6 and 0.96×10^6 (the b-mode Q's ranged from 0.53×10^6 to 1.3×10^6). The c-mode Q's are higher than the

Figure 14 - Blank Defects in Low Q Resonator

Figure 15 - Blank Defects in High Q Resonator

Q's we have been able to achieve for 5 MHz fundamental mode AT-cut resonators of the same blank diameter, regardless of surface finish. This is not too surprising in view of the fact that the capacitance ratios of SC-cut resonators are significantly higher than the corresponding AT-cuts'.

c. Etching Bath Concentration/Temperature Effects

When AT-cut crystals are etched in saturated solutions of $NH_4F.HF$ at temperatures up to 75°C, the etching can be readily monitored by measuring the blank frequencies in an air gap. However, as the etching bath temperature is increased to above 80°C, the blank activities frequently decrease so drastically that it becomes difficult to impossible to measure the frequencies by using only an air gap and a crystal impedance meter. Even when the modes are displayed on an oscilloscope, using a microcircuit bridge system[11], it can be difficult to determine the main mode frequency. After electrodes were deposited onto such low activity 22 MHz blanks, the resonator activities showed no comparable decrease. The mode spectrum, however, did exhibit a significant degradation. We do not have an explanation for these phenomena.

When the surface topographies of the low activity blanks etched in a saturated solution of $NH_4F.HF$ at 90°C were compared with the high activity blanks etched at 70°C, no significant differences could be observed in either the SEM micrographs or the profile meter scans.

Both concentration and temperature appear to play a role in producing suppressed activity. For example, when AT-cut crystals are etched in a saturated solution of $NH_4F.HF$ at 75°C, the crystal activities remain high. If the solution that was saturated at 75°C is heated to 90°C without permitting additional $NH_4F.HF$ to be dissolved, then the solution does produce a drastic loss of activity. If on the other hand a dilute solution, the concentration of which is 25% of a saturated solution's at 75°C, is heated to 90°C, no significant activity loss is observed.

Interestingly, Wolfskill[12] described similar activity anomalies in a patent application filed in 1944. He had studied the etching of AT-cut quartz crystals in hydrofluoric acid as a function of HF concentration, and found that the etching rate was maximum at 40% concentration. He also noted that "...concentrations less than 40% produce the highest quality crystals, while concentrations as high as 60% tend to impair the quality of the crystals..." The activity of crystals decreased with increasing depth of etching for concentrations above 40%. The rate of decrease increased with increasing concentrations. For concentrations above 60% he observed a permanent reduction of activity immediately upon immersing the crystals in the etching solution. For these higher concentration solutions, the activity versus temperature curves were also "extremely erratic", whereas for concentration below 40%, no such anomalies were observed.

Conclusions

Etching solutions capable of chemically polishing SC-cut quartz plates have been found. Chemical polishing can be a simple, inexpensive batch process. If good quality quartz plates are used, the process can provide high yields, with no significant Q degradation at least up to 10 MHz. Chemical polishing produces plates of extremely high strength[1], which reduces yield losses due to breakage during processing and provides the resonators with extremely high shock resistance. The process also reveals defects in the quartz due both to material defects and surface finishing defects. It thereby should also minimize the contribution of such defects to resonator instabilities and failures. The etching solutions which produce a very smooth surface on one side of doubly rotated plates and a rough surface on the other side may be useful for the chemical polishing of doubly rotated surface acoustic wave (SAW) devices, since for SAW devices a rough surface is generally desired on one side of the plate.

Since the etching solutions capable of chemical polishing the SC-cut are not saturated, it is more difficult to control the etching rates. The quantity of etchant in solution decreases as the etching progresses, however, if an open etching container is used, the etchant concentration can increase due to water evaporation. For example, the partial pressure of HF over a 10% HF solution at 80°C is 4.5 torr, whereas the partial pressure of H_2O over the same solution is 312 torr[13].

HF can be a major health hazard. The hazard can be minimized by taking adequate precautions in storage and handling, using appropriate clean-up measures, and by properly dealing with exposure situations.

Acknowledgements

The authors gratefully acknowledge the skillful contributions of D. Eckart and A. Dunlap who provided the SEM micrographs, F. Ivins who provided the profile meter scans, W. Washington who assisted with the etching experiments, D. Boyce who fabricated the etching fixtures, and J. W. LeBus who participated in the early phases of these experiments.

The authors also wish to express their thanks to M. Bloch and B. Goldfrank of FEI and to D. Peters and his collegues at GEND who provided the fabrication and measurements of the Q of 5 MHz 5th overtone resonators.

References

1. J. R. Vig, J. W. LeBus and R. L. Filler, "Chemically Polished Quartz", Proceedings of the 31st Annual Symposium on Frequency Control, pp. 131-143, 1977. Copies available from Electronic Industries Assoc., 2001 Eye St., NW, Washington, DC 20006.

2. Micro Abrasives Corp., 720 Southampton Road, Westfield, MA 01085.

3. Savillex Corp., 5325 Highway 101, Minnetonka, MN 55343.

4. Brooklyn Thermometer Co., 90 Verdi St., Farmingdale, NY 11735.

5. MCB - Manufacturing Chemists, 2909 Highland Avenue, Norwood, OH 45212.

6. Lehigh Valley Chemical Co., P. O. Box 350, Easton, PA 18042.

7. Ashland Chemical Co., Easton, PA 18042.

8. J. S. Judge, "A Study of the Dissolution of SiO_2 in Acidic Fluoride Solutions", Journal of the Electrochemical Society, Vol. 118, pp. 1772-1775, (1975).

9. For a good review of these studies see C. Frondel, "The System of Mineralogy...", Vol. III, Silica Minerals, John Wiley and Sons, Inc., pp. 162-163, (1962).

10. A. W. Warner, "High Frequency Crystal Units for Primary Frequency Standards", Proceedings of the IRE, Vol. 40, pp. 1030-1033, Sept. 1952.

11. G. Malinowski and E. Hafner, "Automatic Microcircuit Bridge for Measurement on Quartz Crystal Units", Proceedings of the 32nd Annual Symposium on Frequency Control, pp. 354-364, 1978. Copies available from Electronic Industries Assoc. 2001 Eye St., NW, Washington, DC 20006.

12. J. M. Wolfskill, "Production of Piezoelectric Crystals", U.S. Patent No. 2,479,286, Aug. 1949.

13. Encyclopedia of Chemical Technology, Wiley Interscience Publisher, Vol. 9, p. 615, 1966.

ANISOTROPY OF ETCHING RATE FOR QUARTZ IN AMMONIUM BIFLUORIDE

P. Suda, A.E. Zumsteg and W. Zingg

OMEGA, Quartz Division, Bienne/Switzerland

Summary

The temperature dependence for the etching rates of synthetic quartz in +X, -X, Y and Z crystallographic directions together with AT-cut in a saturated solution of ammonium bifluoride (NH_4FHF) is reported between 40 and 80°C. For comparison the etching rates in hydrofluoric acid have been measured. In both etchants anisotropy is very large (up to a factor of 1000) and the relation between etching rates are $R(Z) > > R(AT) \gg R(+X) > R(-X) > R(Y)$. The increase of etching rate with temperature is less in HF than in NH_4FHF.

A "polishing" effect was observed on +X-faces in NH_4FHF whilst the pyramidal structure on Z-faces is emphasized by the etch process.

Introduction

Although ammonium bifluoride (NH_4FHF) is an etchant commonly used in the production of quartz resonators we only found some scarce information about etching of quartz during our literature survey. It is well known that the etching rate of quartz primarily depends on the etchant, the temperature and the crystallographic direction after the deformed surface layer has been etched away. According to Ang et al.[1] the change of dimension (let us say thickness) Δt as a function of time τ can be described by the following equation

$$\Delta t = R\tau + C(1 - e^{-\alpha\tau}) \qquad (1)$$

where R is the etch rate in the linear region, C is a constant proportional to the abrasive grain size and α is the etch time constant of the surface layer. Typical curves of etching depth versus time for X , Y- and Z-oriented plates are shown in figure 1. In the initial phase corresponding to region I the behaviour is non-linear. In this paper we are interested only in the linear region II with steady etch rate R.

In previous studies by Vig et al.[2] on AT-crystal plates etched in NH_4FHF and by Lazorina et al.[3] on X-, Y- and Z-faces of crystals etched in HF, the temperature dependence of the etch rate was well fitted by an exponential law

$$R(T) = A e^{-E/kT} \qquad (2)$$

where the constant A contains the nucleation rate of the etch process, E represents its activation energy, k the Boltzmann constant and T the absolute temperature.

Preparation of blanks

For these investigations we used X-, Y-, Z-oriented (direction of the normal to the plate) crystal plates with dimensions 15 x 14 x 0.4 (in mm) and AT-cut plano-convex crystals of 5 MHz fundamental frequency with a diameter of 14 mm. The sides of all plates were lapped with silicon carbide SiC 800 (mean diameter of grain size = 9 μm) and their surfaces with SiC 1200 (3 μm).

Cultured quartz from two different sources has been used (electronic grade quartz from Sawyers and quartz from Russia), but no significant differences were found.

Etching equipment

All experiments were performed in a double-wall beaker closed with a double-wall cover having a hole for agitation of the crystal jig. The whole system was made of polypropylene.

The temperature of the etching bath was stabilized by water, flowing from a conventional thermostat through the walls of the beaker and the cover. The temperature of the water in the thermostat and of the etchant was monitored with thermocouples sheathed with polypropylene. A fairly constant temperature offset between thermostat and etchant of typically 2°C and a

thermal stability of ± 0.6°C of the etchant bath was thus achieved over long periods (up to 70 hours).

The blanks were placed vertically in a polypropylene jig which was moved up and down at a rate of 0.1 Hz (travel 2 cm).

All blanks etched for the same time interval were processed together. None were etched twice and the "state" of all plates at the beginning of the etching was always the same. Once these experiments were carried through, new measurements on some X- and Y-blanks pre-etched for 1 hour at 80°C yielded a perfectly linear time dependence. Altogether approximately 400 blanks have been measured.

Methods of measurement

a) Frequency method

For AT blanks the most common and most exact method to determine the change of thickness $2\Delta t$ is by the change of frequency $\Delta f = f_1 - f_2$ where f_1 and f_2 are the initial and final thickness shear frequencies. If N represents the frequency constant in MHz · mm ($\simeq 1.66$ for AT) and if f_1 and f_2 are expressed in MHz and Δf in kHz, the etch depth on one face Δt is obtained in μm from the equation

$$2\Delta t = N \Delta f / (f_1 f_2) \qquad (3)$$

b) Scale method

In the case of Z and AT-cut plates the depth of etching can be determined accurately by weighing. In our case the resolution of scales was 0.01 mg and the total change of mass usually exceeded 2 mg. The correction arising from etching of the narrow sides is very small for Z-plates due to the surface ratio (approx. 1 to 20) and the slow etch rates in X- and Y-directions compared to Z. In the case of X- and Y-plates this method can give only very crude indication since the loss of mass from the narrow sides can amount to 90% of the total change of mass.

c) Micrometer method

The resolution of thickness measurements with a micrometer is approximately 1 μm. For X- and Y-plates, the total change of thickness used to be in the range 0.5 to 10 μm which yields considerable relative errors.

d) Step method

In opposition to the above methods, it is possible to distinguish between etch depths in direction +X and -X by measuring the height of a step. Therefore we have covered one half of each crystal side with the special black stopping-out varnish used for artistic etching of glass. This masking was insufficient for long etching times, therefore we used the varnish to glue protective quartz plates on half of both sides ot the test plates. After the etching, this sandwich-structure was separated with hot chromic-sulphuric acid. The step on each side was measured with Talysurf (Fig. 2) for all plates except AT. The height can be evaluated by either peak-to-peak or by mean-to-mean differences. The accuracy depends on the surface roughness and is very often limited by the presence of crevices.

Because surfaces are not microscopically flat the first three methods may slightly yield different values. The frequency and the scale methods give average "volumetric" values, e.g. the thickness of an ideal plane-plane plate (if the effect of tension in the deformed surface after lapping is neglected in the former). With the micrometer one gets a peak-to-peak value, i.e. maximal thickness. Since the measured depths of etch are diffrences of either frequency, mass or thickness, the effect due to surface roughness will cancel if the profile does not change significantly.

All measurements made with the four methods described were compatible and thus all values were used to compute the etch rates.

Experimental results

On plates with normal along the Z-axis the change of thickness was measured with scales, micrometer and Talysurf and on AT-plates with scales, micrometer and in terms of frequency change. Etching depths in +X- and -X-directions can be obtained with the step method only. The mean value $\bar{Y}$ and Y were also confirmed by micrometer.

For every orientation and temperature the change of thickness was plotted as a function of etching time (see Fig. 1). After corroboration of the results by the different methods, all values in the linear region were used to compute the etch rates by linear regression. The time of etching was always long enough to guarantee sufficient extension of the linear region. At 80°C it only took a few minutes for Z- and AT-cut plates in order to attain the linear region but for X- and Y-plates the deformed surface layer ($\simeq 2$ μm) is removed only after 1 hour (6 hours at 40°C).

a) Saturated NH_4FHF

Etching rates were plotted in logarithmic scale as a function of inverse temperature (Fig. 3) and the dependence agrees with the exponential of equation (2) at all crystallographic orienta-

tions. Numerical values are reported in table 1.

We were surprised that the etch rate in -X-direction is not negligible compared to +X. It amounts to approximately 30% and the ratio does not depend on temperature. The ratio of etch rates between Z-direction and AT-cut also remains constant with temperature but the slope is less than for X and Y. The deduced values for the activation energy is 0.55 eV (Z-direction) and 0.75 (X-direction). The ratio of etch rates from AT- to Z-orientations is approximately 10% lower than the value (sin 35°) which one would expect from a simple geometric projection. Our experimental etch rate for AT-cut is about 25% less than the corresponding value reported by Vig et al.[2]

b) Unsaturated solution of NH_4FHF

We were interested to know how the etch rates decrease at reduced concentrations. Therefore we used a 1:1 solution (e.g. 1 kg of NH_4FHF in 1 liter of distilled water) which is saturated at 40°C. At 55°C the reduction of etch rate for Z-plates as compared to saturated ammonium bifluoride was about 2% and about 5% at 80°C. In a solution saturated at room temperature (concentration unknown) and heated to 98°C, the etch rate was about 10% below the value extrapolated on figure 3 for Z-direction.

c) Effect of solved SiO_2

In order to evaluate the influence of solved quartz onto the etch rate we added 1.86% SiO_2 (in weight) to saturated ammonium bifluoride. At all temperatures the etch rates measured on Z-plates were about 15% lower than for the original solution which corresponds roughly to a 1% reduction in etch rate per gram of quartz solved in one liter of saturated solution. The effect on other orientations was not investigated.

d) Hydrofluoric acid

A series of experiments was carried out as in part a) but in 38% hydrofluoric acid and on pre-etched plates only. The results at two temperatures (19.4 and 39.9°C) are shown on the right of figure 3 and in table 2. As expected the etch rates are generally larger than in saturated ammonium bifluoride and the 1/T-slopes are smaller. However the ratios of rates in various directions are different. For instance the ratio of etch rates for Z- to AT-orientations is 10 (while it is 2 for NH_4FHF) and for +X to -X the ratio is 12 (3.5 for NH_4FHF). A striking difference occurs between HF and NH_4FHF on Z-plates since the etch rate in the former etchant is almost one order of magnitude higher. The ratios of etch rates between HF an NH_4FHF at 40°C in the different orientations are listed in table 2. It should also be noted that our values for X- and Y-oriented crystal plates are lower at 40°C than those given by Lazorina et al.[3] and that the discrepancy is important for Y-orientation ($\simeq$ 50 times). This remains puzzling.

The effect of concentration onto the etch rate has been checked for Z-plates with 30% and 50% HF. The dependence is linear and the change in etch rate amounts to 0.65 μm/h per percent of concentration change at 20°C.

From figure 3 it can be seen that the etch rate in saturated NH_4FHF will be larger at higher temperature than in 38% HF although the concentration of hydrofluoric acid in ammonium bifluoride is lower. One may surmise the formation of polymeric ions[4] of the type $[HF_2^-]$, $[H_2F_3^-]$ to be involved in this phenomenon but the explanation lies beyond our knowledge.

e) Change of shape

We observed that after long etching some edges and corners were missing. The configurations for X- and Y-plates are shown in figure 4. The edge between X- and Y-planes remains sharp. The effect is much bigger on X-plates than on Y-plates and in both cases increases with time. At some corners small facets occurred. No such effect was found on Z-plates but these were etched for relatively short times.

f) Change of surface structure

The etch figures developed on the different planes of etched crystals agree with those discussed by Cady[5]. We observed the changes of these figures with increasing etch time using an optical microscope with differential interference constrast and the changes in profile with a Talysurf.

On Z-faces small trigonal pyramids appear after short time and their dimensions increase with increasing depth of etch. The surface gets rougher.

On Y-faces typical trapezoidal figures develop very quickly. Their surface increases drastically with etching time but their depth reaches a steady value which is approximately twice the characteristic depth of the lapped surface ($\simeq$ 0.4 μm with SiC 1200).

The -X-surfaces appear like parallel furrows oriented along Z. A profile scan after short etching times shows a few deep grooves ($\simeq$ 1.5 μm) but these irregularities disappear after long etching times. The profile gets very anisotropic in the -X-faces; in Y-direction it remains similar to lapped surface whereas in Z-direction it is much broader.

The most interesting effect was observed on +X-

surfaces. Relatively deep grooves ($\simeq 0.4\ \mu m$) with rhombus-like shapes were found after short etching times. With increased etching the +X-surface becomes much smoother (profile depth about $0.15\ \mu m$) and the structure is isotropic in the plane.

A quantitative analysis of the dependence of surface roughness on the depth of etching has not been attempted.

Conclusions

The etching rates of quartz in ammonium bifluoride like in hydrofluoric acid are very anisotropic. The relations in both etchants are $R(Z) > R(AT) \gg R(+X) > R(-X) > R(Y)$. The etch rates in HF 38% at temperatures $< 40^{o}C$ are generally larger than in saturated NH_4FHF but the temperature dependence is slower. Anisotropy of etching in ammonium bifluoride decreases with increasing temperature. The influence of concentration of bifluoride and also of dissolved SiO_2 on the etch rates is relatively small. The pyramidal structure of Z-plates becomes rougher with longer etching whereas on +X-faces a "polishing" effect takes place. On -X-faces the depth of profile does not change significantly from that of the lapped surface and on Y-surfaces the depth of trapezoidal grooves increases rapidly to a steady value approximately twice that of the initial state.

Acknowledgements

The authors gratefully acknowledge the skillful help of Mr P. Voelgyi from SSIH-Electronic, Quartz Division, who performed the etching and the scale- and micrometer-measurements and of Mr H. Gerber from Laboratory Oméga who provided the Talysurf scans.

References

1) D. Ang, Design and Implementation of an Etch System for Production Use, Proceed. 32nd ASFC, 1978, p 282.

2) J.R. Vig, J.W. LeBus and R.L. Filler, Chemically Polished Quartz, Proceed.31st ASFC, 1977, p 131.

3) E.I. Lazorina and V.V. Soroka, Etching of Quartz and some Features of the Surface Layer, Sov. Phys. Crystallogr. vol. 18, 1974, p 651.

4) J.S. Judge, J. Electrochem. Soc., vol. 118, 1971, p 1772.

5) W.G. Cady, Piezoelectricity, Dover Publ., NY, vol. II, 1964, p 421.

Temperature	Orientation of crystal plates					
(^{o}C)	Z	AT	+X	-X	X	Y
81	45.7	24				
78.5			3.8	1.1	2.5	0.36
54.7	11.4	6				
54			0.62	0.19	0.40	0.06
39.7	4.4	2.2	0.17	0.05	0.11	0.02

Table 1 Etching rates in NH_4FHF ($\mu m/h$)

Temperature	Orientation					
(^{o}C)	Z	AT	+X	-X	X	Y
19.9	16.2	1.22	0.15	0.01	0.08	0.01
39.9	39	3.95	0.35	0.03	0.19	0.019
40 (ref.3)	38.3		1.5	(0)		1.1
$\frac{R(HF)}{R(NH_4FHF)}$ at $40^{o}C$	8.9	1.8	2	0.6	1.7	$\simeq 1$

Table 2 Etching rates in HF 38% ($\mu m/h$)

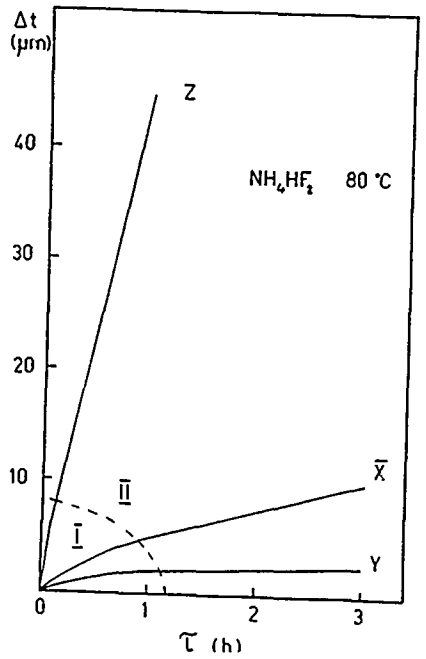

Fig. 1 Etching depth per face as a function of time with non-linear region I and linear region II.

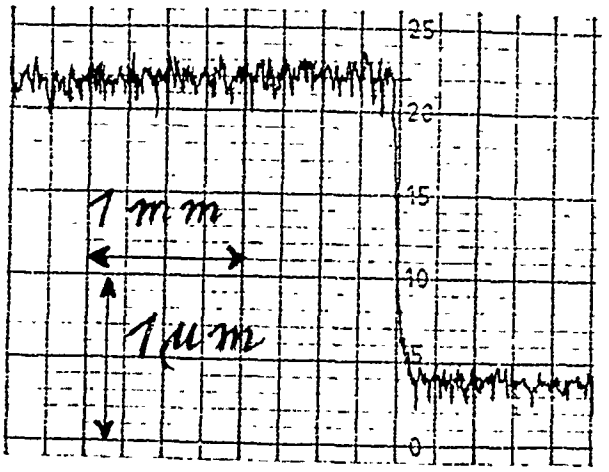

Fig. 2 Talysurf scan on +X-face etched for 30 minutes at 80°C.

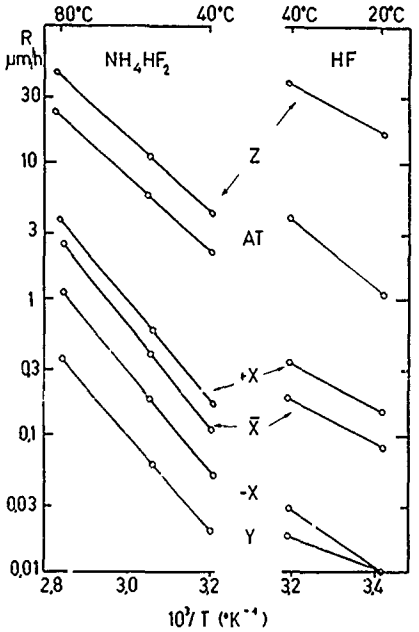

Fig. 3 Temperature dependence of etching rates for all measured crystallographic orientations.

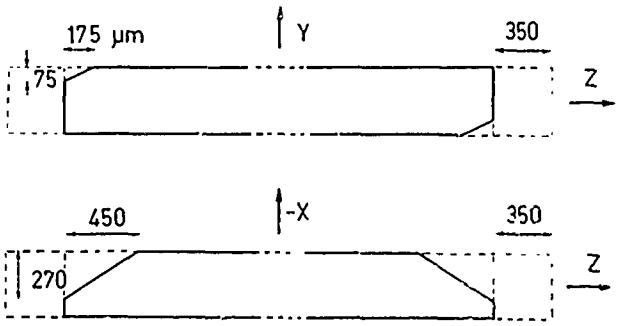

Fig. 4 Shape of edges after etching for 68 hours at 40°C in ammonium bifluoride.

A MICROPROCESSOR ASSISTED ANODIZING APPAKATUS FOR FREQUENCY ADJUSTMENT

Dick Ang

Tyco Crystal Products Inc.,
Phoenix, Az 85019

Summary

Anodizaion of aluminium electrode quartz crystal units have been applied for several years. By controlling the thickness of the oxide on the crystal electrode the frequency of the crystal unit is changed until it reaches the desired frequency. By utilizing a microprocessor assisted instrumentation we have been able to process several crystals simultaneously, but treating each crystal individually as far as the required anox voltage is concerned. Using this technique we are able to process on the order of 1300 crystals per person per day with very high yields.

Introduction

In 1976 V.E. Bottom of Tyco Crystal Products introduced the anodization process on VHF crystal units.[1] Several advantages are readily apparent about this process. Lower aging rate because the Al_2O_3 film is considerably thicker than the natural oxide thickness on the aluminum of non anodized units. The Al_2O_3 film is grown uniformly over the electrode surface, thereby reducing spurious responses on the crystals, (these are crystal responses which may occur below the series resonance frequency because of uneven thickness over the electrode area). Al_2O_3 is a hard material, unlike over plating with other relatively soft metals, it is resistant to scratching during handling between final frequency adjustment and sealing. The problem of "sleeping sickness" appears to be less likely because the Al_2O_3 layer is intimately bonded to the aluminum electrodes.

Anodization involves the build up of aluminum oxide film on the electrode surface of a resonator. The thickness of the oxide film is governed by the applied voltage during anodization. If the frequency of a crystal resonator is X Hz above the target frequency, the required anodizing voltage is approximately[1]:

$$(a)\quad V = Vo + \frac{X}{A} \quad \text{and} \quad (b)\quad A = 0.87\, h f_1^2 \qquad (1)$$

Where:

X = number of Hz above target frequency
A = anox constant in Hz Volt
h = overtone number: 1, 3, 5, ...
f_1 = fundamental frequency of the blank in MHz
Vo = the threshold voltage on the film

In actuality the threshold voltage Vo is not known precisely it is generally less than on the order of 4 volts. Furthermore the anox constant A is slightly dependent on the electrode dimensions and is very sensitive to foreign ion contamination in the solution. Variation on the order of 20% in the constant A is not uncommon and severe contamination of the solution can result in the entire removal of the aluminum film with the ultimate result of an inoperative crystal. Therefore, although the voltage can in principle be computed rather easily from the equations 1 (a) and 1 (b), in actuality the process may not always be that simple to control. Poor knowledge of Vo and variations in the constant A can quickly lead to a trial and error method of adjusting the frequency of the crystal. In the anodization process of quartz resonator crystals which are over anoxed[2] and thus its frequency too low, cannot be raised by "reverse anodization" as a crystal can be "deplated" to raise its frequency. One method to raise the crystal frequency for over anodized crystals is by etching the electrodes in a diluted sodium hydroxide solution. This process, however, consumes the aluminum in the electrodes at a far greater rate than the Al_2O_3. Thus in some cases it can reduce the film conductivity to an unusable level.

In contrast to electroplating for frequency adjustment; where the electrode film can be plated or deplated, to lower or increase the frequency of the resonator respectively; the anox process requires precise control for its success. As a corollary to this, the skills of assembly persons for anodization develops more slowly than skills in other more conventional methods of frequency adjustment.

The advantages in performance of anodized units, however, far outweights the difficulties we mentioned. This paper will attempt to describe what we have learned and applied to gain better control of the anox process with the aid of a micro computer.

Successive Anodization Method

Better control of the anox process can be obtained by performing successive anodization voltages as prescribed in the following sequence. Suppose a crystal which is to be frequency adjusted has a frequency of F_1 and the target frequency is Fo as shown in figure 1. The threshold voltage Fo is unknown, but it can be set to a value which is slightly higher than the upper bound of the natural oxide layer. By applying a 5 volt anodizing voltage to each crystal electrode, we assure that the threshold voltage of the crystal is at 5 volts. The frequency of the crystal will decrease slightly from F_1 let us define this frequency to be Fx.

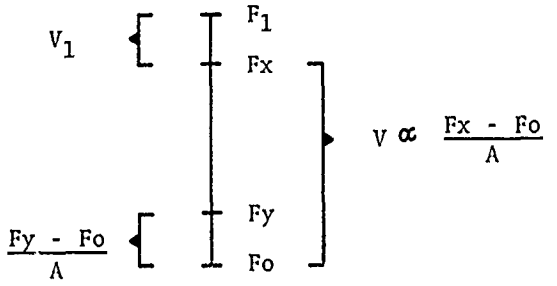

$$V_A = V_0 + \left(\frac{X}{A}\right) \quad ; \quad A \simeq 0.87\ hf_1^2$$

$$V_1 \equiv V_0 \equiv 5V$$

$$V_2 = V_1 + \left(\frac{Fx - Fo}{A}\right) 0.9$$

$$V_3 = V_2 + \left(\frac{Fy - Fo}{A^1}\right)$$

$$A^1 \equiv \frac{(Fx - Fy)\ A}{0.9\ (Fx - Fo)}$$

Figure 1

The next step is to estimate the voltage necessary to reach the target frequency Fo starting from Fx with the 5 volt threshold voltage on the electrodes. Since the constant A, the anox constant, is not known precisely; we use an intermediate step to determine A. To achieve this we can estimate the required voltage using the constant A defined in equation 1 (b); i.e.

$$V = \frac{(Fx - Fo)}{A}$$

however, to assure that we are slightly above the target frequency Fo, we only apply a fraction of this voltage, i.e.

$$V = 0.9\ \frac{(Fx - Fo)}{A}$$

The second anodizing voltage is thus

$$V_2 = V_1 + 0.9\ \frac{(Fx - Fo)}{A}$$

After the second anodization voltage is applied the frequency of the crystal will be at Fy (see figure 1) and as expected still above the target frequency Fo. The difference in the frequency Fx - Fy is a result of applying the voltage of magnitude

$$0.9\ \frac{(Fx - Fo)}{A}$$

We can now determine the exact anox constant for this crystal; i.e.

$$A^1 = \frac{(Fx - Fy)\ A}{0.9\ (Fx - Fo)}$$

The final anodization step can now be applied and the incremental voltage necessary to reach Fo is therefore:

$$V = \frac{(Fy - Fo)}{A^1}$$

The third and last anox voltage is therefore:

$$V_3 = V_2 + \frac{(Fy - Fo)}{A^1}$$

Although the above sequence appears to be tedious and complex to apply, it can easily be performed with the aid of a micro processor assisted apparatus. Furthermore to make more efficient use of the processing time, several crystals can be anodized simultaneously.

Instrument Description

The block diagram of the system we implemented is shown in figure 2. The CRT terminal, floppy disk and 8 bit micro computer with the associated Basic Interpreter comprise the computing part of the system. We choose Basic because it is an easy interactive language to learn and implement. The remaining parts in figure 2 comprise the processing portion of the hardware. The micro computer system incorporated into the apparatus is a North Star Horizon Computer.[3] The D to A and A to D convertors and I/O circuitry is available on the market from Crommenco in the form of card modules.[4] The eight bit resolution of the D to A convertors allows the anox voltages to be varied from 5 to 55 volts in increments of 0.2 volts. This is an equivalent change on the Al_2O_3 film in steps of about 2 Angstroms from about 60 to 560 Angstroms.

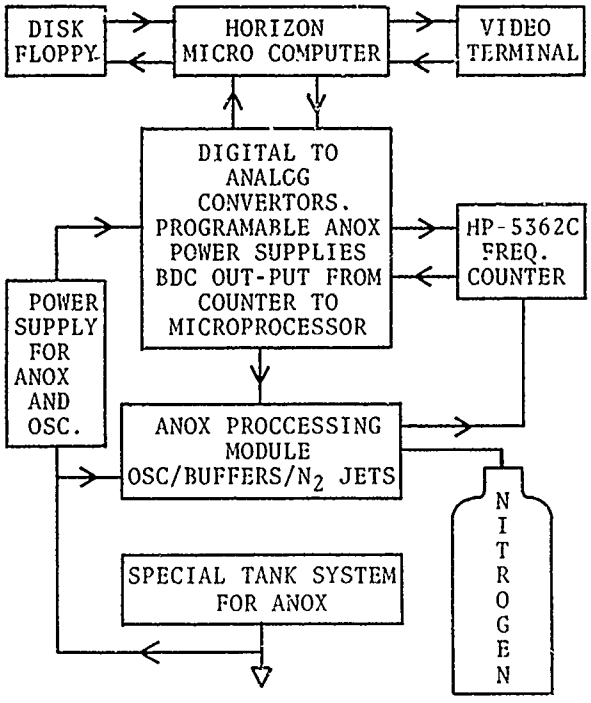

FIGURE 2

The programmable constant voltage power supplies are essentially high voltage operational amplifiers driving a pass transistor. The programmable power supplies converts the low output voltage from the D to A convertors to a maximum of 55 volts. The BCD data from the HP 5326C counter (or any counter with BCD output) is transmitted to the micro computer via the Parallel I/O ports available on the D to A modules.

The anox module provides a platform for processing the crystals. In this system 12 crystals are simultaneously processed and each crystal is treated individually. The only requirement it must have is that the adjustment range must be achievable with less than or equal to 55 volts. The anox module contains 12 individually addressable oscillators and buffer amplifiers, 12 pairs of nitrogen jets for drying the crystals and 12 addressable anox lines. The anox voltage which can reach as high as 55 volts is prevented from damaging the oscillator circuitry by blocking capacitors.

The anox tank is designed to accommodate up to twelve crystals with a minimum amount of interaction between the anodizing electric fields. The negative electrode in the tank is the common electrode for all the crystals in this electrolytic cell. By dividing the tanks into compartments, the electric field from each crystal is directed towards the common aluminum electrode rather than towards other crystals with a lower potential. The tank is constructed out of plexiglass material such that the liquid level can be inspected for proper coverage on the crystal electrodes. To facilitate the draining of the electrolyte in the tank, a solenoid valve is attached to the bottom of the tank.

Anodizing Procedure and Software Outline

Figure 3 shows the anodizing procedure and software outline which we implemented in this instrument.

The crystals which are to be anoxed are inserted into the anox processing module. The module is then lowered into the anox tank for the first 5 volt anox for a length of time of about 5 seconds. The anox tank is equipped with a photodetector which tells the micro porcessor that the processing module is over the tank and anodization should begin on all twelve crystals. The microprocessor times the operation, and after 5 seconds has elapsed it will turn off the 5 volt anodizing voltage and commands the anox operator, via the CRT terminal, to wash and dry the crystals. The operator then picks up the processing module and goes over the washing procedure.

The washing procedure consists of 2 ultrasonic rinses in deionized water and one ultrasonic rinse in methanol. The ultrasonic tanks are equipped with microswitches such that it operates only when the anox module is over the particular ultrasonic station. Solenoid operated drain valves below the ultrasonic tanks facilitate the draining of the liquid inside the ultrasonic vessel. After the last methanol rinse is completed, the anox module is transfered to the drying area where dry nitrogen gas in metered into the drying jets and directed to the crystal surfaces. The drying time is also controlled by the microprocessor by inputting a preprogrammed time into the device.

After the crystals are dry, the microprocessor begins to address each oscillator individually and retrieve the frequency data from each crystal via the HP 5326C frequency counter. After all twelve frequency data are taken, the microprocessor computes the first estimated anox voltages for all twelve crystals. These voltages may and are usually different for all twelve crystals. The microprocessor commands the operator to lower the anox module into the anox tank for the trial anodization; i.e. the crucial anodization step for computing the actual value of the anox constant A^1 for each crystal. Again the photodetector on the tank tells the microprocessor to commence anodization on all the crystals with specific voltages on each crystal and timing each crystal properly; i.e. those crystals with the lower

voltages will be anodized for shorter times and conversely those with higher anox voltages will be anodized for longer times. The anodization is terminated by turning the voltages to Vo = 5 volts. The crystal which requires the highest anox voltage determines the maximum time the anox module spends over the tank. After the completion of this stage, the microprocessor again commands the operator to wash and dry the crystals. Each crystal frequency will again be retrieved by the microprocessor and the anox constant A^1 is calculated for each crystal. The necessary voltage for each crystal to reach target frequency is computed and the operator lowers the anox module for the third and last time. After the anodization is completed the crystals are washed and dried and its frequencies are again read by the microprocessor and compared to the allowed frequency tolerance of the units.

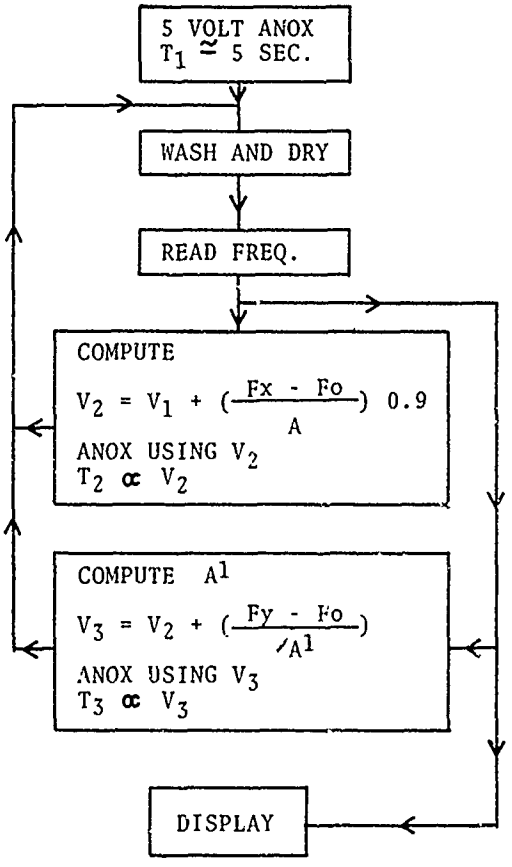

FIGURE 3

The CRT displays all the frequency data and other pertinent data on the screen. It displays which crystals are good and the anox constant A^1 of each crystal. A closely grouped A^1 constants with a mean value close to that defined by equation 1 (b) usually indicates that the process is under excellent control. Conversely wild variations in A^1 from crystal to crystal indicates that the process is out of control. The yield data after each run is stored into the disk and can be retrieved at the end of the day for yield analysis.

Production Notes

Tyco has operated this instrument for over a year at this time. The yield of this particular step in the production is generally 95% or better. The peak troughput is about 1300 crystals per eight hours with a standard deviation of about 3 ppm on the frequency v.s. distribution curve. The crystals were 3rd. overtone units at about 50 MHz. The set up time and cleaning time takes about 5 minutes respectively for an eight hour shift.

The microprocessor part of the system is by far most reliable group of hardware in this system, the individual oscillators in the anox module the worst in terms of maintenance. The oscillators have to be recalibrated periodically (at least once a month) to maintain its correlation. Indeed the anox module receives the most abuse in terms of shock and vibration in everyday service. Incidentally the maximum batch quantity of twelve in this system is by no means a limitation on the computing part of the system. A batch quantity of 100 crystals per run is entirely feasible from the computing standpoint. The problem involves the weight of the processing module. In such applications we recommend a robot arm to move the anox module from the various anodizing and rinsing stations. Our system can also be adapted for batch electroplating by changing the programmable constant voltage power supplies and slight modifications in the tank system.

Acknowledgement

The author would like to thank Mr. A. Klimmuck, Mr. L. Acosta and Mr. S. Cole for their skillful contributions. I am indebted to Dr. V. E. Bottom for many of the priviledged information about the anox process.

References

1. V. E. Bottom "A Novel Method of Adjusting the Frequency of Aluminum Plated Quartz Crystal Resonators" Proc. 30th AFCS, p.p. 249 1976

2. Anox is a trade mark of Tyco Crystal Products Inc.

3. North Star Computers, 2547 Ninth St., Berkeley, Calif. 94710

4. D to A I/O, Crommenco Incorporated, 2400 Charleston Rd., Mountain View, Calif. 94043

CONTINUOUS VACUUM PROCESSING SYSTEM FOR QUARTZ CRYSTAL RESONATORS*

R. J. NEY
General Electric Company, Neutron Devices Department
St. Petersburg, Florida 33733

E. HAFNER
US Army Electronic Technology and Devices Laboratory (ERADCOM)
Fort Monmouth, New Jersey 07703

Abstract

An ultrahigh vacuum continuous cycle quartz crystal fabrication facility has been developed that assures an essentially contamination free environment throughout the final manufacturing steps of the crystal unit. The system consists of five essentially tubular vacuum chambers that are interconnected through gate valves. The unplated crystal resonators, mounted in ceramic flatpack frames and loaded on carrier trays, enter the vacuum system through an entrance air lock, are UV/ozone cleaned, baked at 300°C, plated to frequency, thermocompression sealed, and exit as completed crystal units through an exit air lock, while the bake, plate and seal chambers remain under continuous vacuum permanently. In-line conveyor belts are used, in conjunction with balanced vacuum manipulators, to move the resonator components to the various work stations. Unique high density, highly directional nozzle beam evaporation sources, capable of long term operation without reloading, are used for electroding the resonators simultaneously on both sides. The design goal for the system is a production rate of 200 units per 8 hour day; it is adaptable to automatic operation.

Key Words
Quartz Crystal Units; Ultrahigh Vacuum Systems; Ceramic Flatpack Crystal Units; Nozzle Beam Evaporation Source; In-Vacuum Transport; In-Vacuum Manipulator; Thermocompression Sealing; Hermetic Sealing.

Introduction

The development of the ceramic flatpack crystal unit, it its various stages, has been described in the past[1-4]. The current paper deals with an ultraphigh vacuum system to process the flatpack crystal units in a continuous cycle vacuum system.

*The system has been designed and constructed at the General Electric Neutron Devices Department under an ERADCOM sponsored MM&T contract (Nr. HH 610964CPW3/01), in accordance with ERADCOM supplied visualization and concept design drawings.

The functions to be performed in the system are UV/ozone cleaning, vacuum bake, deposition of gold to a specified resonant frequency and a thermo-compression sealing of the envelope. Unplated resonators, mounted in flatpack frames, are inserted into the system, and exit as completed crystal units.

The major criteria in the design of the system was serviceability and the ability to automate its operation at a later date[5].

Discussion

In order to achieve the above goals, a five-chamber, tubular envelope with in-line conveyor transports and manipulators was developed. Figure 1 is a cross sectional schematic diagram of the system. The five chambers are located as shown: the entrance and UV clean chamber, the bakeout chamber, the plating chamber, the sealing chamber, and the exit chamber. Each chamber is separated from the adjoining chambers by gate valves, and each chamber is individually pumped by cryogenic pumps. Each chamber contains a conveyor-like transport, which carries parts trays to the processing stations. The transports are in line, so that the trays may be transferred from transport to transport over a relatively small gap at the gate valves. Three manipulators are utilized to move the parts, or trays, to the respective work stations, one each at the coarse and fine plating stations, the third at the sealing station. The flatpack components are loaded between guide rails in the parts trays in a lid-frame-lid sequence; experiments to date have been made with ten set trays, adapted to the ceramic flatpack enclosures measuring 1 cm on the side.

The first chamber is used as an "air lock" chamber, so that parts trays may be inserted into the system without exposing the rest of the system to the atmosphere. This chamber is also used as an ultraviolet/ozone cleaning chamber. Special mercury/quartz lamps, with dual envelopes are used, - the outer envelope is intended to minimize the possibility of contaminating the system with mercury.

The components are vacuum baked in the second chamber. Here, tantalum heaters,and reflectors located above the transport, are capable of heating the parts trays to above 300°C. The transport materials and construction permit continuous operation at 300°C and at 10^{-8} torr for extended periods of time.

The third chamber contains two gold plating stations. The first one is for coarse plating, with the crystal resonator at 300°C, the second for fine tuning at the "turn over" temperature. Each station has two deposition sources for simultaneous plating on both sides of the crystal. A nozzle beam gold source was developed for this purpose.[6-8] (The current design of this source will be described later.) Each station has a mask head which contains the mask and associated equipment. The manipulators transfer the substrates from the parts trays into the mask head, and back to the trays after plating. Mask exchange is likewise accomplished with the aid of the carrier trays and manipulators.

In order to maintain high vacuum in the plating chamber for several hundred days continuously, the sources and mask heads are mounted on elevators. These elevators may be retracted through gate valves, into readily demountable auxiliary chambers for maintenance purposes. The elevator shaft to port openings are sealed with metal bellows.

The fourth chamber contains the gold thermocompression press and oven. The parts trays are transferred from the transport into the sealing oven and back to the transport by the third manipulator. The components are heated to 325°C, prior to sealing, at a system pressure of about 5 X 10^{-8} torr; a hydraulically operated ramrod is then used to seal the 10 units in the tray simultaneously. Metal bellows provide the vacuum seal for the ramrod. Operational data to date indicated a sealing yield of 83% for all causes.

The fifth chamber is the exit chamber, which is used as an exit "air lock" so that finished components can be extracted without exposing the rest of the system to the atmosphere.

Figures 2, 3 and 4 are various views of the system hardware during construction. Figure 5 shows the transport. The latter utilizes a commercial stainless steel conveyor belt in the format of 35mm motion picture film. The drive sprocket wheels are standard commercial components. All drive and idler shafts are supported by molybdenum-disulfide coated ball bearings, providing for long-term continuous operation below 10^{-8} torr pressure and at 300°C temperature Several commercial molybdenum-disulfide coated journal bearings failed in the magnetic rotary feedthrough that drives the transport. When the journal bearings were replaced by ball bearings in these devices, no further failures occurred.

The parts tray engages the center holes in the conveyor belt for positive locationing. The trays are 10 inches long, they easily traverse the 3-inch gaps between adjacent transports at the gate valves. Figure 6 shows the transfer of the parts tray through the gate valve "gap".

Figures 7 and 8 show the parts tray with moveable separators. As the ramrod moves the push block, the flatpack components form a solid stack, and the frame/lid separators retract into the rails. Two hooks on the tray are used to engage the Manipulator Tee Bar.

Figure 9 shows a schematic diagram of the manipulator. It contains three metal bellows and a sealed ball joint. Five degrees of freedom are obtained with this device. Atmospheric pressure loading on the bellows is eliminated by rough pumping the inner sealed region of the bellows; this permits direct manual operation of the manipulators.

Figure 10 shows the actual manipulator with forceps that are used to move crystal frames. A Tee Bar substituted for the forceps is used to transport parts trays into the sealing chamber oven.

Figure 11 shows the schematic diagram of the nozzle beam source. It contains two chambers: the source and collimation chambers. The source chamber contains gold in liquid and vapor phases at near equilibrium. The collimation chamber is at relatively high vacuum and it contains liquid gold at the bottom. The gold pools of the two chambers are interconnected by a passageway. The two chambers are also connected by an aperture of diameter d_0. The skimmer, aperture d_1 is used to trim the nozzle beam to the desired size.

The expressions for supersonic free jet flow through the source aperture, and centerline intensity, are shown on Figure 11. From these relations it can be calculated that at about 2360°C source chamber temperature, a 1/2mm aperture is capable of producing a gold beam of about 2000 Å/min deposition rate at 14cm "throw" distance. The pressure in the source tube at this temperature is about 40mm of Hg.

Figure 12 shows the schematic diagram of the device that was developed. It is about 7.5cm long and 2cm in diameter, shown without the radiation shields. The body of the crucible is made of graphite, this material does not react with liquid gold, and it does not crack with repeated temperature cycling between 2400° and 20°C.

The source chamber is a tubular piece of graphite, electrically heated, with a tungsten wick mounted at the center. The wick feeds the liquid gold into the heat zone by surface tension forces, and provides a relatively large surface area for vaporization. Using a sharp VEE aperture of 20mil diameter, an output cone of about 24° included angle was observed. A tungsten skimmer aperture plate, with a 0.076cm aperture is used to trim the beam to approximately 2 1/2° divergence; the excess gold is condensed on the skimmer and it is returned

to the gold reservoir.

Figure 13 shows an X-ray picture of an actual device with the gold reservoir, tungsten wick, and skimmer aperture clearly visible. The first two sources installed into the plating chamber have accumulated over 1100 hours of operating time each and beamed about 2 1/2 ounces of gold each. To date, they are still operating perfectly. The actual device with the skimmer aperture at the front is shown in Figure 14, the source tube, tungsten wick, and two skimmer aperture plates in Figure 15. The sources are enclosed in a water cooled envelope, so that heat transfer into the chamber is minimized.

The actual measured output at 14cm of target distance was 400 Å/min at about 400 W power input to the source tube. The skimmer aperture efficiency was measured to be about 30%.

At power inputs corresponding to about 100 Å/min deposition rates, for final plating, batches of 20 MHz resonators (C_1 = 12fF) had a yield of 90% for 10 ppm deviation through sealing, with the uncertainties in the actual temperature of the resonator during final plating believed to be the major cause of the observed deviations. This aspect is being improved.

Conclusions

The present state of development of the system is illustrated by the following:

1. The entire system was operated for several weeks at a "system check out" production rate of 10 units per day without any mechanical failures.

2. The best pressures obtained so far in the baking and sealing chambers, with the trays at 300°C, are 5 X 10^{-8} torr. The major component of the residual gases is water.

3. The best pressure to date in the plating chamber, during plating is 5 X 10^{-7} torr; this pressure is improving with operating the sources. The major component of the residual gases is water.

4. Plating-to-frequency yields of 90% are typical for 10ppm deviation, and about 50% for 5ppm deviation (20 MHz fundamental resonators).

5. The sealing yield for several hundred units was 83% for all causes. The causes include ceramic part, metallizing and gasket defects.

Work on the system continues toward the 200 unit/8 hour day objective with no major obstacles apparent.

References

1. E. Hafner and J. R. Vig; "Crystal Resonator Housing Configuration", U.S. Patent Nr. 3,931, 388, Jan 6, 1976.

2. J. R. Vig and E. Hafner, "Packaging Precision Crystal Resonators", Technical Report ECOM 4134, US Army Electronics Command, Fort Monmouth, NJ, July, 1973.

3. P. Wilcox, G. Snow, E. Hafner and J. R. Vig, "A New Ceramic Flatpack for Quartz Resonators", Proc. AFCS 28, June 1975, pp 202-210.

4. R. D. Peters, "Ceramic Flatpack Enclosures for Precision Quartz Crystal Units", Proc. AFCS 30, pp 22-231. June 1976.

5. J. M. Frank and R. Ney, "Quartz Crystal Fabrication Facility", First Semi-Annual Report, Contract ECOM HH6l0964CPW3/01 with General Electric Company, Neutron Devices Department, Nov 1977.

6. R. P. Andres, "Design of a Nozzle Beam Type Metal Vapor Source", Proc. AFCS 30, pp 232-236, June 1976.

7. J. R. Vig, E. Hafner and R. P. Andres, "Nozzle Beam Type Metal Vapor Source", U.S. Patent Nr. 4,125,086, Nov 14, 1978.

8. R. Ney and E. Hafner, "Improvement of Nozzle Beam Source", U.S. Patent pending.

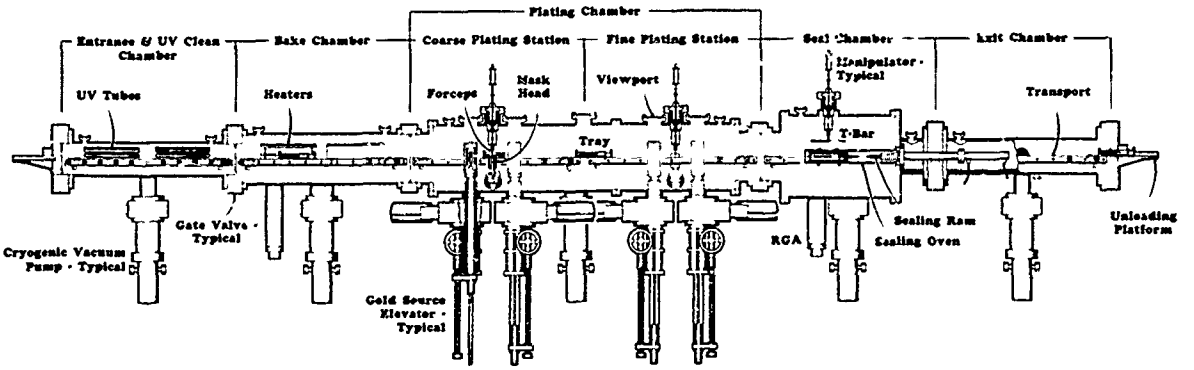

Quartz Crystal Fabrication Facility

1. Cross-sectional Schematic Diagram, Five-Chamber System

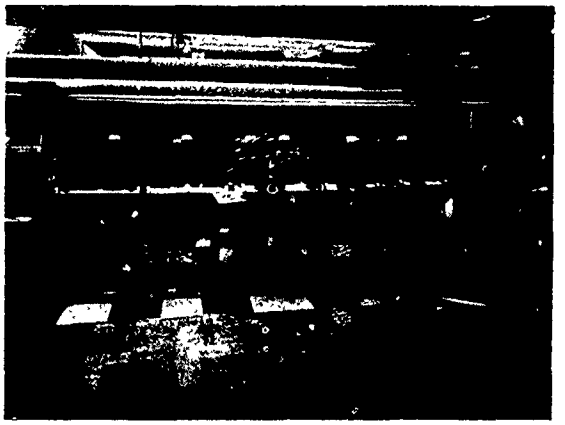

2. Front-Center View of System

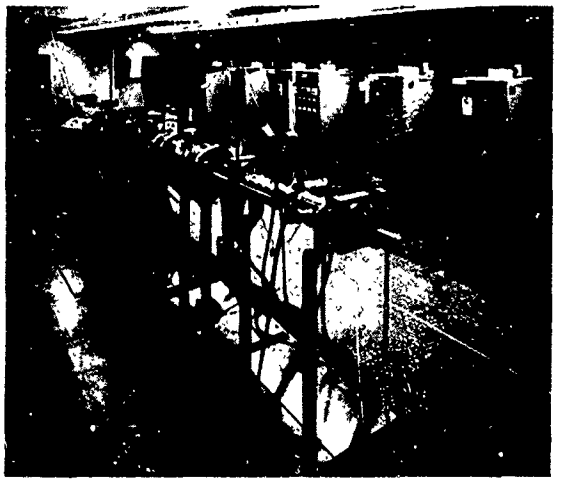

3. Oblique Front End View of System

4. Oblique Back End View of System

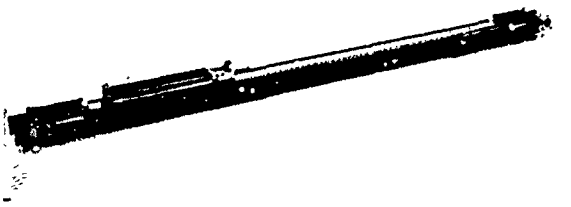

5. Transport

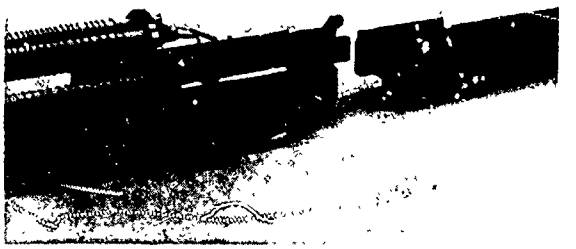

6. Transfer of Tray Through Gate Valve Gap

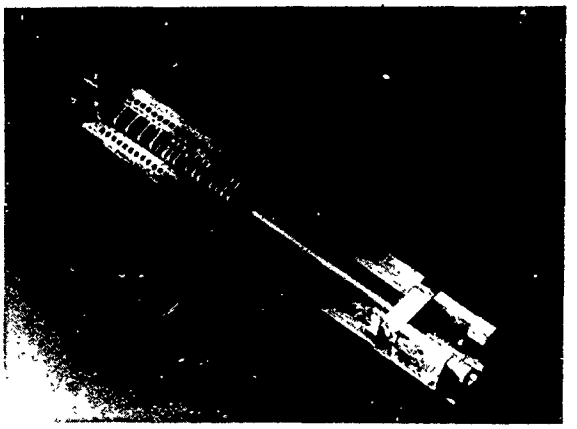

7. Parts Tray

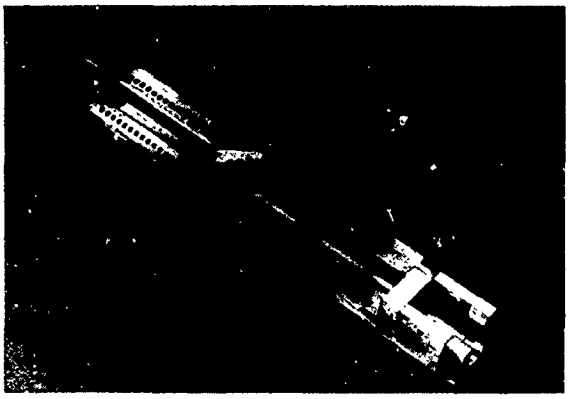

8. Parts Tray

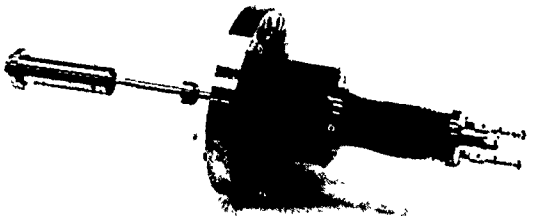

10. Photograph, Manipulator

Vacuum Manipulator

··· Atmospheric Pressure Balanced ···

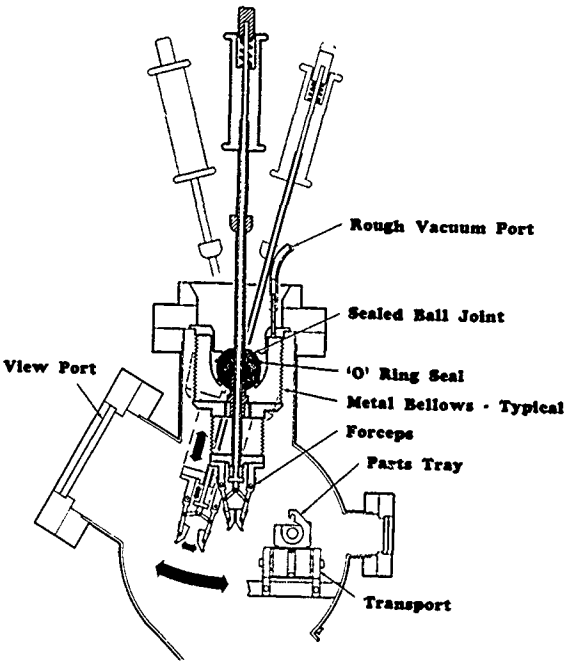

9. Schematic Diagram, Manipulator

NOZZLE BEAM SOURCE

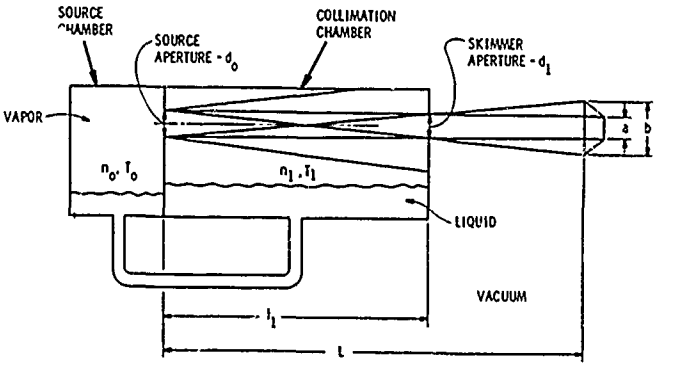

THE EXPRESSIONS FOR SUPERSONIC FREE JET FLOW ARE:

$$f_0 = (0.513) n_0 \left[\frac{2kT_0}{m}\right]^{\frac{1}{2}} \left[\frac{\pi d_0^4}{4}\right] \quad (1)$$

AND $$I(\theta = 0, \ell) = (1.85) f_0 \left[\frac{1}{\pi \ell^2}\right] \quad (2)$$

WHERE f_0 = TOTAL SOURCE FLOW (MOLECULES/SEC)

n_0 = SOURCE DENSITY (MOLECULES/CC)

T_0 = SOURCE TEMPERATURE (°K)

k = BOLTZMANN'S CONSTANT (ERG/°K)

m = MOLECULAR WEIGHT OF VAPOR (GM/MOLECULE)

d_0 = SOURCE APPERTURE DIAMETER (CM)

$I(\theta = 0, \ell)$ = CENTERLINE FLUX INTENSITY (MOLECULES/CM² SEC)

ℓ = DISTANCE FROM SOURCE APPERTURE. (CM).

11. Schematic Diagram, Nozzle Beam Source

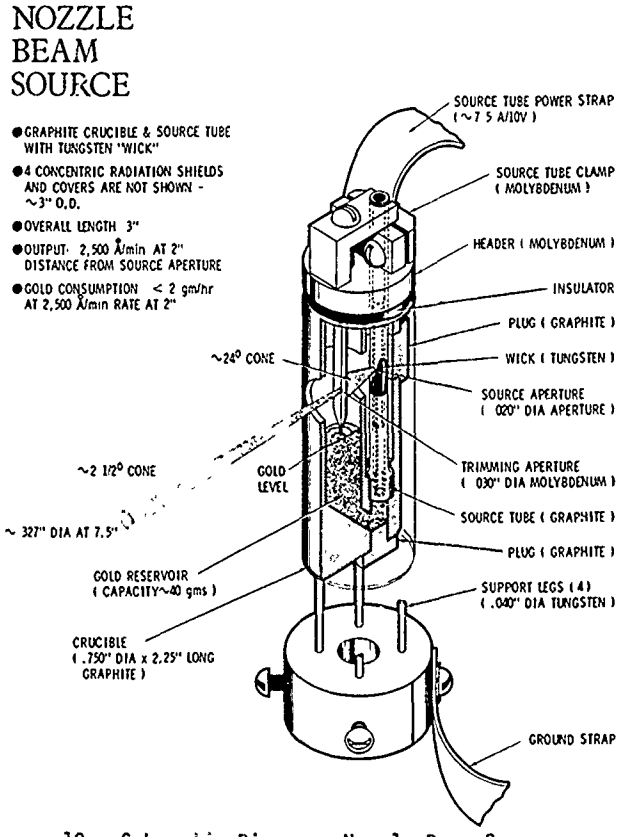

12. Schematic Diagram, Nozzle Beam Source

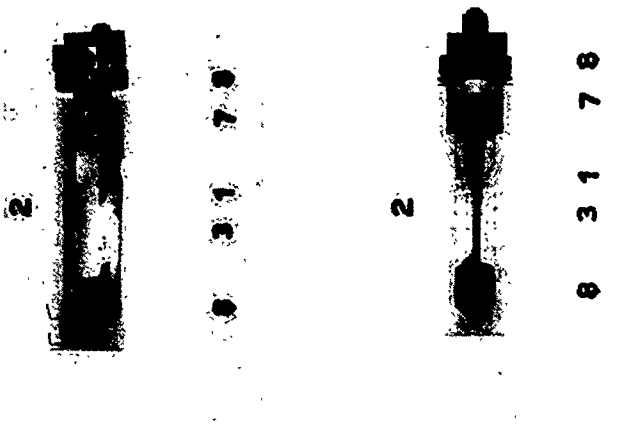

13. X-ray Photograph, Nozzle Beam Source

14. Photograph, Nozzle Beam Source

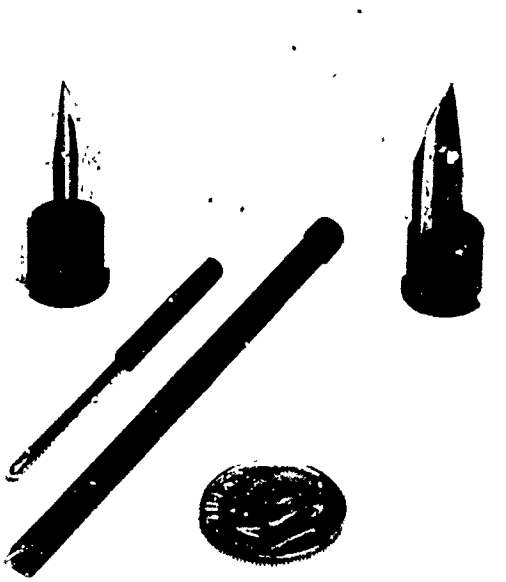

15. Source Tube, Tungsten Wick and Two Skimmer Aperture Plates

HYBRID SAW OSCILLATOR FABRICATION AND PACKAGING

S. J. DOLOCHYCKI, E. J. STAPLES, J. WISE, J. S. SCHOENWALD, AND T. C. LIM

Rockwell International Science Center
Thousand Oaks, California 91360

Abstract

Until recently, fundamental mode quartz oscillator crystals were not available in the 300-400 MHz range. This paper describes the fabrication and packaging of (1) high Q resonators, and (2) a hybrid, hermetically sealed, 400 MHz SAW oscillator. Because of high sensitivity to surface effects, which are inherent in SAW resonator devices, both organic and inorganic surface contamination play a critical role in overall device performance. Cleaning procedures for quartz were investigated using SAW resonators as process monitors. The results of these studies provided an accurate and quantitative measure of the step by step process. Our objective was to evaluate the effect of hybrid fabrication processes on SAW oscillators and to fabricate a completely hybrid 400 MHz oscillator in a common enclosure. Measurement techniques were developed to evaluate resonator stability before being placed in an oscillator circuit. The results of these measurements indicate that much of the instability in SAW oscillators is due to components other than the SAW crystal.

1.0 Introduction

During the 1980's and beyond, there will be a need for low noise, low cost oscillator circuitry in high frequency communications systems, such as JTIDS, packet radio, GPS, as well as in commercial satellite communication systems. Until recently, fundamental mode quartz oscillator crystals were not available in the 400 MHz frequency range. This paper describes the fabrication and packaging of high Q resonators, and a hermetically sealed 400 MHz oscillator.

In this paper, the major process steps associated with high Q SAW resonator fabrication are discussed. Results of chemical cleaning as well as gas loading and stress effects are shown. Hybrid oscillator packaging and overall oscillator performance in terms of hermeticity, and frequency stability are discussed.

2.0 Resonators

The main attraction of SAW chip elements, relative to bulk acoustic devices, is that the signal is propagated on one polished surface of a piezoelectric substrate.[1] The equipment and fabrication techniques used for hybrid SAW oscillators is essentially the same as that used in microwave thin film technology. By use of carefully controlled photolithographic procedures we have been able to produce SAW resonator chips in the 400 MHz frequency range.[1] After cleaning and photoresist applications, the aluminum interdigital electrode pattern was delineated by using a standard contact printing and etching process. Careful control of the line-to-gap ratio and aluminum thickness, resulted in a reproducible frequency from run to run. Following this step, wafers containing approximately 50 patterns were diced into individual chips and then tested with an rf probe and a phase locked network analyzer. A three point measurement technique was used to determine resonant frequency, resistance and resonator Q.[2] The typical SAW resonator filter response, illustrated in Fig. 1, is attributed to the interaction of the two transducers, which gives additional filtering, and sharply reduces harmonic content. Figure 2 shows a SAW resonator equivalent circuit and experimental parameters for a typical device. The equivalent circuit contains a static parallel capacitance, C_o, motional inductance, L_1, motional capacitance, C_1, and motional resistance, R_1. The complex polar impedence shows that a SAW resonator obeys a classical circular resonance with the exception of a spurious mode. Typical parameters for a SAW oscillator crystal at 400 MHz are $R_1 = 50\Omega$, $Q = 20{,}000$, and $C_o = 2$ pf.

Because of the high sensitivity to surface effects which are inherent in SAW resonator devices, both organic and inorganic surface contamination play a critical role in overall device performance. Cleaning procedures for quartz were investigated using SAW resonators as process monitors. The results of these studies provide an accurate and quantitative measure of the step by step process. To show the need and importance of quality control, the chart in Fig. 3 gives an overview of the entire process. It illustrates the need for precise and repeatable rf probe testing to achieve desired results.

3.0 Chemical Effects

The increased demands on performance and reliability of SAW devices and microcircuits in recent years have required the development of improved processing techniques. When surface contamination is minimized or removed, device

SAW Resonator Filter

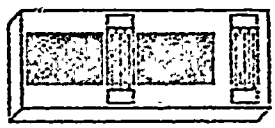

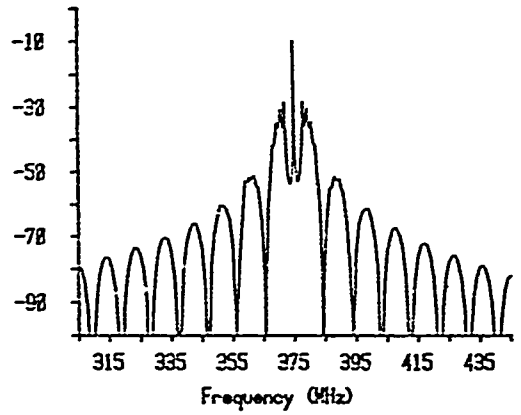

Chips

Processed Wafer

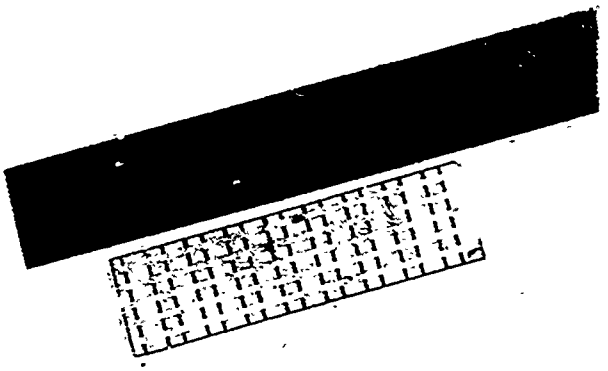

Fig. 1 SAW Resonator Chips

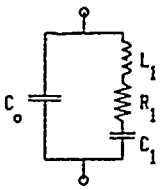

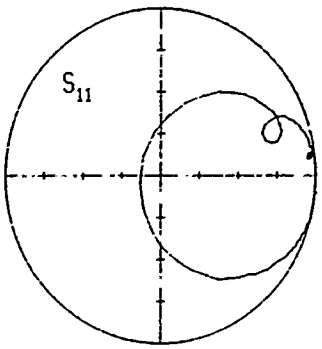

Typical Parameters at 300 MHz

R_1 = 50 ohms	Q = 20,000	C_o = 2 pf

Fig. 2 SAW Resonator Equivalent Circuit

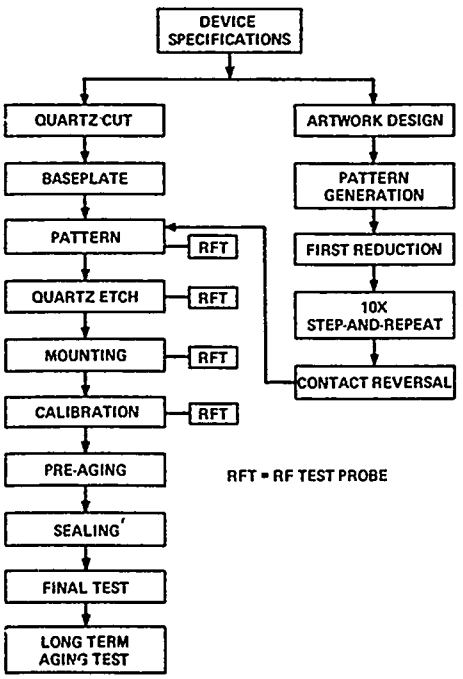

Fig. 3 Quality Control Chart

stability, reproducibility of performance and lifetime are greatly improved. To achieve this goal it is important to determine the effects of cleaning and chemical processing. One unexpected chemical result occurred with the use of heated resist stripper. Typical results of devices repeatedly cleaned in resist stripper are shown in Fig. 4. When surface contamination was reduced the operating frequency increases due to a decrease in mass loading. The chart shows a 50 KHz frequency increase during the first minute of submersion. Very little cleaning effect occurred in the next two min. After measuring the Al electrode thickness with a surface profiler, the last two min in the stripper had etched off 30 Å of aluminum. Plasma etching of the quartz is very important in our process. Although we utilize an all aluminum system,[3] small amounts of contamination are unavoidable. This is verified by etching the resonator chip in diluted nitric acid. The result was typically a 5-10 KHz frequency increase. The use of trichloroethane with quartz is undesirable because of large amounts of residue. It is especially serious when heated since decomposition of the stabilizer in the solvent is known to occur.

4.0 Polyimide Die Attachment

Die attachment of SAW chips to hybrid ceramic substrates has been a primary concern. Die attachment for the SAW chip elements were accomplished by using Ablestik 71-1[4] polyimide compound. This epoxy was chosen because of its low outgassing qualities when cured at the recommended temperatures supplied by Ablestik's outgassing charts.[5]

5.0 Gas Loading and Stress Effects

Gas loading and stress must be fully understood if frequency drift is to be minimized. Experiments were performed utilizing three different SAW resonator mounting methods. The purpose of this experiment was to determine which mounting scheme produced the least amount of frequency drift. The devices were placed in a 50-Ω test fixture in a vacuum system. Transmission measurements were made through the resonantor transducer, and the zero degree phase crossing point at device resonance was tracked by means of a phase locked loop (Fig. 5).

The three different mounting techniques are shown in Fig. 6.

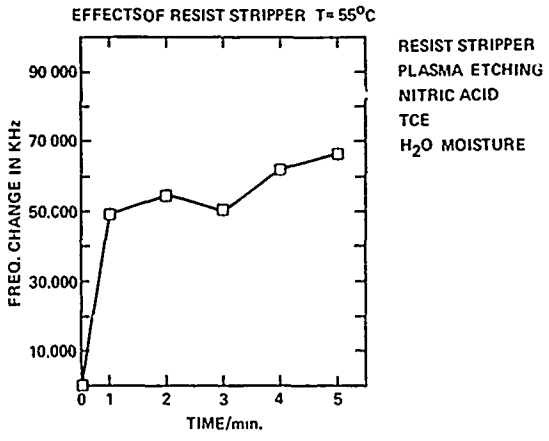

Fig. 4 Chemical Effects

Fig. 5

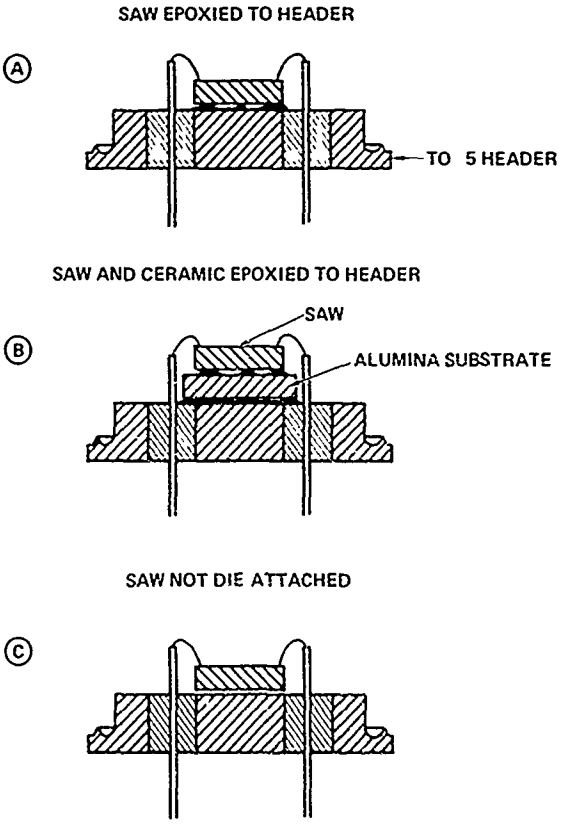

Fig. 6 Effects of gas loading and stress

STABILITY OF PHASE SHIFT ON QUARTZ SAW DEVICES

T. E. Parker and D. L. Lee
Raytheon Research Division
Waltham, Massachusetts 02154

Summary

The stability of phase shift on surface acoustic wave (SAW) devices is important because it determines the stability of frequency control devices and the location of the passband in filters. Several factors affect phase shift stability, and fluctuations may occur on time scales ranging from milliseconds to months. New results involving two types of phase variation will be discussed

Recently it has been observed that short period ($T \lesssim 1$ sec) fluctuations occur in SAW delay lines fabricated on ST-cut quartz. These fluctuations are the dominant source of close-to-carrier FM noise in SAW controlled oscillator. Unexpectedly it has been observed that very clean devices prepared for low aging exhibit the highest FM noise levels, and devices with very thin surface layers of silicone material show the lowest noise levels. As a consequence of the fact that the SAW device itself is the dominant source of close-to-carrier noise, a modified expression for calculating the FM noise power spectrum is presented.

On a longer time scale ($T \gtrsim$ minutes), the temperature dependence of the SAW velocity is the dominant source of variations in phase shift. New interest in the temperature dependence of various cuts of quartz was stimulated by Hauden et al.[1] with the prediction that a doubly rotated cut exists which has both a zero first order and second-order temperature coefficient. However, recent measurements on a device made with this cut show a second-order temperature coefficient only 20 percent smaller than that of ST-cut quartz. A theoretical capability for calculating first- and second-order temperature coefficients has been developed, and these calculations support our experimental results on the doubly rotated cut of Hauden. A comparison between theory and experiment is presented for fourteen different cuts and/or propagation directions.

Introduction

The stability of phase shift (time delay) of a SAW device is an important parameter since it determines the stability of frequency control devices and affects the center frequency of narrow-band filters such as SAW resonators. Fluctuations in phase shift can occur on time scales ranging from milliseconds to months, and may reflect several different physical mechanisms. Recent results from investigations into phase shift stability have provided new information about two different phenomena which result in variations in the phase shift of quartz SAW devices. On a time scale of less than a second, SAW delay lines have been found to be the dominant source of 1/f phase noise in SAW controlled oscillators. In particular, delay lines which have been thoroughly cleaned and hermetically sealed have been found to have the highest noise levels. Results of an investigation of 1/f phase noise are presented in the first section of this report. In the second section, new results on temperature dependence will be discussed. Great interest was stimulated in this area by the prediction of Hauden et al.[1] that there are several doubly rotated cuts of quartz that have a zero second-order temperature coefficient as well as a zero first-order coefficient. We have investigated one cut both theoretically and experimentally, and found the second-order coefficient to be only 20 percent smaller than that of ST-cut quartz. A theoretical analysis of the other cuts also showed relatively large second-order coefficients. To support our theoretical calculations, we have compared predicted and observed temperature dependence at fourteen different cuts and/or propagation directions and have achieved reasonably good agreement.

1/f Phase Noise in SAW Delay Lines

A significant advantage of SAW controlled oscillators over other high frequency sources is the very low FM noise level which can be obtained. For this reason, extensive measurements of the single sideband FM noise power spectrum (phase noise) have been made on numerous delay line-type SAW controlled oscillators. Through the course of these measurements, it was observed that some of the oscillators were noisier than others, and it was quickly established that the SAW delay lines were the source of the noise. Figure 1a shows the single sideband phase noise spectral density, $S_\phi(f_m)/2$, for two open loop SAW oscillators. By open loop, it is meant that the feedback path has been opened and that the circuit is not oscillating, and consists simply of a SAW delay line in series with an amplifier. The phase noise spectral density of this circuit is obtained from the phase fluctuations, $\Delta\phi$, measured as a function of modulation or offset frequency, f_m, on a signal which is passed through the circuit.[2] The relation $(\Delta\phi)^2 = S_\phi(f_m)$ has been used, where $(\Delta\phi)^2$ is normalized to a 1 Hz bandwidth. Figure 1a shows the

noise from two open loop delay line oscillators and the $1/f_m$ dependence of the close-to-carrier noise is clearly seen. This $1/f_m$ noise is commonly called "flicker" or "excess" noise. The $1/f_m$ noise level is nearly 10 dB lower on one of the delay line oscillators, while the far-out noise levels (f_m > 30 KHz) are nearly the same. This is to be expected since the far-out noise level is determined by amplifier parameters such as gain, G, noise figure, F, carrier power, P_c, and thermal noise, kT. The far-out noise level is given by the expression $S_\varphi(f_m)/2 = [(GFkT)/P_c]$ which is independent of f_m and for both oscillators in Fig. 1a has a calculated value of -161 dB. Notice in Fig. 1a that, when the SAW delay line is replaced by a 20 dB attenuator (delay line insertion loss ≈ 20 dB), the noise level remains flat to f_m < 400 Hz. Clearly the SAW devices are the source of the $1/f_m$ noise.

Figure 1b shows the single sideband phase noise spectral density for two oscillators (not the same ones as in Fig. 1a) which are operating closed loop. With the loop closed, the circuit oscillates. However, phase fluctuations in the circuit components of frequency $f_m < 1/(2\pi\tau)$ cause frequency modulation of the oscillator. Here, τ is the group delay ($d\phi/d\omega$) of the SAW device. Consequently, the phase noise of the oscillator takes on an additional $1/(f_m^2\tau^2)$ dependence in the region $f_m < 1/(2\pi\tau)$. Thus a $1/f_m^2$ dependence is observed in the region $f_m < f_\tau$ and $f_m > f_\alpha$, where $f_\tau = 1/(2\pi\tau)$ and f_α equals the frequency at which the flicker noise begins to dominate (see Fig. 1b). Below $f_m = f_\alpha$, a $1/f_m^3$ dependence is observed while for $f_m > f_\tau$ ($f_\tau \approx$ 100 KHz in this case), the spectral density is flat.

The $1/f_m$ noise observed in the open loop circuits clearly manifests itself as $1/f_m^3$ noise for the closed loop oscillators. Thus we will refer to the $1/f_m^3$ region as flicker noise. A surprising factor of the flicker noise is that the highest levels were observed on delay lines that were thoroughly cleaned and hermetically sealed (for aging studies). Devices left unsealed were usually quieter. Furthermore, devices with the quartz substrates mounted with RTV (Dow-Corning 3145, clear) were by far the quietest. RTV was not used with sealed devices because silicone rubber outgasses for an extended period of time and causes excessive aging. To determine what aspect of the RTV mounting was responsible for the reduced flicker noise level, a mechanically mounted (.010" gold wire straps), 400 MHz delay line was measured, and then the mechanical mount was replaced by RTV. After allowing one hour for the RTV to set up, the noise measurement was repeated. Figure 2 shows the single sideband phase noise level at f_m = 100 Hz for this device. (From Fig. 1 it is clear that the noise at f_m = 100 Hz is well into the flicker noise region.) One hour after mounting with the RTV, the noise level had dropped by almost 2 dB, and by three days it was down by more than 6 dB. No further decrease was observed by the seventh day. However, after storing the device at 90°C for 16 hours, a further drop of 4 dB was observed, as measured at room temperature. Further baking produced no additional decrease. The same type of decrease in noise level was also observed when a mechanical mount was used and a small amount of RTV was simply placed inside the SAW package. Furthermore, the noise level could be restored to its original value by cleaning the SAW substrate with ultraviolet light.

From these experiments it is clear that some volatile component of the RTV is affecting the surface of the quartz substrate. Methanol is given off by the RTV, but rinsing with methanol alone had no effect. It therefore appears that volatile silicones are responsible for the flicker noise reduction since surface treatment with other silicone materials also produces a similar noise reduction. The mechanism by which the silicone material reduces the flicker noise level is not fully understood at this time, but it is felt that it is related to surface passivation of the transducer metal in a manner similar to that which occurs on semiconductor devices.

Equation (1) (from Leeson's[3] work on bulk wave oscillators) has been successfully used to predict the phase noise spectral density for SAW oscillators.[4,5]

$$\left\{\frac{P_{SB}}{P_C}\right\}_{dBc} = 10 \log \left\{\frac{GFkT}{P_C}\right\}\left\{\frac{\omega_\alpha}{(\omega_m)^3\tau^2} + \frac{1}{(\omega_m)^2\tau^2} + 1\right\} \qquad (1)$$

where $\omega_m = 2\pi f_m$ and $\omega_\alpha = 2\pi f_\alpha$ and is an experimentally determined flicker noise parameter. Equation (1) is perfectly valid even though the SAW device is the source of the flicker noise, but its form is somewhat misleading. In Eq. (1), ω_α is not a device constant, but is also a function of the amplifier parameters. A more convenient form is shown in Eq. (2),

$$\frac{P_{SB}}{P_C} = 10 \log \left\{\frac{\alpha}{(\omega_m)^3\tau^2} + \left\{\frac{GFkT}{P_C}\right\}\left\{\frac{1}{(\omega_m)^2\tau^2} + 1\right\}\right\} \qquad (2)$$

where α is an experimentally determined flicker noise constant that is dependent only on the SAW substrate. From Eqs. (1) and (2), it is clear that $\omega_\alpha = [(\alpha P_c)/GFkT]$.

To demonstrate that α is independent of the amplifier parameters, flicker noise measurements were made on the same SAW delay line but with several different amplifier configurations. Figure 3 shows the phase noise level at f_m = 100 Hz, for four different values of the parameter $(GFkT/P_c)$. Though there is some scatter to the data (possibly due to varied impedance conditions), the flicker noise level is clearly independent of $(GFkT/P_c)$. The solid line shows how the noise level would vary if it were proportional to the term $(GFkT/P_c)$.

Temperature Dependence

The fractional change in delay time with temperature for a surface acoustic wave is a function of two mechanisms, fractional changes in path length and fractional changes in velocity. Path length changes are directly available from expansion coefficients, but velocity changes must be calculated by computer. Calculation of SAW velocity is facilitated by use of th Christoffel wave equations which describe the

In Group A, the SAW chip was die-attached to a TO-5 header with the polyimide previously mentioned. Devices in Group B were attached to an alumina substrate and then to the header with both attachements using the polyimide compound. In Group C the devices were not die attached. They were held in place by the strength of the two wire bonds (Fig. 6). There are two sets of data for the three different groups (Fig. 7). First the devices were tested unsealed in the vacuum system. Next the devices were hermetically sealed and retested in the vacuum system. The sequence of operation is as follows: one minute in high vacuum, vented to atmosphere and held there for one and a half minutes, and then mechanically pumped to 50 microns, switching to high vacuum and repeating the cycle. The dotted line shows frequency drift primarily due to gas loading. When the resonator package in Group A was sealed, the results show over 3 ppm frequency drift due to stress effects of the crystal mounting. The results of Group B for sealed devices, show only one quarter ppm frequency drift due to stress. The reason for this small change is the use of a ceramic alumina substrate between the SAW and the package. The thermal expansion of the quartz is close to that of the alumina substrate.

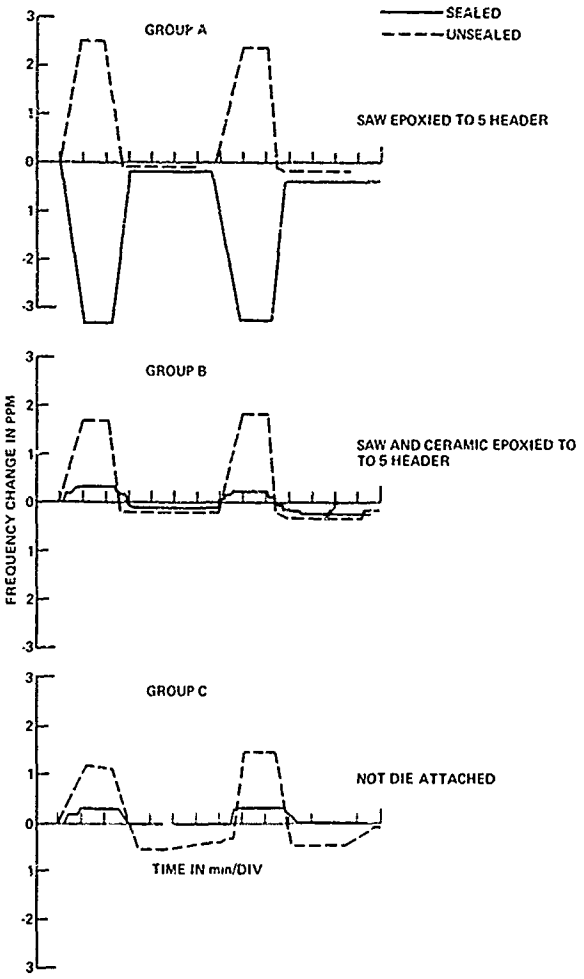

Fig. 7 Gas loading and stress effects

6.0 Packaging

The hybrid microcircuit is a complex network of interconnected components and dissimilar materials. In addition to epoxy outgassing mentioned previously, moisture content is of paramount importance. Moisture will adversely affect the yield, performance, aging, and reliability of the sealed hybrid enclosure. Failure modes associated with moisture include parameter drift, wire bond and metallization corrosion and electro-chemical migration of metals. All of these effects justify the importance of knowing and controlling the internal package ambient condition.

The hermetic leak rates for the resonator packages described here are in the range of 2 to 3 x 10^{-9} Torr (ATM cc/sec He). If a stable, contaminant free environment is to be maintained for a long period of time, leak rates of 2 to 3 x 10^{-9} are necessary.

Because of low outgassing and controlled thermal spreading, capacitive resistance welding was chosen. Packages were placed in a vacuum oven for a minimum of 8 hours to bake off as much accumulated moisture as possible. After the bake cycle, the package was transferred through a moisture monitored N_2 atmosphere to the weld chamber where the unit is evacuated to 2 x 10^{-7} Torr. Once the resistance weld is completed, the package is removed from the weld chamber. The sealed device is immediately tested for leak rate, Q and frequency to determine the weld seal quality. In going from air to a vacuum seal, the device Q increases by 25 to 30% at 400 MHz.

7.0 SAW Oscillator - Experimental Results

The achievement of high Q and a good inductive reactance in SAW resonator crystals, enables many types of oscillator circuits to be considered. A study was made of the following types: Clapp, Colpitts, Pierce, and impedance inverting or negative resistance types. Of these the Pierce, shown in Fig. 8, had the highest frequency stability with moderate power output. In addition, this circuit was the simplest in terms of design and hybrid fabrication.

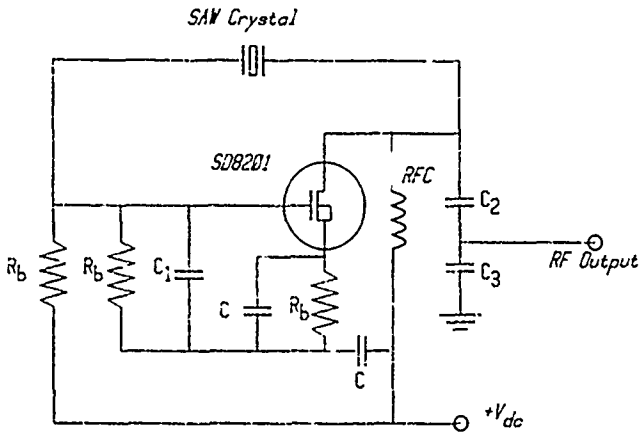

Fig. 8 Pierce oscillator circuit used with SAW oscillator crystals.

Frequency stability for these oscillators was compared with various types of conventional system references, i.e., multiplier chains and PLLs, based on a 5 MHz reference oscillator. Frequency stability was measured in the frequency and time domains using an HP 5390 stability analyzer. Both the SAW oscillator and PLL were analyzed against an HP 8660C frequency synthesizer. Typical results of this comparison for phase noise are shown in Fig. 9. The phase noise of the SAW oscillator in this case was better than the PLL beyond 10 Hz from the carrier because of the higher loop Q of the SAW oscillator. Below 10 Hz, the SAW oscillator showed somewhat higher noise due to temperature fluctuations since the SAW was not ovenized in this case.

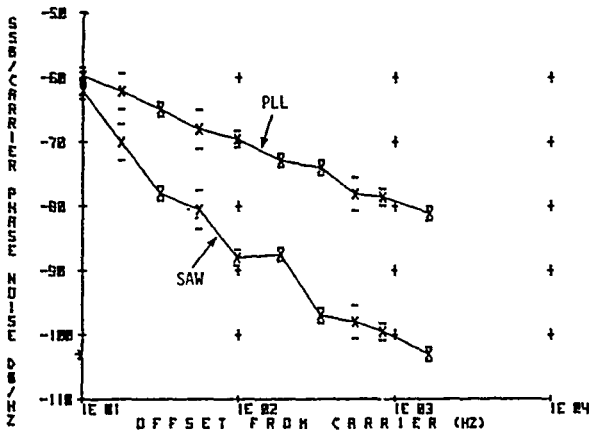

Fig. 9 Comparative phase noise of a 375 MHz PLL, locked to a 5 MHz crystal standard, vs fundamental mode SAW crystal oscillator at 375 MHz.

8.0 Conclusion

Fundamental mode oscillator crystals with Q and impedance values commensurate with low-frequency crystals enable the fabrication of high-stability oscillators in the 300-400 MHz range. The phase noise of these oscillators is considerably lower than conventional system clocks and reference oscillators in this frequency range. The progress of SAW resonators and oscillators will advance with improvements in clean processing, stress relieved mounting and more ideal package enclosures. In addition, SAW technology enables thin film hybrid fabrication techniques to be applied; this results in overall size and weight reductions. These new oscillators will be useful wherever low-noise, low-cost frequency sources are required.

9.0 References

1. J. S. Schoenwald, R. C. Rosenfeld, and E. J. Staples, "Surface Wave Cavity and Resonator Characteristics - VHF to L-Band," 1974 IEEE Ultrasonics Symposium, pp. 253-256.

2. E. Hafner, "The Piezoelectric Crystal - Definitions and Methods of Measurement," Proc. IEEE 57, (2), 179 (1969).

3. C. A. Adams and J. A. Kusters, "Improved Long-Term Aging in Deeply Etched SAW Resonators," Proc. 32nd Annual Symposium on Frequency Control, pp. 74-76, May 1978.

4. Ablestik 71-1 polyimide mounting compound can be obtained from Ablestik Laboratories, Gardena, California.

5. R. L. Filler, J. M. Frank, R. D. Peters, and J. R. Vig, "Polyimide Bonded Resonators," Proc. 32nd Annual Symposium on Frequency Control, pp. 290-298, May 1978.

motion of acoustic plane waves in terms of the temperature-dependent elastic, piezoelectric, dielectric, and mass-density constants. Application of appropriate mechanical and electrical boundary conditions of the surface of a piezoelectric half-space couples plane wave solutions together and in general leads to a solution which represents a SAW propagating at a velocity determined by the substrate material constants.

In order to calculate temperature dependence of velocity, it is necessary to specify accurately the variation of all material constants with temperature. This temperature dependence can be described in an organized manner by expanding each material constant in a Taylor series about a given temperature. The coefficients of the various powers of the temperature in the series expansion have been determined experimentally by several authors, with the largest variation in measured values being for the elastic stiffness constants.[6-9] We have found that the most recent data of Bechmann and Ballato,[8] modified in such a manner as to be consistent with the Christoffel wave formulation, gave reasonable fit with experimental data.

Choice of Constants

When elastic wave propagation in a piezoelectric medium is considered, an additional piezoelectric stress due to an electric field $\bar{E}$ must be included. As a result, two types of measurements of elastic constants, those made at either constant (zero) electric field, $\bar{\bar{c}}^E$, or constant (zero) electric displacement, $\bar{\bar{c}}^D$, lead to slightly different values. Here the double overbar indicates that the elastic constants are represented in abbreviated indices notation as a second rank tensor. The relationship between the two sets is given by[10]

$$c^D_{\lambda\mu} = c^E_{\lambda\mu} + e_{\lambda j}(\varepsilon^{-1})_{ji}\, e_{i\mu} \qquad (3)$$

where ε_{ij} and e_{ij} are the dielectric and piezoelectric stress tensors respectively. The choice of which set of elastic constants is to be used for a given problem is purely a matter of whether electric field or electric displacement is chosen as the independent variable in representing the constitutive relations for the piezoelectric material.

Because the Christoffel wave equation is formulated using constitutive relations in which electric field and electric displacement are independent and dependent variables respectively, it is theoretically consistent to use values of $\bar{\bar{c}}^E$ rather than $\bar{\bar{c}}^D$. Though Bechmann's measurements were made for $\bar{\bar{c}}^D$, in principle, given the temperature coefficients of piezoelectric stress and dielectric constants, $\bar{\bar{c}}^E$ can be determined from $\bar{\bar{c}}^D$.[9] However, only first-order temperature coefficients of piezoelectricity have been published.[11] These are sufficient, however, for calculation of zero and first-order temperature coefficients of elastic constants, $\bar{\bar{c}}^E$ and $T\bar{\bar{c}}^{E(1)}$, and therefore of first-order temperature coefficient of delay.

Using the "Campbell-Jones" program to compute velocity on a quartz half-space,[12] we have found that calculations of first-order temperature coefficients of delay (TCD) made using $\bar{\bar{c}}^E$ and $T\bar{\bar{c}}^{E(1)}$ are in better agreement with experimentally obtained values than those obtained using $\bar{\bar{c}}^D$ and $T\bar{\bar{c}}^{D(1)}$, generally by a few parts per million. Further, we have found that our values for first-order TCD are extremely close to those computed by Lewis et al.,[13] who averaged values of elastic constants and their temperature derivatives, both at constant $\bar{E}$ and $\bar{D}$, from several authors. The improved accuracy allowed a more precise estimate of those crystal orientations which have zero first-order TCD's near or at room temperature. Further, it should be noted that for crystal cuts exhibiting primarily quadratic temperature dependence, this improved accuracy translates into a better determination of turnover temperature. As an example, for a crystal orientation with a second-order TCD comparable to ST-cut quartz, an error of 0.7 ppm in computing the first-order TCD amounts to about a 10°C error in estimation of turnover temperature. Once a crystal orientation which yields zero first-order TCD has been determined in this manner, higher-order TCD's are calculated using values of $T\bar{\bar{c}}^{D(n)}$ up to third order. We found that this choice, while not theoretically correct, gave better results for higher order terms than using $\bar{\bar{c}}^E$ and $T\bar{\bar{c}}^{E(1)}$ in conjunction with $T\bar{\bar{c}}^{D(2)}$ and $T\bar{\bar{c}}^{D(3)}$, presumably because, as was pointed out by Lewis,[13] only the first choice maintains the required symmetry for quartz in the basal plane. Table 1 lists the values of all constants used in our computations.

Results of Our Measurements

To compare our theoretical results with observed temperature dependence, measurements were made on a total of six different cuts of quartz, including one doubly rotated cut. Experimental results of Browning[14] on two rotated X-cuts were also used. One or more transducer orientations were investigated on each cut, for a total of fourteen different configurations. The functions of the angles ϕ, θ, ψ are shown in Fig. 4. (The 1949 convention for quartz has been used here rather than the 1978 IEEE convention.) To facilitate comparison between theory and experiment, small adjustments were arbitrarily made to either psi or theta in our theoretical calculations to make computed turnover temperatures coincide with experimentally measured values. Our results are shown in Fig. 5(a-g). In no case was it necessary to introduce more than a 0.90° angular difference between theoretical values and experimentally measured angles. In all cases we found the theoretical curvature to be greater than or equal to values measured experimentally. Table 2 indicates the calculated values of power flow angle, $\Delta v/v$, and velocity at the turnover temperature for each of the cuts investigated. The angles shown in parentheses are equivalent by symmetry and fall within the reduced ranges $-60° < \phi < +60°$, $0 < \theta < +90°$ and $0 < \psi < +90°$.[1]

It is significant to note that while comparison between experiment and theory indicates reasonable

agreement, we have found discrepancies between our own work and some of the theoretical calculations presented by Hauden on loci of zero first-, second-, and third-order TCD.

We have performed a check of theoretical data presented by Hauden[1] on loci of zero first-order TCD in (ϕ, θ) space for constant values of ψ, and found them to be in reasonable agreement (except $\psi = 54°$) with our own theoretical predictions. However, we have found Hauden's loci of zero second-order TCD to be drastically in error. Specifically, we have investigated theoretically all four cuts, (ϕ,θ,ψ) = (+56, +39, +27), (+73, +21, +27), (-25, +9, +45), (-8, +66, +54), which the author specifies in his curves as having simultaneously zero first- and second-order TCD. Our examination consisted of computing the values of second-order TCD within a shell of ±5° in $\phi/\theta/\psi$ for each of the cuts specified by Hauden. The first two cuts were found to have second-order TCD comparable to ST-cut within the entire "shell." The first cut was also checked experimentally, as shown in Fig. 5g, and is in reasonable agreement with our calculations. The third cut listed had a zero first-order TCD loci displayed somewhat from Hauden's predictions. Again, an examination of second-order TCD in a shell about this region showed no zero or nearly zero second-order TCD. Finally, Hauden's fourth angle was totally incorrect in both first- and second-order TCD. It appears from an examination of his loci of zero first-, second-, and third-order TCD for $\psi = 54°$ that this particular set of curves may have been mislabeled.

Conclusions

Two aspects of phase shift stability on quartz SAW devices have been investigated: 1/f phase noise and temperature dependence. With regard to phase noise, it has been observed that the SAW device is the largest source of 1/f phase noise in a SAW oscillator. Furthermore, SAW substrates that have been thoroughly cleaned and hermetically sealed usually have the highest noise levels. However, the noise level can be reduced by treating the SAW substrate with a very thin layer (a few monolayers) of silicone material.

Temperature stability, including second- and third-order dependence, has been calculated for a number of different cuts and propagation directions and has been compared with experimental results. The predicted cut angles for a given turnover point were never more than 1° in error, while the predicted second-order coefficients averaged about 23 percent larger than the measured values. Included in the cuts that were investigated was one predicted by Hauden to have both zero first- and second-order coefficients. Our results show that the second-order coefficient is not small.

References

1. D. Hauden, M. Michel and D. O. Gangepain, "Higher Order Temperature Coefficients of Quartz SAW Oscillators," Proc. 32nd Annual Symp. on Freq. Control, U. S. Army Elec. Res. and Dev. Comm., Ft. Monmouth, N.J., pp. 77-86 (1978).

2. A. E. Wainright, F. L. Walls, and W. D. McCaa, "Direct Measurement of the Inherent Frequency Stability of Quartz Crystal Resonators," Proc. 28th Annual Symp. on Freq. Control, U. S. Army Elec. Comm., Ft. Monmouth, N.J., pp. 177-180 (1974).

3. D. B. Leeson, "Short Term Stable Microwave Sources," Microwave Journal 13, pp. 59-69 (1970); "A Simple Model of Feedback Oscillator Noise Spectrum," Proc. IEEE 54, pp. 329-330 (1960).

4. T. E. Parker, "Current Developments in SAW Oscillator Stability," Proc. 31st Annual Symp. on Freq. Control, U. S. Army Elec. Res. and Dev. Comm., Ft. Monmouth, N.J., pp. 359-364 (1977).

5. R. Allison and S. J. Goldman, "Vibration Effects on Close-in Phase Noise of a 300 MHz Surface Wave Resonator Oscillator," Proc. 32nd Annual Symp. on Freq. Control, U. S. Army Elec. Res. and Dev. Comm., Ft. Monmouth, N.J., pp. 66-73 (1978).

6. W. P. Mason, "Zero Temperature Coefficient Quartz Crystals for Very High Temperatures," Bell Syst. Tech. J., Vol. 30, pp. 366-380 (1951).

7. I. Koga, M. Aruga, and Y. Yoshihaka, "Theory of Plane Elastic Waves in Piezoelectric Crystalline Medium and Determination of Elastic and Piezoelectric Constants of Quartz," Phys. Rev. 109, pp. 1467-1473 (1958).

8. R. Bechmann, A. D. Ballato, and T. J. Lukaszek, "Higher Order Temperature Coefficients of the Elastic Stiffnesses and Compliances of Alpha-Quartz," Proc. IRE 50, pp. 1812-1822 (1962).

9. J. Zelenka and P. Lee, "On the Temperature Coefficients of the Elastic Stiffnesses and Compliances of Alpha-Quartz," IEEE Trans. Sonics and Ultrasonics SU-18, pp. 79-80 (1971).

10. B. A. Auld, Acoustic Fields and Waves in Solids, Vol. I, Wiley, New York, N.Y. (1973).

11. R. Bechmann, "Temperaturabhängigkeit von Quarzresonatoren," Archiv der Elektrischen Übertragung 5, pp. 89-90 (1951).

12. W. R. Jones, J. J. Campbell, and S. L. Veilleux, Theoretical Analysis of Acoustic Surface Waves, Final Report F19628-69-C-0132, 1 Dec. 1968-30 Nov. 1969, Hughes Aircraft Co., Fullerton, CA. AD-865-352 (1969).

13. M. F. Lewis, G. Bell, and E. Patterson, "Temperature Dependence of Surface Elastic Wave Delay Lines." Journal of Applied Physics 42, pp. 476-477 (1971).

14. I. Browning and M. Lewis, "A New Cut of Quartz Giving Improved Temperature Stability to SAW Oscillators," Proc. 32nd Annual Symp. on Freq. Control, U.S.Army Elec. Res. and Dev. Comm. Ft. Monmouth, N.J., pp. 87-94 (1978).

TABLE 1

MATERIAL CONSTANTS FOR QUARTZ

Piezoelectric Stress Constants[8] and Temperature Derivatives[11]

$e_{11} = 0.171\ C\ m^{-2}$

$e_{14} = 0.0403\ C\ m^{-2}$

$Te_{11}^{(1)} = -1.6 \times 10^{-4}/°C$

$Te_{14}^{(1)} = -14.4 \times 10^{-4}/°C$

Coefficients of Thermal Expansion[8]

$\alpha_{11}^{(1)} = \alpha_{22}^{(1)} = 13.71 \times 10^{-6}/°C$

$\alpha_{33}^{(1)} = 7.48 \times 10^{-6}/°C$

$\alpha_{11}^{(2)} = \alpha_{22}^{(2)} = 6.5 \times 10^{-9}/(°C)^2$

$\alpha_{33}^{(2)} = 2.9 \times 10^{-9}/(°C)^2$

$\alpha_{11}^{(3)} = \alpha_{22}^{(3)} = -1.9 \times 10^{-12}/(°C)^3$

$\alpha_{33}^{(3)} = -1.5 \times 10^{-12}/(°C)^3$

Dielectric Constants[8]

$\varepsilon_{11} = \varepsilon_{22} = 39.97 \times 10^{-12}\ F\ m^{-1}$

$\varepsilon_{33} = 41.03 \times 10^{-12}\ F\ m^{-1}$

Density and Its Temperature Derivatives[8]

$\rho = 2.65 \times 10^{3}\ N\ m^{-4}\ s^{2}$

$T\rho^{(1)} = -34.92 \times 10^{-6}/(°C)$

$T\rho^{(2)} = -15.9 \times 10^{-9}/(°C)^2$

$T\rho^{(3)} = 5.30 \times 10^{-12}/(°C)^3$

Elastic Stiffnesses $c_{\lambda\mu}$ in $10^9 N\ m^{-2}$ at 25°C*[8]

$\lambda\mu$	$c_{\lambda\mu}^{E}$	$c_{\lambda\mu}^{D}$
11	86.72	87.47
33	107.1	107.1
12	6.89†	6.14
13	11.88	11.88
44	57.89	57.93
66	39.92	40.67
14	-17.92	-18.10

Values for the First Order Temperature Coefficients of Stiffness at Constant Electric Field[9]

$\lambda\mu$	$Tc_{\lambda\mu}^{(1)}$ $10^{-6}/°C$
11	+ 44.3
33	- 160.0
12	-2694.0**
13	- 550.0
44	- 175.4
66	+ 187.6
14	+ 117.0

* NOTE: Original values presented at 20°C.

† Original value published incorrectly as 6.99 @ 20°C. Correct value is 6.98 @ 20°C.

** Value corrected to be consistent with change in c_{12}^{E}.

Table 1 (Continued)

Values for the Temperature Coefficients of Stiffness at Constant Electric Displacement[8]

	(1) $Tc_{\lambda\mu}$	(2) $Tc_{\lambda\mu}$	(3) $Tc_{\lambda\mu}$
$\lambda\mu$	$10^{-6}/°C$	$10^{-9}/(°C)^2$	$10^{-12}/(°C)^3$
11	-48.5	- 107	- 70
33	- 160	- 275	- 250
12	-3000	-3050	-1260
13	- 550	-1150	- 750
44	- 177	- 216	- 216
66	+ 178	+ 118	+ 21
14	+ 101	- 48	- 590

TABLE 2

CALCULATED SAW PARAMETERS AT THE TURNOVER TEMPERATURE

Cut Angles (Exp.)			Turnover Temp.	Velocity	Coupling Constant	Power Flow Angle
ϕ	θ	ψ	(°C)	V (m/sec)	2 v/v (%)	(deg)
0	0	34.9	-30	3.35×10^3	.088	3.2
0	0	33.9	+15	3.35	.094	3.1
0	0	32.9	+72	3.35	.098	3.0
0	42.75	0	+20	3.16	.114	0.0
0	34.63	0	+87	3.15	.126	0.0
0	35.0	44.9	+40	3.27	.102	2.8
-90 (+30)	0	34.4	-26	3.18	.072	3.9
-90 (+30)	0	33.4	+80	3.18	.080	2.0
-90 (-30)	0	-26.5 (+26.5)	0	3.58	.088	-12.
-90 (-30)	0	-25.5 (+25.5)	+20	3.57	.094	-12.
90 (-30)	45	64	+12	3.32	.068	- 0.53
90 (-30)	46	64	+65	3.32	.068	- 0.91
56	39	27	- 5	3.58	.112	3.5
56	39	26	+63	3.58	.118	4.1

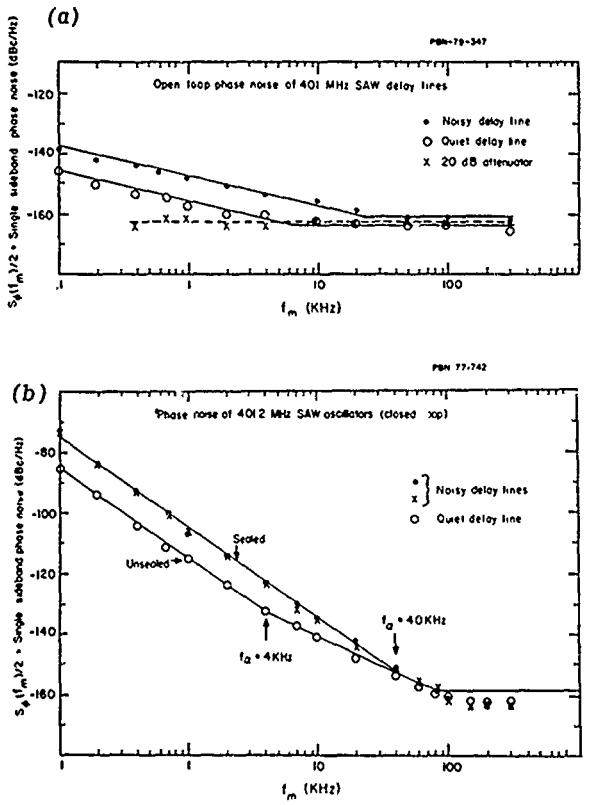

Fig. 1 Open Loop (a) and Closed Loop (b) Phase Noise for SAW Oscillators Showing Differences in Flicker Noise Levels for Different SAW Delay Lines.

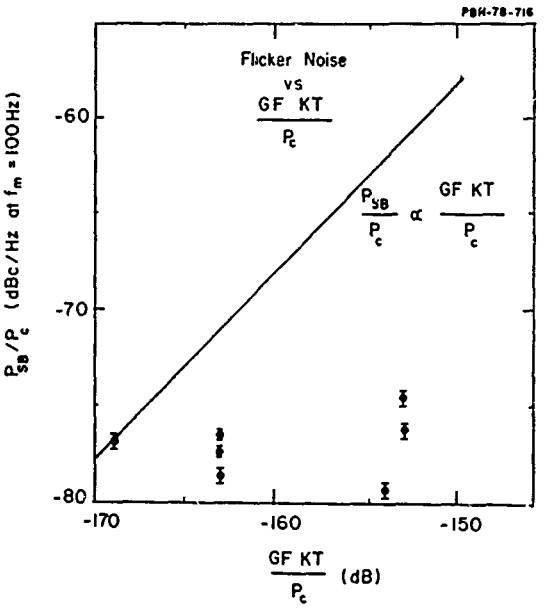

Fig. 3 Observed Flicker Noise Level for Four Values of $\frac{GFkT}{P_c}$. The solid line indicates how the flicker noise level would vary if it were proportional to the term $\frac{GFkT}{P_c}$.

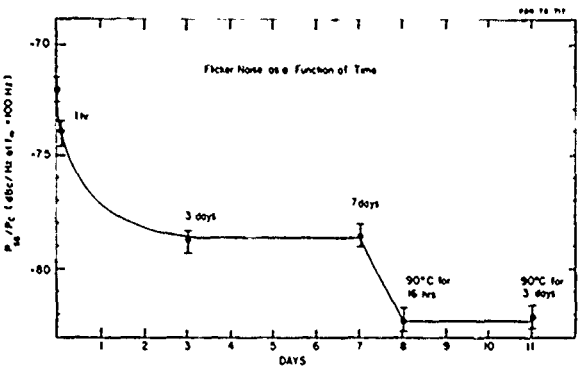

Fig. 2 Flicker Noise as a Function of Time for a SAW Device Mounted with Silicone Rubber.

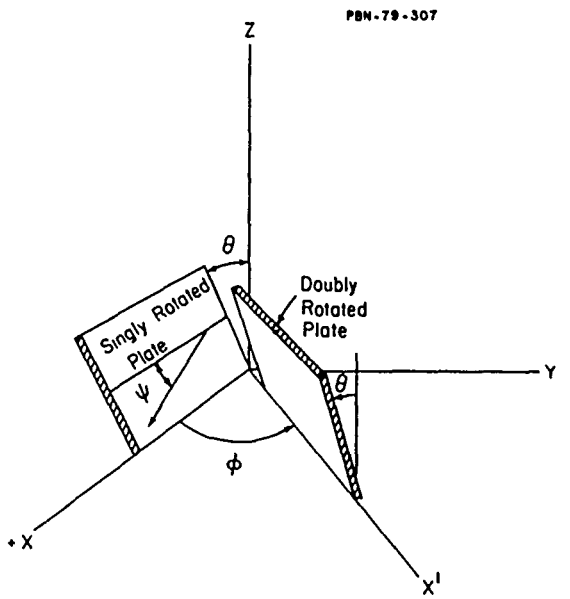

Fig. 4 Definitions of Angles ϕ, θ, and ψ for Rotated Quartz Plates.

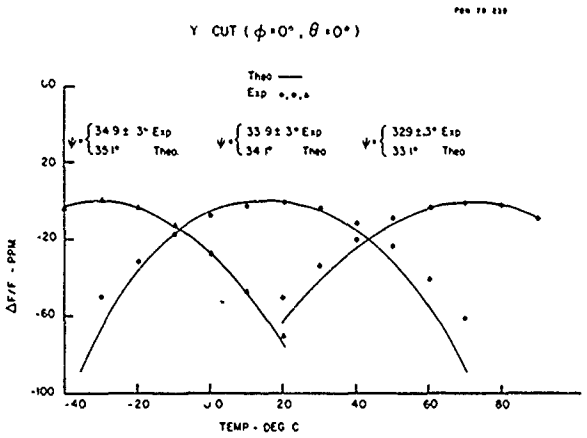

Fig. 5 (a) Comparison Between Theory and Experiment for a Y-Cut Substrate.

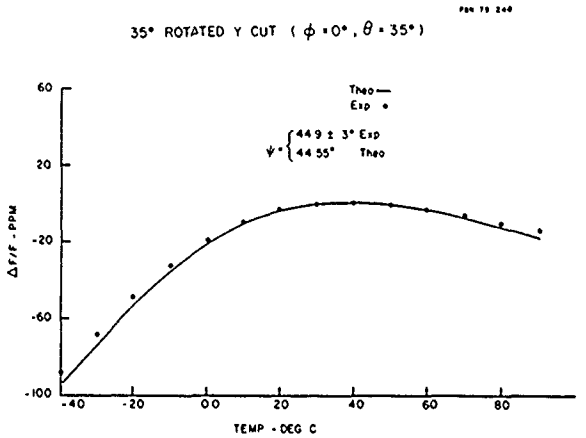

Fig. 5 (c) Comparison Between Theory and Experiment for a Rotated Y-Cut Substrate with Propagation at ≈ 45° from X-Axis.

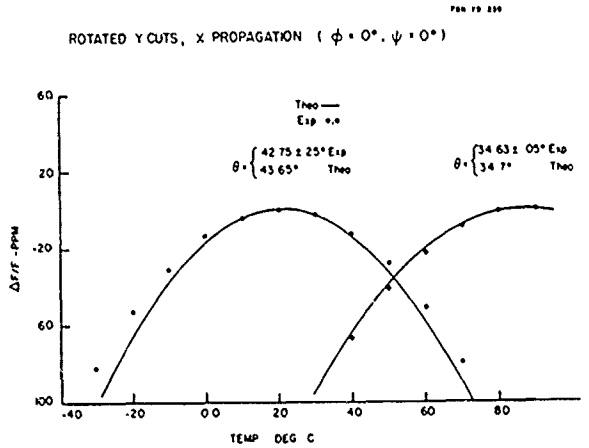

Fig. 5 (b) Comparison Between Theory and Experiment for Two Rotated Y-Cut Substrates.

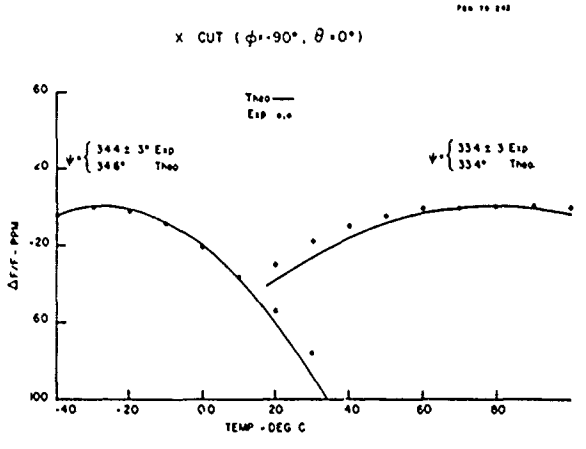

Fig. 5 (d) Comparison Between Theory and Experiment for an X-Cut Substrate.

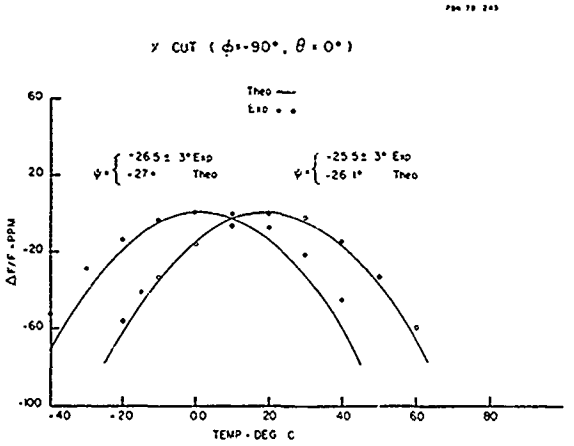

Fig. 5 (e) Comparison Between Theory and Experiment for an X-Cut Substrate.

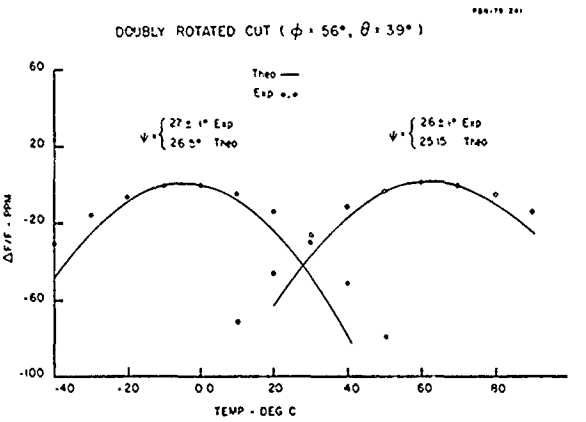

Fig. 5 (g) Comparison Between Theory and Experiment for a Doubly Rotated Cut.

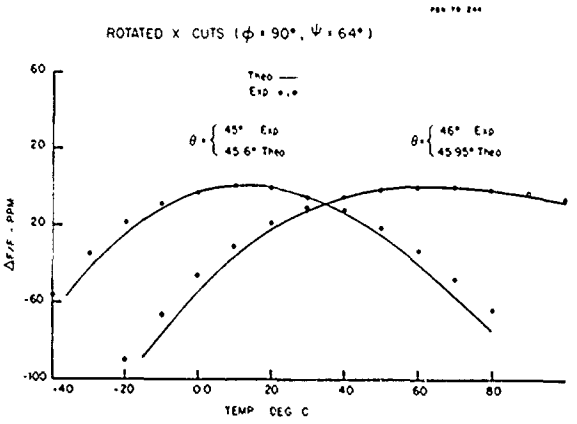

Fig. 5 (f) Comparison Between Theory and Experiment for Rotated X-Cuts. Experiential data from Browning and Lewis.[14]

ANALYSIS OF SHALLOW BULK ACOUSTIC WAVE EXCITATION BY INTERDIGITAL TRANSDUCERS*

K. F. Lau, K. H. Yen, J. Z. Wilcox and R. S. Kagiwada

TRW Defense and Space Systems Group
Redondo Beach, California 90278

Abstract

In this paper, the Shallow Bulk Acoustic Wave (SBAW) in rotated Y-cut quartz is analyzed by first considering the bulk wave generated by a single line source located on the substrate surface. The single line source problem is solved exactly taking into account the full electrical and mechanical boundary conditions. For the case involving multiple line sources, such as that of interdigital transducers, an approximate expression accurate to the order of K_p^2, where K_p^2 is the electromechanical coupling coefficient, is derived. From these calculations, the wave velocity, temperature coefficient of delay, and the equivalent circuit model of the SBAW in rotated Y-cut quartz are derived. It is found that the equivalent circuit model for the SBAW transducer is quite similar to the "in-line" model used in surface acoustic wave calculations. Good agreement between experiment and theoretical prediction has been obtained.

Introduction

Shallow Bulk Acoustic Wave (SBAW) devices promise to have great impact on frequency control due to their compact size, high operating frequency, and excellent short-, medium-, and long-term stabilities.[1-4] A complete understanding of the SBAW excitation, propagation and detection is desirable because it will allow one to design devices with specified characteristics. Theoretical analysis of the SBAW has been performed by several authors,[1-4] and a fairly good understanding of the SBAW properties has been achieved. However, a convenient equivalent circuit model which provides the same simplicity in device design as that of the "cross field" and "in-line" models for the surface acoustic wave device has yet to be proposed. It is the purpose of this paper to derive such a model and to recalculate theoretically some of the wave properties including the wave velocity and temperature coefficient of delay for SBAW in rotated Y-cut quartz. This formulation can also apply to the calculation of SBAW in substrates having similar elastic, piezoelectric and dielectric symmetries as quartz (e.g., rotated Y-cut berlinite). For other types of substrates, the following approach does not rigorously apply, but is expected to provide insight into the various wave properties.

Theoretical Analysis

The configuration of a SBAW device on rotated Y-cut quartz is shown schematically in Figure 1. Interdigital transducers are deposited on the substrate surface with fingers parallel to the X-axis of the quartz crystal. A voltage V_o applied to the transducer launches, through piezoelectric coupling, acoustic waves in the substrate. These waves propagate in the crystalline YZ plane and are detected by a receiving transducer situated at a center-to-center distance r away. The width and length of the transducer are designated by d and ℓ, respectively. Finger-to-finger spacing is designated by $\Delta\vec{r}$.

The analysis of acoustic waves excited by the interdigital transducer will consist of (1) determining the radiation characteristics of a single line source (element factor) and (2) summing the contributions from these individual sources (array factor). In this approach, the interdigital transducer is represented by a series of parallel line sources with alternate polarity. The far-field approximation is used throughout the calculation and the piezoelectric substrate is assumed to be semi-infinite. The aperture of the acoustic wave is assumed to be many wavelengths wide and the field quantities are essentially independent of the y coordinate.

Radiation From a Single Line Source

The configuration of a single line source of time harmonic unit charge located on a piezoelectric medium is illustrated in Figure 2. The solution of electric potential ϕ and particle velocity v can be Fourier-analyzed as[5]

$$\phi^a(x,z) = \frac{1}{2\pi}\int_{-\infty}^{\infty} \phi^a(k_x,z)\, e^{-jk_x x}\, dk_x \tag{1}$$

$$\phi^a(k_x,z) = \frac{1}{2|k_x|\varepsilon_o}\left[e^{-|k_x||z-z'|} + R(k_x)\, e^{|k_x|(z+z')}\right]$$

for $z < 0$ in the air region.

*This work is supported by the Army Research Office under Contract No. DAAG26-78-C-0043.

and

$$v(x,z) = \frac{1}{2\pi}\sum_{i=1}^{4}\int_{-\infty}^{\infty} V_i(k_x)e^{-jk_x x - jk_{zi} z}dk_x$$

$$\phi(x,z) = \frac{1}{2\pi}\sum_{i=1}^{4}\int_{-\infty}^{\infty} \phi_i(k_x)e^{-jk_x x - jk_{zi} z}dk_x \qquad (2)$$

for $z > 0$ in the quartz region.

In these expressions, the quasi-static approximation has been assumed and thus the total number of eigenmodes inside the quartz crystal is four.

By solving the Christoffel Equations,[6] one can show that for rotated Y-cut quartz the longitudinal and vertical shear acoustic modes are decoupled from the electric potential. As a result, the modes of interest inside the quartz medium are the horizontal shear quasi-acoustic mode and the quasi-electrostatic mode. The dispersion relation for these two modes is calculated to be

$$(k_z^2 C_{44} + 2C_{46}k_x k_z + C_{66}k_x^2 - \rho\omega^2) \cdot (\varepsilon_{33}k_z^2 + \varepsilon_{11}k_x^2 + 2\varepsilon_{13}k_x k_z) + + (e_{34}k_z^2 + e_{16}k_x^2 + (e_{14} + e_{36})k_x k_z)^2 = 0 \quad . \qquad (3)$$

They are coupled through the second term and neither of them is purely acoustic or electrostatic.

Solving k_z as a function of k_x, one can obtain a dispersion curve of the quasi-acoustic wave. Figure 3 shows the dispersion curve for AT-cut quartz. Also shown in Figure 3 is the geometrical construction of a $\vec{k}$-vector corresponding to the ray propagating to observation point $\vec{r} = (x,z)$. Due to crystal anisotropy, the $\vec{k}$ vector is not parallel to the energy flow direction. The construction is the graphical representation of the results of the saddle point integration technique.[7]

Of particular interest is the $\vec{k}$ vector which corresponds to the ray directed parallel to the surface of the substrate. This $\vec{k}$ vector determines the phase velocity of the SBAW along the surface of the substrate and is designated $\vec{k}_c$.

The Fourier amplitudes $\phi^a(k_x,z)$, $\phi_i(k_x)$ and $v_i(k_x)$ in Equations (1) and (2) are determined from boundary conditions at the air-substrate interface. The appropriate conditions are (i) continuous electric potential, (ii) continuous normal components of electric displacement, and (iii) stress-free surface. It is important to point out that because of the piezoelectric coupling, the stress-free condition cannot be satisfied by the quasi-acoustic wave itself. Rather, the quasi-acoustic wave must always be accompanied by the quasi-electrostatic mode.

After the Fourier amplitudes are evaluated, the velocity field (v) and the electrostatic potential (ϕ) of each of the modes can be evaluated in the far-field approximation by using the saddle point integration technique.[7] Thus, for a slowly varying $\phi_{AC}(k_x,z)$, the potential inside the bulk crystal due to a line source is

$$\phi_{Ac}(\vec{r}) = \phi_{Ac}(k_x,k_z)\left(\frac{\sqrt{1 + (dk_z/dk_x)^2}}{2\pi r\left|d^2k_z/dk_x^2\right|}\right)^{1/2} \cdot e^{-i(\vec{k}_s \cdot \vec{r}) - i\frac{\pi}{4}\mathrm{sgn}K_s} \qquad (4)$$

where K_s is the curvature of the dispersion curve at the saddle point $\vec{k}_s$,

$$\left.\frac{dk_z}{dk_x}\right|_{\vec{k}_s} = -\tan\theta_r \quad ,$$

and θ_r is the observation angle.

Radiation From Multiple Line Sources

The acoustic field radiated from a multiple line source is obtained by multiplying the radiation pattern of a single line source with the array factor. In terms of radiated power density or Poynting vector, the acoustic field radiated from a single line source can be evaluated from Eq. (4) and the constitutional relations by using the relation

$$\vec{P}_{average}(\vec{r}) = \mathrm{Re}\,\frac{1}{2}(-\vec{v}:T + \phi\frac{\partial}{\partial t}\vec{D}) \qquad (5)$$

where $\vec{D}$ is the displacement field, and T is the stress tensor. The array factor $|f_N(\theta_r)|^2$ is evaluated by using antenna theory.[7] For uniform unweighted transducers,

$$|f_N(\theta_r)|^2 = \left[\frac{\mathrm{Sin}N(\vec{k}_s\cdot\Delta\vec{r}-\pi)}{\mathrm{Sin}(\frac{\vec{k}_s\cdot\Delta\vec{r}\ \pi}{2})}\right]^2 \qquad (6)$$

where N is the number of the finger pairs. Thus, the directional properties of the radiated power density are given by the product of the "element" pattern and the array factor.

Acoustic Poynting Vector Along the Surface

Since the output transducer is located at the substrate surface, the acoustic Poynting vector at $\theta_r = \pi/2$ directly determines the amount of power received by the output transducer. The maximum acoustic power at the surface is achieved when the array factor $|f_N(\pi/2)|^2$ is maximum. This in turn depends on the phase condition,

$$\vec{k}_c \cdot \Delta\vec{r} = \pi \qquad (7)$$

or

$$k_c \cos\gamma_c \Delta r = \pi \quad ,$$

where $\gamma_c = \pi/2 - \theta_{c,s}$.

Thus, if one defines $k_{cx} = k_c \cos\gamma_c$ and lets

$$v_{SBAW} = \omega/k_{cx} \quad , \qquad (8)$$

the center frequency of the SBAW device is given by

$$f_c = \frac{v_{SBAW}}{2\Delta r} \quad . \qquad (9)$$

At f_c, the Poynting vector directed at the output transducer is maximum and is given by

$$P_{max}(r,\theta_r \approx 0) \approx V_o^2 \left(\frac{C_s}{d}\right)^2 \frac{\omega_c N^2}{\pi r} \cdot K_p^2 \cdot \frac{1}{\varepsilon_s}$$

where

$$\varepsilon_s = \left(\varepsilon_o + \sqrt{\varepsilon_{11}\varepsilon_{33} - \varepsilon_{13}^2}\right) \qquad (10)$$

$$K_p^2 = \frac{\left|(e_{14}+e_{34}\bar{n})(C_{46}+C_{44}\bar{n}) \cdot \dfrac{(e_{16}+(e_{14}+e_{36})\bar{n}+e_{34}\bar{n}^2)}{\dfrac{C_{46}^2}{C_{44}} + C_{44}\bar{n}^2 - 2C_{46}\bar{n}}\right|^2}{C_{44}\left(\varepsilon_o + \sqrt{\varepsilon_{11}\varepsilon_{33} - \varepsilon_{13}^2}\right)}$$

$$\omega_c = 2\pi f_c, \quad \text{and} \quad \bar{n} \equiv \frac{-(\varepsilon_{13} + \sqrt{\varepsilon_{11}\varepsilon_{33} - \varepsilon_{13}^2})}{\varepsilon_{33}}$$

In these expressions, the transducer is represented by a capacitor C_T in series with a resistor (see Figure 9). The quantity V_o is the voltage applied to the transducer terminal and c_s is the capacitance per finger pair. For rotated Y-cut quartz, $\varepsilon_s = 4.894\times10^{-11}$ F/m and for uniform transducers, $C_T = NC_s = Nd\,\varepsilon_s$.

The derivation of these expressions is based on Equations (4) and (5). Details of the derivation will be presented in a separate paper elsewhere.[10]

Radiation Resistance and Acoustic Loss

Radiation resistance and acoustic loss are two important parameters for the characterization of SBAW devices. The radiation resistance of a transducer is defined as the ratio

$$R_a = \frac{P_{rad}}{I_T^2} \quad ,$$

where I_T is the total current applied to the transducer and P_{rad} is the radiated acoustic power into the substrate. With this definition, the radiation resistance can be given by

$$R_a(\omega) = \frac{d}{\omega^2 C_T^2 V_o^2} \int_{-\frac{\pi}{2}}^{+\frac{\pi}{2}} d\theta_r \, rP_{av} \quad . \qquad (11a)$$

The frequency dependence of $R_a(\omega)$ depends largely on the array factor $|f(\pi/2)|^2$ and can be approximated by taking the Fourier transform of the impulse function which is determined by the transducer weighting function. This frequency dependence of the SBAW device has been discussed in previous papers.[2]

At center frequency, the integral in Equation (11a) can be replaced by the product of the peak power in Equation (10) and the main lobe halfwidth, $1.54/\sqrt{2}N$. This gives

$$R_a(\omega_c) \approx \frac{2}{\pi} \frac{K_p^2}{\sqrt{N}} \frac{1}{\omega_c C_s} \quad , \qquad (11b)$$

where $C_s = \varepsilon_s d$ is the capacitance per finger pair.

Note that there is no adjustable parameter in this calculation.

The acoustic loss is defined as the ratio of the total received power divided by the total radiated power.

To a good approximation, the power received by the output transducer may be calculated by using the reciprocity arguments. For identical output and input transducers, the acoustic loss, I, is

$$I \equiv 10 \log \frac{P_{received}}{P_{rad}} = 10 \log \frac{\lambda_c}{r} \cdot \left(\frac{P(r,\theta_r \approx \frac{\pi}{2})}{P_{rad}}\right)^2 \qquad (12)$$

where λ_c is the cut-off wavelength. Under matched load conditions, using the same approximation as in Equation (11), Equation (12) becomes

$$I = 10 \log \frac{\lambda_c N}{4.5\, r} \quad . \tag{13}$$

We note that Eq. (13) implies a minimum insertion loss attainable when two identical transducers are placed in close proximity with the center-to-center distance $r = N\lambda_c$. Under matched load conditions,

$$I_{min} = 10 \log \frac{1}{4.5} \approx 6.5 \text{ dB} \quad . \tag{14}$$

This includes the 6 dB bidirectional loss in the transducer. In practice, it is probably not possible to reach I_{min}, since, in the limit where (14) was derived, the far-field approximation is invalid.

Comparison with Experiments

Experimental Arrangements

The experiments discussed in this paper were carried out by fabricating delay lines on various rotated Y-cut quartz substrates and measuring their properties. A single delay line design was used for all experiments. The delay line consisted of two identical interdigital transducers, each with 140 finger pairs. Split finger configuration was used for the electrodes. The delay line had an aperture of 33 wavelengths (λ_c) and the center frequency was 166 MHz when fabricated on ST-cut quartz for SAW propagation. The transducers in the mask were stepped so that delay lines with several different center-to-center separations between transdcuers can be fabricated. The distances between transducers ranges from 150 λ_c to 300 λ_c.

The center frequency, insertion loss and frequency response of the SBAW delay line were obtained by measuring the transmission characteristic of the device on an HP network analyzer. The temperature coefficients of delay were measured by putting the delay line into a feedback loop with an amplifier and forming a SBAW oscillator. The frequency variation of the oscillator as a function of frequency was measured.

Wave Velocity and Temperature Coefficient of Delay

As discussed in the theoretical section, the velocity of the SBAW is given by ω/k_{cx}. This is similar to the cutoff velocity or tilted bulk wave velocity used by previous authors.[3,4] By using Equation (3), the SBAW velocity can be determined taking into account complete piezoelectric, elastic, and dielectric constants. The result of the calculation is shown in Figure 4. In Figure 4, the velocity of the bulk wave with the $\vec{K}$ vector pointing along the surface is also plotted for comparison. The experimental points agree well with the ω/k_{cx} value.

The temperature coefficient of delay can be calculated once the correct expression for the wave velocity is found. The procedure for the temperature coefficeint calculation is shown schematically in Figure 5. It consists of first evaluating the piezoelectric, elastic, and dielectric constants, and density of the quartz substrate at various temperatures. The temperature coefficients of all these quantities have been well documented.[8] After the correct material constants are determined, Equation (3) can be used to determine k_{cx} and thus V_{SBAW} at the particular temperature. The oscillation condition of the SBAW delay line oscillator is given by

$$\frac{2\pi f(T)}{V_{SBAW}(T)} \cdot L + \phi_{ext.} = 2n\pi, \quad L = L_o(1+\alpha(T)) \quad ,$$

where $\alpha(T)$ is the linear expansion coefficient of the substrate. A polynomial fit is then carried out to fit the f(T)'s with 1st, 2nd, and 3rd order temperature coefficients of frequency ($\Delta f/f$). The temperature coefficient of delay ($\Delta\tau/\tau$) is merely the negative of that quantity.

For the SBAW in rotated Y-cut quartz, the first order temperature of delay at 25°C is plotted in Figure 6. The agreement between theory and experiment is excellent. To show the type of agreement achieved, some of the theoretical and experimental data are listed in Table 1. For device applications, the regions where zero first order temperature coefficient exists is of particular interest. A detailed calculation had been made for cuts near AT, and BT cuts which have zero first order temperature coefficient of delay. The frequency shift as a function of temperature for the AT cut region is shown in Figure 7, while Figure 8 shows the temperature shift for the BT-cut region. The results again agree well with experiments.

Equivalent Circuit Model

The expression derived for the radiation resistance and acoustic loss (Equations 11-13) can be used to construct an equivalent circuit model. In this model, the SBAW transducer is represented by radiation resistance in series with the capacitance C_T (see Figure 9). At the center frequency, the radiation resistance is given by Equation (11), i.e.,

$$R_a(\omega_c) \approx \frac{2}{\pi} \frac{K_p^2}{\sqrt{N}} \frac{1}{\omega_c C_s} \quad ,$$

and the capacitive reactance is given by

$$X_c(\omega_c) = \frac{1}{j\omega_c N C_s} \quad ,$$

where K_p^2 is given in Equation (10) and can be identified as the coupling coefficient.

The impedance of the transducer $Z(\omega_c)$ is thus given by

$$Z(\omega_c) = R_a(\omega_c) + \frac{1}{j\omega_c C_T} \quad .$$

It is interesting to point out that the R_a in this SBAW model is quite similar to that used

in the "in-line" model for SAW devices.[9] The major difference is the fact that the effective coupling of the SBAW is inversely proportional to $\sqrt{N}$ while it is independent of N for the SAW case.

A second interesting note is that the K_p^2 is not the same as $2\Delta v/v$, where Δv is the velocity difference of the SBAW with and without considering the piezoelectric effect. Figure 10 shows the $\Delta v/v$ and the K_p^2 for the SBAW in rotated Y-cut quartz. For certain cuts, the two quantities are comparable, whereas at other cuts they can differ by an order of magnitude. Table 2 lists the numbers of several specific cuts.

The insertion loss of the SBAW is the sum of three contributions: conversion loss of input transducer, conversion loss of the output transducer, and acoustic power spreading loss. Following the work in SAW devices, the conversion loss of a transducer is calculated by

$$\text{I. L.} = 10 \log \frac{2 \cdot R_a \cdot R_L}{(R_a+R_L)^2 + \left(\frac{1}{\omega_c C_T}\right)^2} \quad .$$

Here the 3 dB bidirectional loss is included. For SBAW devices, an additional loss is present. This loss is related to the acoustic loss derived in Equation (13).

Not all the acoustic energy radiated toward the output transducer side is received. This so-called acoustic power spreading loss is equal to the acoustic loss given by Equation (13) minus 6 dB, as this has been included in the transducer conversion loss. The expression for the spreading loss is thus given by

$$\text{S. L.} = 10 \log \frac{\lambda_c N}{4.5r} - 6 \quad ,$$

where λ_c is the SBAW wavelength. Using this equivalent circuit model, the Insertion Loss of delay lines fabricated on various rotated Y-cut quartz has been calculated and compared with experiment. Table 3 summarizes the result. In this calcualtion, the capacitance per pair C_s is given by

$$C_s = 1.4\, \varepsilon_s\, d \quad .$$

This is because of the split finger configuration in in the transducer and the finger width influence on the transducer capacitance.[11]

Summary

Starting from the basic electromagnetic and acoustic field equations, expressions for the wave velocity, radiation resistance, and acoustic spreading loss of the SBAW device on rotated Y-cut quartz have been derived. Using these expressions, the wave velocity and temperature coefficient have been calculated. In addition, an equivalent circuit model similar to that of the in-line model used in SAW device calculations has been developed. Initial experiments indicate that the theoretical results agree well with experimental observations.

References

1. Lewis, M., "Surface Skimming Bulk Waves," 1977 IEEE Ultrasonics Symposium Proceedings, pp. 744-752.

2. Lau, K. F., K. H. Yen, R. S. Kagiwada, and K. L. Wang, "Further Investigations of Shallow Bulk Acoustic Waves Generated by Using Interdigital Transducers," 1977 IEEE Ultrasonics Symposium Proceedings, pp. 996-1001.

3. Lee, D., "A Theoretical Analysis of Surface Skimming Bulk Waves," 1978 IEEE Ultrasonics Symposium Proceedings, pp. 675-679.

4. Jhunjhunwala, A., J. F. Vetelino, D. Harmon and W. Soluch, "Theoretical Examination of Surface Skimming Bulk Waves," 1978 IEEE Ultrasonics Symposium Proceedings, pp. 670-674.

5. Vasile, C. F., "Radiation From a Line Charge Source Located Near an Air Piezoelectric Interface," Proceedings of the IEEE, Vol. 64, No. 5, 1976, pp. 636-639.

6. Auld, B.A., Acoustic Fields and Waves in Solids, Vol. 1, Wiley, 1973, p. 298.

7. Felsen, L. B. and R. Rosenbaum, "Ray Optics for Radiation Problem in Anisotropic Regions With Boundaries, I. Line Source Excitation;" Radio Sci., Vol. 2, 1967; and G. Tyras, "Radiation and Propagation of Electromagnetic Waves, Academic Press, 1969.

8. Bechmann, R., A. Ballato and T. Lukaszek, "Higher Order Temperature Coefficients of the Elastic Stiffnesses and Compliances of Alpha Quartz," Proceedings of the IRE, Vol. 50, No. 8, August 1962, pp. 1812-1822.

9. Smith, W. R., H. M. Gerard, J. H. Collins, T. M. Reeder and H. J. Shaw, "Analysis of Interdigital Surface Wave Transducers by Use of an Equivalent Circuit Model," IEEE Trans., 1969, MTT-17, pp. 856-864.

10. Wilcox, J. Z., K. H. Yen, K. F. Lau, and R. S. Kagiwada, in preparation.

11. Engan, H., "Excitation of Elastic Surface Waves by Spatial Harmonics of Interdigital Transducers," IEEE Trans. Electron Devices, ED-16, 1969, pp. 1014

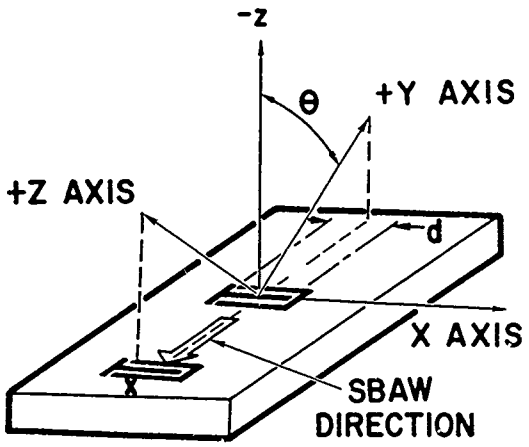

FIGURE 1.
GEOMETRY OF A SBAW DEVICE ON ROTATED Y-CUT QUARTZ; θ = 42.75 FOR ST-CUT QUARTZ.

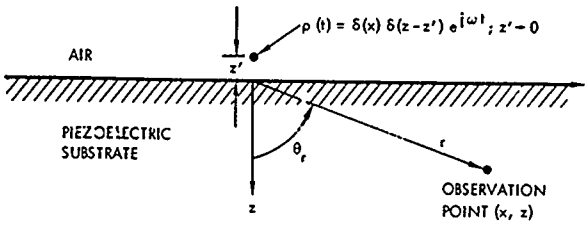

FIGURE 2. GEOMETRY OF A SINGLE LINE SOURCE ON A SEMI-INFINITE SUBSTRATE.

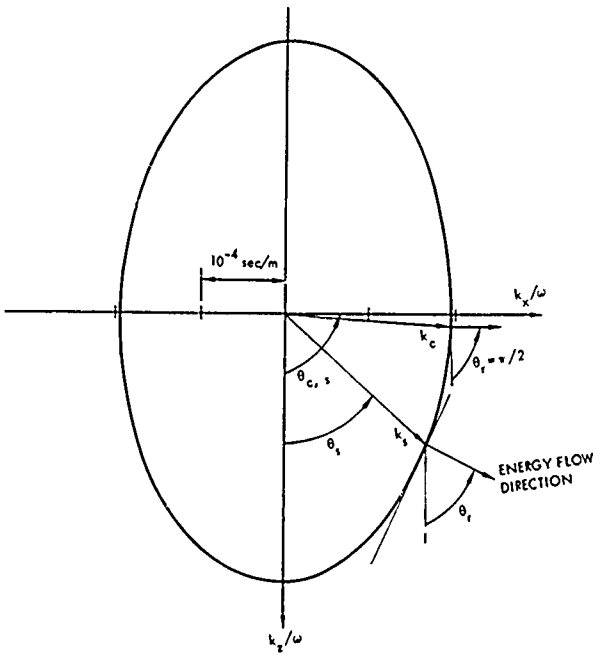

FIGURE 3. INVERSE VELOCITY SURFACE FOR HORIZONTALLY POLARIZED SHEAR WAVE ON ROTATED Y-CUT QUARTZ.

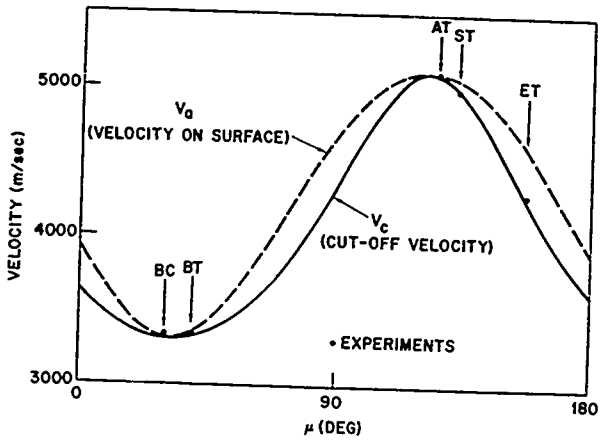

FIGURE 4. CUTOFF VELOCITY AND VELOCITY ON SURFACE OF HORIZONTALLY POLARIZED SHEAR WAVE ON ROTATED Y-CUT QUARTZ.

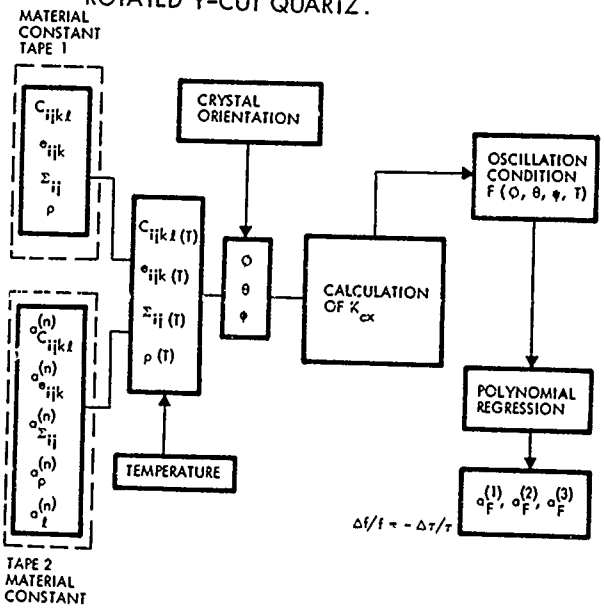

FIGURE 5. FLOW CHART FOR CALCULATING THE TEMPERATURE COEFFICIENT OF DELAY.

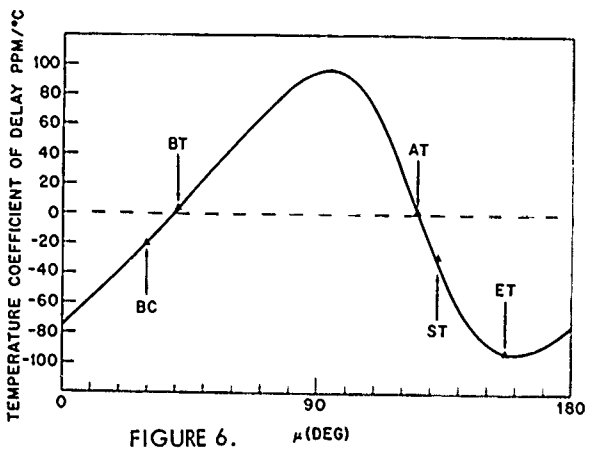

FIGURE 6. FIRST-ORDER TEMPERATURE COEFFICIENT OF DELAY OF SBAW IN ROTATED Y-CUT QUARTZ.

Table 1. Calculated and Measured Wave Velocities and Temperature Coefficients of Delay

Substrate	μ (Deg)	Velocity (m/sec) Theory	Velocity (m/sec) Exp.	Temperature Coefficient of Delay First Order (ppm/°C) Theory	Temperature Coefficient of Delay First Order (ppm/°C) Exp.
ET	156.3	4276	4295	92.9	91.5
ST	132.75	4993	4990	33.2	26.2
AT	125.25	5095	5100	- 2.89	- 2.46
BT	41.0	3338	3340	- 3.75	- 3.15
BC	30.0	3317	3314	19.1	18.5

Table 2. Selected Values of K_p^2 and $\Delta v/v$

Substrate	μ (Degrees)	K_p^2 (%)	Δv/v (%)
ET	156.3	1.488	0.938
ST	132.75	1.899	0.390
AT	125.25	1.436	0.153
BT	41.0	0.413	0.382
BC	30.0	0.485	0.508

Table 3. Calculated and Measured Insertion Losses

Substrate	μ (Deg)	Theoretical Calculation: Conversion Loss per Transducer	Theoretical Calculation: Spreading Loss	Theoretical Calculation: Total Insertion Loss	Measured Insertion Loss
ET	156.3	11.2 dB	1.3 dB	23.7 dB	21.8 dB
ST	132.75	9.9	1.3	21.1	21.0
AT	125.25	11.0	1.3	23.3	25.0
BT	41.0	17.3	1.3	35.9	37.2
BC	30.0	16.5	1.3	34.3	32.0

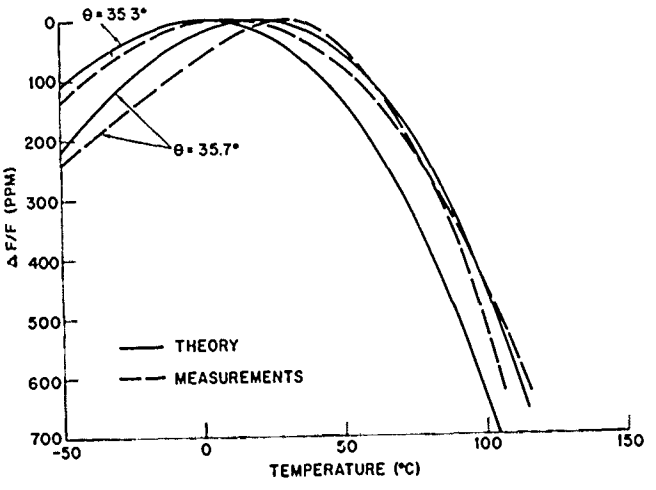

FIGURE 7. TEMPERATURE SHIFT IN FREQUENCY FOR CUTS NEAR AT-CUT.

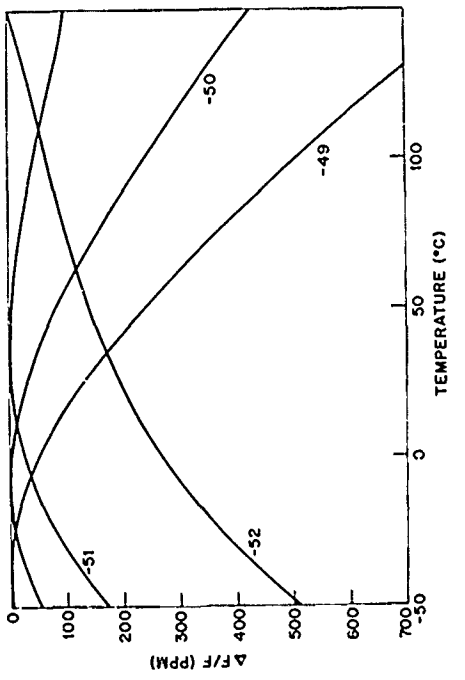

FIGURE 8. CALCULATED TEMPERATURE SHIFT IN FREQUENCY FOR CUTS NEAR BT-CUT.

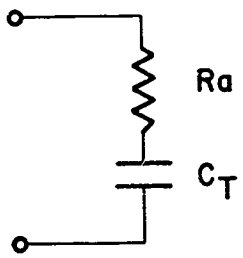

$$Ra \cong \frac{2}{\pi} \frac{1}{\sqrt{N_p}} K_p^2 \frac{1}{\omega_o C_s}$$

$$C_T = N_p C_s$$

$$I.L._{total} = I.L._1 + I.L._2 + S.L.$$

FIGURE 9. EQUIVALENT CIRCUIT MODEL FOR A SBAW TRANSDUCER.

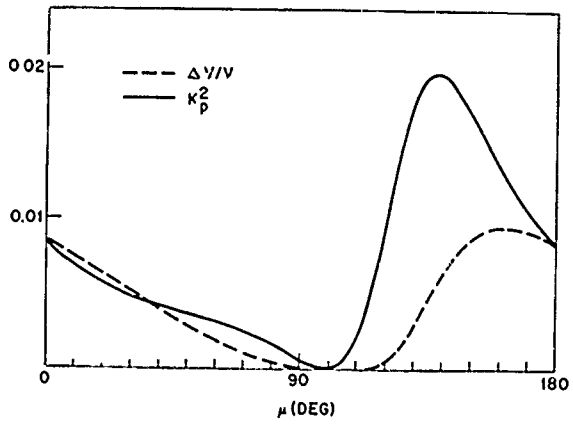

FIGURE 10. $\Delta v/v$ AND K_p^2 OF SBAW IN ROTATED Y-CUT QUARTZ.

L-BAND LOW LOSS SAW FILTERS

Bob R. Potter

Texas Instruments Incorporated
Dallas, Texas 75266

SUMMARY

Conventional and low loss Surface Acoustic Wave (SAW) filters have been used in a remarkable number of system applications from radar to communications, to television tuners. The frequency range for low loss SAW filters has been 30 MHz to 440 MHz. L-band SAW devices can be manufactured using higher resolution fabrication techniques such as E-beam mask making and group-type unidirectional transducer design. Results of a 961 MHz group-type unidirectional fabricated on lithium niobate are presented along with theoretical results. Results of a 250 MHz group-type prototype device are presented along with the series tuned matching technique developed by Malocha.[1]

INTRODUCTION

Low frequency low-loss surface acoustic wave (SAW) filters in the 30 to 440 MHz frequency range are highly developed and insertion loss as low as 2 dB with -50 dB sidelobes have been reported.[2] Greater than 45 dB triple transit suppression is easily achievable and these low frequency SAW devices are being produced regularly.

The 440 MHz upper limit to the three-phase unidirectional transducer is a result of the limitations of the fabrication process of the unidirectional transducer utilizing gold crossovers. (See Reference 2, page 352, paragraph 3). Three masks are required to fabricate the transducer and there is a critical alignment of the via hole mask to the electrode mask. As the via holes become smaller with increasing passband frequency of the transducer the mask alignment becomes impossible above 440 MHz.

The group type unidirectional transducer[3] also requires three masks in the fabrication process, but because the electrodes are arranged in groups the via holes remain large and the mask alignment for the three levels is relatively straightforward.

This work is partially supported by USAERADCOM, Contract No. DAAK20-79-C-0257.

The group-type unidirectional transducer was first described by Yamanouchi.[3] These early group structures utilized a meandering ground line for single level construction and loss as low as -1.0 dB was achieved at 100 MHz. However, at 1 to 2 GHz on ST-quartz a meandering ground line would increase the parasitic losses significantly making the gold crossover technique attractive for reducing insertion loss.

GROUP-TYPE UNIDIRECTIONAL TRANSDUCER THEORY

The group type SAW transducer was first discussed in 1975 by Yamanouchi.[3] A variety of relatively wideband lithium niobate SAW filters have been constructed since that time. These filters use single level construction with a meandering ground line and insertion loss as low as 6 dB has been achieved at 800 MHz.

Transducer Configuration

The configuration is essentially two bi-directional transducers placed 90 degrees out of phase (acoustically) on the substrate. The transducer frequency response will be the same as one of those bi-directional transducers. However the insertion loss will be low due to the power from the two bi-directional transducers adding in phase in one direction and cancelling in the other.

The transducer design approach is shown in Figure 1. Phase 1 is connected

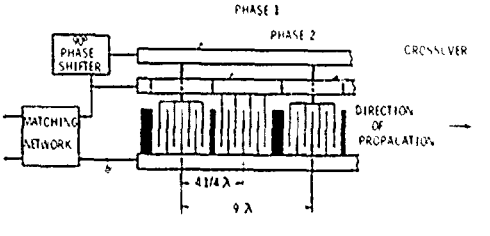

Figure 1. Group-Type Unidirectional Transducer With Crossovers on One Side

to fingers via a line going under a crossover. Phase 2 fingers are connected to the pads that are connected to the gold crossover bar. One contact pad per wavelength at L-band frequencies would make visual alignment of the masks impossible. However, four or five wavelengths per contact pad as shown will result in an adequate pad size.

As shown in Figure 1, the fingers of each transducer will be placed in "packets" of 4 or 5 wavelengths each with every other group 90 degrees or 1/4 wavelength out of phase acoustically with its neighbor. With a +90' electrical phase shift of Phase I from Phase 2, then a wave traveling in the direction of propagation will add in phase with its neighbor. A wave going the opposite direction will then be 180 degrees out of phase with its neighbor and cancellation will occur.

Frequency Response Theory

The Fourier series for the group type unidirectional transducer is given in Reference [3]. When matched, the group type unidirectional will have a large forward wave and a small backward wave. The expression for the frequency response of an unweighted filter is given by:

$$F(\omega)=\sum_{n=-3}^{3}\left[S_a(\pi\tau(f-f_o))\right]\cdot\left[S_a\left[\frac{(\omega-2\pi f_o)-nW}{2}\tau_o\right]\right]\cdot\left[\frac{1}{2}\sqrt{2+2\sin(\frac{5}{2}\pi+\Phi)}\right] \quad (1)$$

where Φ for the backward wave is 180 degrees out of phase from the forward wave.

Definition of variables:

$S_a x = \frac{\sin x}{x}$

ω = $2\pi f$ where f is frequency, MHz

τ = wavelengths in 1/2 of a group, μsec

T = wavelengths in one group

f = frequency, MHz; f_o = device center frequency, MHz

W = $2\pi/T$, rad/sec

τ_o = overall transducer length, μsec

Figure 2 shows the square wave modulation of one group of the group-type unidirectional transducer. The overall length of the transducer, τ_o, influences the main response. The period of the transducer, T, determines how close to the main lobe the spurious lobes will be. The time length, τ, of each group of fingers affects the roll-off of the spurious lobes with respect to

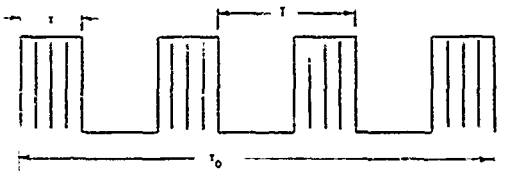

Figure 2. Square Wave Modulation of a Bi-Directional Transducer

the main lobe.

The sidelobe locations are given by:

$$f_\ell = \frac{f_o}{1+\frac{1}{N}} \quad (2)$$

where

f_o = center frequency main lobe, MHz

f_ℓ = spurious lobe frequency, MHz

N = Number of electrodes in a group.

f_ℓ/f_o will be .8 for 4 electrodes per group. Since the spurious lobes will be equally spaced in frequency on either side of the main lobe, there will also be a spurious lobe on the high frequency side at f/f_o = 1.2. Equation 1 automatically places these lobes where they belong.

Theoretical Results

The above expressions have been programmed into our HP 9825 computing system and some theoretical results have been obtained. Figure 3 is a plot of the 250 MHz prototype device frequency theoretical response. The program thus far only uses the above equations and no equivalent circuit model has been used to show rejection of the spurious sidelobes. The response of Figure 3 is for both transducers. Note that the first spurious sidelobe is at 200 and 300 MHz. By equation 2 this would correspond to 4 electrodes per group or two active and 2 grounded electrodes per group.

Another way to find the frequency response of a transducer is to perform a Fast-Fourier-Transform on the time envelope. Figure 4 is a plot of the FFT result on the

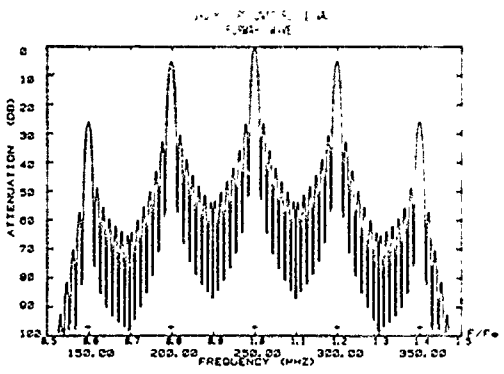

Figure 3. Theoretical Frequency Response of an Unweighted Group-Type SAW Filter at 250 MHz

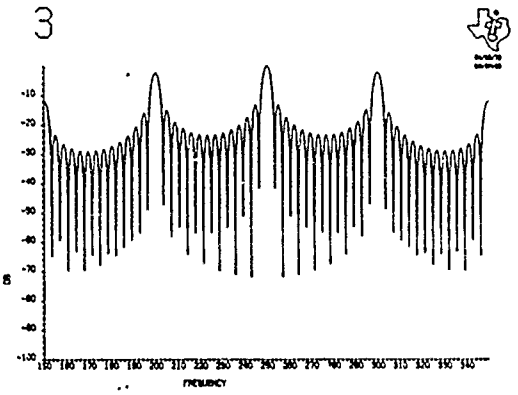

Figure 4. FFT of the Type of Transducer Shown in Figure 2.

250 MHz group-type transducer with N = 4. It must be emphasized that this is for only one transducer whereas Figure 3 was for two transducers.

Note that from Figures 3 and 4 the spurious lobes are down only 4 or 5 dB from the main lobe. For group-type unidirectional filters constructed on lithium niobate this could be a problem. Since the impedance of the lithium niobate transducer is quite low (could be near 50 ohms), the spurious lobes will have relatively low loss unmatched. When the device is matched, only the matching network components will attenuate these lobes. The problem will not be serious on ST-quartz because the transducer has a relatively high impedance unmatched. When the main lobe is matched, the spurious sidelobes should stay suppressed and also be attenuated by the matching network components.

The last theoretical plot shown in Figure 5 is of a 961 MHz group-type unidirectional with N=4. Note that the first suprious lobe occurs at 768.8 MHz and 1153 MHz. Emphirical results will be compared with these theoretical results later in the paper.

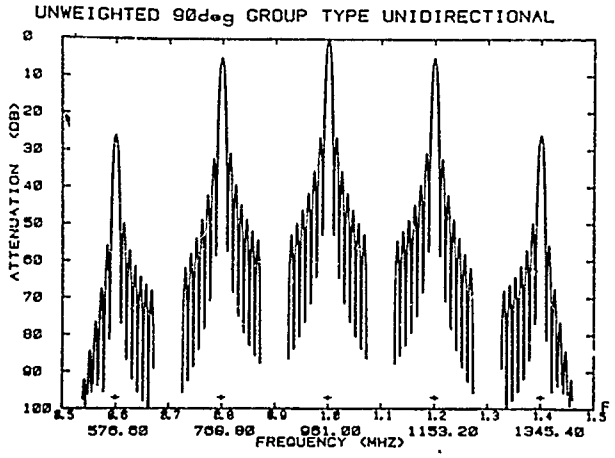

Figure 5. Theoretical Frequency Response of a 961 MHz SAW Filter on Lithium Niobate

Group-Unidirectional Transducer Matching

The first group-type unidirectional transducers used 90 degree lengths of coaxial line to produce the necessary phase shift.[3] This worked well for lithium niobate devices where the transducer impedance was near 50 ohms. However, for devices constructed on ST-quartz matching in and out of the coaxial line would present a difficult problem. Malocha[1] developed a technique for matching and phasing the group-type uni directional transducer on ST-quartz using only two components.

Consider the schematic for the group-type transducer shown in Figure 6. $Z°_{12}$ is the input impedance of the device phased with components X_1 and X_2. The phase shift from phase 1 to phase 2 through X_1 and X_2 will most likely be inductors for ST-quartz and at least one will be a capacitor for lithium niobate substrates. These component values can be calculated from the following:

$$X_1 = A(\cos\Theta + \sin\Theta), \quad (3)$$

$$X_2 = A(\sin\Theta - \cos\Theta), \quad (4)$$

$$Z°_{12} = \left|A\cos\Theta\right|. \quad (5)$$

A and Θ can be calculated from the transducer parameters.

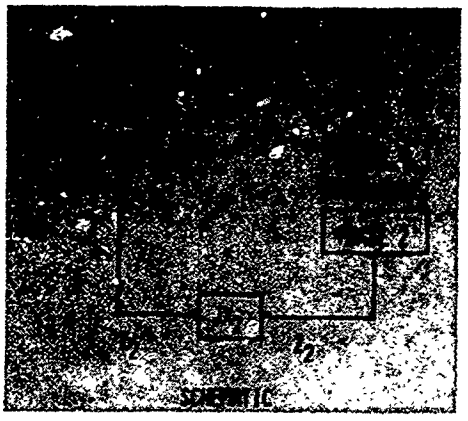

Figure 6. Series Tuning Network for the Group-Type SAW Transducer

$$A = [nf_o C_s \sqrt{(2\pi)^2 + (8k^2 n)^2}]^{-1} \quad (6)$$

and

$$\Theta = \tan^{-1} \left[\frac{\pi}{4k^2 n} \right] \quad (7)$$

where

f_o = center frequency, MHz

n = number of electrodes in 1/2 transducer

C_s = capacitance one finger pair

k^2 = coupling coefficient.

It is interesting to note that Θ only depends on the coupling coefficient and the number of finger pair. However, any significant parasitic capacitance or inductance can change Θ .

Lithium Niobate Design at 961 MHz

The first group-type unidirectional transducer constructed at Texas Instruments was for lithium niobate at 961 MHz. The two transducers were 95 wavelengths long constructed like Figure 1 with crossovers only on one side. The transducer beamwidth was .006 inches or 39 wavelengths. From equations 3-7 this means that X_1 = 22 ohms or an inductor of 4 nh. X_2 - 10 ohm or a capacitor of 16 pf. The transducer beamwidth was not chosen correctly to utilize the series tuned approach to matching and phasing the transducers.

The approach employed to match the device was to use a 90 degree coaxial line with some matching components at each end of the line. This was a crude method and may have caused some insertion loss. The insertion loss after matching was 6.5 dB due to narrow fingers and poor matching.

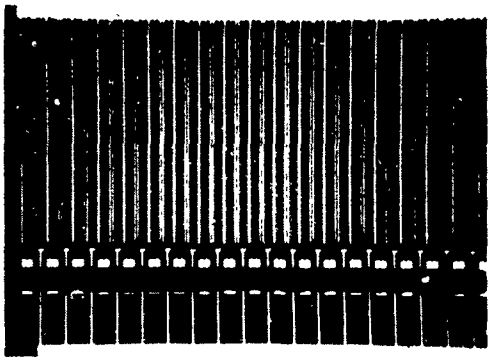

Figure 7. 961 MHz Group-Type Transducer

A photograph of one transducer is shown in Figure 7. Both phases are taken off of one side with the gold crossover going over one phase. This means that the parasitics are not balanced for this transducer which could also lead to insertion loss and inability to totally match the filter.

The main passband response of the device is shown in Figure 8. Since it is an unweighted transducer, the response shows poor sidelobes. RF feedthrough is also an obvious problem with the crosstalk level only 30 dB down from the main passband. This was due to the poor packaging job done on this device. Not shown are the spurious lobes at 768.8 and 1153.2 MHz. These lobes occurred exactly where the theory would have predicted them.

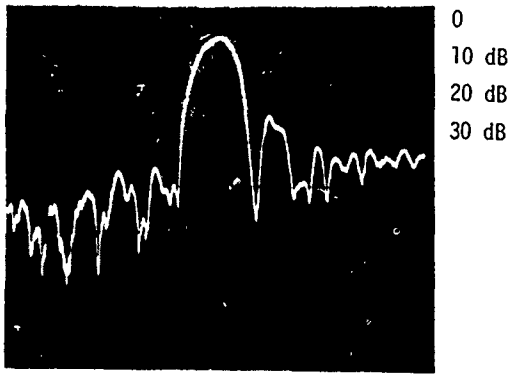

Figure 8. L-Band SAW Filter with 6.5 dB Loss

250 MHz L-Band Prototype on ST-Quartz

To try to understand the group-type unidirectional transducer without the packaging parasitics that occur at L-band frequencies, a device was constructed at 250 MHz on ST quartz. The transducer was 65 wavelengths long, which represents a bandwidth of just over 1 percent at 250 MHz. The period, T, of the transducer was 5 wavelengths long so so that the spurious lobes would appear at .8 x 250 = 200 MHz, and 1.2 x 250 = 300 MHz.

Figure 9. Package for the 250 MHz Filter

The series tuning approach was chosen to see if the technique could be used at L-band frequencies. Θ from equation 7 turned out to be 86.56 degrees and A from equation 6 was 624. The two phasing inductors came out to be 421 nh and 373 nh. $Z°_{12}$ from equation 5 was predicted to be 37^{2} ohms. Parasitic feedthrough capacitance of the package shown in Figure 9 changed considerably the final values Of the phasing inductors from 400 nh to between 100 and 200 nh. More importantly $Z°_{12}$ became very low in impedance and capacitance. Therefore, a matching network was necessary and the total number of components needed per transducer was four.

A photograph of final transducer structure is shown in Figure 10. There are two large ground bars in the interdigital finger structure. One of them, as shown in Figure 1, is 1 wide and the other 1/2 wide with 1/4 between the two. It is hoped that this might cut down on spurious reflections from the large ground bar. The device still has a crossover on only one side as did the 961 MHz device. This can be seen in Figure 10.

The electrical results from the device were good. The insertion loss in the middle of the passband was 3.9 dB, when matched and phased to 50 ohms. Figure 11A shows the

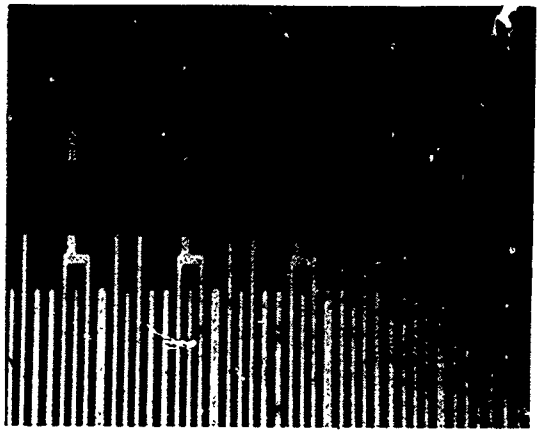

Figure 10. 250 MHz Group-Type Transducer Structure

A. Inband Response and Impedance

B. Frequency Response Showing Spurious Sidelobes

Figure 11. 250 MHz Filter Results

inband response and the Smith chart of the impedance of one transducer. A small amount of ripple still shows in the passband and could be caused by two things. The first is acoustic reflections off the 1/4 wavelength fingers in each group. The second is the possibility that the device is not perfectly phased due to imbalance of parasitics. Figure 11B shows the first spurious sidelobes quite clearly at 200 and 300 MHz. They are suppressed due to the matching and phasing network only acting on the mainlobe.

FUTURE DEVICES

In fabrication at the present time are the following group-type unidirectional devices:

1. 1227.6 MHz ST-quartz unweighted
2. 1227.6 MHz lithium niobate unweighted
3. 1227.6 MHz ST-quartz apodized weighted
4. 250 MHz ST-quartz crossovers both sides.

All of the above devices employ a special technique for suppression of the spurious lobes. The two different transducers have different periods, T, and hence the spurious lobes are at different frequencies for each transducer. Therefore, they will tend to cancel each other.

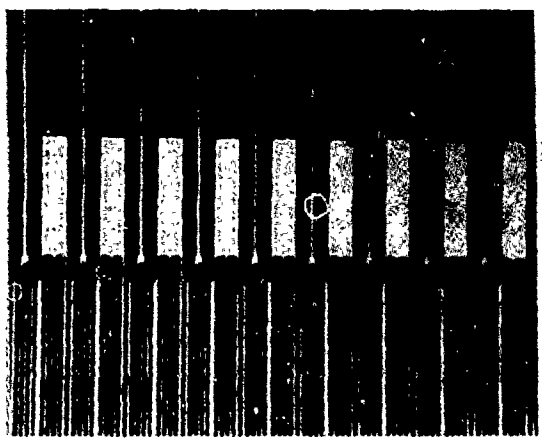

Figure 12. Transducer Structure for a 1227.6 MHz SAW Filter

Figure 12 shows the transducer structure for the 1227.6 MHz ST-quartz device, unweighted, with crossovers on both sides. The parasitics are balanced with the pads shown as ground on both sides and the two phases going between the ground pads on both sides of the transducer.

Packaging for the L-band devices requires some attention because any parasitic capacitance will lower the values of the phasing coils. An alumina ceramic carrier is used to mount the matching components and SAW device. This ceramic board is mounted in an Isotronics 1037 microelectronics package. Matching and phasing components plus a shield and the device are shown.

CONCLUSIONS

The group-type unidirectional transducer structure has been shown feasible for ST quartz devices. However, at L-band frequencies parasitic capacitance will be troublesome and packaging will be a major engineering problem. The packaging problems do not seem insurmountable and good L-band devices should be produced soon.

Apodized weighting techiques look as if they can be implemented easily with crossovers on both sides. Withdrawal weighting[4] may also be implemented in the same filter as the apodized weighted transducer to give an ultimate sidelobe rejection of about 50 dB.

ACKNOWLEDGEMENTS

The author would like to thank Bob Stigall, Gay Spence and Mac Carpenter for their many helpful discussions and work on the project. Also, the help of Charles Shaffer and Bob Vess in fabricating the devices, and Barbara Newell for typing the manuscript is appreciated.

REFERENCES

1. D. C. Malocha and B. J. Hunsinger, "Tuning of Group Type Unidirectional Transducers," IEEE Trans. Son. and Ultras., Vol. SU-26, May 1979, pp. 243-245.

2. B. R. Potter and C. S. Hartmann, "Low Loss Surface-Acoustic-Wave Filters," IEEE Trans. on Parts, Hybrids and Packaging, Vol. PHP-13, No. 4, Dec. 1977, pp. 348-353.

3. K. Yamanouchi, F. Nyffeler, and K. Shibayama, "Low Insertion Loss Acoustic Surface Wave Filter using Group-Type Unidirectional Interdigital Transducer," 1975 Ultrasonics Symp. Proc., IEEE Cat. No. 75 CHO994-4SU, pp. 317-321.

4. C. S. Hartmann, "Weighting Interdigital Surface-Wave Transducers by Selective Withdrawal of Electrodes," 1973 IEEE Ultrasonics Symp. Proc., Cat. No. 73 CHO807-8SU, p. 423.

A NEW CUT OF QUARTZ WITH ORTHOGONAL TEMPERATURE-COMPENSATED PROPAGATION DIRECTIONS FOR SURFACE ACOUSTIC WAVE APPLICATIONS

Robert M. O'Connell

Rome Air Development Center, Deputy for Electronic Technology
Electromagnetic Sciences Division, Hanscom Air Force Base, MA 01731

Abstract

Motivated by increased interest in the reflective array compressor (RAC) and other reflection-grating surface acoustic wave (SAW) devices that employ orthogonal propagation directions, a theoretical search has been performed to find an improved substrate material. This search has produced a new cut of quartz which is temperature-compensated along orthogonal directions and therefore attractive for use in RAC devices. Except for a small electromechanical power flow angle, the SAW properties along the two temperature-compensated directions are similar to those of X propagating, ST-cut quartz. Furthermore, because the attractive propagation paths lie in the plane of a singly-rotated crystal-cut, it should be relatively easy and inexpensive to manufacture.

Introduction

The purpose of this paper is to describe a new surface acoustic wave (SAW) cut of quartz which is temperature-compensated along two orthogonal directions. This result is the product of a theoretical search for an improved substrate material for devices such as the reflective array compressor (RAC) which use reflection-gratings to direct the acoustic energy along orthogonal propagation paths[1,2].

The use of multiple paths in SAW devices is attractive because it provides good rejection of spurious signals and second order effects [3,4]; however, it also places an additional condition on the substrate material if the device is to be temperature-stable without thermostatting. In the operation of a general reflection-grating device, shown schematically in Figure 1, the acoustic wave launched at the input interdigital transducer makes two 90° reflections from the gratings and propagates along the orthogonal paths a and b before reaching the output transducer. For temperature stability, it is necessary first that the substrate material be temperature compensated along the primary propagation axis (a in Figure 1); this is the usual requirement for temperature-stability of the dispersive delay. In addition, to avoid serious reductions in the amplitude of the output signal, it is necessary that the temperature coefficients of delay (TCDS) along both propagation paths be equal [5,6,7]. To meet both of these requirements, it is therefore necessary that the substrate be temperature-compensated along both propagation paths.

Since SAW substrate materials are in general anisotropic, the requirement for temperature-compensated orthogonal propagation directions is not usually satisfied. On the popular ST-cut of quartz, for example, the TCD along the direction orthogonal to the temperature-compensated X-axis is 47 ppm/°C[8] ; hence, orthogonal-direction SAW devices built on ST-cut quartz must be thermostatted. It appears, in fact, that no SAW cut of any material has previously been found which is temperature-compensated along two orthogonal directions. This new cut of quartz should fill that need.

Theoretical Search

In order to find this new crystal-cut, a theoretical search was performed with a previously described set of computer programs which compute the important SAW properties for a desired crystallographic orientation of a given material [9,10] Because it is known to have several temperature-compensated orientations and is available from several manufacturers, quartz was chosen for the search. Furthermore, to maximize crystallographic simplicity and thereby minimize potential manufacturing costs, the search was restricted to the planes of various singly rotated Y-cuts. Two very pertinent examples are the Y-cut itself and the ST-cut. The variation of the TCD in the plane of each of these cuts, taken from reference 8, is shown in Figure 2. These curves provided two observations which further simplified the search. First, because of the symmetry of the crystal, TCD data in the plane of a rotated Y-cut is symmetric about a direction of propagation, θ, equal to 90°; hence, the TCDs at $\theta = 45°$ and 135°, a pair or orthogonal propagation directions, are equal. Second, the sign of the TCD at $\theta = 45°$ in the plane of the Y-cut is opposite to that at $\theta = 45°$ in the plane of the ST-cut; hence, there should be a zero TCD at $\theta = 45°$ (and $\theta = 135°$) in the plane of some intermediate rotated Y-cut. To verify this, it was only necessary to calculate the SAW properties of the boule defined by the Euler angles [8] $\lambda = 0°$, μ varied from 90° (Y-cut) to 132.75° (ST-cut), $\theta = 45°$. The

measured elastic, piezoelectric, and dielectric data of reference 11 were used in the computer model and, as expected, the TCD reversed sign at μ = 125.87°, completing the search.

The Euler angles λ = 0° and μ = 125.87° define the sought-after crystal-cut. The variation of SAW velocity, electromechanical power flow angle, ΔV/V piezoelectric coupling constant, and TCD in the plane of this cut are shown in Figure 3. Note that the TCD is zero along the two orthogonal propagation directions θ = 45° and 135°. For RAC device design, the primary (principal or incident) and secondary axes of propagation [6,7] should be aligned along these directions. A sketch of the crystal-cut, showing the relationship among the XYZ crystal axes, the plate normal, and the primary and secondary propagation directions is shown in Figure 4.

Discussion

The SAW properties along the attractive orthogonal directions of this new cut are listed in Table I, along with the corresponding values for ST-cut quartz for comparison. Note that while the velocities and ΔV/V coupling values are very similar, the new cut has a small but non-zero electromechanical power flow angle along each of its temperature-compensated directions. Depending on the specific device design, this may necessitate a slight shift of either the reflective gratings, the output transducer, or both.

Table II shows the effect on the TCD of the new cut resulting from a slight misorientation of each of the Euler angles. Fortunately, the plate normal μ, which is the most difficult angle to orient, is the least sensitive.

As is the case with any new SAW crystal-cut, theoretical values for the defining Euler angles are only approximate. For this new cut, uncertainty exists only in the value of the second Euler angle, μ, the rotation angle of the plate normal, reported here as nominally 125.87°. To examine the extent to which the calculation of this value depends upon the material constants, the above-described procedure was repeated several times with slightly different, although equally valid, elastic, piezoelectric, and dielectric constants. The plate normal μ for zero TCD was found to vary by as much as 5° from the nominal value; thus, the precise value of μ must be determined experimentally. This is currently being done at RADC/EE and the results will be reported elsewhere.

The development of improved RAC devices need not await the experimental determination of the exact value of μ. One of the more serious problems in RAC design is that temperature variations cause a misalignment of the angle of the reflective gratings in proportion to the difference between the TCDs along the two propagation paths; this results in the above-mentioned reduc- of the amplitude of the output signal of the device.[5,6,7] Since the TCDs at θ = 45° and 135° in the planes of rotated Y-cuts are equal (see Figs. 1 and 2), their differences are zero, and the amplitude reduction problem is minimized independently of the value of μ. The TCDs at θ = 45° and 135° in the plane of the new cut defined by the Euler angles λ = 0° and μ = 125.87° are certainly small, if not zero, and equal. Thus, it should be possible to build greatly improved unthermostatted RAC devices now, without awaiting the results of the above-mentioned experimental determination of μ.

Conclusion

A new SAW cut of quartz has been described which is temperature-compensated along orthogonal directions and therefore attractive for use in RAC and other devices which employ orthogonal propagation paths. While the precise value of the Euler angle μ for the plate normal needs to be determined experimentally, greatly improved RAC devices should be possible using the theoretical values presented here. Finally, because the orthogonal temperature-compensated directions lie in the plane of a rotated Y-cut, it should be relatively easy and inexpensive to manufacture.

References

1. R.C. Williamson, "Properties and Applications of Reflective-Array Devices", Proc. IEEE, Vol. 64, p 702,(1976).

2. R.C. Williamson, in Surface Wave Filters, H. Matthews, Ed., Chap 9, (Wiley, New York, 1977).

3. R.C. Williamson and H.I. Smith, "Large Time-Bandwidth Product Surface-Wave Pulse Compressor Employing Reflective Gratings", Electron Lett., Vol. 8, p 401, (1972).

4. R.C. Williamson and H.I. Smith, "The Use of Surface-Elastic-Wave Reflection Gratings in Large Time-Bandwidth Pulse-Compression Filters" IEEE Trans. Microwave Theory Tech., Vol. MTT-21, p 195, (1973).

5. M.B. Schulz and M.G. Holland, "Materials for Surface Acoustic Wave Components", IEE Conf. Publ. 109, p1, (1973).

6. P.C. Meyer and M.B. Schulz, "Temperature Effects in Reflective Surface-Acoustic-Wave Delay Lines", Electron Lett., Vol. 9, p 523, (1973).

7. P.C. Meyer and M.B. Schulz, "Reflective Surface Acoustic Wave Delay Line Material Parameters", 1973 Ultrasonics Symposium Proceedings, p 500, (IEEE, New York, 1973).

8. A.J. Slobodnik, Jr., "The Temperature Coefficients of Acoustic Surface Wave Velocity and Delay on Lithium Niobate, Lithium Tantalate, Quartz, and Tellurium Dioxide", AFCRL-TR-72-0082 (1971).

9. A.J. Slobodnik, Jr., E.D. Conway, and R.T. Delmonico, Microwave Acoustics Handbook, Vol. 1A, Surface Wave Velocities", AFCRL-TR-73-0597 (1973).

10. R.M. O'Connell and P.H. Carr, "High Piezoelectric Coupling, Temperature Compensated Cuts of Berlinite Al PO_4, for SAW Applications", IEEE Trans. on Sonics and Ultrasonics, Vol. SU-24, p 376,(1977).

11. R. Bechmann, A.D. Ballato, and T.J. Lukaszek, "Higher-Order Temperature Coefficients of the Elastic Stiffnesses and Compliances of Alpha-Quartz", Proc. IEEE, Vol. 5, p 1812, (1962).

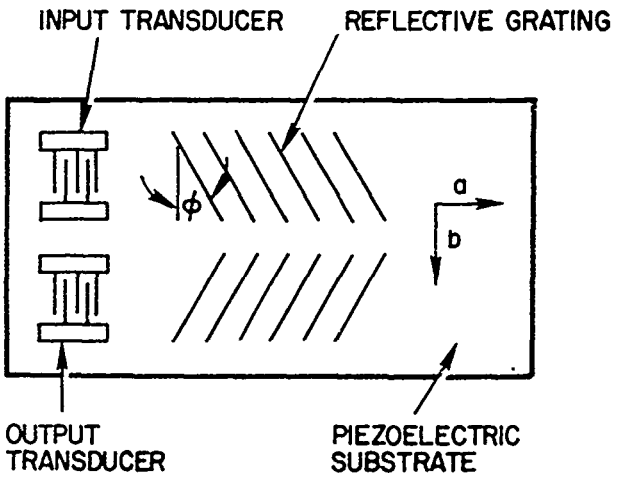

Figure 1:
Schematic diagram of a general reflection-grating SAW device. The acoustic signal makes two 90° reflections and propagates along the orthogonal paths a and b before reaching the output transducer.

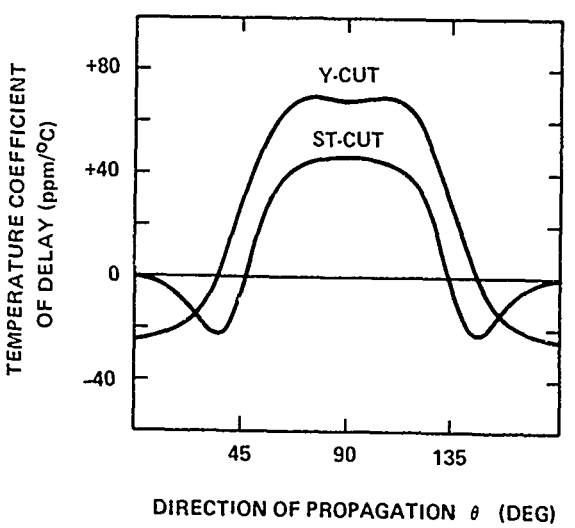

Figure 2:
The variation of temperature coefficient of time delay (TCD) in the planes of Y-cut and ST-cut quartz. Note that each curve is symmetric about a direction of propagation, θ, equal to 90°, and that the TCD at θ = 45° (and 135°) for the Y-cut is opposite in sign to that for the ST-cut.

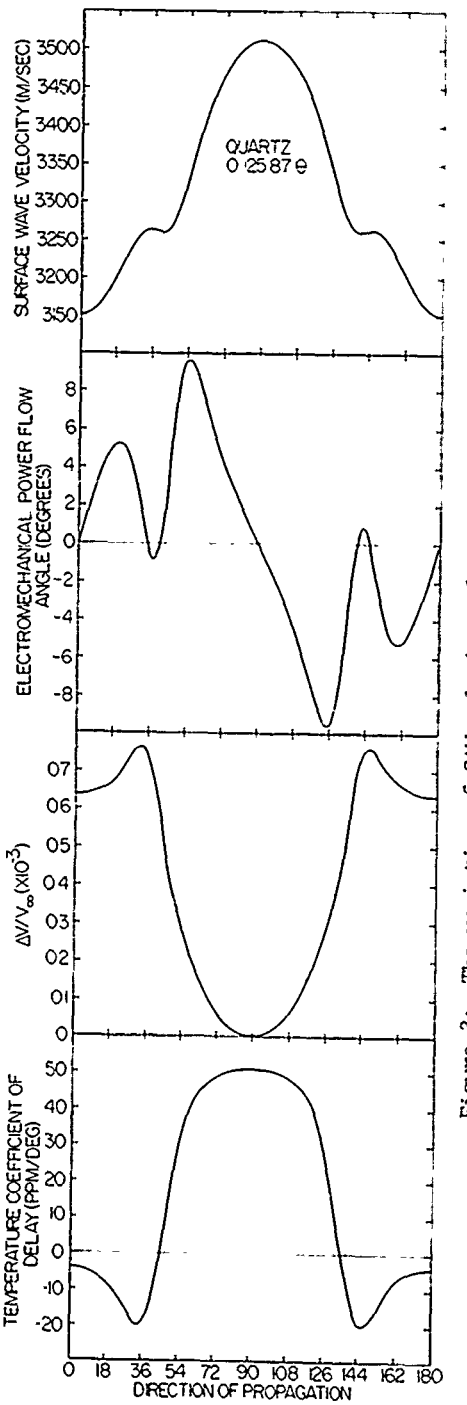

Figure 3: The variation of SAW velocity, electromechanical power flow angle, $\Delta V/V$ piezoelectric coupling constant, and temperature coefficient of time delay (TCD) in the plane of the cut defined by the Euler angles $\lambda = 0.0^{\circ}$ and $\mu = 125.87^{\circ}$. Note that the TCD is zero at $\theta = 45^{\circ}$ and 135°, a pair of orthogonal propagation directions.

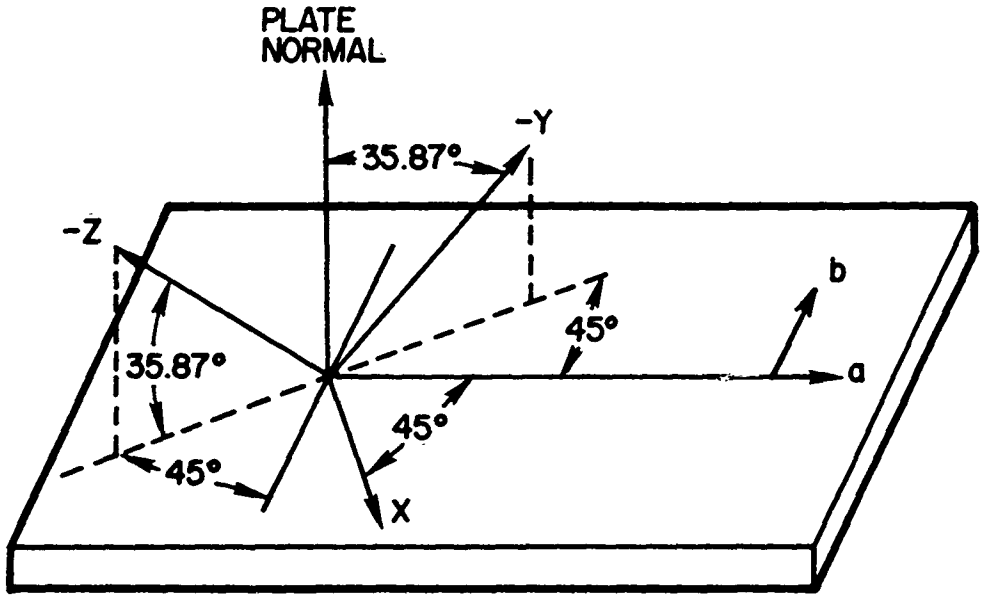

Figure 4: Sketch of the new crystal cut showing the relationship among the XYZ crystal axes, the plate normal, and the primary and secondard propagation directions of a RAC device.

CRYSTAL CUT	EULER ANGLES			TCD	SAW VELOCITY	PIEZOELECTRIC COUPLING ($\Delta V/V$)	POWER FLOW ANGLE (deg)
	λ	μ	θ	(ppm/^{o}C)	(m/sec)	(x10^{-3})	
New RAC Cut	0.0	125.87	45.0	0.0	3267	0.51	+ 3.46
	0.0	125.87	135.0	0.0	3267	0.51	- 3.46
ST-Cut	0.0	132.75	0.0	0.0	3158	0.58	0.0

Table I. Comparison of the SAW properties along the attractive orthogonal directions of the new RAC cut with those of the ST-Cut of quartz.

	Δ TCD (ppm/^{o}C)
$\Delta\lambda = 1^{o}$	-1.3
$\Delta\mu = 1^{o}$	-0.97
$\Delta\theta = 1^{o}$	+3.2

Table II The effect on the TCD of the new cut resulting from a 1^{o} shift in each of the defining Euler angles.

PERFORMANCE RESULTS OF AN OSCILLATOR USING THE SC CUT CRYSTAL

Robert Burgoon and Robert L. Wilson
Hewlett-Packard Company
Santa Clara, Ca.

Summary

An experimental quartz oscillator has been designed to take advantage of the SC cut crystal. The crystal, manufactured by Hewlett-Packard, is a 10 MHz third overtone SC cut used as a single-mode resonator. The crystal temperature is controlled by a single oven and the oscillator is housed in a 5 x 6 x 7 cm package. The design of the experimental oscillator is discussed in another paper entitled "Design Aspects of an Oscillator Using the SC Cut Crystal".

Introduction

The characteristics of the SC cut crystal[1-5] have held great promise for an improved level of oscillator performance. Early tests of the SC cut in modified hp 10544 oscillators gave encouraging results. To further explore the benefits of the SC cut and to test out other oscillator ideas, an experimental oscillator was designed. The performance of this experimental oscillator helped to answer some basic questions regarding the usefulness of the SC cut crystal:

1. The SC cut is relatively insensitive to thermal transient effects. Will the resulting improvement in time domain stability be offset by the increased flicker floor due to the lower crystal Q?

2. Since the SC cut crystal resistance is much higher than that of a BT cut crystal, will crystal drive limitations result in increased phase noise?

3. With thermal transient effects greatly reduced, how fast can an SC cut oscillator be warmed up?

4. What will aging be like?

Warm-Up

Warm-up time is the time span from the application of oscillator power to the point where the oscillator output frequency is stable within a specified relative accuracy. In our data, we have defined warm-up as the time to achieve a frequency accuracy of $\pm 5 \times 10^{-9}$ relative to the oscillator's stabilized frequency 12 hours later. Figure 1 shows a curve of the warm-up time of experimental oscillator #2 versus its warm-up power. For perspective, several data points are plotted for an hp 10544B. The dramatic improvement is largely due to the improved thermal transient characteristics of the SC cut crystal compared to the BT cut used in the hp 10544B.

Warm-up time consists of two stages, cutback time and settling time. Cutback time is the time required to heat the oscillator oven to its required temperature at which time the oven controller reduces (or cuts back) power to the oven. Settling time is the time required for the small temperature changes in the oven to settle out and the crystal and components to recover from the thermal shock. Cutback time is determined by the power applied, the thermal capacitance of the oven, and the thermal insulation around the oven. The cutback time in the experimental oven was reduced about 50% by reducing the thermal capacitance and by increasing the thermal insulation. Also, another difference between the experimental oscillator and the 10544B is in the settling times. Figure 2 shows a warm-up plot for a 10544 with a BT cut crystal (the system resolution of 2×10^{-9} causes the stepped nature of the data. The actual response is quite smooth). Notice how the frequency overshoots considerably before settling down. This is due to the crystal's thermal transient response to the rapid increase in temperature. Increasing the warm-up power increases the frequency overshoot causing even longer settling times. A point is soon reached where the reduction in cutback time is offset by an equal increase in settling time making further improvement in overall warm-up time impossible.

Figure 3 shows the warm-up curve of an early SC cut in a 10544 oscillator (and at a higher warm-up power). Notice the lack of an overshoot. Unlike the hp 10544 with its BT cut crystal, the experimental oscillator's warm-up time may be reasonably approximated by the cutback time for warm-up times greater than 2 minutes. As shown in Figure 1, the actual data flattens out at a minimum time of about 1.8 minutes. The cause for this minimum is not proven, but is believed to be due to thermal effects in the electronics and not the crystal.

Temperature Coefficient

The static temperature coefficient of experimental oscillator #1 is shown in Figure 4 compared to an hp 10544B. The improvement in temperature coefficient is due to the lower crystal temperature

coefficient of the SC cut plus greatly improved oven design. Figure 5 shows the relative temperature coefficients for the AT, BT, and SC cut crystals near their turnover temperatures. The effect of the SC cut is especially dramatic for ovens whose temperature is off more than 0.5° from the crystal turnover temperature.

Normally, oscillator temperature coefficient refers to static temperature coefficient. However, the dynamic or transient effect can be important. Figure 6 is a plot showing the effect of changing the ambient temperature of an experimental oscillator and a 10544B both in the same temperature chamber. The experimental oscillator is the stable trace at the top of Figure 6. Notice the smooth response to temperature change. In contrast, notice the thermal transient overshoot of the 10544B. It nearly spans the full-scale frequency change scale of 1×10^{-8}. Also interesting are the apparent oscillations on the 10544B trace. They are actually the thermal transient response to the small temperature changes in the chamber as the temperature chamber cycles to maintain a fixed temperature. The data in Figure 6 makes clear the dramatic improvement in both static and dynamic temperature response. Of course, slowing down the rate of ambient temperature change will reduce the magnitude of the overshoots.

Low steady-state power consumption in the experimental oscillator was achieved by increasing the thermal insulation and putting the control transistors inside the oven. Figure 7 shows a comparison of the steady-state oven power between experimental oscillator #1 and 10544B. The major difference between the two curves is due to the location of the control transistors. The 10544B uses a resistive winding to heat the oven; the heater winding current is controlled by and passes through a control transistor located outside the oven. This external control transistor causes the nonlinear oven power characteristic as well as high power consumption. The "A" version of the 10544 uses a more power efficient design which keeps power consumption low in the control transistor by switching at 3 KHz. The switching does give spurious frequencies which are unacceptable in some applications. The experimental oscillator combines the best of both characteristics by eliminating the heater winding and using two control transistors to heat the oven with dc current only.

Noise

Oscillator noise may be considered as random and periodic processes and may be viewed in either the time domain or the frequency domain. When viewed from the frequency domain as in a phase noise plot, the continuous random and discrete periodic components are easily separable. In the time domain, as in a plot of the two sample deviation (square root of Allen variance), $\sigma_y(\tau)$, the discrete spurious frequencies are not so easy to separate and are often mistaken for a higher value of random noise. Figure 8 shows the time domain stability plot for oscillator #1 vs #2, showing the combined noise of both, with no two oscillator correction factor applied. Figure 9 compares the experimental oscillator performance with the time domain stability of a 10544B. The upward slope of the 10544B after τ=0.4 seconds shows the effect of the thermal transient sensitivity of the BT cut crystal. Shielding the 10544B from thermal variations by putting it in a box or otherwise protecting it from air currents will reduce the noise in that region. In this same region, the experimental oscillator is quite flat due to the insensitivity of the SC cut crystal to thermal transients. The flat region is the "flicker floor", so called because this power law noise process corresponds to the flicker frequency modulation noise of the frequency domain. The hp 10544B data does not show that flat flicker floor region due to masking by the dominant thermal transient effects. The actual flicker floor lies at or below the 10544B's minimum data point. The experimental oscillators' flicker floor is therefore higher than that of the 10544B. This is not unexpected since the SC cut crystal has a lower Q than the BT. Historically, though, unit to unit variations in flicker floor would not allow any hard conclusions on relative flicker floor levels based on a sample of one comparison.

Figure 10 shows the combined phase noise of experimental oscillator #2 vs. a reference oscillator. (The reference oscillator is a highly modified hp 10544B using a BT cut crystal). Asymptotes were drawn to show the dominant power law noise processes. The asymptotes were then added together to form the smooth curve that runs through the data. The roll-off at 2 Hz is caused by the gain roll-off of the phase noise measurement system. The noise contribution of the reference oscillator is no more than 2 dB from 1 Hz to 10 Hz and above 10 Hz it is less than 1 dB. The measurement system noise contribution is negligible. Its floor is -173 dB, and closer into the carrier the system phase noise is more than 10 dB below the measured data.

Aging

The aging rates of the two experimental oscillators were 2 and 5 parts in 10^{10} per day. Oscillator #1 achieved 2×10^{-10} per day after one week aging and oscillator #2 achieved 5×10^{-10} per day after three weeks of aging.

References

1. J. Kusters and J. Leach, "Further Experimental Data on Stress and Thermal Gradient Compensated Crystals," Proc. IEEE, Vol. 65, pp. 282-284 Feb. 1977

2. A. Ballato, "Doubly Rotated Thickness Mode Plate Vibrators," Physical Acoustics, Vol. XIII, pp 115-181, Academic Press, New York, 1977.

3. J. Kusters, "Transient Thermal Compensation for Quartz Resonators," IEEE Trans. Sonics and Ultrasonics, SU-23, pp. 273-276, July 1976.

4. E. EerNisse, "Quartz Resonator Frequency Shifts Arising from Electrode Stress," in Proc. 29th Annual Symposium on Frequency Control, pp. 1-4, 1975.

5. J. A. Kusters, M. C. Fischer, J. G. Leach, "Dual Mode Operation of Temperature and Stress Compensated Crystals," Proc. 32nd FCS, 1978, pp. 389-397.

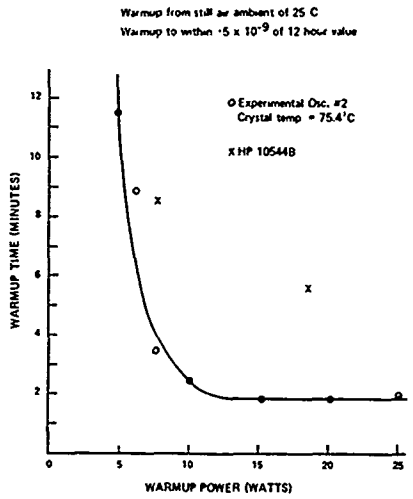

Figure 1. Warmup Time vs Warmup Power for Experimental Oscillator #2

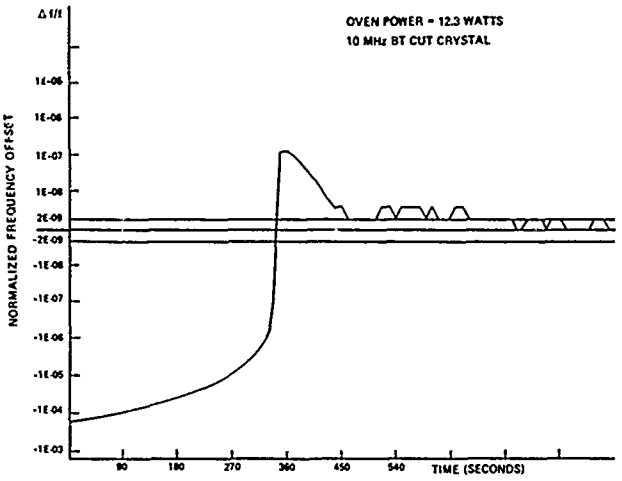

Figure 2. Oscillator Warmup for an HP 10544 Oscillator with BT Cut Crystal

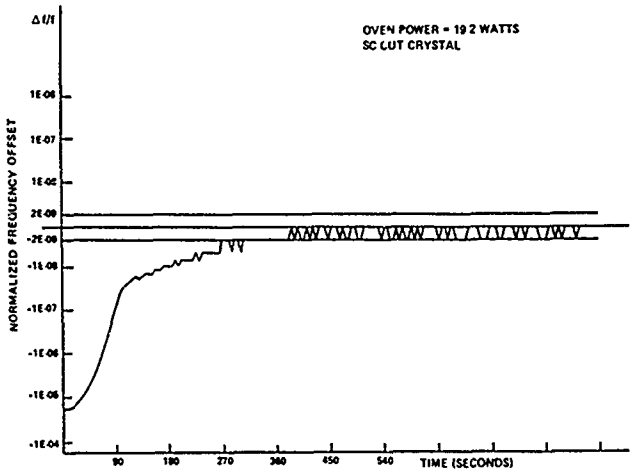

Figure 3. Oscillator Warmup for an HP 10544 Oscillator with SC Cut Crystal

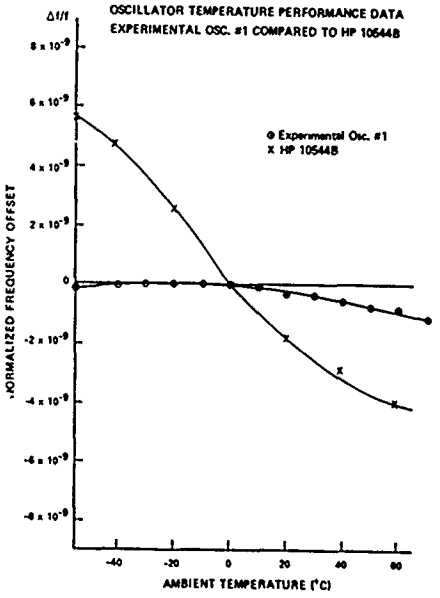

Figure 4. Temperature Performance Data

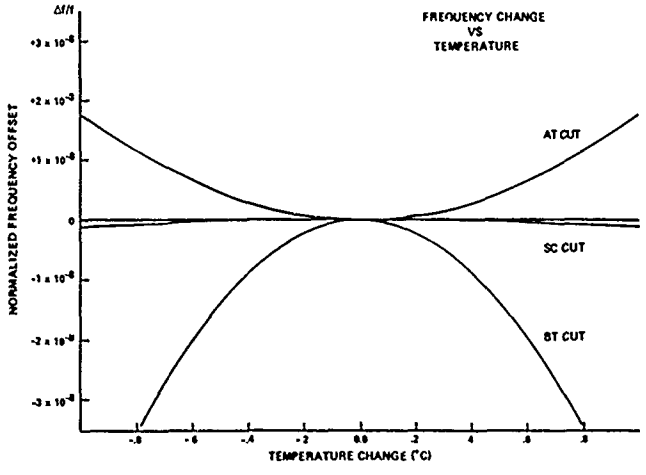

Figure 5. Crystal Temperature Performance Close to the Turnover Temperature

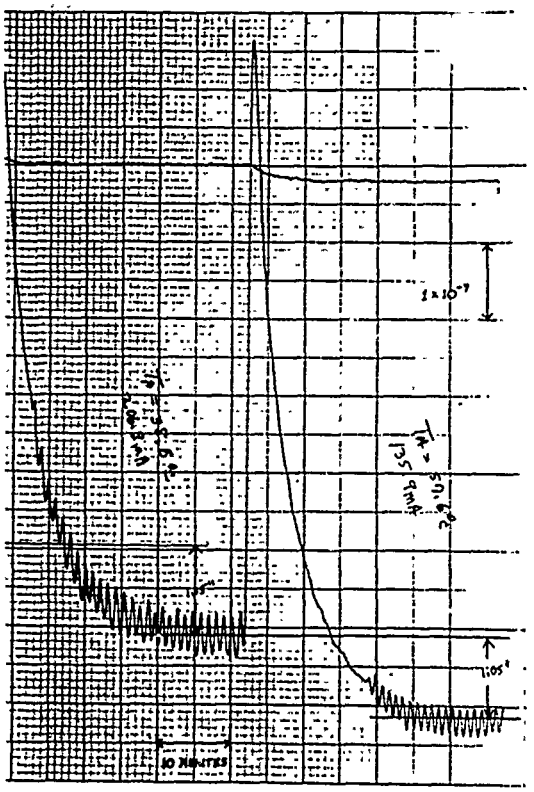

Figure 6.
Temperature Performance Data Showing Transient Overshoots

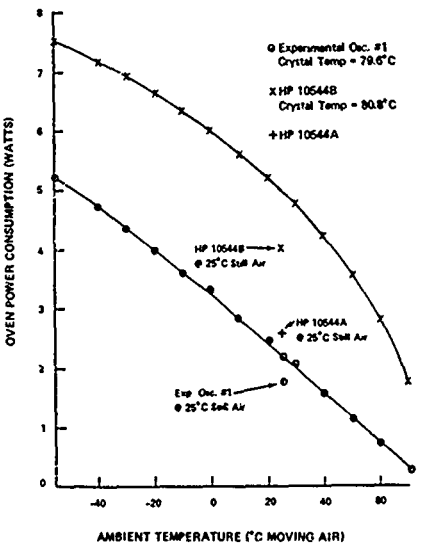

Figure 7. Steady-State Oven Power Consumption vs Ambient Temperature

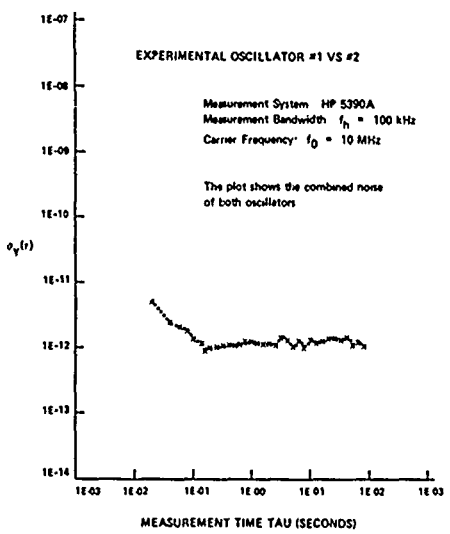

Figure 8. Time Domain Stability of Experimental Oscillator #1 vs #2

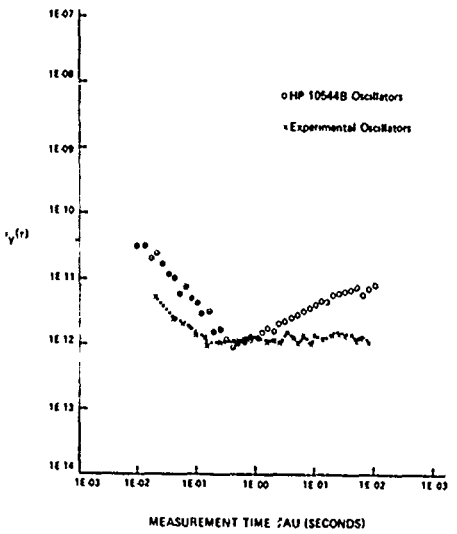

Figure 9. Time Domain Stability Comparison Between HP 10544B and Experimental Oscillators

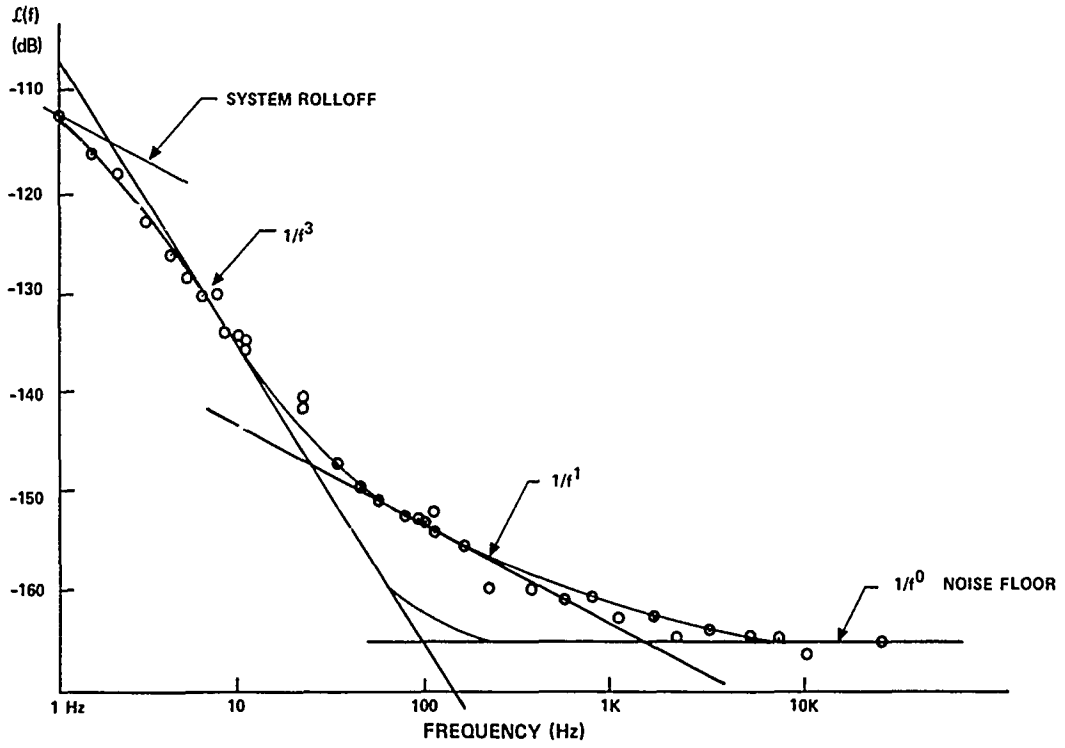

Figure 10. Combined Phase Noise of Experimental Oscillator #2 and Reference Oscillator

DESIGN ASPECTS OF AN OSCILLATOR USING THE SC CUT CRYSTAL

Robert Burgoon and Robert L. Wilson
Hewlett-Packard Company
Santa Clara, Ca.

Summary

An experimental oscillator has been designed to take advantage of the SC cut crystal as well as to improve other areas of oscillator performance relative to the hp 10544 oscillators. The oscillator is a single oven design using a 10 MHz, third overtone SC cut crystal as a single-mode resonator. Performance data is given in the preceding paper entitled "Performance Results of an Oscillator Using the SC Cut Crystal".

Introduction

In recent years there have been a number of papers describing the doubly rotated SC cut crystal and its properties.[1-5] Among these properties are multi-mode capability, low static temperature coefficient, reduced sensitivity to certain mechanical stresses, and insensitivity to thermal transients. This new crystal was the starting point for an experimental oscillator design. The design objective was to use the SC cut to build an experimental 10 MHz high performance component quartz oscillator similar in size and function to the hp 10544 type oscillators.

The multimode capability of the SC cut consists of three thickness modes, A, B, and C, and their overtones. The A mode is of little interest. The B mode has a substantial and approximately linear temperature coefficient while the C mode can have a very low temperature coefficient in the vicinity of a turnover or inflection point. These two shear modes are orthogonal to each other and thus may be run simultaneously and independently. These properties can be used in a "dual mode" oscillator in which the C mode is the reference frequency and the B mode provides temperature information about the quartz crystal itself.[5] However, dual mode operation has the disadvantage of discrete spurious outputs at the B mode frequency. In our case, the 10 MHz C mode is accompanied by a 10.9 MHz B mode and a 900 kHz difference frequency. For this reason it was necessary to suppress the A and B crystal modes and hold the crystal temperature tightly with an oven.

Figure 1 shows a block diagram of the total oscillator. The oscillator loop includes a 10 MHz SC cut crystal which is mode suppressed to allow only C mode operation. The buffer stage transfers the 10 MHz signal to the output stage while isolating the oscillator loop from output effects. The buffer stage also drives the AGC (automatic gain control). The AGC holds the output level constant but more importantly holds crystal current constant to prevent frequency changes due to drive level variations. The oven controller circuitry monitors the temperature of a thermistor embedded in the oven mass, and accurately controls the temperature by applying power to the two heaters. The specific oven temperature depends on the individual crystal and is about 82°C. Because of their power dissipation, the output amplifier and the oven controller are left outside the oven.

Mode Suppression

The SC cut crystal is capable of resonating in many different modes. The crystal we used was cut for a third overtone C mode resonance at 10.0 MHz. The third overtone B mode is above this at 10.9 MHz. Below 10 MHz, the next mode is the fundamental A mode at 7 MHz and further below that, the strong fundamental B and C modes. As with other overtone crystals, the fundamental modes will dominate if they are not suppressed. This leads to the common high pass mode suppression techniques such as low pass traps or tanks. The high pass techniques are not sufficient to suppress any modes above the desired frequency such as the third overtone B mode at 10.9 MHz. One way to implement a bandpass mode suppression is illustrated in Figure 2. The capacitive shunt arms C_2 and C_3 are replaced with parallel and series tank circuits. By properly selecting the component values, the conditions for oscillation will occur over a selected band of frequencies. This frequency band is from ω_p to ω_s, where ω_p is the resonant frequency of the parallel tank circuit and ω_s is the resonant frequency of the series tank circuit. This circuit is described here and shown in Figure 3. At frequencies below ω_p the parallel tank looks inductive and the series tank looks capacitive. With one shunt arm inductive and the other shunt arm capacitive, it is not possible to produce in-phase feedback for oscillation.[6]

At frequencies above ω_s, the result is similar. Here the parallel tank looks capacitive and the series tank looks inductive. Again, no oscillation is possible due to the mixed capacitive and inductive shunt arms. At mid-frequencies (inside the bandpass) the frequency is above the parallel tank resonance and below the series tank resonance. Thus, both shunt arms are capacitive and the circuit is capable of producing the proper phase shift for oscillation. If the crystal has a resonant mode inside the passband and the loop has enough gain, the

circuit will oscillate.

Implementing such a mode suppression is best illustrated by calculating actual circuit values used in an oscillator. For this oscillator the desired oscillation frequency is the third overtone C mode at 10 MHz. The closest interfering modes are the third overtone B mode at 10.9 MHz and the fundamental A mode at 7 MHz. Picking bandpass limits comfortably inside these points gives desired upper and lower frequencies of 10.6 MHz and 8 MHz. Loop gain and sensitivity considerations determine the desired equivalent capacitances of the shunt arms (at the oscillation frequency). For this circuit, they are 60 pF and 4nF for C_2 and C_3 respectively.

where $f_p \simeq 8$ MHz

and $C_2 \simeq 60$ pF at $f_1 = 10$ MHz.

These equations for a parallel tank circuit can be manipulated to solve for L_x and C_x,

$$L_x = \frac{1}{C_2}\left(\frac{1}{\omega_p^2} - \frac{1}{\omega_1^2}\right)$$

$$C_x = C_2 + \frac{1}{\omega_1^2 L_x}$$

Substituting in the above values for f_p and C_2 and solving for L_x gives

ideally, $L_x = 2.37 \times 10^{-6}$ H.

or choosing, $L_x = 2.2$ µH.

therefore sets, $C_x = 180$ pF and $C_2 = 65$ pF

The series tank is calculated in a similar manner

where $f_s = 10.6$ MHz

and $C_3 = 4$nF at $f_1 = 10$ MHz

with $$L_y = \frac{1}{\omega_1^2 \cdot C_3\left(\frac{\omega_s^2}{\omega_1^2} - 1\right)}$$

and $$C_y = \frac{1}{\omega_s^2 \cdot L_y}$$

thus ideally, $L_y = 0.51 \times 10^{-6}$ H.

or choosing, $L_y = 0.47$ µH

therefore sets $C_y = 480$ pF and $C_3 = 4.4$ nF.

The final mode suppression circuit is shown in Figure 4.

For the bandpass mode suppression to work, it is not important which type of tank circuit (series or parallel) replaces C_2 as long as C_3 is replaced by the other type of tank circuit. In fact, the mode suppression may be lumped into only one shunt arm, the other left as a capacitor. Figure 5 shows such an arrangement where the shunt arm appears capacitive only over a band of frequencies. Another arrangement of this one arm technique is shown in Figure 6. Again, these one arm mode suppression networks may be used to replace either C_2 or C_3 as desired.

Phase Noise

When considering the phase noise of an oscillator, it is convenient to consider the total oscillator as being composed of two parts, an oscillating loop section and a buffer amplifier section. If properly designed, the buffer amplifier section contributes only 1/f and white phase noise and the oscillating loop section contributes only $1/f^3$ and $1/f^2$ phase noise processes. It is the filter action of the crystal that provides the extra $1/f^2$ factor for the oscillating loop section.

The method of extracting the signal from the oscillating loop is very important in achieving good phase noise. Since the crystal is a very good filter, the crystal current is a very clean signal. One simple way to cleanly extract the signal is shown in Figure 7 and was used on the hp 10544 oscillator. A capacitor is placed in series with the crystal so that the crystal current flows through the capacitor. The voltage across the capacitor is proportional to the crystal current and is used to drive the buffer amplifier stage. All the oscillator loop noise (except crystal noise) is filtered by the crystal. The output voltage level is proportional to the capacitor impedance and the crystal drive current. For a good signal to noise ratio in the buffer stage, it is desirable to make the loop output voltage large. One way to increase the loop output voltage is to decrease the capacitance. This becomes a problem because as this capacitor approaches the value of the tuning capacitance, it severely restricts tuning range. A compromise is required to balance the tuning range and noise requirements.

In the experimental oscillator, a new approach was taken. The circuit, shown in Figure 8, allows the capacitor to be made small without affecting the tuning. The crystal current is run through a common base stage which in turn feeds the crystal current to the capacitor. The amplifier isolates the capacitor from the tuning circuits since the oscillating loop sees the amplifier as an impedance of $(r_e' + \frac{r_{bb}'}{\beta})$. This is small compared to the crystal resistance and so it does not affect the crystal Q significantly. Since the capacitor is no longer in series with the tuning, it may be made quite low to get a large loop output voltage. The other factor affecting the voltage is the crystal current. A value of 1 mA was chosen giving a crystal dissipation of 50 µW.

Oven Power Consumption

An important oven design requirement was to reduce the normal operating power consumption to below that of the hp 10544B, while still utilizing a linear controller. The 10544B, with a linear controller, requires 4.5 W of oven power in an ambient temperature of 25°C. Because this oven uses a resistive heater, at 25°C, about half of this power is dissipated in the pass transistor located on the outside of the package. This power is effectively wasted. To eliminate this wasted power, the experimental oscillator employs two Darlington transistors as heaters (Figure 9). The heaters Q_1 and Q_2 are bolted to the oven cavity. R_1, a small valued resistor, develops a voltage V_1 which is proportional to the heater current. This voltage is used to limit the warm-up current and provide feedback for the main oven control loop. During warm-up, for $V_{CC} = 20$ V and $I_H = 0.4$A, R_1 dissipates about 1% of the total oven power. While R_1 is not located in the oven cavity, it is on a PC board within the foam insulation and therefore its power is utilized in warming the oven cavity.

The thermal resistance between the oven cavity temperature and the ambient temperature is 25% higher than that in the hp 10544B. This was accomplished by

reducing the physical size of the oven assembly, thus allowing the foam insulation to be slightly thicker. The result of these efforts is an ovenized oscillator that draws less than 2 watts in still air at 25°C.

Warm-Up Time

The warm-up time of the hp 10544B oscillator is limited due to the thermal transient behavior of its BT cut crystal. The warm-up time typically is 10 minutes to 5×10^{-9} of the 12 hour value for V_{CC} = 20V (8 watts). Because the SC cut crystal is much less sensitive to thermal transients, the warm-up time for the experimental oscillator is limited by the most temperature sensitive electronic components and of course, the thermal capacitance of the oven assembly. To minimize total thermal capacitance, and to improve heat transfer to the electronics, the oven assembly was made as compact as possible (see Figures 12, 13). The oven cavity and lids are made of aluminum while the oven cavity in the hp 10544B is made of copper. Aluminum has a lower thermal capacitance per volume than copper by a factor of 0.76. The most temperature sensitive components are located on the two PC boards which are folded into the oven cavity. When the two lids are screwed in place, these components are surrounded by heated aluminum walls.

Because power transistors are used for the heat sources, the input supply voltage and current requirements are flexible. Warm-up current I_H, is set with resistors R_4 and R_5 and, as shown in Figure 9, is independent of V_{CC}. By connecting Point A to V_{CC} instead of V_R, the warm-up current becomes a linear function of V_{CC} and as such, simulates a resistive heater winding. The maximum limit on I_H is determined by the collector current limits on Q_1 and Q_2. Various values of V_{CC} were used between 15V and 35V with no degradation in oven performance. The advantage of all of this is that any combination of V_{CC} and I_H within the above limits can be utilized by this controller so long as the power dissipated in either of Q_1 and Q_2 does not exceed 20 watts. This limit is set by the maximum allowable junction temperature of the heater transistors. The warm-up time to within 5×10^{-9} of the frequency 12 hours after turn-on was measured for the two experimental oscillators. The warm-up power was set at 8.0 watts. The average time was 3.5 minutes which is about 1/3 of that for a typical hp 10544B.

Temperature Coefficient

In an ovenized oscillator, the purpose of the oven is to reduce the effect of ambient temperature fluctuations on the temperature sensitive components in the oscillator. A measure of the ability to do this is termed thermal gain. Thermal gain is defined as the ratio of the change in ambient temperature T_A, divided by the resultant change in temperature of the region in the oven that it is desired to control, T_C. Thermal gain = $\Delta T_{A/\Delta T_C}$. In the experimental oscillator, even though the SC cut crystal has an improved temperature coefficient, it is still 10 times more temperature sensitive than any other component in the oscillator. This means that if all of the components of the oscillator, including the crystal, were to experience the same temperature change, the resultant change in frequency due to the crystal would be 10 times more than that due to any other component. It follows then that the thermal gain to the crystal must be 10 times greater than the thermal gain to the rest of the oscillator electronics for both areas to contribute equally to the oscillator's temperature coefficient.

The temperature coefficient of the crystal varies according to the difference between the actual crystal operating temperature and the turnover temperature of that particular crystal. Turnover temperature is the temperature at which the derivative of crystal frequency with respect to crystal temperature is zero, i.e., $\frac{d\Delta f/f}{dT} = 0$. (See Figure 10.) As will be discussed later, the oven provides a high thermal gain to the crystal. The combination of this high thermal gain and the SC cut crystal's lower sensitivity to temperature allowed the oven temperature to be set merely by installing a fixed resistor. This resistor was chosen individually for each of the two experimental oscillators based on the particular crystal's turnover temperature, T_0. The total tolerance with this process determines how far the oven temperature will be from the crystal's turnover temperature. A worst-case analysis of all the tolerances combined yields a crystal temperature coefficient of $5 \times 10^{-9}/°C$. Since the thermal gain to the crystal (explained below) in the experimental oscillator was greater than 1000, the crystal's maximum contribution to the overall oscillator temperature coefficient was less tnan $5 \times 10^{-12}/°C$.

To achieve a high thermal gain to a particular region in a structure, i.e., the crystal in the oven cavity, two loop gains must be considered; the controller loop gain (partially electrical) and the mechanical gain. The controller loop gain can be defined as the resulting change in heater temperature divided by the change in thermistor temperature assuming it is separate from the heater. This gain can easily be made very large, and in the experimental oscillator is about 10^5. The mechanical gain, like thermal gain, is defined as the change in ambient temperature divided by the resulting change in crystal temperature. The mechanical gain is a function of the thermal properties of the structure, the locations of the two heaters, and the thermistor location. The difference between mechanical gain and thermal gain is as follows: the thermal gain is dependent upon both the controller loop gain and the mechanical gain and can be no larger than the smaller of these two. If it can be assured that the controller loop gain is more than 10 times greater than the desired thermal gain, the resultant thermal gain approximately equals the mechanical gain. This is the case in the experimental oscillator since the controller loop gain was designed to be 100 times the desired minimum thermal gain of 1000. Therefore, with the controller defined, it then was necessary to locate the heaters, thermistor and crystal such that the mechanical gain to the crystal, $\Delta T_{ambient}/\Delta T_{crystal}$, would be greater than 1000.

Normally, when one heater winding is the only source of heat for an oven, the crystal and thermistor must mechanically be rearranged on a trial and error basis until the desirable mechanical gain is obtained. And, if later on in the design a mechanical change occurs, this may change the thermal behavior of the oven enough that the above process would have to be repeated. With two heaters, adjusting the ratio of the power dissipated in each heater transistor achieves the same result that physically moving the thermistor or crystal achieves. With the first experimental oscillator, several trials were required initially to locate the thermistor, crystal, and heaters. After that, it took several hours to "fine tune" the oven to a thermal gain of ≈ -10,000. This fine tuning was accomplished by adjusting the ratio of resistors R_2 and R_3 (Figure 9). Later, when the second oscillator was constructed using a mechanical design identical to #1, the same ratio of R_2 to R_3 was used. No further attempts were made to optimize the thermal gain

of the second oven. The thermal gain to the crystal was measured to be ≈ -3,000.

Mechanical Aspects

A combination rigid-flexible printed circuit board concept was implemented in the experimental oscillators to evaluate its potential for future oscillator development. (Figure 11). The printed circuit board is constructed of a flexible 5 layered Kapton and copper laminate, cemented to a standard G10 fiberglass stiffener. The stiffener is only required for mechanical support since all traces and pads are contained in the flexible laminate. Since the stiffener boards are initially part of a single large sheet, it is possible to leave small, cut-away tabs temporarily connecting the individual boards to the remaining support board. Later on, these tabs are cut with a pair of side cutters to release the boards. While still connected to the support board, the individual boards were loaded with components and wave-soldered in the conventional manner.

During the assembly procedure, no hand wiring was required to interconnect any of the 4 rigid boards. The edge connector, the oven controller board, and the two ovenized boards all are inherently interconnected with this rigid-flexible printed circuit board concept. No appreciable problems were encountered with the rigid-flex concept suggesting that high performance oscillator development may be a viable application of this new technology.

References

1. J. Kusters and J. Leach, "Further Experimental Data on Stress and Thermal Gradient Compensated Crystals," Proc. IEEE, Vol. 65, pp. 282-284 Feb. 1977.
2. A. Ballato, "Doubly Rotated Thickness Mode Plate Vibrators," Physical Acoustics, Vol. XIII, pp. 115-181, Academic Press, New York, 1977.
3. J. Kusters, "Transient Thermal Compensation for Quartz Resonators," "IEEE Trans. Sonics and Ultrasonics, SU-23, pp. 273-276, July 1976.
4. E. EerNisse, "Quartz Resonator Frequency Shifts Arising from Electrode Stress," in Proc. 29th Annual Symposium on Frequency Control, pp. 1-4, 1975.
5. J. A. Kusters, M. C. Fischer, J. G. Leach, "Dual Mode Operation of Temperature and Stress Compensated Crystals", Proc. 32nd FCS, 1978, pp.389-397.
6. Marvin E. Frerking, Crystal Oscillator Design and Temperature Compensation, New York, Van Nostrand Reinhold Co., 1978, pg. 70.

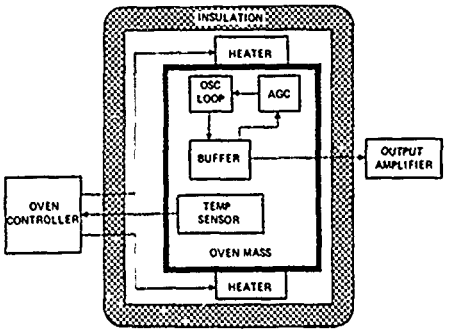

Figure 1. Oscillator Block Diagram

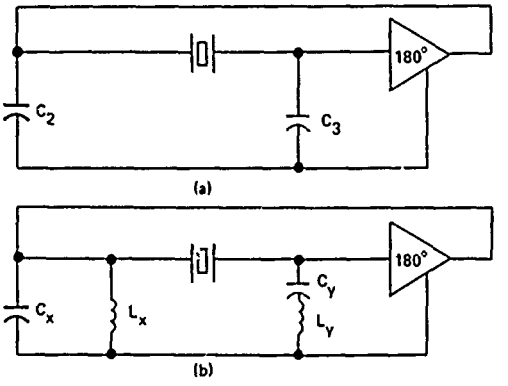

Figure 2. (a) Standard Colpitts Type Oscillator and
(b) The Same Oscillator with Two Arm Mode Suppression

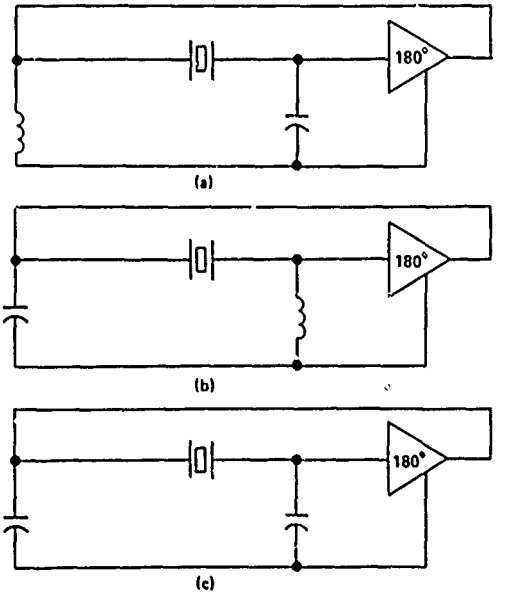

Figure 3. (a) Low Frequency, (b) High Frequency, and (c) Passband Frequency Equivalents for the Mode Suppression Circuit of Figure 2b.

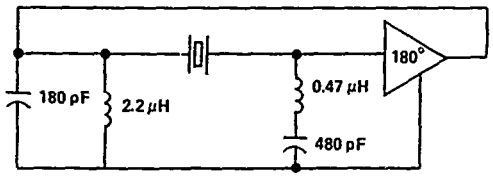

Figure 4. Mode Suppression Circuit to Resonate 10 MHz While Avoiding Resonances at 7 MHz and 10.9 MHz

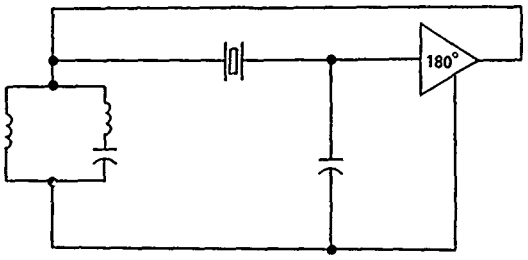

Figure 5. A One Arm Mode Suppression Circuit

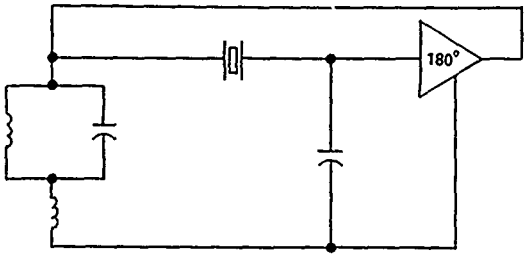

Figure 6. Another One Arm Mode Suppression Circuit

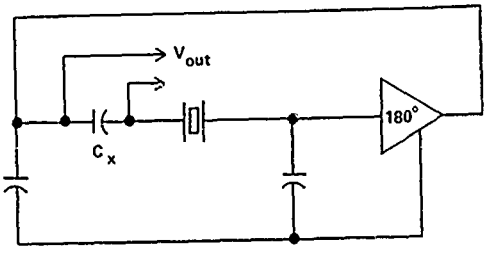

Figure 7. Loop Signal Extraction Used in the HP 10544 Oscillators

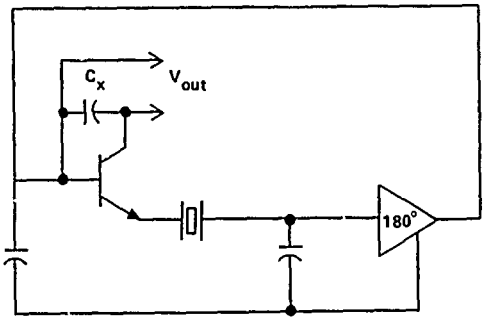

Figure 8. Improved Loop Signal Extraction

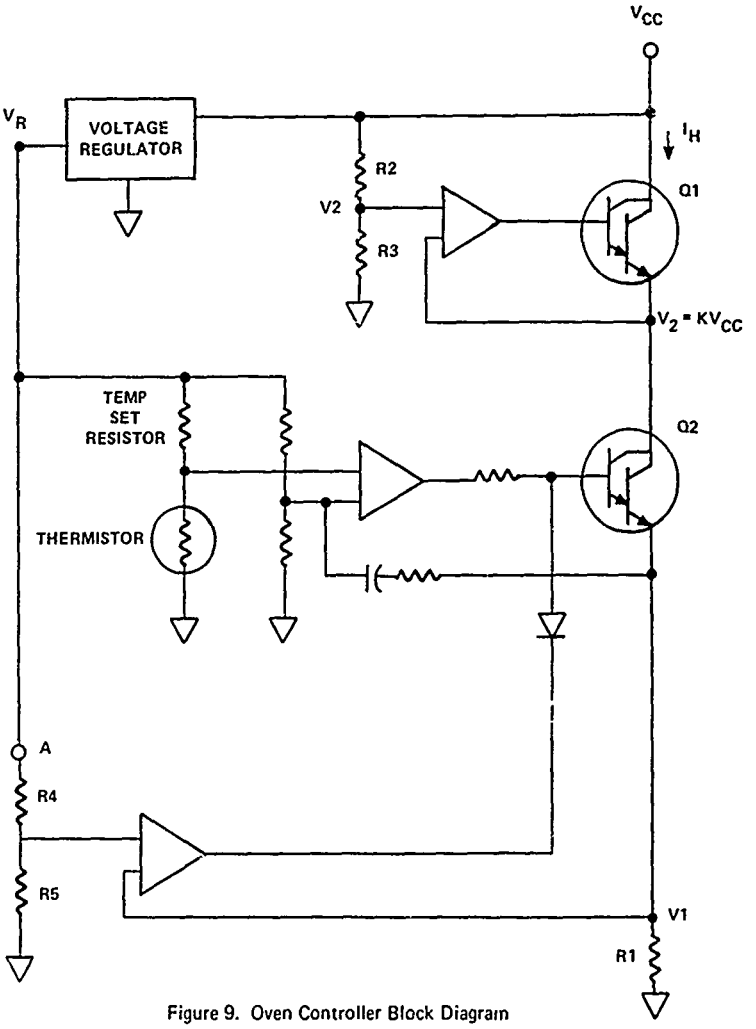

Figure 9. Oven Controller Block Diagram

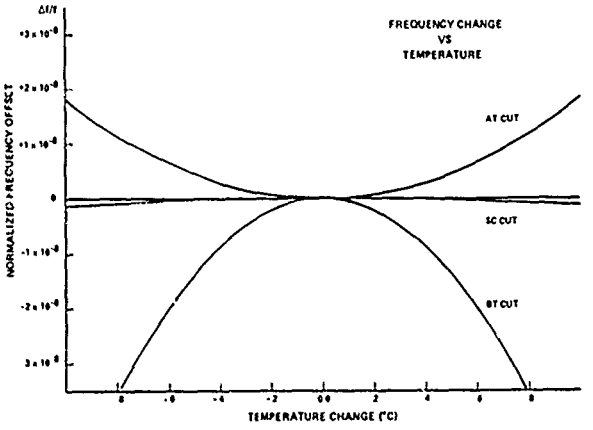

Figure 10. Crystal Temperature Performance Close to the Turnover Temperature

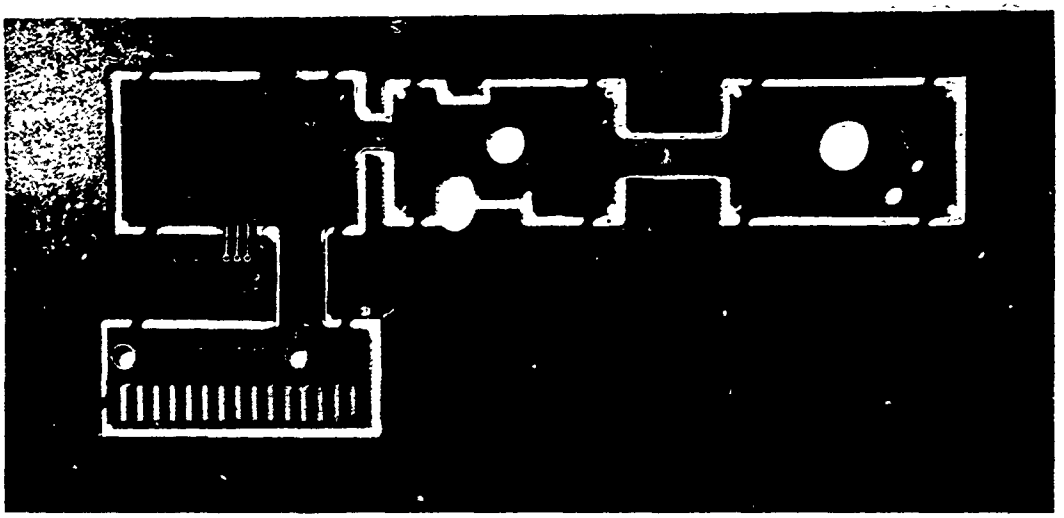

Figure 11. Rigid-Flexible Printed Circuit Board

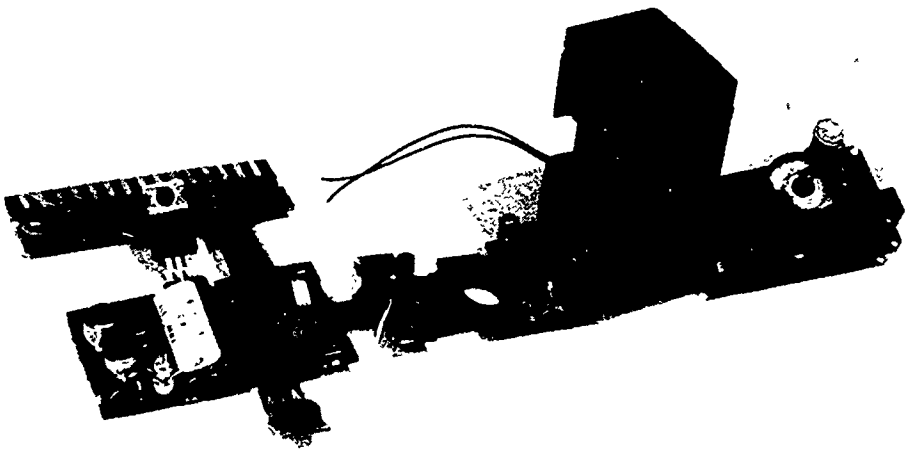

Figure 12. Mechanical Detail of Experimental Oscillator

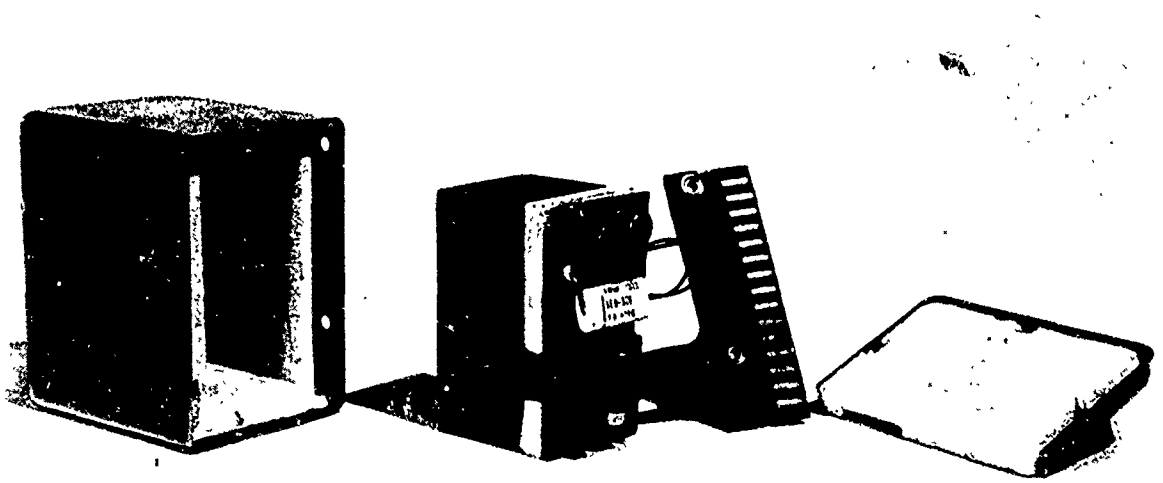

Figure 13. Mechanical Detail of Experimental Oscillator

AN ANALYSIS OF UNWANTED FREQUENCY OSCILLATION IN A CRYSTAL CONTROLLED OSCILLATOR

Shigenori Kodama and Yoshikatsu Sato

Transmission Division, Nippon Electric Company, Ltd.
Kawasaki City, 211 Japan

Summary

In a crystal oscillator, a condition is analyzed that wanted frequency oscillation is caused to occur but unwanted frequency oscillation is suppressed.

In this analysis, nonlinear differential equations are set up from an oscillator equivalent circuit, taken account of wanted and unwanted frequencies. And the stationary solution is obtained from these equations.

From this stationary solution, it is shown that wanted frequency oscillation and unwanted one occur respectively in accordance with oscillator condition. And the condition for only the wanted frequency oscillation is obtained.

Furthermore, this analysis is experimentally proved to be valid by measuring oscillator loop gain depending on the signal amplitude in the case that the wanted signal and the unwanted one coexist in the circuit, and by observing the oscillating amplitude transient phenomena under various oscillator conditions.

Introduction

A quartz crystal resonator has an infinite number of vibration modes because it is a distributed vibrating system. Hence it is important in the design of a crystal oscillator to select one and only mode for oscillation and to suppress all other unwanted modes.

Useful means to suppress unwanted oscillation have been to reduce the loop gain of an oscillator circuit for unwanted modes and to increase equivalent resistances of unwanted modes. These are not quite enough to suppress an unwanted oscillation, when the unwanted mode is located in a close neighbourhood of the wanted mode. This is especially true for simple oscillator circuits without any special automatic gain control (AGC).

This paper presents an analysis of a crystal oscillator which has two closely located modes of vibration. Curves which satisfy the condition of unity loop gain for each mode are obtained as functions of the amplitude level of another mode. An unwanted oscillation is likely to occur when the curves cross each other.

Experiments show a good agreement with results of the analysis. A method for measuring loop gain is developed when signals of two different frequencies coexist. This method has been found to be a convenient way to select oscillator circuits as well as crystal resonators which have enough margin for suppressing unwanted oscillation.

Analysis

Stationary Solution of Oscillation Amplitude

A Colpitts type crystal oscillator shown in Fig. 1 is analyzed. Its characteristics can be represented by the equivalent circuit shown in Fig. 2.

Two closely located modes of vibration are represented by two resonant circuits, (L_1, C_1, R_1) and (L_2, C_2, R_2). Only the nonlinearity of an amplifier is taken into account. The nonlinearity of all other components including the crystal resonator is neglected.

The nonlinear amplitude dependence of the amplifier can be well approximated by the following equation. Here the input current is expanded in terms of odd powers of the output current.

$$i\ell = -\sum_{n=0}^{\infty} a_{2n+1} \cdot i^{2n+1}$$

The inverse function is expressed as

$$i = f(i\ell)$$

From the equivalent circuit in Fig. 2, the following equations are obtained.

$$L_1 i_1'' + R_1 i_1' + \frac{1}{C_1} i_1 = \frac{1}{C0} i0 \qquad (3)$$

$$L_2 i_2'' + R_2 i_2' + \frac{1}{C_2} i_2 = \frac{1}{C0} i0 \qquad (4)$$

$$ia = i - (i_1 + i_2 + i_0) \qquad (5)$$

$$ib = i_1 + i_2 + i_0 - i\ell \qquad (6)$$

$$ib = Cb\, R\ell\, i\ell \qquad (7)$$

$$\frac{1}{Ca} ia = \frac{1}{Cb} ib + \frac{1}{C0} i0 \qquad (8)$$

$$i = f(i\ell) \qquad (2)$$

The eliminating of i_a, i_b and i_o yields the following equations.

$$i_1'' + \alpha_1 i_1' + \omega_1^2 i_1 + \nu_1^2 i_2 - u_1^2(i+k_3 i_\ell) = 0 \quad (9)$$

$$i_2'' + \alpha_2 i_2' + \omega_2^2 i_2 + \nu_2^2 i_1 - u_2^2(i+k_3 i_\ell) = 0 \quad (10)$$

$$k_1(-\tau_\ell i_\ell' + i_\ell) - (i_1+i_2) - k_2(i+k_3 i_\ell) = 0 \quad (11)$$

where,

$$\left.\begin{aligned} &\alpha_i = \frac{R_i}{L_i},\ \omega_i^2 = \frac{1}{C_i L_i} - \nu_i^2, \\ &\nu_i^2 = \frac{1}{L_i(C_0+C_L)},\ u_i^2 = \frac{C_L}{C_a}\nu_i^2 \\ &k_1 = 1 + \frac{C_0}{C_L},\ k_2 = \frac{C_0}{C_a},\ k_3 = \frac{C_a}{C_b} \\ &\tau_\ell = R_\ell C_b,\ \frac{1}{C_L} = \frac{1}{C_a} + \frac{1}{C_b} \quad (i = 1, 2) \end{aligned}\right\} \quad (12)$$

A stationary solution is obtained by assuming only two frequency components in i, i_1 and i_2 as follows;

$$i = I_1 \sin(x_1 t+\theta_1) + I_2 \sin(x_2 t+\theta_2) \quad (13)$$

$$i_1 = I_{11} \sin(x_1 t+\theta_1+\varphi_{11}) + I_{12}(x_2 t+\theta_2+\varphi_{12}) \quad (14)$$

$$i_2 = I_{21} \sin(x_1 t+\theta_1+\varphi_{21}) + I_{22}(x_2 t+\theta_2+\varphi_{22}) \quad (15)$$

The substitution of Eq. (13) into Eq. (1) yields two frequency components of i_ℓ;

$$i_\ell \doteq -\sum_{n=0}^{\infty}\sum_{p=0}^{n} a_{2n+1}(I_1^2)^{n-p}(I_2^2)^p \{K_{1p} I_1 \sin(x_1 t+\theta_1) + K_{2p} I_2 \sin(x_2 t+\theta_2)\} \quad (16)$$

where,

$$\left.\begin{aligned} K_{1p} &= \frac{1}{2^{2n}} \cdot {}_{2n+1}C_{2p} \cdot 2(n-p) + 1 \, {}_{n-p}C_{2p} \\ K_{2p} &= \frac{1}{2^{2n}} \cdot {}_{2n+1}C_{2p+1} \cdot 2(n-p) \, {}_{n-p}C_{2p+1} \end{aligned}\right\} \quad (17)$$

These equations show that the amplitude of each component depends on the amplitude of another component.

The nonlinear differential equations Eqs. (2), (9), (10), (11) and (12) are transformed to algebraic equations by approximating of the nonlinearity (Eq. (1)) and assuming the stationary solution (Eqs. (13) ∿ (15)). These algebraic equations are rearranged concerning the stationary amplitude of the amplifier output current (I_1, I_2), as follows;

$$[C_L F_j + k_2 C_a \Delta_j - \{k_3 C_L F_j - (k_1 - k_2 k_3) C_a \Delta_j\} N_{jn}] I_j = 0 \quad (j=1,2) \quad (18)$$

$$[C_L H_j - (k_3 C_L H_j + k_1 \tau_\ell C_a x_j \Delta_j) N_{jn}] I_j = 0 \quad (j=1,2) \quad (19)$$

where,

$$\left.\begin{aligned} &F_j = \nu^4\{2(\nu^4 + \gamma_{1j}\gamma_{2j} - \beta_{1j}\beta_{2j}) - \nu_1^2\beta_{2j} - \nu_2^2\beta_{1j} \\ &\quad + \nu_1^2\beta_{1j}(\beta_2^2{}_j + \gamma_2^2{}_j) + \nu_2^2\beta_{2j}(\beta_1^2{}_j + \gamma_1^2{}_j) \\ &H_j = \nu_1^2\gamma_{1j}(\beta_2^2{}_j + \gamma_2^2{}_j) + \nu_2^2\gamma_{2j}(\beta_1^2{}_j + \gamma_1^2{}_j) \\ &\quad - \nu^4\{2\gamma_{1j}\beta_{2j} + 2\gamma_{2j}\beta_{1j} - \nu_1^2\gamma_{2j} - \nu_2^2\gamma_{1j}\} \\ &A_j = (\beta_1^2{}_j + \gamma_1^2{}_j)(\beta_2^2{}_j + \gamma_2^2{}_j) + 2\nu^4(\gamma_{1j}\gamma_{2j} \\ &\quad - \beta_{1j}\beta_{2j}) + \nu^8 \\ &\beta_{ij} = \omega_i^2 - x_j^2,\ \gamma_{ij} = \alpha_i x_j,\ \nu^4 = \nu_1^2\,\nu_2^2 \\ &N_{jn} = \sum_{n=1}^{\infty}\sum_{p=0}^{n} a_{2n+1}(I_1^2)^{n-p}(I_2^2)^p K_{jp} \\ &\qquad\qquad (i \text{ or } j = 1,2) \end{aligned}\right\} \quad (20)$$

Since a crystal resonator has a high Q value generally, the following equations are obtained from Eqs. (18) ∿ (20) concerning oscillation frequencies and oscillation amplitudes.

Frequency:
$$X^2{}_j \doteq \frac{\omega_1^2+\omega_2^2 \pm \sqrt{(\omega_1^2-\omega_2^2)^2+4\nu^4}}{2} \doteq \omega_1^2,\ \omega_2^2 \quad (j=1,2) \quad (21)$$

Amplitude:
$$I_j\left[A_j - \sum_{n=1}^{\infty}\sum_{p=1}^{n} a_{2n+1}K_{jp}(I_1^2)^{n-p}(I_2^2)^p\right] = 0 \quad (22)$$

where,

$$A_j = \frac{1}{k_3 + k_1{}^2 C_a C_b \omega^2 j R_L R_j} - a_1 \quad (j=1,2) \quad (23)$$

The solutions (I_1, I_2) of Eq. (22) are stationary oscillation amplitudes of the wanted frequency ω_1 component and the unwanted frequency ω_2, respectively.

These solutions (I_1, I_2) are given by the four solution pairs ([a] ∿ [d]) as follows.

Solution [a]:

$$A_1 - \sum_{n=1}^{\infty}\sum_{p=0}^{n} a_{2n+1}K_{1p}(I_1^2)^{n-p}(I_2^2)^p = 0 \quad (24)$$

$$I_2 = 0 \quad (25)$$

Solution [b]:

$$I_1 = 0 \quad (26)$$

$$A_2 - \sum_{n=1}^{\infty}\sum_{p=0}^{n} a_{2n+1}K_{2p}(I_1^2)^{n-p}(I_2^2)^p = 0 \quad (27)$$

Solution [c]:

$$I_1 = 0 \quad (28)$$

$$I_2 = 0 \quad (29)$$

Solution [d]:

$$A_1 - \sum_{n=1}^{\infty}\sum_{p=0}^{n} a_{2n+1}K_{1p}(I_1^2)^{n-p}(I_2^2)^p = 0 \quad (30)$$

$$A_2 - \sum_{n=1}^{\infty}\sum_{p=0}^{n} a_{2n+1}K_{2p}(I_1^2)^{n-p}(I_2^2)^p = 0 \quad (31)$$

Moreover, these solutions are shown in the coordinates of I_1 and I_2, as in Fig. 3 (a) or (b). In this figure, the curves I , II , III and IV show the equations (30), (31), (29) and (28), respectively.

Oscillation Amplitude Condition

In the case that a wanted frequency ω_1 signal and an unwanted frequency ω_2 coexist in an oscillator circuit, oscillator loop gain concerning each frequency signal is analyzed as follows.

$$G_1 = \frac{A_1 + a_1}{a_1 + \sum_{n=1}^{\infty} \sum_{p=0}^{n} a_{2n+1} (I_1^2)^{n-p} (I_2^2)^p Z_{1p}} \quad (32)$$

$$G_2 = \frac{A_2 + a_1}{a_1 + \sum_{n=1}^{\infty} \sum_{p=0}^{n} a_{2n+1} (I_1^2)^{n-p} (I_2^2)^p Z_{2p}} \quad (33)$$

Where, G_1 is the loop gain at the frequency ω_1 and G_2 at the frequency ω_2. Z_{1p}, Z_{2p}, A_1 and A_2 are shown by Eqs. (17) and (23).

When G_1 or G_2 is equal to 1, it corresponds with Eq. (30) or (31), respectively. Therefore the curve [I] or [II] satisfies the condition that the loop gain at the frequency ω_1 or ω_2 is equal to 1, respectively. And the inner region of each curve satisfies the condition that the loop gain is larger than 1, and the outer region, smaller than 1.

In this analysis, the condition is named "Oscillation Amplitude Condition" that the signal amplitude satisfies the unity loop gain, like curve [I] or [II] of Fig. 3 and Eq. (30) or (31).

When the loop gain is larger than 1, the oscillation amplitude increases. If smaller than 1, it decreases. Accordingly, solutions [a] and [b] are stable and solutions [c] and [d] are instable. And it depends on the oscillation starting condition, which of these two solutions [a] and [b] becomes steady state.

Therefore, to ensure that only the wanted frequency ω_1 oscillation occurs, curve [I] must cover curve [II] completely as Fig. 3 (b). This condition is obtained by comparing the amplifier output current I_2 of curve [I] with one of curve [II], when I_1 is equal to zero.
In the case that the term of 2n+1 order nonlinearity is dominant, the condition for causing only the wanted frequency oscillation is as the next equation.

$$A_1 > (n+1)A_2 \quad (34)$$

This equation is transformed to Eq. (35) by Eqs. (12) and (23).

$$\frac{1}{\frac{Ca}{Cb} + (1+\frac{Co}{C_L})^2 CaCb\omega_1^2 R_1 R_\ell} > \frac{n+1}{\frac{Ca}{Cb} + (1+\frac{Co}{C_L})^2 CaCb\omega_2^2 R_2 R_\ell} - na_1 \quad (35)$$

Furthermore, when $C_L \gg Co$ and $Ca=Cb$, this equation is transformed as follows.

$$\frac{(1+na_1)Y_2^2}{R_1} - \frac{(n+1-na_1)Y_1^2}{R_2} + na_1 Y_1^2 Y_2^2 R_\ell - \frac{n(1-a_1)}{R_\ell R_1 R_2} > 0 \quad (36)$$

where,

$$Y_1^2 = \omega_1^2 CaCb, \quad Y_2^2 = \omega_2^2 CaCb \quad (37)$$

As known above, in order to cause only the wanted frequency oscillation without fail, not only crystal resonator equivalent resistance, but various other oscillator parameters such as amplifier gain and amplifier nonlinearity should be taken into account.
The condition required for the crystal resonator equivalent resistances can be calculated by Eq. (36), and illustrated as in Fig. 4.

Experiment

Experimental Oscillator Circuit

The experimental crystal oscillator circuit is shown in Fig. 5. The amplifier circuit characteristic is obtained by the measurement circuit as in Fig. 6, and the result is shown in Fig. 7. From this measurement result, the constant a_{2n+1} of the oscillator amplifier nonlinearity (Eq. (1)) is obtained by converting voltage into current through the amplifier input impedance and its load impedance. The parameters of two oscillator circuit (OSC1, OSC2) are shown in Table 1.

The Oscillation Amplitude Condition concerning I_1 and I_2 is calculated by substituting these parameters into Eqs. (30) and (31). These Oscillation Amplitude Conditions are converted concerning amplifier input voltage by Eq. (16) and the amplifier input impedance. The converted Oscillation Amplitude Condition is shown in Fig. 8. Fig. 8 (a) shows that, in OSC1, both wanted frequency oscillation and unwanted frequency oscillation occur and become steady, respectively. Fig. 8 (b) shows that, in OSC2, only the wanted frequency oscillation becomes steady.

Experimental Results

These analyses are experimentally proved to be valid through the following measurement and observation.

Oscillator Loop Gain

Oscillator loop gain is measured by the measurement circuit shown in Fig. 9. The oscillation loop is opened at the input part of the amplifier circuit. Both a wanted frequency ω_1 signal and an unwanted frequency ω_2 are applied to the opened amplifier input terminal at the same time, and at the other opened terminal, the same impedance ($R\ell$) as the amplifier input one is loaded. And both amplitudes are measured that satisfy the condition of unity loop gain at the frequency ω_1 or ω_2. Namely, the Oscillation Amplitude Condition is experimentally obtained. As the results, the measurement values show a good agreement with calculated values. They are shown in Fig. 10.

Oscillation Level Locus

Transient phenomena are observed by using the measurement circuit of Fig. 11, in order to make sure that the steady state of oscillation level depends on the oscillation starting condition.

Various oscillation starting conditions are established by exciting the crystal resonator previously through the synthesizer. And the transient phenomena are observed concerning the unwanted frequency amplitude as well as the wanted frequency amplitude. Photo. 1 shows the transient oscillation level obtained by the Oscilloscope. Fig. 12 shows the oscillation level locus obtained by the X-Y recorder.

After all, it depends on the oscillation starting condition, which of the wanted frequency level and the unwanted frequency becomes steady. Maximum values of the oscillation level locus nearly show a good agreement with the Oscillation Amplitude Condition curves.

Measurement of Wanted Frequency Oscillation Condition

To make sure the condition (Eq. (34)) for only the wanted frequency oscillation, the oscillation steady states for various oscillator conditions are observed by using the measurement circuit of Fig. 11.

The measurement result is shown in Fig. 13. In this figure, the circle marks denote that the wanted frequency oscillation is stationary, and the cross marks denote that both wanted frequency oscillation and unwanted frequency are stationary, respectively.

These results mean that only the wanted frequency oscillation is stationary when Eq. (34) is satisfied, and the availability of the theoretical result is assured.

OSC1 uses a crystal resonator whose equivalent resistance at the unwanted frequency is smaller than that at the wanted one. In such type of oscillator, conventionally it was very difficult to oscillate only the wanted frequency. From the result of this analysis, the design method is given by which even this kind of oscillator is caused to occur only the wanted frequency oscillation.
For example, OSC1 can be activated to cause only the wanted frequency oscillation by setting up the terminating capacitor Cb more than 390 pF.

Conclusions

The condition required for causing only the wanted frequency oscillation is obtained by analyzing the nonlinear differential equations and the oscillator loop gain under the oscillator equivalent circuit with its amplifier nonlinearity.

And the availability of this analysis is assured by measuring the oscillator loop gain and by observing the transient phenomena of the oscillation level.

Since the condition for suppressing the unwanted oscillation, obtained through this analysis, is available even when the crystal equivalent resistance at the wanted frequency is near to that at the unwanted, it is widely applicable in designing crystal oscillators.

Various measurement and observation methods developed for experimentally proving this analysis are also applicable to the confirmation test, whether or not oscillator circuits have enough margin for suppressing unwanted oscillation, and contribute to the quality improvement of manufactured oscillators.

Acknowledgements

We are deeply indebted to many persons in the process of the analysis, and wish to express our thanks to professor Morio Onoe, Institute of Industrial Science University of Tokyo, for helpful advices. We would also like to express our appreciation to Mr. Tasuku Yuuki, Manager, and Mr. Hisashi Uchida, Section Chief, of Transmission Division, for helpful and valuable discussions.

References

1. Van Der Pol, "The Nonlinear Theory of Electric Oscillators", Proceedings of the I.R.E., Volume 22, No. 9, September 1934.

2. W.P. Mason, "Physical Acoustics", Volume 1, Part A, Academic Press, 1964.

3. Morio Onoe, "Analysis and Detection of Unwanted Modes in Quarz Crystal Units for Oscillator", Journal of the I.E.C.E., Japan, No. 3677, 1959.

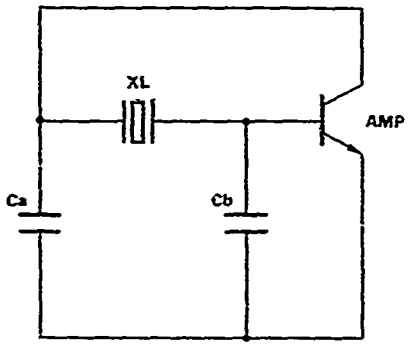

Fig. 1 Crystal Oscillator Circuit

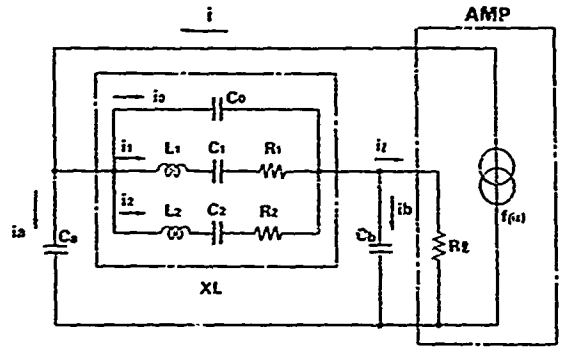

Fig. 2 Equivalent Circuit of Crystal Oscillator

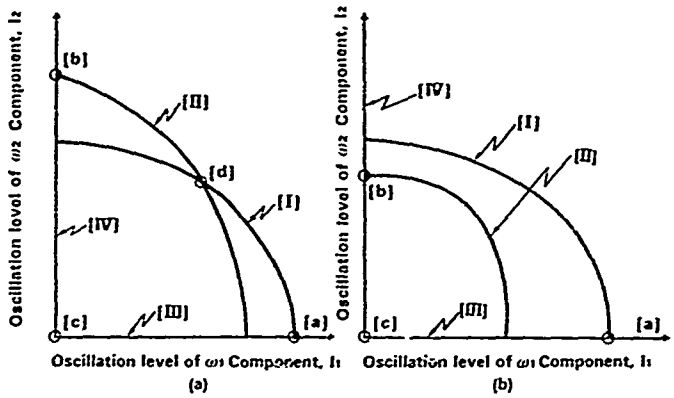

Fig. 3 Oscillation Amplitude Condition Chart

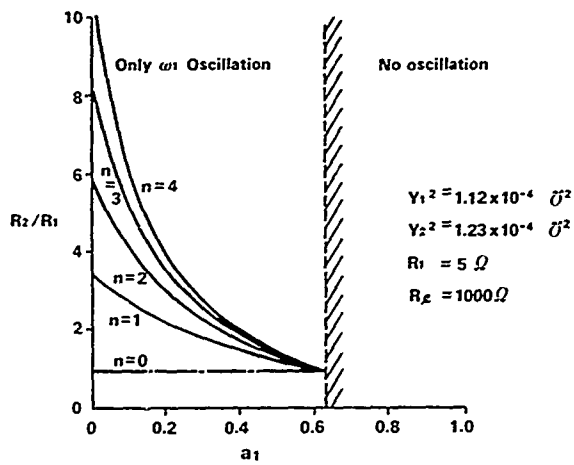

Fig. 4 R_2/R_1 Ratio for Only a Wanted Frequency Oscillation (ω_1)

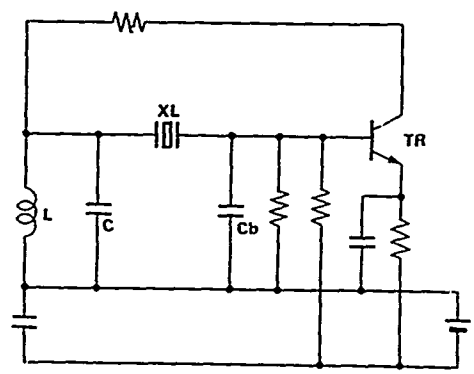

Fig. 5 Experimental Crystal Oscillator Circuit

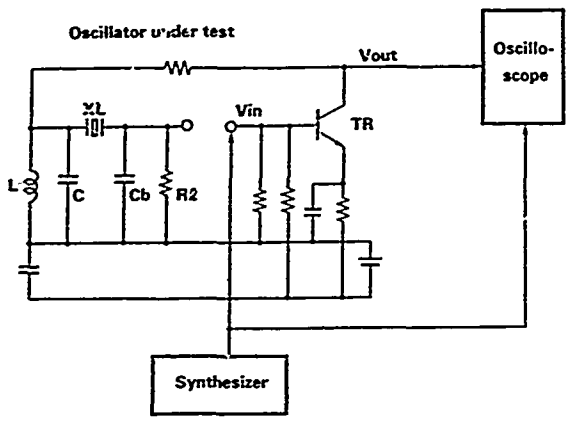

Fig. 6 Amplifier Characteristic Measurement Circuit

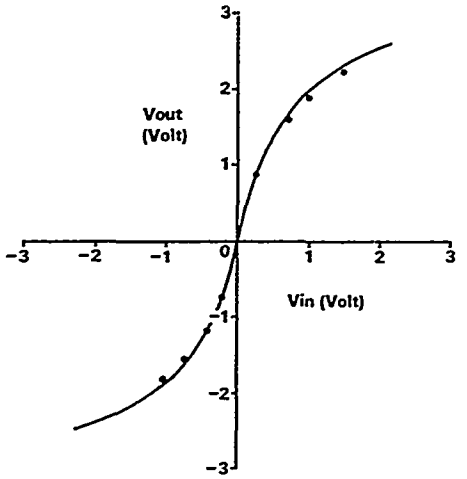

Fig. 7 Amplifier Characteristic

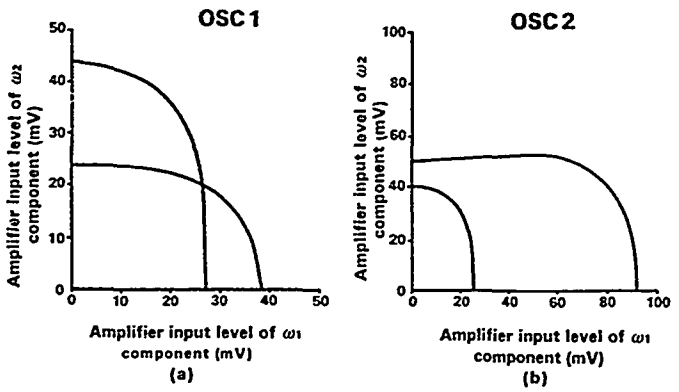

Fig. 8 Calculated Results of Oscillation Amplitude Condition

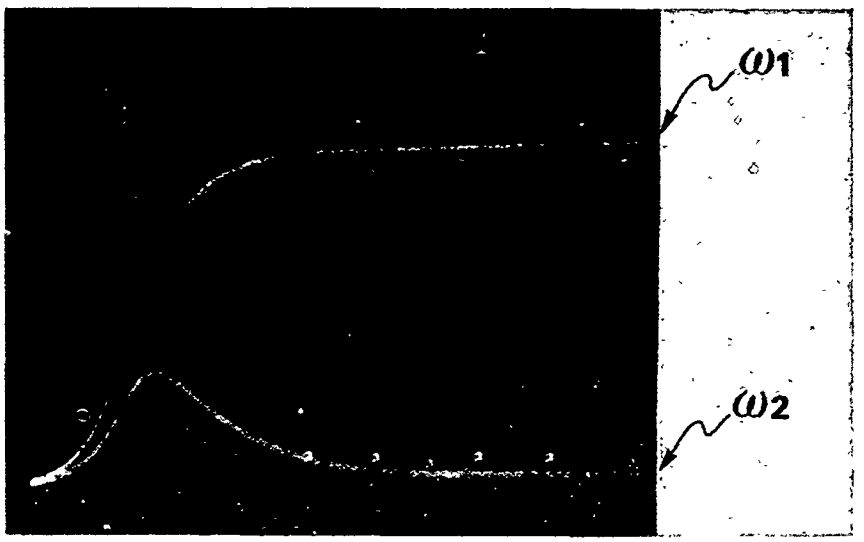

Photo. 1 ω_1 and ω_2 Oscillation levels to elapsed time. (OSC1)

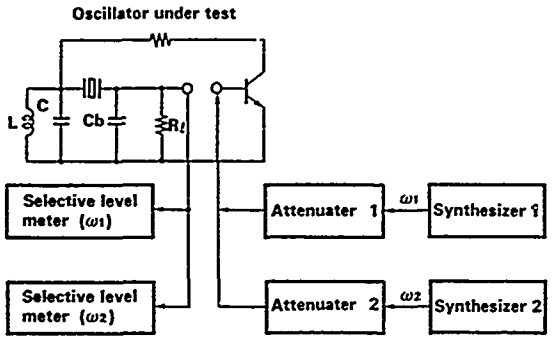

Fig. 9 Oscillator Loop Gain Measurement Circuit

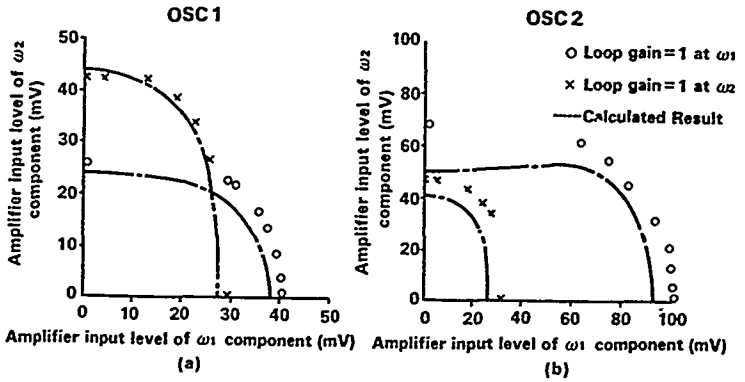

Fig. 10 Experimental Results of Oscillation Amplitude Condition

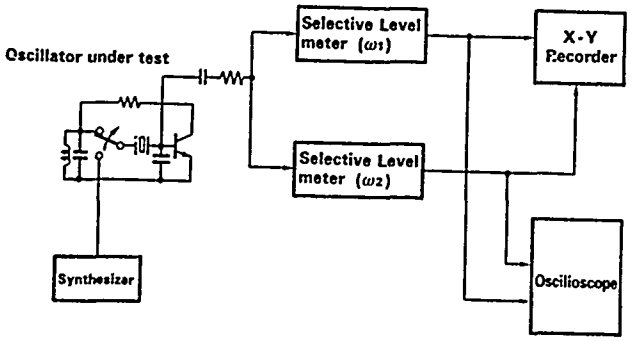

Fig. 11 Oscillation Level Locus Measurement Circuit

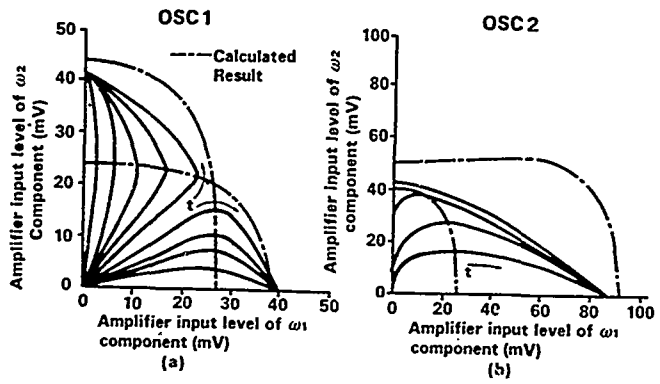

Fig. 12 Experimental Results of Oscillation Level Locus

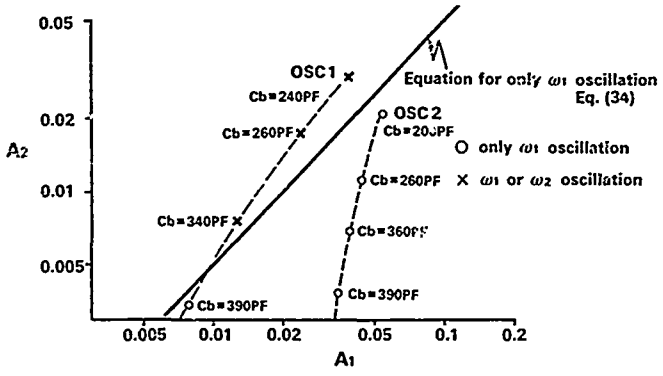

Fig. 13 Measurement Result of Wanted Frequency Oscillation Condition

Table 1 Parameters of Experimental Oscillators

		OSC 1	OSC 2	remark
XL	L_1	3.0 H	3 0 H	
	C_1	1.28×10^{-3} pF	1.28×10^{-3}pF	
	R_1	179 Ω	162 Ω	
	L_2	2.9 H	2.9 H	
	C_2	1.125×10^{-3} pF	1.125×10^{-3} pF	
	R_2	114 Ω	169 Ω	
	C_0	4.5 pF	4 5 pF	
	$f_1\left(\frac{\omega_1}{2\pi}\right)$	2,560 kHz	2,560 kHz	
	$f_2\left(\frac{\omega_2}{2\pi}\right)$	2,785 kHz	2,785 kHz	
$Ca(\omega_1)$		739 pF	600 pF	$Ca(\omega_1)=C\left\{1-\frac{1}{\omega_1^2LC}\right\}$
$Ca(\omega_2)$		860 pF	720 pF	$Ca(\omega_2)=C\left\{1-\frac{1}{\omega_2^2LC}\right\}$
Cb		240 pF	200 pF	
AMP	a_1	0 07	0 07	
	a_3	1.35×10^5	1.35×10^5	
	R_L	1.0 kΩ	1.0 kΩ	

A NON-ITERATIVE SOLUTION FOR A TWO-THERMISTOR TCXO

C. T. Swanson and E. S. McVey

University of Virginia, Charlottesville, Virginia

Theoretical work is presented on optimum error and sensitivity for a well known TCXO network containing two thermistors, three resistors, and a varactor. Ideal temperature placement for zeros of frequency deviation, as well as thermistor temperature coefficient selection, is presented using a third-order AT-type crystal model. The method used yields, without iteration, two realizable solutions predicting frequency compensation to parts in 10^{-7} over a temperature range of -55 to 60°C for an idealized situation.

Introduction

The circuit of Fig. 1 is well known [1] and is used by industry for temperature compensation of crystal oscillators. Solutions for the network presented in literature suggest an iterative procedure for determining the values of the components. A simpler non-iterative method is presented here which requires crystal parameters, specified temperature points for zero error in desired frequency, and thermistor temperature coefficients. The method used generates two realizable solutions, the better of which is in common use today. The other solution apparently is not documented in literature but is presented here as an alternative. In addition, sensitivity of each of the two solutions is presented as well as the effects of varactor selection, crystal-cut angle, and input voltage. The work presented is theoretical (idealized) and is consequently subject to the inaccuracies due to factors such as irregular crystal characteristics, measurement errors, etc.

Crystal Models

An approximate equivalent model of a crystal circuit is shown in Fig. 2. The shunt capacitance, series capacitance, and inductance of the crysal are represented by c_o, c_m, and L, respectively. An external capacitor c_x, is placed in series with the crystal for circuitry needs and to pull the frequency over a range of a few parts per million (ppm) for compensating purposes. The form of this capacitance is defined by the elements of Fig. 3. The frequency behavior of the crystal circuit is approximately

$$\frac{\Delta f}{f} = \frac{C_m \, \Delta C \times 10^6}{2(C_o + C_x)^2} \qquad (1)$$

$$= \frac{P \Delta C}{C_o + C_x} \quad \text{ppm}$$

for small variations in load capcitance, ΔC, about C_x. The quantity P in ppm is defined by the equation also. As is well known, the resonant frequency of the crystal varies as a function of temperature and it is this undesired variation that is to be compensated. Bechmann [2] has modeled AT-type crystals with the third-order polynomial equation

$$\frac{\Delta f}{f} = a(T - T_i) + b(T - T_i)^2 + c(T - T_i)^3 \text{ ppm} \qquad (2)$$

which is illustrated in Fig. 4 for several values of angle where

$a = -5.5\theta \quad {}^{o}C^{-1}$
$b = 0.39 \times 10^{-3} - 4.7 \times 10^{-3}\theta \quad {}^{o}C^{-2}$
$c = 109.5 \times 10^{-6} - 2.0 \times 10^{-6}\theta \quad {}^{o}C^{-3}$
θ = crystal-cut angle in degrees referenced to AT-cut zero degrees
T = actual temperature in degrees C
T_i = inflection temperature (approximately 28°C)

By combining (1) and (2), an expression relating change in load capacitance about C_x is obtained as a function of temperature. This makes $\Delta f/f$ remain zero for all temperatures (within the accuracy of the approximations, of course). It is

$$\Delta C = \left(\frac{C_o + C_x}{P}\right)[a(T-T_i) + b(T-T_i)^2 + c(T-T_i)^3]\text{pf} \qquad (3)$$

External Capacitor

To realize ΔC required by (3), a network of two capacitors and a varactor may be used, as shown in Fig. 3, where C_1 is variable to obtain set point adjustment, C_2 for scaling the total load capacitance, and C_D is a varactor (or tuning diode) used to produce the ΔC component. Variation of voltage across the varactor produces capacitance equal to

$$C_D = 0.18 + \frac{C_{oo}}{\left(1 + \frac{V}{0.6}\right)^{0.44}} \text{ pf} \qquad (4)$$

in a typical case where C_{oo} is the zero voltage value of capacitance exclusive of the 0.18 pf lead capacitance .

From the circuit of Fig. 3 and (3) and (4), an expression for the voltage, V, required by the varactor to achieve zero change in frequency over a specified temperature range is obtained. A graphical representation of this function for a typical

set of parameters is given in Fig. 5.

Resistor-Thermistor Selection

A network of resistors and thermistors is desired such that as temperature is varied, the voltage curve of Fig. 5 will be reproduced. A network to approximate this behavior is included in Fig. 1 where A, B, and D are temperature-independent resistors and C and G are thermistors whose resistance is of the form

$$\begin{aligned} R &= R_o \xi_R(T) \\ &= R_o e^{\beta(\frac{1}{T} - \frac{1}{T_o})} \\ &= R_o r^{[1763.58(\frac{1}{T} - \frac{1}{T_o})]} \end{aligned} \tag{5}$$

where

R_o = resistance at 298°K

r = ratio of resistance at 273°K to that of 323°K

β = a specified thermistor coefficent (1763.58 $\log_e r$)

T = temperature variable in degrees K

T_o = 298°K

Defining the voltage ratio ϕ as $(V_{in}-V_o)/V_o$ the resistor-thermistor network equation becomes

$$\phi = \frac{A + \frac{BC\xi_c(T)}{B + C\xi_c(T)}}{D + G\xi_g(T)} \tag{6}$$

If C is assigned the value 1 ohm for convenience, four unknowns remain which are scaled up or down with changes in C. The value of r (or β) for each thermistor must be given. Calculation of the unknowns may be achieved by specifying four temperature points at which the frequency error is to be zero and solving the resulting four circuit equations. The network output voltage approximates the values required at temperatures other than the four temperatures chosen. The basic circuit equation from (6) may be written for resistor A as

$$A = \phi_n(D + G\xi_{gn}) - \frac{BC\xi_{cn}}{B + C\xi_{cn}} \qquad n = 1,2,3,4 \tag{7}$$

where ϕ_n (defined by (6)) is the required voltage ratio to the varactor at temperature T_n and ξ_{cn} and ξ_{gn} are the corresponding thermistor factors. This yields four nonlinear simultaneous equations to be solved.

The following equations are obtained after successive elimination of variables:

$$mB^2 + pB + q = 0 \tag{8}$$

where

$$m = K_5 + K_4 + K_3 - 1$$

$$p = \xi_{c1}(K_4+K_3-1) + \xi_{c2}(K_5+K_3-1) + \xi_{c3}(K_5+K_4+K_3) + \xi_{c4}(K_5+K_4-1)$$

$$q = \xi_{c1}\xi_{c2}(K_3-K_3') + \xi_{c1}\xi_{c4}(K_4-K_4') + \xi_{c1}\xi_{c4}(K_5-K_5')$$

$$K_1 = \phi_1\phi_2(\xi_{g2}-\xi_{g1}) + \phi_1\phi_4(\xi_{g1}-\xi_{g4}) + \phi_2\phi_4(\xi_{g4}-\xi_{g2})$$

$$K_2 = \phi_1\phi_2(\xi_{g2}-\xi_{g1}) + \phi_1\phi_3(\xi_{g1}-\xi_{g3}) + \phi_2\phi_3(\xi_{g3}-\xi_{g2})$$

$$K_3' = \frac{K_2}{K_1}$$

$$K_4' = \frac{1}{\phi_2-\phi_1}[\phi_3-\phi_1-K_3'(\phi_4-\phi_1)]$$

$$K_5' = 1 - K_3' - K_4'$$

$$K_3 = K_3'\frac{\xi_{c4}}{\xi_{c3}}$$

$$K_4 = K_4'\frac{\xi_{c2}}{\xi_{c3}}$$

$$K_5 = K_5'\frac{\xi_{c1}}{\xi_{c3}} \tag{9}$$

and

$$G = \frac{1}{K_1}[(\phi_2 - \phi_1)(E_4 - E_1) - (\phi_4 - \phi_1)(E_2 - E_1)] \tag{10}$$

$$D = \frac{1}{\phi_2 - \phi_3}[G(\phi_3\xi_{g3} - \phi_2\xi_{g2}) + E_2 - E_3] \tag{11}$$

$$A = \phi_3(D + G\xi_{g3}) - E_3 \tag{12}$$

where

$$E_n = \frac{B\xi_{cn}}{(B + \xi_{cn})} \qquad \text{for } n = 1,2,3,4 \tag{13}$$

Two values of B are obtained from (8) which yields two complete solutions by using both values in calculations which occur after the solution for B. Given ϕ_n, ξ_{cn} and ξ_{gn}, K_1 and K_2 may be calculated. Then calculate K_3', K_4', K_5', K_3, K_4 and K_5 in order listed. Next calculate E from (13). Resistors G, D and A may then be calculated in order listed.

Program Results

A computer program was written to solve the equations for a specific example. V_1 was selected as 5 volts with the varactor bias at a nominal 2.5 volts at 25°C. This supply voltage is relatively low, but some TCXOs have to work with this value. For example, a value of 8 volts would be easier to use as a practical matter. Crystal parameters C_m, C_o, C_x and T_i were chosen to be 0.0112 pf, 3.56 pf, 32 pf, and 28°C, respectively, with C_2 equal to 123 pf. In addition, C_1 was calculated to be 1.8 pf for a C_D of 85 pf at 4 volts (not a practical value but it serves as an illustration). Through trial and error, the best value of crystal angle found for these parameters was 7 minutes, requiring the varactor input voltage to vary between 1.5 and 4 volts for compensation. The selection of thermistor parameters should be based on the best (optimal) value commercially available. Best results were obtained for values of r between 15 and 18 (β = 4800 to 5100).

Two methods were considered for the selection of temperatures at which the zeros of frequency error occur. In the first method values were chosen to minimize deviation from desired frequency over a specified temperature range in an equal ripple fashion, i.e. positive and negative frequency error extremes are equal. In the second method one temperature point was fixed at a value such as 25°C, and the other points were chosen to produce minimum peak errors. Figure 6 shows an example of each method. Method 1 resulted in a seven-minute AT-cut crystal error reduction from a deviation of ±17 ppm to ±0.22 ppm. Method 2 resulted in ±0.28 ppm peak error for the same crystal characteristic. Both results are for a temperature range of -40°C to +60°C.

The two resistor solutions and thermistors from (8) are available for use with either of the two methods. Table 1 gives optimum temperature values and thermistor parameters for the four possible examples. Table 2 shows the resulting values of the resistors and thermistors for these cases. Solutions 1 and 2 produce nearly indistinguishable results for each of the methods.

Tables 1 and 2 were constructed with the purpose of optimizing frequency variation over the temperature range of -40°C to +60°C; but, as will later be shown in sensitivity diagrams, some of the resistor and thermistor values become relatively critical at lower temperatures. It is therefore possible to move the lower end of the specified temperature range from -40°C to -55°C by increasing the thermistor parameter G to 18 for Solution 1 at the expense of only ±0.02 ppm increase in frequency variation. Figure 7 shows this graphically for Solution 1, Method 1.

Sensitivity

Each of the parameters chosen has an effect on the optimum solution for compensation. Below is a list of how each of the more critical parameters affect the outcome in general:

1. C_D tends to affect the overall circuit most in the low temperature range. Increasing C_D, in general, is desirable if good voltage stability can be obtained. Its maximum value is limited by both C_2 and C_X.

2. Stability of V_1 is critical for precise matching of the network to the required characteristic. It will become less critical if it is made larger and C_D is made smaller.

3. The best value of crystal angle is determined by the four temperature points at which zero frequency occurs and the thermistor ratios. Generally, angles in the range of 5 to 8 minutes will yield realable solutions for Method 1. Selection of crystal angles becomes slightly more critical for Method 2.

Figures 8, 9, and 10 show the sensitivity of the optimal solution to one-percent increases in network parameters. For Solution 1, the most critical component values are resistors; whereas, in Solution 2, the critical values are the thermistors. This would seem to indicate an overall advantage of Solution 1 to Solution 2, because precision resistors are less expensive than thermistors and the thermistor temperature constants will enter into the accuracy problem.

Conclusions

New information on an established method has been presented that gives network parameters of a resistor-thermistor network to achieve thermal compensation of crystal oscillators. Although the network used is well known, several factors are presented which apparently are not well documented in the literature. The method is non-iterative and it is shown that two solutions are possible. Sensitivity studies have led to the conclusion that one of the solutions is generally superior to the other. This seems to be in agreement with solutions used by industry. Results given in Table 2 indicate temperature compensation accuracy is theoretically ±0.3 ppm for a temperature range of -40 to +60°C; however, if the thermistor ratio of G can be increased, the effective temperature range is -55° to +60°C. Results this good should not be expected in practice. The results presented can be extended to studies such as error versus crystal angle for different temperature ranges.

References

1. Newell, D. E., and Bangert, R. H., "Temperature Compensation of Quartz Crystal Oscillators," Symp. on Freq. Cont.: Proc., Vol. 17, pp. 491-507, 1963.

2. Bechmann, R., "Frequency-Temperature-Angle Characteristics of AT-Type Resonators Made of Natural and Synthetic Quartz," Inst. of Radio Engrs., Vol. 44, pp. 1600-1607, Nov. 1956.

3. Comptrometer Corp., Union Thermoelec. Div., Quartz Resonator Handbook, Cont. #DA36-039-50-71061, File #27473-PC-56-B1-51, NILFS, 1L, p. 86, 1960.

Solution	Method	T_1	T_2	T_3	T_4	r_C	r_G	θ
1	1	-32.2	-8.8	15.9	57.5	16.4	15.6	7
1	2	-32.3	-7.5	25.0	57.12	15.9	15.8	7
2	1	-32.0	-8.8	16.0	57.5	16.6	16.5	7
2	2	-32.3	-7.5	25.0	57.14	16.0	16.0	7

TABLE I

Optimum temperature point placement and thermistor ratios

Solu-tion	Method	A	B	C	D	G
1	1	1.112	206.60	100	76.476	0.45073
1	2	0.0310	198.10	100	73.368	0.41344
2	1	1.174	18612.	100	75.812	37.200
2	2	0.1317	18196.	100	73.341	37.104

TABLE II

Resulting resistor and thermistor values from optimum placements

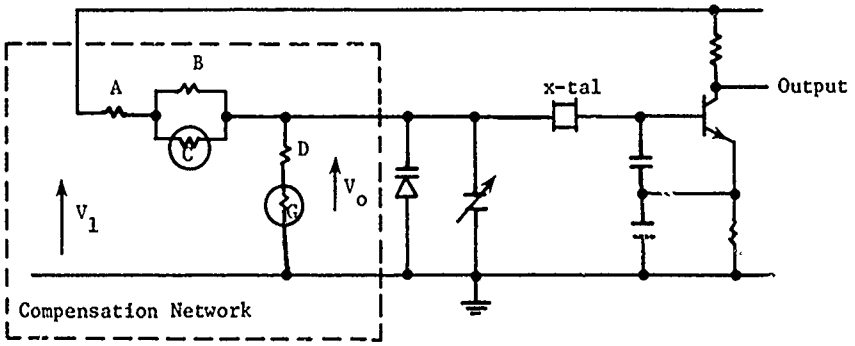

Figure 1 Oscillator and temperature compensation network

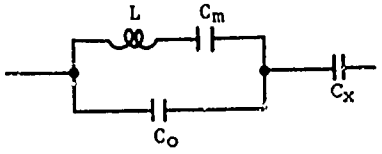

Figure 2 An approximate crystal model

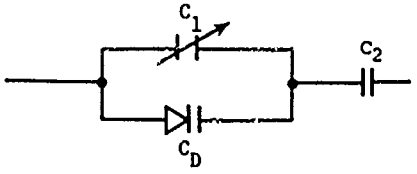

Figure 3 Equivalent compensating capacitance network

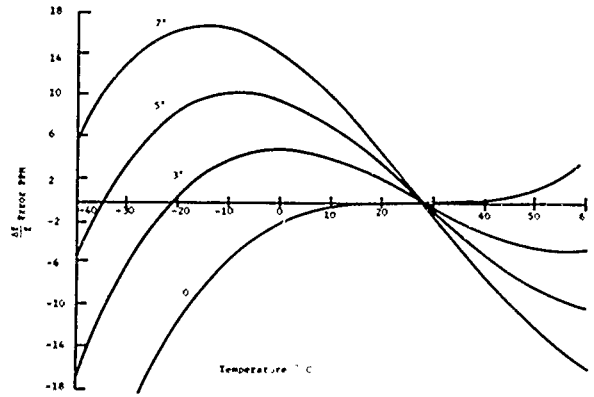

Figure 4 Generalize AT-type crystal curves

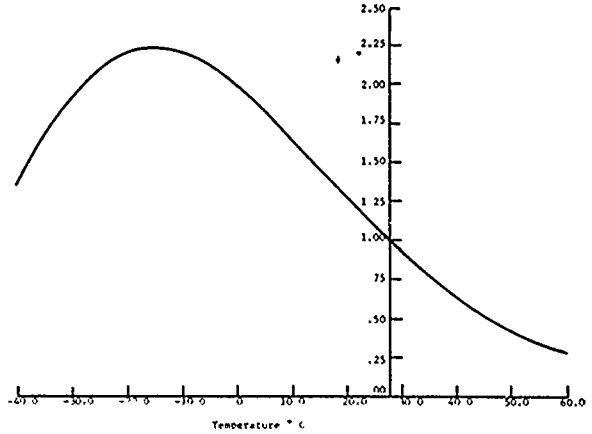

Figure 5 Voltage required by varactor to produce compensation

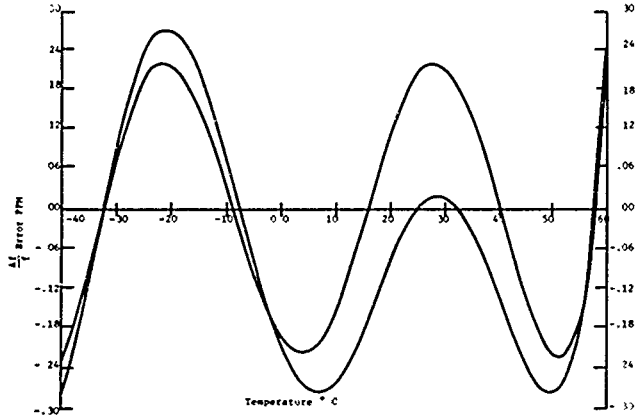

Figure 6 Optimum temperature compensation curves for methods 1 and 2

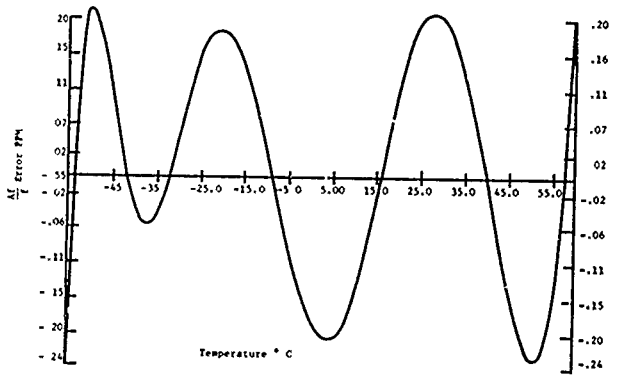

Figure 7 Temperature compensation from -55 to +60°C

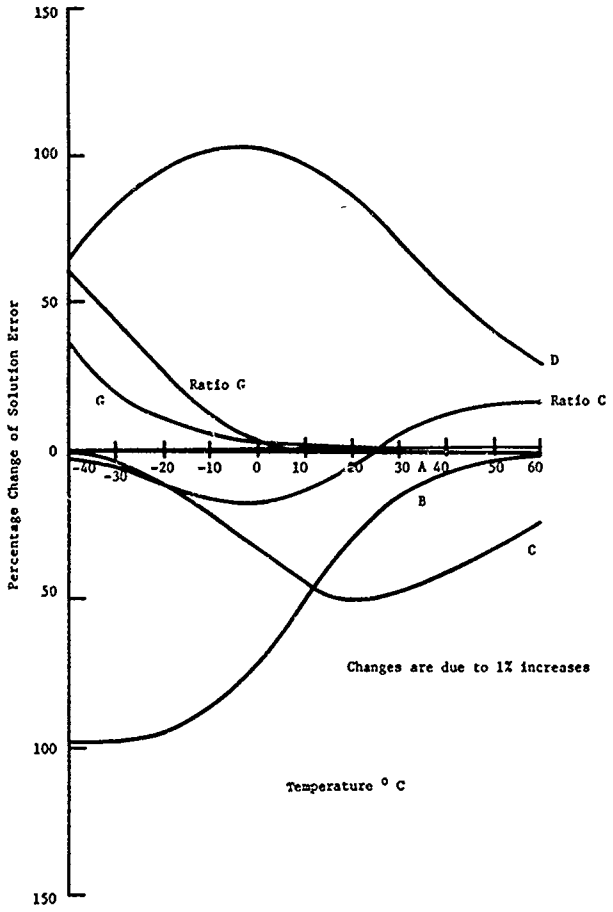

Figure 8 Component sensitivity data for solution 1

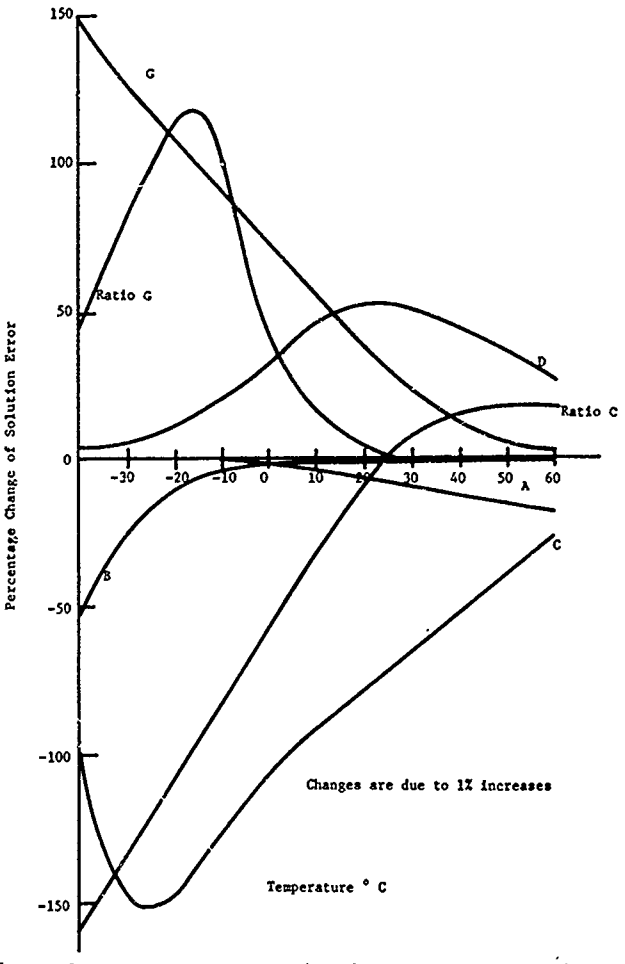

Figure 9 Component sensitivity data for solution 2

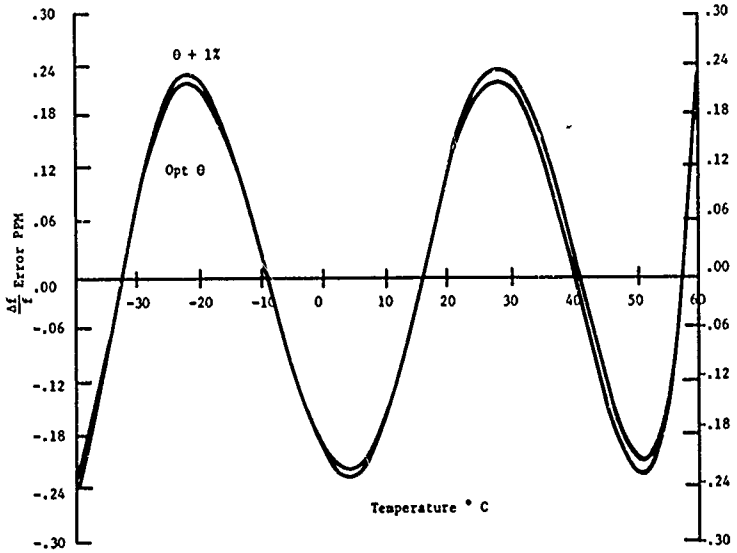

Figure 10 Sensitivity of crystal-cut angle

THE APPLICATION OF MICROPROCESSORS TO COMMUNICATIONS EQUIPMENT DESIGN

Marvin E. Frerking

Collins Telecommunications Products Division
Rockwell International

Summary

The availability of small low cost microprocessors has generated a variety of applications in the communication's field. Many of these applications are described in the paper. The microprocessor, in addition to replacing existing analogue and digital functions, has made it possible to add new features to the equipment and several of these are enumerated. Among them are microprocessor compensation of a crystal oscillator. The basic approach to this application is described including the method of compensation, the program flow chart, and the errors involved. The mathematics is derived to determine the optimum digital word lengths for a given accuracy.

Introduction

A large reduction in the size and cost of microcomputer systems has generated a host of applications in radio communications equipment. It is not surprising that a new technology such as the microcomputer has enabled us to simplify our designs, reduce parts count and costs, and to improve the specifications by a few more db. Another effect has taken place as well, and this the introduction of new features and capabilities which were previously not practical to implement.

Each new generation of communications equipment therefore, tends to be about as complex as its predecessor even though the individual components are greatly superior to those previously used. The introduction of the microcomputer has opened a myriad of such applications and engineers are limited only by their ability to discover the applications.

General Description

In describing some of the applications of microcomputers to communications equipment it is perhaps appropriate to begin by commenting on several equipments which are in the design phase or have recently been designed using microprocessor technology. The applications are not limited to radio communications since the microcomputer is well suited for imputting data, storing it and outputting it either continuously or in a burst mode. It is thus extensively used for data communications and data encryption. The applications also include handshaking, key management, and self test. The use of a microcomputer in these areas has reduced the hardware by a factor of five or more over digital logic in some cases. It should be noted that the design time has not decreased proportionally to the hardware, however, because of the significant programming effort and documentation of the software.

In radio communications there is a trend in some equipments to use a number of dedicated microprocessors to perform all the desired functions. We are presently involved in the design of a frequency hopping radio for the Army which will most likely employ five microprocessors. This may soon become the rule rather than the exception and serves to illustrate that the microprocessor equipment design era is truly a reality.

We can describe some of the functions implemented by the microcomputer in terms of the block diagram for a communications transceiver. The block diagram is shown in Figure 1. This diagram is not intended to apply to a specific equipment, but incorporates the major elements found in a typical military transceiver. The microcomputer is shown in the lower right. During normal operation the microcomputer scans the controls to determine the preset channel number. It then uses this number to enter a non-volitle RAM and look up the frequency corresponding to the selected channel. This information is frequently stored in BCD form to facilitate entry and display in decimal form. The processor then scans the display mode selected and outputs either the channel number or the corresponding frequency to the display. It then scans the PTT line to determine if transmission or reception is desired. Assuming that reception is desired, the processor offsets the frequency by the IF frequency (BCD addition or subtraction) and transmits it to the frequency synthesizer. The frequency synthesizer uses the

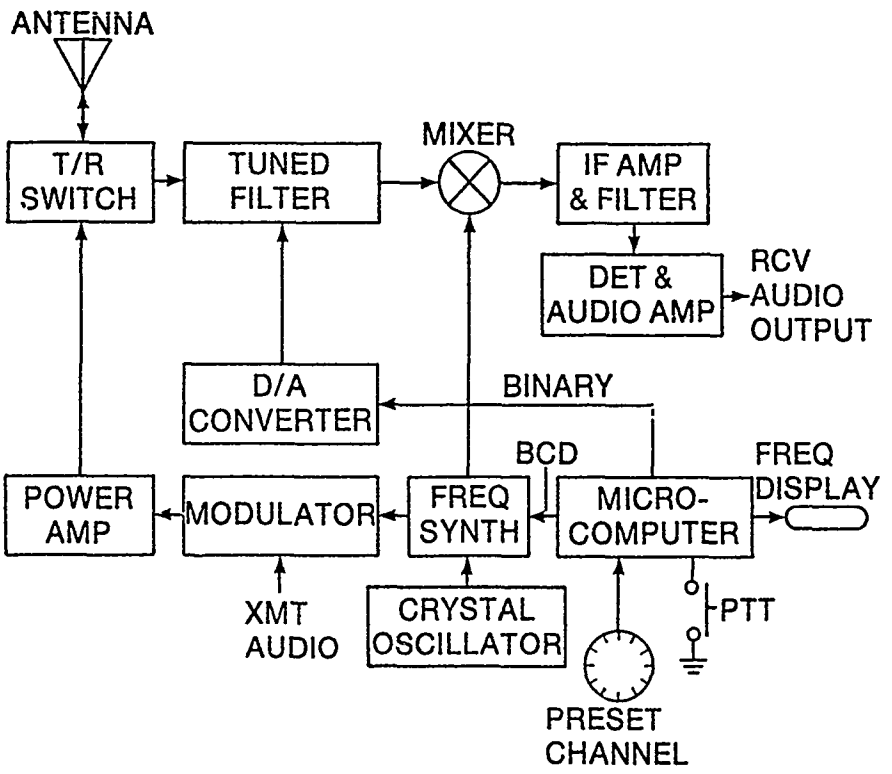

Figure 1. Block Diagram of Typical Military Transceiver

digital input along with the frequency from the temperature compensated crystal oscillator to generate the local injection for the mixer. The microcomputer then converts the channel frequency to a binary number and outputs it to the D/A converter which tunes the preselector. If the transceiver had been in the transmit mode, the channel frequency, rather than an offset, might have been used for the frequency synthesizer.

As indicated earlier, new features are being incorporated in the equipment which were previously not generally implemented because of the cost. One of these is fault isolation. Many military equipments have incorporated self test features for many years. This capability has frequently been limited to a go/no go test. The microcomputer can, with the aid of a series of signal sources and sensors, isolate a fault to a particular module and display the number of the faulty module on the frequency display. A typical test might be to turn on a noise diode, modulated at a 1KHZ rate, coupled to the T/R switch. A sensor at the receiver output then detects the demodulated 1KHZ tone. In the absence of a tone, an intermediate signal source at the input of the mixer or IF amplifier might be turned on to determine where the signal is being lost.

Other functions which can be performed by the microprocessor include frequency scanning, remote control, optimum frequency selection, squelch calibration, time keeping, schedule storage, frequency hopping, spread spectrum control, error correction, data encryption, temperature compensation of the crystal oscillator and others. Both frequency hopping and spread spectrum systems as well as single sideband tend to require stable oscillators. Because of the increasing requirements for high stability and because of the interest of the frequency control community it is appropriate to elaborate on this application of temperature compensation.

Crystal Oscillator Temperature Compensation

It has been possible, for some time, to temperature compensate crystal oscillators to within the hysteresis of the crystal frequency temperature characteristic using hybrid analogue-digital techniques. The microcomputer makes it less difficult to accomplish this task and without the need for analogue coarse compensation. Even with relatively modest stability specifications it may be desirable to use a microcomputer with digital compensation because of the ease of automation in production.

The general block diagram of a microprocessor compensated crystal oscillator is shown in Figure 2. A fairly linear temperature sensor such as a thermistor resistor network or a poorly biased transistor is used to convert the temperature to a voltage. The A/D converter digitizes this voltage for an input to the microcomputer. The microcomputer then determines the correction voltage needed at that temperature and outputs the digital correction to the D/A converter. The D/A converter changes this value to an analogue voltage for application to the varactor in the VCXO.

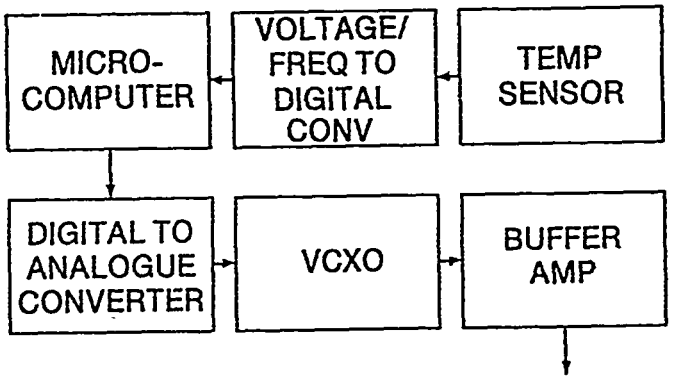

Figure 2. Basic Microprocessor TCXO

The program for the microcomputer is straight forward, and a flow chart is shown in Figure 3. After initialization of the I/O ports, the microcomputer reads in the temperature in digital form and searches for the closest stored values in its memory. The closest stored values can be found using a linear search if both temperature and the corresponding corrections were stored in memory. If only the corrections were stored for evenly spaced temperature points, the most significant bits of the temperature can address the memory directly.

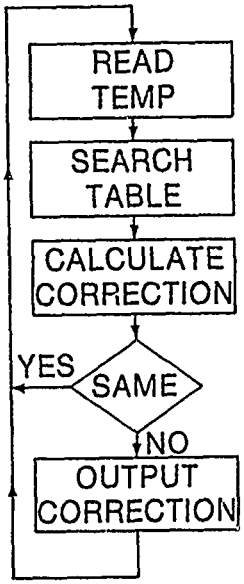

Figure 3. Program Flow Chart

The program then interpolates between the stored correction words using the equation:

$$V = V_n + \frac{(V_{n+1} - V_n)(t - t_n)}{t_{n+1} - t_n} \qquad (1)$$

where V_n is the prestored correction voltage at temperature t_n, and V_{n+1} is the voltage at temperature t_{n+1}. It is assumed here that the ambient temperature, t, falls between t_n and t_{n+1}. Programs have been written for both the INTEL 8080 and the single chip 8048. In each case the compensation values are stored in an external CMOS PROM. Obviously, as single chip CMOS microcomputers become available the power consumption and self heating can be greatly reduced. This is manditory in high precision TCXOs.

It is also desirable to minimize the number of I/O lines from the processor as well as to optimize the number of bits required in the A/D converter and in the D/A converter to achieve a given accuracy. It is not difficult to show that the maximum frequency error due to finite word length is given by[1]

$$\Delta F = \frac{S}{2}\left(\frac{T}{2^{b_t}}\right) + \frac{F}{2}\left(\frac{1}{2^{b_v}}\right) \qquad (2)$$

where:

b_t = no. of bits in the temperature word.
b_v = no. of bits in the correction voltage word.
S = maximum frequency-temperature slope of the crystal, in PPM per ^oC.
T = total temperature range over which the oscillator must be compensated.
F = maximum peak to peak frequency excursion of the crystal in PPM.
ΔF = maximum frequency error allowed, in PPM.

For simplicity here we have assumed that the cost of the A/D and D/A conversion doubles for every bit of accuracy. (This may be approximately true for high accuracy units where we are most concerned about an optimum design.) We may then represent cost by the function

$$C = 2^{b_t} + 2^{b_v} \qquad (3)$$

Using this function we find that the cost is minimized if*

$$b_t = \log_2 \frac{1}{2\Delta F}\left(ST + \sqrt{STF}\right) \qquad (4)$$

and

$$b_v = \log_2 \frac{F}{2\Delta F}\left(1 + \sqrt{\frac{ST}{F}}\right) \qquad (5)$$

As an example, suppose that:

$\Delta f = \pm 0.5$ PPM

F = 35 PPM

$T = 90^oC - (-40^oC) = 130\ C^o$

S = 1.3 PPM / ^oC

We find from equations 4 and 5 that $b_t = 7.94$, and $b_v = 6.81$. We would thus consider an 8 bit A/D converter and a 7 bit D/A converter if these were the only errors involved. In order to allow for the interpolation error we choose $b_t = b_v = 8$. Then from equation 2, $\Delta f = 0.4$PPM. Thus the interpolation error can be as large as $\pm$ 0.1PPM. This error results from using a linear interpolation to approximate the cubic equation of the

* See Appendix

crystal between stored correction points. This error is largest at the temperature extremes where the cubic term of the crystal temperature characteristic is most significant. It is minimal around the inflection point temperature where the crystal behavior is more linear. If we allow ± 0.1 PPM for interpolation error then the stored correction values can be about 3°C apart at the temperature extremes while 10°C could be tolerated at room temperature. The frequency errors due to interpolation have been analyzed in the previously cited reference on Crystal Oscillator Design where it is shown that the error is given by:

$$\delta_{MAX} = \frac{\Delta T^2}{4}\left[1.5b_3\Delta T + b_2 + 3b_3 t\right]$$

where: ΔT is the distance between stored temperature points,
t is temperature at the lower end of the interval,
and b_2 and b_3 are constants of the crystal being used,
see cited reference, p. 172.

Figure 4 shows the frequency versus temperature behavior for a microcomputer compensated crystal oscillator which holds $\pm 3 \times 10^{-7}$ over the temperature range from -26°C to + 82°C. These results were obtained using 8 bit temperature and correction voltage accuracy.

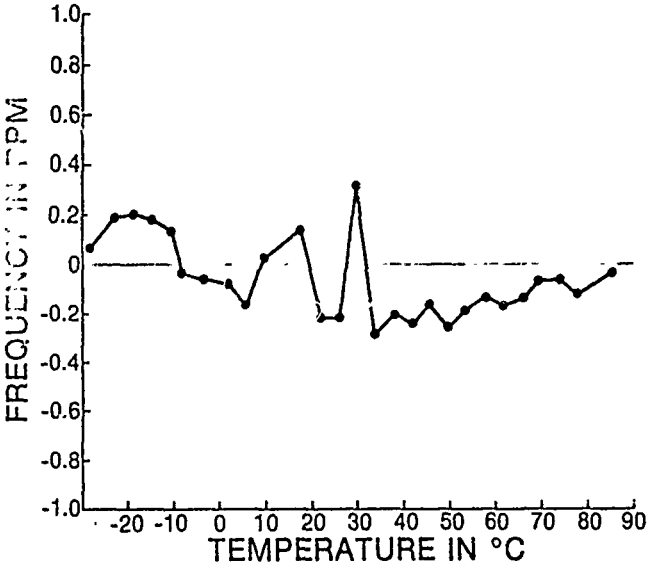

Figure 4. Frequency versus temperature for a microcomputer compensated crystal oscillator.

Conclusions

The future is quite promising for the application of microcomputers to temperature compensation, and we can expect a great deal of innovation in the years ahead. This technique promises to reduce the power of precision TCXO's as well as to decrease the size. Indeed, at the present time, CMOS microprocessors are available which will operate on a few microwatts at slow clocking rates. We can look forward to self compensating TCXO's as additional progress is made with non-volatile memories, and perhaps we may soon be able to model transient effects in the crystal and to temperature compensate dynamically as well as statically. It is not unreasonable to suppose that microcomputers with built-in A/D and D/A converters will become available and allow temperature compensation with a single chip plus the oscillator.

We have singled out temperature compensation here as an example of the application of a microcomputer to communications equipment. Many of the other applications cited are equally exciting and challenging. It is anticipated that digital signal processing, which is presently limited by the processing speed, will also evolve as a major breakthrough in the application of microcomputers to communications equipment. Truly, the microcomputer with its multiple applications in communications will have as large an impact on the electronics industry as the transistor or digital logic.

Appendix

Determination of Optimum Word Lengths in a Microcomputer Compensated Crystal Oscillator.

From equation 2, of the paper, we see that the frequency error due to finite word length is given by:

$$\Delta f = \frac{S}{2}\left(\frac{T}{2^{bt}}\right) + \frac{F}{2}\left(\frac{1}{2^{bv}}\right) \qquad (A\text{-}1)$$

where the terms have been previously defined. This equation assumes that we optimize both the temperature compensation table and the compensation voltage to pick the nearest voltage level. This is contrasted to the case where we simply input and output the digital words without regard to the truncation error. In the latter case, one extra bit will be required in each word since S/2 in equation A-1 becomes S and F/2 becomes F.

The cost criterion used is given by equation A-2 below:

$$C = (2)^{bt} + (2)^{bv} \qquad (A\text{-}2)$$

which assumes that adding one bit doubles the cost of the A/D or D/A converter. This is obviously pessimistic for low precision units. For high precision, however, where it is most important to obtain the optimum design, the criterion becomes more realistic.

$$\text{Now let} \quad X = s^{bt} \qquad (A\text{-}3)$$

$$\text{and} \quad Y = 2^{bv} \qquad (A\text{-}4)$$

$$\text{Then} \quad C = X + Y \qquad (A\text{-}5)$$

$$\text{and} \quad \Delta f = \frac{S}{2}\,\frac{T}{X} + \frac{F}{2}\,\frac{1}{Y} \qquad (A\text{-}6)$$

Solving for Y we have

$$Y = \frac{(F/2)}{\left(\Delta f - \frac{S}{2}\,\frac{T}{X}\right)} \qquad (A\text{-}7)$$

Substituting for Y from equation A-5 gives

$$C = X + \frac{(F/2)}{\left(\Delta f - \frac{S}{2}\ \frac{T}{X}\right)} \qquad (A\text{-}8)$$

We can minimize the expression for C by differentiating with respect to X and setting the derivative equal to zero.

$$\frac{dC}{dX} = 1 - \frac{F/2\ \left(\frac{ST}{2X^2}\right)}{\left(\Delta f - \frac{S}{2}\ \frac{T}{X}\right)^2} = 0 \qquad (A\text{-}9)$$

Now solving this expression for X gives

$$\left(\Delta f - \frac{S}{2}\ \frac{T}{X}\right)^2 = \frac{F}{2}\left(\frac{ST}{2X^2}\right) \qquad (A\text{-}10)$$

$$\Delta f - \frac{S}{2}\ \frac{T}{X} = \frac{\sqrt{FST}}{2X} \qquad (A\text{-}11)$$

$$\Delta f = \frac{\sqrt{FST}}{2X} + \frac{ST}{2X} \qquad (A\text{-}12)$$

$$X = \frac{1}{2\Delta f}\left(\sqrt{FST} + ST\right) \qquad (A\text{-}13)$$

and $$b_t = \log_2 \frac{1}{2\Delta f}\left(\sqrt{FST} + ST\right) \qquad (A\text{-}14)$$

Also from equations A-7 and A-13

$$Y = \frac{F/2}{\Delta f - \frac{ST}{2}\ \frac{2\Delta f}{\sqrt{FST} + ST}}$$

$$= \frac{F}{2\Delta f\left(1 - \frac{ST}{\sqrt{FST} + ST}\right)} \qquad (A\text{-}15)$$

$$Y = \frac{F}{2\Delta f\left(\frac{\sqrt{FST}}{\sqrt{FST} + ST}\right)} \qquad (A\text{-}16)$$

$$Y = \frac{F}{2\Delta f}\left(1 + \sqrt{\frac{ST}{F}}\right) \qquad (A\text{-}17)$$

And finally:

$$b_y = \log_2 \frac{F}{2\Delta f}\left(1 + \sqrt{\frac{ST}{F}}\right) \qquad (A\text{-}18)$$

Reference

1. Frerking, Marvin E., Crystal Oscillator Design and Temperature Compensation, Van Nostrand Reinhold Company, New York, 1978, p. 155.

USE OF FIBER OPTIC FREQUENCY AND PHASE DETERMINING ELEMENTS IN RADAR

by
Arnold M. Levine

ITT Gilfillan
Van Nuys, California

Abstract

The application of fiber optics to modern radar systems and circuits is examined. This paper presents the more unconventional use of fiber optics stable transmission delay characteristics to form active elements within a radar. This technology may be utilized in the design of such radar circuits as a high frequency oscillator, phased array antennas, precision pulse generation, A/D converter, MTI system and an identical chirp curve matching generator. Some systems applications are shown with the benefits and problems indicated.

These circuits, besides being precision devices, are stable enough for radar where long time exact frequency is not as important as short term stability and reliability. These circuits are EMI and EMP resistant and avoid conventional feedback circuit problems. They are low in cost to build, even at current prices, and properly used, are long life components.

Color multiplexing will also be discussed as a means of greatly reducing the amount of fiber optic cable required in these circuits.

Introduction

One of the early optical voice bandwidth communications systems was demonstrated by Alexander Graham Bell prior to 1874. Since the signal was transmitted on a mechanically modulated focused beam of light it may have been considered a semicontained optics link. Light contained and bent is as old as nature, since this is the phenomenon that takes place in a waterfall. It was not until the early 1950's that fiber optics (FO) was placed on a practical foundation.(1) Since then, rapid progress has been made to increase the usable bandwidths, decrease losses, improve manufacturing procedures, reduce cost and extend use into the IR region.(2) In addition, technology of small energy sources for transmission and detection devices for receiving has been vastly improved. This paper will not attempt to go into the device technology as there is adequate data available in current literature. It will review the use of fiber optics in a nonconventional mode as may be utilized in radar systems for circuit and major subsystems, as indicated in Table I. Some of the radar circuits will be described but not all items in the matrix will be covered in this paper.

One characteristic of glass fiber optics is its stable time delay. Curves indicating the stability characteristic can be seen in Figure 1 showing that in the case of Borosilicate the index of refraction does not change more than 30 parts/million from -80° to +60°C. There is also a relatively flat portion of the curve for a more stable operation when temperature control (coarse) is available. The type of optical fibers to be discussed are all graded glass of the silica variety, and are available with attenuations of approximately 1 dB/km at a wavelength of 1.06 μm and 2 dB/km at 0.8 μm. Stack fibers of the graded type are available at 5 dB/km, and for most of the suggested uses, losses are not a major problem. The delay in a typical fiber is given as $n\,L/c$ where n is the refractive index of the fiber core, c the free-space velocity of light, and L the total length. For fused silica, $n = 1.46$ and the delay approximately 4.9 μs/km.(3) Dispersion limits the bandwidths for long delays so that most of the wide bandwidth or high frequency operations discussed are for comparatively short run fibers.

Radar Circuits

In the following section a number of block diagrams and circuits covering RF, antenna, and signal processing, which may be utilized in radar will be described.

Oscillator or Narrowband Regeneration Amplifier

Figure 2 shows two somewhat different arrangements of an oscillator (2a), and an amplifier or oscillator (2b). These circuits operate on the principle of a 180-degree shift in the FO delay line as to cause the input to be in phase with the output of a 180-degree phase shifter amplifier. Assuming there is enough gain available, either circuit will oscillate with what amounts to a FO nonmagnetic coil. By adding negative feedback the gain characteristics of the circuitry can be made more stable and controlled, and the shapes of the filter can be modified as the Q or signal gain is modified. When Figure 2(b) is used as an oscillator or amplifier its frequency may be changed by diode switching different fiber lengths and an active synthesizer may be obtained. This is somewhat different from those generally utilized for communication where switching time is not as important. To prevent operation at multiple frequencies and to reduce harmonic content, C has been added to all such circuits. A further refinement to the

above principles, but in a different circuit arrangement, is shown in Figure 3.

Delay Stabilized Variable Oscillator

In a frequency scan radar system, i.e., where the beam position is dependent on the frequency of the radar, a series of programmed base frequencies must be established.* One of the older methods for doing this is to utilize bands of crystal oscillators and establish a switching system for selecting these oscillators at some low frequency where crystals are easily available. This output is then multiplied upwards to the required transmitted frequency. Since the frequencies are being multiplied, a high degree of frequency stability and accuracy is required plus a large number of crystals for even frequency spacing. This is complex, has a certain degree of unreliability, and is expensive. In addition, multiplying adds noise to the system, so that when improved MTI is desired the conventional system is self limiting. There are several more modern techniques for frequency synthesis. One method for establishing the same basic frequency generation requirement is utilization of a stable FO delay line in a voltage controlled oscillator. As shown in Figure 3 the radar beam position would be coded, and that code would then establish a quantized voltage. This voltage would then be applied to an oscillator so as to position it to a coarse frequency position. By utilizing a precision stable delay line in the feedback control loop of the Voltage Control Oscillator (VCO), the oscillator can be forced to oscillate at only multiple frequencies of the delay in the prior mentioned line. This oscillator can also be made to oscillate at frequencies approximately 10 times the current crystal frequencies. Hence, the stability requirement is less and the cost of multiplying reduced. Instead of a rack of equipment, this total package would be much smaller and have fewer components, with ease of serviceability and high reliability. The fibers can be hand cut for frequency selection without a great deal of skill and with conventional tools. For an improved noise figure, it would appear desirable to follow the oscillator with the aforementioned amplifier filter combinations.

Fiber Optic Phased Array Antenna

The following description covers utilization of fiber optic cables to give precision delay in lightweight phased array antennas for radar or communication systems.

Much work has been done on trying to reduce costs of phased array antennas. One particular type uses frequency change to obtain a beam position. Another type uses fixed incremental delay devices whose combination moves the beam to incremental positions. The latter type, consisting of ferrites with driver mechanisms, diode networks and their associated circuitry, and other similar types, are heavy and consume a large amount of power. In addition, phase stability becomes a problem in wide environmental conditions.

This proposed technique would utilize high quality FO cable for the time delay network. Basically, the system operates as shown in Figure 4(a). The laser input is optically modulated by the RF frequency so that the main output from the optical system contains all the required signal information. This optical output is then optically coupled to multifiber cables where the optical information is transmitted to the antenna proper. At each antenna there is a power amplifier connected directly to a dipole or other radiating device for power combining in space. The number of fibers required per multicable would depend on the beamwidth desired and the number of degrees of beam motion. Each transmitter output stage requires a similar FO bundle. As shown in Figure 4(b) or (c), switching may be carried on at either end of the FO cable and may be switched on an RF or optical basis in order to choose the particular phase delay required. Switching is controlled by a center timing generator and may be digital or analog as indicated in the drawings. Other arrangements may be made from this basic concept but the main goal is to obtain a lightweight phased array antenna having the capability of low cost, high stability, and rapid beam positioning. Its use may be readily seen for radars in general, GCA in particular, communications, missile tracking, and lightweight airborne radars. The transmission of 1 GHz already has been demonstrated at ITT over these comparatively short lengths using a General Optronics laser and a Telefunken BPG28 avalanche diode.

Signal Processing

Fiber optic cable may also be used in signal processing for pulse generation, analog-to-digital conversion, and a special case of MTI.

Precision Pulse Generation

State of the art in the area of pulse generation and timing is quite sophisticated and precise. Most of the precision is dependent upon some form of accurate timing generator. The diagrams, as shown in Figures 5(a) and 5(b), obtain their pulsewidth precision from the fact that a fixed and stable delay device, in this case FO, has been used in the timing loop. All other time constants in this common multivibrator circuit are much longer than the pulsewidth.

Passive Analog-to-Digital Conversion

The state of the art contains many known analog-to-digital conversion devices, but in general, these are highly susceptible to electromagnetic pulse due to nuclear activity and/or lightning and high level electrical impulse noise plus power supply variations. Much of this takes place in triggered devices due to active circuitry and the effect can continue on for a much longer period than the impulse itself. A means of lowering this false pulse information output and having a more EMP resistant system is to utilize the characteristic of FO cables as a compact delay device to set up coding. This is applicable to digital MTI, computers, telemetry, communications systems, CFAR, etc.

Basically, the system samples the signal input on a time sampling basis and the amplitude sampled then goes through a compressor for maximum signal-to-noise (s/n). The output is then applied to a sampling quantizer so that discrete amplitude levels may be established. At each level, there is a cable or set of FO cables whose length determines the pulse position and hence pulse code at the output for the various levels. These are combined, limited, and put through an adder whose output is time sampled to be coincident with the basic sampling pulse frequency. Both the block diagram and waveforms are shown in Figures 6(a) and (b). The block diagram for digital-to-analog conversion

* This excursion is about 10 percent of the transmitted center frequency.

unit is shown in Figure 7. This represents a FO delay line for coanecting and timing the coded pulses so that the original amplitude is established.

Fiber Optic MTI System by Color Reiteration

In order to obtain stable MTI in current radar systems, the usual analog technique utilizes a many-sided quartz crystal. This requires extremely stable conditions, since cancellation takes place on an RF cycle-to-cycle basis and any change in phase characteristics causes a deterioration in MTI capability. Another way of establishing an MTI system would be at video, except the problem here is establishment of wideband, long-time stable delays within a reasonably sized system. The advantage of course, would be a lesser requirement on stability since the video cancellation would not be as critical as cycle-to-cycle RF cancellation. One means of establishing this delay is by utilization of FO cable. Fused silica is a common, low cost, FO cable material and is readily available with low attenuation. However, a single fiber that would give adequate delay for low-pulse sampling rates would have excessive length. One means for reducing this cable length is by color reiteration. As shown in Figure 8, the first scan is detected and the video portion modulates an optical laser modulator. The output travels a FO cable whose length, L, is $D'dN_f \times$ km, where D is total needed delay, d is delay per kilometer and N_f if the number of colors used. At the far end, the particular color selected is demodulated and remodulates another color F_2, which goes down through the same cable. This is again detected and retransmitted on color F_N until an adequate number of reiterations takes place to establish the required delay time for cancellation of the following scan. As a practical example an airport surveillance detection equipment (ASDE) radar has a high repetition rate of 14 kHz or about 71.4 μsec delay requirement. Using the above described technique, a FO cable of only 2.43 km would be required with a six-color selection. The above color division system is not limited to radar, but may be utilized in communications, telemetry, or whenever multiplexing on FO cables is required.

A recent development, as shown in Figure 9, indicates current activity by Hitachi. This IC will contain six different colored lasers with grating feedback.[4]

Automatic Failure Resistant Radar

Several techniques have been proposed for a *Fault Tolerant Transmitter* using solid state devices. Most of these have some component switching mechanism for replacing failed power transistors. The following technique combines all transistors including spares, and operates under lower power per transistor for the same radar range, but changes the system to compensate for the power transistor failures. This further extends transistor life by utilizing lower power per unit.

In solid state combined transistors, it is common to form some sort of combiner so that the transistors may be effectively operated in parallel and be connected in such a mode so that failure of one transistor will not load any of the others. Because of the peak voltage limitations, the transistors are operated in parallel to obtain the power output, and the pulsewidth is made wide enough to obtain the proper power on target. However, when we combine additional spares, more than adequate power is available. The required power on target may be obtained by reducing pulsewidths, thereby reducing the power placed on each transistor and extending the life of each individual solid state device and hence, the total life of the transmitter (Figure 10). Further, as each transistor begins to fail or fails, the pulse is automatically widened to keep the power on target constant. This technique is particularly applicable to *chirp* systems. The main purpose of utilizing some form of frequency chirping and receiver compression is to obtain range resolution equivalent to a narrow pulse radar system. Many types of frequency chirping techniques are in the literature, but as an example, a step scan system is shown in Figure 11. Figure 12 is a block diagram of the system and indicates the method of operation. The transmitter output is maintained at a specific power and the pulsewidth and hence, the number of chirp steps in the pulsewidth available to the transmitter is varied. In order to avoid some matching problems of chirping and dechirping, a technique, shown in Figure 13, may be used. This uses the stable characteristics of fiber optics to form both the source unit for chirp generation and compression and operates independent of pulsewidth. This combines some of the previously described frequency synthesizer techniques with conventional Bragg Cell technology. Figure 14 shows, in schematic form, a combination of the previously described oscillator utilizing the same fibers for frequency generation and filtering, plus the associate delays for a chirp demodulator. This becomes temperature insensitive so that curve matching between transmit and receive is no longer a problem. The curve may also be tailored for best sidelobe suppression.

Experimental Results

Figures 15a and 15b show the breadboard arrangement utilized to demonstrate a fiber optics oscillator. The FO coil was cut for about 5 MHz and fed through a series of broadband amplifiers to have the proper phase reversal (180°). The unit oscillated as predicted, however there was too much gain in the amplifier used and more noise appeared on the output than expected. No additional filtering was employed, but the amplifier bandwidth only extended to 52 MHz. Properly matched, a 20-30 dB gain in s/n is expected over that indicated in Figure 16 showing the oscillator output up to 50 MHz with 5 MHz spacing.

Outlook

As time progresses new technologies become available and what seems like limitations placed on the system by EO components or a particular optical frequency becomes an incentive for further investigations. Recent developments with new materials have indicated that IR tranmission over fiber optic cable is not only possible but has already been utilized by the medical profession.[2] The prediction for future cables are the development of material (Thallium Bromide) with a loss of about 1×10^{-5} dB/km, making transmission from New York to London feasible with no repeaters. There have been many other suggestions in literature for improvements in radar technology, such as using FO for a transversal filter.[5,3]* Many more will come to the readers' mind. As the bandwidths of radar systems become wider more use will be made of analogue technology and, where appropriate, fiber optics will play a role in helping to keep costs down with possibly improved performance.

* See references following Figure 16

TABLE I. FIBER OPTIC TECHNOLOGY USE MATRIX FOR RADAR

Fiber Optic Technology \ Radar Use	EMP Resistance	Low Cost Power Phase Shifters	Lightweight	Wide Δf at L-Band	Solid State Module Use	Electronic Scan	Frequency Synthesizer	Hi Power Control	Hi Stability	Fault Indicator	Feedback Loops	Wideband Receivers/ECCM	Wide Bandwidth	Waveform Design	Chirp Scan	Adapter Analog Log MTI	Wideband Circuitry	Display
	Antenna							**Radio Frequency**						**Signal Processing**				
RF/IFF Video Transmission	X		X	X	X						X	X	X				X	X
Data Bus								X		X			X				X	X
Interchassis Feed-Back Loops								X	X	X	X	X	X				X	
Data Remoting Polar/ Raster Scan																		X
Wideband Intra-Chassis Connect											X	X	X	X		X	X	X
Stabilized Oscillators						X	X		X						X			
Compression & Coding Techniques					X		X		X			X	X	X	X		X	
Display Storage																	X	X
Antenna Control System	X	X	X															
Phased Arrays		X	X	X	X	X			-									
Bragg CSLC												X						
Hi-V Indicators								X		X								
BiDirection Trans										X								
Antenna Diode ϕ Switch	X	X	X		X	X												
A/D-D/A Digital Techniques													X	X		X	X	
EO Autogate														X		X	X	
Precision Pulse Generation													X	X		X	X	

9537-1

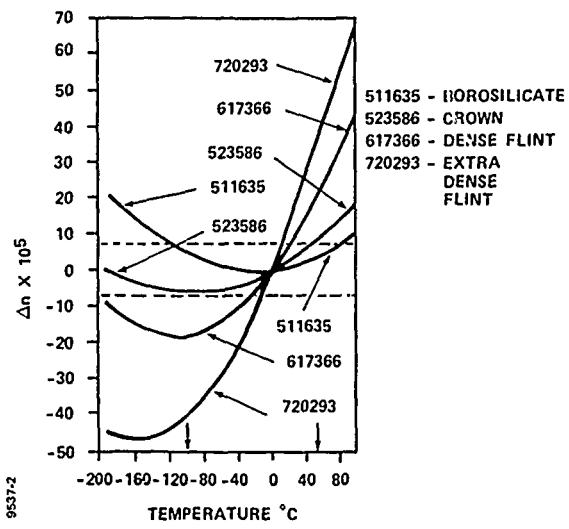

Figure 1. Temperature Dependence of Refractive Index, $\Delta n \times 10^5$ at 589.3 mμ

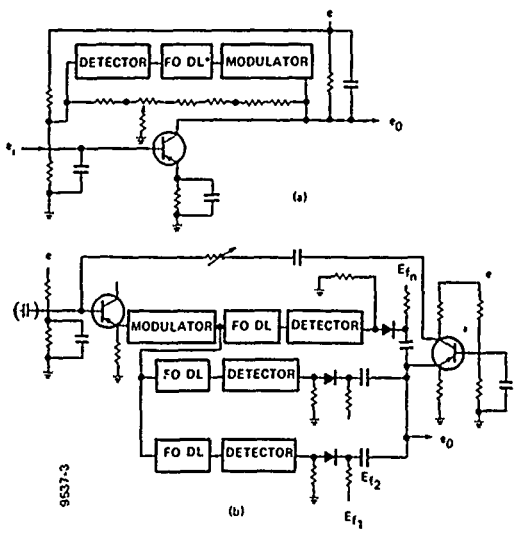

Figure 2. Oscillator or Narrowband Regeneration Amplifier

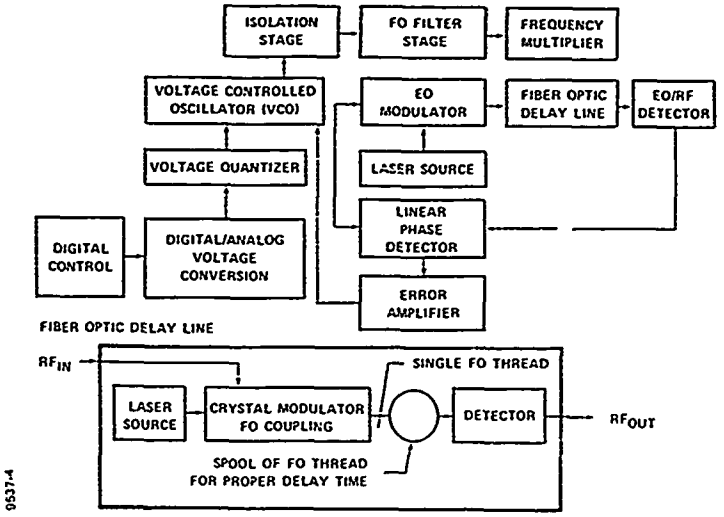

Figure 3. Frequency Synthesizer Block Diagram

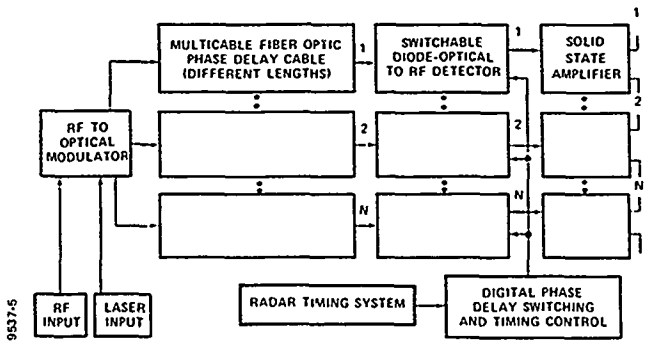

(a) Basic System

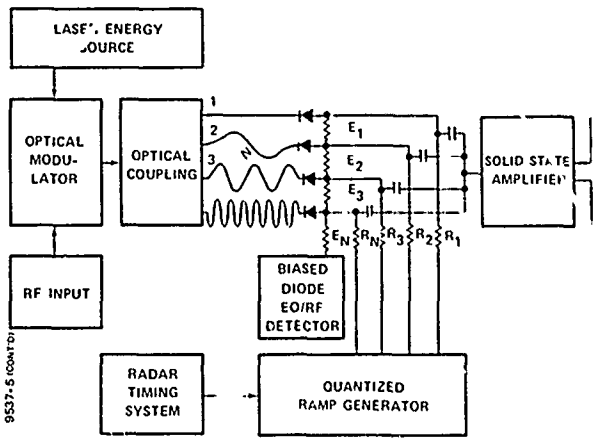

(b) Single Fiber Optic Cable Phase Shifter

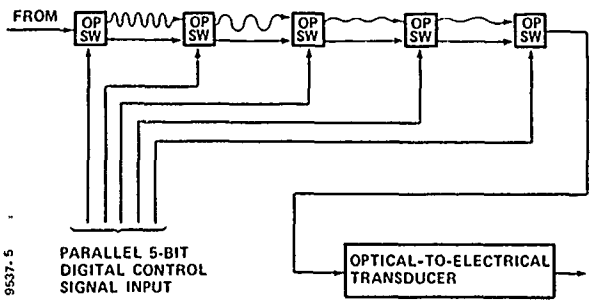

(c) Alternate Series Arrangement Utilizing Digital Techniques

Figure 4. Fiber Optic Delay Cable Phase Shifted RF Drive and Transmitter Output for Electronically Scanned Beam

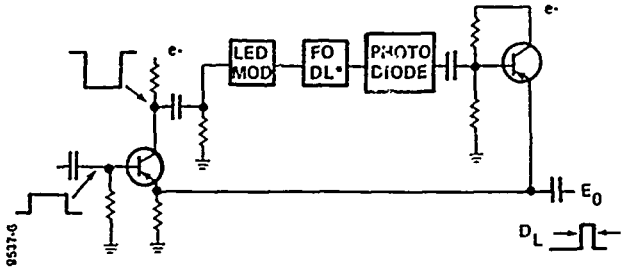

Figure 5(a). Single Trigger Pulse Forming Flip-Flop

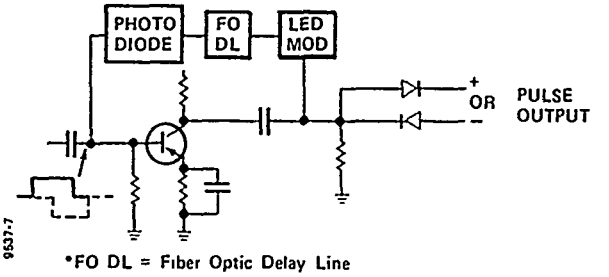

Figure 5(b). Nonactive Pulse Shaping Circuit

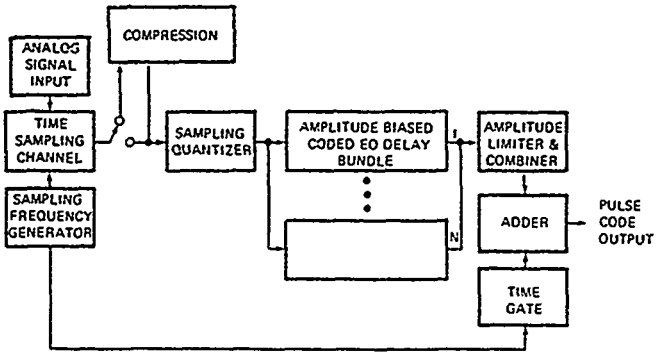

(a)

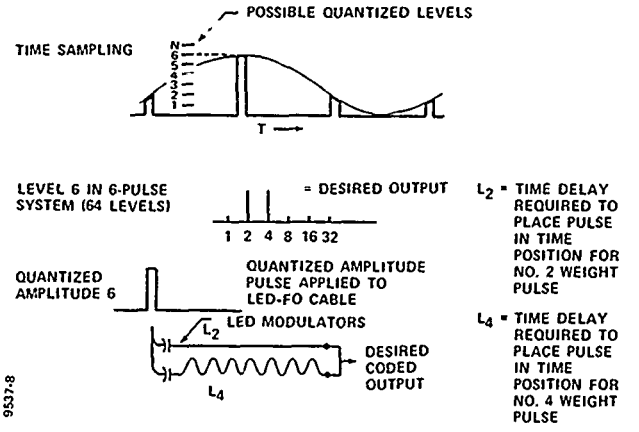

(b)

Figure 6. Fiber Optic Analog-to-Digital Conversion

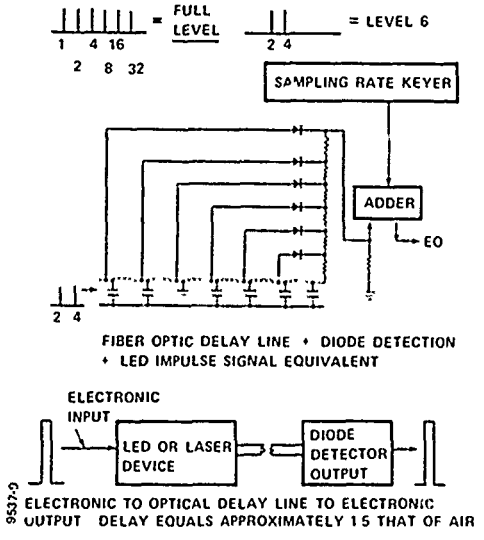

Figure 7. Fiber Optic Digital-to-Analog Conversion

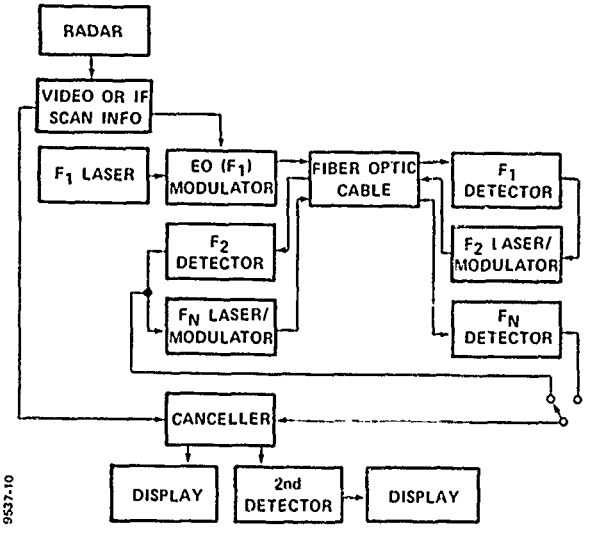

Figure 8. Long Delay Fiber Optic System for Incremental and Stable MTI by Color Reiteration

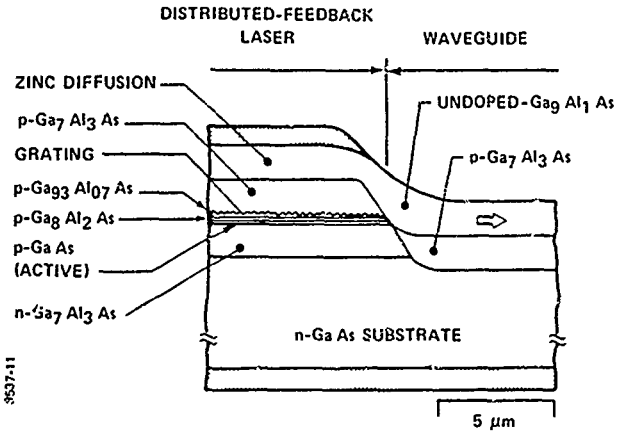

Figure 9. Six-Color Laser IC

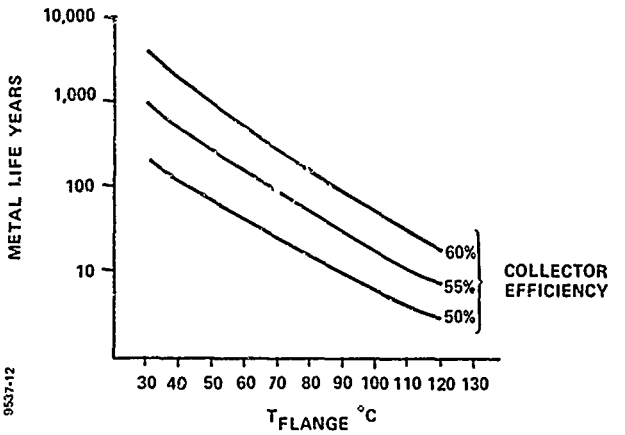

Figure 10. Transistor Life Time vs Flange Temperature

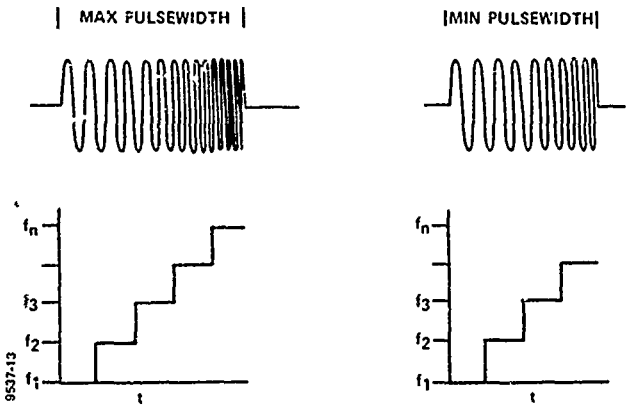

Figure 11. Frequency Chirping Techniques

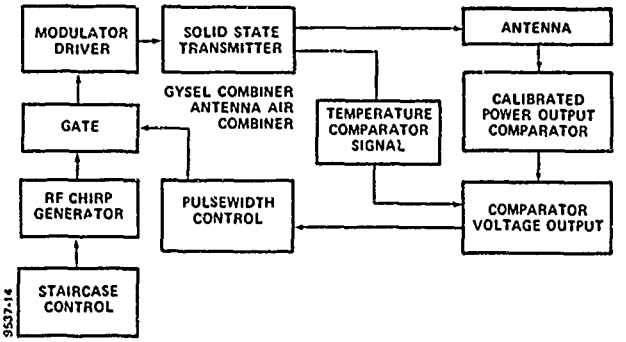

Figure 12. Transmitter Block Diagram

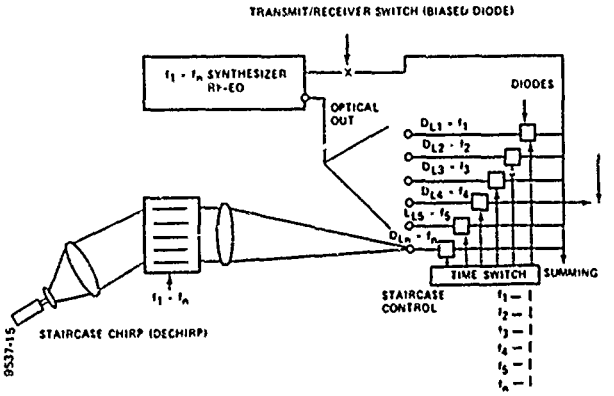

Figure 13. Chirping and Dechirping Techniques

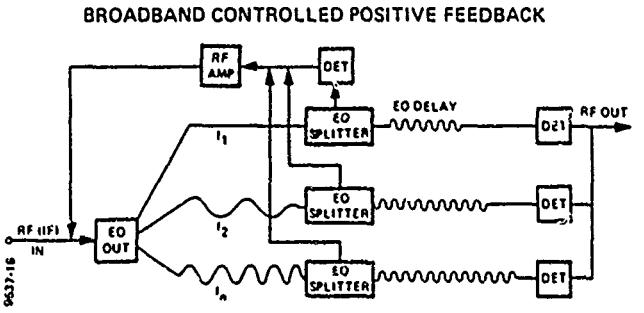

Figure 14. Combined Delay Line Filter and Time Sequence for "Dechirping"

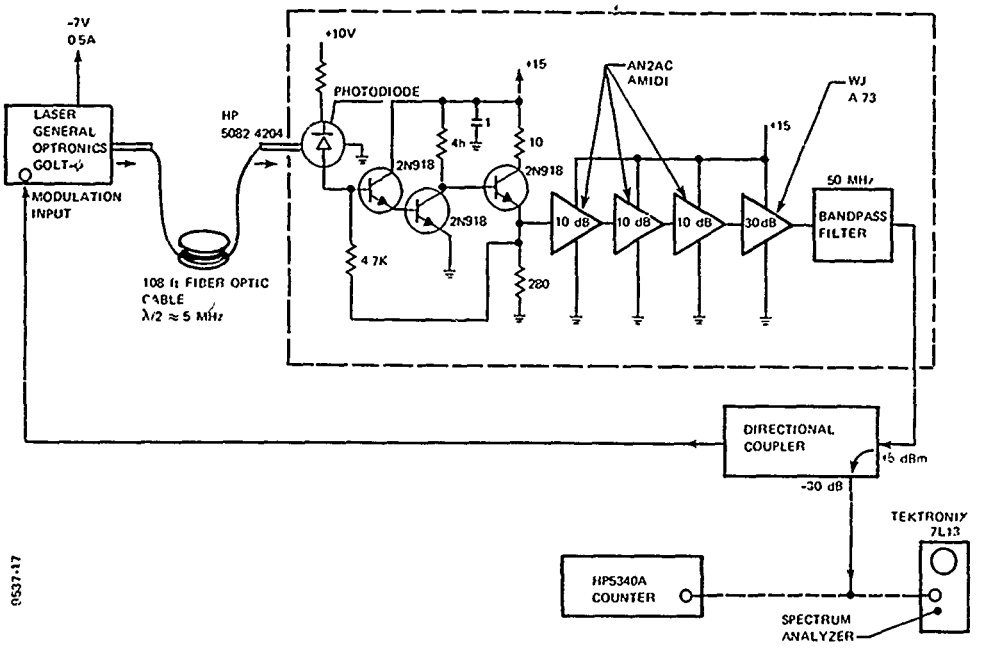

Figure 15a. Fiber Optic Oscillator Test Setup

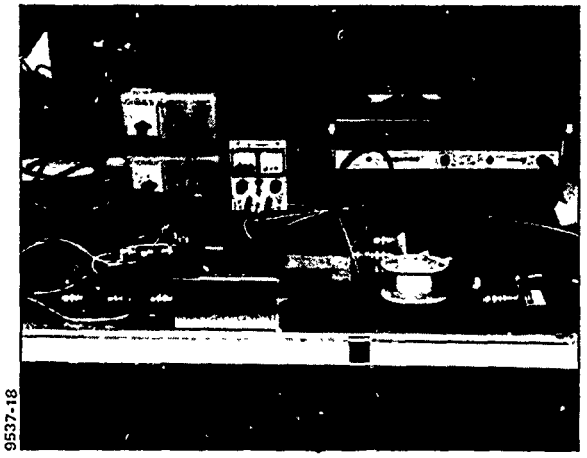

Figure 15b. Breadboard Oscillator Used in Tests

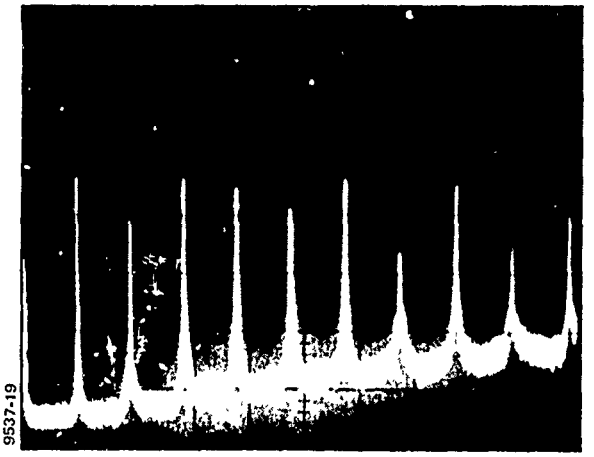

Figure 16. Output Spectrum without Bandpass Filter
Center Frequency – 25 MHz
Horizontal Scanwidth – 5 MHz/Div
Vertical Amplitude – 10 dB/Div
IF Bandwidth – 30 kHz

References

(1) Applied Optics and Optical Eng., R. Kingslake, Academia Press, Vol. IV, 1967.

(2) Dr. Douglas A. Pinnow, HAC, May 18, 1978, IEEE Fellows Meeting, Los Angeles, California.

(3) George M. Dillard, Radar Signal Processing using Fiber and Integrated Optics, IEE/IEEE Radar 77.

(4) Electronics/February 2, 1978, pp. 63, 64.

(5) Skolnik, "Radar Handbook" pp. 20-35, McGraw-Hill, Copyright 1970.

BULK ACOUSTIC RESONATORS FOR MICROWAVE FREQUENCIES*

R.A. Moore, F.W. Hopwood, T. Haynes
Westinghouse Defense & Electronics System Center
Baltimore, MD 21203

B.R. McAvoy
Westinghouse R & D Center
Pittsburgh, PA 15235

Abstract

Bulk acoustic resonators are under development for control of low noise microwave oscillators operating directly at microwave frequencies. Q's greater than 5000 are typical for the frequency range of 1 to 10 GHz and have been fabricated to 20,000.

The combination of high Q and useful electroacoustical coupling is achieved through geometry which includes a substrate of high acoustical Q medium, which is large compared with the wavelength at the operating frequency. Sapphire, ruby, spinel, YAG and diamond are under investigation. External coupling is provided through a piezoelectric transducer.

The use of a separate body and electroacoustical coupling mechanism has two key advantages:

a. A much higher overtone resonance can be used usefully.
b. The resonator itself is not restricted to being piezoelectric.

By using a separate transducer, coupling is not limited by high overtone levels of operation. Operation at these frequencies is allowed even with resonator thickness up to a large fraction of a millimeter. This provides for greater physical rigidity and lower vibration sensitivity than even high Q VHF quartz resonators demonstrate. Because the substrate need not be piezoelectric for coupling, a large variety of media which have Q's which are an order of magnitude greater than quartz are available.

Comprehensive computer modeling of propagation characteristics for various media has provided design data for many crystalographic directions for bulk mode acoustic resonators and delay lines. Experimental verification of the computer data thus far, has been accomplished for sapphire and diamond.

Introduction

The main contribution to improving the stability of fundamental frequency microwave oscillators comes from the design of a high Q cavity with a suitable low temperature co-efficient. Bulk acoustic resonators are under development for control of low noise microwave oscillators operating directly at microwave frequencies. Q's greater than 5000 are typical and have been fabricated to 20,000 for frequency range of 1 to 10 GHz. The very wideband of accessible frequencies made available for oscillator control is suggested by Figure 1. The figure displays a series of resonances from 8GHz to 10 GHz offering the complete range for frequency stabilization applications. Each resonance or overtone response of a high Q nonpiezoelectric substrate is driven by thin film piezoelectric transducers. Though the high Q substrate is operated in an overtone mode, the piezoelectric (ZnO film transducer is operating in its fundamental frequency range. The Q of this resonator is over 4500.

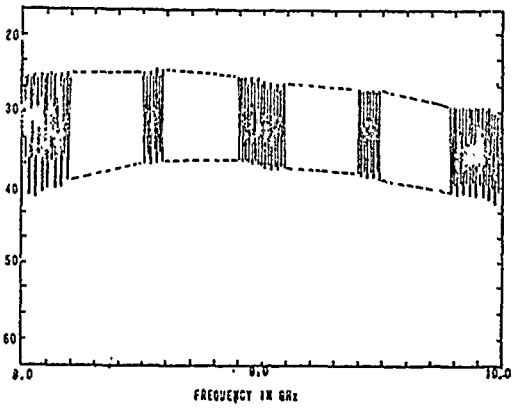

Figure 1. Transmission characteristics of X-band bulk acoustic resonator with wideband ZnO film transducers and spinel substrate. Though only 8 to 10 GHZ is shown for clarity, the resonator respondens from 6 to 10 GHz. Q is 4500.

Application requirements place increasing demands on designers to achieve high-Q operation in decreasing volumes. Figure 2 illustrates the Q's available for operation directly at microwave frequencies. Except for the bulk acoustic resonators the chart illustrates a tendency for decreasing Q's with decreasing volume. The bulk acoustic resonator is clearly the first technology to depart from this trend illustrated by the first three techniques and is the only technique which offers the possibility of Q's equivalent to electromagnetic cavities in sufficiently compact form to be considered for many applications.

*The work reported on this paper has been supported in part by Contact F19628-78-C-0108, Rome Air Development Center, Deputy for Electronic Technology, Hanscom Air Force Base, Massachussetts, 01731

To achieve an equivalent phase noise performance to quartz crystals, resonator Q's must meet or exceed the value governed by the relation $FQ = 10^{13}$ shown in Figure 3. Illustrated on the graph are typical crystal resonators of 10^6 and 10^7 at 10MHz and 100MHz, respectively. Also superimposed on this plot is a number of points representing measured Q's for SAW resonators taken from the literature [2,3,4,5] and those for various bulk acoustic microwave resonators.

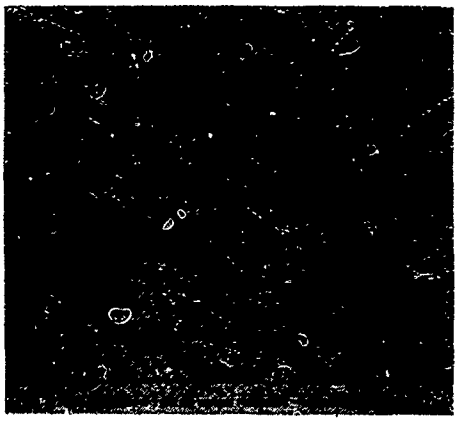

FIGURE 2

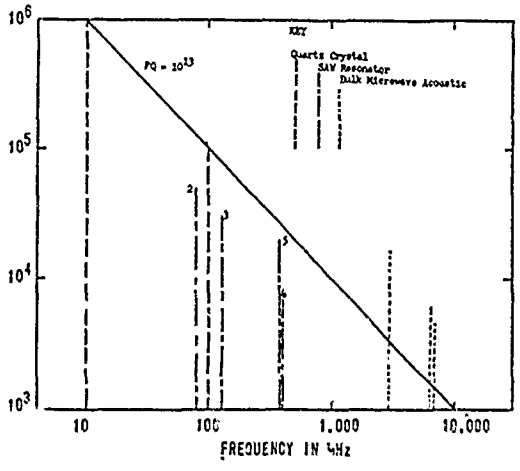

Figure 3. Required Q to meet noise performance of high quartz crystal stabilized oscillators.

It suggests that bulk acoustic resonators have genuine potential for providing low noise stabilization of oscillators operating fundamentally at microwave frequencies.

Description

The use of a separate body and electroacoustical coupling mechanism has two key advantages:

a. A much higher overtone resonance can be used usefully.

b. The resonator itself is no longer restricted to being piezoelectric.

By using a separate transducer where coupling is not limited by high overtone levels, operation through X-band is allowed even with resonator thickness up to a large fraction of a millimeter. This provides for greater physical rigidity and lower vibration sensitivity than even high Q VHF quartz resonators demonstrate.

Because the substrate need not be piezoelectric for coupling, a large variety of media (as suggested by Figure 4) have Q's which are an order of magnitude greater than quartz. (Q is related to propagation attenuation by the relation $\pi/(\alpha\lambda_a)$ when λ_a is the acoustic wavelength. A number of materials have been under investigation including sapphire, YAG, diamond and spinel.

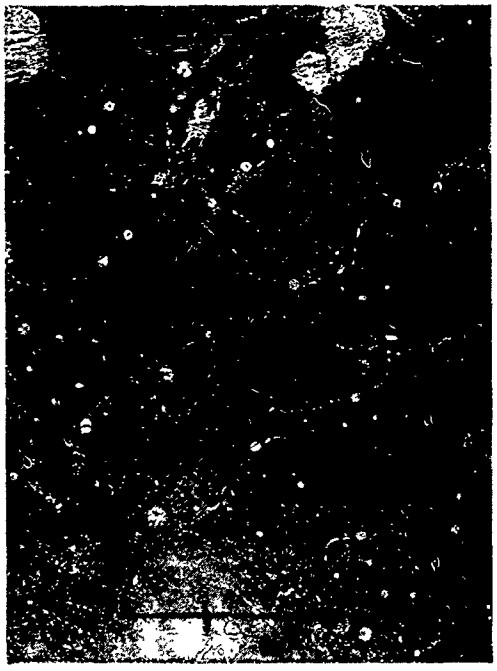

Figure 4. Graph of propagation loss and Q's of substrate media suitable for microwave acoustic resonator. Note that except for lithium niobate, non-piezoelectric media are superior to piezoelectric media.

The latter material, (111) spinel, has been tested to x-band with encouraging results. Figure 5 is an example of a transmission resonance at 7.5 GHz. The Q in this instance is about 6000 and the FQ product exceeds 4×10^{13}. The substrate thickness for this unit is 10 milli-inches providing an overtone separation of 35 MHZ from 7 GHz to 8 GHz as shown in the top portion of Figure 5.

Details of the transducer design on a sapphire substrate (a-axis propagating) are shown in Figure 6. The botton contact of the transducer is a layer of (111) gold on which is r.f. sputtered a thin film of

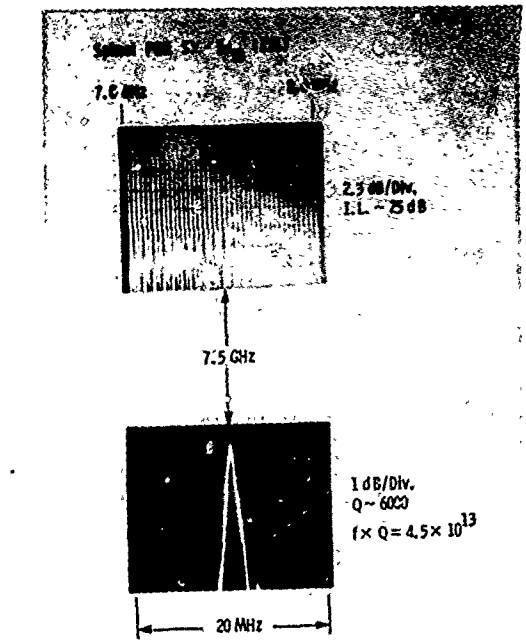

Figure 5. Response of X-band spinel resonator which provides Q of 6000.

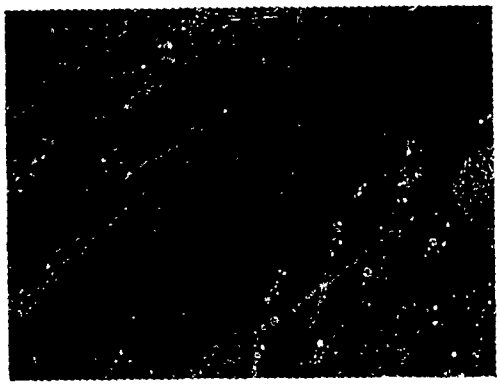

Figure 6. Geometry of Microwave Acoustic Resonator showing substrate and transducer detail.

ZnO, the top contact is made with a film of chrome aluminum. With the application of a high frequency potential a longitudinal bulk mode standing wave is generated in the substrate. We have found that the longitudinal bulk mode resonance will stay relatively free of spurious (shear mode) interference if the substrates are defect and strain free and if the surface substrate is a good perpendicular boundary to impinging waves. This latter remark requires that the surface contain no pits and be free of subsurface damage. Special polishing techniques have been developed for the substrates to satisfy this condition.

A further condition for optimum resonator performance is that non-divergent power flow directions be chosen for the longitudinal mode. The selection of substrate resonator direction is substantially simplified by the examination of specific cases using a computer program which treats all the anisotropic properties of candidate media. The direction for which shear mode do not couple to the substrate and for which longitudinal mode energy is confined due to anisotrophy is the ideal case. An additional very important consideration is that the temperature coefficients of delay be as small as possible consistent with the above criteria.[7] The latter goal requires a compensating mechanism in the substrate medium where a temperature induced dimensional change is mitigated by a velocity change so that the propagation delay (resonant frequency) remains unchanged. As a general rule this means a sign reversal among the elastic moduli and the temperature coefficients of these moduli. A resonator is the most sensitive check on previously measured materials parameters.

Analysis of Substrate Media

The temperature analysis of substrates is aided by computer generated plotting formats - one polar and other rectilinear. Hidden line drawings of 3-dimensional temperature coefficient data are planned in determining the most suitable directions for low temperature coefficient resonance because they are visualized easily.

Our previous experiences with optimization routines in searching for zero temperature SAW directions showed that in general many cases require a large amount of computer time. Also, our experience has been that larger numbers of manual runs are necessary, especially for high resolution data.

The Christoffel equation[8] and the equation for the power flow angle form the basis of the calculation carried out by the computer program. The Christoffel equation is the third order matrix equation whose roots are equal to the mass density of the crystal multiplied by the squares of the phase velocity of one of the planar wave solutions. The normalized eigenvectors are the corresponding particle velocity components. The computer phase and particle velocities are used to compute the power flow vector. With knowledge of the temperature coefficients of the elastic moduli a simple iterative procedure over desired temperature increments yields the velocity change with frequency. This result, corrected for acoustic path length change, gives the temperature coefficient of delay.

Provision has been made to present data in terms of a set of Miller indices and Euler angle coordinate transformations, is made somewhat easier with this presentation. As mentioned, 3-D hidden line drawings are expected to be the most useful. Data input can be read from punched cards or from a previously prepared data element stored in a user defined file. A conversational routine with prompts is used to call out crystal planes of interested and what data is required.

Any crystal cut (scan plane) is available as is shown in Figure 7, which is the temperature coefficient delay for an arbitrary cut in spinel ($MgAl_2O_4$).

Figure 7.

The longitudinal mode (solid line) is seen to slightly vary about the 24 ppm/°C coordinate as a function of direction in the plane. The dashed lines in the plot are the two shear modes. Figure 8, shows the temperature coefficient plot for Lithium Niobate in the X-Z plane. Along the X direction the temperature coefficient exceeds 70 ppm/°C for the longitudinal mode decreasing to about half what value in the Z direction. Figure 9 shows (010) plane normal sapphire which includes the "a" cut for which propagation is along the X coordinate. The temperature coefficient of delay is 32 ppm/°C.

Diamond, at present, seems to be a very good candidate for bulk mode resonators as is shown in Figure 10. Here, again, the X-Z plane (cube face)

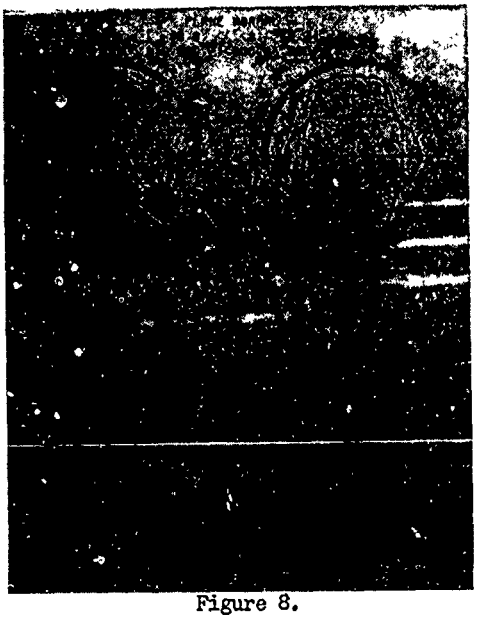

Figure 8.

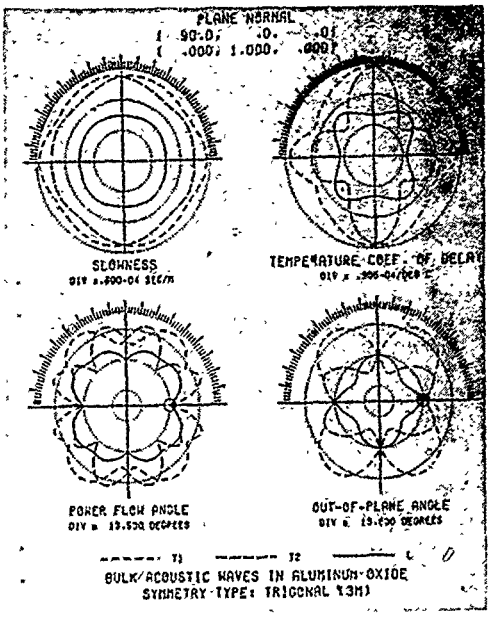

Figure 9.

is presented, but the maximum temperature coefficient for any propagation direction in the plane is less than 8.0 ppm/°C.

Results of Measurement

A measurement of the frequency shift with has been carried out on resonators of "a" oriented sapphire and (111) cut diamond. For those cuts the compensated temperature sensitivity is 32 ppm/°C and 8 ppm/°C, respectively. The substrates have been used both for a first order evaluation of the effect of the transducers on temperature sensitivity and, in the case of diamond, a first test of a material which may lead to temperature stability. In all regards, except temperature stability, both ma-

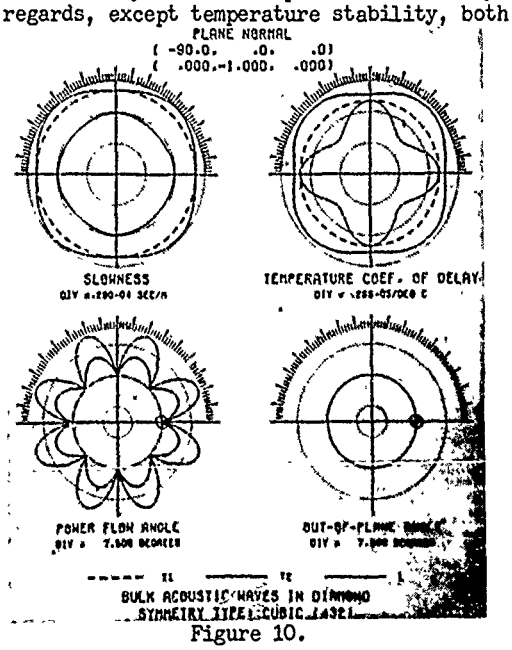

Figure 10.

terials would be suitable for resonator fabrication.

Data was taken the range of 0°C and 100°C. The sapphire resonator displayed 31.7 ppm/°C and the diamond 7.5 ppm/°C. Though these are preliminary measurements being within 1 ppm/°C of the computer temperature sensitivity suggests that actual resonator temperature stability is close to that of the substrate medium.

Preliminary measurements of phase noise as a measure of oscillator stability have been carried out by using the bulk acoustic mode resonator. The results, taken with a delay line phase bridge, are equivalent to anything which has been achieved with a VHF quartz crystal controlled oscillator multiplied to the same frequency range.

Conclusions

Bulk acoustic microwave resonators are described which demonstrate Q's of over 15,000 and have operated through 1-10 GHz frequency range. Favorable temperature characteristics and control of a low noise oscillator operating directly at microwave frequencies have been shown. The oscillator has equivalent phase noise characteristics to quartz crystal controlled oscillators multiplied to the same frequency.

Acknowledgement

Acknowledgement is given to R. Sundelin for fabrication and test of resonators and to M. Meiseles for guidance in oscillator design.

References

1. Haruo Yokouchi, "Cavity Stabilization of MW Oscillators," Microwave Journal, Vol. 21, P. 68, December 1978

2. C. Lardat, "Experimental Performance of Grooved Reflective Array Compressors and Resonators," 1976 Ultrasonics Symposium Proceedings. IEEE Cat. No. 76CH 1120-5SU, pp. 272-276.

3. L.A. Coldrum, R.L. Rosenberg, J.A. Rentschler, "Monolithic Transversely Couple SAW Resonator Filters," 1977 Ultrasonics Symposium Proceedings, IEEE Cat. No. 77 CHI 264-150, pp. 888-893.

4. T.R. Joseph, "Phase Lock SAW Delay Line and Resonators Oscillators," 1976 Ultrasonics Symposium Proceedings, IEEE Cat. No. 76 CH1120-550, pp. 234-239.

5. E.J. Staples, J.S. Schoenwald, S.J. Dolochycki, J. Wise, T.C. Lin, "Application of SAW oscillator to Low-Noise Communications Systems," Int. Microwave Symposium Digest, IEEE Cat. No. 79CH1439-9, MTT-S, pp. 168-170, 1979.

6. J. Murphy, M.M. Gad, "A Versatile Program for Computing and Displaying the Bulk Acoustic Wave Properties," IEEE Cat. No. 78CH-1344-157, pp. 172-181.

7. R.A. Moore, B.A. Newman, B.R. McAvoy, and J. Murphy, "Temperature Characteristics at Microwave Acoustic Resonators," 1979 IEEE International Microwave Symposium Digest, IEEE Cat. No. 79CH1439-9 MTT-S, pp. 171-173.

8. B.A. Auld, "Acoustic Fields and Waves in Solids," Vol. 1, p. 165, Wiley and Sons, 1973.

THE EFFECT OF THE SAMPLING ACTION OF PHASE COMPARATORS ON FREQUENCY SYNTHESIZER PERFORMANCE

M.J. Underhill and R.I.H. Scott

Philips Research Laboratories
Redhill, Surrey, U.K.

Summary

A simple phase-locked loop frequency synthesizer can be treated as a pair of phase-locked oscillators. The sampling action of the PLL phase comparator can limit the synthesizer switching speed both theoretically and in practice. The sampling action also limits the output spectrum improvement which can be achieved by phase locking. Some results are given and compared with continuous and sampled data analyses of a model of the frequency synthesizer system.

Introduction

A frequency synthesizer is a system which attempts to transfer the stability and spectral purity of a fixed frequency reference oscillator to a digitally set variable frequency output. Frequency synthesizers are also often required to switch as rapidly as possible from one frequency to another.

The simple phase locked loop (PLL) type of digital frequency synthesizer is effectively two oscillators phase locked together. All phase comparators are in fact sampling devices and in this paper we show how this limits the switching speed and the degree to which the output oscillator spectrum can be improved by phase locking.

Until now the loop bandwidth has usually had to be much lower than the sampling frequency in order to reduce the effect of phase comparator noise, In this case the sampling action has little effect on the shape of the output spectrum or on the switching speed and these can be predicted by treating the frequency synthesizer as a linear continuous feedback control system. However with the new Philips low noise phase comparator [1] the loop cut-off frequency and switching speed can be increased until the effect of the sampling action is very apparent. This paper aims to explain and characterise some of the effects that are observed. To do this both continuous and sampled data system analysis is used.[2]

The System Model

Figure 1. gives the block diagram of a typical PLL frequency synthesiser. The output signal from the voltage controlled oscillator (VCO) at frequency F_o after division by a programmable ratio N is phase compared with the stable fixed reference at frequency F_r. Any frequency or phase error detected by the phase comparator corrects the VCO frequency until a stable locked condition is achieved with $F_o = NF_r$.

For analysis all signals and transfer functions are defined in terms of the output phase C(s) and so any control voltage in the feedback loop is considered to be equivalent to a phase value.

The phase comparator is taken to be of the sample-hold type as shown. A digital phase comparator of the type which gives its output signal in the form of pulses can be considered as a sampler without the zero order hold section. However as will be seen later, only with the sample-held type of phase comparator can the theoretical performance of the system be approached in practice. Thus the sample-hold case is used in the following analysis.

Three noise sources are shown. $U_1(s)$ represents the spectrum of noise from the reference together with any noise from the programmable divider. In practice $U_1(s)$ is made very small and can be neglected in the analysis. $U_2(s)$ represents the noise generated in the phase comparator. It has two components. The first is a flat white noise spectrum which is assumed to be generated by the active devices and output resistance of the phase comparator. There can also be a 1/f noise spectrum components from the active devices, but in general this is usually found to occur below the frequencies of interest and so is ignored here. The second component is a discrete signal at the sampling frequency. This ideally should not exist, but in practice it occurs because of crosstalk in the sampling switch or because of leakage in the hold circuit. The third noise source $U_3(s)$ is the VCO phase noise which is assumed to dominate other VCO noise sources in the region of interest. It causes the VCO spectrum to have a $1/f^2$ characteristic so that as shown in Fig. 1 $U_1(s)$ will represent a flat spectrum with the VCO acting as an integrator (with a pole not quite at s = 0).

The loop filter is shown split into two parts. The proportional plus integral section determines the type of the feedback control system. For example if the integral gain is set to zero a type 1 control characteristic is obtained. This settles with a zero frequency error but finite phase error, this latter being indicated by the final value of the phase comparator output voltage not being the same value for any frequency setting. A finite integrator gain makes the system type 2 so that no phase error remains in the steady state. If the integrator gain is made much lower than optimum what is called a "quasi-type one" system is obtained. This can give a faster reduction in frequency error than a type 2 system with an optimum integrator gain but at the expense of a slowly decaying final phase error.[3]

The second part of the loop filter is a low pass section which is used to reduce the effect of both phase comparator noise components. The cut-off frequency and number of poles may either be determined by the wish to reduce the effect of one, or the other, or both noise components depending on their relative values and the synthesizer noise and transient response specification.

The usual strategy for choosing the loop filter is to aim for an overall system with the fastest transient response without any serious degradation of the VCO spectrum at any point by the phase comparator noise. When this results in a loop cut-off frequency which is much lower than the sampling frequency it is easier to analyse the synthesizer as a continuous control system rather tna by using a sampled data model.

Analysis as a Continuous System

A very common frequency synthesiser system choice is the type 2 system of order 3 which has a single extra low pass loop filter section. This is therefore taken as an example for continuous system analysis. It is by such an analysis that one can see if the sampling action of the phase comparator is likely to become a limiting factor particularly on the transient response. The criterion for this will be seen to be whether the optimum design given by continuous system analysis requires a loop cut-off frequency which approaches or exceeds about one sixth of the sampling frequency,

Transient Response

The transient response of the synthesiser to frequency steps can be obtained in the following way. For the chosen example the loop transfer function is of the form

$$K\,G(s) = \frac{K(s+a)}{s^2(s+b)} \qquad \ldots.(1)$$

where the low pass section pole is at $s = -b$ and $a = K_i/K$ being the ratio of the integral gain K_i to the proportional gain K.

A fractional frequency jump of δF_o required in the output frequency F_o can be considered to be effected by a sudden phase ramp change of $2\pi\delta F_o$ appearing at the input to the programmable divider and having a Laplace transform of $2\pi\delta F_o/s^2$. The phase ramp in effect is caused by a sudden change in the programmable divider ratio. The closed loop transfer function from this input point to the error signal point is $(1+KG(s))^{-1}$ so that for the frequency change δF_o the putput phase error is given by the Laplace transform

$$E(s) = \frac{2\pi\delta F_o}{s^2(1+K\,G(s))} \qquad \ldots.(2)$$

Figure 2 is a root locus plot for this with the gain K as a parameter. The open loop poles are of course those of equation 1. If we choose $a = b/9$ and $K = b^2/3$ we obtain a triple closed loop pole at $s = -c = -3a$. This is defined as an optimum because it represents the time response with the fastest decay rate and minimum of overshoot.

We now have for the optimum

$$E(s) = \frac{2\pi\delta F_o(s+3c)}{(s+c)^3} \qquad \ldots.(3)$$

and for the time response of the phase error by taking the inverse Laplace transform of E(s):

$$e(t) = 2\pi\delta F_o e^{-ct}(t-2ct^2) \qquad \ldots.(4)$$

The time to settle for a given frequency step is thus solely determined by the parameter c. For convenience c is defined as the loop cut-off frequency. In this case it is the frequency where the loop gain has dropped to unity, this representingthe knee of the final 12 dB/octave closed loop response roll off. c is now chosen to be as large as possible whilst still allowing the output spectrum requirements to be fulfilled.

The Output Spectrum

The three noise sources, reference noise, phase comparator noise and VCO noise can be respectively represented by their power spectral densities $U_1(\omega)$, $U_2(\omega)$ and $U_3(\omega)$. The baseband output spectrum $C(\omega)$ is then the sum of the noise source contributions each modified by their repsective power spectrum transfer functions from input points to the common output.

The baseband spectrum is transferred to r.f. by the frequency or phase modulation process which occurs in the VCO. But frequency modulation is a highly non-linear process where all components of the input signal intermodulate with each other. However, in our case one signal is much stronger than the rest and it has a very narrow spectrum. This corresponds to d.c or $\omega = 0$ in the baseband

and to the carrier or output frequency signal at r.f. In this case all baseband components appear reflected about the carrier frequency in the r.f. spectrum as if frequency modulation were a linear modulation process. But if there is a second discrete component in the baseband, such as arises from sampling frequency cross-talk for example, two discrete sidebands will be created on either side of the carrier and these will have spectra which are exact copies of the main carrier spectrum with its noise sidebands. Effectively each discrete component has the same phase modulation as is present on the main carrier. This effect is apparent in the frequency synthesizer spectrum shown in Figure 3a. It illustrates how the non-linear FM modulation process can cause difficulties in interpreting baseband noise process from observations of the r.f. spectrum.

In order to relate theory with practice it is useful to be able to predict spectra in the form in which they appear on a practical spectrum analyser. The main difference in the displayed spectra shape arises from the shape and bandwidth of the spectrum analyser filter function. The effect is negligible on smoothly varying noise spectra but it means that narrow spectral lines appear with the shape of the filter characteristic and width a peak amplitude almost equal to the total power of the line.

Most of our spectrum measurements are made on an Adret spectrum analyser with a fixed bandwidth of 10 Hz. In the following calculations of predicted spectra we model this as having a filter with a fifth order pole with a damping such that the noise filter bandwidth is 10 Hz. Thus any spectral components of power A which are substantially narrower than 10 Hz are assumed to have a power density spectrum which gives a spectrum analyser output of

$$AF_1 = A.\left(\frac{33.9}{f^2+33.9}\right)^5 \qquad \ldots.(5)$$

To calculate the theoretical spectrum, first we assume the spectral distributions but not amplitudes of the noise sources. Next we calculate the closed loop transfer function G(s) from a noise source to output and convert it to a power spectrum transfer function by one of the following expressions:

$$G(\omega) = |G(j\omega)|^2 = G(j\omega)G(-j\omega) = G(s)G(-s)\Big|_{s=j\omega} \qquad \ldots.(6)$$

The product of the noise source spectral distribution and its $G(\omega)$ then gives its contribution to the output spectrum. The amplitude of the contribution is usually back calculated by an appropriate spot measurement on the observed spectrum that is being modelled. Finally any discrete signals present are given the same noise spectral distribution as the main carrier.

For example applying this method to the type 2 order 3 system under consideration we obtain for the spectrum analyser output in terms of cyclic (not angular) frequency f

$$S(f) = 10\log_{10}\left[F_1+F_2F_3+10PF_4+A_r(F_{11}+F_{12}F_{13}+10PF_{14})\right] \qquad \ldots.(7)$$

where F_1 is the carrier component with a distribution given by the analyser filter i.e.

$$F_1 = \left(\frac{33.9}{f^2+33.9}\right)^5 \qquad \ldots.(8)$$

If the reference oscillator is very noisy then its spectrum shape should be used instead of F_1 as above.

F_2 is the VCO output natural phase noise spectrum which is assumed to have a 6 dB per octave roll-off. F_2 is designed to take account of the analyser 10 Hz bandwidth in that $F_2 \leq 1$ for all f. It is defined in terms of a parameter x which is determined by the VCO noise N_d relative spectral density at frequency d from the carrier. Thus

$$F_2 = \frac{10x}{f^2+10x} \qquad \ldots.(9)$$

$$\text{with } x = N_d \times d^2 \qquad \ldots.(10)$$

F_3 is the transfer function of the VCO noise to the output; it represents the improvement that the negative feedback loop provides. It is therefore a function of the closed loop system in question, in this case an optimum type 2 order 3 system. It can therefore be shown to be

$$F_3 = \frac{f^4(f^2+9c^2)}{(f^2+c^2)^3} \qquad \ldots.(11)$$

where c is in Hz and not rad sec^{-1} as previously.

P is the assumed flat phase noise level. It can be estimated in practice by measuring the synthesizer noise spectrum close to the carrier.

F_4 is the power spectrum transfer function for the phase noise and for the system in question is

$$F_4 = \frac{c^4(9f^2+c^2)}{(f^2+c^2)^3} \qquad \ldots.(12)$$

A_r is the amplitude of the spurious component at baseband frequency r.

F_{11}, F_{12}, F_{13} and F_{14} are respectively F_1, F_2, F_3 and F_4 shifted in frequency by $\pm r$ where r is the spurious frequency, This is effected by letting f become

$$f \rightarrow |f|-r \qquad \ldots.(13)$$

Results of Continuous System Analysis

The spectrum analyser output predicted by equation 7 has been programmed on a Hewlett Packard 9825A desk calculator so that on the associated X-Y plotter it produces spectrum plots of the same size as those obtained from an Adret spectrum analyser. In this way the predicted and measured results can be directly compared.

For example, Figure 3b shows a predicted spectrum which displays similar features to those shown in the measured spectrum of Figure 3a. The repetition of the main carrier spectrum can be correctly observed on the spurs. But as will be seen, the predicted spectrum shown here ignores the suppression of the carrier sideband noise at the sampling frequency effected by the sampling action of the phase comparator. The VCO spectrum that would be observed in the absence of phase locking is also plotted in Figure 3b for comparison purposes and on all subsequent predicted plots.

Figures 4a and 4b show another comparison between practice and theory. In this case the synthesizer had been correctly adjusted for an optimum transient response. This can easily be achieved by observing the phase comparator output with a square wave either applied to the VCO input directly or used to switch one of the digits of the programmable divider. The proportional and integral loop gains are then trimmed until the fastest exponential decay of the transient output of the phase comparator is observed. The close agreement between theory and practice in this case also confirms the validity of the assumption of a flat spectrum phase comparator noise. The VCO used in this case was in fact a VCXO. This was used in order to be able to observe the phase comparator noise uncorrupted by any VCO noise.

Figure 5 shows how for a given phase comparator noise the predicted output spectrum changes rapidly as the loop cut-off frequency c is changed. If the phase noise is low a high value of c can be used without the VCO spectrum being degraded excessively at any point. If then the phase comparator sampling frequency is low we find in practice that this continuous system model is no longer valid and a sampled data model is required to predict the system characteristics.

Analysis as a Sampled Data System

In the following we show how the sampling action limits the transient response and effects the output spectrum of a frequency synthesiser. In this case we assume a system model as in Figure 1 with a type 2 order 2 system in which the low pass loop filter section is not present.

Sampled Data Transient Response

Using sampled data z-transform analysis the open loop transfer function including the sampler and zero order hold is

$$KG(z) = Z\left[\frac{K(s+a)(1-e^{-sT})}{s^3}\right] = \frac{K'(z+a')}{(z-1)^2} \qquad \ldots.(14)$$

where $K' = KT(aT+1)$, $a'=(aT-1)/(aT+1)$, $a=Ki/K$ as before and T is $(F_r)^{-1}$ the sampling period

The z-plane root locus in Figure 6a shows that the closed loop poles can be moved into the optimum response position at the centre of the unit circle if we have $a'=\frac{1}{2}$ and $K'=2$. It also shows that if the loop gain K' in an attempt to increase the loop cut-off frequency is increased beyond $2\frac{2}{3}$ the system becomes unstable.

A frequency jump of δF_o is represented by a ramp transform

$$R(z) = 2\pi\delta F_o \frac{Tz}{(z-1)^2} \qquad \ldots.(15)$$

and the closed loop error transform is $(1+K'G(z))^{-1}$ so that the optimum phase error response with $a' = \frac{1}{2}$, corresponding to $a = 1/3T$, and $K' = 2$, corresponding to $K = 3/2T$, is

$$E(z) = 2\pi\delta F_o T/z \qquad \ldots.(16)$$

This has a sampled time response corresponding to a single error signal impulse at time $t = T$ after the step. At time $t = 2T$ there is no residual error.

Thus the optimum type 2 order 2 system has a dead-beat response with no phase error remaining two sampling periods (2T) after the frequency jump. This is clearly a very fast response.

By a similar argument one can show that an ideal type 1 order 1 system comes to rest after only one sampling period. See Figure 6b for root locus.

Sampled System Spectra

For a sinusoidal component of VCO noise $V(j\omega)$ at frequency ω, we can calculate the resulting contribution to the phase output signal C(s) as

$$C_V(j\omega) = \frac{V(j\omega)}{1+K\,G^*(j\omega)} \qquad \ldots.(17)$$

For a sinusoidal component of phase noise $P(j\omega)$ the contribution is

$$C_p(j\omega) = \frac{P(j\omega)KG(j\omega)}{1+KG^*(j\omega)} \qquad \ldots.(18)$$

$KG^*(j\omega)$ is the sampled sinusoidal signal loop transfer function. For the type 2 order 2 system we can put $z = e^{st} = e^{j\omega T}$ in this case so that we have:

$$B(j\omega) = \frac{1}{1+KG^*(j\omega)} = \frac{1}{1+K'G(z)} = \frac{(z-1)^2}{z^2} = (1-e^{-j\omega T})^2 \quad \ldots.(19)$$

$$= 4\, e^{j\omega T}\, \mathrm{Sin}^2(\omega T/2) \quad \ldots.(20)$$

To convert this to a power spectrum transfer function we put

$$B(\omega) = |B(j\omega)|^2 = 16\, \mathrm{Sin}^4(\omega T/2) \quad \ldots.(21)$$

Implicit in putting $z = e^{j\omega T}$ in the above is that one is treating only the primary signal component of the impulse sampler assumed in the z-transform analysis. Further examination of the system shows that in practice the secondary spectrum components are swamped by the primary component spectrum.

Using equations 17, 18 and 21 we can deduce the following new expressions for F_3 and F_4 to be used in equation 7 to derive the predicted sampled system spectrum. F_3 for the VCO noise becomes

$$F_3 = 16\, \mathrm{Sin}^4(\pi\, fT) \quad \ldots.(22)$$

where $T = F_r^{-1}$ is the sampling frequency.

For the phase noise transfer function we have

$$F_4 = \frac{(9f^2T^2+1)\ \mathrm{Sin}^4(\pi fT)}{(\pi fT)^4} \quad \ldots.(23)$$

Figure 7 shows the predicted optimum 2 order 2 spectrum for the case of no phase comparator noise. It is clear that some degradation of the VCO spectrum occurs at half the sampling frequency although the close-in noise and the noise at the sampling frequency is suppressed.

Figure 8a shows the on the predicted plot how the comparator noise of the system is also suppressed at the reference frequency. Figure 8b shows a predicted spectrum with reference spurs. Figure 8c shows a measured spectrum of a synthesiser with effectively no extra loop filter. The spurs at a spacing of $F_r/3$ are due to pickup and should be ignored.

In practice it is never possible to achieve a type 2 order 2 system. Always there are extra poles introduced by such practical limitations as the necessity to r.f. decouple the VCO input or the fact that the sample hold switch always has a finite on resistance.

On the basis that the optimum proportional gain value for the sampled data system would have resulted in a continuous system unity gain frequency of $c = 3/4\pi \simeq \frac{1}{4}$ times the sampling or reference frequency, this value can be chosen as indicating the limit of the validity of the continuous analysis. For the pulse type digital phase comparator the limit is $1/2\pi \simeq 1/6$. For simplicity the limit of $c = 1/6 \times F_r$ is chosen as covering both cases.

Limitations of Digital Phase Comparators

A digital phase comparator differs from the sample-hold phase comparator in that it provides its output signal in the form of pulses. For example, in the Philips frequency synthesiser chip[1] there is a digital phase comparator which acts as a back-up for the low noise phase comparator when large frequency steps are made. Such a phase comparator has a tristate output such that for no phase error the output can be considered to be at half the supply voltage i.e. at V/2. Then a positive phase error for instance gives positive pulses going from V/2 to V with a length proportional to the error whilst a negative error similarly gives pulses going to V/2 to 0 volts. The total phase range in this case is from -2π to $+2\pi$ radians implying a gain after averaging the output of $V/4\pi$.

For a sampled data analysis the digital phase comparator can be modelled as a perfect impulse sampler which provides impulses at the sampling instants equal in amplitude to the area of the error pulses. It then has an equivalent gain associated with the sampler of $K_2 = VT/4\pi$.

For the open loop transfer function we have from Figure 9

$$K\,G(z) = Z\left[\frac{K(s+a)e^{-sT}}{s^2}\right] = \frac{K''(z+a)}{(z-1)^2} \quad \ldots.(24)$$

where $K'' = K$ and $a'' = aT - 1$

The extra e^{-sT} represents the fact that the phase comparator responds to any new phase error one period T late.

As before the optimum system is obtained when $K'' = 2$ and $a'' = \frac{1}{2}$. In terms of the component gain values for the synthesizer system shown in Figure 9 we have

$$2 = K'' = K = \frac{K_1K_2R_2}{NR_1} = \frac{K_1VTR_2}{4\pi NR_1} = \frac{K_1'VR_2}{2F_oR_1} \quad \ldots.(25)$$

where the VCO output frequency in Hz is $F_o = N/T$, and $K_1' = K_1/2\pi$ is the VCO sensitivity in Hz per volt.

From equation 25 we have for the proportional gain part of the operational amplifier transfer function

$$\frac{R_2}{R_1} = \frac{4F_o}{VK_1'} \quad \ldots.(26)$$

In a typical practical synthesiser at $F_o = 100$ MHz the VCO sensitivity K_1 would not exceed about 10 MHz/volt, and V = 10 volts, say. This then requires that

$$\frac{R_2}{R_1} = \frac{4 \times 100}{10 \times 10} = 4$$

corresponding to an a.c. gain of four in the operational amplifier stage.

But if the phase comparator is giving out V/2 = 5 volt pulses the operational amplifier output must saturate and only give 5 volt pulses rather than the 20 volt pulses called for. This is true for any practical system unless the VCO sensitivity is excessively high. The a.c. gain of the operational amplifier stage can never exceed an effective value of unity and so in this case the effective loop gain will be a factor 4 too low. Hence the optimum fastest system can never be achieved and one must accept a system with a much longer transient response and switching time.

This effect prevents any frequency synthesizer containing a digital phase comparator from being operated with an optimum dead-beat response.

Conclusions

Linear analysis of the PLL as a continuous system has shown how a PLL digital frequency synthesizer can be designed for the best compromise between the switching speed and output noise spectrum.

Sampled data analysis of the system shows that there is an absolute limit on the transient response and switching speed which cannot be exceeded. Comparison with the continuous system analysis shows that this limit can come into play even if the synthesizer is only designed for low noise and not fastest response time. The limit of applicability of the continuous method is when the required loop cut-off frequency approaches one sixth of the sampling frequency.

The sampling action of the phase comparator can improve the output noise spectrum around the reference frequency sidebands but at the expense of increased noise elsewhere. However, in practice cross-talk in the sampling switch can produce reference frequency spurs having the same noise spectra as the main carrier component. These can mask the noise improvement obtained around the reference frequency sidebands.

Comparisons of practical spectrum measurements with the theoretical predictions derived here from continuous and sampled-data systems analysis have shown good agreement between theory and practice.

Acknowledgements

The authors acknowledge with grateful thanks the help of Peter A. Lewis in producing the calculator programme for plotting the theoretical predictions.

References

1. Underhill, M.J., Jordan, P.A., Clarke, M.A.G. and Scott, R.I.H., "A General Purpose LSI Frequency Synthesizer System", Proceedings, 32nd Annual Symposium on Frequency Control, US Army Electronics Command, Fort Monmouth, N.J. pp365-372 (1978).

2. Saucedo, R. and Schiring, E.E., "Introduction to Continuous and Digital Control Systems", Macmillan Company, 1968, New York.

3. Underhill, M.J. and Jordan, P.A.J., "The Split Loop Method for a Wide Range Frequency Synthesiser with Good Dynamic Performance". To be published.

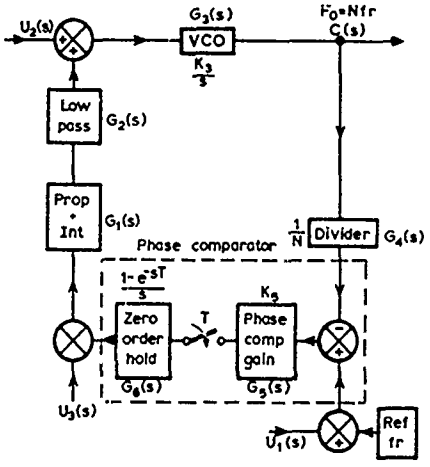

Figure 1 Frequency synthesizer block diagram

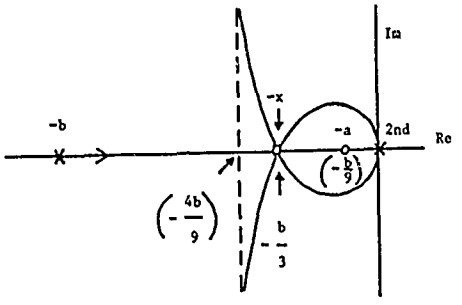

○ = zero

× = open loop poles

□ = closed loop triple pole K = $\frac{b^2}{3}$

Figure 2 Type 2 optimum root locus

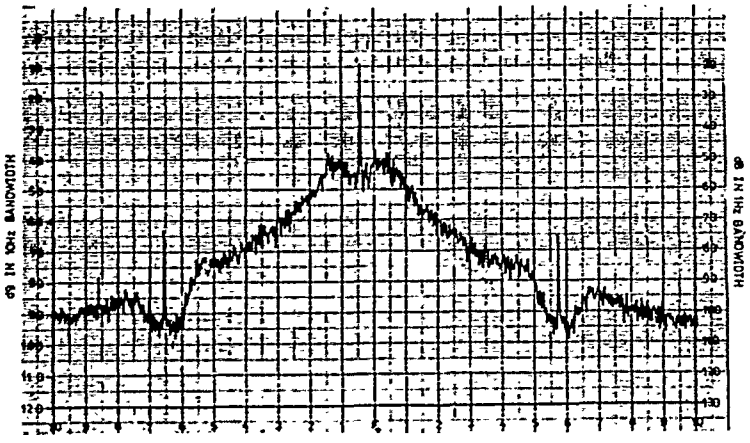

Figure 3a Measured spectrum with reference spurious

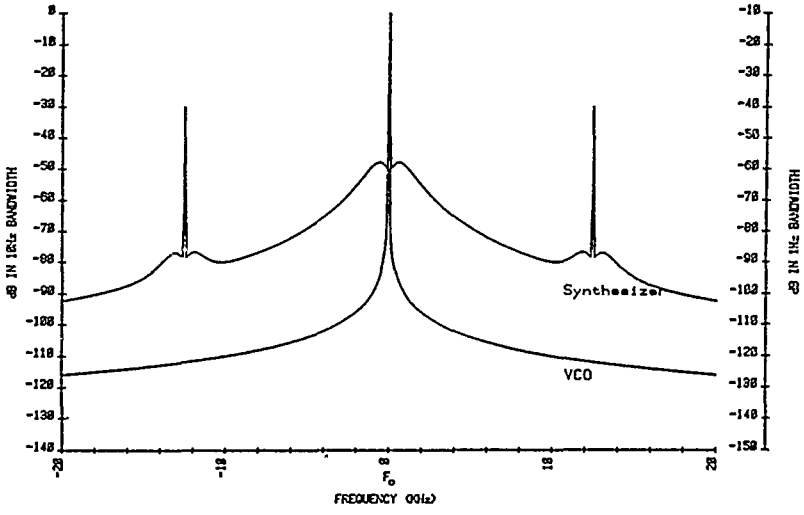

Figure 3b Predicted spectrum with reference spurious

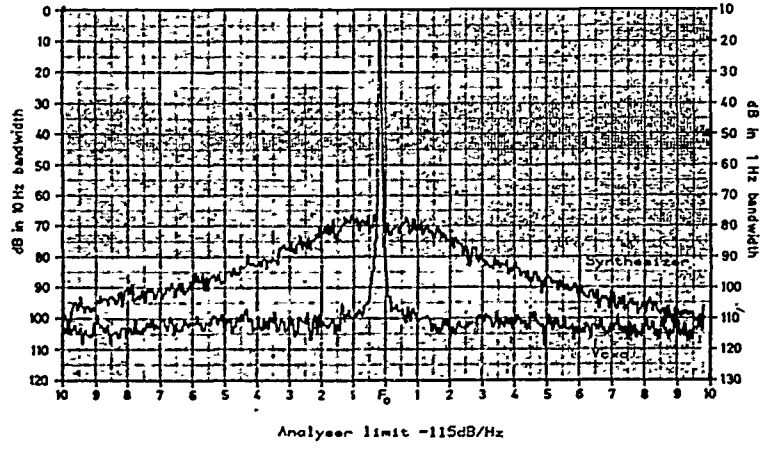

Figure 4a Measured optimum type 2 spectrum

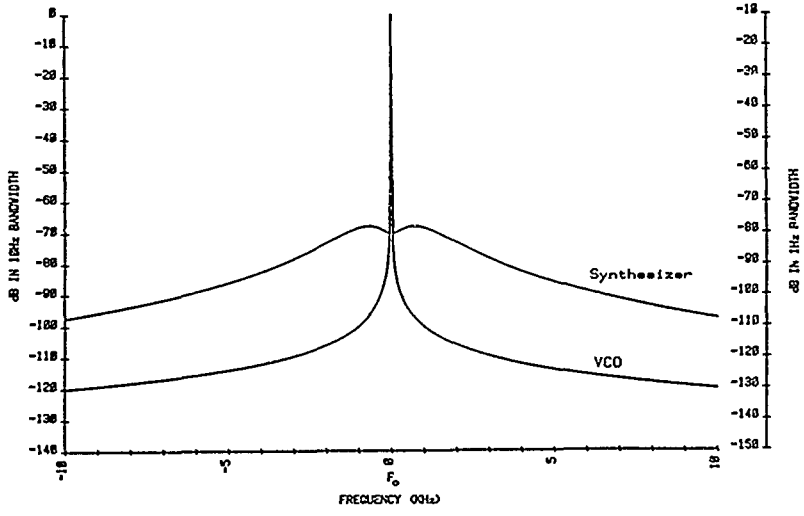

Figure 4b Predicted optimum type 2 spectrum

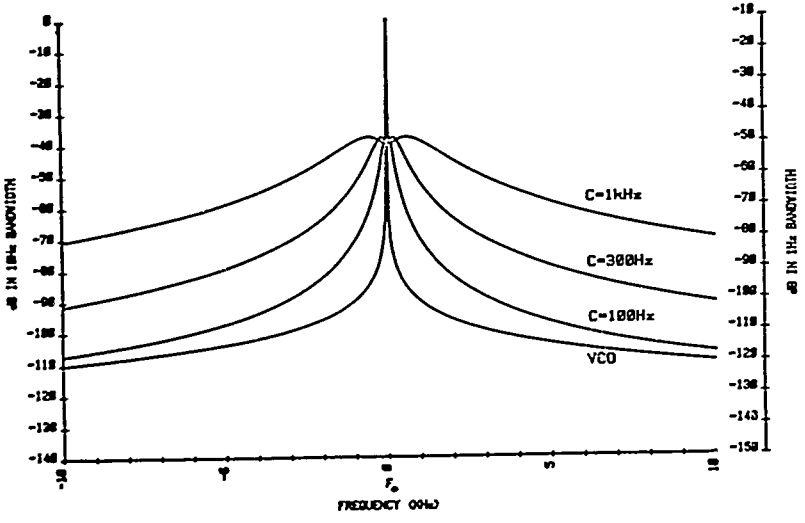

Figure 5 Effect of loop bandwidth on spectrum

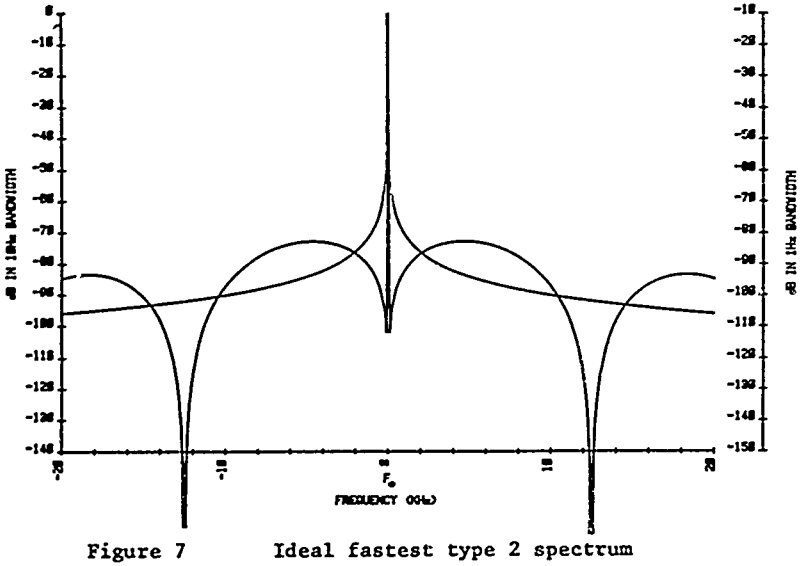

Figure 7 Ideal fastest type 2 spectrum

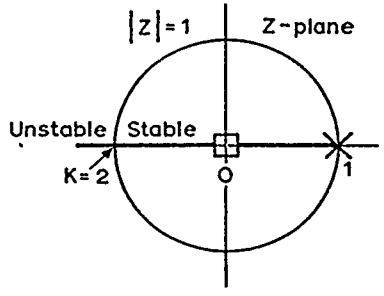

□ = Closed loop pole for K = 1

× = Open loop pole

Figure 6a Fastest type 1 Z plane root locus

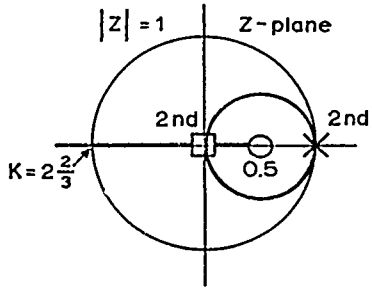

□ = Closed loop double pole per K=2

○ = Open loop zero

× = Open loop poles

Figure 6b Fastest type 2 Z plane root locus

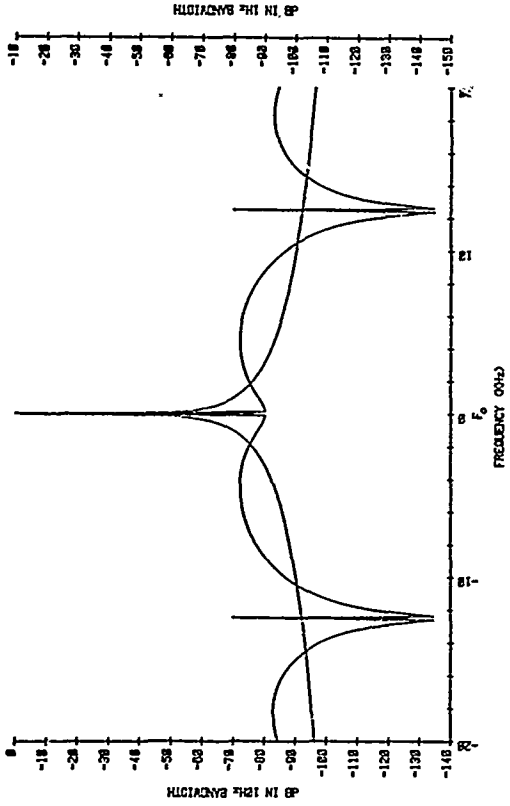

Figure 8b Predicted type 2 wich PC noise and spurious

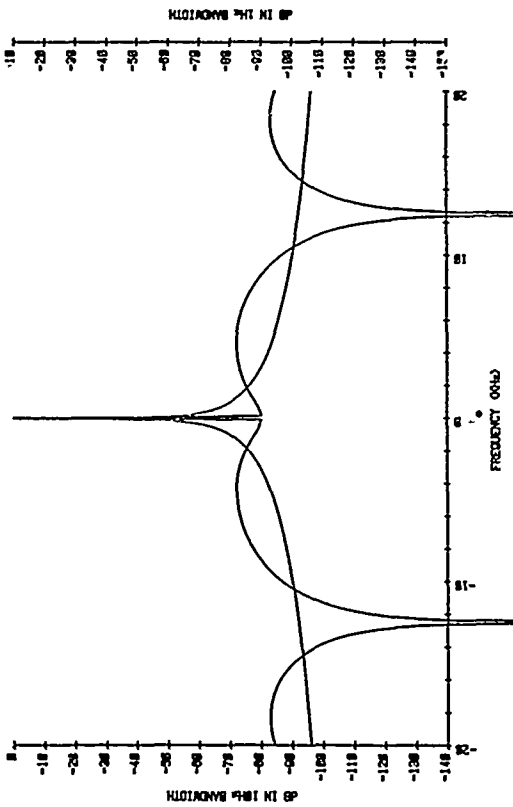

Figure 8a Predicted fastest type 2 with PC noise

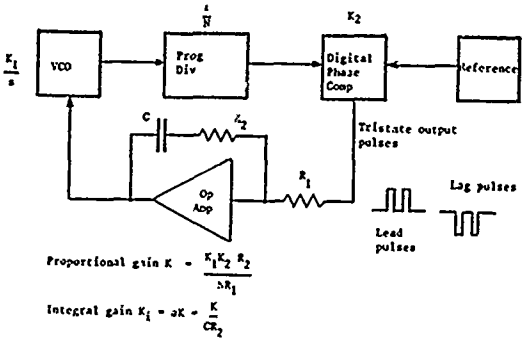

Figure 9

Frequency synthesizer with digital phase comparator

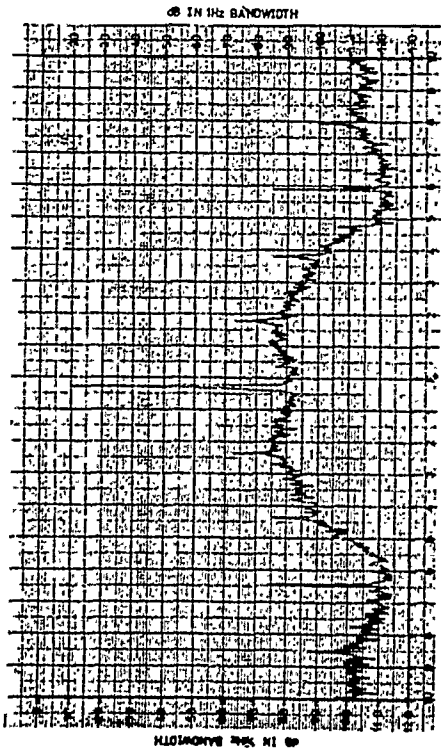

Figure 8c Measured fastest type 2 with PC noise

AN m/n FREQUENCY DIVIDER USING A LAMBDA(Λ)-SHAPED THREE-TERMINAL NEGATIVE RESISTANCE DEVICE

Y. Sekine, M. Suyama, K. Nakamura, H. Sekine and Y. Sakuta

College of Science & Technology, Nihon University
1-8, Kanda Surugadai, Chiyoda-ku, Tokyo, 101, Japan

Summary

In this paper the authors studied the m/n frequency synchronization characteristics, as itemized below.

(1) Derived the equations for calculating m/n frequency-dividing ranges and substantiated the derived equations by experiments.

(2) From the equations derived as above, proved the mutually-adjoining frequency-dividing ratios within the synchronization range are of Farey series.

(3) Ascertained that the frequency divider using the Λ-shaped three-terminal negative resistance device enables m/n frequency division with a large synchronization margin, and verified this by experiments.

Introduction

As negative resistance devices of voltage controlled type in addition to the conventional N-shaped devices, Λ-shaped devices are announed lately and two terminal device is analyzed and studied[1].

We have been engaged in provements and applications of Λ-shaped three-terminal negative resistance devices[2)-4)]. Earlier the authors developed 2 elements Λ-shaped three-terminal negative resistance devices of which operating principle is essentially different from that of the traditional three-terminal negative devices. We found that these new type negative resistance devices have such excellent features as the Λ-characteristics are translated by an amount corresponding to the voltage change. We found further that the CR oscillator which employs the three-terminal negative resistance device is a new type oscillator with a low power consumption, its oscillating frequency is very stable against the supply voltage change, the output voltage remains constant, the oscillating frequency range is as wide as ten times of that uses the conventional element, and the oscillation start supply voltage is as low as 1 volt or lower[4)].

At first, we will show the characteristics of the Λ-shaped negative resistance devices to make clear its characteristics and also the characteristics when such devices are applied to a CR oscillator. In this study we are going to discuss the theory of m/n frequency synchronization range, m/n frequency division synchronization range when external pulse voltage is applied to this CR oscillator and have found that the Farey series is applicable to its result. Last we will indicate that an m/n frequency divider of a large synchronization margin can be obtained with the frequency divider using this Λ-shaped three-terminal negative resistance device.

A Λ-Shaped Three-Terminal Negative Resistance Device and the CR Oscillator

Device

Fig.1 shows equivalent circuits of the Λ-shaped negative resistance devices. Fig.1(a) shows an equivalent circuit of the two terminal Λ-shaped negative resistance device which is called as a Λ-shaped diode, and consists of two complementary depletion type field effect transistors(FET). Fig.1(b) and (c) show the Λ-shaped three-terminal negative resistance devices (hereafter we call them Λ-shaped transistor). Fig.1(b) shows a conventional Λ-shaped transistor which consists of 3 elements so that the current flowing through Λ-shaped diode can be controlled with the third FET. We call this type of Λ-shaped transistor as TΛ-shaped transistor. Fig.1(c) shows a new type Λ-shaped transistor which consists of 2 elements, and this type of Λ-shaped transistor does not need comlementary FET's. We call this type of Λ-shaped transistor as BΛ-shaped transistor. We use the symbol of Fig.1(d) to express Λ-shaped transistor. These devices can be analyzed the operation by means of the characteristics of each transistor.

Fig.2 shows the results of BΛ-shaped transistor. Fig.2(a) shows the I_S vs V_{AS} characteristics with V_{AG} as parameter, (b) shows the I_G vs V_{AS} characteristics with V_{AG} as parameter. The solid lines are theoretical values, and the dotted lines are experimental values. Their two types of values conform quite well.

The characteristics of these BΛ-shaped transistors can be summarized as follows.

1) When Q_1 is saturated, I_S vs V_{AS} characteristics with V_{AG} as parameter are translated into the direction of higher V_{AS} by an amount corresponding to increment ΔV_{AG} of V_{AG}, while, its shape remains unchanged.

2) Translation domain of Q_1 is its saturation domain and can be expressed as follows;

$$V_{AS} \geqq \left| V_{pn} \right| , \tag{1}$$

V_{pn}; pinch off voltage of Q_1.

3) In the domain where Eq.(1) is satisfied, the peak current I_{SP} of I_S remains constant irrespective of V_{AG}.

Judging from these characteristics, application for the CR oscillator to stabilized its oscillating frequency can be considered and application for high-stability frequency divider will be possible.

A CR Oscillator

Fig.3 shows a CR oscillator using the Λ-shaped transistor such like shown in Fig.1(b) and (c), is organized respectively by connecting capacitor C across anode(A) and gate(G), resistor R across G and ground(E), R across source(S) and E.

The voltage across G and E, V_{GE} is dertermined by the following equation.

$$V_{GE} = V_A - V_{AG} + I_S R_{SE} . \tag{2}$$

Thus, when oscillating conditions are satisfied by superimposing load line which represents load R_{SE} on Fig.2(a) to read the cross points with characteristic curves and substituting its values at cross points to Eq.(2), the relation between V_{GE} and I_S is determined as solid line in Fig.4, and oscillation occurs with a cycle of a → b → c → d → e → a.

Oscillating frequency f is approximated by considering the charge of C in the period of V_{Ga} to V_{Gc} in Fig.4 as following equation.

$$f \fallingdotseq 1 / [\, CR_{GE} (\ln V_{Ga} - \ln V_{Gc}) \,] . \tag{3}$$

Eq.(3) signifies that when the external passive elements C and R_{GE} are constant, oscillating frequency f depends on V_{Ga} and V_{Gc}. Therefore, in order that V_{Ga} and V_{Gc} remained constant with respect to the change in V_A, the relationship between V_{GE} and I_S must be maintained constant. Therefore from Eq.(2) in order that the relationship between V_{GE} and I_S remains constant under the condition of that R_{SE} is constant, the changes in V_{AS} and V_{AG} must be equal. Further, the output voltage V_{out} is expressed as

$$V_{out} = I_{SP} R_{SE} , \tag{4}$$

then provide I_{SP} is constant, V_{out} remains constant.

As the I_S vs V_{AS} characteristics of the BΛ-shaped transistor satisfy Eq.(1), it can be said that so far as Eq.(5) is satisfied, the oscillating frequency and the output voltage of the CR oscillator using the BΛ-shaped transistor remained constant irrespective of the supply voltage change.

$$V_A \geqq \left| V_{pn} \right| + I_{SP} R_{SE} . \tag{5}$$

Fig.5 shows the oscillating characteristics against source voltage variation and oscillating frequency deviations characteristic against source voltage variations. These curves indicate that the oscillations start voltage is 0.6V, and when the source voltage is higher than 2V, the change in the output voltage is small and $\Delta f/f$ is as small as 2×10^{-4}/V.

An m/n Frequency Divider

Fig.6(a) shows the waveform of V_{GE} of the circuit depicted in Fig.3. As this gate waveform is linear between V_{Ga} and V_{Gc} via a, b and c, we approximate it as a straight line. This is a significant characteristic if compared to that of a multivibrator which has non-linear part in charge curve at discharge-starting voltage. Fig.6(b) shows a waveform when external voltage is applied and synchronized at division ratio m/n. On Fig.6, regarding to external input pulse, V_p stands for pulse voltage, T_p for period and β for duty factor. Since f equal 1/T, f_p equal $1/T_p$, the following equation can be written for the frequency division ratio m/n.

$$\frac{V_p}{V_{Ga} - V_{Gc}} \geqq \frac{mT - nT_p}{T} = m - n\frac{f}{f_p} \geqq 0 . \tag{6}$$

The low limit voltage $V_{s(m,n)}$ of V_p can be expressed below.

$$\frac{V_{s(m,n)}}{V_{Ga} - V_{Gc}} = m - n\frac{f}{f_p} . \tag{7}$$

The upper limit of V_p is determined when the trading edge of the pulse which is denoted as n'th pulse($1 \leqq n' < n$) and which is nearist to the V_{Gc} has reached V_{Gc}. Therefore Eq.(8) stands by the upper limit voltage $V_{h(m,n)}$ when the circuit is in synchronization with the frequency division ratio of m/n and assuming that the n'th external input pulse is within the m'th cycle($1 \leqq m' \leqq m$) of the CR oscillator output,

$$\frac{V_{h(m,n)}}{V_{Ga} - V_{Gc}} = m' - (n' + \beta)\frac{f}{f_p} . \tag{8}$$

Next we explain how to find m' and n'. m' and n' are determined as integers which minimize $\tau(m',n')$, difference between $m'T$ and $n'T_p$. However

a $\tau(m',n')$ is required to be positive. m' and n' are expressed with the following equations.

$$\tau(m',n') = m'T - n'T_p = 0 \ . \qquad (9)$$

Also because the circuit is synchronizing other frequency division ratio of m/n, $\tau(m,n)$ is expressed by the following equation.

$$\tau(m,n) = mT - nT_p \ . \qquad (10)$$

$\tau(m',n')$ can be written by Eq.(11) from Eq.(9) and Eq.(10).

$$\tau(m',n') = \frac{1}{m}\left[LT_p + m'\tau(m,n) \right] , \qquad (11)$$

where,

$$L = m'n - mn' . \qquad (12)$$

Now because $L \geq 1$, m' and n' for a making minimum, $\tau(m',n')$ can be found to be L=1 by solving Diophantine equation of Eq.(12). From this equation m' and n' can be found using Euclidean algorithm as follows.

$$\begin{aligned} n &= d_1 m + a_3 \\ m &= d_2 a_3 + a_4 \\ a_3 &= d_3 a_4 + a_5 \\ &\ \ \vdots \\ a_{k-1} &= d_{k-1} a_k + a_{k+1} \\ a_k &= d_k a_{k+1} + 1, \end{aligned}$$

from this relationship

$$\begin{aligned} 1 &= a_k - d_k a_{k+1} \\ &= a_k - d_k(a_{k-1} - d_{k-1}a_k) \\ &= -d_k a_{k-1} + (1 + d_{k-1}d_k)a_k \\ &\ \ \vdots \end{aligned}$$

In this method, the subscript of "a" is sequentially reduced and converted into a following equation.

$$1 = Mn - Nm . \qquad (13)$$

Where, both M and N have a same sign. Therefore the solutions are found as follows;

$$M(N) > 0 \qquad m'=M,\ n'=n \qquad (14)$$
$$M(N) < 0 \qquad m'=m-M,\ n'=n-N . \qquad (15)$$

Thus synchronization range at the frequency division ratio of m/n can be obtained as below.

$$0 = m - n\frac{f}{f_p} \leqq \frac{V_p}{V_{Ga} - V_{Gc}} \leqq m' - (n' + \beta)\frac{f}{f_p} \qquad (16)$$

Fig.7 to 10 show the synchronization ranges with β=0. In these figures, (a) is the theoretical values and (b) is the experimental values. Fig.7 shows the synchronization range for a overall region of frequency division with detail omitted Fig.8 is the magnified view of the section from $0.5 \leqq f/f_p \leqq 1$, $0 \leqq V_p/(V_{Ga}-V_{Gc}) \leqq 0.5$, Fig.9 is for $0 \leqq f/f_p \leqq 0.5$, $0 \leqq V_p/(V_{Ga}-V_{Gc}) \leqq 0.5$ and Fig.10 is further expansion of f/f_p for the section $0 \leqq f/f_p \leqq 0.1$.

The above relationship is similar to that of Farey series. Presenting the Farey series as Fig.11, the already explained upper limit voltage of m/n frequency division synchronization is determined by the rational number at the tail end of allow on the right hand which is pointed toward m/n. Therefore when the duty factor β=0, the upper limit voltage of 3/5 frequency division synchronization is the lower limit voltage of 2/3 frequency division synchronization. Thus the synchronization range for frequency division ratio m/n can be easily found by using Farey series

Fig.12 is the frequency division characteristics of the CR oscillator using the conventional TΛ-shaped transistor and Fig.13 is that of the CR oscillator using the BΛ-shaped transistor both are for a frequency division of 1/1, 2/3, 3/5, 4/7 and 5/9.

Now the width of synchronization range is defined in terms of the synchronization margin which is given as the ratio between the maximum source voltage variation range within which synchronization for a division ratio m/n is attainable and the maximum source voltage with which the synchronization is attainable. As shown in Fig.14 denoted by the minimum source voltage $V_{L(m,n)}$ of the widest allowable source voltage change for m/n and by the maximum source voltage $V_{H(m,n)}$, the synchronization margin can be expressed with the following equation.

$$\eta_{(m,n)} = \frac{V_{H(m,n)} - V_{L(m,n)}}{V_{H(m,n)}} = 1 - \frac{V_{L(m,n)}}{V_{H(m,n)}} \ . \qquad (17)$$

Now we explain the synchronization margin by comparing the aforementioned two types of oscillators at a frequency division ratio of 3/5. The synchronization margin $\eta_{(3,5)}$ for V_A in the cace of TΛ-shaped transistor is 2.6 %, and that of the BΛ-shaped transistor is 97 %. Even when the section where the synchronization range is parallel to V_A is taken into consideration, the synchronization margin is 93 %, which is as several tens times of that in the case of the conventional TΛ-shaped transistor.

Fig.15 shows the result of measurement on synchronization range to the divider using BΛ-shaped transistor under the condition where f/f_p is selected as 0.35 at V_A=15 V. The synchronization margin for source voltage V_A at frequency ratio 5/14 was 87 %.

Fig.16 shows the gate to ground voltage waveform and output voltage waveform at frequency division ratio 3/8. The top waveform is that between gate and ground and bottom one is the output waveform.

Fig.17 shows an example of short-term frequency stability characteristics with apparatus depicted in Fig.18. In Fig.17, it is evaluated as a square root of Allan variance. The solid lines are for

the divider using a BΛ-shaped transistor and the dotted lines for one using PLL. From these data it is derived that the short-term frequency stability is as good as that of PLL.

Conclusion

Through our study on m/n frequency divider using the Λ-shaped three-terminal negative resistance device which is called the TΛ-shaped transistor, we found the following:

1) We made the m/n frequency division synchronization region clear.

2) We found that by using Farey series the m/n region can be easily found.

3) The BΛ-shaped transistor is more stable for an m/n frequency divider. A synchronization margin as high as 90 % or over for source voltage variation can be attained.

4) The BΛ-shaped transistor is suitable to be assembled in an IC.

5) It provides a short-term frequency stability as good as that of PLL.

References

1) G. Kano and H. Iwasa: "A new Λ-type negative resistance device of integrated complementary FET structure," IEEE, Trans., ED-21, 7, pp.448 - 449 (July 1974).

2) Y. Sekine and M. Suyama: "A CR Oscillator Circuit Using a Three-Terminal Negative Resistance Device," IECE Japan, J59-C, 5, pp.318 - 319 (May 1976).

3) Y.Sekine, M. Suyama and K. Nakamura: "Utilization of a Lambda(Λ)-shaped Three-Terminal Negative Resistance Device for a CR Oscillator," IECE Japan, J60-C, 10, pp.631 - 638 (Nov. 1977).

4) Y. Sekine, M. Suyama and K. Nakamura: "Two-Element Λ-Shaped Transistor and Its Application to CR Oscillator and High Stability Frequency Divider," IECE Japan, J62-C, 2, pp.145 - 152 (Feb. 1979).

5) S. M. Sze: "Physics of semiconductor devices," New York; Willey, pp.347 (1969).

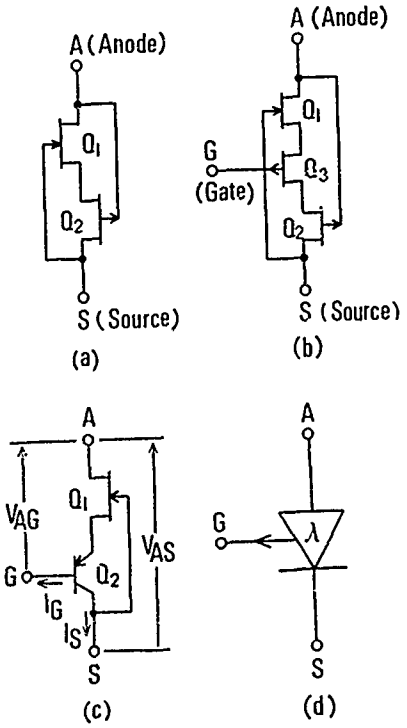

Fig. 1 Λ-shaped negative resistance device.

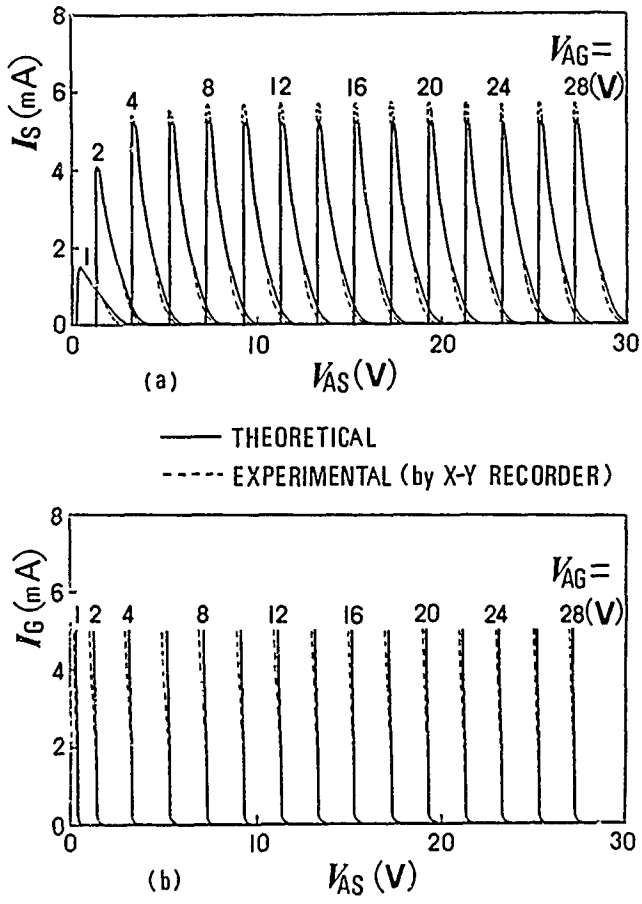

Fig. 2 Static characteristics of the BΛ-shaped transistor.

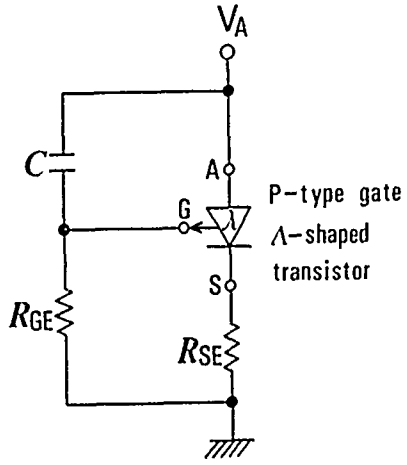

Fig. 3 The CR oscillator circuit.

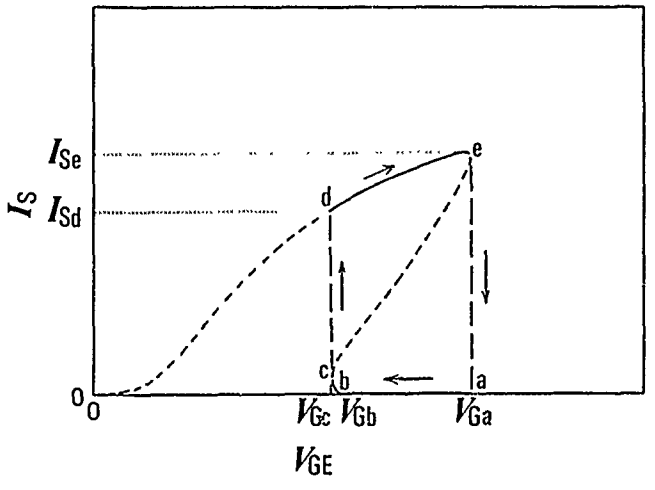

Fig. 4 I_S - V_{GE} characteristic of the CR oscillator.

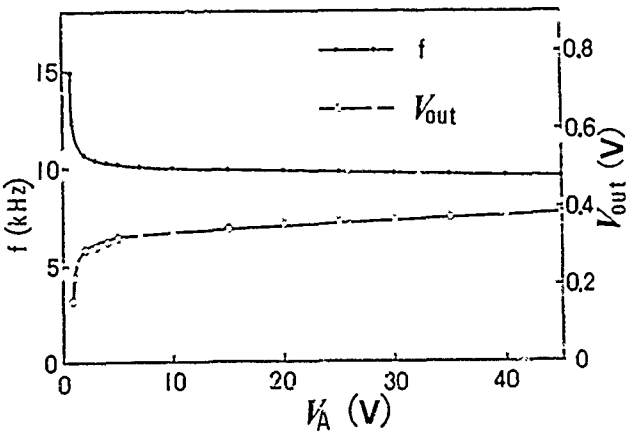

Fig. 5 Oscillating characteristics against source voltage variation.

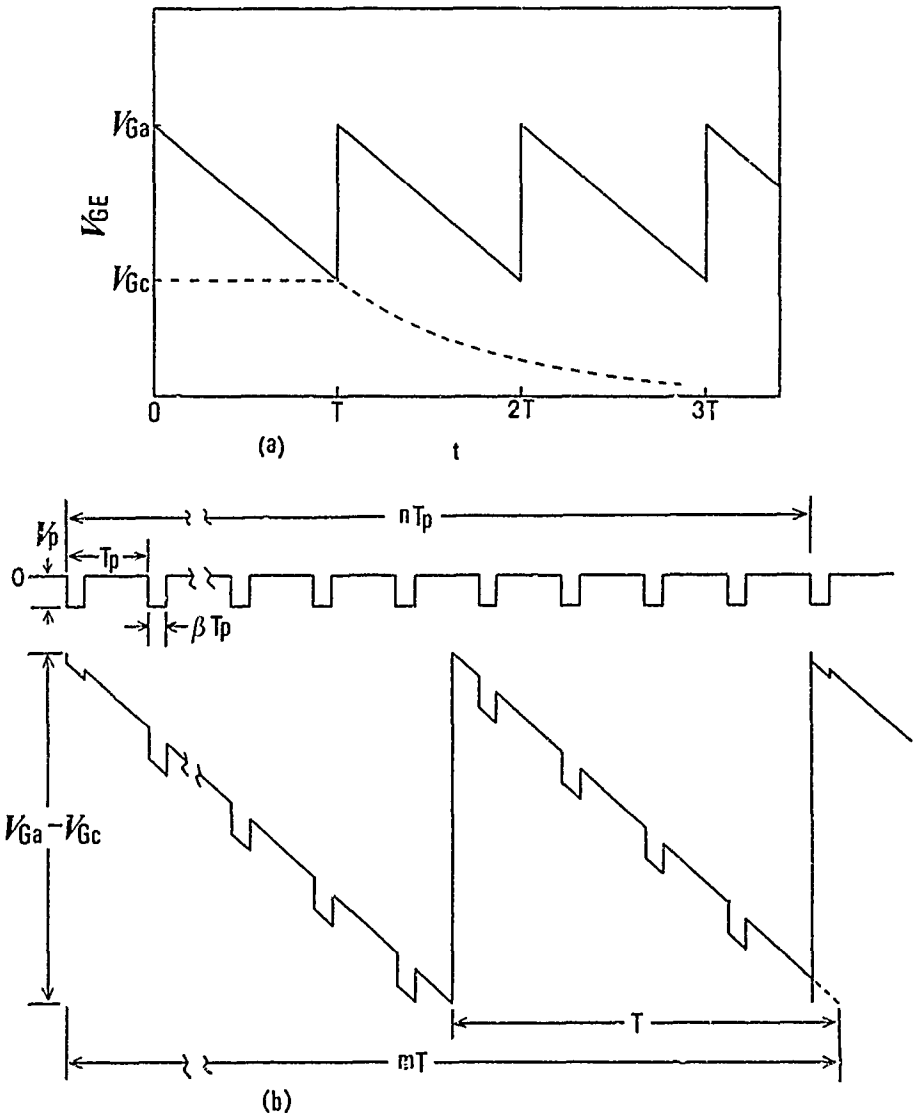

Fig. 6 Waveforms of the gate terminal voltage.

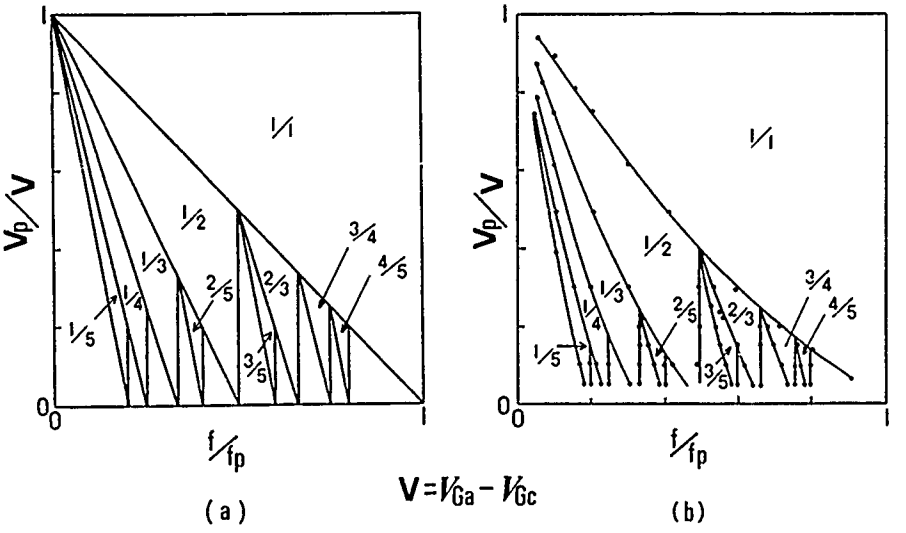

Fig. 7 The synchronization range for a overall region.

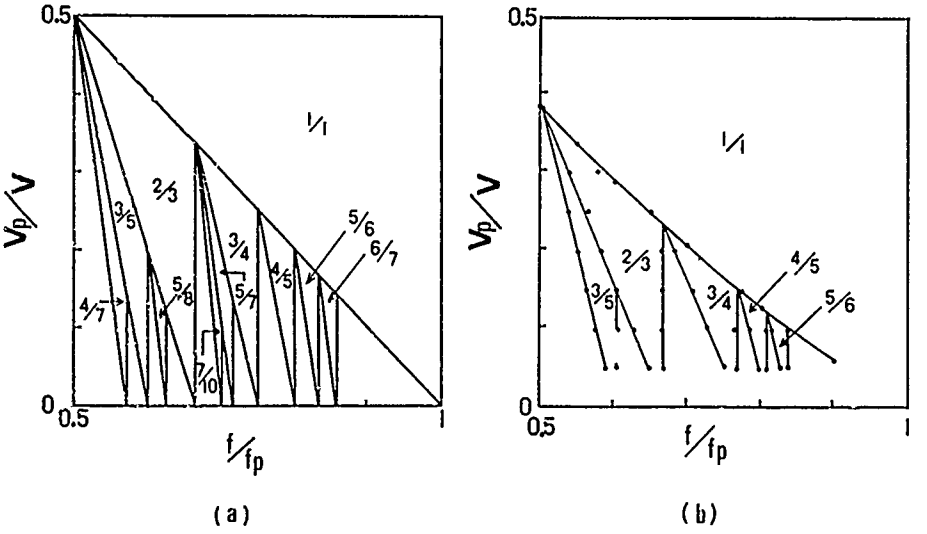

Fig. 8 The synchronization range for $0.5 \leqq f/f_p \leqq 1$, $0 \leqq V_p/V \leqq 0.5$.

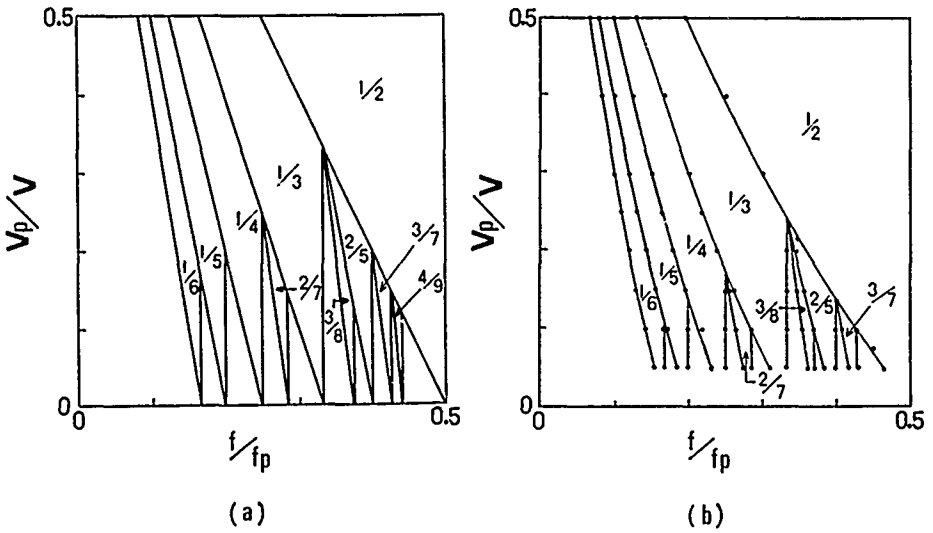

Fig. 9 The synchronization range for $0 \leqq f/f_p \leqq 0.5$, $0 \leqq V_p/V \leqq 0.5$.

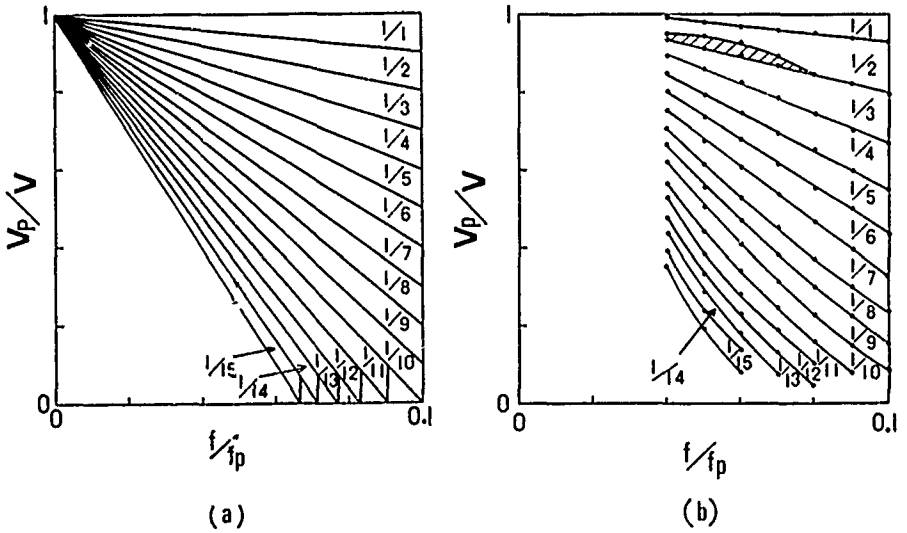

Fig. 10 The synchronization range for $0 \leqq f/f_p \leqq 0.1$, $0 \leqq V_p/V \leqq 1$.

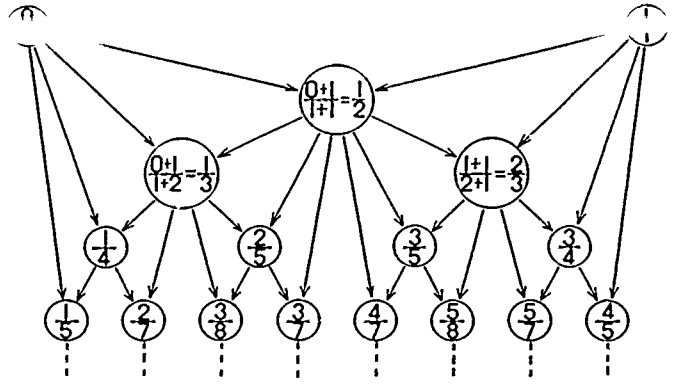

Fig. 11 Schematic Farey series.

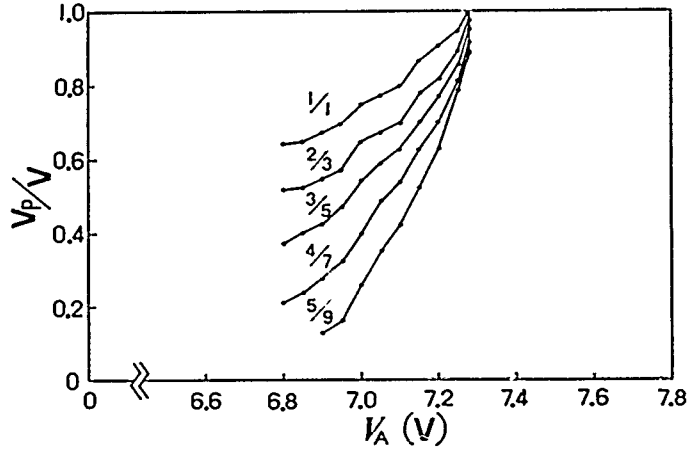

Fig. 12 The frequency division characteristic for the conventional TA-shaped transistor.

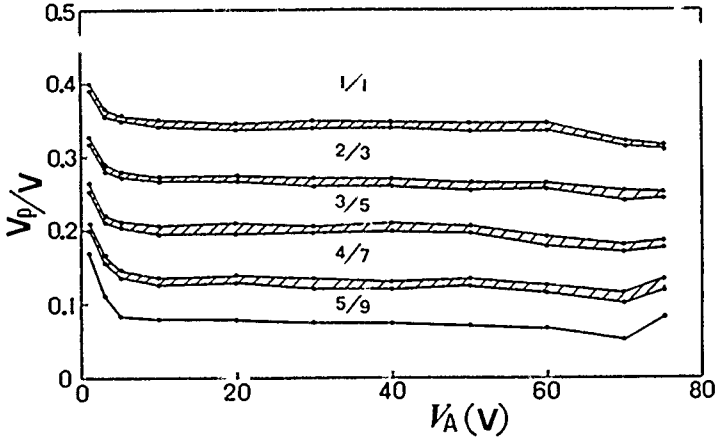

Fig. 13 The frequency division characteristic for the BA-shaped transistor.

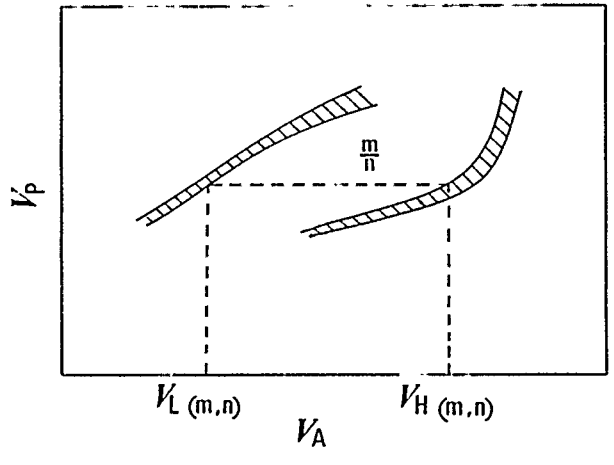

Fig. 14 Schematic of the synchronization range against source voltage variation.

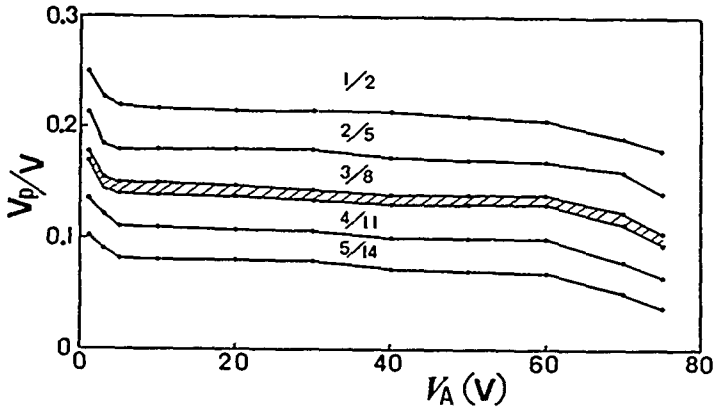

Fig. 15 The frequency division characteristic for the BA-shaped transistor.

Fig. 16 Oscillating waveform. (frequency division ratio 3/8)

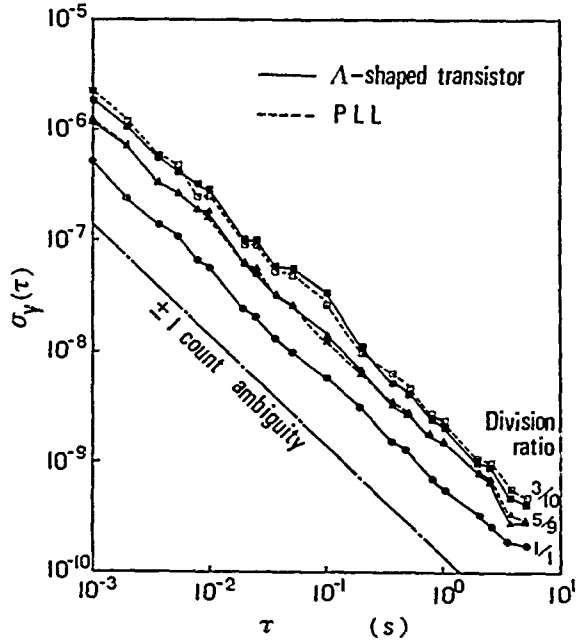

Fig. 17 Short-term frequency stability characteristics.

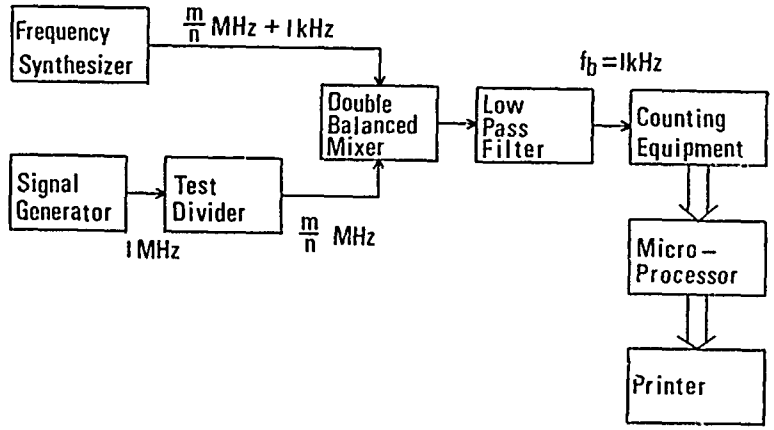

Fig.18 Short-term frequency stability measurment.

A NEW APPROACH TO DATA MANAGEMENT AND ITS IMPACT ON FREQUENCY CONTROL REQUIREMENTS

David L. Blanchard, Arthur J. Fuchs, and Andrew R. Chi
NASA/Goddard Space Flight Center
Greenbelt, Maryland

Abstract

A new approach to data/information management has developed during the past couple of years. This new total system concept is being analyzed and proof demonstrated in the NASA End-to-End Data System (NEEDS) Program. Spacecraft and data/information autonomy are two of the attributes considered essential to this new system concept. An autonomous spacecraft is capable of functioning without external intervention for up to 72 hours by enabling the sensors to make observations, by maintaining its own health and safety, and by going into logical safety modes when anomalies occur. Data/information are made autonomous by associating all relevant ancillary data such as time, position, attitude, and sensor identification with the data/information record of an event onboard the spacecraft. This autonomous data record, called an instrument data packet, is constructed such that the record of the event can be physically identified in a complete and self-contained record that is independent of all other data. All data within a packet will be time tagged to the needed accuracy of the experimenter, and the time markings from packet to packet will be coherent to a UTC time scale. To accomplish all of this, functions such as attitude/orbit determination and universal time should be provided onboard. The need for a satellite-borne frequency oscillator with which to generate the needed time interval as well as the UTC time scale is obvious.

This paper will present the system concept and its requirements for frequency control devices in future autonomous spacecraft.

Introduction

As NASA spaceflight programs approach the era of the 1980's, several enlightening characteristics emerge. When these characteristics are viewed in light of NASA's current data management capabilities, it becomes evident that a new, systematic plan for an efficient data/information system is necessary. This paper will review some of the emerging features that specifically impact our data system and will introduce the system concepts that are currently being developed to meet the challenges of the future. These system concepts are incorporated into a program called the NASA End-to-End Data System (NEEDS). Integral concepts of the NEEDS program are spacecraft and data autonomy which imply the availability of ancillary data including precision time on-board the spacecraft. The features of the onboard ancillary data module and specifically, the procedures required for maintaining precision time onboard the spacecraft are described. Some of the characteristics revealed by the NASA mission model for the 1980's are. An increase in the volume of the data that must be handled, an increase in the sensor resolution required by experimenters, and a decrease in the delivery time being requested by the experimenters.

Figure 1 depicts the evolution of the volume of data being received in terms of the average daily bit rate per spacecraft for both imaging and non-imaging spacecraft. It is obvious from this figure the amount of data that must be accommodated in the 1980's is increasing by orders of magnitude from that in the 1960's and a data system to handle these large volumes of data must be developed.

The resolution of sensor data such as that required by Landsat is also increasing by orders of magnitude as shown in Figure 2 which depicts the ground resolution of sensor data for specific spacecraft. The significance of the increase in sensor resolution is that higher data resolution requires a commensurate increase in the accuracy of the ancillary data. The basic ancillary data are spacecraft position, spacecraft attitude, and event time.

Another characteristic emerging from our projected future requirements is the demand for timely data Figure 3 depicts the evolution of delivery time-demands being made by experimenters. Delivery time is defined in terms of the delay imparted by the system in transmitting data to the users, from the time of detection on the spacecraft to the time when each user has received the sensed data in an engineering format together with all of the ancillary data required for the information extraction process. We are approaching the time where data must be delivered to the users in near real-time without any system delay.

To fully understand the impact of these emerging requirements on the data system, we must first understand the present NASA data system. Figure 4 portrays the current NASA data management system. Sensor data from an instrument shown in the top left portion of the figure is sequentially sampled and multiplexed with other sensor data as a telemetry frame and stored on the spacecraft for later transmission to the ground or relayed to the ground immediately if a ground contact is available. When the data from near-earth free-flyers is received at a ground station, the station forwards the data to Goddard Space Flight Center (GSFC). Here at the processing and distribution center (lower center of Figure 4), the data is decommutated and combined with the ancillary data such as orbit, attitude and time which is determined in a separate facility at GSFC shown in the center of the figure. The data processing facility thus undoes the multiplexing done on the spacecraft and merges each instrument's data with this ancillary data to form data packets The data packets are distributed to the experimenters where, in the reduction and analysis block (lower right of Figure 4), information is extracted. Although this system has worked well in the past, it cannot accommodate large volumes of data in a timely and cost-effective manner. The NEEDS program was instituted several years ago in an attempt to understand, analyze and quantify the present system, to develop concepts for a new, more efficient and cost effective end-to-end data/information system, to design and demonstrate these concepts such that

future requirements could be met in an efficient and cost-effective manner.

The NEEDS Program

Figure 5 indicates that the principal functions performed by a Data/Information (DI) System are sensing an event, transferring data, extracting information, learning, planning, feedback, and sensor conditioning. The objective of a DI system is to efficiently and effectively provide information to the user that will increase understanding of the phenomena being investigated by the mission.

The NEEDS program as the name implies, is an end-to-end data system that functions from the sensing of an event to the delivery of information to a user and from the feedback to condition a sensor for an event detection. Details describing the evolution of the NEEDS program as well as a detailed description of the program, may be found in References 1, 2, and 3. A summary of the main concepts and elements of the program follows.

The main objective of the program is to demonstrate concepts which will provide investigators with the means to efficiently carry out their experimental investigation of the data/information in a form appropriate for immediate analysis, interpretation and feedback for instrument control and subsequent observation. The program is organized into the following teams. systems analysis and integration; information adaptive systems, modular data transport systems; data base management, and software technology The program has identified six general principles which are essential to the development of an operational philosophy and necessary to satisfy the requrements for a NASA data/information system of the 1980's. The essential concepts (principles) are given in Table 1.

The NEEDS functional elements are shown in Figure 6 which encompasses the sensor at one end of the spectrum and the user at the other. The relationship of the NEEDS functional elements to the NEEDS program is shown in Figure 7.

The Information Adaptive System performs the functions at the spacecraft of preselecting the data from an event of interest, performing corrections for instrument distortions to the data, and associating appropriate ancillary data with the event prior to transmission to the ground.

The Modular Data Transport System performs the function of developing packets of autonomous data and moving them efficiently from the sensor or sensor processor through a data base to a user. It includes standardized interfaces and protocols, data bases and the generation of measurement data sets or data packets which include all ancillary data.

The Data Base Management System performs the service to allow users to quickly and effectively locate data/information contained in very large data bases.

The Software Technology System is concentrating on the verification and testing of flight software.

The Systems Analysis and Integration effort analyzes the performance of the present system and NEEDS data/information concepts. The work of all NEEDS subsystems is coordinated so that an integrated demonstration of the system can be made to mission planners.

Ancillary Data Module and Data Packets

A useful data package (packet) should be complete and self-contained. This implies that the measured data and all ancillary data necessary for the identification and successful reduction of data to information should be contained in the package. When an experiment is conducted in any laboratory it is essential to record at the time of the experiment not only the measured data, but also other auxiliary data such as the time and place of the experiment, the environmental conditions, apparatus used, etc. It would not be convenient to record only the measured data and then in a data reduction facility one week later try to recall the time, place, etc. of the experiment. This concept holds true whether the laboratory is on ground or in space. Thus, when data is sensed onboard the spacecraft, it is essential to note.

1. The data that was sensed.
2. The apparatus used (i.e., the sensor ID and mode of operation).
3. Significant ambient conditions (i.e., electron density, etc.)
4. The precise time of the event.
5. The location of the event (i.e., the position and attitude of the spacecraft).

This information forms the basic data packets which are transported to the user. Items 1 through 3 are available on the spacecraft. To accomplish the NEEDS objectives, the precise event time and the position and attitude of the event (Items 4 and 5) must be made available at the spacecraft. Procedures for computing spacecraft position onboard the spacecraft are being developed utilizing data from the Global Positioning System (GPS) or the Tracking and Data Relay Satellite System (TDRSS), references 4 and 5. The spacecraft attitude may be determined as it is on several current spacecraft, through the use of onboard star trackers, gyros and microprocessors as described in Reference 6.

The remaining element of the data packet which must be addressed is the precision time.

Autonomous Spacecraft Clock

It was stated earlier in this paper that experimental data were time tagged by an onboard clock. When the accuracy requirements for time in the early days of the space program (late 50's and early 60's) were on the order of seconds and hundreds of milliseconds per day, they were relatively easy to meet. Even with a crystal oscillator, whose frequency stability was in the order of one part per million per day, there were enough safety margins for refinement when the data were transmitted to and recorded in a ground tracking station. This was because the ground station clocks could be maintained accurately by the use of WWV to about milliseconds order throughout the NASA worldwide network. As the space program achieves maturity and the sensor designs became sophisticated, the requirements for time became more stringent. The requirements were first increased to the order of milliseconds for unmanned spacecraft such as OSO and GOES and then to the order of hundreds of microseconds (μs) for manned spacecraft such as the Apollo. The timing requirements took a leap after the Apollo program as illustrated in Figure 8 which depicts a history of NASA timing requirements including present and projected requirements.

It was during the Apollo program that NASA saw the need for an improved worldwide time distribution technique and

system. While the Manned Space Flight Network was instrumental with more stable atomic oscillators, NASA coordinated and cooperated with the National Bureau of Standards and the United States Naval Observatory in the development of new and improved time distribution techniques. With the use of more stable oscillators and portable clocks, we could maintain our station clocks synchronized to the order of 100 μs worldwide. Through the cooperative effort of the above agencies, we saw synchronization of the Loran C chains to 25 μs and better in the northern hemisphere and the implementation of the dual VLF frequency technique developed from WWVL on the OMEGA navigation system. More advanced systems such as the use of satellites to distribute more precise and accurate time were also developed. The use of a satellite to transfer time was an obvious one because of the reduced effect due to the propagation medium. Cooper and Chi (Reference 7) recently reviewed the satellite time transfer technology. Table 2 gives a summary of the experiments conducted in the past decade and a half. It can be seen from this table that the development of the satellite time transfer technology and the conducting of the experiments are a true representation of international participation.

To meet the needs of spacecraft autonomy and a new generation of data handling and management systems, we are developing an autonomous spacecraft clock, ASC. The ASC is designed to provide, in a future planned spacecraft, the time standard required by all experimenters in the spacecraft which is operated in the autonomous mode. The ASC is to be synchronized as often as necessary by such systems as the Tracking and Data Relay Satellite System (TDRSS) or the Global Positioning System (GPS). TDRSS is a two-way satellite communication system through which user satellites and the ground system can maintain communication with each other. It is under construction by Western Union as a leased service satellite system to NASA. A simple configuration of the use of the satellite system is shown in Figure 9. TDRSS provides nearly worldwide coverage as shown in Figure 10 for elevations angles at 10 and 15 degrees. GPS is a Department of Defense sponsored navigation system. It provides a navigation fix in space giving both a position coordinate (x,y,z) and time (t). It is in the demonstration and validation phase of development.

A conceptual block diagram of the autonomous spacecraft clock is shown in Figure 11. The oscillator may be a crystal controlled oscillator with a long term stability of 1 part in 10^{11} per day or an atomic oscillator when the requirement dictates. Through the parallel binary time code generator a time word will be supplied as the secondary header of the source packet to the telemetry data packet format. In addition, reference frequency sources and pulse signals will be provided to the experimenters for phase clock time synchronization and marking, and other applications.

Most of the TDRSS satellite time transfer programs and ASC are under development. The expected completion date is in the early 1980's when TDRSS and GPS are also expected to be implemented.

Conclusion

The formation of the data packets onboard the satellite will allow us to transmit data to the users in near real-time, thus satisfying the delivery time demands requirements projected in Figure 3 and will, along with the TDRSS, avoid any system bottlenecks, thus accommodating the data volume projections of Figure 1, as well as the delivery time demands of Figure 3. By computing the position and attitude of the spacecraft utilizing GPS, TDRSS, Gyro and Star Trackers, the accuracy requirements levied by the increased sensor resolution depicted in Figure 2 can also be met. This is made possible not only by the high quality of this data, but also by the nature of the real-time computations which avoids unnecessary prediction intervals. The development of the autonomous spacecraft clock which will take place in the early 1980's will provide the most fundamental element of the data packets. This capability is a necessary step for providing the essential concepts formulated under the NEEDS Program.

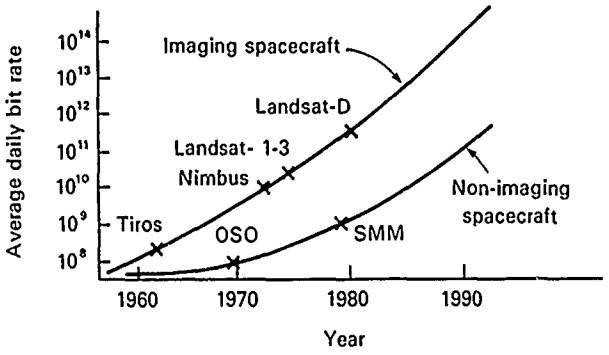

Figure 1. Past, present and future data volume

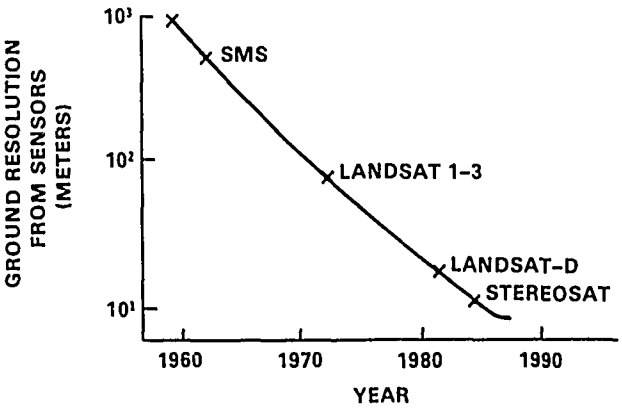

Figure 2. Past, present and future sensor resolution

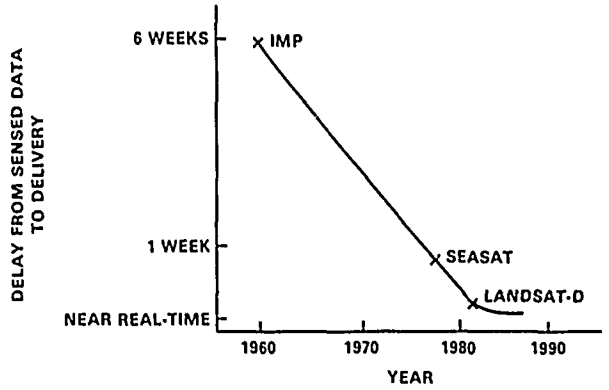

Figure 3. Delivery time demands

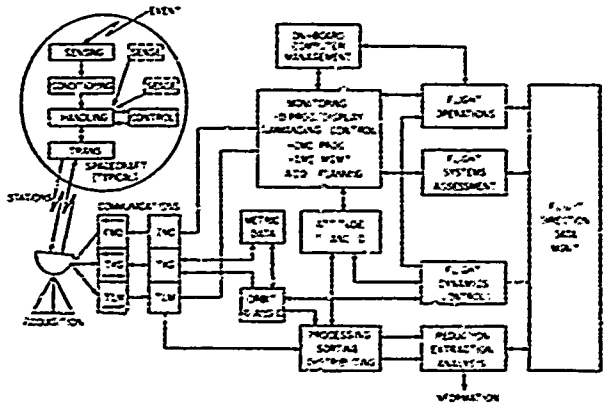

Figure 4. Present data management system

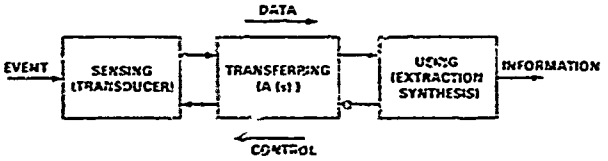

FROM THE DETECTION OF AN EVENT TO THE OUTPUT OF INFORMATION, INCLUDING THE PLANNING AND FEEDBACK OF CONDITIONING FOR EVENT DETECTION

Figure 5. The NASA end-to-end data/information system

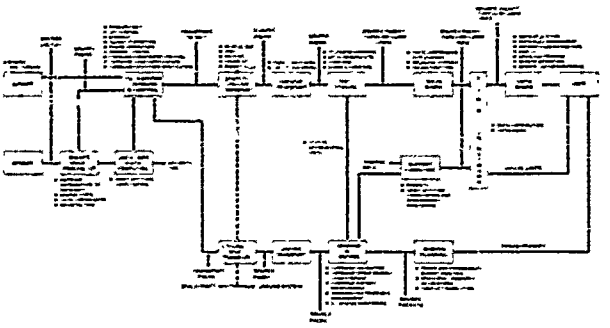

Figure 6. Needs functional elements

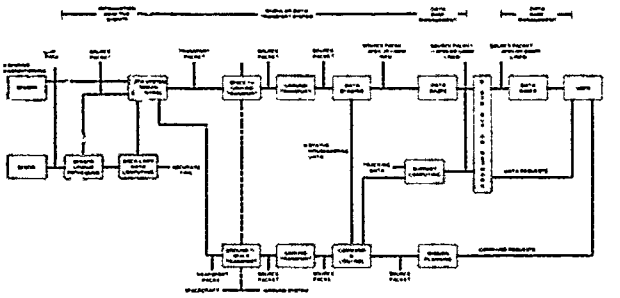

Figure 7. Relationship of needs program elements to needs functional elements

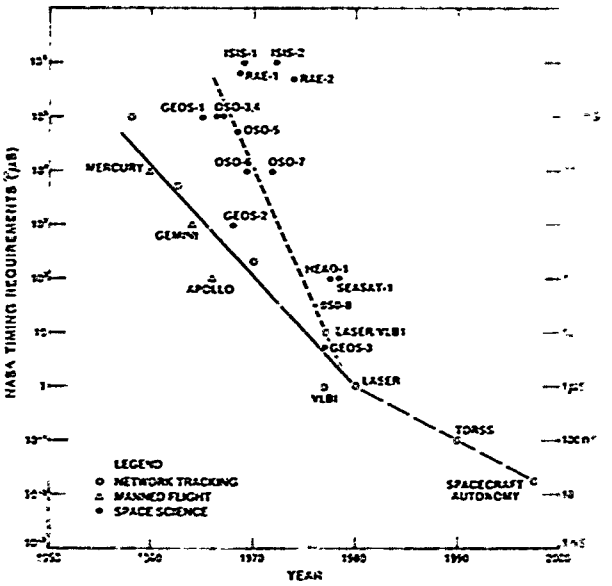

Figure 8. NASA present and future timing requirements

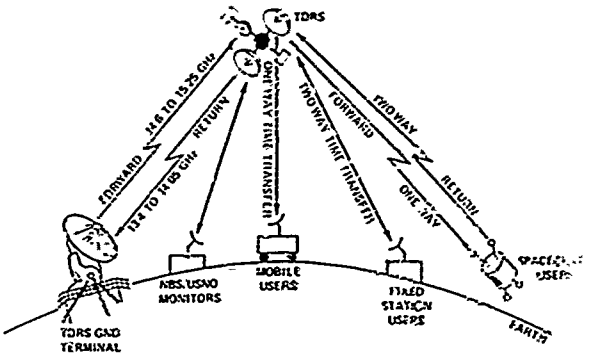

USER	MODE	FORWARD LINK		RETURN LINK	
1	MA	2106.14	MHz	2287.5	MHz
2	SSA	2025–2120	MHz	2200–2300	MHz
3	KSA	13.775	GHz	15.0034	GHz

Figure 9. TDRSS time transfer and user configuration

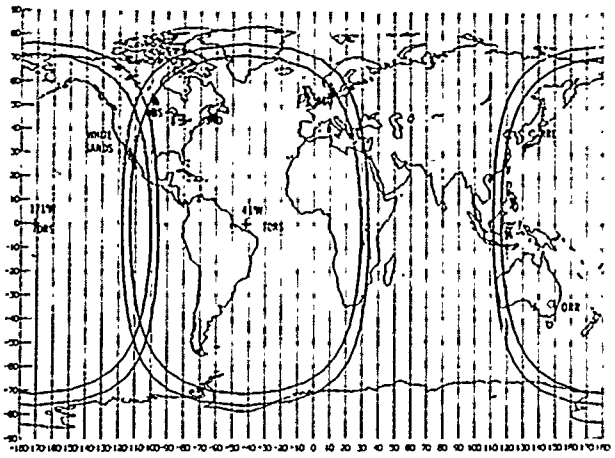

Figure 10. National primary clock sites from which the two-way time transfer system can be calibrated (map shows contours of 5° and 10° elevation viewing angles for TDRSS at 41°w and 171°w)

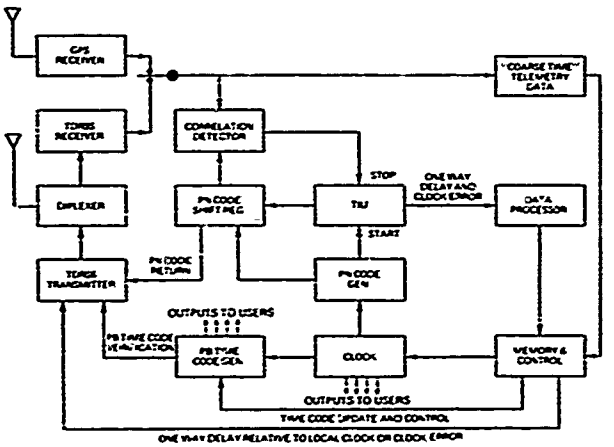

Figure 11. Conceptual functional block diagram of satellite time transfer terminal

TABLE 1

Relationship of essential needs concepts to program elements

ESSENTIAL CONCEPT	PROGRAM ELEMENT				
	SYSTEMS ANALYSIS AND INTEGRATION	MODULAR DATA SYSTEM	INFORMATION ADAPTIVE	DATA BASE MANAGEMENT	SOFTWARE V & V
1) DATA AND INFORMATION AUTONOMY	x	x		x	
2) SPACECRAFT (PLATFORM) AND INSTRUMENT AUTONOMY	x	x	x		
3) DATA REDUCTION TO INFORMATION IN REAL TIME	x		x		
4) STANDARD INTERFACE AND FUNCTIONAL DEFINITIONS	x	x	x	x	x
5) SYSTEM COMMONALITY FOR INTEGRATION TESTING & SPACE FLIGHT	x	x	x		x
6) REDUNDANT MODULAR HARDWARE AND SOFTWARE COMPONENTS	x	x	x		x

TABLE 2

A summary of satellite time transfer experiments

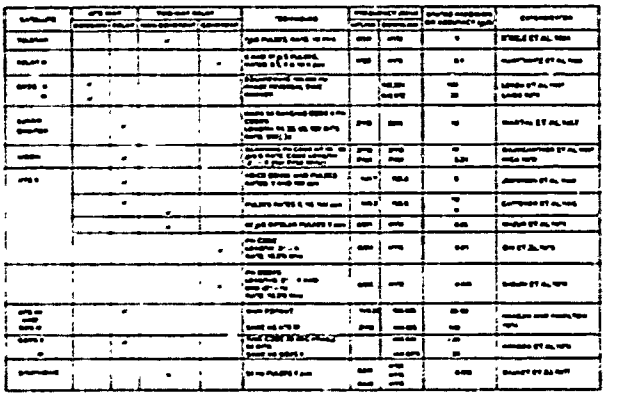

TABLE 2 (cont'd)

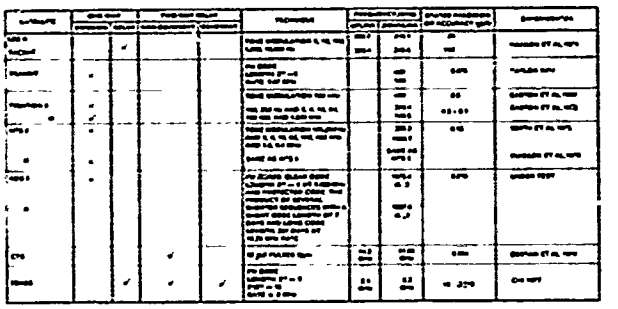

References

1. Price, R.D., The NEEDS Program, AIAA/NASA Smart Sensor Conference, Hampton, Va., November 14-16, 1978.
2. Blanchard, D.L., "Smart" From a NEEDS Perspective, AIAA/NASA Smart Sensor Conference, November 14-16, 1978.
3. NEEDS Systems Team (J. Sos, et.al.), NEEDS System Concept, February 1979.
4. Hoffman, E.J. and Birmingham, W.P., GPSPAC: A Spaceborne GPS Navigation Set, IEEE Conference, San Diego, Ca., November 1978.
5. Fuchs, A.J. and Pajerski, R.S., The Role of Autonomous Satellite Navigation in the NEEDS Program, AIAA/NASA Smart Sensor Conference, Hampton, Va., November 14-16, 1978.
6. Martin Marietta Aerospace, Onboard Attitude Determination System (OADS), Final Study Report Contract NAS4-23428, Mod. 27, MCR-78-514, April 1978.
7. Cooper, R.S. and Chi, A.R., "A Review of Satellite Time Transfer Technology: Accomplishments and Future Applications," to be published in special issue of Radio Science on Time and Frequency, July/August, 1979.

TWO-WAY TIME TRANSFERS BETWEEN NATIONAL RESEARCH COUNCIL (OTTAWA) AND PARIS OBSERVATORY VIA THE "SYMPHONIE" SATELLITE

C.C. Costain, J.-S. Boulanger, H. Daams, L.G. Miller
National Research Council, Canada

G. Fréon, P. Parcelier
Laboratoire Primaire du Temps et des Fréquences, France

M. Brunet
Centre National d'Etudes Spatiales, France

J. Azoubib, B. Guinot
Bureau international de l'Heure, France

Summary

Since July 1978, time comparisons between National Research Council of Canada and Paris Observatory, France, are regularly made via the geostationary telecommunication satellite "Symphonie". The experiment is planned to last at least two years. Until February 1979, the time comparisons were made daily, then twice a week.

A two-way technique is used between earth stations in Ottawa and Pleumeur-Bodou, on the 4-6 GHz channels. The link is complemented by passive television between earth stations and time laboratories.

The random uncertainty of the space link is of the order of 1-2 ns, but the overall random uncertainty is strongly increased by the television method and reaches 24 ns. The results still contain a constant error of the order of a few 0.1 μs, due to the lack of precise calibrations of instrumental delays ; the calibration methods are under study.

These time comparisons require a reasonable amount of work, compatible with routine operation. The work can still be reduced by various technical improvements which are in progress. The results appear especially fitted to detect rapidly frequency changes and such a link would be very useful between laboratories developping primary standards.

Introduction

The lack of precision and accuracy of time comparisons over distances of a few hundreds to a few thousands kilometers remains a major obstacle to the development of time metrology.

Two-way time transfers via geostationary telecommunication satellites originated in 1962. Many experiments of this method were performed ; the recent ones by Saburi et al.[1] have shown that random and systematic uncertainties can be reduced respectively to 1 ns and 10 ns. Following a feasability experiment of time comparisons using the german-french satellites Symphonie, in December 1976, by Brunet et al.[2], Hübner and Hetzel[3], Brunet[4], an operational time link was established, starting in July 1978, between National Research Council of Canada (NRC) and Laboratoire Primaire du Temps et des Fréquences in Paris Observatory (OP), using one of these satellites. The experiment is planned until June 1980.

Organization of the time link

The telecommunication ground stations linked by Symphonie (at the longitude 11°5 W) are the Communication Research Center (CRC) in Ottawa, and the Center of Pleumeur-Bodou (PBS) in France. Until February 1979, reflectors of 10 m diameter in CRC and 16 m diameter in PBS were used ; after this date smaller antennas were affected to the time experiment.

In CRC and PBS, NRC and OP have installed auxiliary time stations equipped respectively with rubidium and cesium clocks, here designated by H(CRC) and H(PBS). The terminal time links with the master clocks of NRC and OP, producing the time scales designated as UTC(NRC) and UTC(OP), are realized by the well known passive television method.

Space link

The method consists in sending quasi-simultaneous second pulses of H(CRC) and H(PBS) via Symphonie. Figure 1 shows the time diagram of the link, R(PBS), for instance, is the measured time interval between the departure of a pulse of H(PBS) and the reception of the corresponding pulse of H(CRC). Let us define Δ by

$$\Delta = \frac{1}{2}\left[R(CRC) - R(PBS)\right] . \qquad (1)$$

Neglecting the instrumental delays, the relativistic corrections, and assuming that the propagation delay is the same in both ways, one should have :

$$H(CRC) - H(PBS) = \Delta .$$

To this raw value, corrections are to be added to ensure accuracy. These corrections are associated to the implementation of the method which will be considered first.

The second pulses of the clocks (30 ns rise-time) are sent directly to the station modulators and also start the intervallometers. The frequencies of the links ground/satellite are 6 GHz upward, 4 GHz downward. Two different transponders of Symphonie are used, according to the direction of the transmission. The received pulses, having a rise-time of the order of 150 ns, stop the intervallometers. Measurements are made every second during about 20 minutes, and registered on magnetic floppy disks. The time comparisons were made every working day until February 1979, then twice a week.

Let us consider the corrections to the raw Δ and their uncertainties.

(a) Instrumental delays in the stations. The correction is

$$0.5\left[\tau E(CRC) - \tau R(CRC)\right] - 0.5\left[\tau E(PBS) - \tau R(PBS)\right], \quad (2)$$

where τE and τR are the delays at emission and reception due to instruments, coaxial links, and the rise-times of the signals. A global measurement of the $\tau E - \tau R$ was attempted in 1976, using a transponder on a truck, in parallel with coaxial link : the experiment was disappointing, the variations of the results being of the order of several tens of nanoseconds, depending on the position of the transponder. A new method is under study ; in the meantime, local loop measurements made every second or every 5 seconds over intervals of 5 minutes are used to check the stability of the $\tau E + \tau R$ in CRC and PBS, each time the time link is established. These measurements give the sum of $\tau E + \tau R$ and of various delays, including the local transponder delay. Thus the measured values of 1.3 µs in CRC and 1.7 µs in PBS represent maximums of $\tau E + \tau R$. The rms residuals are 2 ns in CRC, where no systematic variations were observed, except for the changes in intervallometers threshold, which are taken into account. In PBS, the rms residuals are 8 ns and peak to peak variations reach 30 ns ; some of these variations are due to knonwn instrumental changes which were determined and taken into account.

(b) Transponder delays in the satellite. The correction is $0.5(\tau 1 - \tau 2)$, $\tau 1$ being the transponder delay for the transmission CRC to PBS, and $\tau 2$ for PBS to CRC. $\tau 1$ and $\tau 2$ are of the order of 10 ns and the correction should be, at the most, a few ns. As it is not known, it is neglected.

(c) Tropospheric and ionospheric corrections. These corrections are due to the different frequencies of the upward and downward transmissions. The tropospheric effect is smaller than 1 ns. The ionospheric correction is 6 ns at the most.

(d) Relativistic correction and effects of the satellite motion. The relativistic correction to Δ is 159 ns. The effects of the residual motion of Symphonie, direct (change of path during the measurements), and indirect (change of the relativistic correction) are smaller than 1 ns and are neglected.

The conclusion is that, apart from a fixed correction, which is not measured, the other corrections are sufficiently small or known to ensure an accuracy of the order of 5 ns. As they are also nearly constant, the Δ corrected only for some variations as stated in (a) are considered.

The neglected fixed correction, according to equation (2) and the results of the loop measurements, could be theoretically 1.5 µs in the worst case. But equation (2) shows that compensations can be expected and it is reasonnable to believe that the correction is of the order of a few 0.1 µs. Thus Δ should represent the true values of the clock differences in CRC and PBS with a constant systematic error of a few 0.1 µs, as long as the same equipment is used.

Television links

In Ottawa, CRC and NRC are 35 km apart, and in view of the same television transmitter. The time comparisons are made 15 minutes before and after the space link. The TV link is calibrated by frequent clock transportations.

In France, the distance between OP and PBS is 450 km, and the TV method involves microwave links. The measurements are made daily on UHF and VHF channels. The TV link is calibrated and checked by clock transportations.

Computations and results

The computation of Δ was first made according to equations (1). Until March 1979, the data in PBS were recorded on printed tapes, and only 30 samples at 10s intervals were processed for each daily time comparison. Figure 2 shows the histogram of the standard deviation of individual values of Δ : it can be seen that it is normally 5 ns, leading to a standard deviation on the average of the order of 1 ns. It was checked that extending the averages over larger intervals or the totality of the 1 s time comparisons brings very small changes : usually 1 to 2 ns. The origin of occasional bad measurements is probably in the reception channel at PBS.

Work at NRC showed that a least square fit of a cubic in the reception times allowed to condense the full set of data in four numbers, without loss of information. Starting in April 1979, the time comparisons were derived from the coefficients of the cubics, thus facilitating the data transmission and the computations.

Concerning OP and PBS, in order to take advantage of the stability of the cesium clock H(PBS), the raw values of UTC(OP) - H(PBS) are filtered with a low-pass filter having a frequency cut-off at 0.12 cycle per day. The residuals between raw and filtered values allowed to detect a few wrong values, probably due to changes in the television microwave links, which were rejected. The residuals also give an estimate of the random

uncertainty of the time comparisons between OP and PBS : 19 ns.

As one of the goals of the experiment is to demonstrate the feasability of the operational time link, the percentage of successful operation may be interesting. From 1978 July 12 to 1979 February 9, 106 time links were attempted, and 73 results (69% of success) were retained. The lack of some results is due to various causes : non-establishment of the space link, missing TV links; only 3 results were rejected on account to a poor space link leading to excessively noisy recordings. From 1976 February 26 to 1979 May 5, the percentage of success reached 83%.

An interruption extended from 1978 August 18 to 1978 October 15. This corresponds to the eclipses period of the satellite ; during this period the antennas were used for another purpose. As this interruption was most inconvenient, the eclipses period of March 1979 was bridged using other antennas, thus changing the delays, although this is not observable on the results. The quality of the link was improved with these new antennas, as shown by the histogram of the standard deviation of Δ (fig. 3). This improvement is tentatively explained by (a) the increasing of the EIRP emitted in Ottawa (b) the smaller number of users of Symphonie.

The results are given by figure 4 referred to TA(NRC) and TA(F). TA(NRC) is produced by the laboratory cesium standard NRC CsV in continuous operation ; TA(F) is a paper time scale derived from the data of about 15 commercial cesium standards. For comparison purpose, the LORAN-C time comparisons and the results of the clock transportations are also represented.

It is rather difficult to know whether there has been frequency irregularities in October 1978, after the link was re-established. But the frequency change by 1×10^{-13} at the beginning of December 1979 is certainly real. Its date of occurence can be determined with an uncertainty of a few days, which is impossible with the LORAN-C.

The stability of TA(NRC) and H(PBS) allows to derive the standard deviation of a daily time comparison between NRC and PBS, which is 14 ns. Taking into account the above mentioned uncertainty of H(PBS) - UTC(OP), the global random uncertainty of UTC(NRC) - UTC(OP), and of TA(NRC) - TA(F) is 24 ns.

Conclusion

Time comparisons using the 4-6 GHz channels of a communication satellite, between Canada and France, were achieved with a reasonnable amount of work, on a routine basis. Their precision between telecommunication terminals is of the order of 1 ns, but the accurate calibration of instrumental delays is an important problem which has not yet been solved. The other systematic errors can be corrected with a total uncertainty of the order of 5 ns.

Another problem which awaits solution is the transmission of time between telecommunication terminals and the standard laboratories, at distances of 10-500 km, with a matching precision. Presently most of the random uncertainty between NRC and OP comes from these segments of the time link.

Nevertheless, in its present state, the experiment appears most useful to make measurements of differences of frequencies of remote standards, the other methods available requiring excessively long averaging times.

Recent experiments between the National Bureau of Standards (USA), the U.S. Naval Observatory, NRC and PBS have shown that simultaneous time comparisons using two satellites can extend the geographical coverage of the method, without loss of precision. It could be considered to organize a world-wide coverage with a relatively small number of ground stations and satellites.

References

1 - Saburi Y., Yamamoto M., and Harada K. IEEE Trans. on Instrumentation and Measurement, IM-25, 4, p. 473, 1976.

2 - Brunet M., Fréon G., Parcelier P., Actes du Colloque intern. sur la Mesure en Télécommunications, organisé par l'URSI (Lannion, France, 3-7 octobre 1977).

3 - HUbner U., Hetzel P., Kleinheubacher Berichte 21, 459, 1978.

4 - Brunet M., Proceedings of the Open Symposium on Time and Frequency, URSI, Helsinki, 1-4 Aug. 1978.

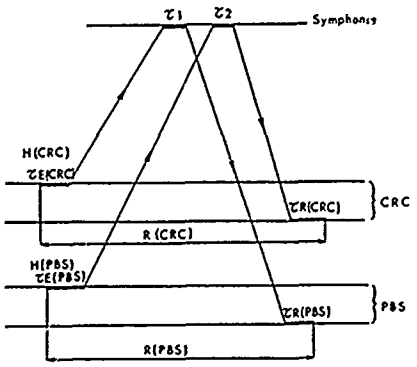

Fig. 1. Time diagram.

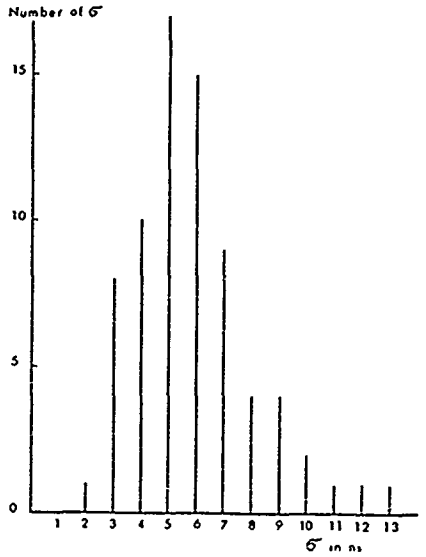

Fig. 2. Histogram of the standard deviations σ of a single one-second time comparison between Ottawa and Pleumeur-Bodou, July 1978 - February 1979 (73 values).

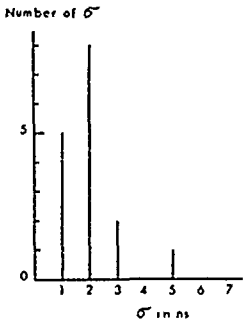

Fig. 3.

Histogram of the standard deviations σ of a single one-second time comparison February - April 1979 (16 values).

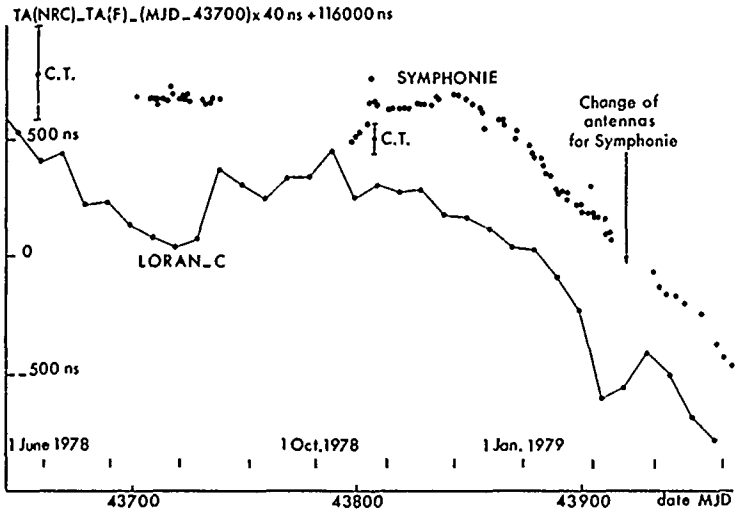

Fig. 4. TA(NRC) - TA(F), corrected for a constant and a drift of 40 ns per day. The dots represent the raw Δ (see text) obtained via "Symphonie". The LORAN-C values are averaged over 10 days and calibrated by clock transportations in 1976. The clock transportations (C.T.) are given with ± one σ error bars.

STUDY OF THE DEPENDENCE OF FREQUENCY UPON MICROWAVE POWER OF WALL-COATED AND BUFFER-GAS-FILLED PASSIVE Rb^{87} FREQUENCY STANDARDS

A. Risley and Stephen Jarvis, Jr.
(National Bureau of Standards, Boulder, Colorado)

and

J. Vanier, (Université Laval, Quebec, Canada)

Summary

Previous studies of a commercial passive gas cell Rb^{87} frequency standard showed a strong dependence of the output frequency, ν_{Rb}, upon the microwave power, $P_{\mu\lambda}$. A major conclusion of that work was that the dependence of ν_{Rb} upon $P_{\mu\lambda}$ was due to a line inhomogeneity effect. The line inhomogeneity interpretation suggested that substituting a wall coating for the usual buffer gas would reduce the dependence upon $P_{\mu\lambda}$. As a part of the present work a wall coating (a form of paraffin) was used and a reduction of this dependence by a factor of 100 was obtained.

The present work has led to a more convincing theoretical demonstration of the line inhomogeneity effect. The paper discusses some of the details of the analytical procedure.

There are certain major requirements that a wall coating would have to satisfy if it were to be superior to the usual buffer gas and these are discussed in the text. The advantages demonstrated by the present work indicate that further studies are warranted to determine if an improved standard could be built based on a wall coating.

Background

The passive Rb^{87} gas cell frequency standard is the most prevalent type of atomic frequency standard in the field. It gives good performance at a fairly low cost. The results of the work reported here suggest that the use of a wall coating instead of the usual buffer gas might improve its medium and long term frequency stability.

Earlier work on a prevalent commercial Rb^{87} standard demonstrated a very strong frequency dependence upon the microwave power, $P_{\mu\lambda}$.[1] This effect appears to be due to a combination of relatively immobile Rb^{87} atoms and a frequency gradient across the absorption cell. The immobility is due to the use of a buffer gas in the cell.

The work reported here demonstrated that a strong signal can be obtained by substituting a wall coating for the buffer gas. Making this substitution results in a drastically reduced dependence of the output frequency, ν_{Rb}, upon $P_{\mu\lambda}$. In the commercial unit studied in reference 1, the dependence upon $P_{\mu\lambda}$ caused by the line inhomogeneity was probably the predominant cause of frequency instability for averaging times of the order of one month and longer. Thus, the ability to use wall coating in lieu of buffer gas might be important commercially.

In section II we discuss the experimental results of the present work. Section III gives the results of the line inhomogeneity analysis which represents our understanding of the dependence of ν_{Rb} upon $P_{\mu\lambda}$ when a buffer-gas is used. In section IV we discuss some pros and cons of using wall coatings.

Experimental Results

Experimental Setup

The experimental arrangement used in these experiments is shown in figure 1. An optical package capable of giving a strong resonance of the $F = 2$, $M_F = 0$ to $F = 1$, $M_F = 0$ transition was used to lock the frequency of a crystal oscillator driving a frequency synthesizer. The frequency was measured then with a counter. The arrangement gave a resolution of 1×10^{-10} which was sufficient for the types of phenomena studied. The optical package--consisting of a rubidium 87 lamp, an isotopic filter, and a TE_{011} exciting cavity--was equipped with a special cell. This cell, made of quartz, was coated with a form of paraffin and connected to a vacuum system. It contained a few milligrams of rubidium 87 in a tail, whose temperature could be controlled independently of the cavity. In our work a typical tail temperature was 70° C. The cell was 3.2 cm in diameter and typically was held at 71° C. The cavity was 5.7 cm in diameter and about 7 cm long. (In the unit studied in reference 1, the cell filled the entire cavity.)

It is important to say that the experimental arrangement was considerably different (and more controlled) here than in reference 1. Nevertheless, our earlier conclusion about line inhomogeneity as the mechanism producing the dependence upon $P_{\mu\lambda}$ is strongly supported by the present work. An additional aspect of the present work was that the Q of the cavity was sufficiently high that a cavity pulling effect could be observed although the system was operated in the passive mode. These results will be reported elsewhere.[2]

In order to study the effects of power shift in the presence of frequency gradients across the cell, special coils were mounted at the end of the cavity. These coils were about 4.5 cm in diameter and were separated by 7 cm. Each consisted of 150 turns. The coils could produce a magnetic field

gradient which was then translated by the rubidium 87 atomic ensemble to a frequency gradient.

The effect of gradients of this sort could then be studied under controlled conditions, and in circumstances where the atom was free to average the magnetic gradient and light shift in the case of the coated cells, or where the atoms were fixed in space with a buffer gas. In this last case, the field gradients and light shift are not averaged by the atomic motion and inhomogeneous broadening and shifting of the resonance line occurs. This shifting and broadening depends on the level of $P_{\mu\lambda}$ and, thus, the frequency dependence upon $P_{\mu\lambda}$ results.

Results

ν_{Rb} versus $P_{\mu\lambda}$ and Magnetic Gradient. Figure 2 shows ν_{Rb} versus $P_{\mu\lambda}$, with the voltage applied to the gradient coils as a parameter. The level of $P_{\mu\lambda}$ is determined by the microwave attenuator and, for an attenuator setting of 50 dB, the power absorbed by the cavity is approximately 1×10^{-10} watts. The data of figures 2 through 5 were taken with the cavity frequency no more than 25 kHz away from ν_{Rb}. Based on our cavity pulling measurements, we conclude that the worst case pulling of ν_{Rb} would be no more than 0.25 Hz due to this offset. Since the precision of the frequency measurements is about 0.7 Hz, cavity pulling effects are negligible.

The resonant frequency of any given atom has a quadratic dependence upon the magnetic field and the coils produce a linear field gradient across the cell. For the maximum voltage (1.6 volts) applied to the gradient coils, the resonant frequencies of the atoms vary across the cell by about 2,500 Hz. This is, of course, a much larger gradient than would be encountered in a working standard. The purpose in applying such a large gradient was twofold. First--since the spatial variation of the magnetic gradient is more accurately known than that of the light shift--we wanted to have a condition where the total gradient was primarily due to the magnetic gradient. Second, we wanted to clearly show the dramatic change in sensitivity to $P_{\mu\lambda}$ when the buffer gas is removed. On the other hand, for applied gradient voltages less than about 0.2 volts, the light shift gradient dominates.

In figure 3 we have plotted the data in a different form. On the right ordinate scale, to emphasize the change in frequency with change in power, we have plotted a frequency change due to a 20 dB change in $P_{\mu\lambda}$ versus the gradient voltage. The microwave change is from an attenuator setting of 40 dB to one of 20 dB. (As a point of further information, the maximum signal level at the lock-in amplifier occurs for a microwave attenuator setting of about 35 dB. The 100 Hz modulation voltage [see figure 1] used in all these measurements is one that produces a maximum signal level at the lock-in when the frequency of the microwave source is just slightly displaced from ν_{Rb}. [This is an open loop test.] This is a way of assuring that the microwave source is not being overmodulated.) This change in $P_{\mu\lambda}$ is, of course, vastly larger than would be encountered in a commercial unit, and our purpose was to emphasize the difference between a buffer gas filled cell and one with only a wall coating. Also shown in figure 3 on the left ordinate is the resonant frequency as a function of applied gradient voltage at a 50 dB attenuation setting for the microwave power.

Figures 4 and 5 give the same information for the paraffin-coated unsealed cell attached to the vacuum system. For applied gradient voltages of 0.8 volts and less, there is no $P_{\mu\lambda}$ dependence to within the precision of the measurement.

The larger dependence of ν_{Rb} upon changes in $P_{\mu\lambda}$ shown in figures 2 and 3 should be contrasted with figures 4 and 5. Note also, the very different character of the center frequency, ν_{Rb}, in figure 3, as compared to figure 5. To understand this difference in the behavior of ν_{Rb} versus magnetic gradient (for fixed $P_{\mu\lambda}$), some additional information is needed.

First, the portion of the cell which is nearest the light source (the "input end" of the cell), is very near the center of the cavity so that the microwave field intensity, β, is near its maximum there. At the $P_{\mu\lambda}$ = 50 dB level, and in this region, $P_{\mu\lambda}$ is just about at its optimum level for inducing transitions. Thus, for smaller attenuator settings, this region is in microwave saturation to a greater or lesser degree. Second, the magnetic field due to the gradient coils has a null just at the "input end" of the cell and so any atom's hyperfine frequency is the higher the further into the cell it finds itself.

Now, the response at the photocell is a weighted average of the absorption throughout the cell. For $P_{\mu\lambda}$ = 50 dB, the major contribution is near the input end of the cell and this group of atoms experinces a weaker field (and, thus, a lower frequency) than the average field experienced by atoms that are free to move in the cell. If the theoretical results for ν_{Rb}--at $P_{\mu\lambda}$ = 50 dB--are displayed as in figure 3, then a large decrease in slope at increasing values of V_g is also observed. If a large value of $P_{\mu\lambda}$ ($P_{\mu\lambda}$ = 20 dB) is used in the calculation, then a larger initial slope is obtained and this slope is roughly independent of V_g. This behavior is qualitatively consistent with the idea that a larger value of $P_{\mu\lambda}$ would increase the weighting of atoms nearer the center of the cell. But a person might expect that, for a fixed value of $P_{\mu\lambda}$, the weighting would be fixed, i.e., independent of V_g. However, for large values of V_g, the frequency change over even a small segment of the cell near the output end is large compared to the low-power, non-homogeneity broadened linewidth (see section II.B.2). This means that the number of atoms available for microwave absorption--per unit bandwidth of the microwave source--is severely decreased near the output end of the cell. Thus--for a fixed value of $P_{\mu\lambda}$--the resonant frequency of all atoms in the cell

rises with increasing V_g, but those segments of the cell for which it rises the most become increasingly less effective at determining the center frequency. This causes the weighting to be shifted toward the front of the cell as V_g increases. A comparison with data (not shown here) for larger values of $P_{\mu\lambda}$ gives the same qualitative behavior as for the theory. Moreover, even in the worst case, the ratio of the theoretical to the experimental value is less than 2.

Linewidth versus $P_{\mu\lambda}$ and Pumping--Light Intensity.

At the $P_{\mu\lambda}$ = 20 dB level--which is 15 to 20 dB higher than that which produces the maximum signal (with the low modulation level that was used)--microwave power broadening is responsible for about 60 percent of the linewidth.

If the magnetic gradient is turned off and $P_{\mu\lambda}$, I_o (the pumping--light intensity), and the modulation voltage reduced to as low a value as possible for obtaining a usable signal (about a factor of 4 lower than was typical for I_o and the modulation voltage), then the linewidth, $\Delta\nu_{Rb}$, is about 170 Hz in the case of 1730 Pascals (13 Torr) of N_2, and about 230 Hz in the cell without buffer gas. We conclude that there is a slightly higher relaxation rate when using the paraffin wall coating than when using the buffer gas.

Further evidence for the validity of the idea of spatial averaging comes from the behavior of $\Delta\nu_{Rb}$ versus magnetic gradient. For example, in the case of just the wall coating, $\Delta\nu_{Rb}$ = 280 Hz with a gradient voltage of 1.2 volts and 260 Hz with no magnetic gradient. For the buffer gas case--at the same level of $P_{\mu\lambda}$ of 50 dB--the values are 850 Hz and 230 Hz. Still further evidence comes from the asymmetry of the line. For the buffer gas case, at 1.2 volts gradient voltage, the low frequency side of the line is 220 Hz wide and the high frequency side is 630 Hz. On the other hand, without buffer gas, the two sides differ by only 3 Hz, which is less than the precision of the linewidth measurement.

Theoretical Results

The theoretical model (based on the buffer gas case) assumes that the Rb^{87} atoms are fixed in space and that their resonant frequency depends upon their position within the cell. In the experiment, the buffer gas produces the immobility, with the intentionally applied magnetic gradient, plus the spatially changing light shift producing the frequency gradient. Figures 6 and 7 show a comparison between the theory and the data. In these figures, V_g is the voltage applied to the gradient coils; β is the microwave field intensity; K is a constant; $\delta\nu_{Rb}$ is the change in frequency between the measured (or calculated) value of ν_{Rb} and its value at V_g = 0 when the minimum value of microwave field is applied.

The equations used in the present calculations are based upon earlier work done by one of us (JV) and others.[3,4,5] The values of some of the parameters that appear in the equations were determined from our or others' measurements. However, the value of pumping light intensity, I_o, used in computing figures 6 and 7 was obtained by fitting to the data. Approximate values of I_o, with which to begin, were obtained from reference 4.

In our calculation we assumed a gaussian optical absorption line and that, at the input end of the cell, I_o also had a gaussian distribution. Because the pumping light is strongly absorbed as it traverses the cell, the light shift varies rapidly along the length of the cell (see figure 8). Based on a measured average light shift of 35 Hz we estimate a light shift of 100 Hz at the entrance to the cell. Then, by adjusting the offset between the centers of the pumping and absorption lines, we attempted to get agreement with the data for no magnetic gradient (V_g = 0.0 of figure 6). The calculated values--at $P_{\mu\lambda}$ = 20 dB, were typically too small by a factor of 2 or greater. With the probable asymmetry of the spectrum of the pumping light, it does not seem surprising to us that the agreement is poor when the gradient is due primarily to the light shift.

To perform the calculation (since the diameter of the cell is small compared to the diameter of the cavity) we assume that there is no variation of I_o, or β, (or of the atom's frequency) across the cell, i.e., at right angles to the axis of the cell. Along the axis we use the distribution for β according to the known mode in the cavity. (In reference 1, the Q of the cavity and the cavity configuration were such that β was inadequately known for useful calculations.)

The amplitudes of a discrete (Gaussian-Hermite) spectrum of pumping light frequencies satisfy a system of first-order differential equations in the axial coordinate, Z. These were solved numerically by a Runge-Kutta method. The center of the dip in the amplitude distribution is the system frequency, ν_{Rb}.

In the measurement process we actually measure a dispersion curve rather than an absorption curve. Thus, the measured linewidth, $\Delta\nu_{Rb}$, is the width between the two dispersion peaks. To make the theoretical procedure compatible with the measurement, the first derivative is taken of the theoretical absorption curve and a theoretical $\Delta\nu_{Rb}$ obtained from the resulting dispersion curve.

On the average, the agreement of the theory with the data is sufficiently good to reinforce our belief that the two basic assumptions of the model are correct. On the other hand, there is sufficient uncertainty about the values of the experimental parameters that further attempts to fit the data presented here do not seem warranted.

Additional Thoughts On The Use of Wall Coatings

In the work reported in reference 1 we found that a change in $P_{\mu\lambda}$ of 0.4 dB about the operation

point caused a fractional change in ν_{Rb} of about 1 x 10^{-11}. The present work shows that, for strong gradients, there is a reduction in the $P_{\mu\lambda}$ dependence by a factor of about 100 due to the use of the wall coating. We presume that (in first order) this factor also holds at weak gradients. (Our theoretical model can address itself to this question and we are proceding to do this. A new experimental setup is being prepared which should have measurement precision of a few parts in 10^{13}.)

Some of the major questions that need to be answered with regard to wall coatings are:

1. Will the frequency shift due to the coating be sufficiently stable (say one part in 10^{12} or better) over periods of many months?
2. Will its temperature dependence be sufficiently small?
3. If a material can be found which satisfies items 1 and 2, is its use commercially feasible?

Despite these uncertainties, the use of a wall coating has made a very large reduction in a major instability. Further studies seem warranted to determine if a significantly improved Rb standard could be developed based on a wall-coated cell.

Acknowledgments

This work was supported in part by contract SMS-80218 from the Space and Missiles Systems Organization of the U.S. Air Force, the Natural Sciences and Engineering Research Council of Canada and the Department of Education of the Province of Quebec. The authors would also like to thank Dr. Peter Bender of JILA and Dr. David Wineland of NBS for discussions regarding the data and its implications. One of us (AR) would also like to thank Mr. David Allan of NBS and Dr. Helmut Hellwig (now of Frequency & Time Systems, Inc.) for their continued interest and support.

References

1. A. Risley and G. Busca, "Effect of line inhomogeneity on the frequency of passive Rb^{87} frequency standards," Proc. 32nd Ann. Symp. on Freq. Control, pp. 506-513 (1978).

2. A. Brisson, J. Vanier, and A. Risley (unpublished).

3. Jacques Vanier, "Relaxation in rubidium-87 and the rubidium maser," Phys. Rev., Vol. 168, p. 129.

4. G. Busca, M. Tetu, and J. Vanier, "Light shift and light broadening in the ^{87}Rb maser," Can. J. Phys., Vol. 51, No. 13, July 1, 1973, pp. 1379-1387.

5. Gilles Missout and Jacques Vanier, "Some aspects of the theory of passive rubidium frequency standards," Can. J. Phys., Vol. 53, 1975, pp. 1030-1043.

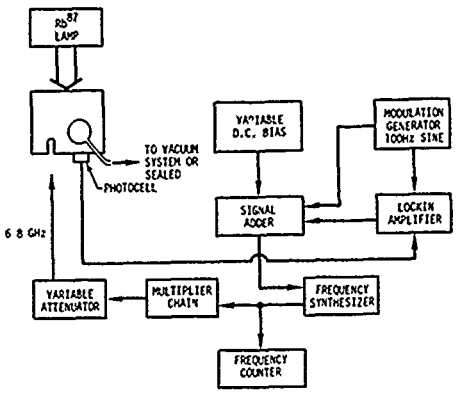

Figure 1. A schematic of the measurement system.

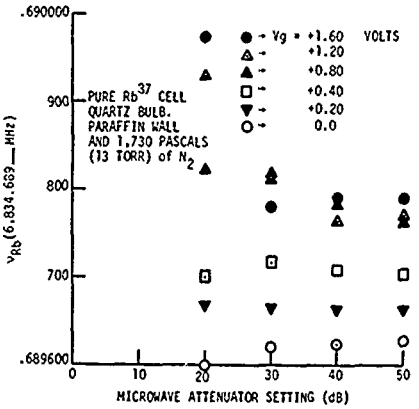

Figure 2. The output frequency, ν_{Rb}, versus applied microwave power on a cell filled with 1730 Pascals (13 Torr) of N_2. Minimum microwave power corresponds to an attenuator setting of 50 dB. The voltage applied to the gradient coils is the parameter. A voltage, V_g, of 1.6 volts applied to the gradient coils causes a frequency change across the cell of about 2,500 Hz.

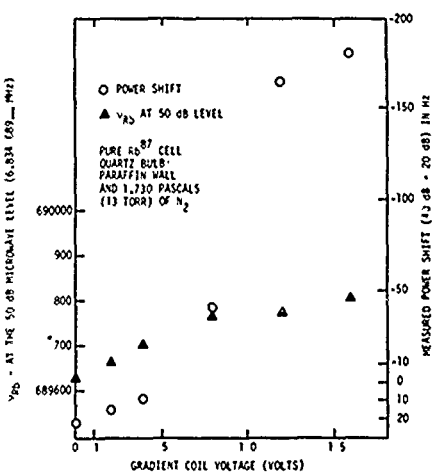

Figure 3. The data was taken on the same cell as used in figure 2. The right hand ordinate represents a frequency change due to a 20 dB change in microwave power, $P_{\mu\lambda}$. The abscissa is the voltage applied to the gradient coils and is a measure of the frequency gradient across the cell. The left hand ordinate is the output frequency at the $P_{\mu\lambda}$ = 50 dB level.

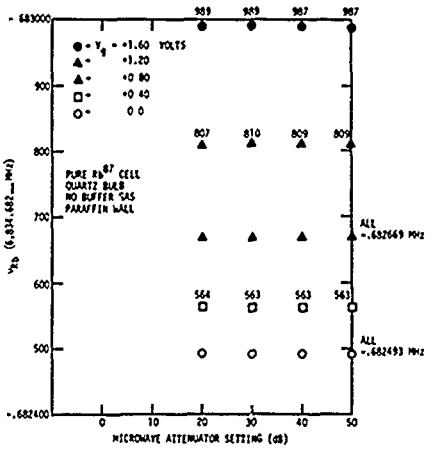

Figure 4. Same as for figure 2 except that the cell wall is coated with paraffin and the cell was kept under vacuum.

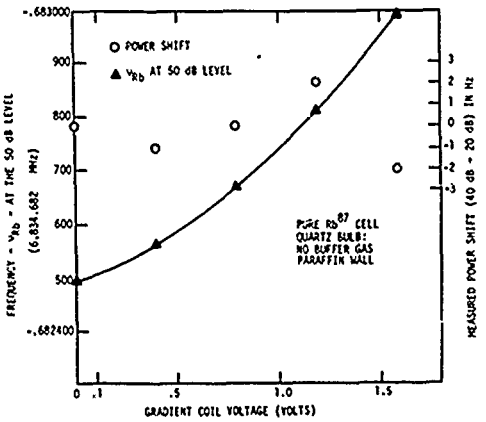

Figure 5. Same cell as for figure 4. The two ordinates and the abscissa are the same as for figure 3.

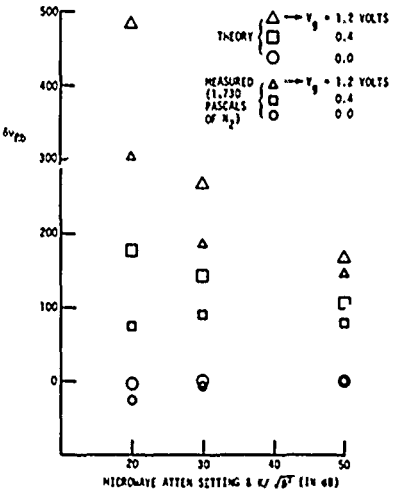

Figure 6. The theoretically obtained frequency change, $\delta\nu_{Rb}$, versus $P_{\mu\lambda}$. Also shown for comparison is some of the data of figure 2 (expressed as a frequency change).

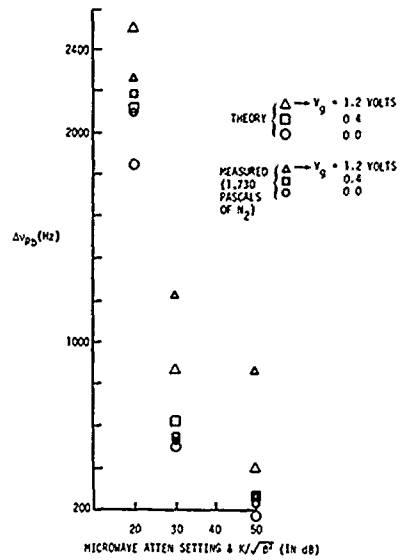

Figure 7. The theoretically obtained linewidth, $\Delta\nu_{Rb}$, versus $P_{\mu\lambda}$. The data shown corresponds to the same cell as in figures 2 and 3.

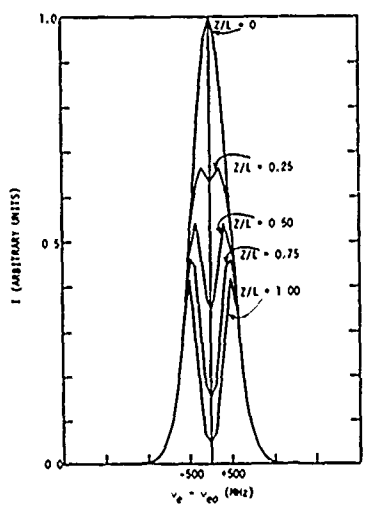

Figure 8. Calculated (theoretical) pumping light distribution, I, at several planes along the cell axis. The total length of the cell is L and Z is measured from the end of the cell where the light enters. The center of the distribution, at Z = 0, is at the frequency ν_{eo}.

DEVELOPMENT OF A LIGHT WEIGHT, MILITARY, CESIUM STANDARD

Iancu Pascaru and Marvin Meirs

Frequency Electronics, Inc.
New Hyde Park, New York

Summary

Frequency Electronics, Inc. is presently developing a lightweight, military, Cesium Beam Frequency Standard which represents a further development and improvement of the Master Regulating Clock TD-1251/U, presently being manufactured. The weight will be reduced from the present 60 lbs to less than 30 lbs. This severe requirement made necessary the redesign of the Cesium Beam Resonator as well as the electronic system.

Introduction

The Portable Real Time Clock (PRTC) was designed for use as a portable, aircraft atomic standard using the transition of Cesium ^{133} (3,0 ↔ 4,0). The PRTC is used as a precision clock for the communication system on the 616A program.

ELECTRICAL SPECIFICATIONS

ACCURACY:	$\pm 3 \times 10^{-11}$, -28°C to +65°C
REPRODUCIBILITY:	$\pm 1 \times 10^{-11}$
SETTABILITY (FREQUENCY):	$\pm 2 \times 10^{-12}$
ADJUSTMENT RANGE:	6×10^{-11}
LONG TERM STABILITY:	$\pm 1 \times 10^{-11}$
SHORT TERM STABILITY	
AVERAGING TIME (SEC.):	Δ F/F
1	7×10^{-11}
10	2.2×10^{-11}
100	7×10^{-12}
1,000	2.2×10^{-12}
WARM-UP TIME:	20 MINUTES FROM -28°C
SINUSOIDAL OUTPUTS:	5 MHZ, 1 MHZ, VIA FRONT PANEL OUTPUTS
OUTPUT VOLTAGE:	0.9 TO 1.5 VRMS INTO 50 OHMS
SQUARE WAVE	
OUTPUT 3 MHz:	2.5 VP-P MINIMUM INTO 75 OHMS, REAR PANEL ONLY.
VOLTAGE REQUIRED:	115 OR 230 VAC ± 10%, SINGLE PHASE. 50 TO 400 HZ; OR 22 TO 31 VDC.
STANDBY BATTERY CAPACITY:	1 HOUR @ 25°C 1/2 HOUR @ -28°C AND +65°C
STANDBY CHARGING RATE:	16 HOURS
BATTERY SWITCHOVER:	AUTOMATIC

TABLE I

ENVIRONMENTAL SPECIFICATIONS

OPERATING TEMPERATURE:	-28°C TO +65°C. FREQUENCY CHANGE $<2 \times 10^{-11}$
HUMIDITY:	95% HUMIDITY. FREQUENCY CHANGE $<1 \times 10^{-11}$
ALTITUDE:	FREQUENCY CHANGE 0 TO 15.2 KM (50,000 ft.), $<2 \times 10^{-12}$
MAGNETIC FIELD:	0 TO 0.2 MILLITESLA (0 TO 2 GAUSS) DC OR PEAK AC AT 50, 60 AND 400 HZ; FREQUENCY CHANGE LESS THAN $\pm 2 \times 10^{-12}$
VIBRATION:	MIL-E-16400 MIL-E-5400 FREQUENCY SHIFT $<2 \times 10^{-11}$
SHOCK:	MIL-E-5400
CRASH SAFETY:	MIL-E-5400
EMC:	MIL-STD-461 AND MIL-STD-462

TABLE II

In its ready mode, the PRTC will be running on a.c. or d.c. external power. When required in the aircraft, the external power is disconnected, and the PRTC automatically switched to its internal batteries. The PRTC will then be carried to the aircraft, where it is plugged into the equipment rack in the plane, which again supplies external power. The PRTC lends itself to any requirement where a portable cesium standard is needed. The small size and light weight of these modules also makes it ideally suited for use as a space lock.

Specification Requirements

A summary of the electrical requirements is shown in Table I. The basic accuracy of the standard is $\pm 3 \times 10^{-11}$ over all operating conditions. The basic environmental specifications are shown in Table II. Frequency Electronics currently manufactures a cesium standard (TD-1251/U) meeting all of these requirements, except for the 30 lbs. This standard is shown in Figure 1. The description and operation of this clock was reported in the 31st Frequency Control Symposium [1].

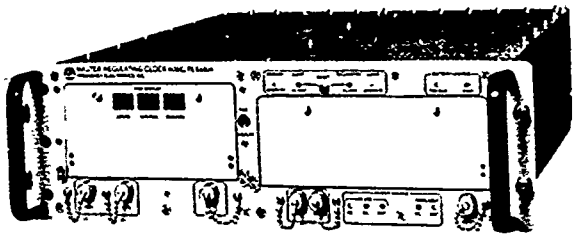

FIGURE 1
Master Regulating Clock, TD-1251/U

System Description

Figure 2 is a simplified block diagram of the new Cesium Beam Standard. The 5 MHz OCVCXO, which has extremely low phase noise and excellent short term stability, is multiplied to f_1 = 9,200 MHz by the multiplier (X40) and harmonic generator (X46). The synthesizer produces a frequency f_2 = 7.368,228,40 MHz from the 5 MHz OCVCXO. The difference between f_1 and f_2 is 9192.631,771,59 MHz which feeds the resonator input. The 5 MHz in the multiplier is phase modulated at an 83 Hz rate.

The signal from the Cesium Beam Resonator is amplified, demodulated and integrated in the Error Signal Controller. The error signal is used to lock the 5 MHz oscillator to the Cesium transition.

The standard provides 1 MHz, 3 MHz and 5 MHz frequency outputs, as well as precision second marks, minute marks, and time of day information. The real time clock also provides a visual time-of-day display.

The front panel controls are shown in Figure 3. A front panel meter is available to check internal circuit functions. A thumbwheel switch provides the ability to advance the output pulse in 100 nanosecond steps up to 1 second. The physical layout of the modules is shown in Figure 4. These same modules were reconfigured to form a space cesium standard (Figure 5). This space standard does not require the front panel controls, real time clock, or battery power supply and will therefore be smaller and consume less power.

Table III shows the weight allocation for the modules of the PRTC. The power distribution is shown in Table IV.

Performance

A breadboard of the system was fabricated and tested. The design of the 5 MHz oscillator has been completed and results of its testing are shown in Table V. This low phase noise oscillator weighs only 0.6 lbs. The oscillator uses miniaturized hybrid components and was made with a glass dewar flask, although provisions were made to use a titanium dewar flask if necessary (Figure 6).

In order to meet the 30 lb. weight requirement, it was necessary to redesign the cesium resonator. All the resonator components, except the cesium oven assembly, are enclosed in a rectangular structure in vacuum. The components are firmly secured to a precision ground base plate, which is the main structure support of the resonator. The only movable component is the cesium detector assembly, which is mounted on a single movable plane platform joined by a metal bellows assembly. The detector assembly is secured by a lock nut when optimum signal to noise ratio is attained during cesium beam alignment.

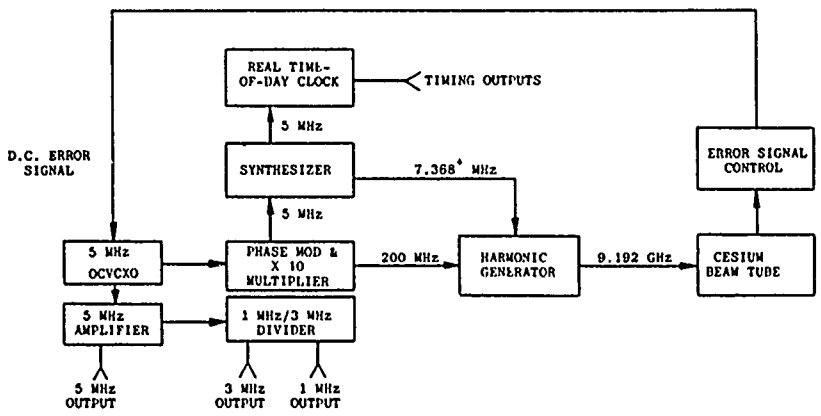

FIGURE 2
PRTC Block Diagram, Model FE-5450A

WEIGHT ALLOCATION

	MODULE	PRTC	TD-1251/U	SPACE APPLICATION
	CHASSIS	8		
A1	CESIUM BEAM TUBE	11.0		
A3	ERROR SIGNAL CONTROLLER	1.0		
A5	MULTIPLIER	.9		
A7	SYNTHESIZER	.7		
A8	5 MHZ OCVCXO	.8		
A9	CLOCK	2.0		
A10	1 MHZ/3 MHZ DIVIDER	.3		
A11	POWER SUPPLY	2		
A17	BATTERY PACK	3		
	TOTAL	29.7 LBS	62 LBS	22.6 LBS

TABLE III

POWER DISTRIBUTION

	MODULE	PRTC	TD-1251/U	SPACE APPLICATION
A1	CESIUM BEAM TUBE	10.0		
A3	ERROR SIGNAL CONTROLLER	1.5		
A5	MULTIPLIER	2.5		
A7	SYNTHESIZER	1.0		
A8	5 MHZ OCVCXO	1.6		
A9	CLOCK	4.5		
A10	1 MHZ/3 MHZ DIVIDER	1.5		
A11	POWER SUPPLY	7.8		
A17	BATTERY PACK	0.9		
	TOTAL	31.3 WATTS	42.5 WATTS	17.8 WATTS

TABLE IV

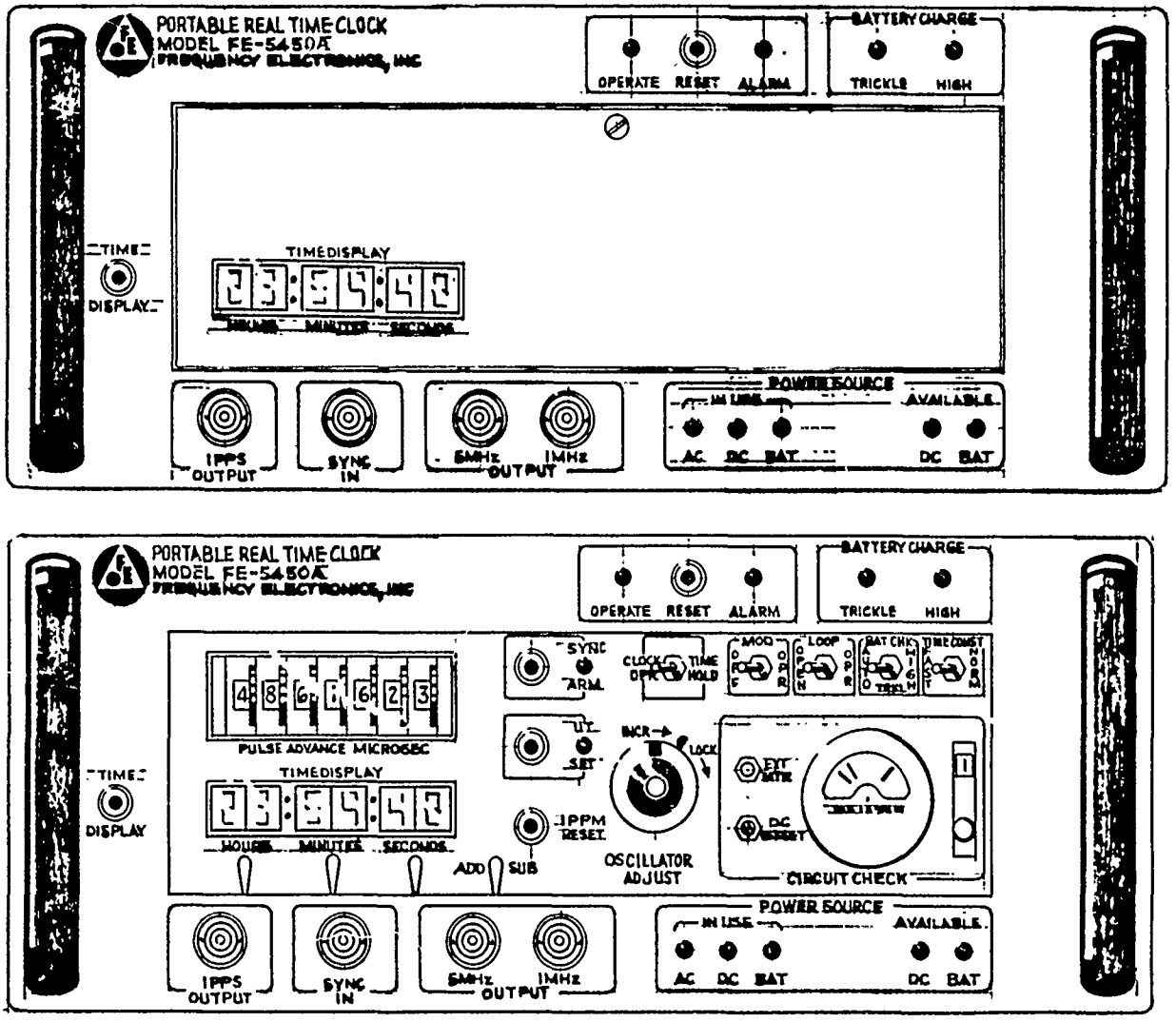

FIGURE 3
Front Panel Detail

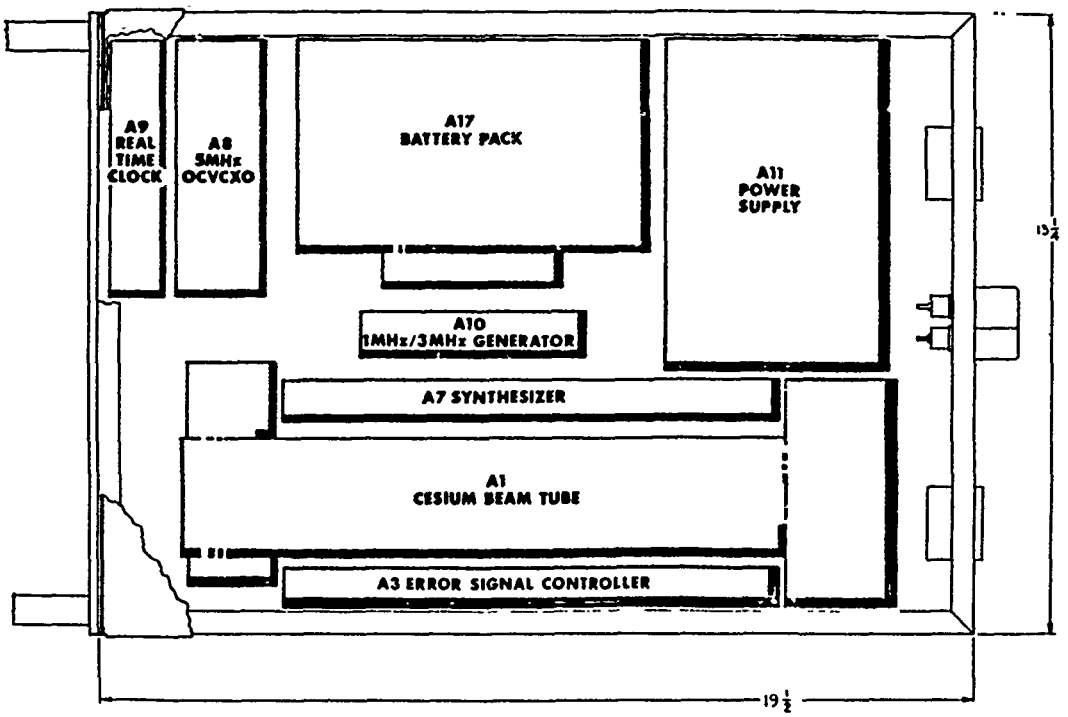

FIGURE 4
PRTC Module Layout

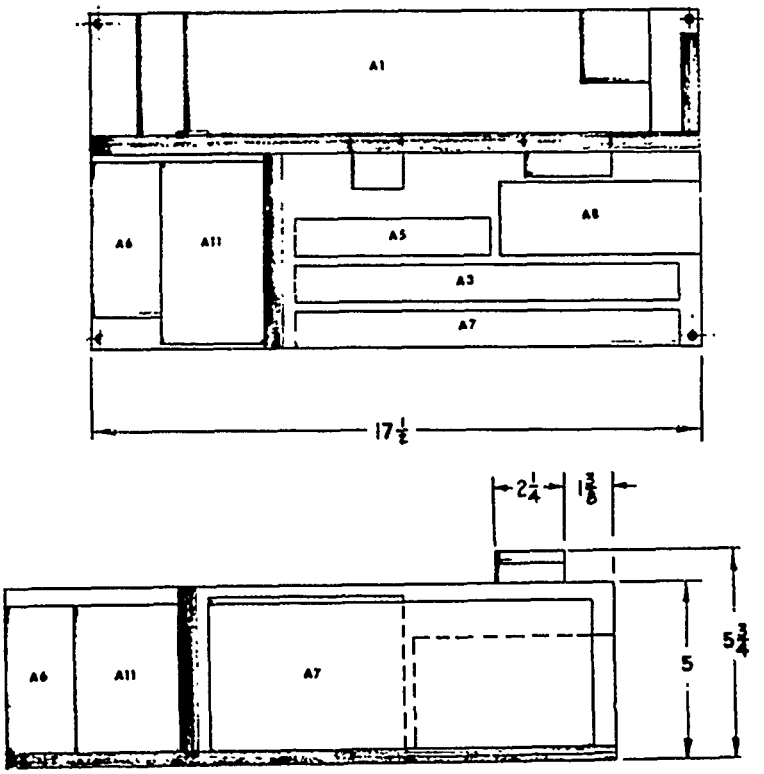

FIGURE 5
Space Application Module Layout

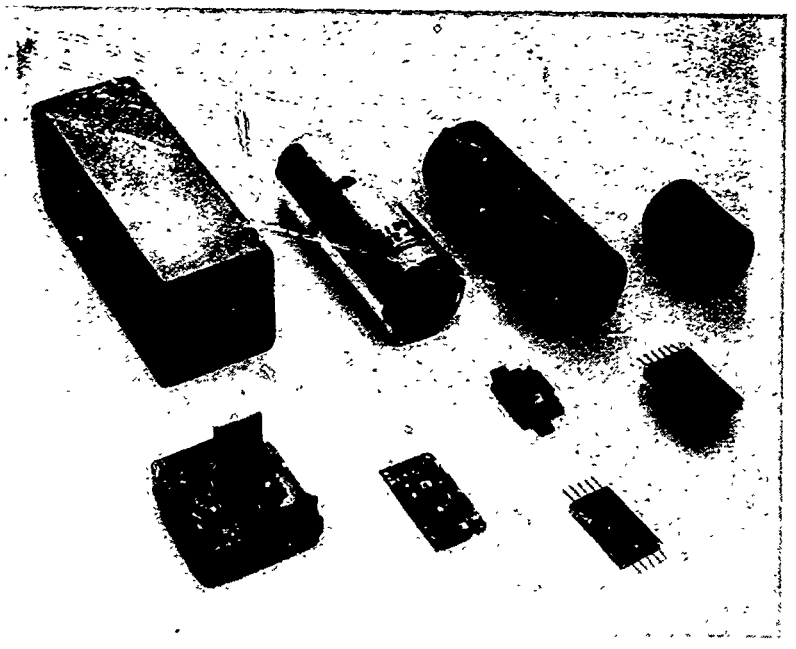

FIGURE 6
Miniaturized Hybrid Oscillator

5 MHZ OSCILLATOR PERFORMANCE

INPUT POWER: 1.6 WATTS
SIZE: 2" X 2" X 5.5"
WEIGHT: 0.6 LBS

STS		PHASE NOISE	
TIME	ALLEN VAR	FREQ.	DB
1 MSEC	1.5×10^{-10}	1 HZ	-116
1 SEC	1.0×10^{-12}	10 HZ	-135
10 SEC	1.2×10^{-12}	100 HZ	-142
100 SEC	1.5×10^{-12}	1 KHZ	-150
		10 KHZ	-160
		100 KHZ	-165

TABLE V

The basic cesium beam optics alignment is simple and straight-forward, i.e., A and B energy state selector magnets, C-field/shield and microwave structure are positioned on the centerline of the precision base plate of the resonator. Preliminary performance data on the new resonator are:

Resonance Linewidth @ I /2:	900 Hz
S/N Ratio (AC error signal):	$\geq$54 dB in 1 Hz B.W.
STS:	$5 \times 10^{-11}/\sqrt{T}$
Resonator Volume:	115 cubic inches
Resonator Weight:	11 lbs.

Much of the data taken on the Cesium resonators used the 1st derivative of the Ramsey curve as shown in Figure 7. The symmetry of this spectrum and the well resolved lines indicates a good uniformity of the C-field and a high degree of accuracy for the phase in the microwave field of the Ramsey cavity. Figure 8 is the derivative curve at the (3,0)$\leftrightarrow$(4,0) transition used for locking the frequency of the standard. The recording of the first derivative of the Ramsey curves represents a sensitive and accurate method of measuring the performance of a cesium beam tube. Figure 9 shows the set-up for recording of this spectrum. By adding a frequency synthesizer, X-Y recorder, and a low pass filter, it is possible to transform the Cesium Standard into a spectrometer for recording the first derivative of the Cesium transitions.

Summary

We have described the development of a lightweight Cesium Frequency Standard that meets stringent military requirements. Breadboard results have shown an accuracy of better than 4×10^{-12}. Hardware is presently being fabricated for the first two prototype systems.

Acknowledgment

The authors wish to acknowledge the support of Alfred Kahane and Nick Zannoni of Electronic Systems Division for their support. This was supported in part by Contract F19628-78-C-0094 from Electronic Systems Division, Air Force Systems Command, USAF.

[1] J. George & A. I. Vulcan, "Development of a Cesium Beam Clock for Satellite Application." Proc. 31st Annual Symposium on Frequency Control, pp. 542-550, 1977.

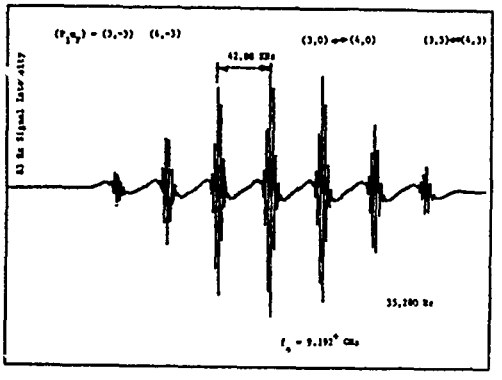

FIGURE 7
Ramsey Derivative Curves for C_S^{133}
- Full Spectrum -

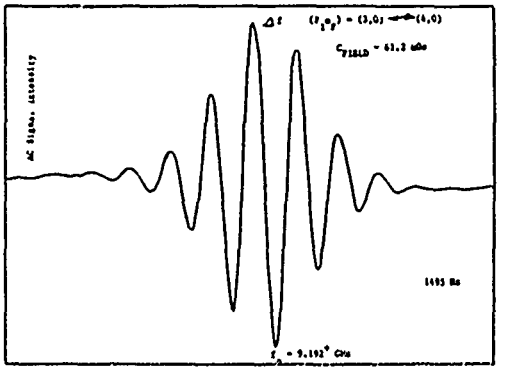

FIGURE 8
Ramsey Derivative Curves for C_S^{133}
(3,0)⟷(4,0) Transition

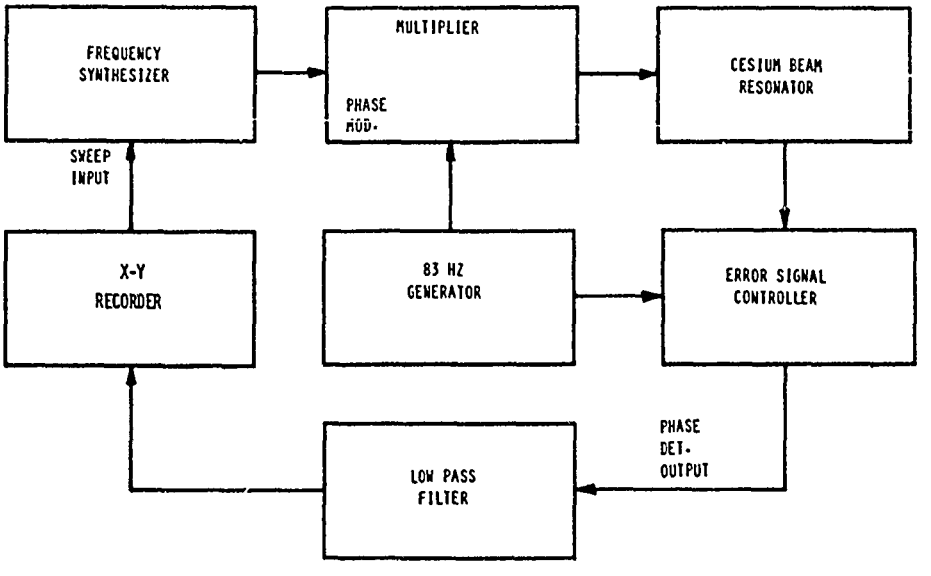

FIGURE 9
Derivative Ramsey Spectrum Test Set-Up

NEW CESIUM BEAM TUBE UTILIZING HEXAPOLE / DOUBLE-DIPOLE OPTICS*

Donald A. Emmons
Paul J. Rogers

Frequency and Time Systems, Inc.
Danvers, Massachusetts 01923

SUMMARY

A prototype hexapole/double dipole cesium beam tube has been operated successfully. The overall length is 37.5 cm and weight of the sealed-off tube is 5.1 kg.

A low frequency flop-to-background ratio of 1.7 indicates that the optics design is successful to first order, and that Majorana transitions and unwanted background are not swamping the signal.

The measured line width is less than 430 Hz which is unusually narrow for a beam tube of this length, and is consistent with a velocity spectrum estimated to peak at approximately 100 m/sec. When the tube optics was trimmed with external magnets, a signal-to-noise ratio of approximately 2,100 was obtained. The line width was subsequently decreased to 320 Hz by external trimming of the hexapole and double-dipole fields.

In view of these observed effects, it is likely that the beam flux can be further increased by improved design. The tube has been operated in a cesium standard with results consistent with measured S/N.

Key Words (for information retrieval) Cesium Beam Tube, Hexapole, Double-Dipole, Frequency Standard.

INTRODUCTION

In operational frequency standard systems for navigation and communications it is of interest to improve the available signal-to-noise performance, to attain smaller frequency uncertainties over relatively short averaging times, while maintaining the presently available size, weight and required power, or even reducing them.

We have constructed an experimental hexapole/double-dipole cesium beam tube (Kartaschoff's design)[1] as a means of exploring an alternative to the standard dipole state-selection beam optics used in all commercial cesium standards at present.

The standard dipole - dipole optics exhibits a large spatial dispersion coupled with a rather wide spectrum in atom velocities.

*Supported in part by the U.S. Navy under Contract N00014-78-C-0416.

The use of a multipole state selector is appealing for several reasons:

1. The velocity selected spectrum can be quite narrow.
2. A particular velocity slice suffers less spatial divergence than for the dipole magnet case.
3. Cesium atoms emitted from the oven are more narrowly confined to the active cavity axis and are thus more readily gettered.
4. As a consequence of the hexapole's (weak) focussing, potential signal strength is increased.

Several multipole - multipole optics systems using hexapole and quadrupole magnets have been explored in the past. One difficulty in the practical realization of a high accuracy, small size device is in the beam detection. The optimal detector location, a small spot on the beam center line, must be shielded from on-axis background. Therefore, the detector is responsive only to flop-out signal and the background tends to be high and the signal-to-noise (short term stability) low. (A "flop-in" annular detector was described by Holloway and Lacey but it suffers from a number of mechanical difficulties.) Nevertheless, the primary standard of the PTB, which uses hexapoles, as well as a more recent Japanese effort have been reported with adequate S/N ratios[3,4].

A scheme using a hexapole state selector and a double-dipole detector-analyzer, was described by Kartaschoff a decade ago[1]. Although this configuration does not retain the cylindrical symmetry of multipole - multipole optics, there are a number of other advantages. The flop-in detector is a simple ribbon, easily shielded from on-axis rays, and should permit good signal-to-background discrimination without rejecting large amounts of useful signal.

The experimental tube to be described was designed to include several features of scale and manufacturability aimed at realizing a highly reliable and rugged device. The hexapole magnet is of minimum size and weight since that will ultimately be a strong consideration in acceptance of such a new design. By way of contrast this hexapole magnet weighs 0.64 kg as compared to 3.4 kg in Kartaschoff's original design, and the double-dipole magnet is similarly

one-fifth the original weight and size.

The beam tube is shown in Figure 1, along with the hexapole magnet and the double-dipole pole piece construction. Overall length of the tube is 37.5 cm (14.75 inches), and the weight is 5.1 kg.

HEXAPOLE DOUBLE-DIPOLE OPTICS

General Principles

The general scheme of state selection and detection is shown in Figure 2. The figure is not to scale and is a top view showing the width greatly exaggerated. The cesium source is a simple effusive channel, placed as close as possible (for highest efficiency) to the entrance aperture of the hexapole "A" magnet. The exit aperture has a beam stop to eliminate on-axis trajectories.

The "C" field is transverse, not solenoidal, thus allowing the use of existing "C" field windings, Ramsey microwave cavity structure and magnetic shielding.

During tube construction, Hall probe measurements at the "B" end inside the doubly shielded "C" field region showed a rapid and smooth decrease of leakage field strength to the 57 milligauss level required at the position of the microwave cavity.

The hot wire detector is a 1mm wide ribbon, shown in cross section. A mass spectrometer selects for cesium ions, and is followed by an electron multiplier in the usual manner.

The operation is as follows. Atoms with negative magnetic moment (μ), traveling out from and along the axis are deflected toward the axis in the "A" magnet. In the strong field approximation they experience a force proportional to radial displacement, and undergo harmonic motion. If the traversal time is, for example, one-quarter of the harmonic period, then the atoms emerge approximately paraxially to travel through the Ramsey cavities. Positive μ atoms are deflected outward, to nearby getters. Atoms in the (4,0) state can undergo r.f. transitions to the (3,0) state. Having now positive μ as they enter the inhomogeneous "B" magnet, they are again deflected toward the axis and strike the detector, whether they go through the left hand or right hand gap.

The hot wire detector is well shadowed by the central pole piece which has additional aperture definition, not shown. This makes it unlikely for atoms not having the proper "signal" characteristics to be detected.

The spatial dispersion of atom velocities is symmetrical to some extent. It is still true that atom velocity will be a function of radial distance, from the axis, of the trajectory of the atom emerging from "A". However, this is in contrast to the strong asymmetries associated with dipole optics. These considerations are important because the clock transition frequency is a function of relative phase across the cross-section of the microwave interaction region[5].

At the "A" magnet exit, beam stops and field trimmers were used to minimize the contribution of Majorana transitions to the background signal. The beam stops were also expected to intercept some of the background states for which the effective magnetic moment μ changes sign between low field regions (near the axis) and high field regions. This will occur for some of the (3, -3) and (3, -2) flux which is deflected first toward the axis center line, then procedes through the "C" field to a high field "B" region, where μ is now negative. These atoms are then deflected toward the hot wire. However, not all such atoms are excluded by the beam stops, particularly when skewed trajectories are considered. Atoms in the state (4, -3) similarly change sign of μ at intermediate field strength and so can contribute "signal-like" trajectories.

In general terms, the hexapole selects a narrow range of atom velocities and provides a state-selected beam which is more or less paraxial. The velocity of an emerging atom is some function of radial distance, but to first order, the velocity range of atoms traveling through the detector magnet gaps, is dictated by the "A" magnet field strength. Assuming strong fields (μ = constant) the expected probable velocity was less than 100 m/sec. which in turn implied a linewidth of about 380 Hz.

Efficiency

The hexapole field may be thought of as focussing, in that a point source of mono-velocity atoms is imaged on a small detector spot. In practice, the source must be of finite size, and the optics is far from perfect. For example, angular momentum of atoms about the axis spreads out the detector plane pattern.

On the basis of oversimplified solid angle considerations alone, the acceptance angle for the hexapole would give considerable advantage over the standard optics. However, a full description of the flux efficiency involves detailed consideration of all possible trajectories, field dependencies and transition probabilities.

It is of interest to know, even approximately, how overall efficiency depends on selected velocities. Becker[6] has calculated the efficiency for various combinations of hexapole and quadrupole magnets. If his assumptions can be applied in our case, with a projected source image larger than the detector aperture, then the dependence of S/N ratio on velocity would go as $(v)^{1.5}$, where v is the velocity of the atoms. Since linewidth is proportional to v, we might expect the quantity (S/N)/W, ("figure-of-merit") where W is linewidth, to increase as $(v)^{0.5}$. However, a more ideal geometry would make use of much smaller source dimensions (at the expense of total flux). In that case Becker's analysis would show (S/N)/W to go as $(v)^{-0.5}$ thus making low velocity selection preferred.

The experimental tube initially exhibited a linewidth consistent with ≅ 113 m/sec. It is useful to recall that available beam intensity from the oven is a steep function of v. At v = 100 m/sec the intensity is 20% of that at the thermal distribution peak, which occurs at 260 m/sec.

RESULTS

The tube was initially run with variable oven temperature. A 20 kHz excitation coil in the center of the C field region allowed observation of the low frequency flop signal. Flop to background ratio was 1.7, an encouraging indicator that

the signal was not lost in a background of Majorana flop and unwanted trajectories. Beam signal was approximately 0.5 pA and this was consistent with the observed noise figure.

Initially, the Ramsey resonance linewidth was 430 Hz and the S/N ratio was 1200, measured as peak minus valley signal current, divided by the noise in a 1/4 Hz bandwidth at the modulation frequency. It was found that it was possible to increase the signal by perturbing the beam optics and trimming the internal fields with external magnets. By this means it was possible to increase the S/N ratio to above 2100.

It was suspected that an even larger signal was prevented in part due to a mis-match between the "A" and "B" magnet field strengths. The trajectory calculations based on measured magnet gap fields, and the placement of the detector, had pointed toward a lower velocity cut than that observed. Thus an attempt was made to decrease the focussing field strengths by small increments, using external degaussing pulses.

In these experiments it was possible to increase the signal by 50%, but without improving S/N ratio. Further efforts then resulted in decreasing signal. During this process the measured Ramsey linewidth decreased from 430 Hz to 320 Hz, the latter indicating a velocity peak at about 84 m/sec.

Figure 3 shows the (4,0) → (3,0) microwave ("clock transition") resonance in detail. This scan was made under conditions of less than 1200 S/N ratio. No external trimming fields were in place.

Figure 4 is a lower resolution scan of the same resonance, showing the centering of the 0 → 0 transition on the pedestal.

The cesium beam tube was operated as a frequency standard using modified FTS Model 4000 cesium standard electronics. Operating conditions were such that the figure-of-merit was approximately 2. Figure 5 shows the preliminary frequency stability measurements. Long term data taking is not yet complete.

CONCLUSION

Some of the vital statistics of the experimental tube are shown in Figure 6, along with a brief summary of results. The overall length of the tube is only 37.5 cm (14.75 inches), weight is 5.1 kg. The hexapole magnet bore diameter is 0.3 cm.

A S/N ratio of more than 2100 (1/4 Hz noise bandwidth) was obtained, under conditions of magnetic trimming, at a linewidth of 430 Hz. This indicated a figure-of-merit of better than 4, which is encouraging for a first cut at this new type of beam optics, in a relatively short tube.

It is clear from the observed response of the beam tube to perturbing forces, that the optics configuration is not yet optimal. A reasonable goal is to have a tube of length and weight similar to this, exhibiting a signal-to-noise ratio greater than 10,000 with a linewidth of 330 Hz, and thus achieve frequency uncertainties approaching 1×10^{-14} for averaging times of one day.

REFERENCES

1. P. Kartaschoff and P. E. Debely "Resonateur a Cesium de Conception Nouvelle", Proc. "Colloque International de Chronometrie", September 1969, Paris, p. A3-1.

2. J. H. Holloway and R. F. Lacey "Performance of Cesium Beam Tubes with Multipole Optics", Proc. "Colloque International Chronometrie" September 1969, Paris

3. ". Becker "Performance of the Primary Cesium - Standard of the Physikalisch - Technische Bundestalt", Metrologia 13 (1977), p. 99.

4. M. Kobayashi, et al., "Design and Preliminary Result on a Cesium Beam Standard at the RRL" IEEE Transactions IM-27 (1978) p. 343.

5. H. Hellwig "The Realization of the Second" Proc. 5th Conf. on Atomic Masses and Fundamental Constants, ed. by J. Sanders and A. Wapstra, Plenum Press (1976), p. 330.

6. G. Becker "Research on Cesium Beam Frequency Standards at the PTB: Beam Optics, Majorana Transitions" IEEE Transactions IM-27 (1978) p. 319.

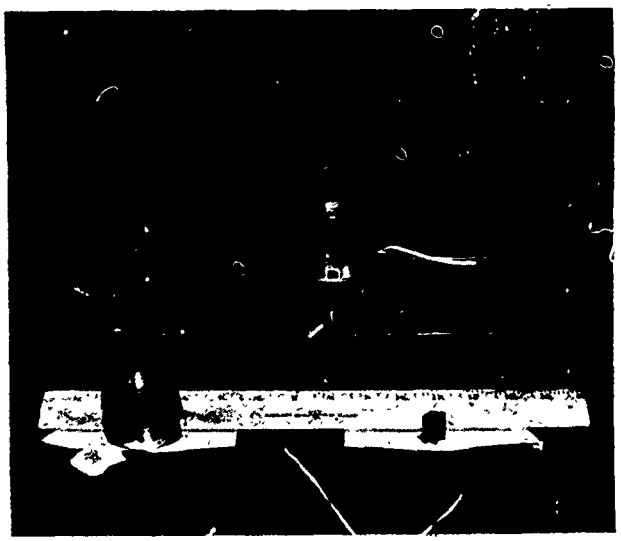

1. Hexapole/Double Dipole Beam Tube

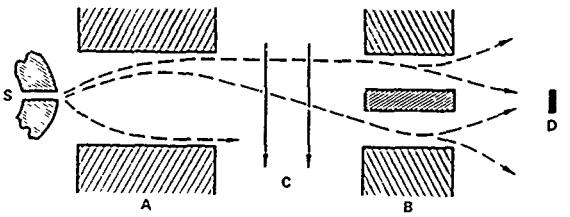

FIGURE 2. HEXAPOLE DOUBLE DIPOLE BEAM OPTICS

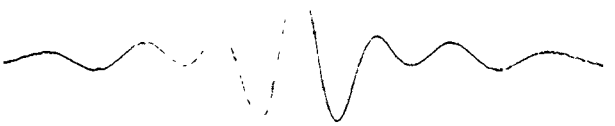

FIGURE 3. MICROWAVE RESONANCE (4,0) → (3,0) TRANSITION; LINEWIDTH 320 Hz

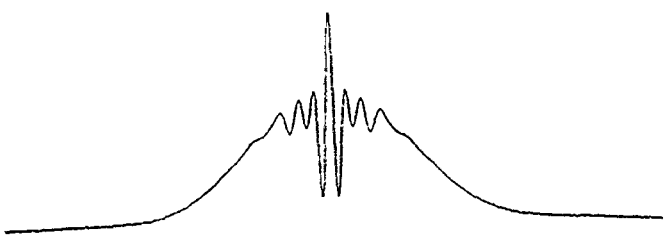

FIGURE 4. (4,0) → (3,0) RESONANCE AT LOW RESOLUTION

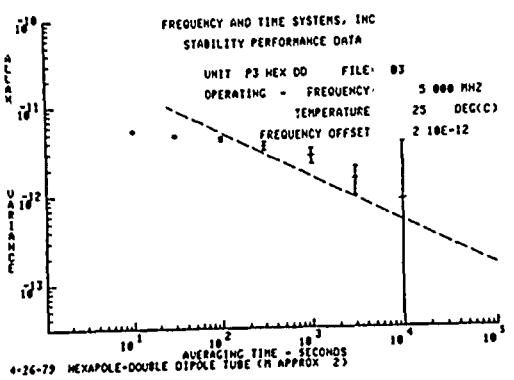

FIGURE 5. FREQUENCY STABILITY

HEXAPOLE DOUBLE DIPOLE CESIUM BEAM TUBE

OVERALL LENGTH	37.5 cm
WEIGHT	6.1 Kg
HEXAPOLE BORE	0.3 cm
LENGTH	4 cm
DOUBLE DIPOLE LENGTH	2 cm
SIGNAL TO NOISE RATIO	2100
LINEWIDTH	<430 Hz

FIGURE 6. SUMMARY DATA

LASER TO MICROWAVE FREQUENCY DIVISION USING SYNCHROTRON RADIATION II

J. C. Bergquist and D. J. Wineland
Frequency and Time Standards Group
National Bureau of Standards
Boulder, CO 80303
(303) 499-1000, ext. 4459

Abstract

We present a review of theoretical calculations which demonstrate the feasiblity of obtaining one step frequency division from optical or infrared laser frequencies to a subharmonic in the microwave spectral region, and include current experimental designs toward a practical realization of this goal. We plan to drive the cyclotron orbit of a single relativistic electron, which is confined in a Penning ion trap, with a laser beam focused to a spot diameter $\sim \lambda$. This method is an extension of a common technique used in cyclotrons and synchrotrons where the orbit of high energy particles is driven at a harmonic of the orbit frequency. Our experiment is designed to measure this orbit frequency which is then a subharmonic of the driving (laser) frequency. This technique requires that the uncertainty in the electron orbit dimensions be limited to $\leq \lambda/2$, which is possible by radiative cooling and the method of motional sideband excitation. The possibility of a unified optical wavelength/frequency standard is evident.

Introduction

It is our intent in this paper to summarize and extend the theoretical analysis of a broadband laser to microwave frequency divider proposed earlier.[1] We also give a brief description of experimental designs being considered for the realization of this division. The importance of accurate freuqency division from the optical spectrum derives primarily from frequency (time) and wavelength metrology and the extreme likelihood that the most accurate, reproducible, and stable oscillators may be realized in that part of the electromagnetic spectrum. Certainly, there is great value of such a device in the area of atomic and molecular spectroscopy.

Principle of Operation

The proposed synchrotron divider is based on the principle that a purely harmonic oscillator can be coherently driven (pumped) by a spatially nonuniform, higher order harmonic driving field. This method has been used for years in cyclotrons, synch ocyclotrons, and synchrotrons to accelerate charged particles to relativistic speeds. In these devices, particles are frequently driven by radiation from microwave cavities, which is localized to a small portion of the cyclotron orbit, at frequencies integrally related to the cyclotron orbit frequency. For a significant transfer of energy from the RF driving field into the cyclotron orbit it is necessary that the interaction time of the charged particles with the radiation field be comparable to or less than one-half period of the RF frequency. Longer interaction times quickly average the transfer of energy to zero.

It would seem possible to straightforwardly extend this technique to driving fields of shorter wavelengths in order to drive the cyclotron orbit of a single electron in a magnetic field at a very high harmonic of the cyclotron frequency. Theoretically, this is the case, however, shorter wavelengths entail special practical considerations discussed below. If the orbit is stable then the power absorbed by the electron from the harmonic excitation is balanced by the emitted synchrotron radiation. The cyclotron frequency is then a phaselocked submultiple of the driving frequency.

We illustrate the important features of the proposed method in fig. 1.

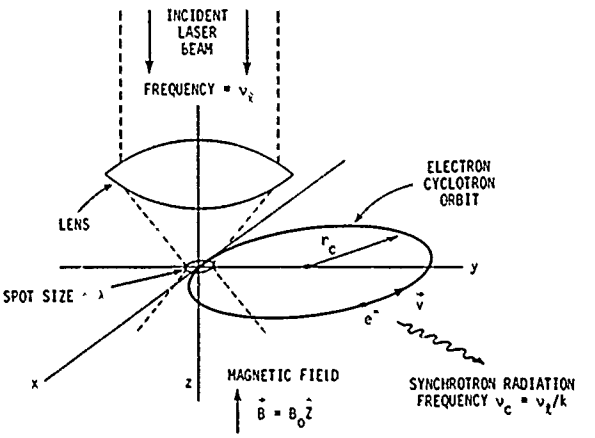

SYNCHROTRON FREQUENCY DIVIDER

Radiation from a well collimated, Gaussian laser beam, linearly polarized in the x direction and traveling in the -z direction is focused into a spot with diameter $\sim \lambda$ by a lens. If it is possible to provide that the electron orbit, which is confined to lie in the x,y plane, pass through this focus, then the electron will absorb energy from

the radiation field. Assuming that the envelope for the electric field vector is approximately Gaussian and that the absorbed energy per pass (ΔW) is small compared to the total electron energy, we have

$$\Delta W \cong \int_{-\infty}^{\infty} eE_x dx = \sqrt{2}\, eA \cos\delta \exp\left\{-\left[\frac{\pi c S_o}{2v\lambda}\right]^2\right\} \qquad (1)$$

where

A = field amplitude factor
δ = phase of laser field
v = electron's velocity
S_o = actual diameter of focused line ($\sim \lambda$)
c = speed of light

Note that ΔW shows a double exponential dependence on the ratio $cS_o/\lambda v$. Thus the energy transferred to the electron is extremely small unless this ratio is approximately equal to one. This is because the oscillating driving field will rapidly average the energy transfer to zero unless we can arrange that the electron spend approximately one cycle or less in the radiation field. If the extent of the interaction region could be made substantially less than λ then the speed of the electron could be made correspondingly less while maintaining an effective energy transfer. A possibility may be a dielectric waveguide with transverse dimensions less than λ that is projected into the trap and is cut off within about λ of the electron orbit.

Confinement of the circular electron orbit path to $\lesssim \lambda/2$, which is necessary to prevent $\Delta W \to 0$, is accomplished by trapping the electron in a Penning trap with hyperbolic electrodes immersed in a static magnetic field $\vec{B} = B_o \hat{z}$. The electrostatic potential is given by $\psi = V_o(r^2 - 2(z^2 - z_o^2))/(r_o^2 + 2z_o^2)$ where r is the radial coordinate, z is the axial coordinate, r_o and z_o are the characteristic dimensions of the trap,[2] and V_o the voltage applied between the trap electrodes. The axially symmetric, static electromagnetic trap is thus formed with two endcap electrodes which are constructed to lie on the $\psi = 0$ equipotential surface and a ring electrode which conforms to the equipotential $\psi = V_o$. The motion of the electron is given by the synthesis of three separate oscillations. First there is the harmonic motion parallel to the z axis at frequency $\nu_z = (eV_o/m\pi^2(r_o^2 + 2z_o^2))^{\frac{1}{2}}$ due solely to the applied electric field. In the radial plane the motion is comprised of the sum of two vectors $\vec{r}_c$ and $\vec{r}_m$ which rotate at frequencies ν_c' and ν_m. These frequencies are approximated by $\nu_m \cong \nu_z^2/(2\nu_c)$ and $\nu_c' \cong \nu_c = (eB_o/2\pi mc)$, when $\nu_c \gg \nu_z$. In order to satisfy our requirement to confine the electron orbit path to $\leq \lambda/2$, $|\vec{r}_m|$ and z must be held to $\leq \lambda/4$. This can be accomplished by radiatively cooling the axial (z) motion and suppressing the magnetron (r_m) motion by the method of motional sideband excitation.[1,3] The electron orbit is then nearly circular with cyclotron frequency ν_c'.

The minimum r_m is given by[1]

$$r_m^2 \cong 2\,(\omega_m/\omega_z)\,\langle z^2\rangle \qquad (2)$$

where $\langle z^2\rangle$ is the mean square thermally excited axial amplitude. As a quantitative example, assume that $r_o \cong 1.6\, z_o = 0.1$ cm, $V_o = 10$ kV, $v/c = 0.8$, $S_o = \lambda$, $B_o \cong 1$T with $\nu_c \sim 15$ GHz, and $T_z = 4$ K. These conditions will give $\nu_z \cong 7.8$ GHz, $\sqrt{\langle z^2\rangle} \cong 175$ nm, and $r_m \sim 150$ nm and an orbit confined to less than $\lambda/2$ provided $\lambda \gtrsim 700$ nm. We note that V_o is extremely large in order to confine the axial z excursions to $< \lambda/4$. This requirement is greatly reduced if the focus is a cylindrical line parallel to z rather than a spot of dimensions λ on all sides. This focus ($\lambda \times \lambda \times 20\lambda$) could be obtained with a softly focused beam followed by a strong focusing cylindrical lens. A smaller value of V_o reduces the likelihood of spurious field emission currents which could give rise to extraneous trapped electrons. Since $\langle z^2\rangle \propto V_o^{-1}$ and $\nu_z \propto V_o^{\frac{1}{2}}$, a reduction of V_o by 10^2 increases $\sqrt{\langle z^2\rangle}$ by 10 and reduces ν_z by the same factor. From Eq. 2, the minimum value of r_m increases by only a factor of three. Thus, this change in V_o to 100 V, allowed by the cylindrical lens focus, gives $\nu_z \cong 780$ MHz, $\sqrt{\langle z^2\rangle} \sim 1.75$ μm, and $r_m = 0.45$ μm, permitting $\lambda \gtrsim 600$ nm. (It is further noted that the electron orbit confinement problem is greatly reduced by choosing longer wavelength lasers).

If we now provide an energy balance between the energy absorbed by the electron and the energy lost through synchrotron radiation, which is efficiently coupled out to the frequency measurement electronics, the the cyclotron frequency will phase lock to a subharmonic of the laser frequency. Given that the laser has only minimum amplitude and frequency stability,[1] the phase lock condition will occur for $0 < \delta < \pi/2$. Consider that $\delta = \pi/4$ initially and that the laser power incident on the cylindrical lens is approximately 20 mW. The power absorbed and subsequently radiated by the electron, confined as described above, is about 1.4×10^{-10} W.

Feedback

Stability of the phase lock is automatically achieved since, for example, an increase in the energy of the electron results in a corresponding

decrease in the cyclotron frequency owing to the increase in relativistic mass. The electron thus experiences a slightly advanced phase of the laser on the next pass through the focus. This implies that ΔW decreases slightly and therefore the electron energy decreases. It is in this manner that the electron phase locks to the laser frequency.

We note that if initially, or at any later time, an energy imbalance exists between the energy absorbed and the energy radiated, then the automatic tracking of the electron to the balance point is not critically damped. Rather, the electron slews to the lock point in a slowly damped oscillatory fashion with a time constant equal to the trap coupled radiative decay time[1] of approximately 1 ms.

To be more quantitative, we write the change of phase of the microwave field (Φ) as

$$\frac{d\Phi(t)}{dt} = \dot{\phi}(t) + \omega_c'$$

where $\dot{\phi}(t)$ is the frequency deviation from the normal "locked" cyclotron frequency ω_c'. We have

$$\dot{\phi}(t) = \Delta\omega(t) = \Delta\omega_{fb}(t) + \Delta\omega_d(t) \qquad (3)$$

where $\Delta\omega_{fb}$ is the is the instantaneous frequency deviation of the electron from ω_c' due to the energy imparted by the laser, and $\Delta\omega_d$ is the frequency deviation due to the radiation decay. Writing $\delta = \pi/2 - \theta$ and assuming we are in the high power limit of the laser then the nominal value of $\delta \to \pi/2$ so that Eq. (1) becomes $\Delta W \cong W_o\theta$, where $W_o \equiv \sqrt{2}\, eA \exp[-(\pi c S_o/2v\lambda)^2]$. Now $\theta = k\phi$ where k is the division factor v_ℓ/v_c' so that $\Delta W \cong W_o k\phi$.

Noting that

$$\frac{d(\Delta\omega_{fb})}{dt} \cong -\frac{\omega_c'}{E}\left(\frac{dE}{dt}\right)_{fb}$$

where E is the total energy of the electron, then

$$\frac{d(\Delta\omega_{fb})}{dt} = -\omega_\ell\left(\frac{W_o v_c'}{E}\right)\phi \qquad (4)$$

To estimate $\frac{d(\Delta\omega_d)}{dt}$ we first note that

$$\frac{d(\Delta\omega_d)}{dt} \cong -\frac{\omega_c'}{E}\left(\frac{dE}{dt}\right)_d$$

An accurate expression for the energy decay due to synchrotron radiation $(dE/dt)_d$ in the absence of coupling structures is given in Ref. 1. Using this expression, we can find the dependence of $d(\Delta\omega_d)/dt$ on the difference frequency ($\Delta\omega$) and obtain

$$\frac{d(\Delta\omega_d)}{dt} \cong -\left(\frac{4e^2\gamma^2\omega_c'^2}{3Ec}\right)\Delta\omega \equiv -\frac{2}{\tau}\Delta\omega \qquad (5)$$

where τ is approximately equal to the damping time at low energy. We will assume that this expression is also valid when τ is decreased by coupling the electron to the trap electrodes. Differentiating Eq. 3 with respect to time and using Eqs. (4) and (5) we obtain

$$\ddot{\phi} + \frac{2}{\tau}\dot{\phi} + (\omega_\phi)^2\,\phi = 0 \qquad (6)$$

where $\omega_\phi = (\omega_\ell v_c' W_o/E)^{1/2}$. Thus phase oscillations around the nominal "locked" phase occur at frequency ω_ϕ and are damped with approximately the radiation damping time. For a laser power of 200 mW (λ = 3.39 μm) in the above example $W_o \cong 1.8 \times 10^{-13}$ ergs, and $\omega_\phi/2\pi \cong 1.7 \times 10^8$ Hz.

Spread of the electron wave packet

To estimate the restrictions placed on the model by quantum mechanics we start with the uncertainty relation $\Delta\phi\,\Delta n \gtrsim 1$, where $\Delta\phi$ is the uncertainty in phase of the cyclotron orbit of the electron and Δn represents the corresponding uncertainty in energy for the electron. Neglecting the electric field and electron spin, the electron energy is given by

$$E = [(mc^2)^2 + mc^2\hbar\omega_c(n + \tfrac{1}{2})]^{1/2} \qquad (7)$$

We want to build a wave packet which has its phase defined with an accuracy $\Delta\phi \lesssim (2\pi\lambda/10)/(2\pi r_c) \cong 1.3 \times 10^{-4}$ rad. From the uncertainty relation this requires a spread in energy quantum number of $\Delta n \lesssim 0.75 \times 10^4$. From Eq. (7) this corresponds to a range of natural frequencies $\Delta\omega \cong \omega_c'\,\Delta n/n \cong 1.3 \times 10^{-6}\,\omega_c'$. Classically, if we assume that the initial conditions for Eq. 6 are given by these values of $\Delta\phi$ and $\Delta\omega$, then we see that the phase is bound and initially oscillates with amplitude 1.75×10^{-4} rad. Quantum mechanically, it therefore seems likely that the electron will phase lock if the initial wave packet has a limited range of values of n and ϕ. Clearly this treatment is not rigorous and a more careful analysis of the quantum fluctuations must be made.

Acknowledgments

The authors acknowledge input from others; in particular we thank Wayne M. Itano and P. L. Bender for useful discussions concerning the uncertainty problem and S. R. Stein for helpful input on the electronics problems.

References

1. D. J. Wineland, J. Appl. Phys. 50, 2528 (1979).

2. H. G. Dehmelt and F. L. Walls, Phys. Rev. Lett. 21, 127 (1968); H. Dehmelt, in Advances in Atomic and Molecular Physics, D. R. Bates and I. Esterman, eds. (Academic, New York, 1967, 1969), Vols. 3 and 5. D. J. Wineland, P. Ekstrom and H. Dehmelt, Phys. Rev. Lett. 31, 1279 (1973). Note that in general one needs only axially symmetric electrodes, for simplicity the case of hyperbolic electrodes is discussed here.
3. R. S. Van Dyck, Jr., P. B. Schwinberg, and H. G. Dehmelt, in New Frontiers in High-Energy Physics, Kursunoglu, Perlmutter, and Scott, eds., (Plenum, New York, 1978) p. 159.

AN IMPROVED MULTIPLIER CHAIN FOR PRECISE FREQUENCY MEASUREMENTS UP TO 20 THz

A. Godone, A. De Marchi, E. Bava

Istituto Elettrotecnico Nazionale "Galileo Ferraris"

Abstract

The measurement of frequencies in the THz region requires a highly clean, reliable and stable multiplier chain to relate this spectral range with the one where standard frequencies are available. Most critical is the low frequency section of such a device. The multiplier realized at IEN is here described.

The 5 MHz signal from a highly pure quartz oscillator drives a commercial x5 multiplier and then a second x5 stage realized with two transistors in a differential amplifier configuration using Schottky diodes as switching elements, which was measured not to significantly increase the phase noise of the incoming signal.

After quartz filtering and amplification at 125 MHz, the XBand is reached with two overlay-transistor doublers and a step recovery diode.

The measured temperature and time dependent variations of the output amplitude remain within a few percent without amplitude control under laboratory conditions, and the phase noise promises a useful carrier-to-pedestal noise ratio at about 20 THz, with 100 Hz IF bandwidth.

A millimetric klystron is phaselocked to the XBand signal and used for obtaining the beat note with the submm signal under measurement.

Introduction

In several fields of technology and science it's very useful to synthesize signals with high spectral purity in the submillimetric region starting from stable quartz oscillators in the MHz region. As examples of applications for metrological purposes one may consider the study of atomic and molecular transitions or the phase locking of the far infrared lasers used in the frequency synthesis from microwave to the visible spectrum.

Some problems arising from the high multiplication order inherent in such a harmonic generation were discussed in [1] and [2], whereas in [3] experimental results showing a signal to phase noise ratio $S/N\phi \simeq 17$ dB in a bandwidth Bw = 10 kHz at 761 GHz were reported without using cryogenic components.

In this paper a new multiplier chain is described in which a particular attention was payed to the origin of phase noise in the first stages of the chain and to its reduction. The experimental results give an improvement, compared to the previous data, greater than 10 dB in $S/N\phi$ in the submillimetric region and as a consequence frequency measurements with coherent reference signals are now possible up to 20 THz.

Review of VHF multipliers

The availability of 5 MHz quartz oscillators with a white phase noise spectral density of -177 dBc has recently allowed a sizable improvement in far infrared synthesis [4]. However the complete exploitation of such characteristics requires to keep very low the additive noise in the multiplier chain. In fig. 1 the experimental results obtained at IEN on some VHF multipliers are reported. As it is well known class C transistors exhibit an additive noise high enough to spoil the spectral purity of the driven quartz. The lowest values of $S_\phi(f)$ obtained for multipliers using different class C transistor configurations fell in the dashed band of figure 1. Little variations within these limits were obtained changing the transistors operation point, the resonant circuit Q,

the multiplication order, the assembly method. As far as step-recovery diodes are concerned the white phase noise is comparable with class C transistors whereas the flicker noise is even worse. Problems in impedance matching and the possibility of hysteresis make not advisable the use of varactors below 100 MHz [5].

Furthermore one must take into account that, even if at higher frequencies the natural increase of phase noise in principle puts less stringent specifications for the multipliers, more difficult efficiency problems are to be faced and a multiplier stage not carefully studied and assembled can deteriorate the spectral purity of the synthesized signal.

The new multipliers in VHF

In a class C transistor multiplier with an input voltage $v_i(t) = V_p \cos\omega_i t$ and an equivalent temperature noise T_e, the phase noise may be written as:

$$S_\phi \propto \frac{f(T_e)}{\left|\frac{dv_i(t)}{d(\omega_i t)}\right|^2_{\omega_i t = \frac{\vartheta}{2}}} = \frac{f(T_e)}{V_p^2 \sin^2 \vartheta/2}$$

being ϑ the conduction angle.

In order to keep $S\phi$ low it is advisable to use low noise components and high V_p. A compromise can be reached between the advantage of high V_p and the correspondingly increasing shot noise, but the values obtained for S_ϕ are not sufficient for our purposes, as one can see in fig. 1. A limiting amplifier can afford a higher slope

$$\left|\frac{dv_i(t)}{d(\omega_i t)}\right|$$

than a class C amplifier with a comparable contribution to $S\phi$ from T_e, so it seems to be a good choice. However in this case amplification takes place at ν_1 on higher power level signals and the maximum allowable currents in the circuit may riduce the obtainable output power with respect to a class C multiplier; the power level of the n^{th} harmonic $P(n\nu_1)$ must be sufficiently high over the thermal noise level and hence the following inequality [6] must hold:

$$P(n\nu_i) \gg \frac{2KT_e}{n^2 S\phi^W(\nu_i)}$$

where KT_e is the available noise power of the circuit in a bandwidth of 1 Hz.

Following the above mentioned principles, a multiplier from 25 MHz to 125 MHz was built and the electrical circuit is reported in fig. 2. The input signal ($V_{pp} \sim 2.8$ V on 50 Ω) after a linear amplification of 7 dB in T_1 enters a differential stage. Here two Schottky diodes D_1 and D_2 square the sinusoidal signal while the two transistors T_2 and T_3 work in their linear region in order to avoid saturation storage responsible for amplitude to phase conversion. Introducing the AM-PM conversion factor K', defined as the output phase variation per 1 dB of input variation divided by the multiplication order, it was shown in [7] that the inequality $K' \leq 6°/dB$ must hold in order to avoid significant noise contribution due to AM-PM conversion.

Multiplier chain up to X band

The block diagram of the chain from 5 MHz to the X band is shown in fig. 3a. Two multipliers of the type described in the previous section transfer the quartz signal to 125 MHz. A_1, A_2 and A_3 are isolator amplifiers using cascode transistor stages and F_1 is a quartz filter for limiting the noise bandwidth [4]. A quadrupler with overlay transistors followed by an interdigital filter F_2 feeds a step-recovery diode. A cavity F_3 selects the wanted line of the comb with spacing 0.5 GHz.

Noise measurements at 125 MHz

The experimental points of $S\phi(f)$, obtained at 125 MHz (point M in fig. 3a) and reported to the input frequency 5 MHz, are shown in fig. 4 where they may be compared with those measured when the 25-125 MHz multiplier is replaced with a step-recovery stage. The white phase noise is cut at f = 12 kHz by F_1. According to the analysis reported in [2], a collapse frequency of 30 THz is expected as a consequence of the phase noise measured at 125 MHz. The output phase variations as a function of the input power for both the differential x5 multiplier and a step-recovery stage are shown in fig. 5. The differential stage with clipping diodes has a smaller AM-PM conversion factor and the input power required for the operation with $K' \simeq 0$, does not require further amplification.

Millimetric and submillimetric section

A harmonic mixer M_1, fed by the X band output, is used for phase-locking an E band millimetric klystron. In fig. 6 the beat note between the klystron at 69.2 GHz and the 6th harmonics of the X band output at 11.5 GHz is drawn (closed loop, point A in fig. 3b). The klystron feeds a submillimetric harmonic mixer M_2 equipped with a Schottky barrier diode. Fig. 7 is a sketch from a photograph showing the beat note (point B in fig. 3b) between the klystron's 11th harmonic and the 761 GHz radiation from a HCOOH laser optically pumped by 9R(18) line of a CO_2 laser. The experimental result is $S/N\phi \simeq 32$ dB (Spectrum Analyzer IF bandwidth 10 kHz) with a white phase noise bandwidth 2B = 200 kHz whereas theoretically it should be $S/N\phi \simeq 36$ dB and 2B = 25 kHz. For the HCOOH radiation at 403 GHz pumped by CO_2 9R(40) $S/N\phi$ = 37 dB with the same IF bandwidth was observed.

Comparing the experimental data with previous results [3] an increment of 15B in $S/N\phi$ is observed. From the measurements taken at 125 MHz one can infer that the stages above this frequency are responsible for a residual degradation of 4 dB in $S/N\phi$ and a broadening of the phase noise pedestal limited to 200 kHz by the klystron phase-lock.

In fig. 8 the improvements obtained at IEN in the past few years are pointed out. The last step shows a 15 dB improvement in $S/N\phi$ for any frequency up to 12 THz. Frequency measurements with coherent signals are now possible up to 20 THz.

Final remarks

An increment of 4 dB in $S/N\phi$ is still possible, as well as a reduction of the noise pedestal width to 25 kHz rising in this way to about 30 THz the carrier collapse frequency of the chain. If one should want to reach this goal the UHF section of the chain, the SRD stage and the klystron phase-lock would have to be reconsidered. In this case it would be also advisable to resort to an E band impatt oscillator and repackage the whole synthesizer in a single three unit rack. In any case the visible region does not appear to be reachable with the source used here.

Acknowledgements

The authors wish to thank Mr. D. Rovera for his substantial contribution to this work and Mr. L. Canarelli for his cooperation.

References

[1] F.L. Walls, A. De Marchi: IEEE Trans. on Instr. and Meas. vol. IM-24, N. 3, Sep. 1975 (210-217).

[2] E. Bava, A. De Marchi, A. Godone: IEEE Trans. on Instr. and Meas. vol. IM-26, N. 2, June 1977 (128-132).

[3] A. Godone, C.O. Weiss, G. Kramer: IEEE Journ. of Quant. Electr. vol. QE-14, N. 5, May 1978 (339-342).

[4] E. Bava, A. De Marchi, A. Godone: Proceedings 31st Annual Symposium on Freq. Control., Atlantic City 1977.

[5] E. Bava, G.P. Bava, A. Godone, G. Rietto: IEEE Trans. on Microwave Theory and Tech. vol. MTT-27, N. 2, Feb. 1979 (141-147).

[6] E. Bava, A. De Marchi, A. Godone: Alta Frequenza, N. 12, vol. XLVII, 1978 (851-858).

[7] E. Bava, G.P. Bava, A. De Marchi, A. Godone: IEEE Trans. on Instr. and Meas. vol. IM-26, N. 1, March 1977 (33-38).

Figure captions

Fig. 1 - Phase noise power spectral densities reported at 5 MHz for the devices discussed in the text.

Fig. 2 - Electrical circuit of the 25 - 125 MHz multiplier.

Fig. 3 - Block diagram of the chain a) section from 5 MHz to X band; c) section from X band to FIR.

Fig. 4 - Measurements of phase noise power spectral densities reported to 5 MHz for two 25 - 125 MHz multipliers compared to the characteristic of the quartz oscillator used.
SRD, Step recovery diode multiplier;
Diff., Differential pair multiplier.

Fig. 5 - Output phase deviation versus input power for the two considered multipliers.

Fig. 6 - Closed loop IF signal of the E band klystron. Spectrum analyzer IF bandwidth: 1 kHz.

Fig. 7 - Beatnote between the 761 GHz line of HCOOH and the chain. Spectrum analyzer IF bandwidth: 10 kHz.

Fig. 8 - Summary of the recent improvements in the FIR synthesis program at IEN.

- Work supported by Consiglio Nazionale delle Ricerche of Italy.

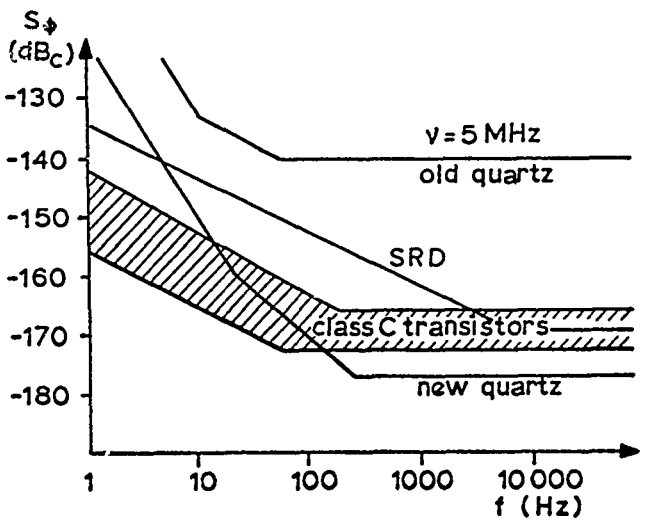

Fig. 1

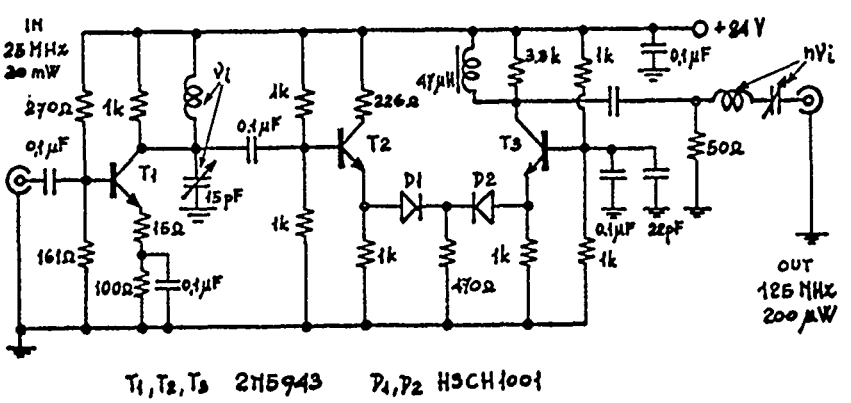

Fig. 2

Fig. 3

Fig. 4

Fig. 5

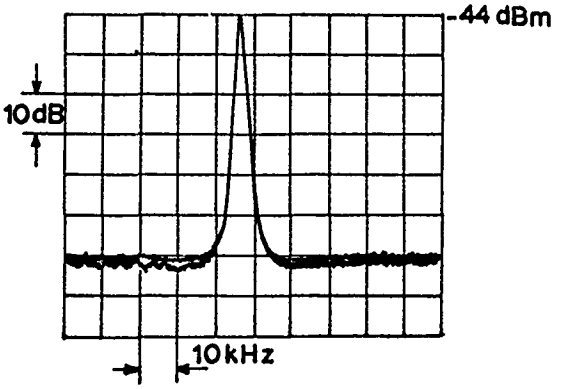

Fig. 6

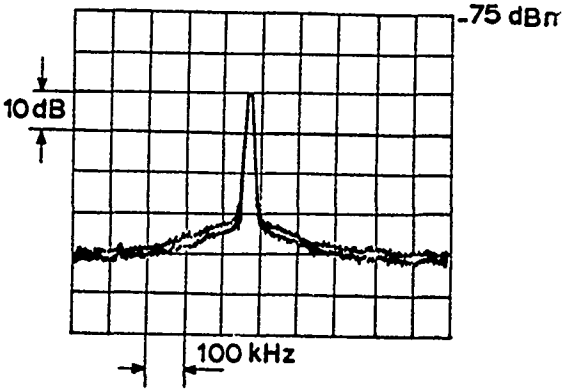

Fig. 7

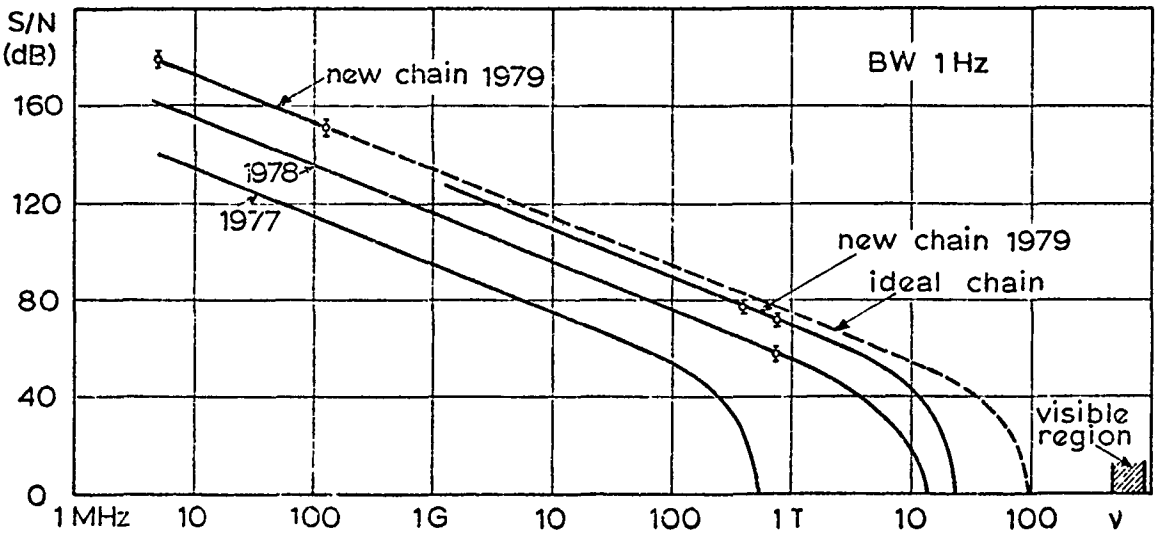

Fig. 8

COMPARISON OF DIFFERENT TUNING AND MODULATION TECHNIQUES FOR F.I.R. LASERS

A. De Marchi, A. Godone, E. Bava

Istituto Elettrotecnico Nazionale "Galileo Ferraris"

Abstract

Frequency and phase modulation of laser sources in the Far Infra Red region has been recently given increasing attention as its potential scientific and technological applications in frequency metrology and communications have been recognized.

Different modulation methods can be used; the characteristics of some of them are here described and the results obtained by beating the modulated signal with a synthesized spectrally pure reference are given.

Movements of mechanical parts driven by PZT give high depth of FM modulation with bandwidths up to about 10 kHz and low AM, while Stark effect on the lasing medium gives a wider bandwidth, limited by the laser cavity selectivity, but more evident and undesired AM at high modulation depth.

Other methods can derive from extension to the FIR region of techniques commonly used in different frequency ranges, like modulation of the refraction index, as is done at optical wavelengths, and coupling of a variable reactance to the cavity, as is done in the mw region.

Results obtained with both these latter methods are here described which show the possibility of obtaining characteristics comparable or better than the first two.

Introduction

Frequency tuning and modulation of sources and signals in any range is always an important task since it increases the versatility of the oscillator, allows its stabilization and makes it possible to build communication channels.

Main characteristics of any particular technique are tuning range and linearity on one side, and modulation depth and bandwidth on the other. Also important is the degree of immunity from spurious variations of parameters other than the desired one (e.g. power variations with frequency modulation). Handling of sources and signal processing have been for long time widely developed for various applications at frequencies up to the microwave region, and in the last decade a variety of studies and technical realizations have been made in this direction on optical and infra-red lasers and coherent signals.

In the far-infra-red region instead a large number of coherent sources have been only recently made available [1] with optically pumped lasers working on vibro-rotational levels of simple organic molecules, and tuning/modulation techniques for this kind of oscillator have not yet been thoroughly studied. In this paper are presented some results on this latter subject obtained with an open resonator optically pumped laser using different techniques, and their characteristics and potentialities are compared.

General considerations

The output frequency ν of an oscillator can be calculated with the equation

$$(\nu-\nu_o) = (\nu_c-\nu)\frac{Q_c}{Q_o} \qquad (1)$$

where ν_o, Q_o and ν_c, Q_c are center frequencies and quality factors of the oscillator gain profile (if any) and electromagnetic resonant structure (e.g. cavity), respectively.

Frequency tuning and modulation(*) of

(*) The terms tuning and modulation refer here to the same phenomenon and differ only by the range of Fourier frequencies they are used to select; in fact we speak about tuning when slow modulation is used. In the following we will use only the term modula

the source can then be obtained through variations of either ν_o, Q_o or ν_c, Q_c depending on what is more convenient. When $Q_o \gg Q_c$, like in microwave masers (e.g. H, Rb masers), the output frequency depends much more strongly on gain profile tuning (C-field adjustment) than on electromagnetic resonance changes; on the other side when $Q_c \gg Q_o$, like in optical lasers, the frequency is determined by the cavity resonance and follows most readily any change in the electromagnetic configuration of the oscillator.

In the FIR region the same order of magnitude is usually obtained for the two quality factors ($Q_o \approx 2\text{+}5\times10^5$; $Q_c \approx 0.5\text{+}3\times10^5$) and as a consequence modulation of a FIR laser can be done either way with comparable efficiency. When a control parameter p is chosen the variation $\delta\nu$ in output frequency can be expressed as follows:

$$\delta\nu = \left(\frac{\partial\nu}{\partial\nu_c}\frac{d\nu_c}{dp} + \frac{\partial\nu}{\partial Q_c}\frac{dQ_c}{dp} + \frac{\partial\nu}{\partial\nu_o}\frac{d\nu_o}{dp} + \frac{\partial\nu}{\partial Q_o}\frac{dQ_o}{dp}\right)\delta p \quad (2)$$

where

$$\frac{\partial\nu}{\partial\nu_c} = F\,(Q_o/Q_c) \quad (3a)$$

$$\frac{\partial\nu}{\partial Q_c} = \frac{\Delta}{Q_o}F^2(Q_c/Q_o) \quad (3b)$$

$$\frac{\partial\nu}{\partial\nu_o} = F\,(Q_c/Q_o) \quad (3c)$$

$$\frac{\partial\nu}{\partial Q_o} = -\frac{\Delta}{Q_c}F^2(Q_o/Q_c) \quad (3d)$$

with

$$\Delta = \nu_c - \nu_o \text{ and } F(x) = 1/(1+x).$$

Each one of the total derivatives with respect to p can be conveniently separated into a DC amplitude component $(d/dp)_o$ and a normalized transfer function H(f) in the Fourier frequency domain.

The fractional frequency deviation induced by p through the quantity α ($\alpha = \nu_o$, Q_o, ν_c, Q_c) can then be written as

$$\frac{\delta\nu}{\nu} = \frac{\partial\nu}{\partial\alpha}\,G_p^{\alpha}(\nu,p)\;H(f)\;\frac{\delta p}{p} \quad (4)$$

where

$$G_p^{\alpha}(\nu,p) = \frac{p}{\nu}\left(\frac{d\alpha}{dp}\right)_o \quad (5)$$

(*) tion: tuning range will be treated together with modulation depth and described by figures of fractional frequency deviation.

Linearity, tuning range and modulation depth are taken into account by G; bandwidth and phase shift with Fourier frequency are described by H.

In our experiments different parameters of an optically pumped FIR laser were modulated and the resulting output frequency variations were measured by analyzing the beatnote between the laser emission and a reference signal. The latter is directly synthesized from a 5 MHz crystal source and guarantees a resolution of a few Hz in the spectral analysis [2]. The measurement sensitivity limit was set by the jitter of the FIR laser whose peak to peak fractional frequency fluctuation was about 10^{-8}.

Some theoretical considerations follow about each method analyzed.

Modulating the gain profile

1) Stark effect

Stark effect in the active medium can produce variations of line quality factor Q_o (low electric field) or gain profile center frequency ν_o (fields high enough to resolve the different pressure broadened Stark sublevels), causing displacements in the FIR laser output frequency according to (2) where (3c) and (3d) are in this case the important terms [3].

In the first case (3d) must be used for the modulation and the cavity must be detuned from line center with the consequence of a frequency displacement according to (3a). For a given Δ maximum FM is obtained if $Q_c = Q_o$; a decrease in output power and high AM must be accepted in this situation. While this method is not convenient to modulate a laser, it can be of some help in studying the structure of molecules which do not show first order Stark effect.

In the second case when Stark sublevels are resolved the cavity should be tuned to the chosen one of them and (3c) gives then the pulling factor. A decrease in output power must be still faced in this situation, but low AM is obtained for a modulation depth much smaller than the line or the cavity halfwidth [4]. Frequency tuning up to 170 MHz [5] and modulation indexes greater than 1 have been demonstrated [4] by this technique with molecules and tran-

sitions highly sensitive to the electric field. Simple theoretical calculations can be performed for symmetric top molecules to determine analytically the frequency deviation due to the electric field [6]. Non-symmetric tops must be analyzed one by one and formulas have been calculated in some cases [7]. The modulation bandwidth appears to be limited by the line or cavity quality factor.

2) Pump frequency variation

Steering of the optically pumped FIR laser output frequency can be obtained by pump frequency variation within the Doppler broadened profile of the absorption line. The pulling factor (3c) multiplied by the FIR to pump frequency ratio gives directly $\delta\nu/\delta\nu_{pump}$. In special cases, when a good coincidence of the pump with the absorption line of the molecule is found, a tuning range of a few hundred kHz is achievable, corresponding to a pump variation of the order of 10 MHz. Otherwise the AM turns out to be severe, the tuning range small, and no serious use can be done of this approach. If the pump frequency is steered by a PZT ceramic, resonance problems arise and one should limit oneself to narrow band modulation and tuning applications.

Modulating the cavity

A shift in the cavity resonance ν_c produces an output frequency shift according to (3a). Virtually no AM is obtained in this case until the modulation depth becomes comparable to the linewidth of the gain profile. In order to increase the pulling factor, Q_c must be kept high when acting on the cavity to steer the laser. Care must be put in obtaining a low loss mode and external couplings must be studied and optimized.

1) Mechanical tuning

Movements of mechanical parts electromagnetically coupled to the FIR cavity produce shifts in its resonance. In fact a mechanical movement can change the equivalent optical length L_{FIR} of the cavity by δl_{FIR} causing a fractional change in its frequency of $\delta\nu_c/\nu_c = -\delta l_{FIR}/L_{FIR}$. If a mirror is axially moved by δl we have $\delta l_{FIR} = \delta l$. Manual, motor driven, PZT or otherwise driven movements can all give good tuning range, but wide modulation band appears difficult to obtain.

2) Refraction index modulation

Another way of changing the optical length of the cavity is to change the refraction index in part or all of its length. This is done in the visible by electric field sensitive crystals (Kerr cells) or by current modulation of the electron density in discharge pumped lasers. No electro optical material being available in the FIR as yet and discharge being absent in optically pumped lasers, this technique appears not accessible unless a plasma is produced within the cavity. Whether or not this may spoil the stability of the laser, which is believed to be an advantage of these lasers due to optical pumping, must be verified. In fact an advantage can be seen here with respect to discharge pumped lasers in the fact that the power output is not directly dependent in this case on plasma excitation. A proposed scheme is to produce a cold plasma in a cell containing a few Torr of some gas, for example neon or N_2, at the far end of the FIR cavity. This would allow sufficient optical pumping by the radiation coming in from the near end. The window should be made of a material with low loss for the FIR radiation and able to withstand or reflect the incoming pump power. A glow discharge could be set in the cell by dc or rf excitation and modulated in intensity (electron density) by acting on the excitation power.

The refraction index n in the plasma region is given by

$$n^2 = 1 - \frac{N e^2}{4\pi^2 m \varepsilon_0 \nu^2} = 1 - 80.5 \frac{N}{\nu^2} \qquad (6)$$

where N, e and m are the electron density, charge and mass, and ε_0 is the permittivity of vacuum. Electron densities of $10^{10}/cm^3$ can be expected for a glow discharge in a low pressure gas [8]. Once the glow discharge is established for a length L_p within the cavity, and the resonator is tuned to the shifted frequency, the fractional frequency deviation of the cavity is

$$\frac{\delta\nu_c}{\nu_c} \simeq -\frac{L_p}{L}\frac{\delta_n}{n} \qquad (7)$$

The modulation bandwidth is limited by the free electrons mean life and increases with the gas pressure in the plasma cell; for a pressure of 20 Torr it is about 15 kHz [8].

3) Electrically variable reactance

As an extension of a technique common

in the microwave region, convenient coupling of a lumped electrically variable reactance to the FIR laser cavity can provide another means to modulate the resonance frequency and hence the laser output frequency [9]. In this attempt Schottky barrier diodes with cutoff frequency above 1 THz can be reverse biased and used as a variable capacitance C. When the diode is coupled to the cavity it modifies its resonance frequency by:

$$\frac{\delta\nu_c}{\nu_c} = G_C^{\nu_c}(\nu_c, C)\, H(f)\, \frac{\delta C}{C} = \qquad (8)$$

$$= G_C^{\nu_c}(\nu_c, C) H(f)\, (1 - 1/\sqrt{1 - V_d/V_{bi}})$$

where V_d and V_{bi} are the voltage across the diode and the barrier built in potential, while $G_C^{\nu_c}$ is a factor which takes into account the overall coupling between junction and resonator; a dependence on ν_c is explicitly shown in it to remind that coupling problems must be solved differently according to the operation frequency. In fact the coupling may be quite straightforward up to about 300 GHz where fundamental mode waveguides are still available, but become problematic for higher frequencies where antenna lobe matching is necessary. An array of diodes would be required in this case to guarantee sufficient coupling. For a reasonable modulation depth high Q_c and good coupling between the junction and the mode oscillating in the resonator must be contemporarily attained. Wide bandwidth, limited only by line or cavity quality factors, is inherent to this technique as well as low values of the control parameters (voltage across the junction).

Experimental results

Experiments were carried out with an open resonator optically pumped FIR laser using the techniques described above on several lines of the formic acid (HCOOH) from 400 GHz to 800 GHz.

The resonator structure was a subconfocal plano-spherical one 70 cm long with gold plated mirrors 9 cm in diameter. Mirrors with different diameter coupling holes could be used at both ends and suitable structures could be matched to them or added to the cavity to adapt the resonator for the different techniques.

The various set-ups used are described in the following together with the results obtained.

a) The characteristics of Stark modulation for FIR lasers using symmetric or quasi-symmetric top molecules are described in the literature [4,5,7]. Here some results of Stark modulation of a formic acid laser are reported. Although the observed lines of this molecule are known not to show first order Stark effect, Stark modulation experiments were done on them both to evaluate the versatility of our apparatus without changing molecule and synthesized frequency, and to obtain some data useful to characterize the molecule. Two Al rectangular plates kept parallel to each other, 4.4 cm apart, by two 15 mm thick plexiglass sheets provided a very overmoded hybrid waveguide between the two cavity mirrors. Measurements were taken on different lines of HCOOH; the output power was between -10 dBm and +10 dBm in all cases and Q_c of the

Line		Experimental conditions			pol.*	measured**	inferred
pump	ν_{FIR}(GHz)	$F(Q_o/Q_c)\cdot\Delta$(MHz)		$\frac{\partial\nu}{\partial Q_o}$(Hz)		$\delta\nu$(kHz)	$-\delta Q_o$
9R(40)	403.7	0.1	12	-5.2	//	< 10	2×10^3
					⊥	< 10	2×10^3
9R(20)	692.9	0.2	7.5	-3	//	< 30	1×10^4
					⊥	< 30	1×10^4
9R(18)	761.6	0.1	14	-3.4	//	40	1.1×10^4
					⊥	80	2.3×10^4

* // → $E_{Stark} // E_{FIR}$; ⊥ → $E_{Stark} \perp E_{FIR}$
** The values reported refer to E = 100 V/cm

TAB. I

order of $2 \times 10^4 + 1 \times 10^5$ were obtained for the used oscillation modes. The results obtained for δQ_o, relative to a $\delta \nu$ measured at E = 100 V/cm, are reported in table I.

b) The modulation with the pump frequency was tried with the 403.7 GHz and the 761.6 GHz line. A PZT ceramic was used to move the pump frequency and a fractional deviation of it as high as 5.5×10^{-9}/V could be obtained in this way. With $Q_c = 2.3 \times 10^4$ and $Q_o = 2 \times 10^5$ ($F(Q_c/Q_o) = 0.9$) a maximum deviation of 5×10^{-9}/V was measured as expected from the PZT sensitivity. The tuning range was ± 50 kHz and the modulation bandwidth was obviously limited by the ceramic characteristics.
For the 761 GHz line a smaller value was obtained ($\delta\nu/\nu \approx 4 \times 10^{-9}$/V); this can be probably explained by the fact that in this case the pump is more out of resonance with the absorption line than in the other case.

c) PZT driven modulation of the cavity length was done at 761.6 GHz by moving the whole plane mirror or a short coupled to the resonator through a hole in the mirror. In the first case a modulation depth was obtained of 240 kHz $_{pp}$ with 213 V_{pp} on the ceramic, which corresponds to a fractional variation of 3×10^{-7}. Being $\delta 1/L = 9 \times 10^{-7}$ we have $F(Q_o/Q_c) = 0.3$ as expected from the measured values $Q_o \approx 4 \times 10^5$, $Q_c \approx 2 \times 10^5$. In the second case with a similar set-up only 20 kHz $_{pp}$ were measured.

d) For a fast check of the possibilities connected with plasma refraction index modulation a low partial pressure (≈50 mTorr) of some gas with low breakdown voltage was added within the cavity and a dc glow discharge was excited at 90 ÷ 100 V/cm between the two 4.4 cm distant Stark plates. An electronic concentration N of the order of $10^{10}/cm^3$ was produced in this way and a laser output frequency shift of 200 kHz was measured. This corresponds to a cavity resonance shift of 1.8 MHz ($Q_o \approx 4 \times 10^5$; $Q_c \approx 5 \times 10^4$; $F(Q_o/Q_c) = 0.11$) and hence to an electronic concentration of $3.4 \times 10^{10}/cm^3$. With the cavity retuned to the new frequency an overimposed signal of 40 V_{pp} (field of ≈ 10 V_{pp}/cm) yielded a peak to peak modulation depth of 200 kHz. Modulation bandwidth as low as 2 kHz was obtained at the used pressure due to the time constant of afterglow quenching [8]. Since higher pressure operation is not allowed with this set-up by lasing conditions, a separate cell containing higher pressure plasma should be inserted in the cavity in order to obtain a wider modulation bandwidth.

e) Measurements were taken of resonators' frequency modulation by an externally coupled varactor mode biased Schottky barrier diode at 100 GHz and 403 GHz [9]. In the first case a klystron was locked to the cavity by self-injection ($Q_c \gg Q_o$) and a frequency deviation of 3×10^{-7} was measured for 5 V variation of the diode voltage. In the second case the set-up described in fig. 1 was used and the laser line of HCOOH was cavity pulled by $F(Q_o/Q_c) = 6 \times 10^{-2}$; a maximum cavity resonance deviation of 1.5×10^{-8} was observed for a variation of 5 V across the diode, Fig. 2. Better pulling factors can be easily obtained by selecting resonator modes with higher Q_c, but coupling between the diode and the selected mode would require a closer analysis and a careful design. An increase of a factor of 10 in the pulling factor as well as in the matching of the diode should be obtainable and would provide a modulation depth of few tens of kHz. The bandwidth of this technique is limited by line and/or cavity quality factors in this utilization, while much higher bandwidth should be obtainable in phase modulation of a travelling wave.

Conclusions

In this paper a review was made of the possible techniques that one can use to tune and frequency modulate an optically pumped FIR laser, and shortcomings or advantages of each one of several different approaches were underlined. Some experimental results were also reported, obtained on a versatile structure by modulating different parameters and analyzing the laser output frequency variations thereby induced by means of a FIR synthesizer. The problem of frequency modulation of these lasers appears far from being solved. In fact Stark modulation gives wide band and convenient modulation depth, but is not usable for all molecules and all lines, while a variable reactance, or a variable electron density plasma, coupled to the resonator work in

all cases but have their own defects because of coupling or bandwidth problems.

Acknowledgements

The authors wish to thank Dr. Fiscella and Dr. Wrixon for their cooperation in making available the Schottky barrier diodes used for this work, and Ing. A. Guiducci and Prof. G.C. Rumi for valuable discussions about the physics of wave propagation in a plasma.

References

[1] D.J.E. Knight: Ordered list of optically-pumped laser lines with frequencies – 4th issue March 78, NPL Report No. Qu 45.

[2] A. Godone, A. De Marchi, E. Bava: An improved multiplier chain for precise frequency measurements up to 20 THz – 33rd Annual Frequency Control Symposium, Atlantic City, May-June 1979.

[3] M. Inguscio, P. Minguzzi, F. Strumia: Stark Tunability of a CH_3F Far Infrared Laser – Infrared Physics, 1976, vol.16, pp. 453-456.

[4] S.R. Stein, A.S. Risley, H. Van de Stadt, F. Strumia: High speed frequency modulation of far infrared lasers using the Stark effect – Applied Optics, vol. 16, July 77, pp. 1893-96.

[5] G. Bionducci, M. Inguscio, A. Moretti, F. Strumia: Design of Molecular FIR Lasers Frequency Tunable by Stark Effect: Electric Breakdown of CH_3OH, CH_3F, CH_3I and CH_3CN – Infrared Physics, in press.

[6] C.H. Townes, A.L. Schawlow: Microwave Spectroscopy – Ch. 10 – McGraw-Hill, New York 1955.

[7] M. Inguscio, P. Minguzzi, A. Moretti, F. Strumia, M. Tonelli: Stark Effect on CH_3OH and CH_3F FIR Lasers: Large Frequency Tuning and Resolved Structures – Applied Physics, 18, 1979, pp. 261-270.

[8] Proc. 4th Internat. Conf. Ionization Phenomena in Gases – North Holland Publishing Co., Amsterdam, 1960.

[9] A. Godone, E. Bava, A. De Marchi: mm-wavelength Fabry-Perot Tuning and Modulation by Electrically Variable External Reactance – To be published.

– Work supported by Consiglio Nazionale delle Ricerche of Italy.

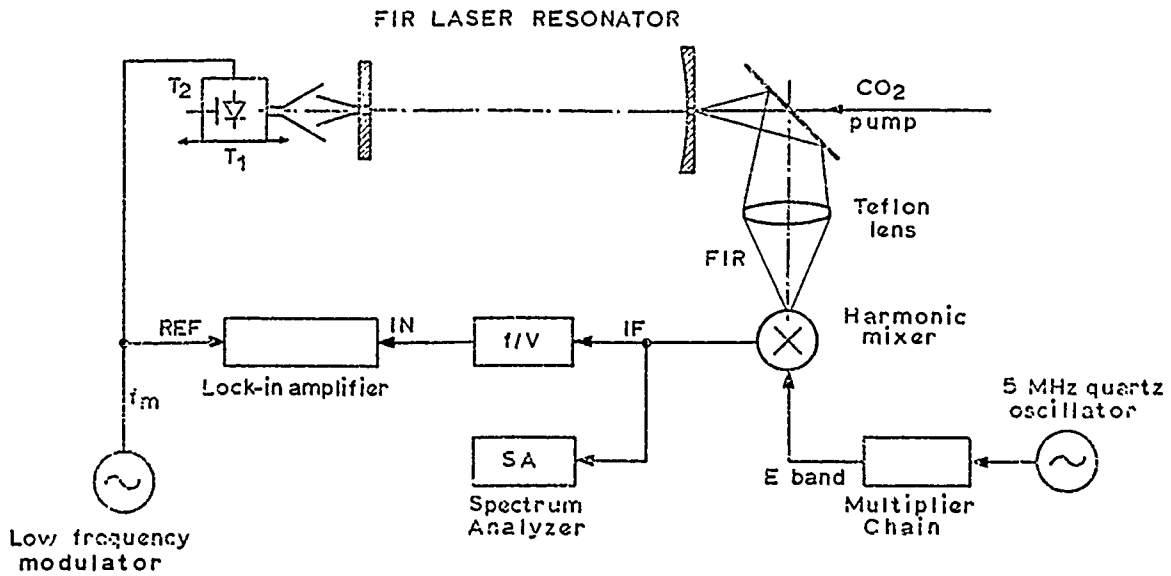

Fig. 1 – Experimental set-up for measurements of frequency modulation with a variable reactance. T_1 = linear translator, T_2 = sliding short.

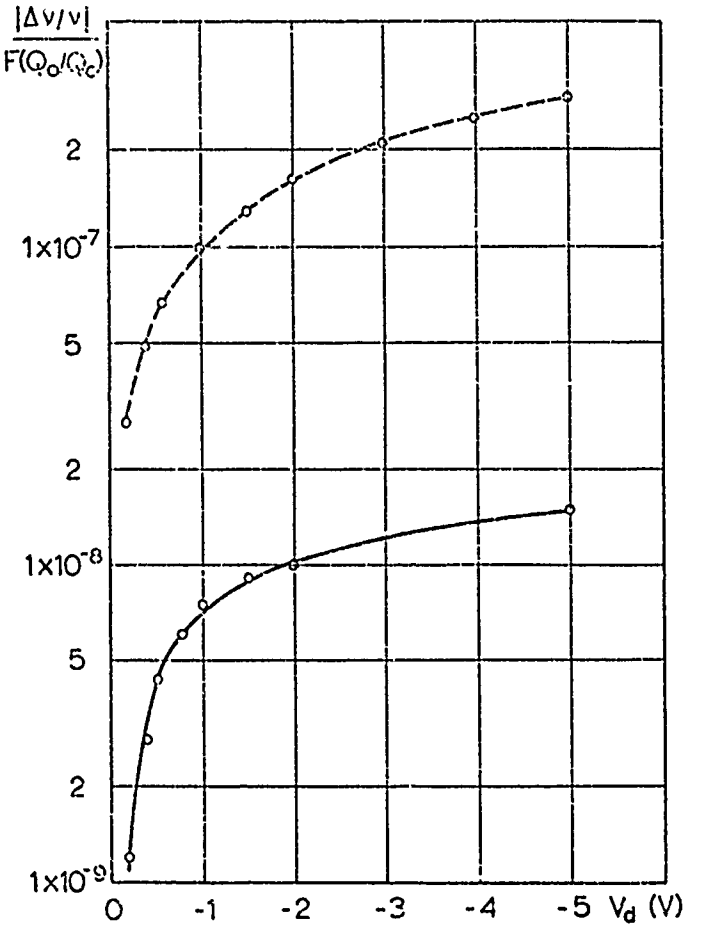

Fig. 2 - Cavity fractional frequency shift as a function of the voltage across the diode. Experimental results at 100 GHz (dashed line) and at 403 GHz (continuous line).

RESEARCH WITH A COLD ATOMIC HYDROGEN MASER*

R.F.C. Vessot, E.M. Mattison and E.L. Blomberg

Smithsonian Astrophysical Observatory
Cambridge, Massachusetts

Summary

The frequency stability of the hydrogen maser is limited by thermal noise within the atomic linewidth and by additive noise at the receiver. By lowering the maser's temperature its stability can be improved both through reduced thermal noise and more favorable kinetic effects in the storage process. Predicted values of the fractional frequency stability are in the range of 10^{-17} to 10^{-18} for averaging intervals of 10^2 to 10^3 seconds.

We have measured the wall shift and atomic line Q of an oscillating maser at temperatures of 77K to 25K. Below 50K this was accomplished by coating the storage bulb with tetrafluoromethane (CF_4) applied through the dissociator. We present the results of these experiments and discuss directions for future research.

Introduction

The invention of the hydrogen maser in 1960 opened new possibilities for atomic frequency standards of extremely high stability. The maser's long atom storage time provides a very narrow resonance linewidth, and because of its active self-oscillation eliminates the need for an electronic servo to generate a stable reference signal. The output signal must be transformed to a useful frequency at a suitable power level, usually by means of a phase-coherent receiver. Such a receiver perturbs the maser signal with additive white phase noise whose bandwidth is determined by the characteristics of the phaselock system. The resulting stability, when characterized by the two-sample (or Allan) variance $\sigma(\tau)$, varies as τ^{-1}, where τ is the averaging interval over which frequency measurements are made. The proportionality factor depends on the noise bandwidth and the noise figure of the receiver and on the maser's output power level.

A second, and in a sense more fundamental, source of maser instability arises from thermal noise lying within the linewidth of the quantum mechanical oscillator itself. This noise results in an Allan variance proportional to $\tau^{-\frac{1}{2}}$. For many years observed maser stability data have been dominated by the τ^{-1} behavior for averaging intervals between one and 100 seconds. In 1977 SAO's VLG-11 series hydrogen masers achieved stability such that the underlying $\tau^{-\frac{1}{2}}$ stability behavior was observed[1]. The measured Allan variance of these masers closely follows the predicted limitation: between 100 and 3,600 seconds the stability varies as $\tau^{-\frac{1}{2}}$ and is controlled by the oscillator linewidth, oscillator power and temperature, while below 100 seconds its behavior is determined by the receiver noise figure, noise bandwidth, and input power level, and is proportional to τ^{-1}.

The realization of the theoretical frequency stability limits has provided a strong motivation to study these limits in greater detail in terms of the oscillation parameters of the maser. We have reported[2] on the possible improvement in stability that could be achieved by operating the quantum mechanical interaction region of the maser at low temperature. This is a natural direction to explore since the chief limitation on instability is thermal noise. In the course of the work, we found that there are several very interesting characteristics of low-temperature operation, which we classify as follows:

Advantages resulting from reduced thermal noise. The thermal noise reduction at low temperature is fundamental to physics and well understood. In the case of a device such as a maser, whose signal level can be raised only at the expense of broadening the atomic resonance linewidth[3], any trade-off ultimately is limited by fundamental noise.

Advantages from the kinetic behavior of atoms at low temperatures. The storage process of the hydrogen maser depends directly on the kinetic behavior of the atoms. Both the wall relaxation rate and the bulb storage time depend on the collision rate of atoms with the wall and, therefore, on the atoms' velocity. Another important kinetic effect is the interatomic spin exchange relaxation, which is the chief limitation to output power. Under low temperature conditions, both the atom-atom collision rate and the spin exchange cross section itself diminish with velocity. The spin exchange reduction is a very important feature for

*This work was supported by the Office of Naval Research under contract N00014-77-C-0777 and by the Smithsonian Institution.

cold maser operation.

Advantages of low temperature properties of materials. The properties of materials at low temperature are well suited to their application in masers. Superconducting magnetic shields would make possible almost complete immunity from external magnetic effects. One could, by using a superconducting cavity coating, achieve nearly perfect power transfer from the atoms to the receiver system by over-coupling the cavity. Reducing the loaded Q by controlled overcoupling would reduce the pulling effect. If 4K operation is assumed, the combination of improved atomic line Q and reduced cavity Q reduces the pulling by a factor of approximately 2,000. At low temperatures the mechanical and thermal properties of materials are favorable and we can expect that improved thermal and mechanical control of the dimensions of the cavity will result.

During the past year we have conducted low temperature experiments on hydrogen masers. As discussed below, we have recently shown that a coating of tetrafluoromethane (CF_4) frozen to the interior surfaces of the cavity permits a hydrogen maser to oscillate at temperatures as low as 25K. This breakthrough, which even at 30K promises stability below 10^{-16}, is most encouraging.

The Experiment

Our experiments on cryogenic maser operation have been performed in an aluminum, liquid-nitrogen-shielded dewar equipped with an internal vacuum well into which is placed a heavy-walled copper TE_{111}-mode septum cavity. Radiation shields within the well help reduce heat leaks to the cavity. The cavity's temperature is measured by a copper against gold-cobalt thermocouple. A hydrogen beam source is mounted on the top of the dewar and is connected to a turbo-molecular vacuum pump. The dewar is surrounded by a solenoid that creates a longitudinal magnetic field at the location of the cavity, and sits in a set of nested open-ended magnetic shields that excludes most of the earth's field. The dewar and cavity are shown in Figure 1.

Prior to an experimental run the cavity is baked in the evacuated well for several days at 60°C to clean its Teflon surface. The dewar is then cooled with liquid nitrogen until the cavity reaches a temperature of 77K. Because the connection between the dewar and the hydrogen beam source is a narrow tube, the system does not have sufficient pumping speed to achieve maser oscillation under these conditions. As soon as liquid helium is transferred into its reservoir, however, the inner surface of the vacuum well acts as a cryopump, reducing the pressure and permitting oscillation.

Maser oscillation allows us to measure directly both the atomic line Q and the wall shift as functions of temperature. As the cavity cools below 77K the cavity resonance frequency increases and pulls the maser output frequency, which is measured by comparison with a room-temperature maser. We periodically retune the cavity to the hydrogen hyperfine frequency of 1420.405752MHz, measuring both the cavity resonance frequency and the output frequency before and after retuning. These data yield the line Q, from which we can calculate the probability of relaxation per wall collision. The behavior of the output frequency at the retuned cavity condition gives the change in wall shift with temperature.

In our early experiments the maser stopped oscillating at approximately 47-50K, although we observed the pulsed decay of the atoms in the cavity down to approximately 20K. These experiments yielded the following values for p(T), the relaxation probability per wall collision:

T (Kelvins)	p(T)
70	5.67×10^{-5}
60.5	1.15×10^{-4}
52.0	1.96×10^{-4}

The value of p(70) agrees well with measurements made by M. Desaintfuscien, who obtained

$$p(77) = 4.8 \times 10^{-5}.$$

The rapid increase of p with decreasing temperature was due, we believe, to contamination of the Teflon surface with condensed volatile matter.

We later performed the experiment in a different way by providing a means of re-coating the interior of the cavity with condensed and frozen tetrafluoromethane gas. A ballast tank connected by a needle valve to the hydrogen beam source allows a controllable amount of the gas to be sent through the hydrogen source collimator directly into the storage volume of the cavity. (The r.f. dissociator was turned off and the gas was admitted to the source. The stopping disc had been removed from the state selecting magnet so that the undeflected molecules could pass through.) We repeated the low-temperature procedure and when at about 50K the maser output power and line Q dropped significantly, we introduced the CF_4 into the cavity. The output immediately rose from -111dbm to -103 dbm, and after a second application of CF_4 the line Q increased from 1.1×10^9 to 1.7×10^9. These data indicate that the relaxation probability per wall collision decreased by a factor of approximately 2 (from 2.5×10^{-4} to 1.4×10^{-4}) as a result of the second CF_4 coating. By applying the CF_4 a third time we were able to maintain maser oscillation to 25K. The measured behavior of maser output power and wall relaxation probability with temperature is shown in Figure 2.

Discussion

Since these results have only recently been obtained, and represent initial findings, many questions concerning maser operation at low temperature remain to be answered. Perhaps the major question concerns the increase in wall relaxation, and the manner in which maser oscillation quenches as temperature decreases. The most likely source of relaxation is contamination of the cold maser storage surface by condensation of foreign atoms or molecules that quench the hydrogen spins or cause hydrogen recombination or reaction with the surface. We suspect this because at 30K the relaxation probability decreased when we renewed the CF_4 wall coating; this suggests that the second coat covered contamination overlaying the first coat. Another mechanism that could contribute to increased wall relaxation is an increase in the hydrogen-wall interaction time resulting from the decreased kinetic energy of the hydrogen atoms. We plan to investigate this by applying coatings of different atoms and molecules to the storage surface. A third relaxation mechanism that may be operating in our present apparatus results from the use of a room temperature dissociator and hydrogen beam. The hot atoms entering the cavity may require many bounces to come to thermal equilibrium with the cold walls, and thus experience a range of wall shifts that decorrelate their phases. We are considering several methods of cooling the beam

before it enters the cavity. One approach would be to direct the atoms into a cold antechamber where they would come to thermal equilibrium before entering the rf interaction region. This would work only if state selection is maintained during cooling. A second option, which is more attractive, is to precool the beam before state selection. This would allow the use of a shorter state selection magnet, and could be done by operating the hydrogen dissociator at low temperature[4].

The prospects for cryogenic maser operation are encouraging. From calculations based on receiver bandwidth and noise temperature and on maser temperature, line Q and power output, we can predict the maser stability at low temperatures. Figure 3 shows the predicted stability for masers operating at about 30K and at 4K. The practical problems of cold maser operation do not appear insuperable. Temperature control, mechanical stability and magnetic field control are readily handled with existing techniques. Magnetic shielding, in particular, can take advantage of superconducting materials. The chief difficulty may be control of surface contamination within the storage vessel. This may require extra care in providing a clean vacuum system and hydrogen supply, and it may necessitate frequent or constant renewal of the condensed storage coating during operation. In addition, a lower temperature limit to maser oscillation may be imposed by wall relaxation due to fundamental hydrogen-surface interactions. We plan to pursue these topics further, and hope to obtain actual stability data between two hydrogen masers operating at low temperatures.

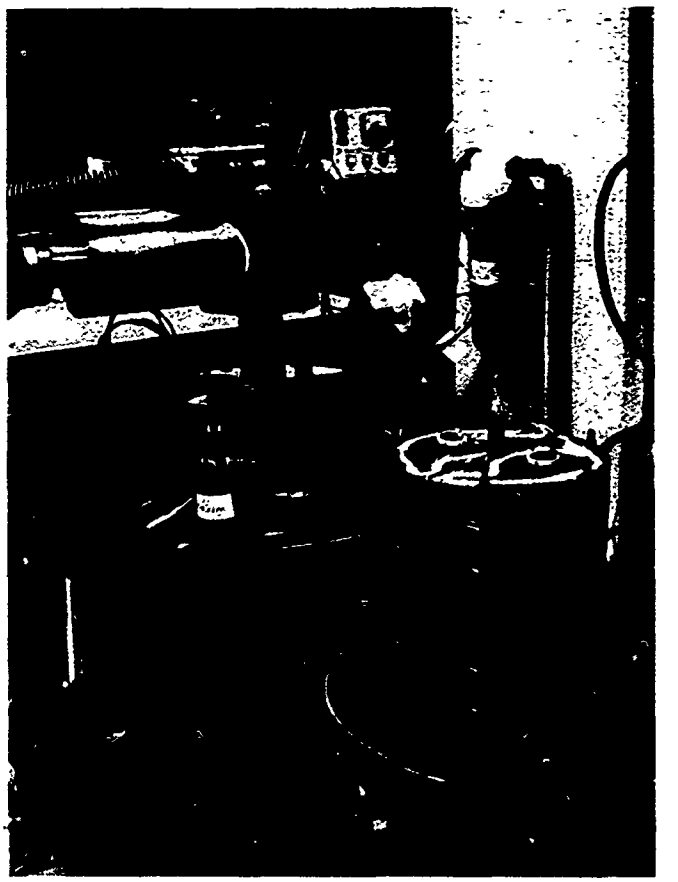

1. Cryogenic hydrogen maser, with TE_{111} - mode resonant cavity in foreground.

References

1. Levine, M.W., R.F.C. Vessot and E.M. Mattison, Performance Evaluation of the SAO VLG-11 Atomic Hydrogen Masers. Proc. 32nd Symposium on Frequency Control, U.S. Army Electronics Research and Development Command, Atlantic City, New Jersey; June 1978. Pp. 477-485.

2. Vessot, R.F.C., M.W. Levine and E.M. Mattison. Comparison of theoretical and observed hydrogen maser stability limitation due to thermal noise and the prospect for improvement by low-temperature operation. Proc. Ninth Annual Precise Time and Time Interval Applications and Planning Meeting, Goddard Space Flight Center, Greenbelt, Maryland; March 1978. Pp. 549-566.

3. Vessot, R.F.C., et. al., Recent Developments Affecting the Hydrogen Maser as a Frequency Standard. Proc. International Conference on Precision Measurement and Fundamental Constants, N.B.S. special publication 343; August 1971. P. 27.

4. Crampton, S.B., et. al., Hyperfine Resonance of Gaseous Atomic Hydrogen at 4.2K. Phys. Rev. Lett. 42, 1039 (1979).

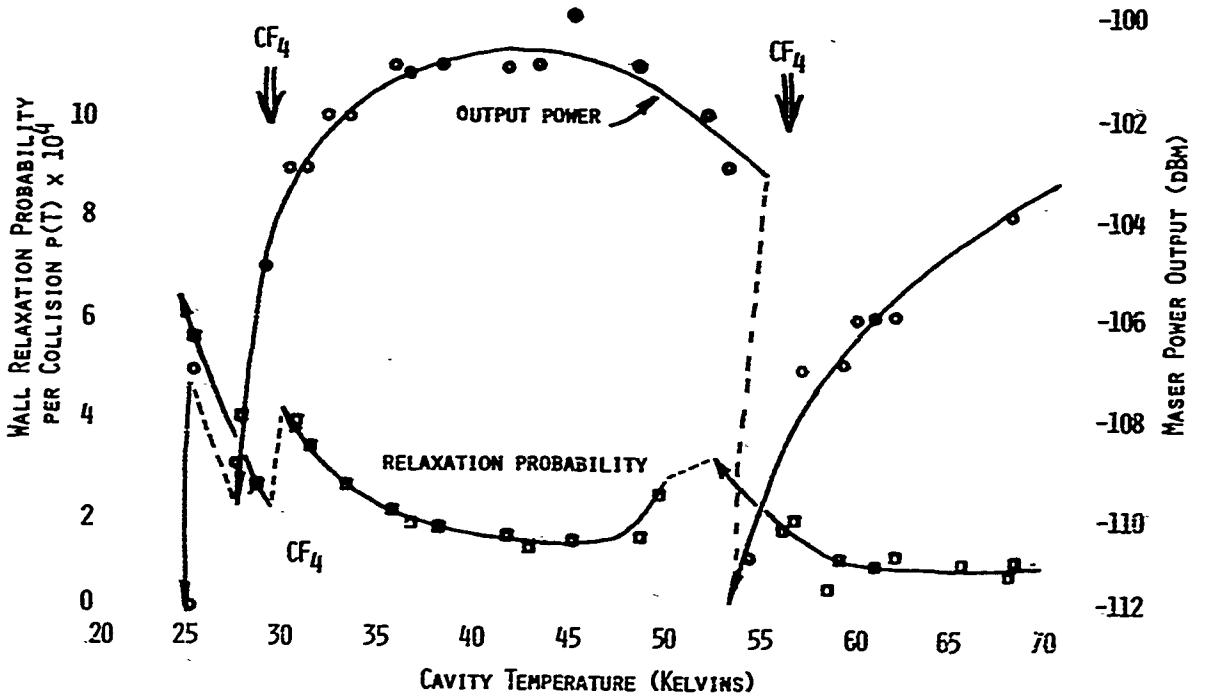

2. Wall relaxation probability and maser power output during low temperature operation

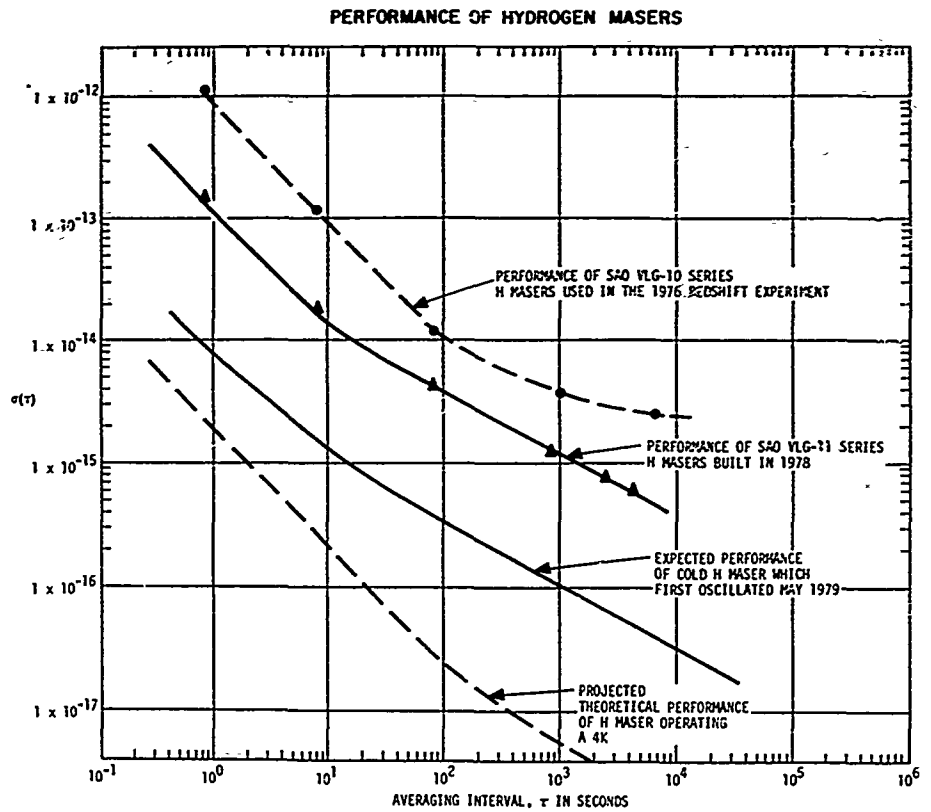

3. Predicted and measured maser stability as functions of averaging interval and maser temperature.

AMPLITUDE NOISE IN PASSIVELY AND ACTIVELY OPERATED MASERS

P. Lesage and C. Audoin

Laboratoire de l'Horloge Atomique
Equipe de Recherche du CNRS, associée à l'Université Paris-Sud
Bât. 221 - Université Paris-Sud
91405 - Orsay - France

and M. Têtu

Laboratoire d'Electronique Quantique
Département de Génie Electrique
Université Laval
Quebec G1K 7P4 - Canada

Summary

A calculation of the power spectral density of amplitude fluctuations in masers is presented, which gives results in close agreement with others. The maximum of this power spectral density, which appears in specified conditions, for a Fourier frequency related to the Rabi frequency of atoms is observed for the first time both in a hydrogen and a rubidium maser.

The given model is completed to include a coherent excitation, as required in passively operated masers. Two methods for the interrogation of the atoms are considered. In the first one, the maximum of the atomic emission line is probed and in the second one, the null of the atomic dispersion line is observed. The power spectral density of fractional frequency fluctuations of the slaved frequency generator is calculated in both cases, including the effect of thermal noise in the microwave cavity and of noise added by the microwave receiver. Optimum operating conditions are specified. The cavity pulling factor is specified for both methods of interrogation and the effect of noise in the control of the microwave cavity resonant frequency is considered. Finally a useful design criterion is given for passively operated masers.

1. Introduction

Theory of amplitude and phase noise has been established soon in the history of ammonia [1] and hydrogen masers [2,3,4] and the validity of results has been further extended to the rubidium maser [5,6]. Although, amplitude noise in the ammonia maser used as a spectrometer has been considered [7,8], most of the interest in this field has been devoted to phase noise, in order to specify the frequency stability which can be expected from masers operating as oscillators. Frequency stability corresponding to the limit fixed by thermal noise in the microwave cavity, and by noise added to the maser signal in the microwave receiver has been effectively observed for measuring times τ up to 4×10^3 s [9].

In the work reported here, we calculate the power spectral density of amplitude noise in actively operated hydrogen and rubidium masers, using a specified model. Theoretical results are in close agreement with others, and are confirmed by experimental measurements on hydrogen and rubidium masers. The validity of theoretical analysis being thus established, amplitude noise in passively operated masers is considered. Indeed, contrary to the case of an oscillating maser, the frequency stability of a frequency generator, which is frequency locked to a passively operated maser is mainly determined by amplitude noise. Two different methods for the derivation of the frequency error signal are considered. Discussion of achieved results give information on the operating conditions which are able to give the best frequency stability when the amplitude noise added in the microwave receiver is taken into account.

2. Model and notations used

A model has been introduced which represents, in terms of an analog system, the behavior of masers [10,11]. As shown on figure 1, it comprises two coupled tuned circuits representing the microwave cavity and the amplifying atomic medium, respectively. The level stabilization is due to atomic saturation which limits the gain of the active medium when the oscillation level increases. Masers then belong to the class of oscillators in which the amplitude limiting effect depends on the amplitude of oscillation (the square of the amplitude here), with a delay in the level control [12], which is to be attributed to the longitudinal relaxation time constant.

The model describes the steady state as well as the transient regime [11]. It has been further completed to take into account the effect of a c.w. excitation externally applied to the microwave cavity, and to describe the amplification properties [13] and the synchronization phenomenon [14] when the maser is operated below and above oscillation threshold, respectively.

A random excitation will be now added to represent thermal noise in the microwave cavity*.

* Quantum noise is negligible for transition frequencies in the microwave region.

Notations of reference 13 and 14 are used.

The magnetic field in the microwave cavity is represented by H_1 such as :

$$H_1 = b \cos(\omega t + \varphi) \qquad (1)$$

where ω is a constant. b represents the amplitude of this field (this is the Rabi frequency of atoms in the microwave field) and φ denotes its phase. Quantities b and φ are allowed to be slowly varying functions of time i.e. their relative variations are small during a period of the microwave field.

This field creates a magnetization M_1 of the atoms in the storage bulb, at frequency ω, and modifies the population difference M_3 between levels involved in the atomic transition.
We set :

$$M_1 = m \sin(\omega t + \psi) \qquad (2)$$

The quantities m, ψ and M_3 are also slowly varying functions of time.

In the case of passively operated masers, we will assume that a monochromatic signal is applied to the microwave cavity via an appropriate coupling loop. We call it H_e defined by :

$$H_e = p \sin \omega t \qquad (3)$$

where p is a constant. The amplitude p is defined in such a way that we have b = p for a cavity without atoms and for $\omega = \omega_c$, where ω_c is the cavity resonant frequency. It will thus not be required to specify the coupling factor of the input loop.

3. Representation and power spectral density of considered noise sources

3.1. Thermal noise in the microwave cavity

Thermal noise in the considered mode of the microwave cavity will be represented as follows. We assume that the microwave cavity is at a temperature of 0 Kelvin, but that is coupled to a generator of a white noise signal H_n, with appropriate power spectral density. We suppose that this signal is band-limited, in order to use its Rice's representation [15], but that its bandwidth is large enough compared to the cavity bandwidth. We then set :

$$H_n = p_1 \cos \omega t + p_2 \sin \omega t \qquad (4)$$

In this model, H_n is white noise for frequencies around ω_c whereas p_1 and p_2 are white noises for low angular Fourier frequencies Ω. It is easy to show that we then have [16] :

$$S_{H_n} = \frac{1}{2} S_{p_1} = \frac{1}{2} S_{p_2} \qquad (5)$$

where S_{H_e}, S_{p_1} and S_{p_2} are one-sided power spectral densities.

Furthermore, we assume that noise magnetic field fluctuations in the microwave cavity are small enough compared to the coherent magnetic field amplitude b, i.e. :

$$p_1 \ll b \quad , \quad p_2 \ll b \qquad (6)$$

As shown in Appendix 1, thermal noise in the useful cavity mode is properly represented when we have :

$$S_{p_1}/b^2 = S_{p_2}/b^2 = 4\,kT/P \qquad (7)$$

where P is the power delivered by atoms to the loaded microwave cavity. An useful expression for P is given in Appendix 2.

It is worth noticing that the effect of the amplitude and phase noises of the interrogating signal H_e could be represented -if necessary- as a contribution to the noise signal H_n, and could then be accounted for as an increase of the cavity temperature.

It can be shown that the shot noise of the source of atoms in the upper quantum level excites amplitude and phase fluctuations which are negligible compared to those considered here *.

3.2. Noise added by the microwave receiver

The microwave receiver adds noise to the signal delivered by the maser at its output port. This noise is not correlated with maser noise and can be considered independently. We then assume that the received maser signal is represented by a pure sinusoïd b' cosωt. The noise signal provided by the receiver is denoted as $p'_1 \cos\omega t + p'_2 \sin\omega t$. As before (equation 6), we assume that p'_1 and p'_2 are much smaller than b'. We then have :

$$S_{p'_{1,2}}/(b')^2 = S_{p'_{1,2}} Q_{ext}/b^2 Q_c \qquad (8)$$

where Q_{ext} is the cavity quality factor connected with the output coupling loop.

By analogy with equation 7, it comes :

$$S_{p'_1}/b^2 = S_{p'_2}/b^2 = 4\,kT'/P = 4\,kT(F-1)/P \qquad (9)$$

where T' and F are the noise temperature and the noise factor of the microwave receiver, respectively.
We then have :

$$S_{p'_1}/(b')^2 = S_{p'_2}/(b')^2 = 4kT(F-1)Q_{ext}/P\,Q_c \qquad (10)$$

4. Basic equations for the maser noise

One can show that the set of differential equations which describes completely the maser behavior, when driven by H_e and H_n is the following

$$T_2\dot{m} + m = M_3\, b\, T_2 \cos\theta \qquad (11)$$

$$T_1\dot{R}_3 + R_3 = -T_1\, bm \cos\theta + T_1\, I \qquad (12)$$

$$T_c\dot{b} + b = KQ_c m\cos\theta + p\cos\varphi + p_1 \sin\varphi + p_2\cos\varphi \qquad (13)$$

$$\dot{\psi} = \omega_o - \omega + M_3 \frac{b}{m} \sin\theta \qquad (14)$$

* Analysis shows that this is true when $kT/P \gg 1/I$ where I is the creation rate of the atomic population difference, as defined in Section 4.

$$\dot{\varphi} = \omega_c - \omega - \frac{1}{T_c}\left[KQ_c \frac{m}{b}\sin\theta + \frac{p}{b}\sin\varphi - \frac{p_1}{b}\cos\varphi + \frac{p_2}{b}\sin\varphi\right] \quad (15)$$

$$\theta = \varphi - \psi \quad (16)$$

where the dot means time derivative. T_1 and T_2 are the longitudinal and the transverse relaxation times of atoms, respectively. T_c is the microwave cavity time constant. ω_o is the atomic transition frequency. I is the difference between the creation rate of atoms in the upper and the lower $m_F = 0$ quantum states. K is a factor which characterizes the coupling between the atomic medium and the microwave cavity field. We have, in S.I.units,

$$K = \mu_o \eta \mu_B^2/\hbar V_c \quad (17)$$

where $\mu_o = 4\pi \times 10^{-7}$, η is the filling factor[2,17,18] μ_B is Bohr magneton, $\hbar$ is Planck constant divided by 2π and V_c is the volume of the microwave cavity.

For $p = 0$ and $p_1 = p_2 = 0$, equations 11 to 16 describe steady state and transient behavior as well [10,11]. For $p \neq 0$ and $p_1 = p_2 = 0$, the considered equations have been used to describe properties of passively operated masers, in the steady state regime [13].

For $p = 0$ and $p_1 \neq 0$, $p_2 \neq 0$, we will obtain results on noise properties of actively operated masers, and for $p \neq 0$, $p_1 \neq 0$ and $p_2 \neq 0$, useful informations on noise properties of passively operated masers will be derived.

In the following, differential equations for the amplitude b and the phase φ are derived from equations (11) to (15) and they are linearized around steady state conditions. Fluctuations on the amplitude b and the phase φ are then described by linear differential equations [19].

Equations (11) to (15) have been established for the hydrogen maser. Although the atomic line is not homogeneous in the rubidium maser -due to trapping effect by the buffer gas- they can be used at least as a first approximation , to describe the noise behavior of this maser also.

5. Power spectral density of amplitude and phase fluctuations in actively operated masers

We set $p = 0$, and in order to simplify the reported results, we will only consider here the case where the microwave cavity is tuned to the atomic transition. We then have :

$$\omega = \omega_c = \omega_o \quad (18)$$

Conditions (6) and (18) allow to solve amplitude equations (11 to 13) independently of phase equations (14) and (15).

5.1. Amplitude noise

Fluctuations of the amplitude of oscillation are small. We then set

$$b(t) = b_o + \Delta b(t) \quad (19)$$

with

$$\Delta b(t)/b_o \ll 1 \quad (20)$$

where b_o is the amplitude of oscillation in steady state condition, for $\omega = \omega_c = \omega_o$ and without any random excitation. b_o is given by the following equation :

$$T_1 T_2 b_o^2 = \alpha - 1 \quad (21)$$

with

$$\alpha = KQ_c T_1 T_2 I \quad (22)$$

The parameter α characterizes the maser operating conditions relatively to oscillation threshold. In this section we have, obviously, $\alpha > 1$.

It can be shown that the differential equation for amplitude fluctuations is the following :

$$T_c \frac{d^3(\Delta b)}{dt^3} + \frac{d^2(\Delta b)}{dt^2} + \frac{1}{T_1}\frac{d(\Delta b)}{dt} + 2b_o^2 \Delta b = \frac{d^2 p_2}{dt^2} + \left(\frac{1}{T_1} + \frac{1}{T_2}\right)\frac{dp_2}{dt} + \left(b_o^2 + \frac{1}{T_1 T_2}\right) p_2 \quad (23)$$

where the verified condition $T_c \ll T_1$ has been taken into account.

The power spectral density of fractional amplitude fluctuations ε, where ε is given by :

$$\varepsilon = \frac{\Delta b}{b_o} \quad (24)$$

is then easily obtained. It comes, when equation (7) is also used :

$$S_\varepsilon(\Omega) = \frac{4kT}{P_o} \frac{\left(b_o^2 + \frac{1}{T_1 T_2} - \Omega^2\right)^2 + \left(\frac{1}{T_1} + \frac{1}{T_2}\right)^2 \Omega^2}{\left(2b_o^2 - \Omega^2\right)^2 + \left(\frac{1}{T_1} - T_c\Omega^2\right)^2 \Omega^2} \quad (25)$$

where P_o is the power delivered by atoms to the tuned cavity,which depends on b_o (see Appendix 2).

It can be seen that for $\Omega T_c \gg 1$, $S_\varepsilon(\Omega)$ varies as $(1 + T_c^2\Omega^2)^{-1}$, which represents the filtering effect of the microwave cavity. For $\Omega^2 \ll (T_1 T_c)^{-1}$ equation (25) becomes identical to the result derived by Cutler [3]. The very slight discrepancy, for $T_c^{-1} > \Omega > (T_c T_1)^{-1/2}$ is related to the fact that we did take into account the time constant of the response of the microwave cavity to its excitation by the atomic magnetization (it is represented by the term $T_c \dot{b}$ in equation 13).

In order to discuss equation (25), it is of interest to introduce the saturation factor S_o which is, under condition (18) defined as :

$$S_o = T_1 T_2 b_o^2 \quad (26)$$

and to assume

$$T_1 = T_2 = T \quad (27)$$

An useful approximation of equation (25) is then, for $0 < \Omega < T_c^{-1}$:

$$S_\varepsilon(\Omega) = \frac{4kT}{P_o} f_\varepsilon(\Omega) \quad (28)$$

with

$$f_\varepsilon(\Omega) = \frac{\left(1 + S_o - T^2\Omega^2\right)^2 + 4T^2\Omega^2}{\left(2S_o - T^2\Omega^2\right)^2 + T^2\Omega^2} \quad (29)$$

Figure 2 shows the variation of $f_\varepsilon(\Omega)$ for several values of S_o. One sees that i) for $\Omega T \gg 1$,

$f_\varepsilon(\Omega)$ tends towards a constant, equal to unity which means that far enough from line bandwidth, amplitude fluctuations ignore the presence of the active medium and that we then have additive amplitude noise, ii) for $\Omega = 0$, power spectral density of fractional amplitude fluctuations is a decreasing function of the saturation factor and for $S_o \gtrsim 1$, amplitude fluctuations "saturates" much and becomes smaller than for $\Omega T >> 1$, iii) for S_o small enough (maser just above oscillation threshold) $S_\varepsilon(\Omega)$ is a monotonously decreasing function of the Fourier frequency and iv) for S_o large enough ($S_o \gtrsim 0.2$) a hump appears in the S_ε-curves[3,4].

This maximum of $S_\varepsilon(\Omega)$ is related to the nature of the dynamical response of the maser amplitude to a perturbation. If the oscillation level is small, for $S_o \lesssim 1/8$ this response is exponentially damped whereas it has an oscillatory component if the level of oscillation is large enough, for $S_o \gtrsim 1/8$ [11]. In this last event, the maximum of $S_\varepsilon(\Omega)$ then occurs at a value which is roughly equal to Ω_1 given by :

$$\Omega_1^2 = 2b_o^2 - 1/4T_1^2 \qquad (30)$$

5.2. Phase fluctuations

The differential equation for phase fluctuations $\Delta\varphi$ can be derived from equations (14, 15). One obtains :

$$T_c \frac{d^2\Delta\varphi}{dt^2} + \frac{d\Delta\varphi}{dt} = \frac{dp_1}{dt} + \frac{1}{T_2}\frac{p_1}{b_o} \qquad (31)$$

The power spectral density $S_{\Delta\varphi}(\Omega)$ of phase fluctuations is then given by :

$$S_{\Delta\varphi}(\Omega) = \frac{4kT}{P_o}\left(1 + \frac{1}{\Omega^2 T_2^2}\right)\frac{1}{(1 + T_c^2\Omega^2)} \qquad (32)$$

in complete agreement with Cutler [3]. The term $1/T_2^2\,\Omega^2$ represents the white frequency noise which constitutes the fundamental thermodynamical limit to the long term frequency stability. It has been observed in time domain measurements [9]. The other term of the parenthesis represents the additive white phase noise contribution of the microwave cavity thermal noise.

5.3. Effect of receiver noise

We will only consider the amplitude noise. Observed amplitude fluctuations have their origin : i) in the interaction of atoms with thermal noise and ii) in the microwave receiver. The observed power spectral density $S'_\varepsilon(\Omega)$ of fractional amplitude fluctuations is then, in the useful Fourier frequency range :

$$S'_\varepsilon(\Omega) = \frac{4kT}{P_o}\left[f_\varepsilon(\Omega) + (F-1)\frac{Q_{ext}}{Q_c}\right] \qquad (33)$$

The hump in $f_\varepsilon(\Omega)$ can then be observed only if $(F-1)Q_{ext}/Q_c$ is small enough.

6. Experimental results on amplitude noise

Measurement of the spectrum of the amplitude response of an ammonia maser to a sinusoïdal excitation[8] showed a good qualitative agreement with results given here, for small S_o, close to oscillation threshold.

We here report experimental results achieved with hydrogen and rubidium masers in which the hump of $S_\varepsilon(\Omega)$ is observed for the first time.

The signal generated by actively operated masers is amplified in a heterodyne receiver, whose output is linearly detected. Amplitude fluctuations are then obtained. They are processed in a FTT spectrum analyzer which gives their power spectrum density.

6.1. Experiments with a hydrogen maser

Figure 3 shows the power spectrum density of amplitude fluctuations in a hydrogen maser with $Q_c = 47\,000$ and $S_o \simeq 0.6$. One sees very good qualitative agreement with figure 2.

Afterwards, in order to study in more details the validity of equation (25) and to provide an easy change of the parameter S_o, we have equipped the maser with an external feedback loop which allowed us to vary the quality factor of the cavity. The experimental set-up is depicted on figure 4. Values of the parameter S_o as large as 8 have been achieved, with $Q_c = 6.5 \times 10^5$.

Figure 5 shows the experimentally recorded variations of $S_\varepsilon(\Omega)$ for $T_1 = 0.175$ s, $T_2 = 0.230$ s and $b_o^2 = 141\ s^{-2}$ (giving $S_o \simeq 5.67$). Quantities T_1 and b_o^2 have been measured by recording a transient of the level of oscillation [11,14] which has been induced by state mixing. The value of T_2 has been obtained via cavity pulling effect. The dotted line represents the theoretical variations of $S_\varepsilon(\Omega)$ as computed from equation (25). The theoretical graph has been adjusted to the recorded one for $\Omega/2\pi = 10$ Hz. One can see that the agreement between theoretical and experimental results is excellent.

Figure 6 compares the theoretical and experimental values of the frequency for which $S_\varepsilon(\Omega)$ shows a maximum, for four different values of S_o. Both values agree within a few percent, the uncertainty being mainly related to measurement of T_1 and b_o^2.

6.2. Experiments with a rubidium maser

Similar experiments have been performed with a rubidium maser. An external feedback loop, such as shown on figure 4 has been used to increase the oscillation level, and therefore the value of S_o. Figure 7 represents the recorded variations of the power spectral density of amplitude fluctuations. A pronounced maximum also appears at a Fourier frequency of 32 Hz. In the rubidium maser, relaxation times are smaller than in the hydrogen maser. It results that a saturation factor of the order of unity requires a larger Rabi frequency. Consequently, the frequency for which the maximum of $S_\varepsilon(\Omega)$ occurs is larger in the rubidium maser than in the hydrogen maser.

6.3. Conclusion

Experimental results confirm theoretical ones. This gives confidence in the validity of the model used to describe amplitude noise in actively operated masers. In the following, it will be completed to describe amplitude noise in passively operated masers, and to predict the frequency stability of a controlled frequency generator.

7. Amplitude and phase noise in passively operated masers

7.1. Statement of the considered problem

When the interrogating frequency ω differs from ω_o, amplitude and phase equations (11) to (15) are coupled together and the algebra becomes heavy. However, as we will see in sections 8 and 9, the calculation of the power spectral density of amplitude and phase fluctuations for $\Omega = 0$ is of special interest to determine the effect of the maser noise on the frequency stability of the generator controlled by the atomic transition.

The assumption $\Omega = 0$ allows one to withdraw all time derivatives in equations (11) to (15) and to derive more easily the equations for amplitude and phase increments Δb and $\Delta\varphi$, respectively, related to thermal noise.

7.2. Recalls on the steady state results

The passive mode of operation is obtained for $\alpha < 1$. An interrogating signal is required to probe the atomic transition. We thus have $p \neq 0$. We assume that the cavity mistuning is small and that the following condition is satisfied :

$$T_c(\omega_c - \omega) \ll 1 \tag{34}$$

On the contrary, no condition is set -except when otherwise stated- on the quantity $T_2(\omega_o - \omega)$.

As shown in reference 13, the following condition then holds for $p_1 = p_2 = 0$:

$$\frac{p}{b}\sin\varphi = T_c(\omega_c - \omega) - \frac{\alpha}{1+S}\sin\theta\cos\theta \tag{35}$$

$$\frac{p}{b}\cos\varphi = 1 - \frac{\alpha}{1+S}\cos^2\theta \tag{36}$$

with

$$\cos^2\theta = \left[1 + T_2^2(\omega_o - \omega)^2\right]^{-1} \tag{37}$$

$$S = T_1 T_2 b^2 \cos^2\theta \tag{38}$$

where S is the saturation factor of the atomic transition.

The modulus G of the maser gain is defined as :

$$G = b/p \tag{39}$$

We have, under condition (34) :

$$G^2 = \frac{(1+S)^2}{(1+S)^2 - \alpha(2+2S-\alpha)\cos^2\theta} \tag{40}$$

For $\omega = \omega_c = \omega_o$ the gain shows a maximum G_o given by :

$$G_o = \frac{1+S_o}{1+S_o-\alpha} \tag{40}$$

where S_o is the value of the saturation factor for $\omega = \omega_o$. The relation between S and S_o is specified in Appendix 4.

Figure 8 depicts the variation of G as a function of α for negligible saturation and figure 9 illustrates the effect of saturation on the gain. It will be shown in section 9 the interest to consider also the imaginary part of the complex gain $\bar{G}$ given by :

$$\mathrm{Im}(\bar{G}) = \frac{b}{p}\sin\varphi = G^2\frac{p}{b}\sin\varphi \tag{42}$$

where $p\sin\varphi/b$ is given by equation (35). Figures 10 and 11 show the variation of $\mathrm{Im}(\bar{G})$ for several values of α and S_o, under condition $\omega_c = \omega_o$.

7.3. Spectral density of amplitude and phase fluctuations

Calculation of amplitude and phase departures from the steady state regime, Δb and $\Delta\varphi$ respectively, give the following results when only the very low frequency components of H_n are considered :

$$\frac{\Delta b}{b}\left[(1+S)^3 - \alpha(2-\alpha+\alpha S+2S)\cos^2\theta\right] = \frac{p_2}{p}(1+S)\left[(1+S)^2 - \alpha(2-\alpha+2S)\cos^2\theta\right] \tag{43}$$

and

$$\Delta\varphi = \frac{p_1}{b} + \frac{1+S}{1+S-\alpha}\left[\frac{p_2}{p} - \frac{\Delta b}{b}\right]\mathrm{tg}\theta \tag{44}$$

In general, the quantities b, S and θ in the two above equations have to be evaluated for $\omega \neq \omega_o$.

Equation (43) shows that, under the specified conditions, amplitude fluctuations are only related to p_2, the amplitude of the noise component which is in phase with the coherent excitation H_e. Phase fluctuations (equation 44) depends on the amplitude p_1 of the noise component in quadrature with H_e, and also on p_2 if $\omega \neq \omega_o$.

The power spectral densities of $S_\varepsilon(\Omega = 0)$ and $S_{\Delta\varphi}(\Omega = 0)$ are then given by :

$$S_\varepsilon = \frac{4kT}{P}\frac{(1+S)^4\left[(1+S)^2 - \alpha(2-\alpha+2S)\cos^2\theta\right]}{\left[(1+S)^3 - \alpha(2-\alpha+\alpha S+2S)\cos^2\theta\right]^2} \tag{45}$$

and

$$S_{\Delta\varphi} = \frac{4kT}{P}G^2\left[1 + \frac{4\alpha^2S^2(1+S)^2\sin^2\theta\cos^2\theta}{\left[(1+S)^3 - \alpha(2-\alpha+\alpha S+2S)\cos^2\theta\right]^2}\right] \tag{46}$$

8. Control of a frequency generator by the atomic line. General statements

There are many ways to control the frequency of a quartz crystal oscillator by the atomic line. One may look either at the wave which is transmitted or at the wave which is reflected by the maser. On the other hand, information on the atomic transition frequency may be inferred either from : i) the phase shift between the output and the input waves, ii) the amplitude of the output wave, or iii) the atomic dispersion curve.

We will limit ourselves to the consideration of the transmitted wave, and to control of the frequency of a quartz crystal oscillator by probing either the maximum of the atomic emission line, or the null of the atomic dispersion curve.

In both cases, a quantity which depends on the

amplitude of the maser response to an appropriate frequency modulation is measured. The maser amplitude noise has then to be considered.

9. Control of a frequency generator by the atomic emission line. Slow frequency modulation

9.1. Power spectral density of frequency fluctuations of the controlled generator

The input wave is frequency modulated in order to probe the maximum of the gain curve. Amplitude modulation of the transmitted wave is detected and coherently demodulated.

We assume square-wave frequency modulation and we set :

$$\omega = \omega_1 \pm \omega_m \tag{47}$$

where ω is the frequency of the input wave, ω_1 is the mean value of this frequency and ω_m is the frequency modulation depth. In this technique, *the frequency of the modulation must be appreciably smaller than the atomic linewidth,* which justifies the consideration of noise power spectral density for $\Omega = 0$.

The error signal is given by the difference δb between the amplitude of the maser response at frequencies $\omega_1 + \omega_m$ and $\omega_1 - \omega_m$. For ω_1 close to ω_o, we have :

$$\delta b = 2(\omega_1 - \omega_o)\left.\frac{\partial b}{\partial \omega}\right|_{\omega_o \pm \omega_m} + \Delta b(\omega_1 + \omega_m) - \Delta b(\omega_1 - \omega_m) \tag{48}$$

where $\Delta b(\omega_1 + \omega_m)$ and $\Delta b(\omega_1 - \omega_m)$ represent amplitude fluctuations, due to thermal noise at frequencies $\omega_1 + \omega_m$ and $\omega_1 - \omega_m$, respectively.

$\left.\frac{\partial b}{\partial \omega}\right|_{\omega_o \pm \omega_m}$ is the slope of the gain curve at frequencies $\omega_o \pm \omega_m$.

One finds :

$$\frac{1}{b}\left|\frac{\partial b}{\partial \omega}\right| = \alpha T_2 \frac{(2 - \alpha + \alpha S + 2S)\, x \cos^4\theta}{(1+S)^3 - \alpha\,(2 - \alpha + \alpha S + 2S)\cos^2\theta} \tag{49}$$

with

$$x = T_2(\omega_o - \omega) = T_2\,\omega_m \tag{50}$$

The servo system function is to impose the condition $\delta b = 0$. The power spectral density of fractional frequency fluctuations of the controlled generator is h_o given by * :

$$h_o = \frac{S'_\varepsilon(\Omega = 0)}{2\omega_o^2\left[\frac{1}{b}\frac{\partial b}{\partial \omega}\right]^2} \tag{51}$$

where S'_ε is the power spectral density of fractional amplitude fluctuations including maser and receiver noise.

We will at first discuss separately the effect of this two noise sources.

* The time domain measure of frequency stability is then $\sigma_y(\tau) = (h_o/2\tau)^{1/2}$.

9.2. Effect of maser noise

With equations (45), (49) and(A-12), it comes, assuming again $T_1 = T_2$:

$$h_o(\text{maser}) = \frac{4kT}{\hbar\omega_o^3} KQ_c \frac{(1+S)^4\left[(1+S)^2 - \alpha(2-\alpha+2S)\cos^2\theta\right]}{\alpha^2 S\left[2+2S-\alpha+\alpha S\right]^2 x^2 \cdot \cos^6\theta} \tag{52}$$

A more rapid but heuristic derivation of equation (52) is given in Appendix 3.

Equation (52) shows that the frequency stability depends on the maser design through the quantities K and Q_c, and on its operating conditions via the parameters α, S and x ($\cos^2\theta$ is a function of x, see equation (37) and (50)). Optimum operating conditions which minimizes h_o have been computed. In this computation it has been assumed that relaxation times T_1 and T_2 do not depend on the atomic density in the bulb, which is true for small enough beam intensities.

One finds that for a given value of α, it exists an optimum value for S_o (the saturation factor for $\omega = \omega_o$) and x, but that the corresponding value of h_o is a decreasing function of α in the range $0 < \alpha < 1$. Curves a on figures 12 and 13 show the optimum values of S_o and $T_2\omega_m$, respectively.

It is worth noticing that the quantities $T_2\omega_m$, α and S_o are easily measurable ones[12] and that optimum adjustments can then readily be made.

The solid line (curve a) on figure 14 shows the corresponding value of h_o for a hydrogen maser of ordinary design, with a cavity volume of 15.5 dm^3, $\eta = 2.8$ (bulb diameter of 16 cm) and $Q_c = 30\,000$.

9.3. Effect of receiver noise

With equations (10), (49) and(A-12), it comes, assuming $T_1 = T_2$:

$$h_o(\text{receiver}) = \frac{4kT}{\hbar\omega_o^3}(F-1)KQ_{ext}\frac{\left[(1+S)^3 - \alpha\,(2 - \alpha + 2S + \alpha S)\cos^2\theta\right]^2}{\alpha^2 S\,[2 + 2S - \alpha + \alpha S]^2 x^2\, \cos^6\theta} \tag{53}$$

It still exists optimum conditions of operation relatively to the receiver noise considered alone. They are shown on figure 12 and 13, curves b.

The solid line (curve a) on figure 15 shows the corresponding value of h_o, for a hydrogen maser, with $V_c = 15.5$ dm^3, $\eta = 2.8$, $Q_{ext} = 60\,000$ and $F = 2$.

9.4. Discussion of results

One sees that optimum operating conditions are quite different according to the considered noise source.

Furthermore, figure 14, curve b shows that, with data specified in sections 9.2. and 9.3., receiver noise will limit the frequency stability if conditions are adjusted to minimize the maser noise. Similarily, figure 15, curve b shows that optimization for receiver noise may not be the best one.

As the contribution of maser and receiver noises are very comparable, it then appears that, in the given example, it is the quantity

$$h_o = h_o(\text{maser}) + h_o(\text{receiver}) \qquad (54)$$

which must be optimized.

Curves c on figures 12 and 13 then specify optimum operating conditions and curves c on figures 14 and 15 show the corresponding values of h_o. One sees that for $\alpha = 0.5$, one has $h_o = 1.5 \times 10^{-25}$ Hz^{-1} giving a frequency stability measure $\sigma_y(\tau) = 2.7 \times 10^{-13}\ \tau^{-1/2}$ and for $\alpha = 0.75$ it comes $h_o = 4.3 \times 10^{-26}$ Hz^{-1} and $\sigma_y(\tau) = 1.5 \times 10^{-13}\ .\ \tau^{-1/2}$.

Figure 16 gives the related values of the gains G and G_o when h_o, as defined in equation (54) is minimized. The two following remarks are of interest :

1. Comparison of equation (52) and (53) shows that the quantity $(F-1)Q_{ext}/Q_c$ should be as small as possible to reduce the contribution of the receiver noise. This implies a good noise figure of the receiver and a coupling factor of the microwave cavity output loop which is larger than in actively operated masers.

2. Curves a and b on figures 12 and 13 are valid for hydrogen and rubidium masers as well and they do not depend on F, Q_{ext} and Q_c. On the contrary, the position of curve c between curves a and b depends on the values of F and Q_{ext}/Q_c.

10. Control of a frequency generator by the atomic dispersion line. Fast frequency modulation

10.1. Calculation of the error signal

The well known Pound technique for the stabilization of a frequency generator on the resonance of a microwave cavity has been successfully applied to the control of a Gunn diode oscillator on a superconductive cavity [20]. In this method, the interrogating signal is frequency modulated at a frequency which is much larger than the bandwidth of the selective circuit. The carrier frequency is reflected depending on its frequency offset relatively to the resonant frequency, and the sidebands are totally reflected.

This technique can be transposed to passively operated masers [21,22]. The existence of two resonant circuits in a maser (the atomic medium and the microwave cavity) allows to use the transmitted wave. The transmission of the carrier depends on its frequency relatively to that of the atomic resonance frequency. *The frequency of the modulation being much larger than the atomic linewidth,* (but equal to, or smaller than, the cavity bandwidth), the sidebands are transmitted by the microwave cavity, as if the atomic medium were absent.

The great advantage of this interrogating process is to allow a much faster frequency modulation than the previously considered one, described in section 9. This offers more freedom for the choice of the attack time of the servo control loop of the frequency generator.

We denote w_i the incident coherent wave at the input port of the maser. We have [20] :

$$w_i = p e^{i\omega t}\left[1 + m\left(e^{i\omega_m t} - e^{-i\omega_m t}\right)\right] \qquad (55)$$

where ω_m is the modulation frequency and m is the amplitude of the two first sidebands relative to that of the carrier.

Assuming that frequency ω is close to the atomic resonant frequency ω_o, whereas frequencies $\omega \pm \omega_m$ are well outside the atomic line width, the transmitted wave will then be the following :

$$w_t = e^{i\omega t}\left[b e^{i\varphi} + mp\,(e^{i\omega_m t} - e^{-i\omega_m t})\right] \qquad (56)$$

where attenuation of the sidebands has been neglected.

This wave drives a square law detector, the output of which is demodulated by multiplication by $\sin\omega_m t$ followed by low pass filtering. The error signal is then V given by :

$$V = k\,\overline{w_t\, w_t^*\, \sin\omega_m t} \qquad (57)$$

where k is a constant and the bar means time averaging.
We get :

$$V = 2k\,p^2\,\frac{b}{p}\sin\varphi \qquad (58)$$

It can be seen that $b \sin\varphi / p$ represents the imaginary part of the maser complex gain, i.e. its dispersion. It is depicted on figures 10 and 11. Under condition $\omega_c = \omega_o$ and $T_2(\omega_o - \omega) \ll 1$, equations (35) and (42) give :

$$\sin\varphi = \frac{b_o}{p}\,\frac{\alpha T_2}{1+S_o}\,(\omega_o - \omega) \qquad (59)$$

10.2. Effect of maser noise

As previously, we represent thermal noise in the microwave cavity by adding a random component to the input wave. We then have now :

$$w_i = e^{i\omega t}\left[(p + p_2 + ip_1) + (mp + p_2^+ + ip_1^+)e^{i\omega_m t} - (mp + p_2^- + ip_1^-)\,e^{-i\omega_m t}\right] \qquad (60)$$

where the subscripts 1 and 2 refer to noise components out of phase and in phase with the coherent excitation, respectively. The superscripts + and - characterize noise components at frequencies very close to $\omega + \omega_m$ and $\omega - \omega_m$, respectively.

The long term frequency stability of the slaved frequency generator is determined by very slow frequency fluctuations of the error signal. We then consider again variations at Fourier frequency $\Omega = 0$. The transmitted wave is then

$$w_t = e^{i\omega t}\left[b e^{i\varphi} + \Delta(b e^{i\varphi}) + (mp + p_2^+ + ip_1^+)\,e^{i\omega_m t} - (mp + p_2^- + ip_1^-)\,e^{-i\omega_m t}\right] \qquad (61)$$

where $\Delta(be^{i\varphi})$ denotes the effect of noise at frequency ω on the maser output.
The error signal becomes :

$$V = 2kpb\left(\sin\varphi - \frac{1}{2m}\,\frac{p_1^+ + p_1^-}{p} + \Delta\varphi\right) \qquad (62)$$

where we have, here, to consider phase fluctuation $\Delta\varphi$. For $|T_2(\omega_o - \omega)| \ll 1$ it is given by :

$$\Delta\varphi = p_1/p \qquad (63)$$

as shown by equation (44).

The servo system imposes V = 0 and the power spectral density of fractional frequency fluctuations of the controlled oscillator determined by maser noise, is then :

$$h_o(\text{maser}) = \frac{4kT}{P_o}\left(1 + \frac{1}{2m^2}\right)\frac{(1+S_o)2}{\alpha^2\omega_o{}^2T_2{}^2} \qquad (64)$$

or, assuming $T_1 = T_2$

$$h_o(\text{maser}) = \frac{8kT}{\hbar\omega_o{}^3}KQ_c\left(1 + \frac{1}{2m^2}\right)\frac{(1+S_o)^2}{\alpha^2 S_o} \qquad (65)$$

For a maser of given design, h_o is minimized for $2m^2 >> 1$ and $S_o = 1$. Curve a on figure 17 then shows the variation of h_o with α for $V_c = 15.5$ dm^3 $\eta = 2.8$ and $Q_c = 30\,000$.

10.3. Effect of receiver noise

We now assume that the microwave cavity is noiseless, but we introduce the noise added by the microwave receiver. One obtains :

$$V = 2k\,p\,b\left[\sin\varphi - \frac{1}{2m}\frac{p'_1 + p'_1}{p} + \frac{p'_1}{p}\right] \qquad (66)$$

where the prime characterizes receiver noise. It then comes, assuming $T_1 = T_2$

$$h_o(\text{receiver}) = \frac{8kT}{\hbar\omega_o{}^2}KQ_{ext}(F-1)\left(\frac{1}{G_o{}^2} + \frac{1}{2m^2}\right)\frac{(1+S_o)^2}{\alpha^2 S_o} \qquad (67)$$

where G_o is given by equation (41).

If m is large enough so that we have $2m^2 >> G_o{}^2$, h_o(receiver) is optimized for $S_o = 1 - \alpha$. As for the other considered method of frequency control, the saturation factor should be smaller when receiver noise dominates than when the maser noise is the largest one.

10.4. Discussion of results

Curve b on figure 17 shows the contribution of the receiver noise ($2m^2 >> G_o{}^2$, F = 2, Q_{ext} = 60 000) when operating conditions are optimized for maser noise. One sees that, as before, it is the quantity

$$h_o(\text{maser}) + h_o(\text{receiver})$$

which must be optimized.
Curve c on figure 18 then shows the value of S_o which minimizes the useful quantity. Curve c on figure 17 gives the power spectral density of fractional frequency fluctuations in the considered example for $2m^2 >> G_o{}^2$. One has $h_o = 8 \times 10^{-26}$ Hz^{-1} and $\sigma_y(\tau) = 2 \times 10^{-13}\,\tau^{-1/2}$ for $\alpha = 0.5$ and $h_o = 3 \times 10^{-26}$ Hz^{-1} and $\sigma_y(\tau) = 1.2 \times 10^{-13}\,\tau^{-1/2}$ for $\alpha = 0.75$.

Considering that the value of m is actually finite, one concludes that the two methods of frequency control have equal capabilities as far as frequency stability is concerned.

11. Cavity pulling and cavity tuning

In passively operated masers, the microwave cavity needs to be tuned at the atomic resonance frequency. The servo system introduces noise on the cavity resonant frequency ω_c and this will affect the transition frequency via cavity pulling effect.

11.1. Cavity pulling in the observation of the emission line

Cavity mistuning distorts the emission line and the condition that the control loop of the frequency generator provides a null of the error signal is the origin of the cavity pulling effect. The cavity pulling factor [13] P_e in the observation of the emission line is then given by :

$$P_e = \frac{\left.\frac{\partial b}{\partial\omega_c}\right|_{\omega_o + \omega_m,\ \omega_c = \omega_o}}{\left.\frac{\partial b}{\partial\omega}\right|_{\omega_o + \omega_m,\ \omega_c = \omega_o}} \qquad (68)$$

It then comes :

$$P_e = \frac{Q_c}{Q_\ell}\frac{(1+S)^2}{(2 - \alpha + 2S + \alpha S)\cos^2\theta} = C\frac{Q_c}{Q_\ell} \qquad (69)$$

where Q_c and Q_ℓ are the quality factors of the cavity and the atomic line, respectively. The parameters S and $\cos^2\theta$ have to be taken for $\omega = \omega_o \pm \omega_m$ (see also Appendix 4).

When operating conditions are optimized for maser plus receiver noises, one has, in the given example : $P_e = 0.98\ Q_c/Q_\ell$ for $\alpha = 0.5$ and $P_e = 0.97\ Q_c/Q_\ell$ for $\alpha = 0.75$.

11.2. Cavity pulling in the observation of the dispersion line

According to equations (35) and (42), the condition that the imaginary part of the complex gain is equal to zero, is the source of the cavity pulling effect. The cavity pulling factor, in the observation of the dispersion line is then given by :

$$P_d = \frac{Q_c}{Q_\ell}\frac{1+S_o}{\alpha} \qquad (70)$$

One then has $P_d = 3.42\ Q_c/Q_\ell$ for $\alpha = 0.5$ and $P_d = 2.15\ Q_c/Q_\ell$ for $\alpha = 0.75$. The pulling effect is then larger than for the other method, in which the emission line is observed. It would even be worse for smaller values of α. This is the drawback of the method based on the observation of the dispersion line.

11.3. Effect of cavity tuning noise

The equation for the power spectral density of fractional fluctuations of the cavity resonant frequency h_c can easily be derived for cavity tuning methods similar to those considered for sensing the atomic transition frequency.

We will mainly consider square wave frequency modulation and measurement of the amplitude of the transmitted wave. The optimum value of the amplitude of the frequency modulation is half the cavity bandwidth. We then have :

$$h_c = \frac{2kT}{P_1}\frac{1}{Q_c{}^2}\left[1 + (F-1)\frac{Q_{ext}}{Q_c}\right] \qquad (71)$$

where P_1 is the power dissipated in the loaded mi-

crowave cavity at the applied frequencies.
The power spectral density h'_o of fractional frequency fluctuations which are due to noise in cavity tuning is then :

$$h'_o = \frac{2kT}{P_1} C^2 \frac{1}{Q_\ell^2} \left[1 + (F-1)\frac{Q_{ext}}{Q_c}\right] \qquad (72)$$

where C is defined in equation (69).
With equation (A 12), where it is assumed $T_1 = T_2$, it comes the following equation :

$$h'_o = \frac{16kT}{\hbar\omega_o^3}\left[1 + (F-1)\frac{Q_{ext}}{Q_c}\right]\frac{P}{P_1}\frac{C^2}{S} KQ_c \cos^2\theta \qquad (73)$$

which looks similar to equations (52) and (53).When operating conditions are optimized for maser plus receiver noises, one has $h'_o = 7.5 \times 10^{-26}$ Hz^{-1} for $P_1 = P/2$ and $\alpha = 0.5$.One sees that the value of h'_o is only 3 dB below the corresponding value of h_o.

It would then be wise to enlarge the power P_1 on sidebands used to probe the cavity resonant frequency.

Similar conclusions can be derived for other methods of control of the frequency generator by the atomic line, and of control of the microwave cavity frequency.

12. A brief comparison of frequency stability of actively and passively operated masers

We will only consider here the fundamental effect of noise in the microwave cavity.

For actively[21] as well as passively operated masers, one can write :

$$\sigma_y(\tau) = C' \frac{1}{Q_\ell}\left(\frac{kT}{2P_o\tau}\right)^{1/2} \qquad (74)$$

where τ is the sampling time. C' is a constant which is equal to unity in oscillating masers.In passive masers, C' depends on the technique used to control the frequency generator, and on the value of the caracteristic parameters α, S_o and, when necessary, $\cos^2\theta$.

Equation (74) shows that there is no major difference between active and passive operation, as far as frequency stability is concerned.

Numerical examples given in the text show that frequency stability of a passively operated maser of classical design (TE_{011} mode cavity without dielectric load) should be $1 \times 2 \times 10^{-13} \times \tau^{-1/2}$ when operated close to oscillation threshold. This is only a little worse than the frequency stability figure of $4 \times 10^{-14}\ \tau^{-1/2}$ which has been obtained with well designed oscillating masers [8].

13. Conclusion : a design criterion for passively operated masers

As a result of the reported analysis, it appears that the power spectral density of frequency fluctuations of the frequency generator slaved to a passive maser operated at optimum conditions varies roughly as $KQ_c/\alpha^2 = (KQ_c T_1^2 T_2^2 I^2)^{-1}$ as shown by equations (52) and (65) and curves c on figures 14,15 and 17. One of the design goals of miniaturized masers should then be to make this quantity as small as possible.

Appendix 1

Power spectral density of p_1 and p_2 representing thermal noise

Let us consider the microwave cavity, without atoms, nor any coherent field, but driven by the random excitation H_n defined by equation (4). The time variation of the microwave cavity field is then solution of the following differential equation [13]

$$\ddot{H}_1 + \frac{2}{T_c}\dot{H}_1 + \omega_c^2 H_1 = -\frac{2\omega_c}{T_c} H_n \qquad (A.1)$$

where a dot represent first order time derivative. ω_c is the cavity resonant frequency, T_c is the cavity time constant which is related to the cavity quality factor Q_c by the following equation :

$$\omega_c T_c = 2 Q_c \qquad (A.2)$$

If $S_{H_1}(\omega)$ and $S_{H_n}(\omega)$ denote the spectral power densities of H_1 and H_n around $\omega = \omega_c$, respectively, we have :

$$S_{H_1}(\omega) = \left[1 + Q_c^2\left(\frac{\omega_c}{\omega} - \frac{\omega}{\omega_c}\right)^2\right]^{-1} S_{H_e}(\omega) \qquad (A.3)$$

The mean quadratic value of H_1 is then $\overline{H_1^2}$ given by :

$$\overline{H_1^2} = \frac{1}{\pi}\int_0^\infty S_{H_1}(\omega)d\omega = \frac{\omega_c}{2Q_c} S_{H_n}(\omega) \qquad (A.4)$$

The quantity $\overline{H_1^2}$ is proportional to kT, the thermal noise energy stored in the useful cavity mode. It is of interest to compare $\overline{H_1^2}$ to the energy W stored in the microwave cavity when atoms are present and when the microwave field H_1 is given by equation (1). It is easy to see that the stored energy is then proportional to $b^2/2$. The proportionality constant is the same in both cases because we are dealing with the same cavity mode. We then have :

$$2\overline{H_1^2}/b^2 = kT/W \qquad (A.5)$$

Energy W is related to the power P delivered by atoms to the loaded microwave cavity according to :

$$P = \omega_c W/Q_c \qquad (A.6)$$

Comparison of equations (5), (A.4), (A.5) and (A.6) gives :

$$S_{p_1}/b^2 = S_{p_2}/b^2 = 4kT/P \qquad (A.7)$$

Appendix 2

Expression of the power delivered to the loaded microwave cavity

The total energy stored in the loaded microwave cavity is W given by :

$$W = \frac{1}{2\mu_o} V_c \langle B^2 \rangle_{cav} \qquad (A.8)$$

where $\mu_o = 4\pi \times 10^{-7}$, V_c is the volume of the microwave cavity and $\langle B^2 \rangle_{cav}$ is the mean value of the squared amplitude of the magnetic field in the microwave cavity.

In the hydrogen maser, the filling factor η is defined as [2,17] :

$$\eta = \frac{< B_z >^2_{bulb}}{< B^2 >_{cav}} \qquad (A.9)$$

where $< B_z >_{bulb}$ is the mean value of the axial component of the amplitude of the magnetic field, averaged on the storage bulb volume.

The amplitude b is such as [10,13] :

$$b = -\frac{\mu_B}{\hbar} < B_z >_{bulb} \qquad (A.10)$$

where μ_B is Bohr magneton. It then comes :

$$W = \frac{V_c \hbar^2 b^2}{2\mu_o \mu_b^2 \eta}$$

With equations (A.6) and (17) the following equation for the power P dissipated in the loaded cavity is obtained :

$$P = \frac{1}{2} \hbar\omega_o \frac{b^2}{KQ_c} \qquad (A.11)$$

It can be shown that equation (A.11) is also valid for the rubidium maser [18].

Another useful expression of P is the following :

$$P = \frac{1}{2}\hbar\omega_o \frac{S}{T_1 T_2 K Q_c \cos^2\theta} = \frac{1}{8}\hbar\omega_o 3\left(\frac{T_2}{T_1}\right)\frac{S}{Q_\ell^2 K Q_c \cos^2\theta} \qquad (A.12)$$

where the expression of the saturation factor S (equation 38) has been introduced. Q_ℓ is the atomic linewidth.

Equations (A.11) and A.12) are valid for actively and passively operated masers as well.

Appendix 3

Rapid derivation of equation 52

If one admits that only the noise component $p_2 \sin\omega t$ which is in phase with the coherent excitation H_e provides amplitude noise for $\omega \neq \omega_o$ (this statement is proved in the text), one has :

$$\Delta b = \frac{\partial b}{\partial p} p_2 \qquad (A.13)$$

It then comes :

$$h_o(\text{maser}) = \frac{\left(\frac{\partial b}{\partial p}\right)^2}{2\omega_o^2 \left(\frac{1}{b}\frac{\partial b}{\partial \omega}\right)^2} S \frac{p_2}{b} \qquad (A.14)$$

One finds :

$$\left(\frac{\partial b}{\partial p}\right)^2 = \frac{(1+S)^4\left[(1+S)^2 - \alpha(2-\alpha+2S)\cos^2\theta\right]^2}{\left[(1+S)^3 - \alpha(2-\alpha+2S+\alpha S)\cos^2\theta\right]^2} \qquad (A.15)$$

One can check that equations (A.14), A.15), (49) and (7) give equation (52).

Appendix 4

Relation between S and S_o

We have :

$$S = T_1 T_2 b^2 \cos^2\theta \qquad (A.16)$$

$$S_o = T_1 T_2 b_o^2 \qquad (A.17)$$

whence

$$S = S_o \frac{G^2}{G_c^2}\cos^2\theta \qquad (A.18)$$

where G is itself a function of S given by equation (40), and G_o a function of S_o specified by equation (41). When necessary in this report, numerical values of S are obtained from S_o using i) curve c of figure 13 which provides $\cos^2\theta$ via equation (37) and ii) values of G and G_o which are given on figure 16.

References

1. K. Shimoda, T.C. Wang and C.H. Townes, Phys. Rev. 102 1308 (1956)
2. D. Kleppner, H.M. Goldenberg and N.F. Ramsey, Phys. Rev. 126 603 (1962)
3. L.S. Cutler, Ph. D. Thesis (1966) unpublished
4. J.H. Shirley, American Journal of Physics 36 949 (1968)
5. M. Têtu, Ph. D. Thesis (1972) unpublished
6. M. Têtu, G. Busca and J. Vanier, IEEE Trans. on Instr. and Meas. IM-22 250 (1973)
7. J.P. Gordon, H.J. Zeiger and C.H. Townes, Phys. Rev. 99 1264 (1955)
8. J. Hardin and J. Uebersfeld, Revue de Physique Appliquée 6 169 (1971)
9. R.F.C. Vessot, M.W. Levine and E.M. Mattison, Proc. 9th Annual PTTI 549 (1977)
10. A.Z. Grazyuk and A.N. Orayevskiy, Radio Eng. Electronic Phys. 3 424 and 443 (1964)
11. C. Audoin, Revue de Physique Appliquée 2 309 (1967)
12. M.J.E. Golay, Proc. of the IEEE 52 1311 (1964)
13. J. Viennet, C. Audoin and M. Desaintfuscien, IEEE Trans. on Instr. and Meas. IM-21 204 (1972)
14. C. Audoin, J.P. Schermann and P. Grivet *in* Advances in Atomic Physics Vol. 7 pp. 1-45 (1971)
15. S.O. Rice, Bell Tech. J. 23 282 (1944)
16. A. Papoulis *in* Probability, Random Variables and Stochastic Processes, p. 380, Mc Graw Hill (1965)
17. D. Kleppner, H.C. Berg, S.B. Crampton, N.F. Ramsey, R.F.C. Vessot, H.E. Peters and J. Vanier, Phys. Rev. A 138 972 (1965)
18. J. Vanier, Phys. Rev. 168 129 (1968)
19. A. Blaquière, Annales de Radio-Electricité 8 36 and 153 (1953)
20. S.T. Stein and J.P. Turneaure, Proc. of the 27th Annual Symposium on Frequency Control pp. 414-420 (1973)
21. C. Audoin, private communication
22. G. Busca, private communication
23. L.S. Cutler and C.L. Searle, Proc. of the IEEE 54 136 (1966)

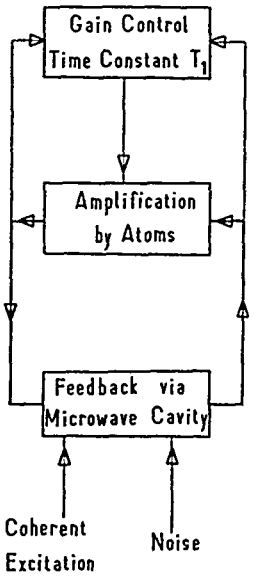

Fig.1

1 - Schematic representation of the model describing the behavior of a maser. Coherent excitation is applied to interrogate atoms in the passive mode of operation. Thermal noise in the microwave cavity can be represented by a noise generator.

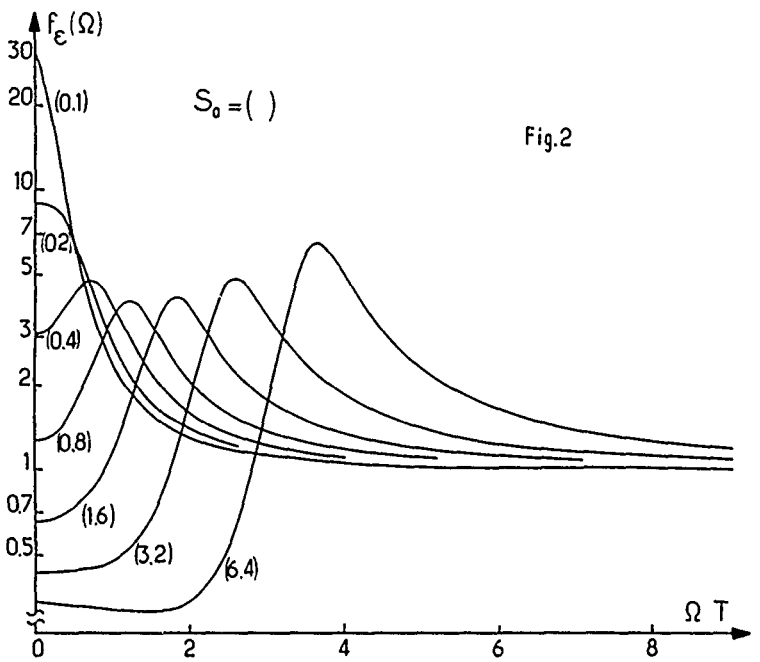

Fig.2

2 - Variation of the factor $f_\varepsilon(\Omega)$ as a function of ΩT for several values of S_o, which are specified within parenthesis.

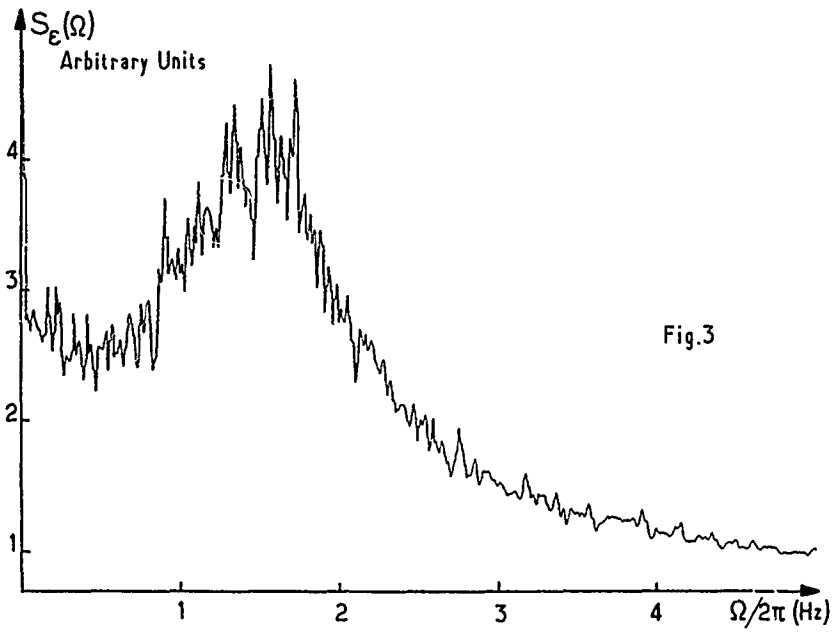

Fig.3

3 - Variation of the power spectral density of amplitude fluctuations in a hydrogen maser with Q_c = 47 000 and S_o = 0.6.

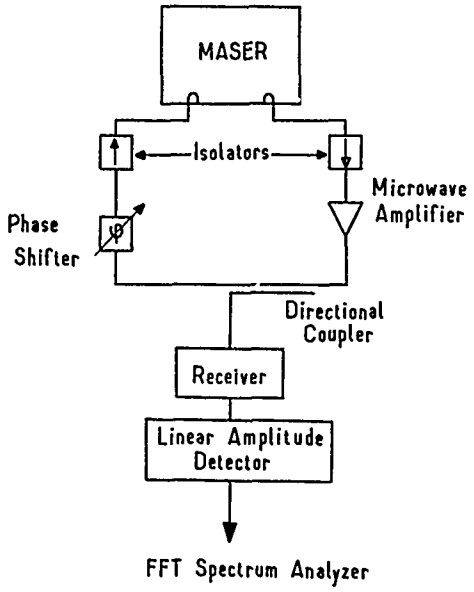

Fig.4

4 - Schematic of the feedback loop which allows to increase the quality factor of the microwave cavity, and consequently, the level of oscillation of the maser.

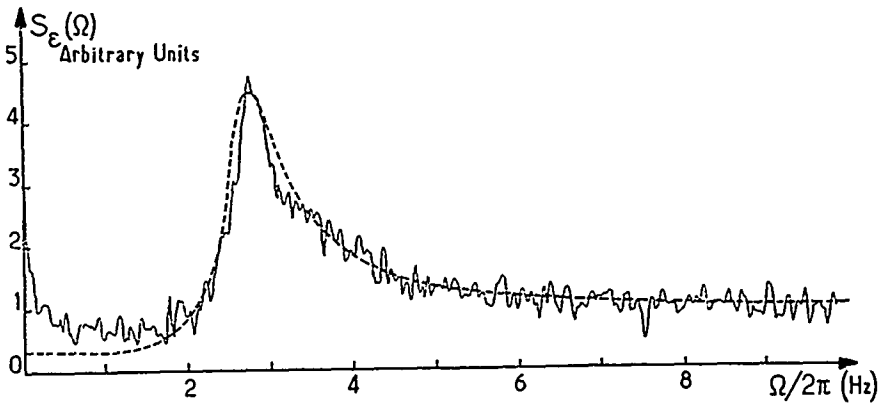

Fig.5

5 - Comparison between recorded and calculated (dotted line) spectral densities of amplitude fluctuations in an actively operated hydrogen maser.

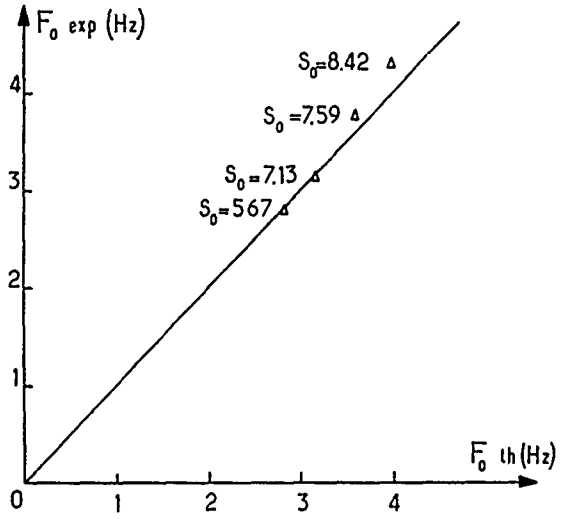

Fig.6

6 - Comparison between experimental (F_o exp) and theoretical (F_o th) frequencies of the maximum of $S_\varepsilon(\Omega)$.

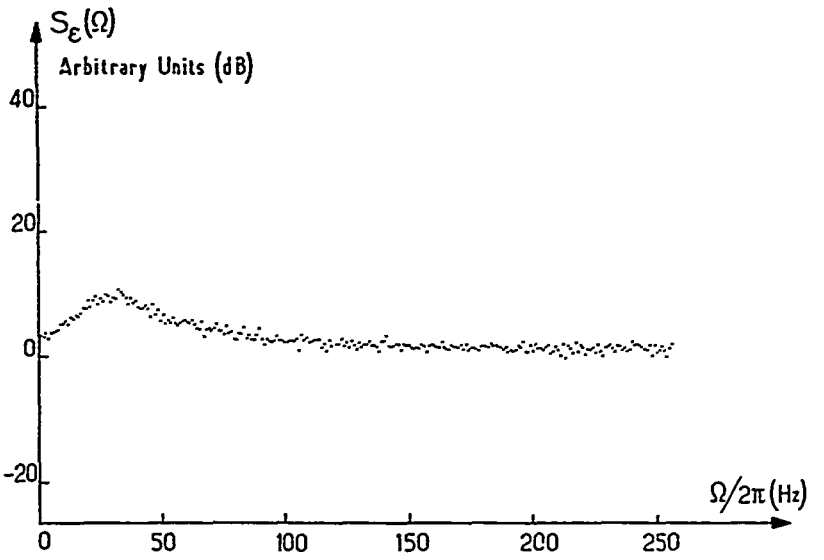

Fig.7

7 - Variation of the power spectral density of amplitude fluctuation in a rubidium maser.

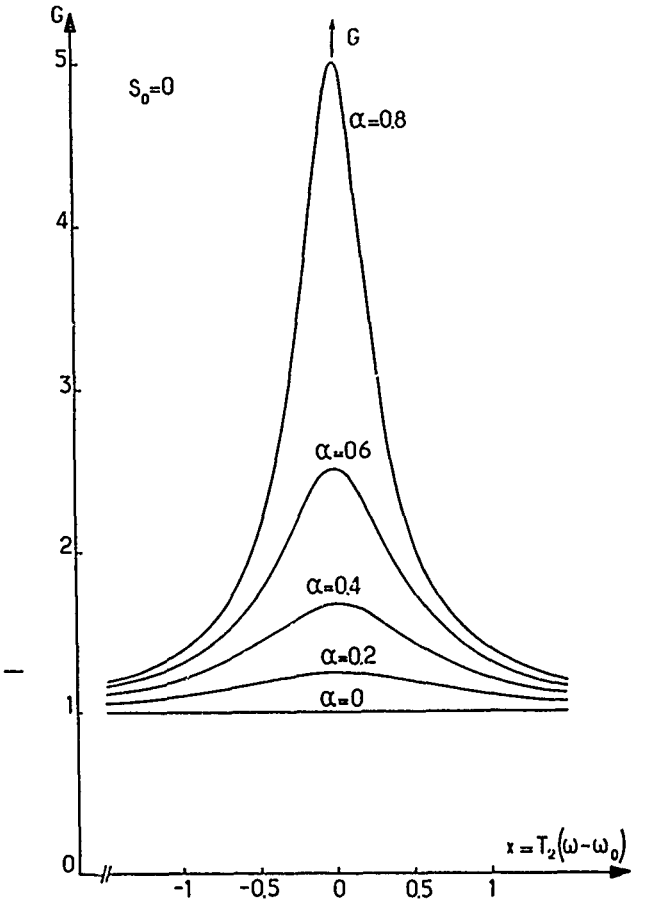

Fig.8

8 - Variation of the maser gain versus interrogating frequency for several values of α, and at negligible saturation.

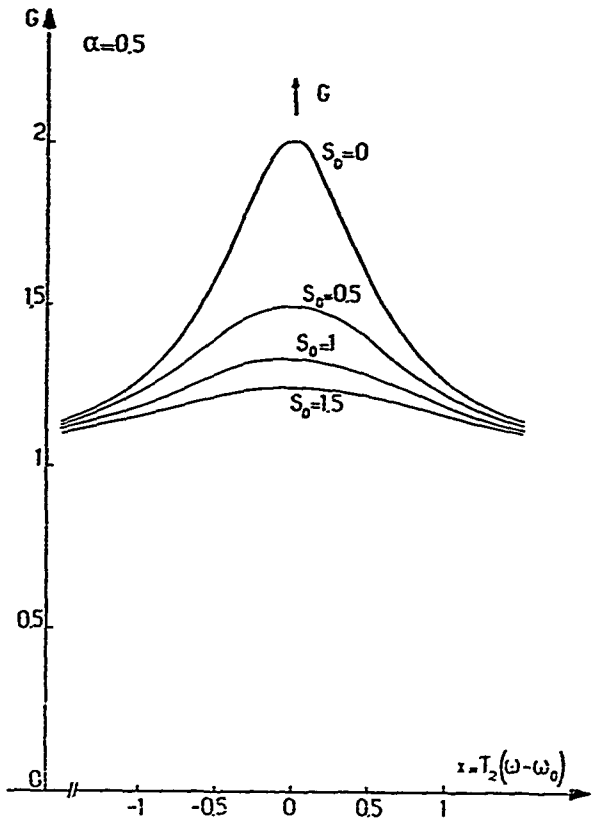

Fig.9

9 - Variation of the maser gain versus interrogating frequency for several values of the saturation parameter S_o, and for $\alpha = 0.5$

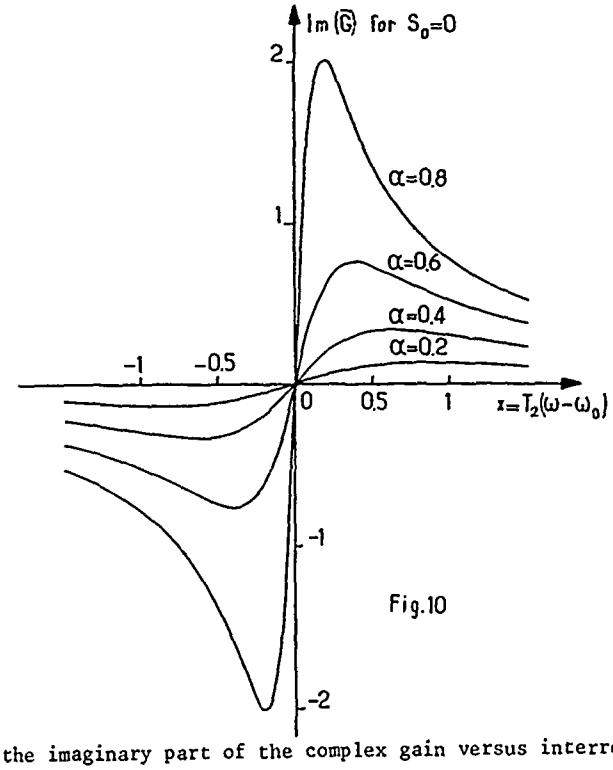

Fig.10

10 - Variation of the imaginary part of the complex gain versus interrogating frequency for several values of α, and at negligible saturation.

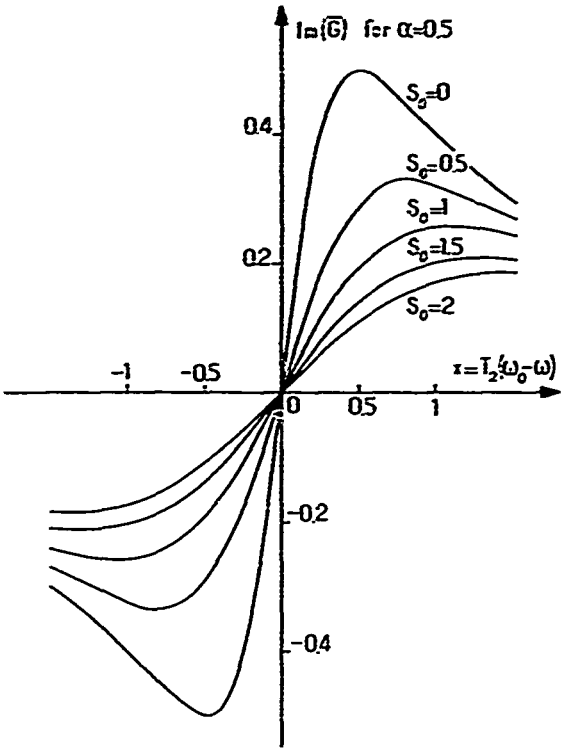

Fig.11

11 - Variation of the imaginary part of the complex gain versus interrogating frequency for several values of the saturation parameter S_0, and for $\alpha = 0.5$.

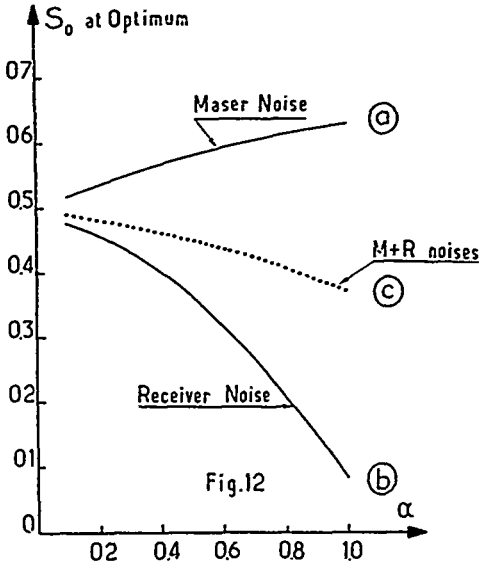

12 - Values of the saturation factor S_0 (for $\omega = \omega_0$) which optimize frequency stability in a passive maser. Frequency control via the *emission line*.

Curve a : maser noise considered alone.

Curve b : receiver noise considered alone.

Curve c : in the presence of maser and receiver noises, but with F = 2 and $Q_{ext}/Q_c = 2$.

See remark n°2 at the end of section 9.4.

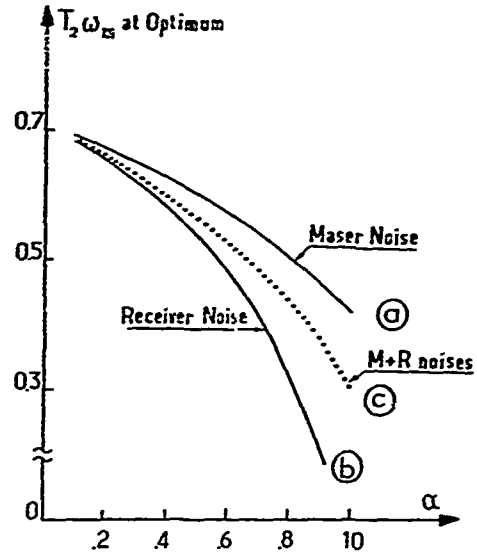

Fig.13

13 - Values of $T_2\omega_m$ which optimize frequency stability in a passively operated maser. Frequency control via the *emission line*.

Curve a : maser noise considered alone.

Curve b : receiver noise considered alone.

Curve c : in the presence of maser and receiver noises, but with $F = 2$ and $Q_{ext}/Q_c = 2$

See remark n° 2 at the end of section 9.4.

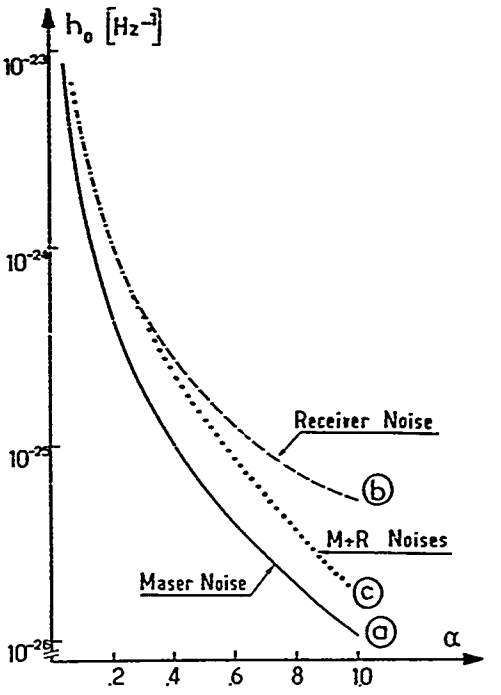

Fig.14

14 - Power spectral density of fractional frequency fluctuations h_o, for a passively operated hydrogen maser. Frequency control via the *emission line*.

Curve a : contribution of *maser noise* when operating conditions are optimized for *maser noise*.

Curve b : contribution of *receiver noise* when operating contributions are optimized for *maser noise*.

Curve c : operating contributions are optimized for maser noise *plus* receiver noise.

V_c = 15.5 dm^3 ; η = 2.8 ; Q_c = 30 000, Q_{ext} = 60 000 and F = 2.

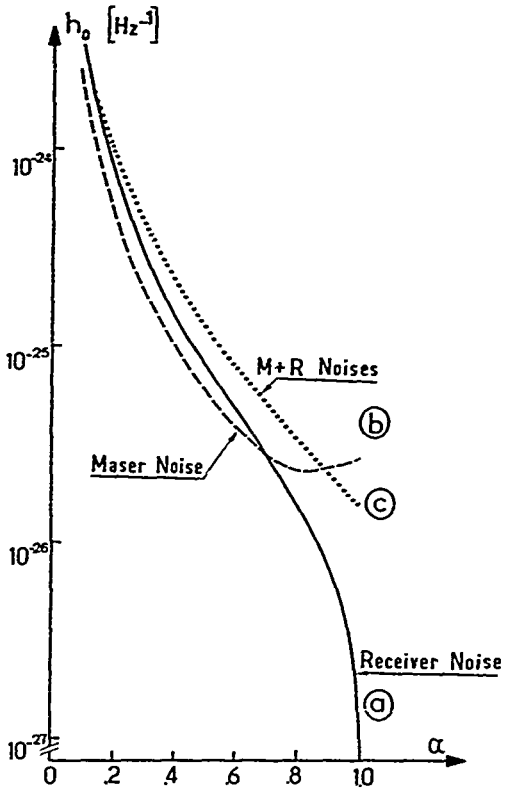

Fig.15

15 - Power spectral density of fractional frequency fluctuations h_o, for a passively operated hydrogen maser. Frequency control via the *emission line*.

Curve a : contribution of *receiver noise* when operating conditions are optimized for *receiver noise*.

Curve b : contribution of *maser noise* when operating conditions are optimized for *receiver noise*.

Curve c : operating conditions are optimized for maser noise *plus* receiver noise.

V_c = 15.5 dm^3 ; η = 2.8; Q_c = 30 000; Q_{ext} = 60 000 and F = 2

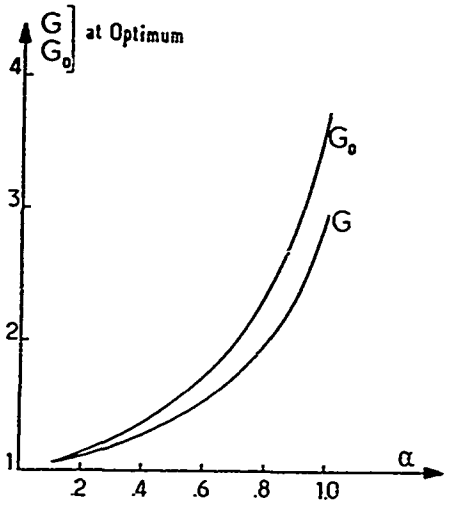

Fig.16

16 - Variation of the gains G and G_o when operating conditions are optimized for maser *plus* receiver gain in the frequency control via the *emission line*. Same data as for figures 14 and 15.

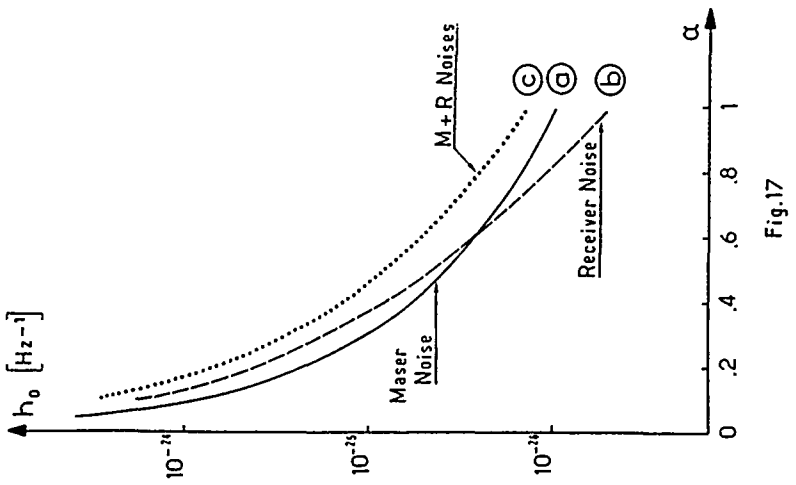

Fig.17

17 - Power spectral density of fractional frequency fluctuations h_o, for a passively operated hydrogen maser. Frequency control via the *dispersion line*.
Curve a : contribution of *maser noise* when operating conditions are optimized for *maser noise*.
Curve b : contribution of *receiver noise* when operating conditions are optimized for *maser noise*.
Curve c : operating conditions are optimized for maser noise *plus* receiver noise.
V_c = 15.5 dm^3 ; η = 2.8 ; Q_c = 30 000 ; Q_{ext} = 60 000 and F = 2.
It is assumed $2m^2 >> G_o^2$.

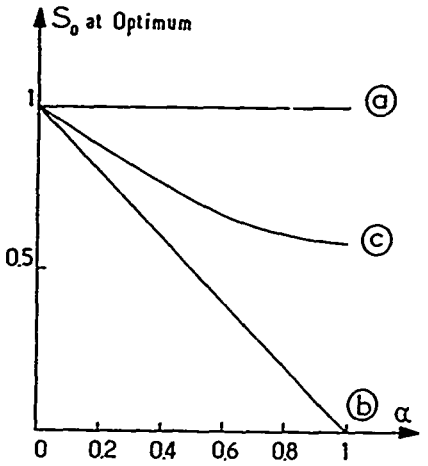

Fig.18

18 - Values of the saturation factor S_o which optimize frequency stability in a passively operated maser. Frequency control via the *dispersion line*.

Curve a : maser noise considered alone.

Curve b : receiver noise considered alone.

Curve c : in the presence of maser and receiver noises, but with F = 2 and $Q_{ext}/Q_c = 2$.

Remark n° 2 at the end of section 9.4. applies.

HYDROGEN FREQUENCY STANDARD USING FREE-INDUCTION TECHNIQUE*

Harry T.M. Wang

Hughes Research Laboratories
Malibu, California

Summary

A hydrogen frequency standard using the free-induction technique is described. The technique permits the use of compact cavities where the oscillation condition need not be met. Unlike the cw method, the atom transition frequency is measured in the absence of external stimulation leading to smaller sensitivity of cavity pulling. The technique also provides a new method of cavity tuning by varying the stimulating pulse parameters. A theory of operation and preliminary experimental results are described.

Key Words
Frequency standard, hydrogen maser, compact microwave cavity, free induction.

Introduction

The inherently excellent stability characteristics of the atomic hydrogen maser frequency standard are well known. However, the conventional maser oscillator is a relatively bulky device whose size is governed by the high-Q cavity resonating at the 21-cm maser transition frequency. There is considerable interest in a compact hydrogen frequency standard, particularly for spaceborne applications where size and weight are distinct constraints. This interest has stimulated developments in compact cavities and methods of atom interrogation. At present, the characteristics of the compact cavities are such that sustained maser oscillation has not been obtained. Some form of external excitation is therefore required for operating the compact hydrogen standard.

A method for atomic interrogation[1] is to use a phase-modulated cw test signal. The dispersive resonance signal is coherently detected. The error voltage is used to control the frequency of a crystal oscillator (VCXO) from which the test signal is synthesized. There are disadvantages to this method. Systematic errors can arise from rf excitation level variations and from drift of the phase-sensitive amplifier stages. These stringent electronics stability requirements for the cw method can be relaxed considerably with the free-induction technique described in this paper.

Principle of Operation

The operation of a hydrogen frequency standard using the free-induction technique can be summarized with the aid of Fig. 1 as follows. State-selected hydrogen atoms are confined in a storage bulb placed in a microwave cavity as in the well-known hydrogen maser oscillator. The atoms are prepared in a radiating state by a short pulse of microwave radiation at the atom transition frequency. The freely decaying atomic resonance signal, after down conversion to a convenient frequency, is counted for a predetermined number of zero crossings set by signal-to-noise and decay-rate considerations. The difference between the measured frequency and a preset value can be summed in an accumulator, the content of which is used with a digital-to-analog converter to update the frequency of the slave VCXO. Alternatively, a pulsed-phase-lock loop using digital phase comparators can be employed. In either case, the receiver must be designed with consideration given to the nature of the exponentially decaying signal as well as to the voltage transients after each repetitive rf excitation pulse. These constraints are not encountered in the cw method.

It should be noted that the responses of the atoms to pulsed and cw stimulations form a Fourier transform pair. Therefore, spectroscopic information about the atoms can be obtained by either technique. The fact that the free-induction signal is observed in the absence of a stimulating microwave radiation means that frequency shift caused by cavity detuning would be much smaller compared with a cw excited standard. The practical significance is the prospect for improved long-term stability of the standard compared with that for an oscillating maser, which is limited by drift of the cavity resonant frequency.

Theory

To understand quantitatively the effects of relaxation phenomena and the parameters of the stimulating rf pulse on the operation of the free-induction hydrogen standard, it is necessary to solve the density matrix rate equation describing the system:

$$\dot{\rho} = \dot{\rho}_{flow} + \dot{\rho}_{rf} + \dot{\rho}_{spin\ exch} + \dot{\rho}_{rel} \qquad (1)$$

*This work was supported by the Office of Naval Research under Contract N00014-78-C139, administered by the Naval Research Laboratory.

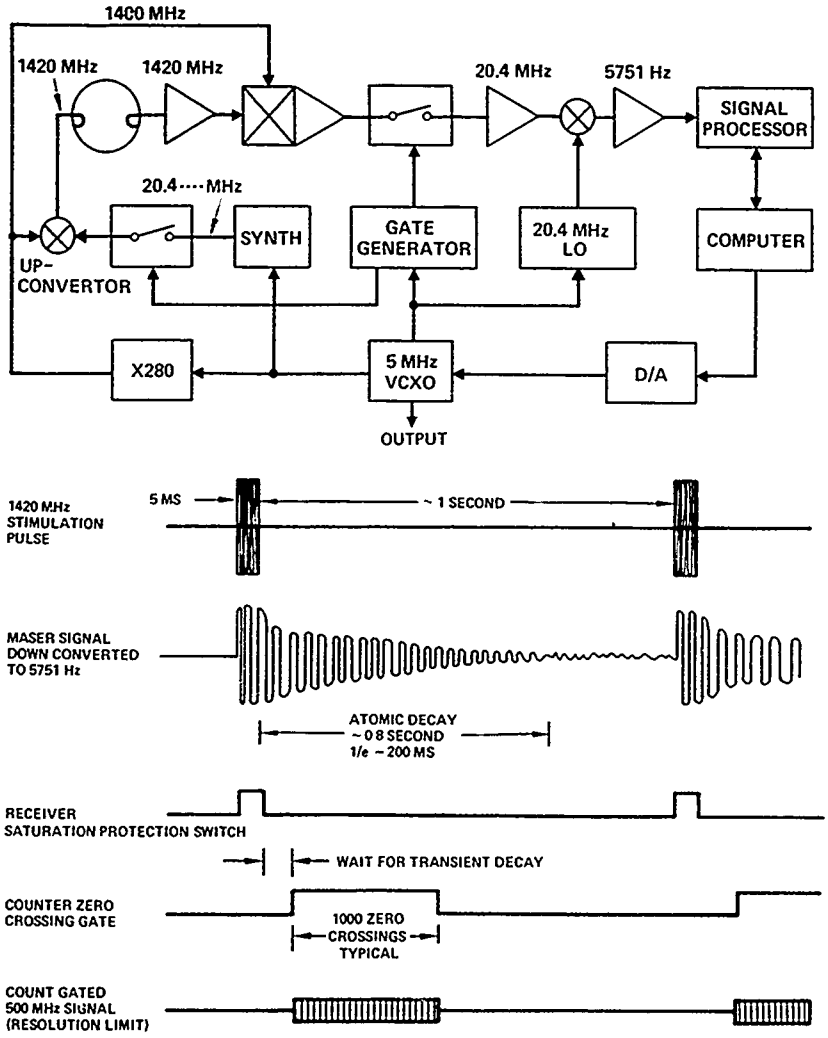

Fig. 1. Schematic of a hydrogen standard using the free-induction technique.

where ρ°_{rel} is caused by relaxation other than flow, rf and spin exchange. For the field-independent, hyperfine transition in the ground-state hydrogen atom, the transition of interest, the general Eq. (1) reduces to[2]

$$\dot{\rho}_{22} - \dot{\rho}^{\circ}_{44} = -\gamma\left[(\rho_{22} - \rho_{44}) - \frac{1}{2}\xi\right] - 2\,\mathrm{Im}\left(x^{*}\,\rho_{24}\,e^{i\omega t}\right) - \frac{1}{T_H}\left(\rho_{22} - \rho_{44}\right)$$
$$\dot{\rho}_{24} = -(\Gamma - i\omega_0)\,\rho_{24} + \frac{1}{2}ix\left(\rho_{22} - \rho_{44}\right)e^{-i\omega t} - \frac{1}{2T_H}\left[1 - i\frac{\lambda}{2\sigma}(\rho_{22} - \rho_{44})\right] \quad (2)$$

where

$$\xi = (\gamma T_g)^{-1}$$
$$\gamma = T_1^{-1} + T_g^{-1} \quad (3)$$
$$\Gamma = T_2^{-1} + T_g^{-1}$$

T_1, T_2 are longitudinal and transverse relaxation times, respectively, as a result of processes other than flow and spin exchange (such as wall collisions and magnetic gradients)

T_g = geometrical storage time

T_H = spin exchange relaxation time

$x = \frac{\mu_o H_1}{2\hbar}$ is the interaction, in frequency units, of the atomic magnetic moment μ_o with the rf magnetic field, $H_1 \cos\omega t$.

σ = H-H spin exchange cross section

λ = H-H spin exchange shift parameter

ω_o = free atom resonance frequency.

The solution of Eq. (2) is facilitated by transforming to a rotating coordinate system. Define

$$P = (\rho_{22} - \rho_{44})$$

$$\rho_{24} = (A + iB)e^{-i\omega t} \quad , \tag{4}$$

where A and B are slowly time varying complex amplitude components of the oscillating magnetic moment.

Furthermore, the power radiated by the atom is detected by the field induced in the cavity. The relationship between the oscillating moment and the induced field may be written as[3]

$$x \equiv 2K(\alpha + i\beta) \tag{5}$$

with

$$\alpha = B\cos\phi + A\sin\phi$$

$$\beta = -A\cos\phi + B\sin\phi$$

$$\tan\phi = \frac{2Q}{\omega}(\omega - \omega_c) \tag{6}$$

$$K = \frac{\pi\mu_o^2\eta Q T_g}{V_c\hbar} I \tag{7}$$

where η, Q are the filling and quality factors, respectively, of the microwave cavity of volume V_c, and I is the total flux of atoms into the storage bulb. Substituting Eq. (4) through (6) in (2) gives

$$\dot{P} = \gamma\left[\frac{\xi}{2} - \left(1 + \frac{1}{\gamma T_H}\right)P\right] - 4K(A^2 + B^2)\cos\phi$$

$$\dot{A} = -\left(\Gamma + \frac{1}{2T_H} - KP\cos\phi\right)A - \left(\delta + \frac{\lambda}{4\sigma T_H}P + KP\sin\phi\right)B \tag{8}$$

$$\dot{B} = -\left(\Gamma + \frac{1}{2T_H} - KP\cos\phi\right)B + \left(\delta + \frac{\lambda}{4\sigma T_H}P + KP\sin\phi\right)A \quad , \tag{8}$$

where $\delta = \omega - \omega_o$.

The experimentally observed quantitites are the "polarization," P, and the "magnetization," M. If we define

$$M \equiv \sqrt{A^2 + B^2}\; e^{i\psi} \tag{9}$$

where $\tan\psi = A/B$, Eq. (8) can be rewritten as

$$\dot{P} = \gamma\left[\frac{\xi}{2} - \left(1 + \frac{1}{\gamma T_H}\right)P\right] - 4KM^2\cos\phi$$

$$\dot{M} = -\left(\Gamma + \frac{1}{2T_H} - KP\cos\phi\right)M$$

$$\dot{\psi} = -\left(\delta + \frac{\lambda}{4\sigma T_H}P + KP\sin\phi\right) \quad . \tag{10}$$

The solution of the nonlinear Eq. (10) with appropriate initial conditions describes the operation of the device. However, the nonlinearity makes a general solution in closed form impossible to obtain. Approximate solution in the special case where the device is operated well below the threshold of oscillation will provide significant physical insight.

Initial Conditions

The atoms are prepared in the radiating state by a short pulse of resonant radiation of duration τ applied at time $t = -\tau$. During the pulse, we have

$$x >> \gamma,\ \Gamma,\ \frac{1}{T_H} \quad , \tag{11}$$

and since the stimulating microwave signal can have arbitrary phase, x is taken to be real. If we also assume that the period between pulses, T, is long compared with all relaxation times and precedes the pulse, the system has reached flow equilibrium so that

$$A(-\tau) = B(-\tau) = 0$$

$$P(-\tau) = \frac{\gamma\xi/2}{\gamma + \frac{1}{T_H}} = \xi_o \quad . \tag{12}$$

Then, the solutions of Eq. (8) give the initial conditions

$$P(0) = \frac{\xi_o}{a^2}\,(\delta^2 + x^2 \cos a\tau)$$

$$A(0) = \frac{\xi_o}{2a^2}\,\delta \times (1 - \cos a\tau)$$

$$B(0) = \xi_o \frac{x}{2a} \sin a\tau \quad , \qquad (13)$$

where $a^2 = \delta^2 + x^2$.

Note that at the end of the stimulating pulse, the power radiated by the atoms is proportional to

$$M^2(0) = A^2(0) + B^2(0)$$

$$= \left(\frac{\xi_o}{2}\right)^2 \left(\frac{x}{a}\right)^2 \left[\left(\frac{\delta}{a}\right)^2 (1 - \cos a\tau)^2 + \sin^2 a\tau\right] . \qquad (14)$$

The signal is optimized if the rf frequency is exactly on resonance (i.e., $\delta = 0$) and the pulse amplitude, x, and duration, τ, are adjusted so that $x\tau = \pi/2$.

Low Flux Solution

In the limit of low flux where the device is operated well below threshold for oscillation, the effect of radiation damping can be neglected. In other words, the power feedback factor K is negligible compared with the relaxation rates (including spin exchange collisions) $\gamma' = \gamma + (1/T_H)$ and $\Gamma' = \Gamma + (i/2T_H)$. In this limit, Eq. (10) can be rewritten as

$$\dot{P} = \gamma'(\xi_o - P)$$
$$\dot{M} = \Gamma' M \quad . \qquad (15)$$

The solution, using initial conditions given by Eq. (13), is

$$P(t) = \xi_o \left[1 - \left(1 - \frac{\delta^2 + x^2 \cos a\tau}{a^2}\right) e^{-\gamma' t}\right]$$

$$M(t) = \xi_o \frac{x}{2a} \left[\left(\frac{\delta}{a}\right)^2 (1 - \cos a\tau)^2 + \sin^2 a\tau\right]^{1/2} e^{-\Gamma' t} \qquad (16)$$

For optimized pulse parameters ($\delta = 0$ and $x\tau = \pi/2$), these solutions are simple exponentials. The polarization and the magnetization approach their equilibrium values at rates governed by the longitudinal and transverse relaxation rates, respectively, as expected.

Cavity Pulling

After the stimulating pulse, although the atoms radiate freely, the resonance is detected through the induced electromagnetic field in the cavity. In the rotating reference frame, the resonance condition requires that the phase of the magnetization, ψ, be stationary;

$$\dot{\psi} = 0 \quad .$$

From Eq. (10), this condition leads to the cavity-pulling relation

$$\delta = KP \left(-\sin\phi - \frac{m\lambda}{4\sigma}\right) ,$$

where

$$m = \frac{1}{T_H K} = \frac{v_c \bar{\nu} \sigma h}{\pi \eta Q \mu_o^2 v_b}$$

$\bar{\nu}$ = relative velocity of colliding atoms

v_c, v_b = volume of microwave cavity and storage bulb.

For small cavity detuning,

$$\sin\phi \simeq \tan\phi \simeq \frac{2Q}{\omega_o}(\omega_o - \omega_c) \quad .$$

It should be noted that, in the free-induction case, the polarization, P(t), is a function of time. The cavity pulling, therefore, depends on the interval during which a measurement is made. The average cavity pulling during an interval (t_1, t_2) after a stimulating pulse can be written as

$$\bar{\delta} \simeq K\left[\frac{2Q}{\omega_o}(\omega_c - \omega_o) - \frac{m\lambda}{4\sigma}\right] \frac{1}{t_2 - t_1} \int_{t_1}^{t_2} P(t)dt \quad . \qquad (18)$$

If we use the low flux solution (16) for P(t) with resonant radiation, $\delta = 0$, Eq. (18) becomes

$$\bar{\delta} = \left[\frac{2Q}{\omega_o}(\omega_c - \omega_o) - \frac{m\lambda}{4\sigma}\right] K\xi_o \left[1 - (1 - \cos\theta) \frac{e^{-\gamma' t_1} - e^{-\gamma' t_2}}{\gamma'(t_2 - t_1)}\right] \quad . \qquad (19)$$

This is to be compared with the cavity-pulling

relation for an oscillating maser

$$\dot{\delta}_{osc} = \left[\frac{2Q}{\omega_o}(\omega_c - \omega_o) - \frac{m\lambda}{4\sigma}\right]\Gamma' \quad . \quad (20)$$

For the free-induction case, signal-to-noise considerations dictate that a frequency measurement be made in an interval so that $\gamma' t_2 \leq 1$. It can also be shown that below the threshold flux for oscillation $K\xi_o < \Gamma'$. From Eqs. (19) and (20) we have

$$\overline{\delta}_{F.I.} \leq \frac{1}{2}\,\delta_{osc} \quad .$$

Equation (19) also shows that the conventional flux-modulated spin-exchange cavity-tuning procedure can still be applied in the free-induction case. In addition, a new method of cavity tuning, by varying the pulse parameter such as the rf level, is indicated. This method varies the angular deflection θ of the atomic spin, which for resonant-stimulating radiation is given by the product of the Z-component rf field amplitude x and the pulse duration τ.

Note that by proper choice of pulse parameters and measurement interval, the second bracketed term of Eq. (19) can be made to vanish, thus eliminating the effect of cavity pulling. However, the burden is shifted to keeping the pulse parameters constant. Conversely, when the cavity is spin exchange tuned, variations in pulse parameters do not cause a frequency shift.

Preliminary Experimental Test

Experimental test of the free-induction technique had been conducted on a test bed maser using compact cavities described in a separate paper in this symposium.[4] Storage bulbs of various dimensions and coatings designed to fit specific cavities under test had been used. Most of the data, however, were taken with a 3-in. i.d. by 4-in.-long quartz cylindrical bulb coated with FEP Teflon by a conventional technique.

The synthesized rf test signal was gated on and off periodically using a pair of diode switches connected in series to provide isolation of about 100 dB. The switches were driven by a timing oscillator with adjustable repetition rate and pulse duration. A variable delayed output was also provided to activate the zero crossing counter that determined the atom transition frequency. This delay ensured that the switching transients did not interfere with the resonance frequency measurement. The rf pulse width was typically about 5 msec and off for about three signal decay time constants. The free-induction atomic signal was down converted to 5.751 kHz and then amplified in a bandpass filter with a 3-dB bandwidth of ~600 Hz. This relatively large receiver bandwidth was designed to improve its transient response. The time interval for a predetermined number of zero crossings was measured in an averaging time-interval counter for multiple pulse measurement. The counter output was inverted to give the atom transition frequency. All reference frequencies were derived from an oscillating hydrogen maser.

During this initial experimental test, no attempt was made to close the phase lock loop to obtain an operating frequency standard. The attention was focused on the physics of the devices as discussed in the previous section.

In an earlier experiment, a 2-in. i.d. by 4-in.-long cylindrical storage bulb was used. The free-induction signal decay time was limited to less than 100 msec and the signal-to-noise ratio was not satisfactory. Nevertheless, the equivalence of free-induction and cw techniques was demonstrated as shown in Fig. 2. The exponentially decaying free-induction signal input to a fast Fourier transform analyzer is shown on the left and the Lorentzian output on the right. The signal-to-noise ratio improved significantly with multiple pulse averaging. Unfortunately, the FET analyzers on the market do not have the desired frequency resolution capability within the limited measurement time window.

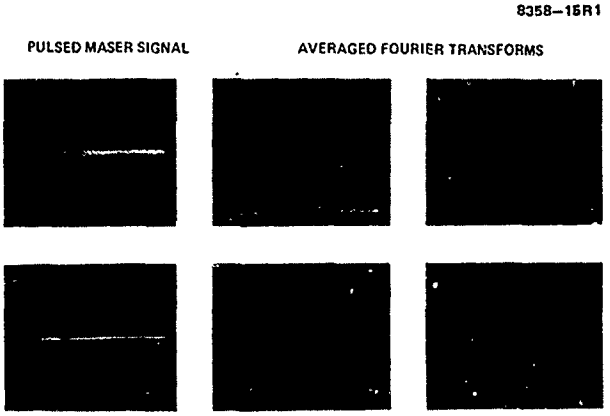

Fig. 2. Lorentzian lineshape of a fast-Fourier-transformed free-induction signal.

The improved signal decay time obtained with a 3-in. i.d. x 4-in.-long cylindrical quartz bulb permits quantitative frequency measurements to be made. Figure 3 shows an oscilloscope display of the down converted 5.75 kHz free-induction signal. The lower trace shows the input to the time interval counter for 1,000 zero crossings. The bulb was designed to have a storage time of 0.28 sec. The observed signal decay time was typically 0.18 sec, as shown, and, of course, is a function of the flux level. The resonance frequency monitored over a period of several hours is shown in Fig. 4. The time interval counter was set at 100 sec gate time. Since the duty cycle (time for 1,000 signal zero crossings divided by pulse spacing) was only 33%, the total elapsed time was 300 sec for each counter reading; 5 readings were taken to compute the statistics of each indicated point.

Figure 5 shows the measured resonance frequency against the cavity frequency. The dotted

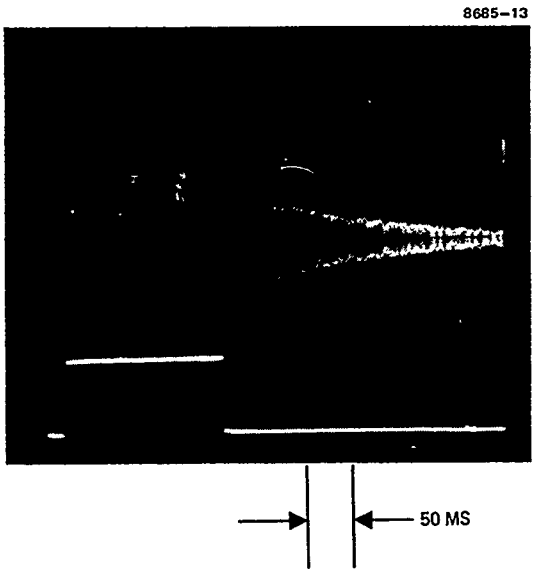

Fig. 3. Free-induction signal with input to the average time interval counter shown in the lower trace.

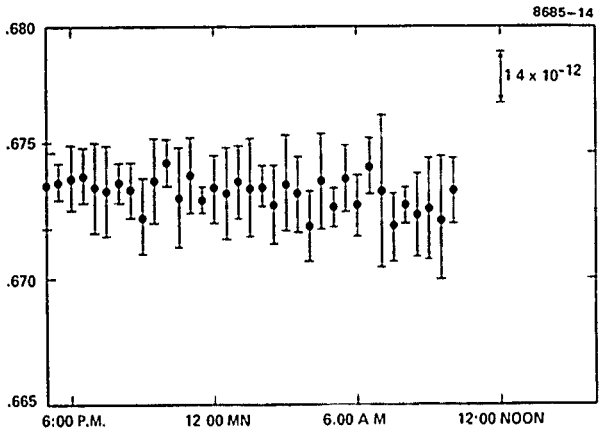

Fig. 4. Free-induction signal frequency monitored over an interval of several hours.

line represents the expected cavity-dependent shift if sustained oscillation were obtained in the same cavity (Q = 7,000) with the same transition linewidth. As expected, the slope for the free-induction technique is substantially smaller.

Finally, the dependence of cavity shift on the stimulating rf power level is shown in Fig. 6. For this measurement, the cavity was purposely offset by amounts equal to ±10% of its half-power bandwidth. The fluctuation of the measured frequency was correspondingly higher as a result of the sensitivity to flux variations. A third case where the cavity is approximately tuned (at varactor bias of 7.5 V) is also shown. The qualitative agreement with theory is very good.

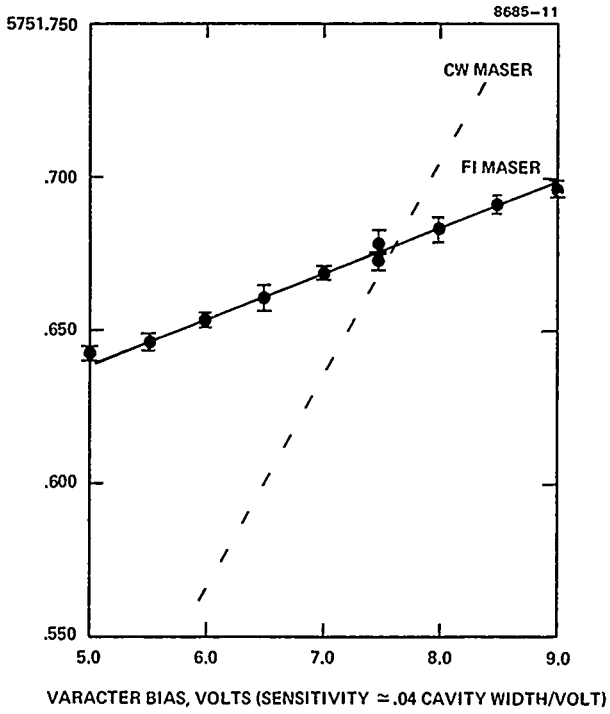

Fig. 5. Atom transition frequency versus cavity resonance frequency. Dotted line is expected cavity shift for an oscillating maser using the same cavity.

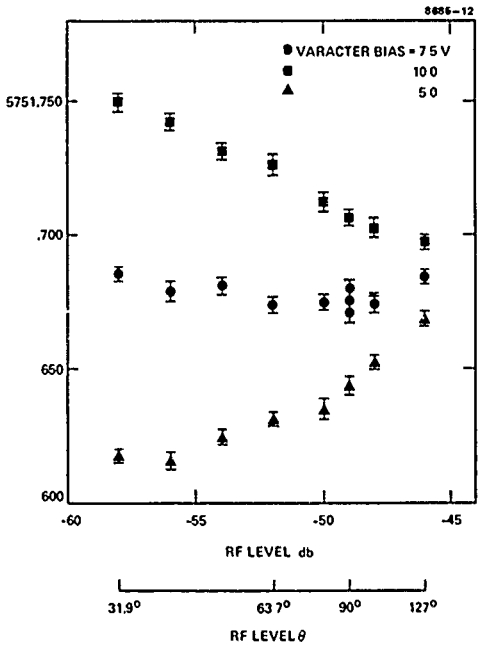

Fig. 6. Cavity shift versus rf pulse level. Cavity was purposely offset by about one-tenth cavity width for varactor biases of 5 and 10 V. The cavity was approximately tuned at a varactor bias of 7.5 V.

Conclusion

These initial results of the compact hydrogen standard using the free-induction technique are encouraging. Although significant developmental work needs to be done, particularly in the area of signal processing and frequency determination, the results indicate the feasibility of a compact hydrogen standard with excellent long-term stability.

References

1. F.L. Walls, and D.A. Howe, Proc. 32nd Annual Symposium on Frequency Control, 1978, pp. 492-498.

2. S.B. Crampton, Phys. Rev. 158, 57 (1967).

3. P.F. Winkler, D. Kleppner, T. Myint, and F.G. Walther, Phys. Rev. A5, 83 (1972).

4. H.T.M. Wang, J.B. Lewis and S.B. Crampton, "Compact Cavity for Hydrogen Frequency Standard" (these proceedings).

Compact Cavity for Hydrogen Frequency Standard*

H.T.M. Wang and J.B. Lewis
Hughes Research Laboratories
Malibu, California

and

S.B. Crampton
Department of Physics, Williams College
Williamstown, Massachusetts

Summary

Progress in the development of a compact and light weight cavity resonating at 1,420 MHz for use in hydrogen frequency standards is reported. Features of the cavity include reasonably high Q, a good filling factor, and the flexibility of trading off the desired degree of compactness for cavity performance parameters. Design theory and experimental tests, including tests for maser action, are described.

Key Words
Frequency standard, hydrogen maser, microwave cavity.

Introduction

This paper reports on the progress in the development of a compact and light weight cavity resonating at 1,420 MHz for use in hydrogen frequency standards. The work was motivated by interest in a compact hydrogen standard: the size and weight of the conventional maser is limited by the high-Q microwave cavity. Crampton[1] has constructed a compact cavity for spectroscopic studies at cryogenic temperatures. The design was based on the empirically successful magnetron resonator theory.[2]

We have adopted that design as a prototype and have conducted further development to make it more suitable for applications in hydrogen frequency standards. In addition to reasonably high Q and good filling factor, the design allows the flexibility of trading off the desired degree of compactness for cavity performance parameters.

An independent design study with a different approach by Peters[3] produced a design that has many similarities to the cavities discussed in this paper. However, there are also significant differences since they are based on very different design equations. Another way to reduce the size of the cavity is by capacitive loading using materials with high dielectric constants and low loss tangents to fill all or part of the volume of the cavity not occupied by the experimental medium. This technique has been successfully applied with sapphire** as the loading material. The relatively high Q obtained with this technique is counterbalanced by its relatively high temperature coefficient of resonant frequency and its weight. Moreover, material limitations may make it difficult to scale up the useful volume for atomic hydrogen storage. Thus, wall collision relaxation may severely limit the atomic transition linewidth and, consequently, the performance of the standard.

In this paper, we outline a theory for designing compact cavities for hydrogen frequency standard applications. The experimental verification of the theory on a prototype cavity is described, followed by test results of an empirical extension to more complicated geometry and larger hydrogen atom storage volume.

Design Theory

The atomic hydrogen frequency standards operate on the field-independent hyperfine transition in the ground-state hydrogen atom. The transition is coupled to an rf magnetic field parallel to the axis of quantization, and preferably there is no axial variation of the field over the experimental volume. Conventionally, a high-Q cylindrical TE_{011} mode cavity is used to produce the desired field configuration. On the other hand, this field configuration can also be produced in a cavity of the geometry shown schematically in Fig. 1. It consists of a closed metal cylindrical shell of inner diameter 2c and length h enclosing an inner concentric metal cylinder of the same length. This inner cylindrical capacitor is 2b o.d. by 2a i.d. with N slots (N = 4 in the illustration) of width d each milled along the length of the cylinder. The cacpacitance may be increased by filling the slots with a dielectric of thickness ℓ. The material is chosen to have a high dielectric constant and a low loss tangent. Two rf magnetic field lines are also indicated.

A rigourous solution to the Maxwell equations for this complicated geometry is hard to obtain.

*This work has been supported by the Office of Naval Research under Contract N00014-78-0139, administered by the Naval Research Laboratory.

**R. Easton and his coworkers at the U.S. Naval Research Laboratory have designed and fabricated several sapphire-loaded cavities. They have kindly supplied us with one for experimentation.

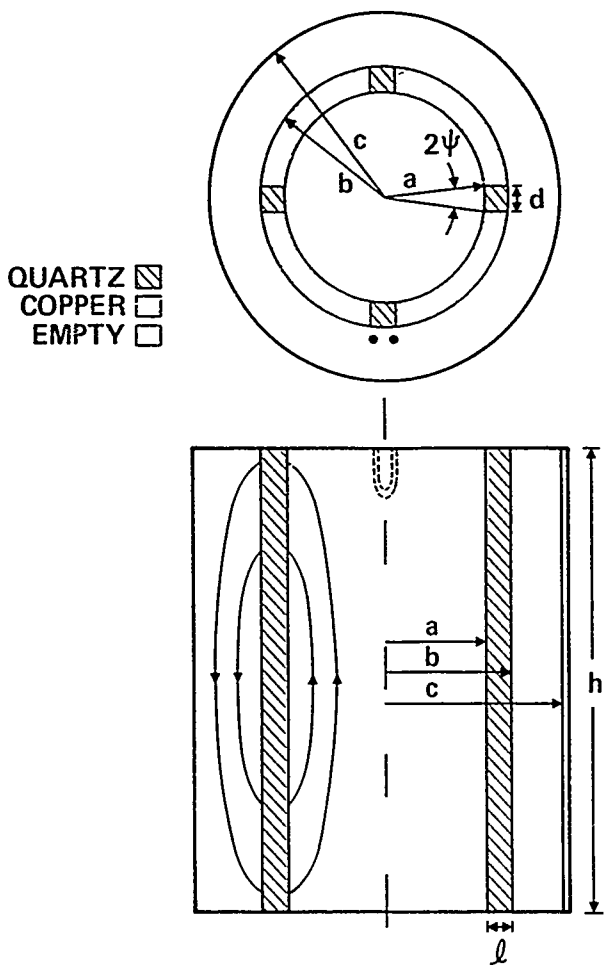

Fig. 1. Schematics of a cavity to generate field configuration similar to a TE_{011} mode field configuration.

However, the empirically successful magnetron resonator theory[2] has shown that field distributions could be approximately matched from one simple geometry to another by matching the complex admittances

$$Y = \frac{h\int_A^B \vec{E} \times \vec{H} \cdot \vec{n}\,dS}{\left|\int_A^B \vec{E} \cdot d\vec{S}\right|^2}, \qquad (1)$$

where the path of integration AB and the length h form a surface connecting the two simple geometries, and $\vec{n}$ is the normal to that surface. The match consists of calculating Y for the field $\vec{E}$ and $\vec{H}$ for each of the two simple geometries separately and then adjusting the parameters so that the two admittances are equal. The weakness of the method is that it requires that the configuration of fields along the path AB be assumed. For example, for the geometry shown in Fig. 1, the electric field in the interior region r < a is chosen to be a superposition of TE_{p11} modes with coefficients so that the electric field has a constant value E along the dielectric surface at r = a and zero along the metal surface at r = a. The electric field in each slot is assumed to be the lowest-order TE rectangular waveguide mode having electric field amplitude E at the (inner) entrance to the slot. With this choice of electric field along the surfaces bounding the two regions, the continuity of the tangential components of the electric fields across that surface is assured. Because the constant electric field along that surface is not an exact solution of the Maxwell equations for that geometry, the magnetic fields determined by the choice of constant electric field across the surface are not continuous but match up only on the average when the admittance match is satisfied. The simple theory is useful as a starting point for empirical design improvements or more sophisticated computer modeling studies.

With the preceding remarks in mind, the electric and magnetic fields in the interior region r < a can be written in the form

$$E_\phi^{in} = \frac{NE\psi}{\pi} \sum_{p=-\infty}^{\infty} \left(\frac{\sin pN\psi}{pN\psi}\right) \frac{J'_{pN}(kr)e^{jpN\phi}}{J'_{pN}(ka)} \sin\frac{\pi Z}{h}$$

$$H_Z^{in} = -j\frac{k}{\mu_o\omega}\frac{NE\psi}{\pi} \sum_{p=-\infty}^{\infty} \left(\frac{\sin pN\psi}{pN\psi}\right) \frac{J_{pN}(kr)e^{jpN\phi}}{J'_{pN}(ka)} \sin\frac{\pi Z}{h}, \qquad (2)$$

where $J_{pN}(kr)$ is the pN^{th}-order Bessel function of argument kr, and $J'_{pN}(kr)$ is its derivative with respect to its argument. The vacuum radial wave vector k satisfies the relation

$$\left(\frac{\omega_o}{v}\right)^2 = k^2 + \left(\frac{\pi}{h}\right)^2 \qquad (3)$$

where v is the velocity of light, and ω_o is the cavity resonant frequency. Using Eqs. (1) and (2), we obtain the admittance at the slot entrance at r = a:

$$Y_{in} = -j\frac{k}{\mu_o\omega}\frac{Nh}{2\pi a}\left[\frac{J_o(ka)}{J_1(ka)} - 2\sum_{p=1}^{\infty}\left(\frac{\sin pN\psi}{pN\psi}\right)^2 \frac{J_{pN}(ka)}{J'_{pN}(ka)}\right]. \qquad (4)$$

Exterior to the slots, the electric field is zero at r = b at the metal surfaces and also at r = c. It is assumed to have a constant value e at the dielectric surfaces at r = b. The exterior electric field can be written in the form

$$E_{\phi}^{out} = \frac{Ne\theta}{\pi} \sum_{p=-\infty}^{\infty} \left(\frac{\sin pN\theta}{pN\theta}\right) \frac{Z'_{pN}(kr)e^{jpN\phi}}{Z'_{pN}(kb)} \sin \frac{\pi z}{h} , \quad (5)$$

where

$$\sin \theta = \frac{d}{2b}$$

$$Z_{pN}(kr) = J_{pN}(kr) - \frac{J'_{pN}(kc)}{N'_{pN}(kc)} N_{pN}(kr)$$

and $N_{pN}(kr)$ are Bessel functions that are irregular at the origin. The admittance at the slot exit at r = b is

$$Y_{out} = -j \frac{k}{\mu_o \omega} \frac{Nh}{2\pi b} \left[\frac{Z_o(kb)}{Z'_o(kb)} + 2 \sum_{p=1}^{\infty} \left(\frac{\sin pN\theta}{pN\theta}\right)^2 \frac{Z_{pN}(kb)}{Z'_{pN}(kb)} \right] . \quad (6)$$

The fields in the slots are determined by assuming that the distribution is the lowest-order TE rectangular waveguide mode. The electric field is assumed to have a value E at the interior entrance and a value e at the exterior exit of each slot. The effects of matching to the slot fields can be understood as transforming the impedance at one end of the slot to its value at the other end. The overall admittance match becomes

$$-Y_{in} = j \frac{h}{d} \frac{K}{\mu_o \omega} \frac{\sin K\ell + \frac{d}{h} \frac{\mu_o \omega}{jK} \cos K\ell \cdot Y_{out}}{\cos K\ell - \frac{d}{h} \frac{\mu_o \omega}{jK} \sin K\ell \cdot Y_{out}} , \quad (7)$$

where the radial wave vector K in the slots is given by

$$K^2 = \frac{\varepsilon}{\varepsilon_o} \left(\frac{\omega}{v}\right)^2 - \left(\frac{\pi}{h}\right)^2 , \quad (8)$$

and $\varepsilon/\varepsilon_o$ is the dielectric constant of the material filling the slots.

Finally, the Q and the fill factor η' can be computed from the equations

$$Q = \frac{2}{\delta \mu_o} \frac{\int \varepsilon E^2 \, dV_c}{\int \left|H_\perp\right|^2 dS}$$

and

$$\eta' Q = \frac{2}{\delta} \cdot \frac{\frac{1}{V_b}\left(\int H_z dV_b\right)^2}{\int \left|H_\perp\right|^2 dS} , \quad (9)$$

where δ is the skin depth of the metal. The surface integral is performed over all metal surfaces in the cavity of volume V_c containing an atom storage region of volume V_b.

The Prototype Cavity

From the previous section, it is seen that H_z in the interior region r < a is a superposition of the TE_{p11} modes in which the relative contribution of higher (non-zero p) modes is quadratic in ka. Since the higher modes add nothing to the filling factor of an azimuthally symmetric storage volume but do contribute to ohmic losses at the cavity walls, $\eta'Q$ is degraded as ka becomes greater than about one-third. Thus it is advantageous to keep k small, and from Eq. (3), this can be done by choosing the length h so that π/h is slightly less than ω_o/v. In the small k limit, the matching condition expressed by Eq. (7) becomes

$$\frac{N}{\pi a^2}\left[1 - \frac{k^2a^2}{8} - \frac{k^2a^2}{N}\left\{\frac{3}{2} - \ell n\, 2N\psi + \frac{N^2\psi^2}{36}\right\}\right] \approx \frac{K}{d} \frac{\pi K(c^2 - b^2)\tan K\ell - Nd(1-\xi)}{\pi K(c^2 - b^2) + Nd(1-\xi)\tan K\ell} \quad (10)$$

where

$$\xi = \frac{2K^2(c^2 - b^2)(c^{2N} + b^{2N})}{N(c^{2N} - b^{2N})} .$$

The approximate expressions for the Q and the filling factor η' are

$$Q \simeq \frac{N\frac{\varepsilon}{\varepsilon_0}\ell d + \left(\frac{N\psi}{\pi}\right)^2 \pi a^2 \left[1 + \frac{4}{N}\left(\frac{3}{2} + \ell n 2N\psi\right)\right]}{\delta D}$$

$$\eta' Q \simeq \frac{10h^2\left(\frac{N\psi}{\pi^2}\right)^2}{\delta D} \quad (11)$$

where

$$D \simeq N\ell\left[1 + d\frac{\varepsilon}{\varepsilon_0}\frac{\tan\delta}{\delta}\right] + \left\{aN\psi + \frac{a}{\pi}\left(\frac{2hN\psi}{\pi a}\right)^2 \left[1 + \frac{a^3 b}{(c^2 - b^2)^2}\right]\right\}\left(1 - \frac{N\psi}{\pi}\right) ,$$

and $\tan\delta$ is the dielectric loss tangent.

For the prototype cavity, the parameters were chosen to satisfy Eq. (10). The ratio of the length ℓ to the width d of each slot was fixed at roughly equality by the boundary condition. The width was made as large as it was to hold down ohmic losses. The number of slots was chosen to be four instead of one so that each slot would be about one-fourth as wide and the theoretical prediction of the resonant frequency would be more reliable. Higher order mode ohmic losses would also be less because there were one-fourth as many higher modes. Quartz rods were used to fill the slots because of their relatively low-loss tangent and availability. Figure 2 is a photograph of the prototype cavity. The design parameters, as well as the measured resonant frequency and loaded Q, are given in Table 1. In view of fabrication tolerances and sensitivity to imperfections in the quartz rods, the agreement between theory and experiment is very good.

8685-26

Figure 2. Prototype compact cavity.

Table 1. Parameters of Prototype Cavity

8685-27

DESIGN FREQUENCY:	1420 MHz
OUTER CYLINDER (2c x h):	3 625 IN x 4.50 IN.
CYLINDRICAL CAPACITOR	
(2a x 2b x h) COMPUTED:	2 054 IN. x 2.577 IN. x 4 50 IN.
ACTUAL:	2 060 IN. x 2.562 IN. x 4 50 IN.
SLOT (ℓ x d x h)/N:	0 250 IN. x 0 250 IN. x 4 50 IN./4
DIELECTRIC:	CLEAR FUSED QUARTZ
QUALITY FACTOR, Q	
COMPUTED (UNLOADED):	4200
MEASURED (2 PORT COUPLED):	3200
FILLING FACTOR, η' (COMPUTED):	.43

Empirical Extension

The observed Q of the prototype cavity is dominated by losses in the slots and on the surfaces. Slot losses occur when the cylindrical capacitor runs the full length of the cavity and the continuity of the rf magnetic field lines requires the field lines to squeeze through the slots. The resultant high-current density leads to proportionally larger ohmic loss. However, if the cylindrical capacitor ran only part of the length of the cavity, the field lines could close by going around its ends thus reducing the losses in the slots. Surface losses can be reduced by reducing the outside diameter of the cylindrical capacitor except at the boundries of the slots. Thus, a four-slot cylindrical capacitor could be fabricated from four equally spaced segments. Each segment is fabricated from a thin copper sheet bent outward along the length on each side to form the boundries of adjacent slots, as shown in Figure 3. The segments are attached to the Teflon-coated quartz storage bulb, which provides the necessary mechanical support. Although the design Eq. (10) does not apply directly to this more complex geometry, it was found empirically that it still provides a useful estimation of the parameters.

8685-29

Figure 3. Cylindrical capacitor for a 6-in. i.d. by 5-1/2-in. length cavity. Mechanical support is provided by a 3-in. i.d. quartz storage bulb mounted on one of the cavity end plates.

Furthermore, the prototype cavity had been used to observe the ground-state atomic-hydrogen hyperfine transition in a testbed maser. Storage bulbs 2-1/16-in. diamemter by 4-in. long with 0.5 sec design geometrical storage time were fabricated from 0.005-in. type-A FEP Teflon film.

The observed free-induction decay time was limited to less than 0.1 sec, even at very low flux levels. To overcome this large wall-collision relaxation, the obvious solution was to go to a larger storage volume. Estimates using Eqs. (10) and (11) indicated that this was feasible without excessive sacrifice in the overall dimension and performance of the cavity. Tests were made with several cavities ranging in diameters from 4 to 5 in. with various experimental volumes as summarized in Table 2.

Table 2. Compact Cavities with Large Atom Storage Volume

OUTER CYLINDER (2c x h) *	4 50 IN x 5 94 IN	5 00 x 6 00	6 00 x 5.56	6 00 x 6 00	6 00 x 6 00
CYLINDRICAL CAPACITOR					
DIMENSION (I D x L)	1 84 IN x 4 00 IN	3 09 x 4 00	3 09 x 4 00	4 00 x 4 00	4 00 x 4 00
SLOT (ℓ x d) (4)	0.25 IN x 0 35 IN	0.25 x 0 75	0.25 x 0 75	0.25 x 1 17	0.25 x 1 30
DIELECTRIC* (T x W x L) (SAPPHIRE)	08x.26x4.5 (4 RODS)	08x.26x4.5 (4 RODS)	---	19x.75x4.5 (2 RODS)	----
RESONANT FREQUENCY, MHz	1490	1441	1419	1424	1514
Q (2 PORT COUPLED)	8470	6860	7700	7100	5800

*IN ADDITION TO QUARTZ STORAGE BULB WHICH PROVIDED MECHANICAL SUPPORT

Several cavities also were subjected to tests for maser action. The features of the design can be illustrated with the results obtained with the cavity shown in Figure 3 and summarized in Table 3. The outer cylinder was clear fused quartz, silver plated on the inside surface, 6 in. i.d. by 5-1/2 in. long, the end plates were made of aluminum. The storage bulb was fabricated from standard clear fused quartz tubing, 3-3/32 in. o.d. by 0.06 in. wall by 4 in. long. The design geometrical storage time was 0.28 sec. The bulb was coated conventionally with FEP Teflon. The cylindrical capacitor was fabricated from 0.02-in. copper shims and attached to the storage bulb using polystyrene Q-dope. The four identical segments were 4 in. long and spaced 11/16 in. apart; the slot depth was one-quarter inch. No dielectric loading other than that provided by the quartz storage bulb was required for frequency tuning. Although the validity of Eqs. (10) and (11) for this complex geometry was doubtful, the unloaded Q and the filling factor were estimated using Eq. (11) and found to be 10,000 and 0.57, respectively. The measured loaded Q for two-port coupling (coupling coefficient $\beta_1 = \beta_2 = 0.22$) was 7,500 and the measured filling factor η' was 0.54. The cavity had a temperature coefficient of 14 kHz/°C, which is about six times smaller than that for a sapphire-loaded cavity and which we believe can be further reduced by the design and fabrication technique of the cylindrical capacitor. For

Table 3. Test Data for a 6-In Cavity

CAVITY DIMENSION	:	6 IN. I.D. x 5-1/2 IN. LONG
CYLINDRICAL CAPACITOR	:	4 SEGMENTS OF 0 02 IN. THICK COPPER SHIM MOUNTED ON QUARTZ STORAGE BULB
SLOT DIM	.	1/4 IN. DEEP x 11/16 IN. WIDE x 4 IN. LONG
STORAGE BULB	·	3-3/32 O D. x 0 06" WALL x 4" LONG (COATED WITH FEP TEFLON)
Q ESTIMATED	:	10,000 (UNLOADED)
MEASURED	:	7500 (LOADED, $\beta \simeq$ 22)
η' ESTIMATED	:	0 57
MEASURED	:	0 54
TEMP COEFF	:	14 KHz/°C
ELECTRONIC TUNING	:	8 KHz/VOLT
RANGE	:	~1 CAVITY WIDTH

electronic tuning, a varactor reactance tuner with a linear tuning range of about one cavity width was incorporated (not shown in Figure 3). The tuner had an insignificant effect on the Q of the cavity over the entire linear tuning range. The relatively large atom-storage volume provided good signal-to-noise ratio as well as the desired narrow transition linewidth. A free induction signal with a 0.18 sec decay time constant observed with the cavity and the storage bulb is shown in Figure 4.

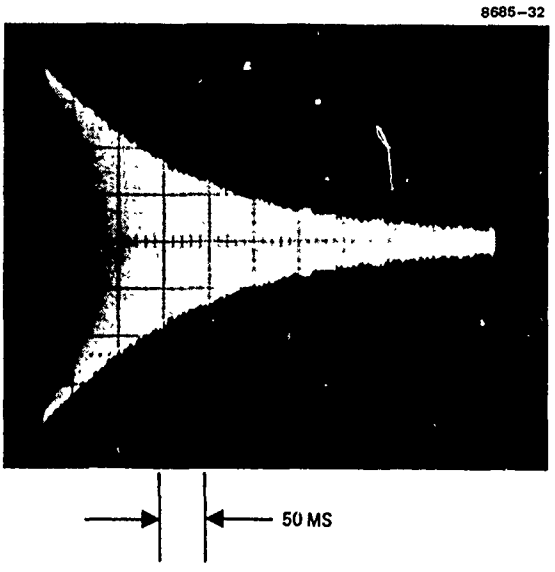

Figure 4. Free-induction signal with 0.18 sec decay time constant observed with the cavity and storage bulb shown in Figure 3.

Conclusion

The progress to date toward the development of a compact and light weight cavity suitable for hydrogen frequency standard applications has been encouraging. The expectations of the approximate design theory were achieved. Undoubtly, great improvements will be made, and computers could be used to simulate the field distribution and optimize the design. It is, therefore, feasible that a truly portable, high-performance hydrogen-frequency standard will soon become a reality.

References

1. S.B. Crampton, T.J. Greytak, D. Kleppner, W.D. Phillips, D.A. Smith, and A. Weinrib, "Hyperfine Resonance of Gaseous Atomic Hydrogen at 4.2 K" (Preprint, paper submitted to the Physical Review Letters).
2. G.B. Collins, Ed., Microwave Magnetrons (McGraw Hills, N.Y., 1948) Ch.2.
3. H.E. Peters, Small, Very Small, and Extremely Small Hydrogen Masers Proc. 32nd Annual Frequency Control Symposium, 1978, pp. 469-475.

DESIGN, CONSTRUCTION AND TESTING OF A SMALL PASSIVE HYDROGEN MASER

E.M. Mattison, E.L. Blomberg, G.U. Nystrom and R.F.C. Vessot

Smithsonian Astrophysical Observatory
Cambridge, Massachusetts

Summary

We have designed, built and tested the development model of a passive hydrogen maser intended for use by the Naval Research Laboratory (NRL) in the Global Positioning System satellite system. The aim was to build a maser physics unit of light weight, small size and low power consumption that embodied in its design the mechanical ruggedness needed for space-qualified hardware. In addition, the development model was designed to be readily demountable so that repairs or changes could be made quickly and easily. The physics unit connects to a vacuum system and hydrogen beam source supplied by NRL. In the course of this work we developed a new method of RF cavity coupling derived from slotline and microstrip techniques.

Two maser physics units were built, operated and delivered. Each is 8.0 inches (20.3 cm) in diameter and 18.5 inches (50.0 cm) long, and weighs 37.2 pounds (16.92 kg).

Maser Design

The maser employs a thick-walled, dielectrically loaded cylindrical sapphire resonant cavity[1-3] designed and supplied by NRL. We coated the cavity with silver on its outer surface to form the electromagnetic resonant cavity, and with Teflon on its inner surface to form the hydrogen storage region. The first maser uses a FEP Teflon sheet liner as the storage surface, while the second has a Teflon coating FEP dispersion. The RF coupling schemes also differ: the first maser has copper cavity endplates and coupling loops surrounded by solid Teflon bulkheads, while the second has Teflon-coated quartz endplates employing the slot coupling technique.

The environment of the resonant cavity is carefully controlled. The cavity is mounted so that it is isolated from movements of the vacuum tank walls caused by changes in temperature or barometric pressure. Its temperature is stabilized by two sets of servo-controlled multi-zone heat stations, in conjunction with foam thermal insulation. The hydrogen interaction region is shielded by four layers of magnetic shields designed by NRL, while two printed circuit solenoids establish uniform field within the innermost shield.

The construction of the maser is shown in Figures 1- , which show the assembly of the components. The cavity (Figure 1) is contained in a titanium vacuum tank. The cavity cylinder and endplates are clamped in a holddown can (Figure 2) that fastens to the vacuum tank at one end, thus isolating the cavity from the deflections of the tank walls. Each end of the tank is supported by a thin-walled titanium neck tube that provides radial and axial support and thermal isolation. The vacuum tank forms the mechanical base for the thermal and magnetic control systems. Heaters are wound on the tank cylinder and end covers. The entire tank is coated with thermally conductive epoxy that provides a smooth cylindrical mounting surface for the magnetic field solenoids and magnetic shields. Figure 3 shows the main printed circuit solenoid mounted on the vacuum tank, with the conical endcaps of the four magnetic shields visible above the flange that joins the physics unit to the vacuum system.

The cavity is thermally coupled to the vacuum tank by radiation and conduction. Therefore the primary temperature control surface is the vacuum tank, whose temperature is held constant at approximately 38°C. (The exact value of the tank temperature is adjusted to fine-tune the cavity's resonance to the hydrogen hyperfine frequency.) Temperature stability is achieved by isolating the vacuum tank as much as possible from outside temperature changes and by maintaining its elevated temperature by means of feedback-controlled heaters. Passive isolation is accomplished by forming the supporting tubes of thin-walled, low-conductivity titanium alloy and by surrounding the tank wall with several layers of foam insulation that separate and support the magnetic shields; active control is achieved by winding heaters on the tank, by surrounding the tank with a temperature-controlled guard oven at the position of the third magnetic shield (Figure 4), and by connecting all wires and coaxial cables that leave the maser to a temperature-controlled heat station. The total power dissipated by the tank and oven heaters and the control electronics (including magnetic field controller) is 7.1 watts at an ambient temperature of 23°C. The temperature stability of the vacuum tank is estimated to be ±.008°C or less.

The DC magnetic field within the cavity must be spatially uniform and temporally constant.

These goals are approached by several means. Four nested molypermalloy shields, designed and supplied by NRL[4], exclude the ambient field from the cavity. The internal longitudinal field is established by a solenoid made in the form of a multi-layer printed circuit. This construction eliminates transverse field components caused by non-cancelled return currents. The shield solenoid contains three windings, a main coil occupying most of its length and two shorter trim coils that remove gradients from the field configuration. Directly beneath the field solenoid is a second printed circuit containing the Zeeman coils used to measure the magnitude of the magnetic field in the cavity, and a set of Helmholtz coils that can be used to cancel quadratic variations in the longitudinal field pattern.

The outer magnetic shield is surrounded by additional foam insulation, and the entire unit is contained in a support cylinder (Figure 5) that carries the mechanical load of the tank.

Slot Coupling Technique

The RF coupling scheme of the first maser has several drawbacks. The large thermal coefficient of expansion of the copper endplates differs from that of the sapphire cylinder and can contribute to temperature-induced stress changes in the cavity. The coupling loops are outside of the sapphire cavity and thus do not sample the maximum field intensity, which occurs within the sapphire dielectric. Consequently, only small values of the coupling factor are attainable. The loops are of necessity formed of small diameter wire and thus lack physical rigidity. Finally, the endplates are isolated from the hydrogen storage region by bulkheads machined from solid Teflon, and the tubular collimator is made in the same way, causing those parts of the storage surface to be of uncertain cleanliness and composition.

To provide sufficiently strong RF coupling in a mechanically stable design we developed slot coupled endplates (Figure 6). These consist of quartz discs coated with silver using printed-circuit techniques. One endplate has an integral quartz collimator tube and an uninterrupted silver coating. On the second endplate, we created sections of 100 ohm slotline in the silvered surface that contacts the cavity, and printed sections of 50 ohm microstrip conductor on the opposite face. The coupling slots are separated from the sapphire only by a thin layer of Teflon and thus couple well to the RF field; by adjusting the dimensions of the slots we achieved coupling coefficients between 0.1 and 0.5, which was the desired range. The quartz and printed circuit construction is inherently rigid and stable, minimizing the possibility of change in the coupling factor or cavity frequency, and allows the Teflon storage surface to be applied directly to the endplates from a dispersion. Ultimately the endplates could be made of sapphire to match exactly the thermal characteristics of the cavity cylinder.

Operation and Test Results

Cavity characteristics. The silver-coated cavities have unloaded Qs of 1.5×10^4 and 1.7×10^4, (the lower-Q cavity has a thinner than usual silver coating). The Q of an uncoated sapphire cavity cylinder enclosed in a snug-fitting brass tube with copper endplates is 1.7×10^5; thus, losses in the silver coating are insignificant compared with those in the sapphire dielectric. The resonance frequency of the cavity changes with temperature at a rate of approximately 50kHz per degree Celsius.

RF coupling. The first maser uses three symmetrically placed loops for coupling RF power into and out of the cavity, each of which has a coupling factor β of approximately 0.08. The slot-coupled endplate of the second maser was designed for stronger coupling. Two of the ports have $\beta \approx 0.15$ while the third has $\beta \approx 0.42$. The different values of β were achieved by adjusting the lengths of the symmetrically located slots.

Magnetic Shielding. To measure the maser's magnetic shielding factor we applied an external field with a pair of four-foot diameter Helmholtz coils and observed the Zeeman frequency of the pulsed atoms to determine the resulting magnetic field change within the cavity. Because of their small size and novel design[4], the magnetic shields are particularly effective, as shown below:

ΔH_{ext} (O_e)	ΔH_{ext}
0.19	4.0×10^4
1.5	6.1×10^4

Hydrogen Atom Storage Time. The maser's receiver will lock a local oscillator to the atomic resonance frequency. The stability of the lock depends upon the narrowness of the atomic resonance Δf, which is determined by the total transverse relaxation rate $1/T_2$:

$$\Delta f = \frac{1}{\pi T_2}$$

Thus a large value of the storage time T_2 is desirable.

We measured the storage times of both masers with several storage surface coatings by observing the free induction decay of the signal produced by the hydrogen atoms when put in a radiative state by a short pulse of RF power at the hyperfine frequency. The free induction signal was displayed on an oscilloscope (Figure 7) and compared with a calibrated exponentially decaying trace to determine the value of T_2.

The original storage surface in the first maser consisted of the solid Teflon bulkheads covering the copper endplates, and a cylindrical type L Teflon sleeve cemented to the inner surface of the cavity cylinder. The collimator, which was machined from solid Teflon and was integral with one of the bulkheads, was 1.5 inches (3.81 cm) long and 0.14 inches (.36 cm) in diameter, while the cavity storage region was 5.43 inches (13.8 cm) long and 1.75 inches (4.44 cm) in diameter. These dimensions give a calculated geometrical, or bulb, storage time T_b of 0.31 seconds. Assuming that all relaxation not due to atom loss from the storage region is caused by relaxation on the walls, we have

$$\frac{1}{T_2} = \frac{1}{T_b} + \frac{1}{T_w}$$

where $1/T_w$ is the wall relaxation rate. The measured values of T_2 were between 40 and 50 msec, giving a wall storage time $T_w \approx 60$ msec. This implies a probability of wall relaxation per collision, p, of approximately 2.5×10^{-4}, which is roughly 2.5 times greater than the values of p commonly measured. To investigate whether the large relaxation rate was caused by the cement used in the cavity liner or by the presence of machined Teflon we disassembled the maser and replaced the storage surfaces. We inserted a new type L liner sleeve assembled by heat welding, and covered the bulkheads with closely fitting discs of the same material. The inner surface of the collimator was not changed. The reassembled maser again had a total storage time of 40 to 50 msec. Because the liner cement was eliminated from the cavity and the area of solid Teflon storage surface was greatly

reduced, this result suggests that the excess wall relaxation is due to the sheet Teflon.

Slot coupling endplates were installed in the second maser. The collimator tube was 0.200 inches (0.51 cm) in diameter and 1.5 inches (3.81 cm) long, giving a geometrical storage time of 0.11 seconds. The inside surfaces of the cavity cylinder and of the collimator, and the faces of the endplates, were coated with FEP Teflon from a dispersion. The total storage time of the maser was measured at SAO by observation of the free conduction decay, which gave a value of T_2 = 80 msec, and at NRL by observing the absorption of an RF signal transmitted through the cavity. The absorption linewidth of 3 Hz gives a storage time of 88 msec, which is consistent with the decay measurement. Using T_2 = 80 msec and T_b = 112 msec we find T_w = 280 msec, and p = 5.2. x 10^{-5}, a very low value of relaxation probability.

Conclusion

The passive masers described here are small, rugged, light weight, low-power frequency standards whose design makes them adaptable to space applications. The slot coupling technique provides a convenient and mechanically stable method of RF cavity coupling, and permits the use of a storage coating that gives excellent relaxation rates.

Acknowledgment

This work was supported by the U.S. Naval Research Laboratory under Contract N00014-78-C-0120.

References

1. Repair of Government-furnished Spherical Fused Quartz Hydrogen-Maser Cavity, Smithsonian Astrophysical Observatory, Cambridge, MA, February 1971. U.S. Army Contract DAAB 07-70-C-A108.

2. Mattison, E.M., and R.F.C. Vessot, Evaluation of Dielectric-loaded Maser Cavities, Smithsonian Astrophysical Observatory, Cambridge, MA, April 1975. U.S. Navy Contract N00014-71-A-0110-0003.

3. Mattison, E.M., R.F.C. Vessot, and M.W. Levine, A Study of Hydrogen Maser Resonators and Storage Bulbs for Use in Ground and Satellite Masers, Proc. Seventh Annual PTTI Planning Meeting, Goddard Space Flight Center, Greenbelt, MD; 1976. P. 243.

4. Wolf, S.A., D.U. Gubser, and J.E. Cox, Shielding of longitudinal magnetic fields with thin, closely spaced, concentric cylindrical shells with applications to atomic clocks, Proc. Tenth Annual PTTI Applications and Planning Meeting, Goddard Space Flight Center, Greenbelt, MD; 1978. P. 131.

1. Sapphire cavity with copper endplates and epoxy-coated vacuum tank.

Fig 2. Assembly of cavity holddown can. Solid teflon collimator is visible at center of near end of cavity.

Fig 3. Magnetic field solenoid installed on vacuum tank. Support tube is visible at top, conical magnetic shield endcaps at bottom.

Fig. 4 Assembly of thermal guard oven.

Fig. 5 Assembly of outer support cylinder.

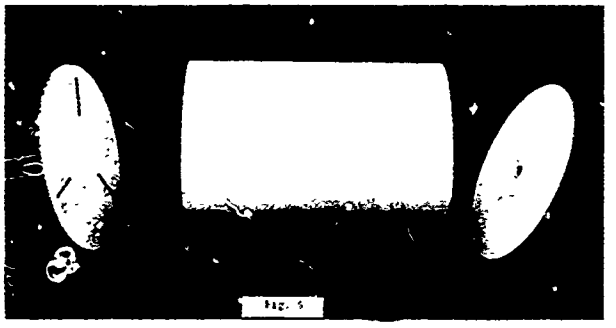

Fig. 6 Cavity cylinder with quartz endplates. Slot coupled endplate is at the left, endplate with integral quartz collimator is at right.

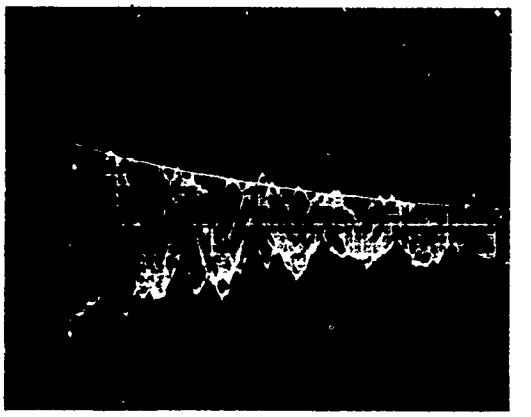

Fig. 7 Simultaneous oscilloscope traces of maser free induction decay and calibrated exponential signal.

A SMALL, PASSIVELY OPERATED HYDROGEN MASER

D. A. Howe, F. L. Walls, Howard E. Bell, and Helmut Hellwig

Frequency and Time Standards Group
National Bureau of Standards
Boulder, CO 80303

Abstract

A compact passive hydrogen maser with many unique features, including a significant reduction in size over previous hydrogen masers, is described. It uses the passive mode of operation, thereby permitting use of a small microwave TE_{011} cavity which is dielectrically loaded by a low-loss alumina (Al_2O_3). The cavity is 14.6 cm O.D. and 13.7 cm high, weighing only 4.4 kg. The unloaded cavity Q factor is about 6000. With a conventional source, hexapole state selector, and 4 magnetic shields the volume of the entire H-maser resonator package is only about 20 ℓ.

The teflon coated quartz bulb which is common in other masers has been replaced by a teflon coating on the inside wall of the cavity. This has yielded a simpler design and more rugged H-maser package. The technique for the application of liquid emulsion FEP 120 is discussed.

The cavity and attached endcaps comprise the vacuum envelope, thus allowing use of a single vacuum system. The dimensional stability of the ceramic cavity under barometric changes is sufficiently within the range of the electronic cavity servo that a second vacuum system is not needed. For temperature control, a single oven is located in the magnetic shield nest.

The electronics for this small passive hydrogen maser is very similar to that previously developed at NBS. Preliminary measurements on a prototype small maser system yield a frequency stability of approximately $\sigma y(\tau) = 6.6 \times 10^{-12}\ \tau^{-\frac{1}{2}}$ to at least one day, with a measurement bandwidth of 1 kHz.

Introduction

The construction details of a small, passively operated hydrogen maser are presented. The concept of the passive maser was introduced in order to obtain better long term stability than that seen using active maser designs.[1,2,3] A quartz oscillator is locked to the hyperfine resonance using a design reminiscent of optical pumping and atomic and molecular beam devices. Two important requirements of conventional oscillating masers have been relaxed: (1) A relatively high cavity Q (needed for oscillation), (2) excellent cavity frequency stability as a function of temperature, pressure, voltage, and time. The second point is possible because in the passive mode of operation one has the ability to lock the frequency of the cavity to the H resonance. Passive electronics has been successfully deployed on a conventional full size maser.[1,2,3] The development of this new electronics makes possible a reevaluation of the design parameters used in the maser (the so-called "physics package").

The maser works on the magnetic dipole transition of the ground state of free hydrogen atoms contained in a storage volume. Figure 1 shows the F = 0 and F = 1 states as a function of applied magnetic field. This hyperfine transition in hydrogen has a frequency of 1420405751.77 Hz. RF interrogation of the hydrogen atoms at this frequency takes place within a teflon coated storage volume. This wall-coating typically permits the hydrogen atoms to bounce 2×10^4 times within this volume before loosing their phase relative to the RF magnetic field.

In order to achieve high filling factors the instantaneous RF magnetic field needs to be singly directed over the entire hydrogen storage volume.[4] With the use of low loss alumina dielectric material, one can develop cavity designs which yield small size and relatively high filling factor over a given volume. The cavity design used here is a right circular cylinder of low-loss ceramic with a bore down the central axis and a silver jacket on the outside surface. The ends are capped with Al_2O_3 plates. The closed central bore is the hydrogen storage volume. Along with good filling factor this geometry has the benefit of good symmetry about all axes of the RF magnetic field in the storage volume. The TE_{011} mode is used. In this new design the microwave cavity therefore forms the vacuum envelope and storage volume. With currently available dielectric materials this is only made possible because of the passive electronic scheme.

Passive Maser Electronics

Figure 2 shows a block diagram of the electronics used in previous work with a full size hydrogen maser. The same scheme was deployed in the small maser described here. A thorough explanation of the operation of the servo system is described in references 1, 2, and 3. The interrogation (exciter) signal at 1420 MHz which enters the cavity is phase modulated at two frequencies, f1 and f2. Frequency f1 is a high frequency (12

kHz) phase modulation component used to probe the hydrogen cavity. Modulation component f2 is used to probe the hydrogen resonance. Figure 3 shows the spectrum of the exciter signal. This FM spectrum, after going through the cavity, then contains amplitude modulation components at frequencies f1 and f2. The transmitted microwave signal is envelope detected to recover f1 and f2 amplitude modulation components. Phase sensitive (synchronous) detectors are referenced to f1 and f2 and are used respectively to (1) determine the cavity frequency relative to the probe frequency, and (2) determine the probe frequency relative to the narrow hydrogen resonance. First, a correction signal is applied to the quartz oscillator which generates the probe frequency so that it is centered on the hydrogen resonance. Second, the cavity is tuned so that it is centered symmetrically about the probe frequency.

Concept of the Dielectrically Loaded Cavity

Figure 4 shows a development sequence of the small cavity design. Most masers use a conventional TE_{011} mode microwave cavity with approximately a diameter of 21 cm and a length of about 50 cm. The lumped constant equivalent circuit for such a cavity consists of an inductance L in series with a capacitance C in series with a resistance R. The insertion of a dielectric which affects the propagation constant ε will increase C, thus decreasing the frequency of the cavity. The overall dimension of the cavity can then be reduced to compensate for the added dielectric. Symmetry, dielectric constant, overall dimension and filling factor are then traded against each other to achieve a given geometry. The effect of the frequency of the TE_{011} mode needs to be factored into the design at this stage. Solving for the frequency requires the solution to a boundary value problem involving a differential equation describing the electromagnetic propagation within the cavity. The dielectric loading of the cavity affects the electric field; the RF magnetic field (which excites the atoms) is pinned to the defined orientation of the electric fields within the cavity. It is possible to choose a cavity bore diameter so that the oscillating axial H-field does not reverse sign in this region. Consequently, the inside bore can substitute for the conventional storage bulb with little compromise in the filling factor.

Details of the Fabrication of the Cavity

The small hydrogen maser uses a ceramic cavity (Al_2O_3) of AD-99.5 which has a loss tangent less than 10^{-4}. Using a silver coat which is fired on the outside surface of cavities cut to 1.42 GHz has yielded unloaded Q's of typically 6,000. The silver solution used is Englehard Industries' #A-2405.[5] This solution consists of silver suspended with a glass frit in a binder solution. The entire solution is first thinned with 1½ cm^3 toluene to 5 grams of A-2405. This mixture is stirred and immediately loaded into a miniature spray gun. This solution is sprayed directly on the cylinder outside surface until a black matte finish is achieved. The solution is allowed to dry for 10 minutes, after which time the coated cylinder is loaded into a firing furnace. The firing furnace has a temperature profile which brings the cylinder up to 600° C in about 2 hours, and the cylinder soaks for 10 minutes at 600° C. Cooling to room temperature takes about 4 hours.

The cooling rate should not be too short. It is relatively easy to form hairline cracks in the ceramic cylinder due to non-uniform cooling. This does not appear to be as much of a problem during heating.

The cylinder is covered on both bottom and top so that stray silver paint which is blown inside the furnace is not redeposited on the inside wall of the cylinder, nor on the top and the bottom. The procedure for coating the silver must be repeated three times in order to achieve sufficiently high Q's, i.e., spray-dry-fire, spray-dry-fire, spray-dry-fire. If a cylinder is improperly coated, no satisfactory method exists for removing faulty coats other than grinding the finish off using a lathe designed for ceramic grinding. There is a deterioration of the ceramic loss tangent due to the diffusion of the glass frit in the silver paint through the ceramic. Normally, after three fires the glass has not noticeably deteriorated the Q of the cavity; however, after six or seven fires deterioration becomes apparent and Q's of below 5,000 are observed.

Figure 5 shows the silver-coated ceramic cylinder alongside two storage bulbs used in conventional full-size masers. The cylinder is approximately 14 cm O.D., 10 cm I.D., and 15 cm long.

The disks which seal the open ends of the cylinder are similarly fired with three silver coats. Each ceramic disk or endcap is cut to a thickness of 6.35 mm and a diameter equal to the outside diameter of the cylinder. One of the endcaps has a 6 mm hole centered in it for the collimator which determines the relaxation rate of the storage volume. It is only necessary to coat the surface of each of the endcaps which face the cylinder.

At this point, the cavity is tuned to the hydrogen resonance at 1.420 GHz for an oven temperature of 45° C. The tuning of the cavity is accomplished by grinding both the length and inside bore of the ceramic cylinder. Each end of the cylinder is first ground flat to 0.01 mm. This requires usually that about 0.05 to 0.1 mm be taken off each end. Grooves are ground into each end which resemble an O-ring gland with a depth of penetration of 6.35 mm and width of 3 mm. These grooves are used as RF mode suppressors. No RF current flows axially in the desired mode (TE_{011}), but undesired modes do require axial RF currents which are suppressed by this gap due to the groove in the outside electrical boundary at the endcaps. The frequency sensitivity due to changing length of the cylinder is about 400 kHz per mm. The cylinder frequency is now checked using the RF slots located midway between top and bottom of the cylinder and

on opposite sides. The TE_{011} mode is readily identifiable by its high Q and cylindrically symmetric field lines. The resonant frequency of the cavity should be about 1.422 GHz at room temperatures for operation in an oven 20° above room temperature, since the cavity frequency coefficient is 100 kHz per degree centigrade. An increase in the temperature causes a decrease in the resonant frequency. The increase in the inside diameter of the cylinder is computed using a cavity frequency coefficient of +4 MHz per 0.1 mm of diameter change. The grinding operation may require several steps in order to come close to 1.422 GHz. If the resonant frequency is cut too high, then the operating oven temperature may be increased to compensate.

With the properly cut cavity with a silver coat and two endcaps each silver coated, the cavity has a symmetric TE_{011} resonance at 1.422 GHz. Symmetry of the resonance over ±10 MHz is better than 3 dB. A spurious mode high in frequency by about 30 MHz is down by 30 dB or more and has very low Q due to the grooves which are cut at the top and bottom ends.

Figure 6 shows a mechanical drawing of the maser and a picture of the complete (sealed) cavity. A copper plate with a slotted, threaded bushing provides a method of fastening a semi-rigid coax line to the cavity sidewall. The end of the coax terminates in an RF coupling loop which penetrates a slot in the ceramic cavity. A nut tightened down on the bushing causes it to compress down to the diameter of the coax. This collet action allows straightforward adjustment of coupling factor. The receiver link is near critical coupling, whereas the exciter link has a coupling coefficient below 0.1.

The cavity is centered lengthwise inside the first magnetic shield using plastic foam at each end of the cavity. An aluminum disc is used at the bottom end for added strength. The C-field is wound on a mylar form located just inside the first magnetic shield, and extends along its entire length (see fig. 7). The windings are one turn per centimeter and are wound from top to bottom to top in a double helix. In this way the tilt of the axis of the C-field due to the coarse pitch of the individual helical windings is subtracted out. Two single turn loops are located at opposing faces of the C-field mylar cylinder for excitation of the Zeeman transition.

There are a total of four magnetic shields concentrically spaced one-half inch apart in a nest. The magnetic shields are fabricated in two halves joined together at the waist with a 5 cm wide overlap joint. The uniformity of the C-field was measured using a rubidium magnetometer. Results showed a homogeneity of at least ± 0.5 nT (± 5 μG) (the resolution of the magnetometer) at an ambient field of 10 nT (100 μG). An axial magnetic shielding coefficient of 1.5×10^5 was measured using these shields. Figure 8 shows the bottom halves of the four nested shields with cavity and C-field coil in place.

A single oven is used to control the temperature of the cavity. Temperature determines a coarse frequency adjustment for the cavity and sensitivity is -100 kHz/°C. The oven is located between the second and third magnetic shields and it is shown in fig. 9. It is an aluminum cylinder with four equally spaced 6Ω titanium heaters running the length of the cylinder. Two precision thermistors with stabilities of about several mK per year are thermally attached to the aluminum cylinder. One thermistor used for the oven controller is located near one of the titanium heaters. The second thermistor, located midway between two heaters, is used as a monitor.

Teflon Coating Technique

The conventional hydrogen maser uses a quartz storage bulb which is coated with teflon. The characteristics of hydrogen wall relaxation depend on the technique of teflon application and the type and purity of teflon.[6] In the small passive maser, no quartz bulb is used and the teflon coat is applied directly to the inside wall of the ceramic dielectric. This is possible because the phase of the axial component of RF magnetic field does not reverse in the hydrogen storage volume, but rather reverses inside the dielectric. The teflon coat serves two purposes. The first is to provide a surface which minimally perturbs the phase of the hydrogen atoms; the second is to vacuum seal the endcaps to the main cylinder.

The teflon coat is made using Dupont FEP 120 emulsion.[5] FEP 120 resins in solution normally contain 50 percent water and about 8 percent triton X-100 stabilizer. The stabilizer tends to (1) keep solid teflon uniformly dispersed, and (2) lower the surface tension by acting as a wetting agent. The liquid emulsion is mixed at 38 percent FEP 120 to 52 percent H_2O to 10 percent triton X-100. This new solution yields a thinner coat, slower initial drying phase, and better wetting of the ceramic surface than the original solution.

The liquid teflon is applied to the ceramic endcaps with a polypropelene squeeze bottle. The surface is uniformly wetted and allowed to dry under a heat lamp for about fifteen minutes. The endcap is placed in a kiln with a heat rise of about 6 K per minute. Pure oxygen is flowed through the kiln during the heating cycles. FEP 120 is fused by melting at a temperature of 360° C. Aluminum foil is placed around the endcap to deflect direct radiant heat from the kiln's heating elements. The rate of heating as one approaches 360° C is important because the high thermal mass of the ceramic causes the ceramic endcap to lag the temperature of the kiln. Thus, fusing of the teflon first takes place at the outside surface of the teflon, trapping stabilizers and other impurities within the teflon. In order to avoid this the rate of temperature increase should be reduced to approximately 1K/min. Three coats of teflon are applied to the ceramic. This lowers the probability that microscopic cracks will increase the effective surface area and that ceramic may be exposed at the bottom of such cracks. Subsequent coats of teflon are applied by using the previous

mix and allowing the solution to dry to a very thin overlayer. Milky lumps of teflon may tend to form but this is of no consequence. After an initial dry, the teflon solution is reapplied, wetting is more pronounced, and the lumps dissolve. The surface then dries as before in a uniform thin film, and the same kiln temperature cycle is used After the first coat the surface has a matte finish. By the third coat the surface is glazed and clear.

The application of the teflon mix on the cylinder wall is very similar. It is useful to mount the cylinder in a lathe so that it can be rotated slowly while the liquid solution rolls on the inside wall. The wall is first uniformly wetted, then removed from the lathe and allowed to stand so that the liquid can drip to one end and the solution allowed to dry. Glass endcaps fitted with tubes which go out of the kiln are placed on the top and bottom of the cylinder during the oven cycle so that oxygen can be flowed through the inside bore of the cylinder. Here the oxygen serves two purposes: (1) to oxidize the stabilizer, and (2) to keep the outside surface of the teflon cool relative to the temperature of the heating ceramic cylinder. This is done to insure that fusing first begins at the teflon-ceramic boundary. A thermocouple is mounted in one of the RF slots of the cavity to monitor the temperature profile. Three coats of teflon are applied to the inside wall of the cylinder. Teflon coats can be removed by increasing the oven temperature to about 650° C.

Small Hydrogen Maser Source

The source for the small hydrogen maser is a conventional design. A tank of hydrogen loaded to about 20 atmospheres pressure is fitted with a regulator and mechanical PZT leak valve. From the PZT valve, hydrogen enters the dissociator bulb. A manometer pressure transducer (capacitance type) measures the pressure difference between the hydrogen inlet to the dissociator bulb and the rest of the maser vacuum system, i.e., that portion of the system on the outside of the collimator of the bulb. The discharge bulb is typically 40 μ bar (3×10^{-2} Torr). An electronic servo system controls the flow of hydrogen by comparing the output of the manometer gauge with a preset value and providing a correction voltage to be applied to the PZT valve.

In the preparation of the 5 cm O.D., 6 cm long, cylindrical dissociator bulb, no etching solution such as chromic acid is used. The bulb is formed with a fire-polish finish on the inside surface. The collimator has bore dimensions of .304 cm length x .039 cm diameter. After fabrication of the bulb, it is epoxied in a hole in a stainless steel conflat baseplate located at the bottom of the hydrogen maser vacuum system. This is shown in the mechanical drawing of fig. 10. The glass-to-epoxy-to-stainless interconnection is made at a point on the stainless plate where a thin membrane has been cut to yield to differing expansion coefficients.

A cylindrical aluminum cover bolts onto the stainless conflat and protects the dissociator bulb. The cover carries the dissociator electronics. The RF source used in the discharge is a 155 MHz crystal controlled oscillator followed by two buffer amplifiers and a 30 watt LSI power module made by TRW.[5] The RF source electronics draws no more than 15 watts of power; about 8 watts is delivered to the discharge. Measurements indicate that one source bottle of H_2 should last more than four years under normal operating conditions.

Small Hydrogen Maser Vacuum System

The stainless steel vacuum flange carrying the hydrogen source is bolted to the underside of a tubular vacuum system of a total length of 25 cm. The state selector hexapole magnet is supported by the flange. Two 20 l/s vac-ion pumps flank the hexapole state selector and are used to pump away the off-axis beam atoms. A separate 20 l/s vac-ion pump evacuates the top portion. Its function is to pump away the scattered unfocused states in the beam as well as to pump those atoms which have escaped from the cavity. Pump lifetime is estimated at 10 years. A diaphragm separates the source region from the cavity region. A small tubulation in the center of the diaphragm maintains a 20 to 1 pressure difference between these two regions. This tubulation does not affect the beam.

Note that no vacuum system is used on the outside of the cavity. Barometric changes cause only a kHz or so change in cavity tuning which is fully compensated and corrected by the cavity servo system.

Figure 11 shows a picture of the so-called "physics package" of the small maser. The receiver front end and first conversion through a doubly-balanced mixer to an IF frequency of 20 MHz can be seen underneath the outside magnetic shield. Contained here also is the cavity tuning scheme described in ref. 1 and shown in the block diagram of fig. 2.

Frequency Stability Data

Figure 12 shows the two-sample $\sigma_y(\tau)$ data for the first small maser versus NBS-6, one of our primary cesium standards. The length of the data set allowed a determination of frequency stability out to one day of $6.6 \times 10^{-12}\ \tau^{-\frac{1}{2}}$. Also shown is a frequency stability of $2 \times 10^{-12}\ \tau^{-\frac{1}{2}}$ of the full-size passive maser using similar electronics. Currently under test is a second small maser which exhibits improved cavity vacuum performance and a better teflon wall coating. The first small maser yielded a hydrogen linewidth of 4.5 Hz. The second maser yields a 1.6 Hz linewidth. From linewidth and signal-to-noise considerations a factor of approximately 5 improvement in frequency stability is expected.

The frequency change of the small maser for a 2 dB increase in excitation power was $2 \pm 2 \times 10^{-13}$ while doubling the hydrogen source pressure resulted in a frequency shift of $2 \pm 4 \times 10^{-13}$.

Fractional frequency stabilities of 10^{-15} for long periods of time ($\tau > 100{,}000$ s) appear possible.

Conclusion

We have described the details of a small, passive hydrogen maser using a dielectrically loaded microwave cavity with integral storage bulb and vacuum container. Frequency stability of $6.6 \times 10^{-12}\ \tau^{-\frac{1}{2}}$ has been observed using this first device. The linewidth of a new small maser has been improved by a factor of 3 to 1.6 Hz. Based on the linewidth and signal-to-noise we expect a factor of approximately 5 improvement in frequency stability.

Acknowledgments

This work was supported in part by the Naval Research Laboratory and the Jet Propulsion Laboratory. We thank Steve Jarvis for the computer program which determines the cavity modes. We also thank James E. Gray, Charles Manney and Mike Mohler for their help in putting together the small maser electronics.

References

1. F. L. Walls and D. A. Howe, "A Passive Hydrogen Maser Frequency Standard," Proc. 32nd Ann. Symp. on Freq. Control, 492, 1978.

2. F. L. Walls and H. Hellwig, "A New Kind of Passively Operating Hydrogen Frequency Standard," Proc. 30th Ann. Symp. on Freq. Control, 473, 1976.

3. F. L. Walls, "Design and Results from a Prototype Passive Hydrogen Maser Frequency Standard," Proc. 8th Ann. Precise Time and Time Interval (PTTI) Planning Meeting, 369, 1976.

4. Daniel Kleppner, H. Mark Goldenberg, and Norman F. Ramsey, "Properties of the Hydrogen Maser," Applied Optics, Vol. 1, no. 1, 55, 1962.

5. Commercial equipment is identified in this paper in order to specify adequately the experimental procedure. This identification does not imply recommendation or endorsement by NBS, nor does it imply that the equipment is the best available for the purpose.

6. Jacques Vanier and Robert Larouche, "A comparison of the Wall Shift of TFE and FEP Teflon Coating in the Hydrogen Maser," Metrologia, 14, 31, 1978.

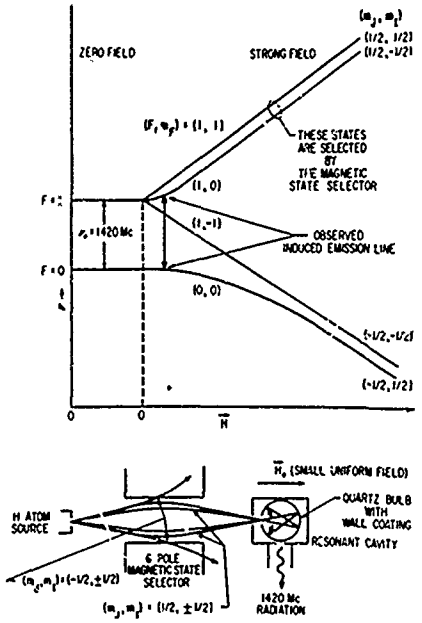

Fig. 1. Magnetic hyperfine transition of hydrogen atom, and maser schematic.

Fig. 2. Block diagram of passive maser electronics

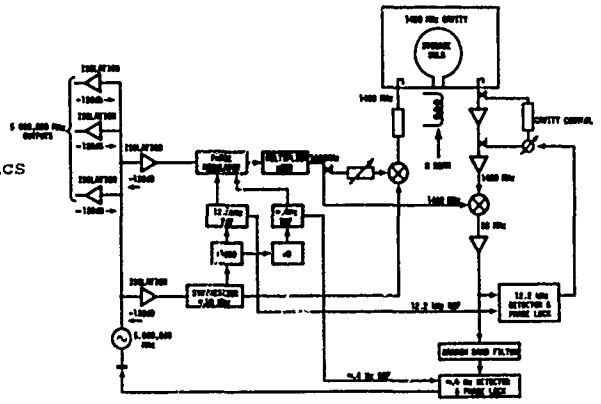

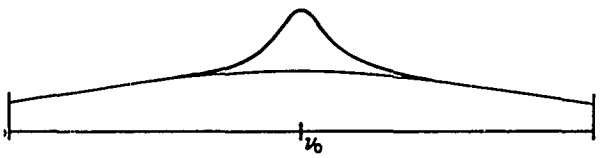

Fig. 3. FM spectrum of exciter signal

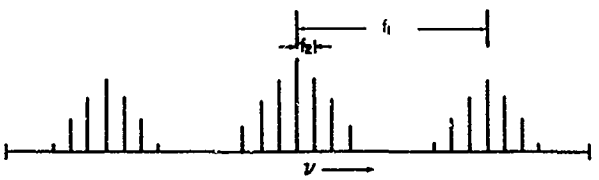

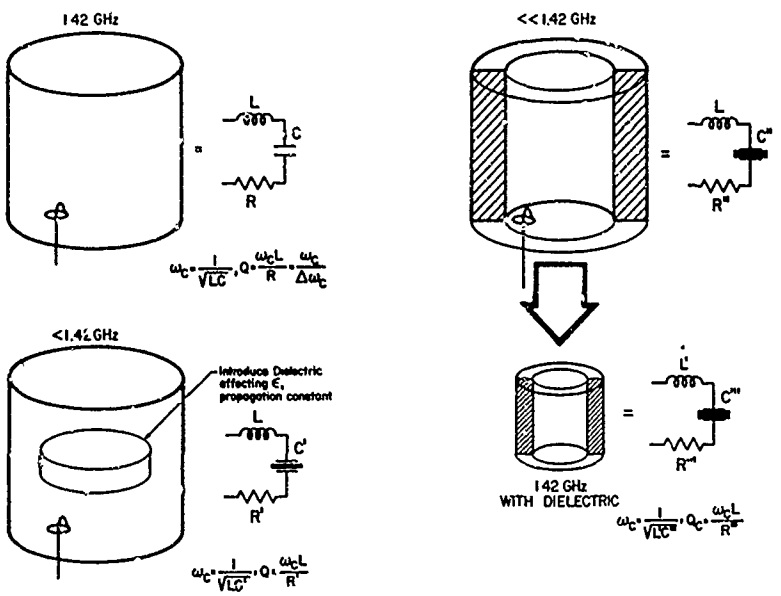

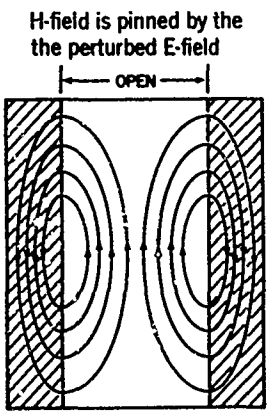

A geometry is chosen so that the oscillating H-field does not reverse sign in the open bore.

No bulb is needed to confine the interrogated atoms to a volume of non-reversing H-field

Fig. 4. Dielectric loading of TE_{011} mode cavity allows a reduction in size.

Fig. 5. Size comparison of the dielectrically loaded cavity with storage bulbs of typical full size masers.

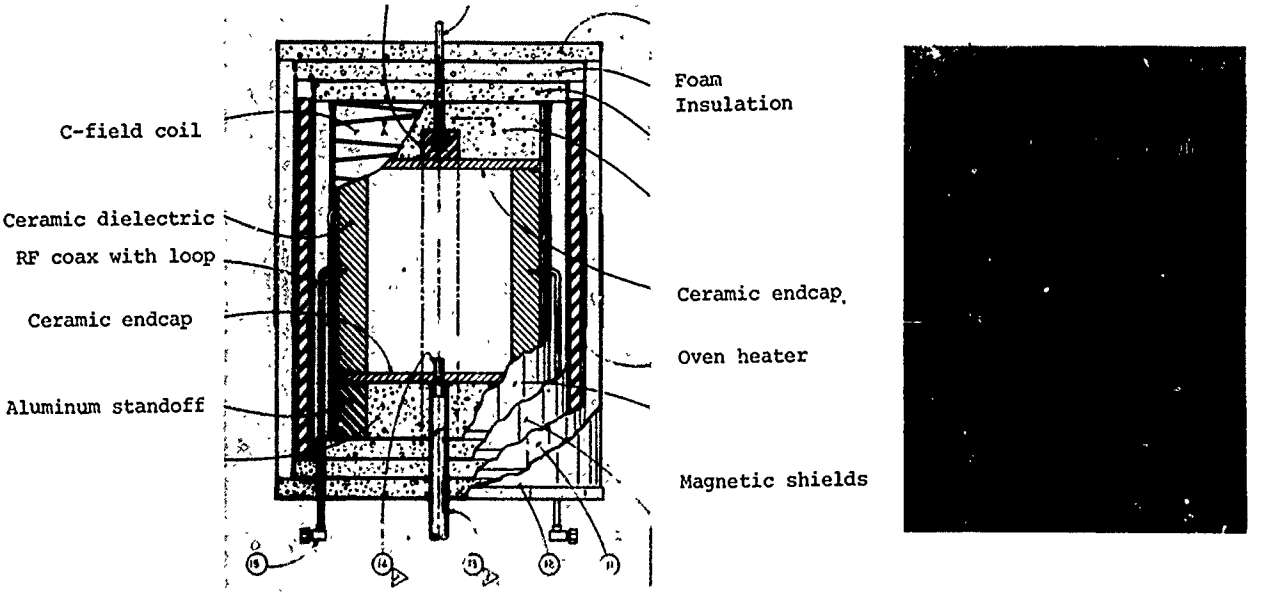

Fig. 6.
Portion of a mechanical drawing showing cavity and shield assembly and picture of cavity collet which accepts semi-rigid coax loop.

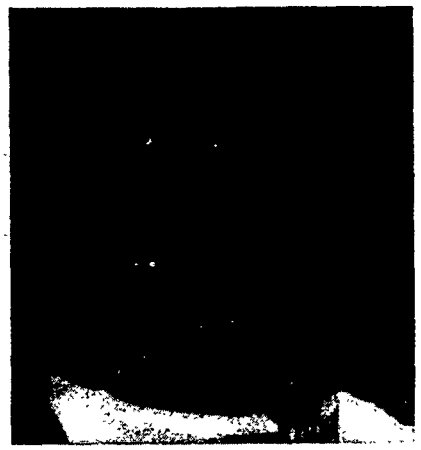

(A). Aluminum standoff (top) and degauss strap.

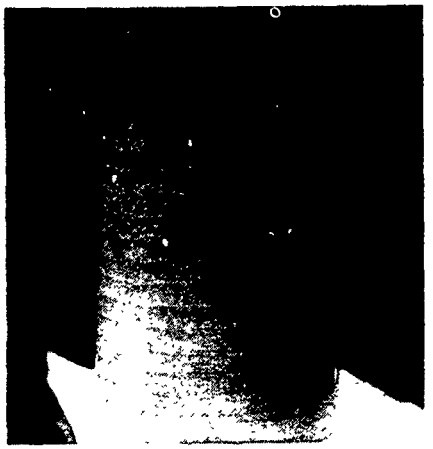

(B). C-field coil.

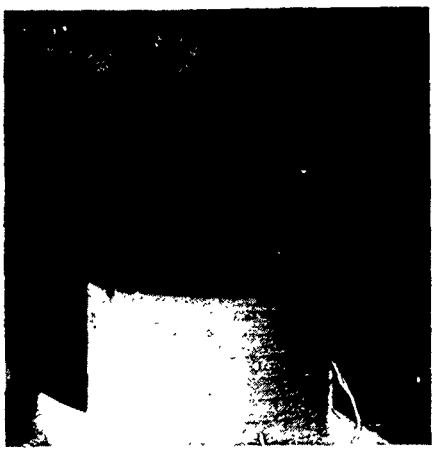

(C). Bottom of first magnetic shield.

Fig. 7.
Assembly of maser parts inside first magnetic shield.

Fig. 8. Picture showing nested shields and sidewall coax RF coupling.

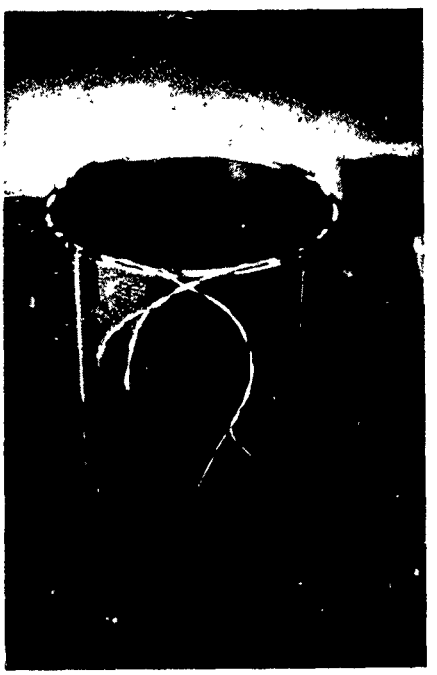

Fig. 9. Oven heater which fits between second and third magnetic shields.

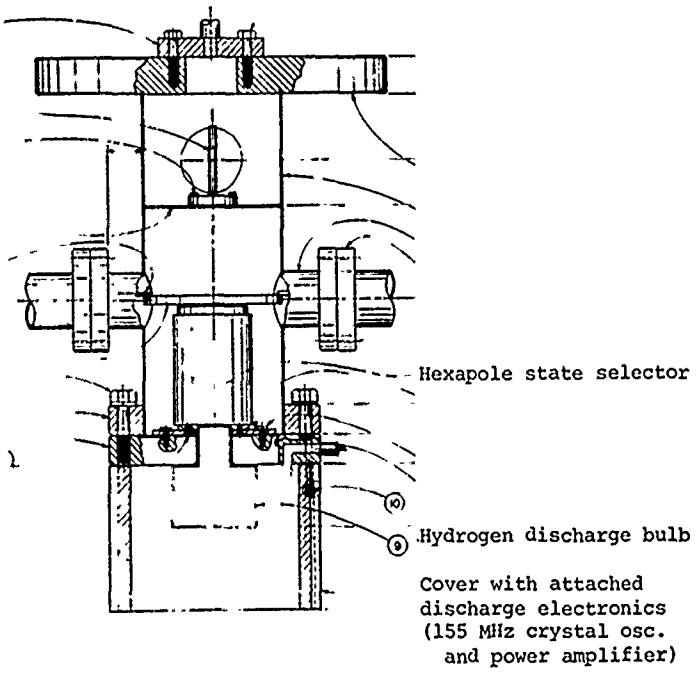

Fig. 10. Mechanical details of source and vacuum system.

Fig. 11. Complete maser "physics package".

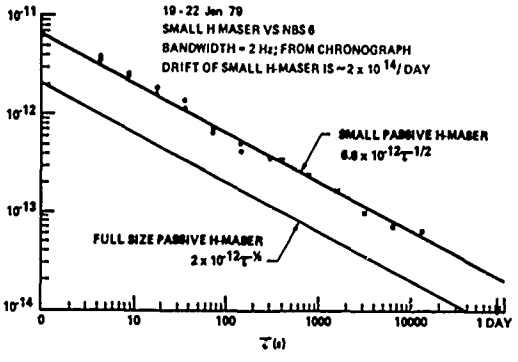

Fig. 12.
Frequency stability of small and full size passive masers.

"PASSIVE H MASER"

Giovanni Busca
Helmut Brandenberger

EBAUCHES S.A.
2000-NEUCHATEL(Switzerland)

Summary

The present work describes a new improved technique for the passive H servo loops consisting in the use of a single modulation frequency and phase discrimination for the separation of the cavity and H line error signals. The cavity resonance is interrogated with the "absorption lock" technique and the H resonance with the "dispersion lock" technique. Preliminary measurements of the frequency stability obtained by comparison of two passive H masers are also reported.

Introduction

In the past two modulation frequencies have been used for the servo control of the maser cavity tuning and the frequency lock to the atomic resonance.[1] The simultaneous use of two modulation frequencies leads to certain practical difficulties due to the interaction of the two control signals (Appendix I). The method described here overcomes these problems by using a single modulation frequency, an absorption lock for cavity tuning and a dispersion lock for the atomic resonance.

Absorption and Dispersion lock

In the passive H maser the error signals for the cavity and H line are derived from a direct detection of an R.F. spectrum. This situation is different from that occurring in other atomic frequency standards, like Cesium and Rubidium, which are based respectively on a direct or optical detection of atoms. Simple expressions for the error signal with RF detection, are not available and are given here. Following the typical frequency lock loop diagram, illustrated in Fig. 1, the resonance is interrogated by a pure single-tone phase modulated signal. The RF output is analysed by the envelope detector, the band-pass filter centered on the modulation frequency (ω_m), the phase sensitive detector and the integrator. For the more widely used frequency locks, the modulation frequency (ω_m) is less or approximately equal to the resonance half-width (γ) as shown in Fig. 2. We call this lock an "absorption lock", because the error signal is due to the interaction of the carrier and sidebands with the resonance. There are also some examples of frequency locks, like those used in superconducting cavity[2] or quartz resonators[3] frequency lock loops, which use a modulation frequency (ω_m) much greater than the resonance width (γ), as shown in Fig. 3. This has been called a "Dispersion Lock". In this case, only the carrier can interact with the resonance, while sidebands are unaffected. The resonance is detected by measuring the reflected signal.

Absorption lock

A simple mathematical analysis of the error signal can be made using the steady state or Fourier method, considering, for simplicity, only the carrier and the first sidebands of the interrogation signal, a square-law detector and a linear system. Alternatively the error signal can be obtained from inspection of the vector diagram shown in Fig. 4.

The error signal (E), after the envelope detector and the filter at frequency ω_m, is found to be :

$$E = 2xJ_o(m)J_1(m)\left[A_o\varepsilon(\omega_m)+D_o\lambda(\omega_m)\right] \qquad (1)$$

$$\varepsilon(\omega_m) = (A_+-A_-)\cos\omega_m t + (D_+ + D_-)\sin\omega_n t$$

$$\lambda(\omega_m) = (D_+-D_-)\cos\omega_m t - (A_+ + A_-)\sin\omega_m t$$

where $\varepsilon(\omega_m)$ and $\lambda(\omega_m)$ represent the AM contribution obtained by the projection of the rotating vectors, appearing in Fig. 4, respectively along the carrier and the quadrature component,

$J_o(m)$, $J_1(m)$ are Bessel functions representing the input signal $V = V_o \cos(\omega t + m \sin \omega_m t)$; A_o, A_+, A_- represent the real part of the normalized resonance response :

$$A(\omega) = \frac{\gamma^2}{\gamma^2+(\omega-\omega_o)^2} \qquad (2)$$

calculated respectively for the carrier frequency (ω), and the upper and lower sideband frequencies

$\omega + \omega_m$, $\omega - \omega_m$; D_o, D_+, D_- are values of the imaginary part of the resonance response :

$$D(\omega) = \frac{-\gamma(\omega - \omega_o)}{\gamma^2 + (\omega - \omega_o)^2} \qquad (3)$$

calculated for the same previous frequencies; γ and ω_o are respectively the resonance half-width and center frequency. The phase angle (θ) of the error signal (E), for near tuning condition and referred to cos $\omega_m t$, is given by :

$$\theta = \arctan \frac{2\gamma\omega_m}{\omega_m^2 - \gamma^2} \qquad (4)$$

For small error, differentiation of eq.(1) with respect to the modulation frequency ω_m, shows that maximum error signal is obtained when :

$$\omega_m \approx \gamma \qquad (5)$$

and the maximum error signal is :

$$E = 2\, J_o(m) J_1(m) \cdot \frac{\omega - \omega_o}{\gamma} \qquad (6)$$

The inconveniences of this type of lock are evident for H line-width of about 1 Hz. The limitation $\omega_m \leqslant \gamma$ implies long servo time constant and imposes severe restrictions on the flicker of phase noise generally present in the electronics at this low modulation frequency.

Dispersion lock

For a general dispersion lock (i.e. $\omega_m >> \gamma$) and resonance detection in reflection mode, the reflected signal is properly described by :

$$R = J_o A_o \left[\cos \omega t + D_o \sin \omega t\right] + J_1 \cos(\omega+\omega_m)t - J_1 \cos(\omega+\omega_m)t \qquad (7)$$

After detection and filtering the error signal (E) is given by :

$$E = 2\, J_o(m) J_1(m) D_o \approx 2\, J_o(m) J_1(m) \frac{\omega - \omega_o}{\gamma} \qquad (8)$$

The same result can be obtained by an analysis of the vector model shown in Fig. 5. The main advantages of this technique are : no upper limit for the modulation frequency (ω_m), possibility of fast servo loop also with very narrow resonance, flicker free electronics due to the high modulation frequency allowed and wider servo acquisition range associated with the broad response of the dispersion curve.

H Dispersion lock

Passive H maser response to a monochromatic input. The general idea of absorption and dispersion lock can be applied to the passive H maser. However we cannot use simple response functions as those illustrated by eq. 2, and 3. A quantum-mechanical calculation is needed. We start from a system of differential equations describing the R.F. field in the cavity (F), the population difference (W) and the coherence (M) of a two level system.[4] We calculate the total response (cavity + atoms) to a monochromatic input signal of amplitude βr_0 and frequency ω, by solving the system :

$$\Gamma_2 M = i\, b\, W\, F$$
$$\Gamma_2 F = -ibM + \beta r_0$$
$$W = \frac{I}{\gamma_1}\left(M^* F - M F^*\right) \qquad (9)$$

where, following mostly the notations given in reference (4),

$\Gamma_2 = \gamma_2 - i(\omega - \omega_a)$, $\Gamma_c = \beta - i(\omega - \omega_c)$, γ_2 is the transverse relaxation rate corresponding to the resonance half-width γ used previously, γ_1 is the longitudinal relaxation rate, ω_a is the atomic resonance frequency, β and ω_c are respectively the cavity half-width and resonant frequency, I is the beam flux in the upper energy level of the H atom and b is defined by the Rabi frequency bF. The solution of the system (9) gives the steady state value for the complex field F in the cavity :

$$F = \frac{\Gamma_2 \beta r_0}{\Gamma_2 \Gamma_c - b^2 W} \qquad (10)$$

where

$$W = \frac{I/\gamma_1}{1 + s(\omega)} \qquad (11)$$

and $s(\omega)$, the saturation parameter is defined by :

$$s(\omega) = \frac{4b\, F\, F^*}{\gamma_1 \gamma_2} \cdot \frac{\gamma_2^2}{\gamma_2^2 + (\omega - \omega_a)^2} \qquad (12)$$

It is convenient to write eq. 11 in the form :

$$W = Z \frac{\beta \gamma_2}{b^2} \qquad (13)$$

where Z = 1 corresponds to the oscillation limit and Z < 1 to the passive maser operation. From eq.13, Z has the meaning of a normalized population difference. Solving for the real and the imaginary part of F ($F = A_r + iA_i$), we obtain :

$$A_r = \frac{\gamma_2^2(1-Z) + (\omega - \omega_a)\left[\omega - \omega_a + \frac{\gamma_2}{\beta}(\omega - \omega_c)\right]}{\left[\gamma_2(1-Z)\right]^2 + \left[\omega - \omega_a + \frac{\gamma_2}{\beta}(\omega - \omega_c)\right]^2} \cdot r_0 \qquad (14)$$

and

$$A_i = \frac{\gamma_2\left[(\omega - \omega_a)Z + \frac{\gamma_2}{\beta}(\omega - \omega_c)\right]}{\left[\gamma_2(1-Z)\right]^2 + \left[\omega - \omega_a + \frac{\gamma_2}{\beta}(\omega - \omega_c)\right]^2} \cdot r_0 \qquad (15)$$

A_r and A_i represent respectively the in phase and quadrature response of the cavity + atoms system to the monochromatic excitation.

Passive H maser response to single-tone phase modulated signal. Supposing a modulation frequency (ω_m) much higher than γ_2 and of the order of β, we realise the conditions for an absorption lock for the cavity resonance and a dispersion lock for the H resonance. The calculation reproduces the eq. (1) in which A_o and D_o are now replaced by the real and the imaginary part of the total (cavity + atoms) response, i.e. A_r and A_i given by the eqs (14, 15) calculated for the carrier frequency. The error signal (E) can be written in a more convenient form, as :

$$E = 2J_o(m)J_1(m)r_o\left[A_r(\omega)\varepsilon(\omega_m)+A_i(\omega)\lambda(\omega_m)\right] \qquad (16)$$

The quantity ε is sensitive to the cavity tuning and λ, on the contrary is practically independent of the cavity tuning. The first term $2xJ_o(m)J_1(m)A_r(\omega)\varepsilon(\omega_m)r_o$ constitutes the cavity error signal and appears with a phase angle θ_c, referred to cos $\omega_m t$, given by :

$$\theta_c = \arctan \frac{\beta^2 - \omega_m^2}{2\beta\omega_m} \quad , \qquad (17)$$

the term $2x\ J_o(m)J_1(m)A_i(\omega)\lambda(\omega_m)r_o$ is the H dispersion error signal and his phase angle θ_H is given by :

$$\theta_H = \arctan \frac{\beta}{\omega_m} \qquad (18)$$

The phase difference beetwen the two phase angle θ_H and θ_c is exactly 90^0 for a modulation frequency ω_m given by :

$$\omega_m = \frac{\beta}{\sqrt{3}} \qquad (19)$$

System realisation

Using two synchronous detectors driven in quadrature after the filter at the single modulation frequency ω_m, we can separate the two error signals for cavity and H lines. A maximum independence of the two servos will be obtained for $\omega_m = \frac{\beta}{\sqrt{3}}$ from eq. (19). A single modulation frequency and phase discrimination of the error signals is, in our opinion, the best answer to the passive H maser problem. This system is illustrated in Fig. 6. The H dispersion lock will maintain a zero value for the numerator A_i (in eq.15) and the carrier frequency ω will be given by:

$$\omega - \omega_a = + \frac{1}{Z} \frac{\gamma_2}{\beta} (\omega_c - \omega) \quad ; \qquad (20)$$

this equation represents the normal cavity pulling multiplied by the factor $\frac{1}{Z}$.

The parameter Z can be defined alternatively from the voltage gain (G) at the H resonance frequency (eventually displaced by the cavity pulling) :

$$G = \frac{1}{1-Z} \qquad (21)$$

A typical value of the gain at resonance is 2, which corresponds t a cavity pulling factor $\frac{1}{Z} = 2$.

Experimental results

Two Masers of traditional type where converted to passive operation using the single modulation technique. These masers have a full size quartz cavity operating on a TE_{011} mode and are equipped with 3 coupling loops, two for transmission measurements and one for cavity frequency control by a varactor. The typical parameters of the two masers in passive operation are listed in table I.

TABLE I

Passive masers typical parameters

Cavity Q	33 000
Cavity temp. coeff.	≃ 300 Hz/°C
Coupling parameter (β)	0.1 ÷ 0.3
Output power	≃ 5×10^{-14} W
H line-width	0.7 Hz
Voltage gain	2
Density dependent shift	< 5×10^{-13} for flux change of 50 %
Power shift	< 5×10^{-13} for microw. power change of 3 dB
Modulation frequency ($\omega_m \simeq \frac{\beta}{\sqrt{3}}$)	≃ 12 kHz

The H servo loop time constant was typically less than 1 second and the cavity servo loop time constant was few seconds. The system used for the measurements of the frequency stability is shown in Fig. 7 and the experimental results obtained are illustrated in Fig. 8. These results are very close to the predictions based on the measurements of the spectral density of the amplitude fluctuations (S_ε) of the signal after the envelope detector. Experimentally we found $S_\varepsilon = 2 \times 10^{-7} x f^0$, which produces an equivalent reference noise of approximately $\sigma_y(\tau) = 2 \times 10^{-13} \times \tau^{-\frac{1}{2}}$. This figure can be obtained from the theoretical slope of the H dispersion which corresponds typically to an AM modulation index of $\simeq 2 \times 10^{-4}$ for a relative frequency deturning of 1×10^{-13}. Further work is in progress for extending the frequency stability measurements to longer averaging times.

Appendix

The two modulation system previously used[1] with the intention of realising two absorption locks, one, at the frequency $\omega_{m,c} \simeq \beta$, for the cavity and one, at the frequency $\omega_{m,H} \simeq \gamma_2$, for the H line, suffers from the fact that the cavity error signal is greatly dominated by the H signal. A calculation gives, in first approximation, for the true cavity error signal (E_c):

$$E_c = 2J_o^2(m_1)J_o(m_2)J_1(m_2)r_o\left[A_r(\omega)\varepsilon(\omega_{m,c}) + A_i(\omega)\lambda(\omega_{m,c})\right] \quad , \qquad (22)$$

for the H line error signal (E_H) :

$$E_H = 2J_o(m_1)J_o^2(m_2)J_1(m_1)r_o\left[A_r(\omega)\varepsilon_H(\omega_{m,H}) + A_i(\omega)\lambda_H(\omega_{m,H})\right] \qquad (23)$$

and for the spurious signal (E_s), on the cavity error signal :

$$E_s = 2J_o(m_1)J_o(m_2)J_1(m_1)J_1(m_2)r_o\left[\varepsilon(\omega_{m,c})\,\varepsilon_H(\omega_{m,H}) + \lambda(\omega_{m,c})\lambda_H(\omega_{m,H})\right] \quad , \qquad (24)$$

where m_1 and m_2 refer respectively to the phase modulation index for cavity and H lines interrogation, ε and λ are defined by eq. 1 and are calculated at $\omega_{m,c}$, ε_H and λ_H are equivalent expressions for the total response of the cavity + atoms evaluated for $\omega_{m,H}$. The spurious signal exist also for a tuned carrier (i.e. $A_i = 0$ and $\varepsilon_H = 0$) and a tuned cavity (i.e. $\varepsilon = 0$). It consists of two strong sidebands adjacent to the cavity signal. Theoretically the mean value of the spurious signal can be averaged to zero. However the peak value of this signal is several order of magnitude higher than the true signal and the process of averaging to a zero value requires equivalent conditions on the phase detector symetry, which could be unrealistic.

Acknowledgment

We gratefully acknowledge the collaboration of all the members of the Groupe des Etalons de Fréquence, in particular the contribution of Fr. Addor and L. Prost for several parts of the electronics. Thanks are also due to C. Menoud of the Laboratoire Suisse de Recherches Horlogères (LSRH) for his work on the physics part of the masers.

References

1. F.L. Walls and H. Hellwig,
   Proc. 30th Ann. Symp. on Freq.Control 473, 1976

   F.L. Walls and D.A. Howe,
   Proc. 32th Ann. Symp. on Freq.Control 492, 1978

2. S.R. Stein and J.P. Turnover,
   Proc. 27th Ann. Symp. on Freq.Control 414, 1973

3. F.L. Walls and S.R. Stein,
   IEEE Trans. Instrum. Meas. 27, 249,1978

4. J.H. Shirley
   AM. J. of Physics 36, 949, 1968.

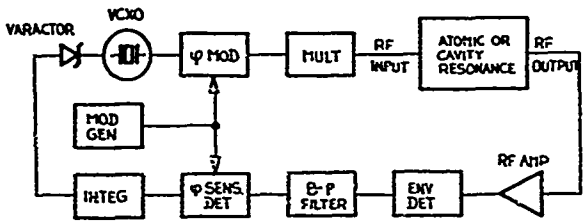

Fig. 1. General Frequency lock loop diagram for the passive H maser.

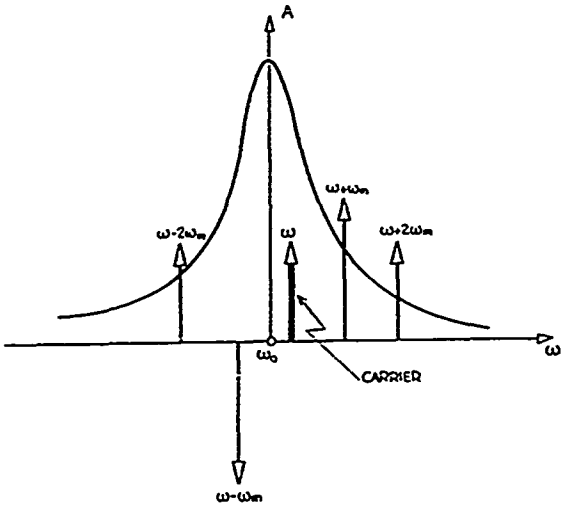

Fig. 2. Representation of signals for the "Absorption lock".

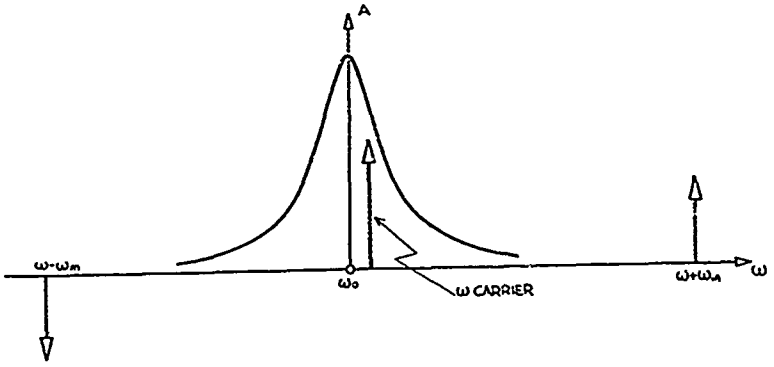

Fig. 3. Representation of the signal for the "Dispersion lock".

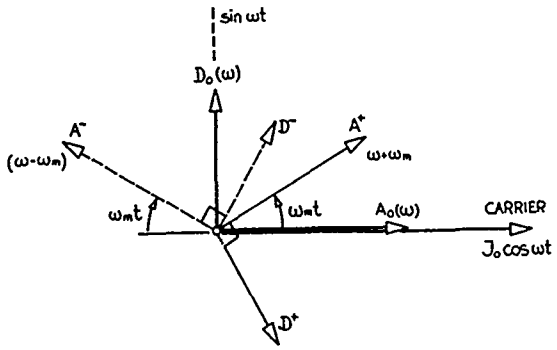

Fig. 4. Vector diagram allowing the calculation of the error signal for the "Absorption lock". The quantities are defined in the text.

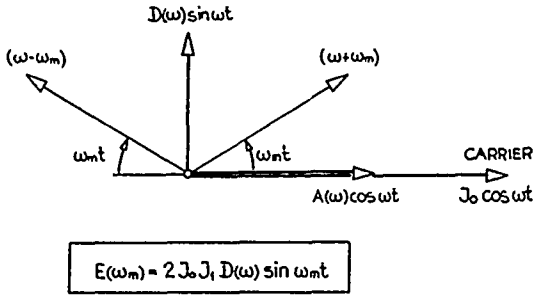

Fig. 5. Vector diagram allowing the calculation of the error signal for the "Dispersion lock"

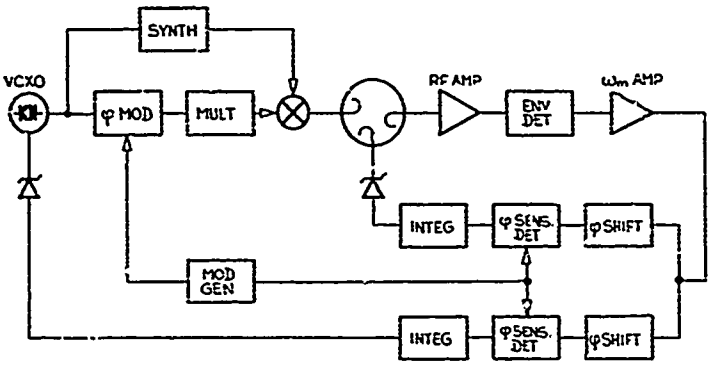

Fig. 6. Single modulation technique block diagram.

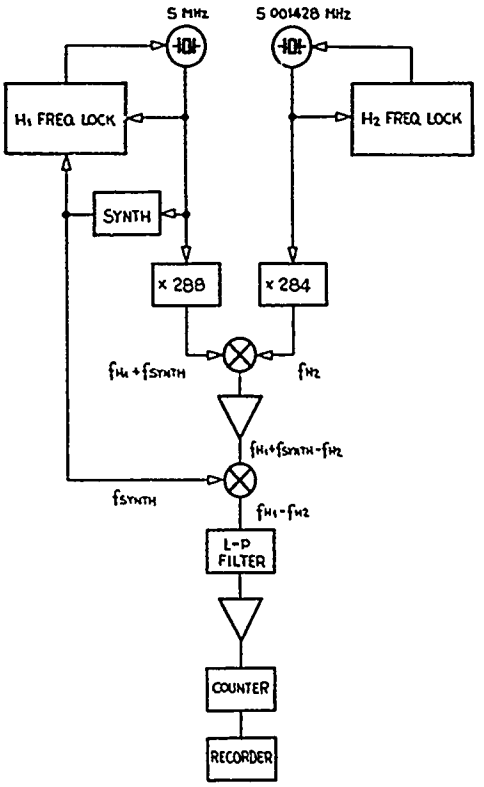

Fig. 7.

System for the measurements of the frequency stability.

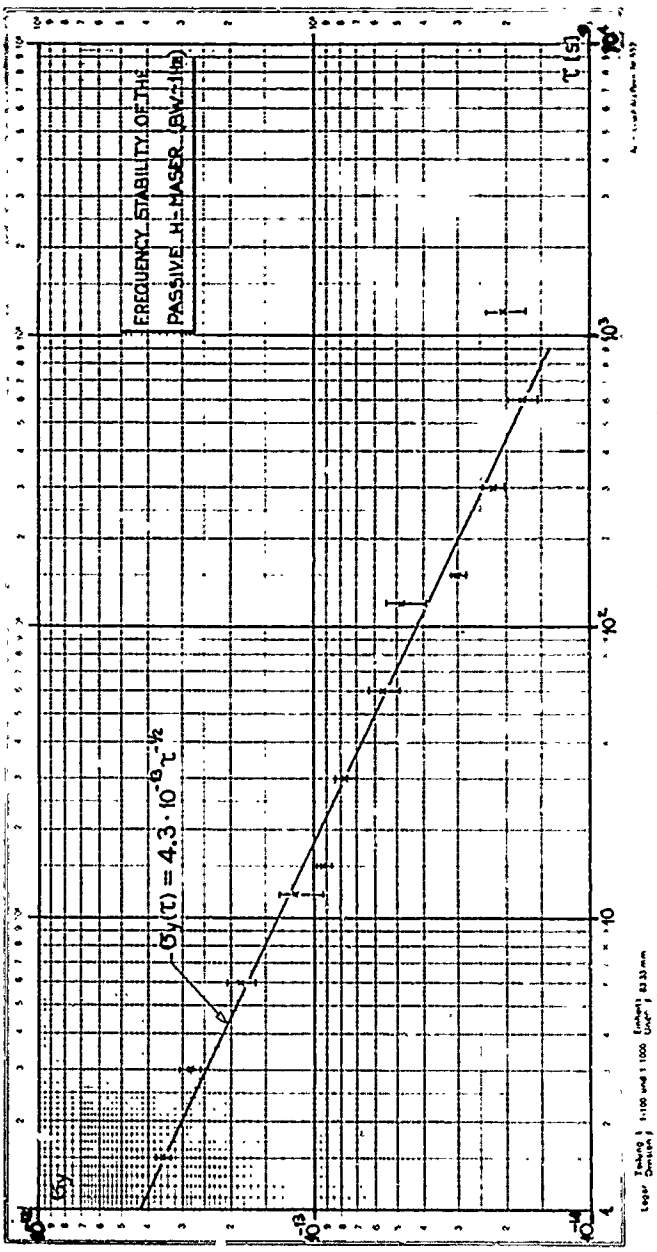

Fig. 8. Frequency stability obtained by comparison of two passive H masers.

PRECISION FREQUENCY CONTROL AND SELECTION

A Bibliography

E. A. GERBER
US Army Electronic Technology and Devices Laboratory (ERADCOM)
Fort Monmouth, New Jersey 07703

The bibliography covers the years 1966-1978. A total of over 3,000 references were found for this period using Science Abstracts A and B and studying the major journals, the Proceedings of the Frequency Control Symposium, sponsored by the US Army Electronic Research and Development Command. This bibliography, together with the index to the Proceedings of the Frequency Control Symposium, published in the Proceedings of 1976, should furnish a complete survey of the literature in this field.

The attribute "Precision" in the title of this bibliography is restricting the contents to papers on those devices whose Q-value and frequency stability far exceed that of an ordinary LC circuit. Consequently, the reader will not find papers on ceramic resonators and ceramic filters listed in this bibliography. Material on polycrystalline and similar devices will only be included if it has some bearing on the behavior of high Q devices, for instance on the theory of vibration of anisotropic bodies. On the other hand, superconductive LC devices with their high Q are included in this bibliography.

Another remark pertaining to the selection of references for acoustic resonators and devices is pertinent. The main application of bulk wave monocrystalline devices lies in the area of frequency control and selection, whereas surface wave devices are being used in many other fields. Therefore, papers on the fundamental properties of bulk wave devices are included to a fuller extent. As far as surface wave monocrystalline devices are concerned, only such papers are included which treat those aspects of their material and resonator properties which are considered pertinent for the application to precision control and selection.

In the area of microwave frequency and time standards, obviously only references on gaseous masers are included. On the other hand, an excessive number of references may be found in the area of laser frequency standards. It is thought that, in this new and proving field, valuable information may be found in papers on gas lasers that are not directly concerned with frequency standards.

The bibliography is organized in terms of 4 main divisions and 16 chapters as follows:

1. Acoustic Resonators and Devices
   - 1.1 Properties of Natural and Synthetic Piezoelectric Crystals and Materials
     - 1.1.1 Quartz
   - 1.2 Theory and Properties of Piezoelectric Resonators and Waves
     - 1.2.1 Bulk Acoustic Waves (BAW) and Resonators
     - 1.2.2 Surface Acoustic Waves (SAW) and Resonators
   - 1.3 Radiation Effects on Resonators
   - 1.4 Resonator and Devices Technology
   - 1.5 Piezoelectric and Electromechanical Filters
     - 1.5.1 Bulk Acoustic Wave Filters
     - 1.5.2 Surface Acoustic Wave Filters
       - 1.5.2.1 SAW Bandpass and Bandstop Filters
   - 1.6 Stability, Reliability and Aging of Resonators
   - 1.7 Resonator and Device Measurement and Specifications
   - 1.8 Precision Oscillators
     - 1.8.1 Bulk Acoustic Wave Oscillators
     - 1.8.2 Surface Acoustic Wave Oscillators
     - 1.8.3 Frequency Standards and Clocks (other than Quantum Devices)
   - 1.9 Temperature Control and Compensation
2. Quantum Electronic Devices and Standards
   - 2.1 Microwave Frequency and Time Standards
     - 2.1.1 (Passive) Beam Standards
     - 2.1.2 Gas Cell Standards
     - 2.1.3 Hydrogen Maser
     - 2.1.4 Other Gas Masers
   - 2.2 Laser Frequency Standards
     - 2.2.1 He-Ne Lasers
     - 2.2.2 Other Laser Standards

3. Other Topics

3.1 Frequency and Time, Their Measurement and Stability
3.1.1 Digital Measurements

3.2 Frequency and Time Coordination, Comparison and Distribution

3.3 Other Means for Precision Frequency Control

3.4 Applications

3.5 Miscellaneous

4. Anonymous/Unknown Authors

Adachi, M., Kawabata, A.
"Piezoelectric Properties of Potassium Tantalate-Niobate Single Crystal", Jap. J. Appl. Phys. (Japan), Vol 11, No. 12, p. 1855 (Dec. 1972).

Arlt, G., Quadflieg, P.
"Piezoelectricity in III-V Compounds with a Phenomenological Analysis of the Piezoelectric Effect", Phys. Status Solidi (Germany), Vol. 25, No. 1, p. 323-30 (1968).

Adhav, R. S.
"Piezoelectric Effect in Tetragonal Crystals", J. Appl. Phys. (USA), Vol 46, No. 6, p. 2803 (Jan. 1975).

Avdienko, K. I., Bogdanov, S. V., Kidyarov, B. I., Semenov, V. I., Sheloput, D. V.
"Optical, Acoustic, and Piezoelectric Properties of α- $LiIO_3$ Crystals", (Inst. of Phys. of Semiconductors, Acad. of Sci., USSR). Bull. Acad Sci, USSR, Phys. Ser. (USA), Vol. 41, No. 4, p. 40-5 (1977). Translation of: Izv. Akad. Nauk SSSR Ser. Fiz, Vol. 41, No. 4, p. 700-6 (1977). (Proceedings of the 1st Soviet-Japanese Symposium on Ferroelectricity, Novosibirsk, USSR, 30 Aug - 3 Sept. 1976).

Avdienko, K. I., Kidyarov, B. I., Sheloput, D. V.
"Growth of α-$LiIO_3$ Crystals of High Piezoelectric and Optical Quality", (Inst. of Semiconductor Phys., Acad. of Sci., Novosibirsk, USSR). J. Cryst. Growth (Netherlands), Vol. 42, p. 228-33 (Dec. 1977). (Fifth International Conference on Crystal Growth, Cambridge, MA, USA, 17-22 July 1977).

Ballman, A. A., Rudd, D. W.
"Czochralski Growth of Ferroelectric Lithium Tantalate for Piezoelectric Filter Devices", Second National Conference on Crystal Growth (abstracts only), Princeton, N. J., USA, 30 July - 3 Aug. 1972 (USA: American Assoc, Crystal Growth 1972), p. 110.

Barsch, G. R.
"X-Ray Determination of Piezoelectric Constants", (Dept. of Phys., Pennsylvania State Univ., University Park, PA, USA). Acta Crystallogr. A (Denmark), Vol. A32, Pt 4, p. 575-86 (1 July 1976).

Barybin, A. A.
"A Theorem for the Kinetic Power of the Charge Carrier Motion in Piezoelectric Crystals", Radiotekhnika i Elektronika (USSR) Vol. 12, No. 10, 1842-4 (Oct 1967). In Russian. English translation in: Radio Engrg. Electronic Phys. (USA).

Battaglia, A., Della Croce, U.
"Apparatus for Determining the Piezoelectricity of Crystalline Powders", (Laboratorio Fisica Atomica Molecolare Consiglio Nazionale Ricerche, Pisa, Italy). Alta Freq. (Italy), Vol. 41, No. 5, p. 375-8 (May 1972).

Belikova, G. S., Pisarevskii, Yu. V., Sil'vestrova, I. M.
"Piezoelectric and Elastic Properties of Crystals of Rubidium Biphthalate", (Inst. Crystallography, Acad. Sci., USSR). Sov. Phys.-Crystallogr. (USA), Vol. 19, No. 4, p. 545-6 (Jan.-Feb. 1975). Translation of: Kristallografiya (USSR), Vol. 19, p. 878-9 (July-Aug. 1974).

Booyens, H., Vermaak, J. S., Proto, G. R.
"Dislocations and the Piezoelectric Effect in III-V Crystals", (Phys. Dept., Univ. of Port Elizabeth, Port Elizabeth, S. Africa). J. Appl. Phys. (USA), Vol. 48, No. 7, p. 3008-13 (July 1977).

Brandle, C. D., Miller, D. C.
"Czochralski Growth of Large Diameter $LiTaO_3$ Crystals", (Bell Labs., Murray Hill, N. J., USA). J. Cryst. Growth (Netherlands), Vol. 24-25, p. 432-6 (Oct. 1974). (Proceedings of the 4th International Conference on Crystal Growth, Tokyo, Japan, 24-29 March 1974).

Chen, P. J., Montgomery, S. T.
"Boundary Effects on the Normal-Mode Response of Linear Transversely Isotropic Piezoelectric Materials", (Sandia Labs., Albuquerque, NM, USA). J. Appl. Phys. (USA), Vol. 49, No. 2, p. 900-4 (Feb. 1978).

Chowdhury, K. L. Glockner, P. G.
"Constitutive Equations for Elastic Dielectrics", (Dept of Math., Simon Fraser Univ., Burnaby, BC, Canada). Int. J. Non-Linear Mech. (GB), Vol. 11, No. 5, p. 315-24 (1976).

Cousins, C. S. G.
"Standard Choice of Axes for Crystal Class $\bar{6}$m2, with Reference to Elastic and Piezoelectric Properties", (Univ. Exeter, England). J. Phys. C. (GB), Vol. 5, No. 16, p. L201-3, (21 Aug. 1972).

Crisler, D. F., Cupal, J. J., Moore, A. R.
"Dielectric, Piezoelectric, and Electromechanical Coupling Constants of Zinc Oxide Crystals", Proc. Inst. Elect. Electronics Engrs. (USA), Vol. 56, No. 2, p. 225-6 (Feb. 1968).

Cross, L. E., Newnham, R. E.
"Ferroelectric, Piezoelectric, and Electroptic Materials", (Pennsylvania State Univ., University Park, USA). In book: Digest of Literature on Dielectrics, Vol. 34, 1970, p. 374-432, Washington, D.C., USA: National Academy of Sciences (1972), xi+515 pp.

Czechowska, Z., Weiss, K.
"Elastic Surface Waves in Piezoelectric Materials", (Osrodek Baden Jakosci Normalizacji, Poland). Elektronika (Poland), Vol. 15, No. 9, p. 383-7 (1974).

de Jong, M.
"Materials with Stronger Piezoelectric Properties", (N. V. Phillips' Gloeilampenfabrieken, Eindhoven, Netherlands). Ingenieur (Netherlands), Vol. 83, No. 23, p. E65-74 (11 June 1971). In Dutch.

Deshmukh, K. G., Ingle, S. G.
"Optical and Etching Studies on Single Crystals of Potassium Niobate", (Visvesvaraya Regional Coll. Engng., Nagpur, India). Indian J. Pure and Appl. Phys., Vol. 10, No. 12, p. 881-4 (Dec. 1972).

Dokmeci, M. C.
"Variational Principles in Piezoelectricity", (Northwestern Univ., Evanston, Ill., USA). Lett. Nuovo Cimento (Italy), Vol. 7, Ser. 2, No. 11, p. 449-54 (14 July 1973).

Firsova, M. M.
"Piezoelectric and Elastic Properties of Hexagonal α -ZnS.", (M. V. Lomonosov Moscow State Univ., USSR). Sov. Phys.-Solid State (USA), Vol. 16, No. 2, p. 350-1 (Aug. 1974).

Fukuda, T., Hirano, H.
"Growth and Characteristics of $LiNbO_3$ Plate Crystals", (Toshiba Res. & Dev. Center, Tokyo Shibaura Electric Co. Ltd., Kawasaki, Japan). Mater. Res. Bull. (USA), Vol. 10, No. 8, p. 801-6 (Aug. 1975).

Gavrilyachenko, V. G., Fesenko, E. G.
"Piezoelectric Effect in Lead Titanate Single-Crystals", Kristallografiya (USSR), Vol. 16, No. 3, p. 640-1 (1971). In Russian, English translation in: Sov. Phys. Crystallogr. (USA)

Graham, R. A.
"Strain Dependence of the Piezoelectric Polarization of Z-Cut Lithium Niobate", (Sandia Labs., Albuquerque, N. Mex., USA). Solid-State Commun. (USA), Vol. 12, No. 6, p. 503-6 (15 March 1973).

Graham, R. A.
"Linear and Nonlinear Piezoelectric Constants Quartz, Lithium Niobate and Lithium Tantalate", (Sandia Labs., Albuquerque, N. Mex., USA). Satellite Symposium of the 8th International Congress on Acoustics on Microwave Acoustics, Lancaster, England, 31 July - 2 Aug. 1974 (Lancaster, England: Univ. Lancaster 1974). p. 124-9.

Graham, R. A., Chen, P. J.
"A New Electrical to Mechanical Coupling Effect for Nonlinear Piezoelectric Solids", (Sandia Labs., Albuquerque, N. Mex., USA). Solid State Commun. (USA), Vol. 17, No. 4, p. 469-71 (15 Aug. 1975).

Graham, R. A.
"Second- and Third-Order Piezoelectric Stress Constants of Lithium Niobate as Determined by the Impact-Loading Technique", (Sandia Labs., Albuquerque, NM, USA). J. Appl. Phys. (USA), Vol 48, No. 6, p. 2153-63 (June 1977).

Greaves, R. W.
"The Piezoelectric Effect, Transducers and Their Applications", (Vibro-meter SA, Fribourg, Switzerland). Ferroelectrics (GB), Vol. 14, No. 1-2, p. 691 (1976). (3rd European Meeting on Ferroelectricity, Zurich, Switzerland, 22-26 Sept. 1976).

Hamid, S. A.
"Piezoelectric Properties of $Li_{1-x}H_xIO_3$", (Mineralogisches Inst., Tech. Univ. Hannover, Hannover, Germany). Phys. Status Solidi A (Germany), Vol. 43, No. 1, p. K29-30 (16 Sept. 1977).

Hartemann, P.
"Characteristics of Non-Crystalline Films Obtained by Implanting Ions in Piezoelectric Materials", (Lab. Central de Recherches Thomson, CSF, Orsay, France). Rev. Phys. Appl. (France), Vol. 12, No. 5, p. 843-8 (May 1977). In French. (Proceedings of the Meeting on Characterization of Non-crystalline Solids, Lyon, France, 8-10 Dec. 1976).

Haussühl, S.
"Piezoelectric and Electrical Behaviour of Lithium Iodate", Phys. Status Solidi (Germany), Vol. 29, No. 2, p. K159-62 (1968). In German.

Haussühl, S.
"Piezoelectric, Elastic and Optical Properties of O", (Univ. Koln, Germany). Z. Kristallogr. (Germany), Vol. 135, Nos. 3-4., p. 287-93 (July 1972). In German.

Holland, E. P.
"Accurate Method for Measuring Piezoelectric Coefficients", EerNisse, E., (Sandia Lab., Albuquerque, N.M., USA). IEEE Trans. Sonics Ultrasonics (USA), Vol. SU-16, No. 1 Suppl., p. 21 (Jan 1969). (1968 IEEE Ultrasonics Symposium, New York, USA, 25-27 Sep. 1968).

Iwasaki, H., Miyazawa, S., Yamada, T., Uchida, N., Niizeki, N.
"Single Crystal Growth and Physical Properties of $LiTaO_3$", Rev. Elec. Commun. Lab. (Japan), Vol. 20, Nos. 1-2, p. 129-37 (Jan.-Feb. 1972).

Jarzebski, Z. M.
"Review of Proposed Defect Structures in $LiNbO_3$", (Res. Center Crystals, Warsaw, Poland). Mater. Res. Bull. (USA), Vol. 9, No. 3, p. 233-40 (March 1974).

Jhunjhunwala, A., Vetelino, J. F., Field, J. C.
"Berlinite, A Temperature Compensated Material for Surface Acoustic Wave Applications", (Dept. of Electrical Engng., Univ. of Maine, Orono, ME, USA). 1976 Ultrasonics Symposium Proceedings, Annapolis, MD., USA, 29 Sept. - 1 Oct. 1976 (New York, USA: IEEE 1976). p. 523-7.

Jhunjhunwala, A., Vetelino, J. F., Field, J. C.
"Temperature Compensated Cuts with Zero Power Flow in Tl_3VS_4 and Tl_3TaSe_4", (Dept. of Electrical Engng., Univ. of Maine, Orono, ME, USA). Electron. Lett. (GB), Vol. 12, No. 25, p. 683-4 (9 Dec. 1976).

Jhunjhunwala, A., Field, J. C., Vetelino, J. F.
Berlinite, a Temperature-Compensated Material for Surface Acoustic Wave Applications", (Electrical Engng. Dept., Univ. of Maine, Orono, ME, USA). J. Appl Phys. (USA), Vol. 48, No. 3, p. 887-92 (March 1977).

Jipson, V.B., Vetelino, J.F., Jhunjhunwala, A., Field, J.C.
"Lithium Iodate - A New Material for Surface Acoustic Wave Applications". (Dept. of Electrical Engng., Univ. of Maine, Orono, ME, USA). Proc. IEEE (USA), vol 64, no. 4, p. 568-9 (April 1976)

Khromova, N. N.
"Elastic, Piezoelectric, and Dielectric Constants of Polydomain and Nonstoichiometric Crystals of Lithium Niobate", (Leningrad Inst. of Aviation Instrument Engng., Leningrad, USSR). Inorg. Mater. (USA), Vol. 11, No. 8, p. 1233-6 (Aug. 1975). Translation of Izv. Akad. Nauk. SSR Neorg. Mater. Vol. 11, No. 8, p. 1444-8 (Aug. 1975).

Kim, C. S., Yamanouchi, K., Karasawa, S., Shibayama, K.
"Temperature Dependence of the Elastic Surface Wave Velocity on $LiNbO_3$ and $LiTaO_3$", (Seoul Nat. Univ., Korea). Jap. J. Appl. Phys. (Japan), Vol. 13, No. 1, p. 24-7 (Jan. 1974).

Kimura, M., Doi, K., Nanamatsu, S., Kawamura, T.
"A new Piezoelectric Crystal $Ba_2Ge_2TiO_8$", (Nippon Electric Co. Ltd., Shimonumabe, Kawasaki). Appl. Phys. Lett. (USA), Vol. 23, No. 10, p. 531-2 (15 Nov. 1973).

Kiseley, D. F., Tirsova, M. M.
"Measurements of the Piezoelectric Coefficients of Lithium Niobate by the Interference Dilatometer Method", (MV Lomonosov Moscow State Univ., USSR). Sov. Phys. Solid State (USA), Vol. 15, No. 1, p. 198-9 (July 1973). Translation of: Fiz. Tverdogo Tela (USSR), Vol. 15, No. 1, p. 279-81 (Jan. 1973).

Kolb, E. D., Laudise, R. A.
"Hydrothermal Synthesis of Aluminum Orthophosphate", (Bell Labs, Murray Hill, NJ USA). 31st Annual Frequency Control Symposium, Atlantic City, NJ, USA, 1-3 June 1977 (Washington, DC, USA: Electronic Industries Assoc. 1977). p. 178-81.

Korobov, A. I., Lyamov, V. E.
"Nonlinear Piezoelectric Coefficients of $LiNbO_3$", (M.V. Lomonosov State Univ., Moscow, USSR). Sov. Phys. Solid State (USA), Vol. 17, No. 5, p. 932-3 Translation of: Fiz. Tverdogo Tela (USSR), Vol. 17, No. 5, p. 1448-50 (May 1975).

Korolyuk, A. P., Matsakov, L. Ya., Vasil'chenko, V. V.
"Determination of the Elastic and Piezoelectric Constants of Lithium Niobate Singic Crystals", Kristallografiya (USSR), Vol. 15, No. 5. p. 1028-32 (Sept. 1970).

Kosmodemianskii, A. S., Lozhkin, V. N.
"Generalized Plane Stress State of a Thin Piezoelectric Plate", Prikl. Mekh. (USSR). Vol. 13, No. 10. p. 75-9 (Oct. 1977). In Russian. English translation in: Sov. Appl. Mech. (USA).

Lissalde, F.
"X-Ray Determination of Piezoelectric Coefficients in Ferroelectric Crystals", (CNRS, Grenoble France). Beme Colloque International sur les Methodes analytiques par rayonnements X. (3rd International Symposium on X-Ray Analytical Methods), Nice, France, 16-20 Sept. 1974 (Issy-les-Moulineaux, France: Compaignie Generale de Radiologie 1974). p. 52-7 In French.

Lissalde, F., Peuzin, J. C.
"X-Ray Determination of Piezoelectric Coefficient in Lithium Niobate", (CNRS Lab. de Rayons, Grenoble, France). Ferroelectrics (GB), Vol. 14, No. 1-2, p. 579-82 (1976).

Ljamov, V. E.
"Nonlinear Acoustical Parameters of Piezoelectric Crystals", (Moscow State Univ. USSR). J. Acoust. Soc. Am. (USA), Vol. 52, No. 1, Pt. 2, p. 199-202 (July 1972).

Marculescu, L., Hauret, G.
"Study of the Brillouin Effect at Room Temperature in $LiNbO_3$", (Univ. Paris-Sud, Orsay, France). C. R. Hebd. Seances Acad. Sci. B (France), Vol 276, No. 13, p. 555-8 (26 March 1973). In French.

Mathur, S.S., Gupta, P. N.
"Higher Order Elastic Constants in Piezoelectric Crystals in the Presence of Ultrasonic Waves", (Indian Inst. Technol, Hauz Khas. New Delhi). Acustica (Germany), Vol. 23, No. 3, p. 160-4 (1970). In English.

Mathur, S. S., Gupta, P. N., Sharma, Y. P.
"Effect of Piezoelectricity on the Second Order Elastic Constants of Piezoelectric Crystals", (Indian Inst. Technol., Hauz Khas. New Delhi). Acustica (Germany), Vol. 24, No. 2, p. 108-10 (Feb. 1971).

McMahon, D. H.
"Acoustic Second-Harmonic Generation in Piezoelectric Crystals", (Sperry Rand Research Center, Sudbury, Massachusetts, USA). J. Acoust. Soc. Amer., Vol. 44, No. 4, p. 1007-13 (Oct. 1968).

Morency, D., Soluch, W., Harmon, D., Vetelino, J. F., Mittleman, D.
"Experimental Determination of the Saw Properties of X-Axis Boule Cuts in Berlinite", Department of Electrical Engineering, University of Maine, Orono, ME 04473. Ultrasonic Symposium Proceedings, Cherry Hill, NJ, USA, 25-27 Sept. 1978. (New York, USA: IEEE 1978), p. 594-597.

Nakagawa, Y., Yamanouchi, K., Shibayama, K.
"Third-Order Elastic Constants of Lithium Niobate", (Tohoku Univ., Sendai-shi, Japan). J. Appl. Phys. (USA), Vol. 44, No. 9, p. 3969-74 (Sept. 1973).

Nakazawa, M.
"Generalized Hooke's Law in Piezoelectric and Elastic Body", (Shinshu Univ., Nagano, Japan). J. Fac. Eng. Shinshu Univ. (Japan), No. 34, p. 147-53 (July 1973). In Japanese.

Nanamatsu, S., Doi, K., Takahashi, M.
"Piezoelectric, Elastic and Dielectric Properties of $LiGaO_2$ Single Crystal", NEC Res. & Dev. (Japan), No. 28, p. 72-9 (Jan. 1973).

Nasalski, W., Zorski, H.
"On the Equations of Classical and Quantrum Piezoelectricity", (Inst. of Fundamental Technol. Res., Polish Acad of Sci, Warsaw, Poland). Bull. Acad. Pol. Sci. Ser. Sci. Tech (Poland), Vol. 23, No. 6, p. 479-87 (1975).

Newnham, R. E., Miller, C. S., Cross, L. E., Cline, T. W.
"Tailored Domain Patterns in Piezoelectric Crystals", (Materials Res. Lab., Pennsylvania State Univ., University Park, PA, USA). Phys. Status Solidi A (Germany), Vol. 32, No. 1, p. 69-78 (16 Nov. 1975).

Newnham, R. E., Cross, L. E.
"Tailored Domains in Quartz and Other Piezoelectrics", (Materials Res. Lab., Pennsylvania State Univ., University Park, PA, USA). Proceedings of the 30th Annual Symposium on Frequency Control, Atlantic City, NJ, USA, 2-4 June 1976 (Washington, DC, USA: Electronic Industries Assoc. 1976), p. 71-7.

Nikiforov, L. G.
"Directed Search for New Piezoelectric Materials", (Rybinsk Aviation-Technol., Inst. of Rybinsk, USSR). Inorg. Mater. (USA), Vol. 13, No. 6, p. 872-4 (June 1977). Translation of Izv. Akad. Nauk SSSR Neorg. Mater., Vol. 13, No. 6, p. 1071-4 (June 1977).

O'Connell, R. M., Carr, P. H.
"New Materials for Surface Acoustic Wave (SAW) Devices", (RADC/AFSC, Hanscom AFB, MA, USA). Opt. Eng. (USA), Vol. 16, No. 5, p. 440-5 (Sept.-Oct. 1977).

O'Connell, R. M.
"Cuts of Lead Potassium Niobate, $Pb_2KNb_5O_{15}$, For Surface Acoustic Wave (SAW) Applications", (Rome Air Dev. Center, Hanscom AFB, MA, USA). J. Appl. Phys. (USA), Vol. 49, No. 6, p. 3324-7 (June 1978).

O'Connell, R. M., Carr, P. H.
"New Materials for Surface Acoustic Wave Devices", (Rome Air Development Center, Deputy for Electronic Technology, Hanscom AFB, MA, USA). Ultrasonic Symp. Proceedings, Cherry Hill, NJ, USA, 25-27 Sept. 1978. (New York, USA: IEEE 1978), p. 590-593.

Pajewski, W.
"New Piezoelectric Materials", Przeglad Elektron (Poland), Vol. 10, No. 2, p. 53-65 (1969). In Polish.

Picot, C.
"Piezoelectricity", Toute Electron. (France), No. 385, p. 27-32 (Feb. 1974). In French.

Rudd, D. W., Ballman, A. A.
"Growth of Lithium Tantalate Crystals for Transmission Resonator and Filter Devices", Western Electric Eng. (USA), Vol. 17, No. 2, p. 14-18 (April 1973).

Rusu, E.
"A Reciprocity Theorem and a Variational Theorem for Coupled Mechanical and Thermoelectric Fields in Piezoelectric Crystals", (Dept of Mech., Polytech. Inst., Jassy, Rumania). Bul. Inst. Politeh. Jasi I (Rumania), Vol. 21, No. 3-4, p. 85-8 (1975).

Scheiding, C., Schmidt, G.
"Piezoelectric d_{36} Coefficient of Gadolinium Molybdate", (Martin-Luther Univ., Halle,Germany). Phys. Status Solidi (Germany), Vol. 53, No. 2, p. K95-8 (1 Oct. 1972).

Schichl, H.
"Piezoelectric Materials for Electromechanical Filters", (Firma Standard Elecktrik Lorenz AG, Unternehmensgruppe Bauelemente, Germany). Nachrichtentech. Z. (NTZ) (Germany), Vol. 29, No. 4, p. 299-301 (April 1976). In German.

Shibayama, K.
"Some Aspects on $LiNbO_3$ Crystals for Surface Acoustic Wave Devices", (Res. Inst. of Electrical Communication, Tohoku Univ., Sendai, Japan). Bull. Acad. Sci. USSR, Phys. Ser. (USA), Vol. 41, No. 4, p. 19-23 (1977). Translation of: Izv. Akad. Nauk SSSR Ser. Fiz., Vol. 41, No. 4, p. 672-8 (1977). (Proceedings of the 1st Soviet-Japanese Symposium on Ferroelectricity, Novosibirsk, USSR, 30 Aug. - 3 Sept. 1976).

Shimura, F., Fiyino, Y.
"Crystal Growth and Fundamental Properties of $LiNb_{1-y}Ta_yO_3$". J. Cryst. Growth (Netherlands), Vol. 38, No. 3, p. 293-302 (June 1977).

Singh, K., Deshmukh, K. G.
"Surface Dendrite in Lithium Niobate Crystals", (Visvesvaraya Regional Coll. Engng., Nagpur, India). Mater. Res. Bull. (USA), Vol. 8, No. 10, p. 1139-41 (Oct. 1973).

Smith, R. T.
"Elastic, Piezoelectric and Dielectric Properties of Lithium Tantalate", Appl. Phys. Letters (USA), Vol. 11, No. 5, 146-8 (1 Sept. 1967).

Smith, R. T., Welsh, F. S.
"Temperature Dependence of the Elastic, Piezoelectric, and Dielectric Constants of Lithium Tantalate and Lithium Niobate", (Bell Telephone Labs. Inc., Allentown, PA., USA). J. Appl. Phys. (USA), Vol. 42, No. 6, p. 2219-30 (May 1971).

Sorge, G., Beige, H.
"Determination of the Piezocoefficients d_{mi} from the Frequency Dependence of the Dielectric Permittivity", (Martin Luther-Univ., Halle-Wittenberg, Halle/Saale, Germany). Exp. Tech. Phys. (Germany), Vol. 23, No. 5, p. 489-93 (1975).

Srinivasan, T. P.
"Invariant Piezoelectric Coefficients for Crystals", (Indian Inst. Technol., Madras). Phys. Status Solidi (Germany), Vol. 41, No. 2, p. 615-20 (1970).

Sugii, K., Iwasaki, H., Miyazawa, S., Niizeki, N.
"An X-Ray Topographic Study on Lithium Niobate Single Crystals", (Nippon Telegraph & Telephone Public Corp., Musashino-shi, Tokyo). J. Cryst. Growth (Netherlands), Vol. 18, No. 12, p. 159-66 (Feb. 1973).

Tamura, M., Yonezawa, M.
"Piezoelectric Ceramics for Acoustic Surface Wave Devices", (Tohoku Metal Industries Ltd., Japan), J. Acoust. Soc. Jap (Japan), Vol. 30, No. 10, p. 574-7 (Nov. 1974). In Japanese.

Viktorov, I. A., Zubova, O. M.
"Two Types of Surface Waves in Cubic Crystals", (Acoustics Inst., Acad of Sci., USSR). Sov. Phys.-Acoust. (USA), Vol. 20, No. 6, p. 556-7 (May-June 1975). Translation of: Akust. Zh. (USSR), Vol. 20, No. 6, p. 912-14 (Nov.-Dec. 1974).

Warner, A. W., Onoe, M., Coquin, G. A.
"Determination of Elastic and Piezoelectric Constants for Crystals in Class (3m)", J. Acoust. Soc. Amer., Vol. 42, No. 6, 1223-31 (Dec. 1967).

Weinert, R. W., Isaacs, T. J.
"New Piezoelectric Materials Which Exhibit Temperature Stability for Surface Waves", (Westinghouse Res. Labs., Pittsburgh, PA, USA). Proceedings of the 29th Annual Frequency Control Symposium, Fort Monmouth, NJ, USA, 28-30 May 1975 (Washington, DC, USA: Electronic Industries Assoc. 1975). p. 139-42.

Yakovlev, L. A., Kirov, E. A.
"Ultrasonic Method of Determining the Piezoelectric and Elastic Constants of Piezoelectric Materials", (Ul'yanov Leningrad Electrotechnical Inst., USSR). Zavod. Lab. (USSR), Vol. 37, No. 12, p. 1460-3 (Dec. 1971). In Russian. English translation in: Ind. Lab. (USA), Vol. 37, No. 12, p. 1881-4 (Dec 1971).

Yamada, T.
"Single-Crystal Growth and Piezoelectric Properties of Lead Potassium Niobate", (Nippon Telegraph & Telephone Public Corp., Musashino-shi, Tokyo, Japan). Appl. Phys. Lett. (USA), Vol. 23, No. 5, p. 213-14 (1 Sept 1973).

Yamada, T.
"Elastic and Piezoelectric Properties of Lead Potassium Niobate", (Nippon Telegraph & Telephone Public Corp., Musashino-shi, Tokyo, Japan). J. Appl. Phys. (USA), Vol. 46, No. 7, p. 2894-8 (July 1975).

Yamaguchi, S., Wada, H.
"Electron Diffraction Measuring Technique for the Investigation of the Pyro- or Piezoelectricity of Crystals", (Nat. Inst. Res., Bunkyo, Tokyo, Japan). Messtechnik (Germany), Vol. 79, No. 6, p. S135-6 (June 1971). In German.

Zelenka, J.
"Electromechanical Properties of Bismuth Germanium Oxide ($Bi_{12}GeO_{20}$)", (Electrotech. Dept., Coll. of Mech. & Textile Engng., Liberec, Czechoslovakia). Czech J. Phys. Sect. B (Czechoslovakia), Vol. B28, No. 2, p. 165-9 (1978).

1.1.1

Anderson, T. L., Newnham, R. E., Cross, L. E., Laughner, J. W.
"Laser-Induced Twinning in Quartz", (Materials Res. Lab., Pennsylvania State Univ., University Park, PA, USA). Phys. Status Solidi A (Germany), Vol. 37, No. 1, p. 235-45 (16 Sept. 1976).

Anderson, T. L., Newnham, R. E., Cross, L. E.
"Coercive Stress for Ferroelastic Twinning in Quartz", (Materials Res. Lab., Pennsylvania State Univ., University Park, PA, USA). 31st Annual Frequency Control Symposium, Atlantic City, NJ, USA, 1-3 June 1977 (Washington, DC, USA: Electronic Industries Assoc. 1977). p. 171-7.

Annaka, S., Nemoto, A.
"Piezoelectric Constants of α -quartz Determined from Dynamical X-Ray Diffraction Curves", (Tokyo Univ. of Mercantile Marine, Tokyo, Japan). J. Appl. Crystallogr. (Denmark), Vol. 10, pt 4, p. 354-5 (1 Aug. 1977).

Asahara, J., Takazawa, K., Yazaki, E., Okuda, J., Asanuma, N.
"Defects in Synthetic Quartz Crystals and their Influence on the Electrical Characteristics of Quartz Crystal Resonators", (Toyo Communication Equipment Co. Ltd., Tsukagoshi, Saiwai-ku, Kawasaki, Japan). Proceedings of the 28th Annual Frequency Control Symposium 1974, Atlantic City, NJ, USA, 29-31 May 1974 (Washington, DC, USA: Electronic Industries Assoc. 1974). p. 117-24.

Baranovskii, S. N., Panov, V. I.
"Effect of Uniaxial Compression on the Piezoelectric Modulus of Quartz", (Novosibirsk Electrical Engng. Inst., USSR). Sov. Phys.-Acoust (USA), Vol. 20, No. 1, p. 71-2 (July-Aug. 1974). Translation of: Akust. Zh. (USSR), Vol. 20, No. 1, p. 122-4 (Jan.-Feb. 1974).

Barns, R. L., Kolb, E. D., Key, P. L., Laudise, R. A., Simpson, E. E., Kroupa, K. M.
"Production and Perfection of 'R-Face' Quartz", (Bell Labs., Murray Hill, NJ, USA). Proceedings of the 29th Annual Frequency Control Symposium, Fort Monmouth, NJ, USA, 28-30 May 1975 (Washington, DC, USA: Electronic Industries Assoc. 1975). p. 98-104.

Barns, R. L., Kolb, E. D., Laudise, R. A., Simpson, E. E., Kroupa, K. M.
"Production and Perfection of 'Z-Face' Quartz", (Bell Labs, Murray Hill, NJ, USA). J. Cryst. Growth (Netherlands), Vol. 34, No. 2, p. 189-97 (July 1976).

Barns, R. L., Freeland, P. E., Kolb, E. D., Laudise, R. A., Patel, J. R.
"Dislocation-Free and Low-Dislocation Quartz Prepared by Hydrothermal Crystallization", (Bell Labs. Inc., Murray-Hill, NJ, USA). J. Cryst. Growth (Netherlands), Vol. 43, No. 6, p. 676-86 (July 1978).

Besson, R., Mesnete, P.
"Electrostriction of α- Quartz. New High Sensitivity Static Method for the Measurement of Electrostriction and Piezoelectric Coefficients of an α - Quartz Crystal Layer", C. R. Acad. Sci. Ser. B (France), Vol. 270, No. 16, p. 994-6 (20 April 1970). In French.

Besson, R.
"Measurement of Nonlinear Elastic, Piezoelectric, [and] Dielectric Coefficients of Quartz Crystal. Applications", (Univ. Besançon, France). Proceedings of the 28th Annual Frequency Control Symposium 1974, Atlantic City, NJ, USA, 29-31 May 1974 (Washington, DC, USA: Electronic Industries Assoc. 1974). p. 8-13.

Besson, R.
"Nonlinearity of the Direct Piezoelectric Effect of Quartz", (Ecole Nat. Sup. Chronometrie, Besançon, France). C.R. Hebd. Seances Acad. Sci. B. (France), Vol. 279, No. 13, p. 325-8 (23 Sept. 1974). In French.

Bottom, V. E.
"Measurement of the Piezoelectric Coefficient of Quartz Using the Fabry Perot Dilatometer", (McMurry Coll., Abilene, Tex., USA). Proceedings of the 23rd Annual Frequency Control Symposium, Atlantic City, NJ, USA, 6-8 May 1969 (Washington, DC, USA: Electronic Industries Assoc. 1969), p. 21-5.

Bottom, V. E.
"Measurement of the Piezoelectric Coefficient of Quartz Using the Fabry-Perot Dilatometer", (McMurry Coll., Abilene, Tex, USA). J. Appl. Phys. (USA), Vol. 41, No. 10, p. 3941-4 (Sept. 1970).

Bottom, V. E.
"Dielectric Constants of Quartz", (McMurry Coll., Abilene, Tex., USA). J. Appl. Phys. (USA), Vol. 43, No. 4, p. 1493-5 (April 1972).

Buisson, M. X., Regreny, M. A.
"Industrial Production of Synthetic Quartz Crystals", (SICN, Annecy, France). Colloque International sur les Materiaux pour les Components Electroneques (International Symposium on Materials for Electronic Components, Paris, France, 2-4 April 1975 (Paris, France: Comm. d'Organisation du Colloque de Paris 1975), p. 106-12. In French.

Capone, B. R., Kahan, A., Sawyer, B.
"Evaluation of Quartz for High Q Resonators", Programme of the 25th Annual Frequency Control Symposium (abstracts), Atlantic City, NJ, USA, 26-28 Apr. 1971 (Fort Monmouth, NJ., USA: US Army Electronics Command 1971), p. 22.

Ching, Ho-Chen, Yang, Kuan-Ch'i., Wang, Chun-Min, Chang Ching-Chu.
"Studies on Synthetic Quartz", Acta Electronica Sinca, No. 1, p. 127-36 (1965). In Chinese.

Conlee, L., Reifel, D.
"Analysis of Synthetic Quartz for Stringent Frequency Versus Temperature Applications", (Motorola Inc., Franklin Park, Ill., USA). Proceedings of the 28th Annual Frequency Control Symposium 1974, Atlantic City, NJ, USA, 29-31 May 1974 (Washington, DC, USA: Electronic Industries Assoc. 1974), p. 125-8

Fowles, R.
"Dynamic Compression of Quartz", J. Geophys. Res. (USA), Vol. 72, No. 22, 5729-42 (15 Nov. 1967).

Fukuyo, H., Oura, N., Shishido, F.
"The Quality Evaluation of Quartz by Measuring the Q-Value of the Second Overtone of a Y-Bar", (Tokyo Inst. of Technol., Tokyo, Japan). Bull. Tokyo Inst. Technol. (Japan), No. 131, p. 1-5 (1975).

Fukuyo, H., Oura, N., Shishido, F.
"A New Quality Evaluation Method of Raw Quartz by Measuring the Q-Value of Y-Bar Resonator", (Tokyo Inst. of Technol., Nagatsuta, Midoriku, Yokohama, Japan). 31st Annual Frequency Control Symposium, Atlantic City, NJ, USA, 1-3 June 1977 (Washington, DC, USA: Electronic Industries Assoc. 1977). p. 117-21.

Golan'sk, R., Kosecki, T.
"Synthetic Quartz in the Modern Manufacturing of Quartz Resonators", Elektronika (Poland), No. 1, p. 18-24 (1971). In Polish.

Graham, R. A., Halpin, W. J.
"Dielectric Breakdown and Recovery of X-Cut Quartz under Shock-Wave Compression", (Sandia Lab., Albuquerque, NM, USA). J. Appl. Phys. (USA), Vol. 39, No. 11, p. 5077-82 (Oct. 1968).

Graham, R. A.
"Strain Dependence of Longitudinal Piezoelectric, Elastic, and Dielectric Constants of X-Cut Quartz", (Sandia Labs., Albuquerque, NM, USA). Phys. Rev. B (USA), Vol. 6, No. 12, p. 4779-92 (15 Dec. 1972).

Hair, M. L.
"The Molecular Nature of Adsorption on Silica Surfaces", (Xerox Corp., Rochester, NY, USA). Proceedings of the 27th Annual Frequency Control Symposium, Cherry Hill, New Jersey, USA, 12-14 June 1973 (Washington, DC, USA: Electronic Industries Assoc. 1973), p. 73-8.

Hruska, K., Janik, L.
"Change in Elastic Coefficients and Moduli of α-Quartz in an Electric Field", Czech. J. Phys. B, Vol. 18, No. 1, 112-16 (1968).

Hruska, K., Kazda, V.
"The Polarizing Tensor of the Elastic Coefficients and Moduli for α-Quartz", Czech. J. Phys. B, Vol. 18, No. 4, 500-3 (1968).

Julian, C. L., Lane, F. O. Jr.
"Calculation of the Elastic Constants of Alpha Quartz from a Model", J. Appl. Phys. (USA), Vol. 39, No. 8, 3931-2 (July 1968).

Kolb, E. D., Nassau, K., Laudise, R. A.
"New Sources of Quartz Nutrient for the Hydrothermal Growth of Quartz", (Bell Labs., Murray Hill, NJ, USA), J. Cryst. Growth (Netherlands), Vol. 36, No. 1, p. 93-100 (Nov. 1976).

Krefft, G. B.
"Effects of High-Temperature Electrolysis on the Coloration Characteristics and OH-Absorption Bands in Alpha-Quartz", (Sandia Labs., Albuquerque, NM, USA). Radiat. Eff. (GB), Vol. 26, No. 4, p. 249-59 (1975).

Ludanov, A. G., Yakovlev, L. A., Fotchenkov, A. A.
"Variation of the Elastic Constants of Piezoelectric Quartz", (All-Union Sci.-Res. Inst. for Synthetics of Mineral Raw Materials, USSR). Sov. Phys.-Acoust. (USA), Vol. 22, No. 4, p. 343-4 (July-Aug 1976). Translation of: Akust. Zh. (USSR), Vol 22, No. 4, p. 612-13 (July-Aug. 1976).

Lynch, W. T.
"Calculation of Electric Field Breakdown in Quartz as Determined by Dielectric Dispersion Analysis", (Bell Labs., Murray Hill, NJ, USA). J. Appl. Phys. (USA), Vol. 43, No. 8, p. 3274-8 (Aug. 1972).

Mindlin, R. D., Toupin, R. A.
"Acoustical and Optical Activity in Alpha Quartz", (Columbia Univ., NY, USA). Programme of the 25th Annual Frequency Control Symposium (abstracts), Atlantic City, NJ, USA, 26-28 Apr 1971 (Fort Monmouth, NJ, USA: US Army Electronics Command 1971), p. 12.

Moriya, K., Ogawa, T.
"Observation of Growth Defects in Synthetic Quartz Crystals by Light-Scattering Tomography", (Dept. of Phys., Gakushuin Univ., Tokyo, Japan). J. Cryst. Growth (Netherlands), Vol. 44, No. 1, p. 53-60 (Aug. 1978).

Mullen, A. J.
"Temperature Variation of the Piezoelectric Constant of Quartz", (Bryn Mawr Coll., Pa., USA). J. App. Phys. (USA), Vol. 40, No. 4, p. 1693-6 (March 1969).

Nadatowska, B., Pacewicz, J.
"Structural Investigation of Quartz for Resonators", Prace Inst. Tele- & Radiotech. (Poland), Vol. 16, No. 1, p. 57-68 (1972). In Polish.

Park, D. S., Nowick, A. S.
"Dielectric Relaxation of Point Defects in α-Quartz", (Columbia Univ., New York, USA). Phys. Status Solidi A (Germany), Vol 26, No. 2, p. 617-26 (16 Dec. 1974).

Parpia, D. Y.
"Growth Sector Boundaries and their Influence on Quartz Resonator Performance", (Cavendish Lab., Cambridge Univ., Cambridge, England). J. Mater. Sci. (GB), Vol. 12, No. 4, p. 844-8 (April 1977).

Rabbetts, R. W. T.
"Man-Made Quartz Crystal", Elect. Commun. (USA), Vol. 42, No. 1, 73-83 (1967).

Regreny, A., Autmont, R.
"Hydrothermal Recrystallization of Quartz", Ann. Telecommun. (France), Vol. 25, No. 7-8, p. 294-306 (July 1970). In French.

Regreny, A.
"Hydrothermal Recrystallisation of Quartz and Characterisation with a View to Radioelectrical Applications", Ann. Telecommun. (France), Vol. 28, No. 3-4, p. 111-22 (1973).

Rudd, D. W., Fiore, A. R., Lias, N.C.
"Computerized Process Control for Synthetic Quartz Growth", (Western Electric Co., North Andover, Mass., USA). Proceedings of the 23rd Annual Frequency Control Symposium, Atlantic City, NJ, USA. 6-8 May 1969 (Washington, DC, USA: Electronic Industries Assoc. 1969), p. 171-7.

Sawyer, B.
"Q Capability Indications from Infrared Absorption Measurements for Na_2CO_3 Process Cultured Quartz", (Sawyer Res. Products Inc., Eastlake, Ohio, USA). IEEE Trans. Sonics & Ultrasonics (USA), Vol. SU-19, No. 1, p. 41-4 (Jan 1972).

Sherman, J. H. Jr.
"Characterization of Cultured Quartz for Use in Precision AT-Cut Quartz Resonators", (General Electric Co., Lynchburg, VA, USA). Proceedings of the 28th Annual Frequency Control Symposium 1974, Atlantic City, NJ, USA, 29-31 May 1974 (Washington, DC, USA: Electronic Industries Assoc. 1974), p. 129-42.

Shevel'ko, M. M., Yakoviev, L. A.
"Precision Measurements of the Elastic Characteristics of Synthetic Piezoelectric Quartz", (V. I. Yl'yanov Lenin Leningrad Inst. of Electrical Engng., Leningrad, USSR). Sov. Phys.-Acoust (USA), Vol. 23, No. 2., p. 187-8 (March-April 1977). Translation of: Akust Zh (USSR), Vol. 23, No. 2, p. 331-2 (March-April 1977).

Stern, R., Smith, R. T.
"On the Third-Order Elastic Moduli of Quartz", J. Acoust. Soc. Amer., Vol. 44, No. 2, 640-1 (Aug. 1968).

Suchanek, J.
"The Use of Infrared Absorption in the Comparison of Synthetic Quartz Quality", Cesk. Cas. Fis. A. (Czechoslovakia), Vol. 21, No. 4, p. 393-5 (1971). In Czech.

Uspyenskaya, A. B., Sobolev, G. A.
"The Piezoelectric Field of a Quartz Layer", Izv. Akad. Nauk. SSSR Fiz. Zemli. No. 4., P. 51-7 (April 1969). In Russian. English translation in: Izv. Acad Sci. USSR Phys. Solid Earth (USA), No. 4, p. 234-7 (1969).

Weil, J. A.
"The Aluminum Centers in α -Quartz", (Univ. Saskatchewan, Saskatoon, Canada). Proceedings of the 27th Annual Frequency Control Symposium, Cherry Hill, NJ, USA, 12-14 June 1973 (Washington, DC, USA: Electronic Industries Assoc. 1973), p. 153-6.

Weil, J. A.
"The Aluminum Centers in α -Quartz", (Dept. of Chem & Chem. Engng., Univ. of Saskatchewan, Saskatoon, Canada). Radiat. Eff. (GB), Vol. 26, No. 4, p. 261-5 (1975).

Yoda, H.
"Synthetic Crystals of Japan", (Nihon Dempa Kogyo Co. Ltd., Japan). JEE (Japan), No. 67, p. 41-8 (June 1972).

Yoda, H.
"Technical Aspects of Crystals from Material Cultivation to Finished Product", (Nihon Dempa Kogyo Co. Ltd., Japan). JEE (Japan), No. 79, p. 39-45 (June 1973).

Zakirova, A. D., Balitskii, V. S., Chuvyrov. A. N.
"Investigation of Optical and Piezoelectrical Properties of Quartz with Germanium Additions", Pis'ma V Zh. Tekh. Fiz. (USSR). Vol. 3, No. 22, p. 1206-8 (26 Nov 1977).

Balakirev, M. K., Gorchakov, A. V.
"Leakage of an Elastic Wave across a Gap between Piezoelectrics", (Inst. of Semiconductor Phys., Acad. of Sci., Novosibirsk, USSR). Sov. Phys.-Solid State (USA), p. 327-8 (Feb 1977). Translation of: Fiz. Tverdogo Tela (USSR), vol 19, No. 2, p. 571-2 (Feb. 1977).

Ballato, A.
"Bulk and Surface Acoustic Wave Excitation and Network Representation", (US Army Electronics Technol. & Devices Lab., Fort Monmouth, NJ). Proceedings of the 28th Annual Frequency Control Symposium 1974, Atlantic City, NJ, USA, 29-31 May 1974 (Washington, D.C., USA: Electronic Industries Assoc. 1974), p. 279-9

Camarero, E. G.
"Acousto-Electromagnetic Propagation Modes in Hexagonal Piezoelectric Crystals", (Dept. de Fisica Aplicada, Univ. Autonoma de Madrid, Madrid, Spain). An. Fis. (Spain), Vol. 72, No. 2, p. 138-44 (April-June 1976).

Datta, S., Hunsinger, B. J.
"Analysis of Line Acoustical Waves in General Piezoelectric Crystals", (Univ. of Illinois, Urbana, IL, USA). Phys. Rev B (USA), Vol. 16, No. 10, p. 4224-9 (15 Nov. 1977).

Epstein, S.
"Elastic-Wave Formulation for Electroelastic Waves in Unbounded Piezoelectric Crystals", (US Army Electronics Command Labs., Fort Monmouth, NJ, USA). Phys. Rev. B (USA), Vol. 7, No. 4, p. 1636-44 (15 Feb. 1973).

Feldmann, M.
"Piezoelectric Waves in Insulators", (CNET, Moulineaux, France). Onde Electr. (France), Vol. 53, No. 5, p. 189-93 (May 1973). In French.

Garcia-Camarero, E.
"Equations of Motion of Acousto-Electromagnetic Waves", (Dept. de Fisica, Univ. Automona de Madrid, Madrid, Spain). An. Fis. (Spain), Vol. 70, No. 3, p. 289-91 (July-Sept. 1974). In Spanish.

Goruk, W. S., Stegeman, G. I.
"Surface to Bulk Mode Conversion at Interfaces on Y-Z $LiNbO_3$", (Dept. of Phys., Univ. of Toronto, Toronto, Ontario, Canada). Appl. Phys. Lett (USA), Vol. 32, No. 5, p. 265-6 (1 March 1978).

Guslchenko, E. K.
"Acoustic and Electric Fields in a Piezoelectric Plate", Sov. Phys.-Acoust. (USA), Vol. 20, No. 4, p. 328-31, (Jan-Feb. 1975). Transl. of Akust. Zk. (USSR), Vol. 20, No. 4, p. 543-9 (July-Aug. 1974).

Hruska, K.
"Relation Between the General and the Simplified Condition for the Velocity of Propagation of Ultrasonic Waves in a Piezoelectric Medium", Czech. J. Phys. B, Vol. 18, No. 2, 214-21 (1968).

Jones, G. L., Henneke, E. G.
"Reflection of an Elastic Wave From a Free Surface in Quartz", (Virginia Polytech. Inst. & State Univ., Blacksburg, USA). Program of the 83rd meeting of the Acoustical Society of America, Abstracts only. Buffalo, New York, USA, 18-27 Apr. 1972 (New York, USA: Acoust. Soc. America 1972), p. 83-4.

Kagawa, Y., Yamabuchi, T.
"A Finite Element Approach to Electromechanical Problems with an Application to Energy-Trapped and Surface-Wave Devices", (Dept. of Electrical Engng., Nat. Univ. of Toyama, Takaoka Toyama, Japan). IEEE Trans. Sonics & Ultrason. (USA), Vol. SU-23, No. 4, p. 263-72 (July 1976).

Kessenikh, G. G., Shuvalov, L. A.
"Energy Flow and Group Velocity of Sound Waves in Piezoelectric Crystals", (Inst. of Crystallography, Acad. of Sci. USSR). Sov. Phys.-Crystallogr. (USA), Vol. 21, No. 5, p. 587-8 (Sept.-Oct. 1976). Translation of: Kristallografiya (USSR), Vol. 21, No. 5, p. 1022-3 (Sept.-Oct. 1976).

Kraut, E. A.
"New Mathematical Formulation for Piezoelectric Wave Propagation", (North American Rockwell Corp., Thousand Oaks, Calif., USA). Phys. Rev. (USA), Vol. 188, No. 3, p. 1450-5 (Dec. 1969).

Lmanov, V. V., Sherman, A. B., Smolenskii, G. A., Angert, N. B., Klyuev, V. P.
"Excitation and Propagation of Longitudinal Elastic Waves of 200-2000 MHz Frequency in Lithium Niobate Crystals", Fiz. Tverdogo Tela (USSR), Vol. 10, No. 6, 1720-4 (June 1968). In Russian. English translation in: Soviet Phys. Solid State (USA).

Lyubimov, V. N.
"Elastic Waves in Crystals in the Presence of the Piezoelectric Effect", Fiz. Tverdogo Tela (USSR), Vol. 12, No. 3, p. 947-9 (March 1970). In Russian, English translation in: Soviet Phys. Solid State (USA)

Ljamov, V. E.
"Nonlinear Acoustical Parameters of Piezoelectric Crystals", (Moscow State Univ., USSR). J. Acoust. Soc. Am. (USA), Vol. 52, No. 1, Pt 2, p. 199-202 (July 1972).

Matthaei, G. L.
"Variational Solutions for Acoustic Resonator Problems from the "Reaction" Point of View", Dept. of Elec. Engng. and Comp. Sci., Univ. of Calif., Santa Barbara, Calif. 93106. Ultrasonics Symposium Proceedings Cherry Hill, NJ, USA, 25-27 Sept. 1978 (New York, USA: IEEE 1978), p. 157-162.

Singh, A.
"Transverse Wave Interaction in Piezoelectric Material", (Banaras Hindu Univ., Varanasi, U.P., India). Internat. J. Electronics (GB), Vol. 25, No. 5, p. 495-6 (Nov. 1968).

Spivak, G. V., Antoshin, M. K., Luk'yanov, A. E., Pau, E. I., Ushakov, O.A., Atishin, A. I., Tokarev, G. A., Lyamov, V. E., Bartel, I.
"Observation of the Propagation of Elastic Waves in Piezoelectrics Using Scanning and Mirror Electron Microscopes", Izv. Akad. Nauk SSSR Ser. Fiz., Vol. 36, No. 9, p. 1954-6 (Sept. 1972). In Russian. English translation in: Bull. Acad Sci. USSR, Phys. Ser (USA).

Togami, Y., Chiba, T.
"Observation of Bulk Waves and Surface Waves Through Side Planes of Several Cuts of $LiNbO_3$ SAW Devices", (NHK Tech. Res. Labs., Japan Broadcasting Corp., Tokyo, Japan). J. Appl. Phys. (USA), Vol. 49, No. 6, p. 3587-9 (June 1978).

Van Dalen, P. A.
"Propagation of Transverse Electroacoustic Waves in Piezoelectric Plate of Symmetry C_{6V} or $C_{\infty V}$", Philips Res. Rep. (Netherlands), Vol. 27, No. 4, p. 323-39 (Aug. 1972).

Vekovishcheva, I. A.
"Plane Electroelasticity Theory for a Piezoelectric Plate", Prkl. Mekh. (USSR), Vol. 11, No. 2, p. 85-9 (Feb 1975). In Russian. English translation in: Sov. Appl. Mech (USA).

Wilson, L. O.
"Vibrations of a Lithium Niobate Fiber", Bell Syst. Tech. J. (USA), Vol. 56, No. 8, p. 1387-404 (Oct. 1977).

Yamabuchi, T., Kagawa, Y.
"Finite Element Method for Electromechanical Problems with Application to Energy-Trapped and Surface-Wave Devices", (Dept. of Electrical Engng. Toyama Univ., Takaoka, Japan). J. Acoust. Soc. Jap (Japan), Vol. 32, No. 3, p. 65-75 (Feb. 1976). In Japanese.

1.2.1

Alekseev, A. N., Bondarenko, V. S.
"Electroelastic Coefficients of a $Bi_{12}GeO_{20}$ Crystal", (Engng. Phys. Inst. Moscow, USSR). Sov. Phys.-Solid State (USA), Vol. 18, No. 9, p. 1595-7 (Sept. 1976). Translation of: Fiz. Tverdago Tela (USSR), Vol. 18, No. 9, p. 2736-8 (Sept. 1976).

Allik, H., Hughes, T. J. R.
"Finite Element Method for Piezoelectric Vibration", (General Dynamics, Groton, Conn., USA). Int. J. Numerical Methods Engng. (GB), Vol. 2, No. 2, p. 151-7 (April 1970.

Ariga, M., Sato, M.
"A High Electromechanical-Coupling Resonator and its Application to Filter-Synthesis", Mem. Fac. Technol Tokyo Metrop. Univ. (Japan), No. 23, p. 2033-42 (1973).

Ashida, T., Sawamoto, K., Nuzeki, N.
"Temperature Dependence of X-Cut $LiTaO_3$ Crystal Resonator Vibrating in Thickness Shear Mode of Motion", Rev. Elec. Commun. Lab. (Japan), Vol. 18, No. 11-12, p. 854-61 (Nov.-Dec. 1970).

Ballato, A.
"Resonance Phenomena in Piezoelectric Vibrators", Report ECOM 3181 (AD-697114), Army Electronics Command, Fort Monmouth, N. J., USA (Sept. 1966). 18 pp.

Ballato, A., Bertoni, H. L., Tamir, T.
"Transmission-Line Analogs for Stacked Crystals with Piezoelectric Excitation", (US Army Electronics Command, Fort Monmouth, NJ), Program of the 83rd Meeting of the Acoustical Society of America. Abstracts only, Buffalo, New York, USA, 18-27 Apr 1972 (New York, USA: Acoust. Soc. America 1972), p. 85.

Ballato, A., Lukaszek, T.
"Mass Effects on Crystal Resonators with Arbitrary Piezo-Coupling", (US Army Electronics Technol. & Devices Lab., Fort Monmouth, NJ). Proceedings of the 27th Annual Frequency Control Symposium, Cherry Hill, New Jersey, USA, 12-14 June 1973 (Washington D.C., USA: Electronic Industries Assoc. 1973), p. 20-9.

Ballato, A., Lukaszek, T. J.
"Mass-Loading of Thickness-Excited Crystal Resonators Having Arbitrary Piezo-Coupling", (US Army Electronics Command Labs., Fort Monmouth, N. J.). IEEE Trans. Sonics & Ultrason. (USA), Vol. SU-21, No. 4, p. 269-74 (Oct. 1974).

Ballato, A., Lukaszek, T. J.
"Mass-Loading Effects on Crystal Resonators Excited by Thickness Electric Fields", Report ECOM-4270, Army Electronics Command, Fort Monmouth, N. J., USA (Oct. 1974), 80 pp. ($4.75).

Ballato, A., Lukaszek, T. J.
"Distributed Network Modelling of Bulk Acoustic Waves in Crystal Plates and Stacks", Report ECOM-4311, Army Electronics Command, Fort Monmouth, N. J., USA (May 1975), 19 pp. ($3.25).

Ballato, A., Lukaszek, T. J.
"Higher-Order Temperature Coefficients of Frequency of Mass-Loaded Piezoelectric Crystal Plates", (US Army Electronics Technol. & Devices Lab., Fort Monmouth, NJ, USA). Proceedings of the 29th Annual Frequency Control Symposium, Fort Monmouth, NJ, USA, 28-30 May 1975 (Washington, DC, USA: Electronic Industries Assoc. 1975), p. 10-25.

Ballato, A., Iafrate, G. J.
"The Angular Dependence of Piezoelectric Plate Frequencies and their Temperature Coefficients", (US Army Electronics Technol. & Devices Lab., Fort Monmouth, NJ, USA). Proceedings of the 30th Annual Symposium on Frequency Control, Atlantic City, NJ, USA, 2-4 June 1976 (Washington, DC, USA: Electronic Industries Assoc. 1976), p. 141-56.

Baranovskii, S. N., Shestopal, V. O.
"Variation of the Frequency of a Piezoelectric Resonator under the Influence of Friction Forces as a Function of the Pressure on the Contact Surfaces", (Novosibirsk Inst. of Electrical Engng., USSR). Sov. Phys.-Acoust. (USA), Vol. 21, No. 1, p. 7-9 (July-Aug. 1975). Translation of: Akust. Zh. (USSR), Vol. 21, No. 1, p. 11-15 (Jan.-Feb. 1975).

Bardati, F., Barzilai, G., Gerosa, G.
"Elastic Wave Excitation in Piezoelectric Slabs", IEEE Trans. Sonics Ultrasonics (USA), Vol. SU-15, No. 4, 193-202 (Oct. 1968).

Beaver, W. D.
"Analysis of Elastically Coupled Piezoelectric Resonators", J. Acoust Soc. Amer., Vol. 43, No. 5, 972-81 (May 1968).

Bleustein, J. L., Tiersten, H. F.
"Forced Thickness-Shear Vibrations of Discontinuously Plated Piezoelectric Plates", J. Acoust. Soc. Amer., Vol. 43, No. 6, 1311-18 (June 1968).

Borisov, V. Yu., Zyruyukin, Yu. A., Shevchik, V. N.
"Features of the Propagation of Elastic Waves through Hexagonal Piezoelectric Crystals", Izv. VUZ Fiz (USSR), No. 5, p. 101-5 (1977). In Russian. English translation in: Sov. Phys. J. (USA).

Browning, T. I., Lewis, M. F.
"New Family of Bulk-Acoustic-Wave Devices Employing Interdigital Transducers", (RSRE, Malvern, England). Electron. Lett. (GB), Vol. 13, No. 5, p. 128-30 (3 March 1977).

Burgess, J. W., Porter, R. J.
"Single Mode Resonance in Lithium Niobate/Lithium Tantalate for Monolithic Crystal Filters", (Plessey Co. Ltd., Towcester, England). Proceedings of the 27th Annual Frequency Control Symposium, Cherry Hill, New Jersey, USA, 12-14 June 1973 (Washington, DC, USA: Electronic Industries Assoc. 1973), p. 246-52.

Burgess, J. W., Hales, M. C., Potter, R. J.
"Equivalent-Circuit Parameters for $LiTaO_3$ Plate Resonators", (Allen Clark Res. Centre, Plessey Co. Ltd., Caswell, Towcester, England). Electron. Lett. (GB), Vol. 11, No. 19, p. 449-50 (18 Sept. 1975).

Burgess, J. W., Hales, M. C.
"Temperature Coefficients of Frequency in $LiNbO_3$ and $LiTaO_3$ Plate Resonators", (Allen Clark Res. Centre, Plessey Co. Ltd., Caswell, Towcester, England). Proc. Inst. Electr. Eng (GB), Vol. 123, No. 6, p. 499-504 (June 1976).

Burov, J., Anastasova, N.
"Synchronous Amplification and Generation of Flexural Waves in Reasonator Platelets of Cadmium Sulphide", (Dept. of Solid State Phys. Univ. of Sofia, Sofia, Bulgaria). Bulg. J. Phys. (Bulgaria), Vol. 5, No. 2, p. 164-70 (1978).

Capparelli, F., Liberatore, A.
"On the Possibility of Increasing the Separation between the Series and Parallel Frequencies of a Piezoelectric Resonator", (Univ. Pisa, Italy). RC Riun. Ass. Elettotec. Ital. (Italy), Vol. 45, No. 2, 8.4.01/6pp (1970). In Italian. (Associatione Elettrotecnica ed Elettronica Italiana 71st Annual Meeting, Milan, Italy. 16-18 Nov. 1971).

Carr, P. H., O'Connell, R. M.
"New Temperature Compensated Materials with High Piezoelectric Coupling", (RADC/AFSC, Hanscom AFB, MA, USA). Proceedings of the 30th Annual Symposium on Frequency Control, Atlantic City, NJ, USA. 2-4 June 1976 (Washington, DC, USA: Electronic Industries Assoc 1976). p. 129-31.

Cernik, K.
"The Problems of Evaluating Piezoelectric Units and of the Accuracy of Calculating the Elements of their Equivalent Circuits", XII International Scientific Colloquium. Ilmenau, Germany, 11-15 Sept. 1967 (Ilmenau: Abt. Wissenchaftliche Publikationen der TH Ilmenau 1968), p. 25-32. In German.

Cheng, N. C., Sun, C. T.
"Wave Propagation in Two-Layered Piezoelectric Plates", (Purdue Univ. West Lafayette, Ind., USA). J. Acoust. Soc. Am. (USA), Vol. 57, No. 3, p. 632-8 (March 1975).

Chen, P. J., Montgomery, S. T.
"Normal Mode Responses of Linear Piezoelectric Materials with Hexagonal Symmetry", (Sandia Labs., Albuquerque, NM, USA). Int. J. Solids & Struct (GB), Vol. 13, No. 10, p. 947-55 (1977).

Chin, T. H., Grossman, P. L.
"Flexural Vibrations of Circular Plates Including those with Elastic Support at the Surface", (Bell Telephone Labs., Whippany, USA). Trans. ASME Ser. E (USA), Vol. 37, No. 2, p. 535-7 (June 1970).

Comparini, A. A., Hannon, J. J.
"Flexural, Width-Shear, and Width-Twist Vibrations of thin Rectangular Crystal Plates", (Bell Telephone Labs., Allentown, Pa., USA). IEEE Trans. Sonics & Ultrason. (USA), Vol. SU-21, No. 2, p. 130-5 (April 1974).

de Jong, G.
"Generation of Thickness-Twist Modes in a Piezoceramic Plate", (Delft Univ. Technol., Netherlands). J. Appl. Phys. (USA), Vol. 45, No. 3, p. 996-1000 (March 1974).

de Jong, G.
"Piezoelectric Trapped Energy Resonators Vibrating in Thickness-two Modes", (Delft Univ., Technol. Netherlands). J. Acoust Soc. Am. (USA). Vol. 56, No. 4, p. 1158-64 (Oct. 1974).

Demidenko, A. A., Piskovoi, V. N., Chi Tkhi Nguen.
"Calculation of the Electromechanical Parameters of Substances by the Resonance-Antiresonance Method in the Presence of Losses", (Kiev Semiconductor Inst., Acad. Sci., Ukrainian SSR). Ukr. Fiz. Zh. (USSR), Vol. 20, No. 6, p. 1028-31 (July 1975). In Russian.

Détaint, J., Langon, R.
"Temperature Characteristics of High Frequency Lithium Tantalate Plates", (CNET, Issy-les-Moulineaux, France). Proceedings of the 30th Annual Symposium on Frequency Control, Atlantic City, NJ, USA, 2-4 June 1976 (Washington, DC, USA: Electronic Industries Assoc. 1976), p. 132-40.

Detaint, J.
"Zero Temperature Coefficients in Overtone Lithium-Tantalate Thickness-Mode Resonators", (Centre Nat. d'Etudes des Telecommunications, Issy-les-Moulineaux, France). Electron. Lett. (GB), Vol. 13, No. 1, p. 20-1 (6 Jan 1977).

Dokmeci, M. C.
"A Theory of High Frequency Vibrations of Piezoelectric Crystal Bars", (Northwestern Univ., Evanston, Ill., USA). Int. J. Solids & Struct. (GB), Vol. 10, No. 4, p. 401-09 (April 1974).

Dokmeci, M. C.
"On The Higher Order Theories of Piezoelectric Crystal Surfaces", (Cornell Univ., Ithica, NY, USA). J. Math. Phys., New York (USA), Vol. 15, No. 12, p. 2248-52 (Dec. 1974).

EerNisse, E. P.
"Parametric and Other Nonlinear Elastic Effects in Piezoelectric Resonators", (Sandia Lab., Albuquerque, NM, USA). Proceedings of the 22nd Annual Frequency Control Symposium, Atlantic City, NJ, USA, 22-24 Apr. 1968 (Fort Monmouth, NJ, USA: Electronic Components Lab. 1968), p. 2.14.

EerNisse, E. P., Holland, R.
"Resonant Piezoelectric Devices, Design of", Cambridge, Mass., USA: MIT Press (1969), x + 258 pp.

Epstein, S., Benson, J.
"Rotation of Characteristic Vectors with Piezoelectric Coupling", (US Army Electronics Command, Fort Monmouth, NJ, USA). IEEE Trans. Sonics & Ultrason (USA), Vol. SU-21, No. 3, p. 214-16 (July 1974).

Fischler, C.
"Propagation and Amplification of Shear-Horizontal Waves in Piezoelectric Plates", (General Telephone and Electronics Labs., Inc., Bayside, NY, USA). J. Appl. Phys. (USA), Vol. 42, No. 3, p. 919-24 (1 March 1971).

Fukumoto, A., Watanabe, A.
"Temperature Dependence of Resonant Frequencies of $LiNbO_3$ Plate Resonators", Proc. IEEE (USA), Vol. 56, No. 10, p. 1751-3 (Oct. 1968).

Genis, A., Newell, D. E.
"Using the X-Y Flexure Watch Crystal as a Pressure-Force Transducer", (Northern Illinois Univ., DeKalb, IL, USA). 31st Annual Frequency Control Symposium, Atlantic City, NJ, USA, 1-3 June 1977 (Washington, DC, USA: Electronic Industries Assoc. 1977), p. 71-7.

Ghosh, N. C., Pal, A. K.
"Wave Propagation in an Infinite Piezoelectric Crystal under a Thermal Field", (Dept. of Math., Jadavpur Univ., Calcutta, India). Czech. J. Phys. Sect. B (Czechoslovakia), Vol. B28, No. 7, p. 807-12 (1978).

Glowinski, A.
"Thickness Vibrations of Piezoelectric Slabs", Ann. Telecommun. (France), Vol. 27, No. 3-4, p. 147-58 (March-April 1972). In French.

Glowinski, A., Lancon, R., Lefevre, R.
"Effects of Asymmetry in Trapped Energy Piezoelectric Resonators", (Centre Nat. Etudes Telecommunications, Issy les Moulineaux, France). Proceedings of the 27th Annual Frequency Control Symposium, Cherry Hill, New Jersey, USA, 12-14 June 1973 (Washington, DC, USA: Electronic Industries Assoc. 1973), p. 233-42.

Godenhielm, B.
"The Piezoelectric Characteristics of the Oscillator Crystal", ERT Elektron. Radio Telev. (Finland), Vol. 25, No. 2, p. 17-19 (1972). In Finnish).

Gopinath, A., Daview, H.
"Frequency Tuning of CdS Platelets", (Univ. College North Wales, Bangor, Wales). Electronics Letters (GB), Vol. 5, No. 24, p. 622-3 (27 Nov. 1969).

Graham, R. A.
"Strain Dependence of the Piezoelectric Polarization of Z-Cut Lithium Niobate", (Sandia Labs., Albuquerque, N.Mex., USA). Solid State Commun. (USA), Vol. 12, No. 6, p. 503-6 (15 March 1973).

Gregoire, J. P., Nedelec, J. C., Planchard, J.
"Calculating the Eigenfrequencies of an Acoustic Resonator", (TIEM, Ciarmart, France). Bull. Dir. Etud. & Rech. C (France), No. 2, p. 5-22 (1973). In French.

Grinchenko, V. T., Kariash, V. L., Meleshko, V. V., Ulitko, A. F.
"Planar Vibrations of Rectangular Piezoelectric Plates", Prikl. Mekh. (USSR), Vol. 12, No. 5, p. 71-8 (May 1976). In Russian. English translation in: Sov. Appl. Mech. (USA).

Hafner, E.
"The Role of Crystal Parameters in Circuit Design", Proceedings of the 22nd Annual Frequency Control Symposium, Atlantic City, NJ, USA, 22-24 Apr. 1968 (Fort Monmouth, NJ, USA: Electronic Components Lab. 1968), p. 269-81.

Hafner, E.
"Filters and Resonators - A Review", (US Army Electronics Command Labs., Fort Monmouth, N. J.). IEEE Trans. Sonics & Ultrason. (USA), Vol. SU-21, No. 4, p. 220-37 (Oct. 1974).

Hales, M. C., Burgess, J. W., Porter, R. J.
"Energy Trapped Vibrations in Lithium Tantalate and Lithium Niobate Resonators", (Plessey Co. Ltd., Towcester, England). Proceedings of the 28th Annual Frequency Control Symposium 1974, Atlantic City, NJ, USA, 29-31 May 1974)Washington, DC, USA: Electronic Industries Assoc. 1974), p. 43.

Hammond, D. L., Benjaminson, A.
"The Crystal Resonator - A Digital Transducer", (Hewlett-Packard Labs., Palo Alto, CA., USA). IEEE Spectrum (USA), Vol. 6, No. 4, p. 53-8 (April 1969).

Hannon, J. J., Lloyd, P., Smith, R. T.
"Lithium Tantalate and Lithium Niobate Piezoelectric Resonators in the Medium Frequency Range with Low Ratios of Capacitance and Low Temperature Coefficients of Frequency", (Bell Telephone Labs. Inc., Allentown, Pa., USA). IEEE Trans. Sonics Ultrasonics (USA), Vol. SU-17, No. 4, p. 239-46 (Oct 1970).

Heyman, J. S., Miller, J. G.
"Verification of Sensitivity Enhancement Factors for CW Ultrasonic Resonators", (NASA, Hampton, VA, USA). J. Appl. Phys. (USA), Vol. 44, No. 8, p. 3398-400 (Aug. 1973).

Holland, R.
"Contour Extensional Resonant Properties of Rectangular Piezoelectric Plates", IEEE Trans. Sonics Ultrasonics (USA), Vol. SU-15, No. 2, 97-105 (April 1968).

Holland, R., Eernisse, E. P.
"Variational Evaluation of Admittances of Multielectroded Three-Dimensional Piezoelectric Structures", IEEE Trans Sonics Ultrasonics (USA), Vol. SU-15, No. 2, 119-32 (April 1968).

Holland, R.
"Resonant Properties of Piezoelectric Ceramic Rectangular Parallelepipeds", J. Acoust. Soc. Amer., Vol. 43, No. 5, 988-97 (May 1968).

Hoppmann, W. H. II, Kunukkasseril, V. X.
"Normal-Mode Vibrations of Model of Centrosymmetric Cubic Crystal", J. Acoust. Soc. Amer., Vol. 42, No. 1, 42-9 (July 1967).

Horton, W. H., Smythe, R. C.
"The Work of Mortley and the Energy-Trapping Theory for Thickness-Shear Piezoelectric Vibrators", Proc. Inst. Elect. Electronics Engrs. (USA), Vol. 55, No. 2, 222 (Feb. 1967).

Hruska, K.
"Vibration of Piezoelectric Plates with a Small Non-Zero Potential across their Electrodes", (Univ. Khartoum, Sudan). Czech. J. Phys. B., Vol. 19, No. 11, p. 1315-21 (1969). In Polish.

Hruska, K.
"Polarizing Effect with Piezoelectric Plates and Second-Order Effects", (Univ. Khartoum, Sudan). IEEE Trans. Sonics Ultrasonics (USA), Vol. SU-18, No. 1, p. 1-7 (Jan. 1971).

Ikeda, T.
"On the Relations between Electromechanical Coupling Coefficients and Elastic Constants in a Piezoelectric Crystal", (Tohoku Univ., Sandai, Japan). Jap. J. Appl. Phys. (Japan), Vol. 11, No. 4, p. 463-71 (April 1972).

Ikeda, T., Inawashiro, S.
"Depolarizing- or Demagnetizing-Field in Electromechanical Extensional Vibrators. I. Depolarizing-field Effect in a Piezoelectric Rod under the Longitudinal-Effect Extensional Vibration", (Dept. of Appl. Phys. Faculty of Engng., Tohoku Univ., Sendai, Japan). J. Acoust. Soc. Jpn. (Japan), Vol. 34, No. 4, p. 223-33 (April 1978).

Ikegami, S., Ueda, I., Kobayashi, S.
"Frequency Spectra of Resonant Vibration in Disk Plates of $PbTiO_3$ Piezoelectric Ceramics", (Matsushita Electric Industrial Co. Ltd., Kadoma, Osaka, Japan). J. Acoust. Soc. Am. (USA), Vol. 55, No. 2, p. 339-44 (Feb. 1974).

Jhunjhunwala, A., Vetelino, J. F., Field, J. C.
Temperature Compensated Cuts with Zero Power Flow in Tl_3VS_4 and Tl_3TaSe_4", (Dept. of Electrical Engng., Univ. of Maine, Orono, ME, USA). Electron. Lett. (GB), Vol. 12, No. 25, p. 683-4 (9 Dec. 1976).

Jumonji, H.
"Analysis of Characteristics of Multiple-Mode Resonators Vibrating in Longitudinal and Flexural Modes", (Univ. Tokyo, Japan). Trans. Inst-Electron. Commun. Eng. Japan. A.B.C., Vol. 53, No. 4, p. 3-5 (April 1970).

Kagawa, Y., Gladwell, G. M. L.
"Finite Element Analysis of Flexure-Type Vibrators with Electrostrictive Transducers", IEEE Trans. Sonics Ultrasonics (USA), Vol. SU-17, No. 1, p. 41-9 (Jan. 1970).

Kaliski, S.
"A Perfect Self-Excited Piezoelectric Resonator", Proc. Vibration Problems (Poland), Vol. 8, No. 1, p. 3-20 (1967).

Kaliski, S.
"Self-Excited Perfect Piezoquartz Resonator with an External Electron Stream", Proc. Vibration Problems (Poland), Vol. 9, No. 4, p. 429-36 (1968).

Kaliski, S.
"Some Properties of The Equations of Piezoelectric Vibration of Lithium Niobate and Tantalate Crystals", Proc. Vib. Probl. (Poland), Vol. 12, No. 1, p. 63-70 (1971).

Kaname, Y., Nagata, T., Tanake, T.
"Piezoelectric Ceramic Disk Resonator Vibrating in Thickness-Shear Mode", J. Inst. Elect. Commun. Engrs. Japan. Vol. 50, No. 1, 13-14 (Jan. 1967).

Kantor, V. M.
"Calculation of the Parameters of Energy-Trapping Piezoelectric Resonators", (Leningrad Branch, Central Sci. Res. Inst. of Communication, USSR). Sov. Phys. Acoust. (USA), Vol. 20, No. 6, p. 516-18 (May-June 1975). Translation of: Akust. Zh. (USSR), Vol. 20, No. 6, p. 843-7 (Nov.-Dec. 1974).

Karaul'nik, A. E., Shin, V.
"Spectral Characteristics of Vibrating Crystals as Affected by the Direction of the Exciting Electrical Field", Kristallografya (USSR), Vol. 14, No. 1, p. 84-9 (1969). In Russian. English translation in: Soviet Phys. Cryst. (USA).

Kaul, R. K.
"Low Frequency Extensional Vibrations of Thin Anisotropic Discs", Report ECOM 01731-2 (AD 681348), Columbia Univ., New York, USA (Aug. 1968), 70 pp Contract DA-28-043-AMC-01731(E) Available from CFSTI, Springfield, VA 22151, USA.

Kee, Pek Yaw
"Simple Tuning Fork", Pract. Electron. (GB), Vol. 13, No. 3, p. 221 (March 1977).

Keuning, D. H.
"Exact Resonant Frequencies for the Thickness-Twist Trapped Energy Mode in a Piezoceramic Plate", (Univ. Gronigen, Netherlands). J. Eng. Math. (Netherlands), Vol. 6, No. 2, p. 143-54 (April 1972).

Kokorin, Yu. I., Zaitseva, M. P., Sysoev, A. M.
"Mechanical Nonlinearity Accompanying the Oscillations of Ferroelectric Crystal Resonators", Izv. Akad. Nauk SSSR Ser. Fiz., Vol. 39, No. 4, p. 816-21 In Russian. English Translation in: Bull. Acad. Sci. USSR, Phys. Ser. (USA).

Koneval, D. J., Sliker, T. R.
"Shear Mode CdS-Quartz Composite Resonators", (Clevite Corp., Cleveland, OH, USA). IEEE Trans. Sonics Ultrasonics (USA), Vol. SU-16, No. 1, Suppl., p. 21 (Jan. 1969). (1968 IEEE Ultrasonics Symposium, New York, USA, 25-27 Sept. 1968).

Kosek, M.
"The Influence of Electrode Thickness on the Frequency Response of a Piezoelectrical Transducer", Slaboproudy Obzor (Czechoslovakia), Vol. 33, No. 7, p. 311-15 (1972). In Czech.

Kumath, P., Mager, R.
"Analysis of a Circular Piezoelectric Plate", (TH Karl Marx Stadt, Karl Marx Stadt, Germany). Z. Elektr. Inf. & Energietech. (Germany), Vol. 5, No. 6, p. 435-42 (1975). In German.

Kusakabe, C.
"Suppression of Spurious Responses of a Flexural Piezoelectric Vibrator with Split-Electrode", (Faculty of Education, Yamagata Univ., Yamagata, Japan). J. Acoust. Soc. Jpn (Japan), Vol. 34, No. 2, p. 73-8 (Feb. 1978). In Japanese.

Langon, R.
"Mechanical Resonances of Asymmetric Monolithic Structures", Ann. Telecommun. (France), Vol. 28, No. 9-10, p. 406-12 (Sept.-Oct. 1973). In French.

Lazutkin, V. N., Mikhailov, A. I.
"Equivalent Circuit of a Radically Vibrating Disk", Akust. Zh. (USSR), p. 58-62 In Russian. English translation in: Sov. Phys. Acoust. (USA), Vol. 18, No. 1, p. 45-8 (July-Sept. 1972).

Lee, P. C. Y.
"Extensional Flexural, and Width-Shear Vibrations of Thin Rectangular Crystal Plates", (Princeton, Univ., NJ, USA). J. Appl. Phys. (USA), Vol. 42, No. 11, p. 4139-44 (Oct. 1971).

Lee, P. C. Y., Wang, Y. S., Markenscoff, X.
"Elastic Waves and Vibrations in Deformed Crystal Plates", (Princeton Univ., NJ, USA). Proceedings of the 27th Annual Frequency Control Symposium, Cherry Hill, New Jersey, USA, 12-14 June 1973 (Washington, DC, USA: Electronic Industries Assoc. 1973). p. 1-5.

Lee, P. C. Y., Wang, Y. S., Markenscoff, X.
"Effects of Initial Bending on the Resonance Frequencies of Crystal Plates", (Princeton Univ., NJ, USA). Proceedings of the 28th Annual Frequency Control Symposium 1974, Atlantic City, NJ, USA, 29-31 May 1974 (Washington, DC, USA: Electronic Industries Assoc. 1974). p. 14-18.

Lee, P. C. Y., Syngellakis, S.
"Waves and Vibrations in an Infinite Piezoelectric Plate", (Dept of Civil Engng., Princeton Univ., Princeton, NJ, USA). Proceedings of the 29th Annual Frequency Control Symposium, Fort Monmouth, NJ, USA, 28-30 May 1975 (Washington, DC, USA: Electronic Industries Assoc. 1975), p. 65-70.

Lee, P. C. Y., Wu, Kuang-Ming
"Effects of Acceleration on the Resonance Frequencies of Crystal Plates", (Dept. of Civil Engng., Princeton Univ., Princeton, NJ, USA). Proceedings of the 30th Annual Symposium on Frequency Control, Atlantic City, NJ, USA, 2-4 June 1976 (Washington, DC, USA: Electronic Industries Assoc. 1976). p. 1-7.

Lemanov, V. V., Yushin, N. K.
"Generation of Harmonics of Transverse Elastic Waves in Crystals", (A. F. Ioffe Physicotech. Inst., Acad. Sci., Leningrad, USSR). Sov. Phys. Solid State (USA), Vol. 14, No. 8, p. 2053-6 (Feb. 1973). Translation of: Fiz. Tverdogo Tela (USSR), Vol. 14, No. 8, p. 2373-7 (Aug. 1972).

Lemanov, V. V., Yushin, N. K.
"Nonlinear Effects in the Propagation of Elastic Waves in Piezoelectric Crystals", (A. F. Ioffe Physicotech. Inst., Acad. Sci., Leningrad, USSR). Sov. Phys. Solid State (USA), Vol. 15, No. 11, p. 2140-2 (May 1974). Translation of: Fiz. Tverdogo Tela (USSR), Vol. 15, No. 11, p. 3206-10 (Nov. 1973).

Lloyd, P.
"Equations Governing the Electrical Behavior of an Arbitrary Piezoelectric Resonator Having N Electrodes", Bell Syst. Tech. J. (USA), Vol. 46, No. 8, 1881-900 (Oct. 1967).

Lozhkin, V. N.
"Flexure of a Thin Piezoelectric Plate with an Elliptic Opening", Mat. Fiz. (USSR), No. 20, p. 90-4 (1976). In Russian.

Madorskii, V. V., Ustanov, Yu. A.
"Construction of a System of Homogeneous Solutions and Analysis of the Roots of the Dispersion Equation of Antisymmetric Vibrations of Piezoelectric Plate", J. Appl. Mech. & Tech. Phys. (USA), Vol. 17, No. 6, p. 867-73 (Nov.-Dec. 1976). Translation of: Zh. Prikl. Mekh. & Tekh. Fiz. (USSR), Vol. 17, No. 6, p. 138-45 (Nov.-Dec. 1976).

Malyshev, V. A.
"On the Equivalency of Resonators and Tank Circuits", Radio Eng. & Electron. Phys. (USA), Vol. 21, No. 8, p. 37-43 (Aug. 1976). Translation of: Radiotekh. & Elektron. (USSR), Vol. 21, No. 8, p. 1631-8 (Aug. 1976).

Mamateva, T. A., Fokina, L. A., Lyamov, V. E.
"Effect of Domain Structure on the Propagation of Elastic Waves in Lithium Niobate", (M. V. Lomonosov Moscow State Univ., USSR). Sov. Phys. Solid State (USA), Vol. 15, No. 2., p. 393-4 (Aug. 1973). Translation of: Fiz. Tverdogo Tela (USSR), Vol. 15, No. 2, p. 569-70 (Feb. 1973).

Markenscoff, X.
"Higher-Order Effects of Initial Deformation on the Vibrations of Crystal Plates", (Engng. Sci. Dept., Virginia Polytech. Inst. & State Univ., Blacksburg, VA, USA). J. Acoust. Soc. Am. (USA), Vol. 61, No. 2, p. 436-8 (Feb. 1977).

Mashonis, A.
"Pulse Response of Radial Vibration of Piezoelectric Disk", (Lab. of Ultrasonics, Kaunas Polytech. Inst., Lithuanian SSR). Period. Polytech. Electr. Eng. (Hungary), Vol. 19, No. 1, p. 3-11 (1975).

McAvoy, B. R., de Klerk, J.
"High Q Microwave Bulk Mode Resonators", (Westinghouse Res. Labs., Pittsburgh, PA, USA). 1976 Ultrasonics Symposium Proceedings, Annapolis, Md., USA, 29 Sept. - 1 Oct. 1976 (New York, USA: IEEE 1976), p. 590-2.

McMahon, D. H.
"Acoustic Second-Harmonic Generation in Piezoelectric Crystals", (Sperry Rand Research Center, Sudbury, Massachusetts, USA). J. Acoust. Soc. Amer., Vol. 44, No. 4, p. 1007-13 (Oct. 1968).

Mitchell, W. S., Muster, D.
"The Vibrational Response of a Thick, Circular, Piezoelectric Plate", (Univ. Houston, Tex., USA). Acustica (Internat.), Vol. 22, No. 6, p. 321-8 (1969). In English.

Mindlin, R. D.
"Lattice and Continuum Theories of Simple Modes of Vibration in Cubic Crystal Plates and Bars", Report TR-11 (AD-677041), Columbia Univ., NY, USA (Aug. 1968), 17 pp. Contract Nonr-4259(13). Available from CFSTI, Springfield, VA 22151, USA.

Mindlin, R. D.
"High Frequency Vibrations of Piezoelectric Crystal Plates", Report TR-8 (AD-735956), Columbia Univ., New York, USA (Jan. 1972), 27 pp. Contract DAAB07-72-Q-0166. Available from NTIS, Springfield, VA, 22151, USA.

Mindlin, R. D.
"High Frequency Vibrations of Piezoelectric Crystal Plates", (Columbia Univ., New York, USA). Int. J. Solids & Struct. (GR), Vol. 8, No. 7, p. 895-906 (July 1972).

Mindlin, R. D.
"Electro-Mechanical Vibrations in Centrosymmetric Crystals", (Columbia Univ., New York, USA). Proceedings of the 22nd Annual Frequency Control Symposium, Atlantic City, NJ, USA, 22-24 Apr 1968 (Fort Monmouth, NJ, USA: Electronic Components Lab. 1968), p. 1.

Mochizuki, Y.
"Simple Exact Solutions for Thickness Shear Mode of Vibration of a Crystal Strip", (Shizuoka Univ., Ooya, Shizuoka-Shi, Japan). Proceedings of the 29th Annual Frequency Control Symposium, Fort Monmouth, NJ, USA, 28-30 May 1975 (Washington, DC, USA: Electronic Industries Assoc. 1975), p. 35-41.

Morrison, J. A., Seery, J. B., Wilson, L. O.
"Propagation of High-Frequency Elastic Surface Waves along Cylinders with Various Cross-Sectional Shapes", (Bell Labs., Murray Hill, NJ, USA). Bell Syst. Tech. J. (USA), Vol. 56, No. 1, p. 77-114 (Jan. 1977).

Mowbray, D. F.
"Vibrations of an Infinite Plate Based on the Dynamic Theory of Thermoelasticity", Rensselaer Polytech. Inst., Troy, NY, USA, thesis, 185 pp. Available from Univ. Microfilms, Ann Arbor, Mich., USA Order No. 69-2471.

Mukherjee, S.
"A Note on Vibration of a Piezoelectric Flexural Vibrator", (R. K. Mission Vidyamandira, Belurmath, Howrah, India). Indian J. Theor. Phys., Vol. 21, No. 3, p. 89-93 (Sept. 1973).

Nagata, T., Nakajima, Y., Sasaki, R.
"$PbTiO_3$ Ceramic Resonators Operating in VHF Band", (Matsushita Electric Industrial Co. Ltd., Kadoma, Japan). Electron. & Commun. Jap. (USA), Vol. 55, No. 7, p. 93-8 (1972).

Nagata, T., Nakajima, Y., Sasaki, R.
"A New Trapped-Energy Mode of the Thickness-Dilatational Wave", (Matsushita Electric Industries Co. Ltd., Kadoma, Japan). Electron. & Commun. Jap. (USA), Vol. 57, No. 3, p. 19-24 (March 1974).

Nakajima, Y., Nagata, T.
"A Trapped Energy Ceramic Resonator with Improved Unwanted Response Characteristics", (Wireless Res. Lab., Matsushita Electric Industrial Co. Ltd., Osaka, Japan). J. Acoust. Soc. Jpn. (Japan), Vol. 33, No. 7, p. 368-75 (July 1977). In Japanese.

Nakamura, K., Shimizu, H.
"Analyses of Two-Dimensional Energy Trapping in Piezoelectric Plates with Rectangular Electrodes", (Faculty of Engng., Tohoku Univ., Sendai, Japan). 1976 Ultrasonics Symposium Proceedings, Annapolis, Md., USA, 29 Sept. - 1 Oct. 1976 (New York, USA: IEEE 1976). p. 608-9.

Nakaura, K., Watanabe, H., Shimizu, H.
"Analysis of Trapped-Energy Resonators and Monolithic Filters by the Equivalent Distributed-Constant Circuits", (Faculty of Engng., Tohoku Univ., Sendai, Japan). Trans. Inst. Electron. & Comunun. Eng. Jpn. Sect. E (Japan), Vol. E59, No. 11, p. 26-7 (Nov. 1976).

Nelson, R. A. Jr., Royster, L. H.
"On the Electromechanical Coupling and Electrical Impedance of a Thin Piezoelectric Disk with an Arbitrary Impedance on the Boundary", Report TR-4 CAS-39 (AD689 206), North Carolina State Univ., Raleigh, USA (May 1969), 13 pp. Contract NONR-486(11). Available from CFSTI, Springfield, VA 22151, USA

Nelson, R. A. Jr., Royster, L. H.
"On the Vibration of a Thin Piezoelectric Disk with an Arbitrary Impedance on the Boundary", (North Carolina State Univ., Raleigh, USA). J. Acoust. Soc. Amer., Vol. 46, No. 3, pt. 2, p. 828-30 (Sept. 1969).

Niizeki, N., Sawamoto, K.
"Zero Temperature Coefficient of Resonant Frequency in $LiTaO_3$ Length Expander Bars", (Nippon Telegraph Telephone Public Corp., Mussasino-si, Tokyo). Proc. IEEE (USA), Vol. 58, No. 8, p. 1289-90 (Aug. 1970).

Onoe, M., Yano, T.
"Analysis of Flexural Vibrations of a Circular Disk", IEEE Trans. Sonics Ultrasonics (USA), Vol. SU-15, No. 3, 182-5 (July 1968).

Onoe, M.
"Relationship between Temperature Behavior of Resonant and Antiresonant Frequencies and the Electromechanical Coupling Factors of Piezoelectric Resonators", Proc. IEEE (USA), Vol. 57, No. 4, p. 702-3 (April 1969).

Onoe, M., Okada, K.
"Analysis of Contoured Piezoelectric Resonators Vibrating in Thickness-Twist Modes", (Univ. Tokyo, Roppongi, Japan). Proceedings of the 23rd Annual Frequency Control Symposium, Atlantic City, NJ, USA, 6-8 May 1969 (Washington, DC, USA: Electronic Industries Assoc. 1969). p. 26-38.

Onoe, M., Ashida, T., Sawamoto, K.
"Zero Temperature Coefficient of Resonant Frequency in an X-Cut Lithium Tantalate at Room Temperature", Proceedings IEEE (USA), Vol. 57, No. 8, p. 1446-7 (Aug. 1969).

Onoe, M.
"Thickness-Twist Vibrations of a Piezoelectric Plate", (Univ. Tokyo, Japan). Trans. Inst. Electronics Commun., Engrs. Japan. ABC, Vol. 52, No. 10 (Oct. 1969). In Japanese. English translation in: Electron. Commun. Jap. (USA). Vol. 52, No. 10, p. 38-43 (Oct. 1969).

Onoe, M.
"Thickness-Twist Vibrations of a Piezoelectric Plate", (Univ. Tokyo, Minato-ku, Japan). J. Acoust. Soc. Amer., Vol. 46, No. 5, Pt. 1, p. 1087-9 (Nov. 1969).

Onoe, M., Kasai, Y.
"Quarter or Half Wavelength Mounting of Low Frequency Flexural Vibrators", (Univ. Tokyo, Japan). J. Acoust. Soc. Japan, Vol. 27, No. 10, p. 515-23 (Oct 1971). In Japanese.

Onoe, M., Shinada, T., Itoh, K., Miyazaki, S.
"Low Frequency Resonators of Lithium Tantalate", Proceedings of the 27th Annual Frequency Control Symposium, Cherry Hill, NJ, USA, 12-14 June 1973 (Washington, DC, USA: Electronic Industries Assoc. 1973). p. 42-9

Onoe, M., Araki, F.
"Simplified Equivalent Circuit for a Piezoelectric Resonator with High Electromechanical Coupling", (Univ. Tokyo, Japan). J. Acoust. Soc. Jap. (Japan), Vol. 30, No. 9, p. 492-7 (Sept. 1974).

Onoe, M., Araki, F.
"Simplified Equivalent Circuit for a Piezoelectric Resonator with High Electromechanical Coupling", (Univ., Tokyo, Roppongi, Japan). Proc. IEEE (USA), Vol. 62, No. 10, p. 1392-3 (Oct. 1974).

Onoe, M., Yamagishi, I.
"Thickness-Twist Vibration of a Plate with Tilted Edges", (Inst of Industrial Sci., Univ. of Tokyo, Tokyo, Japan). Electron & Commun. Jap. (USA), Vol. 58, No. 5, p. 9-18 (May 1975).

Onoe, M.
"Piezoelectric Application of Lithium Tantalate", (Inst. of Industrial Sci., Univ. of Tokyo, Tokyo, Japan). Bull. Acad. Sci. USSR, Phys. Ser. (USA), Vol. 41, No. 1, p. 52-6 (1977). Translation of: Izv. Akad. Nauk, SSSR Ser. Fiz., Vol. 41, No. 4, p. 715-20 (1977). (Proceedings of the 1st Soviet-Japanese Symposium on Ferroelectricity, Novosibirsk, USSR, 30 Aug. - 3 Sept. 1976).

Paul, H. S.
"Vibrational Waves in a Thick Infinite Plate of Piezoelectric Crystal", J. Acoust. Soc. Amer., Vol. 44, No. 2, 478-82 (Aug. 1968).

Pauley, K. E., Dong, S. B.
"Analysis of Plane Waves in Laminated Piezoelectric Plates", (Mech. & Structures Dept., Univ. of California, Los Angeles, CA, USA). Wave Electron. (Netherlands), Vol. 1, No. 4, p. 265-85 (Feb. 1976).

Pietrzak, J., Ostafin, M., Blaszak, K.
"Piezoelectric Radio-Frequency Resonance in Triglycine Sulphate Crystals", (Solid State Spectroscopy Lab., Inst. of Phys., Acta Phys. Pol. A (Poland), Vol. A50, No. 5, p. 713-17 (Nov. 1976).

Pol'skii, A. I., Rizunenko, V. I.
"Bending Resonance Vibrations of a Free Two-Layer Disc", (Kirenskii Phys. Inst., Acad. Sci., USSR). Fiz. Met. & Metalloved. (USSR), Vol. 42, No. 5, p. 1095-8 (Nov. 1976). In Russian. English Translation in: Phys. Met. & Metallogr. (GB).

Pozdnyakov, P. G.
"Piezoelectric Excitation of Torsional Vibrations in Crystalline Rods", Kristallografya (USSR), Vol. 16, No. 5, p. 944-6 (1971). In Russian. English Translation in: Sov. Phys. Crystallogr. (USA).

Preobrazhenskii, N. S., Ikin, V. K.
"Method of Determining Quality of Piezoelectrics", (Kurmakov Inst. of General & Inorganic Chem., Acad. of Sci, Moscow, USSR). Ind. Lab (USA), Vol. 42, No. 9, p. 1421-3 (Sept. 1976). Translation of: Zavod Lab. (USSR), Vol. 42, No. 9, p. 1098-1100 (Sept. 1976).

Roy, P.
"Note on Responses in a Piezoelectric Crystal with Divided Electrodes", (Victoria Coll., Cooch Behar, India). Proc. Nat. Inst. Sci. India A, Vol. 35, No. 5, p. 612-18 (Sept. 1969).

Sang, K. C.
"Temperature Characteristics of Elastic Layer Mode Propagating on Piezoelectric Crystal", (Seoul Nat. Univ., Korea). J. Korean Inst. Electron. Eng., Vol. 10, No. 6, p. 53-61 (Dec. 1973). In Korean.

Sannomiya, T., Chubachi, N.
"An Overtone Composite Resonator for UHF Range", (Tohoku Univ., Sendai, Japan). Rec. Electr. & Commun. Eng. Conversazione Tohoku Univ. (Japan), Vol. 46, No. 2, p. 53-9 (May 1977). In Japanese.

Sawomoto, K.
"Energy Trapping in a Lithium Tantalate X-Cut Resonator", Programme of the 25th Annual Frequency Control Symposium (abstracts), Atlantic City, NJ, USA, 26-28 Apr. 1971 (Fort Monmouth, NJ, USA: US Army Electronics Command 1971), p. 43.

Schmidt, G. H.
"Extensional Vibrations of Piezoelectric Plates", (Univ. Groningen, Netherlands). J. Eng. Math. (Netherlands), Vol. 6, No. 2, p. 133-42 (April 1972).

Schmidt, G. H.
"On Anti-Symmetric Waves in an Unbounded Piezoelectric Plate with Axisymmetric Electrodes", (Dept. of Civil Engng., Univ. of Technol., Delft, Netherlands). Int. J. Solids & Struct. (GB), Vol. 13, No. 3, p. 179-95 (1977).

Schmidt, G. H.
"Resonances of an Unbounded Piezoelectric Plate with Circular Electrodes", (Dept. of Civil Engng, Univ. of Technol, Delft, Netherlands). Int. J. Eng. Sci. (GB), Vol 15, No. 8, p. 495-510 (1977).

Schnabel, P.
"Frequency Equations for n Mechanically Coupled Piezoelectric Resonators", (Philips Zentrallab. GmbH. Lab. Aachen. W. Germany). Acustica (Internat.), Vol. 21, No. 6, p. 351-7 (1969). In English.

Schulz, M. B., Holland, M. G., Fukumoto, A., Watanabe, A.
"Comments on Temperature Dependence of Resonant Frequencies of $LiNbO_3$ Plate Resonators", (Raytheon Res. Div., Waltham, Mass., USA). Proc. IEEE (USA), Vol. 58, No. 3, p. 477 (March 1970).

Schwarz, R.
"Digital Computer Simulation of a Piezoelectric Thickness Vibrator", (Siemens AG, Munchen, Germany). J. Acoust. Soc. Am. (USA) Vol. 62, No. 2, p. 463-7 (Aug. 1977).

Schweppe, H.
"Excitation of Two Adjacent Resonances With a Chosen Frequency Separation in a Ceramic Piezoelectric Resonator", IEEE Trans. Sonics Ultrasonics (USA), Vol. SU-17, No. 1, p. 12-17 (Jan. 1970).

Schweppe, H.
"Double-Mode Piezoelectric Ceramic Resonator", (Phillips Zentrallaboratorium GmbH, Aachen, Germany). IEEE Trans. Sonics Ultrasonics (USA), Vol. SU-17, No. 1, p. 59-60 (Jan. 1970). (Abstract only).

Schweppe, H.
"High-Coupling Piezoelectric Flexural Resonator", (Phillips Forschungslaboratorium GmbH, Aachen, Germany). Proceedings of the 7th International Congress on Acoustics, Budapest, Hungary, 18-26 Aug. 1971 (Budapest, Hungary: Akademiai Kiado 1971), p. 389-92.

Sedlacek, J.
"Torsional Thickness Oscillations in a $Bi_{12}GeO_{20}$ Plate Featuring a (110) Cut", (Tesla Hradec Kralove n.p., Hradec Kralove, Czechoslovakia). Slaboproudy Obz. (Czechoslovakia), Vol. 38, No. 3, p. 106-8 (March 1977). In Czech.

Sneiko, Yu. A.
"Equivalent Circuit of a Flexurally Vibrating Multielectrode Piezoelectric Bar", (Kiev Polytech. Inst., Kiev Ukrainian SSR). Sov. Phys.-Acoust. (USA), Vol. 24, No. 2, p. 154-6 (March-April 1978). Translation of: Akust. Zh. (USSR), Vol. 24, No. 2, p. 279-83 (March-April 1978).

Sinha, D. K.
"Mechanical Response of a Free Piezoelectric Plate", (Jadavpur Univ., Calcutta, India). Indian J. Phys. Vol. 43, No. 9, p. 516-18 (Sept. 1969).

Sinkevich, E. L., Fedorchenko, A. M.
"Thermal Fluctuations in a Piezoelectric Plate", Izv. VUZ Fiz. (USSR), No. 6, p. 95-101 (1978). In Russian. English Translation in: Sov. Phys. J. (USA).

Sliker, T. R., Koneval, D. J.
"Frequency-Temperature Behavior of X-Cut Lithium Tantalate Resonators", Proc. IEEE (USA), Vol. 56, No. 8, 1402 (Aug. 1968).

Sliker, T. R., Koneval, D. J., Hora, C. J. Jr.
"Frequency-Temperature Behavior of CdS Thickness Mode Resonators", IEEE Trans. Sonics Ultrasonics (USA), Vol. SU-16, No. 1, p. 15-18 (Jan. 1969).

Slobodnik, A. J. Jr.
"Microwave Acoustic Resonances in Thin Piezoelectric Disks", (Air Force Cambridge Res. Labs., L. G. Hanscom Field, Bedford, Mass., USA), IEEE Trans. Sonics Ultrasonics (USA), Vol. 17, No. 3, p. 196-9 (July 1970).

Smith, A. B., Kostigian, M., Kedzie, R. W., Grace, M. I.
"Shear-Wave Attenuation in Lithium Niobate", J. Appl. Phys. (USA), Vol. 38, No. 12, 4928-9 (Nov. 1967).

Smith, W. L.
"The Application of Piezoelectric Coupled-Resonator Devices to Communication Systems", (Bell Telephone Labs. Inc., Allentown, Pa., USA). Proceedings of the 22nd Annual Frequency Control Symposium, Atlantic City, NJ, USA, 22-24 Apr. 1968 (Fort Monmouth, NJ, USA: Electronic Components Lab. 1968), p. 206-25.

Smythe, R. C.
"Intermodulation in Thickness-Shear Resonators", (Piezo Technol. Inc., NY, USA). Proceedings of the 28th Annual Frequency Control Symposium 1974, Atlantic City, NJ, USA, 29-31 May 1974 (Washington, DC, USA: Electronic Industries Assoc. 1974), p. 5-7.

Stavsky, Y., Adelman, N. T.
"Radial Vibrations of Composite Piezoelectric Ceramic Disks", (Dept of Mech., Technion-Israel Inst. of Technol., Haifa, Israel). Appl. Sci, Res. (Netherlands), Vol. 31, No. 2, p. 123-38 (Aug. 1975).

Stefan, O.
"The Coupling between the Radial and Thickness Vibration of the Circular Resonator", (Res. Inst. Electroceramics, Hradec Kralove, Czechoslovakia). Czech. J Phys. B., Vol. 19, No. 11, p. 1425-8 (1969).

Stefan, O.
"Contour Oscillations of Circular Ceramic Resonators", Cesk. Casopis Fys. A (Czechoslovakia), Vol. 20, No. 2, p. 113-22 (1970). In Czech.

Stefan, O.
"Electric Equivalent Circuit of the Circular Piezoelectric Resonator", (Res. Inst. Electrochemical Ceramics, Hradec Kralove, Czechoslovakia), Czech J. Phys. B., Vol. 20, No. 4, p. 432-40 (1970).

Stefan, O.
"Parameters of an Electrical Equivalent Circuit of a Piezoelectric Disc Resonator", (Res. Inst. of Electroceramics, Hradec Kralove, Czechoslovakia). TESLA Electron. (Czechoslovakia), Vol. 10, No. 2, p. 45-50 (June 1977).

Stefan, O.
"Describing the Performance of a Piezoceramic Resonator by Circle Diagrams", (Res. Inst. of Electroceramics, Hradec Kralove, Czechoslovakia). TESLA Electron. (Czechoslovakia), Vol. 10, No. 2, p. 51-8 (June 1977).

Stevenson, J. K., Redwood, M.
"The Motional Reactance of a Piezoelectric Resonator - A More Accurate and Simpler Representation for Use in Filter Design", IEEE Trans. Circuit Theory (USA), Vol. CT—16, No. 4, p. 568-72 (Nov. 1969).

Suk, J.
"A Contribution to the Question of the Frequencies of Piezoelectric Plates", (Research Inst. Radiocommunications, Prague, Czechoslovakia). Czech. J. Phys. B., Vol. 19, No. 10, p. 1271-80 (1969).

Suk, J.
"An Influence of the Electrodes on the Frequency of Piezoelectric Bars", (Res. Inst. Radiocommunication, Prague, Czechoslovakia). Czech. J. Phys. B., Vol. 20, No. 4, p. 441-6 (1970).

Suk, J.
"The Dependence of Inter-Resonator Coupling Coefficient on the Orientation of Electrodes (crystal resonators)", (TESLA, Praha, Czechoslovakia). Slaboproudy Obz. (Czechoslovakia), Vol. 38, No. 4, p. 159-62 (April 1977). In Czech.

Syngellakis, S., Lee, P. C. Y.
"An Approximate Theory for the High-Frequency Vibrations of Piezoelectric Crystal Plates", (Dept. of Civil Engng., Princeton Univ., Princeton, NJ, USA). Proceedings of the 30th Annual Frequency Control Symposium, Atlantic City, NJ, USA, 2-4 June 1976 (Washington, DC, USA: Electronic Industries Assoc. 1976), p. 184-90.

Tabarrok, B., Sakaguchi, R. L.
"Complementary Formulation for Plate Vibrating Problems", (Univ. Toronto, Canada). Z. Angew. Math. Phys. (Switzerland), Vol. 20, No. 3, p. 423-8 (25 May 1969). In English.

Takahashi, S., Oyama, S., Konno, M.
"Vibration Nodal Point Movement of Free-Free Flexural Bar Vibrator" (Central Res. Labs., Nippon Electric Co., Ltd., Kawasaki, Japan), Trans. Inst. Electron. & Commun. Eng. Jpn. Sect. E (Japan), Vol. E59, No. 11, p. 20-1 (Nov. 1976).

Tanaka, H., Shimizu, H.
"Flexural Modes of Wave Propagation in a Piezoelectric Plate Poled in its Plane", Rec. Elec. & Commun. Eng. Conversazione Tohoku Univ. (Japan), Vol. 41, No. 2, P. 146-51 (June 1972). In Japanese.

Thery, P., Bridoux, E., Moriamez, M.
"Interactions Between High-Frequency Acoustical Waves in Lithium Niobate", (Faculte Scis. Lille, France). J. Acoust. Soc. Amer., Vol. 48, No. 3, Pt. 2, p. 772-3 (Sept. 1970).

Tiersten, H. F.
"The Relation of Electromechanical Coupling Factors to the Fundamental Material Constants for Thickness Vibrating Piezoelectric Plates", (Bell Telephone Lab., Inc., Murray Hill, NJ, USA). IEEE Trans. Sonics Ultrasonics (USA), Vol. SU-16, No. 1, Suppl., p. 30 (Jan. 1969). (1968 IEEE Ultrasonics Symposium, New York, USA, 25-27 Sep. 1968).

Tiersten, H. F.
"Piezoelectric Plate Vibrations, Linear", New York, USA: Plenum (1969), xv+212 pp.

Tiersten, H. F.
"Electromechanical Coupling Factors and Fundamental Material Constants of Thickness Vibrating Piezoelectric Plates", (Rensselaer Polytechnic Inst., Troy, NY, USA). Ultrasonics (GB), Vol. 8, No. 1, p. 19-23 (Jan. 1970).

Tiersten, H. F.
"Analysis of Trapped Energy Resonators Operating in Overtones of Thickness-Shear", (Rensselear Polytech. Inst., Troy, NY, USA). Proceedings of the 28th Annual Frequency Control Symposium 1974, Atlantic City, NJ, USA, 29-31 May 1974 (Washington, DC, USA: Electronic Industries Assoc. 1974), p. 44-8.

Tiersten, H. F.
"Analysis of Intermodulation in Thickness-Shear and Trapped Energy Resonators", (Rensselear Polytech. Inst., Troy, NY, USA). J. Acoust. Soc. Am. (USA), Vol. 57, No. 3, p. 667-81 (March 1975).

Tiersten, H. F.
"Analysis of Trapped Energy Resonators Operating in Overtones of Coupled Thickness-Shear and Thickness-Twist", (Dept. of Mech Engng. Rensselear Polytech. Inst., Troy, NY, USA). Proceedings of the 29th Annual Frequency Control Symposium, Fort Monmouth, NJ, USA, 28-30 May 1975 (Washington, DC, USA: Electronic Industries Assoc. 1975), p. 71-5.

Tiersten, H. F.
"Analysis of Nonlinear Resonance in Thickness-Shear and Trapped-Energy Resonators", (Dept. of Mech. Engng., Rensselear Polytech. Inst., Troy, NY, USA). J. Acoust. Soc. Am. (USA), Vol. 59, No. 4, p. 866-78 (April 1976).

Tiersten, H. F.
"Analysis of Trapped-Energy Resonators Operating in Overtones of Coupled Thickness Shear and Thickness Twist", (Dept. of Mech. Engng., Rensselear Polytech. Inst., Troy, NY, USA). J. Acoust. Soc. Am. (USA), Vol. 59, No. 4, p. 879-88 (April 1976).

Tiersten, H. F., Smythe, R. C.
"An Analysis of Overtone Modes in Contoured Crystal Resonators", (Dept. of Mech. Engng., Aeronautical Engng. & Mech., Rensselear Polytech. Inst., Troy, NY, USA), 31st Annual Frequency Control Symposium, Atlantic City, NJ, USA, 1-3 June, 1977 Washington, DC, USA: Elec. Indust. Assoc. 1977 p. 44-7.

Tiersten, H. F., Sinha, B. K., McDonald, J.F. Das, P. K.
"On the Influence of a Tuning Inductor on the Bandwidth of Extensional Trapped Energy Mode Transducers", Rensselear Polytechnic Institute, Troy, New York, 12181.

Tiersten, H. F., Sinha, B. K.
"An Analysis of Extensional Modes in High Coupling Trapped Energy Resonators", Rensselaer Polytechnic Institute, Troy, New York, 12181. Ultrasonic Symposium Proceedings, Cherry Hill, NJ, USA, 25-27 Sept. 1976 (New York, USA: IEEE 1978), p. 167-171.

Tomikawa, Y., Hirose, S., Konno, M.
"Equivalent Constants of a Disk Vibrator with Double Resonance", Bull. Yamagata Univ. (Eng.) (Japan), Vol. 12, No. 1, p. 67-91 (Jan. 1972). In Japanese.

Tomikawa, Y., Miura, H., Dong, S. B.
"Analysis of Electrical Equivalent Circuit Elements of Piezotuning Forks by the Finite Element Method", (Dept. of Electrical Engng. Yamagata Univ., Yonezawa, Japan). IEEE Trans. Sonics & Ultrasonics (USA), Vol. SU-25, No. 4, p. 206-12 (July 1978).

Tsuzuki, Y., Hirose, Y., Iijima, K.
"Measurement of Vibrational Modes of Piezoelectric Resonators by Means of Holography", (Yokohama Nat. Univ., Japan). Programme of the 28th Annual Frequency Control Symposium (abstracts), Atlantic City, NJ, USA, 26-28 Apr. 1971 (Fort Monmouth, NJ, USA: US Army Electronics Command 1971), p. 23

Tyutekin, V. V., Shkvarnikov, A. P.
"Calculation of the Resonance Frequencies of Flexurally Vibrating Nonuniform Rods by the Impedance Method", (Inst. Acoustics, Academy of Sci. of the USSR, Moscow, USSR). Akust. Zh. (USSR), Vol. 14, No. 2, p. 305-7 (Apr. 1968). In Russian. English translation in: Soviet Phys. Acoustics (USA), Vol. 14, No. 2, p. 257-8 (Oct. 1968).

Ueda, I., Ikegami, S.
"Vibrational Waves in a Thick Infinite Plate of Piezoelectric Crystal", Japan. J. Appl. Phys., Vol. 7, No. 3., 236-42 (March 1968).

Van der Pauw, L. J.
"Impedance Matrix of Coupled Piezoelectric Resonators", (N. V. Phillips' Gloeilampenfabrieken, Eindhoven, Netherlands). Philips Res. Rep. (Netherlands), Vol. 28, No. 2, p. 158-78 (April 1973).

Vekovishcheva, I. A.
"Simple Cases of Flexure of Thin Piezoelectric Plates", Prikl. Mekh. (USSR), Vol. 13, No. 12, p. 127-30 (Dec. 1977). In Russian. English Translation in Sov. Appl. Mech. (USA).

Volluet, G., Thomson, C. S. F.
"Computed Characteristics of Tl_3VS_4 Bulk Wave Resonators", Research Center - Domaine de Corbeville - 91401 Orsay, France. Ultrasonics Symposium Proceedings, Cherry Hill, NJ, USA, 25-27 Sept 1978 (New York, USA: IEEE 1978), p. 182-187.

Watanabe, A., Yano, T.
"Direction of Displacement in $LiNbO_3$ X-Cut Plate Shear Transducer", (Matsushita Res. Inst. Tokyo Inc., Kawasaki, Kanagawa, Japan). IEEE Trans. Sonics & Ultrason. (USA), Vol. 25, No. 3, p. 159-60 (May 1978).

Wilfinger, R. J., Bardell, P. H., Chhabra, D. S.
"The Resonsistor: A Frequency Selective Device Utilizing the Mechanical Resonance of a Silicon Substrate", IBM J. Res. Developm. (USA), Vol. 12, No. 1, 113-18 (Jan. 1968).

Yamabuchi, T., Kagawa, Y.
"Finite Element Approach for a Piezoelectric Circular Rod", (Dept. of Electrical Engineering, National Univ., Toyama, Takoaka, Toyama, Japan). IEEE Trans. Sonics & Ultrason (USA), Vol. SU-23, No. 6, p. 379-85 (Nov. 1976).

Yamabuchi, T., Kagawa, Y.
"Finite Element Approach for a Piezoelectric Circular Rod", (Dept. of Electrical Engng., Nat. Univ. Toyama, Takaoka, Japan). Trans. Inst. Electron & Commun. Eng. Jpn. Sect. E (Japan), Vol. E59, No. 10, p. 21-2 (Oct. 1976).

Yamada, T., Niizeki, N.
"Admittance of Piezoelectric Plates Vibrating under the Perpendicular Field Excitation", (Nippon Telegraph & Telephone Public Corp., Tokyo, Japan). Proc. IEEE (USA), Vol. 58, No. 6, p. 941-2 (June 1970).

Yamada, T., Niizeki, N.
"A New Formulation of Piezoelectric Plate Thickness Vibration", Rev. Elec. Commun. Lab. (Japan), Vol. 19, Nos. 5-6, p. 705-13 (May-June 1971). In English.

Yao, S. K., Young, E. H.
"Properties and Applications of Composite Bulk Acoustic Resonators", (Electro-Optics Dept., Harris Corp., Melbourne, Australia. 1976 Ultrasonics Symposium Proceedings, Annapolis, Md., USA, 29 Sept. - 1 Oct. 1976 (New York, USA: IEEE 1976), p. 593-6.

Yu-Huan, Xu
"Temperature Stability Analysis of the Resonant Frequency of a Piezoelectric Ceramic Vibrator", (Dept. of Phys., Chung Shan Univ., Canton, China). Acta Phys. Sin (China), Vol. 27, No. 2, p. 146-59 (March 1978). In Chinese.

Zelenka, J.
"Thickness Vibrations of Rectangular Piezoceramic Plates", (Vysoka Skola Strojni a Textilni, Liberec, Czechoslovakia). 4th Conference on Ceramics for Electronics, Spinderuv Mlyn, Czecnoslovakia.

Zelenka, J., Petrzilka, V., Vrzal, J., Michalec, R.
Chalupa, B., Sedlakova, L.
"Equivalent Electrical Circuit of a Bar Excited
in Longitudinal Vibrations as an Electromech-
anical Resonator", (Hochschule Maschinenbau & Textil.
Liberec, Czechoslovakia). Acustica (Germany),
Vol. 27, No. 3, p. 159-65 (Sept. 1972).
In German.

1.2.1.1

Allington, R. W.
"A Length-Thickness Flexure Mode Quartz Resonator", (Instrumentation Specialties Co., Lincoln, NE, USA). Proceedings of the 29th Annual Frequency Control Symposium, Fort Monmouth, NJ, USA, 28-30 May 1975 (Washington, DC, USA: Electronic Industries Assoc. 1975), p. 195-201.

Androsova, V. G., Pozdnyakov, P. G., Biryukov, V. I.
"Temperature Dependence of Shear Oscillation Frequency in Quartz Bars", Sov. Phys.-Dokl. (USA), Vol. 19, No. 11, p. 723-4 (May 1975). Translation of: Dokl. Akad. Nauk SSSR, Vol. 219, No. 1-3, p. 88-90 of Vol 219, No. 1 (Nov. 1974).

Asahara, J., Yazaki, E., Takazawa, K., Kita, K.
"Influences of the Inclusions in Synthetic Quartz Crystals on the Electrical Characteristics of Quartz Crystal Resonator", (Toyo Communication Equipment Co. Ltd., Tsukagoshi, Saiwai-ku, Kawasaki, Japan). Proceedings of the 29th Annual Frequency Control Symposium, Fort Monmouth, NJ, USA, 28-30 May 1975 (Washington, DC, USA: Electronic Industries Assoc. 1975), p. 211-19.

Bahadur, H., Parshad, R.
"Effect of Magnetic Field on Oscillating Properties of Quartz Crystals", (Nat. Phys. Lab., New Delhi, India). Indian J. Pure & Appl. Phys., Vol. 13, No. 10, p. 696-8 (Oct. 1975).

Bahadur, H., Parshad, R.
"Effect of Magnetic Field on Oscillating Properties of Quartz Crystals Vibrating in the Fundamental and Overtone Modes", (Nat. Phys. Lab., New Delhi, India). Indian J. Pure & Appl. Phys., Vol. 14, No. 10, p. 855-6 (Oct 1976).

Bahadur, H., Parshad, R., Hepworth, A., Lall, V.K.
"Electron Contrast Effects from Oscillating Quartz Crystals Seen by the Scanning Electron Microscope", (Nat. Phys. Lab., New Delhi, India), IEEE Trans. Sonics & Ultrason. (USA), Vol. SU-25, No. 5, p. 309-13 (Sept. 1978).

Ballato, A.
"Apparent Orientation Shifts of Mass-Loaded Plate Vibrators", (US Army Electronics Technol. & Devices Lab., Fort Monmouth, NJ, USA). Proc. IEEE (USA), Vol. 64, No. 9, p. 1449-50 (Sept. 1976).

Ballato, A., EerNisse, E. P., Lukaszek, T.
"The Force-Frequency Effect in Doubly Rotated Quartz Resonators", (US Army Electronics Technol. & Devices Lab., ECOM, Fort Monmouth, NJ, USA), 31st Annual Frequency Control Symposium, Atlantic City, NJ, USA, 1-3 June 1977. (Washington, DC, USA: Electronic Industries Assoc. 1977), p. 8-16.

Ballato, A.
"The Fluency Matrix of Quartz", (US Army Electronics Technol. & Devices Lab., ECOM, Fort Monmouth, NJ, USA). IEEE Trans. Sonics & Ultrason. (USA), Vol. SU-25, No. 2, p. 107-8 (March 1978).

Ballato, A.
"Force-Frequency Compensation Applied to Four-Point Mounting of AT-Cut Resonators", (US Army Electronics Technol. & Devices Lab., Fort Monmouth, NJ, USA). IEEE Trans. Sonics & Ultrason. (USA), Vol. SU-25, No. 4, p. 223-6 (July 1978).

Ballato, A., EerNisse, E. P., Lukaszek, T. J.
"Experimental Verification of Stress Compensation in the SC Cut", (Sandia Laboratories, Albuquerque, NM 87115). Ultrasonics Symposium Proceedings, Cherry Hill, NJ, USA, 25-27 Sept. 1978. (New York, USA: IEEE 1978), p. 144-147.

Barcus, L. C.
"Nonlinear Effects in the At-cut Quartz Resonator", (Lowell Technol. Inst., Lowell, MA, USA). IEEE Trans. Sonics & Ultrason. (USA), Vol. SU-22, No. 4, p. 245-50 (July 1975).

Bayle, D.
"On the Resonance Vibrations of Quartz and the Disturbance of the Normal Frequencies Following Two Preferred Directions", (Univ. Bordeaux, France). Acustica (Germany), Vol. 30, No. 6, p. 336-41 (June 1974). In French.

Beaver, W. D.
"Design Equations for Bi- and Plano-Convex AT-cut Resonators", (Comtec Economation, Santa Ana., Calif., USA). Proceedings of the 27th Annual Frequency Control Symposium, Cherry Hill, NJ, USA, 12-14 June 1973 (Washington, DC, USA: Electronic Industries Assoc. 1973), p. 11-19.

Berté, M.
"Acoustic-Bulk-Wav Resonators and Filters Operating in the Fundamental Mode at Frequencies Greater than 100 MHz. (Lab. Central de Recherches, Thomson-CSF, Orsay, France). Electron. Lett. (GB), Vol. 13, No. 9, p. 248-50 (28 April 1977).

Berté, M., Hartemann, P.
"Quartz Resonators at Fundamental Frequencies Greater than 100 MHz", Thomson-CSF - Research Center, Domaine de Corbeville 91401 Orsay, France. Ultrasonics Symposium Proceedings, Cherry Hill, NJ, USA, 25-27 Sept. 1978 (New York, USA: IEEE 1978), p. 148-151.

Besson, R. J., Dulmet, B. M., Gillet, D. P.
"Analysis of the Influence of Some Parameters in Quartz", Ecole Nationale Superieure de Chronometrie et de Micromecanique La Bouloie, Route de Gray - 25030 Besançon Cedex, France. Ultrasonics Symposium Proceedings, Cherry Hill, NJ, USA, 25-27 Sept. 1978 (New York, USA: IEEE 1978), p. 152-156.

Birch, J., Weston, D. A.
"Frequency-Temperature, Activity/Temperature Anomalies in High Frequency Quartz Crystal Units", (Hirst Res. Centre, General Electric Co. Ltd., Wembley, England). Proceedings of the 30th Annual Symposium on Frequency Control, Atlantic City, NJ, USA, 2-4 June 1976 (Washington, DC, USA: Electronic Industries Assoc. 1976), p. 32-9.

Borisov, M., Stoytchev, K. T., Kovachev, M. I.
"Holographic Study of Vibrations of Piezoelectric AT-cut Quartz Resonators", (Faculty of Phys., Sofia Univ., Sofia, Bulgaria). C. R. Acad. Bulg. Sci. (Bulgaria), Vol. 29, No. 4, p. 477-80 (1976).

Burgess, J. W., Muir, A. J. L.
"Quartz-Resonator Inductance", (Allen Clark Res. Centre, Plessey Co. Ltd., Caswell, Towcester, England), Electron. Lett. (GB), Vol. 11, No. 21, p. 502-3 (16 Oct. 1975).

Byrne, R. J., Lloyd, P., Spencer, W. J.
"Thickness-Shear Vibration in Rectangular AT-Cut Quartz Plates with Partial Electrodes", J. Acoust. Soc. Amer., Vol. 43, No. 2, 232-8 (Feb. 1968).

Chernykh, G. G., Yaroslavskii, M. I., Gruzinenko, V. B.
"Temperature-Frequency Characteristics of Quartz Piezoelements Developing Displacement Oscillations at the Boundary", Sov. Phys.-Crystallogr. (USA), Vol. 19, No. 4, p. 512-13 (Jan.-Feb. 1975). Translation of: Kristallografiya (USSR), Vol. 19, p. 828-31 (July-Aug. 1974).

Chernykh, G. G., Bogush, M. E., Fedorkov, A. P.
"Spectral and Temperature-Frequency Characteristics of Regular X-Cut Quartz Piezoelements", Sov. Phys.-Dokl. (USA), Vol. 19, No. 12, p. 818-19 (June 1975). Translation of: Dolk. Akad. Nauk SSSR, Vol. 219, No. 4-6, p. 1355-8 of Vol. 219, No. 6 (Dec. 1974).

Choi, S. K., Chung, K. H., Lee, M. Y.
"Utilization of Domestic Natural Quartz as Electric Resonators; Feasibility Study", J. Korean Inst., Electron. Eng., Vol. 13, No. 3, p. 84-8 (July 1976). In Korean.

Cooper, M.
"The Quartz Crystal Comes of Age", 1967 Eighteenth Annual Conference of the IEEE Vehicular Technology Group, New York, (1967) New York Institute of Electrical and Electronics Engineers, p. 72-7 (1968).

Cowdrey, D. R., Willis, J. R.
"Finite Element Calculations Relevant to AT-Cut Quartz Resonators", (Univ. Cambridge, England), Proceedings of the 27th Annual Frequency Control Symposium, Cherry Hill, NJ, USA, 12-14 June 1973 (Washington, DC, USA: Electronic Industries Assoc. 1973). p. 7-10.

Driscoll, M. M.
"Q-Multiplied Quartz Crystal Resonator for Improved HF and VHF Source Stabilization", (Westinghouse Electric Corp., Baltimore, Md., USA). Proceedings of the 27th Annual Frequency Control Symposium, Cherry Hill, NJ, USA, 12-14 June 1973 (Washington, DC, USA: Electronic Industries Assoc. 1973), p. 157-69.

Drukker, Yu. M., Gruzinenko, V. B., Yaroslavskii, M. I.
"Mechanically Coupled Bending and Contour Shear Vibrations of Piezoelectric Plates", Kristallografya (USSR), Vol. 13, No. 4, p. 714-17 (July 1968). In Russian. English translation in: Soviet Phys. Crystl. (USA).

EerNisse, E. P.
"Quartz Resonator Frequency Shifts Arising from Electrode Stress", (Sandia Labs., Albuquerque, NM, USA). Proceedings of the 29th Annual Frequency Control Symposium, Fort Monmouth, NJ, USA, 28-30 May 1975 (Washington, DC, USA: Electronic Industries Assoc. 1975), p. 1-4.

EerNisse, E. P.
"Calculations on the Stress Compensated (SC-Cut) Quartz Resonator", (Sandia Labs., Albuquerque, NM, USA). Proceedings of the 30th Annual Symposium on Frequency Control, Atlantic City, NJ, USA, 2-4 June 1976 (Washington, DC, USA: Electronic Industries Assoc. 1976), p. 8-11.

EerNisse, E. P., Lukaszek, T. J., Ballato, A.
"Variational Calculation of Force-Frequency Constants of Doubly Rotated Quartz Resonators", (Sandia Labs., Albuquerque, NM, USA). IEEE Trans. Sonics & Ultrason. (USA), Vol. 25, No. 3, p. 132-8 (May 1978).

Flanagan, T. M.
"Hardness Assurance in Quartz Crystal Resonators", (Intelcom. Rad. Tech., San Diego, Calif., USA). IEEE Trans. Nucl. Sci. (USA), Vol. NS-21, No. 6, p. 390-2 (Dec. 1974). (Annual Conference on Nuclear and Space Radiation Effects, Fort Collins, Colo., USA, 15-18 July 1974).

Fukuyo, H., Oura, N., Yokoyama, A., Nonaka, S.
"Thickness-Shear Vibration of Circular Biconvex AT-Cut Plates", (Tokyo Inst. of Technol., Japan), Electr. Eng. Jap. (USA), Vol. 94, No. 3, p. 36-42 (May-June 1974) Translation of: Trans. Inst. Electr. Eng. Jap. (Japan), Vol. 94, No. 3 (May-June 1974).

Gagnepain, J. J.
"Study of Non-Linearities of Quartz and Demonstration of the Isochronism Defect", C. R. Acad. Sci. B. (France), Vol. 266, No. 11, 711-13 (11 March 1968). In French.

Gagnepain, J. J., Besson, R.
"A Study of Quartz Crystal Nonlinearities: Application to X Cut Resonators", (Ecole Nat. Superieure Chronometrie & Micromecanique, Besançon, France). Phys. Lett. A (Netherlands), Vol. 41A, No. 5, p. 443-4 (23 Oct. 1972).

Gagnepain, J. J., Besson, R.
"A Study of Quartz Crystal Nonlinearities: Application to X Cut Resonators", (Ecole Nat. Superieure Chronometrie & Micromecanique, Besançon, France). Phys. Lett. A (Netherlands), Vol. 41A, No. 5, p. 443-4 (23 Oct. 1972).

Gagnepain, J. J.
"Nonlinear Evaluation of the Moving Elements of the Equivalent Scheme of Quartz", (Ecole Nat. Superieure Chronometrie Micromechanique, Besançon, France). C. R. Hebd. Seances Acad. Sci. B (France), Vol. 276, No. 7, p. 231-3 (12 Feb. 1973). In French.

Gagnepain, J. J.
"Influence of a Continuous Electric Field on the Resonance Frequency of a Quartz Crystal", (Ecole Nat Superieure Chronometrie & Micromecanique, Besançon, France). C. R. Hebd. Seances Acad. Sci. B (France), Vol. 276, No. 11, p. 491-4 (19 March 1973) In French.

Gagnepain, J. J.
"Fundamental Noise Studies of Quartz Crystal Resonators", (Ecole Nat. Superieure de Chronometrie et Micromecanique, Besançon, France). Proceedings of the 30th Annual Symposium on Frequency Control, Atlantic City, NJ, USA, 2-4 June 1976 (Washington, DC, USA: Electronic Industries Assoc. 1976), p. 84-91.

Gagnepain, J. J., Ponçot, J. C., Pegeot, C.
"Amplitude-Frequency Behavior of Doubly Rotated Quartz Resonators", (CNRS, Besançon, France), 31st Annual Frequency Control Symposium, Atlantic City, NJ, USA, 1-3 June 1977 (Washington, DC, USA: Electronic Industries Assoc. 1977), p. 17-22.

Ganguly, S. N.
"A Note on Vibration of a Piezoelectric Crystal with Dissipative Mechanical Parameters", (Dept. of Math., Hindu Coll., Gobardanga, Parganas, India). Indian J. Theor. Phys., Vol. 23, No. 2, p. 63-8 (June 1975).

Gerdes, R. J., Wagner, C. E.
"Study of Frequency Control Devices in the Scanning Electron Microscope", (Georgia Inst. Technol., USA). Programme of the 25th Annual Frequency Control Symposium (abstracts), Atlantic City, NJ, USA, 26-28 Apr. 1971 (Fort Monmouth, NJ, USA: US Army Electronics Command 1971), p. 24.

Glowinski, A., Lançon, R.
"Resonance Frequencies of Monolithic Quartz Structures", (Centre Nat. D'Etudes des Telecommunications, Issy-les-Moulineaux, France). Proceedings of the 23rd Annual Frequency Control Symposium, Atlantic City, NJ, USA, 6-8 May 1969 (Washington, DC, USA: Electronic Industries Assoc. 1969), p. 39-55.

Gniewinska, B.
"Effect of Oscillator Circuit and Ambient Conditions on Parameters of Quartz Crystal Unit", Elektronika (Poland), Vol. 18, No. 7-8, p. 309-12 (1977). In Polish.

Goodall, F. N., Wallace, C. A.
"The Analysis of Unwanted-Mode Vibration Patterns in AT-Cut Quartz Oscillator Crystals, Revealed by X-Ray Diffraction Topography. II. A Partial Theoretical Description of the Unwanted Mode", (Central Res. Labs., GEC Ltd., Wembley, England). J. Phys. D (GB), Vol. 8, No. 15, p. 1843-50 (21 Oct. 1975).

Graham, R. A.
"Strain Dependence of Longitudinal Piezoelectric, Elastic, and Dielectric Constants of X-Cut Quartz", (Sandia Labs., Albuquerque, NM, USA). Phys. Rev. B (USA), Vol. 6, No. 12, p. 4779-92 (15 Dec. 1972).

Graham, R. A.
"Shock-Wave Compression of X-Cut Quartz as Determined by Electrical Response Measurements", (Sandia Labs., Albuquerque, NM, USA). J. Phys. & Chem. Solids (GB), Vol. 35, No. 3, p. 355-72 (March 1974).

Haines, D. W.
"Bechmann's Number for Harmonic Overtones of Thickness-Shear Vibrations of Rotated-Y-Cut Quartz-Plates", (Columbia Univ., NY, USA). Internat. J. Solids Structures (GB), Vol. 5, No. 1, p. 1-16 (Jan. 1969).

Hammond, D. L., Adams, C. A., Benjaminson, A.
"Hysteresis Effects in Quartz Resonators", (Hewlett-Packard Co., Palo Alto, Calif., "SA). Proceedings of the 22nd Annual Frequency Control Symposium, Atlantic City, NJ, USA, 22-24 Apr. 1968 (Fort Monmouth, NJ, USA: Electronic Components Lab., 1968), p. 55-66.

Hermann, J.
"Determination of the Electromechanical Coupling Factor of Quartz Bars Vibrating in Flexure or Length-Extension", (Centre Electronique Horloger SA, Neuchatel, Switzerland). Proceedings of the 29th Annual Frequency Control Symposium, Fort Monmouth, NJ, USA, 28-30 May 1975 (Washington, DC, USA: Electronic Industries Assoc. 1975), p. 26-34.

Hermann, J.
"DT-Cut Torsional Resonators", (Centre Electronique Horloger SA, Neuchatel, Switzerland). 31st Annual Frequency Control Symposium, Atlantic City, NJ, USA, 1-3 June 1977 (Washington, DC, USA: Electronic Industries Assoc. 1977), p. 55-61.

Hermann, M. J.
"Quartz Torsion Resonators", (Centre Electronique Horloger SA, Neuchatel, Switzerland). Bul. Ann. Soc. Swisse Chronom. & Lab. Swisse Rech. Horlogers (Switzerland), Vol. 7, No. 3, p. 299-303 (1977). In French.

Hirose, Y., Tsuziki, Y., Iijima, K.
"Measurement of Contour Vibrations of Quartz Plates by Holographic Technique", (Yokohama Nat. Univ., Japan). Trans. Inst. Electron. Commun. Eng. Jap. A.B.C. (Japan) In Japanese. English translation in: Electron. & Commun. Jap. (USA), Vol. 53, No. 6, p. 49-54 (June 1970).

Holland, R.
"Nonuniformly Heated Anisotropic Plates. I. Mechanical Distortion and Relaxation [Quartz Resonator]", (Sandia Labs., Albuquerque, NM, USA). IEEE Trans. Sonics & Ultrason. (USA), Vol. SU-21, No. 3, p. 171-8 (July 1974).

Hruska, K., Khogali, A.
"Polarizing Effect with Alpha-Quartz Rods and the Electroelastic Tensor", (Univ. Khartoum, Sudan). IEEE Trans. Sonics & Ultrasonics (USA), Vol. 18, No. 3, p. 169-74 (July 1971).

Hruska, K.
"The Electroelastic Tensor and Other Second-Order Phenomena in Quasilinear Interpretation of the Polarizing Effect with Thickness Vibrations of α -Quartz Plates", (Dept. of Math., York Univ., Toronto, Ontario, Canada). 31st Annual Frequency Control Symposium, Atlantic City, NJ, USA, 1-3 June 1977 (Washington, DC, USA: Electronic Industries Assoc. 1977), p. 159-70.

Hruska, K.
"Second-Order Phenomena in α -Quartz and the Polarizing Effect with Plates of Orientation (xzl) ψ ", (York Univ., Toronto, Ontario, Canada). IEEE Trans. Sonics & Ultrason. (USA), Vol. SU-25, No. 4, p. 198-203 (July 1978).

Isherwood, B. J., Wallace, C. A.
"The Analysis of Unwanted-Mode Vibration Patterns in AT-Cut Quartz Oscillator Crystals, Revealed by X-Ray Diffraction Topography. I. Interpretation of the X-Ray Diffraction Topographs", (Central Res. Lab., GEC Ltd., Wembley. England). J. Phys. D (GB), Vol. 8, No. 15, p. 1827-42 (21 Oct. 1975).

Jamiolkowski, J.
"High Stability Quartz Resonators for Extended Frequency Range 4.5 to 5.5 MHz", Pr. Inst. Tele- & Radiotech. (Poland), Vol. 12, No. 1, p. 55-7 (1973). In Polish.

Janiaud, D.
"Influence of Supports on the Accelerometric Sensitivity of Quartz Resonators", (Office Nat. d'Etudes et de Recherche Aerospatiales, Chatillon-sous-Bagneux, France). C. R. Hebd. Seances Acad. Sci. Ser. B (France), Vol. 285, No. 4, p. 69-72 (12 Sept. 1977). In French.

Kagawa, Y., Arai, H., Yakuwa, K., Okuda, S., Shirai, K.
"Finite Element Simulation of Energy-Trapped Electromechanical Resonators", (Dept. of Electrical Engng., Toyama Univ., Takaoka, Toyama, Japan). J. Sound & Vib. (GB), Vol. 39, No. 3, p. 317-35 (8 April 1975).

Keyes, R. W., Blair, F. W.
"Stress Dependence of the Frequency of Quartz Plates", Proc. IEEE (USA), Vol. 55, No. 4, 565-6 (April 1967).

King, P. J., Luukkala, M.
"Subharmonic Generation in Quartz Plates", (Helsinki Univ. Technol., Finland). J. Phys. D (GB), Vol. 6, No. 9, p. 1047-51 (11 June 1973).

Koga, I.
"Anomalous Vibrations in AT-Cut Plates", (Kokusai Denshin Denwa Co., Naka-meguro, Tokyo, Japan). Proceedings of the 23rd Annual Frequency Control Symposium, Atlantic City, NJ, USA, 6-8 May 1969 (Washington, DC, USA: Electronic Industries Assoc. 1969), p. 128-31.

Koga, I.
"Anomalous Vibration (Activity Dips) in AT-Cut (R_1) Plates", (Kokusai Denshin Denwa Co. Tokyo, Japan). Trans. Inst. Electronics Commun. Engrs. Japan. p. 1-12 English translation in: Electronics Commun. Japan (USA), Vol. 52, No. 6 (June 1969).

Kusters, J. A., Adams, C. A., Karrer, H. E., Ward, R. W.
"Analytical and Experimental Investigations of 32 kHz Quartz Tuning Forks", (Hewlett-Packard Labs., Palo Alto, CA, USA). Proceedings of the 30th Annual Symposium on Frequency Control, Atlantic City, NJ, USA, 2-4 June 1976 (Washington DC, USA: Electronic Industries Assoc. 1976), p. 175-83.

Kusters, J. A.
"Transient Thermal Compensation for Quartz Resonators", (Hewlett-Packard Labs., Palo Alto, CA, USA). IEEE Trans. Sonics & Ultrason. (USA), Vol. SU-23, No. 4, p. 273-6 (July 1976).

Lee, P. C. Y., Spencer, W. J.
"Shear-Flexure-Twist Vibrations in Rectangular AT-Cut Quartz Plates with Partial Electrodes", (Dept. Civil and Geological Engineering, Princeton Univ., NJ, USA). J. Acoust. Soc. Amer., Vol. 45, No. 3, p. 637-45 (March 1969).

Lee, P. C. Y.
"Extensional, Flexural and Width-Shear Vibrations of Thin Rectangular Quartz Resonator Plates", (Princeton Univ., NJ, USA). Programme of the 25th Annual Frequency Control Symposium (abstracts), Atlantic City, NJ, USA, 26-28 Apr. 1971 (Fort Monmouth, NJ, USA: US Army Electronics Command 1971), p. 13.

Lee, P. C. Y., Zelenka, J.
"The Resonance Frequency Temperature Dependence of Coupled Vibrations of + ϕ X-Cut Quartz Plates", (Dept. Civil & Geological Engng., Princeton, NJ, USA). Proceedings of the 7th International Congress on Acoustics, Budapest, Hungary, 18-26 Aug. 1971 (Budapest, Hungary: Akademiai Kiado 1971), p. 201-4.

:, P. C. Y., Zelenka, J.
ıe Frequency Temperature Dependence of Coupled
:ensional, Flexural, and Width-Shear Vibrations
Rotated X-Cut Quartz Plates", (Princeton
'v., NJ, USA). J. Appl. Phys. (USA), Vol. 43,
. 8, p. 3325-8 (Aug. 1972).

:, P. C. Y., Tameroglu, S., Cakmak, A. S.
:tensional, Flexural, Width-Shear and Width-
'etch Vibrations of Thin Rectangular Resonators",
:pt. of Civil Engng., Princeton Univ.,
:nceton, NJ, USA). Ultrasonics International
75, London, England, 24-26 March 1975 (Guild-
rd, Surrey, England: IPC Sci. & Technol.
ess 1975), p. 162-5.

' e, P. C. Y., Wu, Kuang-Ming
ıe Influence of Support-Configuration on the
:eleration Sensitivity of Quartz Resonator
:tes", (Dept. of Civil Engng., Princeton
:v., Princeton, NJ, USA). IEEE Trans. Sonics
Jltrason. (USA), Vol. SU-25, No. 4, p. 220-3
uly 1978).

' wis, O., Lu, Chih-shun
elationship of Resonant Frequency of Quartz
' ystal to Mass Loading", (Xerox Corp., Webster.
' , USA). Proceedings of the 29th Annual Freq-
' ncy Control Symposium, Fort Monmouth, NJ, USA,
' -30 May 1975 (Washington, DC, USA: Electronic
' dustries Assoc. 1975), p. 5-9.

L kaszek, T. J.
' ode Control and Related Studies of VHF Quartz
Filter Crystals", (USAECOM, Fort Monmouth, NJ,
USA). IEEE Trans. Sonics & Ultrasonics (USA),
Vol. SU-18, No. 4, p. 238-46 (Oct. 1971).

M rkenscoff, X.
" ffects of Initial Bending on Resonance
' equencies of Crystal Plates", Princeton Univ.,
' , USA thesis, 1974, 122 pp. Available from
' iv. Microfilms, Ann Arbor, Mich., USA, Order
' . 75-20648.

M vrov, N. P.
" alculation of Parameters of Circular Quartz
' sonators with Energy-Trapping", Bulg. J. Phys.
(ulgaria), Vol. 4, No. 2, p. 167-78 (1977). In
Russian.

Meeker, T. R.
"Plate Constants and Dispersion Relations for
Width-Length Effects in Rotated Y-Cut Quartz
Plates", (Bell Telephone Labs. Inc., Allentown,
P , USA). Proceedings of the 29th Annual Freq-
u ncy Control Symposium, Fort Monmouth, NJ, USA,
2 -30 May 1975 (Washington, DC, USA: Electronic
Industries Assoc. 1975), p. 54-64.

M eker, T. R.
" l and X3 Flexure, Face-Shear, Extension,
' ickness-Shear and Thickness-Twist Modes in
' ctangular Rotated Y-Cut Quartz Plates", (Bell
lephone Labs. Inc., Allentown, PA, USA). 31st
' ual Frequency Control Symposium, Atlantic
ty, NJ, USA, 1-3 June 1977 (Washington, DC, USA:
' ectronic Industries Assoc 1977), p. 35-43.

Mesnage, P.
"Bulk Waves Quartz Resonator", (EMSCM, Besançon,
France). Onde Electr. (France), Vol. 56, No. 6-7,
p. 289-92 (June-July 1976). In French.

Mindlin, R. D.
"Optimum Sizes and Shapes of Electrodes for
Quartz Resonators", J. Acoust. Soc. Amer., Vol.
43, No. 6, 1329-31 (June 1968).

Mindlin, R. D., Spencer, W. J.
"Anharmonic, Thickness-Twist Overtones of Thick-
ness-Shear and Flexural Vibrations of Rectangular,
AT-Cut Quartz Plates", J. Acoust. Soc. Amer.,
Vol. 42, No. 6, 1268-77 (Dec. 1967).

Mindlin, R. D.
"Thickness-Twist Vibrations of Quartz Strip",
Report TR-3 (AD-708057), Columbia Univ., New
York, USA (July 1970). 13 pp. Contract DA-28-043-
AMC-01731(E). Available from CFSTI, Springfield,
VA, 22151, USA.

Mindlin, R. D.
"Electromagnetic Radiation from a Vibrating
Quartz Plate", Report TR-23 (AD-744312), Columbia
Univ., New York, USA (July 1972). 18 pp. Contract
N00014-67-A-0027. Available from NTIS, Springfield
VA, 22151, USA.

Mindlin, R. D.
"Electromagnetic Radiation from a Vibrating
Quartz Plate", (Columbia Univ., NY, USA). Int.
J. Solids & Struct. (Gb), Vol. 9, No. 6, p.
697-702 (June 1973).

Mindlin, R. D.
"Coupled Piezoelectric Vibrations of Quartz
Plates", (Columbia Univ., NY, USA). Int. J.
Solids & Struct. (GB), Vol. 10, No. 4, p. 453-9
(April 1974).

Munk, S.
"Facts about the Quartz Crystal", Elektronik
(Denmark), No. 4, p. 10, 12, 14 (April 1977).
In Danish.

Musha, T.
"1/f Resonant Frequency Fluctuation of a Quartz
Crystal", (Tokyo Inst. of Technol., Meguroka,
Tokyo, Japan). Proceedings of the 29th Annual
Frequency Control Symposium, Fort Monmouth, NJ,
USA, 28-30 May 1975 (Washington, DC, USA: Elec-
tronic Industries Assoc. 1975), p. 308-10.

Nakazawa, M.
"Pure- and Quasi-Plane Elastic Waves in Thickness
Quartz Crystal Plate", (Shinshu Univ., Nagano,
Japan). J. Fac. Eng. Shinshu Univ., (Japan),
No. 34, p. 155-56 (July 1973). In Japanese.

Nonaka, S., Yuuki, T., Hara, K.
"The Current Dependence of Crystal Unit Resistance
at Low Drive Level", Programme of the 25th Annual
Frequency Control Symposium (abstracts). Atlantic
City, NJ, USA, 26-28 Apr. 1971 (Fort Monmouth, NJ,
USA: US Army Electronics Command 1971), p. 33.

Onoe, M., Obazaki, M.
"Miniature AT-Cut Strip Resonators with Tilted Edges", (Inst. of Industrial Sci., Univ. of Tokyo, Roppongi, Tokyo, Japan). Proceedings of the 29th Annual Frequency Control Symposium, Fort Monmouth, NJ, USA, 28-30 May 19[illegible] (Washington, DC, USA: Electronic Industries Assoc. 1975), p. 42-8.

Oomura, Y.
"Miniaturized Circular Disk AT-Cut Crystal Vibrator", (Faculty of Engng., Tokyo Metropolitan Univ., Setagaya, Tokyo, Japan). Proceedings of the 30th Annual Symposium on Frequency Control, Atlantic City, NJ, USA, 2-4 June 1976 (Washington, DC, USA: Electronic Industries Assoc. 1976), p. 202-8.

Comura, Y.
"The Frequency Temperature Behavior of Miniaturized Circular Disk AT-Cut Crystal Vibrator". (Faculty of Engng., Tokyo Metropolitan Univ., Tokyo, Japan). Trans. Inst. Electron. & Commun. Eng. Jpn. Sect E (Japan), Vol. E61, No. 2, p. 93-4 (Feb. 1978).

Oura, N., Fukuyo, H., Yokoyama, A.
"The Vibration of a Biconvex Circular AT-Cut Plate", (Tokyo Inst. of Technol., Midoriku, Yokohama, Japan). Proceedings of the 30th Annual Symposium on Frequency Control, Atlantic City, NJ, USA, 2-4 June 1976 (Washington, DC, USA: Electronic Industries Assoc. 1976), p. 191-5.

Pearman, G. T.
"Thickness-Twist Vibrations in Beveled AT-Cut Quartz Plates", (Bell Telephone Lab., Inc., Allentown, PA, USA). J. Acoust. Soc. Amer., Vol. 45, No. 4, p. 928-34 (April 1969).

Pozdnyakov, P. G., Vasin, I. G.
"Quartz Torsional-Vibration Resonators", Dokl. Akad. Nauk. SSSR, Vol. 185, No. 4, p. 809-12 (April 1969). In Russian., p. 377-9.

Pozdnyakov, P. G.
"Quartz Resonators for Torsional Vibrations", Kristallografiya (USSR), Vol. 15, No. 1, p. 78-85 (Jan. 1970). In Russian. English translation in: Soviet Phys. Cryst. (USA).

Pozdnyakov, P. G., Bankov, V. N., Vasin, I. G.
"The Overtones of Torsional Vibrations of Quartz Rods", Kristallografiya (USSR), Vol. 15, No. 5, p. 1033-7 (Sept. 1970). In Russian.

Pozdnyakov, P. G., Fedotov, I. M.
"Thermal-Probing of Oscillating Piezoelectric Plates", Sov. Phys.-Dokl. (USA), Vol. 17, No. 8, p. 807-9 (Feb. 1973). Translation of: Dokl. Akad. Nauk SSSR, Vol. 205, No. 4-6, p. 1339-42 Vol. 205, No. 6 (Aug. 1972).

Ratajski, J. M.
"Force-Frequency Coefficient of Singly Rotated Vibrating Quartz Crystals", IBM J. Res. Developm. (USA), Vol. 12, No. 1, p. 92-9 (Jan 1968).

Ristic, V. M., Gehrels, J. F.
"Real Time Visualization of Thickness Modes in Crystal Resonators", (Univ. Toronto, Canada). Int. J. Electron. (GB), Vol. 35, No. 2, p. 281-3 (Aug. 1973).

Roberts, G. E.
"The Design of Coupled-Resonator AT-Cut Quartz Crystals for Operation on the Third Thickness-Shear Overtone", (General Electric Co., Lynchburg, VA, USA). Proc. IEEE (USA), Vol. 63, No. 10, p. 1527-9 (Oct. 1975).

Rohde, R. W., Jones, O. E.
"Mechanical and Piezoelectric Properties of Shock-Loaded X-Cut Quartz at 573°K", Rev. Sci. Instrum. (USA), Vol. 39, No. 3, p. 313-6. (March 1968).

Royer, J. J.
"A New DT Quartz Resonator", IEEE Trans. Sonics Ultrasonics (USA), Vol. SU-17, No. 1, p. 18-22 (Jan. 1970).

Sasaki, E., Jumonji, H.
"Effects of Electrode Dimensions on Resonant Q of Energy-Trapped AT-Cut Quartz Resonators", (NIT, Musashino, Japan) Electron. & Commun. Jap. (USA), Vol. 56, No. 10, p. 69-77 (Oct. 1973).

Sauerbrey, G., Jung, G.
"Vibration Modes of Plano Convex Quartz Plates", Z. Angew. Phys. (Germany), Vol. 24, No. 2, 100-8 (Jan. 1968) In German.

Schmidt, P. K.
"High-Q BT-Cut Resonators in Flat Configuration", (AEG-Telefunken Res. Inst., Ulm, Germany). Proceedings of the 28th Annual Frequency Control Symposium 1974, Atlantic City, NJ, USA, 29-31 May 1974 (Washington, DC, USA: Electronic Industries Assoc. 1974), p. 67-72.

Schnabel, P.
"Frequency Equations for n Mechanically Coupled Piezoelectric Resonators", (Phillips Zentrallab. GmbH, Lab. Aachen, W. Germany). Acustica (Internat.), Vol. 21, No. 6, p. 351-7 (1969). In English.

Sharma, R. S.
"Effect of Magnetic Field on Oscillating Properties of a Quartz Crystal", (Dept. of Phys., Univ. of Kashmir, Srinagar, India). Indian J. Pure & Appl Phys., Vol. 15, No. 4, p. 293-5 (April 1977).

Sheahan, D. F.
"An Improved Resonance Equation for AT-Cut Quartz Crystals", (Lenkurt Elec. Co. Inc., Calif, USA). Proc. IEEE (USA), Vol. 58, No. 2, p. 260-1 (Feb. 1970).

Sherman, J. H. Jr.
"A Novel Algorithm for the Design of the Electrodes of Single-Mode AT-Cut Resonators", (General Electric Co., Lynchburg, VA, USA). Proceedings of the 23rd Annual Frequency Control Symposium, Atlantic City, NJ, USA, 6-8 May 1969 (Washington, DC, USA: Electronic Industries Assoc. 1969), p. 143-56.

Smagin, A. G., Nikol'skaya, V. I.
"Quartz Resonator with Q Close to 120 x 10^6 at Temperature 2°K", Zh. Eksper. Teor. Fiz. Pis'ma (USSR), Vol. 6, No. 3, 556-8 (1 Aug. 1967). In Russian. English translation in: JETP Letters (USA), Vol. 6, No. 3, 72-4 (1 Aug. 1967).

Smagin, A. G.
"A 1-MHz Quartz Resonator with a Q Factor of 4.2 x 10^9 at a Temperature of 2K", (All-Union Civil Engng. Correspondence Inst. Moscow, USSR). Instrum. & Exp. Tech. (USA), Vol. 17, No. 6, Pt. 2, p. 1721-3 Translation of: Prib. Tekh. Eksp. (USSR), Vol. 17, No. 6, Pt. 2, p. 143-5 (Nov.-Dec. 1974).

Smagin, A. G.
"A Quartz Resonator for a Frequency of 1 MHz with a Q-Value of 4.2 x 10^9 at a Temperature of 2K", (All-Union Correspondence School of Engng. Construction Inst. Moscow, USSR). Cryogenics (GB), Vol. 15, No. 8, p. 483-5 (Aug. 1975).

Smagin, A. G.
"Amplitude-Frequency Effect as an Evidence of Anharmonicity of Oscillations", Radio Eng. & Electron. Phys. (USA), Vol. 22, No. 4, p. 343-5 (April 1977). Translation of: Radiotekh. & Elektron. (USSR), Vol 22, No. 4, p. 857-8 (April 1977).

Smolarski, A.
"Nonlinear Modification of the Quartz Crystal Equivalent Circuit", Przeglad Elektron. (Poland), Vol. 9, No. 10, p. 475-89 (1968). In Polish.

Spencer, W. J., Pearman, G. T.
"X-Ray Diffraction from Vibrating Quartz Plates", (Bell Telephone Labs Inc., Allentown, PA, USA). Advances in X-Ray Analysis, Denver, Colo., USA, 6-8 Aug. 1969 (London, England: Plenum 1970), p. 507-25.

Tichy, J., Tolman, J., Zelenka, J.
"The Dependence of the Resonance Frequency of Quartz Oscillator Crystals on the Electric Field", Conference on Frequency Generation and Control for Radio Systems, London, (1967) (London Institution of Electrical Engineers, 1967: Conference Publication No. 31) 72-7.

Tiersten, H. F.
"Analysis of Intermodulation in Rotated Y-Cut Quartz Thickness-Shear Resonators", (Rensselaer Polytech. Inst., Troy, NY, USA). Proceedings of the 28th Annual Frequency Control Symposium 1974, Atlantic City, NJ, USA, 29-31 May 1974 (Washington, DC, USA: Electronic Industries Assoc. 1974), p. 1-4.

Tiersten, H. F.
"Analysis of Intermodulation in Thickness-Shear and Trapped Energy Resonators", (Rensselaer Polytech. Inst., Troy, NY, USA). J. Acoust. Soc. Am. (USA), Vol. 57, No. 3, p. 667-81 (March 1975).

Tiersten, H. F.
"Analysis of Nonlinear Resonance in Rotated Y-Cut Quartz Thickness-Shear Resonators", (Dept. of Mech. Engng. Rensselaer Polytech. Inst., Troy, NY, USA). Proceedings of the 29th Annual Frequency Control Symposium, Fort Monmouth, NJ, USA, 28-30 May 1975 (Washington, DC, USA: Electronic Industries Assoc. 1975), p. 49-53

Tiersten, H. F., Sinha, B. K.
"Temperature Induced Frequency Changes in Electroded AT-Cut Quartz Thickness-Shear Resonators", (Dept. of Mech. Engng., Aeronautical Engng. & Mech. Rensselaer Polytech. Inst., Troy, NY, USA). 31st Annual Frequency Control Symposium, Atlantic City, NJ, USA, 1-3 June 1977 (Washington, DC, USA: Electronic Industries Assoc. 1977). p. 23-8.

Topa, V. I., Matescu, I., Velicescu, B.
"The Design and the Realization of Quartz Low-Frequency Resonators", Posta & Telecommunicatii (Rumania), Vol. 3, No. 6, p. 304-07 (June 1973). In Rumanian.

Topolevsky, R. B., Redwood, M.
"A General Perturbation Theory for Elastic Resonators and its Application to the Monolithic Crystal Filter", (Queen Mary Coll., Univ. London, England). IEEE Trans. Sonics & Ultrason. (USA), Vol. SU-22, No. 3, p. 152-61 (May 1975). (Ultrasonics Symposium (Abstracts only), Milwaukee, Wis., USA, 11-14 Nov. 1973).

Tsuzuki, Y.
"Parametric Interaction between Two Contour Modes of Vibration in X-Cut Quartz Bars", Proc. Inst. Elect. Electronics Engrs. (USA), Vol. 56, No. 1, 98 (Jan. 1968).

Tsuzuki, Y., Hirose, Y., Iisima, K.
"Holographic Observation of the Parametrically Excited Vibrational Mode of a X-Cut Quartz Plate", Proc. IEEE (USA), Vol. 56, No. 7, 1229-30 (July 1968).

Valdois, M., Janiaud, D.
"The Quartz Resonator: Existence of a Direction of Zero Acceleration Effect", (ONERA, Chatillon, France). Mes. Regul. Autom. (France), Vol. 43, No. 1, p. 57-8 (Jan. 1978). In French.

Van Ballegooijen, E. C., Boersma, F., Van der Steen, C.
"Influence of the Thickness of Tabs on the Resonating Properties of a Quartz Crystal", (Dept. of Phys., Eindhoven Univ. of Technol, Eindhoven, Netherlands). J. Acoust. Soc. Am. (USA), Vol. 62, No. 5, p. 1189-95 (Nov. 1977).

Van der Steen, C., Boersma, F.
Van Ballegooyen, E. C.
"The Influence of Mass Loading outside the Electrode Area on the Resonant Frequencies of a Quartz-Crystal", (Dept. of Phys., Eindhoven Univ. of Technol., Eindhoven, Netherlands). J. Appl. Phys. (USA), Vol. 48, No. 8, p. 3201-5 (Aug. 1977).

Vichmann, L.
"A Monolithic Quartz for Portable and Mobile Communications Equipment", (ITT Bavelemente Gruppe Europa, Nürnberg, Germany). Funk-Tech. (Germany), No. 23, p. 891-3 (Dec. 1973). In German.

Wallace, C. A., Isherwood, B. J.
"Ultrasonic Vibrations in Quartz Crystals", GEC J Sci. Technol. (GB), Vol. 35, No. 2, 87-90 (1968).

Wilson, C. J.
"X-Ray Topography of Quartz Crystal Resonators: An Investigation of Band Breaks", (Cambridge Univ. England). Proceedings of the 27th Annual Frequency Control Symposium, Cherry Hill, NJ, USA, 12-14 June 1973 (Washington, DC, USA: Electronic Industries Assoc. 1973), p. 35-8.

Wilson, C. J.
"Vibration Modes of AT-Cut Convex Quartz Resonators", (Univ. Cambridge, England). J. Phys. D (GB), Vol. 7, No. 18, p. 2449-54 (11 Dec. 1974).

Yamagata, S., Yamamoto, K., Fuskai, I., Yasuda, I.
"Thickness-Shear Stress Distributions of the Oscillating Planoconvex AT-Cut Quartz-Crystal Resonator", (Phys. Lab., Hokkaido Univ. of Education, Hokkaido, Japan), Electron. Lett. (GB), Vol. 14, No. 14, p. 450-1 (6 July 1978).

Yamagata, S., Fukai, I., Yasuda, I.
"Analysis of Vibrations in AT-Cut Quartz Crystal Plates Using a Light Modulated Oscillator", (Phys. Lab., Hokkaido Univ. of Education, Hokkaido, Japan), IEEE Trans. Sonics & Ultrason. (USA), Vol. SU-25, No. 4, p. 192-8 (July 1978).

Yen, K. H., Wang, K. I., Kagiwada, R. S.
"Efficient Bulk Wave Excitation on ST Quartz", (TRW Defense & Space Systems Group, Redondo Beach, CA, USA). Electron. Lett. (GB), Vol. 13, No. 2, p. 37-8 (20 Jan. 1977).

Loza, Yu. Kh., Molchanov, A. A., Yalovega, G. I.
"Analysis of Triggering Phenomena in a Quartz-Crystal Resonator, Controlled by p-n Junction Capacitance", Izv. VUZ Radioelektron. (USSR), Vol. 17, No. 12, p. 90-2 (Dec. 1974). In Russian.

Zelenka, J.
"Temperature Dependence of Resonant Frequency in Accurate AT and BT-cut Quartz Resonators and its Dependence on Excitation Level", (Tesla Hradec Kralove, Czechoslovakia). Tesla Electronics (Czechoslovakia), Vol. 2, No. 3, p. 67-74 (Sept. 1969).

Zelenka, J.
"Type DY Quartz Resonators, Having the Form of Rectangular Plates", Slaboproudy Obzor (Czechoslovakia), Vol. 31, No. 10, p. 437-42 (1970). In Czech.

Zelenka, J., Lee, P. C. Y.
"On the Temperature Coefficients of the Elastic Stiffness and Compliances of Alpha-Quartz", (Princeton Univ., NJ, USA). IEEE Trans. Sonics & Ultrasonics (USA), Vol. SU-18, No. 2, p. 79-80 (April 1971).

Zelenka, J.
"The Frequency Spectrum of NT-Cut Quartz Plates", (Coll. Mech. Textile Eng., Liberec, Czechoslovakia). Czech. J. Phys. B. (Czechoslovakia), Vol. B23, No. 7, p. 696-702 (1973).

Zelenka, J.
"The Influence of Electrodes on the Resonance Frequency of AT-Cut Quartz Plates", (Electrotech. Dept., Coll. of Mech. and Textile Engng., Liberec, Czechoslovakia). Int. J. Solids & Struct. (GB), Vol. 11, No. 7-8, p. 871-6 (July-Aug. 1975).

Zelenka, J.
"A Calculation of the Resonant Frequencies of Metallized AT-Cut Square Quartz Plates", (Liberec Machine Construction & Textile Inst., Czechoslovakia). Sov. Phys.-Crystallogr. (USA). Vol. 20, No. 5, p. 590-3 Translation of: Kristalografiya (USSR), Vol. 20, No. 5, p. 960-4 (Sept.-Oct. 1975).

Zelenka, J., Petrzilka, V., Michalec, R., Mikula, P.
"The Comparison of the Thickness Vibrations of Circular and Square Quartz Plates", (Vysoka Skola Stronjni a Textilni, Liberec, Czechoslovakia). Cesk. Cas. Fis. A (Czechoslovakia), Vol. 25, No. 5, p. 492-4 (1975). In Czech.

Zumsteg, A. E., Suda, P.
"Properties of a 4 MHz Miniature Flat Rectangular Quartz Resonator Vibrating in a Coupled Mode", (SSIH-Quartz Div., Omega, Bienne, Switzerland). Proceedings of the 30th Annual Symposium on Frequency Control, Atlantic City, NJ, USA, 2-4 June 1976 (Washington, DC, USA: Electronic Industries Assoc. 1976). p. 196-201.

Adams, C. A., Kusters, J. A.
"Deeply Etched SAW Resonators", (Hewlett-Packard Labs., Palo Alto, CA, USA). 31st Annual Frequency Control Symposium, Atlantic City, NJ, USA, 1-3 June 1977 (Washington, DC, USA: Electronic Industries Assoc. 1977), p. 246-50.

Alippi, A., Palma, A., Palmieri, L., Socine, G.
"Phase and Amplitude Relations between Fundamental and Second Harmonic Acoustic Surface Waves on SiO_2 and $LiNbO_3$", (Institute di Fisica, Univ. of Perugia, Italy). J. Appl. Phys. (USA), Vol. 48, No. 6, p. 2182-90 (June 1977).

Auld, B. A., Yeh, Bing-Hui.
"Piezoelectric Shear Surface Wave Grading Resonators", (W. W. Hansen Labs. of Phys., Stanford Univ., Stanford, CA, USA). 31st Annual Frequency Control Symposium, Atlantic City, NJ, USA, 1-3 June 1977 (Washington, DC, USA: Electronic Industries Assoc. 1977), p. 251-7.

Balakirev, M. K., Gorchakov, A. V.
"Coupled Surface Waves in Piezoelectrics", (Inst. of Semiconductor Phys., Acad. of Sci., Novosibirsk, USSR). Sov. Phys.-Solid State (USA), p. 355 (Feb. 1977). Translation of: Fiz. Tverdogo Tela (USSR), Vol. 19, No. 2, p. 613-14 (Feb. 1977).

Bell, L. T. Jr., Li, R. C. M.
"Surface Acoustic Wave Resonators", (Texas Instruments Inc., Dallas, TX, USA). Proc. IEEE (USA), Vol. 64, No. 5, p. 721-21 (May 1976).

Bermann, H.
"Acoustic Surface Waves - A Review", Elektron Int. (Austria), No. 10, p. 346-7 (1975). In German.

Bleustein, J. L.
"A New Surface Wave in Piezoelectric Materials", (Yale Univ., New Haven, CT, USA). Appl. Phys. Letters (USA), Vol. 13, No. 12, p. 412-13 (15 Dec. 1968).

Browning, T. I., Lewis, M. F., Milsom, R. F.
"Surface Acoustic Waves on Rotated Y-Cut $LiTaO_3$", R.S.R.E., Malvern, Worcs., UK, Plessey Co., Caswell, UK. Ultrasonics Symposium Proceedings, Cherry Hill, NJ, USA, 25-27 Sept. 1978 (New York, USA: IEEE 1978), p. 586-589.

Budreau, A. J., Carr, P. H.
"Temperature Dependence of the Attenuation of Microwave Frequency Elastic Surface Waves in Quartz", (Air Force Cambridge Res. Labs., Bedford, Mass., USA). Appl. Phys. Lett. (USA), Vol. 18, No. 6, p. 239-41 (15 March 1971).

Cambiaggio, E., Azan, F., Lantz, A.
"SAW Reflection from Metallic Gratings of Periodicity λ and Applications to Resonators", Nice University, Parc Valrose, 06034 Nice, France. Conservatoire National des Arts et Metiers, Paris, France. Ultrasonics Symposium Proceedings, Cherry Hill, NJ, USA, 25-27 Sept. 1978, (New York, USA: IEEE 1978), p. 643-646).

Campbell, J. J., Jones, W. R.
"A Method for Estimating Optimal Crystal Cuts and Propagation Directions for Excitation of Piezoelectric Surface Waves", IEEE Trans. Sonics & Ultrasonics (USA), Vol. SU-15, No. 4, 209-17 (Oct. 1968).

Coldren, L. A., Rosenberg, R. L.
"Scattering Matrix Approach to SAW Resonators", (Bell Telephone Labs. Inc., Holmdel, NJ, USA). 1976 Ultrasonics Symposium Proceedings, Annapolis, MD, USA, 29 Sept. - 1 Oct. 1976 (New York, USA: IEEE 1976), p. 266-71

Coldren, L. A.
"Characteristics of Surface Acoustic Wave Resonators Obtained from Cavity Analysis", (Bell Labs., Holmdel, NJ, USA). IEEE Trans. Sonics & Ultrason (USA), Vol. SU-24, No. 3, p. 212-17 (May 1977).

Coldren, L. A.
"Effects of Anisotropy of SAW Resonator Transverse Modes", (Bell Telephone Labs., Holmdel, NJ, USA). Appl. Phys. Lett. (USA), Vol. 31, No. 7, p. 409-12 (Oct. 1977).

Coldren, L. A., Haus, H. A., Wang, K. I.
"Experimental Verification of Mode Shape in SAW Grating Resonators", (Bell Telephone Labs., Holmdel, NJ, USA), Electron. Lett. (GB), Vol. 13, No. 21, p. 642-4 (13 Oct. 1977).

Coldren, L. A., Lemons, R. A.
"Variable Frequency SAW Resonators on Ferroelectric-ferroelastics", (Bell Labs., Holmdel, NJ, USA). Appl. Phys. Lett. (USA), Vol. 32, No. 3, p. 129-31 (1 Feb. 1978).

Coussot, G., Bridoux, E.
"Study of the Harmonic Generation of a Surface Wave in Piezoelectric Crystals", (Thomson-CSF, Orsay, France). J. Phys. (France), Vol. 33, No. 11-12, Suppl., p. C6/276-80 (Nov.-Dec. 1972). In French.

Cross, P. S., Smith, R. S., Haydl, W. H.
"Electrically Cascaded Surface-Acoustic-Wave Resonator Filters", (Inst. Angewandte-Festkorperphys., Fraunhofer-Gesellschaft, Freiburg, Germany). Electron. Lett. (GB), Vol. 11, No. 11, p. 244-5 (29 May 1975).

Cross, P. S., Haydl, W. H., Smith, R. S.
"Electronically Variable Surface-Acoustic-Wave Velocity and Tunable SAW Resonators", (Inst. fur Angewandte Festkorperphys. Fraunhofer-Gesellschaft, Freiburg, Germany). Appl. Phys. Lett. (USA), Vol. 28, No. 1, p. 1-3 (1 Jan. 1976).

Cross, P. S., Haydl, W. H., Smith, R. S.
"Design and Applications of Two-Port SAW Resonators on YZ-Lithium Niobate", (Inst. für Angewandte Festkorperphysik, Fraunhofer-Gesellschaft, Freiburg, Germany), Proc. IEEE (USA), Vol. 64, No. 5, p. 682-5 (May 1976).

Cross, P. S.
"Properties of Reflective Arrays for Surface Acoustic Resonators", (Inst. für Angewandte Festkorperphys., Fraunhofer-Gesellschaft, Freiburg, Germany). IEEE Trans. Sonics & Ultrasonics (USA), Vol. SU-23, No. 4, p. 255-62 (July 1976).

Cross, P. S., Schmidt, R. V.
"Coupled Surface-Acoustic-Wave Resonators", Bell Syst. Tech. J. (USA), Vol. 56, No. 8, p. 1447-82 (Oct. 1977).

Czechowska, Z., Weiss, K.
"The Application of Surface Waves in Piezoelectric Materials", Elektronika (Poland), Vol. 15, No. 10, p. 425-30 (1974). In Polish.

Danicki, E.
"Acoustic Surface Waves in Electronic Devices", Elektronika (Poland), Vol. 19, No. 2, p. 52-60 (1978). In Polish.

Daniel, M. R., De Klerk, J., Jones, C. K., Patterson, A.
"Surface Wave Propagation in Crystalline Quartz", (Westinghouse Research Lab., Pittsburgh, PA, USA). IEEE Trans. Sonics Ultrasonics (USA), Vol. SU-16, No. 1, Suppl., p. 23 (Jan. 1969). (1968 IEEE Ultrasonics Symposium. New York, USA, 25-27 Sept. 1968).

Engan, H., Hanebrekke, H., Ingebrigsten, K. A., Jergan, E.
"Numerical Calculations on Surface Waves in Piezoelectrics", (Norwegian Inst. Tech., Norway). Appl. Phys. Letters (USA), Vol. 15, No. 8, p. 239-41 (15 Oct. 1969).

Farnell, G. W., Lim, T. C.
"Properties of Elastic Surface Waves", (McGill Univ., Montreal, Canada). IEEE Trans. Sonics Ultrasonics (USA), Vol. SU-16, No. 1, Suppl., p. 20 (Jan. 1969). (1968 IEEE Ultrasonics Symposium, New York, USA, 25-27 Sept. 1968).

Farnell, G. W.
"SAW Propagation in Piezoelectric Solids", (Dept. of Electrical Engng., McGill Univ., Montreal, Canada). Wave Electron. (Netherlands), Vol. 2, No. 1-3, p. 1-24 (July 1976). (European Workshop on Computer Aided Design of SAW Devices, Bologna, Italy, 7-9 April 1976).

Feldmann, M., Henaff, J.
"Acoustic Surface Wave Propagation: Atlas of Calculated Configurations for Quartz, Lithium Tantalate, Lithium Niobate and Thallium Vanadosulphide in Relation to Temperature Coefficien and Piezoelectric Coupling", (CNET, Issy-les-Moulineaux, France). Rev. Phys. Appl. (France), Vol. 12, No. 11, p. 1775-88 (Nov. 1977). In Fre

Field, M. E., Chen, C. L.
"Bistable Surface Acoustic Wave Resonators", School of Electrical Engineering, Purdue Univers[illegible], W. Lafayette, IN 47907. Ultrasonics Symposium Proceedings, Cherry Hill, NJ, USA, 25-27 Sept. 1978 (New York, USA: IEEE 1978), p. 469-473.

Fildes, R. D., Hunsinger, B. J.
"Application of Unidirectional Transducers to Resonator Cavities", (Coordinated Sci. Lab., Univ. of Illinois, Urbana-Champaign, IL, USA). 1976 Ultrasonics Symposium Proceedings, Annapolis, MD, USA, 29 Sept. - 1 Oct. 1976 (New York, USA: IEEE 1976), p. 303-5.

Hanebrekke, H., Ingebrigtsen, K. A., Solie, L.
"A Note on the Perturbation Theory for Piezoelectric Coupling to Surface Waves", (Norwegian Inst. Technol., Trondheim). In book: Acoustic Surface Wave and Acousto-Optic Devices. T. Kallord (Ed.)., p. 117-24. New York, USA: Optosonic Press (1971), vii-221 pp. (0 87739 003 7).

Hartemann, P.
"Surface-Acoustic-Wave Guidance Produced by Ion Implantation in Quartz", (Thomson-CSF, Orsay, France). Electron. Lett. (GB), Vol. 10, No. 7, p. 110-11 (4 April 1974).

Hartemann, P.
"Ion-Implanted Acoustic-Surface-Wave Resonator", (Lab. Central de Recherches, Thomson-CSF, Orsay, France). Appl. Phys. Lett. (USA), Vol. 2-, No. 2, p. 73-5 (15 Jan. 1976).

Haus, H. A.
"Scattering Loss of SAW Resonators", (Res. Lab. of Electronics, MIT, Cambridge, MA, USA). Electron. Lett. (GB), Vol. 12, No. 9, p. 214-15 (29 April 1976).

Haus, H. A.
"Modes in SAW Grating Resonators", (Dept. of Electrical Engng. & Computer Sci., MIT, Cambridge, MA, USA). Electron Lett. (GB), Vol. 13, No. 1, p. 12-13 (6 Jan. 1977).

Haus, H. A.
"Bulk Scattering Loss of SAW Grating Cascades", (Res. Lab. of Electronics, MIT, Cambridge, MA, USA). IEEE Trans. Sonics & Ultrason. (USA), Vol. SU-24, No. 4, p. 259-67 (July 1977).

Haydl, W. H., Hiesinger, P., Smith, R. S., Dischler, B., Heber, K.
"Design of Quartz and Lithium Niobate SAW Resonators Using Aluminum Metalization", (Inst. for Angewandte Festkorperphys. Fraunhofer Geselschaft, Freiburg, Germany).

Haydl, W. H.
"Surface Acoustic Wave Resonators", (Inst. für Angewandte Festkorperphys., Fraunhofer Gesellschaft Freiberg, Germany). Microwave J. (USA), Vol. 19, No. 9, p. 43-6 (Sept. 1976).

Haydl, W. H., Dischler, B., Hiesinger, P.
"Multimode SAW Resonators -- A Method to Study the Optimum Resonator Design", (Inst. for Appl. Solid State Phys., Fraunhofer Gesellschaft, Freiburg, Germany). 1976 Ultrasonics Symposium Proceedings, Annapolis, MD, USA, 29 Sept. - 1 Oct. 1976 (New York, USA: IEEE 1976), p. 287-96.

Heighway, J.
"Surface Acoustic Wave Devices and Appliances", (Allen Clark Res. Centre, Plessey Co. Ltd., Towcester, England). Syst. Technol. (GB), No. 23, p. 2-6 (March 1976).

Hiesinger, P., Schmidt, K. H.
"Scanning Electron Microscopy of Resonating Surface Acoustic Wave Devices", Institut fur Angewandte Festkorperphysik der Fraunhofer Gesellschaft, Eckerstr. 4, D-7800 Freiburg, W. Germany. Ultrasonics Symposium Proceedings, Cherry Hill, NJ, USA, 25-27 Sept. 1978 (New York, USA: IEEE 1978), p. 611-616.

Hoffmann, L.
"Propagation of Surface Waves on Piezoelectric Ceramic", (Siemens, AG, Munchen, Germany). Ber. Dirsch. Keram. Ges. (Germany), Vol. 51, No. 11, p. 311-7 (Nov. 1974). In German.

Ingebrigtsen, K. A.
"Surface Waves in Piezoelectrics", (Norwegian Inst. Technology, Trondheim, Norway). J. Appl. Phys. (USA), Vol. 40, No. 7, p. 2681-6 (June 1969).

Ishihara, F., Yoshikawa, S.
"Elastic Surface Wave Devices, their Application to Communication and Processing", (NIT, Tokyo, Japan). J. Acoust. Soc. Jap. (Japan), Vol. 30, No. 10, p. 557-62 (Nov. 1974). In Japanese.

Joseph, T. R., Lakin, K. M.
"Equivalent Circuit and Properties of Surface Wave Planar Resonators", (Univ. of Southern California, Los Angeles, CA, USA). Proceedings of the 29th Annual Frequency Control Symposium, Fort Monmouth, NJ, USA, 28-30 May 1975 (Washington, DC, USA: Electronic Industries Assoc. 1975), p. 158-66.

Joshi, S. G., White, R. M.
"Excitation and Detection of Surface Elastic Waves in Piezoelectric Crystals", (Univ. of California, Berkley, USA). J. Acoust. Soc. Amer., Vol. 46, No. 1, Pt. 1, p. 17-27 (July 1969).

Joshi, S. G.
"Excitation, Detection, and Dispersion of Surface Elastic Waves in Piezoelectric Crystals", Univ. California, Berkley, USA, thesis 171 pp. Available fm Univ. Microfilms, Ann Arbor, MI, USA Order No. 69-10319.

Kaliski, S., Kapelewski, J., Makowski, Z.
"Surface Waves in Piezoquartz", Proc. Vibration Problems (Poland), Vol. 7, No. 4, 403-17 (1966).

Kim, C. S.
"Temperature Characteristics of Elastic Surface Wave", J. Korean Inst. Electron. Eng., Vol. 10, No. 3, p. 141-8 (June 1973). In Korean.

Kinoshita, Y., Kojima, H., Tabuchi, T.
"Two-Port SAW Resonator Utilizing Piezoelectric Surface Shear Wave Mode", (Central Res. Lab., Hitalchi Ltd., Kokubunji, Tokyo, Japan). 1978 IEEE MTT-S International Microwave Symposium Digest, Ottawa, Canada, 27-29 June 1978 (New York, USA: IEEE 1978), p. 472-4.

Koerber, G.
"Uncoupled Piezoelectric Surface-Wave Modes", (Iowa State Univ., Ames, USA). IEEE Trans. Sonics & Ultrasonics (USA), Vol. SU-18, No. 2, p. 73-8 (April 1971).

Kohlbacher, G., Schmitt, P.
"Components with Surface Acoustic Waves", (AEG-Telefunken, Ulm, Germany). Nachr. Elektron. (Germany), Vol. 32, No. 6, p. 181-7 (June 1978). In German.

Koyamada, Y., Yoshikawa, S., Ishihara, F.
"Analysis of SAW Resonators Using Long IDTs and their Applications", (Musashino Electrical Communication Lab., NTT, Musashino, Japan). Trans. Inst. Electron. & Commun. Eng. Jpn. Sect E (Japan), Vol. E60, No. 9, p. 481-2 (Sept. 1977).

Koyamada, Y., Yoshikawa, S.
"A Two-Port SAW Resonator Using Long IDTs", (Musashino Electrical Communication Lab., NIT, Tokyo Japan). J. Acoust. Soc. Jpn. (Japan), Vol. 33, No. 10, p. 557-64 (Oct. 1977). In Japanese.

Laker, K. R., Szabo, T. L., Kearns, W. J.
"High-Q-Factors SAW Resonators at 780 MHz", (RADC/AFSC, Hanscom AFB, MA, USA). Electron. Lett. (GB), Vol. 13, No. 4, p. 97-9 (17 Feb 1977).

Lakin, K. M., Joseph, T., Penunuri, D.
"A Surface Acoustic Wave Planar Resonator Employing an Interdigital Electrode Transducer", (Univ. Southern California, Los Angeles, USA). Appl. Phys. Lett. (USA), Vol. 25, No. 7, p. 363-5 (1 Oct. 1974).

Lardat, C.
"Surface Acoustic Wave Components", (Thomson-CSF, Cagnes-sur-Mer., France). Rev. HF (Belgium), Vol. 10, No. 9, p. 245-54 (1978). In French.

Larosa, R., Vasile, C. F., Zagardo, D. V.
"Comparison of Surface-Wave Reflection Coefficients for Different Metals on Quartz", (Hazeltine Corp., New York, USA). Electron. Lett. (GB), Vol. 9, No. 21, p. 495-6 (18 Oct. 1973).

Leah, E. G. H., Tseng, C. C.
"Nonlinear Effects in Surface Acoustic Waves", (IBM Watson Res. Center, Yorktown Heights, NY, USA). IEEE Trans. Sonics Ultrasonics (USA), Vol. SU-17, No. 1, p. 53 (Jan. 1970).

Lewis, M. F., Patterson, E.
"Some Properties of Acoustic Surface Waves on X-Cut Quartz", (GEG Ltd., Wembley, England). J. Acoust. Soc. Am. (USA), Vol. 49, No. 5, Pt. 2, p. 1667-8 (May 1971).

Li, R. C. M., Alusow, J. A., Williamson, R. C.
"Surface-Wave Resonators Using Grooved Reflectors", (MIT, Lincoln Lab., Lexington, MA, USA). Proceedings of the 29th Annual Frequency Control Symposium, Fort Monmouth, NJ, USA, 28-30 May 1975 (Washington, DC, USA: Electronic Industries Assoc. 1975), p. 167-76.

Li, R. C. M.
"310-MHz SAW Resonator with Q at the Material Limit", (Lincoln Lab., MIT, Lexington, MA, USA). Appl. Phys. Lett. (USA), Vol. 31, No. 7, p. 407-9 (Oct. 1977).

Lothe, J., Barnett, D. M.
"Further Development of the Theory for Surface Waves in Piezoelectric Crystals", (Inst. of Phys., Univ. of Oslo, Oslo, Norway), Phys. Norv. (Norway), Vol. 8, No. 4, p. 239-54 (1976).

Mason, I. M., Chambers, J., Lagasse, P. E.
"Laser-Probe Analysis of Field Distributions within Acoustic-Surface-Wave Planar Resonators", (Dept. of Electronic & Electrical Engng., Univ. Coll. London, London, England), Electron. Lett. (GB), Vol. 11, No. 14, p. 288-90 (10 July 1975).

Matthaei, G. L., O'Shaughnessy, B. P., Barman, F.
"Relations for Analysis and Design of Surface-Wave Resonators", (Dept. of Electrical Engng. & Computer Sci., Univ. of California, Santa Barbara CA, USA). IEEE Trans. Sonics & Ultrason. (USA), Vol. SU-23, No. 2, p. 99-107 (March 1976).

Matthaei, G. L., Barman, F., Savage, E. B.
"Acoustic Surface-Wave Resonators for Band-Pass Filter Applications", (Univ. of California, Electrical Engng. & Computer Sci., Santa Barbara, CA, USA). 1976 IEEE MIT-S International Microwave Symposium, Cherry Hill, NJ, USA, 14-16 June 1976 (New York, USA: IEEE 1976), p. 283-5.

Matthaei, G. L., Barman, F.
"SAW Resonators Using Low-Loss 'Waffle-Iron' Reflectors", (Electrical Engng. & Computer Sci., Univ., of California, Santa Barbara, CA, USA). 1976 Ultrasonics Symposium Proceedings, Annapolis, MD, USA, 29 Sept. - 1 Oct. 1976 (New York, USA: IEEE 1976), p. 415-18.

Matthaei, G. L., Barman, F.
"A Study of the Q and Modes of SAW Resonators Using Metal 'Waffle-Iron' and Strip Arrays", (Dept. of Electrical Engng. & Computer Sci., Univ. of California, Santa Barbara, CA, USA). IEEE Trans. Sonics & Ultrason. (USA), Vol. 25, No. 3, p. 138-46 (May 1978).

Minagawa, S., Okamoto, T., Tsubouchi, K., Mikoshiba, N.
"Saw Tunable Resonator on Monolithic MIS Structure", (Clarion Co., Kamitoda, Toda, Saitama, Japan & Research Institute of Electrical Communication, Tohoku University, Sendai, Japan). Ultrasonics Symposium Proceedings, Cherry Hill, NJ, USA, 25-27 Sept. 1978 (New York, USA: IEEE 1978), p. 464-468.

Mitsuyu, T., Ohji, K., Ono, S., Yamazaki, O. Wasa, K.
"Thin-Film Surface-Acoustic-Wave Devices", Natl. Tech. Rep. (Japan), Vol. 22, No. 6, p. 905-23 (Dec. 1976). In Japanese.

Morency, D. G., Soluch, W., Vetelino, J. F. Mittleman, S. D., Harmon, D., Surek, S., Field, J. C.
"Experimental Measurement of the SAW Properties of Berlinite", (Dept. of Electrical Engng., Univ. of Maine, Orono, ME, USA). Appl. Phys. Lett. (USA), Vol. 33, No. 2, p. 117-19 (15 July 1978).

Moriamez, M., Bridoux, E., Desrumaux, J. M. Rouvaen, J. M., Delannoy, M.
"Propagation of Acoustic Surface Waves in Piezoelectric Crystals", (Centre Univ. Valenciennes, France). Revue Phys. Appl. (France), Vol. 6, No. 3, p. 333-9 (Sept. 1971). In French.

Nevesely, M., Szekely, J.
"The Possibilities of Applications of Surface (Rayleigh) Elastic Waves in Microwave Technology", Elektrotech. Cas. (Czechoslovakia), Vol. 27, No. 10, p. 775-82 (1976). In Slovak.

O'Connell, R. M., Carr, P. H.
"High Piezoelectric Coupling Temperature-Compensated Cuts of Berlinite ($AlPO_4$) for SAW Applications", (Deputy for Electronic Technol., RADC/AFSC, Hanscom Air Force Base, MA, USA). IEEE Trans. Sonics & Ultrason. (USA), Vol. SU-24, No. 6, p. 376-84 (Nov. 1977).

O'Connell, R. M., Carr, P. H.
"New Materials for Surface Acoustic Wave (SAW) Devices", (RADC/AFSC, Hanscom AFB, MA, USA). Opt. Eng. (USA), Vol. 16, No. 5, p. 440-5 (Sept.-Oct. 1977).

O'Connell, R. M.
"Cuts of Lead Potassium Niobate, $Pb_2KNb_5O_{15}$, for Surface Acoustic Wave (SAW) Applications", (Rome Air Development Center, Hanscom AFB, MA, USA). J. Appl. Phys. (USA), Vol. 49, No. 6, p. 3324-7 (June 1978).

Ono, S., Yamazaki, O., Ohji, K., Wasa, K., Hayakawa, S.
"SAW Resonators Using RF-Sputtered ZnO Films on Glass Substrates", (Materials Res. Lab., Matsushita Electric Industrial Co. Ltd., Kadoma, Osaka, Japan). Appl. Phys. Lett. (USA), Vol. 33, No. 3, p. 217-18 (1 Aug. 1978).

Owens, J. M., Smith, C. V. Jr., Adam, J. D., Patterson, R.
"Magnetostatic Wave Devices: A Status Report", (The University of Texas at Arlington, Arlington, TX and Westinghouse Research, Pittsburg, PA). Ultrasonics Symposium Proceedings, Cherry Hill, NJ, 25-27 Sept. 1978 (New York, USA: IEEE 1978), p. 684-698.

Parker, T. E., Schulz, M. B., Wichansky, H.
"Temperature Stable Materials for SAW Devices", (Raytheon Res. Div., Waltham, MA, USA), Proceedings of the 29th Annual Frequency Control Symposium, Fort Monmouth, NJ, USA, 28-30 May 1975 (Washington, DC, USA: Electronic Industries Assoc. 1975), p. 143-9.

Rosenberg, R. L., Coldren, L. A.
"Reflection-Dependent Coupling between Grating Resonators [Passband Filter]", (Bell Telephone Labs. Inc., Holmdel, NJ, USA). 1976 Ultrasonics Symposium Proceedings, Annapolis, MD, USA, 29 Sept. - 1 Oct. 1976 (New York, USA: IEEE 1976), p. 281-6.

Rosenfeld, R. C., O'Shea, T. F., Ameson, S. H.
"Tuning Quartz SAW Resonators by Opening Shorted Reflectors", (Communications Div., Motorola Inc., Schaumburg, IL, USA). 31st Annual Frequency Control Symposium, Atlantic City, NJ, USA, 1-3 June 1977 (Washington, DC, USA: Electronic Industries Assoc. 1977). p. 231-9.

Richardson, B. A., Kino, G. S.
"Probing of Elastic Surface Waves in Piezoelectric Media", (Stanford Univ., Calif., USA). Appl. Phys. Letters (USA), Vol. 16, No. 2, p. 82-5 (15 Jan. 1970).

Sabine, H., Cole, P. H.
"Surface Acoustic Waves in Communications Engineering", (Univ. Adelaide, Australia). Ultrasonics (GB), Vol. 9, No. 2, p. 103-13 (April 1971).

Sato, H., Meguro, T., Yamanouchi, K., Shibayama, K.
"Optimum Cut for Rotated Y-Cut $LiNbO_3$ Crystals Used as the Substrate of Elastic Surface Wave Filters", (Tohoku Univ., Sendai, Japan). J. Acoust. Soc. Jap. (Japan), Vol. 30, No. 10, p. 549-56 (Nov. 1974). In Japanese.

Schmitt, P., Waller, W.
"Resonators With Surface Acoustic Waves", Wiss. Ber. AEG-Telefunken (Germany), Vol. 50, No. 3, p. 100-6 (1977). In German.

Schoenwald, J. S., Shreve, W. R.
"Surface Acoustic Wave Resonator Development", (Texas Instruments Inc., Dallas, TX, USA). Proceedings of the 29th Annual Frequency Control Symposium, Fort Monmouth, NJ, USA, 28-30 May 1975 (Washington, DC, USA: Electronic Industries Assoc. 1975), p. 150-7.

Schoenwald, J. S.
"Progress in SAW Resonator Development", (Teledyne MEC, Palo Alto, CA, USA). Proceedings of the 1976 IEEE International Symposium on Circuits and Systems, Munich, Germany, 27-29 April 1976 (New York, USA: IEEE 1976), p. 698-701.

Schoenwald, J. S.
"Optical Waveguide Model for SAW Resonators", (Teledyne MEC, Palo Alto, CA, USA). Proceedings of the 30th Annual Symposium on Frequency Control, Atlantic City, NJ, USA, 2-4 June 1976 (Washington, DC, USA: Electronic Industries Assoc. 1976), p. 340-5.

Schoenwald, J. S.
"Tunable Variable Bandwidth/Frequency SAW Resonators", (Teledyne MEC, Palo Alto, CA, USA). 31st Annual Frequency Control Symposium, Atlantic City, NJ, USA, 1-3 June 1977 (Washington, DC, USA: Electronic Industries Assoc. 1977). p. 240-5.

Schulz, M. B., Matsinger, B. J., Holland, M. G.
"Temperature Dependence of the Surface Acoustic Wave Velocity in Quartz", IEEE Trans. Sonics Ultrasonics (USA), Vol. SU-17, No. 1, p. 59 (Jan. 1970).

Schulz, M. B., Holland, M. G.
"Temperature Dependence of Surface Acoustic Wave Velocity in Lithium Tantalate", (Raytheon Res. Div., Waltham, Mass., USA). IEEE Trans. Sonics & Ultrasonics (USA), Vol. SU-19, No. 3, p. 381-4 (July 1972).

Schwelb, O., Adler, E. L.
"Guided Modes and Proximity Coupling in SAW Resonators", (Dept. of Electrical Engng., Concordia Univ., Montreal, Canada and Dept. of Elect. Engng., McGill Univ., Montreal, Canada). Ultrasonics Symposium Proceedings, Cherry Hill, NJ, USA, 25-27 Sept. 1978 (New York, USA: IEEE 1978), p. 651-657.

Shibayama, K., Uchiyama, H.
"The Velocity of Elastic Surface Wave on X-Cut Quartz Plates", Rep. Res. Inst. Elect. Commun. Tohoku Univ. (Japan), Vol. 19, No. 1, 9-15 (1966).

Shibayama, K., Yamanouchi, K., Sato, H., Meguto, T.
"Optimum Cut for Rotated Y-Cut $LiNbO_3$ Crystal Used as the Substrate of Acoustic Surface-Wave Filters", (Res. Inst. of Electrical Communication, Tohoku Univ., Sendai, Japan). Proc. IEEE (USA), Vol. 64, No. 5, p. 595-7 (May 1976).

Shimizu, Y., Terazaki, A., Sakaue, T.
"Temperature Dependence of SAW Velocity for Metal Film on α -Quartz", (Tokyo Inst. of Technol., Tokyo, Japan). 1976 Ultrasonics Symposium Proceedings, Annapolis, MD, USA, 29 Sept. - 1 Oct. 1976 (New York, USA: IEEE 1976), p. 519-22.

Shimzu, M., Tsutsumi, M.
"The Coupling of Elastic Surface Waves in Piezoelectric Crystals", (Faculty of Engng., Osaka Univ., Suita, Japan). Trans. Inst. Electron. & Commun. Eng. Jpn. Sect. E (Japan), Vol. E60, No. 1, p. 48 (Jan. 1977).

Shimizu, Y., Sakaue, T., Terazaki, A., Kaneaki, T.
"Temperature Dependence of Surface-Acoustic-Wave on α -Quartz", (Tokyo Inst. of Technol. Tokyo, Japan). Trans. Inst. Electron. & Commun. Eng. Jpn. Sect E (Japan), Vol. E61, No. 2, p. 94-5 (Feb. 1978).

Shreve, W. R.
"Two-Port Quartz SAW Resonators", (Texas Instruments Inc., Dallas, TX). Proceedings of the 30th Annual Symposium on Frequency Control, Atlantic City, NJ, USA, 2-4 June 1976 (Washington, DC, USA: Electronic Industries Assoc. 1976), p. 328-33.

Shreve, W. R., Stigall, R. E.
"Surface Acoustic Wave Devices for Use in a High Performance Television Tuner", (Texas Instruments Inc., Dallas, TX, USA). IEEE Trans. Consum. Electron. (USA), Vol. CE-24, No. 1, p. 96-104 (Feb. 1978).

Sinha, B. K., Tiersten, H. F.
"On the Temperature Dependence of the Velocity of Surface Waves in Quartz", Rensselaer Polytechnic Institute, Troy, NY, USA. Ultrasonics Symposium Proceedings, Cherry Hill, NJ, USA, 25-27 Sept. 1978 (New York, USA: IEEE 1978), p. 662-666.

Slobodnik, A. J. Jr.
"Surface Acoustic Waves and SAW Materials", (Air Force Cambridge Res. Labs., AFSC, Hanscom AFB, MA, USA). Proc. IEEE (USA), Vol. 64, No. 5, p. 581-95 (May 1976).

Slobodnik, A. J. Jr., Silva, J. H., Kearns, W. J., Szabo, T. L.
"Lithium Tantalate SAW Substrate Minimal Diffraction Cuts", (RADC/AFSC, Hanscom AFB, MA, USA). IEEE Trans. Sonics & Ultrason. (USA), Vol. SU-25, No. 2, p. 92-7 (March 1978).

Solodov, I. Yu.
"Collinear Nonlinear Interaction of Elastic Surface Waves in Quartz", (Dept. Acoustics, Moscow Univ., USSR). Vestn. Mosk. Univ. Fiz. Astron. (USSR), Vol. 13, No. 1, p. 35-9 (1972). In Russian.

Soluch, W., Lee, K., Latuszek, A.
"Properties of Elastic Surface Waves in $LiIO_3$", Bull. Acad. Pol. Sci, Ser. Sci. Tech. (Poland), Vol. 20, No. 6, p. 473-6 (1972).

Spaight, R. N., Koerber, G. G.
"Piezoelectric Surface Waves on $LiNbO_3$", IEEE Trans. Sonics & Ultrasonics (USA), Vol. SU-18, No. 4, p. 237-8 (Oct. 1971).

Staples, E. J.
"UHF Surface Acoustic Wave Resonators", (Texas Instruments, Inc., Dallas, USA). Proceedings of the 28th Annual Frequency Control Symposium, 1974, Atlantic City, NJ, USA, 29-31 May 1974 (Washington, DC, USA: Electronic Industries Assoc. 1974), p. 280-5.

Staples, E. J., Smythe, R. C.
"SAW Resonators and Coupled Resonator Filters", (Piezo Technol. Inc., Orlando, FL, USA). Proceedings of the 30th Annual Symposium on Frequency Control, Atlantic City, NJ, USA, 2-4 June 1976 (Washington, DC, USA: Electronic Industries Assoc. 1976), p. 322-7.

Tanski, W. J., Van de Vaart, H.
"The Design of SAW Resonators on Quartz with Emphasis on Two Ports", (Sperry Res. Center, Sudbury, MA, USA). 1976 Ultrasonics Symposium Proceedings, Annapolis, MA, USA, 29 Sept. - 1 Oct. 1976 (New York, USA: IEEE 1976), p. 260-5.

Tanski, W. J.
"A Configuration and Circuit Analysis for One-Port SAW Resonators", (Sperry Res. Center, Sudbury, MA, USA). J. Appl. Phys. (USA), Vol. 49, No. 4, p. 2559-60 (April 1978).

Tanski, W. J.
"High Q and GHz SAW Resonators", (Sperry Research Center, 100 North Road, Sudbury, Mass.) Ultrasonics Symposium Proceedings, Cherry Hill, NJ, USA, 25-27 Sept. 1978 (New York, USA: IEEE 1978), p. 433-437.

Toda, K.
"The Influence of External Tensile Stress on Surface Elastic Waves on Piezoelectric Ceramic Plates", (Dept. of Electrical Engng., Nat. Defense Acad., Hashirimizu, Yokosuka, Japan). Appl. Phys. (Germany), Vol. 10, No. 2, p. 161-3 (June 1976).

Vandewege, J.
"Acoustic Resonators for VHF and UHF", Rev HF (Belgium), Vol. 10, No. 4, p. 111-20 (1976). In Dutch.

Vella, P. J., Stegeman, G. I., Ristic, V. M.
"Surface-Wave Harmonic Generation on y-z, x-z, and 41-1/2 x Lithium Niobate", (Dept. of Phys., Univ. of Toronto, Toronto, Canada). J. Appl. Phys. (USA), Vol. 48, No. 1, p. 82-5 (Jan. 1977).

Wagers, R. S.
"Plate Mode Coupling in Acoustic Surface Wave Devices", (Texas Instruments Inc., Dallas, TX, USA). IEEE Trans. Sonics & Ultrason. (USA), Vol. SU-23, No. 2, p. 113-27 (March 1976).

Wagers, R. S.
"Spurious Acoustic Responses in SAW Devices", (Central Res. Labs., Texas Instruments Inc., Dallas, TX, USA). Proc. IEEE (USA), Vol. 64, No. 5, p. 699-702 (May 1976).

Welsh, F. S.
"Surface-Wave Temperature Coefficients on Lithium Tantalate", (Bell Telephone Labs. Inc., Allentown, PA, USA). IEEE Trans. Sonics & Ultrasonics (USA), Vol. SU-18, No. 2, p. 108-9 (April 1971).

Wested, J.
"New High Frequency Component: SAW-Crystal Resonator", EC-Nyt (Denmark), No. 43, p. 12-14 (April 1975). In Danish.

White, R. M.
"Surface Elastic Waves", (Univ. California, Berkley, USA). Proc. IEEE (USA), Vol. 58, No. 8, p. 1238-76 (Aug. 1970).

White, P. D., Stevens, R., Mitchell, R. F.
"Surface Acoustic Wave Resonators in Communications", (Philips Res. Labs., Redhill, England). Communications 78. Conference on Communications Equipment and Systems, Birmingham, England, 4-7 April 1978 (London, England: IEE 1978), p. 270-3.

White, P.D., Mitchell, R.F., Stevens, R.
"Synthesis and Design of Weighted Reflector Banks for SAW Resonators", Ultrasonics Symposium Proceedings, Cherry Hill, NJ, USA, 25-27 Sept. 1978 (New York, USA: IEEE 1978). p. 634-638.

Yashiro, K., Groto, N.
"Analysis of Generation of Acoustic Waves on the Surface of a Semi-Infinite Piezoelectric Solid", (Dept. of Electrical & Electronic Engng., Tokyo Inst. of Technol., Tokyo, Japan). IEEE Trans. Sonics & Ultrason. (USA), Vol. 25, No. 3, p. 146-53 (May 1978).

Yasuda, T.
"Research Works on Elastic Surface Waves in United States and European Countries", (Tokyo Inst. Technol., Japan). J. Acoust. Soc. Jap. (Japan), Vol. 30, No. 10, p. 578-83 (Nov. 1974) In Japanese.

Yen, K. H., Lau, K. F., Kagiwada, R. S.
"Second Harmonic SAW Resonators", (TRW Defense and Space Systems Group, One Space Park, Redondo Beach, CA, USA). Ultrasonics Symposium Proceedings, Cherry Hill, NJ, USA, 25-27 Sept. 1978 (New York, USA: IEEE 1978), p. 442-447.

1.3

Aoki, T., Norisawa, K., Sakisaka, M.
"Frequency Change of Quartz Resonators Irradiated by 1 MeV Electrons", (Dept. of Engng. Phys. Chubu Inst. of Technol., Kasugai, Japan). Mem. Chubu Inst. Technol. (Japan), Vol. 11A, p. 113-19 (Dec. 1975).

Aoki T., Norisawa, K., Sakisaka, M.
"Frequency Change and Elastic Constants of Quartz Irradiated by 1 MeV Electrons", (Dept. of Engng. Phys., Chubu Inst. of Technol., Kasugai, Japan). Jap. J. Appl. Phys. (Japan), Vol. 15, No. 5, p. 749-54 (May 1976).

Aoki, T., Norisawa, K., Sakisaka, M.
"Optical Absorption Study for Quartz Resonators Irradiated by Electrons", (Dept. of Engng. Phys., Chubu Inst. of Technol., Kasugai, Japan), Jap. J. Appl. Phys. (Japan), Vol. 15, No. 11, p. 2131-5 (Nov. 1976).

Aoki, T., Norisawa, K., Sakisaka, M.
"Frequency Change of Quartz Resonators Irradiated by Alpha Particles", (Dept. of Engng. Phys., Chubu Inst. of Technol., Kasugai, Japan). Jap. J. Appl. Phys. (Japan), Vol. 15, No. 12, p. 2307-10 (Dec. 1976).

Aoki, T., Wada, K.
"Optical and Anelastic Absorptions and Resonator Frequency of Electron-Irradiated Quartz", (Dept. of Engng. Phys., Chubu Inst. of Technol., Kasugai, Aichi, Japan). Jpn. J. Appl. Phys. (Japan), Vol. 17, No. 6, p. 1015-22 (June 1978).

Benedikter, H. J., Sherman, J. H., Gillespie, R. D.
"The Effect of Gamma Irradiation on the Temperature-Frequency Characteristics of AT-Cut Quartz", (General Electric Co., Lynchburg, VA, USA). Proceedings of the 28th Annual Frequency Control Symposium 1974, Atlantic City, NJ, USA, 29-31 May 1974 (Washington, DC, USA: Electronic Industries Assoc. 1974), p. 143-9.

Berg, C. A., Erickson, J. R.
"Effects of Gamma Irradiation on Frequency Stability of 5th Overtone Crystal Oscillators", (Gibbs Mfg. & Res. Corp., Jamesville, Wis, USA). Proceedings of the 23rd Annual Frequency Control Symposium, Atlantic City, NJ, USA, 6-8 May 1969 (Washington, DC, USA: Electronic Industries Assoc. 1969), p. 178-86.

Dowell, M., Lefkowitz, I., Taylor, G. W.
"Radiation Damage in $LiNbO_3$", (Frankford Arsenal, Philadelphia, PA, USA). 2nd International Meeting on Ferroelectricity, Kyoto, Japan, 4-9 Sept. 1969 (Tokyo, Japan: Phys. Soc. Japan 1969), p. 158-9.

Draggoo, V. G., Chian-Yao, S., McAllister, G. L.
"Effects of Laser Mode Structure on Damage in Quartz", (Colorado State Univ., Fort Collins, USA). IEEE J. Quantum Electron. (USA), Vol. QE.8, No. 2, Pt. 1, p. 54-7 (Feb. 1972).

Esquivel, A. L., Sagara, H. I.
"Effects of Ionizing Radiation on Swept and Unswept Synthetic Quartz Metals", (Space Electronics Lab., Hughes Aircraft Co., Culver City, CA, USA). Electrochemical Society, Fall Meeting. (Extended abstracts of Battery Division, New York, USA, 13-17 Oct. 1974 (Princeton NJ, USA: Electrochem. Soc. 1974), p. 395-6.

Felden, M., Comets, J. C., Haug, R.
"Modification of the Resonance Frequency of Various Quartz Crystal Cuts Subjected to Various Types of Particle Irradiation", Ann. Telecomm. (France), Vol. 22, No. 11-12, 284-92 (Nov.-Dec. 1967). In French.

Flanagan, T. M., Wrobel, T. F.
"Radiation Effects in Swept-Synthetic Quartz", (Gulf General Atomic Inc., San Diego, Calif, USA). IEEE Trans. Nuclear Sci. (USA), Vol. NS-16, No. 6, p. 130-7 (Dec. 1969). (Annual Conference on Nuclear and Space Radiation Effects, University Park, PA, USA, 8-11 Jul 1969).

Hartman, E. F., King, J. C.
"Calculation of Transient Thermal Imbalance within Crystal Units Following Exposure to Pulse Irradiation", (Sandia Labs., Albuquerque, NM, USA). Proceedings of the 27th Annual Frequency Control Symposium, Cherry Hill, NJ, USA, 12-14 June 1973 (Washington, DC, USA: Electronic Industries Assoc. 1973), p. 124-7.

Hartman, E. F., King, J. C.
"Calculation of Transient Thermal Imbalance within Crystal Units Following Exposure to Pulse Irradiation", (Sandia Labs., Albuquerque, NM, USA). Radiat. Eff. (GB), Vol. 26, No. 4, p. 219-23 (1975).

Hughes, R. C.
"Electronic and Ionic Charge Carriers in Irradiated Single Crystal and Fused Quartz", (Sandia Labs., Albuquerque, NM, USA). Radiat. Eff. (GB), Vol. 26, No. 4, p. 225-35 (1975).

Krebs, M.
"The Influence of X-Rays on the Resonance Frequency of DKT Piezoelectric Resonators", Cesk. Casopis Fys. A (Czechoslovakia), Vol. 19, No. 4, p. 415-17 (1969). In Czech.

Krebs, M.
"Effect of Different Kinds of Radiation on Velocity and Attenuation of Elastic Waves in Quartz and DKT", Fiz. Cas. (Czechoslovakia), Vol. 21, No. 2-3, p. 132-5 (1971). In English. (2nd seminar on Absorption and Velocity of Ultrasonic Waves in Solids, Zilina, Czechoslovakia, 9-11 Sept. 1970).

Kurin, M. N., Krivobokov, V. P., Koshelev, F. P., Mal'tseva, V. V., Darymov, V. J.
"Radiation Corrosion of the Silver Electrodes of Quartz Piezoelements", Izv. VUZ Radioelektron. (USSR), Vol. 21, No. 3, p. 116-19 (March 1978). In Russian.

King, J. C., Sander, H. H.
"Rapid Annealing of Frequency Change in Crystal Resonators Following Pulsed X-Irradiation", (Sandia Labs., Albuquerque, NM, USA). IEEE Trans. Nucl. Sci. (USA), Vol. NS-19, No. 6, p. 23-32 (Dec. 1972). (Annual Conference on Nuclear and Space Radiation Effects, Seattle, WA, USA, 24-27 July 1972).

King, J. C., Sander, H. H.
"Rapid Annealing of Frequency Change in High Frequency Crystal Resonators Following Pulsed X-Irradiation at Room Temperature", (Sandia Labs., Albuquerque, NM, USA). Proceedings of the 27th Annual Frequency Control Symposium, Cherry Hill, NJ, USA, 12-14 June 1973 (Washington, DC, USA: Electronic Industries Assoc. 1973), p. 113-19.

King, J. C., Sander, H. H.
"Transient Change in Q and Frequency of AT-Cut Quartz Resonators Following Exposure to Pulse X-Rays", (Sandia Labs., Albuquerque, NM, USA). IEEE Trans. Nucl. Sci. (USA), Vol. NS-20, No. 6, p. 117-25 (Dec. 1973). (Annual Conference on Nuclear and Space Radiation Effects, Logan, Utah, USA, 23-26 July 1973).

King, J. C., Sander, H. H.
"Transient Changes in Quartz Resonators Following Exposure to Pulse Ionization", (Sandia Labs., Albuquerque, NM, USA). Radiat. Eff. (GB), Vol. 26, No. 4, p. 203-12 (1975).

Lobanov, Ye. M., Chubarov, L. B., Zverev, B. P.
"Effect of Radiation in the Active Region of a Nuclear Reactor on Signal Frequency of Quartz Slabs", Radiotekhnika I Elektronika (USSR), Vol. 13, No. 10, p. 1864-6 (Oct. 1968). In Russian. English translation in: Radio Engng. Electronic Phys. (USA).

Ludanov, A. G., Fotchenkov, A. A., Yakolev, L. A.
"Variation of the Elastic Constants of Piezoelectric Quartz", (All-Union Sci.-Res. Inst. for Synthetics of Mineral Raw Materials, USSR). Sov. Phys.-Acoust. (USA), Vol. 22, No. 4, p. 343-4 (July-Aug. 1976). Translation of: Akust. Zh. (USSR), Vol. 22, No. 4, p. 612-13 (July-Aug. 1976).

Mattern, P. L.
"Effects of ^{60}Co Gamma Ray Irradiation on the Optical Properties of Natural and Synthetic Quartz from 85 to 300K", (Sandia Labs., Livermore, CA, USA). Proceedings of the 27th Annual Frequency Control Symposium, Cherry Hill, NJ, USA, 12-14 June 1973 (Washington, DC, USA: Electronic Industries Assoc. 1973), p. 139-52.

Mattern, P. L., Lengweiler, K., Levy, P. W.
"Effects of ^{60}Co Gamma-Ray Irradiation on the Optical Properties of Natural and Synthetic Quartz from 85 to 300K", (Sandia Labs., Livermore, CA, USA). Radiat. Eff. (GB), Vol. 26, No. 4, p. 237-48 (1975).

Paradysz, R. E., Smith, W. L.
"Crystal Controlled Oscillators for Radiation Environments", (Bell Telephone Labs., Allentown, PA, USA). Proceedings of the 27th Annual Frequency Control Symposium, Cherry Hill, NJ, USA, 12-14 June 1973 (Washington, DC, USA: Electronic Industries Assoc. 1973), p. 120-3.

Paradysz, R. E., Smith, W. L.
"Crystal Controlled Oscillators for Radiation Environments", (Bell Telephone Labs., Allentown, PA, USA). Radiat. Eff. (GB), Vol. 26, No. 4, p. 213-18 (1975).

Smith, R. W.
"Gamma Radiation Effects in Lithium Niobate", (WADCO, Corp., Richland, WA, USA). Proc. IEEE (USA), Vol. 59, No. 4, p. 712-13 (April 1971).

Soroka, V. V., Khromova, N. N.
"Elastic and Piezoelectric Properties of γ -Irradiated and Annealed Lithium Niobate Crystals", (Inst. of Aviation Instrument Construction, Leningrad, USSR). Sov. Phys.-Solid State (USA), p. 371-2 (Feb. 1977). Translation of: Tverdogo Tela (USSR), Vol. 19, No. 2, p. 638-40 (Feb. 1977).

Sosin, A.
"The Kinetics of an Atom Diffusing in One Dimension: Hydrogen in Quartz", (Univ. of Utah, Salt Lake City, UT, USA). Radiat. Eff. (GB), Vol. 26, No. 4, p. 267-71 (1975).

Vecchi, M. P., Nava, R.
"Propagation of Ultrasonic Shear Waves in γ -Ray Irradiated Quartz Crystals", (Inst. Venezolano de Investigaciones Cientificas, IVIC, Caracas, Venezuela). Appl. Phys. (Germany), Vol. 13, No. 2, p. 171-3 (June 1977).

1.4

Andres, R. P.
"Design of a Nozzle Beam Type Metal Vapor Source", (Dept. of Chem. Engng., Princeton Univ., Princeton, NJ, USA). Proceedings of the 30th Annual Symposium on Frequency Control, Atlantic City, NJ, USA, 2-4 June 1976 (Washington, DC, USA: Electronic Industries Assoc. 1976), p. 232-6.

Bahadur, H., Parshad, R.
"Operation of Quartz Crystals in their Overtones New Methods", (Nat. Phys. Lab., New Delhi, India). Indian J. Pure & Appl. Phys., Vol. 13, No. 12, p. 862-5 (Dec. 1975).

Berenshtein, B. Sh., Bobrikov, V. S.
"The Restoration of Quartz Resonators that are Used to Measure the Thickness and Rate of Vacuum Deposition of Thin Films", (Sci. Res. Phys. Inst. Voron'egh State Univ., USSR). Instrum. & Exp. Tech. (USA), Vol. 16, No. 5, Pt. 2, p. 1518 (Sept.-Oct. 1973). Translation of: Prib. Tekh. Eksp. (USSR), Vol. 16, No. 5, Pt. 2, p. 185 (Sept.-Oct. 1973).

Berenshtein, B. Sh., Karpova, L. N.
"Restoration of Quartz Resonators", (Voronezh State Univ., USSR). Instrum. & Exp. Tech. (USA), Vol. 18, No. 2, Pt. 2, p. 626 (March-April 1975). Translation of: Prib. Tekh. Eksp. (USSR), Vol. 18, No. 2, pt. 2, p. 236 (March-April 1975).

Bernstein, M.
"Quartz Crystal Units for High G Environments", (US Army Electronics Command, Fort Monmouth, NJ, USA). 1970 International Telemetering Conference, Los Angeles, CA, USA, 13-15 Oct. 1970 (Woodland Hills, CA, USA: Internat. Found. Telemetering 1970), p. 452-60.

Bernstein, M.
"Quartz Crystal Units for High G Environments", Programme of the 25th Annual Frequency Control Symposium (abstracts), Atlantic City, NJ, USA, 26-28 Apr. 1971 (Fort Monmouth, NJ, USA: US Army Electronics Command 1971), p. 25.

Berte, M.
"Acoustic Bulk Wave Resonators and Filters Operating in the Fundamental Mode at Frequencies Greater than 100 MHz", (Res. Center, Thomson-CSF, Orsay, France). 31st Annual Frequency Control Symposium, Atlantic City, NJ, USA, 1-3 June 1977 (Washington, DC, USA: Electronic Industries Assoc. 1977), p. 322-5.

Besson, R.
"A New Piezoelectric Resonator Design", (Ecole Nat. Superieure de Chronometrie et de Micromecaniqué, Besançon, France). Proceedings of the 30th Annual Symposium on Frequency Control, Atlantic City, NJ, USA, 2-4 June 1976 (Washington, DC, USA: Electronic Industries Assoc. 1976), p. 78-83.

Besson, R. J.
"A New 'Electrodeless' Resonator Design", (Ecole Nat. Superieure de Chronometrie et de Micromecanique, Besançon, France). 31st Annual Frequency Control Symposium, Atlantic City, NJ, USA, 1-3 June 1977 (Washington, DC, USA: Electronic Industries Assoc. 1977), p. 147-52.

Bond, W. L., Kusters, J. A.
"Making Doubly Rotated Quartz Plates", (Stanford Univ., Stanford, CA, USA). 31st Annual Frequency Control Symposium, Atlantic City, NJ, USA, 1-3 June 1977 (Washington, DC, USA: Electronic Industries Assoc. 1977), p. 153-8.

Bottom, V. E.
"A Novel Method of Adjusting the Frequency of Aluminum-Plated Quartz Crystal Resonators", (Tyco Crystal Products Inc., Pomona, CA, USA). Proceedings of the 30th Annual Symposium on Frequency Control, Atlantic City, NJ, USA, 2-4 June 1976 (Washington, DC, USA: Electronic Industries Assoc. 1976), p. 249-53.

Caruso, R. D., Setter, G. A.
"Frequency Adjusting a Crystal Device Utilizing the Device Header as a Seal", (Western Electric Merrimack Valley, NH, USA). Tech. Dig. (USA), No. 45, p. 9-10 (Jan. 1977).

Caruso, R. D.
"Hermetically Sealed Crystal Device Having Glass Lasing Window", Tech. Dig. (USA), Vol. 48, p. 9-10 (Oct. 1977).

Castellano, R. N., Hokanson, J. L.
"A Survey of Ion Beam Milling Techniques for Piezoelectric Device Fabrication", (Bell Telephone Labs. Inc., Allentown, PA, USA). Proceedings of the 29th Annual Frequency Control Symposium, Fort Monmouth, NJ, USA, 28-30 May 1975 (Washington, DC, USA: Electronic Industries Assoc. 1975), p. 128-34.

Castellano, R. N., Meeker, T. R., Sundahl, R. C.
"The Relationship between Quartz Surface Morphology and the Q of High Frequency Resonators", (Bell Telephone Labs. Inc., Allentown, PA, USA). 31st Annual Frequency Control Symposium, Atlantic City, NJ, USA, 1-3 June 1977 (Washington, DC, USA: Electronic Industries Assoc. 1977), p. 126-30.

Costa, P., Piacentini, G. F., Stacchiotti, G.
"LC Conventional, Electro-mechanical Quartz and Polylithic Filters", Telettra (Italy), No. 27, p. 3-22 (Nov. 1975).

Deacon, J., Heighway, J.
"SAW Technology", (Plessey Co. Ltd., Allen Clark Res. Centre, Caswell, England). Commun. Int. (GB), Vol. 3, No. 3, p. 14-16-17 (March 1976).

Engdahl, J., Matthey, H.
"32 kHz Quartz Crystal Unit for High Precision Wrist Watch", (OMEGA, SSIH-QUARTZ Division, Bienne, Switzerland). Proceedings of the 29th Annual Frequency Control Symposium, Fort Monmouth, NJ, USA, 28-30 May 1975 (Washington, DC, USA: Electronic Industries Assoc. 1975), p. 187-94.

Engdahl, J., Zumsteg, A., Weber, C.
"New SSIH Miniature 32 kHz Quartz Resonator", (SSIH Electronic SA, Bienne, Switzerland). Bul. Ann. Soc. Swisse Chronom. & Lab. Swisse Rech. Horlogers (Switzerland), Vol. 7, No. 3, p. 347-9 (1977). In French.

Field, M. E., Chen, C. L.
"On the Fabrication Tolerances of Surface Acoustic Wave Resonators, Reflectors, and Interdigital Transducers", (School of Electrical Engng., Purdue Univ., West Lafayette, IN, USA). 1976 Ultrasonics Symposium Proceedings, Annapolis, MD, USA, 29 Sept. - 1 Oct. 1976 (New York, USA: IEEE 1976), p. 510-13.

Filler, R. L., Vig, J. R.
"The Effect of Bonding on the Frequency vs. Temperature Characteristics of AT-Cut Resonators", (US Army Electronics Technol. & Devices Lab., Fort Monmouth, NJ, USA). Proceedings of the 30th Annual Symposium on Frequency Control, Atlantic City, NJ, USA, 2-4 June 1976 (Washington, DC, USA: Electronic Industries Assoc. 1976), p. 264-8.

Filler, R. L., Vig, J. R.
"The Effect of Bonding on the Frequency vs. Temperature Characteristics of AT-Cut Resonators", Report ECOM-4433, Army Electronics Command, Fort Monmouth, NJ, USA (Sept. 1976). 15 pp.

Fischer, H
"Some Results of Frequency Response Measurements of 1 MHz Precision Quartzes", (Tech. Univ. Dresden. Dresden, Germany). Nachrichtentech. Elektron. (Germany). Vol, 27, No. 4, p. 154-5 (1977). In German.

Fischer, H., Schulzke, L.
"Direct Plating to Frequency - A Powerful Fabrication Method for Crystals With Closely Controlled Parameters", Proceedings of the 30th Annual Symposium on Frequency Control, Atlantic City, NJ, USA, 2-4 June 1976 (Washington, DC, USA: Electronic Industries Assoc. 1976), p. 209-23.

Fukuyo, H., Oura, N.
"Surface Layer of a Polished Crystal Plate", (Tokyo Inst. of Technol., Nagatsuta, Midoriku, Yokohama, Japan). Proceedings of the 30th Annual Symposium on Frequency Control, Atlantic City, NJ, USA, 2-4 June 1976 (Washington, DC, USA: Electronic Industries Assoc. 1976), p. 254-8.

Fyfe, W. A.
"Lead Attaching Machine for Quartz Crystals", Tech. Dig. (USA), No. 25, p. 25-6 (Jan. 1972).

Fyfe, W. A.
"Quartz Crystal Turnover Mechanism for a Lead Soldering Machine", Tech. Dig. (USA), No. 25, p. 27-8 (Jan. 1972).

Giannotto, J. M.
"Multiple Crystal Holder", Report ECOM 2972 (AD672064), Army Electronics Lab., Fort Monmouth, NJ, USA (May 1968), 19 pp. Available from CFSTI, Springfield, VA, USA

Greutter, A.
"Some Remarks Concerning Flexural Type Quartz Vibrators for Wristwatches", Eurocon 71 Digest. Lausanne, Switzerland, 18-22 Oct 1971 (New York, USA: IEEE 1971), 1 pp.

Grzegorzewicz, J.
"High Temperature Bond to Thin Films Coating Quartz Crystal Plates", (Inst. Teli i Radiotechniczny, Warsaw, Poland). Thin Solid Films (Switzerland), Vol. 36, No. 2, p. 409 (2 Aug. 1976). (3rd International Conference on Thin Films, Budapest, Hungary, 25-29 Aug. 1975).

Guttwein, G. K., Ballato, A. D., Lukaszek, T. J.
"Design Considerations for Oscillator Crystals", Proceedings of the 22nd Annual Frequency Control Symposium, Atlantic City, NJ, USA, 22-24 Apr 1968 (Fort Monmouth, NJ, USA: Electronic Components Lab. 1968), p. 67-88.

Hafner, E.
"The Piezoelectric Crystal Unit--Definitions and Methods of Measurement", Proc. IEEE (USA), Vol. 57, No. 2, p. 179-201 (Feb. 1969).

Hall, M.
"Quartz Crystals: Familiar Component but too much Mystique?", Electron (GB), No. 114, p. 49-50 (14 April 1977).

Hara, K.
"Surface Treatment of Quartz Oscillator Plate by Ion Implantation", (JC-Division, Nippon Denso Co. Ltd., Showa-cho, Kariya, Atchi, Japan). Oyo Buturi (Japan), Vol. 47, No. 2, p. 145-6 (Feb. 1978). In Japanese.

Hart, R. K., Hicklin, W. H., Phillips, L. A.
"Methods of Cleaning Contaminants from Quartz Surfaces During Resonator Fabrication", (Georgia Inst. Technol., Atlanta, USA). Proceedings of the 28th Annual Frequency Control Symposium 1974, Atlantic City, NJ, USA, 29-31 May 1974 (Washington, DC, USA: Electronic Industries Assoc. 1974), p. 89-95.

Hart, R. K.
"Precision Single Sideband Crystal Units", Report GIT-A-1536-F ECOM-0172-F, Georgia Inst. Technol., Atlanta, USA (Aug. 1974), 60 pp ($4.25) Contract DAAB07-73-C-0172-0004. Available from NTIS, Springfield, VA, USA.

Heighway, J.
"Surface Acoustic Wave Devices", (Plessey Co. Ltd., Towcester, England). Wireless World (GB), Vol. 82, No. 1488, p. 39-43 (Aug. 1976).

Hertzog, W.
"On the Adjustment of the Inductance of Oscillator Crystals in Filter Circuits", Bull. Ass. Swisse Elec. (Switzerland), Vol. 62, No. 9, p. 451-4 (1 May 1971). In French.

Hokanson, J. L.
"Laser Matching Thin Film Electrode Arrays on Quartz Crystal Substrates", (Bell Telephone Labs. Inc., Allentown, PA, USA). Proceedings of the 23rd Annual Frequency Control Symposium, Atlantic City, NJ, USA, 6-8 May 1969 (Washington, DC, USA: Electronic Industries Assoc. 1969), p. 163-70.

Huguenin, R., Matthey, H.
"Manufacture of Quartz Clock Resonators", Rev. Polytech. (Switzerland), No. 11, p. 1517-19 (Nov. 1974). In French.

Husgen, D., Calmes, C. C. Jr.
"A Method of Angle Correction", (Savoy Electronics Inc., Ft. Lauderdale, FL, USA), Proceedings of the 30th Annual Symposium on Frequency Control, Atlantic City, NJ, USA, 2-4 June 1976 (Washington, DC, USA: Electronic Industries Assoc. 1976), p. 259-63.

Jamiolkowski, J., Sobocinski.
"Technology of Cold-Welding of High Stability Quartz Crystal Units", Pr. Inst. Tele- & Radiotech. (Poland), Vol. 18, No. 2, p. 5-15 (1974). In Polish.

Knowles, J. E.
"On the Origin of the 'Second Level of Drive' Effect in Quartz Oscillators", (Mullard Res. Labs., Redhill, England). Proceedings of the 29th Annual Frequency Control Symposium, Fort Monmouth, NJ, USA, 28-30 May 1975 (Washington, DC, USA: Electronic Industries Assoc. 1975), p. 230-6.

Koga, I.
"Specifying Quartz Crystal Cuts Without Regard to Handedness", (Kokusai Denshin Denwa Co., Tokyo, Japan). Proc. IEEE (USA), Vol. 57, No. 12, p. 2171-2 (Dec. 1969).

Kosecki, T.
"New Calibration Method for Piezoelectric Quartz Resonators by Gold Plating", Prace Inst. Tele & Radiotech. (Poland), Vol. 14, No. 3, p. 67-70 (1970). In Polish.

Kulischenko, W.
"Tuning Crystals with AJM", (S. S. White Industrial Products, Pennwalt Corp., Piscataway, NJ, USA). Solid State Technol. (USA), Vol. 18, No. 10, p. 20-1 (Oct. 1975).

Kusters, J. A., Adams, C. A., Yoshida, H., Leach, J. G.
"TICs-Further Developmental Results", (Hewlett-Packard Labs., Palo Alto, CA, USA). 31st Annual Frequency Control Symposium, Atlantic City, NJ, USA, 1-3 June 1977 (Washington DC, USA: Electronic Industries Assoc. 1977). p. 3-7.

Lee, P. C. Y., Wu, Kuang-Ming
"The Influence of Support-Configuration on the Acceleration Sensitivity of Quartz Resonator Plates", (Dept. of Civil Engng., Princeton Univ., Princeton, NJ, USA). 31st Annual Frequency Control Symposium, Atlantic City, NJ, USA, 1-3 June 1977 (Washington, DC, USA: Electronic Industries Assoc. 1977), p. 29-34.

Lorant, M.
"New Replacement for Quartz", Radio & Electron. Constructor (GB), Vol. 31, No. 9, p. 529 (May 1978).

Matistic, A. S.
"Quartz-Crystal Timing Accuracy Is Hard to Beat", (Quartz Time Products, Communications Div., Motorola Inc., Franklin Park, IL, USA). Electron. Des. (USA), Vol. 24, No. 2, p. 74-9 (19 Jan. 1976).

Matsuzawa, H., Kamiryo, K., Kano, T.
"Temperature Control of Quartz Crystals for Deposited Thin-Film Thickness Monitors", Rec. Electr. & Commun. Eng. Conversazione Tohoku Univ. (Japan), Vol. 42, No. 4, p. 211-14 (Nov. 1973). In Japanese.

McDermott, J.
"Focus on Crystals for Frequency Control", Electron. Des. (USA), Vol. 24, No. 14, p. 40-5 (5 July 1976).

Metcalf, W. S.
"Crystal Frequency Control", Electron (GB), No. 12, p. 15-17 (28 Sept. 1972).

Metcalf, W. S.
"Quartz Crystals", (Cathodeon Crystals Ltd., Cambridge, England). Elektron. Prax. (Germany), Vol. 13, No. 1-2, p. 79-80, 82 (Feb. 1978). In German.

Mindlin, R. D.
"Optimum Sizes and Shapes of Electrodes for Quartz Resonators", J. Acoust. Soc. Amer., Vol. 43, No. 6, 1329-31 (June 1968).

Mitsuyu, T., Ohji, K., Ono, S., Yamazaki, O., Wasa, K.
"Thin-Film Surface-Acoustic-Wave Devices", Natl. Tech. Rep. (Japan), Vol. 22, No. 6, p. 905-23 (Dec. 1976). In Japanese.

Nemetz, G. E.
"Using a Pendulum Suspension Diffractometer to Improve Precision of X-Raying Quartz Crystals", Programme of the 25th Annual Frequency Control Symposium (abstracts), Atlantic City, NJ, USA. 26-28 Apr. 1971 (Fort Monmouth, NJ, USA: US Army Electronics Command 1971), p. 26.

Noda, J., Suzui, J., Furusawa, Y.
"Fabrication of AT-Cut Quartz for MCF Substrates", Electr. Commun. Lab. Tech. J. (Japan), Vol. 23, No. 1, p. 79-93 (1974). In Japanese.

Okano, S.
"Quartz Crystals--A Continuing Search", (Toyo Communication Equipment Co. Ltd., Kanagawa, Japan). JEE (Japan)., No. 121, p. 39-41 (Jan. 1977).

Onoe, M., Kamada, K., Okazaki, M., Tajika, F., Manabe, N.
"4 MHz AT-Cut Strip Resonator for Wristwatch", (Inst. of Industrial Sci., Univ. of Tokyo. Roppongi, Tokyo, Japan). 31st Annual Frequency Control Symposium, Atlantic City, NJ, USA, 1-3 June 1977 (Washington, DC, USA: Electronic Industries Assoc. 1977), p. 48-54.

Oomura, Y.
"Miniaturized Circular Disk R1-Cut (AT) Crystal Vibrator by Means of Side Wire Mounting", (Faculty of Engng., Tokyo Metropolitan Univ., Tokyo, Japan). Trans. Inst. Electron. & Commun. Eng. Jpn. Sect. E (Japan), Vol. E59, No. 10, p. 17-18 (Oct. 1976).

Pantani, L.
"Temperature Stabilization and Design Criteria in Some SAW Devices", (Istituto di Ricerca sulle Onde Elettromagnetiche, CNR, Firenze, Italy). Ultrasonics International 1975, London, England, 24-26 March 1975 (Guildford, Surrey, England: IPC Sci. & Technol. Press 1975), p. 138-41.

Peters, R. D.
"Ceramic Flat Pack Enclosures for Precision Quartz Crystal Units", (Neutron Devices Dept., General Electric Co., St. Petersburg, FL USA). Proceedings of the 30th Annual Symposium on Frequency Control, Atlantic City, NJ, USA, 2-4 June 1976 (Washington, DC, USA: Electronic Industries Assoc. 1976), p. 224-31.

Piwonski, W.
"Modern Technological Processes in Quartz Resonators Manufacturing", Elektronika (Poland), No. 1, p. 14-17 (1971). In Polish.

Pogson, I.
"LF Quartz Crystals in TO-5 Case", Electron. Aust. (Austrailia), Vol. 37, No. 7, p. 53, (Oct. 1975).

Rankin, D. H.
"Vacuum Techniques in the Quartz Crystal Industry", (Hy-Q Electronics Pty, Ltd., Frankston, Victoria, Austrailia). Vacuum (GB), Vol. 22, No. 9, p. 377-80 (Sept. 1972).

Royer, J. J.
"Rectangular AT-Cut Resonators", (Bell Telephone Labs., Inc., Allentown, PA, USA). Proceedings of the 27th Annual Frequency Control Symposium, Cherry Hill, NJ, USA, 12-14 June 1973 (Washington, DC, USA: Electronic Industries Assoc. 1973), p. 30-4.

Salim, M.
"Piezoelectricity with Special Reference to Piezoelectric Analogous Relationships, Design and Development of Testing and Measuring Methods", (Pakistan Atomic Energy Comm. Karachi). Nucleus (Pakistan), Vol. 8, No. 3, p. 53-8 (July-Sept. 1971).

Schiavone, L. M.
"Electroless Gold Metallization for Polyvinylident Fluoride Films [Piezoelectric Device Application]", (Bell Labs., Holmdel, NJ, USA). J. Electrochem. Soc. (USA), Vol. 125, No. 4, p. 522-3 (April 1978).

Seed, A.
"Theoretical Studies of Microminiature Quartz Crystal Units", Conference on Frequency Generation and Control for Radio Systems, London, 1967 (London: Institution of Electrical Engineers, 1967: conference Publication No. 31) pp. 29-32.

Seed, A., Smith, D. W.
"Quartz Crystals for Timepieces", Electron. Components (GB), Vol. 14, No. 3, p. 122-6, 128 (9 Feb. 1973).

Sherman, J. H.
"Measurement of the Characteristic Frequency of an AT-Cut Plate", (General Electric Co., Lynchburg, VA, USA). 31st Annual Frequency Control Symposium, Atlantic City, NJ, USA, 1-3 June 1977 (Washington, DC, USA: Electronic Industries Assoc. 1977), p. 108-16.

Simpson, E. E.
"Manufacturing High-Reliability Quartz Crystal Units under Contamination Control", West. Elect. Engr. (USA), Vol. 14, No. 1, p. 44-9 (Jan. 1970).

Smagin, A. G.
"Frequency Correction to 10^{-8} by Ruby Laser for Precision Quartz Crystals", (All-Union Extramural Engng. Construction Inst., Moscow, USSR). Instrum. & Exp. Tech. (USA), Vol. 17, No. 5, Pt. 2, p. 1397-8 (Sept.-Oct. 1974). Translation of: Prib. Tekh. Eksp. (USSR), Vol. 17, No. 5, Pt. 2, p. 127-8 (Sept.-Oct. 1974).

Snell, F. E.
"Method for Automatically Controlling Plating Rates of Material on Crystal Resonators", Tech. Dig. (USA), No. 38, P. 41-2 (April 1975).

Snell, F. E.
"Method for Controlling Gold Usage in the Plating of Crystal Resonators", Tech. Dig. (USA), No. 38, p. 43-4 (April 1975).

Sobocinski, J., Marzec, A.
"Ultra-High Vacuum System for Final Pumping down of Quartz Crystal Resonators", Pr. Inst. Tele.- & Radiotech. (Poland), Vol. 18, No. 1, p. 55-9 (1974). In Polish.

Staudte, J. H.
"Micro-Resonators in Integrated Electronics", Proceedings of the 22nd Annual Frequency Control Symposium, Atlantic City, NJ, USA, 22-4 Apr, 1968 (Fort Monmouth, NJ, USA: Electronic Components Lab. 1968), p. 226-31.

Staudte, J. H.
"Subminiature Quartz Tuning Fork Resonator", Proceedings of the 27th Annual Frequency Control Symposium, Cherry Hill, NJ, USA, 12-14 June 1973 (Washington, DC, USA: Electronic Industries Assoc. 1973), p. 50-4.

Takeda, J.
"Oscillator Crystals Keep on Shrinking as Watch Demand Heats Up", (Kinsekisha Lab. Ltd., (Japan). JEE (Japan), No. 101, p. 15-18 (April 1975).

Thompson, E. C.
"Double Mount for Each Electrode of Crystal to Prevent Failure", Tech. Dig. (USA), No. 26, p. 59-60 (April 1972).

Toki, M., Tsuzuki, Y., Mikami, T.
"Precise Design of Motional Inductance of Longitudinal Mode X-Cut Quartz Crystal Resonator", (Faculty of Engng., Yokohama Nat. Univ., Yokohama, Japan). Trans. Inst. Electron. & Commun. Eng. Jpn. Sect. E (Japan), Vol. E-61, No. 4, p.315-16 (April 1978).

Vasin, L. N., Shushkov, A. G.
"Mechanical Processing of Quartz Resonator Plates", Sov. J. Opt. Technol. (USA), Vol. 41, No. 8, p. 477-8 (Aug. 1974). Translation of: Opt.-Mekh. Prom.-st (USSR), Vol. 41, p. 78-9 (Aug. 1974).

Vig, J., Wasshauzen, H., Cook, C., Katz, M., Hafner, E.
"Surface Preparation and Characterization Techniques for Quartz Resonators", (US Army Electronics Technol. & Devices Lab., Fort Monmouth, NJ, USA). Proceedings of the 27th Annual Frequency Control Symposium, Cherry Hill, NJ, USA, 12-14 June 1973 (Washington DC, USA: Electronic Industries Assoc. 1973), p. 98-112.

Vig, J. R., Cook, C. F. Jr., Schwidtal, K., Lebus, J. W., Hafner, E.
"Surface Studies for Quartz Resonators", (US Army Electronics Technol. & Devices Lab., Fort Monmouth, NJ , USA). Proceedings of the 28th Annual Frequency Control Symposium 1974, Atlantic City, NJ, USA, 29-31 May 1974 (Washington, DC, USA: Electronic Industries Assoc. 1974), p. 96-108.

Vig, J. R.
"A High Precision Laser Assisted X-Ray Goniometer for Circular Plates", (US Army Electronics Technol. & Devices Lab., Fort Monmouth, NJ, USA). Proceedings of the 29th Annual Frequency Control Symposium, Fort Monmouth, NJ, USA, 28-30 May 1975 (Washington, DC, USA: Electronic Industries Assoc. 1975), p. 240-7.

Vig, J. R., LeBus, J. W., Filler, R. L.
"Further Results on UV Cleaning and Ni Electrobonding", (US Army Electronics Technol. & Devices Lab., Fort Monmouth, NJ, USA). Proceedings of the 29th Annual Frequency Control Symposium, Fort Monmouth, NJ, USA, 28-30 May 1975 (Washington, DC, USA: Electronic Industries Assoc. 1975), p. 220-9.

Vig, J. R., LeBus, J. W., Filler, R. L.
"Chemically-Polished Quartz", (US Army Electronics Technol. & Devices Lab., ECOM, Fort Monmouth, NJ, USA). 31st Annual Frequency Control Symposium, Atlantic City, NJ, USA, 1-3 June 1977 (Washington, DC, USA: Electronic Industries Assoc. 1977), p. 131-43.

Vig, J. R., LeBus, J. W., Filler, R. L.
"Chemically Polished Quartz", Report ECOM-4548, US Army Electronics Command, Fort Monmouth, NJ, USA (Nov. 1977), 37 pp.

Wasshausen, H.
"Processing Techniques for Shock Resistant Precision Quartz Crystal Units", Report ECOM-3524 (AD-735685), Army Electronics Command, Fort Monmouth, NJ, USA (Dec. 1971), 41 pp Available from NTIS, Springfield, VA, USA.

Werner, J. F., Dyer, A. J.
"The Relationship Between Plateback, Mass Loading and Electrode Dimensions for AT-Cut Quartz Crystals Having Rectangular Resonators Operating at Fundamental and Overtone Modes", (Hirst Res. Centre, General Electric Co. Ltd., Wembley, England). Proceedings of the 30th Annual Symposium on Frequency Control, Atlantic City, NJ, USA, 2-4 June 1976 (Washington, DC, USA: Electronic Industries Assoc. 1976), p. 40-53.

White, M. L.
"Clean Surface Technology", (Bell Telephone Labs. Inc., Allentown, PA, USA). Proceedings of the 27th Annual Frequency Control Symposium, Cherry Hill, NJ, USA, 12-14 June 1973 (Washington, DC, USA: Electronic Industries Assoc. 1973), p.79-88.

Wilcox, P. D., Snow, G. S., Hafner, E., Vig, J. R.
"A New Ceramic Flat Pack for Quartz Resonators", (Sandia Labs., Albuquerque, NM, USA). Proceedings of the 29th Annual Frequency Control Symposium, Fort Monmouth, NJ, USA, 28-30 May 1975 (Washington, DC, USA: Electronic Industries Assoc. 1975), p. 202-10.

Wolfskill, J. M.
"Advancements in Production of 5 MHz Fifth Overtone High Precision Crystal Units", Proceedings of the 22nd Annual Frequency Control Symposium, Atlantic City, NJ, USA, 22-24 Apr 1968 (Fort Monmouth, NJ, USA: Electronic Components Lab. 1968), p. 89-117.

Albsmeier, H., Gunther, A. E., Volejnik, W.
"Some Special Design Considerations for a Mechanical Filter Channel Bank", (Siemens AG, Hanau, Germany). IEEE Trans. Commun. (USA), Vol. COM-22, No. 7, p. 935-40 (July 1974).

Albsmeier, H.
"Important Process Steps in Mechanical Channel Filter Fabrication" (Siemens, AG, Munich, Germany). Proceedings of the 1976 IEEE International Symposium on Circuits and Systems, Munich, Germany, 27-29 April 1976 (New York, USA: IEEE 1976), p. 758-60.

Albrechans, W.
"New Channel-Changer with Electromechanical Filters", Fernmelde Praxis (Germany), Vol. 48, No. 20, p. 923-6 (25 Oct. 1971). In German.

Amstutz, P., Bon, M., Bosc, R., Carru , H., Loyez, P.
"Design and Realization of an Electromechanical Filter Model for Voice Channel I", (CNET Issy-les-Moulineaux, France). Onde Electr. (France), Vol. 58, No. 4, p. 307-11 (April 1978). In French.

Ardelean, G. H., Niculescu, T., Simonescu, M.
"Optimum Filter with Magnetostrictive Line", Telecomunicati (Rumania), Vol. 12, No. 12, p. 481-8 (Dec. 1968). In Rumanian.

Ariga, M., Sato, M.
"A High Electromechanical-Coupling Resonator and its Application to Filter-Synthesis", Mem. Fac. Technol. Tokyo Metrop. Univ. (Japan), No. 23, p. 2033-42 (1973).

Ashida, T.
"Design of Piezoelectric Transducers for Temperature Stabilized Mechanical Filters" (Musashino Electrical Communication Lab., NTT, Mussashino, Japan). Electron. & Commun. Jap. (USA), Vol. 57, No. 5, p. 10-17 (May 1974).

Birn, B.
"A Modified Insertion Loss Theory for Mechanical Channel Filter Synthesis", (Fachbereich Weitverkehr und Kabeltech., AEG-Telefunken, Backnang, Germany). Proceedings of the 1976 IEEE International Symposium on Circuits and Systems, Munich, Germany, 27-29 April 1976 (New York, USA: IEEE 1976), p. 754-7.

Bon, M., Bosc, R., Loyez, P.
"New Materials for Transducers and Resonators Tolerances Assignment in Electromechanical Filters", Proceedings of the 1976 IEEE International Symposium on Circuits and Systems, Munich, Germany, 27-29 April 1976 (New York, USA: IEEE 1976), p. 739-42.

Bon, M., Bosc, R., Loyez, P.
"New Design of Electromechanical Filters at 128 kHz", (Centre Nat. d'Etudes des Telecommunications, Issy-Les-Moulineaux, France). 1977 IEEE International Symposium on Circuits and Systems Proceedings, Phoenix, Ariz., USA, 25-27 April 1975 (New York, USA: IEEE 1977), p. 239-42.

Bosc, R., Loyez, P.
"Design of an Electromechanical Filter at 128 kHz in a Two Step Modulation System", (Centre Nat. Etudes Telecommunications, Issy-Les-Moulineaux, France). Proceedings of the 1974 IEEE International Symposium on Circuits and Systems, San Francisco, CA, USA, 22-25 April 1974 (New York, USA: IEEE 1974), p. 111-14.

Bosc, R., Cobiombat, F., Herreng, C., Loyez, P.
"An Electromechanical Filter 12 Channel Project", (EST-DEF, Issy-les-Moulineaux, France). Echo Rech. (France), No. 79, p. 30-9 (Jan. 1975). In French.

Braun, A. R.
"Filters and Resonators--A Review", IEEE Trans. Sonics & Ultrason. (USA), Vol. SU-21, No. 4, p. 219 (Oct. 1974).

Bremon, C., Villela, G., Duchet, C. H.
"Single Crystal-Metal Composite Transducer for Electromechanical Filter Devices", (Lab. Filtres, CIT-Alcatel, Montihery, France), Onde Electr. (France), Vol. 58, No. 6-7, p. 464-9 (June-July 1978). In French.

Bunger, D. A.
"Composite Tuning Fork Filters", D. H. Baldwin Co., Patent USA 3437850, 19 Aug. 1963: publ. 8 April 1969, USA 303060.

Caviglia, F., Gamerro, R.
"Linear Band-Pass Filters Synthesis Method Developed for the Design of Electromechanical Filters", (CSELT, Torino, Italy). Alta Freq. (Italy), Vol. 46, No. 10, p. 463-76 (Oct. 1977). In Italian.

Chang, J. H., Tuteur, F. B.
"Adaptive Tapped Delay Line Filters", (Yale Univ., New Haven, CT, USA), Proceedings of the Second Annual Princeton Conference on Information Sciences and Systems, Princeton, NJ, USA, 25-26 Mar. 1968 (New York, NY, USA: IEEE 1968), p. 164-8.

Chelovechkov, A. J., Sharov, N. V.
"The Use of Narrow-Band Tuning Fork Filters in Geophysical Apparatus", Geofiz. Appar. (USSR), No. 51, p. 186-9 (1973). In Russian.

Court, I. N.
"Microwave Acoustic Devices for Pulse Compression Filters", IEEE Trans. Microwave Theory. Tech. (USA), Vol. MTT-17, No. 11, p. 968-86 (Nov. 1969).

Cucchi, S., Molo, F.
"Bridging Elements in Mechanical Filters: Design Procedure and an Example of Negative Bridging Element Realization", (FDM Div. Labs., Teletra SpA, Milan, Italy). Proceedings of the 1976 IEEE International Symposium on Circuits and Systems, Munich, Germany, 27-29 April 1976 (New York, USA: IEEE 1976), p. 746-9.

Deckert, J., Guls, P.
"Mechanical Filters for Channel Converters", Tech. Mitt. AEG-Telefunken (Germany), Vol. 64, No. 2-3, p. 74-6 (1974). In German.

Deschamps, R.
"Longitudinal Resonance Filters with Magnetostrictive Beams and Two Oblong Holes", Cables & Transm., (France), Vol. 31, No. 1, p. 87-108 (Jan. 1977). In French.

Dydyk, M.
"Dielectric Resonators Q to MIC Filters", (Motorola Inc., Government Electronics Div., Scottsdale, AZ, USA). Microwaves (USA), Vol. 16, No. 12, p. 150-1, 154-6 (Dec. 1977).

Ecotiere, B.
"Mechanical Resonant Filters: Problems of Construction and Design", Cables & Transm. (France), Vol. 27, No. 1, p. 126-36 (Jan. 973). In French.

Ernyei, H. H.
"Simplified Bridge Calculation and Realization of a Pole Type Mechanical Filter", (Lognes Telegraphiques et Telephoniques, Paris, France). 1977 IEEE International Symposium on Circuits and Systems Proceedings, Phoenix, AZ, USA, 25-27 April 1975 (New York, USA: IEEE 1977), p. 235-8.

Ey, K., Hornung, F., Volejnik, W.
"Channel Modern Features Electromechanical Filters", (Siemens AG., Munich, Germany). Siemens Rev. (Germany), Vol. 39, No. 7, p. 293-8 (July 1972).

Ey, K., Hornung, F., Volejnik, W.
"Electromechanical Filter Channel Modem", (Siemens Munich, Germany). Onde Electr. (France), Vol. 53, No. 8, p. 297-302 (Sept, 1973). In French.

Faktor, Z.
"Spurious Vibrations in Component Parts of Electromechanical Filters and their Investigation", Slaboproudy Obzor (Czechoslovakia), Vol. 30, No. 10, p. 444-50 (1969). In Czech.

Freris, L. L., Nunes de Carvalho, J.
"An Electromechanical Harmonic Filter", (Imperial Coll. Sci. & Technol., London, England). International Conference on High Voltage DC and/or AC Power Transmission, London, England, 19-23 Nov. 1973 (London, England: IEE 1973), p. 11-15.

Freris, L. L., Nunes de Carvalho, J.
"Electromechanical Filter and its Performance in DC Transmission Systems", (Imperial Coll. Sci. & Technol., London, England). Proc. Inst. Electr. Eng. (GB), Vol. 122, No. 1, p. 55-60 (Jan. 1975).

Galvan-Ruiz, J.
"Electromechanical Filters", Rev. Telecomun. (Spain), Vol. 29, No. 114, p. 3-13 (March 1974). In Spanish.

Grant, P. M., Collins, J. H., Darby, B. J., Morgan, D. P.
"Potential Applications of Acoustic Matched Filters to Air-Traffic Control Systems", (Univ. Edinburgh, Scotland). IEEE Trans. Microwave Theory & Tech. (USA), Vol. MIT-21, No. 4, p. 288-300 (April 1973).

Guenther, A. E.
"High-Quality Wide-Band Mechanical Filters Theory and Design", (Siemens AG, Munich, Germany). IEEE Trans. Sonics & Ultrasonics, (USA), Vol. SU-20, No. 4, p. 294-301 (Oct. 1973).

Gunther, A.
"High-Quality Wide-Band Filters of Ultrasonic Resonators Technique and Design", (Siemens AG, Munchen, Germany). IEEE Trans. Sonics & Ultrasonics (USA), Vol. SU-19, No. 3, p. 406 (July 1972). (1971 IEEE Ultrasonics Symposium, Miami Beach, FL, USA, 6-8 Dec. 1971).

Gunther, A.
"Remarks on the Design of Mechanical Wide-Band Filters", (Siemsn AG, Munchen, Germany). Nachrichtentech. Z. (NTZ) (Germany), Vol. 25, No. 8, p. 345-51 (Aug. 1972). In German.

Gunther, A. E.
"Electromechanical Filters -Satisfying Additional Demands", (Siemens AG, Munchen, Germany). International Symposium on Circuit Theory 1973, Toronto, Canada, 9-11 April 1973 (New York, USA: IEEE 1973), p. 142-5.

Halsig, C.
"Mechanical Filters of Kombinat VEB Elektronische Bauelemente Teltow and their Application", (Kombinat VEB Elektronische Bauclemente, Teltow, Germany). Proceedings of the 1976 IEEE International Symposium on Circuits and Systems, Munich, Germany, 27-29 April 1976 (New York, USA: IEEE 1976), p. 761-6.

Halsig, C.
"Mechanical Frequency Selection--Present Status of Development and Perspective", (VEB Elektronische Bauelemente Teltow, Germany). Nauchrichtentech. Elektron. (Germany), Vol. 27, No. 1, p. 10-13 (1977). In German.

Hartmann, C. S.
"Matched Filters", (Texas Instruments Inc., Dallas, TX, USA). International Specialist Seminar on the Impact of New Technologies ir Signal Processing, Aviemore, Scotland, 20-24 Sept. 1976 (London, England: IEE 1976), p. 78-83.

Johnson, R. A.
"New Single Sideband Mechanical Filters", (Collins Radio Co., Newport Beach, CA, USA). 1970 WESCON Technical Papers, Vol. 14, Western Electronic Show & Convention, Los Angeles, CA, USA, 25-28 Aug. 1970, 10 pp.

Johnson, R. A., Borner, M., Konno, M.
"Mechanical Filters--A Review of Progress", (Collins Radio Co., Newport Beach, CA, USA). IEEE Trans. Sonics & Ultrasonics (USA), Vol. 18, No. 3, p. 153-68 (July 1971).

Johnson, R. A.
"Mechanical Filters", (Collins Radio Co., Newport Beach, CA, USA). IEEE Trans. Sonics & Ultrasonics, (USA), Vol. SU-19, No. 3, p. 410 (July 1972). (1971 IEEE Ultrasonics Symposium, Miami Beach, FL, USA, 6-8 Dec. 1971.

Johnson, R. A.
"Mechanical Filters", (Collins Radio Co., Newport Beach, CA, USA). International Symposium on Circuit Theory 1973, Toronto, Canada, 9-11 April 1973 (New York, USA: IEEE 1973), p. 402-5.

Johnson, R. A., Winget, W. A.
"FDM Equipment Using Mechanical Filters", (Collins Radio Co., Newport Beach, CA, USA). Proceedings of the 1974 IEEE International Symposium on Circuits and Systems, San Francisco, CA, USA, 22-25 April 1974 (New York, USA: IEEE 1974), p. 127-31.

Johnson, R. A., Guenther, A. E.
"Filters and Resonators--A Review. III. Mechanical Filters and Resonators", (Rockwell Internat. Newport Beach, CA, USA). IEEE Trans. Sonics & Ultrasonics (USA), Vol. SU-21, No. 4, p. 244-56 (Oct. 1974).

Johnson, R. A.
"The Design of Mechanical Filters with Bridged Resonators", (Collins Radio Group, Rockwell Internat., Newport Beach, CA, USA). 1975 IEEE International Symposium on Circuits and Systems, Newton, Mass., USA, 21-23 April 1975 (New York, USA: IEEE 1975), p. 313-6.

Johnson, R. A.
"The Design and Manufacture of Mechanical Filters", (Collins Radio Group, Rockwell International, Newport Beach, CA, USA). Proceedings of the 1976 IEEE International Symposium on Circuits and Systems, Munich, Germany, 27-29 April 1976 (New York, USA: IEEE 1976), p. 750-3.

Johnson, R. A.
"Mechanical Filters Take on Selective Jobs", (Collins Radio Group, Rockwell Internat. Corp., Newport Beach, CA, USA). Electronics (USA), Vol. 50, No. 21, p. 81-5 (13 Oct. 1977).

Johnson, R. A.
"Mechanical Filters Using Disk and Bar Flexure-Mode Resonators", (Electronic Devices Div., Rockwell Internat. Corp., Newport Beach, CA, USA). Onde Elektr. (France), Vol. 58, No. 2, p. 141-8 (Feb. 1978). In French.

Johnson, R. A., Yakuwa, K.
"Miniaturized Mechanical Filters", (Filter Products, Rockwell Internat., Newport Beach, CA, USA). Proceedings of the 1978 IEEE International Symposium on Circuits and Systems, New York, USA, 17-19 May 1978 (New York, USA: IEEE 1978), p. 330-5.

Jones, J. S.
"A Metal Reed Mechanical Filter for Channel Bank Application", Bell Laboratories, Allentown, PA, USA. Ultrasonics Symposium Proceedings, Cherry Hill, NJ, USA, 25-27 Sept 1978 (New York, USA: IEEE 1978), Manuscript not available.

Jungwirt, J.
"The Design of Electromechanical Filters for Telecommunications", (TESLA, Prague, Czechoslovakia). TESLA Electron. (Czechoslovakia), Vol. 7, No. 1, p. 3-9 (March 1974).

Jutzi, W.
"Active Tapped Delay Line Filter", IBM Tech. Disclosure Bull. (USA), Vol. 12, No. 9, p. 1359-60 (Feb. 1970).

Kagawa, Y.
"Analysis and Design of Electromechanical Filters by Finite Element Method", (Univ. Southampton, England). J. Acoust. Soc. Japan, Vol. 27, No. 4, p. 201-14 (April 1971). In Japanese.

Kagawa, Y., Yamabuchi, T.
"Finite Element Stimulation of Two-Dimensional Electromechanical Resonators", (Toyama Univ., Takaoka, Japan). JEE Trans. Sonics & Ultrason. (USA), Vol. SU-21, No. 4, p. 275-83 (Oct. 1974).

Kaminski, F.
"Method of Electromechanical Filter Synthesis by Means of Equivalent Circuits with Distributed Constants", Arch. Elekrotech (Poland), Vol. 17, No. 3, p. 449-67 (1968). In Polish.

Kaminski, F.
"On the Synthesis of Supernarrow Band-Pass Electromechanical Chain Filters with Regular Structure", Bull. Acad. Polon. Sci. Ser. Sci. Tech. (Poland), Vol. 17, No. 1, p. 101-4 (1969). In Russian.

Kaminski, F.
"The Synthesis of Electromechanical Chain Filters by Means of Equivalent Circuits with Distributed Parameters", Rozprawy Elektrotech. (Poland), Vol. 15, No. 4, p. 717-49 (1969). In Polish.

Kaminski, F.
"On the Synthesis of a Certain Group of Electromechanical Filters by Means of Equivalent Networks with Distributed or Lumped Constants", Arch. Elektrotech. (Poland), Vol. 22, No. 2, p. 517-21 (1973). In Polish.

Kaminski, F.
"Synthesis of an Electromechanical Filter with Simple Couplers", Arch. Elektrotech. (Poland), Vol. 22, No. 3, p. 525-37 (1973). In Polish.

Kaminski, F.
"Outline of the Theory of the Regular-Structure Mechanical and Microwave Filter Synthesis", (PAN, Warsaw, Poland). Rozpr. Electrotech. (Poland), Vol. 20, No. 2, p. 295-312 (1974). In Polish.

Kampfhenkel, H.
"Iterative Synthesis of Symmetrical Electromechanical Filters", (Standard Elektrik Lorenz AG, Stuttgart, Germany). Nachrichtentech. Z. (NTZ) (Germany), Vol. 26, No. 9, p. 401-7 (Sept. 1973). In German.

Kantor, V. M., Lanne, A. A.
"Bandpass Limitations of Electromechanical Filters", Izv. VUZ Radioelektron. (USSR), Vol. 16, No. 12, p. 66-72 (Dec. 1973). In Russian. English translation in: Radio Electron. & Commun. Syst. (USA).

Kidokoro, M., Kawana, T.
"Mechanical Filters Take Over", (Nippon Electric Co. Ltd., Kawasaki, Japan). JEE (Japan), No. 130, p. 48-52 (Oct. 1977).

Koh, Y.
"The Mechanical Filter: Evolution to Technical Maturity", (Kokusai Electric Co., Ltd., Japan). JEE (Japan), No. 79, p. 32-7 (June 1973).

Kogan, S. S., Stepanov, A. S.
"Electromechanical Channel Filters", (Elektrosvyaz (USSR), p. 58-65. In Russian. English translation in: Telecommun. & Radio Eng. Pt. J (USA), Vol. 25, No. 11, p. 44-50 (Nov. 1971).

Kohlhammer, B., Schussler, H.
"A Mechanical Torsion Filter with Piezoelectric Transducers as Channel and Signal Filters for a New Carrier-Frequency System", (AEG-Telefunken Forschungsinstitut, Ulm, Germany). Proceedings of the 7th International Congress on Acoustics, Budapest, Hungary, 18-26 Aug. 1971 (Budapest, Hungary: Akademai Kiado 1971), p. 341-4. In German.

Kohlhammer, B., Schussler, H.
"Remarks on the Influence of the Mechanical Vibration Quality on the Transmission Properties of Channel Filters", (AEG-Telefunken, Ulm, Germany). Frequenz (Germany), Vol. 25, No. 9, p. 287-8 (Sept. 1971).

Konno, M., Tomikawa, Y.
"An Electromechanical Filter Consisting of a Flexural Vibrator with Double Resonances", J. Inst. Elect. Commun. Engrs, Japan, Vol. 50, No. 8, 1426-33 (Aug. 1967). In Japanese.

Konno, M., Tomikawa, Y.
"Electromechanical Filters, I. Introduction", (Yamagata Univ., Yonezawa-si, Japan). Denshi Tsushin Gakkai Zasshi (Japan), Vol. 52, No. 3, p. 303-12 (March 1969). In Japanese (59 refs).

Konno, M., Aoshima, K., Nakamura, H.
"H-Shape Resonator and its Application to Electromechanical Filter", (Yamagata Univ., Japan). Bull. Yamagata Univ. (Eng.) (Japan), Vol. 10, No. 2, p. 261-85 (March 1969). In Japanese.

Konno, M., Tomikawa, Y., Tacano, T., Izumi, H.
"Electromechanical Filters Using Degeneration Modes of a Disk or a Ring", (Yamagata Univ., Yonezawa, Japan). Trans. Inst. Electronics Commun. Engrs. Japan, A.B.C., p. 19-28 (May 1969). In Japanese. English translation in: Electronics Commun. Japan (USA), Vol. 52, No. 5, (May 1969).

Kopp, H.
"A Mechanical Filter Channel Bank", (Siemens AG, Munchen, Germany). 7th International Conference on Communications, Montreal, Canada, 14-16 June 1971 (New York, USA: IEEE 1971), p. 6-19-24.

Kuenemund, F.
"Materials for High-Grade Electromechanical Frequency Filters", (Siemsn AG, Munich, Germany). Inst. Eng. Aust. Elec. Eng. Trans. (Austrailia), Vol EE8, No. 1, p. 41-2 (April 1972).

Kunemund, F.
"Channel Filters with Longitudinally Coupled Flexural Mode Resonators", (Siemens AG, Munchen, Germany). Siemens Forsch - & Entwicklungsber. (Germany), Vol. 1, No. 4, p. 325-8 (1972). In English.

Kunemund, F. L.
"Electromechanical Filters", (Siemens AG, Berlin, Germany). NTG-Fachber. (Germany), Vol. 54, p. 159-70 (1975). In German.

Luder, E.
"Mechanical Oscillators in Filters for Low Frequencies", Arch Electrotech. (Germany), Vol. 51, No. 6, 351-7 (1968). In German.

Martinelli, G., Salerno, M., Masiani, G., Orlandi, G.
"Constrained Synthesis for Mechanical Filters", (Istituto di Communicazioni Elettriche, Rome, Italy). Proceedings of the 1978 IEEE International Symposium on Circuits and Systems, New York, USA, 17-19 May 1978 (New York, USA: IEEE 1978), p. 59-63.

Mifune, H., Tanaka, T.
"Reed Filters and their Characteristics", (Matsushita Electric Industrial Co. Ltd., Osaka, Japan). Nat. Tech. Rep. (Japan), Vol. 16, No. 4, p. 541-50 (Aug. 1970). In Japanese.

Nakamura, H., Konno, M., Tanno, K.
"Electromechanical Filter Consisting of Frame-Vibrator with Double Resonance", (Yamagata Univ., Japan). Bull. Yamagata Univ. (Eng.) (Japan), Vol. 10, No. 2, p. 431-45 (March 1969). In Japanese.

O'Clock, J. D. Jr.
"Matched Filters Boost Receiver Gain by Improving the Signal-to-Noise Ratio", Electron. Des. (USA), Vol. 25, No. 11, p. 162-6 (24 May 1977).

Ohyama, M., Uehara, K., Yoshida, N., Yano, T.
"N-5000 Series FDM Channel Bank Using New Mechanical Filters", (Transmission Div., Nippon Electric Co. Ltd., Tokyo, Japan). NEC Res. & Dev. (Japan), No. 49, p. 98-109 (April 1978).

Onoe, M., Yano, T.
"Electromechanical Wave-Separating Filters", (Univ. Tokyo, Minatoku, Japan). Proceedings of the 1970 Electronic Components Conference, Washington, DC, USA, 13-15 May 1970 (New York, USA: IEEE 1970), p. 269-76.

Papandakis, E. P.
"Improvements in a Broadband Electromechanical Bandpass Filter in the Voice Band", (Panametrics Inc., Waltham, MA, USA). IEEE Trans. Sonics & Ultrasonics, (USA), Vol. SU-22, No. 6, p. 406-15 (Nov. 1975).

Pfleiderer, R., Wollmershauser, P.
"Electromechanical Pilotfilter with Improved Temperature Characteristics", (Standard Elektrik Lorentz AG, ITT, Stuttgart, Germany). Proceedings of the 1976 IEEE International Symposium on Circuits and Systems, Munich, Germany, 27-29 April 1976 (New York, USA: IEEE 1976), p. 743-5.

Plourde, J. K., Linn, D. F.
"Microwave Dielectric Resonator Filters Utilizing $Ba_2Ti_9O_{20}$ Ceramics", (Bell Telephone Labs, Allentown, PA, USA). 1977 International Microwave Symposium Digest, San Diego, CA, USA, 21-23 June 1977 (New York, USA: IEEE 1977), p. 290-3.

Prache, P. M.
"Introduction to Linear Electromechanical Networks Theory", (Societe Lignes Telegraphiques & Telephoniques, Paris, France). Cables & Transm. (France), Vol. 28, No. 4, p. 304-27 (Oct. 1974). In French.

Psenicka, B., Trnka, J.
"Electromechanical Filters with Poles of Attenuation at Finite Frequencies", (CVUT-FEL, Praha, Czechoslovakia). Proceedings of the 5th Colloquium on Microwave Communication. Vol. II. Circuit Theory and Computer Aided Design (Preprints), Budapest, Hungary, 24-30 June 1974 (Budapest, Hungary: Akad Kiado 1974), p. CT-23/203-12.

Pshenichka, V., Trnka, I.
"Design of Electromechanical Filters with Polar Coupling", Izv. VUZ Radioelektron. (USSR), Vol. 18, No. 11, p. 21-6 (Nov. 1975). In Russian.

Reushkin, N. A.
"Method of Tuning a Multiresonator Filter", Telecomm. & Radio Eng. Part I (USA), Vol. 30, No. 6, p. 25-8 (June 1976). Translation of: Elektrosvyaz (USSR), Vol. 30, No. 6, p. 36-9 (June 1976).

Sasaki, E., Shinzaki, K.
"Torsional Mode Transducer for Mechanical Filter", Electr. Commun. Lab. Tech. J. (Japan), Vol. 23, No. 1, p. 111-24 (1974). In Japanese.

Sawamoto, K., Kondo, S.
"Torsional Mode Mechanical Filters", Electr. Commun. Lab. Tech. J. (Japan), Vol. 23, No. 1, p. 95-110 (1974). In Japanese.

Sawamoto, K., Sasaki, E., Kondo, S., Ashida, T., Shinozaki, K.
"Torsional-Mode Mechanical Filters", (Musashino Electrical Communication Lab., NTT, Musashino, Japan). Electron. & Commun. Jap. (USA), Vol. 57, No. 8, p. 17-24 (Aug. 1974).

Sawamoto, K., Kondo, S., Watanabe, N., Tsukamoto, K., Kiyomoto, M., Ibaraki, O.
"A Torsional-Mode Pole-Type Mechanical Channel Filter", (Nippon Telegraph & Telephone Public Corp., Electrical Communication Lab., Tokyo, Japan). IEEE Trans. Sonics & Ultrasonics (USA), Vol. SU-23, No. 3, p. 148-53 (May 1976). (IEEE Ultrasonics Symposium, (Abstracts only). Los Angeles, CA, USA, 22-24 Sept. 1974).

Sawamoto, K., Kondo, S., Sasaki, E.
"A Torsional Mode Mechanical Channel Filter", (NTT, Tokyo, Japan). Rev. Electr. Commun. Lab. (Japan), Vol. 23, No. 5-6, p. 429-38 (May-June 1975).

Sawamoto, K., Yano, T., Yakuwa, K., Koh, Y., Konno, M.
"Electromechanical Filters Developed in Japan. II. Channel EM Filters", (Trunk Transmission System Dev. Div., Nippon Telegraph & Telephone Public Corp., Kanagawa, Japan). Onde Electr. (France), Vol. 58, No. 6-7, p. 482-7 (June-July 1978). In French. For Pt 1, see ibid., Vol. 58, No. 5, p. 401 (1978).

Schaffler, K.
"The Piezoelectric Tuning Fork as a New Filter Element for the Audio-Frequency", BBC Nachr. (Germany), Vol. 49, No. 8, 395-401 (Aug. 1967). In German.

Schussler, H.
"Filters with Mechanical Resonators", Bull. Assoc. Swisse Elect. (Switzerland), Vol. 60, No. 6, p. 216-21 (15 March 1969). In German.

Schussler, H.
"Consideration about Channel Filters for a New Carrier Frequency System with Mechanical Filters", Programme of the 25th Annual Frequency Control Symposium (abstracts), Atlantic City, NJ, USA, 26-28 Apr. 1971 (Fort Monmouth, NJ, USA: US Army Electronics Command 1971), p. 45.

Schussler, H.
"Filters for Channel Bank Filtering with Mechanical Resonators, Quartz Crystals and Gyrators", (AEG-Telefunken, Ulm, Germany). Proceedings of the 1974 IEEE International Symposium on Circuits and Systems, San Francisco, CA, USA, 22-25 April 1974 (New York, USA: IEEE 1974), p. 106-10.

Sekine, T., Konno, M.
"Narrow Band Mechanical Filter Consisting of Differential-Couplers", (Faculty of Engng., Gifu Univ., Kakamigahara, Japan). Trans. Inst. Electron. & Commun. Eng. Jpn. Sect. E (Japan), Vol. E-59, No. 10, p. 28 (Oct. 1976).

Sheahan, D. F., Johnson, R. A.
"Crystal and Mechanical Filters", (GTE Lenkurt Inc., San Carlos, CA, USA). IEEE Trans. Circuits & Syst. (USA), Vol. CAS-22, No. 2, p. 69-89 (Feb. 1975).

Shibayama, K., Sato, H.
"Bar-Shaped Mechanical Filters Under the Consideration of Higher Mode Effects", (Tohoku Univ., Sendai, Japan). Proceedings of the 7th International Congress of Acoustics, Budapest, Hungary, 18-26 Aug. 1971 (Budapest, Hungary: Akademiai Kiado 1971). p. 349-52.

Takahashi, I., Yoshida, N., Ishizaki, Y.
"An Analysis of a Torsional Mode Transducer for Electromechanical Filters", (Transmission Div., Nippon Electric Co. Ltd., Shimonumabe, Kawasaki, Japan). 1976 Ultrasonics Symposium Proceedings, Annapolis, MD, USA, 29 Sept. - 1 Oct. 1976 (New York, USA: IEEE 1976), p. 602-5.

Tanno, K., Hacchome, T., Konno, M.
"Band Eliminators Consisting of Electromechanical Vibrators", Bull. Yamagata Univ. (Eng.) (Japan), Vol. 11, No. 2, p. 101-22 (March 1971). In Japanese

Tomikawa, Y., Konno, M.
"Electromechanical Filter with Attenuation-Poles Consisting of Multi-Mode Resonators", (Yamagata Univ., Yonezawa, Japan). Proceedings of the 7th International Congress on Acoustics, Budapest, Hungary, 18-26 Aug. 1971 (Budapest, Hungary: Akademiai Kiado 1971), p. 637-40.

Tomikawa, Y.
"Electromechanical Filter with Attenuation Poles Consisting of Multi-Mode Vibrators", (Yamagata Univ., Yonezawa-shi, Japan). Electron. & Commun. Jap. (USA), Vol. 54, No. 9, p. 19-25 (Sept. 1971). In Japanese.

Tomikawa, Y., Sugawara, S., Havens, D. P.
"Resonances in Flexure-Mode Mechanical Filters", (Faculty of Electrical Engng., Yamagata Univ., Yonezawa, Japan). 1976 Ultrasonics Symposium Proceedings, Annapolis, MD, USA, 29 Sept. - 1 Oct. 1976 (New York, USA, IEEE 1976), p. 597-601.

Tsuzuki, Y., Hirose, Y., Takada, S., Iyima, K.
"Holographic Investigation of Spurious Modes of Mechanical Filters", (Yokohama Nat. Univ., Yokohama-shi, Japan). Electron. & Commun. Jap. (USA), Vol..54, No. 3, p. 31-8 (March 1971). In Japanese.

Velikin, Ya. I., Gel'mont, Z. Ya., Zelyakh, E. V., Ivanova, A. I.
"Magnetostrictive Ladder Filters", Elektrosvyaz., p. 40-6 In Russian. English translation in: Telecomm. Radio Engn. Pt. 1 (USA), Vol. 23, No. 11 (1969).

Wasiak, M.
"Electromechanical 200 kHz Channel Filter", Prace Inst. Tele.- & Radiotech. (Poland), Vol. 15, No. 1, p. 5-25 (1971). In Polish.

Yakuwa, K.
"Electromechanical Filters. II. High Frequency Electromechanical Filters", (Fujitsu, Kawasaki-si, Japan). J. Inst. Electronics Commun. Engrs. Japan, Vol. 52, No. 5, P. 568-77 (May 1969). In Japanese.

Yakuwa, K., Okuda, S., Shirai, K., Kasai, Y.
"128 kHz Pole-Type Mechanical Channel Filter", (Fujitsu Ltd., Nakahara-Ku, Kawasaki, Japan). 31st Annual Frequency Control Symposium, Atlantic City, NJ, USA, 1-3 June 1977 (Washington, DC, USA: Electronic Industries Assoc. 1977), p. 207-12.

Yano, T., Futami, T., Kanazawa, S.
"New Torsional Mode Electromechanical Channel Filter", NEC Res. & Dev. (Japan), No. 39, p. 30-6 (Oct. 1975).

Yoda, H., Nakazawa, Y., Okano, S., Korbori, N.
"High Frequency Crystal Mechanical Filters", (Toyo Communication Equipment Co., Kawasaki, Japan). Proceedings of the 22nd Annual Frequency Control Symposium. Atlantic City, NJ, USA, 22-24 Apr. 1968 (Fort Monmouth, NJ, USA: Electronic Components Lab. 1968), p. 188-205.

Yuki, T., Yano, T.
"Electromechanical Filters. III. Low Frequency Electromechanical Filters", (Nippon Electric Co. Ltd., Kawasaki-si, Japan). J. Inst. Electronics Commun. Engrs. Japan, Vol. 52, No. 6, p. 727-32 (June 1969). In Japanese. English translation in: Elect. Engng. Japan (USA). For Pt. II see ibid Vol. 52, No. 5, p. 568 (1969).

Ainger, F. W., Burgess, J. W., Hales, M. C., Porter, R. J.
"The Use of Lithium Tantalate in Monolithic Crystal Filters", (Allen Clark Res. Centre, Plessey Co. Ltd., Caswell, Towcester, England). Ferroelectrics (GB), Vol. 10, No. 1-4, p. 75 (1976). (1975 IEEE Symposium on Applications of Ferroelectrics. I, Albuquerque, NM, USA, 9-11 June 1975).

Akcakaya, E.
"An Equivalent Circuit Applicable to Design Monolithic Crystal Filters", (Tech. Univ. of Istanbul, Istanbul, Turkey). Proceedings of the 1976 IEEE International Symposium on Circuits and Systems, Munich, Germany, 27-29 April 1976 (New York, USA: IEEE 1976), p. 359-61.

Akcakaya, E.
"New Approach to the Analysis of Monolithic Crystal Filters", (Marmara Sci. & Industrial Res. Inst. Kadikoy-Istanbul, Turkey). J. Acoust. Soc. Am. (USA), Vol. 60, No. 2, p. 492-502 (Aug. 1976).

Albsmeier, H.
"A Comparison of the Realizability of Electromechanical Channel Filters in the Frequency Range 12 KHz to 10 MHz", (Siemens AG, Munchen, Germany). Frequenz (Germa-y), Vol. 25, No. 3, p. 74-9 (March 1971). In German.

Amsler, H.
"The Quartz Miniature Receiver for Hasler Radio Paging Systems", Hasler Rev. (Switzerland), Vol. 2, No. 1, p. 20-2 (April 1969).

Aoshima, T.
"Ceramic Filter Frequency Limits Expand to 27 MHz", (Toko Inc., Tokyo, Japan). JEE (Japan), No. 130, p. 60-4 (Oct. 1977).

Ashida, T.
"Eigenfrequencies of Monolithic Filters", (NTT, Musashino, Tokyo, Japan). Electron. & Commun. Jap. (USA), Vol. 54, No. 6 (June 1971). In Japanese. p. 41-9.

Ashida, T.
"Design and Characteristic Analysis of Monolithic Crystal Filters", (Musashino Electrical Communication Lab., NTT, Musashino, Japan). Electron. & Commun. Jap. (USA), Vol. 57, No. 5, p. 1-9 (May 1974).

Austin, B. A.
"Single-Sideband Transceiver Design. Underground Application Uses Simple Ceramic Sideband Filter", (Res. Labs., Chamber of Mines, Johannesburg, S. Africa). Wireless World (GB), Vol. 84, No. 1506, p. 75-6 (Feb. 1978).

Ballato, A., Lukaszek, T.
"A Novel Frequency Selective Device: The Stacked-Crystal Filter", (US Army Electronics Technol. & Devices Lab., Fort Monmouth, NJ, USA). Proceedings of the 27th Annual Frequency Control Symposium, Cherry Hill, NJ, USA, 12-14 June 1973 (Washington, DC, USA: Electronic Industries Assoc. 1973), p. 262-9

Ballato, A., Lukaszek, T.
"Stacked-Crystal Filters", (US Army Electronics Command, Fort Monmouth, NJ, USA). Proc. IEEE (USA), Vol. 61, No. 10, p. 1495-6 (Oct. 1973).

Ballato, A., Bertoni, H. L., Tamir, T.
"Systematic Design of Stacked-Crystal Filters by Microwave Network Methods", (US Army Electronics Command, Fort Monmouth, NJ, USA). IEEE Trans. Microwave Theory & Tech. (USA), Vol. MTT-22, No. 1, p. 14-25 (Jan. 1974).

Ballato, A.
"The Stacked-Crystal Filter", (US Army Electronics Technol. & Devices Lab., Fort Monmouth, NJ, USA). 1975 IEEE International Symposium on Circuits and Systems, Newton, Mass, USA, 21-23 April 1975 (New York, USA: IEEE 1975), p. 301-4.

Bastelaer, P. H.
"The Design of Band-Pass Filters with Piezoelectric Resonators", Rev. HF (Belgium), Vol. 7, No. 7, p. 193-206 (1968).

Beaver, W. D., Frymoyer, E. M.
"The Effect of Variations in Fabrication on the Transmission Properties of Monolithic Crystal Filters", (Collins Radio Co., Newport Beach, CA, USA). IEEE Trans. Sonics Ultrasonics (USA), Vol. SU-17, No. 1, p. 59 (Jan. 1970).

Beck, E.
"Monolithic Crystal Filters", (Hasler Ltd., Berne, Switzerland). Hasler Rev. (Switzerland), Vol. 8, No. 2, p. 44-9 (Summer 1975). In English.

Beck, E., Schultze, E., Meyer, H.
"An Admittance Approach to the Dual Monolithic Crystal Filter", (Res. Div., Hasler Ltd., Berne, Switzerland). Proceedings of the 1976 IEEE International Symposium on Circuits and Systems, Munich, Germany, 27-29 April 1976 (New York, USA: IEEE 1976), p. 316-19.

Beck, E., Schultze, E., Meyer, H.
"Chain Matrix Description of Polylithic Crystal Filters", (Res. Div., Hasler Ltd., Berne, Switzerland). Journees d'Electronique et de Mecanique sur Interactions Electronique-Micromecanique. (1976 Electronic and Micromechanical Meeting on Electronic-Micromechanical Interactions). Lausanne, Switzerland, 19-21 Oct. 1976 (Lausanne, Switzerland: Ecole Polytech. Federale de Lausanne 1976), p. 273-85.

Beletskiy, A. F., Lebedev, A. T., Ovchinnikov, A. A.
"Synthesis of T-Shaped Quartz Matched Filters for Rectangular Pulses", Telecommun. & Radio Eng. Pt. I (USA), Vol. 26, No. 8, p. 45-7 (Aug. 1972). Translation of: Elektrosvyaz (USSR), Vol. 26, No. 8, p. 59-61 (Aug. 1972).

Belevitch, V., Kamp, Y.
"Theory of Monolithic Crystal Filters Using Thickness-Twist Vibrations", Philips Res. Rep. (Netherlands), Vol. 24, No. 4, p. 331-69 (Aug. 1969).

Bezemer, J. A.
"The Monolithic Quartz Crystal Filter", PTT Bedriff (Netherlands), Vol. 18, No. 1, p. 29-37 (April 1972). In Dutch.

Bezemer, J. A.
"The Single Quartz Crystal in the Monolithic Crystal Filter", Data (Netherlands), Vol. 75, No. 1, p. 1-25 (March 1974). In Dutch.

Bidart, M.
"Crystal Filter Modern Conception", Onde Elec. (France), Vol. 51, No. 4, p. 311-19 (April 1971). In French.

Bidart, L.
"Semi-Monolithic Quartz Crystal Filters and Monolithic Quartz Filters", Programme of the 25th Annual Frequency Control Symposium (abstracts), Atlantic City, NJ, USA, 26-28 Apr. 1971 (Fort Monmouth, NJ, USA: US Army Electronics Command, 1971), p. 46.

Blinchikoff, H. J.
"Low-Transient Intermediate-Band Crystal Filters", (Westinghouse Electric Corp., Baltimore, MD, USA). IEEE Trans. Circuits & Syst. (USA), Vol. CAS-22 No. 6, p. 509-15 (June 1975).

Bucherl, E.
"Bandstop Filters Incorporating Double-Tuned Monolithic Crystal Units", (Siemens AG, Munich, Germany). Siemens Forsch. - & Entwicklungsber. (Germany), Vol. 2, No. 5, p. 238-7 (1973). In English.

Camurri, F., Costamagna, E.
"On the Design of Monolithic Crystal Filters", (Univ. Genova, Italy). Alta Freq. (Italy), Vol. 42, No. 8, p. 341-5 (Aug. 1973). In English.

Cawley, H. F., Jennings, J. D., Pelc, J. I., Perri, P. R., Snell, F. E., Miller, A. J.
"Manufacture of Monolithic Crystal Filters for A-6 Channel Bank", (Western Electric Co., North Andover, MA, USA). Proceedings of the 29th Annual Frequency Control Symposium, Fort Monmouth, NJ, USA, 28-30 May 1975 (Washington, DC, USA: Electronic Industries Assoc. 1975), p. 113-19.

Chelmonski, J., Wrobel, T., Koczynski, B.
"Band-Stop Quartz Filter FZ-256 kHz", Prace Inst. Tele & Radiotech. (Poland), Vol. 14, No. 3, p. 55-7 (1970).

Chohan, V. C., Dillon, C. R.
"Specification, Design and Synthesis of F.S.K. Filters Using Double-Resonator Monolithic Crystal Filter (MCF) Sections", (CERN, Geneva, Switzerland). Arch. Elektron. & Uebertagungstech. (Germany), Vol. 29, No. 3, p. 121-4 (March 1975).

Colin, J. E.
"Formulae for the Calculation of Narrow Band Pass Filters with Identical Piezoelectric Crystals and Maximally Flat Attenuation Behavior", Cables et Transm. (France), Vol. 22, No. 2, p. 132-5 (Apr. 1968). In French.

Colin, J. E.
"Example of a Balanced Parametric Band-Pass Filter Using Piezoelectric Crystals at both Filter Ends", (Societe Anonyme de Telecommunications, Paris, France). Cables & Transm. (France), Vol. 29, No. 4, p. 427-32 (Oct. 1975). In French.

Costa, P., Stacchiotti, G.
"Polylithic Crystal Filters--Reasons for the Choice", (Telettra SpA., Vimercate, Milano, Italy). Alta Freq. (Italy), Vol. 43, No. 12, p. 1040-3 (Dec. 1974).

Dillon, C. R., Lind, L. F.
"Cascade Synthesis of Monolithic-Crystal Filters Possessing Finite Transmission Zeros", (Univ. Essex, Colchester, England). Int. J. Circuit Theory & Appl. (GB), Vol. 3, No. 1, p. 101-7 (March 1975).

Lind, L. F.
"Cascade Synthesis of Polylithic Crystal Filters Containing Double-Resonator Monolithic Crystal Filter (MCF) Elements", (Faculty of Technol., Open Univ., Milton Keynes, England). IEEE Trans. Circuits & Syst. (USA), Vol. CAS-23, No. 3, p. 146-54 (March 1976).

Folk, A.
"Simple Ladder Type Quartz Crystal Filter", Przeglad Telekommun. (Poland), 1968, No. 2, 38-42. In Polish.

Garrison, J. L., Georgiades, A. N., Simpson, H. A.
"The Application of Monolithic Crystal Filters to Frequency Selective Networks", (Bell Telephone Labs., Inc., North Andover, Mass., USA). Digest of Technical Papers of the 1970 IEEE International Symposium on Circuit Theory, Atlanta, GA, USA, 14-16 Dec. 1970 (New York, USA: Lewis Winner 1970), p. 177-8.

Gehrels, J.
"Monolithic Crystal Filters Reduce Space Requirements by Factor of Ten", Can. Electron. Eng. (Canada), Vol. 16, No. 5, p. 28-30 (May 1972).

Glowinski, A.
"Integrated Quartz Filters: Synthesis and Adjustment Problems in Monolithic Filters", (CNET, Issy-les-Moulineaux, France). Proceedings of the International Conference on Advanced Microelectronics, Paris, France, 6-10 Apr. 1970 (Paris, France: Federation Nationale des Industries Electroniques 1970), 2pp

Goodwin, M. W., Wood, A. F. B.
"The Use of Crystal Filters in Mobile Communications Systems", (Standard Telephones and Cables Ltd., Harlow, England). Communications 74, Brighton, Sussex, England, 4-7 June 1974 (London, England. IPC Business Press 1974), p. 13-2/1.

Goral, A.
"Monolithic Filters", Elektronika (Poland), No. 11, p. 460-4 (1972). In Polish.

Grenier, R. P.
"Automatic Frequency Adjustment of Monolithic Crystal Filters", W. Elec. Eng. (USA), Vol. 15, No. 1, p. 15-19 (Jan. 1971).

Haggarty, R. D., Hart, L. A., O'Leary, G. C.
"A 10,000:1 Pulse Compression Filter Using a Tapped Delay Line Linear Filter Synthesis Technique", (MITRE Corp., Bedford, Mass, USA). Electronics and Aerospace Systems Record, Washington, DC, USA, 9-11 Sept. 1968 (New York, USA: Institute and Electrical and Electronics Engineers 1968), p. 306-14.

Haine, J. L.
"Simple Design Procedure for Single-Sideband Crystal Filters", (Dept. of Electrical & Electronic Engng., Univ. of Leeds, Leeds, England). Electron. Lett. (GB), Vol. 12, No. 23, P. 637-8 (10 Nov. 1977).

Hales, M. C., Burgess, J. W.
"Wide Band Monolithic Crystal Filters Using Lithium Tantalate", (Allen Clark Res. Centre, Plessey Co. Ltd., Towcester, England). Electrocompon. Sci. & Techrol. (GB), Vol. 3, No. 1, p. 43-9 (June 1976).

Hales, M. C., Burgess, J. W.
"Design and Construction of Monolithic-Crystal Filters Using Lithium Tantalate", (Allen Clark Res. Centre, Plessey Co. Ltd., Caswell, Towcester, England). Proc. Inst. Electr. Eng. (GB), Vol. 123, No. 7, p. 657-61 (July 1976).

Hardcastle, J. A.
"Some Experiments with High-Frequency Ladder Crystal Filters. I. Construction", Radio Commun. (GB), Vol. 52, No. 12, p. 896-8, 905 (Dec. 1976).

Hardcastle, J. A.
"Some Experiments with High-Frequency Ladder Crystal Filters. II. Test Equipment", Radio Commun. (GB), Vol. 53, No. 1, p. 28-9 (Jan. 1977).

Hardcastle, J. A.
"Some Experiments with High-Frequency Ladder Crystal Filters. III.", Radio Commun. (GB), Vol. 53, No. 2, p. 122-4 (Feb. 1977).

Haruta, K., Lloyd, P., Hokanson, J. L.
"Monolithic Crystal Filter. II. Normal Mode Frequencies and Displacements", (Bell Telephone Lab. Inc., Allentown, PA, USA). IEEE Trans. Sonics Ultrasonics (USA), Vol. SU-16, No. 1, Suppl., p. 21 (Jan. 1969). (1968 IEEE Ultrasonics Symposium, New York, USA, 25-27 Sept. 1968).

Herzig, P. A., Swanson, T. W.
"A Polylithic Crystal Filter for a Satellite Channel Application", (E-Systems, ECI Div., St. Petersburg, FL, USA). Proceedings of the 1978 IEEE International Symposium on Circuits and Systems, New York, USA, 17-19 May 1978 (New York, USA: IEEE 1978), p. 64-5.

Hirst, J., Vlach, Z.
"Frequency Characteristics Analysis of Directly Connected Filters with Piezoelectric Elements Using Digital Computers", Elektrotech. Casopis (Czechoslovakia), Vol. 20, No. 1, p. 59-69 (1969). In Czech.

Hokanson, J. L.
"The Monolithic Crystal Filter: The Device, its Operation and Choice of Piezoelectric Materials", (Bell Telephone Lab., Inc., Allentown, PA, USA). 6th Annual Integrated Circuits Seminar, Hoboken, NJ, USA, 9 Apr. 1969 (New York, USA: IEEE 1969), p. 32-43.

Horton, W. H., Smythe, R. C.
"Experimental Investigations of Intermodulation in Monolithic Crystal Filters", Proceedings of the 27th Annual Frequency Control Symposium, Cherry Hill, NJ, USA, 12-14 June 1978 (Washington, DC, USA: Electronic Industries Assoc. 1973), p. 243-5.

Horwood, P. J.
"A 5.2 MHz Crystal Filter for SSB", Radio Commun. (GB), Vol. 48, No. 6, p. 366 (June 1972).

Hribsek, M. F., Newcomb, R. W.
"High-Q Selective Filters Using Mechanical Resonance of Silicon Beams", (Faculty of Electrical Engng., Univ. of Belgrade, Belgrade, Yugoslavia). IEEE Trans. Circuits & Syst. (USA), Vol. CAS-25, No. 4, p. 215-32 (April 1978).

Jain, J. D., Walther, L.
"Application of Piezoelectric, Ceramic, Torsional Resonators in Filters", Hochfrequenztech. & Elektroakust. (Germany), Vol. 79, No. 4-5, p. 128-32 (Oct. 1970). In German.

Jennings, J. D., Perri, P. P.
"A Monolithic Channel Filter Manufacture with a New Technology", (Western Electric Co. Inc., North Andover, Mass., USA). Proceedings of the 21st Electronic Components Conference, Washington, DC, USA, 10-12 May 1971 (New York, USA: IEEE 1971), p. 365-73.

Jennings, J. D.
"Fine Tuning Monolithic Crystal Filters", (Western Electric Co., Merrimack Valley, NH, USA). Tech. Dig. (USA), No. 42, p. 23-4 (April 1976).

Jumonji, H., Watanabe, N., Tsukamoto, K.
"Design of High Performance Monolithic Crystal Filters", (NTT, Tokyo, Japan). Rev. Electr. Commun. Lab. (Japan), Vol. 23, No. 5-6, p. 439-52 (May-June 1975).

Kantor, V. M., Lanne, A. A.
"The Synthesis of Low- and High-Pass Piezoelectric Filters from their Effective Parameters", Elektrosvyaz (USSR), 1967, No. 4, In Russian. English translation in: Telecomm. Radio Engng. Pt. 1. (USA), 1967, No. 4, 6-14 (April).

Kantor, V. M.
"The Design of Piezoelectric Band-Elimination Filters with Given Working Parameters", Telecommun. & Radio Eng. Pt. 2 (USA), Vol. 27, No. 4, p. 88-95 (April 1973). Translation of: Radiotekhnika (USSR), Vol. 27, No. 4, p. 41-50 (April 1973).

Kerboull, J.
"2.5 MHz Crystal Filters for a 12 Channel Multiplex Telephon System", (Compagnie d'Electronique et de Piezo-Electricite, Sartrouville, France). Onde Electr. (France), Vol. 58, No. 6-7, p. 458-63 (June-July 1978). In French.

Kohlbacher, G.
"Use of Electrical Low-Pass Equivalent Circuits for the Design of Multiple-Tuned Crystal and Ceramic Filters from Monolithic Single-Filter Elements", (AEG-Telefunken, Ulm, Donau, Germany). Arch. Elek. Uebertrag. (Germany), Vol. 25, No. 11, p. 492-501 (Nov. 1971). In German.

Kohlbacher, G.
"Monolithic Quartz- and Ceramic Filters", (AEG-Telefunken-Forschunsinst., Ulm, Germany). Int. Elektron. Rundsch. (Germany), Vol. 26, No. 9, p. 203-9 (Sept. 1972). In German.

Kohlbacher, G.
"Monolithic Crystal Filters for the VHF Range", Wiss. Ber. AEG-Telefunken (Germany), Vol. 49, No. 6, p. 248-53 (1976). In German.

Kollmann, M.
"Wide-Band Crystal Filters for Higher Frequency Bands", (TESLA Radio Engineering Labs., Prague, Czechoslovakia). Tesla Electronics (Czechoslovakia), Vol. 2, No. 1, p. 12-16 (1969).

Kollmann, M.
"A Wide-Band Crystal Filter", Sdelovaci Tech. (Czechoslovakia), Vol. 25, No. 3, p. 99-103 (March 1977). In Czech.

Komori, N.
"Crystal Filters--Designs Enhanced to Meet Expanding Requirements", (Toyo Communication Equipment Co. Ltd., Kanagawa, Japan). JEE (Japan), No. 130, p. 57-60 (Oct. 1977).

Kostarev, V. Ye., Osipov, V. G.
"Synthesis of Bandpass Piezoelectric Filters with an Attenuation Characteristic which is Monotonic in the Passband and Extremal in the Stop Band", Elektrosvyaz (USSR), p. 77 et seq. In Russian. English Translation in: Telecommun. & Radio Eng. Pt. 1 (USA), Vol. 25, No. 11, p. 61-3 (Nov. 1971).

Krause, G.
"A Coilless Bandpass Half-Section for Realizing Quartz Poles in the Lower Cut-Off Range", (KDT, Dresden, Germany). Nachrichtentechnik (Germany), Vol. 20, No. 1, p. 30-3 (Jan. 1970). In German.

Krause, G.
"Design of Wideband Crystal Bandpass Filters with Assymmetrical Attenuation on the Basis of the Theory of Recurrent m-Sections", (Hochschule Verkehrswesen 'Friedrich list', Dresden, Germany). Fernmeldetechnik (Germany), Vol. 11, No. 4, p. 113-15 (April 1971). In German.

Krause, G.
"Matching Problems in Bandpass Crystal Filters with Sharp Cutoffs Calculated by the Theory of Wave Parameters", Nachrichtentechnik (Germany), Vol. 21, No. 4, p. 130-3 (April 1971). In German.

Krause, G.
"Design of Wideband Pass Filters with Unsymmetrical Damping, Using Resonant Crystals, According to the Theory of m-Chains. II", (Hochschule Verkehrswesen. 'Friedrich List' Dresden, Germany). Fernmeldetecknik (Germany), Vol. 11, No. 5, p. 141-5 (May 1971). In German.

Krause, G.
"Design of Wideband, Attenuation Unsymmetrical Band-Pass Filters with Oscillating Crystals, Based on the M-Section Theory", (Hochschule Verkehrwesen 'Friedrich List' Dresden, Germany). Fernmeldetechnik (Germany), Vol. 11, No. 6, p. 171-4 (June 1971). In German.

Lampe, L.
"A New Monolithic 10.7 MHz Piezo-Filter", Radio Fernsehen Elektron. (Germany), Vol. 26, No. 1, p. 27-8 (1977). In German.

Lee, M. S.
"Polylithic Crystal Filters with Loss Poles at Finite Frequencies", (GTE Lenkurt Inc., San Carlos, CA, USA). 1975 IEEE International Symposium on Circuits and Systems, Newton, Mass., USA, 21-23 April 1975, p. 297-300.

Lefevre, R.
"Application of Monolithic Quartz Crystal to the Telephone Voice Channel Filter in Analog Systems", (CNET, Issy-les-Moulineaux, France). Onde Electr. (France), Vol. 58, No. 6-7, p. 475-81 (June-July 1978). In French.

Lin, C. C.
"Design of Symmetrical Polylithic Crystal Filters", (Communications Div., Motorola Inc., Franklin Park, IL, USA). Electron. Lett. (GB), Vol. 12, No. 8, p. 202-4 (15 April 1976).

Lloyd, P., Haruta, K.
"Monolithic Crystal Filter., I. The Theoretical Model", (Bell Telephone Lab., Inc., Allentown, PA, USA). IEEE Trans. Sonics Ultrasonics (USA), Vol. SU-16, No. 1, Suppl. p. 21 (Jan. 1969). (1968 IEEE Ultrasonics Symposium, New York, USA, 25-27 Sept. 1968).

Lloyd, P.
"Monolithic Crystal Filters for Frequency Division Multiplex", Programme of the 25th Annual Frequency Control Symposium (abstracts), Atlantic City, NJ, USA, 26-28 Apr. 1971 (Fort Monmouth, NJ, USA: US Army Electronics Command 1971), p. 47.

Lloyd, P.
"Monolithic Crystal Filters", (Bell Telephone Labs., Allentown, PA, USA). Proceedings of the 7th International Congress on Acoustics, Budapest, Hungary, 18-26 Aug. 1971 (Budapest, Hungary: Akademiai Kiado 1971), p. 309-12.

Lu, S. K. S.
"Cascade Synthesis of Monolithic Crystal Filters with Transmission Zeros at Finite Frequencies", (Dept. of Electrical Engng., Univ. of Malaya, Kuala Lumpur, Malaysia). Electron. Lett. (GB), Vol. 14, No. 2, p. 45-6, (19 Jan. 1978).

Lu, S. K. S.
"Comments on 'Cascade Synthesis of Polylithic Crystal Filters Containing Double-Resonator Monolithic Crystal Filter (MCF) Elements'", (Dept. of Electrical Engng., Univ. of Malaya, Kuala Lumpur, Malaysia). IEEE Trans. Circuits & Syst. (USA), Vol. CAS-24, No. 5, p. 274-5 (May 1977).

Lukaszek, T. J.
"Mode Control and Related Studies of VHF Quartz Filter Crystals", (USAECOM, Fort Monmouth, NJ, USA). IEEE. Trans. Sonics & Ultrasonics (USA), Vol. SU-18, No. 4, p. 238-46 (Oct. 1971).

Markvoort, J. A.
"On the Modeling of Monolithic Quartz Crystal Filters", (Eindhoven Univ. Technol., Netherlands). Appl. Sci. Res. (Netherlands), Vol. 29, No. 5, p. 361-79 (Sept. 1974).

Mason, W. P.
"Constants of a Trapped-Energy Electromechanical Transducer Made by Evaporating a Thin Layer of a Piezoelectric Crystal on Each Side of a Quartz Plate", (Columbia Univ., New York, USA). J. Acoust. Soc. Amer., Vol. 46, No. 3, Pt. 2, p. 687-92 (Sept. 1969).

Masuda, Y., Kawakami, I., Kobayashi, M.
"Monolithic Crystal Filters", Oki Rev. (Japan), Vol. 38, No. 4, p. 39-44 (1971). In Japanese.

Masuda, Y., Kawakami, I., Kobayashi, M.
"Monolithic Crystal Filter with Attenuation Poles Utilizing 2-Dimensional Arrangement of Electrode", (Oki Electric Industry Co. Ltd., Tokyo, Japan). Proceedings of the 27th Annual Frequency Control Symposium, Cherry Hill, NJ, USA, 12-14 June 1973 (Washington, DC, USA: Electronic Industries Assoc. 1973), p. 227-32.

Masuda, Y., Kawakami, I., Kobayashi, M., Gunji, K.
"Monolithic Crystal Filters Having Attenuation Poles", (Oki Electric Industry Co. Ltd., Tokyo, Japan). Electron. & Commun. Jap. (USA), Vol. 57, No. 12, p. 8-16 (Dec. 1974).

Mavrov, N. P.
"Problems of Optimum Design of Quartz Filter Resonators with Energy Trapping", Bulg. J. Phys. (Bulgaria), Vol. 4, No. 5, p. 516-22.

Metel'kova, T. F., Stein, M. I.
"A Quartz Crystal Through-Connection Filter for Master Groups", Telecommun. & Radio Eng. Pt. 1 (USA), Vol. 30, No. 1, p. 12-16 (Jan. 1976). Translation of: Elektrosvyaz (USSR), Vol. 30, No. 1, p. 17-22 (Jan. 1976).

Miles, R. H. A., Cooper, R. G.
"Monolithic Dual Quartz Crystal Filters", Electronic Compon. (GB), Vol. 11, No. 1, p. 84-5 (Jan. 1970).

Morse, W. C., Rennick, R. C.
"Adjusting Frequency of Monolithic Crystal Filters with an Automatic Vapor Plater", (Western Electric Co., North Andover, Mass., USA). J. Vac. Sci. & Technol. (USA), Vol. 9, No. 1, p. 28-32 (Jan.-Feb. 1972). (Proceedings of the 5th International Vacuum Congress Part I, Boston, Mass, USA, 11-15 Oct. 1971).

Mortley, W. S.
"Wave Propagation in Alpha-Quartz Dispersive Filters", Marconi Rev. (GB), Vol. 34, No. 182, p. 173-206 (1971).

Muir, A. J. L.
"Monolithic Crystal Filters", (Plessey Telecommunications Res., Taplow, England). Syst. Technol. (GB), No. 17, p. 16-23 (Sept. 1973).

Muller, O.
"Monolithic Filters on Single Chips or Analog Sampling Filters with Charge Transfer Elements (Q-Filters)", (General Electric Co., MRD Lynchburg, VA, USA). Elektroniker (Switzerland), Vol. 15, No. 7, p. EL6-11 (July 1976). In German.

Matthes, H.
"Crystal-Band-Stop Filters with Improved Spurious Resonance Behavior", (Central Communication Labs., Siemens AG, Munich, Germany). Int. J. Circuit Theory & Appl. (GB), Vol. 4, No. 1, p. 25-42 (Jan. 1976).

Nakajima, Y., Hagiwara, K., Kitani, T., Nagata, T.
"Piezoelectric Ceramic Filter in the Fundamental Thickness-Extensional Mode for VHF Range", (Wireless Res. Lab., Matushita Electric Industrial Co. Ltd., Kadoma, Japan). Trans. Inst. Electron. & Commun. Eng. Jpn. Sect. E (Japan), Vol. E60, No. 9, p. 505-6 (Sept. 1977).

Okuno, K., Watanabe, T.
"A Hybrid Integrated Monolithic Crystal Filter", (Nippon Electric Co. Ltd., Kawasaki City, Kanagawa, Japan). Proceedings of the 30th Annual Symposium on Frequency Control, Atlantic City, NJ, USA, 2-4 June 1976 (Washington, DC, USA: Electronic Industries Assoc. 1976), p. 109-18.

Olster, S. H., Oak, I. R., Pearman, G. T., Rennick, R. C., Meeker, T. R.
"A6 Monolithic Crystal Filter Design for Manufacture and Device Quality", (Western Electric Co. Inc., North Andover, MA, USA). Proceedings of the 29th Annual Frequency Control Symposium, Fort Monmouth, NJ, USA, 28-30 May 1975 (Washington, DC, USA: Electronic Industries Assoc. 1975), p. 105-12.

O'Neill, J. F., Ghausi, M. S.
"Design of Frequency Selective Networks Using Only Resonators", Conference Record Tenth Midwest Symposium of Circuit Theory, Lafayette, (1967) (New York: Institute of Electrical and Electronics Engineers, Inc., 1967), Paper No. X-5.

Orsucci, M., Reggiani, M., Stacchiotti, G.
"Synthesis of Bridged Polylithic Crystal Filters", (FDM Div. Labs., Telettra SpA, Milano, Italy). Alta Freq. (Italy), Vol. 45, No. 12, p. 747-51 (Dec. 1976).

Oshima, Y.
"Quartz Crystal Filters for Export", Meidensha Rev. (Int. Ed.) (Japan), Vol. 37, No. 2, p. 1-9 (1971).

Owens, J. M., Smith, C. V. Jr., Collins, J. H.
"Magnetostatic Wave Bandpass Filters and Resonators", (Dept. of Electrical Engng., Univ. of Texas, Arlington, TX, USA). Proceedings of the 1978 IEEE International Symposium on Circuits and Systems, New York, USA, 17-19 May 1978 (New York, USA: IEEE 1978), p. 563-8.

Pearman, G. T., Rennick, R. C.
"Filters and Resonators - A Review", (Bell Telephone Labs., Inc., Allentown, PA, USA). IEEE Trans. Sonics & Ultrason. (USA), Vol. SU-21, No. 4, p. 238-43 (Oct. 1974).

Pearman, G. T., Rennick, R. C.
"Unwanted Modes in Monolithic Crystal Filters", (Bell Telephone Labs. Inc., Allentown, PA, USA). 31st Annual Frequency Control Symposium, Atlantic City, NJ, USA, 1-3 June 1977 (Washington, DC, USA: Electronic Industries Assoc. 1977), p. 191-6.

Pochet, J.
"Crystal Ladder Filters", Wireless World (GB), Vol. 83, No. 1499, p. 62-3 (June 1977).

Pond, C. W.
"Phased Matched Crystal Filters", (Hughes Aircraft Co., Newport Beach, CA, USA). 1970 WESCON Technical Papers, Volume 14, Western Electronic Show and Convention, Los Angeles, CA, USA, 25-28 Aug. 1970 (Los Angeles, CA, USA: WESCON 1970), 6 pp.

Przesmyski, O.
"Application of Narrow Band-Stop Filters with Quartz Crystal Resonators", (Warsaw Polytechnic, Poland). Elektronika (Poland), No. 6, p. 252-3 (1971). In Polish.

Przesmyski, O.
"A Novel Type of Stop-Band Filter with Piezoelectric Resonators", (Inst. Telelektroniki Politechniki Warszawskiej, Poland). Pr. Inst. Tele.- & Radiotech. (Poland), Vol. 19, No. 1, p. 51-62 (1975). In Polish.

Reilly, N. H. C., Redwood, M.
"Wave-Propagation Analysis of the Monolithic-Crystal Filter", Proc. Instn. Electr. Engrs. (GB), Vol. 116, No. 5, p. 653-60 (May 1969).

Rennick, R. C.
"An Equivalent Circuit Approach to the Design and Analysis of Monolithic Crystal Filters", (Bell Labs., Inc., Allentown, PA, USA). IEEE Trans. Sonics & Ultrason. (USA), Vol. SU-20, No. 4, p. 347-54 (Oct. 1973).

Rennick, R. C.
"Modelling and Tuning Methods for Monolithic Crystal Filters", (Bell Telephone Labs. Inc., Allentown, PA, USA). 1975 IEEE International Symposium on Circuits and Systems, Newton, Mass, USA, 21-23 April 1975 (New York, USA: IEEE 1975), p. 309-12.

Revankar, G. N., Bapat, V. B.
"High-Q Active Crystal Band-Pass Filter", (Electrical Engng. Dept., Indian Inst. of Technol., Bombay, India), Stud. J. Inst. Electron. & Telecommun. Eng. (India). Vol. 17, No. 4, p. 197-8 (Oct. 1976).

Roberts, D. A.
"CdS-Quartz Monolithic Filters for the 100-500 MHz Frequency Range", Programme of the 25th Annual Frequency Control Symposium (abstracts), Atlantic City, NJ, USA, 26-28 Apr. 1971 (Fort Monmouth, NJ, USA: US Army Electronics Command 1971), p. 44.

Sasaki, R., Nagata, T., Matsushita, S.
"Piezoelectric Resonators as a Solution to Frequency Selectivity Problems in Color TV Receivers", (Matsushita Electric Industrial Co. Ltd., Osaka, Japan). IEEE Trans. Broadcast. & Telev. Receivers (USA), Vol. BTR-17, No. 3, p. 195-201 (Aug. 1971). (IEEE-BTR Chicago Spring Conference, Chicago, IL, USA, 7-8 June 1971).

Sasaki, R., Tsukamoto, K.
"Resonant Q of Quartz Crystal Resonator for Monolithic Crystal Filter", Electr. Commun. Lab. Tech. J. (Japan), Vol. 23, No. 1, p. 67-78 (1974). In Japanese.

Sauerland, F.
"Design of Piezoelectric Ladder Filters", International Symposium on Circuit Theory, Digest, San Francisco, CA, USA, 8-10 Dec. 1969 (New York, USA: IEEE 1969), p. 9.

Seed, A., Wood, A. F. B., Goodwin, M. W.
"Monolithic Filters for Mobile Radio Applications", (Internat. Telephone & Telegraph Corp., Harlow, England). Proceedings of the International Conference on Advanced Microelectronics, Paris, France, 6-10 Apr. 1970 (Paris, France: Federation Nationale des Industries Electroniques 1970), 2pp

Sivkov, B. V., Pashkovskii, N. A.
"Measuring the Secondary Resonances of Quartz Filter Resonators", Meas. Tech. (USA), Vol. 18, No. 1, p. 122-4 (Jan. 1975). Translation of: Izmer. Tekh. (USSR), Vol. 18, No. 1, p. 74-6 (Jan. 1975).

Sheahan, D. F., Schmidt, C. E.
"Coupled Resonator Quartz Crystal Filters", Papers Presented at the Western Electronic Show and Convention, San Francisco, CA, USA, 24-27 Aug. 1971 (North Hollywood, CA, USA: Western Periodicals Co. 1971), 8/3 6 pp.

Sheahan, D. F.
"Crystal Filters", (GTE Lenkurt Inc., San Carlos, CA, USA). International Symposium on Circuit Theory 1973, Toronto, Canada, 9-11 April 1973) (New York, USA: IEEE 1973), p. 394-7.

Sheahan, D. F.
"Polylithic Crystal Filters", (GTE Lenkurt Inc., San Carlos, CA, USA). Proceedings of the 29th Annual Frequency Control Symposium, Fort Monmouth, NJ, USA, 28-30 May 1975 (Washington, DC, USA: Electronic Industries Assoc. 1975), p. 120-7

Sherman, J. H. Jr.
"Dimensioning Rectangular Electrodes and Arrays of Electrodes on AT-Cut Quartz Bodies", (Mobile Radio Products Dept., General Electric Co., Lynchburg, VA, USA). Proceedings of the 30th Annual Symposium on Frequency Control, Atlantic City, NJ, USA, 2-4 June 1976 (Washington, DC, USA: Electronic Industries Assoc. 1976), p. 54-64.

Simpson, H. A., Finch, E. D. Jr., Weeman, R. K.
"Composite Filter Structures Incorporating Monolithic Crystal Filters and L-C Networks", Programme of the 25th Annual Frequency Control Symposium (abstracts), Atlantic City, NJ, USA, 26-28 Apr. 1971 (Fort Monmouth, NJ, USA: US Army Electronics Command (1971), p. 48.

Singhi, B. M., Datta, M. R.
"Modified Crystal Selective Network", (Dept. of Electrical Engng., G. S. Inst. of Tech. & Sci., Indore, India). J. Inst. Electron. & Telecommun. Eng. (India), Vol. 21, No. 9, p. 495-8 (Sept. 1975).

Smythe, R. C.
"Communications Systems Benefit from Monolithic Crystal Filters", (Piezo Technol. Inc., Orlando, FL, USA). Electronics (USA), Vol. 45, No. 3, p. 48-51 (31 Jan. 1972).

Spasov, L., Borisov, M.
"Studies on Monolithic Quartz Filters", (Inst. of Solid State Phys., Bulgarian Acad. of Sci. Sofia, Bulgaria). Bulg. J. Phys. (Bulgaria), Vol. 4. No. 5, p. 523-32.

Spencer, W. J.
"A New Functional Device -- The Monolithic Crystal Filter", IEEE Trans. Mag. (USA), Vol. MAG-4, No. 3, p. 221 (Sept. 1968).

Stearns, C. M., Wanuga, S., Tehon, S. W., Kachelmyer, A.
"Multi-Mode Stacked Crystal Filter", (General Electric Co., Syracuse, NY, USA). 31st Annual Frequency Control Symposium, Atlantic City, NJ, USA, 1-3 June 1977 (Washington, DC, USA: Electronic Industries Assoc. 1977), p. 197-206.

Stevenson, J. K.
"Synthesis of Narrowband Cascaded Crystal-Capacitor Lattice Filters", (Hirst Res. Centre, Wembley, England). Radio & Electron. Eng. (GB), Vol. 44, No. 6, p. 326-30 (June 1974).

Stevenson, J. K.
"Simple Design Formulae for Third and Fourth-Order Crystal Lattice Filters and Finite Attenuation Poles", (General Electric Co. Ltd., Hirst Res. Centre, Wembley, England). Int. J. Electron. (GB), Vol. 38, No. 6, p. 697-710 (June 1975).

Stevenson, J. K.
"Design Formulae for Multi-Lattice Crystal Filters", (CEC Ltd., Telecommunications Res. Labs., Hirst Res. Centre, Wembley, England). Int. J. Electron. (GB), Vol. 41, No. 2, p. 105-23 (Aug. 1976).

Stevenson, J. K.
"Transformation for Modifying the Lumped-Element Equivalent Circuit for Metal-Encapsulated Crystals in Unbalanced Semi-Lattice Filters", (Dept. of Electrical & Electronic Engng., Polytech. of South Bank, London, England). Radio & Electron. Eng. (GB), Vol. 46, No. 12, p. 614-16 (Dec. 1976).

Sykes, R. A., Smith, W. L., Spencer, W. J.
"Monolithic Crystal Filters", IEEE International Convention Record, New York (1967), (New York: Institute of Electrical and Electronics Engineers, Inc., 1967), Pt. 11, 78-93.

Szentirmai, G.
"The Synthesis of Narrowband Crystal Band-Elimination Filters", (Bell Telephone Lab., USA). 1968 International Symposium on Circuit Theory Digest, Miami Beach, FL, USA, 4-6 Dec. 1968 (New York: Institute of Electrical and Electronics Engineers 1968), p. 65.

Szentirmai, G.
"Problems of Crystal Filter Design", (Cornell Univ., Ithica, NY, USA). Digest of Technical Papers of the 1970 IEEE International Symposium on Circuit Theory, Atlanta, GA, USA, 14-16 Dec. 1970 (New York, USA: Lewis Winner 1970), p. 108.

Szentirmai, G.
"Crystal and Ceramic Filters" (Cornell Univ., Ithica, NY, USA). 4th Annual Contemporary Filter Design Seminar, Coral Gables, FL, USA, 19-21 Apr. 1971 (Coral Gables, FL, USA: Univ. Miami, USA 1971). 59 pp.

Tenen, O.
"Crystal Filters--Their Design and Engineering", (Pye Pty. Ltd., Clayton, Victoria, Australia). Proc. Inst. Radio Electron. Eng. Aust. (Australia), Vol. 32, No. 5, p. A9 (May 1971). (13th National Convention of the Institution of Radio and Electronics Engineers, Australia (abstracts), Melbourne, Australia, 24-28 May 1971).

Tenen, O.
"Wide-Band Crystal Filter Design", Telecommun. J. Aust. (Australia), Vol. 27, No. 1, p. 71-80 (1977).

Tiersten, H. F.
"An Analysis of Overtone Modes in Monolithic Crystal Filters", (Dept. of Mech. Engng., Aeronaut. Engng. & Mech., Rensselaer Polytech. Inst., Troy, NY, USA). Proceedings of the 30th Annual Symposium on Frequency Control, Atlantic City, NJ, USA, 2-4 June 1976 (Washington, DC, USA: Electronic Industries Assoc. 1976), p. 103-8.

Tiersten, H. F.
"Analysis of Overtone Modes in Monolithic Crystal Filters", (Mech. Engng. Dept., Rensselaer Polytech. Inst., Troy, NY, USA). J. Acoust. Soc. Am. (USA), Vol. 62, No. 6, p. 1424-30 (Dec. 1977).

Tiersten, H. F.
"Electric Field Effects in Monolithic Crystal Filters", (Rensselaer Polytechnic Inst., Troy, NY, USA). Proceedings of the 23rd Annual Frequency Control Symposium, Atlantic City, NJ, USA, 6-8 May 1969 (Washington, DC, USA: Electronic Industries Assoc. 1969), p. 56-64.

Todorov, P., Tsvetanski, R.
"Passive Integral Filters [Quartz Resonator]", Tekh. Misul (Bulgaria), Vol. 12, No. 3, p. 33-9 (1975). In Russian.

Todorov, M. I., Dimitriev, A. P.
"Device for the Automatic Selection of Piezoceramic Resonators for Multi-Unit Filters", Elektro. Prom.-st. & Priborostr. (Bulgaria), Vol. 13, No. 2, p. 62-4 (1978). In Bulgarian.

Topolevsky, R. B., Redwood, M.
"The Electrical Characteristics of Symmetric and Asymmetric Monolithic Crystal Filters: A New Analytical Approach", (Queen Mary Coll., Univ. London, England). IEEE Trans. Sonics & Ultrason. (USA), Vol. SU-22, No. 3, p. 162-8 (May 1975). (Ultrasonics Symposium (abstracts only), Milwaukee, Wis, USA, 11-14 Nov. 1973).

Topolevsky, R., Burgess, J. W.
"Interresonator Coupling for Overtone Monolithic Quartz Filters", (Plessey Co. Ltd., Towcester, England). Electron. Lett. (GB), Vol. 10, No. 23, p. 476-7 (14 Nov. 1974).

Toyama, K., Matsumoto, A., Nishide, T.
"Synthesis of Image Band-Pass Filters with Two-Crystal Unsymmetrical Lattice Structures", (Toyo Communications Equipment Co. Ltd., Kawasaki, Japan), Trans. Inst. Electronics Commun. Engrs. Japan A.B.C., p. 7-13. In Japanese. English Translation in: Electronics Commun. Japan (USA), Vol. 52, No. 2, (Feb. 1969).

Uno, T.
"200 MHz Thickness Extensional Mode $LiTaO_3$ Monolithic Crystal Filter", (Nippon Telegraph & Telephone Public Corp., Tokyo). IEEE Trans. Sonics & Ultrason. (USA), Vol. SU-22, No. 3, p. 168-74 (May 1975). (Ultrasonics Symposium (Abstracts only), Milwaukee, Wis, USA, 11-14 Nov. 1973).

Uno, T.
"Thickness Extensional Mode $LiTaO_3$ Monolithic Crystal Filter", (Nippon Telegraph & Telephone Public Corp., Tokyo, Japan). Electr. Commun. Lab. Tech. J. (Japan), Vol. 24, No. 7, p. 1337-46 (1975). In Japanese.

Vostrova, I. N., Spivak, S. Kh., Cherne, Kh. I.
"Equivalent-Circuit Transformation of a Crystal-Controlled Filter", Izv. VUZ Radioelektron. (USSR), Vol. 16, No. 7, p. 102-4 (July 1973). In Russian. English Translation in: Radio Electron. & Commun. Syst. (USA).

Vostrova, I. N., Kantor, V. M.
"Monolithic Quartz Filters", Telecommun. & Radio Eng. Pt. 1, (USA), Vol. 29-30, No. 1, p. 61-6 (Jan. 1975). Translation of: Elektrosvyaz (USSR), Vol. 29, No. 1, p. 69-74 (Jan. 1975).

Waddington, D. E. O. N.
"Narrow Band Crystal Filter Design", Marconi Instrum. (GB), Vol. 15, No. 1, p. 10-13 (Spring 1975).

Watanabe, N., Tsukamoto, K.
"High-Performance Monolithic Crystal Filters with Stripe Electrodes", (Musashino Electrical Communication Lab., NTT, Musashino, Japan). Electron. & Commun. Jap. (USA), Vol. 57, No. 4, p. 53-60 (April 1974).

Watanabe, N., Tsukamoto, K., Jumonji, H.
"Design of High Performance Monolithic Crystal Filters", Electr. Commun. Lab. Tech. J. (Japan), Vol. 23, No. 1, p. 53-65 (1974). In Japanese.

Watanabe, N., Shimizu, H.
"Image Parameter Design of Monolithic Filters with Two Electrode Pairs Using a High-Electro Mechanical-Coupling Piezoelectric Plate. I Conventional Image Parameter Design Using the Distributed Constant Equivalent Circuit", (Res. Inst. of Electrical Communication, Tohoku, Univ., Sendai, Japan).

Watanabe, N., Shimizu, H.
"Image Parameter Design of Monolithic Filters with Two Electrode Pairs Using a High-Electromechanical-Coupling Piezoelectric Plate. III. A Design Method of Making the Pass Band to be the Frequency Range Between the Two Resonances", (Tohoku Univ., Sendai, Japan). Rec. Electr. & Commun. Eng. Conversazione Tohoku Univ. (Japan). Vol. 44, No. 3, p. 42-51 (Aug. 1975). In Japanese.

Watanabe, N., Nakamura, K., Shimizu, H.
"Image-Parameter Design of Monolithic Filters with Two Electrode Pairs Using a High-Electromechanical-coupling Piezoelectric Plate. IV. Design and Experiment of Piezoelectric-Strip Monolithic Filters", Rec. Electr. & Commun. Eng. Conversazione Tohoku Univ. (Japan), Vol. 45, No. 1, p. 11-6, (Feb. 1976). In Japanese.

Watanabe, N., Shimizu, H.
"Image-Parameter Design of Multi-Electrode-Pair Monolithic Filters. I. A New Method of Designing Multiple-Mode Filters", Rec. Electr. & Commun. Eng. Conversazione Tohoku Univ. (Japan), Vol. 45, No. 4, p. 181-5 (Nov. 1976). In Japanese.

Watanabe, N., Shimizu, H.
"Image-Parameter Design of Multi-Electrode-Pair Monolithic Filters. II. Four-Electrode-Pair Monolithic Filter", Rec. Electr. & Commun. Eng. Conversazione Tohoku Univ. (Japan), Vol. 46, No. 1, p. 15-22 (Feb. 1977). In Japanese.

tanabe, H., Shimizu, H.
mage-Parameter Design of Multi-Electrode-
ir Monolithic Filters. III. Four-Electrode-
ir Bilithic Filter", Rec. Electr. & Commun.
g. Conversazione Tohoku Univ. (Japan),
l. 46, No. 1, p. 23-9 (Feb. 1977). In Japanese.

tanabe, H., Shimizu, H.
mage-Parameter Design of Two-Electrode-Pair
nolithic Filters on High-Electromechanical-
upling Piezoelectric Plates", (Faculty of
gng., Tohoku Univ., Sendai, Japan).
ans. Inst. Electron. & Commun. Eng. Jpn. Sect.
(Japan), Vol. E60, No. 3, p. 146-7 (March
77).

rner, J. F., Dyer, A. J., Birch, J.
he Development of High Performance Filters
ing Acoustically Coupled Resonators on AT-Cut
artz Crystals", (General Electric Co. Ltd.,
mbley, England). Proceedings of the 23rd
nual Frequency Control Symposium, Atlantic
ty, NJ, USA, 6-8 May 1969 (Washington, DC,
A: Electronic Industries Assoc. 1969), p. 65-75.

rner, J. F.
he Bilithic Quartz-Crystal Filter", J. Sci.
Technol. (GB), Vol. 38, No. 2, p. 74-82 (1971).

'e, H. K. H.
inite-Pole Frequencies in Monolithic Crystal
lters", (Northern Electric Co. Inc., Montreal,
nada). Proc. IEEE (USA), Vol. 59, No. 1,
88-9 (Jan. 1971).

e, H. K. H.
mplitude Distortion Compensation in Two-Pole
nolithic Crystal Filters", (Northern Electric
. Ltd., Montreal, Canada). Proc. IEEE (USA),
l. 59, No. 8, p. 1286-7 (Aug. 1971).

da, H., Nakazawa, Y., Kobori, N.
igh Frequency Crystal Monolithic (HCM)
.lters", (Toyo Communication Equipment Co.
Ltd. (Japan). Proceedings of the 23rd Annual
Frequency Control Symposium, Atlantic City, NJ
A, 6-8 May 1969 (Washington, DC, USA: Elec-
onic Industries Assoc. 1969), p. 76-92.

da, H., Endo, A., Hasegawa, K.
rystal Filters: With Performance Up and Cost
own, They are Ready to Uncrowd the Spectrum",
E (Japan), No. 108, p. 24-7 (Nov.-Dec. 1975).

lenka, J.
. Twin-Resonator Monolithic Piezoelectric
Filter with a Common Electrode", (VSST, Liberec,
zechoslovakia). Slaboproudy Obz. (Czechoslovakia),
Vol. 35, No. 7, p. 311-14 (July 1974). In Czech.

elyakh, E. V., Krukhmaleva, V. D.
. Crystal Band-Elimination Filter", Elektrosvyaz
USSR), p. 40-4 In Russian. English Translation
in: Telecomm. Radio Engng. Pt. 1. (USA), Vol.
23, No. 5, (May 1969).

Akitt, D. P.
"70 MHz Surface-Acoustic-Wave Resonator Notch
Filter", (Div. of Electrical Engng., Nat. Res.
Council of Canada, Ottawa, Ontario, Canada).
Electron. Len. (GB), Vol. 12, No. 9, p. 217-18
(29 April 1976).

Akitt, D. P.
"High Q Acoustic Surface Wave Filters", (Div. of
Elect. Engng., Nat. Res. Council of Canada, Ottawa,
Ontario, Canada). Canadian Communications and
Power Conference, Montreal, Canada, 20-22 Oct.
1976 (New York, USA: IEEE 1976), p. 200-1.

Armstrong, G. A.
"The Design of SAW Dispersive Filters Using
Interdigital Transducers", (Microwave & Electronic
Systems Ltd., Newbridge, Scotland). Wave Electron.
(Netherlands), Vol. 2, No. 1-3, p. 155-76
(July 1976). (European Workshop on Computer Aided
Design of SAW Devices, Bologna, Italy, 7-9 April
1976).

Atzeni, C., Masotti, L., Teodori, E.
"Acoustic Surface-Wave Matched Filters", Alta
Freq. (Italy), Vol. 40, No. 6, p. 506-12 (June
1971). In English.

Atzeni, C.
"Sensor Number Minimization in Acoustic Surface-
Wave Matched Filters", (Consiglio Nazionale
Ricerche, Florence, Italy). IEEE Trans. Sonics
& Ultrasonics (USA), Vol. SU-18, No. 4, p. 193-201
(Oct. 1971).

Atzeni, C., Masotti, L.
"Acoustic Surface-Wave Transversal Filters", In
book: Acoustic Surface Wave and Acousto-Optic
Devices, T. Kallord (Ed.), p. 69-80, New York,
USA: Optosonic Press (1971), vii+221 pp.
[0 87739 003 7].

Atzeni, C., Masotti, L.
"Interdigital Electrode Minimization in Acoustic
Surface Wave Filters" (Consiglio Nazionale Ricerche,
Florence, Italy). IEEE Trans. Sonics & Ultra-
sonics (USA), Vol. SU-19, No. 3, p. 401 (July 1972).
(1971 IEEE Ultrasonics Symposium, Miami Beach,
FL, USA, 6-8 Dec. 1971).

Atzeni, C., Manes, G., Masotti, L.
"Design of Surface Acoustic Wave Filters", (Facolta
Ingeneria, Firenze, Italy). Alta Freq. (Italy),
Vol. 43, No. 10, p. 865-75 (Oct. 1974).

Atzeni, C., Manes, G., Masotti, L.
"New Insights into SAW Filter Design", (Italian
Nat. Res. Council, Florence, Italy). Ultrasonics
International 1975, London, England, 24-26 March
1975 (Guildford, Surrey, England: IPC Sci. &
Technol. Press 1975), p. 133-7.

Atzeni, C., Manes, G., Masotti, L.
"Surface-Acoustic-Wave Phase-Interference Filters", (Italian Nat. Res. Council & Electronic Engng. Dept., Univ. of Florence, Italy). Wave Electron. (Netherlands), Vol. 1, No. 2, p. 97-104 (July 1975).

Autran, J.-M., Maloney, E. D.
"Application of CAD Techniques to SAW Filters", (Electron Tube Div., Thomson-CSF, Paris, France). Electron. Eng. (GB), Vol. 49, No. 592, p. 51-4 (May 1977).

Balek, R., Bunc, V.
"The Applicability of Surface Elastic Waves", Sdelovaci Tech. (Czechoslovakia), Vol. 23, No. 4, p. 130-2 (April 1975). In Czech.

Balek, R., Bunc, V.
"Surface Elastic Wave Filters", Sdelovaci Tech. (Czechoslovakia), Vol. 23, No. 11, p. 419-20 (Nov. 1975). In Czech.

Boege, T. J., Chao, G., Drummond, W. S.
"Design of Arbitrary Phase and Amplitude Characteristics in SAW Filters", (Tektronix Labs., Tektronix Inc., Beaverton, OR, USA). 1976 Ultrasonics Symposium Proceedings, Annapolis, MD, USA, 29 Sept. - 1 Oct. 1976 (New York, USA: IEEE 1976), p. 313-16.

Borisov, M. I., Stojanov, D. V., Velkov, V. V., Burov, J. I.
"Electrically Controlled Acoustic-Surface-Wave Filters", (Sofia Univ., Bulgaria). Electron. Lett. (GB), Vol. 10, No. 24, p. 519-20 (28 Nov. 1974).

Bristol, T. W.
"Acoustic Surface-Wave-Device Applications", (Hughes Aircraft Co., Fullerton, CA, USA). Microwave J. (USA), Vol. 17, No. 1, p. 25-7, 63 (Jan. 1974).

Budreau, A. J., Carr, P. H., Laker, K. R.
"Frequency Synthesizer Using Acoustic Surface-Wave Filters", (Air Force Cambridge Res. Labs., Bedford, Mass, USA). Microwave J. (USA), Vol. 17, No. 3, p. 65-6, 68-9 (March 1974).

Budreau, A. J., Laker, K. R., Carr, P. H.
"Compact Microwave Acoustic Surface Wave Filter Bank for Frequency Synthesis", (Air Force Cambridge Res. Labs., Laurence G. Hanscom Air Force Base, Bedford, MA, USA). Proceedings of the Symposium on Optical and Acoustical Micro-Electronics, New York, USA, 16-18 April 1974 (Brooklyn, NY, USA: Polytech. Press 1975), p. 471-83.

Burgess, A. S., Cole, P. H.
"Design of Acoustic Surface-Wave Devices Using an Admittance Formalism", (Univ. Adelaide, Australia). IEEE Trans. Microwave Theory & Tech. (USA), Vol. MTT-21, No. 10, p. 611-18 (Oct. 1973).

Burnsweig, J.
"Surface-Wave Signal Processing Filters", (Hughes Aircraft Co., Culver City, CA, USA).
Papers presented at the Western Electronic Show and Convention, San Francisco, CA, USA, 24-27 Aug. 1971 (North Hollywood, CA, USA: Western Periodicals Co. 1971), 8/4 10 pp.

Claiborne, L.T.
"New Surface Wave Components", (Texas Instruments, Dallas, TX, USA). Int. Elektron. Rundsch. (Germany), Vol. 25, No. 8, p. 206-7 (Aug. 1971). In German.

Claiborne, L.T., Staples, E. J.
"Surface Wave Filters Integrated Circuits", (Texas Instruments Inc. Dallas, TX, USA). IEEE Trans. Sonics & Ultrasonics (USA), Vol. SU-19, No. 3, p. 413 (July 1972). 1971 IEEE Ultrasonics Symposium, Miami Beach, FL, USA, 6-8 Dec 1971.

Claiborne, L.T.
"A Survey of Current SAW Device Capabilities", (Texas Instruments Inc., Dallas, TX, USA). Proceedings of the 29th Annual Frequency Control Symposium, Fort Monmouth, NJ, USA, 28-30 May 1975 (Washington, DC, USA: Electronic Industries Assoc. 1975), p. 135-8.

Coldren, L. A., Rosenberg, R. L.
"Saw Resonator Filter Overview: Design and Performance Tradeoffs", (Bell Laboratories, Holmdel, NJ, USA). Ultrasonics Symposium Proceedings, Cherry Hill, NJ, USA, 25-27 Sept. 1978 (New York, USA: IEEE 1978), p. 422-432.

Collins, J., Owens, J.
"SAW Devices Meet High-Rel Systems Needs", Microwave Syst. News (USA), Vol. 7, No. 10, p. 58, 60, 64, 66, 70 (1 Oct. 1977).

Coussot, G.
"Investigation of Intermodulation in Acoustic-Surface-Wave Filter", (Thomson-CSF, Orsay, France). Electron. Lett. (GB), Vol. 11, No. 5, p. 116-17 (6 March 1975).

Coussot, G.
"Surface Acoustic Wave Filters", (Lab. Central de Rechenches da la Thomson, CSF, France). Rev. Polytech. (Switzerland), No. 6, p. 787, 789, 791 (25 June 1975). In French.

Coussot, G.
"Filters for Surface Elastic Waves", (Lab. Centrale di Richerche della Thomson-CSF, Orsay, France). Electrificazione (Italy), No. 11, p. 521-4 (Nov. 1975). In Italian.

Coussot, M., van den Driessche, M.
"Surface [acoustic] Wave Filters", Toute Electron. (France), No. 418, p. 37-43 (Feb. 1977). In French.

Costanza, S. T., Hagon, P. J., MacNevin, L. A.
"Analog Matched Filter Using Tapped Acoustic Surface Wave Delay Line", (North American Rockwell Corp., Anaheim, CA, USA). IEEE Trans. Microwave Theory. Tech. (USA), Vol. MTT-17, No. 11, p. 1042-3 (Nov. 1969).

Cross, P. S.
"Surface Acoustic Wave Resonator Filters Using Tapered Gratings", (Bell Telephone Labs., Holmdel, NJ, USA). IEEE Trans. Sonics & Ultrason. (USA), Vol. SU-25, No. 5, p. 313-19 (Sept. 1978).

Danicki, E.
"A 30 MHz Filter Based on Acoustic Surface Waves", Bull. Acad. Pol. Sci. Ser. Sci. Tech. (Poland), Vol. 20, No. 4, p. 289-95 (1972).

Darby, B. J., Grant, P. M., Collins, J. H.
"Performance of Surface Acoustic Wave Matched Filter Modems in Noise and Interference Limited Environments", (Univ. Edinburgh, Scotland). Ultrasonics International 1973 Conference Proceedings, London, England, 27-29 March 1973 (Guildford, Surrey: IPC Sci. & Technol. Press 1973), p. 314-21.

De, Zhang
"Suppression of Direct Transmission in SAW Resonator Filters by Inverse Phase IDT", (Acoustics Lab., Nanjing Univ., Nanjing, China). Acta Phys. Sin. (China), Vol. 27, No. 3, p. 349-52 (May 1978). In Chinese.

Deacon, J. M., Heighway, J., Jenkins, J. A.
"Multistrip Coupler in Acoustic-Surface-Wave Filters", (Plessey Co., Caswell, Towcester, England). Electron. Lett. (GB), p. 235-6 (17 May 1973).

DeVries, A. J., Dias, J. F., Rypkema, J. N., Wojcik, T. J.
"Characteristics of Surface Wave Intergratable Filters (SWIFS)", (Zenith Radio Corp., Chicago, IL, USA). Proceedings of the National Electronics Conference, Chicago, IL, USA, 7-9 Dec. 1970 (Oak Brook, IL, USA: National Electron. Conf. Inc., 1970), p. 537-40.

DeVries, A. J., Dias, J. F., Rypkema, J. N., Wojcik, T. J.
"Characteristics of Surface-Wave Integratable Filters (SWIFS). (Zenith Radio Corp., Chicago, IL, USA). IEEE Trans. Broadcast. & Telev. Receivers (USA), Vol. BTR. 17, No. 1, p. 16-23 (Feb. 1971).

Dieulesaint, E., Hartemann, P.
"Acoustic Surface Wave Filters", (Thomson CSF, Domaine Corbeville, Orsay, France). Ultrasonics (GB), Vol. 11, No. 1, p. 24-30 (Jan. 1973).

Drummond, W. S., Roth, S. A.
"Application of High Performance SAW Transversal Filters in a Precision Measurement Instrument", (TV Products Engineering, Tektronix, Inc., PO Box 500, Beaverton, OR, USA). Ultrasonics Symp, Cherry Hill, NJ, USA, 25-27 Sept. 1978.

El-Diwany, M. H., Campbell, C. K.
"Modification of Optimum Impulse Response Techniques for Application to SAW Filter Design", (Dept. of Electrical Engng., McMaster Univ., Hamilton, Ontario, Canada). IEEE Trans. Sonics & Ultrason. (USA), Vol. SU-24, No. 4, p. 277-9 (July 1977).

Engan, H.
"Interdigital Transducer Techniques for Specialized Frequency Filters SAW Transversal Filters", (Norwegian Inst. of Tech., Trondheim, Norway). Wave Electron. (Netherlands), Vol. 2, No. 1-3, p. 133-54 (July 1976). (European Workshop on Computer Aided Design of SAW Devices, Bologna, Italy, 7-9 April 1976).

Feldmann, M., Henaff, J., Carel, M.
"A.S.W. Filter Bank Using a Multistrip Reflective Array", (Dept. EST/DEF, Centre Nat. d'Etudes des Telecommunications, Issy-les-Moulineaux, France). Electron. Lett. (GB), Vol. 12, No. 5, p. 118-19 (4 March 1976).

Feldmann, M., Henaff, J.
"An ASW-Filter Using Two Fan-Shaped Multistrip Reflective Arrays", (CNET, Dept. EST/DEF, Issy-les-Moulineaux, France). 1976 Ultrasonics Symposium Proceedings, Annapolis, MD, USA, 29 Sept. - 1 Oct. 1976 (New York, USA: IEEE 1976), p. 397-400.

Feldmann, M., Henaff, J.
"Design of SAW Filter with Minimum Phase Response", (C.N.E.T., Department TCR/DEF, 92131 Issy-les-Moulineaux, France). Ultrasonics Symposium, Proceedings, Cherry Hill, NJ, USA, 25-27 Sept. 1978 (New York, USA: IEEE 1978), p. 720-723.

Fisk, J. R.
"New Acoustic Surface-Wave Devices", Electron. Aust. (Australia), Vol. 33, No. 4, p. 24-7 (July 1971).

Ganguly, A. K., Vassell, M. O., Zucker, J.
"A New, First Principles Approach to Acoustic Surface Wave Filter Analysis", (GTE Labs., Bayside, NY, USA). IEEE Trans. Sonics & Ultrasonics (USA), Vol. SU-19, No. 3, p. 400 (July 1972). (1971 IEEE Ultrasonics Symposium, Miami Beach, FL, USA, 6-8 Dec. 1971).

Ganguly, A. K., Vassell, M. O.
"Frequency Response of Acoustic Surface Wave Filters", (GTE Labs. Inc., Waltham, Mass, USA). J. Appl. Phys. (USA), Vol. 44, No. 3, p. 1072-85 (March 1973).

Gerard, H. M., Judd, G. W., Pedinoff, M. E.
"Phase Corrections for Weighted Acoustic Surface-Wave Dispersive Filters", (Hughes Aircraft Co., Fullerton, CA, USA). IEEE Trans. Microwave Theory & Tech. (USA), Vol. MTT-20, No. 2, p. 188-92 (Feb. 1972).

Gerard, H. M., Otto, O. W., Weglein, R. D.
"Wideband Dispersive Surface Wave Filters", Report ECOM-73-0110-F, Hughes Aircraft Co., Fullerton, CA, USA (Dec. 1974). 51 pp. ($4.25) Contract DAAB07-73-C-0110.

Guenther, A. E.
"Rapid Approximate Analysis of SAW Filters", (Zentrallab. fur Nachrichtentechnik, Siemens AG, Munchen, Germany). Proceedings of the 1976 IEEE International Symposium on Circuits and Systems, Munich, Germany, 27-29 April 1976 (New York, USA: IEEE 1976), p. 363-6.

Guerard, A., Glowinski, R., Feldmann, M.
"Synthesis by Optimization of Acoustic Surface Wave Frequency Filters", Ann. Telecommun. (France), Vol. 32, No. 1-2, p. 37-48 (Jan.-Feb. 1977). In French.

Hagon, P. J., Micheletti, F. B., Seymour, R. N., Wrigley, C. Y.
"A Programmable Surface Acoustic Wave Matched Filter for Phase-Coded Spread Spectrum Waveforms", (North American Rockwell Corp., Anaheim, CA, USA). IEEE Trans. Microwave Theory & Tech. (USA), Vol. MTT-21, No. 4, p. 303-6 (April 1973).

Hagon, P. J., Wheatley, C. E.
"Programmable Analog Matched Filters", (Rockwell International, Anaheim, CA, USA). Microwave J. (USA), Vol. 17, No. 7, p. 42-5 (July 1974).

Hartemann, P., Dieulesaint. E.
"Acoustic-Surface-Wave Filters", Electronics Letters (GB), Vol. 5, No. 25, p. 657-8 (11 Dec. 1969).

Hartmann, C. S., Claiborne, L. T., Buss, D. D., Staples, E. J.
"Programmable Transversal Filters Using Surface Waves, Charge Transfer Devices, and Conventional Digital Approaches", (Texas Instruments Inc., Dallas, TX, USA). International Specialist Seminar on Component Performance and Systems Applications of Surface Acoustic Wave Devices, Aviemore, Scotland, 25-28 Sept. 1973 (London, England: IEE 1973), p. 102-14.

Hartmann, C. S.
"Acoustic Surface Wave Devices [Signal Processing Functions]", (Texas Instruments Inc., Dallas, TX, USA). Communications Systems and Technology Conference, Dallas, TX, USA, 30 April - 1 May 1974 (New York, USA: IEEE 1974), p. 122-8.

Hartmann, C. S.
"Recent Advances in Surface Acoustic Wave Devices", (Texas Instruments Inc., Dallas, TX, USA). NTC '77 Conference Record, Pt. I, Los Angeles, CA, USA, 5-7 Dec. 1977 (New York, USA: IEEE 1977), p. 16-2/1-5.

Haydl, W. H., Cross, P. S.
"Fine Tuning of Surface-Acoustic-Wave Resonator Filters with Metallization Thickness", (Inst. for Angewandle Festkorperphys. Fraunhofer-Gesselschaft, Freiburg, Germany).

Hewes, C. R., Claiborne, L. T., Hartmann, C. S., Buss, D. D.
"Filtering with Analog CCDs and SWDs", (Texas Instruments Inc., Dallas, TX, USA). Proceedings of the 30th Annual Symposium on Frequency Control, Atlantic City, NJ, USA, 2-4 June 1976 (Washington, DC, USA: Electronic Industries Assoc. 1976), p. 123-8.

Hickernell, F. S., Bush, H. J.
"Monolithic Programmable SAW Transversal Filters", (Motorola Government Electronics Div., Scottsdale, AZ, USA). Proceedings of the 1978 IEEE International Symposium on Circuits and Systems, New York, USA, 17-19 May 1978 (New York, USA: IEEE 1978), p. 386-9.

Hirosaki, B.
"Systematic Jitter Reduction Effect by Inherent Delay of Acoustic Surface Wave Filter", (Central Res. Labs., Nippon Electric Co. Ltd., Kawasaki, Japan). Trans. Inst. Electron & Commun. Eng. Jpn. Sect. E (Japan), Vol. E-59, No. 7, p. 20-1 (July 1976).

Hohkawa, K., Ishihara, F., Yoshikawa, S.
"Acoustic Surface-Wave Filters without Apodisation Loss with Electrodes with Inclined Apodisation", (Musashino Electrical Communications Lab., Nippon Telegraph & Telephone Public Corp., Massashino, Tokyo, Japan). Electron. Lett. (GB), Vol. 11, No. 12, p. 259-61 (12 June 1975).

Hohkawa, K., Yoshikawa, S., Ishihara, F.
"Design of SAW Filters Using Linear Programming Technique", (Nippon Telegraph & Telephone Public Corp., Tokyo, Japan). J. Acoust. Soc. Jap. (Japan), Vol. 32, No. 9, p. 531-9 (Sept. 1976). In Japanese.

Hunsinger, B. J., Kansy, R. J.
"SAW Filter Sampling Techniques", (Coordinated Sci. Lab., Univ. Illinois, Urbana, IL, USA). IEEE Trans. Sonics & Ultrason. (USA), Vol. SU-22, No. 4, p. 270-3 (July 1975).

Jack, M. A.
"Fast-Fourier-Transform Processor Using SAW Chirp Filters", (Dept. of Electrical Engng., Univ. of Edinburgh, Edinburgh, Scotland). Electron. Lett. (GB), Vol. 14, No. 19, p. 634-5 (14 Sept. 1978).

Janus, A. R.
"Progress Report on Surface Acoustic Wave Device MMT [Filters and Delay Lines]", (Hughes Aircraft Co., Fullerton, CA, USA). Proceedings of the 30th Annual Symposium on Frequency Control, Atlantic City, NJ, USA, 2-4 June 1976 (Washington, DC, USA: Electronic Industries Assoc. 1976), p. 157-66.

Janus, A. R., Dyal, L. III.
"Progress Report on Surface Acoustic Wave Device MMT-II", (Hughes Aircraft Co., Fullerton, CA, USA). 31st Annual Frequency Control Symposium, Atlantic City, NJ, USA, 1-3 June 1977 (Washington, DC, USA: Electronic Industries Assoc. 1977), p. 281-4.

Jones, W. S., Kempf, R. A., Hartmann, C. S.
"Practical Surface Wave Chirp Filters for Modern Radar Systems", (Texas Instruments Inc., Dallas, TX, USA). Microwave J. (USA), Vol. 15, No. 5, p. 43-6, 8, 50, 76 (May 1972).

Jones, R. R., Schellenberg, J., Tanski, W. J., Moore, R. A.
"Transplexing SAW Filters for ECM. I.", Microwaves (USA), Vol. 13, No. 12, p. 43-4, 46, 50, 52, (Dec. 1974).

Jones, R. R., Schellenberg, J., Tanski, W. J., Moore, R. A.
"Transplexing SAW Filters for ECM. II", (Westinghouse Electric Corp., Baltimore, MD, USA). Microwaves (USA), Vol. 14, No. 1, p. 63-70, 72-3 (Jan. 1975).

Judd, G.
"Acoustic Pulse Compression Filters", Report FR-74-14-665, Hughes Aircraft Co., Fullerton, CA, USA (Sept. 1974), 51 pp ($4.25) Contract DAAB07-73-C-0121. Available from NTIS, Springfield, VA, 22151, USA.

Karnopp, D., Reed, J., Margolis, D., Dwyer, H.
"Computer-Aided Design of Acoustic Filters Using Bond Graphs", (Univ. of California, Dept of Mech. Engng., Davis, CA, USA). Noise Control Eng. (USA), Vol. 4, No. 3, p. 114-18 May-June 1975).

Kearns, W. J., Slobodnik, A. J. Jr.
"Fabrication of Micrometer Line Width SAW Filters Using Direct Optical Projection", Report AFCRL-TR-75-0055, Acad. Natural Sci., Philadelphia, PA, USA (Jan. 1975), 11 pp.

Kerber, G. L., White, R. M., Wright, J. R.
"Surface-Wave Inverse Filter for Non-Destructive Testing", (Naval Undersea Center, San Diego, CA, (USA). 1976 Ultrasonics Symposium Proceedings, Annapolis, MD, USA, 29 Sept. - 1 Oct. 1976 (New York, USA: IEEE 1976), p. 577-81.

LaGrante, J. B., Daniels, W. D., Lewandowski, R. L.
"SAW Devices: The Answer for Channelized Receivers? Radar'", (Texas Instruments Inc., Dallas, TX, USA). Microwave Syst. News (USA), Vol. 7, No. 12, p. 87-8, 90, 93-4, 96 (1 Dec. 1977).

Laker, K. R., Budreau, A. J., Carr, P. H.
"A Circuit Approach to SAW Filterbanks for Frequency Synthesis", (Air Force Cambridge Res. Labs., Hanscom AFB, MA, USA). Proc. IEEE (USA), Vol. 64, No. 5, p. 692-5 (May 1976).

Laker, K. R., Cohen, E., Slobodnik, A. J. Jr.
"Electric Field Interactions within Finite Arrays and the Design of Withdrawal Weighted SAW Filters at Fundamental and Higher Harmonics", 1976 Ultrasonics Symposium Proceedings, Annapolis, MD, USA, 29 Sept. - 1 Oct. 1976 (New York, USA: IEEE 1976), p. 317-21.

Langer, E.
"Surface Wave Filters", (Siemens AG, Munchen, Germany). 6th International Congress on Microelectronics, Munich, Germany, 25-27 Nov. 1974 (Munich, Germany: Internat. Electronics Assoc. 1976), 10pp. In German.

Langer, E.
"Surface Wave Filters for More Integration", (Bereich Bauelemente. Siemens AG, Munchen, Germany), Radio Mentor Electron. (Germany), Vol. 42, No. 12, p. 491-4 (Dec. 1976). In German.

Lardat, C.
"Experimental Performance of Grooved Reflective Array Compressors and Resonators", (Thomson-CSF, ASM Div., Cagnes-sur-Mer, France). 1976 Ultrasonics Symposium Proceedings, Annapolis, MD, USA, 29 Sept. - 1 Oct. 1976 (New York, USA: IEEE 1976), p. 272-6.

La Rosa, R., Kerbel, S. J.
"Synthesis of Transfer Functions by Parallel-Channel SAW filter Banks", (Hazeltine Corp., Greenlawn, NY, USA). 1976 Ultrasonics Symposium Proceedings, Annapolis, MD, USA, 29 Sept. - 1 Oct. 1976 (New York, USA: IEEE 1976), p. 322-7.

Lawrence, M. W.
"Surface Acoustic Waves and their Application", (AWA Res. Lab., North Ryde, New South Wales, Australia). Aust. Electron. Eng. (Australia), Vol. 8, No. 10, p. 19-22 (Oct. 1975).

Lever, K. V., Patterson, E., Stevens, P. C., Wilson, I. M.
"SAW 350 microsecond Binary Phase-Shift-Keyed Matched Filter", (Hirst Res. Centre, GEC Ltd., Wembley, England). Electron. Lett. (GB), Vol. 12, No. 5, p. 116-17 (4 March 1976).

Lever, K. V., Patterson, E., Stevens, P. C., Wilson, I. M.
"Surface Acoustic Wave Matched Filters for Communications Systems", (General Electric Co. Ltd., Hirst Res. Centre, Wembley, England). Radio & Electron. Eng. (GB), Vol. 46, No. 5, p. 237-46 (May 1976).

Lever, K. V., Patterson, E., Stevens, P. C., Wilson, I. M.
"Surface-Acoustic-Wave Matched Filters for Multi-frequency Shift Keyed Communication Systems", (Hirst Res. Centre, Wembley, England). Proc. Inst. Electr. Eng. (GB), Vol. 123, No. 8, p. 770-4 (Aug. 1976).

Lewis, M. F.
"Surface-Acoustic-Wave Devices", GEC J. Sci. & Technol. (GB), Vol. 39, No. 4, p. 156-62 (1972).

Lewis, M. F.
"Surface-Acoustic-Wave Filters Employing Symmetric Phase-Weighted Transducers", (Royal Radar Establ., Great Malvern, England). Electron. Lett. (GB), Vol. 9, No. 6, p. 138-40 (22 March 1973).

Maines, J. D.
"Advances in Surface Acoustic Wave Pulse Compression Filters", 1972 European Solid State Devices Research Conference, Lancaster, England, 12-15 Sept. 1972 (London, England: Inst. Phys. 1973), p. 181.

Maines, J. D., Moule, G. L., Newton, C. O., Paige, E. G. S.
"A Novel SAW Variable-Frequency Filter", (RRE, Malvern, England). Journees d'Electronique 1975 sur Technologie de Pointe pour le Traitement des Signaux. (1975 Electronic Meeting on Advanced Signal Processing Technology), Lausanne, Switzerland, 14-16 Oct. 1975 (Lausanne, Switzerland: Ecole Polytech. Federale de Lausanne 1975), p. 215-20.

Matthaei, G. L.
"Acoustic Surface-Wave Transversal Filters", (Univ. CA, Santa Barbara, USA). IEEE Trans. Circuit Theory (USA), Vol. CT-20, No. 5, p. 459-70 (Sept. 1973).

Matthaei, G. L., Wong, D. Y., O'Shaughnessy, B. P.
"Synthesis of Two Classes of Acoustic Surface-Wave Filter Tap Weights", (Dept. of Electrical Engng. & Computer Sci., Univ. of California, Santa Barbara, CA, USA). IEEE Trans. Microwave Theory & Techniques (USA), Vol. MTT-24, No. 1, p. 1-9, (Jan. 1976).

Matthaei, G. L., Savage, E. B., Barman, F.
"Synthesis of Acoustic-Surface-Wave-Resonator Filters Using any of Various Coupling Mechanisms", (Electrical Engng. & Computer Sci., Univ. of CA, Santa Barbara, CA, USA). 1977 International Microwave Symposium Digest, San Diego, CA, USA, 21-23 June 1977 (New York, USA: IEEE 1977), p. 328-31.

McCusker, J. H., Perlman, S. S., Veloric, H. S.
"Microsonic Pulse Filters--Replacements for Traditional Butterworth Designs", (RCA Labs., Princeton, NJ, USA). RCA Rev. (USA), Vol. 37, No. 3, p. 389-405 (Sept. 1976).

McIngails, J., Flynn, G. T.
"16-Channel Surface-Acoustic-Wave Grating-Filter Bank for Real-Time Spectral Analyzer", (MIT, Lexington, Mass., USA). Electron. Lett. (GB), Vol. 10, No. 7, p. 107-9 (4 April 1974).

Miller, R. L., DeVries, A. J.
"A Simple 'Building Block' Method for the Design of SAW Filters Having Non-Linear Phase Response", (Zenith Radio Corp., Elk Grove Village, IL, USA). 1976 Ultrasonics Symposium Proceedings, Annapolis, MD, USA, 29 Sept. - 1 Oct. 1976 (New York, USA: IEEE 1976), p. 553-7.

Minowa, J., Nakagawa, K., Yokosuka, E. C. L.
"400 MHz SAW Timing Filter for Optical Fiber Transmission Systems", (Nippon Telegraph and Telephone Public Corp., Yokosuka, Japan. Ultrasonics Symposium Proceedings, Cherry Hill, NJ, USA, 25-27 Sept. 1978, (New York, USA: IEEE 1978), p. 486-489.

Mitchell, R. F.
"Acoustic Surface-Wave Filters", (Mullard Res. Le Redhill, England). Philips Tech. Rev. (Netherlan Vol. 32, No. 6-8, p. 179-89 (1971).

Mitchell, R. F.
"Acoustic Surface Wave Filters", (Mullard Res. Lab., Leatherhead, England). Eurocon-71 Digest, Lausanne, Switzerland, 18-22 Oct. 1971 (New York, USA: IEEE 1971), 2pp.

Mitchell, R. F.
"Surface Acoustic Wave Transversal Filters: Their Use and Limitations", (Mullard Res. Labs., Redhil England). International Specialist Seminar on Component Performance And Systems Applications of Surface Acoustic Wave Devices, Aviemore, Scotland, 25-28 Sept. 1973 (London, England: IEE 1973), p. 130-40.

Mitchell, R. F., Parker, D. W.
"Synthesis of Acoustic-Surface-Wave Filters Using Double Electrodes", (Mullard Res. Labs., Redhill, England). Electron. Lett. (GB), Vol. 10, No. 24, p. 512 (28 Nov. 1974).

Mitchell, R. F., Stevens, R.
"Diffraction Effects in Small-Aperture Acoustic Surface Wave Filters", (Mullard Res. Labs., Redhil England). Wave Electron. (Netherlands), Vol. 1, No. 3, p. 201-18 (Oct. 1975).

Mitchell, R. F.
"Basics of SAW Frequency Filter Design: A Review" (Mullard Res. Labs., Redhill, England). Wave Elec (Netherlands), Vol. 2, No. 1-3, p. 111-32 (July 1976). (European Workshop on Computer Aided Desig of SAW Devices, Bologna, Italy, 7-9 April 1976.)

Moore, P. A., Redwood, M.
"Acoustically Coupled Surface-Wave Resonators 'Filters'", (Dept. of Electrical and Electronic Engng., Queen Mary Coll., Univ. of London, London, England). Electron. Lett. (GB), Vol. 12, No. 18, p. 449-50 (2 Sept. 1976).

Morgan, D. P.
"Surface Acoustic Wave Devices and Applications. I. Introductory Review", (Univ. Edinburgh, Scotlan Ultrasonics (GB), Vol. 11, No. 3, p. 121-31 (May 1973).

Mortley, W. S.
"Wave Propagation in Alpha-Quartz Dispersive Filters", Marconi Rev. (GB), Vol. 34, No. 182, p. 173-206 (1971).

Murphy, P. V.
"Surface Acoustic Wave Devices", J. R. Electr. & Mech. Eng. (GB), No. 25, p. 63-7 (April 1975).

Nagy, J.
"Computational Methods for Acoustic Surface Wave Filters", (Kando Kalman Coll., Electrical Engng., Budapest, Hungary). Proceedings of the 5th Colloquium on Microwave Communication. Vol. III. Electromagnetic Theory, Antennas and Propagation, Budapest, Hungary, 24-30 June 1974 (Budapest, Hungary: Akad. Kiado 1974), p. ET-127/227-35.

Newton, C. O., Paige, E. G. S.
"Surface Acoustic Wave Dispersive Filter with Variable, Linear, Frequency--Time Slope", (Royal Radar Estab., Malvern, England). 1976 Ultrasonics Symposium Proceedings, Annapolis, MD, USA, 29 Sept. - 1 Oct. 1976 (New York, USA: IEEE 1976), p. 424-7.

O'Clock, G. D. Jr., Gandololfo, D. A., Bush, W. J.
"Acoustic Surface-Wave Matched Filters Using a MOSFET Array", (RCA Advanced Technol. Labs., Van Nuys, CA, USA). Proc. IEEE (USA), Vol. 61, No. 8, p. 1165-7 (Aug. 1973).

Otomo, J., Nishiyama, S., Konno, Y.
"UHF Range SAW Filters Using Group-Type Uni-Directional Interdigital Transducers", (Nihon Dempa Kogyo Co. Ltd., Tokyo, Japan). 31st Annual Frequency Control Symposium, Atlantic City, NJ, USA, 1-3 June 1977 (Washington, DC, USA: Electronic Industries Assoc. 1977), p. 275-80.

Otto, O. W., Gerard, H. M.
"Nonsynchronous Scattering Loss in Surface-Acoustic-Wave Reflective-Array-Compression Filters", (Hughes Res. Labs., Malibu, CA, USA). J. Appl. Phys. (USA), Vol. 49, No. 6, p. 3337-40 (June 1978).

Paige, E. G. S.
"Surface Acoustic Wave Devices: Against the Digital Tide", (Royal Radar Estab., Malvern, England). 1972 European Solid State Devices Research Conference (Invited papers and abstracts of contributed papers), Lancaster, England, 12-15 Sept. 1972 (London, England: Inst. Phys. 1973), p. 39-54.

Panasik, C. M., Hunsinger, B. J.
"Precise Impulse Response Measurement of SAW Filters", (Coll. of Engng., Univ. of Illinois, Urbana, IL, USA). IEEE Trans. Sonics & Ultrason. (USA), Vol. SU-23, No. 4, p. 239-49 (July 1976).

Parker, D. W., Pratt, R. G., Smith, F. W., Stevens, R.
"Acoustic Surface Wave Filter", (Mullard Res. Labs., Redhill, England). Funk-Tech. (Germany), Vol. 31, No. 24, p. 811-14 (Dec. 1976). In German.

Potter, B. R., Hartmann, C. S.
"Low Loss Surface-Acoustic Wave Filters", (Texas Instruments Inc., Dallas, TX, USA). IEEE Trans. Parts, Hybrids & Packag. (USA), Vol. PHP-13, No. 4, p. 348-53 (Dec. 1977).

Ragan, L. H.
"Surface Acoustic Wave Resonator Filters", (Texas Instruments Inc., Dallas, TX, USA). 1976 IEEE MTT-S International Microwave Symposium, Cherry Hill, NJ, USA, 14-16 June 1976 (New York, USA: IEEE 1976), p. 286-8.

Redwood, M., Topolevsky, R. B., Mitchell, R. F., Palfreeman, J. S.
"Coupled-Resonator Acoustic-Surface-Wave Filter", (Dept. of Electrical & Electronic Engng., Queen Mary Coll., London, England). Electron. Lett. (GB), Vol. 11, No. 12, p. 253-4 (12 June 1975).

Ronnekliev, A., Skeie, H., Hanebrekke, H.
"Design Problems in Surface Wave Filters", (Univ. Trondheim, Norway). International Specialist Seminar on Component Performance and Systems Applications of Surface Acoustic Wave Devices, Aviemore, Scotland, 25-28 Sept. 1973 (London, England: IEE 1973), p. 141-51.

Rosner, B., Puspoki, S., Andrasi, A.
"Examination of Structures of Acoustic Surface Wave Filters", Hiradastechnika (Hungary), Vol. 25, No. 11, p. 333-7 (Nov. 1974). In Hungarian.

Sabine, H., Cole, P. H.
"Acoustic Surface Wave Devices: A Survey", (Univ. Adelaide, Australia). Proc. Inst. Radio Electron. Eng. Aust. (Australia), Vol. 32, No. 12, p. 445-58 (Dec. 1971).

Sandy, F., Parker, T. E.
"Surface Acoustic Wave Ring Filter", (Raytheon Res. Div., Waltham, MA, USA). 1976 Ultrasonics Symposium Proceedings, Annapolis, MD, USA, 29 Sept. - 1 Oct. 1976 (New York, USA: IEEE 1976), p. 391-6.

Sato, H., Yamanouchi, K., Shibayama, K., Nishiyama, S.
"On the Design of Elastic Surface Wave Filters with No Tuning Coil", (Tohoku Univ., Sendai, Japan). Proceedings of the 28th Annual Frequency Control Symposium 1974, Atlantic City, NJ, USA, 29-31 May 1974 (Washington, DC, USA: Electronic Industries Assoc. 1974), p. 286-98.

Schoenwald, J. S.
"Ultra-Low-Shape Factor SAW Filters Using Asymmetrically Truncated Transducers", Science Center, Rockwell International, PO Box 1085, Thousand Oaks, CA, USA.

Seifert, F., Reichard, H.
"Reduction of Bulk Waves in Surface Acoustic Wave (SAW) Filters", (Inst. fur Phys. Elektronik, Tech. Univ., Wien, Austria). Arch. Elektron & Uebertragungstech. (Germany), Vol. 32, No. 5-6, p. 206-8 (May-June 1978). In German.

Shimizu, Y., Sakaue, T.
"A Simple Technique of Fine Tuning of Surface-Acoustic Wave Filters", (Cradle, Tokyo Inst. of Technol., Tokyo, Japan). Trans. Inst. Electron. & Commun. Eng. Jpn. Sect. E (Japan), Vol. E-60, No. 2, p. 92 (Feb. 1977).

Shoquist, T. L., Stigall, R. E., Hays, R. M.
"Surface Acoustic Wave Components: Products and Applications", (Texas Instruments Inc., Dallas, TX, USA). EASCON-77, Arlington, VA, USA, 26-28 Sept. 1977 (New York, USA: IEEE 1977), 18-5A/1pp.

Sinista, V. N., Basov, V. G., Sprin, V. A., Chirkin, N. M., Kotova, I. F.
"An Acoustic Surface-Wave Non-Dispersive Filter",
Izv. VUZ Radioelektron. (USSR), Vol. 18, No. 1, p. 98-9 (Jan. 1975). In Russian.

Skudera, W. J. Jr., Gerard, H. M.
"Some Practical Design Considerations of Dispersive Surface Wave Filters", (US Army Electronics Technol. & Devices Lab., Fort Monmouth, NJ, USA). Proceedings of the 27th Annual Frequency Control Symposium, Cherry Hill, NJ, USA, 12-14 June 1973 (Washington, DC, USA: Electronic Industries Assoc. 1973), p. 253-61.

Skudera, W. J. Jr.
"The Versatility of the 'In-Line' SAW Chirp Filter", (US Army Electronics Technol. & Devices Lab., Fort Monmouth, NJ, USA). 31st Annual Frequency Control Symposium, Atlantic City, NJ, USA, 1-3 June 1977 (Washington, DC, USA: Electronic Industries Assoc. 1977), p. 285-90.

Slobodnik, A. J. Jr., Laker, K. R.
"Improved Frequency and Time Domain Response-Surface Acoustic Wave Filters for Pulse Applications", (Air Force Cambrdige Res. Labs., Hanscom AFB, Bedford, MA, USA), 1975 IEEE International Symposium on Circuits and Systems, Newton, Mass., USA, 21-23 April 1975 (New York, USA: IEEE 1975), p. 143-6.

Slobodnik, A. J. Jr.
"Surface Acoustic Wave Filters at UHF: Design and Analysis", Report AFCRL-TR-75-0311 (AD-A017 106/6GA), Air Force Cambridge Res. Labs., Hanscom AFB, Mass., USA (3 June 1975), 672 pp. Available from NTIS, Springfield, VA, 22161, USA.

Slobodnik, A. J. Jr., Laker, K. R.
"Periodic Frequency Response SAW Filters for a Tree Approach to Many-Tone Frequency Synthesis", (Deputy for Electronic Technol., Hanscom AFB, MA, USA). 1976 IEEE MTT-S International Microwave Symposium, Cherry Hill, NJ, USA, 14-16 June 1976 (New York, USA: IEEE 1976), p. 300-2

Slobodnik, A. J. Jr., Budreau, A. J. Jr., Kearns, W. J., Szabo, T. L., Roberts, G. A.
"SAW Filters for Frequency Synthesis Applications", (Hanscom AFB, MA, USA). 1976 Ultrasonics Symposium Proceedings, Annapolis, MD, USA, 29 Sept. - 1 Oct. 1976 (New York, USA: IEEE 1976), p. 432-5.

Slobodnik, A. J. Jr., Roberts, G. A., Silva, J. H., Kearns, W. J., Sethares, J. C., Szabo, T. L.
"UHF Switchable SAW Filterbanks", (Rome Air Development Center, Deputy for Electronic Tech. Hanscom AFB, MA, USA). Ultrasonics Symposium Proceedings, Cherry Hill, NJ, USA, 25-27 Sept. 1978 (New York, USA: IEEE 1978), p. 486-489.

Speiser, J. M., Whitehouse, H. J.
"Surface Wave Transducer Array Design Using Transversal Filter Concepts", (Naval Undersea Res. & Dev. Center, San Diego, CA, USA). In book: Acoustic Surface Wave and Acousto-Optic Devices, T. Kallord (Ed.), p. 81-90. New York, USA: Optosonic Press (1971), vii-221pp.

Staples, E. J., Clairborne, L. T.
"A Review of Device Technology for Programmable Surface-Wave Filters", (Texas Instruments Inc., Dallas, TX, USA). IEEE Trans. Microwave Theory & Tech. (USA), Vol. MTT-21, No. 4, p. 279-87 (April 1973).

Stevens, M. R., Parker, D. W., Penna, D. E., Pratt, R. G.
"Acoustic Surface Wave Filters", (Mullard Res. Labs., Redhill, England). Colloque International sur les Materiaux pour les Composants Electroniques (International Symposium on Materials for Electronic Components), Paris, France, 2-4 April 1975 (Paris, France: Comm. d'Organisation du Colloque de Paris, 1975), p. 291.

Sugiyama, K., Yoshikawa, S.
"Design of Acoustic Surface Wave Filters Using Phase Coded Transducers", (Musashino Electrical Communication Lab., NTT, Musashino, Japan). Trans. Inst. Electron. & Commun. Eng. Jpn. Sect. E (Japan), Vol. E-60, No. 3, p. 142-3 (March 1977).

Sugiyama, K., Yoshikawa, S.
"Design of Acoustic Surface Wave Filter Using Multielectrode Pair", (Nippon Telegraph & Telephone Public Corp., Tokyo, Japan). Electr. Commun. Lab. Tech. J. (Japan), Vol. 26, No. 6, p. 1755-80 (1977). In Japanese.

Suzuki, Y., Shimizu, H., Takeuchi, M., Nakamura, K., Yamada, A.
"Some Studies on SAW Resonators and Multiple-Mode Filters", (Faculty of Engng., Tohoku Univ., Sendai, Japan). 1976 Ultrasonics Symposium Proceedings, Annapolis, MD, USA, 29 Sept. - 1 Oct. 1976 (New York, USA: IEEE 1976), p. 297-302.

Szabo, T. L., Slobodnik, A. J. Jr.
"Diffraction Compensation in Periodic Apodized Acoustic Surface Wave Filters", (AFSC, Laurence G. Hanscom Field, Bedford, MA, USA). IEEE Trans. Sonics & Ultrason. (USA), Vol. SU-21, No. 2, p. 114-19 (April 1974).

Takahashi, S., Kodma, T.
"SAW Filter TTE Source and Load Impedance Dependence Estimation", (Toshiba Res. & Dev. Center, Kawasaki, Japan). Trans. Inst. Electron. & Commun. Eng. Jpn. Sect. E (Japan), Vol. E-60, No. 3, p. 141-2 (March 1977).

Takahashi, S., Hirano, H., Kodama, T., Miyashiro, F., Suzuki, B., Onoe, A., Adachi, T., Fujinuma, K.
"SAW IF Filter on $LiTaO_3$ for Color TV Receivers", (Toshiba R&D Center, Saiwai-Ku, Kawasaki, Japan). IEEE Trans. Consum. Electron. (USA), Vol. CE-24, No. 3, p. 337-48 (Aug. 1978). (1978 IEEE Chicago Spring Conference, Arlington Heights, IL, USA, 5-6 June 1978).

Tancrell, R. H., Holland, M. G.
"Acoustic Surface Wave Filters", (Raytheon Res. Div., Waltham, MA, USA). Proceedings of the 1970 Ultrasonics Symposium, San Francisco, CA, USA, 21-23 Oct. 1970 (New York, USA: IEEE 1971), p. 48-64.

Tancrell, R. H., Holland, M. G.
"Acoustic Surface Wave Filters", (Raytheon Res. Div., Waltham, Mass, USA). Proc. IEEE (USA), Vol. 59, No. 3, p. 393-409 (March 1971).

Tancrell, R. H.
"Improvement of an Acoustic-Surface-Wave Filter with a Multistrip Coupler", (Raytheon Res. Div., Waltham, Mass, USA). Electron. Lett. (GB), Vol. 9, No. 14, p. 316-17 (12 July 1973).

Terstegge, H.
"Acoustical Surface Waves Used in a Novel Filter Unit", (AEG Telefunken, Heilbronn, Germany). Int. Elektron. Rundsch. (Germany), Vol. 24, No. 11, p. 279-82 (Nov. 1970). In German.

Theodossiou, L.
"Surface Acoustic Wave Filters", Television (GB), Vol. 26, No. 12, p. 645-9 (Oct. 1976).

Tiemann, J. J., Young, J. D.
"Acoustic Surface Wave Filter Using Chirp Transform for NDT", (General Electric Corp., Res. & Dev. Center, Schenectady, NY, USA). 1976 Ultrasonics Symposium Proceedings, Annapolis, MD, USA, 29 Sept. - 1 Oct. 1976 (New York, USA: IEEE 1976), p. 382-5.

Tiersten, H. F.
"Guided Acoustic-Surface-Wave Filters", (Dept. of Mech. Engng., Aeronaut. Engng. & Mech., Rensselaer Polytech. Inst., Troy, NY, USA). Appl. Phys. Lett. (USA), Vol. 28, No. 3, p. 111-13 (1 Feb. 1976).

Trankle, E.
"The Surface-Wave Effect and its Application in Filters and Ultrasonic Delay Lines", Nachrichtech. Z. (NTZ) (Germany), Vol. 23, No. 9, p. 436-9 (Sept. 1970). In German.

Umkauf, M. G., Schulz, M. B., Gadoury, J. B. II.
"A Programmable Surface Wave Ultrasonic Matched Filter", Report RADC-TR-74-260, Raytheon Co., Norwood, Mass., USA (Oct. 1974), 120pp., Contract F30602-72-C-0095. Available from NTIS, Springfield, VA, USA.

Vasile, C. F., Larosa, R.
"1000 Bit Surface-Wave Matched Filter", (Hazeltine Corp., Greenlawn, NY, USA). Electron Lett. (GB), Vol. 8, No. 19, p. 479-80 (21 Sept. 1972).

Vasile, C. F.
"Two-Port Description of an SAW Filter", (Sci. Center, Rockwell Internat. Thousand Oaks, CA, USA). Electron. Lett. (GB), Vol. 13, No. 11, p. 326-8 (26 May 1977).

Van de Vaart, H., Solie, L. P.
"A SAW Pulse Compression Filter Using the Reflective Dot Array", (Sperry Res. Center, Sudbury, MA, USA). 1977 International Microwave Symposium Digest, San Diego, CA, USA, 21-23 June 1977 (New York, USA: IEEE 1977), p. 321-3.

Watatsuki, N., Namikota, T.
"Suppression of Bulk Wave in SAW Filter by Metal Over-Lay Design", (Fujitsu Ltd., Kawasaki, Japan). 1976 Ultrasonics Symposium Proceedings, Annapolis, MD, USA, 29 Sept. - 1 Oct. 1976 (New York, USA: IEEE 1976), p. 332-5.

Waldner, M., Pedinoff, M. E., Gerard, H. M.
"Broadband Surface Wave Nonlinear Convolution Filters", (Hughes Aircraft Co., Los Angeles, CA, USA). IEEE Trans. Sonics & Ultrasonics (USA) Vol. SU-19, No. 3, p. 399 (July 1972). (1971 IEEE Ultrasonics Symposium, Miami Beach, FL, USA, 6-8 Dec. 1971.

Walther, F. G., Budreau, A. J., Carr, P. H.
"Multiple UHF Frequency Generation Using Acoustic Surface-Wave Filters", (Air Force Cambridge Res. Labs., Laurence G. Hanscom Field, Bedford, Mass., USA). Proc. IEEE (USA), Vol. 61, No. 8, p. 1162-3 (Aug. 1973).

Weglein, R. D.
"The Characteristics of Acoustic Surface Wave Grating Filters", (Hughes Res. Labs., Malibu, CA, USA). 1973 European Microwave Conference, Vol. II, Brussels, Belgium, 4-7 Sept. 1973 (Ghent, Brussels: Univ. Ghent 1973), C8.4/4pp.

Weglein, R. D., Otto, O. W.
"Characteristics of Periodic Acoustic-Surface-Wave Grating Filters", (Hughes Res. Labs., Malibu, CA, USA). Electron. Lett. (GB), Vol. 10, No. 6, p. 68-9 (21 March 1974).

Weglein, R. D.
"SAW Chirp Filter Performance Above 1 GHz", (Electron Device Phys. Dept., Hughes Res. Labs., Malibu, CA, USA). Proc. IEEE (USA), Vol. 64, No. 5, p. 695-8 (May 1976).

Weinert, R. W., Isaacs, T. J., Aalgas, F., Godfrey, J. T., Morre, R. A.
"Performance of SAW Filters on Sulfosalt-Type Substrates", (Westinghouse Res. Labs., Pittsburgh, PA, USA). 1976 Ultrasonics Symposium Proceedings, Annapolis, MD, USA, 29 Sept. - 1 Oct. 1976 (New York, USA: IEEE 1976), p. 532-5.

Yakovkin, I., Kohler, E.
"Components Based on Elastic Surface Waves", (Inst. for Halbleterphys., Akad. der Wissenschaften, Ukrainian SSR). Nachrichtentech. Elektron. (Germany), Vol. 25, No. 5, p. 186-9 (1975). In German.

Yamaguchi, M., Kogo, H.
"Design of Surface-Acoustic-Wave Filters by Taking Account of Electrical Terminations and Matching Circuits", (Faculty of Engng., Chiba Univ., Chiba-shi, Japan). Electron. Lett. (GB), Vol. 12, No. 8, p. 181-2 (15 April 1976).

Yamaguchi, M., Temma, T., Takato, K., Kogo, H.
"Frequency Response of a Surface-Acoustic-Wave Filter Using a Waveguide", (Faculty of Engng., Chiba Univ., Chiba-shi, Japan). Electron. Lett. (GB), Vol. 13, No. 7, p. 204-5 (31 March 1977).

Yamanouchi, K., Nyffeler, F. M., Shibayama, K.
"Low Insertion Loss Acoustic Surface Wave Filter Using Group-Type Unidirectional Interdigital Transducers", (Res. Inst. of Electrical Communication, Tohoku Univ., Sendai, Japan). J. Acoust. Soc. Jpn. (Japan), Vol. 33, No. 10, p. 532-9 (Oct. 1977). In Japanese.

Yamaguchi, M., Kogo, H.
"Design of Surface-Acoustic-Wave Television i.f. Filters by Use of Constrained Damped Least Squares", (Faculty of Engng., Chiba Univ., Chiba-shi, Japan). IEE J. Microwave Opt. & Acoust. (GB), Vol. 2, No. 2, p. 60-4 (March 1978).

Zucker, J., Ganguly, A. K.
"Frequency Response of Acoustic Surface Wave Filters. II.", (GTE Labs. Inc., Waltham, Mass., USA). J. Appl. Phys. (USA), Vol. 44, No. 3, p. 1086-8 (March 1973).

1.5.2.1

Arranz, T.
"Lithium Tantalate Channel Filters for Multiplex Telephony", (Compaignie d'Electronique et de Piezoelectricite, Sartrouville, France). 31st Annual Frequency Control Symposium, Atlantic City, NJ, USA, 1-3 June 1977 (Washington, DC, USA: Electronic Industries Assoc. 1977). p. 213-24.

Artzeni, C., Masotti, L.
"Weighted Interdigital Transducers for Smoothing of Ripples in Acoustic-Surfacewave Bandpass Filters", (CNR, Firenze, Italy). Electron. Lett. (GB), Vol. 8, No. 19, p. 485-6 (21 Sept. 1972).

Atzeni, C., Masotti, L.
"Band-Pass Filtering by Acoustic Planar Processing Techniques", (Consiglio Nazionale delle Ricerche, Firenze, Italy). Alta Freq. (Italy), Vol. 42, No. 2, p. 84-92 (Feb. 1973). In English.

Borner, M., Kohlbacher, G.
"Surface Acoustic Wave (SAW) Devices with Coupled Resonators", Wiss. Ber. AEG-Telefunken (Germany), Vol. 48, No. 2-3, p. 79-82 (1975). In German.

Bristol, T. W., Meyer, W. E.
"Surface Acoustic Wave UHF Frequency Filters", (North American Rockwell Corp., Anaheim, CA, USA). IEEE Trans. Sonics & Ultrasonics (USA), Vol. SU-19, No. 3, p. 400-1 (July 1972). (1971 IEEE Ultrasonics Symposium, Miami Beach, FL, USA, 6-8 Dec. 1971).

Broux, G., Claes, R., Deleers, J. J.
"Surface-Wave Filters for TV Receiver IF Stages I. Acoustic Surface-Wave Technology", (Radio Mentor Electron. (Germany), Vol. 44, No. 5, p. 189-92 (May 1978). In German.)

Burgess, J. W., Hales, M. C., Airger, F. W.
"Single-Mode Resonance in $LiNbO_3$ for Filter Design", (Plessey Co., Caswell, Towcester, England). Electron. Lett. (GB), Vol. 9, No. 11, p. 251-2 (31 May 1973).

Chauvin, D., Coussot, G., Dieulesaint, E.
"Acoustic Surface-Wave Television Filters", (Thomson-CSF, Orsay, France). Electron. Lett. (GB), Vol. 7, No. 17, p. 491-2 (26 Aug. 1971).

Claiborne, L. T.
"Surface Wave Bandpass Filters: Components and Subsystems", (Texas Instruments Inc., Dallas, TX, USA). Proceedings of the Symposium on Optical and Acoustical Microelectronics, New York, USA, 16-18 April 1974 (Brooklyn, NY, USA: Polytech. Press 1975), p. 461-9

Claiborne, L. T., Hartmann, C. S., Hays, R. M., Rosenfeld, R. C.
"UHF/VHF Bandpass Filters Using SAW Device Technology", (Texas Instruments Inc., Dallas, TX, USA). Microwave J. (USA), Vol. 17, No. 5, p. 35-8, 40 (May 1974).

Coldren, L. A., Rosenberg, R. L.
"Multipole SAW Resonator Filters", (Bell Telephone Labs., Holmdel, NJ, USA). Proceedings of the 1978 IEEE International Symposium on Circuits and Systems, New York, USA, 17-19 May 1978 (New York, USA: IEEE 1978), p. 548-52.

Craven, G., Lush, D. M.
"Surface-Acoustic-Wave Rejection Filters Using Mode Conversion/Reconversion", (Stand. Telecommunication Labs. Ltd., Harlow, England). Electron. Lett. (GB), Vol. 10, No. 11, p. 218-19 (30 May 1974).

Coussot, G., Menager, O.
"Experimental Investigation of Mass-Producible Acoustic Surface Wave Filter", (Thomson-CSF Labs., Domaine de Corbeville, Orsay, France). Proceedings of the 29th Annual Frequency Control Symposium, Fort Monmouth, NJ, USA, 28-30 May 1975 (Washington, DC, USA: Electronic Industries Assoc. 1975), p. 181-6.

Coussot, G., Van Den Driessche, M.
"Design of a TV Receiver's Intermediate Frequency Stage Employing a Surface Wave Filter", Rev. Tech. Thomson-CSF (France), Vol. 8, No. 3, p. 585-605 (Sept. 1976). In French.

Cross, P. S., Schmidt, R. V., Haus, H. A.
"Acoustically Cascaded ASW Resonator-Filters", (Bell Telephone Labs., Holmdel, NJ, USA), 1976 Ultrasonics Symposium Proceedings, Annapolis, MD, USA, 29 Sept. - 1 Oct. 1976 (New York, USA: IEEE 1976), p. 277-80.

Devries, A. J., Adler, R.
"Case History of a Surface Wave TV IF Filter for Color Television Receivers", (Zenith Radio Corp., Chicago, IL, USA). Proc. IEEE (USA), Vol. 64, No. 5, p. 671-6 (May 1976).

Fujishima, S., Ishiyama, H., Inoue, A., Ieki, H.
"Surface Acoustic Wave VIF Filters for TV Using ZnO Sputtered Film", Proceedings of the 30th Annual Symposium on Frequency Control, Atlantic City, NJ, USA, 2-4 June 1976 (Washington DC, USA: Electronic Industries Assoc. 1976), p. 119-22.

Gerard, H. M., Judd, G. W.
"500 MHz Bandwidth RAC Filter with Constant Groove Depth", (Hughes Aircraft Co., Fullerton, CA, USA). Ultrasonics Symposium Proceedings, Cherry Hill, NJ, USA, 25-27 Sept. 1978 (New York, USA: IEEE 1978), p. 734-738.

Grice, D. C., Pi, S. C., Wilk, J. M.
"Acoustic Surface Wave Filter for TV Tuning Circuits", (IBM, Armonk, NY, USA). IBM Tech. Disclosure Bull. (USA), Vol. 19, No. 3, p. 971-4 (Aug. 1976).

Hartemann, P.
"Narrow-Bandwidth Rayleigh-Wave Filters", (Thompson CSF, Orsay, France). Electron. Lett. (GB), Vol. 7, No. 22, p. 674-5 (4 Nov. 1971).

Hartemann, P.
"Narrowbandwidth Rayleigh Wave Filters", (Thomson CSF, Domaine de Corbeville, Orsay, France). IEEE Trans. Sonics & Ultrasonics (USA), Vol. SU-19, No. 3, p. 401 (July 1972). (1971 IEEE Ultrasonics Symposium, Miami Beach, FL, USA, 6-8 Dec. 1971).

Hartmann, C. S., Vollers, H. G., Cheek, T. F.
"VHF/UHF Bandpass Filters Using Interdigital Surface Wave Transducers", (Texas Inst. Inc., Dallas, TX, USA). IEEE Trans. Sonics & Ultrasonics (USA), Vol. SU-19, No. 3, p. 400 (July 1972). (1971 IEEE Ultrasonics Symposium, Miami Beach, FL, USA, 6-8 Dec. 1971).

Hartman, C. S., Bell, D. T. Jr., Rosenfeld, R. C.
"Impulse Model Design of Acoustic Surface-Wave Filters", (Texas Instruments, Inc., Dallas, TX, USA). IEEE Trans. Microwave Theory & Tech. (USA), Vol. MTT-21, No. 4, p. 162-75 (April 1973).

Hays, R. M., Rosenfeld, R. C., Hartmann, C. S.
"One Hundred Channel Selectable Surface Wave Bandpass Filter", (Texas Instruments Inc., Dallas, TX, USA). Microwave Symposium Digest of Technical Papers, Atlanta, GA, USA, 12-14 June 1974 (New York, USA: IEEE 1974), p. 236.

Hickernell, F. S., Kline, A. J., Allen, D. E., Brown, W. C.
"Surface Elastic Wave Bandpass Filters for Frequency Synthesis", (Motorola Government Electronics Div., Scottsdale, AZ, USA). IEEE Trans. Microwave Theory & Tech. (USA), Vol. MTT-21, No. 4, p. 300-2 (April 1973).

Hohkawa, K., Yoshikawa, S.
"Design of Surface Acoustic Wave Filters Using Linear Programming Techniques", (Nippon Telegraph & Telephone Public Corp., Tokyo, Japan). Elect. Commun. Lab. Tech. J. (Japan), Vol. 26, No. 10, p. 2875-88 (1977).

Jordan, P. M., Lewis, B.
"A Tolerance-Related Optimized Synthesis Scheme for the Design of SAW Bandpass Filters with Arbitrary Amplitude and Phase Characteristics", (Plessey Research, Caswell Limited, Caswell, Towcester, Northamptonshire, England). Ultrasonics Symposium Proceedings, Cherry Hill, NJ, USA, 25-27 Sept. 1978 (New York, USA: IEEE 1978), p. 715-719

Kaverina, G. M., Kleshnev, Yu. A., Nikitin, V. I., Sirotin, G. F., Ul'yanov, G. K.
"Ultrasonic Surface-Wave Piezoelectric Filters for Television Receivers", Telecommun. & Radio Eng., Pt. 2 (USA), Vol. 29, No. 4, p. 121-2 (April 1974). Translation of: Radiotekhnika, Moskva (USSR), Vol. 29, No. 4, p. 90-1 (April, 1974).

Komatsu, Y., Yanagisawa, Y.
"A Surface Acoustic Wave Filter for Colour TV Receiver VIF", (Sony Corp. Res. Center, Yokohama, Japan). IEEE Trans. Electron Devices (USA), Vol. ED-24, No. 3, p. 230-3 (March 1977).

Koyamada, Y., Ishihara, F., Yoshikawa, S.
"Band-Elimination Filter Employing Surface-Acoustic-Wave Resonators", (Nippon Telegraph & Telephone Public Corp., Tokyo, Japan). Electron. Lett. (GB), Vol. 11, No. 5, p. 108-9 (6 March 1975).

Koyamada, Y., Ishihara, F., Yoshikawa, S.
"Narrow-Band Filters Employing Surface-Acoustic-Wave Resonators", (Electrical Communication Labs., Nippon Telegraph & Telephone Public Corp., Musashino, Tokyo, Japan). Proc. IEEE (USA), Vol. 64, No. 5, p. 685-7 (May 1976).

Kuwano, Y.
"Applications of Surface Acoustic Wave Filter to TV Receiver", (Res. Center, Sanyo Electric Co. Ltd., Osaka, Japan). J. Inst. Telev. Eng. Jpn. (Japan), Vol. 31, No. 11, p. 845-52 (Nov .1977). In Japanese.

Lagasse, P. E., Vandewege, J., Naten, T.
"Distributed Feedback Acoustic Surface Wave Resonators for Use in Large Bandwidth Filters", (Univ. of Ghent, Ghent, Belgium). Ultrasonics Symposium Proceedings, Cherry Hill, NJ, USA, 25-27 Sept. 1978 (New York, USA: IEEE 1978), p. 438-441.

Laker, K. R., Cohen, E., Szabo, T. L., Pustaver, J. A.
"Computer-Aided Design of Withdrawal Weighted SAW Bandpass Transversal Filters", (RADC/AFSC, Hanscom AFB, MA, USA). 1977 IEEE International Symposium on Circuits and Systems Proceedings, Phoenix, AZ, USA, 25-27 Apr. 1975 (New York, USA: 1977), p. 126-30.

Laker, K. R., Cohen, E., Szabo, T. L., Pustaver, J. A. Jr.
"Computer-Aided Design of Withdrawal-Weighted SAW Bandpass Filters", (Electromagnetic Sci. Div., Hanscom Air Force Base, Bedford, MA, USA). IEEE Trans. Circuits & Syst. (USA), Vol. CAS-25, No. 5, p. 241-51 (May 1978).

Lever, K. V.
"An Appraisal of Bandpass Filter Techniques", (GEC Ltd., Hirst Res. Centre, Wembley, England). International Specialist Seminar on the Impact of new Technologies in Signal Processing, Aviemore, Scotland, 20-24 Sept. 1976 (London, England: IEE 1976), p. 72-7.

Malocha, D. C., Wilkus, S.
"Low Loss Capacitively Weighted TV IF Filter", (Texas Instruments Inc. Dallas, TX, USA). Ultrasonics Symposium Proceedings, Cherry Hill, NJ, USA, 25-27 Sept. 1978 (New York, USA: IEEE 1978), p. 500-503.

Matthaei, G. L., Savage, E. B., Barman, F.
"Synthesis of Acoustic-Surface-Wave-Resonator Filters Using any of Various Coupling Mechanisms", (Dept. of Electrical Engng., Univ. of California, Santa Barbara, CA, USA). IEEE Trans. Sonics & Ultrason. (USA), Vol. SU-25, No. 2, p. 72-84 (March 1978).

Matthaei, G. L., Savage, E. B., Barman, F.
"Synthesis of Surface-Acoustic-Wave-Resonator Band-Pass Filters Using the 'Direct-Coupled-Filter' Point of View", (Dept. of Electrical Engng. & Computer Sci., Univ. of California, Santa Barbara, CA, USA). Proceedings of the 1978 IEEE International Symposium on Circuits and Systems, New York, USA, 17-19 May 1978 (New York, USA: IEEE 1978), p. 541-7.

Minowa, J., Tanaka, K.
"Surface Acoustic Wave Filters with Narrow Pass Band", Electr. Commun. Lab. Tech. J. (Japan), Vol. 27, No. 2, p. 419-28 (1978). In Japanese.

Minowa, J., Morikawa, T., Abe, H.
"Stability for Surface Acoustic Wave Filters with Narrow Passband", Electr. Commun. Lab. Tech. J. (Japan), Vol. 27, No. 2, p. 429-40 (1978). In Japanese.

Mitchell, R. F.
"Surface Acoustic Wave Devices and Applications IV. Bandpass Filters", (Mullard Res. Labs., Redhill, England). Ultrasonics (GB), Vol. 12, No. 1, p. 29-35 (Jan. 1974).

Murakami, T.
"New Color TV Receiver with SAW IF Filter", (Hitachi Consumer Products Res. Center, Lyndhurst, NJ, USA). IEEE Trans. Consum. Electron. (USA), Vol. CE-24, No. 1, p. 89-95 (Feb. 1978).

Murray, R. J., Read, E.
"Surface-Acoustic-Wave Transversal Bandpass Filters", (Central Res. Labs., Hirst Res. Centre, Wembley, England). GEC J. Sci. & Technol. (GB), Vol. 44, No. 1, p. 3-12 (1977).

Murray, R. J., Neylon, S.
"The Design, Fabrication and Performance Limitations of Narrow-Band Fast Cut-Off Surface Wave Filters", (GEC Hirst Research Centre, Wembley, England). Ultrasonics Symposium Proceedings, Cherry Hill, NJ, USA, 25-27 Sept. 1978 (New York, USA: IEEE 1978), p. 482-485.

Parker, D. W.
"Acoustic Surface Wave Bandpass Filters", (Mullard Res. Labs., Redhill, England). Proceedings of the 1976 IEEE International Symposium on Circuits and Systems, Munich, Germany, 27-29 April 1976 (New York, USA: IEEE 1976), p. 689-92.

Parker, D. W., Pratt, R. G., Stevens, R.
"A Television IF Acoustic-Surface-Wave Filter on Bismuth Silicon Oxide", (Mullard Res. Labs., Redhill, England). Proc. IEEE (USA), Vol. 64, No. 5, p. 677-81 (May 1976).

Parker, D. W., Pratt, R. G., Smith, F. W., Stevens, R.
"Acoustic Surface-Wave Bandpass Filters", (Mullard Res. Lab., Redhill, England). Philips Tech. Rev. (Netherlands), Vol. 36, No. 2, p. 29-43 (1976).

Parker, D. W., Pratt, R. G., Smith, F. W., Stevens, R.
"Acoustic Surface-Wave Bandpass Filters", (Mullard Res. Labs., Reigate, England). Mullard Tech. Commun. (GB), Vol. 14, No. 133, p. 110-24 (Jan. 1977).

Parker, D. W., Pratt, R. G., Smith, F. W., Stevens, R.
"Filters Based on Acoustic Surface Waves. III.", (Mullard Res. Lab., Redhill, England). Funk.-Tech. (Germany), Vol. 32, No. 1, p. F&E 4-7 (Jan. 1977). In German.

Parker, D. W.
"Acoustic Surface Wave Bandpass Filters", (Mullard Res. Labs., Redhill, England). Electron. & Power (GB), Vol. 23, No. 5, p. 389-92 (May 1977).

Parker, D. W., Pratt, R. G., Smith, F. W., Stevens, R.
"Acoustic Surface-Wave Bandpass Filters", (Philips Res. Labs., Redhill, England). Electron. Appl. Bull. (Netherlands), Vol. 35, No. 1, p. 24-39 (Nov. 1977).

Peach, R. C., Dix, C.
"A Low Loss Medium Bandwidth Filter on Lithium Niobate", (Hirst Research Centre, Wembley, England). Ultrasonics Symposium Proceedings, Cherry Hill, NJ, USA, 25-27 Sept. 1978 (New York, USA: IEEE 1978), p. 509-512.

Piwonski, W.
"Surface Wave Piezoelectric Filters", Wiad. Telekommun. (Poland), Vol. 15, No. 12, p. 7-11 (Dec. 1975). In Polish.

Plass, K. G.
"Acoustic Surface Wave Band-Stop Filter for UHF Frequencies", (Philips Forschungslab. Hamburg, GmbH, Germany). 1973 European Microwave Conf., Vol. II, Brussels, Belgium, 4-7 Sept. 1973 (Ghent, Brussels: Univ. Ghent 1973), C8.3/3pp.

Puspoki, S., Rosner, B., Andrasi, M.
"Surface Acoustic Wave Bandpass Filters with Asymmetric Frequency Response", (Res. Inst. for Technical Phys., Hungarian Acad. of Sci., Budapest, Hungary). Alta Freq. (Italy), Vol. 45, No. 12, p. 766-8 (Dec. 1976).

Reilly, J. P., Campbell, C. K., Suthers, M. S.
"The Design of SAW Bandpass Filters Exhibiting Arbitrary Phase and Amplitude Response Characteristics", (Dept. of Electrical Engng., McMaster Univ., Hamilton, Canada). IEEE Trans. Sonics & Ultrason. (USA), Vol. SU-24, No. 5, p. 301-5 (Sept. 1977).

Rosenfeld, R. C., Hartmann, C. S., Brown, R. B.
"Low-Loss Unidirectional Acoustic Surface Wave Filters", (Texas Instruments Inc., Dallas, TX, USA). Proceedings of the 28th Annual Frequency Control Symposium 1974, Atlantic City, NJ, USA, 29-31 May 1974 (Washington, DC, USA: Electronic Industries Assoc. 1974). p. 299-303.

Rosenfeld, R. C., Hartmann, C. S.
"Subminiature Broadband Filters", Report TI-08-74-59 ECOM 72-0326-F, Texas Instruments Inc., Dallas, TX, USA (Oct. 1974), 62pp., Contract DAAB07-72-C-0326. Available from NTIS, Springfield, VA, USA.

Rypkema, J., DeVries, A., Banach, F.
"Engineering Aspects of the Application of Surface Wave Filters in Television IF's", (Zenith Radio Corp., Chicago, IL, USA). IEEE Trans. Consum. Electron. (USA), Vol. CE-21, No. 2, p. 105-14 (May 1975).

Sandy, F., Parker, T. E.
"Surface Acoustic Wave Ring Filter", (Raytheon Res. Div., Waltham, MA, USA). Proceedings of the 30th Annual Symposium on Frequency Control, Atlantic City, NJ, USA, 2-4 June 1976 (Washington, DC, USA: Electronic Industries Assoc. 1976), p. 334-9.

Sardaryan, V. S., Tatikyan, L. M.
"The Synthesis of Narrow-Band Acoustic Surface Wave Filter", Izv. Akad. Nauk Arm. SSR Fiz. (USSR), Vol. 10, No. 5, p. 397-402 (1975). In Russian.

Sato, H., Meguro, T., Yamanouchi, K., Shibayama, K.
"Piezoelectric Thin Film Unidirectional SAW Transducer and Filter", (Dept. of Electrical Communication, Tohoku Univ., Sendai, Japan). Proc. IEEE (USA), Vol. 66, No. 1, p. 102-4 (Jan. 1978).

Scheibner, J.
"Quartz Resonators and Piezoceramic Vibrators in Bandpass and Bandstop Filters for Data Technology. II.", Wiss. Z. Elektrotech. (Germany), Vol. 13, No. 4, p. 181-92 (1969). In German.

Schmidt, R. V.
"Cascaded SAW Gratings as Passband Filters", (Bell Labs., Holmdel, NJ, USA). Electron. Lett. (GB), Vol. 13, No. 15, p. 445-6 (21 July 1977).

Seiler, D. G., Campbell, C. K., Suthers, M. S.
"A Technique for Measuring and Matching the Input Impedance of a Narrow-Band Surface Acoustic Wave Filter", (Electrical Engng. Dept. McMaster Univ., Hamilton, Ontario, Canada). IEEE Trans. Instrum. & Meas. (USA), Vol. IM-26, No. 2, p. 188-9 (June 1977).

Shiosaki, T., Ieki, E., Kawabata, A.
"58-MHz Surface-Acoustic Wave Video Intermediate-Frequency Filter Using ZnO-Sputtered Film", (Dept. of Electronics, Kyoto Univ., Kyoto, Japan). Appl. Phys. Lett. (USA), Vol. 28, No. 9, p. 475-6 (1 May 1976).

Shiosaki, T., Kawahota, A.
"58 MHz Surface-Acoustic Wave TV-Intermediate-Frequency Filter Using ZnO-Sputtered Film", (Dept. of Electronics, Faculty of Engng., Kyoto Univ., Sakyo-ku, Kyoto, Japan). Jpn. J. Appl. Phys. (Japan), Vol. 16, Supply 1, p. 483-6 (1977). (1976 International Conference on Solid State Devices, Tokyo, Japan, 1-3 Sept. 1976).

Shreve, W. P.
"Surface Wave Resonators and their Use in Narrow-Band Filters", (Texas Instruments Inc., Dallas, TX, USA). 1976 Ultrasonics Symposium Proceedings, Annapolis, MD, USA, 29 Sept. - 1 Oct. 1976 (New York, USA: IEEE 1976), p. 706-13.

Smith, F. W.
"Acoustic Surface Wave Bandpass Filters", (Mullard Res. Lab., Redhill, England). SERT J. (GB), Vol. 9, No. 1, p. 13-15 (Jan. 1975).

Solie, L. P.
"A SAW Filter Using a Reflective Dot Array (RDA)", (Sperry Res. Center, Sudbury, MA, USA). 1976 Ultrasonics Symposium Proceedings, Annapolis, MD, USA, 29 Sept. - 1 Oct. 1976 (New York, USA: IEEE 1976), p. 309-12.

Solie, L. P.
"A SAW Bandpass Filter Technique Using a Fanned Multistrip Complex", (Sperry Res. Center, Sudbury, MA, USA). Appl. Phys. Lett (USA), Vol. 30, No. 8, p. 374-6 (15 April 1977).

Sudhaker, P., Bhattacharyya, A. B., Mathur, B.
"SAW Bandpass Filter with -50 dB Sidelobes Using Unweighted IDTs", (Dept. of Electrical Engng., Indian Inst. of Technol., New Delhi, India). Electron. Lett. (GB), Vol. 14, No. 14, p. 437-9 (6 July 1978).

Szabo, T. L., Slobodnik, A. J. Jr., Laker, K. R.
"Computer-Aided Design of Low Sidelobe SAW Transversal Filters", (Rome Air Develop. Center (AFSC), Hanscom AFB, MA, USA), Proceedings of the 1978 IEEE International Symposium on Circuits and Systems, New York, USA, 17-19 May 1978 (New York, USA: IEEE 1978), p. 376-9.

Takahashi, S., Kodama, T., Miiyashiro, F., Ebata, Y.
"Television IF Surface Acoustic Wave Filter", (Toshiba R&D Center, Tokyo Shibaura Electric Co. Ltd., Kawasaki, Japan). Trans. Inst. Electron. & Commun. Eng. Jpn. Sect. E. (Japan), Vol. E-60, No. 11, p. 1-2 (Nov. 1977).

Takahashi, S., Hirano, H., Kodama, T., Miyashiro, F., Suzuki, B., Onoe, A., Adachi, T., Fujinuma, K.
"SAW IF Filter on $LiTaO_3$ for Color TV Receivers", (Toshiba K&D Center, Saiwai-Ku, Kawasaki, Japan). IEEE Trans. Consum. Electron. (USA), Vol. CE-24, No. 3, p. 337-48 (Aug. 1978). (1978 IEEE Chicago Spring Conference, Arlington Heights, IL, USA, 5-6 June 1978.

Takuro, Koike
"Tunable Bandpass Filters Utilizing the Magnetostatic Wave Propagation", (Dept. of Electronics, Tamagawa Univ., Machida, Tokyo, Japan). Ultrasonics Symposium Proceedings, Cherry Hill, NJ, 25-27 Sept. 1978 (New York, USA: IEEE 1978), p. 689-692.

Tancrell, R. H.
"Analytic Design of Surface Wave Bandpass Filters", (Raytheon Co., Waltham, Mass., USA). IEEE Trans. Sonics & Ultrason. (USA), Vol. SU-21, No. 1, p. 12-22 (Jan. 1974).

Vollers, H. G.
"High Performance Surface Wave Bandpass Filters for Signal Processing Applications", (Texas Instruments Inc., Dallas, USA). 1973 IEEE International Convention and Exposition, Vol. VI, New York, USA, 26-30 March 1973 (New York, USA: IEEE 1973), 42.3/4pp.

Weglein, R. D., Wolf, E. D.
"The Microwave Realization of a Simple Surface Wave Filter Function", (Hughes Res. Labs., Malibu, CA, USA). 1973 IEEE G-MTT International Microwave Symposium Digest of Technical Papers, Boulder, Colo, USA, 4-6 June 1973 (New York, USA: IEEE 1973), p. 120-2.

Worley, J. C.
"Bandpass Filtering Using Surface Wave Delay Line", (Sperry Rand Res. Center, Sudbury, Mass., USA). IEEE Trans. Sonics & Ultrasonics (USA), Vol. SU-19, No. 3, p. 401 (July 1972). (1971 IEEE Ultrasonics Symposium, Miami Beach, FL, USA, 6-8 Dec. 1971).

Worley, J. C.
"Bandpass Filters Using Nonlinear FM Surface-Wave Transducers", (Sperry Rand Res. Center, Sudbury, Mass., USA). IEEE Trans. Microwave Theory & Tech. (USA), Vol. MTT-21, No. 4, p. 302-3 (April 1973).

Yamada, J., Ishigaki, M., Hazama, K., Toyama, T.
"Design and Mass Productive Fabrication Techniques of High Performance SAW TV IF Filter", (Consumer Products Research Center and Yokohama Works, Hitachi, Ltd., 292 Yoshida-machi, Totsuka-ku, Yokohama, Japan). Ultrasonics Symposium Proceedings, Cherry Hill, NJ, USA, 25-27 Sept. 1978 (New York, USA: IEEE 1978), p. 504-508.

Yamaguchi, M., Kogo, H.
"An Elastic Surface Wave Filter for a Television Receiver with Suppressed Triple Transit Echo and Multiple Passband", (Coll. of Engng., Univ. of Chiba, Chiba, Japan). J. Inst. Telev. Eng. Jap (Japan), Vol. 30, No. 3, p. 191-7 (March 1976). In Japanese.

Yen, K. H., Lau, K. F., Kagiwada, R. S.
"Shallow Bulk Acoustic Wave Filters", (TRW Defense and Space Systems Group, Redondo Beach, CA, USA). Ultrasonics Symposium Proceedings, Cherry Hill, NJ, 25-27 Sept. 1978 (New York, USA: IEEE 1978) p. 680-683.

Zelyakh, E. V., Novikov, A. A.
"Active Rejection Filters with Piezoelectric Resonators", Telecomm. & Radio Eng. Part 1 (USA), Vol. 31, No. 1, p. 45-50 (Jan. 1977). Translation of: Elektrosvyaz (USSR), Vol. 31, No. 1, p. 68-73 (Jan. 1977.

1.6

Bell, D. T. Jr., Miller, S. P.
"Aging Effects in Plasma Etched SAW Resonators", (Texas Instruments Inc., Dallas, TX, USA). Proceedings of the 30th Annual Symposium on Frequency Control, Atlantic City, NJ, USA, 2-4 June 1976 (Washington, DC, USA: Electronic Industries Assoc. 1976), p. 358-62.

Belser, R. B., Hicklin, W. H.
"Comparison of Aging Performance of 5 MHz Resonators Plated With Various Electrode Metals", (Georgia Inst. Technol., USA). Proceedings of the 23rd Annual Frequency Control Symposium, Atlantic City, NJ, USA, 6-8 May 1969 (Washington, DC, USA: Electronic Industries Assoc. 1969), p. 132-42.

Bernstein, M.
"Precision Measurement of the Frequency Aging of Quartz Crystal Units", Proceedings of the 22nd Annual Frequency Control Symposium, Atlantic City, NJ, USA, 22-24 Apr. 1968 (Fort Monmouth, NJ, USA: Electronic Components Lab. 1968), p. 232-47.

Bernstein, M.
"Precision Measurement of the Frequency Aging of Quartz Crystal Units", Report ECOM 3227 (AD-703841). Army Electronics Command, Fort Monmouth, NJ, USA (Jan. 1970), 25pp. Available from CFSTI, Springfield, VA, USA.

Bessol'tsev, V. A., Yefremov, O. N., Nevolin, V. K.
"The Effect of the Residual Gas Pressure on the Frequency Instability of Vacuum Quartz Resonators", Radio Eng. & Electron. Phys. (USA), Vol. 21, No. 10, p. 153-4 (Oct. 1976). Translation of: Radiotekh & Elektron. (USSR), Vol. 21, No. 10, p. 2257 et seq. (Oct. 1976).

Bloch, M. B., Denman, J. L.
"Further Development on Precision Quartz Resonators", (Frequency Electronics Inc., New Hyde Park, NY, USA). Proceedings of the 28th Annual Frequency Control Symposium 1974, Atlantic City, NJ, USA, 29-31 May 1974 (Washington, DC, USA: Electronic Industries Assoc. 1974), p. 73-84.

Bruggemann, P., Muller, F.
"A Universal Aging Process for Quartz Resonators", Femmeldetechnik (Germany), Vol. 14, No. 4, p. 134-6 (1974). In German.

Byrne, R. J., Kokanson, J. L.
"Effect of High-Temperature Processing on the Aging Behavior of Precision 5-MHz Quartz Crystal Units", IEEE Trans. Instrum. Meas. (USA), Vol. IM-17, No. 1, 76-9 (March 1968).

Chaban, A. A.
"Instability of Elastic Oscillations in Piezoelectrics in Alternating Electric Fields", Zh. Eksper. Teor. Fiz. Pis'ma (USSR), Vol. 6, No. 11, 967-70 (Dec. 1967). In Russian. English translation in JETP Letters (USA), Vol. 6, No. 12, 381-3 (Dec. 1967).

Demchuk, M. I., Dmitriev, S. M., Chernyavskii, A. F.
"Investigation of Short-Term Fluctuations of the Frequency in Quartz Shock-Excitation Generators", Meas. Tech. (USA), Vol. 20, No. 5, p. 721-5 (May 1977). Translation of: Izmer. Tekh. (USSR), Vol. 20, No. 5, p. 71-3 (May 1977).

Dordevic, L., Samardzija, M.
"Aging of Quartz Crystal Units", Elektroteh. Vestnik (Yugoslavia), Vol. 35, 1-3, 8-11 (Jan. - March 1968). In Slovenian.

Dybwad, G. L.
"Aging Analysis of Quartz Crystal Units with Ti Pd Au Electrodes", (Bell Telephone Labs. Inc., Allentown, PA, USA). 31st Annual Frequency Control Symposium, Atlantic City, NJ, USA, 1-3 June 1977 (Washington, DC, USA: Electronic Industries Assoc. 1977). p. 144-6.

Efremov, O. N., Lyubimov, L. A., Fomicheva, Z. I., Shin, V., Yaroslavskii, M. I.
"Aging of Precision Quartz Resonators", Meas. Tech. (USA), Vol. 18, No. 3, p. 442-3 (March 1975), Translation of: Izmer. Tekh. (USSR), Vol. 18, No. 3, p. 74-5 (March 1975).

Gniewinska, B.
"The Effect of Crystal Current Level on Frequency Stability of Quartz Crystal Oscillators", Prace Inst. Tele. & Radiotech. (Poland), Vol. 15, No. 3, p. 73-9 (1971). In Polish.

Hafner, E., Blewer, R. S.
"Low Aging Quartz Crystal Units", Proc. IEEE (USA), Vol. 56, No. 3, 366-8 (March 1968).

Helmick, C. N. Jr., White, D. J.
"Observations of Aging and Temperature Effects on Dielectric-Coated SAW Devices", (Research Department, Naval Weapons Center, China Lake, CA). Ultrasonics Symposium Proceedings, Cherry Hill, NJ, USA, 25-27 Sept. 1978 (New York, USA: IEEE 1978), p. 580-585.

Jamiolkowski, J.
"High Stability Quartz Crystal Resonator Aging Equipment", Prace Inst. Tele & Radiotech. (Poland), Vol. 15, No. 1, p. 45-59 (1971). In Polish.

Latham, J. I., Saunders, D.
"Aging and Mounting Developments for SAW Resonators", (Texas Instruments Inc., PO Box 225012, Dallas, TX, USA). Ultrasonics Symposium, Proceedings, Cherry Hill, NJ, USA, 25-27 Sept. 1978 (New York, USA: IEEE 1978), p. 513-517.

Malakhov, A. N., Solin, N. N.
"Amplitude and Frequency Fluctuations of Quartz Oscillators", Izv. VUZ Radiofiz (USSR), Vol. 12, No. 4, p. 529-37 (1969).. In Russian.

Payne, J. B.
"Measure and Interpret Short-Term Stability", (Communication Techniques Inc., Parsippany, NJ, USA). Microwaves (USA), Vol. 15, No. 7, p. 34-5, 38, 41, 43-5 (July 1976).

Shreve, W. R., Kusters, J. A., Adams, C. A.
"Fabrication of SAW Resonators for Improved Long Term Aging", (Hewlett-Packard Laboratories, Palo Alto, CA, USA). Ultrasonics Symposium Proceedings (Cherry Hill, NJ, USA, 25-27 Sept. 1978). (New York, USA: IEEE 1978), p. 573-579.

Smolarski, A., Wojicki, M.
"Quartz Crystal Resonator Aging Meter", Pr. Inst. Tele.- & Radiotech. (Poland), Vol. 19, No. 1, p. 77-84 (1975). In Polish.

Skripnik, Yu. A., Kuz'min, Yu. P., Pavlov, V. K.
"Stabilizing the Power Dissipated by Quartz Resonators During the Measurement of their Parameters", Priborostroenic (USSR), No. 17, p. 35-41. In Russian.

Valdois, M., Besson, J., Gagnepain, J. J.
"Influence of Environment Conditions on a Quartz Resonator", (ONERA, Chatillon, France). Proceedings of the 28th Annual Frequency Control Symposium 1974, Atlantic City, NJ, USA, 29-31 May 1974 (Washington, DC, USA: Electronic Industries Assoc. 1974), p. 19-32.

Wainwright, A. E., Walls, F. L., McCaa, W. D.
"Direct Measurements of the Inherent Frequency Stability of Quartz Crystal Resonators", (Nat. Bur. Stand. Boulder, Colo, USA). Proceedings of the 28th Annual Frequency Control Symposium 1974, Atlantic City, NJ, USA, 29-31 May 1974 (Washington, DC, USA: Electronic Industries Assoc. 1974), p. 177-80.

Walls, F. L., Wainwright, A. E.
"Measurement of the Short-Term Stability of Quartz Crystal Resonators and the Implications for Crystal Oscillator Design and Applications", (Nat. Bur. Stand. Boulder, Colo, USA). IEEE Trans. Instrum. & Meas. (USA), Vol. IM-24, No. 1, p. 15-20 (March 1975).

1.7

Adams, C., Kusters, J., Benjaminson, A.
"Measurement Techniques for Quartz Crystals", (Hewlett-Packard Co., Palo Alto, CA, USA). Proceedings of the 22nd Annual Frequency Control Symposium, Atlantic City, NJ, USA, 22-24 Apr. 1968 (Fort Monmouth, NJ, USA: Electronic Components Lab., 1968), p. 248-58.

Allanstein, K.
"Measuring Procedures for Quartz Crystal Parameters", (AEG-Telefunken, Fachbereich Anlagen Hochfrequenz. Berlin, Germany). Tech. Mess. - ATM (Germany), Vol. 45, No. 2, p. 49-55 (Feb. 1978). In German.

Bahadur, H., Parshad, R.
"New Method of Detection of Weak Anharmonic Modes of a Quartz Crystal and its Applications for Generating Multicrystal Resonance Frequencies", (Nat. Phys. Lab., New Delhi, India). J. Appl. Phys. (USA), Vol. 48, No. 7, p. 3141-3 (July 1977).

Bahadur, H., Parshad, R.
"A New Method for Determination of the Frequency Spectrum of a Quartz Crystal and its Applications for Generation of a Number of Precise Frequencies and Time Intervals", (Nat. Phys. Lab., New Delhi, India). European Conference on Precise Electrical Measurement, Brighton, Sussex, England, 5-9 Sept. 1977 (London, England: IEEE 1977), p. 79-82.

Bahadur, H., Parshad, R.
"A New Method for Determination of the Frequency Spectrum of a Quartz Crystal and its Applications", (Nat. Phys. Lab., New Delhi, India). IEEE Trans. Sonics & Ultrason. (USA), Vol. SU-25, No. 1, p. 24-9 (Jan. 1978).

Ballato, A., Oliva, G. R. Jr.
"Admittance Bridge Determination of Quartz Vibrator Parameters Using Augmenting Immittance Elements", (Army Electronics Command, Fort Monmouth, NJ, USA). IEEE Trans. Instrum. Meas. (USA), Vol. IM-19, No. 2, p. 127-34 (May 1970).

Ballato, A., Tilton, R.
"Ovenless Activity Dip Tester 'Crystal Resonator Testing'", (US Army Electronics Technol. & Devices Lab., ECOM, Fort Monmouth, NJ, USA). 31st Annual Frequency Control Symposium, Atlantic City, NJ, USA, 1-3 June 1977 (Washington, DC, USA: Electronic Industries Assoc. 1977). p. 102-7.

Ballato, A., Tilton, R.
"Electronic Activity Dip Measurement", (US Army Electronics Tech & Devices Lab (ECOM), Fort Monmouth, NJ, USA). IEEE Trans. Instrum. & Meas. (USA), Vol. IM-27, No. 1, p. 59-65 (March 1978).

Belostotskii, M. B., Red'ko, Yu. P.
"Determination of the Equipment Dynamic Characteristics of a Frequency Measuring Filter Element", Avtometriya (USSR), No. 4, p. 95-8 (July-Aug. 1977). In Russian. English Translation in: Autom. Monit. & Meas. (GB).

Bryan, P.
"A Rapid and Simple In-Process Test Method Design to Improve Quality of Quartz Resonators in Current Demand Today", (Colorado Crystal Corp., Loveland, CO, USA). Proceedings of the 29th Annual Frequency Control Symposium, Fort Monmouth, NJ, USA, 28-30 May 1975 (Washington, DC, USA: Electronic Industries Assoc. 1975), p. 237-9.

Essler, R.
"Some Problems of the Dynamic Measurement of Equivalent Circuit Values of Piezoelectric Resonators", Wiss. Z. Elektrotech. (Germany), Vol. 11, No. 1-2, p. 1-15 (1968). In German.

Essler, R.
"On the Dynamic Measurement of Equivalent Circuit Parameters of Piezoelectric Filter Elements", Nachrichtentechnik (Germany), Vol. 18, No. 4, 127-30 (April 1968). In German.

Feigen, I., MacKeen, D., Fine, S.
"A Method for Detecting and Measuring Frequency of Surface Vibrations Using a Helium-Neon Laser (Northeastern Univ., Boston, MA, USA). Rev. Sel, Instrum. (USA), Vol. 40, No. 2, p. 381-2 (Feb. 1969).

Fischer, H.
"Some Results of Frequency Response Measurements of 1 MHz Precision Quartzes", (Tech. Univ., Dresden, Dresden, Germany). Nachrichtentech. Elektron. (Germany), Vol. 27, No. 4, p. 154-5 (1977). In German.

Fischer, R., Schulzke, L.
"Extending the Frequency Range of the Transmission Line Method for the Measurement of Quartz Crystals up to 250 MHz", 31st Annual Frequency Control Symposium, Atlantic City, NJ, USA, 1-3 June 1977 (Washington, DC, USA: Electronic Industries Assoc. 1977), p. 96-101.

Forster, H. J.
"Automatic Recording of the Frequency-Temperature Response of Quartz Crystals", (Geschaftsbereich Weitverkehrssysteme, Siemens AG, Munchen, Germany). Frequenz (Germany), Vol. 31, No. 12, p. 375-81 (Dec. 1977). In German.

Franx, C.
"On Precision Measurements of Frequency and Resistance of Quartz Crystal Units", (N. V. Philips' Gloeilampenfabrieken, Eindhoven, Netherlands). Proceedings of the 23rd Annual Frequency Control Symposium, Atlantic City, NJ, USA, 6-8 May 1969 (Washington, DC, USA: Electronic Industries Assoc. 1969). p. 102-10.

Frerking, M. E.
"Vector Voltmeter Crystal Measurement System", (Collins Radio Co., Cedar Rapids, Iowa, USA). Proceedings of the 23rd Annual Frequency Control Symposium, Atlantic City, NJ, USA, 6-8 May 1969 (Washington, DC, USA: Electronic Industries Assoc. 1969), p. 93-101.

Fukada, E.
"An Apparatus for Piezoelectrical Measurements", JEE (Japan), No. 68, p. 24-30 (July 1972).

Ganea, S.
"Quartz Resonator Parameters; Measurement Method and Equipment", Autom. & Electron. (Rumania), Vol. 18, No. 3, p. 93-104 (May-June 1974). In Rumanian.

Gerdes, R. J., Wagner, C. E.
"Study of Frequency Control Devices in the Scanning Electron Microscope", (Georgia Inst. Technol., USA). Programme of the 25th Annual Frequency Control Symposium (Abstracts), Atlantic City, NJ, USA, 26-28 Apr. 1971 (Fort Monmouth, NJ, USA: US Army Electronics Command 1971), p. 24.

Gibert, G., Broussou, S., Morel, J.
"Quartz Crystal Units for Space Applications", (CEPE, Sartrouville, France). Proceedings of the 27th Annual Frequency Control Symposium, Cherry Hill, NJ, USA, 12-14 June 1973 (Washington, DC, USA: Electronic Industries Assoc. 1973), p. 39-41.

Godwin, P. F. Jr., Snider, G. L.
"Methods for Production Screening for Anomalous Responses in Quartz Crystals Intended for High Reliability Applications", (TRW Defense & Space Systems Group, Redondo Beach, CA, USA). 31st Annual Frequency Control Symposium, Atlantic City, NJ, USA, 1-3 June 1977 (Washington, DC, USA: Electronic Industries Assoc. 1977), p. 78-95.

Godwin, P. F. Jr., Snider, G. L.
"Test Techniques Useful in Identifying Sources of Discontinuous Behavior in Quartz Crystals, Crystal Oscillators and Crystal Filters", (TRW Defense & Space Systems Group, Redondo Beach, CA, USA). ATFA 77, Los Angeles, CA, USA: 27-29 Sept. 1977 (New York, USA: IEEE 1977), p. 178-97.

Grachev, V. G., Prozorov, V. A.
"A Quartz Filter Spectrum Analyzer", Izv. VUZ Radiofiz. (USSR), Vol. 19, No. 11, p. 1740-4 (1976). In Russian. English translation in: Radiophys. & Quantrum Electron. (USA).

Grenier, R. P.
"Technique for Crystal Resonance Measurements Based on Phase Detection in a Transmission Type Measurement System," (Western Electric Co. Ltd., North Andover, Mass, USA). Proceedings of the 22nd Annual Frequency Control Symposium, Atlantic City, NJ, USA, 22-24 Apr. 1968 (Fort Monmouth, NJ, USA: Electronic Components Lab. 1968), p. 259-68.

Grenier, R. P.
"Crystal Resonance Frequency Measurement by Phase Detection", W. Elec. Eng. (USA), Vol. 14, No. 3, p. 15-19 (July 1970).

Grigor'ev, V. N.
"Instrument for Measuring the Parameters of Quartz Resonators", Prib. & Sist. Upr. (USSR), No. 9, p. 43-4 (1975). In Russian.

Hafner, E., Riley, W. J.
"Implementation of Bridge Measurement, Techniques for Quartz Crystal Parameters", US Army Electronics Technol. & Devices Lab., Fort Monmouth, NJ, USA). Proceedings of the 30th Annual Symposium on Frequency Control, Atlantic City, NJ, USA, 2-4 June 1976 (Washington, DC, USA: Electronic Industries Assoc. 1976), p. 92-102.

Hartemann, P., Rouvaen, J., Torguet, R., Bridoux, E., Bruneel, C.
"Laser Probing of a Surface-Acoustic-Wave Resonator", (Lab. Central de Recherches, Thomson-CSF, Orsay, France). Electron. Lett. (GB), Vol. 12, No. 7, p. 176-7 (1 April 1976).

Hirose, Y., Tsuziki, Y., Iijima, K.
"Measurement of Contour Vibrations of Quartz Plates by Holographic Technique", (Yokohama Nat. Univ., Japan). Trans. Inst. Electron. Commun. Eng. Jap. A.B.C. (Japan). In Japanese. English translation in: Electron & Commun. Jap. (USA), Vol. 53, No. 6, p. 49-54 (June 1970).

Holland, R., EerNisse, E. P.
"Accurate Method for Measuring Piezoelectric Coefficients", (Sandia Lab., Albuquerque, NM, USA). IEEE Trans. Sonics Ultrasonics (USA), Vol. SU-16, No. 1, Suppl., p. 21 (Jan. 1969). (1968 IEEE Ultrasonics Symposium, New York, USA, 25-27 Sept. 1968).

Iijima, K., Tsuzuki, Y., Hirose, Y., Akiyama, M.
"Laser Interferometric Measurement of Vibration Displacements of Plano-Convex AT-Cut Quartz Crystal Resonator", (Yokohama Nat. Univ., Yokohama, Japan). Proceedings of the 30th Annual Frequency Control Symposium, Atlantic City, NJ, USA, 2-4 June 1976 (Washington, DC, USA: Electronic Industries Assoc. 1976), p. 65-70.

Ikeda, T.
"Errors and Corrections in the Determination of Piezoelectric Parameters by the Resonance-Antiresonance Method", (Tohoku Univ., Sendai, Japan). J. Acoust. Soc. Jap. (Japan), Vol. 30, No. 1, p. 5-13 (Jan. 1974). In Japanese.

Koga, I.
"Precision Measurement of Crystal Frequency by 'Center-Line Method'", (Kokusai Denshin Denwa Co., Tokyo, Japan). Trans. Inst. Electron. Commun. Eng. Jap. A.B.C. (Japan). In Japanese. English Translation in: Electron. & Commun. Jap. (USA), Vol. 53, No. 6, p. 1-8 (June 1970).

Koga, I.
"Precision Determination of Parameters of VHF Crystals", Proceedings of the 28th Annual Frequency Control Symposium 1974, Atlantic City, NJ, USA, 29-31 May 1974 (Washington, DC, USA: Electronic Industries Assoc. 1974), p. 49-56.

Kollmann, M.
"Measuring the Parameters of Piezocrystal Units on a Polyscope", Sdelovaci Tech. (Czechoslovakia), Vol. 24, No. 3, p. 83-5 (March 1976). In Czech.

Ksiazek, J., Smolarski, A.
"Bridge Circuit for Measurement of Parasitic Resonances of Crystal Quartz", Prace Inst. Tele. & Radiotech. (Poland), Vol. 15, No. 4, p. 71-6 (1971). In Polish.

Layden, O. P., Ballato, A., Shibla, C.
"Newly Developed Crystal Measurement Instruments", Proceedings of the 22nd Annual Frequency Control Symposium, Atlantic City, NJ, USA, 22-24 Apr. 1968 (Fort Monmouth, NJ, USA: Electronic Components Lab. 1968), p. 282-97.

Layden, O. P., Ballato, A. D., Shibla, C. L.
"Crystal Parameter Measurement", Instrum. Control Syst. (USA), Vol. 43, No. 2, p. 67-71 (Feb. 1970).

Marshall, F. G.
"Equivalent Circuit for the Acoustoelectric Oscillator", Electronics Letters (GB), Vol. 5, No. 23, p. 581-2 (13 Nov. 1969).

Masiani, G., Zanardi, F.
"RC Bridge Transmission Method for Measurement of Unwanted Resonances in Piezoelectric Crystals", Alta Freq. (Italy), Vol. 46, No. 12, p. 582-91 (Dec. 1977). In Italian.

McDermott, J.
"Focus on Piezoelectric Crystals and Devices", Electron. Des. (USA), Vol. 21, No. 17, p. 44-54 (16 Aug. 1973).

Mel'kanovich, A. F., Perlatov, V. G.
"Measuring the Parameters of Piezoelectric Materials and Cells", (All-Union Sci.-Res. Inst. of Nondestructive Testing, Kishinev, USSR). Sov. J. Nondestr. Test. (USA), Vol. 13, No. 4, p. 384-9 (July-Aug. 1977). Translation of: Defecktoskopiya (USSR), Vol. 13, No. 4, p. 25-32 (July-Aug. 1977).

Merigoux, H.
"Progress in Checking Quartz Crystals", (Univ. Besancon, France). Microtechnic (Switzerland), Vol. 28, No. 1, p. 31 (Feb. 1974). In French.

Metcalf, W. S.
"Practical Crystal Measurements and Standardization", (Cathodeon Crystals Ltd., Cambridge, England). Proceedings of the 27th Annual Frequency Control Symposium, Cherry Hill, NJ, USA, 12-14 June 1973 (Washington, DC, USA: Electronic Industries Assoc. 1973), p. 55-62.

Metcalf, W. S.
"Crystal Measurement and Standardization", Cathodeon Crystals Ltd., Linton, England). Electron. (GB), No. 68, p. 61-3 (13 Feb. 1975).

Michaelis, M.
"Test Equipment for Quartz Oscillators and Filters", Funkschau (Germany), Vol. 49, No. 17, p. 810 (12 Aug. 1977). In German.

Murashov, B. P., Tsvetkov, Yu. P.
"Instrument for Checking Quartz-Crystal Oscillators with Standard Frequency Signals in the Long-Wave and Very-Long-Wave Ranges", Meas. Tech (USA), Vol. 19, No. 7, p. 1012-15 (July 1976). Translation of: Izmer. Tekh. (USSR), Vol. 19, No. 7, p. 51-3 (July 1976).

Nakajima, Y., Nagata, T.
"Method for Measuring Frequency Response of Unplated Piezoelectric Ceramic Plate and its Application", (Wireless Res. Lab., Matushita Electric Industrial Co. Ltd., Osaka, Japan). Trans. Inst. Electron. & Commun. Eng. Jpn. Sect. E (Japan). Vol. E-60, No. 6, p. 325 (June 1977).

Nier, E.
"Piezoelectric Measuring Equipment", (Lab. fur Elektrophys. Dresden, Germany). Meres & Autom. (Hungary), Vol. 24, No. 6, p. 210-17 (1976). In Hungarian).

Oliva, G. R. Jr., Ballato, A.
"Quartz Vibrator Parameter Determination by Parallel Bridge Methods", Report ECOM 3121 (AD-697110), Army Electronics Command, Fort Monmouth, NJ, USA (Aug. 1969). 55pp. Available from CFSTI, Springfield, VA, USA.

Pacuraru, I., Toderean, G.
"Digital Q-Meter for Quartz", (Inst. de Technologie Izotopica si Moleculara, Cluj-Napoca, Rumania). Electrotech. Electron. & Autom. Electrotech (Rumania), Vol. 25, No. 7, p. 281-4 (Oct. 1977). In Rumanian.

Panigati, R., Stacchiotti, G.
"An Automatic System for a Quartz Characterization both at Fundamental and Unwanted Modes", Alta Freq. (Italy), Vol. 44, No. 8, p. 405-11 (Aug. 1975).

Pegeot, C., Gagnepain, J. J.
"Quartz Crystal Parameters Measurement System", (Societe Quartz et Electronique, Asniere, France). IEEE Trans. Instrum. & Meas. (USA), Vol. IM-26, No. 4, p. 300-4 (Dec. 1977).

Preobrazhenskii, N. S., Il'in, V. K.
"Apparatus for Determining Axes of Highest Piezoelectric Activity", (Kurnakov Inst. of General & Inorganic Chem., Acad. of Sci., USSR). Ind. Lab. (USA), Vol. 42, No. 5, p. 732-3 (May 1976). Translation of: Zavod. Lab. (USSR), Vol. 42, No. 5, p. 549-50 (May 1976).

Preobrazhenskii, N. S., Il'in, V. K.
"Method of Determining Quality of Piezoelectrics", (Kurnakov Inst. of General & Inorganic Chem., Acad. of Sci., Moscow, USSR). Ind. Lab. (USA), Vol. 42, No. 9, p. 1421-3 (Sept. 1976). Translation of: Zavod. Lab. (USSR), Vol. 42, No. 9, p. 1098-1100 (Sept. 1976).

Pustarfi, H. S., Smith, W. L.
"An Automatic Crystal Measurement System", (Bell Telephone Labs. Inc., Allentown, PA, USA), Proceedings of the 27th Annual Frequency Control Symposium, Cherry Hill, NJ, USA, 12-14 June 1973, (Washington, DC, USA: Electronic Industries Assoc. 1973), p. 63-72.

Ramadan, B., Kos, J. F.
"Crystal Bridge for Measuring the Equivalent Electrical Parameters of Piezoelectric Crystals", (Dept. of Phys. & Astron., Univ. of Regina, Regina, Saskatchewan, Canada). Rev. Sci. Instrum. (USA), Vol. 49, No. 3, p. 374-7 (March 1978).

Ridley, A. T.
"Measuring Techniques in the Production of Quartz Crystal Components", (ITT Standard Telephones & Cables Ltd., Harlow, England). Radio Mentor Electron. (Germany), Vol. 40, No. 9, p. 359-61 (Sept. 1974). In German.

Saul, R. H., Bauer, C. L.
"Simplified Bridge System for Measurement of Internal Friction and Fractional Variations of Young's Modulus at Kilohertz Frequencies", Rev. Sci. Instrum. (USA), Vol. 38, No. 10, 1449-51 (Oct. 1967).

Schade, R. W.
"Reliable and Repeatable Measurements of Frequency and Resistance Changes of Quartz Crystals due to Wide Temperature Variations", (Defense Electronics Supply Center, Dayton, OH, USA). Proceedings of the 22nd Annual Frequency Control Symposium, Atlantic City, NJ, USA, 22-24 Apr. 1968 (Fort Monmouth, NJ, USA: Electronic Components Lab. 1968), p. 164-7.

Schwartz, R. B.
"Simple System Using One-Crystal Composite Oscillator for Internal Friction and Modulus Measurements 'In Temperature Range 1.7 to 300K'", (Phys. Dept. Univ. of IL, Urbana, IL, USA). Rev. Sci. Instrum. (USA), Vol. 48, No. 2, p. 111-15 (Feb. 1977).

Sedra, R. N., Hanna, F. F.
"Various Methods for the Detection of Harmonic Vibrations of a Quartz Crystal", (Faculty of Sci., Univ. Cairo, Giza, UAR). (Nat. Research Centre, Dokky, Giza, UAR). Proc. Math. Phys. Soc. UAR (Egypt), No. 29, p. 67-72 (June 1965).

Sherman, J. H. Jr.
"Comments on a 'New Method for Determination of the Frequency Spectrum of a Quartz Crystal and its Application'", (General Electric Co., Lynchburg, VA, USA). IEEE Trans. Sonics & Ultrason. (USA), Vol. SU-25, No. 4, p. 226 (July 1978).

Shevel'ko, M. M., Yakovelev, L. A.
"Precision Measurements of the Elastic Characteristics of Synthetic Piezoelectric Quartz", (V. I. Ul'yanov Lenin Leningrad Inst. of Electrical Engng., Leningrad, USSR). Sov. Phys.-Acoust. (USA), Vol. 23, No. 2, p. 187-8 (March-April 1977). Translation of: Akust. Zh. (USSR), Vol. 23, No. 2, p. 331-2 (March-April 1977).

Sladky, P.
"Apparatus for the Measurements of Internal Friction by Means of the Composite Oscillator Technique", (Matematicko-Fyzikalni Fakulta, Univ. Karlovy, Praha, Czechoslovakia). Cesk. Cas. Fis. A (Czechoslovakia), Vol. 25, No. 6, p. 589-95 (1975).

Smolarski, A. J., Wojcicki, M. S.
"Quartz Crystal Units Measurement Method with T-Network", Elektronika (Poland), Vol. 18, No. 7-8, p. 281-5 (1977). In Polish.

Solc, I.
"The Possibility of Determining the Resonant Frequencies of Piezoelectric Crystal Cuts by the Method of Double Excitation", Cesk. Cas. Fis. A (Czechoslovakia), Vol. 21, No. 1, p. 26-8 (1971), in Czech.

Spain, C.
"Measuring Equivalent Series Resistance of Crystals", New Electron. (GB), Vol. 10, No. 22, p. 42 (15 Nov. 1977).

Srinivasan, P., Chopra, O. K.
"Determination of Resonant Frequencies and Mode Shapes of Vibrating Plates by the Use of Solid CO: EXCITER", (Indian Inst. Sci. Bangalore, India). Indian J.-Pure Appl. Phys., Vol. 7, No. 4, p. 256-8 (April 1969).

Stickland, W. J.
"Techniques for the Measurement of Quartz Crystal Parameters", Marconi Instrum. (GB), Vol. 11, No. 4A, p. 2-5 (May 1968).

Toki, M., Tsuzuki, Y.
"Precise Determination of Equivalent Circuit Parameters of a Quartz Crystal Unit", (Faculty of Engng., Yokohama Nat. Univ., Yokohama, Japan). Trans. Inst. Electron. & Commun. Eng. Jpn. Sect. E (Japan), Vol. 59, No. 9, p. 24-5 (Sept. 1976).

Tomikawa, Y.
"Finite Element Method and its Application to Analysis of Equivalent Circuit Elements of Piezo-Tuning Fork", (Dept. of Electrical Engng., Yamagata Univ., Yonezawa, Japan). J. Inst. Telev. Eng. Jpn. (Japan), Vol. 31, No. 6, p. 457-66 (June 1977). In Japanese.

Tsuzuki, Y., Hirose, Y., Iijima, K.
"Measurement of Vibrational Modes of Piezoelectric Resonators by Means of Holography", (Yokohama Nat. Univ., Japan). Programme of the 25th Annual Frequency Control Symposium (abstracts), Atlantic City, NJ, USA, 26-28 Apr. 1971 (Fort Monmouth, NJ, USA: US Army Electronics Command 1971), p. 23.

Tsuzuki, Y., Toki, M.
"Precise Determination of Equivalent Circuit Parameters of Quartz Crystal Resonators", (Dept. of Electrical Engng., Yokohama Nat. Univ., Yokohama, Japan). Proc. IEEE (USA), Vol. 64, No. 8, p. 1149-50 (Aug. 1976).

Viles, R. S.
"Swept Frequency Techniques for Accurate RF Measurements", Marconi Instrum. (GB), Vol. 13, No. 4, p. 88-92 (May 1972).

Wojcicki, M.
"Oscillating Circuit for Measurement of Frequency and Resistance Change in Quartz Crystals", Pr. Inst. Tele.- & Radiotech. (Poland), Vol. 17, No. 3, p. 71-6 (1973). In Polish.

Yasuda, I., Yamagata, S.
"Stress Distribution Measurement in Oscillating Quartz Crystals with a Laser Probe", (Hokkaido Univ., Tokyo, Japan). Conference on Laser and Electrooptical Systems. (Digest of Technical Papers). San Diego, CA, USA, 25-27 May 1976 (New York, USA: IEEE 1976, p. 38.

Zakharov, V. P., Evtikhiev, N N., Snezhko, Yu. A., Tychinskii, V. P.
"Application of Laser Interferometry of the Investigation of Vibratory Processes", (Moscow Inst. of Radio Engng., Electronics & Automation, Moscow, USSR). Sov. Phs.-Acoust (USA), Vol. 22, No. 1, p. 17-19 (Jan.-Feb. 1976). Translation of: Akust. Zh. (USSR), Vol. 22, No. 1, p. 32-6 (Jan.-Feb. 1976).

Babitch, D., Oliverio, J.
"Phase Noise of Various Oscillators at Very Low Fourier Frequencies", (Hewlett-Packard Co., Santa Clar, CA, USA). Proceedings of the 28th Annual Frequency Control Symposium 1974, Atlantic City, NJ, USA, 29-31 May 1974 (Washington, DC, USA: Electronic Industries Assoc. 1974), p. 150-9.

Browning, T. I., Lewis, M. F.
"A New Class of Quartz Crystal Oscillator Controlled by Surface-Skimming, Bulk Waves", (RSRE, Malvern, England). 31st Annual Frequency Control Symposium, Atlantic City, NJ, USA, 1-3 June 1977, (Washington, DC, USA: Electronic Industries Assoc. 1977), p. 258-65.

Butcher, P. N., Janus, H. M.
"The Linear Theory of Acoustoelectric Oscillators with Arbitrary Static Field Distributions", (Tech. Univ. Denmark, Lyngby). J. Phys. C (GB), Vol. 5, No. 5, p. 567-81 (14 March 1972).

Carhianu, G., Marghescu, I.
"Electromechanical Oscillators with Capacitive Transducer Using an Auxiliary IF Carrier", Posta & Telecommunicatii (Rumania), Vol. 3, No. 5, p. 232-6 (May 1973). In Rumanian.

Dantard, F., Payant, A.
"High Stability Frequency Reference Standard Generator", (LTT, Conflans-Sainte-Honorine, France). Cables & Transm. (France), Vol. 29, No. 1, p. 123-6 (Jan. 1975). In French.

Edwards, D.
"A Crystal Locked Musical Tone Generator", Electron. Aust. (Australia), Vol. 36, No. 5, p. 73-7. 115 (Aug. 1974).

Flint, A. F., Pustarfi, H. S.
"L5 System: 39A Precision Oscillator", (Bell Telephone Labs. Inc. New York, USA). Bell Syst. Tech. J. (USA), Vol. 53, No. 10, p. 2097-107 (Dec. 1974).

Goncharuk, N. M., Kotsarenko, N. Ya., Fedorchenko, A. M.
"The Theory of An Acoustic Oscillator with a Resonant Electrical Load", Radio Eng. & Electron. Phys. (USA), Vol. 19, No. 9, p. 84-90 (Sept. 1974). Translation of: Radiotekh. & Elektron. (USSR), Vol. 19, No. 9, p. 1939-47 (Sept. 1974).

Hirai, K., Okikawa, T., Aiba, N.
"New Types of Frequency-Stabilized Gunn Oscillator", (R&D Center, Tokyo Shibaura Electric Co. Ltd., Tokyo, Japan). Toshiba Rev. (Int. Ed.) (Japan), No. 115, p. 37-41 (May-June 1978).

Lesage, P., Audoin, C.
"Frequency Stability of Oscillators: Measurements in the Frequency Domain by a Temporal Method", (CNRS, Orsay, France). Onde Electr. (France), Vol. 55, No. 2, p. 82-9 (Feb. 1975). In French.

Malik, D. N. B., Nag, B. R.
"Free and Forced Oscillations in a Delay Line Oscillator", Internat. J. Electronics (GB), Vol. 23, No. 2, 101-22 (1967).

Manukin, A. B., Tikhonov, M. Yu.
"The Equivalent Circuit of a Capacitive Mechanical Oscillator", Vestn. Mosk. Univ. Fiz. Astron. (USSR), No. 5, p. 584-5 (1970). In Russian.

McLeod, R. B.,
"Stable-Fast Start Electromechanically Controlled Oscillator", (E. W. Bliss Co.) Patent USA 3460057, 20 Sept. 1967; publ. 5 Aug. 1969, USA 669219.

Nadai, C.
"Piezoelectric Tuning Fork Modules", Electron. & Microelectron. Ind. (France), No. 167, p. 39-48 (15 Feb. 1973). In French.

Nardin, R., Ho, J.
"Computer Design and Analysis for High Precision Oscillators", (Frequency Electronics Inc., New Hyde Park, NY, USA). Proceedings of the 28th Annual Frequency Control Symposium, 1974, Atlantic City, NJ, USA, 29-31 May 1974 (Washington, DC, USA: Electronic Industries Assoc. 1974), p. 237-42.

Remy, J.
"Direct Measurement of the Spectral Purity of Stable Oscillators", (Adret Electronique, Trappes, France). Onde Electr. (France), Vol. 55, No. 2, p. 90-4 (Feb. 1975). In French.

Rippy, R.
"A New Look at Source Stability", (Goddard Space Flight Center, NASA, Greenbelt, MD, USA). Microwaves (USA), Vol. 15, No. 8, p. 42-3, 46, 48 (Aug. 1976).

Risley, A. S., Shoaf, J. H.
"Frequency Stabilization of X-Band Sources for Use in Frequency Synthesis into the Infrared", (Nat. Bur. Stand., Boulder, Colo., USA). IEEE Trans. Instrum. & Meas. (USA), Vol. IM-23, No. 3, p. 187-95 (Sept. 1974).

Roubicek, O.
"An Electromechanical Low-Frequency Control Oscillator", Automatizace (Czechoslovakia), No. 9-10, p. 261-7 (1968). In Czech.

Rudoi, A. J.
"High Precision Alternating Signal Source", Probl. Tekh. Elektrodin. (USSR), No. 49, p. 73-6 (1974). In Russian.

Rutman, J.
"Very Short-Term Frequency Instability (Time Domain) of an Oscillator Disturbed by Additive Internal Thermal Noise", (Office Nat. Etudes et de Rech Aerospatiales, Conera, Chatillon, France). Proc. IEEE (USA), Vol. 58, No. 6, p. 958-9 (June 1970).

Tuama, S. S. O.
"Crystallographic Orientation Dependence of Electrical Response of Acoustoelectric Oscillators", (Univ. Glasgow, Scotland). Proc. Inst. Elec. Eng. (GB), Vol. 118, No. 6, p. 746-9 (June 1971).

Tuama, S. S. O., Richter, J.
"Frequency Control and Mode Selectivity in the Acoustoelectric Oscillator", (Coll. Technol., Dublin, Ireland). J. Phys. D. (GB), Vol. 7, No. 3, p. 425-8 (11 Feb. 1974).

Wilson, W. L. Jr.
"Precise Frequency and Phase Control of LSA Oscillators", (Cornell Univ., Ithica, NY, USA). IEEE Trans. Microwave Theory & Tech. (USA), Vol. MTT-21, No. 3, p. 146-9 (March 1973).

1.8.1

Al'tshuller, G. B.
"Variation of the Center Frequency of Frequency-Modulated Quartz Oscillators", Telecommun. & Radio Eng. Pt. I (USA), Vol. 27, No. 12, p. 47-50 (Dec. 1973). Translation of: Elektrosvyaz (USSR), Vol. 27, No. 12, p. 56-9 (Dec. 1973).

Arakelian, R., Driscoll, M. M.
"Linear Crystal Controlled FM Source for Mobile Radio Application", (Communications Div., Iran Electronics Industries, Shiraz, Iran). IEEE Trans. Veh. Technol. (USA), Vol. VT-27, No. 2, p. 43-50 (May 1978).

Arakelian, R., Driscoll, M. M.
"Linear Crystal Controlled FM Source for Mobile Radio Application", 31st Annual Frequency Control Symposium, Atlantic City, NJ, USA, 1-3 June 1977 (Washington, DC, USA: Electronic Industries Assoc. 1977), p. 400-6.

Arias, J.
"A Calibrator with a Crystal Controlled Oscillator", Rev. Esp. Electron. (Spain), Vol. 24, No. 270, p. 50-2 (May 1977). In Spanish.

Artym, A. D., Zelenkov, A. A.
"Frequency Stability of Crystal Oscillators", Radiotekhnika (USSR), Vol. 22, No. 3, 63-70 (March 1967). In Russian. English translation in: Telecomm. Radio Engng. Pt. 2 (USA), Vol. 22, No. 3, (See Abstr. 19228 of 1967). 111-17 (March 1967).

Balaz, I.
"Frequency Control of Crystal Oscillators", (SVST, Bratislava, Czechoslovakia). Elektrotech. Cas. (Czechoslovakia), Vol. 24, No. 3, p. 129-44 (1973). In Slovak.

Barnes, A.
"Sinewave of High Purity from a Crystal Oscillator", New Electron. (GB), Vol. 11, No. 5, p. 18 (7 March 1978).

Beauvy, C.
"Stable Frequency Controlled Oscillators", (CEPE Sartrouville, France). Onde Electr. (France), Vol. 56, No. 6-7, p. 308-10 (June-July 1976). In French.

Beerbaum, R. H.
"Two Inverters and a Crystal Assure Oscillator Start", Electronics (USA), Vol. 49, No. 24, p. 115 (25 Nov. 1976).

Bernard, C.
"Quartz Crystal Oscillators With Low Drift", Tech. Mitti, PTT (Switzerland), Vol. 45, No. 11, 603-9 (1967.) In French.

Belotsvetov, Yu. V., Belousov, A. G.
"Circuit of a Crystal Controlled FM Oscillator", Elektrosvyaz (USSR), No. 11, p. 50-4 (1968). In Russian. English Translation In: Telecomm. Radio Engng. Pt. I (USA), No. 11 (Nov. 1968).

Bertrand, A.
"Crystal Oscillators", Onde Electr. (France), Vol. 56, No. 6-7, p. 303-7 (June-July 1976). In French).

Blagovescenskij, M. V., Balaz, I.
"Project Optimization of Voltage Controlled Crystal Oscillators from the Viewpoint of Frequency Control Characteristic Linearization", (MEI, Moskva, USSR). Elektrotech. Cas. (Czechoslovakia), Vol. 24, No. 10, p. 762-79 (1973). In Slovak.

Blankenburg, F. J., Drumheller, J. E., Worsencroft, D. K.
"A Transistorized 125 kHz Crystal Controlled Oscillator for ESR Field Modulation", (Montana State Univ., Bozeman, USA). Rev. Sci. Instrum. (USA), Vol. 42, No. 9, p. 1377-8 (Sept. 1971).

Bloch, M. B., Meirs, M. P., Robinson, T. M.
"Stable Oscillator for Pioneer Venus Programme", (Frequency Electronics Inc., New Hyde Park, NY, USA). Proceedings of the 30th Annual Symposium on Frequency Control, Atlantic City, NJ, USA, 2-4 June 1976 (Washington, DC, USA: Electronic Industries Assoc. 1976), p. 279-83.

Bloch, M. B., Vulcan, A. I.
"The Stability of Precision Oscillators in Vibratory Environments", (Frequency Electronics Inc., New Hyde Park, NY, USA). Proceedings of the 30th Annual Symposium on Frequency Control, Atlantic City, NJ, USA, 2-4 June 1976 (Washington, DC, USA: Electronic Industries Assoc. 1976), p. 284-91.

Blood, B.
"Crystal VCO uses ECL Line Receiver", (Motorola Phoenix, AZ, USA). Electron. Eng. (GB), Vol. 50, No. 609, p. 23 (July 1978).

Bobkov, Yu. N., Mokrenko, P. V., Necheporenko, V. I.
"Comparison of Frequency Control Methods of Quartz Crystal Generators", Otbor Peredacha Inf. (USSR), No. 27, p. 64-68 (1971). In Russian.

Brendel, R., Groslambert, J., Marianneau, G., Olivier, M., Uebersfeld, J.
"Internal Noise of a Quartz Crystal Oscillator, Influence of the Parallel Capacitance", (Lab. de Phys. et Metrologie des Oscillateurs, CNRS, Besancon, France). Proceedings of the 29th Annual Frequency Control Symposium, Fort Monmouth, NJ, USA, 28-30 May 1975 (Washington, DC, USA: Electronic Industries Assoc. 1975), p. 311-15.

Brendel, R., Olivier, M., Marianneau, G.
"Analysis of the Internal Noise of Quartz-Crystal Oscillators", (Lab. de Physique Metrologie Oscillateurs, Besancon, France). IEEE Trans. Instrum. & Meas. (USA), Vol. IM-24, No. 2, p. 160-70 (June 1975).

Brown, D. E.
"Frequency Measurement of Quartz Crystal Oscillators", Marconi Instrum. (GB), Vol. 11, No. 3, 12-15 (1967).

Buchanan, J. E.
"Crystal-Oscillator Design Eliminates Start-Up Problems", (Westinghouse Electric Corp., Baltimore, MD, USA). EDN (USA), Vol. 23, No. 4, p. 110 (20 Feb. 1978).

Cairns, P.
"Transistor Crystal Marker Unit", Radio Constructor (GB), Vol. 25, No. 8, p. 458-62 (March 1972).

Capparelli, F., Verrazzani, L.
"Microminiature Quartz Crystal Variable Frequency Oscillator for Phase-Lock Receivers", Electrotecnica (Italy), Vol. 42, No. 2, p. B-2.6 (1967), In Italian. (Electrical Rotating Machines, 68th Annual Meeting of the Italian Electrotechnical and Electrical Society, Part 2, San Remo, 1967).

Capparelli, F., Verrazzani, L.
"Comment on 'Variable Frequency Crystal Oscillators'", Proc. Inst. Elect. Electronics Engrs. (USA), Vol. 55, No. 9, 1619-21 (Sept. 1967).

Yung, Chung Man, Ung, Kim Young, Sik, Kim Byung
"Frequency Modulated Quartz Oscillator Using VVC Diode", J. Korean Inst. Electron. Eng., Vol. 8, No. 5, p. 228-40 (Nov. 1971). In Korean.

Collison, R. R., Kmetovicz, R. E.
"Calibrated FM, Crystal Stability, and Counter Resolution for a Low-Cost Signal Generator", Hewlett-Packard J. (USA), Vol. 27, No. 7, p. 11-17 (March 1976).

Curtis, M. A.
"Crystal-Derived 50 Hz for Clocks", Electron. Aust. (Australia), Vol. 37, No. 4, p. 79 (July 1975).

Damijanovic, D. D.
"New Quartz Multivibrator", (Boris Kidric Inst., Vinca, Beograd, Yugoslavia). Proc. IEEE (USA), Vol. 62, No. 5, p. 640-1 (May 1974).

Davies, T.
CMOS Crystal-Controlled Toneburst 'Oscillator'", Radio Commun. (GB), Vol. 53, No. 8, p. 603, 605 (Aug. 1977).

Dilworth, I. J.
"A Channel Scanning Arrangement for Quartz Crystals", Radio Commun. (GB), Vol. 53, No. 9, p. 680-3 (Sept. 1977).

Dowsett, J., Smith, D. A.
"The Trend Towards Packaged Crystal Oscillators", Des. Electron. (GB), Vol. 8, No. 9, p. 20-3 (June 1971).

Driscoll, M. M.
"HF and VHF Source Stabilization Technique Incorporating Q-Multiplied Quartz Crystal Resonator", IEEE Trans. Instrum. & Meas. (USA), Vol. IM-23, No. 2, p. 131-40 (Jan. 1974).

Driscoll, M. M., Healey, D. J.
"Voltage-Controlled Crystal Oscillators", (Westinghouse Electric Corp., Baltimore, MD, USA). IEEE Trans. Electron Devices (USA), Vol. ED-18, No. 8, p. 528-35 (Aug. 1971).

Driscoll, M. M.
"Low Frequency Noise Quartz Crystal Oscillator", (Westinghouse Electric Corp., Baltimore, MD, USA). IEEE Trans. Instrum. & Meas. (USA), Vol. IM-24, No. 1, p. 21-6 (March 1975).

Doktorow, A. A., Morozov, V. A.
"Quartz Oscillator with Automatic Frequency Control", (Inst. of Radio Engng. & Electronics, Acad. of Sci., Moscow, USSR). Instrum. & Exp. Tech. (USA), Vol. 18, No. 1, Pt. 2, p. 187-9 (Jan.-Feb. 1975). Translation of: Prib. Tekh. Eksp. (USSR), Vol. 18, No. 1, Pt. 2, p. 163-4 (Jan.-Feb. 1975).

Dubey, G. C., Singh, R. A.
"Thin Film Hybrid Crystal Oscillator", (Solid State Phys. Lab., Delhi, India). J. Inst. Electron & Telecommun. Eng. (India), Vol. 20, No. 3-4, p. 119-21 (March-April 1974).

Dwyer, D. F. G., Roberts, J., Haynes, G.
"Quartz Crystal Oscillator Circuit without Inductors", Wireless World (GB), Vol. 75, No. 1408, p. 474-6 (Oct. 1969).

Dwyer, D. F. J.
"Characteristics of Quartz Crystal Oscillators", (Quartz Crystal Div., ITT, Harlow, England). Electron. Eng. (GB), Vol. 49, No. 591, p. 24-5 (April 1977).

Eaton, S. S.
"COS/MOS Crystal Oscillators Advance Timekeeping Technology", (RCA Solid State Div., Somerville, NJ, USA). 1973 IEEE International Convention and Exposition, Vol. VI, New York, USA, 26-30 March 1973 (New York, USA: IEEE 1973), 51.3/3pp.

Evans, B.
"Low Cost Crystal Oscillator for the R6500", (Pelco Electronics Ltd., Hove, England). Electron. Eng. (GB), Vol. 50, No. 603, p. 17 (March 1978).

Fiok, A. J.
"One-Stage Quartz Oscillators with Three Reactance Elements", (Inst. Radioelektroniki, Politechniki Warsaw, Warsaw, Poland). Rozpr. Electrotech. (Poland), Vol. 22, No. 4, p. 913-24 (1976). In Polish.

Fomin, N. N.
"Design of a Tunnel Diode Oscillator with a Quartz Crystal in the Capacitive Arm of the Tuned Circuit", Radiotekhnika (USSR), Vol. 22, No. 4, 107-9 (April 1967). In Russian. English translation in: Telecomm. Radio Engng. Pt. 2 (USA), Vol. 22, No. 4, 151-4 (April 1967).

Fomin, N. N.
"Nonlinear Theory of Tunnel-Diode Quartz Oscillators", Radiotekhnika (USSR), Vol. 23, No. 5, 23-30 (May 1968). In Russian. English translation in: Telecomm. Radio Engng. Pt. 2 (USA).

Frank, R.
"Low Frequency Quartz and Quartz Oscillators", Radio TV Electron. (Switzerland), Vol. 34, No. 8, p. 771-4 (Aug. 1974). In German.

Frank, R.
"Building Instructions: A Multiple Quartz Oscillator", Radio TV Electron. (Switzerland), Vol. 35, No. 2, p. 146-8 (Feb. 1975). In German.

Fricher, H.
"Linear Calculation of the Frequency Response of Quartz Oscillators", (Tech. Univ. Dresden, Dresden, Germany). Nachrichtentech. Elektron. (Germany), Vol. 27, No. 4, p. 151-3 (1977). In German.

Gagnepain, J. J., Besson, R.
"High Level Resonators and Crystal Oscillators", Onde Electr. (France), Vol. 52, No. 11, p. 488-92 (Dec. 1972). In French.

Gagnepain, J. J., Uebersfeld, J.
"From Hertz to Gigahertz: Quartz Oscillators", (l'Ecole Nat. Superieure de Chronometria et de Micromechanique, Besancon, France). Onde Electr. (France), Vol. 56, No. 4, p. 175-9 (April 1976).

Gavra, T. D., Shabanov, Yu. V.
"Transistor Crystal-Controlled VHF Oscillator with Improved Operational Frequency Stability", Radiotekhnika (USSR), p. 62-7, In Russian. English Translation in. Telecommun. Radio Eng. Pt 2 (USA), Vol. 26, No. 6, p. 95-8 (June 1971).

Gavra, T. D., Pruzhanskiy, M. M., Shabanov, Yu. V.
"Simple Harmonic Quartz Transistorized Meter-Wave Oscillators", Telecomm. Radio Engng., Pt. 2, (USA), Vol. 22, No. 2, 121-5 (Feb. 1967). Translation of: Radiotekhnika (USSR), Vol. 22, No. 2, 67-73 (Feb. 1967).

Greenhouse, H. M., McGill, R. J., Clark, D. P.
"A Fast Warmup Quartz Crystal Oscillator", (Bendix Corp., Baltimore, MD, USA). Proceedings of the 27th Annual Frequency Control Symposium, Cherry Hill, NJ, USA, 12-14 June 1973 (Washington, DC, USA: Electronic Industries Assoc. 1973), p. 199-217.

Greuter, A.
"Low Power Quartz Crystal Oscillator with a Backward Diode as the Active Elements", Mitt. AGEN Switzerland, No. 10, p. 92-7 (Sept. 1969). In German.

Groslambert, J., Marianneau, G., Olivier, M., Uebersfeld, J.
"The Design and Performance of a Crystal Oscillator Exhibiting Improved Short-Term Frequency Stability", (Lab. Phys. Metrologie Oscillateurs, Besancon, France). Proceedings of the 28th Annual Frequency Control Symposium, 1974, Atlantic City, NJ, USA, 29-31 May 1974 (Washington, DC, USA: Electronic Industries Assoc. 1974), p. 181-3.

Hahn, H.
"Advice for the Circuit Design of Quartz Oscillators", Bauelemente Elektrotech. (Germany), Vol. 4, No. 22, p. 40-50 (March 1969). In German

Hajek, J.
"Crystal Oscillators with TTL Circuits", Sdelovaci Tech. (Czechoslovakia), Vol. 23, No. 11, p. 426-7 (Nov. 1975). In Czech.

Hajek, J.
"A Crystal Oscillator Controlled by a Standard Frequency Transmitter", Sdelovaci Tech. (Czechoslovakia), Vol. 24, No. 12, p. 457-9 (Dec. 1976). In Czech.

Hart, R. K., Hicklin, W. H.
"Tactical Miniature Crystal Oscillator", Report GIT-A-1344 ECOM-0301-1 (AD-74927), Georgia Inst. Tech., Atlanta, USA (Aug. 1972), 50 pp Contract DAAB07-71-C-0301. Available from NTIS, Springfield, VA, USA.

Helle, J.
"VCXO 'Voltage Controlled Crystal Oscillator' - Theory and Practice", (Compaignie d'Electronique et de Piezoelectricite, Sartouville, France). Proceedings of the 29th Annual Frequency Control Symposium, Fort Monmouth, NJ, USA, 28-30 May 1975 (Washington, DC, USA: Electronic Industries Assoc. 1975). p. 300-7.

Helle, J.
"Theory and Practice of Voltage Controlled Crystal Oscillators", Rev. Tech. Thomson-CSF (France), Vol. 8, No. 3, p. 607-37 (Sept. 1976). In French.

Herrero, J. L.
"A New Approach to Provide a Crystal Accuracy Frequency Scale to Microwave Sweepers", Singer Instrum. Rev. (USA), Vol. 2, No. 2, p. 1-8 (Aug. 1970).

Ho, J., Block, M.
"A Fast Warmup Oscillator for the GPS Receiver", (Frequency Electronics Inc., New Hyde Park, NY, USA). 31st Annual Frequency Control Symposium, Atlantic City, NJ, USA, 1-3 June 1977 (Washington, DC, USA: Electronic Industries Assoc. 1977). p. 421-8.

Holmbeck, J. D.
"Frequency Tolerance Limitations with Logic Gate Clock Oscillators", (Northern Engng. Labs. Inc., Burlington, VT, USA). 31st Annual Frequency Control Symposium, Atlantic City, NJ, USA, 1-3 June 1977 (Washington, DC, USA: Electronic Industries Assoc. 1977). p. 390-5.

Honda, S., Watahiki, T.
"On Analysis of Quartz Crystal Oscillator Circuit for Quartz Watches", (Faculty of Engng., Ibaraki Univ., Hitachi, Japan). J. Fac. Eng. Ibaraki Univ. (Japan), No. 23, p. 141-4 (1975). In Japanese.

Iliev, S. G., Rajkov, K. G., Durcev, N. H.
"Matrix Analysis of a Generator with Quartz-Type Frequency Stabilization", Elektro Prom.-st. & Proborostr. (Bulgaria), Vol. 9, No. 8, p. 269-9 (Sept. 1974). In Bulgarian.

Ivanchenko, Yu. S., Plonskii, A. F.
"A Two-Stage Pulse-Excited Crystal-Controlled Self-Running Oscillator", Izv. VUZ Radioelektron. (USSR), Vol. 16, No. 8, p. 95-7 (Aug. 1973). In Russian. English Translation in: Radio Electron. & Commun. Syst. (USA).

Jiru, V., Smid, V.
"A Crystal Bandpass 'filter' with Variable Bandwidth for Telecommunications Measuring Instruments", (TESLA, Vyzkumny Ustav Telekomunikaci, Praha, Czechoslovakia). Slaboproudy Obz. (Czechoslovakia), Vol. 39, No. 4, p. 173-7 (April 1978). In Czech.

Karlinskii, S. I.
"Calculating the Stability and Excitation of One Quartz Oscillator Circuit with a Tunnel Diode", Otbor & Peredacha Inf. (USSR), No. 41, p. 74-9 (1974). In Russian.

Katyl, R. H.
"Monolithic Crystal Oscillator", (IBM Corp., Armonk, NY, USA). IBM Tech. Disclosure Bull. (USA), Vol. 20, No. 3, p. 970-2 (Aug. 1977).

Kennedy, R. J., Foster, I. M.
"A Drive Unit for a Quartz Composite Oscillator", (Dept. of Phys. Univ. of Canterbury, Christchurch, New Zealand). J. Phys. E (GB), Vol. 11, No. 9, p. 889-91 (Sept. 1978).

Komlik, V. V., Uvarov, R. V.
"Control of the Transmission Coefficient at the Resonant Frequency in a Four-Terminal Network with a Paraelectric Piezoresonator", Izv. VUZ Radioelektron. (USSR), Vol. 20, No. 9, p. 84-8 (Sept. 1977). In Russian.

Kupka, K., Thanhauser, G.
"Transistorized Crystal Oscillators in MHz Frequencies for Applications to Carrier Frequencies Technique", (Siemens AG, Munchen, Germany). Frequenz (Germany), Vol. 24, No. 12, p. 357-63 (Dec. 1970). In German.

Kupka, K., Thanhauser, G.
"Phase-Controlled Crystal Oscillators for Integral Frequency Multiplication with Applications in Wide-Band Carrier Frequency Systems", (Siemens AG, Munchen, Germany). Frequenz (Germany), Vol. 26, No. 1, p. 14-18 (Jan. 1972). In German.

Kuznetsov, A. A., Baryshev, V. I.
"Crystal Oscillator Using Field-Effect Transistors", (Acad. Sci., Moscow, USSR). Pribory Tekh. Eksp. (USSR), p. 137-9. In Russian. English Translation in: Instrum. & Exp. Tech. (USA), No. 2, p. 468-70 (March-April 1970).

Layden, O. P., Smith, W. L., Anderson, A. E., Bloch, M. B., Newell, D. E., Sulzer, P. C.
"Crystal-Controlled Oscillators", (US Army Electronics Technol. & Devices Lab., Fort Monmouth, NJ, USA). IEEE Trans. Instrum. & Meas. (USA), Vol. IM-21, No. 3, p. 277-86 (Aug. 1972).

Lean, G. D.
"A Crystal-Controlled Solid-State Source for 10 GHz", Radio Commun. (GB), Vol. 51, No. 8, p. 614-19 (Aug. 1975).

Lega, M. C., Frentzel, R. W.
"Crystal Controlled Frequency Modulator", (Univ. Nac. Cordoba, Argentina). Rev. Telegr. Electron. (Argentina), Vol. 62, No. 730, p. 502-4, 15 (Sept. 1973). In Spanish.

Lipoff, S. J.
"Design of Voltage Controlled Crystal Oscillators", (Arthur D. Little, Inc., Cambridge, MA, USA). Proceedings of the 30th Annual Symposium on Frequency Control, Atlantic City, NJ, USA, 2-4 June 1976 (Washington, DC, USA: Electronic Industries Assoc. 1976), p. 301-8.

Lipsk, H.
"Adjustable Digital Function Generator Using a Quartz Oscillator", Elektronik (Germany), Vol. 24, No. 8, p. 77-8 (Aug. 1975). In German.

Litvinenko, V. P., Novinskii, N. A., Undrevich, A. Ya., Kosogovski, V. V.
"Influence of Quartz-Crystal Dynamical Inductance on Spurious Amplitude Modulation in Frequency-Modulated Crystal-Controlled Oscillators", Izv. VUZ Radioelektron. (USSR), Vol. 19, No. 9, p. 99-101 (Sept. 1976). In Russian.

Lue, J. T.
"A Simple Circuit of a Crystal Oscillator and its Application to a High-Resolution NYR Spectrometer", (Dept. of Phys. Nat. Tsing Hun Univ., Hsinchu, Taiwan). IEEE Trans. Instrum. & Meas. (USA), Vol. IM-25, No. 1, p. 76-8 (March 1976).

Lukyavenko, Ye. B., Ponomarev, M. F., Fursa, E. A.
"A Crystal-Controlled Sinusoidal Transistor Oscillator", Izv. VUZ Radioelektron. (USSR), Vol. 18, No. 1, p. 64-7 (Jan. 1975). In Russian.

Luxmore, T., Newell, D. E.
"The MXO-Monolithic Crystal Oscillator", (CTS Knights Inc., Sandwich, IL, USA). 31st Annual Frequency Control Symposium, Atlantic City, NJ, USA, 1-3 June 1977 (Washington, DC, USA: Electronic Industries Assoc. 1977), p. 396-9.

Makarenko, B. I., Schmidt, V. V., Ovsyannikov, Yu. V., Arkhipov, A. V., Bel'ko, A. A., Bakhtin, V. D.
"Solid-State Three-Frequency, Quartz-Crystal-Stabilized, Millimeter-Range Frequency Source", Radiotekhnika. Kharkov (USSR), No. 39, p. 62-4, (1976). In Russian.

Malakhov, A. N.
"Natural Fluctuations in Quartz Generator", Izv. VUZ Radiofiz. (USSR). 1968, No. 6, 850-65. In Russian. English Translation in: Soviet Radiophys. (USA).

Mancini, R. A.
"A Low Cost, Crystal-Controlled Oscillator Design", (Honeywell Inc., St. Petersburg, FL, USA). Comput. Des. (USA), Vol. 13, No. 1, p. 94-6 (Jan. 1974).

Markus, N., Rogner, R.
"The TN Quartz Pulse Generator", Nachr. Telefonbau & Normalzeit (Germany), No. 77, p. 45-9 (1976). In German.

Marshall, F. G.
"Vibration Mode Patterns of Acoustoelectric Oscillators", (Royal Radar Estab., Great Malvern, England). Electron. Lett. (GB), Vol. 7, No. 9, p. 203-5 (6 May 1971).

Misra, R. K.
"A Network that will Keep a Crystal Oscillator Operating at Zero Phase Angle", (Indian Space Res. Organisation, Ahmedabad). J. Inst. Electron. & Telecommun. Eng. (India), Vol. 19, No. 10, p. 555-7 (Oct. 1973).

Miyajima, S., Asakura, T., Oguchi, T.
"Frequency Stabilization of a Bridge Oscillator", J. Radio Res. Lab. (Japan), Vol. 14, No. 71, 27-56 (Jan. 1967).

Mortley, W. S.
"Comments on 'Voltage-Controlled Crystal Oscillators'", (GEC Ltd., Chelmsford, England). IEEE Trans. Electron Devices (USA), Vol. ED-19, No. 9, p. 1065-7 (Sept. 1972).

Mossuz, G., Gagnepain, J. J.
"Quartz Crystal Oscillator at Very Low Temperature", (Ecole Nat. Superiecute de Chronometrie et Micromechanique, Besançon, France). Cryogenics (GB), Vol. 16, No. 11, p. 652-6 (Nov. 1976).

Nedashkovskii, A. I.
"A Crystal Oscillator with Frequency Trimming", Prib. & Sist. Upr. (USSR), No. 12, p. 47 (1975). In Russian.

Negodenko, O. N., Ponomarev, M. F.
"A Unijunction Quartz-Crystal Transistor", Izv. VUZ Radioelectron. (USSR), Vol. 15, No. 1, p. 87-92 (1972). In Russian. English Translation in: Radio Electron. & Commun. Syst. (USA).

Noble, F. W.
"Need an Adjustable Crystal Oscillator?", (Lab. of Tech. Dev. Nat. Heart & Lung Inst., Bethesda, MD, USA). Electron. Des. (USA), Vol. 24, No. 7, p. 88-90 (29 March 1976).

Nonaka, S.
"Abnormal Crystal Oscillator Frequency Change with Load Capacitance and its Elimination", (Nippon Electric Co. Ltd., Kawasaki City, Japan). Proceedings of the 28th Annual Frequency Control Symposium, 1974, Atlantic City, NJ, USA, 29-31 May 1974 (Washington, DC, USA: Electronic Industries Assoc. 1974), p. 203-10.

Norton, J. R.
"An Ultrastable Low Power 5 MHz Quartz Oscillator Qualified for Space Usage", (Appl. Phys. Lab., Johns Hopkins Univ., Laurel, MD, USA). Proceedings of the 30th Annual Symposium on Frequency Control, Atlantic City, NJ, USA, 2-4 June 1976 (Washington, DC, USA: Electronic Industries Assoc. 1976), p. 275-8.

Novinskii, N. A., Undrevich, A. Ya.
"Design of Quartz Crystal Self-Running Tunnel-Diode Oscillator", Izv. VUZ Radioelektronika (USSR), Vol. 12, No. 5, p. 543-7 (May 1969). In Russian.

Novinskii, N. A., Litvinenko, V. P., Undrevich, A. Ya.
"A Double-Frequency Controlled Quartz-Crystal Oscillator", Izv. VUZ Radioelektron. (USSR), Vol. 17, No. 3, p. 105-7 (March 1974). In Russian. English Translation in: Radio Electron. & Commun. Syst. (USA).

Novinskii, N. A.
"A Crystal Oscillator Based on a Field-Effect Transistor", Izv. VUZ Radioelektron. (USSR), Vol. 21, No. 3, p. 100-3 (March 1978). In Russian.

Nukiyama, D., Miyazaki, N.
"A Type of Oscillator", J. Res. Inst. Technol. Nihon Univ. (Japan), 1967, No. 34, 18-24 (Sept.) In Japanese.

Odess, L.
"Analysis of the Frequency and Sensitivity of Crystal-Controlled Oscillators", (Motorola Israel Ltd., Tel-Aviv). 8th Convention of the Electrical and Electronics Engineers in Israel, Tel Aviv, Israel, 30 April - 3 May 1973 (Israel: Electrical & Electronics Engnrs. in Israel 1973), 66pp.

Odess, L.
"Analysis of the Frequency and Sensitivity of Crystal-Controlled Oscillators", (School of Engng., Tel-Aviv Univ., Ramat-Aviv, Tel-Aviv, Israel). Radio & Electron. Eng. (GB), Vol. 46, No. 3, p. 109-16 (March 1976).

Ohata, Y.
"New Approach to the Design of Crystal Oscillators", (Defense Acad., Yokosuka, Kanagawa, Japan). Proceedings of the 28th Annual Frequency Control Symposium 1974, Atlantic City, NJ, USA, 29-31 May 1974 (Washington, DC, USA: Electronic Industries Assoc. 1974), p. 221-31.

Olivier, M., Marianneau, G.
"High Quality Quartz Oscillator", (CNRS, Besancon, France). Onde Electr. (France), Vol. 56, No. 6-7, p. 293-6 (June-July 1976). In French.

Omlin, L.
"Analysis and Design of Quartz-Oscillators. I.", Elektroniker (Switzerland), Vol. 16, No. 6, p. EL30-6 (1977). In German.

Omlin, L.
"Analysis and Component Sizing of Quartz Oscillators. II.", Elektroniker (Switzerland), Vol. 16, No. 9, p. EL 8-14 (1977). In German.

Ovcharenko, V. V., Ovcharenko, N. F.
"New Tunnel-Diode Oscillators with Quartz Crystal in the Capacitive Arm of the Circuit", Radiotekhnika (USSR), Vol. 25, No. 2, p. 101-3 (Feb. 1970). In Russian. English Translation in: Telecomm. Radio Engng. Pt. 2 (USA).

Paul, E.
"High-Stability Frequency Generator", Posta & Telecommunicatii (Rumania), Vol. 2, No. 8, p. 403-5 (Aug. 1972). In Rumanian.

Pichl, H.
"Crystal Oscillator Module for Electronic Control Systems", News from Rohde and Schwarz (Germany), Vol. 7, No. 25, 9-12 (1967).

Pichler, H.
"Quartz Oscillator with 'SN 74' Series TTL Elements", Radio Elektron Schau (Austria), Vol. 51, No. 4, p. 209-10 (1975). In German

Pionskii, A. F., Samkov, E. Ya.
"On the Modulation Characteristic of a Piezoelectric Oscillator Stabilized by Dipotassium Tartate and Frequency Modulated by means of a p-n Junction Capacitance", Izv. VUZ Radioelektronika (USSR), Vol. 11, No. 4, p. 299-307 (April 1968). In Russian.

Plonskiy, A. F., Tearo, V. I.
"The Frequency Stability of Self-Excited Quartz Oscillator with a Line Section", Telecommun. & Radio Eng. Part 2 (USA), Vol. 31, No. 8, p. 82-7 (Aug. 1976). Translation of: Radiotekhnika, Moskva (USSR), Vol. 31, No. 8, p. 49-54 (Aug. 1976).

Polikarpov, E. D., Undrevich, A. Ya., Khenkin, E. A.
"A Nomographic Design Technique for a Quartz-Crystal Oscillator with a Double Frequency Control", Izv. VUZ Radioelektron. (USSR), Vol. 21, No. 1, p. 34-8 (Jan. 1978). In Russian.

Preston, B., Rignall, M. W.
"Microelectronic Crystal Oscillators", Proceedings 2nd International Congress on Microelectronics, Munich, 1966 (Munich: R. Oldenbourg Verlag, 1967) 641-62.

Pruzhanskii, M. M., Gavra, T. D.
"Bridge Circuits for Transistorized Harmonic Quartz Oscillators", Radiotekhnika (USSR), Vol. 22, No. 10, 50-8 (Oct. 1967). In Russian. English Translation in: Telecomm. Radio Engng. Pt. 2 (USA).

Przjemski, J. M., Konop, P. L.
"Limitations on GPS Receiver Performance Imposed by Crystal-Oscillator G-Sensitivity", (Charles Stark Draper Lab. Inc. Cambridge, MA, USA). Proceedings of the IEEE 1977 National Aerospace and Electronics Conference, NAECON '77, Dayton, Ohio, USA, 17-19 May 1977 (New York, USA: IEEE 1977), p. 319-22.

Przjemski, J. M.
"A Compensation Technique for Accleration-Induced Frequency Changes in Crystal Oscillators", (Charles Stark Draper Lab. Inc., Cambridge, MA, USA). Proceedings of the IEEE 1978 National Aerospace and Electronics Conference NAECON 78, Pt. 2, Dayton, OH, USA, 16-18 May 1978 (New York, USA: IEEE 1978), p. 55-60.

Rapallini, R. E.
"A VXO Oscillator Exciter", Rev. Telegr. Elektron. (Argentina), Vol. 64, No. 757, p. 25, (Jan. 1976). In Spanish.

Rohde, U. L.
"Crystal Oscillator Provides Low Noise", (Rohde & Schwarz Sales Co. Inc., Fairfield, NJ, USA). Electron. Des. (USA), Vol. 23, No. 21, p. 98-9 (11 Oct. 1975).

Rossman, H., Chino, J. J.
"Crystal Oscillator Vibration Isolation for Airborne Radar Applications", (Systems Dev. Div., Westinghouse Electric Corp. Baltimore, MD, USA). IEEE 1977 Mechanical Engineering in Radar Symposium, Arlington, VA, USA, 8-10 Nov. 1977 (New York, USA: IEEE 1977), p. 72-4.

Rozwadowski, M.
"Application of Crystal Oscillators in Modern Telecommunication Equipments", Przegl. Telekomun. (Poland), Vol. 51, No. 5, p. 147 (1978). In Polish.

Ryzhkov, A. V., Kremnev, Yu. V.
"Short-Term Frequency Stability of Meter-Wave Quartz Oscillators", Telecommun. & Radio Eng. Part 2 (USA), Vol - 31, No. 12, p. 82-5 (Dec. 1976). Translation of: Radiotekhnika Moskva (USSR), Vol. 31, No. 12, p. 49-53 (Dec. 1976).

Sabatterie, R.
"Crystal Controlled Low-Frequency Oscillator", IBM Tech. Disclosure Bull. (USA); Vol. 15, No. 10, p. 3075-7 (March 1973).

Saito, T., Ikeda, T., Katsuta, H., Takahashi, I.
"A High Power Transistor Crystal Oscillator", Mem. Defense Acad. (Math., Phys., Chem., Engng.) (Japan), Vol. 7, No. 2A, 451-9 (Sept. 1967).

Schomezler, G., Zwilling, H.
"Digital Level Oscillator 200 Hz to 2 MHz, a Crystal Accurate Level and Sweep Oscillator with Programmable Decade Frequency Control", Entwicklungsber. Siemens und Halske (Germany), Vol. 30, No. 3, 215-21 (Sept. 1967). In German.

Sharma, A. K., Wilson, M. G. F.
"Linear Theory of the Acoustoelectric Oscillator", Proc. Inst. Elec. Eng. (GB), Vol. 117, No. 12, p. 2216-20 (Dec. 1970).

Shevkoplyas, G. B.
"Matrix Capacitor for the Tuning of Thick-Film Hybrid Quartz Crystal Oscillators", Izv. VUZ Radioelektronika (USSR), Vol. 13, No. 5, p. 655-8 (May 1970). In Russian. English translation in: Radio Electronics and Commun. Soyst. (USA), Vol. 13, No. 5 (May 1970).

Singh, D., Garters, J.
"Crystal-Controlled 164 MHz Oscillator/Quadrupler", Electronic Engng (GB), Vol. 39, 769-72 (Dec. 1967).

Siukaev, A. V.
"Using a Crystal Oscillator", No. 4, p. 27, (April 1975). In Russian.

Slavik, M., Zelenka, J.
"Use of the Integrated Gyrator in a Voltage Controlled Crystal Oscillator", Elektrotech. Cas. (Czechoslovakia), Vol. 27, No. 10, p. 772-4 (1976).

Solin, N. N.
"Comparative Analysis of Fluctuations in Various Types of Two-Circuit Quartz Oscillators", Radiotech. & Elektron. (USSR), p. 316-21. In Russian. English Translation in: Radio Eng. & Electron. Phys. (USA), Vol. 16, No. 2, p. 272-6 (Feb. 1971).

Solin, N. N.
"Fluctuations of Single-Stage Crystal-Controlled Valve Oscillators", Izv. VUZ Radioelektron. (USSR), Vol. 14, No. 3, p. 267-75 (March 1971). In Russian. English Translation in: Radio Electron. & Commun. Syst. (USA).

Solin, N. N.
"The Limiting Short-Term Frequency Instability of Self-Excited Quartz Oscillators", Radio Eng. & & Electron. Phys. (USA), p. 69-72. Translation of: Radiotekh. & Elektron. (USSR), Vol. 17, No. 1, p. 86-9 (Jan. 1972). In Russian.

Solov'ev, I. I.
"Automatic Adjustment of the Amplitude of Crystal Oscillators with Tunnel Diodes", Meas. Tech. (USA), Vol. 15, No. 4, p. 599-601 (April 1972). Translation of: Izmer. Tekh. (USSR), Vol. 15, No. 4, p. 60-2 (April 1972). In Russian.

Stolarski, E., Vojtasek, S.
"An Approximate Method for the Solution of an Oscillator with a Piezotransistor", Elektrotech. Obzor (Czechoslovakia), Vol. 21, No. 9, p. 632-45 (1970). In Czech.

Tesic, S., Vasiljevic, D.
"Quartz-Controlled Complementary Multivibrator", (Faculty of Electrical Engng., Univ. of Belgrade, Belgrade, Yugoslavia). Proc. Inst. Electr. Eng. (GB), Vol. 123, No. 9, p. 851-4 (Sept. 1976).

Tesic, S., Vasiljevic, D.
"A Quartz Multivibrator Using Two Regenerative Switches", (Faculty of Electrical Engng., Univ. of Belgrade, Belgrade Yugoslavia). Proc. IEEE (USA), Vol. 65, No. 1, p. 166-7 (Jan. 1977).

Theaker, M. E.
"CMOS Crystal Calibrator", Pract. Wireless (GB), Vol. 51, No. 11, p. 958-75 (March 1976).

Tourki, P.
"Quartz Oscillator in Complementary MOS Technology", (SE SCOSEM Corberville, Orsay, France). Electron. Lett. (GB), Vol. 9, No. 19, p. 451-3 (20 Sept. 1973).

Valdois, M., Moreau, R., Dupuy, A.
"Airborne Quartz Oscillators, Applications", (ONERA, Chatillon, France). Onde Electr. (France), Vol. 56, No. 6-7, p. 297-302 (June-July 1976). In French.

Vasiljevic, D., Tesic, S.
"An Emitter-Coupled Quartz Multivibrator", (Dept. of Electrical Engng., Univ. of Belgrade, Yugoslavia). Int. J. Electron. (GB), Vol. 42, No. 6, p. 551-8 (June 1977).

Vinkler, E., Grebenyuk, V. M., Zinov, V. G.
"Quartz-Crystal Stabilized 150-MHz Oscillator", (Joint Inst. of Nuclear Res., Dubna, USSR). Instrum. & Exp. Tech. (USA), Vol. 20, No. 3, Pt. 1, p. 736-8 (May-June 1977). Translation of: Prib. Tekh. Eksp. (USSR), Vol. 20, No. 3, Pt. 1, p. 113-15 (May-June 1977).

Vovchenko, P. S.
"Flicker Noise in Quartz-Crystal Controlled Oscillator", Izv. VUZ. Radioelektronika (USSR), Vol. 13, No. 6, p. 754-8 (June 1970). In Russian. English Translation in: Radio Electronics and Commun. Syst. (USA).

Walls, F. L., Stein, S. R.
"A Frequency-Lock System for Improved Quartz Crystal Oscillator Performance", (Time & Frequency Div., Nat. Bur. of Stand. Boulder, CO, USA). IEEE Trans. Instrum. & Meas. (USA), Vol. IM-27, No. 3, p. 249-52 (Sept. 1978).

Walker, D. A. S.
"A Stable Crystal Oscillator Employing Digital Integrated Circuitry", Report AECL-4160, Atomic Energy Canada Ltd., Chalk River, Ontario (March 1972), 5 pp.

Watrobski, B.
"Possibilities of Improving Frequency Stability in Generating Devices", Pomiary Autom. Kontrola (Poland), Vol. 18, No. 11, p. 498-9 (Nov. 1972), In Polish.

Yamnyi, V. E.
"Study of Low Frequency Amplitude and Phase Fluctuations of Quartz-Crystal Transistor Oscillators", Izv. VUZ. Radioelektronika (USSR), Vol. 13, No. 5, p. 658-60 (May 1970). In Russian.

Yelfimov, N. N., Al'tshuller, G. B.
"The Amplitude Relations in Quartz Oscillators", Telecommun. & Radio Eng. Pt. 1 (USA), Vol. 30, No. 2, p. 52-4 (Feb. 1976). Translation of: Elektrosvyaz (USSR), Vol. 30, No. 2, p. 68-70, (Feb. 1976).

Yoda, H., Ikeda, H., Yamabe, H.
"Low Power Crystal Oscillator for Electronic Wrist Watch", JEE (Japan), No. 62, p. 24-30 (Jan. 1972).

Zamzow, D.
"Direct Frequency Modulation of Transistorized Quartz Oscillators", (Deutsche Post, Rudfunk- und Fernsehtechnisches Zentralamt, Berlin, West Germany). Tech. Mitt. RFZ (Germany), Vol. 12, No. 3, p. 125-30 (Mar. 1968). In German.

Ziegler, R. R.
"Know Your Crystal Oscillators", (Greenray Industries Inc., Mechanicsburg, PA, USA). Microwave J. (USA), Vol. 19, No. 6, p. 44-47 (June 1976).

Barton, R. K., Gratze, S. C.
"Surface Acoustic Wave Oscillators: Long Term Stability", Electron Engineering (GB), Vol. 47, No. 565, p. 49-51 (March 1975).

Browning, I., Lewis, M. F.
"Theory of Multimoding in SAW Oscillators", 1976 Ultrasonics Symposium Proceedings, Annapolis, MD, USA, 29 Sept. - 1 Oct. 1976 (New York, USA: IEEE 1976), p. 256-9.

Crabb, J., Lewis, M. F., Maines, J. D.
"Surface-Acoustic-Wave Oscillators: Mode Selection and Frequency Modulation", Electron. Lett. (GB) p. 195-7 (17 May 1973).

Cullen, D. E., Gilden, M., Montress, G. K.
"Design of Stable SAW Oscillators Operating above 1 GHz", Ultrasonics Symposium Proceedings, Cherry Hill, NJ, USA, 25-27 Sept. 1978 (New York, USA: IEEE 1978), p. 433-437.

Davies, L. W., Lawrence, M. W.
"Prospects for Surface Elastic Wave Crystal-Controlled Delay Line Oscillators", Proc. Inst. Radio Electron. Eng. Aust. (Australia), Vol. 32, No. 2, p. 61-2 (Feb. 1971).

Desormiere, B., Hartemann, P.
"Acoustic Surface-Wave Oscillators", Onde Electr. (France), Vol. 56, No. 4, p. 186-8 (April 1976).

Gasior, B., Gregorkiewicz, W., Kaliski, S.
"Experimental Realization of a Generator of Spontaneous Oscillations on a Transverse Surface Wave", Proc. Vib. Probl. (Poland), Vol. 12, No. 3, p. 273-84 (1971).

Grant, P. M., Hussian, K. M., Corner, R. C., Collins, J. H.
"Mobile Radio Frequency Synthesizers Based on Surface Acoustic Wave Oscillators", Radio & Electron. Eng. (GB), Vol. 47, No. 5, p. 209-16 (May 1977).

Gratze, S. C.
"Surface Acoustic Wave Oscillators", Electron. Ind. (GB), Vol. 1, No. 3, p. 20-1, 23 (Nov. 1975).

Gratze, S. C.
"The Development of Surface Acoustic Wave Oscillators", Electron. Engineering (GB), Vol. 49, No. 590, p. 41-3 (April 1977).

Gratze, S. C.
"SAW Oscillators-Their Current Status", Microwave J. (USA), Vol. 20, No. 12, p. 45-8, 57 (Dec 1977).

Hartemann, P.
"Programmable Acoustic-Surface-Wave Oscillator", Electron. Lett. (GB), Vol. 11, No. 5, p. 119-20 (6 March 1975).

Hartemann, P.
"Oscillator Temperature Stability Change Induced by Ion-Implantation", 1976 Ultrasonics Symposium Proceedings, Annapolis, MD, USA, 29 Sept. - 1 Oct. 1976 (New York, USA: IEEE 1976), p. 240-2.

Hauden, D., Michel, M., Bardeche, G., Gagnepain, J. J.
"Temperature Effects on Quartz-Crystal Surface-Wave Oscillators", Appl. Phys. Lett. (USA). Vol.31 No. 5, p. 315-17 (1 Sept. 1977).

Henaff, J.
"Elastic Surface Wave Oscillators", Onde Electr. (France), Vol. 56, No. 4, p. 189-96 (April 1976).

Joseph, T. R.
"Phase Locked SAW Delay Line and Resonator Oscillators", 1976 Ultrasonics Symposium Proceedings, Annapolis, MD, USA, 29 Sept. - 1 Oct. 1976 (New York, USA: IEEE 1976), p. 234-9.

Joseph, T. R.
"SAW Oscillators for Phase Locked Applications", 31st Annual Frequency Control Symposium, Atlantic City, NJ, USA, 1-3 June 1977 (Washington, DC, USA: Electronic Industries Assoc. 1977), p. 365-70.

Karrer, H. E., Dias, J. F.
"Surface Acoustic Wave Oscillators", Proceedings of the 28th Annual Frequency Control Symposium 1974, Atlantic City, NJ, USA, 29-31 May 1974 (Washington, DC, USA: Electronic Industries Assoc. 1974), p. 266-9.

Kyuma, K., Hyakutake, J., Morizumi, T., Yasuda, T.
"Proposal and Analysis of SAW Oscillator Using SAW Amplifier with Segmented Structures", Trans. Inst. Electron. & Commun. Eng. Jpn. Sect. E (Japan), Vol. E60, No. 6, p. 308-9 (June 1977).

Lawrence, M. W.
"Surface-Elastic-Wave Delay-Line Oscillators", AWA Tech. Rev. (Australia), Vol. 15, No. 2, p. 67-76 (Dec. 1973).

Lawrence, M. W.
"Surface Acoustic Wave Oscillator", Wave Electron. (Netherlands), Vol. 2, No. 1-3, p. 199-213 (July 1976). (European Workshop on Computer Aided Design of SAW Devices, Bologna, Italy, 7-9 April 1976).

Lee, L. L., Hunsinger, B. J., Cho, F. Y.
"A SAW-Stabilized Pulse Generator", IEEE Trans. Sonics & Ultrason, (USA), Vol. SU-22, No. 2, p. 141-2 (March 1975).

Lewis, M.
"The Design, Performance and Limitations of SAW Oscillators", International Specialist Seminar on Component Performance and Systems Applications of Surface Acoustic Wave Devices, Aviemore, Scotland, 25-28 Sept. 1973 (London, England: IEE 1973), p. 63-72.

Lewis, M. F.
"Surface Acoustic Wave Devices and Applications. VI. Oscillators-the Next Successful Surface Acoustic Wave Device?", Ultrasonics (GB), Vol. 12, No. 3, p. 115-23 (May 1974).

Lewis, M.
"The Surface Acoustic Wave Oscillator-a Natural and Timely Development of the Quartz Crystal Oscillator", Proceedings of the 28th Annual Frequency Control Symposium 1974, Atlantic City, NJ, USA, 29-31 May 1974 (Washington, DC, USA: Electronic Industries Assoc. 1974), p. 304-14.

Lewis, M. F.
"Oscillators and Frequency Synthesisers Using SAW Delay Lines as Control Elements", Proceedings of the 1976 IEEE International Symposium on Circuits and Systems, Munich, Germany, 27-29 April 1976, (New York, USA: IEEE 1976), p. 702-5.

Lewis, M. F., Thorp, T. L.
"Status of SAW and SSBW Oscillators", Proceedings of the 1978 IEEE International Symposium on Circuits and Systems, New York, USA, 17-19 May 1978 (New York, USA: IEEE 1978), p. 553-7.

Mannucci, A., Pantani, L.
"Mode Selection and Transducer Design in Surface-Acoustic-Wave Oscillators", Alta Freq. (Italy), Vol. 43, No. 12, p. 1036-8 (Dec. 1974).

Martin, G.
"Surface Wave Filter with Weighting of Electrode Overlap without Beam Integration", Nachrichien-tech. Elektron, (Germany), Vol. 28, No. 2, p. 65-8 (1978). In German.

Nandi, A. K., Costanza, S. T., Wheatley, C. E., III
"Surface Acoustic Wave Oscillator Experiments", Proceedings of the 28th Annual Frequency Control Symposium 1974, Atlantic City, NJ, USA, 29-31 May 1974 (Washington, DC, USA: Electronic Industries Assoc. 1974), p. 260-5.

Otto, O. W., Weglein, R. D.
"High Frequency Periodic Grating Oscillator", 1976 Ultrasonics Symposium Proceedings, Annapolis, MD, USA, 29 Sept. - 1 Oct. 1976 (New York, USA: IEEE 1976), p. 248-51.

Parker, T. E., Sage, J. P.
"A SAW Oscillator Using Two Acoustic Paths", 1976 Ultrasonics Symposium Proceedings, Annapolis, MD, USA, 29 Sept. - 1 Oct. 1976 (New York, USA: IEEE 1976), p. 243-7.

Parker, T. E.
"Current Developments in SAW Oscillator Stability", 31st Annual Frequency Control Symposium, Atlantic City, NJ, USA, 1-3 June 1977 (Washington, DC, USA: Electronic Industries Assoc. 1977), p. 359-64.

Parker, T. E.
"Frequency Stability of Surface Wave Controlled Oscillators", Proceedings of the 1978 IEEE International Symposium on Circuits and Systems, New York, USA, 17-19 May 1978 (New York, USA: IEEE 1978), p. 558-62.

Pookaiyaudom, S.
"Surface-Acoustic Wave Delay-Line Controlled Low-Frequency Oscillators", Proc. IEEE (USA), Vol. 63, No. 7, p. 1071-2 (July 1975).

Pookaiyaudom, S., Surawatpanya, C.
"Optimum Short-Term Frequency Stability Improvement in Multi-Delay Line Surface-Acoustic-Wave Oscillators", IEEE Trans. Instrum. & Meas. (USA), Vol. IM-27, No. 1, p. 86-9 (March 1978).

Ragan, L. H.
"Voltage Controlled Surface Wave Resonator Oscillators", 1976 Ultrasonics Symposium Proceedings, Annapolis, MD, USA, 29 Sept. - 1 Oct. 1976 (New York, USA: IEEE 1976), p. 252-5.

Schaer, A., Maloney, E. D.
"GHz Fundamental Acoustic-Wave Oscillators", Microwave J. (USA), Vol. 20, No. 1, p. 41-2 (Jan 1977).

Staples, E. J., Lim, T. C.
"300 MHz Oscillators Using SAW Resonators and Delay Lines", 31st Annual Frequency Control Symposium, Atlantic City, NJ, USA, 1-3 June 1977 (Washington, DC, USA: Electronic Industries Assoc. 1977), p. 371-4.

Temmyo, J., Yoshikawa, S.
"Photolithographic Contact Printing of 0.7 μm Linewidth Interdigital Transducer and 1.1 GHz SAW Oscillator", J. Acoustic. Soc. Jpn. (Japan), Vol. 33, No. 10, p. 549-56 (Oct. 1977) In Japanese.

Vollen, H. G., Claiborne, L. T.
"RF Oscillator Control Utilizing Surface Wave Delay Lines", Proceedings of the 28th Annual Frequency Control Symposium 1974, Atlantic City, NJ, USA, 29-31 May 1974 (Washington, DC, USA: Electronic Industries Assoc. 1974), p. 256-9.

Weglein, R. D., Otto, O. W.
"The Periodic Grating Oscillator (PGO)", Proceedings of the 30th Annual Symposium on Frequency Control, Atlantic City, NJ, USA, 2-4 Jun 1976 (Washington, DC, USA: Electronic Industries Assoc. 1976), p. 363-6.

Weglein, R. D., Otto, O. W.
"Effect of Vibration on SAW Oscillator Noise Spectra", Electron. Lett. (GB), Vol. 13, No. 4, P. 103-4 (17 Feb. 1977).

Weglein, R. D., Otto, O. W.
"Effect of Vibration on SAW-Oscillator Noise Spectra", Electron. Lett. (GB), Vol. 13, No. 4, p. 103-4 (17 Feb. 1977).

Weglein, R. D.
"1.2 GHz Temperature-Stable SAW Oscillator", 31st Annual Frequency Control Symposium, Atlantic City, NJ, USA, 1-3 June 1977 (Washington, DC, USA: Electronic Industries Assoc. 1977).

Wilkinson, V. J.
"The Design and Development of a Surface Acoustic Wave Oscillator with a Frequency Modulation Capability", Marconi Rev. (GB), Vol. 38, No. 197, p. 65-76 (1975).

1.8.3

Aker, J. L.
"HP-25 Calculator Serves as Clock", Electronics (USA), Vol. 49, No. 23, p. 116 (11 Nov. 1976).

Aldridge, D., Mouton, A.
"CMOS Industrial Clock/Timer", New Electron, (GB), Vol. 8, No. 9, p. 45, 49 (29 April 1975).

Arnoldt, M.
"1 Hz Quartz Time Base Unit for Digital Watches", Funk-Tech. (Germany), No. 24, p. 873-4 (Dec. 1974). In German.

Arnold, M.
"Integrated Circuit Quartz Frequency Reference", Funk-Tech. (Germany), Vol. 31, No. 15, p. 476-8 (Aug. 1976). In German.

Arnoldt, M.
"Quartz Clock with Six-Digit Liquid Crystal Display", Funk-Tech. (Germany), Vol. 32, No. 17, p. 301-3, 306-7 (Sept. 1977). In German.

Assmus, F.
"The Influence of Electronics on the Development of Clocks and Watches", Feinwerktech. & Messtech. (Germany), Vol. 86, No. 1, p. 9-21 (Jan.-Feb. 1978). In German.

Babbitt, H. S., III
"Precision Oscillators Flown on the LES-89 Spacecraft", 31st Annual Frequency Control Symposium, Atlantic City, NJ, USA, 1-3 June 1977 (Washington, DC, USA: Electronic Industries Assoc. 1977), p. 412-20.

Banner, G. H.
"The Standard Frequency and Time Signal Installation at Rugby Radio Station: GPO Equipment", Colloquium on Definition, Realisation and Use of Time and Frequency, London, 1967 (London: Institution of Electrical Engineers, 1967: Colloquium Digest 1967/16). Paper No. 6/1-6/10.

Becker, G., Rohbeck, L.
"A Standard Frequency Quartz Oscillator, Controlled by the DCF 77 Radio Transmitter", Elektronik (Germany), Vol. 24, No. 2, p. 73-5 (Feb. 1975). In German.

Begley, W. W., Shapiro, A. H.
"Precision Timing Systems. II. Stable Clocks", Instrum. Contr. Syst. (USA), Vol. 43, No. 10, p. 90-4 (Oct. 1970).

Belomestnov, G. I., Dmitrienko, A. D., Emakov, A. S., Korzh, V. F.
"Automatic System for Aquiring, Recording, and Processing Information by Computer for Secondary Time-and-Frequency Standards", Meas. Tech. (USA), Vol. 19, No. 11, p. 1572-4 (Nov. 1976). Translation of: Izmer. Tekh. (USSR), Vol. 19, No. 11, p. 27-8 (Nov. 1976).

Bhat, C. L., Razdan, H., Sapru, M. L., Kaul, I. K.
"An Error Monitoring and Correction Circuit for Clocks", J. Inst. Electron. & Telecommun. Eng. (India), Vol. 24, No. 1, p. 9-13 (Jan. 1978).

Berger, T. V.
"Digital RPM-Meter and Digital Quartz Clock", Radio-TV-Electron. (Switzerland), Vol. 38, No. 4, p. 42-4 (April 1978). In German.

Bogucki, J.
"Frequency Standard for X-Band Range", Wiad. Telekomun. (Poland), Vol. 16, No. 9, p. 255-7 (Sept. 1976). In Polish.

Bourgeois, C.
"Quartz Crystals as Frequency Standards for Wrist Watches", Eurocon 71 digest, Lausanne, Switzerland, 18-22 Oct. 1971 (New York, USA: IEEE 1971). 2pp.

Breuer, R.
"Radio-Controlled Digital Clock", Radio Fernsehen Elektron. (Germany), Vol. 26, No. 21-22, p. 734-6 (1977). In German.

Breuer, R.
"Circuit for the Automatic Regulation of Digital Clocks", Radio Fernsehen Elektron. (Germany), Vol. 26, No. 3, p. 80 (1977). In German.

Buhrer, C. F.
"Color-TV Set Calibrates Standard Oscillators", Electronics (USA), Vol. 49, No. 23, p. 114-15 (11 Nov. 1976).

Bunn, W.
"National Synchronisation Reference Clock", Post Off. Electr. Eng. J. (GB), Vol. 71, pt. 2, p. 132-5 (July 1978).

Burckardt, G.
"Quartz Time-Piece with Gearing Mechanism, I.", Funkschau (Germany), Vol. 47, No. 5, p. 71-4 (28 Feb. 1975). In German.

Cerzelka, G.
"High Precision Standard Frequency Spectrum for Workshop and Amateur", Funk-Tech. (Germany), Vol. 30, No. 6, p. 131-5 (March 1975). In German.

Chi, A. R.
"Projection of Timing Capability and Spacecraft Clock Calibration in 1980's", International Telemetering Conference, Silver Spring, MD, USA, 14-16 Oct. 1975 (Woodland Hills, Calif., USA: Internat. Found.Telemetering 1975), p. 246.

Cierniewski, S., Dominski, I.
"Quartz Generator with $\pm 5.10^{-11}$ Diurnal Stability", Postepy Astron. (Poland), Vol. 21, No. 4, p. 313-15 (Oct.-Dec. 1973). In Polish.

Coelho, H.
"Quartz Crystal Clock", Tecnica (Portugal), Vol. 33, No. 409, p. 519-22 (June 1971). In Portugese.

Cometta, E.
"Electrical Pulse Clocks and Watches", Elettrificazione (Italy), No. 9, p. 401-9 (Sept. 1977). In Italian.

Dick, J. S. B.
"A Perfect...[Musical Standard]", Electron. Today Int. (GB), p. 86 (Dec. 1977).

Dowsett, J.
"Design of a 2.5 Mc/s Standard of Frequency", Conference on Frequency Generation and Control for Radio Systems, London, (1967) (London: Institution of Electrical Engineers, 1967: Conference Publication No. 31) 58-63.

Dowsett, J.
"Design of a 2.5 MHz Frequency Standard", Point to Point Telecomm. (GB), Vol. 12, No. 1, 38-50 (Jan. 1968).

Easton, R. L., Bartholomew, C. A., Phiips, D. H.
"Crystal Oscillator Satellite Experiment", Proceedings of the 22nd Annual Frequency Control Symposium, Atlantic City, NJ, USA, 22-24 Apr. 1968 (Fort Monmouth, NJ, USA: Electronic Components Lab. 1968), p. 342-53.

Flanagan, T. M.
"Hardening Frequency Standards for Space Applications", IEEE Trans. Nucl. Sci. (USA), Vol. NS-24, No. 6, p. 2252-8 (Dec. 1977). (IEEE Annual Conference on Nuclear and Space Radiation Effects, Williamsburg, VA, USA, 12-15 July 1977).

Feichtinger, H.
"Standard Frequency from DCF 77 [Radio Transmitter]", Funkschau (Germany), Vol. 49, No. 3, p. 134-5 (28 Jan. 1977). In German.

Gerz, G., Weissbacker, K.
"Electronic Clock Generator for the National STD Services (EZTGN)", Fernmelde-Praxis (Germany), Vol. 55, No. 5, p. 177-90 (10 March 1978). In German.

Gilabert, K., Larcher, J.
"Modern Frequency Standards", Onde Elect. (France) Vol. 48, 382-92 (April 1968). In French.

Hajek, J.
"The Chrometron Quartz Crystal-Controlled Electronic Clocks", Jemna Mech. & Opt. (Czechoslovakia), Vol. 20, No. 2, p. 55-8 (Feb. 1975). In Czech.

Halford, D., Hellwig, H.
"Progress and Feasibility for a Unified Standard for Frequency, Time and Length", Proc. IEEE (USA), Vol. 60, No. 5, p. 623-5 (May 1972).

Hegendorfer, M.
"Quartz-Clock Module for Screen Display", Radio Elektron. Schau (Austria), Vol. 51, No. 10, p. 562-4 (1975). In German.

Hellwig, H.
"Frequency Standards and Clocks. A Tutorial Introduction", Report NBS TN 616, Nat. Bur. Stand. Washington, DC, USA (April 1972). 65 pp.

Hellwig, H.
"Design Principles and Characteristics of Frequency and Time Standards", IEEE Trans. Nucl. Sci. (USA), Vol. NS-23, No. 6, p. 1629-35 (Dec. 1976). (IEEE Annual Conference on Nuclear and Space Radiation Effects, San Diego, Calif., USA, 27-30 July 1976).

Hers, J.
"Improved Portable Electronic Clock", Mon. Not. Astron. Soc. S. Afr. (S. Africa), Vol. 33, No. 9-10, p. 118-20 (Oct. 1974).

Hinnah, H. D.
"A New Type of Crystal Controlled Clock Oscillator", 26th Electronic Components Conference, San Francisco, Calif., USA, 26-28 April 1976 (New York, USA: IEEE 1976), p. 203-12.

Holmbeck, J. D.
"Standards and the Frequency Control Industry", Programme of the 25th Annual Frequency Control Symposium (abstracts), Atlantic City, NJ, USA, 26-28 Apr 1971, (Fort Monmouth, NJ, USA: US Army Electronics Command 1971), p. 34.

Il'in, V. G., Teverovskii, V. I.
"Design Principles of a Device for Evaluating Time and Frequency Sources", Izmerit. Teckh. (USSR), No. 4, p. 531-5 (April 1969). In Russian. English Translation in: Meas. Tech. (USA), No. 4 (April 1969).

Jenness, C. A., Morris, R. A.
"The Television Colour Burst Signal as a Secondary Frequency Standard", Radio & Electron. Eng. (GB), Vol. 47, No. 12, p. 567-70 (Dec. 1977).

Kramer, G.
"Noise in Passive Frequency Standards", CPEM 74 Digest: Conference on Precision Electromagnetic Measurements, London, England, 1-5 July 1974 (London, England: IEE 1974), p. 157-9.

Kulpinski, R. J.
"Application of Crystal Clocks for Navigation and Time Ordered Communications", Programme of the 25th Annual Frequency Control Symposium (abstracts), Atlantic City, NJ, USA: US Army Electronics Command 1971), p. 18.

Le Fevre, E. N.
"Frequency Standards for H. F. Communications", Proceedings of the 23rd Annual Frequency Control Symposium, Atlantic City, NJ, USA, 6-8 May 1969 (Washington, DC, USA: Electronic Industries Assoc. 1969), p. 198-200.

Loutfy el Sayed, A.
"Frequency Standard Work in Egypt", Proc. IEEE (USA), Vol. 60, No. 5, p. 627-8 (May 1972).

Luckau, H., Sellar, D., Weil, G.
"Integrated Quartz Oscillator Q052", Components Rep. (Germany), Vol. 11, No. 5, p. 162-6 (Nov. 1976).

Malde, M. R., Shahasrabudhe, H. V., Kardile, Y. K., Shah, S. G.
"Digital Clock", J. Inst. Eng. (India) Electron. & Telecommun. Eng. Div., Vol. 53, Pt. ET2, p. 64-8 (Nov. 1972).
(Proceedings of the Seminar on Industrial Electronics, Instrumentation and Control, Baroda, India, 6 Aug. 1972).

McGuigan, D. F., Douglas, D. H.
"Clocks Based upon High Mechanical Q Single Crystals", 31st Annual Frequency Control Symposium, Atlantic City, NJ, USA, 1-3 June 1977 (Washington, DC, USA: Electronic Industries Assoc. 1977).

Miller-Kirkpatrick, J.
"24 Hour Digital Clock with Precision Time Switch", Pract. Wireless (GB), Vol. 53, No. 3, p. 204-9 (July 1977).

Mooser, L.
"Crystal Frequency Standards-Applications and Characteristics", News from Rohde and Schwartz (Germany), Vol. 7, No. 25, 5-8 (1967).

Moynahan, C. F.
"An Improved Crystal Calibrator Using Solid-State Techniques", CQ Radio Amat. J. (USA), Vol. 28, No. 5, p. 18, 20 (May 1972).

Myers, L.
"Understanding Precision Crystal Time Bases", Electronics (USA), Vol. 51, No. 17, p. 114-18 (17 Aug. 1978).

Nazarov, K. I.
"A Transportable Working Frequency Standard", Meas. Tech. (USA), Vol. 17, No. 9, p. 1460-3 (Sept. 1974). Translation of: Izmer Tekh. (USSR), Vol. 17, No. 9, p. 91-3 (Sept. 1974).

Nichols, S.
"A Satellite Frequency Standard System with Digital Control", 1973 National Telecommunications Conference, Vol. I, Atlanta, GA, USA, 26-28 Nov. 1973 (New York, USA: IEEE 1973), p. 19E/1-4.

Nolte, B.
"Patterns of Electronic Luminous Clocks", Electron. Ind. (France), No. 139, p. 775-84 (Dec. 1970). In French.

Nowak, U. Oszczak, S.
"Electronic Corrector of the Digital Quartz Clocks Indications", Postepy Astron. (Poland), Vol. 25, No. 3, p. 187-90 (July 1977) In Polish.

Oakes, J. B., Mauck, R. A.
"A High Stability Crystal Oscillator for the GEOS Spacecraft", Conference on Frequency Generation and Control for Radio Systems, London, 1967 (London: Institution of Electrical Engineers, 1967: Conference Publication No. 31) pp. 53-7.

Penfold, R. A.
"CMOS Crystal Calibrator", Radio & Electron. Constructor (GB), Vol. 30, No. 10, p. 615-21 (May 1977).

Pocza, A.
"Frequency Generators of High Accuracy", Hiradastechnika (Hungary), Vol. 24, No. 2, p. 55-60 (Feb. 1973). In Hungarian.

Pogson, I.
"Frequency Reference Derived from VNG", Electron. Aust. (Australia), Vol. 37, No. 1, p. 42-5, 47, 49 (April 1975).

Prat, M.
"Electronic Clocks and Watches", Rev. Esp. Electron. (Spain), Vol. 21, No. 234, p. 48-50 (May 1974). In Spanish.

Prinz, D.
"A World Time Accessory for Digital Clocks", Funkschau (Germany), Vol. 47, No. 4, p. 63-5 (14 Feb. 1975). In German.

Pustarfi, H. S.
"An Improved 5 MHz Reference Oscillator for Time and Frequency Standard Applications", IEEE Trans. Instrum. Meas. (USA), Vol. IM-15, No. 4, 196-202 (Dec. 1966).

Rayer, F. G.
"1 MHz Crystal Marker", Radio & Electron. Constructor (GB), Vol. 28, No. 1, p. 22-4 (Aug. 1974).

Ronyecz, J., Takacs, J.
"Electronic Clock for the Measurement of Short Times", Fiz. Sz. (Hungary), Vol. 24, No. 3, p. 85-8 (March 1974). In Hungarian.

Rowe, V. J.
"Digital Quartz Clock Module Runs from 12 V", Electron. Aust. (Australia), Vol. 39, No. 2, p. 50-1 (May 1977).

Slabon, W. Ruediger
"Results of Investigations for the Clock Frequency Control and Distribution System in the Digital Telephony and Data Networks of the Deutsche Bundespost and Future Plans", 31st Annual Frequency Control Symposium, Atlantic City, NJ, USA, 1-3 June 1977 (Washington, DC, USA: Electronic Industries Assoc. 1977), p. 455-62.

Saburi, Y.
"Precision of Time Standard and Its Applications", Oyo Buturi (Japan), Vol. 46, No. 12, p. 1203-10 (Dec. 1977). In Japanese.

Schlenk, K. W.
"Electric Clock Installations in Design and Practice", Elektromeister & Dtsch. Elektrohandwerk (Germany), Vol. 51, No. 4, p. 183-6, 199 (Feb. 1976).

Schlenzig, K.
"Crystal-Controlled Clock with Automatic Time Announcement", Radio Fernsehen Elektron. (Germany), Vol. 26, No. 5, p. 168-71 (1977). In German.

Schreiber, H.
"Control of Commercial Clocks by Time-Signal [Radio] Transmitters. I", Funkschau (Germany), Vol. 49, No. 2, p. 96-8 (14 Jan. 1977). In German.

Schreiber, H.
"Radio Controlled Digital Clock with Improved Safety from Disturbances", Funk-Tech. (Germany), Vol. 32, No. 20, p. 358-936 (Oct. 1977). In German.

Sen, A. K., Saha, B.
"Worldwide Standards of Time and Frequency", J. Sci. & Ind. Res. (India), Vol. 32, No. 6, p. 300-11 (June 1973).

Simpson, L.
"Quartz Crystal Drive for Fluorescent Readout Clock", Electron. Aust. (Australia), Vol. 37, No. 6, p. 74-5, 77 (Sept. 1975).

Smagin, A. G.
"Nonthermostated Quartz Generators with an Instability of 10^{-8}", Instrum. & Exp. Tech. (USA), Vol. 18, No. 2, pt. 2, p. 508-10 (March-April 1975). Translation of: Prib. Tekh. Eksp. (USSR), Vol. 18, No. 2, pt. 2, p. 147-9 (March April 1975).

Smagin, A. G.
"A Low-Temperature Oscillator with a Frequency Stability 4 x 10^{-14}", Instrum. & Exp. Tech. (USA), Vol. 18, No. 6, p. 52, p. 1853-5 (Nov.-Dec. 1975). Translation of: Prib. Tekh. Eksp. (USSR), Vol. 18 No. 6, pt. 2, p. 157-9 (Nov.-Dec. 1975).

Smagin, A. G.
"Very Stable Crystal Oscillators Aging Less Than 10^{-10} per Month", Instrum. & Exp. Tech. (USA), Vol. 20, No. 1, pt. 2, p. 188-9 (Jan.-Feb. 1977). Translation of: Prib. Tekh. Eksp. (USSR), Vol. 20, No. 1, pt. 2, p. 166-7 (Jan.-Feb. 1977).

Spadoni, E. R.
"A Versatile Secondary Frequency Standard", CQ Radio Amat. J. (USA), Vol. 31, No. 9, p. 31-2 (Sept. 1975).

Stadler, K.
"Low-Noise Frequency Standard XSS", News Rohde and Schwartz (Germany), Vol. 8, No. 30, p. 22-5 (1968).

Steiner, C.
"From Quartz Clocks to Electronic Quartz Wrist Watches", Jemna Mech. & Opt. (Czechoslovakia), Vol. 15, No. 6, p. 158-60 (1970). In Czech.

Suard, J. G.
"Industrial Aspects of Quartz Clockmaking", Rev. Gen. Electr. (France), Vol. 84, No. 12, p. 931-9 (Dec. 1975). In French.

Uebersfeld, J., Rutman, J.
"Stability Characterization of Frequency Standards", Colloque International sur L'Electronique et la Mesure. (International Conference on Electronics and Measurements), Paris, France, 26-30 May 1975 (Paris France: Comm. d'Organisation du Colloque Internat. sur l'Electronique et la Mesure 1975), p. 101-10. In French.

Veazey, R. L., Nieman, T. A.
"Laboratory Real Time Clock Featuring Computer, Experiment, and Manual Interaction", Anal. Chem. (USA), Vol. 49, No. 9, p. 1466-8 (Aug. 1977).

Viney, K.
"Secondary Standards [Frequency]", Radio Commun. (GB), Vol. 53, No. 11, p. 862-3 (Nov. 1977).

Vovelle, P.
"Technical Aspects of Quartz Clockwork", Rev. Gen. Electr. (France), Vol. 84, No. 12, p. 919-30 (Dec. 1975). In French.

Wilhelmy, H. J.
"New Quartz Clocks", Elektronik (Germany), Vol. 23, No. 7, p. 261-2 (July 1974). In German.

Wilhelmy, H. J.
"Quartz Crystal Clocks and Watches for the Consumer", Elektronik (Germany), Vol. 25, No. 2, p. 67-72 (Feb. 1976). In German.

Yasuda, Y.
"Accuracy of Estimating Clockface and Rate of the Frequency Standards by Normal Regression Theory", Rev. Radio Res. Lab. (Japan), Vol. 19, No. 100, p. 21-30 (Jan. 1973). In Japanese.

Zima, V., Buzek, O., Hrdicka, J., Cermak, J.
"Secondary Frequency Standard Controlled by Radio Signals in the Range of Long Waves and Very Long Waves", Merici Systemy a Jejich Pouziti. (Measuring Systems and Their Applications) EMISCON 73, Brno, Czechoslovakia, Oct. 1973 (Brno, Czechoslovakia,: CSTV House of Technics 1974), p. 314-20 In Czech.

1.9

Al'tshuller, G. B.
"Temperature Compensation for Frequency-Controlled Quartz Oscillators", Telecomm. Radio Engng Pt. 1 (USA), No. 2, 49-51 (1967). Translation of: Elektrosvyaz (USSR), (1967).

Ashida, T.
"Low Temperature Coefficient Lithium Niobate Resonators by Use of Temperature Sensitive Capacitances", Proc. IEEE (USA) Vol. 58, No. 1, p. 146-7 (Jan 1970).

Ballato, A.
"Frequency-Temperature-Load Capacitance Behavior of Resonators for TCXO Application", IEEE Trans. Sonics & Ultrason. (USA), Vol. SU-25, No. 4, p. 185-91 (July 1978).

Batdorf, H. A.
"Temperature-Compensated Crystal-Controlled Oscillators Operating from 800 kHz to 1500 kHz". Proceedings of the 23rd Annual Frequency Control Symposium, Atlantic City, NJ, USA, 6-8 May 1969 (Washington, DC, USA: Electronic Industries Assoc. 1969). p. 192-7.

Berry, B. S., Pritchet, W. C.
"Temperature Compensation for Constant-Frequency Electromechanical Oscillators", IBM Tech. Disclosure Bull. (USA), Vol. 14, No. 4, p. 1237-8 (Sept. 1971).

Bozic, S. M.
"Temperature Compensation of Frequency in Crystal Oscillators Using Varactor Diodes", Electronic Engng. (GB), Vol. 40, No. 490, p. 670-2 (Dec. 1968).

Brekenfeld, H.
"Aspects of Precision Thermostats for Quartz Oscillators", Feingeraete Tech. (Germany), Vol. 24, No. 2, p. 72-6 (Feb. 1975). In German.

Brunner, J.
"Wide-Range Temperature Compensation by Addition of Two Crystal-Resonator Frequencies: Application to Quartz and $LiTaO_3$", Electron. Lett. (GB), Vol. 8, No. 26, p. 639-40 (28 Dec. 1972).

Brunner, J.
"Wide-Range Temperature Compensation by Addition of Two Crystal-Resonator Frequencies: Practical Results with Quartz and $LiTaO_3$", Electron. Lett. (GB), Vol. 11, No. 14, p. 304-5 (10 July 1975).

Buroker, G. E.
"High-Stability Temperature-Compensated Crystal Oscillator Study (HSTCXO)", Report ECOM-0136-1 (AD-738837), Collins Radio Co., Cedar Rapids, Iowa, USA (Jan. 1972), 48 pp. Contract DAAB07-71-C-0136. Available from NTIS, Springfield, VA, 22151, USA.

Buroker, G. E., Frerking, M. E.
"A Digitally Compensated TCXO", Proceedings of the 27th Annual Frequency Control Sypmosium, Cherry Hill, New Jersey, USA, 12-14 June 1973 (Washington DC, USA: Electronic Industries Assoc. 1973), p. 191-8.

Duckett, P., Pedito, R., Chizak, G.
"Temperature Compensated Crystal Oscillators", Proc. 24th Annual Frequency Control Symposium, Atlantic City, NJ, USA, 27-29 April 1970 (Washington, DC, USA: Electronic Industries Assoc. 1970) p. 191-199.

Fewings, D. J., Ince, C. R. S.
"A New Form of Temperature Compensared Crystal Oscillator", Conference on Frequency Generation and Control for Radio Systems, London, (1967) (London: Institution of Electrical Engineers, 1967: Conference Publication No. 31) 38-41.

Fewings, D. J., Ince, C. R.S.
"A Self Compensating Crystal Oscillator", Marconi Rev. (GB), Vol. 31, 57-78 (2nd Qtr. 1968).

Forster, H. J.
"Temperature-Compensated Crystal Oscillators for 2 MHz to 60 MHz", Siemens Rev. (Germany), Vol. 42, No. 12, p. 545-9 (Dec. 1975).

Fujii, S. Uchida, H.
"An Analysis of Frequency Stability for TCXO [Temperature Compensated Crystal Oscillators]", Proceedings of the 29th Annual Frequency Control Symposium, Fort Monmouth, NJ, USA, 28-30 May 1975 (Washington, DC, USA: Electronic Industries Assoc. 1975), p. 294-9.

Fujii, S., Uchida, H.
"Improvement of Frequency Stability for TCXO", NEC Res. & Dev. (Japan), No. 43, p. 75-80 (Oct. 1976).

Grabar, L. I., Stebletsov, V. M.
"Thermal Compensation of Quartz-Crystal Oscillators", Otbor & Peredacha Inf. (USSR), No. 30, p. 90-4 (1971). In Russian.

Grisdale, G. L., Pipe, H. J.
"Miniature Low-Consumption Crystal Ovens", Conference on Frequency Generation and Control for Radio Systems, London, (1967) (London: Institution of Electrical Engineers, 1967: Conference Publication No. 31) 42-6.

Hajek, J.
"Temperature Compensation of a Crystal Oscillator", Sdelovaci Tech. (Czechoslovakia), Vol. 23, No. 4, p. 151 (April 1975). In Czech.

Hamatsuki, T., Goto, T., Uchida, H.
"High Stability Integrator-Controlled Oven for Crystal Oscillators", Proceedings of the 27th Annual Frequency Control Symposium, Cherry Hill, New Jersey, USA, 12-14 June 1973 (Washington DC, USA: Electronic Industries Assoc. 1973), p. 218-26.

Hardingham, C.
"Temperature-Compensated Crystal Oscillators - A Review of Recent Australian Developments", Proc. Instn. Radio Electronics Engrs. Australia, Vol. 28, No. 11, 424-34 (Nov. 1967).

Heile, J.
"VCXO - Theory and Practice", Proc. 29th Annual Frequency Control Symposium, Atlantic City, NJ, USA, 28-30 May 1975 (Washington, DC, USA: Electronic Industries Assoc. 1975), p. 300-307.

Henaff, J., Feldmann, M.
"A SAW Temperature Compensated Oscillator Using the Difference between Metallized and Free Delay Temperature Coefficients on LITAO3", Ultrasonics Symposium Proceedings, Cherry Hill, NJ, USA, 25-27 Sept. 1978 (New York, USA: IEEE 1978), p. 448-451.

Hinnah, H., Newell, D. E.
"Automatic Compensation Equipment for TCXC's", Proc. 22nd Annual Frequency Control Symposium, Atlantic City, NJ, USA, 22-24 April 1968 (Ft. Monmouth, NJ, USA Electronic Components Lab, 1968), p. 298-310.

Hirama, K.
"A Temperature-Compensated Crystal Oscillator Utilizing Three Crystals", Proc. 26th Annual Frequency Control Symposium, Atlantic City, NJ, USA, 6-8 June 1972, (Washington, DC, USA: Electronic Industries Assoc. 1972) p. 132-139.

Hirama, K.
"A Temperature-Compensated Three-Crystal Oscillator", Electron. & Commun. Jap. (USA), Vol. 56, No. 3, p. 33-40 (March 1973).

Hornung, F.
"A New Circuit for Equalizing the Parabolic Temperature Performance of Quartz Oscillators", Frequenz (Germany), Vol. 22, No. 8, p. 223-7 (Aug. 1968). In German.

Hutton-Penman, P. R., Billinshurst, F. M.
"Temperature Control of a Master Oscillator by Deep Burial", Conference on Frequency Generation and Control for Radio Systems, London, (1967) (London: Institution of Electrical Engineers, 1967: Conference Publication No. 31) 64-71.

Ikebe, T.
"Theory of Controlling a Small Thermostatic Oven [Crystal Oscillator Frequency Stability]", Anritsu Tech. Bull. (Japan), No. 33. p. 9-15 June 1975). In Japanese.

Ivanchenko, Yu. S., Medvedev, V. N.
"Computer-Aided Design of Heat-Compensated Quartz-Crystal Oscillators", Izv. VUZ Radioelektron. (USSR), Vol. 21, No. 6, p. 139-42 (June 1978). In Russian.

Jeziorowski, M.
"Analysis of Frequency Variation of Thermally Compensated Oscillators", Pr. Inst. Tele & Radiotech. (Poland), Vol. 16, No. 2, p. 17-28 (1972). In Polish.

Kusters, J. A., Leach, J. G.
"Dual Mode Operation of Temperature and Stress Compensated Crystals", Proc. 32nd Annual Frequency Control Symposium, Atlantic City, NJ, USA, 31 May - 2 June 1978 (Washington, DC, USA: Electronic Industries Assoc. 1978), p. 389-397.

Kwiatkowska, D., Rozwadowski, M.
"Thermostat for Frequency Standards", Pomiary Automat. Kontrol. (Poland), Vol. 16, No. 6, p. 256 (June 1970). In Polish.

Maries, V. A.
"Synthesis and Analysis of an Electric Circuit for the Exact Thermocompensation of Quartz Crystal Oscillators for Three Temperatures", Stud. & Cercet. Energ. & Electroteh. (Rumania), Vol. 24, No. 2, p. 519-30 (1974). In Rumanian.

Maries, V. A.
"Analysis of an Electric Circuit for the Thermo-Compensation of Quartz Crystal Oscillators at Four Temperatures", Rev. Roum. Sci. Tech. Ser. Electrotech. & Energ. (Rumania), Vol. 21, No. 1, p. 75-84 (Jan-March 1976). In English.

Mathieson, P. H.
"Economical Crystal Oven", Electron. Aust. (Australia), Vol. 37, No. 7, p. 77 (Oct. 1975).

McVey, E. S., Swanson, C. T.,
"Capacitor Temperature-Compensated Crystal Oscillators", IEEE Trans. Ind. Electron. & Control Instrum. (USA), Vol. IECI-25, No. 2, p. 164-6 (May 1978).

Michowski, K.
"Computer Aided Design of the Temperature Compensation of Crystal Oscillators", Arch. Elektrotech. (Poland), Vol. 25, No. 2, p. 255-69 (1976). In Polish.

Mroch, A. B., Hykes, G. R.
"A Miniature High Stability TCXO Using Digital Compensation", Proceedings of the 30th Annual Symposium of Frequency Control, Atlantic City, NJ, USA, 2-4 June 1976 (Washington, DC, USA: Electronic Industries Assoc. 1976), p. 292-300.

Nelson-Jones, L.
"Crystal Oven and Frequency Standard", Wireless World (GB), Vol. 76, No. 1416, p. 269-73 (June 1970).

Newell, D. E., Hinnah, H.
"Automatic Compensation Equipment for TCXO's", Proceedings of the 22nd Annual Frequency Control Symposium, Atlantic City, NJ, USA, 22-24 April 1968, (Ft. Monmouth, NJ, USA,: Electronic Components Lab. 1968), p. 298-310.

Newell, D. E., Hinnah, H.
"A Report on TCXO's and Segmented Compensation", Proceedings of the 23rd Annual Frequency Control Symposium, Atlantic City, NJ, USA, 6-8 May 1969 (Washington, DC, USA: Electronic Industries Assoc. 1969), p. 187-91.

O'Connell, R. M., Carr, P. H.
"Temperature Compensated Cuts of Berlinite and β-Eucryptite for SAW Devices", 31st Annual Frequency Control Symposium, Atlantic City, NJ, USA, 1-3 June 1977 (Washington DC, USA: Electronic Industries Assoc. 1977), p. 182-6.

Onoe, M., Yamagishi, I., Hiroshi, N.
"Temperature Compensation of Crystal Oscillator by Microprocessor", Proc. 32th Annual Frequency Control Symposium, Atlantic City, NJ, USA, 31 May - 2 June 1978 (Washington DC, USA: Electronic Industries Assoc. 1978), p. 398-402.

Page, P. B.
"Temperature Compensation of Quartz Crystal Oscillators", Conference on Frequency Generation and Control for Radio Systems, London, (1967) (London: Institution of Electrical Engineers, 1967: Conference Publication No. 31) 33-7.

Page, P. B.
"Wide Range Temperature Compensation of Miniature Quartz Crystal Oscillators", Electron Compon. (GB), Vol. 13, No. 1, p. 22, 4-6 (14 Jan. 1972).

Page, P. B.
"Wide Range Temperature Compensation of Miniature Quartz Crystal Oscillators", Electron. Compon. (GB), Vol. 13, No. 8, p. 381-4 (21 April 1972).

Page, P. B.
"Wide Range Temperature Compensation of Miniature Quartz Crystal Oscillators. III. Compensating Circuit Synthesis", Electron. Compon. (GB), Vol. 13, No. 9, p. 429-31 (5 May 1972).

Page, P. B.
"Wide Range Temperature Compensation for Miniature Quartz Oscillators. I.", Elektron. Anz. (Germany), Vol. 6, No. 10, p. 203-5 (Oct. 1974).

Pichl, H.
"Design of High Quality Thermostats for Crystal Oscillators", Int. Elektron. Rundsch. (Germany), Vol. 25, No. 10, p. 249-51 (Oct. 1971). In German.

Podgorski, A. Gniewinska, B.
"Automatic Production of Thermally Compensated Quartz Generators", Pol. Tech. Rev. (Poland), No. 7, p. 12-13 (1977).

Pogson, I.
"Temperature Compensated Crystal Oscillator", Electron. Aust. (Australia), Vol. 39, No. 5, p. 80-1, 83 (Aug. 1977).

Pompei, J., Kerforne, J. F.
"A Temperature-Compensated Quartz Oscillator", Onde Elect. (France), Vol. 50, No. 514, p. 32-7 (Jan. 1970). In French.

Prak, J. W. L., Peduto, R. J.
"Digital ICs Set Temperature Compensation for Oscillators", Electronics (USA), Vol. 45, No. 17, p. 124-6 (14 Aug. 1972).

Pupeza, D., Maries, V.
"Thermal Compensation of Quartz Oscillators", Electroteh. Electron. & Autom. Autom. & Electron. (Rumania), Vol. 19, No. 4, p. 170-4 (Dec. 1975). In Rumanian.

Roberts, E. A.
"Temperature Compensation of AT Cut Crystals by Thermally Controlled Non-Linear Reactances", Proceedings of the 22nd Annual Frequency Control Symposium, Atlantic City, NJ, USA, 22-24 Apr. 1968 (Fort Monmouth, NJ, USA: Electronic Components Lab. 1968), p. 325-39.

Rozwadowski, M.
"Application of Crystal Oscillators in Modern Telecommunication Equipments", Przegl. Telekomun. (Poland), Vol. 51, No. 5, p. 147 (1978). In Polish.

Sarkar, S. K.
"Explicit Expressions for TCXO [Temperature-Compensated Crystal Oscillator] Design", Proceedings of the 28th Annual Frequency Control Symposium 1974, Atlantic City, NJ, USA, 29-31 May 1974 (Washington, DC, USA: Electronic Industries Assoc. 1974), p. 232-6.

Schodowski, S.
"New Approach to a High Stability Temperature Compensated Crystal Oscillator", Proc. 24th Annual Frequency Control Symposium, Atlantic City, NJ, USA, 27-29 April 1970 (Washington, DC, USA: Electronic Industries Assoc. 1970), p. 200-208.

Scott, P. J.
"Design Considerations for a Digitally Temperature Compensated Crystal Oscillator", 31st Annual Frequency Control Symposium, Atlantic City, NJ, USA, 1-3 June 1977 (Washington, DC, USA: Electronic Industries Assoc. 1977), p. 407-11.

Smirnov, V. I.
"Method of Compensating the Temperature Instability of the Frequency of a Crystal-Controlled Oscillator", Radiotekhnika (USSR), p. 134-6. In Russia. English translation in: Telecommun. & Radio Eng. Pt2 (USA) Vol. 25, No. 10 (Oct. 1970).

Smith, D. A., Holmes, P. A.
"Temperature Compensated Crystal Oscillators", Electron. Equip. News (GB), Vol. 13, No. 4, p. 14-19 (July-Aug. 1971).

Soluch, W.
"Piezoelectric Crystals", Elektronika (Poland), Vol. 19, No. 1, p. 8-12 (1978). In Polish.

Thomann, D. L.
"A Microcircuit Temperature Compensated Crystal Oscillator (MCTCXO)", Proceedings of the 28th Annual Frequency Control Symposium 1974, Atlantic City, NJ, USA, 29-31 May 1974 (Washington, DC, USA: Electronic Industries Assoc. 1974), p. 214-20.

Vasil'yev, Yu. A., Il'ichev, V. A., Chernobylkin, V. V.
"Optimizing the Resistances of Resistors in Temperature-Compensating Networks for Crystal Oscillators", Telecommun. & Radio Eng. Part 2 (USA), Vol. 32, No. 6, p. 143-4 (June 1977). Translation of:Radiotekhnika, Moskva (USSR), Vol. 32, No. 6, p. 105-6 (June 1977).

Vovelle, P. G.
"Recent Improvements to TCXO", Proceedings of the 22nd Annual Frequency Control Symposium, Atlantic City, NJ, USA, 22-24 Apr. 1968 (Fort Monmouth, NJ, USA: Electronic Components Lab. 1968), p. 311-24.

Whitten, S. V., Jr.
"A Practical Approach to the Design of a Temperature Compensated Crystal Oscillator", National Telemetering Conference Record, Washington, DC, USA, 12-15 April 1971 (New York, USA: IEEE 1971), p. 54-9.

2.1

Alekseev, E. I., Bazarov, E. N.
"Light-Induced Shifts of a Quantum Frequency Standard with Optical Pulse Pumping and Optical Display of a Ramsey Line with Suppressed Side Maxima [^{87} Rb]", Sov. J. Quantum Electron. (USA), Vol. 5, No. 5, p. 563-7. Translation of: Kvantovaya Elektron., Moskva (USSR), Vol. 2, No. 5, p. 1035-42 (May 1975).

Allan, D. W., Barnes, J. A.
"Modeling and Optimum Utilization of High Performance Clocks", CPEM 74 Digest: Conference on Precision Electromagnetic Measurements, London, England, 1-5 July 1974 (London, England: IEE 1974), p. 277-8.

Annabi, M., Gillet, D.
"Adiabatic Passage on the Electric Dipole Transitions of a Molecular Beam Traversing an Inhomogenous Magnetic Field", C. R. Hebd. Seances Acad. Sci. B (France), Vol. 277, No. 18, p. 515-17 (5 Nov. 1973). In Franch.

Audoin, C.
"State of the Art in the Field of Very Stable Frequency Generators", Onde Electr. (France), Vol. 53, No. 2, p. 39-45 (Feb. 1973). In French.

Audoin, C.
"Ultrastable Atomic and Molecular Oscillators and Their Applications in Navigation", Navigation (France), Vol. 21, No. 83, p. 281-97, (July 1973) In French.

Audoin, C., Vanier, J.
"Atomic Frequency Standards and Clocks", J. Phys. E (GB), Vol. 9, No. 9, p. 697-720 (Sept. 1976).

Bahadur, H., Parshad, R.
"Atomic Frequency Standards-a Review", J. Sci. & Ind. Res. (India), Vol. 33, No. 11, p. 561-9 (Nov. 1974).

Balogh, F.
"Frequency Standards", Meres & Autom. (Hungary), Vol. 22, No. 11, p. 417-21 (1974). In Hungarian.

Barnes, J. A.
"Frequency Measurement Errors of Passive Resonators Caused by Frequency-Modulated Exciting Signals", IEEE Trans. Instrum. Meas. (USA), Vol. IM-19, No. 3, p. 147-52 (Aug. 1970).

Barnes, J. A., Winkler, G. M. R.
"The Standards of Time and Frequency in the USA", Report NBS-TN-649, Nat. Bur. Stand., Washington, DC, USA (Feb. 1974), 86 pp.

Bashkin, A. S.
"Current Status and Development Prospects of Quantum Frequency Standards (Review)", Kvantovaya Elektron. (USSR), No. 5, p. 3-27 (1971). In Russian.

Basov, N. G., Prokhorov, A. M.
"Possible Methods of Obtaining Active Molecules for a Molecular Oscillator", In book: Maser, the Solid State, p. 114-16, Oxford, England: Pergamon (1970), ix + 283 pp. [08 0068 18 9].

Chachulski, A.
"Atomic Frequency Standards", Pol. Tech. Rev. (Poland), No. 10, p. 2-3 (1975).

Chi, A. R., Major, F. G., Lavery, J. E.
"Frequency Comparison of Five Commercial Cesium Standards with a NASA Experimental Hydrogen Maser", Proc. IEEE (USA), Vol. 58, No.1, p. 142-3 (Jan. 1970).

Clemence, G. M., Szebehely, V.
"Measurement of Small Density Differences: Solutions of Slightly Soluble Gases", Astron. J. (USA), Vol. 72, No. 1355, 1324-6 (Dec. 1967).

Cordwell, C. R.
"Frequency Standards", Vacation school on electrical measurement practice, Manchester, England, 15-26 July 1968 (London: Institution of Electrical Engineers 1968), 14 pp.

Cutler, L. S., Vessot, R. F. C.
"Present Status of Clocks and Frequency Standards" 1968 NEREM Record, Boston, Mass, 6-8 Nov. 1968 (New York: IEEE 1968), p. 68-9.

Elkin, G. A.
"Effect of Output-Signal-Spectrum Sidebands and Resonator Detuning on the Frequency of an Atomic Standard", Meas. Tech. (USA), Vol. 19, No. 11, p. 1587-8 (Nov. 1976). Translation of: Izmer. Tekh. (USSR), Vol. 19, No. 11, p. 35-6 (Nov. 1976).

Essen, L.
"Atomic Standards of Time", Alta Freq. (Italy), Vol. 40, No. 8, p. 679-87 (Aug. 1971). In English.

Fukuyo, H.
"Time and Frequency Standards", J. Soc. Instrum. & Control Eng. (Japan), Vol. 14, No. 7, p. 521-8 (July 1975). In Japanese.

Ganter, W. A.
"Modeling of Atomic Clock Performance and Detection of Abnormal Clock Behavior", Report NBS-TN-636, Nat. Bur. Stand., Washington, DC, USA (March 1973), 30 pp.

Glaze, D. J., Hellwig, H., Allan, D. W., Jarvis, S., Jr., Wainwright, A. E.
"Accuracy Evaluation and Stability of NBS Primary Frequency Standards", IEEE Trans. Instrum. & Meas. (USA), Vol. IM-23, No. 4, p. 489-501 (Dec. 1974). (1974 Conference on precision electromagnetic measurements, London, England, 1-5 July 1974).

Hahn, S. L., Radecki, K. W.
"Features of a Silver Beam Magnetic Resonance Apparatus as a Frequency Standard", CPEM Digest 1978. Conference on Precision Electromagnetic Measurements, Ottawa, Canada, 26-29 June 1978 (New York, USA: IEEE 1978), p. 13-15.

Hall, J. L.
"Problems of Atomic Frequency Standards of Extreme Accuracy and a New Atomic Beam Interaction Geometry", Opt. Commun. (Netherlands), Vol. 18, No. 1, p. 62-3 (July 1976). (9th International Conference on Quantum Electronics. (Digest). Amsterdam. Netherlands, 14-18 June 1976).

Hellwig, H.
"Areas of Promise for the Development of Future Primary Frequency Standards", Metrologia (Germany), Vol. 6, No. 4, p. 118-26 (Oct. 1970).

Hellwig, H.
"Frequency Standards and Clocks. A Tutorial Introduction", Report NBS-TN-616, Nat. Bur. Stand., Washington, DC, USA (April 1972), 65 pp.

Hellwig, H., Jarvis, S., Jr., Halford, D., Bell, H.E.
"Evaluation and Operation of Atomic Beam Tube Frequency Standards Using Time Domain Velocity Selection Modulation", Metrologia (Germany), Vol. 9, No. 3, p. 107-12 (Sept. 1973).

Hellwig, H.
"Status Report on Primary Frequency Standards", Report NBS-TN-646, Nat. Bur. Stand., Washington, DC, USA (Sept. 1973). 12 pp.

Hellwig, H.
"Atomic Frequency Standards: a Survey", Proceedings of the 28th Annual Frequency Control Symposium 1974, Atlantic City, NJ, USA, 29-31 May 1974 (Washington, DC, USA: Electronic Industries Assoc. 1974), p. 315-39.

Hellwig, H. W.
"Atomic Frequency Standards: a Survey", Proc. IEEE (USA), Vol. 63, No. 2, p. 212-29 (Feb. 1975).

Hellwig, H.
"Design Principles and Characteristics of Frequency and Time Standards", IEEE Trans. Nucl. Sci. (USA), Vol. NS-23, No. 6, p. 1629-35 (Dec. 1976). (IEEE Annual Conference on Nuclear and Space Radiation Effects, San Diego, Calif., USA, 27-30 July 1976).

Ivanov, N. I.
"Short-Term Frequency Instability of the Frequency Synthesizer in an Atomic Clock", Meas. Tech. (USA) Vol. 18, No. 2, p. 248-51 (Feb. 1975). Translation of: Izmer. Tekh. (USSR), Vol. 18, No. 2, p. 55-6 (Feb. 1975).

Ivanov, N. I., Leikin, A. Ya., Fertik, N. S.
"Fluctuations in Atomic Clocks", Meas. Tech. (USA) Vol. 18, No. 3, p. 389-90 (March 1975). Translation of: Izmer. Tekh. (USSR), Vol. 18, No. 3, p. 44-5 (March 1975).

Jespersen, J., Fitz-Randolph, J.
"From Sundials to Atomic Clocks", Washington, DC USA: Nat. Bur. Standards (1977), vii + 175 pp.

Kartaschoff, P., Barnes, J. A.
"Standard Time and Frequency Generation", Proc. IEEE (USA), Vol. 60, No. 5, p. 493-501 (May 1972).

Koshel'kov, V. A., Krochik, G. M.
"The Use of a Four-Pass Winding as the Sorting System for a Molecular Generator", Radio Eng. & Electron. Phys. (USA), p. 854-7 (May 1972). Translation of: Radiotekh. & Elektron. (USSR), Radio Eng. & Electron. Phys. (USA), p. 1095-7.

Koshel'kov, V. A.
"On Increasing the Number of Active Molecules in a Molecular Oscillator", Radio Eng. & Electron. Phys. (USA), Vol. 20, No. 5, p. 145-6 (May 1975). Translation of: Radiotekh. & Elektron. (USSR), Vol. 20, No. 5, p. 1107-9 (May 1975).

Kramer. G.
"Noise in Passive Frequency Standards", CPEM, 74 Digest: Conference on Precision Electromagnetic Measurements, London, England, 1-5 July 1974 (London, England: IEE 1974), p. 157-9.

Lender, R., Szepan, R.
"Standard-Frequency-Controlled Digital Clock for High Precision Time Measurements", Nachr. Elektron (Germany), Vol. 32, No. 7, p. 217-19 (July 1978). In German.

Leschiutta, S.
"Atomic Frequency Standards", Elettrotecnica (Italy), Vol. 59, No. 3 [illegible], p. 3[illegible]-8 (March 1972). In Italian.

Leschiutta, S., Strumia, F.
"Atomic Frequency Standards", Alta Freq. (Italy), Vol. 43, No. 10, p. 844-8 (Oct. 1974).

Logachev, V. A., Morozov, V. N., Savva, V. A., Strakhovskii, G. M.
"The Properties of a Molecular Generator in Magnetic Field", Radiotekhnika I Elektronika (USSR), Vol. 13, No. 11, p. 2011-18 (Nov. 1968). In Russian. English translation in: Radio Engng. Electronic Phys. (USA).

McCoubrey, A., Cutler, L.
"Twenty Years of Progress in Atomic Frequency Standards", Proc. 26th Annual Frequency Control Symposium, Atlantic City, NJ, USA, 6-8 June 1972 (Washington, DC, USA: Electronic Industries Assoc. 1972), p. 202-210.

Mehta, A.
"Maser", J. Inst. Eng. (India) Electron. & Telecommun. Eng. Div., Vol. 55, No. ET2-3, p. 47-50 (April 1975).

Meles, H. P.
"The Atomic Standard Aspect", Conference on Frequency Generation and Control for Radio Systems, London, (1967) (London: Institution of Electrical Engineers, 1967: Conference Publication No. 31) 21-3.

Mungall, A. G.
"Atomic Time Standards and Time Scales in Canada", International Electrical, Electronics Conference and Exposition, Toronto, Canada, 26-28 Sept. 1977 (New York, USA: IEEE 1977), p. 118-19.

Percival, D. B.
"A Heuristic Model of Long-Term Atomic Clock Behaviour", Proceedings of the 30th Annual Symposium on Frequency Control, Atlantic City, NJ, USA, 2-4 June 1976 (Washington, DC, USA: Electronic Industries Assoc. 1976), p. 414-19.

Percival, D. B.
"Prediction Error Analysis of Atomic Frequency Standards", 31st Annual Frequency Control Symposium, Atlantic City, NJ, USA, 1-3 June 1977 (Washington, DC, USA: Electronic Industries Assoc. 1977), p. 319-26.

Ramsey, N.
"History of Atomic and Molecular Control of Frequency and Time", 25th Annual Frequency Control Symposium, Atlantic City, NJ, USA, 26-28 April 1971 (Washington, DC, USA: Electronic Industries Association 1971), p. 46-57.

Ramsey, N.
"History of Atomic and Molecular Standards of Frequency and Time", IEEE Trans. Instrum. & Meas. (USA), Vol. IM-21, No. 2, p. 90-9 (May 1972).

Reinhardt, V. S., Lavanceau, J.
"A Comparison of the Cesium and Hydrogen Hyperfine Frequencies by Means of Loran-C and Portable Clocks", Proceedings of the 28th Annual Frequency Control Symposium 1974, Atlantic City, NJ, USA, 29-31 May 1974 (Washington, DC, USA: Electronic Industries Assoc. 1974), p. 379-83.

Risley, A. S.
"The Physical Basis of Atomic Frequency Standards", Report TN 399, Nat. Bur. Stand., Washington, DC, USA (April 1971), 54 pp.

Ritz, V. H., Bermudez, V. M., Folen, V. J.
"Characterization of Degraded Hydrogen Dissociator Envelopes by AES [w.r.t. Atomic Clocks]", J. Appl. Phys. (USA), Vol. 48, No. 5, p. 2096-8 (May 1977).

Sadovskii, A. B., Pashev, G. P., Zeuv, E. V., Pikhtelev, A. I.
"Atomic Clocks and the Time Errors of Adjustable Electronic Clocks", Meas. Tech. (USA), Vol. 18, No. 3, p. 391-2 (March 1975). Translation of: Izmer. Tekh. (USSR). Vol. 18, No. 3, p. 45-6 (March 1975).

Sazhin, V. V., Il'in, V. G.
"New USSR State Time and Frequency Standards", Piroda (USSR), No. 8, p. 16-27 (Aug. 1977). In Russian.

Schuessler, H. A.
"The Ion Storage Tube, a Proposal for a New Atomic Frequency Standard", Metrologia (Germany), Vol. 7 No. 3, p. 103-7 (July 1971).

Schutz. K.
"The Efficiency of Atomic Frequency Standards", Frequenz (Germany), Vol. 22, No. 8, p. 229-25 (Aug. 1968). In German.

Steiner, C.
"Atomic Clocks", Schweiz. Tech, Z (STZ) (Switzerland), Vol. 66, No. 5, p. 61-71 (30 Jan. 1969). In French.

Strumia, F.
"Analysis of New Microwave and Optical Frequency Standards Based on Ions Storage", Proc. 32nd Annual Frequency Control Symposium, Atlantic City, NJ, USA, 31 May-2 June 1978 (Washington, DC, USA: Electronic Industries Association 1978), p. 444-452.

Terrien, J.
"Standards of Length and Time", Rep. Prog. Phys. (GB), Vol. 39, No. 11, p. 1067-108 (Nov. 1976).

Vaillancourt, R., Missout, G., Tetu, M., Vanier, J.
"Study of Atomic Clocks (and Masers)", Abstracts of papers of the 38th ACFAS Congress, Quebec, Canada, 16-17 Oct. 1970 (Quebec, Canada: ACFAS 1970), p. 42. In French.

Vanier, J., Tetu, M, Bernier, L. G.
"Transfer of Frequency Stability from an Atomic Frequency Reference to a Quartz Crystal Oscillator" Proc. 32nd Annual Frequency Control Symposium, Atlantic City, NJ, USA, 31 May-2 June 1978 (Washington, DC, USA: Electronic Industries Association 1978), p. 520-526.

Vessot, R., Peters, H., Vanier, J., Beehler, R., Halford, D., Harrach, R., Allan, D., Glaze, D., Snider, C., Barnes, J., Cutler, L. Bodily, L.
"An Intercomparison of Hydrogen and Cesium Frequency Standards", IEEE Trans. Instrum. Meas. (USA), Vol. IM-15, No. 4, 165-76 (Dec. 1966). [Conference on Precision Electromagnetic Measurements, Boulder, 1966].

Viennet, J., Audoin, C., Desaintfuscien, M.
"Discussion of Cavity Pulling in Passive Frequency Standards", Programme of the 25th Annual Frequency Control Symposium (abstracts), Atlantic City, NJ, USA, 26-28 Apr. 1971 (Fort Monmouth, NJ, USA: US Army Electronic Command 1971) p. 54.

Viennet, J., Audoin, C., Desaintfuscien, M.
"Cavity Pulling in Passive Frequency Standards", IEEE Trans. Instrum. & Meas. (USA), Vol. IM-21, No. 3, p. 204-9 (Aug. 1972).

Walls, F. L., Wineland, D. J., Orullinger, R. E.
"New Possibilities for Frequency Standards Using Laser Cooling", Proc. 32nd Annual Frequency Control Symposium, Atlantic City, NJ, USA, 31 May-2 June 1978, (Washington, DC, USA: Electronic Industries Association 1978), p. 453-459.

Zhabotinskii, M. Ye.
"Quantum Frequency Standards", Radiotekhnika i Elektronika (USSR), Vol. 12, No. 11, 2023-31 (Nov. 1967). In Russian. English translation in: Radio Engng. Electronic Phys. (USA).

Zholnerov, V. S., Korniyenko, V. V.
"On Optimizing the Parameters of the Static Automatic Frequency Control System of a Passive Quantum Frequency Standard in Terms of the Accuracy Characteristics", Radio Eng. & Electron. Phys. (USA), Vol. 21, No. 1, p. 106-9 (Jan. 1976). Translation of: Radiotekh. & Elektron. (USSR), Vol. 21, No. 1, p. 145-9 (Jan. 1976).

Abashev, Yu. G.
"Velocity Distribution in an Atomic Beam", Meas. Tech. (USA), Vol. 15, no. 11, p. 1679-81 (Nov. 1972). Translation of: Izmer. Tekh. (USSR), Vol.15 no. 11, p. 53-5 (Nov. 1972).

Abashev, Yu. G., Voronin, G.F., Nul'chatskii, N.A.
"Investigation of the Angular Distribution of Cesium Atoms Diffusing from Rectangular Channels" (time-frequency standard). Meas. Tech. (USA), Vol. 19, no. 11, p. 1590-4 (Nov, 1976). Translation of: Izmer. Tekh (USSR), Vol 19, no. 11, p. 37-9 (Nov. 1976).

Allan, D. W., Glaze, D. J., Machlan, H.E., Wainwright, A. E., Hellwig, H., Barnes, J. A., Gray, J. E.,
"Performance, Modeling, and Simulation of Some Cesium Beam Clocks",
Proceedings of the 27th Annual Frequency Control Symposium, Cherry Hill, NJ, 12-14 June 1973 (Washington, D.C., USA, Electronic Industries Assoc. 1973), p 334-46.

Allan, D.W., Hellwig, H., Jarvis, S., Jr, Howe, D.A., Garvey, R. M.
"Some Causes and Cures of Frequency Instabilities (Drift and Noise) in Cesium Beam Frequency Standards."
Proceedings of the 31st Annual Frequency Control Symposium, Atlantic City, NJ, 1-3 June 1977, (Washington, DC, USA Electronics Industries Assoc. 1977). p. 555-61.

Andresen, S.G., Mortelmaus, H. O., Wauters, P.J., De Prins, J.
"Some Experimental Results of BaO Applicable to a Molecular Beam Frequency Standard"
Proc. 22nd Annual Frequency Control Symposium, Atlantic City, N.J., USA, 22-24 April, 1968, (Ft. Monmouth, NJ, USA: Electronic Components Laboratory, 1968), p. 517-528

Audoin, C., Lesage, P., Mungall, A. G.
"Second Order Doppler and Cavity Phase Dependent Frequency Shifts in Atomic Beam Frequency Standards."
CPEM 74 Digest: Conference on Precision Electromagnetic Measurements, London, England, 1-5 July 1974 (London, England: IEE 1974), p. 16[illegible]-1

Audoin, C, Leasage, P., Mungall, A. G.
"Second-order Doppler and Cavity Phase Dependent Frequency Shifts in Atomic Beam Frequency Standards"
IEEE Trans. Instrum. & Meas. (USA), Vol. IM-23, no. 4, p. 501-8 (Dec. 1974), (1974 Conference on precision electromagnetic measurements, London, England, 1-5 July 1974).

Audoin, C., Jardino, M.
"Frequency Offset Due to Spectral Impurities in Cesium Beam Frequency Standards".
CPEM Digest 1978, Conference on Precision Electromagnetic Measurements, Ottawa, Canada, 26-29 June 1978 (New York, USA: IEEE 1978), p. 4

Bailey, R, Mungall, A. G., Daams, H.
"The Design, Construction, and Performance of a Cesium-beam Tube".
IEEE Trans Instrum. Meas. (USA), Vol IM-16, no. 4, 319-26 (Dec.1967)

Beehler, R. E.
"Cesium Atomic Beam Frequency Standards"
Programme of the 25th annual frequency control symposium (abstracts), Atlantic City, N. J., USA, 26-28 Apr 1971 (Fort Monmouth, NJ, USA: US Army Electronic Command 1971), p. 49.

Becker, G., Fischer, B., Kramer, G., Muller, E. K.
"The Primary Time and Frequency Standard of the Physikalisch-Technische Bundesanstalt."
Eurocon 71 digest, Lausanne, Switzerland, 18-22 Oct 1971 (New York, USA: IEEE 1971), 1pp.

Becker, G.
"Work on Primary Cs Beam Frequency Standards at the PTB".
1976 Conference on Precision Electromagnetic Measurements, Boulder, Colo., USA, 28 June - 1 July 1976 (New York, USA: IEE 1976), p. 226-7

Becker, G.
"Recent Progress in Primary Cs Beam Frequency Standards at the PTB"
IEEE Trans, Instrum. & Meas. (USA), Vol. IM-25, no. 4, p. 458-65 (Dec. 1976) (1976 Conference on Precision Electromagnetic Measurements, Boulder, Colo., USA 28 June - 1 July 1975)

Becker, G.
"Performance of the Primary Cs-Standard of the Physikalisch-Technische Bundesanstalt"
Metrologia (Germany), Vol. 13, no. 3, p. 99-104 (received: June 1977)

Becker, G.
"Research on Primary Cs-Beam Time and Frequency Standard at the PTB."
CPEM Digest 1978. Conference on Precision Electromagnetic Measurements, Ottawa, Canada, 26-29 June 1978 (New York, USA: IEEE 1978), p. 1-2

Beehler, R.
"Cesium Beam Frequency Standards"
Proc. 25th Annual Frequency Control Symposium, Atlantic City, NJ, USA, 26-29 April 1971 (Washington, D.C., USA: Electronic Industries Association 1971) p. 297-303

Beli, C. M., Babitch, D.
"A System Analysis of the Cesium Beam Atomic Clock", IEEE Trans. Instrum. Meas. (USA), Vol. IM-17, No. 2, 155-66.

Bonsch, G.
"Wavelength Intercomparison Between Methane- and Iodine-Stabilized He-Ne Lasers: Alignment and Error Estimations".
Informative Meeting on Iodine Stablised He-Ne Lasers, Germany, 10-11 Feb. 1977 (Braunschweig, Germany: Physikalisch-Technische Bundesanstalt 1977), p. 151-8

Cerez, P., Bennett, S. J.
"New Developments in Iodine Stabilized He-Ne Lasers"
CPEM Digest 1978. Conference on Precision Electromagnetic Measurements, Ottawa, Canada, 26-29 June 1978 (New York, USA: IEEE 1978), p. 72.

Chartier, J. M., Avrons, D.
"Technological Principles of Iodine Stablized He-Ne Lasers"
Informative Meeting on Iodine Stablised He-Ne Lasers, Germany, 10-11 Feb. 1977 (Braunschweig, Germany: Physikalisch-Technische Bundesanstalt 1977) p. 13-31 In French.

Chartier, J. M., Avrons, D.
"International Comparisons of Iodine Stabilized He-Ne Lasers".
Informative Meeting on Iodine Stabilized He-Ne Lasers, Germany, 10-11 Feb. 1977 (Braunschweig, Germany: Physikalisch-Technische Bundesanstalt 1977), p. 133-8 In French.

Daams, H.
"Cesium Beam Servo System Using Square Wave Frequency Modulation"
Proc. 24th Annual Frequency Control Symposium, Atlantic City, N.J., USA, 27-29 April 1970 (Washington, D.C., USA, Electronic Industries Association 1970), p. 294-300

Daams, H.
"Corrections for Second Order Doppler Shift and Cavity Phase Error in Cesium Atomic Beam Frequency Standards".
CPEM 74 Digest: Conference on Precision Electromagnetic Measurements, London, England, 1-5 July 1974 (London, England: IEE 1974), p 162-3

Daams, H.
"Corrections for Second-Order Doppler Shift and Cavity Phase Error in Cesium Atomic Beam Frequency Standards".
IEEE Trans. Instrum. & Meas. (USA), Vol. IM-23, no. 4, p. 509-14 (Dec. 1974). (1974 Conference on precision electromagnetic measurements, London, England, 1-5 July 1974).

Daams, H.
"Errors in Cesium Beam Frequency Standards Due to Small Asymmetries in the Beam Excitation".
1976 Conference on Precision Electromagnetic Measurements, Boulder, Colo., USA, 28 June - 1 July 1976 (New York, USA: IEEE 1976). p. 235-6

Dittmann,H.,Kalau, M.
"The National Time and Frequency Standard of the German Democratic Republic."
Radio Fernsehen Elektron. (Germany), vol. 27, no.6, p. 381-2 (1978). In German.

Elkin, G. A.
"Effect of Output-Signal-Spectrum Sidebands and Resonator Detuning on the Frequency of an Atomic Standard".
Meas. Tech. (USA), Vol. 19, no. 11, p. 1587-8 (Nov. 1976). Translation of: Izmer. Tekh (USSR), Vol. 19, no. 11, p. 35-6 (Nov. 1976).

Elkin, G. A.
"Doppler Frequency Shift in Atomic Standards".
Meas. Tech. (USA), Vol. 19, no. 11, p. 1594-6 (Nov. 1976). Translation of Izmer. Tekh (USSR). Vol. 19, no. 11, p. 40-1 (Nov. 1976)

Ermakov, V. I., Zemskov, E. M., Sachkov, V. I.
"Certain Errors in Reproducing the Frequency of a Cesium Reference Standard, Which are due to the Electronic Equipment".
Izmerit Tekh, (USSR), 1966, No. 9, 54-7 (Sept.). In Russian. English translation in: Meas. Tech. (USA), 1966, No. 9, 1177-81 (Sept.).

Essen, L., Sutcliffe, D. S.
"Improvement to the National Physical Laboratory Atomic Clock".
Nature (GB), Vol. 223, no. 5206, p. 602-3 (9 Aug. 1969)

Fischer, M.C., Heger, C. E.
"Measured Performance and Environmental Sensitivities of a Rugged Cesium Beam Frequency Standard".
Proceedings of the 30th Annual Symposium on Frequency Control, Atlantic City, N. J., USA, 2-4 June 1976 (Washington, D.C., USA: Electronic Industries Assoc. 1976), p. 463-7

George, J., Vulcan, A. I.
"Development of a Cesium Beam Clock for Satellite Application"
31st Annual Frequency Control Symposium, Atlantic City, NJ, USA, 1-3 June 1977 (Washington, DC, USA: Electronic Industries Assoc. 1977), p. 542-50

Giacomo, P.
"Length Metrology and Iodine Stablized Lasers."
Informative Meeting on Iodine Stabilised He-Ne Lasers, Germany, 10-11 Feb. 1977 (Braunschweig, Germany: Physikalisch-Technische Bundesanstalt 1977) p. 9-11 In French.

Glaze, D. J.
"Improvements in Atomic Cesium Beam Frequency Standards at the National Bureau of Standards"
IEEE Trans. Instrum. Meas. (USA). vol. IM-19, no.3, p. 156-60 (Aug. 1970).

Glaze, D. J., Hellwig, H., Jarvis, Jr.,S.
Wainwright, A. E., Allan, D. W.
"Recent Progress on the NBS Primary Frequency Standard".
Proceedings of the 27th Annual Frequency Control Symposium, Cherry Hill, N. J., USA, 12-14 June 1973 (Washington, D.C., USA: Electronic Industries Assoc. 1973), p. 347-56

Glaze, D. J., Hellwig, H., Allan, D. W., Jarvis,Jr., S., Wainwright, Bell, H. E.
"Accuracy Evaluation and Stability of the NBS Primary Frequency Standards".
CPEM 74 Digest: Conference on Precision Electromagnetic Measurements, London, England, 1-5 July 1974 (London, England: IEE 1974), p.155-6

Glaze, D.J., Hellwig, H., Allan, D. W., Jarvis,Jr., S.
"NBS-4 and NBS-6: The NBS Primary Frequency Standards".
Metrologia (Germany), Vol 13, no. 1, p. 17-28 (1977)

Graf, E., Johnson., L. F., Kern, R. H.
"A New Compact Cesium Beam Frequency Standard".
Proceedings of the 29th Annual Frequency Control Symposium, Fort Monmouth, NJ, USA, 28-30 May 1975, (Washington, D.C., USA: Electronic Industries Assoc. 1975), p. 352-6

Granveaud, M., Azoubib, J.
"TAI (temps atomique international) Frequency".
1976 Conference on Precision Electromagnetic Measurements, Boulder, Colo., USA, 28 June - 1 July 1976 (New York, USA: IEEE 1976), p. 230

Granveaud, M., Azoubib, J.
"TAI Frequency".
IEEE Trans. Instrum. & Meas. (USA), Vol. IM-25, no. 4, p. 469-72 (Dec. 1976) (1976 Conference on Precision Electromagnetic Measurements, Boulder, Colo., USA, 28 June - 1 July 1976)

Gregory, T. K.
"New Cesium Beam Frequency Standards for Flight and Ground Applications.
31st Annual Frequency Control Symposium, Atlantic City, NJ, USA, 1-3 June 1977 (Washington, DC., USA: Electronic Industries Assoc. 1977) p. 551-4

Hahn, S., Chachulski, A., Kunski, R.
"Atomic Caesium Frequency Standard".
Arch. Elektrotech. (Poland), Vol. 16, No. 4, 841-55 (1967) In Polish.

Hahn, S. L., Radecki, K. W.
"Design and Preliminary Experiments with a Silver Beam Atomic Clock".
CPEM 74 Digest: Conference on Precision Electomagnetic Measurements, London, England, 1-5 July 1974, (London, England: LEE 1974), p. 166-8 (6 refs.)

Heger, C.E., Hyatt, R.C., Seavey, G. A.
"A Cesium Beam Frequency Reference for Severe Environments".
Hewlett-Packard J. (USA), Vol. 27, No. 7, p. 2-10 (Mar 1976)

Hellwig, H., McKnight, R., Pannaci, E., Wilson, G.
"Barium Oxide Beam Tube Frequency Standard".
Proc. 22nd Annual Frequency Control Symposium, Atlantic City, N.J., USA, 22-24 April 1968 (Ft. Monmouth, NJ, USA: Electronic Components Laboratory 1968), p. 529-544

Hellwig, H., Barnes, J. A., Glaze, D. J.
"Frequency Biases in a Beam Tube Caused by Ramsey Cavity Phase Differences".
Programme of the 25th Annual frequency control symposium (abstracts), Atlantic City, NJ., USA, 26-28 April 1971 (Fort Monmouth, NJ., USA: US Army Electronic Command 1971), p. 50.

Hellwig, H., Jarvis, Jr., S., Glaze, D. J., Halford, D., Bell, H.E.
"Time Domain Velocity Selection Modulation as a Tool to Evaluate Cesium Beam Tubes".
Proceedings of the 27th Annual Frequency Control Symposium, Cherry Hill, N.J., USA, 12-14 June 1973 (Washington DC, USA: Electronic Industries Assoc. 1973), p. 357-66

Hellwig, H., Jarvis, Jr., S., Halford, D., Bell,H.E.
"Evaluation and Operation of Atomic Beam Tube Frequency Standards Using Time Domain Velocity Selection Modulation."
Metrologia (Germany), Vol. 9, no. 3, p. 107-12 (Sept. 1973)

Howe, D. A., Bell, H.E., Hellwig, H., DeMarchi, A.
"Preliminary Research and Development of the Cesium Tube Accuracy Evaluation System".
Proceedings of the 28th Annual Frequency Control Symposium 1974, Atlantic City, N.J., USA, 29-31 May 1974 (Washington, D.C., USA: Electronic Industries Assoc. 1974), p. 362-72

Howe, D. A., Salazar, H. F.
"A Digital 5.00688 MHz Synthesizer and Squarewave FM Serve System for Cesium Standards".
Proceedings of the 29th Annual Frequency Control Symposium, Fort Monmouth, NJ, USA, 28-30 May 1975 (Washington, D.C., USA: Electronic Industries Assoc. 1975), p. 387-93

Howe, D. A.
"Velocity Distribution Measurements of Cesiam Beam Tubes (Frequency Standard)".
Proceedings of the 30th Annual Symposium on Frequency Control, Atlantic City, NJ, USA, 2-4 June 1976 (Washington, D.C., USA: Electronic Industries Assoc. 1976), p. 451-6

Hyatt, R., Throne, D., Cutler, Holloway, J. J., Mueller, L. F.
"Performance of Newly Developed Cesium Beam Tubes and Frequency Standards".
Programme of the 25th Annual Frequency Control Symposium (abstracts), Atlantic City, NJ, USA, 26-28 April 1971 (Fort Monmouth, NJ, USA: US Army Electronic Command 1971), p. 51.

Hyatt, R. C., Mueller, L. F., Osterdock, T. N.
"A High-Performance Beam Tube for Cesium Beam Frequency Standards".
Hewlett-Packard J. (USA), Vol. 25, no. 1, p. 14-23 (Sept. 1973).

Iijima, S., Fujiwara, K., Kato, T.
"An Experiment on the Effect of Ambient Temperature on the Rate of Cesium Clock".
Tokyo Astron. Bull. (Japan), no. 244, p. 2071-5 (7 July 1976).

Il'in, V. G., Elkin, G. A., Abashev, Yu. G., Purtov, V. I.
"The Metrological Cesium Frequency Standard MTS-1".
Meas. Tech. (USA), Vol. 19, no. 10, p. 1450-5 (Oct. 1976). Translation of: Izmer. Tekh. (USSR), Vol. 19, no. 10, p. 43-7 (Oct. 1976).

Ilyusnina, E. N., Yukhvidin, Ya. A.
"Operating Characteristics of Atomic-Beam Tubes at the Transition between the Hyperfine Structure Levels in the Absence of Zeeman Splitting".
Radio Eng. & Electron. Phys. (USA), vol 21, no. 9, p. 140-1 (Sept. 1976). Translation of: Radiotekh. & Elektron (USSR), Vol.21, no. 9, p. 2010-12 (Sept. 1976).

Jarvis, Jr., S.
"Determination of Velocity Distributions in Molecular Beam Frequency Standards from Measured Resonance Curves."
Metrologia (GErmany), Vol. 10, no. 3, p. 87-8, (1974). In English.

Jarvis, Jr., S., Wineland, D. J., Hellwig, H.
"Two-Frequency Excitation for the Ramsey Separated Oscillatory Field Method",
J. Appl Phys (USA), Vol. 48, no. 12, p. 5336-7 (Dec 1977).

Jumoniy, H., Tanaska, K., Toyanna, J., Takaoka, H., Kariza, K., Kawada, J.
"A New Low Voltage, Maintenance-Free Cesium Beam Tube for a Frequency Standard".
Proc. 32nd Annual Frequency Control Symposium, Atlantic City, NJ, USA, 31 May - 2 June 1978 (Washington, DC, USA: Electronic Industries Assoc. 1978), P. 460-465.

Kartaschoff, P.
"Power - Linewidth Relations in Atomic Beam Tubes".
Eurocon 71 Digest. Lausanne, Switzerland, 18-22 Oct 1971 (New York, USA: IEEE 1971), 2pp.

Kobayashi, M., Nakagiri, K., Urabe, S., Shiburi, Y.
"Design and Preliminary results on a Cesium Beam Standard at the RRL"
CPEM Digest 1978. Conference on Precision Electromagnetic Measurements, Ottawa, Canada, 26-29 June 1978 (New York, USA: IEEE 1978), p. 5-7

Koga, Y., Nakadan, Y., Yoda, J.
"A Cesium Beam Frequency Standard and Its Frequency Stability".
Oyo Buturi (Japan), Vol. 45, No. 8, p. 753-62 (Aug. 1976). In Japanese.

Korobov, V. K., Il'in, V. G., Pushkin, S. B.
"New State Standard of Time and Frequency, and Methods of Realizing its Accuracy."
Meas. Tech. (USA), Vol. 19, no. 10, p. 1444-9 (Oct. 1976). Translation of: Izmer. Tekh. (USSR), Vol 19. no. 10. p. 40-3 (Oct. 1976).

Kupersuirth, F., Thomburg, C., Ho, J.
"New Primary Cesium Beam Frequency Standard"
Proc. 24th Annual Frequency Control Symposium, Atlantic City, NJ., USA, 27-29 April 1970, (Washington, DC., USA: Electronic Industries Assoc. 1970), p. 308-314

Lacey, R. F.
"Thallium Beam Frequency Standards"
Metrologia (Germany), Vol. 3, No. 3, 70-8(July 1967)

Lacey, R. F.
"Phase Shift in Microwave Ramsey Structures". Proceedings of the 22nd annual frequency control symposium, Atlantic City, NJ, USA, 22-24 Apr 1968, (Fort Monmouth, NJ, USA: Electronic Components Lab. 1968), p. 545-58.

Leschiutta, S.
"Experiments with a Commerical Caesium Resonator". Alta Frequenza (Italy), Vol. 37, no. 10, p.916-22 (Oct. 1968). In Italian.

Mungall, A. G., Bailey, R., Daams, H., Morris, D.
"A Re-evaluation of the NRC Long Cesium Beam Frequency Standard".
Metrologia (Germany), vol. 4, no. 4, p. 165-8 (Oct. 1968).

Mungall, A. G., Daams, H.
"Cesium Beam Frequency Standard Cavity Design."
Metrologia (Germany), Vol. 6, No. 2, p. 60-4 (April, 1970).

Mungall, A. G.
"The Second Order Doppler Shift in Cesium Beam Atomic Frequency Standards".
Metrologia (Germany), Vol. 7, no. 2, p. 49-56 (April, 1971).

Mungall, A. G.
"Cavity Phase Dependent Frequency Shifts in Cesium Beam Frequency Standards."
Metrologia (Germany), Vol. 8, no. 1, p. 28-32 (Jan. 1972).

Mungall, A. G., Bailey, R., Daams, H., Morris, D., Costain, C. C.
"A Preliminary Report on Cs V, the New NRC Long Beam Primary Frequency and Time Standard".
Proceedings of the 27th Annual Frequency Control Symposium, Cherry Hill, New Jersey, USA, 12-14 June 1973 (Washington D.C., USA: Electronic Industries Assoc. 1973), p. 317-33

Mungall, A. G., Daams, M., Morris, D., Costain, C.C.
"The Atomic Second - to 13 Significant Figures".
Phys. Can. (Canada), Vol. 29, no.24, p. 40 (1973).

Mungall, A. G., Bailey, R., Daams, H., Morris, D., Costain, C. C
"The New NRC 2.1 Metre Primary Cesium Beam Frequency Standard, Cs V".
Metrologia (Germany), Vol. 9, no. 3, p. 113-27 (Sept.1973).

Mungall, A. G., Daams, H., Morris, D., Costain, C.C.
"Performance and Operation of the NRC Primary Cesium Clock CsV".
Metrologia (Germany), Vol. 12, No. 3, p. 129-39 (1976).

Mungall, A. G.
"The Millman Effect in Cesium Beam Atomic Frequency Standards".
Metrologia (Germany), Vol 12, no. 4, p. 151-8 (1976)

Mungall, A. G., Costain, C. C.
"NRC CsV Primary Clock Performance". Metrologia (Germany, vol. 13, no. 3, P. 105-7 (1977).

Mungall, A. G.
"Atomic Time Standards and Time Scales in Canada" International Electrical, Electronics Conference and Exposition, Toronto, Canada, 26-28 Sept. 1977 (New York, USA: IEEE 1977), p. 118-19.

Mungall, A. G.
"A New Concept in Atomic Time Keeping: The Continuously Operating Long Beam Primary Cesium Clock". CPEM Digest 1978. Conference on Precision Electromagnetic Measurements, Ottawa, Canada, 26-29 June 1978 (New York, USA: IEEE 1978). P. 3.

Oliver, M., Pretot, R.
"Servo-System for Frequency Standard". Rev. Phys. Appl. (France), Vol. 2, no. 1, 17-19 (Mar 1967). In French.

Oraevskiy, A. N.
"Atomichron as an Optical Frequency Standard". Conference on Precision Electromagnetic Measurements, Boulder (1968) Institute of Electrical and Electronics Engineers (1968) 47-8.

Peters, H. E., Reinhardt, V. S.
"Atomic Frequency Standard Relativistic Doppler Shift Experiment." Proceedings of the 28th Annual Frequency Control Symposium 1974, Atlantic City, NJ, USA, 29-31 May 1974 (Washington, DC, USA: Electronic Industries Assoc. 1974), p. 247-55.

Philibert, V.
"The Cesium-Beam Atomic Clock". Electronics World (USA), Vol. 83, no. 6, p. 40-1 (June 1970).

Picque, J. L.
"Hyperfine Optical Pumping of Cesium with a CW GaAs Laser". IEEE J Quantum Electron, (USA), Vol. QE-10 no. 12, p. 892-97 (Dec. 1974)

Rovera, G., De Marchi, A.
"The Optically Pumped Passive Cesium Frequency Standard: Basic Theory and Experimental Results on Buffer Gas Frequency Shifts". IEEE Trans. Instrum. & Meas. (USA), Vol. IM-25, no. 3, P. 203-16 (Sept. 1976).

Sachkov, V. I.
"Phasing of Resonators of a Cesium Frequency Standard". Izmerit. Tekh. (USSR), No. 9, 54-6 (Sept. 1967). In Russian. English translation in: Meas. Tech. (USA), No. 9, 1096-9 (Sept. 1967).

Sachkov, V. I.
"Application of U-shaped Resonators in Cesium Frequency Standards". Izmerit. Tekh. (USSR), no. 7, p. 99-100 (July 1968). In Russian. English Translation in: Meas. Tech. (USA), no. 7, p. 997-8 (July 1968).

Seavey, G. A., Mueller, L.F.
"Performance of a Dual Beam High Performance Cesium Beam Tube (Frequency Standard)". Proceedings of the 30th Annual Symposium on Frequency Control, Atlantic City, NJ, USA, 2-4 June 1976 (Washington, DC, USA: Electronic Industries Assoc. 1976), p. 457-62

Strumia, F.
"A Proposal for a New Absolute Frequency Standard, Using a Mg or Ca Atomic Beam". Metrologia (Germany), vol. 8, no. 3, p. 85-90 (July 1972)

Strumia, F., Minguzzi, P., Franesconi, M., Benedetti, R.
"Mg Frequency Standard: Optimization of the Metastable Atomic Beam". Proceedings of the 28th Annual Frequency Control Symposium 1974, Atlantic City, NJ, USA, 29-31 May 1974 (Washington, DC, USA: Electronic Industries Assoc. 1974). p. 350-4.

Wineland, D. J., Allan, D. W., Glaze, D. J., Hellwig, H. W., Jarvis, Jr., S.
"Results on Limitationsin Primary Cesium Standard Operation." IEEE Trans. Instrum. & Meas. (USA), Vol. IM-25, no. 4, p. 453-8 (Dec. 1976). (1976 Conference on Precision Electromagnetic Measurements, Boulder, Colo., USA, 28 June - 1 July 1976).

Wineland, D. J.
"The Cesium Beam Frequency Standard-Prospects for the Future". Metrologia (Germany), vol. 13, no. 3, p. 121-3 (1977)

Wineland, D. J., Hellwig, H.
"Comment on the Millman Effect in Cesium Beam Atomic Frequency Standards". Metrologia (Germany), Vol. 13, no. 4, p. 173-4, (1977).

Winkler, G. M. R., Hall, R. G., Percival, D. B.
"The US Naval Observatory Clock Time Reference and the Performance of a Sample of Atomic Clocks". Metrologia (Germany), Vol. 6, no. 4, p. 126-34 (Oct. 1970).

Yoda, J., Nakadan, Y., Koga,Y.
"Improvement of the Frequency Stability of the Cs Frequency Standard NRLM-L". Jpn. J. Appl. Phys. (Japan), vol. 17, no. 6, p. 1139-40 (June 1978).

2.1.2

Alekseev, E. I., Bazarov, Ye. N., Grigor'ev, V. I.
"The Effect of the Filtering Conditions of the Light Pump on the Frequency of the 0-0 Transition of the Rb^{87} Atoms". Radiotekhnik i Elektronika (USSR) Vol. 13, No. 6, 1041-44 (June 1968). In Russian. English translation in: Radio Engng. Electronic Phys. (USA).

Alekseev, E. I., Bazarov, E. N., Levshin, A. E.
"Frequency Shifts due to the Luminous Pump in a Passive Frequency Standard Using ^{87}Rb Atoms". Radiotekhnika i Elektronika (USSR), Vol. 14,no. 11, p. 2026-35 (1969). In Russian

Alekseev, E. I., Bazarov, E. N., Levshin, A. E.
"Theory of Frequency Standard with Pulsed Optical Pumping". Radio Eng. & Electron. Phys. (USA), p. 77-83. Translation of: Radiotekh, & Elektron (USSR), Vol. 19, no. 1, p. 103-11 (Jan. 1974).

Alekseyev, E. I., Bazarov, E. N., Telegin, G. I.
"Frequency Shifts in Standard with Pulsed Optical Pumping and a Continuous Microwave Field". Radio Eng. & Electron, Phys. (USA), Vol. 19, no. 7, p. 1457-66, (July 1974),

Alekseyev, E. I., Bazarov, E. N., Telegin, G. I.
"Optical Indication of the Ramsey Structure at the Line of the 0-0 Transition or Rb^{87} Atoms". Radio Eng. & Electron. Phys. (USA), Vol 19, no. 8, p. 88-91, (Aug. 1974). Translation of: Radiotekh. & Elektron. (USSR), Vol. 19, no. 8, p. 1708-12, (Aug. 1974)

Alekseyev, E. I., Bazarov, Ye. N., Gubin, V. P.
"Light Shifts in a Frequency Standard with a Rubidium Cell in the Presence of Spatial Separation of the Optical Pumping and Interactionwith the Microwave Field". Radio Eng. & Electron. Phys. (USA), Vol 19, no. 9, p. 58-63 (Sept. 1974). Translation of: Radiotekh. & Elektron. (USSR), Vol. 19, no. 9, p. 1901-9 (Sept. 1974).

Alekseyev, E. I., Bazarov, Ye. N., Telegin, G. I.
"Light Shifts in a Quantum Frequency Standard with Pulsed Optical Pumping and Optical Indicationof the Ramsey Structure of the 0-0 Transition Line of Rb^{87} Atoms". Radio Eng. & Electron. Phys. (USA), Vol. 20, no. 4, p. 73-80 (April 1975). Translation of: Radiotekh. & Elektron. (USSR), Vol. 20, no. 4, p. 777-85 (April 1975).

Alekseyev, E. I., Bazarov, Ye. N., Telegin, G. I.
"The Change in the Ramsey Structure of the 0-0 Transition Line of Rb^{87} Atoms with an Increase in the Number of Microwave Pulses in the Intervals between the Optical Pumping Pulses". Radio Eng. & Electron. Phys. (USA), Vol.20, no. 4, p. 145-7 (April 1975). Translation of: Radiotekh. & Elektron. (USSR), Vol. 20, no. 4, p. 860-3 (April 1975).

Alekseev, E. I., Bazarov, E. N.
"Light-Induced Shifts of a Quantum Frequency Standard with Optical Pulse Pumping and Optical Display of a Ramsey Line with Suppressed Side Maxima (^{87}Rb)". Sov. J. Quantum Electron (USA), Vol. 5, no. 5, p. 563-7. Translation of: Kvaniovaya Elektron., Moskva (USSR), Vol. 2, no. 5, p. 1035-42 (May 1975).

Arditi, M., Picque, J. L.
"Application of the Light-Shift Effect to Laser Frequency Stablization with Reference to a Microwave Frequency Standard". Opt. Commun. (Netherlands) Vol. 15, No. 2, p. 317-22 (Oct. 1975).

Bahadur, H., Parshad, R.
"Optical Pumping for Alkali Gas Cell Frequency Standard". J. Opt. (India), Vol. 5, no. 3, p. 59-67 (July-Sept. 1976).

Bava, E., De Marchi, A., Rover, G., Beverini, N., Strumia, F.
"Measurements on Optically Pumped Cesium Vapor Frequency Standard". Alta Freq. (Italy), Vol. 44, no. 10, p. 574-8 (Oct 1975).

Bazarov, Ye. N., Grigorev, V. I.
"Frequency Shift of $S_{1/2}$ F=2, m =0 $S_{1/2}$ F=1, m =0 Transition Frequency of Rubidium Atoms using Pulsed Optical Pumping". Radiotekhnika i Elektronika (USSR), Vol. 14, no. 6, p. 1056-64 (June 1969). In Russian. English translation in: Radio Engng. Electronic Phys. (USA).

Vazarov, Ye. N., Gubin, V. P., Telegin, G. I.
"Experimental Study of Shifts of the Frequency of the $S_{1/2}$, F=2, m=0 $S_{1/2}$ F=1, m-0 Transition of Rb^{87} Atoms for Pulsed Optical Pumping". Radio Eng. & Electron. Phys. (USA), Vol. 18, no. 10, p. 1530-5, (Oct. 1973). Translation of: Radiotekh. & Elektron. (USSR), Vol. 18, no. 10, p. 2083-9 (Oct. 1973)

Bennett, T. J., Hayes, R. E. Norton, G. T., Zepler, M. M.
"A Simplified Rubidium Atomic Frequency Source". Syst. Technol. (GB), no. 12, p. 7-11 (April 1971).

Bespalova, M.P., Mishakov, G. A., Pikhtelev, A.I.
"Frequency Shifts of the Standard Atomic Transition in RB^{87} Appearing with Optical Pumping in a Passive Frequency Standard". Radio Eng. & Electron. Phys. (USA). Vol. 18, no. 11, p. 1707.14 (Nov. 1975). Translation of: Radiotekh. & Elektron. (USSR), Vol. 18, no. 11, p. 2356-63 (Nov. 1973).

Beverini, N., Strumia, F.
"On the Population Inversion between the Hyperfine Sublevels of Cs". Opt. Commun. (Netherlands), Vol. 4, no. 1, p. 56-7 (Sept. 1971).

Bespalova, M. P., Bogoslovskii, N. N., Kulagin, E.V., Kisel'nikova, S. I., Pikhtelev, A. L., Ul'yanov, A. A.
"Some Frequency Characteristics of the RB^{87} Pair Quantum Frequency Standard". Izv.VUZ Radiofiz, (USSR), vol 17, no. 5, p. 767-70 (1974). In Russian. English translation in: Radiophys. & Quantum Electron. (USA)

Bottcher, S., Fruhauf, T.
"Rubidium oscillator XSRB". News Rohde & Schwarz (Germany), Vol. 16, no. 73, p. 22-3 (1976). (Received: Aug. 1976).

Cerez, P., Hartmann, F.,
"Theoretical Analysis of the Operation of an Optically Pumped Rubidium Atomic Beam Clock". IEEE J. Quantum Electron. (USA), Vol. QE-13, no. 5, p. 344-51 (May 1977).

Chi, A. R., Roeder, J. H., Wardrip, S. C., Bruger, B.
"Long-term Frequency Stability Measurement of Rubidium Gas Cell Frequency Standards". Proceedings of the 22nd Annual Frequency Control Symposium, Atlantic City, N.J., USA, 22-24 Apr 1968 (Fort Monmouth, NJ., USA: Electronic Components Lab, 1968) p. 592-605.

Ernvien-Pecquenard, J.
"Atomic Clock Using Sequential Optical Pumping". Ann. Radioelect. (France), Vol. 23, 137-54 (April 1968) (In French).

Ernvein-Pecquenard, J., Mainar, L.
"Atomic Clock with Sequencial Optical Pumping". C. R. Acad. Sci. B (France), Vol. 268, no. 12, p. 817-20 (24 Mar 1969). In French.

Farmer, D. J., Long, J. D.
"Atomic Frequency Standards for Special Applications" Conference on Frequency Genration and Control for Radio Systems, London, (1967) (London: Institution of Electrical Engineers, 1967: Conference Publication No. 31) 16-28.

Frerking, M. E.
"Ruggedized Rubidium Frequency Standard". Proc. IEEE (USA), Vol. 60, no. 5, p. 628-9 (May 1972).

Frerking, M. E., Johuson, D. E.
"Rubidrium Frequency & Time Standard for Military Enviroment". Proc. 26th Annual Frequency Control Symposium, Atlantic City, N. J., USA, 6-8 June 1972 (Washington, D. C., USA: Electronic Industries Association 1972), p. 216-222.

Fruhauf, T.
"Improved Rubidium Frequency Standard XSRM". News Rohde & Schwarz (Germany), Vol. 17, no. 78, p. 37 (1977). (Received: Jan. 1978) (no refs)

Fukuyo, H., Iga, K., Kuramochi, N., Mastuda, I., Ishikawa, H.
"Fundamental Characteristics and Frequency Stability in the Early Stage of a Laboratory-Made Rb Atomic Oscillator". Bull. Tokyo Inst. Technol. (Japan), no. 107, p. 75-88 (1971).

Hayes, R. E., Bennett, T. J., Norton, G. T., Zepler, M. M.
"Rubidium Atomic Frequency Source Having Small Size and Fast Warm Up". Electron. Lett. (GB), Vol. 6, no. 23, p. 734-5 (Nov. 1970).

Ivanov, N. I., Kravchenko, V. F.
"Fluctuations in a Rubidium Frequency Standard". Izv. VUZ Radioelekron. (USSR), Vol. 15, no. 7, p. 890-4 (1972). In Russian.

Jeckhart, E., Hubner, G.
"XSR-primary Frequency Standard for Atomic and Universal Time". News Rohde and Schwartz (Germany), Vol. 8, n. 30, p. 26-30 (1968).

Jechart, E.
"A new Miniature Rubidium Gas Cell Frequency Standard". Proceedings of the 27th Annual Frequency Control Symposium, Cherry Hill, New Jersey, USA, 12-14 June 1973 (Washington DC, USA: Electronic Industries Assoc. 1973), p. 387-9.

Jechart, E.
"Miniaturized Rubidium-Gas-Cell Frequency Standard". Elektronik (Germany), Vol. 23, no. 12, p. 457-60 (Dec. 1974) In German.

Kbarchev, O. P.
"Rubidium Cell Frequency Standard with pulse Optical Pumping". Izv. VUZ Priborostr. (USSR), Vol. 19, no. 1, p. 114-18 (1976) In Russian.

Kuramochi, N., Fukuyo, H., Matsuda, I., Shiomi, N.
"Spectral Profiles of the ^{87}Rb Pumping Light Source (for Frequency Standard)". Jap. J. Appl. Phys. (Japan), Vol 15, no. 6, p. 949-54 (June 1976).

Kuramochi, I., Matsuda, I., Kuramochi, N., Naruse, S., Iga, K., Fukuyo, H.
"Measurement of the Frequency Displacement of the ^{87}Rb Pumping Light Passed through the ^{87}Rb Filter Cell". Bull. Res. Lab. Precis. Mach. & Electron. (Japan), no. 38, p. 47-50 (Sept. 1976).

Lacroix, M., Malnar, L.
"The Vapour Rubidium Atomic Clocks among the Atomic Frequency Standards". Onde Elect. (France), Vol. 48, No. 491, 164-71 (Feb. 1968). In French.

Lacroix, M., Malnar, L.
"Rubidium Vapour Atomic Clocks as Atomic Frequency Standards". Onde Elect. (France), Vol. 48, 189-95 (March 1968). In French.

Ya.Leikin, A., YuLinker, B., Samoilovich, A. I.
"A Combined Gas Cell for a Passive Quantum Frequency Standard Based on Rubidium Vapor". Meas. Tech. (USA), Vol. 18, no. 1, p. 88-9 (Jan. 1975), Translation of: Izmer. Tekh. (USSR), Vol. 18 no. 1, p. 53-4 (Jan. 1975).

Leschiutta, S., Strumia, F.
"Optically Pumped Caesium Cell Frequency Standards". CPEM 74 Digest: Conference on Precision Electromagnetic Measurements, London, England, 1-5 July 1974 (London, England: IEE 1974), p. 310-11.

Matsuda,I., Sato, T., Kuramochi, N., Fukuyo, H.,
"Frequency Stability of the Rb Standard TTR-1". Bull. Tokyo Inst. Technol. (Japan), no. 125, p. 9-15 (1974).

Matsuda, I., Shiomi, N., Kuramochi, N., Fukuyo, H.
"^{87}Rb Resonant Frequency Change Due to the Spectral Profile of the Pumping Light". Bull. Res. Lab. Precis. Mach. & Electron. (Japan), no. 40, p. 7-16 (Sept. 1977).

McGuire, M. D.
"The Trapped Mercury Ion Frequency Standard". 31st Annual Frequency Control Symposium. Atlantic City, N. J., USA, 1-3 June 1977 (Washington, DC, USA: Electronic Industries Assoc. 1977), p. 612-15

Missout, G., Vanier, J.
"Theoretical and Experimental Studies of Some Problems Related to the Passive Rubidium Gas Cell Frequency Standard". Proceedings of the 29th Annual Frequency Control Symposium, Fort Monmouth, NJ, USA, 28-30 May 1975 (Washington, DC, USA: Electronic Industries Assoc. 1975), p. 383.

Missout, G., Vanier, J.
"Some Aspects of the Theory of the Passive Rubidium Frequency Standards".
Can. J. Phys. (Canada), vol. 53, no. 11, p. 1030-43 (1 June 1975).

Missout, G., Vanier, J.
"Pressure and Temperature Coefficients of the More Commonly Used Buffer Gases in Rubidium Vapor Frequency Standards".
IEEE Trans. Instrum. & Meas. (USA), Vol. IM-24, no. 2, p. 180-4 (June 1975).

Nichols, S. A., White, J. D, Moore, R. B.
"Evaluation of a Rubidium Standard for Satellite Application". Proceedings of the 27th Annual Frequency Symposium, Cherry Hill, New Jersey, USA, 12-14 June 1973 (Washington D. C., USA: Electronic Industries Assoc. 1973), p. 390-9.

Nichols, S. A., White, J. D., Moore, R. B.
"Performance Evaluation of a Rubidium Standard for Space Environment". 1973 National Telecommunications Conference, Vol. I, Atlanta, GA, USA, 26-28 Nov. 1973 (New York, USA: IEEE 1973), p. 19A/1-6

Nichols, S.A, White, C.
"Satellite Application of a Rubidium Frequency Standard". Proceedings of the 28th Annual Frequency Control Symposium 1974, Atlantic City, N.J., USA, 29-31 May 1974 (Washington, D.C., USA: Electronic Industries Assoc. 1974), p. 401-5.

Oyamada, H., Takahashi, K., Sato, Y., Uchida, H.
"A Consideration of Rubidium Lamp Stability for Rubidium Frequency Standard". Proceedings of the 28th Annual Frequency Control Symposium 1974, Atlantic City, N.J., USA, 29-31 May 1974 (Washington DC, USA: Electronic Industries Assoc. 1974), p. 340-3.

Oyamada, H., Takahashi, K., Sato, Y., Uchida, H.
"Rubidium Lamp Stability and Reliability for Rubidium Frequency Standard". NEC Res. & Dev. (Japan), no. 43, p. 69-74 (Oct. 1976).

Risley, A., Busca, G.
"Effect of Line Inhomogeneity on the Frequency of Passive Rb^{87} Frequency Standards". Proc. 32nd Annual Frequency Control Symposium, Atlantic City, N.J., USA, 31 May - 2 June 1978 (Washington, DC, USA, Electronic Industries Assoc. 1978), p. 506-513.

Rovera, G., De Marchi, A., Vanier, J.
"The Optically Pumped Passive Cesium Frequency Standard: Basic Theory and Experimental Results on Buffer Gas Frequency Shifts". IEEE Trans. Instrum. & Meas. (USA), Vol. IM-25, no. 3, p. 203-16 (Sept. 1976).

Rovera, G., Beverini, N.
"Frequency Stability of the Optically Pumped Passive Cesium Frequency Standard". European Conference on Precise Electrical Measurement, Brighton, Sussex, England, 5-9 Sept. 1977 (London, England: IEEE 1977), p. 83.

Rovera, G., Leschiutta, S., Busca, G.,
"Parameters Affecting the Stability of an Optically Pumped Cesium Frequency Standard". Proc. 32nd Annual Frequency Control Symposium, Atlantic City, N. J., USA, 31 May - 2 June 1978, (Washington, D.C. USA: Electronics Industries Assoc., 1978), p. 466-468.

Sato, Y., Kumamoto, H., Ayamado, H., Uchida, H.
"Automatic Frequency Controlled Rubidium Frequency Standard". Proc. 26th Annual Frequency Control Symposium, Atlantic City, NJ., USA, 6-8 June 1972 (Washington, D.C., USA: Electronic Industries Assoc. 1972), p. 211-215.

Schulten, F.
"Simple Molecular Frequency Standard for Millimeter Waves." Microwave J. (USA), Vol. 10, No.12, 71-4 (Nov. 1967).

Singh, G., DiLavore, P., Alley, C.
"Comments on 'Hyperfine Optical Pumping of Cesium with a CW GaAs Laser'". IEEEJ. Quantum Electron. (USA), Vol. QE-12, no. 2, pt. 1, p. 81-2 (Feb. 1976).

Stadler, K.
"Rubidium Frequency Standard XSRM". News Rohde & Schwarz (Germany), vol.14, no. 64, p. 8-10 (1974).

Stadler, K.
"Calibrating Crystal Oscillators with Frequency Standard XSRM". News Rohde & Schwarz (Germany), Vol. 15, no. 70, p. 12-14 (1975).

Strumia, F., Beverini, N., Moretti, A., Rovera, G.
"Optimization of the Buffer Gas Mixture for Optically Pumped Cs Frequency Standards". Proceedings of the 30th Annual Symposium on Frequency Control, Atlantic City, N.J., USA, 2-4 June 1976 (Washington, D.C., USA: Electronic Industries Assoc. 1976), p. 468-72.

Tank, H., Happe, W.
"Light Modulation at the Rb Syperfine Frequency". Proc. 23rd Annual Frequency Control Symposium, Atlantic City, N.J., USA, 6-8 May 1969 (Washington, D.C., USA: Electronic Industries Association 1969), p. 263-270.

Tetu, M., Fortin, R., Savard, J. Y.
"A New Determination of the Rb^{85} Unperturbed Hyperfine Transition Frequency". 1976 Conference on Precision Electromagnetic Measurements, Boulder, Colo., USA, 28 June - 1 July 1976 (New York, USA, IEEE 1976), p. 233-4

Tetu, M., Fortin, R., Savard, J. Y.
"A New Determination of the Rb^{85} Unperturbed Hyperfine Transition Frequency".
IEEE Trans. Instrum. & Meas. (USA), Vol. IM-25, no. 4, p. 477-80 (Dec. 1976). (1976 Conference on Precision Electromagnetic Measurements, Boulder, Colo., USA, 28 June - 1 July 1976).

Thomsen, M.P.R., Shief, L. J., Fallon, R. J.
"Study of Phenomena Affecting the Composition of Rubidium Vapor Cells". Proc. 22nd Annual Frequency Control Symposium, Atlantic City, N.J., USA, 22-24 April 1968 (Ft. Monmouth, NJ, USA: Electronic Components Laboratory 1968) p. 559-572.

Throne, D. H.
"A Rubidium-Vapor Frequency Standard for Systems Requiring Superior Frequency Stability". Hewlett-Packard J. (USA), Vol. 19, no. 11, p. 8-14 (July 1968).

Throne, D. H.
"A Report of the Performance Characteristics of a New Rubidium Vapor Frequency Standard".
Proceedings of the 23rd annual frequency control symposium, Atlantic City, NJ, USA, 6-8 May 1969 (Washington, DC, USA: Electronic Industries Assoc. 1969), p. 274-8.

Wineland, D. J., Hellwig, H.
"Comment on 'The Millman Effect in Cesium Beam Atomic Frequency Standards'". Metrologia (Germany), Vol. 13, no. 4, p. 173-4 (1977).

Yoshimura, K., Kobayashi, M.
"Analysis of the Servo System of the Rubidium Vapor Frequency Standard". Rev. Radio Res. Lab. (Japan), Vol.19, no. 101, p. 117-27 (Mar 1973).

Yuuki, T., Uchida, H., Sato, Y., Kumamoto, H., Oyamada, H., Kawaji, H., Kondo, K.
"Rubidium Frequency Standard". NEC Res. & Dev. (Japan), no. 31, p. 42-56 (Oct. 1973).

Zepler, M. M.
"Miniaturized, Rapid Warmup Rubidium Frequency Source". Programme of the 25th Annual Frequency Control Symposium (abstracts), Atlantic City, N.J., USA, 26-28 Apr 1971 (Fort Monmouth, NJ, USA: US Army Electronics Command 1971), p. 53.

Zholnerov, V. S.
"Buffer Mixtures for the Gas Cell of an Optically Pumped Frequency Standard". Opt. & Spectrosc, (USA). Vol. 43, no. 5, p. 566-8 (Nov. 1977), Translation of: Opt. & Spektrosk. (USSR), Vol. 43, no. 5, p. 957-61. (Nov. 1977).

2.1.3

Andresen, H. G.
"Atomic Beam Preparation for Hydrogen Maser Operation with Unpolarized Atoms". Z. Phys. (Germany), Vol. 223, no. 1, p. 71-102 (1969), In English.

Andresen, H. G.,
"Hydrogen Maser Atomic Beam Resonances".
Z. Phys., (Germany), Vol. 233, no. 4, p. 293-307 (1970). In English.

Audoin, C.
"The Hydrogen Maser in a Transient Mode".
Rev. Phys. Appl. (France). Vol. 2, No. 4, 309/et/seq. (Dec. 1967).

Audoin, C., Desaintfuscien, M., Schermann, J. P.
"Application of the Transient Behavior to the Study of the Hydrogen Maser".
Proc. 22nd Annual Frequency Control Symposium, Atlantic City, N.J., USA, 22-24 April, 1968 (Ft. Monmouth, NJ, USA: Electronic Components Laboratory 1968), p. 493-56.

Audoin, C., Desaintfuscien, M., Schermann, J. P., Viennet, J.
"Experimental Study of a Synchromised Hydrogen Maser". C. R. Acad. Sci. B. (France), Vol. 266, No. 19, 1264-7 (6 May 1968). In French.

Audoin, C., Benoit, H., Desaintfuscien, M., Piejus, P., Schermann, J. P.
"Triplet Decomposition of the Line M = 0 of a Hydrogen Maser under the Influence of Transitions between the Zeeman Sub-Levels". C. R. Acad. Sci. B. (Frence), Vol. 266, No. 25, 1521-4 (17 June 1968) In French.

Audoin, C., Desaintfuscien, M., Petit, P., Schermann, J. P.
"Design of a Double Focalisation in a Hydrogen Maser". Conference on Precision Electromagnetic Measurements, Boulder, (1968), New York, Institute of Electrical and Electronics Engineers (1968) 49-50.

Audoin, C., Desaintfuscien, M., Piejus, P., Schermann, J. P.
"A New Method for Measurement of the Population Difference of Hyperfine-levels of Stored Atoms". Proceedings of the 23rd Annual Frequency Control Symposium, Atlantic City, N.J., USA, 6-8 May 1969 (Washington, D.C., USA: Electronic Industries Assoc. 1969), p. 288-96.

Audoin, C., Desaintfuscien, M., Petit, P., Schermann, J. P.
"Efficiency of a Single-Hyperfine-State Selector for Hydrogen Masers". Electronics Letters (GB), Vol. 5, no. 13, p.292-3 (26 June 1969).

Audoin, C., Duchene, J. L., Schermann, J. P.
"Measurement of the Populations of the Atomic Jet in a Hydrogen Maser". C. R. Acad. Sci. B (France), Vol. 268, no. 26, p. 1757-60 (30 June 1969). In French.

Audoin, C., Desaintfuscien, M, Piejus,P., Schermann, J. P.
"Double-Resonance Method for the Determination of Level Populations". IEEE J. Quantum Electronics (USA), Vol. EQ-5, no. 9, p. 431-4 (Sept. 1969).

Audoin, C., Desaintfuscien, M., Schermann, J. P.
"Dynamical Time Constants of the Hydrogen Maser and Atomic Relaxation Times". Phys. Letters (Netherlands), Vol. 30A, no. 5, p. 321-2 (3 Nov. 1969).

Audoin, C., Schermann, J. P.
"Physics of the Hydrogen Maser". In Book: Advances in Atomic and Molecular Physics, Vol. 7, D.R. Bates, I. Esterman (ED.), . p. 1-45, London, England: Academic Press (1971), xiii+406pp.

Audoin, C., Lesage, P., Viennet, J., Barrillet, R.
"Analysis of H- Maser Autotuning Systems". Proc. 32nd Annual Frequency Control Symposium, Atlantic City, NJ, USA, 31 May - 2 June 1978 (Washington, DC., USA: Electronic Industries Association 1978), p. 531-541.

Baker, M., Levine, M., Mueller, L., Vessot, R.
"Progress in the Developmentof Hydrogen Masers". Proc. 22nd Annual Frequency Control Symposium, Atlantic City, N.J., USA: Electronic Components Laboratory 1968), p. 605-620.

Bangham, N. J., Donaldson, R. W.
"Hydrogen Maser Work at the NPL". Report NPL-QU-17, Nat. Phys. Lab., Teddington, England (March 1971), 14 pp.

Barillet, R., Audoin, C.
"Electronic Circuits Showing a Level-Independent Phase Shift for Hydrogen-Maser Work Applications". IEEE Trans. Instrum. & Meas. (USA), Vol. IM-25, no. 4, p. 465-8 (Dec. 1976). (1976 Conference on Precision Electromagnetic Measurements, Boulder, Colo., USA, 28 June - 1 July 1976).

Barillet, R., Audoin, C.
"Electronic Circuits Showing a Level Independent Phase Shift for Hydrogen Maser Work Applications". 1976 Conference on Precision Electromagnetic Measurements, Boulder, Colo., USA, 28 June - 1 July 1976 (New York, USA: IEEE 1976), p. 228-9

Bogdan, D. A., Demidov, N. A.
"Measurement of Hydrogen Atom Temperature in the Source of H- Maser Beam". Izv VUZ Radiofiz. (USSR), vol. 14, no. 4, p. 575-9 (1971). English translation in: Radiophys. Quantum Electron, (USA).

Bogdan, D. A., Demidov, N. A., Eshov, E. M., Lavrov, A. I., Logachev, V.A., Sakharov, B. A., Chernov, G. M., Utyanov, A. A., Fateev, B. P., Sharov, Yu. P.
"A Hydrogen Frequency Standard". Meas. Tech. (USA), Vol. 17, no. 11, p. 1704-4 (Nov. 1974), Translation of: Izmer. Tekh. (USSR), Vol. 17, no. 11, p. 41-3 (Nov. 1974).

Brenner, D.
"Absolute Frequency of the Hydrogen Maser Using a Flexible Storage Bulb" J. Appl. Phys. (USA), Vol. 41, no. 7, p. 2942-50 (June 1970).

Brousseau, R., Vanier, J.,
"Stimulated Emission in a Hydrogen Maser". Phys. Can. (Canada), Vol. 27, no. 4, p. 56 (1971). In French. (Canadian Association of Physicists' Annual Congress, Ottawa, Ontario, Canada, 21-24 June 1971).

Crampton,S. B., Wang, H. T. M.
"Density-Dependent Shifts of Hydrogen Maser Standards". Proceedings of the 28th Annual Frequency Control Symposium 1974, Atlantic City, N.J., USA, 29-31 May 1974 (Washington, D.C., USA: Electronic Industries Assoc., 1974), p. 355-61.

Crampton, S. B., Fleri, E. C., Wang, H.T.M.
"Effects of Atomic Reasonance Broadening Mechanisms on Atomic Hydrogen Maser Long-term Frequency Stability". Metrologia (Germany), Vol. 13, no. 3, p. 131-5 (1977).

Debely, P. E.
"Hydrogen Maser with Deformable Storage Bulb". Rev. Sci. Instrum. (USA), Vol. 41, no. 9, p. 1290-2 (Sept. 1970).

Demidov, N. A., Ezhov, E. M., Ul'yanov, A. A., Fedorov, V. A.
"Frequency Shifts of a Hydrogen Generator Due to Hydrogen Atom Collisions with Storage Flask Walls". Meas. Tech. (USA), Vol. 20, no. 7, p. 1000-2 (July 1977), Translation of: Izmer. Tekh. (USSR), Vol. 20, no. 7, p. 45-7 (July 1977).

Desaintfuscien, M., Petit, P., Audoin, C. Schesmann, J. P.
"Oscillation of Hydrogen Master for Ambient Temperatures Between 77 and 293K". C. R. Acad. Sci. Ser. B (France) Vol. 270, no. 14, p. 906-8, (6 April 1970), In French.

Desaintfuscien, M., Andoin, C., Petit, P.
"Method of Measurement of Relaxation Times T1 and T2 of the Hydrogen Maser, for Any Value of Atomic Flux". C. R. Hebd. Sean. Acad. Sci. B (France) Vol. 272, no.11, p. 676-9 (15 March 1971). In French.

Desaintfuscien, M., Audoin, C.
"Measurement of the Time Constant for Filling the 'Storage Flask' of a Hydrogen Maser". C. R. Hebd. Seances Acad. Sci. B (France), Vol. 279, no. 26, p. 657-60 (23 Dec. 1974). In French.

Desaintfuscien, M., Viennet, J., Audoin, C.
"Discussion of Temperature Dependence of Wall and Spin Exchange Effects in the Hydrogen Maser". Metrologia (Germany), Vol. 13, no. 3, p. 127-30 (1977).

Elkina, L. P., Elkin, G. A., Strakhovskii, G. M.
"Measurement of the Frequency Drift of a Hydrogen Standard Owing to Atomic Impacts on the Flask Wall". Izmerit. Tekh. (USSR), no. 6, p. 91 (June 1968). In Russian. English translation in: Meas. Tech (USA), no. 6, p. 841-2 (June 1968).

Elkin, G. A., Zhestkova, N. D., Kurnikov, G. P.
"Error Reproducion of the Frequency of Undisturbed Transition of the Hydrogen Atom". Meas. Tech. (USA), Vol. 16, no. 3, p. 394-7 (March 1973). Translation of: Izmer. Tekh. (USSR), Vol. 16, no. 3, p. 52-4 (March 1973).

Essen, L., Donaldson, R. W., Bangham, M. J., Hope, E. G.
"Frequency of the Hydrogen Maser". Nature (GB), Vol. 229, no. 5280, p.110-11 (8 Jan. 1971).

Essen, L., Donaldson, R. W., Hope, E. G., Bangham., M. J.
"Hydrogen Maser Work at the National Physical Laboratory". Metrologia (Germany), Vol. 9, no. 3, p. 128-37 (Sept. 1973).

Finnie, C., Sydnor, R., Sward, A.
"Hydrogen Maser Frequency Standard". Programme of the 25th Annual Frequency Control Symposium (abstracts), Atlantic City, N.J., USA, 26-28 Apr 1971 (Fort Monmouth, NJ., USA: US Army Electronics Command 1971), p. 56.

Gaigerov, B. A., Elkin, G. A.
"Automatic Turning of the Resonator of the Hydrogen Frequency Standard".
Izmerit, Tekh. (USSR), No. 6, p. 90-1 (June 1968). In Russian. English Translation in: Meas. Tech. (USA), No. 6, p. 839-40 (June 1968).

Elkin, G. A., Elkina, L. P., Zhestkova, N. D., Kurnikov, G. P., Popov, B. P.
"Hydrogen Maser as a Quantum Frequency Standard". Meas. Tech. (USA), Vol. 15, no. 11, p. 1640-3 (Nov. 1972). Translation of: Izmar. Tekh. (USSR), Vol. 15, no. 11, p. 29-32 (Nov. 1972).

Gaigerov, B. A.
"Automatic Stablization of the Magnetic Field in a Hydrogen Generator".
Meas. Tech. (USA), Vol. 16, no. 3, p. 464-5 (March 1973). Translation of: Izmer. Tekh. (USSR), Vol. 16, no.3, p. 91 (March 1973).

Gheorghiu, O., Viennet, T., Petit, P., Audoin, C.
"Automatic Tuning of the Resonant Cavity of Hydrogen Atomic Clocks". C.R. Hebd. Seances Acad. Sci. B (France), Vol. 278, no. 25, p. 109-16 (17 June 1974) In French.

Gheorghiu, O.C., Giurgiu, L.C.
"The Hydrogen Maser of the Institute of Physics in Bucharest, Romania". Rev. Roum. Phys. (Rumania), Vol. 20, no. 3, P. 305-7 (1975)

Gheorghiu, O.C., Gheorghe, V. N.
"Characteristics of a UHF Discharge Used as Atomic Source for a Maser". Int. J. Electron. (GB), Vol. 39, no. 3, p. 329-35 (Sept. 1975).

Gheorghiu, O., Gheorghe, V., Giurgiu, L., Mandache, C.
"Hydrogen Masers as Frequency Standards". Metrol. Apl. (Rumania), Vol. 24, no. 2, p. 75-7 (1977)

Hellwig, H., Pannaci, E.
"Automatic Tuning of Hydrogen Masers".
Proc. IEEE (USA), Vol. 55, no. 4, 551-6 (April 1967)

Hellwig, H., Pannaci, E.
"Maser Oscillations with External Gain". J. Appl. Phys. (USA), Vol. 39, no. 12, p.5496-8 (Nov. 1968).

Hellwig, H.
"Hydrogen Spin Exchange Frequency Shifts".
Report NBS-TN-387 (PB-193701), Nat. Bur. Stand., Washington, DC, USA (March 1970), 19 pp.

Hellwig, H.
"The Hydrogen Storage Beam Tube, a Proposal for a New Frequency Standard", Metrologia (Germany), Vol. 6, No. 2, p. 56-60 (April 1970)

Hellwig, H., Bell., H. E.
"Experimental Results with Atomic Hydrogen Storage Beam Systems".
Proc. 26th Annual Frequency Control Symposium, Atlantic City, NJ, USA, 6-8 June 1972, (Washington, DC., USA; Electronic Industries Assoc. 1972) p. 242-247.

Hellwig, H., Bell., H. E.,
"Some Experimental Results with an Atomic Hydrogen Storage Beam Frequency Standard".
Metrologia (Germany), Vol. 8, No. 3, p. 96-8 (July 1972),

Hernqvist, K. G.
"The Hydrogen Dissociator (H Maser)"
IEEE Trans. Plasma Sci. (USA), Vol. PS-6, No. 3, p. 238-43 (Sept 1978).

Hibbard, L.U.
"The Hydrogen Maser as an Australian Frequency Standard".
Proc. Instn. Radio Electronics Engrs. Australia, Vol. 28, No. 12, 453-61 (Dec. 1967)

Kapitanskii, V. R., Kolosov, A.S., Kostakov, A.V., Livshits, A.I., Metter, I.M.
"Hydrogen Atomic Beam Oscillator with a Multichannel Source Output and a Multichannel Input into a Storage Box".
Zh. Tekh. Fiz. (USSR), Vol. 38, No. 8, p. 1366-9 (Aug. 1968). In Russian. English translation in: Soviet Phys-Tech. Phys. (USA).

Lacey, R.F., Vessot, R. F. C.
"Improved State Selection for Hydrogen Masers".
Proc. of the 23rd Annual Frequency Control Symposium, Atlantic City, NJ., USA, 6-8 May 1969 (Washington, DC., USA: Electronic Industries Assoc. 1969) p. 279-83

Levine, M. W., Vessot, R. F. C.
"Hydrogen Maser Time and Frequency Standard at Agassiz Observatory".
Radio Sci. (USA), Vol. 5, No. 10, p. 1287-92 (Oct. 1970).

Levine, M.W., Vessot, R. F. C., Mattison, E., Nystrom, G., Hoffman, T., Blomberg, E.
"A New Generation of SAO Hydrogen Masers".
Proc. 31st Annual Frequency Control Symposium, Atlantic City, NJ, USA., 1-3 June 1977 (Washington, DC, USA: Electronic Industries Assoc. 1977). p. 525-34.

Levine, M. W., Vessot, R. F. C., Mattison, E. M.
"Performance Evaluation of the SAO VLG-11 Atomic Hydrogen Maser".
Proc. 32nd Annual Frequency Control Symposium, Atlantic City, NJ., USA, 31 May - 2 June 1978 (Washington, DC, USA, Electronic Industries Assoc. 1978), p. 477-485.

Lightfoot, H. W.
"Construction and Investigation of an Atomic Hydrogen Beam Maser".
Univ. Keele, Staffs., England, thesis,(Feb. 1975).

Lightfoot, H. W., Laine, D.C.
"Comments on Oscillation Amplitude Settling Transients in a Hydrogen Maser Evoked by Rapid Frequency Scanning."
J. Phys. D (GB), Vol. 9, No. 15, p. L171-3 (21 Oct. 1976).

Morris, D.
"Hydrogen Maser Wall Shift Experiments at the National Research Council of Canada".
Programme of the 25th Annual Frequency Control Symposium (abstracts), Atlantic City, NJ, USA, 26-28 April 1971 (Ft. Monmouth, NJ, USA, US Army Electronics Command 1971), p. 55.

Morris, D.
"Hydrogen Maser Wall Shift Experiments at the National Research Council of Canada".
Metrologia (Germany), Vol. 7, No. 4, p. 162-6 (Oct. 1971).

Morris, D., Nakagiri, K.
"The Frequency Stability of a Pair of Auto-tuned Hydrogen Masers".
Metrologia (Germany), Vol. 12, No. 1, p. 1-6 (1976).

Morris, D.
"Time-Dependent Frequency Shifts in the Hydrogen Maser".
CPEM Digest 1978. Conference on Precision Electromagnetic Measurements, Ottawa, Canada, 26-29 June 1978 (New York, USA: IEEE 1978). p. 10-12.

Mungall, A.G., Morris, D., Daams, H., Bailey, R.
"Atomic Hydrogen Maser Development at the National Research Council of Canada".
Metrologia (Germany), Vol. 4, No. 3, p.87-94 (July 1968).

Nikitin, A.I., Strakhovskii, G. M.
"Quantum Generator Using a Beam of Hydrogen Atoms with a Superinvar Resonator".
Pribory Tekh. Eksper. (USSR), 1967, No. 1, p. 129-31 (Jan.-Feb.) in Russian. English translation in: Instrum. Exper. Tech (USA), No. 1, p. 134-6 (Jan.-Feb. 1967; publ. Jan.-Feb. 1967).

Nikitin, A.I., Strakhovskii, G. M.
"The Effect of Contamination of the Surface of a Storage Bulb on the Operation of a Hydrogen Maser".
Izv. VUZ Radiofiz (USSR), Vol. 12, No. 4, p. 517-19 (1969). In Russian.

Ohta, Y., Yoshimura, K., Shibuki, M., Nakagiri, K., Morikawa, T., Kobayashi, M., Saburi., Y.
"On an Automatic Cavity Tuner for Hydrogen Frequency Standard".
Rev. Radio Res. Lan. (Japan), Vol. 20, No. 106, p. 39-58 (Jan. 1974). In Japanese.

O'Neill, J. J., Phillips, D. H., Stone, R. R.
"Hydrogen Maser Frequency Translator".
Report NRL-7858, Naval Res. Lab., Washington, DC., USA (June 1975), 10 pp.

Peters, H. E., McGunigal, T.E., Johnson, E. H.
"Hydrogen Standard Work at Goddard Space Flight Center".
Proc. 22nd Annual Frequency Control Symposium, Atlantic City, NJ., USA, 22-24 April 1968 (Ft. Monmouth, NJ., USA, Electronic Components Laboratory 1968), p. 464-492A.

Peters, H. E., Johnson, E. H., McGunigal, T. E.
"Atomic Hydrogen Standards for NASA Tracking Stations".
Proc. 23rd Annual Frequency Control Symposium, Atlantic City, NJ., USA, 6-8 May 1969 (Washington, DC, USA, Electronic Industries Assoc. 1969), p. 297-304.

Peters, H.
"Hydrogen as an Atomic Standard".
Proc. 26th Annual Frequency Control Symposium, Atlantic City, NJ, USA, 6-8 June 1972, (Washington, DC, USA, Electronic Industries Assoc. 1972), p. 230-241.

Peters, H.E., Hall, R. G., Percival, D. B.
"Absolute Frequency of an Atomic Hydrogen Maser Clock".
Proc. 26th Annual Frequency Control Symposium, Atlantic City, NJ, USA, 6-8 June 1972 (Washington, DC., USA, Electronic Industries Association 1972) p. 319-322.

Peters, H.E.
"The Concertina Hydrogen Maser".
Proc. 29th Annual Frequency Control Symposium, Fort Monmouth, NJ, USA, 28-30 May 1975, (Washington, DC, USA, Electronic Industries Assoc. 1975) p. 362-70.

Peters, H.E.
"Small, Very Small, and Extremely Small Hydrogen Masers".
Proc. 32nd Annual Frequency Control Symposium, Atlantic City, NJ, USA, 31 May, 1-2 June 1978 (Washington, DC, USA, Electronic Industries Assoc. 1978) p. 469-476.

Petit, P., Viennet, J., Barillet, R., Desaintfuscien, M., Audoin, C
"Developments of Hydrogen Masers as Frequency Standards at Orsay".
Proc. 27th Annual Frequency Control Symposium, Cherry Hill, NJ, USA, 12-14 June 1973(Washington, DC, USA, Electronic Industries Assoc. 1973), p. 367-75.

Petit, P., Viennet, J., Barillet, R., Desaintfuscien, M., Audoin, C.
"Development of Hydrogen Masers as Frequency Standards at the Laboratoire de l'Horloge Atomique".
Metrologia (Germany), Vol. 10, No. 2, p.61-7 (1974).

Petit, P., Viennet, Barillet, R., Desaintfuscien, M., Audoin, C.
"Atomic Hydrogen Frequency Standards".
International Conference on Electronics and Measurements), Paris, France, 26-30 May 1975 (Paris, France. Comm. d'Organization due Colloque Internat. sur l' Electronique et la Mesure 1975), p. 111-19. In French.

Petit, P., Desaintfuscien, M., Audoin, C.
"Hydrogen Maser with a Double Configuration Bulb for Wall Shift Measurements in the Temperature Range 25 - 120°C."
Proc. 31st Annual Frequency Control Symposium, Atlantic City, NJ, USA, 1-3 June 1977 (Washington, DC, USA, Electronics Industries Assoc. 1977). p. 520-4.

Pepa, A. E., Wang, H. T. M., Bridges, W. B., Chester, A. N., Etter, J.E., Walsh, B. I.
"A Study to Identify Hydrogen Maser Failure Modes".
Proc. 30th Annual Symposium on Frequency Control, Atlantic City, NJ, USA., 2-4 June 1976, (Washington, DC, USA, Electronic Industries Assoc.) p. 489-92.

Ramsey, N. F.
"Atomic Hydrogen Hyperfine Structure".
Proc. of the Arnold Summerfield's centennial memorial meeting and of the international symposium on the physics of the one and two electron atoms, Munich, Germany, 10-14 Sept. 1968 (Amsterdam, Netherlands: North-Holland 1969). p. 218-34.

Ramsey, N. F.
"Hydrogen Maser Research".
Proc. of the Esfahan Symposium on Fundamental and Applied Laser Physics, Esfahan, Iran, 29 Aug.-5 Sept. 1971 (Chichester, Sussex, England; Wiley-Interscience 1973). p. 437-61.

Reinhardt, V. S., Peters, H. E.
"An Improved Method for Measuring the Magnetic Inhomogeneity Shift in Hydrogen Masers".
Proc. of the 29th Annual Frequency Control Symposium, Fort Monmouth, NJ, USA., 28-30 May 1975 (Washington, DC, USA., Electronic Industries. Assoc. 1975). p. 357-61.

Reinhardt, V. S., Kaufmann, D. C., Adams, W. A., De Luca, J. J., Soucy, J. L.
"NASA Atomic Hydorgen Standards Program - An Update".
Proc. 30th Annual Frequency Control Symposium, Atlantic City, NJ, USA., 2-4 June 1976 (Washington, DC, USA., Electronic Industries Assoc. 1976). p. 481-8.

Rueger, L. J., Bates, A., Stillman, L., Reinhardt, V. A.
"NASA NR Hydrogen Maser".
Proc. 32nd Annual Frequency Control Symposium, Atlantic City, NJ., USA., 31 May - 2 June 1978 (Washington, DC., USA., Electronic Industries Assoc. 1978). p. 486-91.

Sabisky, E. S., Peters, H. E.
"Design of a Spacecraft Hydrogen Maser".
Proc. 31st Annual Frequency Control Symposium, Atlantic City, NJ, USA, 1-3 June 1977 (Washington, DC., USA, Electronic Industries Assoc. 1977) p. 510-19.

Sabisky, E. S., Weaklien, H. A.
"An Operating Development Model Spacecraft Hydrogen Maser".
Proc. 32nd Annual Frequency Control Symposium, Atlantic City, NJ, USA., 31 May - 2 June 1978 (Washington, DC., USA, Electronic Industries Assoc 1978), p. 499-505.

Schutz, K.
"Measurements on Hydrogen Masers I".
Frequenz (Germany), Vol. 26, No. 12, p. 338-43 (Dec 1972). In German.

Schutz, K.
"Performance of a Hydrogen Maser II".
Frequenz (Germany), Vol. 27, No. 1, p. 12-17 (Jan. 1973). In German.

Sward, A., Sydnor, R.
"Power Density Spectrum of the Hydrogen Maser".
Proc. IEEE (USA), Vol. 56, No. 9, 1614-16 (Sept. 1968).

Uzgiris, E. E., Ramsey, N. F.
"Large Storage Box Hydrogen Maser".
Proc. 22nd Annual Frequency Control Symposium, Atlantic City, NJ, USA., 22-24 Apr 1968 (Fort Monmouth, NJ, USA., Electronic Components Lab. 1968) p. 452-64.

Uzgiris, E. E., Ramsey, N. F.
"Large Storage Box Hydrogen Maser".
IEEE J. Quantum Electronics Conference, Miami, Fl., (May 14-17, 1968).

Uzgiris, E. E., Zitzewitz, P. W.
"Recent Results Concerning the Hydrogen Maser Wall Shift Problems".
Proc. 23rd Annual Frequency Control Symposium, Atlantic City, NJ, USA, 6-8 May 1969 (Washington, DC, USA, Electronic Industries Assoc. 1969), p. 284-7.

Uzgiris, E. E., Ramsey, N. F.
"Multiple Hydrogen Maser with Reduced Wall Shift".
Phys. Rev. (USA), Vol. 1, No. 2, p. 429-46 (Feb. 1970).

Vessot, R. F. C.
"H Maser Wall Shift"
Metrologia (Germany), Vol. 6, No. 2, p. 52-3 (April 1970).

Vanier, J., Brousseau, R., Larouche, R.
"Simulated Emission in the Hydrogen Maser and the H Spin-Exchange Cross Section".
Can. J. Phys. (Canada), Vol. 51, No. 18, p. 1901-9 (15 Sept. 1973)

Vanier, J., Larouche, R., Audoin, C.
"The Hydrogen Maser Wall Shift Problem".
Proc. 29th Annual Frequency Control Symposium, Fort Monmouth, NJ, USA, 28-30 May 1975 (Washington, DC, USA, Electronic Industries Assoc. 1975) p. 371-82.

Vanier, J., Larouche, R.,
"A Comparison of the Wall Shift of TFE and FEP Coatings in the Hydrogen Maser.
Metrologia (Germany), Vol. 14, No. 1, p. 31-7 (1978).

Vessot, R. F. C., Levine, M. W.
"Atomic Hydrogen Maser for Space Vehicle Application, Phase I, Final Report, 1 Mar 1966 - 31 Mar 1968".
Report NASA-CR-94937, Hewlett-Packard Co. Frequency and Time Div., Available from CFSTI, Springfield, VA 22151.

Vessot, R. F. C., Levine, M., Cutler, L., Baker, M., Mueller, M.
"Progress in Development of Hydrogen Masers".
Proc. 22nd Annual Frequency Control Symposium, Atlantic City, NJ, USA 22-24 Apr 1968, (Fort Monmouth, NJ, USA, Electronic Components Lab. 1968), p. 605-20.

Kleppner, D., Ramsey, N. F.,
"Application of the Hydrogen Maser to Experimental Relativity".
IEEE J. Quantum Electronics (USA), Vol. QE-4, No. 5, p. 376 (May 1968).

Vessot, R. F. C., Levine, M. W.
"Studies of Hydrogen Maser Wall Shift for High Molecular Weight Polytetrafluorethylene"
Proc. 24th Annual Frequency Control Symposium, Atlantic City, NJ, USA., 27-29 April 1970 (Washington, DC, USA., Electronics Industries Assoc. 1970). p. 263-269.

Vessot, R. F. C., Levine, M. W.
"A Method for Eliminating the Wall Shift in the Atomic Hydrogen Maser".
Metrologia (Germany), Vol. 6, No. 4, p. 116-17 (Oct 1970).

Vessot, R. F. C., Levine, M. W.
"Performance Data of Space and Ground Hydrogen Masers and Ionospheric Studies for High Accuracy Comparison between Space and Ground Clocks".
Proc. 28th Annual Frequency Control Symposium 1974, Atlantic City, NJ, USA., 29-31 May 1974(Washington, DC, USA., Electronic Industries Assoc. 1974). p. 408-14.

Vishina, A. V., Gaigerov, B. A.
"Hydrogen Time and Frequency Standards with Redundancy".
Meas. Tech. (USA), Vol. 19, No. 10, p. 1460-1 (Oct 1976). Translation of: Izmer. Tekh. (USSR), Vol. 19, No. 10, p. 50 (Oct 1976).

Walls, F. L., Hellwig, H.
"A New Kind of Passively Operating Hydrogen Frequency Standard".
Proc. 30th Annual Frequency Control Symposium, Atlantic City, NJ, USA, 2-4 June 1976 (Washington, DC, USA, Electronic Industries Assoc. 1976) p. 473-80.

Walls, F. L., Howe, D. A.
"A Passive Hydrogen Maser Frequency Standard". Proc. 32nd Annual Frequency Control Symposium, Atlantic City, NJ, USA, 31 May - 2 June 1978 (Washington, DC, USA, Electronic Industries Assoc. 1978). p. 492-498.

Zhestkova, N. D., Elkin, G. A., Zemskova, V. I.
"Hydrogen Frequency Standard and Undisturbed Frequency Transition Evaluation".
Meas. Tech. (USA), Vol. 19, No. 10, p. 1461-3 (Oct. 1976). Translation of: Izmer. Tekh. (USSR), Vol. 19, No. 10, p. 50-1 (October 1976).

Zitzewitz, P. W., Uzgiris, E. E., Ramsey, N. F.
"Wall Shift of FEP Teflon in the Hydrogen Maser". Rev. Sci. Instrum. (USA), Vol. 41, No. 1, p. 81-6 (Jan. 1970).

Zitzewitz, P. W.
"Surface Collision Frequency Shifts in the Atomic Hydrogen Maser".
Proc. 24th Annual Frequency Control Symposium, Atlantic City, NJ, USA, 27-29 April 1970, (Washington, DC, USA., Electronic Industries Assoc. 1970). p. 263-269.

Zitzewitz, P. W., Ramsey, N. F.
"Studies of the Wall Shift in the Hydrogen Maser". Phys. Rev. A (USA), Vol. 3, No. 1, p.51-61 (June 1971).

2.1.4

Vanier, J., Tetu, M., Brousseau, R.
"Frequency and Time Domain Stability of the Rb^{87} Maser and Related Oscillator: A Progress Report". Proc. 31st Annual Frequency Control Symposium, Atlantic City, NJ., USA, 1-3 June 1977 (Washington, DC, USA: Electronic Industries Association 1977), p. 344-346.

Alekseev, E. I., Bazarov, E. N.
"Theory of a Rubidium Maser Generator Using Optical Pumping". Radiotekhnika i Elektronica (USSR), Vol. 15, no. 5, p. 1044-51 (May 1970). Russian. English translation in: Radio Engng. Electronic Phys. (USA).

Bardo, W. S.
"A Study of CoherencePhenomena in an Ammonia Maser". Univ. Keele. Staffordshire, England, thesis.

Bardo, W. S., Laine, D. C.
"Induced Spiking in an Ammonia-Maser Oscillator" Electronics Letters (GB), Vol. 5, no. 26, p. 688-9 (25 Dec. 1969).

Bardo, W. S., Laine, D. C.
"Ammonia Maser Operated without Cryogenic Pumping". J. Phys. E (GB), Vol. 48, no. 8, p. 595-7 (Aug. 1971).

Bardo, W. S.
"Osillation Transient in a Molecular Q-switched Ammonia Maser". J. Phys. D (GB), Vol. 4, no. 11, p. L42-4 (Nov. 1971).

Bardo, W. S., Laine, D. C.
"On Detuning Phenomena in Cascaded Cavity Molecular Beam Masers". J. Phys. B (GB), vol. 4, no. 11, p. 1523-35 (Nov. 1971).

Basov, N. G., Borisenko, M. I., Vlasov, V. P., Dubonosov, S. P., Ivanov, N. E., Strakhovskii, G.M., Fedorenko, G. M., Chikhakhev, B. M.
"Operating Experience with a Satellite-Borne Maser Oscillator". Kosmicheskie Issledovaniya (USSR), Vo. 5, no. 4, 608-16 (July-Aug. 1967). In Russian. English translation in: Cosmic Res. (USA), Vol. 5, no. 4, 526-32 (July-Aug. 1967).

Bazarov,YE. N.
"Approximate Theory of Optically Pumped Rubidium Vapour Maser Oscillator". Radiotekhnika i Elektronika (USSR), Vol. 14, no. 6, p. 1035-42 (June 1969). In Russian. English translation in: Radio Engng. Electronic Phys. (USA).

Bazarov, Ye. N., Gubin, V. P.
"Experimental Study of a Fixed Operating Range of Optically Pumped Rubidium Vapour Maser Oscillator". Radiotekhnika i Elektronika (USSR), Vol. 14, no. 6, p. 1043-9 (June 1969). In Russian. English Translation in: Radio Engng. Electronic Phys. (USA).

Bazarov, Ye. N., Gubin, V. P.
"Light Frequency Shift in a Rubidium Maser Oscillator Using Modulated Optical Pumping". Radiotekhnika i Elektronika (USSR), Vol. 14, no. 6, p.1050-5 (June 1969). In Russian. English translation in: Radio Engng. Electronic Phys. (USA).

Bazarov, Ye. N., Gubin, V. P.
"Short-term Frequency Instability of an Optically Pumped Rubidium Maser". Radiotek. & Elektron. (USSR). In Russian. English Translation in: Radio Eng. Electron. (USA)., Vol. 15, no. 10, p. 1860-7 (Oct. 1970).

Bazarov, Ye. N., Biketov, V. D., Gubin, V. P., Yukhvidin, Ya. A.
"The Effect of the Buffer Gas on the Operation of an Optically Pumped Rb^{87} Maser". Radio Eng. & Electron Phys. (USA), Vol. 17, no. 3, p. 432-9 (March 1972). Translation of: Radiotekh. & Elektron. (USSR), Vol. 17, no. 3, p. 556-64 (March 1972).

Bazarov, E. N., Biketov, V. D., Gubin, V. P.
"Short-Term Instability of an Optically Pumped Rubidium Maser Standard". Radio Eng. & Electron. Phys. (USA), Vol. 17, no. 4, p. 697-9 (April 1972). Translation of: Radiotekh. & Elektron. (USSR), p. 887-8

Ben-Reuven, A., Kukolich, S. G.
"Relaxation Rates in Molecular Beam Maser Experiments". Chem. Phys. Lett. (Netherlands) vol. 23, no. 3, p. 376-80 (1 Dec. 1973).

Brousseau, R,, Vanier, J.
"An Electronic System for the Tuning of Masers". IEEE Trans. Instrum. & Meas. (USA), Vol. IM-22, no. 4, p. 367-76 (Dec. 1973) (Electrical and Electronic Measurement and Test Instrument Conference, Ottawa, Ontario, Canada, 14-17 May 1973).

Busca, G., Tetu, M., Vanier, J.
"Cavity Tuning and Light-Shift in the Rb^{87} Maser". Proceedings of the 27th Annual Frequency Control Symposium, Cherry Hill, N. J., USA, 12-14 June 1973 (Washington, D. C., USA: Electronic Industries Assoc. 1973), p. 400-3.

Busca, G., Tetu, M., Vanier, J.
"Light Shift and Light Broadening in the ^{87}Br Maser". Can. J. Phys. (Canada), Vol. 51, No. 13, p. 1379-87 (1 July 1973).

Busca, G., Tetu, M., Vanier, J.
"Light Shift Effects in the Rb^{87} Maser". Appl. Phys. Lett. (USA), Vol. 23, no. 7, p. 395-6 (1 Oct. 1973). (6 refs)

Busca, G., Racine, J., Vanier, J.
"A Compact Rb^{87} Maser". Proceedings of the 28th Annual Frequency Control Symposium 1974, Atlantic City, N.J., USA, 29-31 May 1974 (Washington, D. C., USA: Electronic Industries Assoc. 1974), p. 344-7.

Busca, G., Brousseau, R., Vanier, J.
"Long-Term Frequency Stability of the Rb^{87} Maser". IEEE Trans. Instrum. & Meas. (USA), Vol. IM-24, no. 4, p. 291-6 (Dec. 1975).

Busca, G., Savard, J. Y., Rovea, S., Vanier, J., Desaintfuscien, M., Petit, P., Audoin, C.
"Zeeman Effects on H and Rb Masers", 31st Annual Frequency Control Symposium, Atlantic City, N.J., USA, 1-3 June 1977 (Washington, D.C. USA: Electronic Industries Assoc. 1977), p. 535-41.

DeLucia, F., Gordy, W.
"Molecular-Beam Maser for the Shorter-Millimeter-Wave Region: Spectral Constants of HCN and DCN". Phys. Rev. (USA), Vol. 187, no. 1, p. 58-65 (Nov. 1969).

Dyubko, S. F, Efimenko, M.N., Svich, V. A., Fesenko, L. D.
"Stimulated Emission of Radiation from Optically Pumped Vinyl Bromide Molecules". Sov. J. Quantum Electron. (USA), Vol. 6, no. 5, p. 600-1 (May 1976). Translation of: Kvantovaya Elektron. Moskva (USSR), Vol. 3, no. 5, p. 1121-2 (May 1976).

Frayne, P. G.
"Repetitive Q-modulated HCN Gas Maser". J. Phys. B. Proc. Phys. Soc. Ser. 2, Vol. 2, no. 2, p. 247-59 (Feb. 1969)

Fuller, D. W. E., Hines, J., Compton, B.
"Short-term Frequency Stability of the HCN Maser". Electronics Letters (GB), Vol. 5, no. 19, p. 448-9 (18 Sept. 1969).

Gheorghiu, O., Gheorghe, V., Giurgiu, L., Mandache, C., Bocaniciu, T., Iordachescu., T.
"Hydrogen Masers as Frequency Standards". Metrol. Apl. (Rumania), Vol. 24, no. 2, p. 75-7 (1977).

Gubkin, A. N., Novak, M. M., Kholodva, G. K.
"Electric Field of Ring Electrets and Possible Application for State Selection in a Maser". Zh. Tekh. Fiz. (USSR), Vol. 42, no. 4, p. 864-8 (April 1972). In Russian. English translation in Sov. Phys. Tech. Phys. (USA), Vol. 17, no. 4, p. 681-4 (Oct. 1972).

Hardin, J., Uebersfeld, J.
"Radioelectric Scheme Equivalent to an Ammoniacal Maser". CR. Acad. Sci. Ser. B (France), Vol. 270, no. 25, p. 1617-19 (22 June 1970). In French.

Hardin, J., Uebersfeld, J.
"An Ammonia Maser Used for Electron Paramagnetic Resonance". Revue Phys. Appl. (France), Vol. 6, no. 2, p. 165-72 (June 1971). In French.

Hartmann, F.
"Maser Amplification by an Alkali Vapour Submitted to Optical Pumping: Application to the Case of Rubidium 85". Ann. Phys. (France), Vol.2, no. 6, p. 329-42 (Nov. 1967). In French.

Hartmann, F.
"Frequency Stability of the Regenerative Rubidium Maser Oscillator". Phys. Letters (Netherlands), Vol. 28a, no. 3, p. 193-4 (18 Nov. 1968).

Hartmann, F.
"Resonance Line Shape and Filling Factor in an Alkali Vapor Maser: Influence of Atomic Motion". IEEE J. Quantum Electronics (USA), Vol. QE-5, no. 12, p. 595-600 (Dec. 1969).

Hellwig, H., Pannaci, E.
"Maser Oscillations with External Gain". J. Appl. Phys. (USA), vol. 39, no. 12, p. 5496-8 (Nov. 1968).

Iga, Ken-ichi, Fukuyo, H.
"Optical Pumping and Optical Detection Mechanism in Rb Atomic Oscillator". Inst. Electron. Commun. Eng. Jap. A, B, C. (Japan) In Japanese. English translation in: Electron & Commun. Jap. (USA), Vol. 53, no. 1, p. 54-9 (Jan. 1970).

Ivanna, E. P., Ivanov, N. I., Kravchenko, V. F.
"Shortlived Fluctuations in the Frequency of a Rb Maser". Radiotekhnika, Kharkov (USSR), no. 31, p. 142-6 (1974). In Russian.

Jelinek, F., Vrba, J.
"Solid State Microwave Power Source for an Ammonia Maser". Proceedings of the third colloquium on microwave communication, Budapest, (1968), Budapest, Akademiai, Kiado, 693-701 (1968).

Jones, H., Eyer, A.
"Collisional Transfer of Energy in Ammonia; Some Triple Resonance Experiments". Z. Naturforsch. A (Germany) Vol. 28A, no. 10, p. 1703-6 (Oct. 1973).

Khaplanov, G. M., Biketov, V. D., Volkova, N. I., Lukoshkova, G. I., Bazarov, Ye. N., Yukhvidin, Ya.A., Cubin, V. P.
"Rb^{87} Vapour Maser". Radiotekhnika i Elektronika (USSR), Vol.13, No. 1, 165 (Jan. 1968). In Russian. English Translation in: Radio Engng. Electronic Phys. (USA).

Krause, W. H. U.
"Quantum-Mechanical Explanation of Detuning Effect Observed with Two-Cavity Molecular Beam Masers". Phys. Letters (Netherlands) Vol. 28A, No. 5, p.380-1 (16 Dec. 1968).

Krause, W.H. U., Laine, D. C.
"Nuclear Spin Analogue of a Molecular Beam Maser with Cavities in Series". J. Phys. B (GB), Vol. 6, no. 8, p. 1516-30 (Aug. 1973).

Koshurinov, Ye. I.
"Effect of the Symmetry of Potentials at the Separating System and the Reasonator of a Molecular Oscillator". Radiotekhnika i Elektronika (USSR), Vol. 14, no. 10, p. 1840-2 (Oct. 1969).

Kroupnov, A. F., Skvortsov, V. A., Sinegoubko, L.A.
"The Study of Operation Regimes of Two-Resonator Molecular Generator with Opposite Beams". Izv. VUZ Radiofiz. (USSR), 1968, no. 2, 244-50. In Russian. English translation in: Soviet Radiophys. (USA).

Kukolich, J. G.
"Measurements of the 3-2 Inversion Frequency and Frequency Stability of a Two-Cavity Ammonia Maser". Proc. Inst. Elect. Electronics Engrs. (USA), Vol. 56, no. 1, 124-5 (Jan. 1968).

Laine, D. C., Smith, A. L. S.
"Modulation Effects in an Ammonia Beam Maser Oscillator". IEEE J. Quantum Electronics (USA) Vol. QE-2, No. 9, 399-408 (Sept. 1966). (Fourth International Quantum Electronics Conference, Phoenix, 1966).

Laine, D. C.
"Oscillation Quenching in a Molecular-Beam Maser". Electronics Letters (GB), Vol. 3, no. 10, 454-5 (Oct. 1967).

Laine, D. C., Bardo, W.S.
"Transients in an Ammonia-Maser Oscillator". Electronics Letters (GB), Vol. 5, no. 14, p. 323-4 (10 July 1969).

Laine, D. C., Bardo, W. S.
"Comment on an Anomalous Saturation Effect in an Ammonia Beam Maser". J. Phys. B. (GB) Ser. Vol. 3, no. 2, p. 123-4 (Feb. 1970)

Laine, D. C., Smart, G. D. S.
"Ammonia Beam Masers Employing Parallel Plate and Conical Types of Open Resonator". J. Phys. D (GB), Vol. 4, no. 8, p. L23-5 (Aug. 1971).

Laine, D. C., Sweeting, R. C.
"Electret Behaviour of Solid Ammonia Observed in an Ammonia Beam Maser". Phys. Lett. A (Netherlands), Vol. 36A, no. 6, p. 469-70 (11 Oct. 1971).

Laine, D. C., Sweeting, R. C.
"On the Operation of Molecular Beam Masers with Electret Focusers". J. Phys. D (GB), Vol. 4, no.11, p. L44-6 (Nov. 1971).

Laine, D. C., Bardo, W. S.
"Multiple PopulationInversion in a Beam Maser". J. Phys. B (GB),Vol. 4, no. 12, p. 1738-42 (Dec. 1971).

Laine, D. C.
"Molecular Beam Masers". Phys. Bull.(GB), Vol. 24, p. 79-84 (Feb. 1973).

Laine, D. C., Sweeting, R. C.
"Operation of a Molecular Beam Maser with an Electret State Separator". J. Phys. D (GB), Vol.7, no. 4, p. 500-9 (1 March 1974).

Laine, D. C., Matoff, A. K. H.
"Oscillation Pulsations in a Two-Cavity Molecular Beam Maser". Proceedings of the 18th Ampere Congress on Magnetic Resonance and Related Phenomena, Vol. I, Nottingh am, England, 9-14 Sept. 1974 (Amsterdam, Netherlands: North-Holland 1975), p. 199-200.

Lefrere, P. R., Laine, D. C.
"Beat Mode Phase Shifts in a Molecular Beam Zeeman Maser Oscillator Operated with Series". Phys. Lett. A (Netherlands), Vol. 45A, no. 5, p. 405-6 (22 Oct. 1973).

Lefrere, P. R., Laine, D. C.
"Molecular Beam Maser Oscillator Analogue of Forced Phase-Locking in Lasers". J. Phys. D (GB), Vol. 6, no. 18, p. L131-3 (5 Dec. 1973).

Lefrere, P. R.
"Coupled Molecule-Radiation Field Effects in an Ammonia Beam Maser". Univ. Keele, Staffs.,England) thesis, May 1974.

Maroof, A. K. H., Laine, D. C.
"Operation of J=3, K=2, $^{14}NH_3$ Molecular Beam Maser Oscillation without Cryopumping or Time Limit". J. Phys. E (GB), Vol. 7, no. 5, p. 409-11 (May, 1974).

Maroof, A. K. H.
"Design, Construction and Investigation of an Ammonia Beam Maser Operated under Conditions of Strong Oscillation". Univ. Keele, Staffs.,England thesis, Feb. 1975).

Maroof, A. K. H., Laine, D. C.
"Molecular Beam Mass Oscillation on the J=K=1 Inversion Line of $^{14}NH_3$". J. Phys. D (GB), Vol. 9, no. 5, p. 697-700 (1 April 1976).

Matsuda, I., Sato, T., Kuramochi, N., Fukuyo, H.
"Frequency Stability of the Rb Standard TTR-1". Bull. Tokyo Inst. Technol. (Japan), no. 125, p. 9-15 (1974).

Mehta, A.
"Maser". J. Inst. Eng. (India) Electron. & Telecommun. Eng. Div., Vol. 55, no. ET2-3, p. 47-50 (April 1975)

Mukhamedgalieva, A. F., Oraevskii, A. N., Strakhovskii, G. M.
"Investigation of a Molecular Oscillator with a 'Molecular-Ringing' Amplifier". Izv. VUZ Radiofiz. (USSR), Vol. 9, no. 2, 302-7 (March-April 1966).

Olivier, M., Plain, A.
"Extension of the Theory of the Frequency Noise of Maser Oscillators". C. R. Hebd, Seances Acad. Sci. B (France), Vol. 276, no. 14, p. 615-8 (2 April 1974), In French.

Oyamada, H., Takahashi, K., Sato, Y., Uchida, H.
"A Consideration of Rubidium Lamp Stability for Rubidium Frequency Standard". Proceedings of the 28th Annual Frequency Control Symposium 1974, Atlantic City, N.J., USA, 29-31 May 1974 (Washington, D. C., USA: Electronic Industries Assoc., 1974), p. 340-3.

Pankratov, V. A.
"Possible Use of a Rubidium Maser as a Combined Frequency Standard". Sov. J. Quantum Electron. (USA), Vol. 4, no. 4, p. 521-2 (Oct. 1974). Translation of: Kvantovaya Elektron Moskva (USSR), Vol. 1, no. 4, p. 950-2 (April 1974).

Smart, G.D.S.
"Construction and Characteristics of an Ammonia Beam Maser Employing a Fabry-Perot Cavity". Univ. Keele, Staffs., England Thesis, Sept. 1974.

Stern, W. A., Novick, R.
"An Optically Pumped ^{85}Rb Maser Frequency Standard". Proceedings of the 23rd annual frequency control symposium, Atlantic City, N.J., USA, 6-8 May 1969 (Washington, D.C., USA: Electronic Industries Assoc. 1969), p. 271-3.

Stern, W.A., Novick, R.
"A Field-independent Optically Pumped ^{85}Rb Maser Oscillator". Appl. Phys. Lett (USA), Vol. 17, no. 5, p. 216-17 (1 Sept. 1970).

Stern, W. A., Novick, R.
"A Field Independent Optically Pumped 85 Maser Frequency Standard". Programme of the 25th Frequency Control Symposium (abstracts). Atlantic City, N.J., USA, 26-28 Apr 1971 (Fort Monmouth, N.J., USA: US Army Electronics Command 1971), p. 52.

Stern, W. A., Novick, R.
"Light and Buffer-Gas Frequency Shifts in the ^{85}Rb Maser Frequency Standard". IEEE Trans. Instrum. & Meas. (USA), Vol. IM-21, no. 2, p. 99-105 (May 1972).

Stern, W. A., Novick, R.
"Further Results on the Rubidium-87 Maser Frequency Standard". Proc. 26th Annual Frequency Control Symposium, Atlantic City, N.J., USA, 6-8 June 1972 (Washington, D. C., USA: Electronic Industries Association 1972), p. 223-224.

Stern, W. A., Aulich, E., Novick, R.
"Status of the Development of the Rubidium-87 Maser Frequency Standard". Proceedings of the 27th Annual Frequency Control Symposium, Cherry Hill, New Jersey, USA, 12-14 June 1973 (Washington, D. C., USA: Electronic Industries Assoc. 1973),p. 404-5.

Smith, A. L. S., Laine, D. C.
"Fluctuations in the Amplitude of Oscillation of an Ammonia Beam Maser". Electronics Letters (GB), . Vol. 3, no. 2, 90-1 (Feb. 1967).

Smith, A. L. S., Laine, D. C.
"Further Characteristics of a Molecular Beam Maser Oscillator Operated with Two Cavities in Series". Brit. J. Appl. Phys. (J. Phys. D). (GB) Ser. 2, Vol. 1, 727-32 (June 1968).

Temple, R. E.,
"The Operation and Frequency Stability Measurement of a Hydrogen Cyanide Beam Type Maser at 88.6 GHz". Univ. Colorado, Boulder, USA thesis, 1971, 146 pp Available from Univ. Microfilms, Ann Arbor, Mich., USA Order No. 71-25877.

Tessier, M., Vanier, J.
"Theory of the Rubidium 87 Maser". Can. J. Phys. (Canada), Vol. 49, no. 21, p. 2680-9 (1 Nov. 1971) In French.

Tetu, M., Busca, G., Vanier, J.
"Short Term Stability of the Rb^{87} Maser". Proc. 26th Annual Frequency Control Symposium, Atlantic City, N.J., USA, 6-8 June 1972 (Washington, D.C., USA: Electronics Industries Association 1972), p. 225-229.

Tetu, M., Busca, G., Vanier, J.
"Short-term Frequency Stability of the Rb^{87} Maser". IEEE Trans. Instrum. & Meas. (USA), Vol. IM-22, no. 3, p. 250-7 (Sept. 1973).

Truman, M.J., Laine, D. C.
"Anomalous Beahaviour of an Ammonia Beam Maser Employing a Ring Focuser". J. Phys. D (GB), Vol. 9, no. 15, p. L175-8 (21 Oct. 1976).

Valentin, M.
"Study of the Behaviour of a Measer with Eight Ammonia Jets Using a Fabry-Perot Resonator". Nuovo Cimento B (Italy), Vol.44 B, Ser. 2, no. 1, p. 205-27 (11 March 1978). In French.

Varner, J.,Vaillancourt, R., Missont, C, Tetu, M.
"Progress Report on the Rubidium 85 Maser". Proc. 24th Annual Frequency Control Symposium, Atlantic City, N.J., USA, 27-29 April 1970 (Washington, D.C. USA, Electronic Industries Association 1970), p. 280-284.

Vanier, J., Vaillancourt, R., Missout, C., Tetu, M.
"Rubidium-85 Maser-Oscillator". J. Appl. Phys. (USA), Vol. 41, no. 7, p.3188-9 (June 1970).

Vanier, J., Strumia, F.
"Theory of the Optically Pumped Cesium Maser". Can. J. Phys. (Canada), Vol. 54, no. 23, p. 2355-66 (1 Dec. 1976).

Vanier, J., Tetu, M., Brousseau, R.
"Frequency and Time Domain Stability of the Rb^{87} Maser and Related Oscillators: A Progress Report". 31st Annual Frequency Control Symposium, Atlantic City, N.J., USA, 1-3 June 1977 (Washington, D.C., USA: Electronic Industries Assoc. 1977), p. 344-6.

Wineland, D. J., Howe, D. A., Mohler, M. B.
"Results with the Special-Purpose Ammonia Frequency Standard". 31st Annual Frequency Control Symposium, Atlantic City, NJ, USA, 1-3 June 1977 (Washington, DC, USA: Electronic Industries Assoc. 1977), p. 562-73

Zhabotinskii, M. E., Karlov, N. V., Steinshleiger, V. B.
"Masers". Radiotekhnika i Elktronika (USSR), Vol. 12, no. 11, 2032-51 (Nov 1967). In Russian. English translation in: Radio Engng. Electronic Phys. (USA), Vol. 12, no. 11, 1879-94 (Nov. 1967).

2.2

Akimoto, Y., Ohi, M.
"Stability Evaluation of Frequency Stabilized Laser", Oyo Buturi (Japan), Vol. 47, No. 5, p. 425-31 (May 1978).

Arditi, M., Picque, J. L.
"Application of the Light-Shift Effect to Laser Frequency Stabilization with Reference to a Microwave Frequency Standard", Opt. Commun. (Netherlands), Vol. 15, No. 2, p. 317-22 (Oct. 1975).

Bageav, S. N., Chebotaev, N. P., Vasilenko, L. S.
"An Optical Frequency Standard with Two Absorption Cells", Opt. & Spectrosk, (USSR), Vol. 29, No. 2, p. 156-9 (Aug. 1970).

Baird, K. N.
"Laser Stabilization at N.R.C.," Electron Technol. (Poland), Vol. 2, No. 2/3, p. 85-8, (1969).

Baird, K. M., Hanes, G. R.
"Stabilization of Wavelengths from Gas Lasers", Rep. Prog. Phys. (GB), Vol. 37, No. 7, p. 927-50 (1974).

Basov, N. G., Letokhov, V. S.
"Optical Frequency Standards", Electron. Technol. (Poland). Vol. 2, No. 2/3, p. 15-20 (1969).

Basov, N. G., Belenov, E.M., Danileiko, M. V.
"Power Resonances and Frequency Stabilization of a Gas Laser with a Nonlinear-absorption Cell", Kvantovaya Elecktron ,(USSR), No. 1, p. 42-52 (1971).

Belenov, E. M., Danileiko, M. V., Nedavnii, A. P., Shpak, M.T.
"Frequency Shifts in Stabilized Gas Lasers", Ukr. Fiz. Zh. (USSR), Vol. 22, No. 11, p. 1765-79 (Nov. 1977).

Bennett, W. R., Jr.
"Role of Hole Burning in the Self-Stabilization of Gas Laser Frequencies", Comments At. & Mol. Phys. (GB), Vol. 3, No. 3, p. 63-8 (May-June 1972).

Beterov, I. M., Matyugin, Yu. A., Milushkin, G. A., Troshin, B. I., Chebotae, V. P.
"High-Stability Gas Laser Based on Non-Linear Absorption", Avtometriya (USSR), No. 6, p. 64-8 (Nov-Dec. 1972).

Beterov, I. M., Matyugin, Yu. A., Milushkin, G. A., Troshin, B. I., Chebotaev, V. P.
"High-Stability Gas Laser Based on Nonlinear Absorption", Avtometriya (USSR), No. 6, p. 53-64, (Nov.-Dec. 1974).

Birnbaum, G.
"Frequency Stabilized Gas Lasers", Electron. Technol. (Poland), Vol. 2, No. 2/3, p. 67-9 (1969).

Bloom, A. L.
"Gas Lasers and Their Application to Precise Length Measurements", Progress in Optics (Amsterdam), Vol. 9, p. 3-30 (1971).

Bobrik, V. I., Gol'dort, V. G., Kolomnikov, Yu. D., Pecherskii, Yu. Ya.
"Stabilization of Laser Frequencies", Meas. Tech. (USA), Vol. 17, No. 8, p. 1252-3 (Aug. 1974).

Borisovskii, S. P., Vereikin, V. K., Vlasov, A. N., Ostapchenko, E. P., Teselkin, V. V., Chulyaeva, E. G., Yakovlev, Yu. M.
"Measuring Stability and Reproducibility of Gas-Laser Generation Frequency", Meas. Tech. (USA), Vol. 20, No. 8, p. 1161-5 (Aug. 1977).

Boyne, H. S.
"Laser Frequency Stabilization Techniques and Applications", IEEE Trans. Instrum. & Meas. (USA), Vol. IM-20, No. 1, p. 19-22 (Feb. 1971).

Koffend, J. Brooke, Goldstein, S., Bacis, R., Field R. W., Ezekiel, S.
"Doppler-Free Stimulated-Emission Spectroscopy and Secondary Frequency Standards Using an Optically Pumped Laser", Phys. Rev. Lett. (USA), Vol. 41, No. 15, p. 1040-4 (Oct. 1978).

Bulygin, A. S., Kapralov, V. P.
"Synchronization of Laser Radiation with a Quantum Frequency Standard in the Microwave Region", Opt. & Spectrosc. (USA), Vol 42, No. 1. Translation of: Opt. & Spektrosk, (USSR), Vol. 42, No. 1, p. 154-60 (Jan. 1977).

Clark, N. A.
"Laser Frequency Stabilization: Combined Integrating Thermal Proportional Servos", Appl. Opt. (USA), Vol. 15, No. 6, p. 1375 (June 1976).

Domnin, Yu. S., Tatarenkov, V. M., Shumyatskii, P.S.
"Absolute Frequency Measurements of Lasers in Submillimeter and Infrared Ranges", Meas. Tech. (USA), Vol. 19, No. 10, p. 1475-9 (Oct. 1976). Translation of: Izmer. Tekh. (USSR), Vol. 19. No. 10, p. 59-61 (Oct. 1976).

Engelhard, E.J.G.
"The Feasibility of Establishing a New Primary Wavelength Standard of Length by a Laser Line", Electron. Technol. (Poland), Vol. 2, No. 2/3, p. 71-6 (1969).

Eppers, W. C., Jr.
"Fixed Frequency Lasers", Proceedings of the Society of Photo-Optical Instrumentaion Engineers (USA), Vol. 49, p. 19-20(Aug. 1974).

Evenson, K. M., Petersen, F. R.
"Stabilized Lasers and Applications", Laser Applications to Optics and Spectroscopty (USA), p. 367-400 (July 1973).

Evenson, K. M., Jennings, D. A., Petersen, F. R.
"Laser Frequency Measurements: A Review, Limitations, Extension to 197 THz (1.5 μm)." Laser Spectroscopy III (USA), p. 56-68 (July 1977).

Galutin, V. Z., Zenkevich, S. S., Obukhov, I. V., Skibarko, A. P.
"Frequency Stability of a Gas Laser Operating in a Two-Mode Domain", Izv. VUZ Radioelektron (USSR), Vol. 16, No. 9, p. 90-3 (Sept. 1973).

Greenstein, H.
"Theory of a Gas Laser with Internal Absorption Cell", J. Appl. Phys. (USA), Vol. 43, No. 4, p. 1732-50 (April 1972).

Gronchi, M.
"Frequency Stabilized Lasers as Absolute Standards", Riv. Nuovo Cimento (Italy), Vol. 2, No. 2, p. 219-52 (April-June 1970).

Hall, J. L.
"Laser Frequency Stabilization", IEEE J. Quantum Electronics (USA), Vol. QE-5, No. 6, p. 324 (June 1969).

Hartman, F.
"Optical Frequency Standards", Ann. Phys. (France) Vol. 5, No. 4, p. 281-90 (July-Aug. 1970).

Iriarte, M. Jr.
"Lasers and Masers", IEEE Electrolatina (Mexico), Vol. 7, No. 3, p. 17-23 (Sept. 1973).

Jimenez, J. J., Petersen, F. R.
"Recent Progress in Laser Frequency Synthesis", Infrared Phys. (GB), Vol 17, No. 6, p. 541-6 (Nov. 1977).

Kayak, I. K., Kalinin, N. A., Kapralov, V. P.
"Research on Frequency-Stabilised Gas Lasers in the Member Nations of COMECON (Council for Economic Assistance), Meas. Tech. (USA), Vol. 17, No. 6, p. 829-31 (June 1974).

Ketskemety, I., Bor, Zs., Racz, B., Kozma, L.
"Improved Line Narrowing and Wavelength Stabilization Technique of Distributed Feedback Dye Lasers", Opt. Commun. (Netherlands), Vol 22, No. 3, p. 275-7 (Sept. 1977).

Kuznetsiv, V. M.
"Gas Laser Automatic Frequency Stabilization System", Prib. Tekh. Eksp. (USSR), p. 189-91 Translation in English: Instrum. Exp. Tech. (USA) No. 1, p. 218-20 (Jan. 1970).

Le Floch, A., Frere, P., Brun, P.
"Frequency Stabilization of a Gas Laser Using the Magnetic Lamb Dip", Appl. Phys. Letters (USA), Vol. 17, No. 1, p. 40-2 (July 1970).

Le Floch, A., La Naour, R, Stephan, G. Brun, P.
"Frequency Stabilization and Tunability of Lasers; Use of Mobile Dips and Peaks", Appl. Opt. (USA), Vol 15, No. 11, p. 2673-7 (Nov. 1976).

Leikin, A. J., Solovjov, V. S.
"Determination of the Emission Wavelength Stability of a Gas Laser", Electron. Technol. (Poland), Vol. 2, No. 2/3, p. 77-9 (1969).

Leikin, A. Ya., Solov'ev, V. S., Moskienko, N. V.
"Stabilization of Laser Frequency by 'Extremum Storage' Automatic Control Systems", Kvantovaya Elektron, (USSR), No. 4, p. 95-7 (1971).

Leikin, A. Ya., Solov'ev, V. S., Moskienko, N. V.
"Some Problems in the Calculation of Frequency Stabilization of Lasers Using the Lamb Dip", Radiotekhnika (Kharkov) (USSR), No. 22, p. 104-11 (1972).

Naour, R. Le.
"Comparative Analysis of a Laser Frequency Stabilization Method Using a Mobile and a Fixed Lorentzian", Opt. & Quantum Electron (GB), Vol. 10, No. 2, p. 119-29 (March 1978).

Letoklov, V. S., Pavlik, B. D.
"The Stability of the Frequency of Radiation of Laser Beams with Coherent Excitation", Zh. Tekh. Fiz (USSR), Vol. 40, No. 8, p. 1638-48 (1970).

Letokhov, V. S.
"Problems of Laser Frequency Stabilization by Nonlinear Saturation of Absorption Resonance in Gases", Comments At. & Mol. Phys. (GB), Vol. 2, No. 6, p. 181-94 (Feb.-March 1971).

Letokhov, V. S., Chebotaev, V. P.
"Quantum Optical Frequency Standards", Sov. J Quantum Electron (USA), Vol. 4, No. 2, p. 137-48 (Aug. 1974).

Lewandowski, L.
"Methods of Laser Frequency Stabilization", Elektronika (Poland), Vol. 17, No. 2, p. 59-63 (1976).

Likhanskii, V. V., Napartovich, A. P.
"Stability of Single-Mode Emission from a Laser", Sov. J. Quantum Electron, (USA), Vol. 17, No. 6, p. 763-5 (June 1977).

Lisitsyn, V. N., Chebotaev, V. P.
"On the Use of the Zeeman Effect for Stabilization of the Frequency of a Gas Laser with Nonlinear Absorption", Optika i. Spektrosk (USSR), Vol. 26, No. 5, p. 856-8 (May 1969).

Malyshev, Yu. M., Tatarenkov, V. M., Titov, A. N.
"Optical Frequency Standard with a Beam Type Absorbing Cell", ZH. Eksp. Teor. Fiz. Pisma (USSR), p. 522-5. Translation: JETP Lett. (USA) Vol. 13, No. 11, p. 422-4 (June 1971).

Mel'stin
"Experimental Study of the System of Frequency Stabilization of Ring Laser with an External Absorption Chamber", Zh. Prikl. Spektrosk (USSR), Vol. 15, No. 2, p. 214-18 (1971).

Mel'tsin, A. L., Shchegolev, V. V.
"Study of the Stability of the Standard Frequency of an Optical Discriminator,"Zh. Prikl. Spektrosk. (USSR), Vol. 22, No. 6, p. 985-90 (July 1975).

Milovskii, N. D.
"Single-Frequency Laser Stability", Izv. VUZ Radiofiz. (USSR), Vol. 16, No. 4, p. 537-44 (1973).

Oraevskii, A. N.
"Beam Laser as a Frequency Standard", Izv. VUZ. Radiofiz. (USSR), Vol. 11, No. 10, p. 1554-9 (1968). Translation: Soviet Radiophys. (USA).

Pao, Yoh-Han, Knox, J. D., Yusek, R., Goldberg, M. W.
"Frequency Standards Based on Accurately Stabilized Lasers", Proceedings of the 3rd Biennial Cornell Electrical Engineering conference on high frequency generation and amplification devices and application (Ithaca, NY, USA), p. 85-104 (1971).

Privalov, V. E., Strokvskii, G. A.
"Improving the Stability of the Perimeter of a Ring Gas Laser", Izv. VUZ Priborostr. (USSR), Vol. 18, No. 8, p. 111-15 (1975).

Sargent, M.,III.
"Mode Locking in Quantum Optics", Appl. Phys. (Germany), Vol. 1, No. 3, p. 133-9 (March 1973).

Schiller, N., Grant, M., Alfano, R. R.
"Ultrafast Laser Clocks", Phys. Teach. (USA), Vol. 15, No. 7, p. 396-404 (Oct. 1977).

Shotton, K. C., Woods, P. T., Rowley, W. R. C.
"Wavelength Intercomparison of Visible and Infrared Stabilized Lasers", 1976 Conference on Precision Electromagnetic Measurements (USA), p. 186-7 (July 1976).

Shotton, K. C., Rowley, W. R. C.
"An Electronic Servocontrol System for Stabilized Lasers and Similar Applications", Report NPL-QU-28, Nat. Phys. Lab. (England), p. 33 (Sept. 1976).

Simkin, G. S.
"Establishment of a Single Time and Length Standard", Izmerit. Tekh. (USSR), No. 10, p. 1308-14 (Oct. 1968). Translation: Meas. Tech. (USA) No. 10, (Oct. 1968).

Solomakha, D. A., Toropov, A. K.
"Precision of Laser Frequency, Measurements Based on the Dopoler Shift", Sov. J. Quantum Electron. (USA), Vol. 6, No. 5, p. 621-3 (May 1976). Translation: Kvantovaya Elecktron. Moskva (USSR), Vol. 3, No. 5, p. 1148-50 (May 1976).

Titov, E. A.
"Influence of Transit Effects on the Frequency of a Stabilized Gas Laser", Sov. J. Quantum Electron. (USA), Vol. 5, No. 10, p. 1207-10 Translation: Kvantovaya Elektron. Moskva (USSR), Vol. 5, No. 10, p. 2217-22 (Oct. 1975).

Umeda, N.
"Polarization Mode and Frequency Stabilization of an Internal Mirror Laser", Oyo Buturi (Japan), Vol. 47, No. 1, p. 42-9 (Jan. 1978).

Voitovich, A. P., Smirnov, A. Ya.
"The Autostabilization of Intermode Pulse Frequencies in a Gas Laser", Zh. Prikl. Spektrosk (USSR), Vol. 20, No. 3, p. 510-12 (March 1974). Translation: J. Appl. Spectroc. (USA).

Wenk, G. J.
"Frequency Stabilization of Gas Lasers", Proc. Instn. Radio Electronics Engrs. (Australia), Vol. 30, No. 8, p. 250-9 (Aug. 1969).

2.2.1

Akimoto, Y., Ohi, M.
"Frequency Fluctuation Analysis of CH, Stabilized He-Ne Lasers", Jap. J. Appl. Phys. (Japan), Vol. 16, No. 2, p. 385-6 (Feb. 1977).

Ambartsumjan, R. V., Basov, N. G., Letokhov, V. S.
"Frequency Stability of He-Ne Laser with Non-Resonant Feedback", Conference on Precision Electromagnetic Measurements (USA), p. 45 (1968).

Bagaev, S. N., Kolomnikov. Yu. D., Chebotaev, V. P.
"Stabilization and Reproducibility of a Helium Neon Laser Frequency at A=0.63μ". Izmerit. Tekh. (USA), No. 8, p. 27-9 (August 1968). Translation: Meas. Tech. (USA), No. 8, p. 27-9 (Aug. 1968).

Bagaev, S. N., Kolomnikov, Ju. D., Lisitsin, V. N., Chebotaev, V. P.
"Stabilization of Reproducibility of Frequencies of He-Ne Lasers at 0.63μ", IEEE J. Quantum Electronics (USA), Vol. QE-4, No. 11, p. 868-70 (Nov1968)

Bagaev, S. N., Baklanov, E. V., Timov, E. A., Chebotaev, V. B.
"Reproducibility of the Frequency of a He-Ne Laser with a Methane Absorption Cell", Zh. Eskp. & Teor. Fiz. Pis'ma (USSR), Vol. 20, No. 5, p. 292-6 (Sept. 1974). Translation: JETP Letters (USA)

Bagaev, S. N., Chebotaev, V. P.
"Frequency Stability and Reproducibility of the 3.39 μm He-Ne Laser Stabilized on the Methane Line", Appl. Phys. (Germany), Vol. 7, No. 1, p. 71-6 (May 1975).

Bagaev, S. N., Vasilenko, L. S., Gol'dort, V. G., Dmitriev, A. K., Dychkov, A. S.
"Helium-Neon Laser Emitting =3.39 μ Line of 7Hz Width", Sov. J. Quantum Electron (USA), Vol. 7, No. 5, p. 665-6 (May 1977). Translation: Kvantovaya Elecktron. Moskva (USSR) Vol. 4, No. 5, p. 1163-6 (May 1977).

Bagayev, S. N., Chebotayev, V. P., Vasilenko, L. S.
"A Narrow Linewidth (10 Hz) Frequency Scannable 3.39 μm He-Ne Laser and Its Application to Frequency Stabilization and High-Resolution Spectroscopy", IEEE J. Quantum Electron (USA), Vol QE-13, No. 9, p. 33 (Sept. 1977).

Bakumenko, V. M., Valitov, R. A.
"Frequency Stabilization and Instability Measurement of Helium-Neon Lasers at a Wavelength of 0.6328 mu m.", Radiotekh. & Elecktron (USSR),

p. 2289-93. Translation: Radio Eng. & Electron Phys. (USA), Vol. 15, No. 12 (Dec. 1970).

Balhorn, R., Kunzmann, H., Lebowsky, F.
"Frequency Stabilization of Internal-Mirror Helium Neon Lasers", Appl. Opt. (USA), Vol. 11, No. 4, p. 742-4 (April 1972).

Balhorn, R., Lebowsky, F., Ullrich, D.
"Efficiency of the Frequency Stabilization of He-Ne Lasers by the Two-Mode Comparison Method", Report PTB-Me-9, Phys. Tech. (Germany), p. 29, (Dec. 1975).

Bashkin, A. S., Belenov, E. M., Gonchukov, S. A., Oraevskii, A. N., Petrovskii, V. N., Protsenko, E. D.
"Stabilization of the Oscillation of a Gas Laser by Comparison with a Radio-Frequency Standard", Kvantovaya Elektron.,(USSR), No, 2, p. 40-8 (1971).

Basov, N. G., Gubin, M. A., Niktin, V. V., Protsenko, E. D., Stepanov, V. A.
"Frequency Stabilization of a Gas Laser Using Mode-Interaction Effects", Zh. Eksp. Teor. Fiz. Pisma (USSR), Vol. 15, No. 9, p. 525-8 (May 1972). Translation: JETP Lett. (USA) Vol. 15, No. 9, p. 371-3 (May 1972).

Basov, N. G., Belenov, E. M., Vol'nov, M. I., Gubin, M. A., Danileiko, M. V., Niktin, V. V.
"Frequency Reproducibility of a Stabilized Ring Laser", Sov. Phys. Dokl, (USA), Vol. 18, No. 5, p. 316-17 (Nov. 1973). Translation: Dokl. Akäd. Nauk (USSR), Vol. 210, No. 1-3, p. 306-8 (May1973).

Batarchukova, N. R., Glozman, T.,I.,Kartashev, A. I., Irikova, L. A., Ptitsyna, E. A.
"Certifying the Wavelength of He-Ne Laser Stabilized by Means of the Lamb Dip", Meas. Tech. (USA), Vol. 17, No. 7, p1116-17(July 1974) Translated: Izmer.Tekh. (USSR), Vol. 17, No. 7, p. 83 (July 1974).

Bayer-Helms, F., Chartier,J.-M.,Helmcke, J., Wallard,A.
"Evaluation of the International Intercomparison Measurements", Informative Meeting on Iodine Stabilized He-Ne Lasers (Germany), p. 139-46 (1977).

Belenov, E. M., Danileiko, M. V., Nedavnii, A. P., Shpak, M. T.
"Frequency Shifts in Stabilized Gas Lasers", Ukr. Fiz. Zh. (USSR), Vol. 22, No. 11, p. 1765-79 (Nov. 1977).

Bennett, S. J., Ward, R. E., Wilson, D. C.
"Comments on: Frequency Stabilization of Internal Mirror He-Ne Lasers", Appl. Opt, (USA), Vol. 12, No. 7, p. 1406 (July 1973).

Bertinetto, F., Rebaglia, B. I., Liverani, M., Gualini, S.
"Present Development of Iodine Stabilized He-Ne Lasers at the Instituo di Metrologia Gustavo Colonnetti", Alta. Freq. (Italy), Vol. 44, No. 10, p. 569-73 (Oct. 1975).

Bertinetto, F., Rebaglia, B. I.
"Performance of IMGC He-Ne (I_2) Lasers", European Conference on Precise Electrical Measurements (England), p. 38-9 (Sept. 1977).

Bessmel'tsv, V. P., Vorob'ev, V. V., Khanov, V. A.
"Stabilization of the Frequency Difference in a Two-Frequency Laser", Autometriya, (USSR) No. 5, p. 94-6 (Sept-Oct. 1975).

Beterov, I. M., Klement'ev, V. M., Chebotaev, V. P.
"Secondary Frequency Standard Using Mercury Laser at Microwaves", Radioteknika i Elektronika (USSR) Vol. 14, No. 11, p. 2066-9 (1969).

Beterov, I. M., Matyugin, Yu. A., Milushkin, G. A., Troshin, B. I., Chebotaev, V. P.
"High Stability Gas-Filled Laser Based on Non-Linear Absorption" (λ=0.63 microns). II Selection of Modes of Oscillation in a He-Ne Laser at λ =0.63 microns", Avtometriya (USSR), No. 5, p. 59-70 (Oct. 1972).

Beterov, I. M., Matyugin, Yu. A., Milushkin, G. A., Troshin, B. I., Chebotaev, V. P.
"High Stability Gas-Filled Laser Based on Non-linear Absorption (λ =0.63 Microns)", Autometriya (USSR), No. 5, p. 71-85 (Sept.-Oct. 1972).

Beterov, I. M., Matyugin, Yu. A., Milushkin, G. A., Troshin, B. I., Chebotaev, V. P.
"High-Stability Gas Laser Based on Non-linear Absorption (λ=0.63u) III. Optical System of a Stabilized Single Frequency He-Ne Laser atλ =0.63 μm", Autometriya (USSR), No. 6, p. 55-63 (Nov.-Dec.1972)

Bikmukhametov, K. A., Bobrik, V. I., Kolomnikov, Yu. D., Mogil'nitskii, B. S.
"Helium-Neon Lasers as Standard Wavelength Sources", Meas. Tech. (USA), Vol. 20, No. 6, p. 821-3 (June 1977). Translation: Izmer. Tekh. (USSR), Vol. 20, No. 6, p. 35-7 (June 1977).

Blabia, J.
"State of Development of a He-Ne Laser Stabilized by Saturated Absorption in I.", Feingeraetetechnik (Germany), Vol.27, No. 3, p. 111 (March 1978).

Blaney, T. G., Bradley, C. C., Edwards, G. J., Jolliffe, B. W., Knight, D. J. E., Woods, P. T.
"Measurement of the Frequency of the Methane-Stabilized Laser at 3.39 μm and of the R(32) Transition of CO_2 at 10.17 μm ", Nature (GB), Vol. 254, No. 5501, p. 584-5 (April 1975).

Blaney, T. G., Edwards, G. J., Jolliffe, B. W., Knight, D. J. E., Woods, P. T.
"Absolute Frequencies of the Methane-Stabilized He-Ne Laser (3.39 μ m) and the CO_2 R(32) Stabilized Laser (10.17 μm)", J. Phys. D. (GB), Vol. 9, No. 9, p. 1323-30 (June 1976).

Bobrik, V. I., Kolomnikov, Yu. D., Mogil'nitskii, B. S.
"Measuring the Wavelength of a Helium-Neon Laser", Meas. Tech. (USA), Vol. 18, No. 12, p.1788-9 (Dec. 1975). Translated: Izer. Tekh. (USSR), Vol. 18, No. 13, p.43-4 (Dec. 1975).

Bodlaj, V.
"Frequency Stabilization of the He-Ne Laser with an External Ne Absorption Tube in the Magnetic Alternating Field", Frequenz (Germany), Vol. 23, No. 3, p. 92-4 (March 1969).

Bodlaj, V.
"Absolute Frequency Stabilization of a He-Ne Laser by an Expernal Ne-Absorption Cell in an Alternating Field", MOGA 70 8th International Conference on Microwave and Optical Generation and Amplification (summaries) (Netherlands), (Sept. 1970)

Bodlaj, V., "Frequency Stabilization of the He-Ne Laser with an External Ne Absorption Tube in an Alternating Magnetic Field", Opto-Electron. (GB), Vol. 2, No. 4, p. 221-6 (Nov. 1970).

Bodlaj, V.
"Frequency Stabilization of a He-Ne Laser with an External Absorption Tube in an Alternating Magnetic Field", Z. Angew. Phys. (Germany), Vol. 31, No. 2, p. 97-105 (1971).

Bodlaj, V.
"Frequency Stabilization of a He-Ne Laser in an Alternating Magnetic Field", Phys. Lett. A (Netherlands), Vol. 35A, No. 5, p. 381-82 (June 1971).

Bodlaj, V.
"He-Ne Laser Wave as a Secondary Length Standards", Laser & Angew. Strahlentech. (Switzerland), Vol. 3, No. 2, p. 21-8 (June 1071).

Bodlaj, V.
"Ne Absorption Tube in an Alternating Magnetic Field Inside a Laser Cavity as a Frequency Standard", Opt. Commun. (Netherlands), Vol. 6, No. 1, p. 12-14 (Sept. 1972).

Bonsch, G.
"Wavelength Intercomparison Between Methane- and Iodine-Stabilized He-Ne Lasers: Alignment and Error Estimations", Informative Meeting on Iodine Stabilized He-Ne Lasers, (Germany), p. 151-8 (1977).

Brillet, A., Cerez, P., Clergeot, H.
"Frequency Stabilization of He-Ne Lasers by Saturated Absorption", IEEE J. Quantum Electron (USA), Vol. QE-10, No. 6, p. 526-8 (June 1974).

Bruce, C. F.
"Stable Single-Frequency He-Ne Laser", Appl. Opt. (USA), Vol. 10, No. 4, p. 880-3 (April1971)

Cerez, P., Brillet, A., Hajdukovic, S., Man, N.
"Iodine Stabilized He-Ne Laser with a Hot Wall Iodine Cell", Informative Meeting on Iodine Stabilized He-Ne Lasers (Germany), p. 71-84 (1977).

Cerez, P., Brillet, A.
"Factors which Limit the Reproducibility of Iodine Stabilized He-Ne Lasers", Metrologia (Germany), Vol. 13, No. 1, p. 29-33 (1977).

Cerez, P., Brillet, A., Hajdukovic, S., Man, N.
"Iodine Stabilized He-Ne Laser with a Hot Wall Iodine Cell", Opt. Commun. (Netherlands), Vol. 21, No. 3, p. 332-6 (June 1977).

Cerez, P., Brillet, A., Hajdukovic, S., Man, N.
"Iodine Stabilized He-Ne Laser with a Hot Wall Iodine Cell", European Conference on Precise Electrical Measurement, Brighton, Sussex, England, 5-9 Sept. 1977 (London, England: IEEE 1977) p. 37.

Alekseev, V. A., Malyugin, A. V.,
"Influence of the Hyperfine Structure on the Frequency Reproducibility of an He-Ne Laser with a Methane Absorption Cell", Sov. J. Quantum Electron. (USA), Vol. 7, No. 9, p. 1075-81 (Sept. 1977) Translation of: Kvantovaya Elektron., Moskva (USSR), Vol. 4, No. 9, p. 1890-902 (Sept. 1977).

Cerez, P., Audoin, C., Bennett, S. J.
"Frequency Stability of the Helium-Neon Laser Including an Iodine Cell with Warm Walls", C. R. Hebd. Seances Acad. Sci. Ser. B (France), Vol. 286, No. 4, p. 53-6 (30 Jan. 1978). In French.

Chartier, J. M., Helmcke, J., Wallard, A. J.
"International Intercomparison of the Wavelength of Iodine-Stabilized Lasers", IEEE Trans. Instrum. & Meas. (USA), Vol. IM-25, No. 4, p. 450-3 (Dec. 1976). (1976 Conference on Precision Electromagnetic Measurements, Boulder, Colo., USA, 28 June - 1 July 1976).

Chartier, J. M., Avrons, D.
"Technological Principles of Iodine Stabilized He-Ne Lasers", Informative Meeting on Iodine Stabilised He-Ne Lasers, Germany, 10-11 Feb. 1977 (Braunschweig, Germany: Physikalisch-Technische Bundesanstalt 1977), p. 13-31. In French.

Chartier, J. M., Avrons, D.
"International Comparisons of Iodine Stabilized He-Ne Lasers", Informative Meeting on Iodine Stabilised He-Ne Lasers, Germany, 10-11 Feb. 1977 (Braunschweig, Germany: Physikalisch-Technische Bundersanstalt 1977), p. 133-8. In French.

Cole, J. B., Bruce, C. F.
"Iodine Stabilized Laser with Three Internal Mirrors", Appl. Opt. (USA), Vol. 14, No. 6, p. 1303-10 (June 1975).

Cole, J. B.
"Laser Frequency Stabilization Using a Resonator Containing a Saturable Absorber", J. Phys. D (GB), Vol. 8, No. 12, p. 1392-408 (21 Aug. 1975).

Curtis, R. A., McDuff, O. P.
"Stabilizing Single Mode Lasers Using Intracavity Phase Modulation", 1975 International Electron Devices Meeting. (Technical Digest), Washington, DC, USA, 1-3 Dec. 1975 (New York, USA: IEEE 1975) p. 611-14.

Danileiko, M. V., Zubrilin, N. G., Nedavnii, A.P. Shpak, M. T.
"He-Ne Laser with Travelling Wave Phonon Interaction", Ukr. Fiz. Zh. (USSR), Vol. 20, No. 9, p. 1573-5 (Sept. 1975). In Russian.

Dekker, H., Lamberts, C. W.
"Stability Measurements of a Tunable Single Frequency He-Ne Laser by Means of Self-Locking Phenomena", Opt. & Quantum Electron. (GB), Vol. 7, No. 4, p. 239-45 (July 1975).

Evenson, K. M.
"Extension of Absolute Frequency Measurements to the cw He-Ne Laser at 88 THz (3.39μ)", Appl. Phys. Lett. (USA), Vol. 20, No. 3, p. 133-4 (1 Feb. 1972)

Evenson, K. M., Wells, J. S., Petersen, F. R., Danielson, B. L., Day, G. W., Barger, R. L., Hall, J. L.
"Laser Frequency and Wavelength Measurements and the Speed of Light", 1972 Annual Meeting of the Optical Society of America, Abstracts only, San Francisco, Calif., USA, 17-20 Oct. 1972 (Washington, DC, USA: Optical Soc. America 1972), p. 22.

Geller, V. M., Grif, G. I.
"Determination of the Absolute Oscillation Frequency of the $3s_2$ 2p Transition in a Helium-Neon Laser", Sov. J. Quantum Electron. (USA), Vol. 4, No. 8, p. 1052-3 (Feb. 1975). Translation of Kvantovaya Elektron., Moskva (USSR), Vol. 1, No. 8, p. 1883-5 (Aug. 1974).

Giacomo, P.
"Length Metrology and Iodine Stabilized Lasers", Informative Meeting on Iodine Stabilised He-Ne Lasers, Germany, 10-11 Feb. 1977 (Braunschweig, Germany: Physikalisch-Technische Bundesanstalt 1977), p. 9-11. In French.

Gnatovskii, A. V., Belenov, E. M., Danileiko, M.V., Nikitin, V. V., Fedin, V. P., Shpak, M. T.
"Reproducibility of the Frequency of a Laser Stabilised According to the Transition of the Absorbing Gas", Zh. Eskp. & Teor. Fiz. Pis'ma (USSR), Vol. 19, No. 6, p. 368-71 (20 March 1974) In English translation in: JETP Letters (USA).

Hall, J. L.
"The Laser Absolute Wavelength Standard Problem", IEEE J. Quantum Electronics (USA), Vol. QE-4, No. 10, p. 638-41 (Oct. 1968). (1968 International Quantum Electronics Conference, Miami, FL, May 14-17 1968).

Hanes, G. R., Baird, K. M., DeRemigis, J.
"Stability, Reproducibility, and Absolute Wavelength of a 633-nm He-Ne Laser Stabilized to an Iodine Hyperfine Component", Appl. Opt. (USA), Vol. 12, No. 7, P. 1600-5 (July 1973).

Hellwig, H., Bell, H. E., Kartaschoff, P., Bergquist, J. C.
"Frequency Stability of Methane-Stabilized He-Ne Lasers", J. Appl. Phys. (USA), p. 450-2 (Feb. 1972).

Helmcke, J.
"Wavelength-Stabilized He-Ne Laser [for Measurement]", Meeting on Length Measuring Techniques, Braunschweig, Germany, Oct. 1973 (Braunschweig, Germany: Physikalisch-Technische Bundesanstalt 1974), p. 29-39. In German.

Helmcke, J., Bayer-Helms, F.
"Stabilising ^{3}He-^{22}Ne Lasers by Saturated Absorption in $^{129}I_2$", Metrologia (Germany), Vol. 10, No. 2, p. 69-71 (1974). In German.

Helmcke, J., Bayer-Helms, F.
"He-Ne Laser Stabilized by Saturated Absorption in I_2", CPEM 74 Digest: Conference on Precision Electromagnetic Measurements, London, England, 1-5 July 1974 (London, England: IEE 1974) p. 104.

Helmcke, J., Bayer-Helms, F.
"He-Ne Laser Stabilized by Saturated Absorption in I_2", IEEE Trans. Instrum.& Meas. (USA), Vol. IM-23, No. 4, p. 529-31 (Dec. 1974). (1974 Conference on precision electromagnetic measurements, London, England, 1-5 July 1974).

Helmcke, J., Bayer-Helms, F.
"Estimation and Investigation of Instrumental Frequency Offsets of Iodine Stabilized He-Ne Lasers", Informative Meeting on Iodine Stabilised He-Ne Lasers, Germany, 10-11 Feb. 1977 (Braunschweig, Germany: Physikalisch-Technische Bundesanstalt 1977), p. 111-32.

Hochuli, U., Haldemann, P.
"Relative Frequency Stability of Stable He-Ne Gas Laser Structures", International electron devices metering (abstracts), Washington, DC, USA, 28-30 Oct. 1970 (New York, USA: IEEE 1970), p. 92.

Hochuli, U., Haldemann, P.
"Relative Frequency Stability of Stable He-Ne Gas Laser Structures", IEEE J. Quantum Eletron. (USA), Vol. QE-7, No. 12, p. 573-5 (Dec. 1971).

Hochuli, U. E., Haldemann, P., Li, H. A.
"Factors Influencing the Relative Frequency Stability of He-Ne Laser Structures", Rev. Sci. Instrum. (USA), Vol. 45, No. 11, p. 1378-81 (Nov. 1974).

Ito, N., Tanaka, K.
"Absolute Wavelength Measurements of the Iodine 127 Stabilized He-Ne Laser of NRLM", Metrologia (Germany), Vol. 14, No. 2, p. 47-51 (1978).

Jolliffe, B. W., Kramer, G., Chartier, J. M.
"Methane-Stabilized He-Ne Laser Intercomparisons 1976", IEEE Trans. Instrum. & Meas. (USA), Vol. IM-25, No. 4, p. 447-50 (Dec. 1976). (1976 Conference on Precision Electromagnetic Measurements, Boulder, Colo., USA, 28 June - 1 July 1976).

Jolliffe, B. W., Rowley, W. R. C., Shotton, K. C., Wallard, A. J., Woods, P. T.
"Recent Studies on He-Ne Lasers Frequency-Stabilized by Reference to Absorption Transitions in Iodine and Methane, and the Intercomparison of Their Wavelengths", European Conference on Precise Electrical Measurement, Brighton, Sussex, England, 5-9 Sept. 1977 (London, England: IEEE 1977), p. 35-6.

Knight, D. J. E., Edwards, G. J., Blaney, T. G.
"Developments in Laser Frequency Measurement towards realizing the Metre from a Unified Frequency and Length Standard", European Conference on Precise Electrical Measurement, Brighton, Sussex, England, 5-9 Sept. 1977 (London, England: IEEE 1977), p. 40.

Knox, J. D., Pao, Y. H.
"Stabilization of the ^{3}He-^{20}Ne Laser about Inverted Lamb-Dip Components in $^{129}I_2$ Vapor", 1970 Spring meeting of the Optical Society of America, Philadelphia, PA, 7-10 Apr. 1970 (Washington, DC, USA: Optical Soc. America 1970), p. 20.

Knox, J. D., Pao, Y. H.
"Laser Wavelengths and Frequency Standards Based on He-Ne Lasers and $^{129}I_2$ Vapor", International electron devices metering (abstracts), Washington DC, USA, 28-30 Oct. 1970 (New York, USA: IEEE 1970), p. 90.

Konovalov, I. P., Protsenko, E. D.
"Frequency Stabilization of a 3.39 μ He+Ne Laser", Instrum. & Exp. Tech. (USA), Vol. 17, No. 5, pt. 2, p. 1433-6 (Sept.-Oct. 1974). Translation of: Prib. Tekh. Eksp. (USSR), Vol. 17, No. 5, pt. 2, p. 158-60 (Sept.-Oct. 1974).

Koronkevich, V. P., Khanov, V. A.
"Investigation of the Spectral Characteristics of Helium-Neon Lasers with Lamb-Dip Stabilisation", Autometriya (USSR), No. 5, p. 73-80 (Sept.-Oct. 1975). In Russian.

Koshelyaevskii, N. B., Mukhamedgalieva, A. F., Tatarenkov, V. M., Titov, A. N.
"Investigations and Stabilization of the Frequency of a Helium-Neon Laser", Izmer. Tekh. (USSR), p. 38-40. In Russian. English translation in: Meas. Tech. (USA), No. 8, p. 1170-3 (Aug. 1970).

Koshelyaevskii, N. B., Tatarenkov, V. M., Titov, A.N.
"Quantum Freuqency Reference at 3.39μ Wavelength" Zh. Eksp. Teor. Fiz. Pis'ma (USSR), Vol. 15, No. 8, p. 461-4 (20 April 1972). In Russian. English translation in: JETP Lett. (USA), Vol. 15, No. 8, p. 326-7 (20 April 1972).

Koshelyaevskii, N. B., Tatarenkov, V. M., Titov, A. N.
"Frequency Meters Based on He-Ne Lasers", Meas. Tech. (USA), Vol. 15, No. 11, p. 1644-8, (Nov. 1972), Translation of: Izmer. Tekh. (USSR), Vol. 15, No. 11, p. 32-5, (Nov. 1972).

Kramer, G., Weiss, C. O., Helmcke, J.
"Laser Frequency Stabilization by Means of Saturation Dispersion", Z. Naturforsch. A (Germany), Vol. 30A, No. 9, p. 1128-32 (Sept. 1975).

Kuhn, H.
"Stabilised Helium-Neon-Gas Lasers (for Length Measurement)", Feingeraete Tech. (Germany), Vol. 25, No. 6, p. 259-61, (June 1976). In German.

Layer, H. P.
"The Iodine Stabilized Laser as a Realization of the Length Unit", Proceedings of the Society of Photo-Optical Instrumentation Engineers, Vol. 129. Effective Utilization of Optics in Quality Assurance, Arlington, Heights, IL, USA, 14-16 Nov. 1977 (Bellingham, WA, USA: Soc. Photo-Optical Instrumentation Engrs. 1978), p. 9-11.

Leclerc, M. J.
"Measurements of the Wave-Lengths Emitted by Laser Tubes (Type Monomode 3He 20Ne) and Their Stability", 2nd European Electro-Optics Conference, Montreux, Switzerland, 2-5 April 1974 (St. Albans, Herts., England: Mack-Brooks Exhibitions 1974). 1 pp. In French.

Leikin, A. Ya., Solov'ev, V. S.
"Studying the Stability of Wavelengths Radiated by a Gas Laser", Izmerit. Tekh. (USSR), No. 9, 29-32 (Sept. 1967). In Russian. English translation in Meas. Tech. (USA), No. 9, 1060-3 (Sept. 1967).

Leikin, A. Ya., Solov'ev, V. S.
"Stabilization of a Laser Radiation Frequency", Izmerit. Tekh. (USSR), No. 8, p. 19-22 (Aug. 1968). In Russian. English translation in: Meas. Tech. (USA), No. 8, p. 1025-9 (Aug. 1968).

Leikin, A. Ya, Solov'ev, V. S., Fisher, A. M.
"Stabilizing the Generation Frequency of a Helium Neon Laser with a Wavelength of 0.63 μ with Respect to a Generation Frequency with a Wavelength of 3.39 μ. Meas. Tech. (USA), Vol. 16, No. 9, p. 1321-2 (Sept. 1973). Translation of: Izmer. Tekh. (USSR), Vol. 16, No. 9, p. 29-30 (Sept. 1973).

Lokhmatov, A. I., Khanov, C. A.
"Frequency Stabilising System of Gas Laser Using Lamb Depression Effect", Autometriya (USSR), No. 1, p. 16-20 (19/1). In Russian.

Malyshev, Yu. M., Tatarenkov, V. M., Titov, A.N.
"Optical Frequency Standard with a Beam Type Abosrbing Cell", Zh. Eksp. Teor. Fiz. Pisma (USSR) p. 592-5. In Russian. English translation in: JETP Lett. (USA), Vol. 13, No. 11, p. 422-4 (5 June 1971).

Malyshev, G. F., Triotskii, Yu. V., Kahnov, V. A., Khyuppenen, V. P.
"Stabilisation of a Single-Frequency Helium-Neon Laser", Autometriya (USSR), No. 5, p. 86-93 (Sept. Oct. 1972). In Russian.

Matyshev, G. F., Troitskii, Yu. V.
"Frequency Stabilisation of a Single Frequency He-Ne Laser (λ =0.63 micron) with a Diffraction Selector", Autometriya (USSR), No. 6, p. 71-6 (Nov.-Dec. 1974). In Russian.

Matyugin, Yu., A., Troshin, B. I., Chebotaev, V.P.
"Method for Stabilizing He-Ne Laser Frequency Using the Lorentzian Absorption Profile in an External Gas Cell", Opt. & Spektrosk (USSR), p. 111-15. In Russian. English translation in: Opt. & Spectrosc. (USA), Vol. 31, No. 1, p. 56-8 (July 1971).

Melnikov, N. A., Privalov, V. E., Fofanov, Ya. A.
"Experimental Investigation of He-Ne Lasers Stabilized by Saturation Absorption in Iodine", Opt. & Spectrosc. (USA), Vol. 42, No. 4, p. 425-8 (April 1977). Translation of: Opt. & Spektrosk. (USSR), Vol. 42, No. 4, p. 747-51 (April 1977).

Mielenz, K. D., Nefflen, K. F., Rowley, W. R. C., Wilson, D. C., Engelhard, E.
"Reproducibility of Helium-Neon Laser Wavelengths at 633 nm", Appl. Optics (USA), Vol. 7, No. 2, 289-94 (Feb. 1968).

Miekal, K. D.
"Length Measurement and Laser Wavelength Stability", ISA Trans. (USA), Vol. 6, No. 4, p. 293-7, (1968).

Mikhal'tsova, I. A., Lenkova, G. A., Lokhmatov, A. I.
"Single Frequency Stabilised Helium-Neon Laser", Autometriya (USSR), No. 1, p. 10-15 (1971). In Russian.

Morinaga, A., Tanaka, K.
"Stabilization of a Complex Resonator He-Ne Laser by Frequency Offset Lock", Jap. J. Appl. Phys. (Japan), Vol. 16, No. 2, p. 383-4 (Feb. 1977).

Morinaga, A., Tanaka, K.
"Stabilization of a Complex Resonator He-Ne Laser", Jpn. J. Appl. Phys. (Japan), Vol. 17, No. 5, p. 881-7 (May 1978).

Morris, R. H., Ferguson, J. B., Warniak, J. S.
"Frequency Stabilization of Internal Mirror He-Ne Lasers in a Transverse Magnetic Field", Appl. Opt. (USA), Vol. 14, No. 12, p. 2808 (Dec. 1975).

Mukhamedgalieva, A. F., Tatarenkov, V. M., Titov, A. N.
"Investigation of He-Ne Laser with an Absorbing Cell", Izv. VUZ Radiofiz. (USSR), Vol. 12, No. 8, p. 1156-8 (1969). In Russian. English translation in: Soviet Radiophys. (USA).

Nagai, H., Taniguchi, I.,
"A Simple, Single-Frequency He-Ne Laser for Practical Uses", Jap. J. Appl. Phys. (Japan), Vol. 12, No. 3, p. 434-8 (March 1973).

Nishiyama, Y., Shimauchi, A., Kikuchi, M.
"Mode Stabilization by an Axial Magnetic Field for Long Resonator Cases of He-Ne Laser", Jap. J. Appl. Phys. (Japan), Vol. 15, No.11, p. 2195-200 (Nov. 1976).

Ohi, M., Akimoto, Y.
"Improvements in Methane-Stabilized Lasers", Jap. J. Appl. Phys. (Japan), Vol. 15, No. 9, p. 1853-4 (Sept. 1976).

Ohi, M., Akimoto, Y.
"Characteristics of Low Noise Laser Tubes for CH_4 Stabilized Lasers (3.39 μ He-Ne Laser)", Oyo Buturi (Japan), Vol. 46, No. 8, p. 832-5 (Aug. 1977). In Japanese.

Pucek, B.
"Circuits for Stabilization of the Laser Radiation Wavelength", Cesk. Cas. Fis. Sekce A (Czechoslovakia), Vol. 28, No. 3, p. 241-4 (1978). In Czech.

Rapier, J. L., Heimple, H. H., Schawlow, A. L.
"Spontaneous Emission from a Helium-Neon Laser as a Convenient Wavelength Standard", Amer. J. Phys., Vol. 35, No. 9, 890-1 (Sept. 1967).

Rowley, W. R. C., Wilson, D. C.
"Optical Coupling Effects in Frequency Stabilized Lasers", Appl. Opt. (USA), Vol. 11, No. 2, p. 475-6, (Feb. 1972).

Schellekens, P.
"Research on Iodine Stabilized Lasers in the Metrology Laboratory of Eindhoven University of Technology", Informative Meeting on Iodine Stabilized He-Ne Lasers, Germany, 10-11 Feb. 1977 (Braunschweig, Germany: Physikalisch-Technische Bundesanstalt 1977), p. 55-61.

Schweitzer, W. G., Jr., Kessler, E. G., Deslattes, R. D., Layer, H. P., Whetstone, J. R.
"Description, Performance, and Wavelengths of Iodine Stabilized Lasers", Appl. Opt. (USA), Vol. 12, No. 12, p. 2927-38 (Dec. 1973).

Shimoda, K.
"Ultimate Stability of Methane-Stabilized Lasers", Jap. J. Appl. Phys. (Japan), Vol. 12, No. 8, p. 1222-6 (Aug. 1973).

Smith, P. W.
"On the Stabilization of a High-Power Single-Frequency Laser", IEEE J. Quantum Electronics (USA), Vol. QE-2, No. 9, 666-8 (Sept. 1966). Fourth International Quantum Electronics Conference Phoenix, 1966].

Spieweck, F.
"Relating a Laser Frequency to the Atomic Frequency by Means of Sweeping", Naturforsch. (Germany) Vol. 22a, No. 12, 2067-9 (Dec. 1967). In German.

Spieweck, F.
"Classification of I_2 Hyperfine Components and Their Suitability for the Stabilization of Laser Wavelengths", Informative Meeting on Iodine Stabilised He-Ne Lasers, Germany, 10-11 Feb. 1977 (Braunschweig, Germany: Physikalisch-Technische Bundesanstalt 1977), p. 33-42.

Strakhovskii, G. M., Tatarenkov, V. M., Titov, A.N.
"Frequency Stabilization of a Helium-Neon Laser Having an Internal Absorptive Cell, which Operates at a Wavelength of 0.63μ", Izmer. Tekh. (USSR), p. 25-8. In Russian. English translation in: Meas. Tech. (USA), No. 12, p. 1839-43 (Dec. 1970).

Tanaka, K.
"Method for Stabilizing the Frequency of an Unmodulated Laser Output", J. Opt. Soc. Am. (USA), Vol. 62, No. 1, p. 24-9 (Jan. 1972).

Tanaka, K., Seino, S.
"Wavelength Stabilization of He-Ne Lasers and Interferometric Length Measurements", J. Jap. Soc. Precis. Eng. (Japan), Vol. 40, No. 9, p. 716-23 (Sept. 1974). In Japanese.

Tanaka, K., Sakurai, T., Kurosawa, T.
"Frequency Stabilisation of the He-Ne Laser by Means of Saturated Abosrption in Iodine", Trans. Soc. Instrum. & Control Eng. (Japan), Vol. 10, No. 6, p. 669-74 (Dec. 1974). In Japanese.

Tanaka, K., Kurosawa, T.
"Optical Feedback Effect in Iodine Stabilised He-Ne Laser with Long Path Interferometer [Earth Strain Meter]", Jap. J. Appl. Phys. (Japan), Vol. 15, No. 11, p. 2271-2 (Nov. 1976).

Tanaka, K., Sakurai, T., Kurosawa, T.
"Frequency Stability and Reproducibility of an Iodine Stabilized He-Ne Laser", Jpn. J. Appl. Phys. (Japan), Vol. 16, No. 11, p. 2071-2 (Nov. 1977).

Terrien, J.
"Wavelength Standards, Optical Frequency Standards, and the Velocity of Light", Nouv. Rev. Opt. (France), Vol. 4, No. 4, p. 215-20 (July-Aug. 1973). In French.

Tschudi, T., Balser, P., Wuthrich, M.
"Control System for the Frequency Stabilisation of a He-Ne Laser", Uerh. Deut. Phys. Ges. (Germany), No. 10, p. 766 (1971). In German (German Physical Society Spring Meeting, Ulm, Germany, 29 Mar-3 Apr 1971).

Tsetsegova, E. I.
"He-Ne Laser Frequency Stabilization at the Wavelength 3.39 μ Izv. VUZ Radiofiz. (USSR), Vol. 12, No. 8, p. 1159-64 (1969). In Russian. English translation in: Soviet Radiophys. (USA).

Tuma, W., van der Hoeven, C. J.
"Helium-Neon Laser Stabilized on Iodine: Design and Performance", Appl. Opt. (USA), Vol. 14, No. 8, p. 1896-7 (Aug. 1975).

Umeda, N., Tsukiji, M., Takasaki, H.
"Degeneration of Longitudinal Modes and Frequency Stabilization of an Internal Mirror He-Ne Laser with a Transverse Magnetic Field", Oyo Buturi (Japan), Vol. 47, No. 5, p. 432-6 (May 1978). In Japanese.

van Oorschot, B. P. J.
"Frequency Shifts in Iodine Stabilized Lasers", J. Phys. D (GB), Vol. 10, No. 8, p. 1117-24 (1 June 1977).

Vysotskii, V. G., Okunev, R. I., Nikolaev, V. M., Petrun'kin, V. Yu.
"Longitudinal Mode Selection and Frequency Stabilization in the He-Ne Ring Laser", Sov. Phys. Tech. Phys. (USA), p. 560 - 1 Translation of: Zh. Tekh. Fiz, (USSR), Vol. 43, No. 4, p. 881-3 (Oct. 1973).

Wallard, A. J.
"Frequency Stabilization of the Helium-Neon Laser by Saturated Abosrption in Iodine Vapour", J. Phys. E. (GB), Vol. 5, No. 9, p. 926-30 (Sept.1972)

Wallard, A. J.
"Characteristic of the 633 nm He-Ne Laser Stabilized by Saturated Absorption in Iodine Vapour", Proceedings of the 27th Annual Frequency Control Symposium, Cherry Hill, NJ, USA, 12-14 June 1973 (Washington, DC, USA: Electronic Industries Assoc. 1973), p. 376-81.

Wallard, A. J.
"The Reproducibility of 633 nm Lasers Stabilized by $^{127}I_2$", CPEM 74 Digest: Conference on Precision Electromagnetic Measurements, London, England, 1-5 July 1974 (London, Engiand: IEE 1974), p. 106-7.

Wallard, A. J.
"The Reproducibility of 633 nm Lasers Stabilized by $^{127}I_2$", IEEE Trans. Instrum.& Meas. (USA), Vol. IM-23, No. 4, p. 532-5 (Dec. 1974). (1974 Conference on precision electromagnetic measurements, London, England, 1-5 July 1974).

Wallard, A. J.
"Wavelength Measurements of the Iodine Stabilized Helium-Neon Laser", Metrologia (Germany), Vol. 11, No. 2, p. 89-95 (1975).

Wallard, A. J., Jolliffe, B. W.
"International Comparison of the Reproducibility of Iodine and Methane Stabilized Lasers", 1976 Conference on Precision Electromagnetic Measurements, Boulder, Colo., USA, 28 June - 1 July 1976 (New York, USA: IEEE 1976), p. 182-3.

Wallard, A. J.
"Report on NPL Activities", Informative Meeting on Iodine Stabilised He-Ne Lasers, Germany, 10-11 Feb. 1977 (Braunschweig, Germany: Physikalisch-Technische Bundesanstalt 1977), p. 43-53.

Wang, S. C., Byer, R. L., Siegman, A. E.
"Observation of an Enhanced Lamb Dip with a Pure Xe Gain Cell Inside a 3.51-μ He-Xe Laser", Appl. Phys. Letters (USA), Vol. 17, No. 3, p. 120-2 (1 Aug. 1970).

Wellegchausen, B., Guttner, A.
"Relative Frequency Stability Measurements of Single-Mode Lasers", Z. Naturforsch. A. (Germany), Vol. 28a, No. 6, p. 968-72 (June 1973). In German.

Whitford, B. G., Smith, D. S.
"Frequency of the Methane-Stabilized He-Ne Laser at 3.39 μm Measured Relative to the 10.17 μm R(32) Transition of the CO_2 Laser [Measurement Standard]" Opt. Commun. (Netherlands), Vol. 20, No. 2, p. 280-3 (Feb. 1977).

Yepifanov, V. P., Mazan'ko, I. P., Yaroshenko, N.G.
"Study of Build-Up and Stability of Oscillations in a Neon- Helium Laser", Radiotekhnika i Elektronika (USSR), Vol. 12, No. 8, 1517-18 (1967). In Russian. English translation in: Radio Engng. Electronic Phys. (USA).

Zaitsev, Yu. I., Khurtin, L. A.
"Frequency Stabilization of a He-Ne Laser by Means of Low-Frequency Oscillations of Its Intensity", Pribory Tekh. Eksper . (USSR), No. 3, p. 177-9 (May 1969). In Russian. English translation in: Instrum. Exper. Tech. (USA), p. 731-3.

Zakharenko, Yu. G., Mel'nikov, N. A., Privalov, V. E., Fofanov, Ya. A.
"An He-Ne Laser, Stabilised by Absorption Saturation in Vapours of Iodine", Pis'ma V Zn. Tekh. Fiz. (USSR), Vol. 2, No. 4, p. 153-6 (26 Feb. 1976) In Russian.

2.2.2

Abate, J. A.
"Long-Term Frequency and Intensity Stabilization of a c.w. Dye Laser", J. Appl. Phys. (USA), Vol. 47, No. 4, p. 1464-6 (April 1976).

Akimoto, Y., Tako, T.
"A Double Servo System for the CH Stabilized Laser" Oyo Buturi (Japan), Vol. 44, No. 6, p. 635-40 (June 1975). In Japanese.

Ambartsumyan, R. V., Basov, N. G., Letokohv. V. S.
"Investigation of the Frequency Characteristics of a Xe-He Laser with a Diffuse Mirror", Zh. Eksper. Teor. Fiz. Pis'ma(USSR), Vol. 7, No. 3, 88-91 (Feb. 1968). In Russian. English translation in: JETP Letters (USA), Vol. 7, No. 3, 66-7 (Feb. 1968).

Antropov, Ye. T., Kochetkov, Yu. A., Ostapets, V.N. Panov, Ye. I., Podobed, V. S., Silin-Bekchurin, I. A., Sobolev, N. N., Taktarov. S. G.
"Automatic Frequency Control of a Selective CO_2 Laser by Means of a Piezoelectric Device", Radio Eng. & Electron. Phys. (USA), Vol. 19, No. 2, p. 59-62 (Feb. 1975). Translation of: Radiotekh. & Elektron. (USSR), Vol. 19, No. 2, p. 330-5 (Feb. 1974).

Arzumanov, V. N., Zaitsev, G. F., Kruzhalov, S. V., Pakhomov, L. N., Petrun'kin, V. Yu.
"Single-Frequency YAG-Nd Laser Stabilised by a Standard Anisotropic Resonator", Avtometriya (USSR) No. 2, p. 125-7 (March-April 1977). In Russian. English translation in: Autom. Monit. & Meas. (GB).

Bagaev, S. N., Vasilenko, L. S., Matyugin, V. M., Klementev, V. M., Troshin, B. I., Chebotaev. V. P.
"Some Results of an Investigation of the Generation-Frequency Stability of Gas Lasers at 0.63 μm, 1.5 μm, 3.39 μm, and 9.6 μm", Opt. & Spectrosc. (USA), Vol. 32, No. 4, p. 422-5 (April 1972). Translation of: Opt. & Spektrosk. (USSR), Vol. 32, No. 4, p. 802-8 (April 1972). In Russian.

Baird, K. M., Riccius, H. D., Siemsen, K. J., Hart, K. H., Smith, D. S.
"Measurements of Stabilized Laser Wavelengths", 1971 Annual Meeting of the Optical Society of America, Ottawa, Canada, 5-8 Oct. 1971 (Washington, DC, USA: Optical Soc. America 1971) p. 25.

Baird, K. M.
"CO_2 Laser Wavelength Standards", IEEE Trans. Instrum. & Meas. (USA), Vol. IM-25, No. 4, p. 445-7 (Dec. 1976). (1976 Conference on Precision Electromagnetic Measurements, Boulder, Colo., USA, 28 June - 1 July 1976).

Barger, R. L., Sorem, M. S., Hall, J. L.
"Frequency Stabilization of a CW Dye Laser", Appl. Phys. Lett. (USA), Vol. 22, No. 11, p. 573-5 (1 June 1973).

Barger, R. L., English, T. C., West, J. B.
"Frequency Stabilization of a CW Dye Laser and Laser Saturation of Atomic Beams", Proceedings of the 29th Annual Frequency Control Symposium, Fort Monmouth, NJ, USA, 28-30 May 1975 (Washington, DC, USA: Electronic Industries Assoc. 1975), p. 316-20.

Barger, R. L., West, J. B., English, T. C.
"Fast Frequency Stabilization of a CW Dye Laser", Appl. Phys. Lett. (USA), Vol. 27, No. 1, p. 31-3 (1 July 1975).

Basov, N. G., Belenov, E. M., Vol'nov, M. I., Gubin, M. A., Nikitin, V. V., Troshagin, V. N.
"Stabilization of Ring-Laser Frequency", Zh. Eksp. Teor. Fiz. Pis'ma (USSR), p. 659-61. In Russian. English translation in: JETP Lett. (USA), Vol. 15, No. 12, p. 466-8 (5 June 1972).

Bazarov, E. N., Gerasimov, G. A., Gubin, V. P., Posudin, Yu. I.
"Frequency Stabilisation of CO_2-Lasers Using Narrow Resonances in OsO_4", Izv. VUZ Radioelektron. (USSR), Vol. 20, No. 10, p. 39-44 (Oct. 1977). In Russian.

Benedetti, R., Di Lieto, A., Inguscio, M. Minguzzi, P., Strumina, F., Tonelli, M.
"Frequency Modulation of a Far Infrared CH_3F Laser by Stark Effect", 31st Annual Frequency Control Symposium, Atlantic City, NJ, USA, 1-3 June 1977 (Washington, DC, USA: Electronic Industries Assoc. 1977), p. 605-11.

Beterov, I. M., Klement'ev, V. M., Chebotaev, V.P. "Secondary Frequency Standard Using Mercury Laser at Microwaves", Radiotekhnika i Elektronika (USSR, Vol. 14, No. 11, p. 2066-9 (1969). In Russian.

Bikmukhametov, K. A., Klement'ev, V. M. "Investigation of the Stability of the Oscillation Frequency of a Mercury Laser Emmiting at $\lambda = 1.53\,\mu$", Sov. J. Quantum Electron. (USA), Vol. 2, No. 3, p. 254-6 (Nov.-Dec. 1972).Translation of: Kvantovaya Elektron. (USSR), No. 3(9), p. 74-6 (1972).

Bjorkholm, J. E., Danielmayer, H. G. "Frequency Control of a Pulsed Optical Parametric Oscillator by Radiation Injection", Appl. Phys. Letters (USA), Vol. 15, No. 6, p. 171-7 (15 Sept. 1969).

Blaney, T. G., Bradley, C. C., Edwards, G. J., Knight, D. J. E. "Absolute Frequency Measurement of a Lamb-Dip Stabilised Water Vapour Laser Oscillating at 10.7 THz ($28\,\mu$m)", Phys. Lett. A (Netherlands), Vol. 43 A, No. 4, p. 471-2 (9 April 1973).

Blaney, T. G., Bradley, C. C., Edwards, G. J., Knight, D. J. E., Woods, P. T., Jolliffe, B. W. "Absolute Frequency Measurement of the R(12) Transition of CO_2 at $9.3\,\mu$m", Nature (GB), Vol. 244, No. 5417, p. 504 (24 Aug. 1973).

Blaney, T. G., Bradley, C. C., Edwards, G. J., Jolliffe, B. W., Knight, D. J. E., Woods, P. T. "Measurement of the Frequency of the Methane-Stabilised Laser at $3.39\,\mu$m and of the R(32) Transition of CO_2 at $10.17\,\mu$m", Nature (GB), Vol. 254, No. 5501, p. 584-5 (17 April 1975).

Blaney, T. G., Bradley, C. C., Edwards, G. J., Jolliffe, B. W., Knight, D. J. E., Rowley, W. R. C., Shotton, K. C., Woods, P. T. "Measurement of the Speed of Light. I. Introduction and Frequency Measurement of a Carbon Dioxide Laser", Proc. R. Soc. London Ser. A (GB), Vol. 355, No. 1680, p. 61-88 (1977).

Borde, C., Henry, L. "Study of the Lamb Dip and of Rotational Competition in a Carbon Dioxide Laser. Applications to the Laser Stabilization and to the Measurement of Absorption Coefficients of Gases", IEEE J. Quantum Electronics (USA), Vol. QE-4, No. 11, p. 874-80 (Nov. 1968). (1968 International Quantum Electronics Conference, Miami, FL 14-17 May 1968).

Borde, C., Camy, G., Vialle, J. L., Decomps, B. "Frequency Stabilization of an Argon Laser by Saturated Absorption or Dispersion in Iodine at 5145 A", CPEM 74 Digest: Conference on Precision Electromagnetic Measurements, London, England, 1-5 July 1974 (London, England: IEE 1974), p. 105.

Bourdet, G., Orszag, A., de Valence, Y. "Utilization of the Impedance Variation of the Plasma of CO_2 Laser for Frequency Stabilization on the 'Lamb Dip'", C. R. Hebd. Seances Acad. Sci. B (France), Vol. 277, No. 9, p. 207-9 (3 Sept. 1973). In French.

Bradley, C. C., Knight, D. J. E., "Frequency Locking an HCN Laser to a Molecular Absorption Line", Electron. Lett. (GB), Vol. 7, No. 13, p. 381-2 (1 July 1971).

Burmakin, V. A., Korolev, F. A., Lebedeva, V. V., Odintsov, A. I., Salimov, V. M., Sinitsa, L. N. "A Method for Absolute Frequency Stabilization of an Argon-Ion Laser with a Magnetic Field", Radiotekh. & Elektron. (USSR), p. 1292-6. In Russian. English translation in: Radio Eng. & Electron. Phys. (USA), Vol. 16, No. 7, p. 1228-31 (July 1971)

Camy, G., Decomps, B., Gardissat, J. L., Borde, C. J. "Frequency Stabilization of Argon Lasers at 582.49 THz Using Saturated Absorption in $^{127}I_2$", Metrologia (Germany), Vol. 13, No. 3, p. 145-8 (1977).

Clarion, A., Henry, L., "Stabilisation of Carbon Dioxide Gas Lasers by Saturated Absorption", C. R. Hebd. Seances Acad. Sci. B (France), Vol. 279, No. 16, p. 419-22 (14 Oct. 1974). In French.

Clark, N. A. "Laser Frequency Stabilization: Combined Integrating Thermal-Proportional Servos", Appl. Opt. (USA), Vol. 15, No. 6, p. 1375 (June 1976).

Corcoran, V. J. "Frequency Lock of the Hydrogen Cyanide Laser to a Microwave Frequency Standard", IEEE J. Quantum Electronics (USA), Vol. QU-5, No. 8, p. 424-6 (Aug. 1969).

Corcoran, V. J., Cupp, R. E., Smith, W. T., Gallagher, J. J. "Stabilization of a Far-Infrared Molecular Laser" IEEE J. Quantum Electronics (USA), Vol. QE-6, No. 3, p. 184 (March 1970). (Second Conference on chemical and molecular lasers. Digest, St. Louis, MO. USA 22-24 May 1969).

Corcoran, V. J., Gallagher, J. J., Cupp, R. E. "Stabilization of a Submillimeter Wavelength Laser on a Microwave Frequency Standard", Symposium on submillimeter waves (abstracts only received). New York, USA, 31 Mar. - 2 Apr. 1970 (New York, USA: Polytechnic Press. 1970), 2pp.

Cupp, R. E., Corcoran, V. J., Gallagher, J. J. "Phase Lock of a Far-Infrared Laser to an Absolute Frequency Standard", IEEE J. Quantum Electronics (USA), Vol. QE-6, No. 3, p. 160-2 (March 1970).

Danileiko, M. V., Nedavnii, A. P., Nikolaenko, A. N., Fedin, V. P., Shpak, M. T. "Use of Self-Excited Lasing Modes to Increase the Reproducibility of Frequency-Stabilised Ring Lasers", Sov. Phys. Dokl. (USA), Vol. 20, No. 9, p. 625-5. Translation of: Dokl. Akad. Nauk SSSR, Vol. 224, No. 1-3, p. 68-71 (Sept. 1975).

Domnin, Yu. S., Tatarenkov, V. M., Shumyatskii, P. S.,
"D_2O Laser for Absolute Frequency Measurements", Sov. J. Quantum Electron. (USA), Vol. 5, No. 8, p. 991-3. Translation of: Kvantovaya Elektron., Moskva (USSR), Vol. 2, No. 8, p. 1818-21 (Aug. 1975).

Domnin, Yu. S., Tatarenkov, V. M.,Shumyatskii, P.S.
"Laser Translator of Standard Frequency to Submillimetre Range", Sov. J. Quantum Electron. (USA), Vol. 7, No. 5, p. 661-2 (May 1977). Translation of: Kvantovaya Elktron. Moskva (USSR), Vol. 4, No. 5, p. 1158-60 (May 1977).

Dutu, C. A.
"Frequency Stabilization by Phase Control of a Single Frequency-Single Mode CO_2 Laser", Stud. Cercet. Fiz. (Rumania), Vol. 24, No. 5, p. 535-44 (1972). In Rumanian.

Dutu, D.
"Investigation of an Automatic Frequency Stabilized CO_2 Laser", Rev. Roum. Phys. (Rumania), Vol. 19, No. 1, p. 3-15 (1974). In German.

Eng, R. S., Spears, D. L.
"Frequency Stabilization and Absolute Frequency Measurements of a CW HF/DF Laser", Appl. Phys. Lett. (USA), Vol. 27, No. 12, p. 650-2 (15 Dec 1975).

Ezekiel, S., Weiss, R.
"A Molecular Beam Reference for Laser Frequency Stabilization", IEEE J. Quantum Electronics (USA), Vol. QE-4, No. 5, p. 367 (May 1968). (1968 International Quantum Electronics Conference, Miami, FL, USA, 14-17 May 1968).

Ezekiel, S.
"Laser Frequency Stabilization Using a Primary Frequency Reference", Proceedings of the 23rd Annual Frequency Control Symposium, Atlantic City, NJ, USA, 6-8 May 1969 (Washington, DC, USA: Electronic Industries Assoc. 1969), p. 312.

Freed, C.
"Design and Short-Term Stability of Single-Frequency CO_2 Lasers", IEEE J. Quantum Electronics (USA), Vol. QE-4, No. 5, p. 369 (May 1968). (1968 international quantum electronics conference, Miami, FL, USA, 14-17 May 1968).

Freed, C.
"Design and Short-Term Stability of Single-Frequency CO_2 Lasers", IEEE J. Quantum Electronics (USA), Vol. QU-4, No. 6, 404-8 (June 1968).

Freed, C.
"Advances in Stable CO_2 Laser Design and Performance", International electron devices metering (abstracts), Washington, DC, USA, 28-30 Oct 1970 (New York, USA: IEEE 1970), p. 92.

Freed, C.
"Frequency Stabilization of CO_2 Lasers", Proceedings of the 29th Annual Frequency Control Symposium, Fort Monmouth, NJ, USA 28-30 May 1975 (Washington, DC, USA: Electronic Industries Assoc. 1975), p. 330-7.

Freed, C., O'Donnell, R. G., Ross, A. H. M.
"Absolute Frequency Calibration of the CO_2 Laser Transitions [Using Varactor Diode]", IEEE Trans. Instrum. & Meas. (USA), Vol. IM-25, No. 4, p. 431-7 (Dec. 1976). (1976 Conference on Precision Electromagnetic Measurements, Boulder, Colo., USA, 28 June - 1 July 1976).

Freed, C.
"Progress in CO_2 Laser Stabilization", 31st Annual Frequency Control Symposium, Atlantic City, NJ, USA, 1-3 June 1977 (Washington, DC, USA: Electronic Industries Assoc. 1977), p. 592-600.

Freed, C., O'Donnell, R. G.
"Advances in CO_2 Laser Stabilization using the 4.3μm Fluorescence Technique", Metrologia (Germany), Vol. 13, No. 3, p. 151-6 (1977).

Fukuyo, H., Iga, K., Ueno, A., Sano, T.
"Pure Ne Laser and Its Fundamental Characteristics", Bull. Tokyo Inst. Technol. (Japan), No. 107, p. 67-73 (1971).

Galkin, S. L., Kruzhalov, S. V., Nikolaev, V. M., Pakhomov, L. N., Petrun'kin, V. Yu.
"A Stabilised YAG:Nd^{3+} Laser with Synchronisation of Longitudinal Modes", Pis'ma V Zh. Tekh. Fiz. (USSR), Vol. 3, No. 1, p. 18-20 (12 Jan. 1977). In Russian. English translation in: Sov. Tech. Phys. Lett. (USA).

Gallagher, J. J.
"Limitations on Miniature Molecular Frequency Sources", Proceedings of the 29th Annual Frequency Control Symposium, Fort Monmouth, NJ, USA, 28-30 May 1975 (Washington, DC, USA: Electronic Industries Assoc. 1975), p. 344-51.

Galutin, V. Z., Zenkevich, S. S., Obukhov, I. V., Skibarko, A. P.
"Frequency Stability of a Gas Laser Operating in a Two-Mode Domain", Izv. VUZ Radioelektron. (USSR), Vol. 16, No. 9, p. 90-3 (Sept. 1973). In Russian. English translation in: Radio Electron. & Commun. Syst. (USA).

Galutva, G. V., Ryazantsev, A. I.
"Gas-Laser Resonator Stabilized by Thermal Compensation", Kvantovaya Elektron. (USSR), No. 2, p. 32-9 (1971). In Russian.

Gerhardt, H., Bodecker, V., Welling, H.
"Frequency Behaviour of a Frequency-Stable YAG:Nd^{3+} Laser", Z. Angew. Phys. (Germany), Vol. 31, No. 1, p. 11-15 (1971). In German.

Gerhardt, H., Tittel, F. K.
"A Frequency Stabilized, CW Dye Laser for High Resolution Spectroscopy", Opt. Commun. (Netherlands), Vol. 16, No. 3, p. 307-9 (March 1976).

Gerstenhauer, E.
"A Stable CW HCN Laser", Laser & Elektro-Opt. (Germany), Vol. 8, No. 3, p. 20-1 (Sept. 1976). In German.

Goldberg, M. W., Yusek, R.
"Doppler Jitter Stabilization of a CO_2 Laser", Appl. Phys. Lett. (USA), Vol. 18, No. 4, p. 135-7 (15 Feb. 1971).

Goldberg, M. W.
"The Inverted Lamb Dip in Spectroscopy and Laser Stabilization", Case Western Reserve Univ., Cleveland, Ohio, USA,thesis, 1971, 93 pp.

Grove, R. E., We, F. Y., Ezekiel, S.
"Frequency Stabilization of a CW Dye Laser", Proceedings of the Society of Photo-Optical Instrumentation Engineers, Vol. 49. Impact of Lasers in Spectroscopy, San Diego, Calif., USA, 19-20 Aug. 1974 (Palos Verdes Estates, Calif., USA: Soc. Photo-Optical Instrumentation Engrs. 1975), p.75-9.

Gusev, V. M., Kompanets, O. N., Kukudzhanov, A. R., Letokhov, V. S., Mikhailov, E. L.
"Stabilization of the Emission Frequency of a CO_2 Laser to within 10^{-12} with the Aid of Narrow SF_6 and OsO_4 Resonances", Sov. J. Quantum Electron. (USA), Vol. 4, No. 11, p. 1370-2 (May 1975). Translation of: Kvantovaya Elektron., Moskva (USSR), Vol. 1, No. 11, p. 2465-9 (Nov. 1974).

Hackel, L. A., Youmans, D. G., Ezekiel, S.
"Molecular Beam Stabilized Laser", Proceedings of the 27th Annual Frequency Control Symposium, Cherry Hill, NJ, USA, 12-14 June 1973 (Washington, DC, USA: Electronic Industries Assoc. 1973)., p. 382-5.

Hackel, L. A., Hackel, R. P., Ezekiel, S.
"Molecular Beam Stabilized Multiwatt Argon Lasers" Metrologia (Germany), Vol. 13, No. 3, p. 141-3 (1977).

Hackett, C. E., Dewey, C. F., Jr.,
"Improved Temporal Stability of Polymethine Lasers Dyes in Aqueous Solutions", IEEE J. Quantum Electron. (USA), Vol. QE-9, No. 11, p. 1119-20 (Nov. 1973).

Hall, J. L., Borde, C.
"Influence of Hyperfine Structure on Methane-Stabilized Lasers", Proceedings of the 27th Annual Frequency Control Symposium, Cherry Hill, NJ, USA, 12-14 June 1973 (Washington, DC, USA: Electronic Industries Assoc. 1973), p. 386.

Hall, D. R., Jenkins, R. M., Gorton, E. K.
"A Frequency-Stabilised CW Waveguide Carbon Dioxide Laser", J. Phys. D (GB), Vol. 11, No. 6, p. 859-69 (21 April 1978).

Hinchen, J. J., Frieberg, R. J.
"Frequency Stability Associated with a CW HF Laser", Appl. Opt. (USA), Vol. 15, No. 2, p. 459-61 (Feb. 1976).

Hohimer, J. P., Kelly, R. C.
"Frequency Stabilization of a High Power Argon Laser", Appl. Opt. (USA), Vol. 11, No. 3, p. 626-9 (March 1972).

Iga, K., Fukuyo, H.
"Frequency Stabilization of Pure Neon Laser", Bull. Tokyo Inst. Technol. (Japan), No. 112, p. 43-7 (1972).

Ivanov, V. A., Leikin, A. Ya., Solov'ev, V. S., Pavlov, V. G.
"Method for Stabilisation of the Output Frequency of a Carbon Dioxide Laser", Sov. J. Quantum Electron. (USA), Vol. 3, No. 3, p. 272-3 (Nov.-Dec. 1973). Translation of: Kvantovaya Elektron., Moskva (USSR), No. 3, p. 133-4 (1973).

Kasamatsu, M.
"Frequency Stabilization of Gas Lasers", Bull. Electrotech. Lab. (Japan), Vol. 32, No. 1, 48-65 (1968). In Japanese.

Kelly, M. J., Thomas, J. E., Monchalin, J. P., Kurnit, N. A., Javan, A.
"Potential Frequency Accuracy of the CO_2 Fluorescence Saturation Dip", Proceedings of the 29th Annual Frequency Control Symposium, Fort Monmouth, NJ, USA, 28-30 May 1975 (Washington, DC, USA: Electronic Industries Assoc. 1975), p. 338-43.

Kempf, R. A., Cupp, R. E., Smith, W. T., Gallagher, J. J.
"Extension of Frequency Control Techniques to the Submillimeter Wavelength Region", Proceedings of the 22nd Annual Frequency Control Symposium, Atlantic City, NJ , USA, 22-24 Apr 1968 (Fort Monmouth, NJ, USA: Electronic Components Lab, 1968), p. 573-91.

Kleiman, A. S., Leikin, A. Ya., Pestovskii, V. I., Fertik, N. S.
"Measurement of Short-Time Instability of Laser Frequency at $3.3\,^{15}NH_3$ Line", Izv. VUZ Radiofiz. (USSR), Vol. 12, No. 8, p. 1165-8 (1969). In Russian. English translation in: Soviet Radiophys. (USA).

Koffend, Brooke, J., Goldstein, S., Bacis, R., Field, R. W., Ezekiel, S.
"Doppler-Free Stimulated-Emission Spectroscopy and Secondary Frequency Standards Using an Optically Pumped Laser", Phys. Rev. Lett. (USA), Vol. 41, No. 15, p. 1040-4 (9 Oct. 1978).

Kompanets, O. N., Kukudzhanov, A. R., Letokhov, V. S., Mikhailov, E. L.
"Stabilisation of the Emission Frequency of a Carbon Dioxide Laser by an External Nonlinearly Absorbing SF_6 Cell", Sov. J. Quantum Electron. (USA), Vol. 3, No. 4, p. 293-6 (Jan.-Feb 1974). Translation of: Kvantovaya Elektron., Moskva (USSR), No. 4, p. 28-34.

Kompanets, O. N., Kukudzhanov, A. R., Mikhailov, E. L.
"Highly Stable CW CO_2 Lasers Obtained by Automatic Frequency Control", Instrum. & Exp. Tech. (USA), Vol. 18, No. 1, pt. 2, p. 296-7 (Jan.-Feb. 1975). Translation of: Prib. Tekh. Eksp. (USSR), Vol. 18, No. 1, pt. 2, p. 250-1 (Jan.-Feb. 1975).

Kompanets, O. N., Kukudzhanov, A. R., Mikhailov, E. L.
"Problem of Reproducibility of the Output Frequency of a CO_2/OsO_4 Laser", Sov. J. Quantum Electron. (USA), Vol. 7, No. 9, p. 1150-2 (Sept. 1977). Translation of: Kvantovaya Elektron., Moskva (USSR) Vol. 4, No. 9, p. 2016-19 (Sept. 1977).

Kurosawa, T., Kosaki, A., Sakurai, T., Tanaka, K.
"Experiments of a CO_2 Laser Frequency Stabilization", Oyo Buturi (Japan), Vol. 46, No. 3, p. 304-9, (March 1977). In Japanese.

Lachambre, J. L., Otis, G., Lavigne, P.
"Simultaneous Frequency Stabilization and Injection in a TEA-CO_2 Oscillator", Appl. Opt. (USA), Vol. 17, No. 7, p. 1015-17 (1 April 1978).

Le Floch, A., Le Naour, R., Stephan, G., Brun, P.
"Frequency Stabilization and Tunability of Lasers: use of Mobile Dips and Peaks", Appl. Opt. (USA), Vol. 15, No. 11, p. 2673-7 (Nov. 1976).

Lemaire, J., Houriez, J., Lapauw, J. M.
"Frequency Stabilisation of CO_2 or N_2O Laser by a Rapid Sampling Method", Rev. Phys. Appl. (France), Vol. 7, No. 4, p. 323-8 (Dec. 1972). In French.

Letokhov, V. S.
"Self-Stabilization of Laser Optic-Oscillation Frequency by Nonlinear Absorption in Gas", Zh. Eksper. Teor. Fiz. Pis'ma (USSR), Vol. 6, No. 4, 597-600 (15 Aug. 1967). In Russian. English translation in: JETP Letters (USA), Vol. 6, No. 4, 101-3 (15 Aug. 1967).

Letokhov, V. S., Pavlik, B. D.
"Production of Coherent Light by Atomic or Molecular Beams", Zh. Eksper. Teor. Fiz. (USSR), Vol. 53, No. 3, 1107-15 (Sept. 1967). In Russian. English translation in: Soviet Phys. JETP (USA).

Letokhov, V. S., Pavlik, B. D.
"Method for Establishing a Quantum Frequency Standard in the Visible Range Using Atomic Absorption Lines and a CW Dye Laser", Sov. J. Quantum Electron. (USA), Vol. 6, No. 1, p. 32-8. Translation of: Kvantovaya Elektron., Moskva (USSR), Vol. 3, No. 1, p. 60-71 (Jan. 1976).

Lipchak, M. W.
"Improved Frequency Stability of the TEA CO_2 Laser", Opt. Commun. (Netherlands), Vol. 19, No. 2, p. 205-7 (Nov. 1976).

Lourtioz, J. M., Henaux, J. C., Adde, R.
"Design of a Stable and Powerful Oscillator at 891 GHz", C. R. Hebd. Seances Acad. Sci. B (France), Vol. 282, No. 7, p. 161-4 (16 Feb. 1976). In French.

Lourtioz, J. M., Adde, R.
"Design of a Stable CW HCN Laser for Far Infrared Frequency Synthesis", Rev. Phys. Appl. (France), Vol. 11, No. 4, p. 533-40 (July 1976).

Maischberger, K.
"Long Term Frequency Stabilization of a Composite Cavity Argon Laser Using a Reference Frequency Light Source", Report ESRIN-IN-117, European Space Res. Inst., Frascatti, Italy (Dec. 1970). 27 pp. Available from NTIS, Springfield, VA 22151, USA.

Maischberger, K.
"Long Term Frequency Stabilization of a Composite-Cavity Argon Laser", IEEE J. Quantum Electron. (USA), Vol. QE-7 No. 6, p. 250-2 (June 1971).

Man, C. N., Cerez, O., Brillet, A., Hartmann, F.
"A Frequency Stabilized CW Dye Laser for Spectroscopic and Metrological Applications", J. Phys. Lett. (France), Vol 38, No. 14, P. L287-9. (15 July 1977).

Martinot-Largarde, P., Coumes, C.
"Argon Ion Laser in Unique Modes, Stabilized", Nachrichtentech. Fachber. (NTF) Germany, Vol. 35, p. 695-702 (1968). In French. (7th International Conference on Microwave and Optical Generation and Amplification, Hamburg, 16-20 Sept. 1968).

Mathieu, P., Izatt, J. R.
"Laser Frequency Control by Spectrally Depleted Destructive Two-Beam Interference", Opt. Commun. (Netherlands), Vol. 26, No. 1, p. 86-90 (July 1978).

Mel'tsin, A. L.
"Experimental Study of the System of Frequency Stabilisation of Ring Laser with an External Absorption Chamber", Zh. Prikl. Spektrosk. (USSR) Vol. 15, No. 2, p. 214-18 (1971). In Russian.

Meyer, Y. H.
"Frequency Locking of a Dye Laser Using Absorbed Atoms", Opt. Commun. (Netherlands), Vol. 19, No. 3, p. 343-5 (Dec. 1976).

Michalski, W., Nowicki, R., Plinski, E. F.
"Noise, Fluctuations and Output Power Stabilization in a CO_2 Laser", Elektronika (Poland), Vol. 18, No. 7-8, p. 303-5 (1977). In Polish.

Minguzzi, P., Tonelli, M.
"Simple Frequency Stabilization of CO_2 Laser for Far-Infrared Laser Pumping", J. Phys. E (GB), Vol. 10, No. 8, p. 775-6 (Aug. 1977).

Mocker, H. W.
"High Stability CO_2 Waveguide Lasers", EASCON' 76 Record, Washington, DC, USA, 26-29 Sept. 1976 (New York, USA: IEEE 1976), p. 151A/1-4.

Munch, J., Kolpin, M. A., Levine, J.
"Frequency Stability and Stabilization of a Chemical Laser", IEEE J. Quantum Electron. (USA), Vol. QU-14, No. 1, p. 17-22 (Jan. 1978).

Nicholson, J. P., Lipton, K. S.
"A Tunable Stabilized Single-Mode TEA CO_2 Laser", Appl. Phys. Lett. (USA), Vol. 31, No. 7, p. 430-2 (Oct. 1977).

Nussmeier, T. A., Abrams, R. L.
"Stark Cell Stabilization of CO_2 Laser", Appl. Phys. Lett. (USA), Vol. 25, No. 10, p. 615-17 (15 Nov. 1974).

Ohi, M., Akimoto, Y.,
"Performance of Methane-Stabilized Lasers with the Method of Saturated Absorption", Jap. J. Appl. Phys. (Japan), Vol. 15, No. 6, p. 1177-8 (June 1976).

Oraevskii, A. N.
"Beam Laser as a Frequency Standard", Izv. VUZ, Radiofiz. (USSR), Vol. 11, No. 10, p. 1554-9 (1968). In Russian. English translation in: Soviet Radiophys. (USA).

Ouhayoun, M., Borde, C. J.,
"Frequency Stabilization of CO_2 Lasers through Saturated Absorption in SF_6." Metrologia (Germany), Vol. 13, No. 3, p. 149-50 (1977).

Pankratov, V. A.
"Rubidium Laser with Zero Frequency Shift Caused by a Buffer Gas", Sov. J. Quantum Electron. (USA), Vol. 4, No. 3, p. 413 (Sept. 1974). Translation of: Kvantovaya Elektron., Moskva (USSR), Vol. 1, No. 3, p. 720-1 (March 1974).

Rabinowtiz, P., LaTourrette, J. T., Gould, G.
"Proposed Ultrastable CO_2 Oscillator", International electron devices meeting, Washington, DC, USA, 18-20 Oct. 1967 (New York: Institute of Electrical and Electronics Engineers 1967), p. 132.

Reynolds, R. S.
"Stabilized Carbon Dioxide Gas Laser" Final Report, 1 Dec. 1966-30 Jan. 1968", Report NASA-CR-95055, Sylvania Electric Products, Inc., Mountain View, Cal., USA (30 Jan. 1968), 78 pp. Contract NAS5-10309. Available from CFSTI, Springfield, VA 22151, USA.

Reynolds, R. S., Sasnett, M. W.
"Active Frequency Stabilization of a 20-Watt CO_2 Laser with Etalon Wavelength Selection", International electron devices meeting, Washington, DC, USA, 23-25 Oct. 1968 (New York, NY, USA: IEEE 1968), p. 60.

Ryan, T. J.
"Molecular-Beam Stabilized Argon Laser", Appl. Phys. Lett. (USA), Vol. 21, No. 7, p. 320-2 (1 Oct. 1972).

Sasnett, M. W.,
"Frequency Stabilized Gas Laser [Final Report]", Report NASA-CR-102617, Sylvania Electronic Systems West, Mountain View, Calif., USA (Oct. 1969), 81 pp. Contract NAS8-20631. Available from CFSTI, Springfield, VA, 22151, USA.

Sasnett, M. W., Reynolds, R. S.
"Stabilized CO_2 Laser Source for 10.6 Micron Heterodyne Communication System", International electron devices meeting, Washington, DC, USA, 29-31 Oct. 1969 (New York, USA: IEEE 1969), p. 108-10.

Shimoda, K.,
"Absolute Frequency Stabilization of the 3.39 μm Laser on a CH_4 Line", Conference on Precision Electromagnetic Measurements, Boulder (1968) New York, Institute of Electrical and Electronics Engineers (1968) 46.

Shimoda, K.
"Frequency Shifts in Methane-Stabilized Lasers", Jap. J. Appl. Phys. (Japan), Vol. 12, No. 9, p. 1393-1402 (Sept. 1973).

Skolnick, M. L.
"Frequency Stabilized Passively Q-Switched CO_2 Laser", 17th International Electron Devices Meeting (abstracts), Washington, DC, USA, 11-13 Oct., 1971 (New York, USA: IEEE 1971). p. 86.

Smith, P. W.
"Stabilized Single-Frequency Output from a Long Ring Laser", IEEE J. Quantum Electronics (USA), Vol. QE-4, No. 8, 485-90 (Aug. 1968).

Smith, P. W., Maloney, P. J.
"A Self-Stabilized 3.5 μm Waveguide He-Xe Laser", Appl. Phys. Lett. (USA), Vol. 22, No. 12, p. 667-9 (15 June 1973).

Sochor, V.
"Stability and Selectivity of Molecular Laser Resonator", Czech. J. Phys. B, Vol. 18, No. 7, 910-18 (1968).

Sorem, M. S., Barger, R. L., Hall, J. L.
"Frequency Stabilization of a CW Dye Laser", 1973 IEEE/OSA Conference on Laser Engineering and Applications Digest of Technical Papers, Washington, DC, USA, 30 May-1 June 1973 (New York, USA: IEEE 1973), p. 81.

Sorokin, P. P., Lankard, J. R., Moruzzi, V. L., Lurio, A.
"Frequency-Locking of Organic Dye Lasers to Atomic Resonance Lines", Appl. Phys. Letters (USA), Vol. 15, No. 6, p. 179-81 (15 Sept. 1969).

Spieweck, F.
"Wavelength Stabilization of an Ar+ Laser with and External $^{129}I_2$ Absorption Cell", Appl. Phys. (Germany), Vol. 3, No. 5, p. 429-30 (May 1974).

Wallard, A. J.
"The Reproducibility of 633-nm Lasers Stabilized by $^{127}I_2$", IEEE Trans. Instrum. & Meas. (USA), Vol. IM-23, No. 4, p. 532-5 (Dec. 1974). (1974 Conference on precision electromagnetic measurements, London, England, 1-5 July 1974).

Wang, S. C.
"Potential Methods of Frequency Stabilization for the Xenon 3.51 μm Laser Transition", Stanford Univ., Calif., USA thesis, 1971, 75 pp. Available from Univ. Microfilms, Ann Arbor, Mich., USA Order No. 71-19774.

Wang, C. P.
"Frequency Stability of a CW HF Chemical Laser", J. Appl. Phys. (USA), Vol. 47, No. 1, p. 221-3 (Jan 1976).

Welling, H., Schroder, H. W., Wellegehausen, B., Nottbeck, N.
"Frequency-Stable Single-Mode Dye Laser", 1973 IEEE/OSA Conference on Laser Engineering and Applications Digest of Technical Papers, Washington DC, USA, 30 May-1 June 1973 (New York, USA: IEEE 1973), p. 80-1.

Welling, H., Schroder, H. W., Wellegehausen, B.
"Frequency Stability and Linewidth of Single Mode CW Dye Lasers", Spectrosc. Lett. (USA), Vol. 8, No. 9, p. 685-95 (1975).

Wells, N.
"A Stabilized HCN Laser for Infrared Frequency Synthesis", IEEE Trans. Instrum. & Meas. (USA), Vol. IM-22, No. 2, p. 113-18 (June 1973).

Wenk, G. J.
"Frequency Stabilisation of Gas Lasers", National Radio and Electronics Engineering Convention, Sydney, 1967 (Sydney: Institution of Radio and Electronics Engineers, 1967) pp. 170-1.

Woods, P. T., Jolliffe, B. W.
"Stable Single-Frequency Carbon Dioxide Lasers", J. Phys. E (GB), Vol. 9, No. 5, p. 395-402 (May 1976).

Wu, F. Y., Grove, R. E., Ezekiel, S.
"CW Dye Laser for Ultrahigh-Resolution Spectroscopy", Appl. Phys. Lett. (USA), Vol. 25, No. 1, p. 73-5 (1 July 1974).

Wu, F. Y., Ezekiel, S.
"Frequency Stabilization of Commercial CW Dye Lasers for Ultrahigh Resolution Spectroscopy", IEEE J. Quantum Electron. (USA), Vol. QE-13, No. 9, p. 30-1 (Sept. 1977). (1977 IEEE/OSA Conference on Laser Engineering and Applications. (Digest of technical papers), Washington, DC, USA, 1-3 June 1977).

Yusek, R.
"CO_2 Laser Frequency Stabilization Using Resonant Absorption in SF_6", Case Western Reserve Univ., Cleveland, Ohio, USA, thesis, 1970, 129 pp. Available from Univ. Microfilms, Ann Arbor, Mich, USA Order No. 70-25930.

Spieweck, F.
"Wavelength Stabilization of the Green Ar II Line Using Saturated Absorption in an Internal $^{129}I_2$ Cell", Metrologia (Germany), Vol. 12, No. 1, p. 43-6 (1976). In German.

Spieweck, F.
"Development of Wavelength Stabilisers for the Green Ar+ Laser Line at λ = 514.5 nm for Metrological Applications", Feinwerktech. & Messtech. (Germany), Vol. 85, No. 4, p. 155-63 (May-June 1977). In German.

Spieweck, F.
"Wavelength Stabilization of the Ar+ Laser Line at λ = 515 nm for Length Measurements of Highest Precision", Laser 77 Opto-Electronics, Munich, Germany, 20-24 June 1977 (IPC Sci. Technol. Press 1977), p. 130-6.

Stein, S. R., van de Stadt, H.
"Electronic Tuning and Phase-Lock Techniques for Optically Pumped Far Infrared Lasers", 31st Annual Frequency Control Symposium, Atlantic City, NJ, USA, 1-3 June 1977 (Washington, DC, USA: Electronic Industries Assoc. 1977), p. 601-4.

Steiner, M., Walther, H., Zygan, K.
"Highly Stable Dye Lasers", Opt. Commun. (Netherlands), Vol. 18, No. 1, p. 2 (July 1976). (9th International Conference on Quantum Electronics. (Digest), Amsterdam, Netherlands, 14-18 June 1976).

Tako, T., Ohi, M., Akimoto, Y., Sugiyama, A., Shimoda, K.
"Frequency Stabilization of the 3.39 μm Laser on a CH_4 Line", Jap. J. Appl. Phys. (Japan), Vol. 9, No. 12, p. 1535 (Dec. 1970).

Targ, R., French, J. M., Yarborough, J. M.
"Frequency Stabilization and Noise Suppression in the Argon FM Laser", IEEE J. Quantum Electronic (USA), Vol. QE-4, No. 10, p. 644-8 (Oct. 1968). (1968 International Quantum Electronics Conference Miami, FL, May 14-17, 1968).

Thomason, W. H., Elbers, D. C.
"An Inexpensive Method to Stabilize the Frequency of a CO_2 Laser", Rev. Sci. Instrum. (USA), Vol. 46, No. 4, p. 409-12 (April 1975).

Tomlinson, W. J., Fork, R. L.
"Frequency Stabilization of a Gas Laser", Appl. Optics (USA), Vol. 8, No. 1, p. 121-9 (Jan 1969).

Vasilenko, L. S., Skvortsov, M. N., Chebotaev, V.P. Shershneva, G. I., Shishaev, A. V.
"Frequency Stabilization of a CO_2 Laser", Opt. & Spectrosc. (USA), Vol. 32, No. 6, p. 609-12 (June 1972). Translation of: Opt. & Spektrosk. (USSR), Vol. 32, No. 6, p. 1123-9 (June 1972).

Waksberg, A. L.
"Stabilization of a CO_2 Laser Using a Three-Mirror Laser System", IEEE J. Quantum Electronics (USA), Vol. QE-4, No. 9, 532-3 (Sept. 1968).

Ablovich, D., Jr.
"Some Observations Concering Frequency and Time Standardization". Proceedings Twenty-first Instrument Society America Conference, New York, (1966) (Pittsburgh: Instrument Society America), Vol. 21, Pt 1, Paper No. 12, 9-3-66, pp. 20.

Akimochkin, I. K., Denisov, V. P., Cherenkova, E.M.
"Long-term Frequency Comparator". Meas. Tech. (USA), Vol. 16, no. 1, p. 83-5 (Jan. 1973). Translation of: Izmer. Tekh. (USSR), Vol. 16, no.1, p. 54-5 (Jan. 1973). Translation of Izmer Tekh. (USSR), Vol. 16, no. 1, p. 54-5 (Jan. 1973).

Allan, D. W., Gray, J. E., Machlan, H. E.
"The National Bureau of Standards Atomic Time Scales: Generation, Dissemination, Stability, and Accuracy". IEEE Trans. Instrum. & Meas. (USA) Vol. IM-21, no. 4, p. 388-91 (Nov. 1972).

Allan, D. W., Daams, H.
"Picosecond Time Difference Measurement System". Proceedings of the 29th Annual Frequency Control Symposium, Fort Monmouth, N.J., USA, 28-30 May 1975 (Washington, D.C., USA: Electronic Industries Assoc. 1975), p. 404-11.

Allan, D. W., Hellwig, H., Glaze, D. J.
"An Accuracy Algorithm for an Atomic Time Scale". Metrologia (Germany), vol. 11, no. 3, p. 133-8 (1975).

Artyukh, Yu. N., Arnit, M. A., Gotlib, G. I., Zagurskii, V. Ya.
"Instrument for Measuring Time Intervals to an Accuracy of 2 nsec". Instrum. & Exp. Tech. (USA) Vol 20, no. 4, pt. 1, p. 1039-41 (July-Aug. 1977) Translation of: Prib. Tekh. Eksp. (USSR), Vol. 20, no. 4, pt. 1, P. 108-10 (July-Aug. 1977).

Auchterlonie, L. J., Bryant, D. L.,
"A Direct Method of Measuring Small Frequency Shifts Using Two Open Resonators at Millimetre Wavelengths" Int. J. Electron. (GB), Vol. 45, no. 2, p. 113-22 (Aug. 1978).

Ausejo, R.
"Frequency and Time Meters". Mundo Electron. (Spain), no. 50, p. 59-66 (March 1976). In Spanish.

Azoubib, J., Granveaud, M., Guinpot, B.
"Estimation of the Scale Unit Duration of Time Scales". Metrologia, (Germany), vol. 13, no. 3, p. 87-93 (1977).

Baev, A. V., Rozkina, M. S., Torbenkov, G. B.
"Capacitive Method for Measuring Frequency". Meas. Tech. (USA), Vol. 16, no. 7, p. 1034-6 (July 1973). Translation of: Izmer. Tekh. (USSR) Vol. 16, no. 7, p. 53-4 (July 1973)

Bahadur, H.,Parshad, R.
"Measurement of Time". Stud. J. Inst. Electron. & Telecommun. Eng. (India), Vol. 17, no. 2, p. 103-8 (April 1974).

Baidakov, I. G., Pushkin, S.B., Titov, V. P.
"Securing Unanimity of Time and Frequency Measurement in the USSR at the Highest Section of the Reference System". Meas. Tech. (USA), Vol. 16, no. 1, p. 60-3 (Jan. 1973). Translation of: Izmer. Tekh. (USSR), Vol. 16, no. 1, p. 60-3 (Jan. 1973).

Barber, R. E.
"Short-term Frequency Stability of Precision Oscillators and Frequency Generators". Bell Syst. Tech. J. (USA), Vol. 50, no. 3, p. 881-915 (March 1971).

Barnes, J. A., Winkler, G. M. R.
"The Standard of Time and Frequency in the U.S.A.". Proc. 26th Annual Frequency Control Symposium, Atlantic City, N. J., USA, 6-8 June 1972 (Washington D.C., USA: Electronic Industries Association 1972), p. 269-278.

Barnes, J. A.
"Models for the Interpretation of Frequency Stability Measurements". Report NBS-TN-683, Nat. Bur. Stand., Washington, DC, USA (Aug. 1976) 39 pp.

Barnes, J. A.
"A Simulation of the Fluctuations of International Atomic Time". Report NBS-TN-689, Nat. Bur. Stand., Washington, D.C., USA (Nov. 1976), 20 pp.

Barrier, B., Humbert, J.P.
"Numerical Frequency Meters from A to Z". Inter. Electron. (France), vol. 28, no. 81, p. 33-39 (5 Feb. 1973). (In French).

Bastelberger, J.
"Normal Frequencies, Their Investigation and Measurement". Fernmelde-Ingenieur (Germany), Vol. 22, no. 5, p. 23 (May 1968), In German.

Bava, E., de Marchi, A., Godone, A.
"A Narrow Output Linewidth Multipiler Chain for Precision Frequency Measurements in the 1 THz Region". 31st Annual Frequency Control Symposium, Atlantic City, NJ., USA, 1-3 June 1977 (Washington, DC, USA: Electronic Industries Assoc. 1977), p. 578-82.

Bay, Z., Luther, G. G.
"Locking a Laser Frequency to the Time Standard" Appl. Phys. Letters (USA), Vol. 13, no. 9, p. 303-4 (1 Nov. 1968).

Becker, G.
"The Second as Standard Unit of Time". Umsch. Wiss. & Tech. (Germany), Vol. 76, no. 22, p. 706-7 (15 Nov. 1976). In German.

Begley, W. W., Shapiro, A. H.
"Precision Timing Systems. I. Standard Scales". Instrum. Contr. Syst. (USA), Vol. 43, no. 9, p. 87-9 (Sept. 1970).

Behnke, H.
"Standard Frequency Comparison by 'Error Multiplication'". Radio Fernsehen Elektron. (Germany), Vol. 22, no. 19, p. 642-3 (Oct. 1973). In German.

Belotserkovskii, D. Ya., Il'in, V. G., Stepanova, I. V.
"International Cooperation in the Field of Exact Time and Frequency Measurements". Meas. Tech. (USA), Vol. 18, no. 4, p. 517-19 (April 1975). Translation of: Izmer, Tekh. (USSR), Vol. 18, no. 4, p. 28-9 (April 1975).

Belomestnov, G. I., Dmitrienko, A. D., Emakov,A.S., Korzh, V. F.
"Automatic System for Acquiring, Recording, and Processing Information by Computer for Secondary Time-and-Frequency Standards". Meas. Tech. (USA), Vol. 19, no. 11, p. 1572-4 (Nov. 1976). Translation of: Izmer. Tekh. (USSR), Vol. 19, no. 11, p. 27-8 (Nov. 1976).

Berger, F.
"Time Metrology and Quartz Application. I. Time Metrology". Rev. Gen. Electr. (France), Vol 84, no. 12, p. 907-18 (Dec. 1975). In French.

Blachman,N.M.
"The Effect of Noise Upon Polar-Display Instantaneous Frequency Measurement". IEEE Trans. Instrum. & Meas. (USA), Vol. IM-25, no. 3, p. 214-21 (Sept. 1976).

Blair, B. E.
"Time and Frequency: Theory and Fundamentals". Report NBS-Mono-140, Nat. Bur. Stand., Washington, D.C., USA(May 1974), 460 pp.

Body, I., Szemok, I.
"General Problems of Frequency Measurement". Meres & Autom. (Hungary), Vol. 22, no. 11, p. 422-8 (1974). In Hungarian.

Borisochkin, V. V.
"Checking the Frequency of Highly Stable Generators". Meas. Tech. (USA), p. 460-3 Translation of: Izmer. Tekh. (USSR), Vol. 15, no. 3, p. 69-71 (Sept. 1972).

Bowman, J.
"Short and Long Term Stability Measurements Using Automatic Data Recording System". Proceedings of the 27th Annual Frequency Control Symposium, Cherry Hill, N.J., USA, 12-14 June 1973 (Washington, D.C. USA: Electronic Industries Assoc. 1973), p. 440-5.

Bowman,M. J., Whitehead, D. G.
"A Picosecond Timing System", IEEE Trans. Instrum. & Meas. (USA), Vol. IM-26, No. 2, p. 153-7 (June 1977).

Brandenbenberger, H., Hadorn, F., Halford, D., Shoaf, J.H.
"High Quality Quartz Crystal Oscillators: Frequency Domain and Time Domain Stability", Programme of the 25th annual frequency control symposium (abstracts), Atlantic City, NJ, USA, 26-28 Apr. 1971 (Fort Monmouth, NJ, USA: US Army Electronics Command 1971), p. 36.

Brown, D. E.
"Frequency Measurement of Quartz Crystal Oscillators", Marconi Instrum. (GB), Vol. 11, No. 3, 12-15 (1967).

Buisson, J., McCaskill, T., White, J., Stebbins, S.
"NTS-2 Cesium Frequency Stability Results", Proc. 32nd Annual Frequency Control Symposium, Atlantic City, NJ, USA, 31 May-2 June 1978 (Washington, DC, USA: Electronics Industries Association 1978), p. 560-566.

Coates, P. B.
"Fast Measurement of Short Time Intervals", J. Sci. Instrum. (J. Phys. E) (GB), Ser. 2, Vol. 1, No. 12, p. 1123-7 (Dec. 1968).

Cole, H. M.
"Time Domain Measurements", Electron. Electro-Optic Infrared Countermeas. (USA), Vol. 1, No. 4, p. 38-42, 55 (Aug. 1975).

Cordwell, C. R.
"Frequency Measurements", Vacation school on electrical measurement practice, Manchester, England, 15-26 Jul 1968 (London: Institution of Electrical Engineers 1968), 13 pp.

Cordwell, C. R.
"Frequency Measurements", Electronic Radio Tech. (GB), Vol. 3, No. 3, p. 95-103 (Aug. 1969).

Danilevich, V. V., Chernyavskii, A. F., Yakushev, A. K.
"Selectro-Type Time-Interval Analyzer with a Measurement Range of 10^{-10} to 10^{-12} sec.", Instrum. & Exp. Tech. (USA), Vol. 20, No. 1, pt. 2, p. 326-7 (Jan.-Feb. 1977). Translation of: Prib. Tekh. Eksp. (USSR), Vol. 20, No. 1, pt. 2, p. 282 (Jan.-Feb. 1977).

Danilevich, V. V., Kvachenok, V. G., Primak, M. A., Chernyavskii, A. F., Yakushev, A. K.
"Signal Generator for Adjusting and Calibrating Time Measurement Systems", Instrum. & Exp. Tech. (USA), Vol. 20, No. 2, pt. 2, p. 600 (March-April 1977). Translation of: Prib. Tekh. Eksp. (USSR), Vol. 20, No. 2, pt. 2, p. 245 (March-April 1977).

Danzeisen, K.
"Remote Frequency Measurement Using VHF-UHF Receivers", Funk-Tech. (Germany), Vol. 32, No. 11, p. 196-7 (June 1977). In German.

Davis, D. D.
"Calibrating Crystal Oscillators with TV Color-Reference Signals", Electronics (USA), Vol. 48, No. 6, p. 107-12 (20 March 1975).

De Prins, J.
"Timing Systems", ELF-VLF Radio Wave Propagation, Spatind, Norway, 17-27 April 1974 (Dordrecht, Netherlands: Reidel 1974), p. 385-98.

De Prins, J., Cornelissen, G.
"Critique and Discussion about Frequency Stability Definitions with Respect to Various Kinds of Noises", CPEM 74 Digest: Conference on Precision Electromagnetic Measurements, London, England, 1-5 July 1974 (London, England: IEE 1974), p. 54-6.

De Prins, J.
"Aspects of Time and Frequency Measurement", Rev. HF (Belgium), Vol. 10, No. 5, p. 123-34 (1977). In French.

Dombrovskii, A. S., Zaitsev, V. N., Pashev, G. P.
"Apparatus for Time and Frequency Measurement", Meas. Tech. (USA), Vol. 17, No. 6, p. 919-21 (June 1974). Translation of: Izmer. Tekh. (USSR), Vol. 17, No. 6, p. 63-5 (June 1974).

Egidi, G.
"Frequency/Time Metrology at the I.E.N.G.F. (Istituto Elettrotecnico Nazionale Galileo Ferraris)", Rev. Gen. Elect. (France), Vol. 78, No. 3, p. 275-82 (March 1969). In French.

Egidi, C., Leschiutta, S.
"The True Meaning of the Word 'Time'", Alta Frequenza (Italy), Vol. 39, No. 8, p. 689-93 (Aug. 1970).

Egidi, C., Leschiutta, S.
"The Metrology of Time", Riv. Nuovo Cimento (Italy), Vol. 1, Ser. 2, No. 4, p. 496-518 (Oct.-Dec. 1971). In Italian.

Elkin, G. A., Purtov, V. I.
"Automatic System for Comparing the Frequency of a (Quantum) Store with the Transition Frequency of Cesium Atoms", Meas. Tech. (USA), Vol. 19, No. 10, p. 1456-60 (Oct. 1976). Translation of: Izmer. Tekh. (USSR), Vol. 19, No. 10, p. 47-9 (Oct. 1976).

Ely, R. D.
"Frequency Measurements by Frequency Meter or Timer Counter?", Electron. & Power (GB), Vol. 24, No. 1, p. 45-6 (Jan. 1978).

Essen. L.
"Atomic Units and Scales of Time", Colloquium on Definition, Realisation and Use of Time and Frequency, London, 1967 (London: Institution of Electrical Engineers, 1967; Colloquium Digest 1967/16) Paper No. 1.

Essen, L.
"Time Scales", Metrologia (Germany), Vol. 4, No. 4, p. 161-5 (Oct. 1968).

Evenson, K. M., Wells, J. S., Petersen, F. R., Danielson, B. L., Day, G. W., Barger, R. L., Hall, J. L.
"Laser Frequency and Wavelength Measurements and the Speed of Light", 1972 Annual Meeting of the Optical Society of America, Abstracts only, San Francisco, Calif., USA, 17-20 Oct. 1972 (Washington, DC, USA: Optical Soc. America 1972), p. 22.

Fisher, M. C.
"Frequency Stability Measurement Procedures", Onde Electr. (France), Vol. 58, No. 4, p. 291-9 (April 1978). In French.

Freeman, R. L.
"The Science of Time and Its Inverse", Telecommun. J. (Engl. Ed.) (Switzerland), Vol. 44, No. 2, p. 66-72 (Feb. 1977).

Frenkel, L.
"Methods for the Measurement of Frequency and Stability of Laser Generators of Submillimeter Oscillations", Electron Technol. (Poland), Vol. 2, No. 2/3, p. 47-52 (1969).

Fukuyo, H.
"Time and Frequency Standards", J. Soc. Instrum. & Control Eng. (Japan), Vol. 14, No. 7, p. 521-8 (July 1975). In Japanese.

Gabry, A., Faucheron, G., Dubouis, B. Petit, P.
"Distant Comparison of Stable Frequency Standards by Means of the Transmission of a Beat Note between the Carrier of a TV Broadcast Signal and a Frequency Synthesized from the Frequency Standards", 31st Annual Frequency Control Symposium, Atlantic City, NJ, USA, 1-3 June 1977 (Washington DC, USA: Electronic Industries Assoc. 1977), p. 499-502.

Granveaud, M., Azoubib, J.
"The Problem of Ageing in the Derivation of TAI (International Atomic Time)", CPEM 74 Digest: Conference on Precision Electromagnetic Measurements, London, England, 1-5 July 1974 (London, England: IEE 1974), p. 297-80.

Granveaud, M., Guinot, B.
"The Role of Primary Standards in Establishing the International Atomic Time TAI", CPEM Digest 1978. Conference on Precision Electromagnetic Measurements, Ottawa, Canada, 26-29 June 1978 (New York, USA: IEEE 1978), p. 39-41.

Gray, J. E.
"Clock Synchronization and Comparison: Problems, Techniques and Hardware", Report NBS-TN-691, Nat. Bur. Stand., Washington, DC, USA (Nov. 1976) 9 pp.

Greivulis, Ya. P., Blumbergs, E. A.
"Frequency Meter", Izv. VUZ Priborostr. (USSR), Vol. 19, No. 8, p. 13-15 (1976). In Russian.

Grenchik, T. J., Fang, B. T.
"Time Determination for Spacecraft Users of the Navstar Gloval Positioning System (GPS)", 31st Annual Frequency Control Symposium, Atlantic City, NJ, USA, 1-3 June 1977 (Washington, DC, USA: Electronic Industries Assoc. 1977), p. 489-94.

Groslambert, J. M.
"Automatic Measurement System of Oscillator Frequency Stability", Eurocon 71 digest, Lausanne, Switzerland, 18-22 Oct. 1971 (New York, USA: IEEE 1971), 1 pp.

Groslambert, J., Olivier, M., Uebersfeld, J.
"Automatic Plotting Systems for Frequency Stability Curves and Discrete Spectral Density of Frequency Standards", IEEE Trans. Instrum. & Meas. (USA), Vol. IM-21, No. 4, p. 405-9 (Nov. 1972).

Groslambert, J., Olivier, M., Uebersfeld, J.
"Spectral and Short Term Stability Measurements", CPEM 74 Digest: Conference on Precision Electromagnetic Measurements, London, England, 1-5 July 1974 (London, England: IEE 1974), p. 60-1.

Groslambert, J., Olivier, M., Uebersfeld, J.
"Spectral and Short Term Stability Measurments", IEEE Trans. Instrum. & Meas. (USA), Vol. IM-23, No. 4, p. 518-21 (Dec. 1974). (1974 Conference on Precision Electromagnetic Measurements, London England, 1-5 July 1974).

Guignard, A., Berney, J. C.
"A New Series of Electronic Instruments for Time Measurements and Standard-Time Distribution", Mesures, Regulation, Automat. (France), Vol. 32, No. 4, 100 (April 1967). In French.

Guinot, M. B.
"Mean Atomic Time-Scales", Bull. Astron. (France), Vol. 2, No. 3, 449-64 (1967). In French.

Guinot, B.
"Characteristics of a Scale of Time", Alta Freq. (Italy), Vol. 40, No. 8, p. 684-6 (Aug. 1971). In English.

Guinot, B., Granveaud, M.
"Atomic Time Scales", IEEE Trans. Instrum. & Meas. (USA), Vol. IM-21, No. 4, p. 396-400 (Nov. 1972).

Guinot, B.
"Long Term Stability and Accuracy of Time Scales" CPEM 74 Digest: Conference on Precision Electromagnetic Measurements, London, England, 1-5 July 1974 (London, England: IEE 1974), p. 333-5.

Hafner, E.
"Frequency and Time", Proceedings of the conference on new horizons in measurements-trends in theory and application, Morristown, NJ, USA, 8-9 Oct. 1969 (New York, USA: IEE 1969), p. 58-68.

Hocker, L. O., Small, J. G., Javan, A.
"Extension of Absolute Frequency Measurements to the 84 μ Range", Phys. Letters (Netherlands), Vol. 29a, No. 6, p. 321-2 (2 June 1969).

Hoene, J., Holland-Nell, U.
"Time Measuring Equipment for the Delayed Representation of Signals with High Definition", Nachrichtentechnik (Germany), Vol. 20, No. 11, p. 405-11 (Nov. 1970). In German.

Hubner, U.
"Models and Predictions for the Realization of Time Scales", 31st Annual Frequency Control Symposium, Atlantic City, NJ, USA, 1-3 June 1977 (Washington, DC, USA: Electronic Industries Assoc. 1977), p. 327-34.

Hudson, G. E., Barnes, J. A.
"Clock Error Statistics as a Renewal Process" Proc. 22nd Annual Frequency Control Symposium, Atlantic City, NJ, USA, 22-24 April 1968 (Fort Monmouth, NJ, USA: Electronic Components Laboratory 1968), pp. 384-418.

Iijima, S., Fujiwara, K.
"Precise Measurement of Radio Time Signals by Means of Pulsed Oscillator", Tokyo Astron. Obs. Rep. (Japan), Vol. 14, No. 3, p. 273-85 (March 1968).

Il'in, V. G., Lukin, A. E.
"Phase Fluctuations in a Heterodyne Multistage Frequency Multiplier (for Standard Frequency Comparison)", Meas. Tech. (USA), Vol. 15, No. 11, p. 1659-61 (Nov. 1972). Translation of: Izmer Tekh. (USSR), Vol. 15, No. 11, p. 41-3 (Nov. 1972).

Il'in, V. G., Sazhin, V. V., Bolotnikov, M. V., Elkin, G. A.
"High-Precision Time and Frequency Measurements in the National Economy and Scientific Investigations", Meas. Tech. (USA), Vol. 17, No. 7, p. 1033-7 (Jul 1974). Trans. of: Izmer. Tekh. (USSR), Vol. 17, No. 7, p. 36-9 (July 1974).

Ivanov, V. V., Stepanov, B. M.
"Measurement of Small Duration Intervals", Izmer. Tekh. (USSR), p. 25-7. In Russian. English translation in: Meas. Tech. (USA), Vol. 14, No.1, p. 36-40 (Jan. 1971).

Ivanov, N. I., Kravchenko, V. F.
"Short-Term Frequency Instability of an Oscillator" Izv. VUZ Radioelektron. (USSR), Vol. 15, No. 11, p. 1391-3 (1972). In Russian. English translation in: Radio Electron. & Commun. Syst. (USA).

Izohk, V. V., Tabachnik, E. I.
"Mean-Square and Information-Theory Estimates of Time-Interval Measurement Accuracy in the Presence of Noise", Meas. Tech. (USA), Vol. 20, No. 3, p. 343-7 (March 1977). Translation of: Izmer. Tekh. (USSR), Vol. 20, No. 3, p. 23-6 (March 1977).

Jennings, D. A., Peterson, F. R.
"Extension of Absolute Frequency Measurements to 148 THz: Frequencies of the 2.0 and 3.5 μm Xe Laser", Phys. Lett. (USA), Vol. 26, No. 9, p. 510-11 (1 May 1975).

Jimenez, J. J., Petersen, F. R.
"Recent Progress in Laser Frequency Synthesis", Infrared Phys. (GB), Vol. 17, No. 6, p. 541-6 (Nov. 1977). (High Resolution Infrared and Sub-Millimeter Spectroscopy, Bonn, Germany, 8-10 March 1977).

Job, A.
"Short Term Stability of Sinusoidal Generators", Onde Elect. (France), Vol. 49, No. 506, p. 528-34 (May 1969). In French.

Jutzi, K. H.
"Frequency Measurement by Signal Sampling", Frequenz (Germany), Vol. 27, No. 11, p. 309-11 (Nov. 1973). In German.

Kahnt, D.
"ASMW Time and Frequency Signals and Their Applications", Radio Fernsehen Elektron. (Germany), Vol. 26, No. 4, p. 112-13 (1977). In German.

Kamyshan, V. V., Valitov, R. A.
"Heterodyne Method of Frequency Measurement in the Millimeter Range", Prib. Tekh. Eksp. (USSR), No. 4, p. 106-8 (1969). In Russian. English translation in: Instrum. Exper. Tech. USA, No. 4, p. 925-8 (July 1969).

Kartaschoff, P.
"Terms and Methods to Describe Frequency Stability" Tech. Mitt. PTT (Switzerland), Vol. 51, No. 11, p. 520-9 (1973). In German.

Kartaschoff, P.
"Frequency Control & Timing Requirements for Communications Systems", Proc. 31st Annual Frequency Control Symposium, Atlantic City, NJ, USA, 1-3 June 1977 (Washington, DC, USA: Electronic Industries Association), p. 478-483.

Kazi, A. M., Perini, G. J.
"Program Execution Time Measurement", IBM Tech. Disclosure Bull. (USA), Vol. 14, No. 2, p. 428 (July 1971).

Kendall, W. B., Parsons, P. L.
"A Precision Frequency Measurement Technique for a Moving Signal with a Low Signal to Noise Ratio", Conference on Precision Electromagnetic Measurements, Boulder (1968), New York, Institute of Electrical and Electronics Engineers (1968) 54-55.

Klimov, A. I., Meleshko, E. A.
"Monitoring Unit for Time-Interval Analyzers of Nanosecond Range", Instrum. & Exp. Tech. (USA), Vol. 20, No. 4, pt. 1, p. 1058-60 (July-Aug. 1977) Translation of: Prib. Tekh. Eksp. (USSR), Vol. 20, No. 4, pt. 1, p. 125-7 (July-Aug 1977).

Knight, D. J. E., Edwards, G. J., Blaney, T. G.
"Developments in Laser Frequency Measurement towards Realising the Metre from a Unified Frequency and Length Standard", European Conference on Precise Electrical Measurement, Brighton, Sussex, England, 5-9 Sept. 1977 (London, England: IEEE 1977), p. 40.

Kobayashi, M., Osawa, H., Morinaga, N., Namekawa, T.
"Output Signal-to Noise Ratios in Mean Frequency Measurement System", Technol. Rep. Osaka Univ. (Japan), Vol. 23, No. 1121-1154, p. 515-26 (Oct. 1973).

Kobayashi, M., Osawa, H., Morinaga, N., Namekawa, T.
"Mean Frequency and Mean Power Measurement Using Correlation Detection", Trans. Soc. Instrum. & Control Eng. (Japan), Vol. 12, No. 6, p. 613-18 (Dec. 1976). In Japanese.

Kocaurek, R.
"Frequency Comparison Receiver EF 151 K", News Rohde and Schwarz (Germany), Vol. 8, No. 32, p. 23-4 (1968).

Kogan, L. R.
"Oscillator Stability Requirements in Radio Interferometers", Radiotekhnika i Electronika (USSR), Vol. 15, No. 6, p. 1292-4 (June 1970). In Russian. English translation in: Radio Engng. Electronic Phys. (USA).

Kotel'nikov, A. V., Rubailo, G. T., Uvarov, N. E.
"An Instrument for Measuring the Ratio of Time Intervals", Telecommun. & Radio Eng. Pt. 1 (USA), p. 60-1. Translation of: Elektrosvyaz (USSR), Vol. 29, No. 3, p. 67-8 (March 1975).

Kramer, G.
"An Electronic Time Intervalometer with High Resolution", Nachrichtech. Z. (NTZ) (Germany), Vol. 23, No. 9, p. 433-6 (Sept. 1970). In German.

Krause, W. H. U.
"Accurate Time and Frequency Measurement", Frequenz (Germany), Vol. 22, No. 6, 178-82 (June 1968). In German.

Kul'gavchuk, V. M.
"Frequency Meters Using Devices with S-Shaped Volt-Ampere Characteristics", Instrum. & Exp. Tech. (USA), Vol. 18, No. 2, pt. 2, p. 514-16 (March-April 1975). Translation of: Prib. Tekh. Eksp. (USSR), Vol. 18, No. 2, pt. 2, p. 152-3 (March-April 1975).

Kuznetsov, V. P., Reznikov, A. L.
"Adjacent Time Intervals Measured by Two Frequency Meters", Meas. Tech. (USA), Vol. 17, No. 3, p. 474-5 (March 1974). Translation of: Izmer. Tekh. (USSR) Vol. 17, No. 3, p. 93-4 (March 1974).

Leikin, A. Ya., Orlov, E. Z.
"Equipment for Comparing Frequencies of Highly-Stable Generators", Meas. Tech. (USA), Vol. 16, No. 10, p. 1469-70 (Oct. 1973). Translation of: Izmer. Tekh. (USSR), Vol. 16, No. 10, p. 24-5 (Oct. 1973).

Leikin, A. Ya., Tomashenko, I. V., Fertik, N. S.
"Application of a Rubidium Discriminator for the Measurement of Frequency Fluctuations", Izv. VUZ Radiofiz. (USSR), Vol. 17, No. 6, p. 851-4 (1974). In Russian. English translation in: Radiophys. & Quantum Electron. (USA).

Lemesev, S. G., Rachev, B. T., Strugach, V. G., Shub, S. M.
"Statistical Method for Measuring a Recurrent Time Interval Using a Random Pulse Signal", Izv. VUZ Priborostr. (USSR), Vol. 18, No. 11, p. 16-21 (1975). In Russian.

Lesage, P., Audoin, C.
"Characterization of Frequency Stability: Uncertainty Due to the Finite Number of Measurements", IEEE Trans. Instrum. & Meas. (USA), Vol. IM-22, No. 2, p. 157-61 (June 1973).

Lesage, P., Audoin, C.
"Comments on 'Characterization of Frequency Stability: Uncertainty due to the Finite Number of Measurements'", IEEE Trans. Instrum. & Meas. (USA) Vol. IM-24, No. 1, p. 86 (March 1975).

Lesage, P., Audoin, C.
"Estimation of the Two-Sample Variance with a Limited Number of Data (Signal Generator Frequency Stability)", 31st Annual Frequency Control Symposium, Atlantic City, NJ, USA, 1-3 June 1977 (Washington, DC, USA: Electronic Industries Assoc. 1977). p. 311-18.

Lomas, G.
"Signal-Frequency Meter", Wireless World (GB), Vol. 80, No. 429-34 (Nov. 1974).

Lubentsov, V. F., Ashitkov, I. N.
"Device for Measuring the Frequencies and Errors of Crystal Oscillators", Izmerit. Tekh. (USSR), No. 7, p. 38-42 (July 1968). In Russian. English translation in: Meas. Tech. (USA), No. 7, p. 906-11 (July 1968).

Lubentsov, V. F.
"The Errors of the Absolute Method for Measuring Difference-Signal Frequency", Telecommun. & Radio Eng. Pt. 2 (USA), Vol. 28, No. 4, p. 96-9 (April 1973). Translation of: Radiotekhnika, Moskva (USSR), Vol. 28, No. 4, p. 74-9 (April 1973).

Lukas, M.
"An Intermediate Freuqency Measuring Equipment with an Unusual Frequency Indication", Slaboproudy Obzor (Czechoslovakia), Vol. 29, No. 6, 323-6 (1968). In Czech.

Markowitz, W.
"Time and Frequency Measurement; Atomic and Astronomical", Proceedings of the 5th Annual ISA test measurement symposium, advances in metrology, New York, USA, 28-31 Oct. 1968 (Pittsburgh, Pa., USA: Instrument Soc. America 1968), 6pp.

Maton, G. W.
"Thoughts on Frequency Meters and Counter-Timers" Electron (GB), No. 134, p. 24, 27 (27 March 1978).

McCaskill, T. B., Buisson, J. A.
"NTS-1 (TIMATION-III) (Satellite) Quartz and Rubidium Oscillator Frequency Stability Results", Proceedings of the 29th Annual Frequency Control Symposium, Fort Monmouth, NJ, USA, 28-30 May 1975 (Washington, DC, USA: Electronic Industries Assoc. 1975), p. 425-8.

Meer, P.
"Four Function Calculator Can Measure Time", Electron. Eng. (GB), Vol. 49, No. 596, p. 35 (Sept. 1977).

Millham, E. H.
"High-Accuracy Time Meter", IBM Tech. Disclosure Bull. (USA), Vol. 17, No. 4, p. 1143-4 (Sept. 1974)

Mitsenko, I. D., Borisov, S. K.
"Phase-Pulse Descriminator for Measurement of Nanosecond Time Intervals", Instrum. & Exp. Tech. (USA), Vol. 18, No. 1, pt. 1, p. 144-5 (Jan.-Feb. 1975). Translation of: Prib. Tekh. Eksp. (USSR), Vol. 18, No. 1, pt. 1, p. 128-30 (Jan.-Feb. 1975).

Mungall, A. G.
"Atomic Time Scales", Metrologia (Germany), Vol. 7, No. 4, p. 146-53 (Oct. 1971).

Murashov, B. P., Tsvetkov, Yu. P.
"Instrument for Checking Quartz-Crystal Oscillators with Standard Frequency Signals in the Long-Wave and Very-Long-Wave Ranges", Meas. Tech. (USA), Vol. 19, No. 7, p. 1012-15 (July 1976). Translation of: Izmer. Tekh. (USSR), Vol. 19, No. 7, p. 51-3, (July 1976).

Muzychuk, O. V., Shepelevich, L. G.
"On the Determination of Short Time Signal Frequency Instability", Izv. VUZ Radiofiz. (USSR), Vol. 17, No. 6, p. 855-63 (1974). In Russian. English translation in: Radiophys. & Quantum Electron. (USA).

Nakadan, Y., Koga, Y.
"Measurements of Frequency Stability of Precision Oscillators", Oyo Buturi (Japan), Vol. 46, No. 6, p. 572-9 (June 1977). In Japanese.

Offermann, R. W., Schultz, S. E., Trimble, C. R.
"Active Probes Improve Precision of Time Interval Measurements", Hewlett-Packard J. (USA), Vol. 27, No. 2, p. 11-16 (Oct. 1975).

Orte, A.
"Comparison of Various Fundamental Methods of Defining Time, with Special Reference to Astronomical Applications", Navigation (France), Vol. 24, No. 93, p. 72-84 (Jan. 1976).

Osakabe, M., Sasao, K., Kato, E.
"Field Strength and Frequency Measuring Instruments", Annitsu Tech. Bull. (Japan), No. 29, p.52-6, (April 1973). In Japanese.

Parkinson, B. A. R.
"Precise Time and Frequency Measurement. II", Electronic Equip. News (GB), Vol. 12, No. 2, p.60-5 (May 1970).

Parankar, A. R., Nambiar, K. P. P., Sitharaman, M. R.
"An Automatic Electronic Frequency Comparator", J. Inst. Electron. & Telecommun. Eng. (India), Vol. 20, No. 8, p. 405-7 (Aug. 1974).

Paul, F.
"Reciprocal Frequency Meters", Electron and Microelectron. Ind. (France), no. 168, p. 55-9, (March 1973). In French.

Peltz, I. G.
"Highly Stable Audio Generator for Frequency Measurements on Clock Crystals", Elektronik (Germany), Vol. 20, No. 10, p. 345-8 (Oct. 1971). In German.

Percival, D. B., Winkler, G. M. R.
"Timekeeping and the Reliability Problem", Proceedings of the 29th Annual Frequency Control Symposium, Fort Monmouth, NJ, USA 28-30 May 1975 (Washington, DC, USA: Electronic Industries Assoc. 1975), p. 412-16.

Percival, D. B.
"The US Naval Observatory Clock Time Scale", CPEM Digest 1978. Conference on Precision Electromagnetic Measurements, Ottawa, Canada, 26-29 June 1978 (New York, USA: IEEE 1978), p. 42-4.

Perkinson, R. E.
"Time/Frequency Technology in System Development", 24th Annual Frequency Control Symposium, Atlantic City, NJ, USA, 27-29 April 1970 (Washington, DC, USA: Electronic Industries Association 1970) p. 315-321.

Potschke, H.
"Time Measurement", Nachr. Elektron. (Germany), Vol. 30, No. 5, p. 107-8 (May 1976). In German.

Powers, R. S., Snyder, W. F.
"Radio-Frequency Measurements in the NBS Institute for Basic Standards", Report NBS TN 373, Nat. Bur. Stand., Washington, DC, USA (June 1969), 37-2 pp.

Putkovich, K.
"Automated Timekeeping", IEEE Trans. Instrum. & Meas. (USA), Vol. IM-21, No. 4, p. 401-5 (Nov. 1972).

Reid, J. H.
"The Measurement of Time", J. R. Astron. Soc. Can. (Canada), Vol. 66, No. 3, p. 135-48 (June 1972).

Reinhardt, V., Lavanceau, J.
"A Comparison of the Cesium and Hydrogen Hyperfine Frequencies by Means of Loran C and Clocks", Proc. 28th Annual Frequency Control Symposium, 29-31 May 1974 (Washington, DC, USA: Electronic Industries Association 1974), p. 379-383.

Risley, A. S.
"The National Measurement System for Time and Frequency", Report NBS-SP-445-1 Nat. Bur. Stand. Washington, DC, USA (June 1976), 64 pp.

Roth, R.
"Alignment Generator AS5 with Quartz Controlled Frequency Indicator", Grundig Tech. Inf. (Germany), Vol. 24, No. 4, p. 209-16 (1977). In German.

Rozwadowski, M.
"Modern Frequency Stabilisation Methods", Przegl. Telekomun (Poland), Vol. 44, No. 10, p. 335-8 (1971). In Polish.

Rusconi, L., Sedmak, G.
"Estimate of the Limiting Standard Deviation in the Absolute Timing of Periodic Sources", Astrophys. & Space Sci. (Netherlands), Vol. 46, No. 2, p. 301-8 (Feb. 1977).

Rutman, J.
"Comment of 'Characterization of Frequency Stability'", IEEE Trans. Instrum. & Meas. (USA), Vol. IM-21, No. 1, p. 85 (Feb. 1972).

Rutman, J.
"Short Term Frequenct Instability of Signal Generators", Onde Electr. (France), Vol. 52, No. 11, p. 480-7 (Dec. 1972). In French.

Rutman, J.
"Characterization of Frequency Stability: A Transfer Function Approach and Its Application to Measurements via Filtering of Phase Noise", IEEE Trans. Instrum. & Meas. (USA), Vol. IM-23, No. 1, p. 40-8 (March 1974).

Rutman, J., Sauvage, G.
"Measurement of Frequency Stability in Time and Frequency Domains via Filtering of Phase Noise", CPEM 74 Digest: Conference on Precision Electromagnetic Measurements, London, England, 1-5 July 1974 (London, England: IEE 1974), p. 57-9.

Rutman, J., Sauvage, G.
"Measurement of Frequency Stability in Time and Frequency Domains via Filtering of Phase Noise", IEEE Trans. Instrum. & Meas. (USA), Vol. IM-23, No. 4, p. 515-18 (Dec. 1974). (1974 Conference on Precision Electromagnetic Measurements, London, England, 1-5 July 1974)

Rutman, J.
"Oscillator Specifications: A Review of Classical and New Ideas", 31st Annual Frequency Control Symposium, Atlantic City, NJ, USA, 1-3 June 1977 (Washington, DC, USA: Electronic Industries Assoc. 1977), p. 291-301.

Rzewvski, M.
"Freuqency Deviation Measurements by Synchronized Sampling Method", Przegl. Telekomun. (Poland), Vol. 49, No. 1, p. 7-9 (1976). In Polish.

Schneider, R. J.
"Time and Frequency Standardization", Signal (USA), Vol. 25, No. 12, p. 42-5 (Aug. 1971).

Secaze, G.
"Measurement of Time-Standards and Their Marketing", Electron. & Microelectron. Ind. (France), No. 208, p. 71-5 (15 Sept. 1975). In French.

Shoaf, J. H., Halford, D., Risley, A. S.
"Frequency Stability Specification and Measurement: High Frequency and Microwave Signals", Report NBS-TN 632, Nat. Bur. Stand., Washington, DC, USA (Jan 1973), 65 pp.

Smith, H. M.
"Astronomical Time Scales", Colloquium on Definition, Realisation and Use of Time and Frequency. London, 1967 (London: Institution of Electrical Engineers, 1967; Colloquium Digest 1967/16) Paper No. 2.

Stecher, R.
"Electronic Time Interval Measurement with Nanosecond Resolution", Nachrichtentech. Elektron. (Germany), Vol. 23, No. 11, p. 413-16 (1973). In German.

Steele, J. McA.
"Frequency Measurement Using Standard Frequency Emissions", Conference on Frequency Generation and Control for Radio Systems, London, (1967) (London: Institution of Electrical Engineers, 1967: Conference Publication No. 31).

Steer, G.
"A New UHF Frequency Measuring Device", Fernmelde Praxis (Germany), Vol. 50, No. 13, p. 571-6 (10 July 1973). In German.

Steiner, C. I.
"Electronic Methods of Time Measurement", Elektroniker (Germany), Vol. 8, No. 1, p. 3-16 (1969). In German.

Stoyko, A.
"Ephemeris Time According to the Revised Lunar Theory of Brown", Bull. Astron. (France), Vol. 2, No. 2, 411-16 (1967). In French.

Szata, R.
"New Method of Oscilloscopic Frequency Measurement" Pomiary Automat. Kontrola (Poland), Vol. 14, No. 7, 300-1 (July 1968). In Polish.

Taylor, D.
"Time Measurement", Instrum. Rev. (GB), Vol. 15, 173-6 (March 1968).

Taylor, G. W.
"Time - A Precious Commodity", Electron. & Power (GB), Vol. 23, No. 1, p. 61-4 (Jan. 1977).

Tolman, J.
"Accurate Frequency and Time Measurement at the Institute of Radio Engineering and Electronics", Slaboproudy Obzor (Czechoslovakia), Vol. 31, No. 6, p. 286-90 (1970). In Czech.

Trkal, V.
"A New Definition of the Second on a Quantum Basis", Cesk. Casopis Fys. A. (Czechoslovakia), Vol. 18, No. 6, p. 641-69 (1968). In Czech.

Triplet, J. M.
"Ephemeris Time Determination by Lunar Photography" Bull. Astron. (France), Vol. 2, No. 3, 465-527 (1967). In French.

Turrini, A.
"Hererodyne Frequency Meter No. 351C E.I.P.", Antenna (Italy), Vol. 46, No. 2, p. 62-8 (Feb. 1974). In Italian.

Upton, R.
"An Objective Comparison of Analog and Digital Methods of Real-Time Frequency Analysis", Bruel & Kjaer Tech. Rev. (Denmark), No. 1, p. 18-26 (1977).

Valaskova, E.
"Measuring the Frequency of Damped Oscillators", Sdelovaci Tech. (Czechoslovakia), Vol. 19, No. 6, p. 174-5 (1971). In Czech.

Weiss, R.
"Time-Signal and Standard-Frequency Receiver for the DCF 77 with Reserve. I.", Funkschau (Germany), Vol. 48, No. 22, p. 964-8 (22 Oct. 1976). In German.

Westlund, R. C.
"Very Short Time Interval Measurements", New Electron. (GB), Vol. 11, No. 1, p. 13-14 18 (10 Jan. 1978).

Wheeler, K. G.
"An Optimum Solution for Counting and Timing", New Electron. (GB), Vol. 9, No. 20, p. 24,28,32 (19 Oct. 1976).

Wiley, R. G.
"A Direct Time-Domain Measure of Frequency Stability: The Modified Allan Variance", IEEE Trans. Instrum. & Meas. (USA), Vol. IM-26, No. 1, p. 38-41 (March 1977).

Woschni, E. G.
"Errors in High-Precision Frequency Measurements due to Interactive Effects", Wiss. Z. Tech. Hochsch. Karl-Marx-Stadt (Germany), Vol. 17, No. 5, p. 633-9 (1975). In German.

Woschni, E. G.
"On the Optimum Difference Frequency in High Accuracy Frequency Measurements of Industrial Parameters", Mess. Steuern Regein mit Automatisierungsprax. (Germany), Vol. 19, No. 10, p. 334-5 (Oct. 1976). In German.

Wrzesien, M.
"Instantaneous Frequency Measuring Circuit", Pomiary Autom. Kontrola (Poland), Vol. 22, No. 3, p. 90-1 (March 1976). In Polish.

Yasuda, Y.
"Accuracy of Estimating Clockface and Mean Rate of the Frequency Standard by Normal Regression Theory", J. Radio Res. Lab. (Japan), Vol. 21, No. 103, p. 39-60 (1974).

Yosimura, K., Harada, K., Kobayashi, M.
"Measurement of Short-Term Frequency Stability of Frequency Standards", Rev. Radio Res. Labs. (Japan) Vol. 17, No. 92, p. 437-43 (Sept. 1971). In Japanese.

Yoshimura, K.
"The Generation of an Accurate and Uniform Time Scale with Calibrations and Prediction", Report NBS-TN-626, Nat. Bur. Stand., Washington, DC, USA (Nov. 1972), 59 pp.

Zelentsov, V. I., Sulakshin, A. S., Fedorov, N. P.
"Meter for Measuring the Carrier Frequency of Single Ultrahigh-Frequency Pulses", Instrum. & Exp. Tech. (USA), Vol. 19, No. 2, pt. 2, p. 476-7 (March-April 1976). Translation of: Prib. Tekh. Eksp. (USSR), Vol. 19, No. 2, pt. 2, p. 132-3 (March-April 1976).

Zhilin, N. S., Subbotin, L. S.
"Devices for Reproducing Reference Time Intervals", Meas. Tech. (USA), Vol. 20, No. 7, p. 995-9 (July 1977). Translation of: Izmer. Tekh. (USSR), Vol. 20, No. 7, p. 42-5 (July 1977).

Zhuk, A. V., Kazantsev, E. M., Kirianaki, N. K., Mosievich, P. M.
"Computer Investigation of the Metrological Characteristics of Frequency Meters with Digital Positive Feedback and Measures to Improve Them", Otbor & Peredacha Inf. (USSR), No. 50, p. 110-15 (1977). In Russian.

3.1.1

Aldridge, D.
"5 MHz Digital Frequency Meter", Electron (GB), No. 82, p. 61, 63-4, 66, 68 (9 Oct. 1975).

Aldridge, D.
"5 MHz Digital Frequency Measuring Instrument", Elektron. Anz. (Germany), Vol. 10, No. 2, p. 15-18 (Feb. 1978). In German.

Andres, 1.
"Straight Talk on Frequency Counters", Communications (USA), p. 54, 56-60 (March 1977).

Arnoldt, M.
"A Frequency Counter with Time-Multiple Indication", Funk-Tech. (Germany), No. 20, p. 721-4 (Oct. 1974). In German.

Arnoldt, M.
"Frequency Counter for Ultra Short Wave Radio Receivers", Funk-Tech. (Germany), Vol. 32, No. 18, p. 237-42, 244-5 (Sept. 1977). In German.

Balph, T.
"A 200 MHz Autoranging Frequency Counter", Electron Equip. News (GB), p. 17, (April 1976).

Beckman, D.
"How Accurate is Your Timer-Counter?", Electron. Equip. News (GB), Vol. 15, No. 10, p. 32-3 (March 1974).

Bologlu, A.
"Automatic 4.5 GHz Counter Provides 1 Hz Resolution" Hewlett-Packard J. (USA), Vol. 27, No. 1, p. 14-18 (Sept. 1975).

Bordt, A.
"Universal Digital Counter for Frequencies up to 12 MHz. I.", Radio Fernsehen Elektron. (Germany), Vol. 22, No. 11, p. 365-8 (1973). In German.

Bordt, A.
"Universal Digital Counter for Frequencies up to 12 MHz. II.", Radio Fernsehen Elektron. (Germany), Vol. 22, No. 12, p. 402-6 (1973). In German.

Bosnjakovic, P.
"A New Solution of the Precision Line Frequency Measurement", Automatika (Yugoslavia), Vol. 17, No. 5-6, p. 194-6 (1976). In Slovenian.

Buxton, A. J.
"Digital Frequency Meter", Pract. Electron. (GB), Vol. 12, No. 5, p. 376-82 (May 1976).

Cantero, J. A., Pollan, T., Barquilas, J.
"Digital Frequencymeter Uses Variable Measuring Times and Automatic Scale Conversion", Mundo Electron. (Spain), No. 71, p. 34-5 (Feb. 1978). In Spanish.

Charriere, J. J.
"A Digital Chronometer", Rev. Polytech. (Switzerland), No. 6, p. 585, 587 (25 June 1977). In French.

Denbnovetskii, S. V., Kovtun, A. K.
"Time Measurements. Digital Time-Interval Meters", Izmer. Tekh. (USSR), p. 29-31. In Russian. English translation in: Meas. Tech. (USA), Vo. 10, p. 1514-16 (Oct. 1970).

Denbnovetskii, S. V., Shkuro, A. N.
"Principles of Eliminating Ambiguity in Digital Time-Interval Meters (Review)", Instrum. & Exp. Tech. (USA), Vol. 18, No. 6, pt. 1, p. 1659-70 (Nov.-Dec. 1975). Translation of: Prib. Tekh. Eksp. (USSR), Vol. 18, No. 6, pt. 1, p. 7-16 (Nov.-Dec. 1975).

Ghoroury, H. S. El., Gupta, S. C.
"Algorithmic Measurement of Digital Instantaneous Frequency", IEEE Trans. Commun. (USA), Vol. COM-24, No. 10, p. 1115-22 (Oct. 1976).

El-Ghoroury, H. S., Gupta, S. C.
"Algorithmic Measurement of Digital Instantaneous Frequency", IEEE Trans. Commun. (USA), Vol. COM-24, No. 10, p. 1115-22 (Oct. 1976).

Faso, G., Lo
"RTL Micrologic in a Digital Frequency and Time Counter", Internat. Elektronische Rundschau (Germany), Vol. 22, No. 2, 47-50 (1968). In German.

Faso, G., Lo
"Digital Frequency Meter and Chronometer in RTL Micrologic", Internat. Elektronische Rundschau (Germany), Vol. 22, No. 3, 63-6 (March 1968). In German.

Fernandez, A. N.
"Adapting a Frequency Meter into a Digital Clock", Mundo Electron. (Spain), No. 34, p. 92 (Oct. 1974). In Spanish.

Ferrari, H. I.
"Frequency Meter and Digital Counter", Rev. Telegr. Electron. (Argentina), Vol. 64, No. 761, p. 234-8, 241-2 (May 1976). In Spanish.

Fichtenbaum, M. L.
"Counter Inverts Period to Measure Low Frequency", Electronics (USA), Vol. 49, No. 5, p. 100-1 (4 March 1976).

Filin, N. A., Trofimov, A. V.
"Time Counter", Instrum. & Exp. Tech. (USA), Vol. 19, No. 5, pt. 2, p. 1582 (Sept.-Oct. 1976). Translation of: Prib. Tekh. Eksp. (USSR), Vol. 19, No. 5, pt. 2, p. 291 (Sept.-Oct. 1976).

Firth, G. F., Pratt, D. M.
"A Digital Frequency Counter and Timer (Direct Read-Out at 150 MHz)", Radio Commun. (GB), Vol. 52, No. 3, p. 182-9 (March 1976).

Fleys, M.
"Microwave Frequency Counters - Which Conversion Technique to Choose?", Mes. Regul. Autom. (France), Vol. 43, No. 2, p. 31-8 (Feb. 1978). In French.

Fullagar, D.
"Frequency Counter", New Electron. (GB), Vol. 9, p. 28, No. 3, (10 Feb. 1976).

Gutnikov, V. S., Nedashkovskii, A. I., Palkin, V.S.
"A Specialised Digital Frequency Meter Used for Operation with Measuring Frequency Convertors", Prib. & Sist. Upr. (USSR), No. 5, p. 22-4 (1977). In Russian.

Harry, E.
"Counter, Scope Team Up for Precise Timing Measurements", Electronics (USA), Vol. 51, No. 2, p. 126-7 (19 Jan. 1978).

Hutchinson, F.
"Frequency Measurement and Timer-Counters", Electron. Equip. News (GB), p. 22-3 (March 1976).

Hodgkinson, G.
"Counters & Timers, Once Lab Luxuries, Now Everyday Instruments", Electron (GB), No. 120, p. 13, 16, 19 (21 July 1977).

Imshenetskii, V. V., Martyniv, M. S.
"Extending the Frequency Limits of an Electronic Counting Frequency Meter", Otbor & Peredacha Inf. (USSR), No. 39, p. 89-92 (1974). In Russian.

Ioannides, C.
"The 50 MHz Universal Counter UZ56/UZ56s", Grundig Tech. Inf. (Germany), Vol. 21, No. 2, p. 307-10 (1974). In German.

Jayapal, R.
"Measure Power Frequency with a Conventional Counter", Electron. Eng. (GB), Vol. 49, No. 507, p. 17 (Oct. 1977).

Kiehne, F.
"FEGR - A Multi-Purpose 500 kHz Counter", News from Rohde and Schwarz (Germany), Vol. 7, No. 27, 15-16 (1967).

Kirianaki, N. V., Kazantsev, E. M., Mosievich, P.M.
"Multirange Fast Automatic Digital Frequency Meter" Izv. VUZ Priborostr. (USSR), Vol. 20, No. 1, p. 9-14 (1977). In Russian.

Leah, P.
"Frequency Counter/Timer", Pract. Electron. (GB), Vol. 14, No. 1, p. 22-8 (Sept. 1977).

MacLeod, K. J.
"A Portable High-Resolution Counter for Low-Frequency Measurements", Hewlett-Packard J. (USA), Vol. 25, No. 3, p. 10-15 (Nov. 1973).

Maletz, W.
"100 MHz Universal Counter FET 100", News Rohde & Schwarz (Germany), Vol. 14, No. 64, p. 5-7 (1974).

Martin, D.
"Frequency Stability Measurements by Computing Counter System", Hewlett-Packard J. (USA), Vol. 23, No. 3, p. 9-14 (Nov. 1971).

Martin, J. D.
"Digital Methods of Frequency Measurement: A Comparison", Radio & Electron. Eng. (GB), Vol. 42, No. 6, p. 285-94 (June 1972).

Martin, D.
Measure Time Interval Precisely", Electron. Des. (USA), Vol. 22, No. 24, p. 162-7 (22 Nov. 1974).

Mende, F. F., Charkin, V. A.
"Superhigh Frequency Measurement with Electronic-Counter Frequency Meters", Meas. Tech. (USA), Vol. 16, No. 9, p. 1360-2 (Sept. 1973). Translation of: Izmer. Tekh. (USSR), Vol. 16, No. 9, p. 53-4 (Sept. 1973).

Mohos, Z.
"Time Interval Measurement by Averaging", Meres & Autom. (Hungary), Vol. 21, No. 7, p. 268-72 (1973). In Hungarian.

Mroz, T. J.
"Time-Interval Meter Reads Digitally to 99.9 ms on a DVC IC", Electron. Des. (USA), Vol. 25, No. 6, p. 108,110 (15 March 1977).

Muchiauri, A. A.
"A Digital Method of Frequency Measurement for Harmonic Signals", Meas. Tech. (USA), Vol. 16, No. 11, p. 1710-12 (Nov. 1973). Translation of: Izmer Tekh. (USSR), Vol. 16, No. 11, p. 71-3 (Nov. 1973).

Niki, S.
"Automatic Frequency Counter used TRAHET Technique to Count to 32 GHz with -20 dBm Sensitivity", JEE (Japan), No. 107, p. 20-3 (Oct. 1975).

Palamaryuk, G. O., Kholkin, I. I.
"Digital Smoothing Frequency Meter for Variable-Sign Pulse Signals", Izmerit. Tekh. (USSR), 1967, No. 7, 55-7 (July). In Russian. English translation in: Meas. Tech. (USA), 1967, No. 7, 845-7 (July).

Pashev, G. P., Parfenov, G. A.
"Analysis of the Errors of Statistical Devices Measuring Repeated Time Intervals", Meas. Tech. (USA), Vol. 20, No. 3, p. 347-9 (March 1977). Translation of: Izmer. Tekh. (USSR), Vol. 20, No. 3, p. 26-7 (March 1977).

Parykov, V. G., Podlesnyi, S. A., Chmykh, M. K.
"Digital Frequency Meter with High Noise Immunity" Instrum. & Exp. Tech. (USA), Vol. 19, No. 5, pt. 2, p. 1581 (Sept.-Oct. 1976). Translation of: Prib. Tekh. Eksp. (USSR), Vol. 19, No. 5, pt. 2, p. 290 (Sept.-Oct. 1976).

Pokorny, L.
"Modern Frequency Counters", Radio Elektron. Schau (Austria), Vol. 52, No. 1, p. 20-4 (1976). In German.

Pokorny, L.
"Hewlett-Packard 5328A Universal Counter with DVM Options", Elektronikschau (Austria), Vol. 53, No. 11, p. 56 (1977).

Prusakov, V. K., Kilna, A. A.
"About Digital Harmonic Signal Frequency Measuring Accuracy", Liet. TSR Mokslu Akad. Darbai B (USSR), No. 80, p. 141-8 (1974). In Russian.

Reeder, R.
"The Not So Simple Counter", Electron. Equip. News (GB), p. 9-10 (Nov. 1977).

Reussner, J., Weiss, H. J.
"Standard Frequency Receiver for Calibrating Frequency Counters", Radio Fernsehen, Elektron. (Germany), Vol. 22, No. 19, p. 618-40 (Oct. 1973). In German.

Ribenyi, A.
"Digital Frequency Measuring Instruments", Meres es Automat. (Hungary), Vol. 15, No. 11, 436-9 (1967). In Hungarian.

Rikhter, V., Folger, G.
"Influence of Stresses Due to Discontinuous Jamming on the Accuracy of Digital Frequency Measuring Devices", Prib. & Sist. Upr. (USSR), No. 1, p. 21-3 (1977). In Russian.

Runyon, S.
"Focus on Electronic Counters", Electron. Des. (USA), Vol. 25, No. 11, p. 54-63 (24 May 1977).

Sakai, T.
"Frequency Counters become Sophisticated", JEE (Japan), No. 121, p. 20 3 (Jan. 1977).

Senftleben, H.
"A Digital Universal Counter", Radio Fernsehen Elektron. (Germany), Vol. 26, No. 13, p. 441-5 (1977). In German.

Simpson, L.
"A Low-Cost 200 MHz Digital Frequency Meter", Electron. Aust. (Australia), Vol. 38, No. 12, p. 30-5, 37 (March 1977).

Sorden, J. L.
"A New Generation in Frequency and Time Measurements", Hewlett-Packerd J. (USA), Vol. 25, No. 10, p. 2-8 (June 1974). In English.

Spapens, W.
"Accurate Time Measurements with a Counter and an Oscilloscope", Philips Test & Meas. Not. (Netherlands), No. 2, p. 4-8 (1972).

Sarhadi, M., Aitchison, C. S.
"Fast-Sampling Frequency Meter", Electron. Lett. (GB), Vol. 14, No. 12, p. 366-7 (8 June 1978).

Valverde, R. M.
"A Digital Instantaneous Frequency-Meter", Automaz. e Strum. (Italy), Vol. 16, No. 5, p. 216-21 (March 1968). In Italian.

Van Blerkom, R., Freeman, D. G., Crutchfield, R.C.
Frequency Measurement Techniques", IEEE Trans. Instrum. Meas. (USA), Vol. IM-17, No. 2, 133-45 (June 1968).

Van Den Broek, H. G. J.
"Two Frequency Counters for Routine Measurements", Polytech. Tijdschr. Elektrotech. Elektron. (Netherlands), Vol. 32, No. 9, p. 517-18 (Sept. 1977). In Dutch.

Wessel, R.
"A Digital Frequency Meter", Elektromeister + Dtsch. Elektrohandwerk, (Germany), Vol. 48, No. 15, p. 1066-8 (Aug. 1973). In German.

Whittaker, A. E., Westbury, P. R.
"Measuring Low Frequencies", New Electron. (GB), Vol. 9, No. 20, p. 36 (19 Oct. 1976).

Zander, H.
"Measurement of Low Frequencies with Short Duration", Elektronik (Germany), Vol. 26, No. 8, p. 63-4 (Aug. 1977). In German.

Akatsuka, K., Yasuda, Y., Matsuura, T.
"International Time and Frequency Comparison via Loran-C", Rev. Radio Res. Lab. (Japan), Vol. 23, No. 125, p. 165-70 (Dec. 1977). In Japanese.

Allan, D. W., Blair, B. E., Davis, D. D., Machlan, H. E.
"Precision and Accuracy of Remote Synchronization Via Portable Clocks, Loran C, and Network Television Broadcasts", Proc. 25th Annual Frequency Control Symposium, Atlantic City, NJ, USA, 26-28 April 1971 (Washington, DC, USA: Electronic Industries Association 1971), p. 195-208.

Allan, D. W., Blair, B. E., Davis, D. D., Machlan, H. E.
"Precision and Accuracy of Remote Synchronization Via Network Television Broadcasts, Loran-C, and Portable Clocks", Metrologia (Germany), Vol. 8, No. 2, p. 64-72 (April 1972).

Allan, D. W.
"Time Transfer Using Near-Synchronous Reception of Optical Pulsar Signals", Proc. IEEE (USA), Vol. 60, No. 5, p. 625-7 (May 1972).

Allan, D. W., Machlan, H. E., Marshall, J.
"Time Transfer Using Nearly Simultaneous Reception Times from a Common Transmitter", Proc. 26th Frequency Control Symposium, Atlantic City, NJ, USA, 6-8 June 1972 (Washington, DC, USA: Electronic Industries Association 1972), p. 309-16.

Allan, D. W., Hellwig, H., Glaze, D. J.
"An Accuracy Alorithm for an Atomic Time Scale", Metrologia (Germany), Vol. 11, No. 3, p. 133-8 (1975).

Barnes, J. A., Winkler, G. M. R.
"The Standards of Time and Frequency in the USA", Report NBS-TN-649, Nat. Bur. Stand., Washington, DC, USA (Feb. 1974), 86 pp.

Bastelberger, J.
"Transmission of the Standard Frequency of the German Federal Post Office", Fernmelde-Ing. (Germany), Vol. 27, No. 11, p. 1-40 (Nov. 1973). In German.

Becker, G., Kramer, G.
"Methods of International Time and Frequency Comparison with V. L. F.", Frequenz (Germany), Vol. 23, No. 9, p. 256-61 (Sept. 1969). In German.

Becker, G., Enslin, H.
"Exact Time and Frequency Comparisons by Means of Television Picture Pulses", Frequenz (Germany), Vol. 26, No. 12, p. 332-7 (Dec. 1972). In German.

Belotserkovskii, D. Yu., Palii, G. N.
"New System for Transmitting Exact-Time and Standard-Frequency Radio Signals", Izmer. Tekh. (USSR), Vol. 14, No. 11, p. 11-13 (Nov. 1971). In Russian. English translation in: Meas. Tech. (USA), Vol. 14 No. 11, p. 1633 (Nov. 1971).

Besson, J.
"Synchronisation of Clocks to a Precision of a Few Nanoseconds", C. R. Hebd. Seances Acad. Sci. B (France), Vol. 279, No. 7, p. 147-50 (12 Aug 1974). In French.

Besson, J.
"Accurate Synchronisation of Ultra-Stable Clocks", Colloque International sur L'Electronique et la Mesure. (International Conference on Electronics and Measurements), Paris, France, 26-30 May 1975 (Paris, France: Comm. d'Organisation du Colloque Internat. sur l'Electronique et la Mesure 1975), p. 140-50. In French.

Besson, J., Brejaud, H., Moreau, J. P., Parcelier, P., Benavente, J.
"Results of the Laser Synchronization by Flyover between the Observatories of Paris and San Fernando, Spain", CPEM Digest 1978. Conference on Precision Electromagnetic Measurements, Ottawa, Canada, 26-29 June 1978 (New York, USA: IEEE 1978), p. 45-7. In French.

Blouet, J.
"International Comparisons in High Frequencies Measurements", Colloque International sur L'Electronique et la Mesure. (International Conference on Electronics and Measurements), Paris, France, 26-30 May 1975 (Paris, France: Comm. d'Organisation du Colloque Internat. sur l'Electronique et la Mesure 1975), p. 84-93. In French.

Brokaw, A. P.
"Slave Clock Can Run Free at Center Frequency and Lock In within One Cycle", Electron. Des. (USA), Vol. 22, No. 24, p. 196-198 (22 Nov. 1974).

Buisson, J. A.
"International Time Transfer Using the Timation II Satellite", Proceedings of the 27th Annual Frequency Control Symposium, Cherry Hill, NJ, USA, 12-14 June 1973 (Washington, DC, USA: Electronic Industries Assoc. 1973), p. 277-85.

Burns, A. A.
"Preliminary Analysis of a Proposed High-Stability Frequency Standard Distribution System", IEEE Trans. Aerosp. & Electron. Syst. (USA), Vol. AES-7, No. 2, p. 385-91 (March 1971).

Burtop, W. V., Wilson, L. O.
"Precise Frequency Comparison Using a Frequency Tracking Technique", 22nd Annual Frequency Control Symposium, Atlantic City, NJ, USA, 22-24 April 1968 (Ft. Monmouth, NJ, USA: Electronic Components Laboratory 1968), p. 441-451.

Caprioli, G.
"Present Day Requirement of Astronomical and Geodetic Research (for Clock Synchronisation)", 20th International Congress on Electronics, Rome, Italy, 28-31 March 1973. (Rome, Italy: Rassegna Int. Elettronica Nucleare e Teleradiocinematografica 1973), p. TR-I-2/513-16. Italian.

Cherepukhin, M. A., Polyak, A. G.
"Effect of the Parameters of the Propagation Path on Locking Error when Using Signals from a Loran-S Station", Meas. Tech. (USA), Vol. 19, No. 11, p. 1585-6 (Nov. 1976). Translation of: Izmer. Tekh. (USSR), Vol. 19, No. 11, p. 34-5 (Nov. 1976).

Chi, A. R., Fosque, H. S.
"A Step in Time Changes in Standard Frequency and Time Signal Broadcasts", IEEE Spectrum (USA) Vol. 9, No. 1, p. 82-6 (Jan 1972).

Clifford, P. M.
"The Use of Standard Frequency Transmission in Industry", Colloquium on Definition, Realisation and Use of Time and Frequency, London, 1967 (London: Institution of Electrical Engineers, 1967: Colloquium Digest 1967/16), paper no. 8/1-8/7.

Cordwell, C. R.
"N. P. L. Standard Frequency Installation at Rugby Radio Station", Colloquium on Definition, Realisation and Use of Time and Frequency, London, 1967 (London: Institution of Electrical Engineers 1967: Colloquium Digest 1967/16). Paper No. 5/1-5/8.

Costain, C. C.
"Time Dissemination in Canada". International Electrical, Electronics Conference and Exposition, Toronto, Canada, 26-28 Sept. 1977 (New York, USA: IEEE 1977), p. 120-1.

Counselmann, C. C., III, Shapiro, I. I., Rogers, A. E. E., Hinteregger, H. F., Knight, C. A., Whitney, A. R., Clark, T. A.
"VLBI Clock Synchronization", Proc. IEEE (USA), Vol. 65, No. 11, p. 1622-3 (Nov. 1977).

Danzeisen, K.
"Frequency Measured Remotely with VHF-UHF Receivers ESU 2 and ESM 2", News Rohde & Schwartz (Germany), Vol. 17, No. 77, p. 28-30 (1977).

Del Bello, R., Leschiutta, S., Angeli, M. T.
"The Main National Time Scales Compared with the Italian UTC(IEN) Time Scale in the Period 1970-1974", Alta Freq. (Italy), Vol. 44, No. 10, p. 558-68 (Oct. 1975).

Dudnik, B. S., Kashcheev, B. L., Leikin, A. Ya., Smirnov, A. N., Sopel'nikov, M. D.
"Use of Meteoric Reflection of Radio Waves to Compare the Clocks of Time and Frequency-Service Stations", Izmer. Tekh. (USSR), Vol. 14. No. 12, p. 38-42 (Dec. 1971). In Russian. English translation in: Meas. Tech. (USA), Vol. 14, No. 12, p. 1842-7 (Dec. 1971).

Dudnik, V. S., Leman, Yu. A., Chernyr, V. I.
"Equipment for Coordinating Time Standards Using the Meteoric Propagation of Radiowaves", Radiotekhnika, Kharkov (USSR), No. 28, P. 23-31 (1974). In Russian.

Dunne, J. F., Ive, J. G., Wilkinson, J. H.
"Clock Generation and Distribution", IBA Tech. Rev. (GB), No. 8, p. 77-84 (Sept. 1976).

Easton, R. L.
"The Role of Time/Frequency in Navy Navigation Satellites", Proc. IEEE (USA), Vol. 60, No. 5, p. 557-63 (May 1972).

Easton, R. L., Morgan, P., Smith, H. M.
"Satellite Time Transfer from the US Naval Observatory to the Royal Greenwich Observatory and to Australia", CPEM 74 Digest: Conference on Precision Electromagnetic Measurements, London, England, 1-5 July 1974 (London, England: IEE 1974) p. 281-3.

Fisher, L. C., Hanson, D. W., Hellwig, H. W., Rueger, L. J.
"Dissemination of Time and Frequency by Satellite", Proc. IEEE (USA), Vol 64, No. 10, p. 1482-93 (Oct. 1976).

Egidi, C.
"The General Adoption of the Atomic Unit of Time", Elettrotecnica (Italy), Vol. 59, No. 4, p. 430-3 (April 1972). In Italian.

Ehrlich, E.
"The Role of Time-Frequency in Satellite Position Determination Systems", Proc. IEEE (USA), Vol. 60, No. 5, p. 564-71 (May 1972).

Essen, L.
"A Revolution in Time-Keeping", Conference on Frequency Generation and Control for Radio Systems, London, (1967) (London: Institution of Electrical Engineers, 1967: Conference Publication No. 31) 11-15.

Essen, L.
"Atomic Units and Scales of Time", Colloquium on Definition, Realisation and Use of Time and Frequency, London, 1967 (London: Institution of Electrical Engineers, 1967: Colloquium Digest 1967/16), Paper No. 1/1-1/2.

Essen, L.
"Relativity and Time Signals", Wireless World (GB), Vol. 84, No. 154, p. 44-5 (Oct. 1978).

Fedorov, Yu. A.
"Transmission of Timing Information by Means of Continuous Harmonic Oscillations", Izmer. Tekh. (USSR), p. 28-30. In Russian. English translation in: Meas. Tech. (USA), Vol. 14, No. 1, p. 41-4 (Jan. 1971).

Fedorov, Yu. A., Nasidze, N. A., Bol'shakov, V.Ya. Ermilov, N. I.
"Automatic System of Synchronization of Time Scales on the Channel of an All-Union Television Broadcasting Station", Meas. Tech. (USA), Vol. 20, No. 4, p. 502-6 (April 1977). Translation of: Izmer. Tekh. (USSR), Vol. 20, No. 4, p. 32-4 (April 1977).

Fey, L., Looney, C. H., Jr.
"A Dual Frequency V. L. F. Timing System", IEEE Trans. Instrum. Meas. (USA), Vol. IM-15, No. 4, 190-5 (Dec. 1966). (Conference on Precision Electromagnetic Measurements, Boulder, 1966).

Fey, L.
"Time Dissemination Capabilities of the Omega System", 25th Annual Frequency Control Symposium, Atlantic City, NJ, USA, 26-28 April 1971 (Washington, DC, USA: Electronic Industries Association 1971)., p. 167-170.

Ficklin, B. P.
"Standard Time and Frequency Accuracies Obtainable with a Stationary Satellite", Conference on Frequency Generation and Control for Radio Systems, London, 1967 (London: Institution of Electrical Engineers, 1967: Conference Publication No. 31) pp. 174-80.

Fleer, A. G., Stepanov, V. A.
"Probelms of Experimental Investigations of Radiowave Propagation for Time Service", Meas. Tech. (USA), Vol. 15, No. 11, p. 1671-4 (Nov. 1972). Translation of: Izmer. Tekh. (USSR), Vol. 15, No. 11, p. 48-50 (Nov. 1972).

Fleer, A. G., Vorob'ev, L. Ya.
"Dynamics of Seasonal Variations in the Transmission Times of Time Signals and Standard Frequencies in the Short and Very-Long-Wave-Ranges", Meas. Tech. (USA), Vol. 19, No. 6, p. 836-43 (June 1976). Translation of: Izmer. Tekh. (USSR), Vol. 19, No. 6, p. 36-40 (June 1976).

Friedberg, H., Kral, W. A.
"Wireless Time Signals and Wireless Clocks: Receiving of Time Signals for Private and Industrial Use", Nachr. Elektron. (Germany), Vol. 32, No. 8, p. 257-9 (Aug. 1978). In German.

Fujiwara, K., Hara, T., Sakai, T.
"Precise Clock Comparison by Loran-C Signals", Tokyo Astron. Obs. Rep. (Japan), Vol. 15, No. 4, p. 825-37 (March 1972). In Japanese.

Fujiwara, K., Kato, T., Hokugo, S., Miyazaki, K.
"Precise Clock Comparison by Means of TV Signals (between Tokyo Astronomical Obs. and Kanozan Geodetic Obs.)", Tokyo Astron. Obs. Rep. (Japan), Vol. 17, No. 2, p. 261-83 (March 1975). In Japanese.

Gabry, A., Faucheron, G., Dubois, B., Petit, P.
"Distant Comparison of Stable Frequency Standards by Means of the Transmission of a Beat Note between the Carrier of a TV Broadcast Signal and a Frequency Synthesized from the Frequency Standards", 31st Annual Frequency Control Symposium, Atlantic City, NJ, USA, 1-3 June 1977 (Washington, DC, USA Electronic Industries Assoc. 1977), p. 499-502.

Gatterer, L. E., Bottone, P. W., Morgan, A. H.
"World-Wide Clock Synchronization Using a Synchronous Satellite", Conference on Precision Electromagnetic Measurements, Boulder (1968), New York, Institute of Electrical and Electronics Engineers (1968) 58-60.

Gerharz, R.
"Long-Period Time Interval Markers from Mercury Transits", J. Br. Astron. Assoc. (GB), Vol. 85, No. 3, p. 252-4 (April 1975).

Gray, J. E.
"Clock Synchronization and Comparison: Problems, Techniques and Hardware", Report NBS-TN-691, Nat. Bur. Stand., Washington, DC, USA (Nov. 1976), 9 pp.

Grimsley, S. W., Miller, M. J.
"Phase Comparison of Frequency Standards", Proc. Instn. Radio Electronics Engrs. Australia, Vol. 29, No. 1, 14-17 (Jan. 1968).

Guetrot, A., Annal, D. W., Higbie, L. S., Lavancean, J.
"An Application of Statistical Smoothing Techniques on VLF Signals for Comparison of Time between USNO and NBS", Proc. 23rd Annual Frequency Control Symposium, Atlantic City, NJ, USA, 6-8 May 1969 (Washington, DC, USA: Electronic Industries Association 1969), p. 248.

Guillaume, F., Lievin, J. C., De Prins, J.
"Study of LF and VLF Time Signals by Digital Method", 31st Annual Frequency Control Symposium, Atlantic City, NJ, USA, 1-3 June 1977 (Washington, DC, USA: Electronic Industries Assoc. 1977), p. 503-9.

Hall, R. G., Klepczynski, W. J.
"Time Service", Nav. Res. Rev. (USA), Vol. 29, No. 10, p. 28-36 (Oct. 1976).

Hanson, D. W., Hamilton, W. F.
"Clock Synchronization from Satellite Tracking", IEEE Trans. Aerosp. & Electron. Syst. (USA), Vol. AES-7, No. 5, p. 895-9 (Sept. 1971).

Hanson, D. W., Hamilton, W. F.
"Time and Frequency Broadcast Experiments from the ATS-3 Satellite", Report NBS-TN-645, Nat. Bur. Stand., Washington, DC, USA (Nov. 1970), 107 pp.

Hellwig, H., Wainwright, A. E.
"Sub-Microsecond Time Transport with a Rubidium Portable Clock", Proceedings of the 29th Annual Frequency Control Symposium, Fort Monmouth, NJ, USA, 28-30 May 1975 (Washington, DC, USA: Electronic Industries Assoc. 1975), p. 384-5.

Hellwig, H.
"Clocks-Time and Frequency Measurements", Nachrichtentech. Z. (NTZ) (Germany), Vol. 30, No. 1, p. 69 (Jan. 1977). In German.

Hellwig, H., Allan, D. W., Stein, S. R., Prichard, K. A.
"Transcontinental and Intercontinental Portable Clock Time Comparison", 31st Annual Frequency Control Symposium, Atlantic City, NJ, USA, 1-3 June 1977 (Washington, DC, USA: Electronic Industries Assoc. 1977), p. 495-8.

Hellwig, H. W.
"Workdwide Timekeeping Better Than Previously Believed", Dimensions NBS (USA), Vol. 61, No. 9, p. 23-5 (Sept. 1977).

Hellwig, H. W., Allan, D. W., Stein, S. R., Prichard, K. A.
"Transcontinental and Intercontinental Portable Clock Time Comparison", IEEE Trans. Instrum. & Meas. (USA), Vol. IM-27, No. 1, p. 65-8 (March 1978).

Helsby, N. C.
"Atomic Time Receiver", Pract. Wireless (GB), Vol. 53, No. 4, p. 288-92 (Aug. 1977).

Henderson, J. T.
"The Foundation of Time and Frequency in Various Countries", Proc. IEEE (USA), Vol. 60, No. 5, p. 487-93 (May 1972).

Heron, M. L., Rose, R. J.
"The Accuracy of Frequency Standards Disseminated by HF Radio Paths through the Ionosphere", Aust. J. Phys. (Australia), Vol. 31, No. 3-4, p. 333-45 (Aug. 1978).

Herring, J. C., Abby, D. G., Cook, J. A.
"Time Synchronization of Primary Geodetic Sites through Use of Artificial Satellites", Report AFCRL-70-0333 (AD-709360). Air Force Cambridge Res. Labs., Mass., USA (June 1970), 21 pp.

Bodily, LaT. N., Hyatt, R. C.
"Flying Clock" Comparisons Extended to East Europe, Africa and Australia", Hewlett-Packard J., (USA), Vol. 19, No. 4, 12-16 (Dec. 1967).

Higa, W. H.
"Time Synchronization via Lunar Radar", Proc. IEEE (USA), Vol. 60, No. 5, p. 552-7 (May 1972).

Hilberg, W.
"Radio-Controlled Clocks with Digital Standard-Time Indication", Elektronik (Germany), Vol. 16, No. 11, 325-8 (Nov. 1967). In German.

Hirai, K., Okikawa, T., Aiba, N.
"New Types of Frequency-Stabilized Gunn Oscillator", Toshiba Rev. (Int. Ed.) (Japan), No. 115, p. 37-41 (May-June 1978).

Honma, S., Kato, S.
"An Automatic Clock Synchronizer Using the 40kHz Standard Frequency Transmission", Rev. Radio Res. Lab. (Japan), Vol. 21, No. 114, p. 165-76 (May 1975). In Japanese.

Howe, D. A.
"Results of Active Line-1 TV Timing", Proc. IEEE (USA), Vol. 60, No. 5, p. 634-7 (May 1972).

Howe, D. A.
"Nationwide Precise Time and Frequency Distribution Utilizing an Active Code within Network Television Broadcasts", Proc. 26th Annual Frequency Control Symposium, Atlantic City, NJ, USA, 6-8 June 1972 (Washington, DC, USA: Electronic Industries Association 1972), p. 292-308.

Howe, D. A.
"Nationwide Precise Time and Frequency Distribution Utilizing an Active Code within Network Television Broadcasts", IEEE Trans. Instrum. & Meas. (USA), Vol. IM-21, No. 3, p. 263-6 (Aug. 1972).

Howe, D. A.
"Precise Frequency Dissemination Using the 19-kHz Pilot Tone on Stereo FM Radio Stations", IEEE Broadcast, (USA), Vol. BC-20, No. 1, p. 17-20 (March 1974).

Howe, S. L.
"NBS Time and Frequency Dissemination Services", Report NBS-SP-432, Nat. Bur. Stand., Washington DC, USA (Jan. 1976), 16 pp.

Hudson, G. E., Allan, D. W., Barnes, J. A., Hall, R. G., Lavancean, J. D., Winkler, G. M.R.
"A Coordinate Frequency and Time System", Proc. 23rd Annual Frequency Control Symposium, Atlantic City, NJ, USA, 6-8 May 1969 (Washington, DC, USA: Electronic Industries Association 1969) p. 249-62.

Hundertmark, B., Kahnt, D., Kalau, M.
"Standard Frequency Transmission by Stabilised Synchronising Pulses of Television in the DDR", Radio Fernsehen Elektron. (Germany), Vol. 25, No. 9, p. 277-9 (1976). In German.

Il'in, V. G., Palii, G. N., Tel'pukhovskii, N. A., Del'kovich, D. A., Starodubtsev, N. A., Ivanova, Yu. D.
"Comparison of Secondary Time-and-Frequency Standards, and Determination of the Time Required for Radio Waves to Travel over Synchronization Links", Meas. Tech. (USA), Vol. 19, No. 11, p. 1568-72 (Nov. 1976). Translation of: Izmer. Tekh. (USSR), Vol. 19, No. 11, p. 25-7 (Nov. 1976).

Il'in, V. G., Stepanova, I. V.
"Cooperation of the USSR Time and Frequency Service with International Organizations", Meas. Tech. (USA), Vol. 20, No. 4, p. 587-9 (April 1977). Translation of: Izmer. Tekh. (USSR), Vol. 20, No. 4, p. 81-2 (April 1972).

Inouye, T., Nara, M.
"The Stability of Time Comparison by TV Signal of Common Emission", Trans. Soc. Instrum. & Control Eng. (Japan), Vol. 11, No. 3, p. 269-74 (June 1975). In Japanese.

Jeansaume, G.
"The Distribution of Standard Time", Electron & Microelectron. Ind. (France), No. 208, P. 77-81 (15 Sept. 1975). In French.

Jespersen, J. L., Kamas, G., Gatterer, L. E., MacDoran, P. F.
"Satellite VHF Transponder Time Synchronization", Proc. IEEE (SUA), Vol. 56, No. 7, 1202-6 (July 1968).

Jespersen, J. L.
"A Survey of Time and Frequency Dissemination Techniques", 24th Annual Frequency Control Symposium, Atlantic City, NJ, USA, 27-29 April 1970 (Washington, DC, USA: Electronic Industries Association 1970), p. 322-324.

Jespersen, J. L., Blair, B. E., Gatterer, L. E.
"Characterization and Concepts of Time-Frequency Dissemination", Proc. IEEE (USA), Vol. 60, No. 5, p. 502-21 (May 1972).

Joyner, K. H., Butcher, L. C.
"The Effect of the Ionosphere on the Phase of Standard Frequency Transmissions", Aust. Telecommun. Res. (Australia), Vol. 11, No. 3, p. 23-9 (1977).

Kobayashi, S., Satoh, T., Tanaka, M.
"Accuracy of Time Comparison by the Reception of JJY Signals Propagating via the E Region", J. Radio Res. Lab. (Japan), Vol. 24, No. 114, p. 87-100 (July 1977).

Kulpinski, R. J.
"Minimum Variance Methods for Synchronization of Airborne Clocks", Proceedings of the 30th Annual Symposium on Frequency Control, Atlantic City, NJ USA, 2-4 June 1976 (Washington, DC, USA: Electronic Industries Assoc. 1976). p. 401-13.

Laidet, L. M.
"Workdwide Stnchrorization Using the TRANSIT Satellite System", Proc. IEEE (USA), Vol. 60, No. 5, p. 630-2 (May 1972).

Laios, S. C.
"Satellite Time Synchronization of a NASA Network", Proc. IEEE (USA), Vol. 60, No. 5, p. 632-3 (May 1972).

Leschiutta, S.
"Long Term Accuracy of Time Comparisons via TV Signal along Radio Relay Links", IEEE Trans. Instrum. & Meas. (USA), Vol. IM-22, No. 1, p. 84-7 (March 1973).

Leschiutta, S.
"Long-Term Accuracy of Time Comparisons via TV Signal along Radio Relay Links", IEEE Trans. Instrum. & Meas. (USA), Vol. IM-22, No. 1, p. 84-7 (March 1973).

Lobanova, Sh. P., Polyak, A. G., Cherepukhin, M.A.
"Estimating the Error in Determining Propagation Times of Short-Wave Signals", Meas. Tech. (USA), Vol. 19, No. 11, p. 1581-8 (Nov. 1976). Translation of: Izmer. Tekh. (USSR), Vol. 19, No. 11, p. 32-3 (Nov. 1976).

Markus, N.
"Centrally Controlled Electronic Time Service Systems Ranging from the Quartz Master Clock to the Time Service Central Station", Nachr. Telefonbau & Normalzeit (Germany), No. 78, p. 44-51 (1977). In German.

Mazur, W. E., Jr.
"Dual Transponder Time Synchronization at C Band Using ATS-3", Proc. IEEE (USA), Vol. 60, No. 5, p. 633-4 (May 1972).

Mazur, W. E.
"Time Synchronization of NASA Tracking Stations via Loran C", Proc. 27th Annual Frequency Control Symposium, Atlantic City, NJ, USA, 12-14 June 1973 (Washington, DC, USA: Electronic Industries Association 1973), p. 270-276.

Mercz, J. K.
"The Public Indication of Time in the Netherlands. II Conclusion", Polytech. Tijdschr. Elektrotech. Elektron. (Netherlands), Vol. 29, No. 26, p. 862-7 (20 Dec. 1974). In Dutch.

Miller, M. J.
"Synchronization of Distant Clocks by Television Pulse Comparisons", Proc. Astron. Soc. Aust., Vol. 1, No. 7, p. 352 (April 1970).

Milton, J. B.
"Standard Time and Frequency. Its Generation, Control, & Dissemination from the Natural Brueau of Standards Time & Frequency Division", Report NBS-TN-379, Nat. Bur. Stand., Washington, DC, USA (Aug. 1969), 27 pp.

Milton, J. B.
"Standard Time and Frequency: Its Generation, Control, and Dissemination by the National Bureau of Standards", Report NBS-TN-656, Nat. Bur. Stand. Washington, DC, USA (June 1974), 18 pp.

Minullin, R. G., Palii, G. N., Sidorov, V. V., Sukhotskii, A. V., Ivanova, Yu. D.
"Locking In to the State Standard of Time by Using Reflections from Meteors", Izmer. Tekh. (USSR), p. 22-4. In Russian. English translation in: Meas. Tech. (USA), Vol. 14, No. 1, p. 33-5 (Jan. 1971).

Montogomery, L.
"Standard Frequency and Time Service Using Radio Broadcasting Facilities", Proc. 26th Annual Frequency Control Symposium, Atlantic City, NJ, USA, 6-8 June 1972 (Washington, DC, USA: Electronic Industries Association 1972). p. 317-18.

Moreau, J. P.
"Measurement of Time Displacement between Remote Clocks", Mes. Regul. Autom. (France), Vol. 42, No. 5, p. 63-71 (May 1977). In French.

Moreau, J. P.
"High Resolution (100 ps) Optical Process of Synchronization for Remote Atomic Clocks Using Injection Laser Diodes", European Conference on Precise Electrical Measurement, Brighton, Sussex, England, 5-9 Sept. 1977 (London, England: IEEE 1977), p. 84-6.

Mungall, A. G., Daams, H., Bailey, R., Morris, D.
"Mass-Frequency Effect on V. I. F. and Portable Clock Comparisons of Atomic Frequency Standards", Metrologia (Germany), Vol. 5, No. 1, p. 31-2 (Jan. 1969).

Mungall, A. G., Daams, H., Bailey, R.
"Note on Atomic Time Keeping at the National Research Council", Metrologia (Germany), Vol. 5, No. 3, p. 73-6 (July 1969).

Murray, J. A., Pritt, D. L., Blocker, L. W., Leavitt, W. E., Hotten, P. M., Goring, W. D.
"Time Transfer by Defense Communications Satellite", Proc. 25th Annual Frequency Symposium, Atlantic City, NJ, USA, 26-28 April 1971 (Washington, DC, USA: Electronic Industries Association 1971), p. 186-193.

Nazarov, K. I., Unkovskii, K. V., Melikhov, G. G.
"Device for Receiving the Referenced Frequency of 66.(6) kHz", Meas. Tech. (USA), Vol. 16, No. 2, p. 265-7 (Feb. 1973). Translation of: Izmer Tekh. (USSR), Vol. 16, No. 2, p. 67-9 (Feb. 1973).

Nezik, D.
"Atomic Clock-Exact Time with the TN DCF 77 Time Signal Regulating Unit", Nachr. Telefonbau & Normalzeit (Germany), No. 78, p. 54-8 (1977). In German.

Oganyan, N. A., Savinova, V. S.
"Circuit for Automatically Snychronizing Marine Contact Chronometers with the State Time Scale", Izmer. Tekh. (USSR), p. 92-3. In Russian. English translation in: Meas. Tech. (USA), Vol. 14, No.1, p. 149-50 (Jan 1971).

Nasaka, M.
"Comparison among Integrated Atomic Time Systems", Univ. Tokyo, Tokyo Astron. Obs. Rep. (Japan), Vol. 14, No. 4, p. 482-8 (March 1969). In Japanese.

Pakos, P. E.
"Use of Loran-C Systems for Time and Frequency Dissemination", Proc. 23rd Annual Frequency Control Symposium, Atlantic City, NJ, USA, 6-8 May 1969 (Washington, DC, USA: Electronic Industries Association 1969), p. 236-247.

Pakos, P. E.
"Use of the Loran-C System for Time and Frequency Dissemination", Proceedings of the 23rd Annual Frequency Control Symposium, Atlantic City, NJ, USA, 6-8 May 1969 (Washington, DC, USA: Electronic Industries Assoc. 1969), p. 236-47.

Palii, G. N., Luk'yanchenko, Ya. I., Fedorov, Yu.A., Vnukov, E. M.
"Experimental High-Precision System for Transmitting Time Units and Frequency Over Television Channels", Izmer. Tekh. (USSR), Vol. 15, No. 1, p. 34-7 (Jan 1972). In Russian. English translation in: Meas. Tech. (USA), Vol. 15, No. 1, p. 54-9, (Jan. 1972).

Palii, G. N., Ivanova, Yu. D., Malov, A. G., Oksentyuk, A. R.
"Use of Atrificial Earth Satellites to Transmit Exact Time Signals", Meas. Tech. (USA), Vol. 19, No. 10, p. 1480-4 (Oct. 1976). Translation of: Izmer. Tekh. (USSR), Vol. 19, No. 10, p. 62-4 (Oct. 1976).

Palmer, W.
"The Omega Navigation System as a Source of Frequency and Time", 24th Annual Frequency Control Symposium, Atlantic City, NJ, USA, 27-29 April 1970 (Washington, DC, USA: Electronic Industries Assoc. 1970), p. 345-360.

Parcellier, P.
"Frequencies Comparison", Rev. Gen. Elect. (France), Vol. 78, No. 3, p. 287-90 (March 1969). In French.

Parkinson, C. E.
"Time/Frequency Dissemination and Clock Synchronization", Marconi Rev. (GB), Vol. 40, No. 207, p. 225-35 (1977).

Phillips, D. H., Phillips, R. E., O'Neil, J. J.
"Time & Frequency Transfer via Microwave Link",Proc. 24th Annual Frequency Control Symposium, Atlantic City, NJ, USA, 27-29 April 1970 (Washington, DC, USA: Electronic Industries Assoc. 1970), p. 325-331.

Phillips, D. H., Phillips, R. E., Boman, I. A., O'Neil, J. J.
"Methods of Local Time and Frequency Transfer", Proc. 25th Annual Frequency Control Symposium, Atlantic City, NJ, USA, 26-28 April 1971 (Washington, DC, USA: Electronic Industries Assoc. 1971), p. 209-216.

Pogson, I.
"Derived Frequency Reference from North West Cape II", Electron. Aust. (Australia), Vol. 38, No. 5, p. 56-61 (Aug. 1976).

Polyak, A. G.
"Resolving Ambiguity with Multifrequency Transmission of Time Signals", Meas. Tech. (USA), Vol. 19, No. 11, p. 1583-5 (Nov. 1976). Translation of: Izmer. Tekh. (USSR), Vol. 19, No. 11, p. 33-4 (Nov. 1976).

Potts, C. E., Wieder, B.
"Precise Time and Frequency Dissemination via the Loran-C System", Proc. IEEE (USA), Vol. 60, No. 5, p. 530-9 (May 1972).

Powers, R. F.
"Reference Frequency Transmission over Bell System Radio and Coaxial Facilities", Proc. 28th Annual Frequency Control Symposium, Atlantic City, NJ, USA, 29-31 May 1974 (Washington, DC, USA: Electronics Industries Assoc. 1974), p. 373-378.

Pushkin, S. B., Fedorov, Yu. A., Kalau, M., Kant, D.
"Comparison of the National USSR and GDR Time and Frequency Standards by Means of Transportable Clocks and Television Signals", Meas. Tech. (USA) Vol. 19, No. 10, p. 1467-71 (Oct. 1976). Translation of: Izmer. Tekh. (USSR), Vol. 19, No. 10, p. 54-6 (Oct. 1976).

Ramasastry, J., Rosenbaum, B., Michelini, R. D., Kuegler, G. K.
"Clock Synchronization Experiments Performed via the ATS-1 and ATS-3 Satellites", IEEE Trans. Instrum. & Meas. (USA), Vol. IM-22, p. 9-12 (March 1973).

Rovera, G.
"On the Accuracy of TV Timing Method", Alta Freq. (Italy), Vol. 41, No. 11, p. 822-4 (Nov. 1972). In English.

Rueger, L. J.
"One-Way Time Dissemination from Low Altitude Satellites", Proc. 25th Annual Frequency Control Symposium, Atlantic City, NJ, USA, 26-28 April 1971 (Washington, DC, USA: Electronic Industries Assoc. 1971), p. 179-185.

Rueger, L. J., Bates, A. G.
"Frequency Synthesizer for Normalizing the Frequency and Time Scales of Crystal Clocks on Orbiting Satellites", Proc. of the 28th Annual Frequency Control Symposium 1974, Atlantic City, NJ, USA, 29-31 May 1974 (Washington, DC, USA: Electronic Industries Assoc. 1974), p. 395-400.

Rueger, L. J.
"The Remote Synchronization Technology", Proceedings of the 30th Annual Symposium on Frequency Control, Atlantic City, NJ, USA, 2-4 June 1976 (Washington, DC, USA: Electronic Industries Assoc. 1976), p. 444-50.

Saburi, Y., Yamamoto, M., Harada, K.
"Precision Intercontinental Time Comparison via Geostationary Satellite", 1976 Conference on Precision Electromagnetic Measurements, Boulder, Colo. USA, 28 June - 1 July 1976 (New York, USA: IEEE 1976), p. 231-2.

Saburi, Y., Yamamoto, M., Harada, K.
"High Precision Time Comparison via Satellite and Observed Discrepancy of Synchronization", IEEE Trans. Instrum. & Meas. (USA), Vol. IM-25, No. 4, p. 473-7 (Dec. 1976). (1976 Conference on Precision Electromagnetic Measurements, Boulder, Colo. USA, 28 June - 1 July 1976).

Saburi, Y.
"Observed Time Discontinuity of Clock Synchronization in Rotating Frame of the Earth", J. Radio Res. Lab. (Japan), Vol. 23, No. 112, P. 255-65 (Nov. 1976).

Saden, D. S., Au, B. D.
"Daily Veriations of the Frequency of a Very Accurate Radio Frequency", Nature (GB), Vol. 224, No. 5226, p. 1291-3 (27 Dec. 1969).

Saxena, G. M., Nathur, B. S.
"Synchronization to Microsecond Accuracy of Clocks in India through Television Transmission", J. Inst. Electron. & Telecommun. Eng. (India), Vol. 23, No. 2, p. 78-80 (Feb. 1977).

Schreiber, H.
"Digital Clock Controlled by a Signal-Time Station", Mundo Electron. (Spain), No. 69, p. 63-72 (Dec. 1977). In Spanish.

Schreiber, H.
"Control of Electronic Clocks by One-Minute Interval Signals Derived from Standard Frequency Transmitters", Funk-Tech. (Germany), Vol. 33, No. 3, p. 53-4, 59-62 (Feb. 1978). In German.

Schwartz, H. M.
"A New Method of Clock Synchronization without Light Signals", Am. J. Phys. (USA), Vol. 39, No.9, p. 1269-70 (Sept. 1971).

Schwartz, H. M.
"A New Method of Clock Synchronization without Light Signals", Am. J. Phys. (USA), Vol. 39, No. 10, p. 1269-70 (Oct. 1971).

Semenov, S. F., Biadak, V. M., Dudnik, B. S., Motora, A. A.
"Correlation of Dispersed Time Standards", Radiotekhnika, Kharkov, (USSR), No. 29, p. 28-34 (1974). In Russian.

Sen, A. K., Saha, B.
"Worldwide Standards of Time and Frequency", J. Sci. & Ind. Res. (India), Vol. 32, No. 6, p. 300-11 (June 1973).

Sen, A. K.
"Precision of Standard Frequency Radio Signals in Relation to Ionospheric and Trans-Ionospheric Propagation", J. Inst. Electron. & Telecommun. Eng. (India), Vol. 23, No. 6, p. 365-9 (June 1977).

Shapiro, L. D.
"Time Synchronization from Loran-C", IEEE Spectrum (USA), Vol. 5, No. 8, 46-55 (Aug. 1968).

Smith, H.
"International Coordination of Radio Time Signal Emissions", Proc. 23rd Frequency Control Symposium Atlantic City, NJ, USA, 6-8 May 1969 (Washington, DC, USA: Electronic Industries Assoc. 1969), p. 18-20.

Smith, H. M.
"International Time and Frequency Coordination", Proc. IEEE (USA), Vol. 60, No. 5, p. 479-87 (May 1972).

Smith, H. M., Easton, R. L., Buisson, J. A., McCaskill, T. B.
"Sub-Microsecond Intercontinental Time Comparisons by Satellite", European Conference on Precise Electrical Measurement, Brighton, Sussex, England, 5-9 Sept. 1977 (London, England: IEEE 1977), p. 87-9.

Stadler, K.
"Standard Frequency Receiver XKD for Monitoring Secondary Frequency Standards", News Rohde and Schwarz (Germany), Vol. 8, No. 32, p. 20-2 (1968).

Stecher, R.
"Precision Reading Comparison of Time Standards at Long Distance from Each Other", Nachrichtentechnik (Germany), Vol. 17, No. 10, 404-8 (Oct. 1967).

Steele, J. McA.
"Past and Future Development of Standard Frequency Emissions", Colloquium on Definition, Realisation and Use of Time and Frequency, London, 1967 (London: Institution of Electrical Engineers, 1967: Colloquium Digest 1967/16), paper No. 4/1-4/5.

Stone, R. R., Gattis, T. H., Petit, R. C., Lieberman, T. N.
"Time Control of Frequency Shift Keyed Transmissions at VLF", Proceedings 25th Annual Frequency Control Symposium, Atlantic City, NJ, USA, 26-28 April 1971 (Washington, DC, USA: Electronic Industries Assoc. 1971), p. 152-158.

Stow, R. C., Coralnick, P.
"Active and Passive Relative Synchronization of Remote Clocks in a Time Ordered System", Proceedings of the 27th Annual Frequency Control Symposium, Cherry Hill, NJ, USA, 12-14 June 1973 (Washington, DC, USA: Electronic Industries Assoc. 1973), p. 296-303.

Swanson, E. R., Kugel, C. P.
"Omega VLF Timing", Proceedings 25th Annual Frequency Control Symposium, Atlantic City, NJ, USA, 26-28 April 1971 (Washington, DC, USA: Electronic Industries Assoc. 1971), p. 159-166.

Swanson, E. R., Kugel, C. P.
"VLF Timing: Conventional and Modern Techniques Including Omega", Proc. IEEE (USA), Vol. 60, No. 5, p. 540-51 (May 1972).

Takahashi, F.
"Proposal of Accurate Time-Dissemination Method Using a Broadcasting Satellite", Rev. Radio Res. Lab. (Japan), Vol. 22, No. 118, p. 135-42 (June 1976). In Japanese.

Takahashi, F.
"A Proposal of Accurate Time Dissemination Using TV Signals from a Broadcasting Satellite", J. Radio Res. Lab. (Japan), Vol. 23, No. 112, p. 267-83 (Nov. 1976).

Taylor, R. J.
"Satellite to Ground Timing Experiments", Proc. 28th Annual Frequency Control Symposium, Atlantic City, NJ, USA, 29-31 May 1974 (Washington, DC, USA: Electronic Industries Assoc. 1974), p. 384-388.

Vasin, L. D., Kiritsev, E. S., Kireev, B. M.
"Apparatus for Frequency Collation Using the Signals of Super-Long Wave Radio Stations", Meas. Tech. (USA), Vol. 15, No. 11, p. 1656-8 (Nov. 1972). Translation of: Izmer. Tekh. (USSR), Vol. 15, No. 11, p. 39-41 (Nov. 1972).

Ward, K.
"Precision Worldwide Time Transfer Using the GPS" 1976 National Telecommunications Conference, Pt. III, Dallas, Tex., USA, 29 Nov.-1 Dec. 1976 (New York, USA: IEEE 1976), p. 41.2/1.

Weiss, R.
"Time-Signal and Standard Frequency Receiver for DCF 77 with Reserve. III", Funkschau (Germany), Vol. 48, No. 24, p. 1086-8 (19 Nov. 1976). In German.

Weiss, R.
"Standard Time and Frequency Receiver for DCF 77 with Auxiliary Channel", Funkschau (Germany), Vol. 48, No. 25, p. 1122-5 (3 Dec. 1976). In German.

Wieder, B.
"Use of Loran-C Over Land", Proc. 25th Annual Frequency Control Symposium, Atlantic City, NJ, USA, 26-28 April 1971 (Washington, DC, USA: Electronic Industries Assoc. 1971), p. 171-178.

Winkler, G. M. R.
"Recent Improvements in the US Naval Observatory Timekeeping and Time Distribution Operations", Proc. 22nd Annual Frequency Control Symposium, Atlantic City, NJ, USA, 22-24 April 1968 (Ft. Monmouth, NJ, USA: Electronic Components Laboratory 1968), p. 383.

Winkler, G. M. R.
"International Coordinated Clock Time and the Coming Improvements in the System "UTC"", Proc. 25th Annual Frequency Control Symposium, Atlantic City, NJ, USA 26-28 April 1971 (Washington, DC, USA: Electronic Industries Assoc. 1971),p. 217-21.

Winkler, G. M. R.
"Path Delay, Its Variations, and Some Implications for the Field Use of Precise Frequency Standards", Proc. IEEE (USA), Vol. 60, No. 5, p. 522-9 (May 1972).

Yamamoto, M., Harada, K., Saburi, Y.
"A Time Comparison Experiment Performed by SSRA System via ATS-1", J. Radio Res. Lab. (Japan), Vol. 23, No. 110, p. 85-103 (March 1976).

3.3

Anan'ev, L. L., Gerasimova, T. M., Gerasimov, N,P., Golubkov, V. P., Krasnoperov, E. P., Reinov, N. M.
"Superconducting Oscillating Circuit with Lumped Parameters", Pribory. Tekh. Eksper. (USSR), p. 130-1. English translation in: Instrum. Exper. Tech. (USA), Vol 6, p. 1517-18 (Nov. 1969).

Anan'ev, L. L., Gerasimov, N. P., Reinov, N. M., Terent'eva, M. N.
"Temperature Dependence of the Resonance Frequency of a Superconducting Lumped-Parameter Circuit", Zh. Tekh. Fiz. (USSR), Vol. 42, No. 1, p. 222-4 (Jan. 1972). In Russian. English translation in: Soc. Phys. Tech. Phys. (USA), Vol. 17, No. 1, p. 180-1.

Bindal, V. N., Singhal, S. K.
"A Piezoelectric Miniaturized Tuning Fork", Indian J. Pure & Appl. Phys., Vol. 14, No. 5, p. 378-81 (May 1976).

Bjorkholm, J. E., Danielmeyer, H. G.
"Frequency Control of a Pulsed Optical Parametric Oscillator by Radiation Injection", IEEE J. Quantum Electronics (USA), Vol. QE-6, No. 1, p. 7 (Jan. 1970). (1969 IEEE conference on laser engineering and applications (post-deadline papers), Washington, DC, USA, 26-28 May 1969).

Bloomfield, D. L. H., Pointon, A. J.
"Short-Term Frequency Stability of an L Band Oscillator with a Superconducting Cavity", Electron. Lett. (GB), Vol. 9, No. 19, p. 461-2 (20 Sept. 1973).

Bushy, P. W.
"Electronic Tuning Fork", Pract. Electron. (GB), Vol. 11, No. 11, p. 882-8 (Nov. 1975).

Debeau, J., Minet, R.
"Superconductor Highfrequency Filters", Echo Rech. (France), No. 72, p. 14-21 (April 1973). In French.

Dydyk, M.
"Dielectric Resonators Add Q to MIC Filters", Microwaves (USA), Vol. 16, No. 12, p. 150-1 (Dec. 1977).

Herzog, W.
"Narrow-Band Quartz Crystal Filters with Losses", Proc. Instn. Radio Electronics Engrs.Australia, Vol. 29, No. 1, 18-24 (Jan. 1968).

Jimenez, J. J., Viet, N. T., Bernard, J., Septier, A.
"Frequency Standards of Cavity Superconductors", Electron. & Fis. Apl. (Spain), Vol. 16, No. 2, p. 79-84 (1973). In French.

Jimenez, J. J., Septier, A.
"S-and X-Band Superconducting Cavity Stabilized Oscillators", Proc. of the 27th Annual Frequency Control Symposium, Cherry Hill, NJ, USA, 12-14 June 1973 (Washington, DC, USA: Electronic Industries Assoc. 1973), p. 406-13.

Kukushkin, A. V., Nasonov, V. S.
"Phase Fluctuations of the Signal of a Generator with a Traveling-Wave Tube Using a Superconducting Resonator", Pribory. Tekh. Eksper. (USSR), p. 127-9. In Russian. English translation in: Instrum. Exper. Tech. (USA), No. 6, p. 1514-16 (Nov. 1969).

McGuigan, D. F., Donglass, D. H.
"Clocks Based upon High Mechanical Q Single Crystals", Proc. 31st Annual Frequency Control Symposium, Atlantic City, NJ, USA, 1-3 June 1977 (Washington, DC, USA: Electronic Industries Assoc. 1977), p. 616-619.

Minakova, I. I., Minina, G. P., Panov, V. I., Petnikov, V. G.
"A Free-Running Oscillator, Stabilised by a Three-Cavity System with a Superconducting Resonator", Izv. VUZ Radioelektron. (USSR), Vol. 19, No. 10, p. 16-23 (Oct. 1976). In Russian.

Minakova, I. I., Minina, G. P., Nazarov, V. I., Panov, V. I., Popel'nyuk, V. D.
"Stabilizing the Frequency of an Oscillator for High Q-Factors of the Stabilizing Resonator", Vestn. Mosk. Univ. Fiz. Astron. (USSR), Vol. 17, No. 6, p. 722-7 (Nov.-Dec. 1976). In Russian.

Nukiyama, D., Miyazaki, N.
"A Type of Oscillator", J. Res. Inst. Technol. Nihon. Univ. (Japan), 1967, No. 34, 18 et seq. (Sept.). In Japanese.

Ota, M., Nagase, T., Oyanagi, T., Kenmotsu, N.
"Micro Tuning Fork", Hitachi Hyoron (Japan), Vol. 53, No. 6, p. 37-42 (June 1971). In Japanese.

Plourde, J. K., Linn, D. F., Tatsuguchi, I., Swan, C. B.
"A Dielectric Resonator Oscillator with 5 PPM Long Term Frequency Stability at 4 GHz", 1977 International Microwave Symposium Digest, San Diego, Calif., USA, 21-23 June 1977 (New York, USA: IEEE 1977), p. 273-6.

Rose, B. E.
"10 GHz Cavity Stabilized FET Oscillator", Proc. 32nd Annual Frequency Control Symposium, Atlantic City, NJ, USA, 31 May - 2 June 1978 (Washington, DC, USA: Electronic Industries Assoc.), p. 385-388.

Schwarz, H. R.
"Eigenfrequencies of Tuning-Forks", Comput. Methods Appl. Mech. & Eng. (Netherlands), Vol.1, No. 2, p. 159-72 (Aug. 1972).

Stein, S. R., Turneaure, J. P.
"A Superconducting Cavity Stabilized Oscillator", Proc. 26th Annual Frequency Control Symposium, Atlantic City, NJ, USA, 6-8 June 1972 (Washington DC, USA: Electronic Industries Assoc., 1972), p. 257-

Stein, S. R., Turneaure, J. P.
"The Development of the Superconducting Cavity Stabilised Oscillator", Proc. of the 27th Annual Frequency Control Symposium, Cherry Hill, NJ, USA, 12-14 June 1973 (Washington, DC, USA: Electronic Industries Assoc. 1973), p. 414-20.

Stein, S. R.
"The Superconducting-Cavity Stabilized Oscillator and an Experiment to Detect Time Variation of the Fundamental Constants", Stanford Univ., Calif., USA thesis, 1974, 111 pp. Available from Univ. Microfilms, Ann Arbor, Mich., USA. Order No. 75-6932.

Stein, S. R.
"The Superconducting-Cavity Stabilized Oscillator and an Experiment to Detect Time Variation of the Fundamental Constants", Report HEPL-741, Stanford Univ., Calif., USA (Oct. 1974), 111 pp. Contract N00014-67-A-0112-0076. Available from NTIS, Springfield, VA. 22151, USA.

Stein, S. R.
"Application of Superconductivity to Precision Oscillators", Proc. of the 29th Annual Frequency Control Symposium, Fort Monmouth, NJ, USA 28-30 May 1975 (Washington, DC, USA: Electronic Industries Assoc. 1975), p. 321-7.

Stein, S. R., Turneaure, J. P.
"Superconducting-Cavity Stabilized Oscillators with Improved Frequency Stability", Proc. IEEE (USA), Vol. 63, No. 6, p. 992-3 (June 1975).

Stone, J. L., Hartwig, W. H.
"Oscillators Utilizing Superconducting Resonators" Southwestern Institute of Electrical and Electronics Engineers Conference Record of Technical Program, Dallas, 1967 (New York: Institute of Electrical and Eelctronics Engineers, Inc., 1967) paper no. 9-3-1-9-3-8.

3.4

Arai, S., Ieki, H., Kadota, M.
"SAW Filters Are Finding Extensive Applications", JEE (Japan), No. 130, P. 52-6 (Oct. 1977).

Asakawa, K.
"Acoustic Surface Waves and Their Applications", J. Inst. Electron. & Commun. Eng. Jap. (Japan), Vol. 55, No. 1, p. 67-78 (Jan. 1972). In Japanese.

Baker, M. A.
"Vacuum Applications of the Quartz Crystal Microbalance", Vacuum (GB), Vol. 19, No. 7, p. 327-30 (July 1969).

Battison, A. H.
"Ionized Light Emitter Using Piezoelectric Crystal", IBM Tech. Disclosure Bull. (USA), Vol. 14, No. 2, p. 555-7 (July 1971).

Benndorf, C., Keller, G., Scidel, H., Thieme, F.
"High- Resolution Quartz Oscillator Microbalance and Its Application to the Initial Oxidation of Aluminium", J. Vac. Sci. & Technol. (USA), Vol. 14, No. 3, p. 819-21 (May-June 1977).

Berenshtein, B. Sh., Bobrikov, V. S.
"The Restoration of Quartz Resonators That are Used to Measure the Thickness and Rate of Vacuum Deposition of Thin Films", Instrum. & Exp. Tech. (USA), Vol. 16, No. 5, pt. 2, p. 1518 (Sept.-Oct. 1973). Translation of: Prib. Tekh. Eksp. (USSR), Vol. 16, No. 5 pt. 2, p. 185 (Sept. - Oct. 1973).

Bourov, J. I., Velkov, V. J., Stojanov, D. V.
"Surface Acoustic Waves and Some Applications", Elektro Prom. st. & Priborostr. (Bulgaria), Vol. 11, No. 7, p. 252-3 (Aug. 1976). In Bulgarian.

Chao, G.
"Surface Acoustic Wave Devices Move into High-Volume Marktes", EDN (USA), Vol. 22, No. 9, p. 96-9 (5 May 1977).

Collins, J.
"SAW Devices Emerging into Commercial and Military Hardware", Microwave Syst. News(USA), Vol. 7, No. 1, p. 15-21 (Jan. 1977).

Cometta, M.
"Piezoelectricity, (Devices) and Its Applications", Elettrificazione (Italy), No. 2, p. 71-5 (Feb. 1974). In Italian.

Corlet, J.
"A Small Quartz Watch with Automatic Digital Frequency Regulation", Bul. Ann. Soc. Suisse Chronom. & Lab. Suisse Rech. Horlogeres (Switzerland), Vol. 7, No. 3, p. 314-2 (1977). In French.

Daniels, R. G., Musa, F. H.
"The Crystal-Controlled Electronic Wrist-Watch System: A Si-Gate CMOS-MSI Approach", Programme of the 25th Annual Frequency Control Symposium (abstracts), Atlantic City, NJ, USA, 26-28 April 1971 (Ft. Monmouth, NJ, USA: US Army Electronic Command 1971), p. 16.

Deacon, J. M., Heighway, J.
"SAW Filters for TV Receivers", IEEE Trans. Consum. Electron. (USA), Vol. CE-21, No. 4, p. 390-5 (Nov. 1975).

De Klerk, J.
"Past, Present and Future of Surface Elastic Waves", J. Phys. (France), Vol. 33, No. 11-12 Suppl., p. C6/182-8 (Nov.-Dec. 1972). In English

Dietzel, R.
"Passive Resonators with Noise Feeding in Frequency-Analogue Measuring Systems", Mess. Steuern Regeln mit Automatisierungprax. (Germany), Vol. 18, No. 11, p. 389-93 (Nov. 1975). In German.

Dressner, J. M., Del Vecchio, J. P.
"Frequency Control Requirements for the Mallard Communication System", Proceedings of the 23rd Annual Frequency Control Symposium, Atlantic City, NJ, USA, 6-8 May 1969 (Washington, DC, USA: Electronic Industries Assoc. 1969), p. 1-7.

Eykholt, A., Lipetz, N.
"Surface Acoustic Wave Devices - an Emerging Technology", Proceedings of the national electronics conference, Chicago, Ill., USA, 7-9 Dec. 1970 (Oak Brook, Ill., USA: National Electron. Conf. Inc. 1970), p. 991.

Fonjallaz, C., Vittoz, E.
"The Crystal Electronic Wrist-Watch. III. Electronic Circuits for Crystal Wrist-Watches", Schweiz. Tech. Z. (STZ) (Switzerland), Vol. 67, No. 24-25, p. 458-61 (11 June 1970). In French.

Forrer, N.
"The Crystal Electronic Wrist-Watch. I. Synopsis", Schweiz. Tech. Z (STZ) (Switzerland), Vol. 67, No. 24-25, p. 454-5 (11 June 1970). In French.

Gerber, E., Ahlstrom, E. R.
"Solid-State Laser with Vibrating Reflector", IEEE J. Quantum Electronics (USA), Vol. QE-5, No. 8, p. 403-9 (Aug. 1969).

Gniewinska, B., Czarnecki, A., Rozwadowski, M.
"Digital Quartz Thermometer", Pol. Tech. Rev. (Poland), No. 4-5, p. 23-4 (1977).

Guye, R., Chauvy, D., Hubner, K.
"The Crystal Electronic Wrist-Watch. IV. Integrated Circuits of a Crystal Wrist-Watch", Schweiz. Tech. Z. (STZ) (Switzerland), Vol. 67, No. 24-25, p. 461-4 (11 June 1970). In French.

Haas, W.
"Channeling Equipment Technology Using Electromechanical Filters", Electr. Commun. (USA), Vol. 48, No. 1-2, p. 16-20, (1973).

Hama, T.
"Electronic Watches Using Quartz Crystal Oscillators", Jpn. J. Appl. Phys. (Japan), Vol. 16, Suppl. 1, p. 185-9 (1977). (1976 International Conference on Solid State Devices, Tokyo, Japan, 1-3 Sept. 1976).

Hammer, D., Benes, E., Pulker, H. K.
"A Digital Quartz Deposition Monitor Using a Microprocessor", Thin Solid Films (Switzerland), Vol. 32, No. 1, p. 47-50 (16 Feb. 1976). (3rd International Conference on Thin Films, Budapest, Hungary, 25-29 Aug. 1975).

Hammer, M. W.
"A Small Quartz Watch with Automatic Digital Frequency Regulation", Bul. Ann. Soc. Suisse Chronom. & Lab. Suisse Rech. Horiogeres (Switzerland), Vol. 7, No. 3, p. 337-40 (1977). In French.

Hays, R. M., Hartmann, C. S.
"Surface-Acoustic-Wave Devices for Communications" Proc. IEEE (USA), Vol. 64, No. 5, p. 652-71 (May 1976).

Hegendorfer, M.
"Quartz Clock Module Supplies Accurate Time, Programme Number and Tuning Scale to TV Set", Funkschau (Germany), Vol. 47, No. 20, p. 51-3 (26 Sept. 1975). In German.

Hermann, J., Forrer, M., Omlin, L.
"The Crystal Electronic Wrist-Watch. II. Wrist-Watch Crystal Resonator", Schweiz. Tech. Z (STZ) (Switzerland), Vol. 67, No. 24-25, p. 456-8 (11 June 1970). In French.

Hirama, K.
"Quartz Crystal Units in Communications Equipment", JEE (Japan), No. 121, p. 50-2 (Jan. 1977).

Holland, M. G., Claiborne, L. T.
"Practical Surface Acoustic Wave Devices", Proc. IEEE (USA), Vol. 62, No. 5, p. 582-611 (May 1974).

Hordejuk, J.
"Application of Low-Frequency Electromechanical Filters to Seismological Investigations", Acta Geophys. Pol. (Poland), Vol. 19, No. 4, p. 351-64 (1971). In English.

Inamura, T., Yoshikawa, S.
"Applications of Surface Acoustic Wave Devices", Oyo Buturi (Japan), Vol. 45, No. 8, p. 718-28 (Aug. 1976). In Japanese.

Ivanov, G. A., Pekar, I. K. I., Roitbert, M. B., Guglya, V. G.
"Expanding the Temperature Range of a Piezoelectric Quartz Microbalance", Zavod. Lab. (USSR), Vol. 37, No. 7, p. 798-800 (July 1971). In Russian. English translation in: Ind. Lab. (USA), Vol. 37, No. 7, p. 1019-21 (July 1971).

Ivanov, G. A.
"Microweighing with Piezoelectric Quartz Crystals", Ind. Lab. (USA), Vol. 38, No. 6, p. 884-90 (June 1972). Translation of: Zavod. Lab. (USSR), p. 693-9.

Jack, M., Grant, P. M., Collins, J. H.
"New Network Analyzer Employs SAW Chirp Filters", Microwave Syst. News (USA), Vol. 5, No. 4, p. 62 (Aug.-Sept. 1975).

Janghorbani, M., Freund, H.
"Application of a Piezoelectric Quartz Crystal as a Partition Detector Development of a Digital Sensor", Chem. (USA), Vol. 45, No. 2, p. 325-32 (Feb. 1973).

Joshi, N. K., Singh, A.
"Surface Acoustic Wave Devices in Electronic Warfare", Def. Sci. J. (India), Vol. 27, No. 4, p. 157-62 (Oct. 1977).

Kanbayashi, S., Okano, S., Hirama, K., Kudama, T., Konno, M., Tomikawa, Y.
"Analysis of Tuning Fork Crystal Units and Application into Electronic Wrist Watches", Proc. of the 30th Annual Symp. on Frequency Control, Atlantic City, NJ, USA, 2-4 June 1976 (Washington, DC, USA: Electronic Indus. Assoc. 1976), p. 167-74.

Kertzman, J.
"Piezoelectric Sensors for Use as Pollution Detectors, Meteorology Monitors and Research Instruments", Programme of the 25th Annual Frequency Control Symposium (abstracts), Atlantic City, NJ, USA, 26-28 Apr. 1971 (Fort Monmouth, NJ, USA: US Army Electronic Command 1971), p. 20.

Khmurny, Ya., Chernik, K.
"The Use of Piezo-Ceramic Resonators in Selective Transistor Amplifiers", Ivz. VUZ Radioelektronika (USSR), Vol. 11, No. 4, p. 392-5 (April 1968). In Russian.

King, W. H., Jr.,
"The Present State-of-the-Art in Piezoelectric Sensors", Programme of the 25th Annual Frequency Control Symposium (abstracts), Atlantic City, NJ, USA, 26-28 April 1971 (Fort Monmouth, NJ, USA: US Army Electronic Command 1971), p. 21.

Kino, Y., Nakayama, Y., Furuya, N., Watanabe, Y., Aihara, Y., Inaba, R.
"Applications for Surface Acoustic Waves", Natl. Tech. Rep. (Japan), Vol. 22, No. 5, p. 644-50 (Oct. 1976). In Japanese.

Klemperer, W. K.
"Long-Baseline Radio Interferometry with Independent Frequency Standards", Proc. IEEE (USA), Vol. 60, No. 5, p. 602-09 (May 1972).

Kornstein, E., Kikuyama, A., Horiuchi, A.
"The Quartz Analog Watch Still Lives", 1975 WESCON Technical Papers - Western Electronic Show and Convention. Vol. 19, San Francisco, Calif., USA, 16-19 Sept. 1975 (North Hollywood, Calif., USA: Western Periodicals 1975), 12/1, 5pp.

Kuwano, Y.
"Applications of Surface Acoustic Wave Filter to TV Receiver", J. Inst. Telev. Eng. Jpn. (Japan), Vol. 31, No. 11, p. 845-52 (Nov. 1977). In Japanese

Laan, C. J., Frankena, H. J.
"Monitoring of Optical Thin Films Using a Quartz Crystal Monitor", Vacuum (GB), Vol. 27, No. 4, p. 391-7 (1977). (Proceedings of the International Symposium on Vacuum and Thin Film Technology, Uppsala, Sweden, 31 Aug.-3 Sept. 1976).

Laker, K. R., Slobodnik, A. J., Jr.
"Impact of SAW Filters on RF Pulse Frequency Measurement by Double Detection", Report AFCRL-PSRP-621, Air Force Cambridge Res. Labs., Hanscom AFB, Mass., USA (6 Jan. 1975), 194 pp.

Levchuk, E. A., Chudnovskii, A. F., Samuilova, S.I.
"Maximum Sensitivity of Humidity Transducers with Crystal Plates", Izmer. Tekh. (USSR), Vol. 14, No. 10, p. 88 (Oct. 1972). In Russian. English translation in: Meas. Tech. (USA), Vol. 14, No. 10, p. 1608-09 (Oct. 1971).

Lostis, P.
"Control of Thin Films by Piezoelectric Quartz", Vide (France), Vol. 26, No. 154, p. 159-63 (July-Oct. 1971). In French.

Lu, Chih-Shun
"Mass Determination with Piezoelectric Quartz Crystal Resonators", J. Vac. Sci. & Technol. (USA), Vol. 12, No. 1, p. 578-83 (Jan.-Feb. 1975). (21st National Symposium of the American Vacuum Society, Anaheim, Calif., USA, 8-11 Oct. 1974).

Lu, Kee-Siang, S.
"The Application of Quartz Crystals to Discriminators, Filters and Monolithic Filters", Aust. Electron. Eng. (Australia), Vol. 4, No. 3, p.21-4 (Aug. 1971).

Maines, J. D., Paige, E. G. S.
"Surface Acoustic-Wave Devices for Signal Processing Applications", Proc. IEEE (USA), Vol. 64, No. 5, p. 639-52 (May 1976).

Meccea, V., Bucur, R. V.
"The Use of RF Voltage in Quartz Crystal Microbalance Measurements: Application to Nonmetallic Films", J. Phys. E (GB), Vol. 7, No. 5, p. 348-9 (May 1974).

Melngailis, J., Williamson, R. C.
"Surface-Acoustic-Wave Device for Doppler Filtering of Radar Burst Waveforms", 1976 IEEE MTT-S International Microwave Symposium, Cherry Hill, NJ, USA, 14-16 June 1976 (New York, USA: IEEE 1976), p. 289-91.

Miller, R. L., DeVries, A. J.
"Commercial Application of a Surface Wave Television IF Filter", 1976 IEEE MTT-S International Microwave Symposium, Cherry Hill, NJ, USA, 14-16 June 1976 (New York, USA: IEEE 1976), p. 318-20.

Moreau, R.
"The Use of Atomic Clocks in Spacecraft Location", Eurocon 71 Digest, Lausanne, Switzerland, 18-22 Oct. 1971 (New York, USA: IEEE 1971), 2 pp.

Nagy, G.
"Piezoelectric Crystal-Type Thickness Measuring Instrument for Vacuum Evaporated Films", Meres es Automat. (Hungary), Vol. 15, No. 11, 433-5 (1967). In Hungarian.

Nichols, S. A., White, J.
"Satellite Application of a Rubidium Frequency Standard", Proceedings of the 28th Annual Frequency Control Symposium 1974, Atlantic City, NJ, USA, 29-31 May 1974 (Washington, DC, USA: Electronic Industries Assoc. 1974), p. 401-5.

Nichols, S. A., Woodring, D. G.
"Applications of Atomic Frequency Standards to Satcom Spread Spectrum Systems", Proc. 31st Annual Frequency Control Symposium, Atlantic City, NJ, USA, 31 May-2 June 1978 (Washington, DC, USA: Electronics Industries Assoc. 1978), p. 555-559.

Noiray, J. C., Lanteri, H., Bindi, R., Borgnino,J. Martin, F.
"Study and Development of an Oscillating Quartz-Crystal Microbalance - Comparison with Optical and Mechanical Measurement Methods", Thin Solid Films (Switzerland), Vol. 26, No. 2, p. 293-303 (April 1975). In French.

Nunamaker, R. J.
"Frequency Control Devices for Mobile Communications", Programme of the 25th Annual Frequency Control Symposium (abstracts), Atlantic City, NJ, USA, 26-28 Apr. 1971 (Fort Monmouth, NJ, USA: US Army Electronics Command 1971), p. 15.

Nuvolone, R., Boiziau, C.
"Realization of a Very Sensitive Quartz Balance", Vide (France), Vol. 27, No. 157, p. 10-16 (Jan.-Feb. 1972). In French.

Nuvolone, R., Boiziau, C.
"A Very Sensitive Vibrating Quartz Balance Working in Ultra-High Vacuum and at Very Low Temperatures. Application to the Study of Gas-Solid Interactions" Revue Phys. Appl. (France), Vol. 7, No.1, p. 55-60 (March 1972). In French.

Oguey, H., Droz, J. C.
"The Crystal Electronic Wrist-Watch. V. Display Micromotor in the Crystal/Wrist-Watch. Theory", Schweiz. Tech. Z (STZ) (Switzerland), Vol. 67, No. 24-25, p. 464-7 (11 June 1970). In French.

Ohnuki, A.
"Quartz Crystal Units for CB Transceivers", JEE (Japan), No. 121, p. 45-9 (Jan. 1977).

Onoe, M., Furusawa, K., Ishigami, S., Sase, T., Sato, M.
"Quartz Crystal Accelerometer Insensitive to Temperature Variation", 31st Annual Frequency Control Symposium, Atlantic City, NJ, USA, 1-3 June 1977 (Washington, DC, USA: Electronic Industries Assoc. 1977), p. 62-70.

Paige, E. G. S.
"Acoustic Surface Waves and Their Applications in Electronics", Proceedings of the 7th International congress on acoustics, Budapest, Hungary, 18-26 Aug. 1971 (Budapest, Hungary: Akademiai Kiado 1971), p. 141-51.

Porter, W. A., Anderson, S. W.
"The Effects of Temperature on the Accuracy of Crystal Oscillator Thickness Monitors", J. Vac. Sci. & Technol. (USA), Vol. 9, No. 6, p. 1472-4 (Nov.-Dec. 1972).

Prokysek, J.
"Electronic Clocks and Watches with Crystal-Controlled Oscillator", Jemna Mech. & Opt. (Czechoslovakia), Vol. 19, No. 9, p. 248-50 (Sept. 1974). In Czech.

Pulker, H. K.
"Experiments on the Realizable Precision in Continuous Film Thickness Measurement with a Quartz Oscillator", Vide (France), Vol. 26, No. 154, p. 150-8 (July-Oct. 1971). In French.

Pulker, H. K.
"Progress in Monitoring Thin Film Thickness with Quartz Crystal Resonators", Thin Solid Films (Switzerland), Vol. 32, No. 1, p. 27-33 (16 Feb. 1976). (3rd International Conference on Thin Films, Budapest, Hungary, 25-29 Aug. 1975).

Raabe, M.
"Integrated CMOS Circuit with Low Power Consumption for Quartz-Crystal Wristwatches", Elektronik (Germany), Vol. 22, No. 12, p. 424-6 (Dec. 1973). In German.

Robrock, R. B.
"Quartz Crystal Applications in Digital Transmission", Programme of the 25th Annual Frequency Control Symposium (abstracts), Atlantic City, NJ, USA, 26-28 Apr. 1971 (Fort Monmouth, NJ, USA: US Army Electronic Command 1971), p. 14.

Rozwadowski, M., Czarnecki, A.
"Quartz Crystal Resonator with Linear Dependence of Frequency upon Temperature", Pr. Inst. Tele. & Radiotech. (Poland), Vol. 19, No. 1, p. 85-90 (1975). In Polish.

Schilling, H., Pechhold, W.
"Two Quartz Resonator Methods for the Investigation of the Complex Shear Modulus of Polymers", Acustica (Internat.), Vol. 22, No. 5, p. 244-53 (1970) In German.

Schmidt, L.
"The Piezo-Electric Effect and Its Application to Modern Technology", VDE Fachber, (Germany), Vol. 26, p. 139-43 (1970).

Schmidt, L.
"The Piezoelectric Effect and Its Application in the Modern Technology", Messen u. Prufen (Germany) Vol. 6, No. 10, p. 811-16 (Oct. 1970). In German.

Seed, A.
"Quartz Crystals for Timepieces", Eurocon 71 digest Lausanne, Switzerland, 18-22 Oct. 1971 (New York, USA: IEEE 1971), 2pp.

Shiojiri, M., Hasegawa, Y., Mupata, Y., Matsumura, S.
"Quartz Crystal Microbalance Techniques Applicable to the Studies of Sulphuration and Oxidation of Thin Metal Films", Japan J. Appl. Phys., Vol. 8, No. 6, p. 783-91 (June 1969).

Smagin, A. G., Mil'shtein, B. G.
"Quartz Frequency Thermometer", Pribory Tekh. Eksp. (USSR), p. 258-9. In Russian. English translation in: Instrum. & Exp. Tech. (USA), No. 3, p. 932-4 (May-June 1970).

Sollner, E., Benes, E., Biedermann, A., Hammer, D.
"Properties of Heavily Preloaded Quartz Crystals for Thin Film Thickness Monitors", Vacuum (GB), Vol. 27, No. 4, p. 367-71 (1977). (Proceedings of the International Symposium on Vacuum and Thin Film Technology, Uppsala, Sweden, 31 Aug.-3 Sept. 1976).

Staudte, J. H.
"Quartz Crystals for Watches", 1975 WESCON Technical Papers - Western Electronic Show and Convention. Vol. 19, San Francisco, Calif., USA, 16-19 Sept. 1975 (North Hollywood, Calif. USA: Western Periodicals 1975), 17/1, 6 pp.

Stevenson, S. A.
"Developments in the Application of Synthetic Quartz", Electronic Compon. (GB), Vol. 10, No. 12, p. 1465-6 (Dec. 1969).

Suckling, C. W.
"A Crystal-Controlled Frequency Marker for 10 GHz", Radio Commun. (GB), Vol. 52, No. 5, p. 352-3 (May 1976).

Swinbank, E., Heeks, T. R., Shelly, J. H.
"Quartz-Crystal Watches", Electron. & Power (GB) Vol. 20, No. 19, p. 887-91 (31 Oct. 1974).

Takeda, I.
"Transceiver Crystal Techniques: Painstaking Design is Essential", JEI - Jap. Electron. Ind. (Japan), Vol. 23, No. 3, p. 60-70 (March 1976).

Thommen, W., Ruegg, H.
"Bipolar Micropower Circuits for Crystal Controlled Watches", Eurocon 71 Digest, Lausanne, Switzerland, 18-22 Oct. 1971 (New York, USA: IEEE 1971), 2 pp.

van Ballegooijen, Boersma, F., van der Steen, C.,
"Application of a Quartz Crystal with Electrode-Tab Configuration for Simultaneous Mass and Temperature Determination", J. Acoust. Soc. Am (USA), Vol. 63, No. 3, p. 806-14 (March 1978).

Wallace, D. A.
"Use of the Quartz Crystal Microbalance for Outgassing and Optical Contamination Measurements", J. Vac. Sci. & Technol. (USA), Vol. 9, No. 1, p. 462-6 (Jan.-Feb. 1972). (Proceedings of the 5th international vacuum congress part I, Boston, Mass. USA, 11-15 Oct. 1971).

Webb, D. C.
"Surface Acoustic Wave Devices for Communications", International Telemetering Conference, Silver Spring, MD, USA, 14-16 Oct. 1975 (Woodland Hills, Calif, USA: Internat. Found. Telemetering 1975), p. 581-93.

Wiefelsputz, F. G.
"Frequency Control in Radiocommunications", Telecommun. J. (Engl. Ed.) (Switzerland), Vol. 45, No. 7, p. 395-402 (July 1978).

Williams, R. L.
"Making It Clear as Crystal. I.", Communications USA), p. 20-2, 24-6, 28-9 (March 1978).

Yamazaki, S.
"Quartz Thermometers Achieve High Accuracy", JEE (Japan), No. 131, p. 59-61 (Nov. 1977).

Yoda, H.
"Crystal Oscillators Growing Influence in Watch Field", JEE (Japan), No. 87, p. 37-42 (Feb. 1974).

Yoda, H.
"Crystal Watches Herald New Dimension in Timepiece Field. II", JEE (Japan), No. 88, p. 44-8 (March 1974).

Yoda, H., Horie, N.
"Technical Aspects of Crystal Wrist Watches", Proceedings of the 28th Annual Frequency Control Symposium 1974, Atlantic City, NJ, USA, 29-31 May 1974 (Washington, DC, USA: Electronic Industries Assoc. 1974), p. 57-66.

Yoda, H.
"A View of General Trends in Electronic Watches and New Developments in Watch Oscillators", JEE (Japan), No. 101, p. 12-14 (April 1975).

Yoda, H.
"Quartz Crystal Units for Electronic Watches become Standardized", JEE (Japan), No. 121, p. 42-5 (Jan 1977).

Blair, B. E.
"Time and Frequency: A Bibliography of NBS Literature Published July 1955 - December 1970", Report Spec. Publ. 350, Nat. Bur. Stand, Washington, DC, USA (June 1971), 50 pp.

Bowers, K. D.
"Ultrasonics in Communications", Bell Lab. Rec. (USA), Vol. 49, No. 5, p. 139-45 (May 1971).

Dunworth, J. V., Dean, P.
"The National Phtsical Laboratory - Aspects of Work on the Primary Standards of Measurement", Proc. R. Soc. Edinburgh A(GB), Vol. 70, Sec. A, p. 125-41 (1971-72).

Essen, L.
"Electrical Standards in Terms of Frequency and Physical Constants", Alta Freq. (Italy), Vol. 40, No. 8, p. 693-6 (Aug. 1971). In English.

Gerber, E. A., Sykes, R. A.
"A Quarter Century of Progress in the Theory and Development of Crystals for Frequency Control and Selection", Programme of the 25th Annual Frequency Control Symposium (abstracts), Atlantic City, NJ, USA, 26-28 Apr. 1971 (Fort Monmouth, NJ, USA: US Army Electronic Command 1971), p. 10.

Greebe, C. A. A. J.
"Electromagnetic, Elastic and Electro-Elastic Waves", Philips Tech. Rev. (Netherlands), Vol. 33, No. 11-12, p. 311-49 (1973).

Hawkins, D. T.
"Absolute Configuration of Piezoelectrics-A Bibliography", Ferroelectric (GB), Vol. 5, No. 1-2 p. 111-23 (1973).

Lubimov, L. A., Zhourkina, L. I.
"Piezoelectric Devices", IEC Bull. (Switzerland), Vol. 9, No. 31, p. 1-2 (Jan. 1975).

Lubimov, L. A., Zhourkina, L. I.
"Piezoelectric Devices", Etek. Aktuell Elektron. (Sweden), Vol. 18, No. 3, p. 59-61 (March 1975). In English.

Lundbom, P. O.
"On the Activities of URSI Commission I (for Radio Measurements and Standards) During the Last 20 Years and Plans for the Future", CPEM 74 Digest: Conference on Precision Electromagnetic Measurements, London, England, 1-5 July 1974 (London, England: IEE 1974), p. 330.

Mason, W. P.
"Professor Walter G. Cady's Contributions to Piezoelectricity and What Followed from Them", J. Acoust. Soc. Am. (USA), Vol. 58, No. 2, p. 301-9 (Aug. 1975).

Nekrasov, M. M., Lavrineko, V. V., Bozhko, A. A., Kartashev, I. A., Koval, V. S., Miroshincheko, A. P., Yakimenko, Yu. I.
"Elements of Piezo-Electronics and Prospects of Application in Electrical Engineering", Elektririchestvo (USSR), p. 1-8, No. 12 (1971). In Russian. English translation in: Elec. Technol. USSR (GB), Vol. 4, p. 134-5 (1971).

Paige, E. G. S.
"Acoustic Surface Waves and Their Applications in Electronics", Proceedings of the 7th International Congress on Acoustics, Budapest, Hungary, 18-26 Aug. 1971 (Budapest, Hungary: Akademiai Kiado 1971). p. 141-51.

Pajewski, W.
"Development in Research and Technology of Piezoelectric Elements", Elektronika (Poland), No. 1, p. 25-34 (1971). In Polish.

Pajewski, W.
"Piezoelectronics and Acoustoelectronics", Elektronika (Poland), No. 1-2, p. 50-4 (1973). In Polish.

Sabine, H., Cole, P. H.
"Acoustic Surface Wave Devices: A Survey", Proc. Inst. Radio Electron. Eng. Aust. (Australia), Vol. 32, No. 5, p. A12 (May 1971). (13th national convention of the Institution of Radio and Electronics Engineers, Australia (abstracts), Melbourne, Australia, 24-28 May 1971).

Shaw, H. J.
"An Overview of Surface-Wave Methods and Devices", 81st meetings of the Acoustical Society of America (abstracts only received). Washington, DC, USA, 20-23 Apr. 1971 (New York, USA: Acoustical Soc. America 1971), p. 29.

Stone, R. R., Jr., Phillips, D. H., Berg, W. B.,Jr.
"Technology Forecasts: Frequency and Time", Digest of Technical Papers of 1971 IEEE Region 2 Conferernce on Technology Forecasting and Assessment of Electrotechnology, Washington, DC, USA, 8 Oct. 1971 (New York, USA: IEEE 1971), p. 54-5.

Tanaka, T.
"Recent Developments and Promising Applications of Piezo-Resonators", JEE (Japan), No. 80, p. 58-60, 62 (July 1973).

4. Anonymous/Unknown Authors.

1.2.2

"Progress in Microelectronics, Acoustic-Electrical Surface Waves - Building Elements".
VDI Z. (Germany), Vol. 115, No. 8, p. 639-41 (June 1973). In German.

1.4

"Quartz Crystals, Mechanical Resonators for Electronics".
Radio Mentor Electron. (Germany). Vol. 42, No. 8, p. 296 (Aug. 1976). In German.

"Surface Acoustic Wave Technology".
New Electron. (GB), Vol. 10, No. 8, p. 64, 67, 71 (19 April 1977).

1.5

"Testing Resonant Reed Filters".
Dawe Dig. (GB), Vol. 14, No. 1, p. 5-6 (May 1971)

"Testing Resonant Reed Filters".
Electron. Compon. (GB), Vol. 12, No. 12, p. 758-9 (9 July 1971).

1.5.2

"Improved SAW Filters Minimize Sidelobes in Chirp Radar".
Microwave Syst. News (USA), Vol. 6, No. 5, p. 87, 90 (Oct-Nov 1976).

1.5.2.1

"SAW Bandpass Filter".
Microwave J. (USA), Vol. 18, No. 1, p. 32 (Jan 1975)

1.8.1

"A Universal Quartz Crystal Oscillator".
Rev. Esp. Electron (Spain), Vol. 23, No. 263, p.35 (Oct 1976). In Spanish.

"A Voltage Controlled Variable Frequency Ultraliner Quartz Oscillator".
Electronique Industr. (France), No. 128, p. 674-5 (1969). In French.

1.8.2

"Surface Acoustic Wave Oscillator Tuned by Magnetoelastic Effect".
Electron. Lett. (GB), Vol. 13, No. 19, p. 588-90 (15 Sept 1977).

1.8.3

"Characteristics of Electromechanical Resonators as Frequency Standards".
Eurocon 71 digest. Lausanne, Switzerland, 18-22 Oct 1971 (New York, USA; IEEE 1971). 2 pp.

"Crystal Timebase for Synchronous Clocks".
Elektor (GB), Vol. 2, No. 7-8, p. 721 (July-Aug 1976).

"Crystal Controlled Clock Pulse Generator"
ABU Tech. Rev. (Japan), No. 6, p. 10-15 (Jan 1970).

"Development of a Generator of Standard Frequencies".
Toute Electron. (France), No. 378, p. 51-3 (June 1973). In French.

"Economical Crystal Controlled Clock Generator".
Electron. Eng. (GB), Vol. 50, No. 610, p. 19 (Aug 1978)

"MOS Clock II".
Elektor (GB), Vol. 1, No. 4, p. 634-6 (June 1975).

"Radio Frequency Standards".
Bull. Radio & Elect. Engrg. Div., National Research Council, Canada, Vol. 19, No. 4, p. 8 (Oct 1969)

"Review of Frequency and Time Standards".
Instrum. Contr. Syst. (USA), Vol. 43, No. 10, p. 85 (Oct 1970).

"Stable Pierce Oscillator as TTL Clock",
Electron. Aust. (Australia, Vol. 38, No. 11, p. 75, (Feb 1977).

2.1

"Frequency and Time Standard of the Dr. Neher Laboratory".
Data (Netherlands), Vol. 74, No. 4, p. 81-97 (Dec 1973). In Dutch.

2.1.1

"Construction of an Improved Cesium Frequency Standard (NRLM-II)."
Jpn. J. Appl. Phys. (Japan), Vol. 17, No. 4, p. 749-50 (April 1978)

"Cesium Atomic Beam Oscillator Technology for Navigation Satellites".
Report unnumbered. Frequency & Time Systems, Inc. (Jan 1975), 28 pp.

2.1.2

"2.2 pound Rubidium Standard for Systems Uses only 12 W".
Electron. Des. (USA), Vol. 22, No. 5, p. 72 (1 March 1974.

2.1.3

"Hydrogen Frequency Measured Accurately".
Nat. Bur. Stand. Tech. News Bull. (USA), Vol. 55, No. 8, p. 194-205 (Aug 1971)

"Time Studies with Hydrogen Maser".
Sci. Dimension (Canada), Vol. 1, No. 3, p. 3-5 (Aug 1969). In English and French.

"Study of Oscillation Level Saturation of the Hydrogen Maser as a Function of the Atomic Flux Entering the Cavity".
Ann. Phys. (France), Vol. 3, No. 2, p. 145-54 (March 1968). In French.

2.2

Stabilization of a Composite Cavity Single Frequency Laser".
IEEE J. Quantum Electronics (USA), Vol. QE-4, No. 10, p. 699-701 (Oct 1968).

2.2.1

"Single Frequency Superstable Gas Laser".
Sov. J. Quantum Electron. (USA), Vol. 7, No. 11, p. 1425-6, (Nov 1977).

"Informative Meeting on Iodine Stablised He-Ne Lasers".
Braunschweig, Germany; Physikalisch-Technische Bundesanstalt (1977), 158.

3.1

"Analogue Frequency Meter".
Elektor (GB), Vol. 1, No. 5, p. 737, (July-Aug 1975).

"Electromagnetic Radiation in Frequency Measurements".
Electron. Aust. (Australia), Vol. 37, No. 1, p. 31, 33 (April 1975).

"High Accuracy Timing Devices".
Elektron. & Elektrotech. (Netherlands), Vol. 31, No. 769, p. 9-11 (Jan 1976). In Dutch.

"Definition, Realization and Use of Time and Frequency".
London: Institution of Electrical Engineers (1967 Colloquim Digest 1967/16) Paper No. 1/1-8/7.

"Time and Frequency: Two Important Quantities in Modern Measurements".
Tecnol. Eletr. (Italy), No. 12, p. 66-9 (Dec 1976) In Italian.

"Time Measurements: Where are We?".
Mes. Regal. Autom. (France), Vol. 43, No. 2, p. 19-23 (Feb 1978). In French.

"Universal Frequency Reference".
Elektor (GB), Vol. 1.,No. 5, p. 715 (July-Aug 1975).

3.1.1

"50 MHz Counter/Timer"
CSIO Commun. (India), Vol. 4, No 2, p 34, (April-June 1977).

"Precision Timebase for Frequency Counter"
Elektor (GB), Vol. 3, No. 6, p. 22-5 (June 1977)

"Programmable Counter Type Frequency Meter"
Electron. & Microelectron Ind (France), No 211, p. 45-9, (1 Dec 1975). In French

"Universal Counting and Time Measuring Device
Elektron Int (Austria), No 5, P 167-9 (1977)
In German

"Which Counter?"
Automation (GB), Vol 12, No [illegible]9, p 21, 23, 25 (Aug, Sept 1977)

3.2

"UTC Time Scale to Change in 1972
Hewlett Packard J (USA), Vol 23, No 2, p 14 (Oct.1971)

"NBS Frequency and Time Broadcast Service , Radio Stations, WWV, WWVH, WWVB, WWVL
Report Special Publication 236 1969, Nat Bur Stand , Washington, DC , USA, (1969 , 13 pp

"Time Dissemination and Clock Synchronization via Television".
Nat. Bur. Stand. Tech. News Bull. (USA), Vol. 54, No. 6, p. 125-6 (June 1970).

"Standards and Calibration".
Nat. Bur. Stand. Tech. News Bull. (USA), Vol. 55, No. 4, p. 98-99 (April 1971).

"NBS Frequency and Time Broadcast Services".
Report Spec. Publ. 236, Nat. Bur. Stand. Washington, DC, USA, (July 1971). 15 pp.

3.4

"Applications of Mechanical Oscillation in Communication Technology".
Technica (Switzerland), Vol. 18, No. 15, p. 1451-4 (25 July 1969). In German.

"Ultra-Quartz Electronic Quartz Water".
Jemna Mech. & Opt. (Czechoslavkia), Vol. 20, No. 3, p. 86 (March 1975). In Czech.

"The Quartz Era".
Elettrificazione (Italy), No. 11, p. 524-5, (Nov. 1976). In Italian.

"Quartz Timepiece Components".
Microtecnic (Switzerland), Vol. 26, No. 3, p. 157-62 (April 1972).

AUTHOR INDEX

AUTHOR	PAGE
T. Adachi	201
C. Alley	4
Dick Ang	364
A. F. Armington	62, 134
C. Audoin	515
J. Azoubib	473
A. Ballato	293, 311, 322
R. L. Barnes	88
E. Bava	498, 504
W. D. Beaver	189
R. Beeson	337
H. E. Bell	554
J. C. Bergquist	494
D. L. Blanchard	468
E. L. Blomberg	511, 549
J. S. Boulanger	473
C. Bourgeois	255
G. Brandenberger	563
R. Brandmayr	351
R. N. Brown	134
M. Brunet	473
R. Burgoon	406, 411
G. Busca	563
B. H. T. Chai	80
A. R. Chi	468
C. C. Costain	473
S. B. Crampton	543
L. E. Cross	110
H. Daams	473
A. De Marchi	498, 504
J. Detaint	70
S. P. Doherty	134
S. J. Dolochycki	374
A. J. Douglas	346
N. Echigo	277
E. P. EerNisse	300
D. A. Emmons	490
F. Euler	122
M. Feldmann	70
R. L. Filler	351
E. D. Fletcher	346
G. Freon	473
M. E. Frerking	431
E. M. Frymoyer	223
A. J. Fuchs	186
J. J. Gagnepain	239, 337
A. Godone	498
B. Goldfrank	306
A. F. Graziani	166
J. C. Grenier	88
D. L. Griscom	98
B. Guinot	473
E. Hafner	368
L. E. Halliberton	62, 134
T. Haynes	444
H. Helliwig	554
J. Henaff	70
J. Hermann	255
C. R. Hewes	214
F. W. Hopwood	444
M. Horie	235
D. A. Howe	554
M. F. Hribsek	173
N. Inoue	247
D. Janiaud	337
D. M. Jansky	47
S. Jarvis, Jr.	477
R. S. Kagiwada	388
L. A. Kappers	62
H. Kataoka	235
T. Kato	271
S. Kodama	417
D. R. Koehler	118
S. Kogure	247
E. D. Kolb	88
N. Koumvakalis	134
K. Kubota	277
J. Larkin	62
K. F. Lau	388
R. A. Laudise	88
D. L. Lee	379
R. Lefevre	148
P. Lesage	515
A. M. Levine	436
J. B. Lewis	543
P. A. Ligor	122
T. C. Lim	374
H. G. Lipson	182
T. J. Lukaszek	311
G. Marianneau	239
M. Markes	134
J. J. Martin	134
E. M. Mattison	511, 549
B. R. McAvoy	444
D. I. McLean	166
E. S. McVey	425
T. R. Meeker	176, 286
M. Meirs	306, 484
L. G. Miller	473
R. F. Milsom	263
R. D. Mindlin	1
E. Momosaki	247
R. A. Moore	444
S. Motte	277
K. H. Mucke	186
T. Musha	235
K. Nakamura	458
R. J. Ney	368
G. U. Nystrom	549
R. M. O'Connell	402
E. J. Ozimek	80
P. Parcelier	473
T. E. Parker	379
I. Pascaru	484
H. Poignant	70
B. R. Potter	396
R. Pretot	239
A. Risley	477
G. E. Roberts	159
P. J. Rogers	490
M. Rosenfeld	306
R. C. Rosenfeld	220
J. J. Royer	166
Y. Sakuta	458
Y. Sato	417
J. S. Schoenwald	374
R. I. H. Scott	449
H. Sekine	458
Y. Sekine	458
W. E. Van Loben Sels	189
J. H. Sherman, Jr.	181
W. A. Sibley	134
B. K. Sinha	228
R. C. Smythe	209
T. Sonoda	247
E. J. Staples	374
P. Suda	359
M. Suyama	458
C. T. Swanson	425
K. Takahashi	277
Y. Teramachi	235
M. Tetu	515
G. Theobald	239
H. F. Tiersten	228, 293
M. Toki	201
Y. Toudic	70
Y. Tsuzuki	201
K. Uchino	110
H. Ueda	271
M. J. Underhill	449
M. Valdois	337
J. Vanier	477
R. F. C. Vessot	511, 549
J. Vig	351
R. F. Voss	40
F. L. Walls	554
H. T. M. Wang	536, 543
M. Wang	189
A. Warner	306
A. Watanabe	277
R. L. Wilson	406, 411
J. Z. Wilcox	388
D. J. Wineland	494
J. Wise	374
F.J. Witt	206
H. Yamashita	277
K. H. Yen	388
W. Zingg	359
A. E. Zumsteg	359

SPECIFICATIONS AND STANDARDS GERMANE TO FREQUENCY CONTROL

Institute of Electrical and Electronic Engineers

Order through: IEEE Service Center
445 Hoes Lane
Piscataway, NJ 08854
(201/981-0060)

176-1978 Piezoelectricity $ 9.00

177-1966 Piezoelectric Vibrators, Definitions and Methods of Measurements for (ANSI C83.17-1970) $ 4.00

180-1962 Ferroelectric Crystal Terms, Definitions of $ 3.00

319-1971 Piezomagnetic Nomenclature $ 4.00

Electronic Industries Association

Order through: Electronic Industries Assn.
2001 Eye Street, N.W.
Washington, D.C. 20006

(a) Holders and Sockets

RS-192-A, Holder Outlines and Pin Connections for Quartz Crystal Units. (Standard Dimensions for older types.) $ 6.80

RS-367, Dimensional and Electrical Characteristics Defining Receiver Type Sockets. (Including crystal sockets.) $20.20

RS-417, Crystal Outlines (Standard dimensions and pin connections for current quartz crystal units - 1974) $ 7.80

(b) Production Tests

RS-186-E, (All Sections), Standard Test Methods for Electronic Component Parts $42.00

(c) Application Information

Components Bulletin No.6, Guide for the Use of Quartz Crystals for Frequency Control $ 4.90

International Electrotechnical Commission

Order through: American National Standards Institute
1430 Broadway
New York, New York 10018

*ANSI can quote prices on specific IEC publications on a day to day basis only. All IEC and ISO standards have been removed from its Standards Catalog. Call ANSI, NYC (212/354-3300) for prices.

IEC Publication 122-1 (1976). Quartz crystal units for frequency control and selection. Part 1: Standard values and test conditions. (Second edition)

IEC Publication 122-2 (1962) Section 3: Guide to the Use of Quartz Oscillator Crystals, including Amendment 1 (1969)

IEC Publication 122-3 (1977) Part 3: Standard Outlines and pin connections. (Second edition)

IEC Publication 283 (1968) Methods for the Measurement of Frequency and Equivalent Resistance of Unwanted Resonances of Filter Crystal Units

IEC Publication 302 (1969) Standard Definitions and Methods of Measurement for Piezoelectric Vibrators Operating Over the Frequency Range up to 30 MHz

IEC Publication 314 (1970) Temperature Control Devices for Quartz Crystal Units, including Supplement 314A Contents: General Characteristics & Standards; Test Conditions; Pin Connections

IEC Publication 314A (1971) First Supplement to Publication 314 (1970) Contents: Guide to the Use of Temperature Control Devices for Quartz Crystal Units.

IEC Publication 368 (1971) Piezoelectric Filters, including Amendment 1, Amendment 2, and Supplement 368A and 368B Contents: General Information & Standard Values; Test Conditions

IEC Publication 368A (1973) First Supplement to Publication 368 (1971) Contents: Guide to the Use of Piezoelectric Filters

IEC Publication 368B (1975) Second Supplement to Publication 368 (1971) Contents: Piezoelectric Ceramic Filters

IEC Publication 444 (1973) Basic Method for the Measurement of Resonance Frequency and Equivalent Series Resistance of Quartz Crystal Units by Zero Phase Technique in a π - Network

IEC Publication 483 (1976) Guide to Dynamic Measurements of Piezoelectric Ceramics with High Electromechanical Coupling

Department of Defense

Order through: Naval Publication & Form Center
5801 Tabor Avenue
Philadelphia, PA 19120

MIL-C-3098 Crystal Unit, Quartz, General Specification For

MIL-H-10056 Holders (Enclosures), Crystal, General Specifications For

MIL-STD-683 Crystal Units, Quartz; And Holders, Crystal

MIL-F-28734 Frequency Standards, Cesium Beam, General Specifications For

MIL-O-55310 Oscillators, Crystal, General Specification For

MIL-F-18327 Filters, High Pass, Low Pass, Band Pass Suppression and Dual Functioning, General Specification For

MIL-O-39021 Oven, Crystal, General Specification For

MIL-O-55240 Oscillators, Audio Frequency

MIL-F-28811 Frequency Standard, Cesium Beam Tube

ANNUAL FREQUENCY CONTBOL SYMPOSIA

A complete Index to the Proceedings of the Frequency Control Symposium for 1956 (10th) through 1976 (30th) is available as part of the 1976 (30th) Proceedings.

No.	YEAR	DOCUMENT NO.	OBTAIN FROM*	COST
10	1956	AD 298322	NTIS	16.50
11	1957	AD 298323	"	19.00
12	1958	AD 298324	"	19.00
13	1959	AD 298325	"	21.50
14	1960	AD 246500	"	14.00
15	1961	AD 265455	"	12.50
16	1962	PB 162343	"	15.00
17	1963	AD 423381	"	19.00
18	1964	AD 450341	"	19.00
19	1965	AD 471229	"	19.00
20	1966	AD 800523	"	19.00
21	1967	AD 659792	"	16.50
22	1968	AD 844911	"	19.00
23	1969	AD 746209	"	11.75
24	1970		EIA	6.50
25	1971	AD 746211	NTIS	12.50
26	1972	AD 771043	"	12.00
27	1973	AD 771042	"	14.50
28	1974	AD AO11113	"	13.25
29	1975	AD AO17466	NTIS	14.50
30	1976	AD AO46089	NTIS	16.25
31	1977		EIA	10.00
32	1978		EIA	10.00
33	1979		EIA	12.50

*NTIS - National Technical Information Service
Sills Building
5285 Port Royal Road
Springfield, Virginia 22161

NTIS prices are as of September 1979 and are subject to change.

*EIA - Annual Frequency Control Symposium
c/o Electronic Industries Association
2001 Eye Street, N.W.
Washington, D.C. 20006

Remittance must be enclosed with all orders. For orders placed with NTIS from outside the United States, double the domestic price list per copy for handling and mailing.

When referencing these Proceedings, please use the format shown in the following examples:

(1) W. D. Beaver, "Theory and Design of the Monolithic Crystal Filters" Proceedings, 21st Annual Symposium on Frequency Control, US Army Electronics Command, Fort Monmouth, N.J. pp 179-199, (1967). National Technical Information Service Accession NR. AD 659792

(2) Jeff Stuart Schenwald, "Tunable Variable Bandwidth/Frequency SAW Resonators", Proceedings 31st Annual Symposium on Frequency Control, U.S. Army Electronics Command, Fort Monmouth, NJ pp 240-245, (1977). Copies available from the Electronic Industries Association, 2001 Eye Street, N.W., Washington, D.C. 20006

QUARTZ CRYSTALS FOR ELECTRICAL CIRCUITS
by
R. A. Heising

Available from EIA	$10.00 plus Postage and Handling
U.S.	$ 1.50
Europe	5.00
Asia, Africa & East Europe	6.50

This is a reprint of the original text and is available only as long as supplies last. Send check or money order to: *EIA